

**Determination of PEMS Measurement
Allowances for Gaseous Emissions
Regulated Under the Heavy-Duty Diesel
Engine In-Use Testing Program**

Revised Final Report

Determination of PEMS Measurement Allowances for Gaseous Emissions Regulated Under the Heavy-Duty Diesel Engine In-Use Testing Program

Revised Final Report

Assessment and Standards Division
Office of Transportation and Air Quality
U.S. Environmental Protection Agency

Prepared for EPA by
Southwest Research Institute
EPA Contract No. EP-C-05-018
Work Assignment No. 0-6, 1-6, 2-6

NOTICE

This technical report does not necessarily represent final EPA decisions or positions. It is intended to present technical analysis of issues using data generated in the associated test program. The purpose in the release of such reports is to facilitate the exchange of technical information and to inform the public of technical developments which may form the basis for a final EPA decision, position, or regulatory action.



EXECUTIVE SUMMARY

This report documents a program conducted by Southwest Research Institute® (SwRI®), on behalf of the U.S. Environmental Protection Agency (EPA), the objective of which was to determine a set of brake-specific measurement allowances for the gaseous pollutants regulated under the Heavy-Duty In-Use Testing (HDIUT) program. Those pollutants are non-methane hydrocarbons (NMHC), carbon monoxide (CO), and oxides of nitrogen (NO_x). Each measurement allowance represents the incremental error between measuring emissions under controlled conditions in a laboratory with lab-grade equipment, and measuring emissions in the field using Portable Emissions Measurement Systems (PEMS).

The completion of this program was part of the resolution of a 2001 legal suit filed against EPA by the Engine Manufacturer's Association (EMA) and several individual engine manufacturers regarding certain portions of the Not-to-Exceed (NTE) standards. This dispute was settled on June 3, 2003. A portion of the settlement documents stated:

“The NTE Threshold will be the NTE standard, including the margins built into the existing regulations, plus additional margin to account for in-use measurement accuracy. This additional margin shall be determined by the measurement processes and methodologies to be developed and approved by EPA/CARB/EMA. This margin will be structured to encourage instrument manufacturers to develop more and more accurate instruments in the future.”

The program detailed in this report is the result of the aforementioned statement. Therefore, while this program was contracted through EPA, it represented a joint effort between EPA, EMA, and the California Air Resources Board (CARB). The Memorandum of Agreement (MOA) that was part of the settlement documents outlined a process during which a Test Plan would be jointly developed by EPA, EMA, and the California Air Resources Board (CARB). SwRI was chosen as the contractor to carry out this Test Plan. All efforts during the program were conducted under the direction of a joint body, the HDIUT Measurement Allowance Steering Committee, referred to in this report simply as the Steering Committee. This group was composed of representatives of EPA, CARB, EMA, and various individual EMA member companies. The Steering Committee reviewed all decisions and results during this program, and any changes made to the Test Plan were subject to Steering Committee review and approval before being executed.

The measurement allowances determined in this program were meant to be assessed in comparison to certain NTE compliance threshold values. For this program, a single set of NTE threshold values was determined by the Steering Committee. These values served as the basis for calculating the final measurement allowances, as well as for the scaling of various other parameters during this program. The NTE threshold values used for the program are given in Table 1.

This revised version of the final report contains a number of changes made following EPA's peer review of the original final report. None of the results or conclusions of the original report were affected as part of the revision. The changes made to the report primarily involved additional clarifying language in areas where the peer review process indicated that the original report was unclear or vague.

TABLE 1. NTE THRESHOLD VALUES USED FOR MEASUREMENT ALLOWANCE PROGRAM

Pollutant	NTE Threshold, g/hp-hr
NMHC	0.21
NO _x	2.0
CO	19.4

The final Measurement Allowance values determined at the conclusion of this program are summarized in Table 2. These values were unanimously approved by the Steering Committee, and will be the values published by EPA for use during the HDIUT program. The effective date for these values was be March 1, 2007.

TABLE 2. FINAL MEASUREMENT ALLOWANCES

Pollutant	Measurement Allowance, g/hp-hr
NMHC	0.02
NO_x	0.45
CO	0.5

The remainder of this report details the process used to determine the values reported above.

Acknowledgements

This program could not have taken place without significant contributions from a wide variety of participants. SwRI would like to acknowledge EPA, CARB, and the various participating EMA member companies for jointly funding this effort. Numerous other contributions were made as well. Test engines were supplied by Daimler Chrysler, Caterpillar, and International. In addition Caterpillar also supplied the test truck used for validation testing, and International contributed the diesel particulate filters (DPFs) used on that truck. A considerable quantity of PEMS equipment was provided by EPA in order to facilitate the timely completion of this program. Significant support in terms of training, diagnosis, and technical support was also provided by Sensors Inc. as the primary PEMS manufacturer participating in the program. SwRI would like to thank all of the companies who made these contributions. SwRI would also like to acknowledge the efforts of CE-CERT in completing the on-road validation tests that were a key portion of this program.

SwRI would also like to extend a special thanks to the various individual representatives who made up the Steering Committee. Participation in the Committee required a significant amount of time and energy on the part of these individuals, and SwRI would like to acknowledge the commitment of the Committee members to the successful completion of this program.

SwRI would also like to thank Mr. Ed Oelkers for his efforts in developing and executing the Crystal Ball Monte Carlo simulation model.

Program Methodology

Statistical Simulation Approach (Monte Carlo Model)

During the Test Plan development, it was understood that it would not be feasible to conduct enough representative experiments to directly quantify the measurement allowances. Therefore, the Steering Committee chose a methodology which involved the construction of a statistical Model of the measurement errors. The statistical Model incorporated Monte Carlo (random sampling) methodology to simulate the variation in errors over repeat measurements. The Model was then run thousands of times to generate a large data set to allow determination of a robust set of measurement allowances.

The Model incorporates a variety of error components, each of which represents a different source of potential error between the laboratory and the PEMS. Each of these error components was associated with a laboratory experiment designed to characterize and quantify the effect of a potential error source. The result of each experiment was an empirical model, often visualized as a three-dimensional surface, which related the chosen test conditions to the error between a laboratory reference measurement and a PEMS measurement. These empirical models are thus referred to as “error surfaces” in this report. The individual errors are generally referred to as “deltas”, and are typically characterized as the PEMS measurement value minus the laboratory reference value. A positive delta indicates a PEMS measurement higher than the reference, while a negative delta would indicate a PEMS value below that of the laboratory.

A total of 37 error surfaces were incorporated into the Model. The individual error surfaces encompassed a wide variety of error sources. A number of additional potential error sources were investigated during the program beyond those which ultimately resulted in error surfaces. However, in those cases, upon reviewing the experimental data, the Steering Committee deemed that the errors from those sources were not significant; therefore, inclusion in the final Model was not warranted. A wide variety of experiments were conducted to examine the various error terms, but they can be grouped into several major categories.

1. **Steady-State error surfaces.** These error terms characterized precision and bias errors over repeated steady-state measurements. The errors were characterized via steady-state testing in an engine dynamometer test cell. The Model incorporates steady-state surfaces for each gaseous pollutant and exhaust flow rate.
2. **Transient error surfaces.** These error terms characterized precision errors of repeated measurement of 30-second NTE events. Note that bias errors were specifically not included in the transient error surfaces due to concerns about the ability of the reference laboratory methods to accurately quantify emissions over 30-second events. These errors were characterized by repeat transient testing. The transient cycles were composed of a series of 30-second NTE events whose order was randomized for each repeat. This testing was also run in an engine dynamometer test cell. The Model incorporates transient error surfaces for each

gaseous pollutant and exhaust flow rate. Transient error surfaces also were incorporated to look at dynamic errors in the ECM CAN broadcast signals.

3. **Torque and BSFC error surfaces.** These error terms were included to quantify the ability of the engine ECM to accurately predict and broadcast torque and brake-specific fuel consumption (BSFC) in a wide variety of conditions. These experiments involved subjecting the test engines to changes in a variety of different conditions (altitude, temperature, fuel, etc.), and comparing laboratory reference measurements to values generated using parameters broadcast from the engine ECM via the CAN bus. All of these experiments used steady-state tests conducted in an engine dynamometer test cell which was capable of simulating a wide variety of ambient conditions.
4. **Exhaust Flow Measurement error surfaces.** These error terms characterized the effect of various installation/measurement conditions (wind, pipe bends, etc.) on the PEMS exhaust flow meter measurements. These experiments were conducted in an engine dynamometer test cell, with PEMS measurements compared to the laboratory reference flow meters, again using steady-state testing.
5. **Environmental Testing error surfaces.** These error terms were designed to model the effects of various ambient conditions on the PEMS. The conditions examined included ambient temperature and pressure, vibration, electromagnetic interference (EMI), etc. These experiments were conducted using a variety of environmental test facilities at SwRI, each of which was designed to simulate a wide variety of change to a given environmental parameter (such as altitude or EMI interference). In these cases, PEMS were set up to measure standard reference gases during testing, while the environmental conditions were varied according to the design of each experiment. The deltas generated for these tests were between the PEMS measurement and the known reference concentrations.
6. **Miscellaneous error surfaces.** Several additional error surfaces were incorporated in the Model to account for diverse error terms, such as time alignment of data and engine production variability. These error terms involved computational exercises made using data from some of the aforementioned experiments, and in some cases, data supplied by participating engine manufacturers.

Test Methods and Equipment

Engine dynamometer tests were conducted using three different test engines, one Heavy Heavy-Duty (HHD) engine, one Medium Heavy-Duty (MHD) engine, and one Light Heavy-Duty (LHD) engine. These engines were contributed to the program by the engine manufacturers, along with all support needed to insure successful engine operation. These engines were generally model year 2005 or 2006 engines. In order to simulate a post-2007 test environment, SwRI procured several diesel particulate filters (DPFs) which were installed in the exhaust of the various engines during all testing. It should be noted that the filters selected were

designed to regenerate primarily via passive regeneration, as active regeneration systems were not available at the time of this program.

The original intention of the program was to examine PEMS from more than one manufacturer. However, at the time of this program only one equipment manufacturer, Sensors Incorporated, was able to supply commercially available PEMS units to the program. Therefore, the measurement allowance values are based only on measurements made using the Sensors Inc. SEMTECH-DS instrument. Multiple examples of that instrument were used during the program, often in parallel with each other, in order to encompass instrument-to-instrument variation errors. Late in the program, several Horiba OBS-2200 units became available. These units were incorporated into the program as time and resources allowed. However, all Horiba PEMS measurements were performed for information purposes only, and no Horiba PEMS data was used in the generation of the measurement allowances.

The primary engine laboratory reference measurements used for this program were made using a transient capable engine dynamometer test cell, which incorporated a full-flow CVS dilution tunnel. The test cell was capable of simulating a wide variety of ambient conditions in order to facilitate some of the Torque and BSFC error experiments. All of the emission concentration deltas that went into the Model were generated using the dilute laboratory measurements as the reference value. However, raw exhaust laboratory measurements were also conducted during this program for quality assurance purposes, and as an additional check on the primary reference. The laboratory reference values are summarized in Table 3. All calculations were made using methods detailed in 40 CFR Part 1065. Unless otherwise stated, all engine tests were run using U.S. EPA certification grade ultra-low sulfur 2-D diesel fuel.

TABLE 3. LABORATORY REFERENCE METHODS

PEMS Measurement	Laboratory Reference	Reference Method
Gaseous Analyzers – engine testing	Dilute Emission Analyzers ¹	Dilute mass calculated using CVS flow, then raw concentrations back-calculated using laboratory raw exhaust flow
Raw Exhaust Flow	Measured Intake Air Flow and Fuel Flow	Air Flow measured using Laminar Flow Element (LFE). Fuel Flow measured using coriolis type meter.
Predicted Torque (from CAN)	Measured Torque	Shaft mounted in-line torque meter
Predicted BSFC (from CAN)	Measured Fuel flow and Power	see above notes
Gaseous Analyzers – environmental chamber testing	Standard reference gas concentrations	Reference values validated on all bottles at SwRI

¹ Reference NMHC levels were based on laboratory raw measurements due to very low levels.

PEMS and Laboratory Audits

In order to insure that all measurements were conducted at the highest quality level, a full audit of the reference laboratory was conducted prior to the start of testing. In addition, the audit was performed to verify that all requirements given in 40 CFR Part 1065 were met, and that any recommended practices were followed to the extent possible. Quality assurance procedures were in place to insure that all test equipment was maintained within the requirements of Part 1065 throughout the program.

Audits based on 40 CFR Part 1065 were also conducted on all PEMS equipment used in the program. In addition, PEMS equipment was re-audited whenever equipment failures resulted in major repairs to one or more PEMS. This occurred on numerous occasions throughout the program. In general, the PEMS passed the requirements in 40 CFR Part 1065, but there were exceptions. In cases where the requirements were not initially met, the PEMS manufacturer was offered an opportunity to correct the problem. However, in cases where no correction was available, the Steering Committee had the option to approve the deficiency and continue testing.

Individual audit results for each PEMS are detailed in Section 2 of this report. However, there were several general issues which arose during the audits which are summarized here.

Gaseous Analyzer Linearity

Numerous gas analyzers on the various PEMS units failed to meet the 1065 Subpart D linearity criteria during the program. Nearly all of these failures were in the regression line intercept criteria outlined in 1065.307 Table 1, which specify a tolerance on the intercept of 0.5% of the maximum value expected during testing. Because this value was not known at the time of the audits, this maximum value was interpreted as the span gas value used for the instrument. It should be noted that this interpretation resulted in a relatively loose tolerance for this particular check, which the PEMS still failed periodically. A number of the gas analyzers in various PEMS, particularly the NDUV analyzers used for NO and NO₂ measurement tended to fail this requirement high. Certain units passed all linearity criteria.

Sensors Inc. initially re-calibrated one unit as a result of this failure, but numerous other units were deemed by Sensors Inc. to be operating correctly, and Sensors Inc. indicated that they felt there were issues with the linearity procedure as written in 40 CFR Part 1065. Due to the difficulty in continually re-calibrating these units and comments from Sensors Inc., the Steering Committee ultimately elected to allow testing to continue with PEMS units that failed the 1065 linearity verification. However, this remains an issue to be addressed during in-use testing, wherein manufacturers will be legally bound to use equipment that meets all 1065 specifications. It should be noted that the Horiba PEMS passed all 1065 linearity checks.

NO₂ Penetration Checks and NO₂ Measurement

Initially all of the PEMS failed the NO₂ penetration check in 1065.376 due to issues within the sample handling systems of the SEMTECH DS units. This issue turned out to have a measurable effect on NO_x emissions results, due to the relatively high tailpipe NO₂ fractions resulting from the use of the catalyst-based DPFs. The result was a significant low bias in NO_x

measurements from the PEMS units as initially configured. As a result, it became necessary for Sensors Inc. to modify the test equipment during the course of the program. Although such a modification was initially not allowed in the Test Plan, the Steering Committee approved a retrofit in order to address this significant measurement error. This modification was successfully accomplished, and is now commercially available on all new SEMTECH DS units and as a retrofit for existing units. Following this retrofit, all PEMS passed the NO₂ penetration check. All of the data that was used in the Monte Carlo Model reflects the use of this retrofit. However, the issue resulted in significant program schedule delays as the retrofit was designed, tested, and implemented.

Exhaust Flow Meter Linearity and Calibration

The exhaust flow meter linearity checks required considerable effort on the part of both SwRI and Sensors Inc., and may ultimately have been a source of some of the bias errors observed during later testing as well. The issue was directly linked to the size (diameter) of the Sensors Inc. exhaust flow meter (EFM). The 5-inch flow meters had little difficulty with the linearity check at SwRI, with only one failing unit which was re-calibrated by Sensors Inc. and then passed linearity at SwRI. However, the initial linearity checks showed slope problems with all the smaller flow meters, some low and some high. All of the 3-inch and 4-inch meters were sent to Sensors Inc. for re-calibration. Linearity checks on the newly calibrated meters indicated low slopes for the 4-inch flow meters, and even lower on average for the 3-inch flow meters. Considerable effort was directed into determining the root cause for these discrepancies.

A possible cause for the linearity failures was a design difference between the flow stands used by SwRI and Sensors Inc. for calibration and linearity checks. The arrangement of the SwRI flow stand is test flow meter followed by reference flow meter followed by pump, while the Sensors Inc. flow stand uses the reverse order. Thus the Sensors Inc. calibrations were performed with the EFM under a slight positive pressure, while the SwRI linearity checks were performed with the EFM under a slight negative pressure. According to the static pressure measurement in the PEMS EFMs, the 5-inch meters, which showed minimal error, were under a vacuum of about 2 kPa, while the 4-inch and 3-inch meters both experienced slightly higher vacuum levels of about 2.5 kPa.

The Steering Committee ultimately decided to authorize recalibration of the Sensors Inc. flow meters using the SwRI linearity data. The average slope adjustment was on the order of a 4 percent positive offset for both the 3-inch and 4-inch flow meters.

Engine Dynamometer Results

Detailed information on the results of all of the engine dynamometer laboratory experiments performed to generate individual error surfaces is given in Section 3 of this report. However, there were several overall trends which affected the results of several of the dynamometer experiments, which are discussed below.

NMHC Measurement and Low NMHC Emissions

Although the engine experiments were designed to quantify errors in NMHC, CO, and NO_x, the NMHC measurements presented a particular problem due to the very low levels of NMHC observed during testing. This was due to a combination of relatively low engine-out NMHC levels and the use of catalyst-based DPFs. In this program, the DPFs used were CRTs procured from Johnson Matthey. In addition, the DPFs were sized to be larger than normal for these engines in order to keep engine backpressure levels low, because none of these pre-2007 test engines were originally designed to operate with DPFs installed. The resulting DPF-out NMHC levels were at or near zero all of the time.

An attempt was made to address this issue by using a 2007 production-style DPF, which likely had lower precious metal loadings, on one of the test engines. However, NMHC was still at a level of less than 10 percent of the 2007 standard level of 0.14 g/hp-hr. The levels observed were often below the noise limitations of the laboratory reference method for all test engines, thus complicating the generation of meaningful deltas. As a result, the data analysis methods and resulting error surfaces for NMHC were modified considerably from the Test Plan.

An additional issue with NMHC derived from the fact that no commercially viable method of in-field NMHC measurement existed at the time of the experiments. All available PEMS measured only total hydrocarbons (THC). Therefore, the PEMS NMHC measurements were THC measurements multiplied by a factor of 0.98 as allowed in CFR 40 Part 1065.

Engine-PEMS Installation Variability

The Test Plan was designed to capture PEMS variability from unit-to-unit and engine-to-engine. However, it was anticipated that there would be a certain amount of uniformity in the measurement error trends and the response of the PEMS observed from one engine to the next, despite the different installations, and in some cases different measurement equipment (such as different sized exhaust flow meters). When the results of experiments on all three engines were compared, it was apparent that reproducibility from engine installation to engine installation was a more important variable than expected. This resulted in the need to modify some of the initially planned data analysis methods to account for the unexpectedly large source of variation.

CO Measurement

CO measurements throughout the program were generally affected by the relatively poor resolution of the NDIR detector used for CO measurement in the SEMTECH DS. Tailpipe CO levels during this program were orders of magnitude below the CO NTE threshold levels (due to the catalyst-based DPFs). The NDIR detector in the SEMTECH DS uses the same percent scale resolution for CO that is used for CO₂. As a result, the minimum resolution is 0.001 %, or 10 ppm. In addition, it was found that simply switching from the calibration gas port to sample line generally resulted in a reading of roughly 20 to 60 ppm, even when reading zero gas through the sample line. However, this lack of accuracy at low levels is not likely to be a compliance issue, as the tailpipe levels observed with the SEMTECH-DS CO even with resolution and bias issues were still orders of magnitude below the NTE threshold. Therefore, no particular modifications were made to the Test Plan to account for this issue.

Individual Error Surfaces

The following is a brief overview of the results for each of the various engine dynamometer experiments. This summary gives a broad overview of the general magnitude of each error term, as well as any major issue or findings associated with a given experiment. Detailed information for each experiment is given later in the report.

Steady-State Error Surfaces

Considerable effort was expended in the generation of the steady-state data sets, as the data from these experiments was also used in the analysis of data from most of the other engine experiments. These experiments were run on all three engines, with three PEMS run simultaneously for all of these experiments. Due to various equipment failures, the same three PEMS were not used on all three engines. The steady-state error surfaces deal with both bias and precision errors. Steady-state deltas were generated by comparing PEMS measurements to laboratory measurements for each individual data point, and the data were then pooled to generate the error surface. Because these matched pairs of PEMS-laboratory data were used, the steady-state error surfaces were not affected by variability of the test article itself.

The final NMHC error surface incorporated only data from Engine 2, which was the only engine showing a significant number of non-zero PEMS THC readings. The magnitudes of the error deltas for the steady-state error surfaces are summarized in Table 4. For errors which were not level dependent, the size of the error is shown as a percentage of the average value at the appropriate NTE threshold. It should be noted that these average concentration values at the thresholds are only estimates which were calculated by examining NTE data supplied by various engine manufacturers, and that these calculations assume certain average power levels and flow rates. These values are used only as a means to portray the magnitude of the steady-state errors.

TABLE 4. MAGNITUDE OF ERROR TERMS FOR STEADY-STATE ERROR SURFACES

Percentile	Error Magnitudes				
	NMHC, % threshold ¹	CO, % threshold ¹	NO _x , % threshold ¹	CO ₂ , % threshold ¹	EFM, % max ²
5 th	0%	0.3%	-5% ³	0.3%	-1%
50 th	1%	1.1%	0	0.4%	5%
95 th	7%	2.0%	5%	0.8%	11%
¹ %threshold = percent of average concentration at NTE threshold, or for CO ₂ average value during “typical” NTE event (NMHC = 60 ppm, CO = 4450 ppm, NO _x = 290 ppm, CO ₂ = 8 %)					
² %max = percent of maximum value, varies by flow meter size					
³ Above 400ppm, NO _x 5 th percentile appeared level dependent at -14% of point					

The NO_x error surface was complicated by the engine-to-engine variability issues described earlier. Steady-state NO_x errors were generally independent of level. However, at

NO_x concentrations above 400 ppm, larger negative errors were observed. These errors showed a dependency on level; generally at about -14% of point (positive errors remained unchanged). The NO_x errors were due to negative biases observed for some of the PEMS during tests on Engine 3. The reason for this negative bias is not fully understood, as the PEMS passed all NO_x related Part 1065 QA checks during this time.

The steady-state exhaust flow meter error surfaces were also complicated by large variations in observed errors engine and test installation to another. A different size flow meter was used for each of the three test engines, and each size flow meter appeared to have different magnitudes of error. In general, a net positive bias was observed with the PEMS EFMs as compared to the laboratory, with larger biases for the smaller diameter EFMs. Some of this error may have been the result of calibration method differences between Sensors Inc. and SwRI, as discussed earlier, but the calibration differences were not large enough to account for all of the positive bias observed.

Transient Error Surfaces

The transient error surface experiments were also run on all three test engines. This data set was used not only to generate the transient error surfaces, but also to generate other error surfaces dealing with dynamic and time alignment errors that are described later. As with the steady-state experiments, three PEMS were run in parallel for the transient experiments, although the same three PEMS were not used for all three engines.

The transient error surfaces deal with precision errors that result from transient operation. Although bias errors could have been quantified, the Test Plan specifically excluded bias error from the transient error surfaces. As a result, PEMS variability was characterized with respect to the median PEMS value for a given NTE event, without direct reference to the transient laboratory data. A secondary task for this experiment was to provide an initial assessment of the laboratory's ability to repeat such short transient measurements.

The transient error surface data analysis was complicated by the desire to correct for precision errors already characterized by the steady-state measurements, so that the transient surfaces would characterize only the incremental error due to transient operation. The method given in the Test Plan called for the variability of the steady-state measurements to be subtracted from the variability observed for the transient experiments, on an engine-by-engine basis. However, because both of these variability terms are evaluated across all the repeats for a given engine as a pooled data set, the analytical method was particularly vulnerable to issues related to variability in the test article itself (i.e. variability in the pooled NO_x level during steady-state or transient testing).

This vulnerability manifested on several occasions throughout the transient error surface experiments. In some cases, it was addressed by removing selected outliers where the engine did not repeat from the pooled data sets for both steady-state and transient experiments. In other cases, however, this approach was not adequate to address variability problems. For Engine 3, steady-state variability was intermittently higher than transient variability for many concentration levels. As a result, the transient data analysis methodology was modified considerably from the one originally designed in the Test Plan. Because bias errors were not included, all transient

error surfaces have 50th percentile error values of zero. A summary of the magnitude of the transient error surfaces is given in Table 5. The gaseous emissions errors showed a dependency on level, and are therefore given as percent of point values. The EFM transient errors were not as level dependant and are given as a percent of maximum flow.

TABLE 5. MAGNITUDE OF ERROR TERMS FOR TRANSIENT ERROR SURFACES – GASEOUS ANALYZERS AND EXHAUST FLOW

Percentile	Error Magnitudes				
	NMHC, % point	CO, % point	NO _x , % point	CO ₁ , % point	EFM, % max ¹
5 th	-0.03%	0%	-2.5%	1%	-0.7% ²
50 th	0%	0%	0%	0%	0%
95 th	3%	0%	2.5%	1%	0.6% ²

¹ % max = percent of maximum flow rate, varies by flow meter size
² Values represent average across range of range of flow, individual 5th and 95th percentile values varied

Another set of transient error surfaces were generated to capture the effects of transient operations on ECM broadcast signals that are used to predict torque and BSFC. These error surfaces were again designed only to capture precision errors, and therefore the PEMS deltas for each repeat were generated with respect to the median PEMS value for a given event. The magnitude of these ECM-related transient error surfaces is summarized in Table 6.

TABLE 6. MAGNITUDE OF TRANSIENT ERROR TERMS FOR ECM VARIABLES

Percentile	Error Magnitudes			
	CAN-Speed, % point	CAN-Fuel Rate, % max ¹	Interpolated Torque, % max ¹	Interpolated BSFC, % average ²
5 th ³	-0.2%	-0.8%	-0.9%	-0.2%
50 th ³	0%	0%	0%	0%
95 th ³	0.2%	0.6%	0.7%	0.2%

¹ % max = percent of maximum engine torque or fuel rate
² % average = percent of average BSFC over a “typical” NTE event = 245 g/kW-hr
³ Values represent average across range of measurement, individual 5th and 95th percentile values varied and may be as large as 2-3 times averages

Torque and BSFC Error Surfaces

There were a number of engine experiments associated with various sources of error in torque and BSFC estimation. Some of these were run only on selected engines, as noted below for each error surface. The PEMS values for these surfaces were not broadcast directly from the engine ECMs. Rather ECM CAN broadcast speed and CAN broadcast fuel rate were recorded during these experiments. For each test engine, a 40-point steady-state map was run to interpolate torque and/or BSFC from CAN-speed and CAN-fuel rate. The recorded values were

post-processed via interpolation to provide the resulting PEMS values for comparison to the laboratory reference values. A summary of the magnitude of each of the torque and BSFC error surfaces is given in Table 7. Each of the error surface types is summarized briefly below.

TABLE 7. MAGNITUDE OF TORQUE AND BSFC ERROR SURFACES

Error Surface	Error Magnitudes		
	5 th Percentile	50 th Percentile	95 th Percentile
Torque	% max ¹		
Interacting Parameters – DOE ²	-0.5%	0.6%	2.3%
Interacting Parameters – Warm-up	-5.9%	0%	5.9%
Independent Parameters	-1.0%	0%	1.8%
Interpolation	-0.9%	0.06%	1.6%
BSFC	% average ³		
Interacting Parameters – DOE ²	-4.2%	-1.5%	0.8%
Interacting Parameters – Warm-up	-3.6%	0%	3.6%
Independent Parameters	-1.8%	0.2%	1.2%
Interpolation	1.0%	0.3%	3.7%
¹ % max = percent of maximum engine torque			
² DOE percentiles are average percentiles for whole load range, values varied somewhat by level			
³ % average = percent of average BSFC during “typical” NTE event = 245 g/kW-hr			

Interacting Parameters – Design of Experiment

The Design of Experiment (DOE) experiment was designed to characterize errors in predicted torque and BSFC based on a variety of operating and environmental conditions. The conditions included barometric pressure, manifold temperature, exhaust restriction, and inlet restriction. These parameters were all varied according to the DOE test matrix. Using steady-state testing, this experiment was run on two of the three test engines. The data was all pooled together to form a single error surface. A “baseline” set of tests were used to remove interpolation errors from the data set, because those errors are already accounted for elsewhere in the Model.

Interacting Parameters – Warm-up Experiment

The warm-up experiment was designed to capture errors in predicted torque and BSFC related to variations in engine fluid properties and operating temperatures, including viscosity effects. An exhaustive test matrix of these parameters could not readily be conducted; therefore, these errors were dealt with collectively using a relatively simple cold-start warm-up experiment. This experiment was run on all three engines. However, two of the three engines (both of which were EGR equipped) were started from low room temperature condition (roughly 15°C), while a third engine (non-EGR equipped) was soaked to a temperature near 0°C prior to engine start. The error surface values were characterized by finding the maximum error observed during the experiment after the point in time where all engine temperatures had reached the entry point of

the NTE zone, as defined in CFR 40 Part 86. The data from all tests was pooled together to generate a final error surface.

Independent Parameters

The independent parameters experiment characterized errors in predicted torque and BSFC caused by changes in fuel or ambient humidity levels. Three different ULSD fuels were tested which spanned a wide range of properties including aromatic content, density, and cetane number. Three humidity levels were also run from near zero humidity to levels near 28 g/kg. A full nine point test matrix was run testing all nine combinations of these parameters. A clear trend was observed for fuel changes, while humidity changes did not demonstrate an obvious trend. All of the data for all test points was collected into a single error surface. This experiment was run only on the MHD engine.

Interpolation Torque and BSFC Errors

During the design of the Test Plan, it was determined that a 40-point speed-load matrix would be used to define an interpolation grid for predicted torque and BSFC from CAN-speed and CAN-fuel rate. While this matrix served the needs of the program, it was felt that in real-world testing, the test matrix was too dense, placing an excessive mapping burden on individual engine manufacturers. The Steering Committee determined that a 20-point speed-load matrix would be a more acceptable level of effort. However, the less dense grid would likely lead to more interpolation errors in use.

The interpolation error surfaces were designed to capture the incremental error involved in dropping from a 40-point matrix to a 20-point matrix. The generation of this surface was a computational exercise carried out using the initial 40-point steady-state map data generated for each engine. The Steering Committee down-selected 20 points from those 40 to generate the coarser grid. A matrix of several thousand CAN-Speed and CAN-Fuel Rate combinations was run using both 40-point and 20-point grids, and these data sets were compared to generate the final deltas, 20-point values minus the 40-point values. Percentile values from this data set were averaged for all three engines to derive the final error surface.

Exhaust Flow Meter Error Surfaces

There were three exhaust flow meter installation experiments, each of which dealt with a different potential error source. All of these experiments were conducted only using Engine 1, which used a 5-inch diameter Sensors Inc. exhaust flow meter. The first dealt with errors due to pulsations in the exhaust. For this experiment, the DPFs were removed from the exhaust and the flow meter was relocated to a position relatively close to the turbocharger outlet. The second experiment dealt with non-uniform velocity profiles in the EFM introduced by pipe bends upstream of the flow meter. This second experiment was referred to as swirl error. The magnitude of these error terms is summarized below in Table 8.

TABLE 8. MAGNITUDE OF ERROR TERMS FOR EXHAUST FLOW ERROR SURFACES

Percentile	Pulsation Errors, % max ¹	“Swirl” Errors, % max ¹
50 th	0.5% to 2%	0.1% to 0.9%
Total spread 5 th to 95 th ²	0.2% to 0.8%	0.1% to 0.5%
¹ %max = percent of maximum flow rate, varies by flow meter size ² This value is the total width of the error band between the 5 th and 95 th percentile boundaries.		

A third experiment was conducted to examine the possible effects of air currents up to 60 mph across the outlet of the EFM in various directions. The wind experiments resulted in no significant errors; therefore this error surface was removed from the Model.

Miscellaneous Error Surfaces

There were several error surfaces which either did not fit under the above categories, or were based on data taken outside this program. These error surfaces are described below.

OEM Torque and BSFC Error Surfaces

The OEM torque and BSFC error surfaces were generated based on data supplied by the various engine manufacturers directly to EPA. The intention for these error surfaces was to characterize errors based on a variety of terms chosen by joint agreement of the Steering Committee members. Some of these error sources include production variability, the action of various AECs, etc. The data was combined and analyzed by EPA. Discussions were held between EPA and individual engine manufacturers, due to the confidential nature of much of the information being disclosed. At the end of this process, EPA submitted a single set of error surfaces, which was approved by the Steering Committee for inclusion in the Model. The magnitude of these errors is described in Table 9.

TABLE 9. MAGNITUDE OF OEM ERROR SURFACES

Percentile	Error Magnitudes	
	Torque, % point	BSFC, % point
5 th	-5.9%	-6.5%
50 th	0%	0%
95 th	5.9%	6.5%

Time Alignment Errors

The time alignment error surface captured the effect of errors in time alignment of the various continuous PEMS data sources on the final brake-specific emission results. This error source was not originally included in the Test Plan, and no experiment had been designed to examine it. However, during various Steering Committee discussions over the course of the program, it was decided that time alignment was a potentially significant source of error, and that it should be incorporated into the Model. This proved difficult because unlike many of the other terms which dealt with a single measurement term, time alignment is associated with the collection of the various data streams into the final result. Therefore, a single additive delta could not easily be generated.

Ultimately, the Steering Committee settled on a multiplicative adjustment factor which would be applied after all other error terms had been added and the final brake-specific result had been determined. A separate factor was developed for each pollutant, and for each of the three calculation methods allowed in the HDIUT program. The error values were generated using a set of transient data from each engine. Time alignment of three data streams; the gaseous analyzers, the exhaust flow meter, and the ECM vehicle interface data stream, were perturbed relative to one another by increments of 0.5 and 1 second alignment errors in various combinations forward and backward. The brake-specific emission levels for all 30 NTE events in the cycle were calculated for each misaligned data set, and were compared to values calculated using the nominal time alignment values. The errors were pooled across all three engines to arrive at a final set of error terms. Time alignment values were only generated for NO_x and CO, because NMHC values were too low and stable to see any discernible trends in NMHC due to time alignment. The final time alignment values are given in Table 10 below.

TABLE 10. MAGNITUDE OF TIME ALIGNMENT ERROR SURFACES

Calculation Method	Percentile	Error Values, % point (BS emission level)	
		CO	NO _x
1	5 th	-7.5%	-3.2%
	50 th	0.0%	-0.1%
	95 th	4.6%	1.5%
2	5 th	-5.4%	-1.3%
	50 th	0.0%	0.0%
	95 th	5.1%	1.5%
3	5 th	-5.2%	-1.4%
	50 th	0.0%	0.0%
	95 th	12.3%	2.9%

The use of the time alignment error term was not universally accepted by all of the Steering Committee members, due to concerns over the method by which it was applied, and the potential magnitude of its effects compared to all other error terms. However, the majority vote of the Steering Committee was to include this error surface in the final Model.

Environmental Chamber Results

Detailed information on the results of all of the environmental chamber experiments performed to generate individual error surfaces is given in Section 4 of this report. However, several general observations can be made regarding the environmental chamber test results.

These tests were different from the engine dynamometer tests in that they did not involve the sampling of engine exhaust. Rather PEMS errors during environmental chamber testing were conducted while sampling reference gases at various concentrations over an automated sequence. These gases were sampled continuously while the various environmental disturbances were applied to the PEMS. Environmental error sources that were examined included the effects of ambient temperature, ambient pressure (i.e., altitude), vibration, and electromagnetic interference (EMI/RFI). In addition, because the PEMS HC instrument used ambient air for the FID burner air supply, the effect of ambient HC variation was examined on the NMHC measurement.

In most cases, the observed effect of most of the environmental disturbances was relatively small, as compared to other error sources examined during this program. During the course of environmental testing, it was often noted that the PEMS exhibited similar variations on analyzer response whether the environmental disturbances were applied or not. The exception to this general trend was NMHC, which demonstrated considerable variation as a result of both temperature and ambient HC variation. This is despite the fact that a fairly broad range disturbance was applied for each potential error source. It should be noted that in some cases, particularly for the vibration and EMI/RFI experiments, the range of environmental disturbances was actually sufficient to cause occasional functional failures of the PEMS.

The relative magnitude of the environmental error surfaces is given in Table 11. In general, these error surfaces were centered around a zero error, with the table value showing a typical maximum range of the error surface values, as a percentage of average value at the appropriate NTE threshold. Generally, this error could be either positive or negative.

TABLE 11. MAGNITUDE OF ERROR TERMS FOR ENVIRONMENTAL ERROR SURFACES

Error Surface	Maximum Error Magnitudes				
	NMHC, % threshold	CO, % threshold	NO _x , % threshold	CO ₂ , % threshold	EFM, % max ¹
Temperature	7.5 %	0.1 %	2.8 %	0.5 %	0.2 %
Pressure	2.5 %	0.7 %	- ²	- ²	0.5 %
EMI/RFI	- ²	- ²	- ²	- ²	0.3 %
Vibration	- ²	- ²	- ²	- ²	- ²
Ambient HC	10 %	n/a	n/a	n/a	n/a

¹ % max = percent of maximum value, varies by flow meter size
² a dash (-) indicates that error effect was not deemed significant enough to justify inclusion in the model

It should be noted that the effect of the environmental surfaces was limited in the overall model by design. This was done in an attempt to simulate the effect of the drift check criteria in 40 CFR Part 1065. The effect of this drift check was simulated in the model by comparing the brake-specific results of each model run, both with and without the environmental errors applied. If these two results diverged by more than the tolerance allowed in 40 CFR Part 1065, generally 4 percent, the result of that particular model run was discarded for the pollutant in question as having failed the drift check. Therefore, the maximum potential effect of the environmental error surfaces was limited.

Given the magnitude of the environmental error surfaces for NMHC, it was recognized that a large number of model runs were likely to fail this drift check at a 4 percent tolerance. Therefore, EPA agreed to widen the drift check tolerance for NMHC for in-use testing from 4 percent to 10 percent. This change will be applied to 40 CFR Part 1065 Subpart J.

Monte Carlo Model Results and Validation

The results of the Monte Carlo simulation run, as well as the details of procedures used to validate these results are given in Section 5 of this report. A summary of these is given below, including a brief description of the selection of the final Measurement Allowances which were given at the front of the Executive Summary.

The final model run to generate the measurement allowance values using all of the data described above was a significant investment of time and resources. A data set of 195 “reference NTE events” was used to conduct the model run. Each event was run through the model at least 10,000 times and in some cases many more times. During each repeat, all of the error surfaces described above were randomly sampled, and the resulting errors were applied to appropriate terms (i.e., concentrations, exhaust flow, etc.). The model would then calculate several sets of brake-specific results. An “ideal” result would be calculated from the un-perturbed reference data for the event in question. Then a set of perturbed results would be calculated from the data set after all errors had been applied. Calculation of the perturbed results was done using each of the three brake-specific calculations allowed by 40 CFR Part 1065 Subpart J for in-use testing. The perturbed results were then compared to the ideal result to generate a delta. The details of each of the three calculation methods are described in the background information given in Section 1 of this report.

For each of the 195 reference events, the resulting deltas for all of the 10,000 or more repeats were pooled together, and a 95th percentile delta was determined for each pollutant by each of the three calculation methods. These 95th percentile deltas were pooled together for all 195 reference events in order to generate a final potential measurement allowance value. A set of 9 candidate measurement allowance values was determined, three values for each pollutant (NMHC, CO, NO_x), one for each calculation method. The candidate values determined by the model run are given in Table 12. The results of model validation are also shown in this table.

TABLE 12. MODEL RESULTS AND VALIDATION

Measurement Errors (%) at Respective NTE Threshold			
Emission	Method 1 “Torque-Speed”	Method 2 “BSFC”	Method 3 “ECM Fuel Specific”
BSNO_x	22.30	4.45	6.61
BSNMHC	10.08	8.03	8.44
BSCO	2.58	1.99	2.11
Note: values in white cells were validated successfully, while values shown in gray cells were not validated.			

As is the case with all simulation results, no model values should be used until those results are somehow validated against a set of real test data. The generation of a validation data set was a considerable challenge, as it required in-use testing with PEMS to be performed, while at the same time requiring comparison to some acceptable form of reference measurement. This was required because the output of the model is a set of deltas between a PEMS measurement and a laboratory reference measurement.

Two methods of generating validation data were used in this program. The primary method involved on-road field testing using one of the PEMS that was examined during this program. The reference for this on-road validation testing was the CE-CERT Mobile Emission Laboratory, which is operated by the University of California-Riverside. This unique facility incorporates a full-flow CVS dilution tunnel and measurement system into a trailer which can be pulled behind a Class 8 heavy-duty truck. During validation testing, truck exhaust was sampled simultaneously by the PEMS and the mobile laboratory, in order to generate deltas. As an added quality assurance measure, the mobile laboratory was correlated to the SwRI reference laboratory test cell, in order to eliminate any potential effect of biases between the two facilities on the model validation effort.

A secondary validation data set was generated in the SwRI dynamometer laboratory reference test cell. This was done because the on-road validation could not incorporate any form of reference torque and fuel flow measurements, to allow validation of torque and BSFC error terms. Therefore, selected portions of the on-road testing operation were re-played in the dynamometer laboratory, in order to try to validate the errors predicted by the model for torque and BSFC sources.

The final result of these validation exercises is depicted in Table 12. As noted in that table, the model result for NO_x was validated only for calculation Method 1. The model result for NMHC was validated for all three calculation methods, while the CO results did not validate for any of the three calculation methods. As has been noted earlier, the test engines used during this program generated very low levels of CO, orders of magnitude below the NTE thresholds, and therefore the model result based on that data was not likely to be a good predictor of actual measurement errors at the CO compliance threshold. However, the Steering Committee noted

that actual engines which would be evaluated during the HDIUT program are also likely to be several orders of magnitude below the NTE threshold, and therefore the lack of validation of CO was not deemed to be a significant problem.

Efforts were made to examine the reasons for the lack of validation of NO_x for calculations Methods 2 and 3. These involved examination of both the model results and the validation data sets to determine if any errors were made or issues could be resolved. It should be noted that these two methods predicted considerably smaller overall measurement allowances, as compared to Method 1. However, the CE-CERT on-road validation deltas for those same methods were larger, resulting in a lack of validation. As a result, after considerable Steering Committee discussion, the values for Methods 2 and 3 were deemed not usable as candidates for measurement allowance generation.

The methodology for selecting measurement allowance values from among the three calculation methods called for a single method to be chosen for all three pollutants. With CO not considered relevant for this purpose, only Method 1 contained validated values for the other pollutants. Therefore, the candidate measurement allowance values for Method 1 were adopted as the basis for calculating the final measurement allowances. These percentage values were applied to the appropriate NTE thresholds, as given in Table 1, in order to generate the final allowances which were given earlier in Table 2.

It should be noted, however, that as part of the final agreement reached by the Steering Committee on the Method 1 values, EPA indicated its desire to continue to examine the possible reasons for lack of validation, as well as the potential to modify the model and the error surfaces in order to correct the issues. If upon further examination, this path appeared promising in terms of being able to achieve validation of all three calculation methods, then a further cooperative program would be initiated to revise the model result. However, any revised measurement allowance values which were generated as a result of such a future program would not take effect before the 2010 model year.

LIST OF ACRONYMS

Auxiliary Emission Control Device	AECD
American Society for Testing and Materials	ASTM
Brake-Specific	BS
Brake-Specific Fuel Consumption	BSFC
Bulk Current Injection	BCI
California Air Resources Board	CARB
Center for Environmental Research & Technology	CE-CERT
Code of Federal Regulations	CFR
Constant Volume Sampling	CVS
Controller Area Network	CAN
Design of Experiment	DOE
Diesel Particulate Filter	DPF
Electromagnetic Interference	EMI
Electronic Flow Meter	EFM
Electrostatic Discharge	ESD
Empirical Distribution Function	EDF
Engine Coolant Temperature	ECT
Engine Control Module	ECM
Engine Manufacturer's Association	EMA
Environmental Protection Agency	EPA
Heavy Duty In-Use Testing	HDIUT
Heavy Heavy Duty	HHD
Intake Manifold Temperature	IMT
Laminar Flow Element	LFE
Light Heavy Duty	LHD
Median Absolute Deviation	MAD
Mobile Emissions Laboratory	MEL
Medium Heavy Duty	MHD
Memorandum of Agreement	MOA
Non-Dispersive Ultraviolet	NDUV
Non-Dispersive Infrared	NDIR
Nonmethane Cutter	NMC
Nonmethane Hydrocarbon	NMHC
Not To Exceed	NTE
Portable Emission Measurement System	PEMS
Power Spectral Density	PSD
Radio Frequency Interference	RFI
Root Mean Square	RMS
SEMTECH-DS SN G05-SDS04	PEMS 1
SEMTECH-DS SN G05-SDS02	PEMS 2
SEMTECH-DS SN G05-SDS03	PEMS 3
SEMTECH-DS SN G05-SDS01	PEMS 4

SEMTECH-DS SN D06-SDS01
SEMTECH-DS SN D06-SDS06
SEMTECH-DS SN F06-SDS02
Society of Automotive Engineers
Southwest Research Institute
Ultra-Low Sulfur Diesel
Wide Open Throttle

PEMS 5
PEMS 6
PEMS 7
SAE
SwRI
ULSD
WOT

TABLE OF CONTENTS

	<u>Page</u>
EXECUTIVE SUMMARY	i
LIST OF ACRONYMS	xx
LIST OF FIGURES	xxvi
LIST OF TABLES	xxxv
1.0 INTRODUCTION	1
1.1 Objective	1
1.2 Background	1
1.2.1 Measurement Allowance Program Test Plan	1
1.2.2 PEMS Steering Committee	2
1.2.3 Portable Emission Measurement Systems (PEMS) Description and Function	2
1.2.4 PEMS Operations at SwRI	5
1.2.5 Emission Calculation Methods for In-Use Testing	6
1.2.5.1 Calculation Method 1 – “Torque” Method	6
1.2.5.2 Calculation Method 2 – “BSFC” Method	7
1.2.5.3 Calculation Method 3 – “Fuel Specific” Method	7
1.3 Monte Carlo Model Simulation	8
1.4 1065 PEMS and Laboratory Audit	9
1.5 Engine Dynamometer Laboratory Testing	9
1.6 Environmental Chamber Testing	10
1.7 Exhaust Flow Meter Testing	10
1.8 Model Validation	11
1.9 Measurement Allowance Generation	12
2.0 MONTE CARLO MODEL	14
2.1 Model Background	14
2.1.1 Reference NTE Events	14
2.1.2 Error Surfaces	19
2.1.3 Error Surface Sampling and Interpolation	25
2.1.4 Brake-Specific Emissions Calculations	27
2.1.5 Periodic Drift Check	29
2.1.6 Time Alignment for NO _x and CO	30
2.1.7 Convergence and Number of Trials	31
2.1.8 Simulation Output	32
2.1.9 Step-by-Step Simulation Example	33
2.1.10 Measurement Allowance	36
2.1.11 Validation	37
3.0 1065 PEMS AND LABORATORY AUDIT	45
3.1 Audit Objective	45
3.2 Overview of 1065 Audit Activities	45
3.2.1 Laboratory Audits	46
3.2.2 PEMS Audits	47
3.3 Gas Analyzer Linearity Verifications	47
3.4 1065 Gas Analyzer Verifications	59

3.4.1	1065.350 H ₂ O Interference for CO ₂ NDIR.....	63
3.4.2	1065.355 H ₂ O and CO ₂ Interference for CO NDIR	63
3.4.3	1065.360 FID Optimization Methane Response.....	64
3.4.4	1065.362 Non-stoichiometric Raw FID O ₂ Interference	64
3.4.5	1065.365 Nonmethane Cutter Penetration Fractions	64
3.4.6	1065.370 CO ₂ and H ₂ O Quench Verification for NO _x CLD	65
3.4.7	1065.372 HC and H ₂ O Interference for NO _x NDUV	65
3.4.8	1065.376 Chiller NO ₂ Penetration	66
3.4.9	1065.378 NO ₂ -to-NO Converter Conversion	69
3.5	1065 Exhaust Flow Meter Linearity Verification.....	70
3.5.1	Five-Inch Exhaust Flow Meter Linearity.....	71
3.5.2	Four-Inch Exhaust Flow Meter Linearity	74
3.5.3	Three-Inch Exhaust Flow Meter Linearity	76
4.0	ENGINE DYNAMOMETER LABORATORY TESTING	79
4.1	Engine Testing Objectives	79
4.2	Test Engines and Dynamometer Laboratory	79
4.3	40-Point Torque and BSFC Map Generation and Error Surface	82
4.4	Steady-State Repeat Engine Testing and Error Surfaces.....	85
4.4.1	Engine 1 Detroit Diesel Series 60 Steady-State.....	86
4.4.2	Engine 2 Caterpillar C9 Steady-State	92
4.4.3	Engine 3 International VT365 Steady-State	98
4.4.4	Steady-State Concentration Error Surface Generation	104
4.5	Transient Engine Testing and Error Surfaces	108
4.5.1	Engine 1 Detroit Diesel Series 60 Transient.....	110
4.5.2	Engine 2 Caterpillar C9 Transient	116
4.5.3	Engine 3 International VT365 Transient	119
4.5.4	Transient Concentration Error Surface Generation	122
4.5.5	Transient Flow Meter Error Surface Generation	129
4.5.6	Transient Dynamic Error Surface Generation	132
4.6	Interacting Parameters - Warm-Up Test Error Surface	136
4.6.1	Interacting Parameters - Warm-Up Test Procedure.....	136
4.6.2	Interacting Parameters - Warm-Up Data Analysis	138
4.6.3	Interacting Parameters – Warm-Up Error Surface Generation.....	141
4.7	Torque and BSFC Interacting Parameters - Design of Experiment.....	144
4.7.1	Interacting Parameters - DOE Data Analysis	146
4.7.2	Engine 1 Detroit Diesel Series 60 DOE.....	146
4.7.3	Engine 3 International VT365 DOE	148
4.7.4	Interacting Parameters - DOE Error Surface Generation	150
4.8	Torque and BSFC Independent Parameters Sensitivity Analysis.....	155
4.8.1	Independent Parameters Data Analysis	158
4.8.2	Independent Parameters Error Surface Generation.....	159
4.9	Torque and BSFC Interpolation Errors.....	161
4.9.1	Interpolation Error Surface Generation	164
4.10	Exhaust Flow Meter Testing.....	166
4.10.1	Pulsation Test.....	166
4.10.2	Pulsation Error Surface Generation	168

4.10.3	Non-Uniform Velocity Profile Swirl Test	169
4.10.4	Swirl Error Surface Generation	171
4.10.5	Tailpipe Wind Test	172
4.11	Torque and BSFC - OEM Supplied Error Surfaces.....	176
4.12	Time Alignment Error Surfaces.....	177
5.0	ENVIRONMENTAL CHAMBER TESTING	181
5.1	Environmental Testing Objective	181
5.2	Environmental Testing Procedure.....	181
5.3	Baseline Testing.....	185
5.4	Temperature Chamber Testing	193
5.4.1	Temperature Error Surface Generation.....	200
5.5	Pressure Chamber Testing	207
5.5.1	Pressure Error Surface Generation.....	217
5.6	Radiation Chamber Testing	220
5.6.1	Bulk Current Injection	220
5.6.2	Radiated Immunity.....	227
5.6.3	Electrostatic Discharge	233
5.6.4	Conducted Transients.....	238
5.6.5	Radiation Error Surface Generation.....	245
5.7	Vibration Table Testing	250
5.8	Ambient Hydrocarbon Testing	257
5.8.1	Ambient Hydrocarbon Error Surface Generation	263
6.0	MODEL RESULTS AND VALIDATION	266
6.1	Model Results	266
6.2	Results of Drift Correction.....	266
6.3	Convergence Results from MC Runs	270
6.4	Delta BS Emissions Plots for 95 th Percentiles	277
6.5	Sensitivity Based on Variance	282
6.6	Sensitivity Based on Bias and Variance	295
6.7	CE-CERT Mobil Emission Laboratory Correlation	307
6.8	CE-CERT On Road Validation Testing.....	313
6.9	Laboratory Replay Testing	314
6.10	Validation Results.....	340
7.0	MEASUREMENT ALLOWANCE GENERATION AND CONCLUSIONS	352
7.1	Measurement Error Allowance Results	352
7.2	Conclusions.....	364
7.2.1	Engine-Installation-PEMS Variability.....	365
7.2.2	PEMS 1065 Audit Failures	365
7.2.3	Method 2 and Method 3 Validation for NO _x	366
7.2.4	PEMS Sampling Handling System Issues and Overflow Checks	369
7.2.5	Lessons Learned for Future Programs	370

Appendix

No. of Pages

A	PEMS Operation Log.....	11
B	Brake-Specific Emission Calculations for NO _x , CO, and NMHC.....	5
C	Crystal Ball Output File Description	15
D	Monte Carlo Spreadsheet Computations	19
E	40-Point Torque and BSFC Map Data.....	6
F	Steady-State Error Surface Data	30
G	Transient Error Surface Data	19
H	Interacting Parameters – DOE Error Surface Data	9
I	Interpolation Torque and BSFC Error Maps	3
J	Evaluation of Manufacturer Supplied Error Surfaces.....	4
K	Environmental Chamber Testing Results and Error Surfaces	39
L	Measurement Allowance Test Plan – Final Version.....	75
M	CE-CERT On-road Validation Testing Report.....	93

LIST OF FIGURES

<u>Figure</u>		<u>Page</u>
1	Sensors Inc. SEMTECH-DS Portable Emissions Analyzer	3
2	SEMTECH EFM2 Exhaust Flow Meter and Control Unit.....	5
3	Method 1 BSNO _x Values for Reference NTE Events	17
4	Method 1 BSCO Values for Reference NTE Events	17
5	Method 1 BSNMHC Values for Reference NTE Events.....	18
6	Error Surface Construction: PEMS vs. Laboratory Results.....	23
7	Error Surface Construction: (PEMS - Lab) vs. Laboratory Results	24
8	Error Surface Construction: Error at Variability Index vs. Laboratory Results ..	25
9	Truncated Standard Normal and Uniform Probability Density Functions	26
10	Steady-State NO _x Error Surface with Example Sampling for a Reference NTE Event	27
11	Periodic Drift Check Flowchart	30
12	Overview of Monte Carlo Simulation for BSNO _x	33
13	Error Surfaces Included in Monte Carlo Simulation	35
14	Plot of Model-Generated Empirical Distribution Functions for Two Percentiles	40
15	Plot of On-Road and Model-Generated Empirical Distribution Functions	41
16	STEC Inc. Model SGD-710C Gas Divider with SEMTECH-DS PEMS	48
17	SwRI Gas Humidification and Blending Cart	60
18	NO ₂ Chiller Penetration Audit Results.....	67
19	NO _x Concentration Pooled Delta Data From Engine 1 Steady-State Repeat Testing Prior to Chiller NO ₂ Penetration Retrofit Installation.....	68
20	NO _x Concentration Pooled Delta Data From Engine 1 Steady-State Repeat Testing After Chiller NO ₂ Penetration Retrofit Installation	69
21	SwRI LFE Flow Stand Manometers and Reference LFEs	70
22	Sensors Inc. EFM Mounted on the SwRI LFE Flow Stand.....	71
23	5-Inch Sensors EFM Exhaust Flow Pooled Delta Data From Engine 1 Steady- State Repeat Testing	73
24	5-Inch Horiba Exhaust Flow Meter Pooled Delta Data From Engine 3 Steady- State Repeat Testing	74
25	4-Inch EFM Exhaust Flow Pooled Delta Data From Engine 2 Steady-State Repeat Testing.....	76
26	3-Inch EFM Exhaust Flow Pooled Delta Data From Engine 3 Steady-State Repeat Testing.....	78
27	PEMS Instrumentation Setup in Dynamometer Test Cell	79
28	Engine 1 (HHD) - 14L DDC Series 60.....	80
29	Engine 2 (MHD) - Caterpillar C9	80
30	Engine 3 (LHD) - International VT 365	81
31	Test Cell Exhaust System showing PEMS Flowmeters and Sampling Points	82
32	Engine 1 - Detroit Diesel Series 60 Lug Curve and 40-Point Map	83
33	Engine 2 - Caterpillar C9 Lug Curve and 40-Point Map	84
34	Engine 3 - International VT365 Lug Curve and 40-Point Map	84

35	NO _x Concentration Pooled Deltas for repeat steady-state testing on engine 1 after NO ₂ Penetration Upgrade	88
36	CO Concentration Pooled Deltas for Repeat Steady-State Testing on Engine 1..	89
37	Mean Raw HC Concentrations for Engine 1 Steady-State Testing	90
38	PEMS NMHC Concentrations for Engine 1 Steady-State Testing.....	91
39	Pooled EFM Deltas for Engine 1 Steady-State Testing – 5-inch Flow Meter.....	92
40	Corroded RH Sensor (Left) Compared to a New RH Sensor (Right).....	93
41	Disassembled RH Sensor Manifold with RH Sensor	94
42	Engine 2 Initial Steady-State Repeat NO _x Results Showing Time Dependent Concentration Shift	95
43	Raw Hydrocarbon Levels for Engine 2 Steady-State Testing	96
44	PEMS NMHC Concentrations for Engine 2 Steady-State Testing.....	96
45	Pooled EFM Deltas for Engine 2 Steady-State Testing – 4 Inch Flow Meter.....	98
46	PEMS NO _x Concentration versus Mean Laboratory Reference for Engine 3 Steady-State Testing	99
47	International VT365 Point 35 NO _x Concentrations During Steady-State Repeat Testing.....	100
48	International VT365 Point 30 NO _x Concentrations During Steady-State Repeat Testing.....	101
49	Pooled EFM DelTas for Engine 3 Steady-State Testing – 3-Inch Flow Meter ..	102
50	Pooled Horiba OBS-2200 Exhaust Flow Rate Deltas For Engine 3 Steady-State Testing.....	102
51	Pooled NO _x Deltas for the Horiba OBS-2200 During Engine 3 Steady-State Testing.....	103
52	Pooled THC Measurements for the Horiba OBS-2200 During Engine 3 Steady-State Testing.....	104
53	Combined Error Surface for Steady-State NO _x Concentration.....	105
54	Final Error Surface for Steady-State NO _x Concentration	106
55	Combined Error Surface for Steady-State Exhaust Flow Rate.....	107
56	Final Error Surface for Steady-State Exhaust Flow Rate	108
57	Engine 1 Example Speed Traces During Transient Testing	111
58	Engine 1 Example Torque Traces During Transient Testing	112
59	Engine 1 NO _x Concentration Traces During Transient Testing Showing Outlying Events.....	113
60	Engine 1 Pooled Transient Test NTE Brake-Specific NO _x Results	114
61	Engine 1 Pooled Transient Test NTE Brake-Specific NO _x MAD Results	114
62	Engine 1 Pooled PEMS NTE NO _x Concentration Data Versus the Laboratory Mean	115
63	Engine 1 Pooled PEMS NTE Exhaust Flow Rate Data Versus the Laboratory Mean	116
64	Engine 2 Pooled Transient Test NTE Brake-Specific NO _x Results	117
65	Engine 2 Pooled Transient Test NTE Brake-Specific NO _x MAD Results	117
66	Engine 2 Pooled PEMS NTE NO _x Concentration Data Versus the Laboratory Mean	118
67	Engine 2 Pooled PEMS NTE Exhaust Flow Rate Data Versus the Laboratory Mean	119

68	Engine 3 Pooled Transient Test NTE Brake-Specific NO _x Results	120
69	Engine 1 Pooled Transient Test NTE Brake-Specific NO _x MAD Results	120
70	Engine 3 Pooled PEMS NTE NO _x Concentration Data Versus the Laboratory Mean	121
71	Engine 3 Pooled PEMS NTE Exhaust Flow Rate Data Versus the Laboratory Mean	122
72	Engine 1 Uncorrected Transient Flow-Weighted NO _x Concentration Errors	123
73	Engine 1 Transient and Interpolated Steady-State MAD Values with Resulting Scaling Factor	124
74	Error Surface for Engine 1 Transient Flow-Weighted NO _x Concentration	125
75	Engine 3 Transient and Interpolated Steady-State MAD Values with Resulting Scaling Factor	126
76	Error Surface for Engine 3 Transient Flow-Weighted NO _x Concentration	127
77	Final Error Surface for Transient Flow-Weighted NO _x Concentration	128
78	Error Surface for Engine 1 Transient Exhaust Flow Rate	130
79	Error Surface for Engine 2 Transient Exhaust Flow Rate	131
80	Error Surface for Engine 3 Transient Exhaust Flow Rate	131
81	Final Error Surface for Transient Exhaust Flow Rate	132
82	Final Error Surface for Dynamic ECM Fuel Rate	133
83	Final Error Surface for Dynamic ECM Speed	134
84	Final Error Surface for Dynamic Interpolated Torque	135
85	Final Error Surface for Dynamic Interpolated BSFC	136
86	Caterpillar C9 Engine Partially Enclosed in the Insulating Box Prior to the Warm- Up Test.....	138
87	Caterpillar C9 Engine Fully Enclosed in the Insulating Box Prior to the Warm-Up Test.....	138
88	Example of Warm-up Test Bias Correction, DDC Engine Part Load Test	140
89	Example of Determination of NTE Zone Entry for Warmup Test, DDC Engine Part Load Point	141
90	Error Surface for Interacting parameters - Warm-Up Delta Torque.....	143
91	Error Surface for Interacting parameters Warm-Up Delta BSFC.....	143
92	Error Surface for Interacting Parameters - DOE Engine 1 Delta Torque	151
93	Error Surface for Interacting Parameters - DOE Engine 1 Delta BSFC.....	152
94	Error Surface for Interacting Parameters - DOE Engine 3 Delta Torque	153
95	Error Surface for Interacting Parameters - DOE Engine 3 Delta BSFC.....	153
96	Error Surface for Interacting Parameters - DOE Delta Torque Final	154
97	Error Surface for Interacting Parameters - DOE Delta BSFC Final	155
98	Intake Air Low Humidity Control SYSTEM.....	158
99	Error Surface for Independent Parameters Delta Torque	160
100	Error Surface for Independent Parameters Delta BSFC	161
101	Detroit Diesel Series 60 Down Selected 20-Point Map.....	162
102	Caterpillar C9 Down Selected 20-Point Map	162
103	International VT365 Down Selected 20-Point Map	163
104	Interpolated Torque Error (% Peak Torque) by Speed (rpm) and Fuel Rate (g/s) for Engine #1.....	164
105	Torque Interpolation Error Surface.....	165

106	BSFC Interpolation Error Surface	166
107	Pulsation Test SEMTECH-DS Exhaust Flow Rate Deltas – Raw Data	167
108	Pulsation Test SEMTECH-DS Exhaust Flow Rate Delta - Corrected for Steady- State Bias	168
109	Error Surface for Pulsation Exhaust Flow Rate	169
110	Swirl Test SEMTECH-DS Exhaust Flow Rate Deltas – Raw Data	170
111	Swirl Test SEMTECH-DS Exhaust Flow Rate Deltas - Corrected for Steady-State Bias	171
112	Error Surface for Swirl Exhaust Flow Rate	172
113	High Velocity Blower System	173
114	EFM Wind Test Flow Schematic.....	173
115	Swirl Test SEMTECH-DS Exhaust Flow Rate Deltas – Raw Data	174
116	Wind Test SEMTECH-DS Exhaust Flow Rate Deltas - Corrected for Steady- State Bias	175
117	Wind Test Mean Delta Values With 95 % Confidence Level Bars.....	176
118	Pooled and Weighted Brake-Specific Time Alignment Error Data for NO _x and CO	180
119	Systematic High CO ₂ Bias During Zero Air Reference Gas Measurement.....	184
120	CO ₂ Concentration Decay During Zero Air Measurement Following the Quad Blend Span Reference Gas.....	184
121	PEMS NO ₂ Delta Data During Initial Environmental Baseline Testing	187
122	PEMS 2 NO and NO ₂ Response During Hour 1 of Initial Environmental Baseline Testing.....	188
123	PEMS 2 NO ₂ and NO Response With Thermoelectric Chiller Bypassed and Reconnected.....	189
124	PEMS 2 Environmental Baseline Zero Delta Measurements	190
125	PEMS 2 Environmental Baseline Audit Delta Measurements	191
126	PEMS 2 Environmental Baseline Span Delta Measurements.....	192
127	5-Inch EFM Environmental Baseline Zero Delta Measurements.....	193
128	Temperature Histograms for NEI Model and Test Profile	194
129	Temperature Test Profile and Moving Average	195
130	Thermotron SM-32 Temperature Control Chamber with Supplemental Liquid Nitrogen Cylinder	196
131	PEMS 2 Environmental Temperature Zero Delta Measurements	197
132	PEMS 2 Environmental Temperature Audit Delta Measurements.....	198
133	PEMS 2 Environmental Temperature Span Delta Measurements.....	199
134	5-Inch EFM Environmental Temperature Zero Delta Measurements	200
135	Error Surface for Environmental Temperature NO _x Concentration Zero Delta Measurements	202
136	Error Surface for Environmental Temperature NO _x Concentration Audit Delta Measurements	202
137	Error Surface for Environmental Temperature NO _x Concentration Span Delta Measurements	203
138	Final Error Surface for Environmental Temperature NO _x Concentration	204
139	Corrected CO Deltas Measured During Environmental Temperature Testing...	205
140	Final Error Surface for Environmental Temperature CO Concentration.....	206

141	Error Surface for Environmental Temperature Exhaust Flow Rate Delta Measurements	207
142	Pressure Histograms for NEI Model and Test Profile	208
143	Pressure Test Profile and Moving Average	210
144	Altitude Chamber Top – Removed From Base.....	211
145	PEMS Equipment on Altitude Chamber Base	212
146	Altitude Chamber and Pressure Control Equipment During Testing	213
147	PEMS 2 Environmental Pressure Zero Delta Measurements	214
148	PEMS 2 Environmental Pressure Audit Delta Measurements.....	215
149	PEMS 2 Environmental Pressure Span Delta Measurements.....	216
150	5-Inch EFM Environmental Pressure Zero Delta Measurements	217
151	NMHC Corrected Delta Data for the Environmental Pressure Testing.....	218
152	Final Error Surface for Environmental Pressure NMHC Concentration	219
153	Error Surface for Environmental Pressure Exhaust Flow Rate	220
154	Bulk Current Injection Probe	221
155	Calibration Device for the Bulk Current Injection Probe	222
156	PEMS 7 in the Radiation Chamber Undergoing Bulk Current Injection Testing.....	223
157	PEMS 7 Environmental Radiation BCI Zero Delta Measurements.....	224
158	PEMS 7 Environmental Radiation BCI Audit Delta Measurements	225
159	PEMS 7 Environmental Radiation BCI Span Delta Measurements	226
160	5-Inch EFM Environmental Radiation BCI Zero Delta Measurements	227
161	PEMS 7 and Radiation Antenna in the Absorber-Lined Radiation Chamber During Radiated Immunity Testing	228
162	Signal Generators, Amplifiers, Oscilloscopes and Other Electronics Used to Perform Radiation Testing.....	229
163	PEMS 7 Environmental Radiation Radiated Immunity Zero Delta Measurements	231
164	PEMS 7 Environmental Radiation Radiated Immunity Audit Delta Measurements	232
165	PEMS 7 Environmental Radiation Radiated Immunity Span Delta Measurements	232
166	5-Inch EFM Environmental Radiation Radiated Immunity Zero Delta Measurements	233
167	Electrostatic Discharge Simulator Used During Electrostatic Discharge Testing	234
168	Electrostatic Voltmeter Used to Calibrate the Electrostatic Discharge Simulator	235
169	PEMS 7 Environmental Radiation Electrostatic Discharge Zero Delta Measurements	236
170	PEMS 7 Environmental Radiation Electrostatic Discharge Audit Delta Measurements	237
171	PEMS 7 Environmental Radiation Electrostatic Discharge Span Delta Measurements	237
172	5-Inch EFM Environmental Radiation Electrostatic Discharge Zero Delta Measurements	238
173	Schaffner NSG 5200 Automotive Electronics Test System	239

174	Example Voltage Trace During a Voltage Spike with Slow Recovery	240
175	Example Voltage Trace During a Voltage Spike with Quick Recovery	241
176	Example Voltage Trace During a Voltage Burst	242
177	PEMS 7 Environmental Radiation Conducted Transient Zero Delta Measurements	243
178	PEMS 7 Environmental Radiation Conducted Transient Audit Delta Measurements	244
179	PEMS 7 Environmental Radiation Conducted Transient Span Delta Measurements	244
180	5-Inch EFM Environmental Radiation Conducted Transient Zero Delta Measurements	245
181	Combined Radiation Chamber Zero Delta Test Results	246
182	Combined Radiation Chamber Audit Delta Test Results	247
183	Combined Radiation Chamber Span Delta Test Results	247
184	Pooled Exhaust Flow Rate Zero Deltas Measured During Environmental Radiation Testing	249
185	Error Surface for Environmental Radiation Exhaust Flow Rate Delta Measurements	250
186	PEMS 3 in an Environmental Enclosure During Vibration Testing Using an Unholtz-Dickie Shaker System	251
187	Army M915A2 Semi-Tractor Used to Generate Vibration Spectra for Vibration Testing	252
188	Power Spectral Densities Evaluated For Vibration Testing	253
189	PEMS 3 Environmental Vibration Zero Delta Measurements	254
190	PEMS 3 Environmental Vibration THC Zero Delta Measurements	255
191	PEMS 3 Environmental Vibration Audit Delta Measurements	256
192	PEMS 3 Environmental Vibration Span Delta Measurements	256
193	PEMS 3 Environmental Vibration NO _x Span Delta Measurements	257
194	THC Measurements for Test 1 of the Ambient Hydrocarbon Test Sequence	260
195	THC Measurements for Test 2 of the Ambient Hydrocarbon Test Sequence	262
196	THC Measurements for Test 6 of the Ambient Hydrocarbon Test Sequence	263
197	PEMS 3 NMHC Response Versus FID Air Methane Contamination Measured During Ambient Hydrocarbon Testing	264
198	Error Surface for Ambient Hydrocarbon Testing	265
199	Percent of Trials Deleted for Each Reference NTE Event Due to Periodic Drift Check for BSNO _x Method 1	267
200	Percent of Trials Deleted for Each Reference NTE Event Due to Periodic Drift Check for BSNO _x Method 2	267
201	Percent of Trials Deleted for Each Reference NTE Event Due to Periodic Drift Check for BSNO _x Method 3	268
202	Percent of Trials Deleted for Each Reference NTE Event Due to Periodic Drift Check for BSNMHC Method 1	269
203	Percent of Trials Deleted for Each Reference NTE Event Due to Periodic Drift Check for BSNMHC Method 2	269
204	Percent of Trials Deleted for Each Reference NTE Event Due to Periodic Drift Check for BSNMHC Method 3	270

205	Convergence Interval Width as a Percent of Threshold for BSNO _x Method 1 ..	271
206	Convergence Interval Width as a Percent of Threshold for BSNO _x Method 2 ..	272
207	Convergence Interval Width as a Percent of Threshold for BSNO _x Method 3 ..	272
208	Convergence Interval Width as a Percent of Threshold for BSNMHC Method 1	273
209	Convergence Interval Width as a Percent of threshold for BSNMHC Method 1274	
210	Convergence Interval Width as a Percent of Threshold for BSNMHC Method 3	274
211	Convergence Interval Width as a Percent of Threshold for BSCO Method 1	275
212	Convergence Interval Width as a Percent of Threshold for BSCO Method 2	276
213	Convergence Interval Width as a Percent of Threshold for BSCO Method 3	276
214	Box Plot of 95 th Percentile Delta BSNO _x for Three Methods from 195 Reference NTE Events	278
215	Box Plot for 95 th Percentile Delta BSCO for Three Methods from 195 Reference NTE Events	279
216	Box Plot for 95 th Percentile Delta BSCO for Three Methods for 195 Reference NTE Events	280
217	Comparison of 95 th Percentile Delta BSNO _x for Methods 1, 2, and 3 for 195 Reference NTE Events	281
218	Comparison of 95 th Percentile Delta BSNMHC for Methods 1, 2, and 3 from 195 Reference NTE Events	281
219	Comparison of 95 th Percentile Delta BSCO for Methods 1, 2, and 3 from 195 Reference NTE Events	282
220	Box Plot of Error Surface Sensitivity Based on Variance for BSNO _x Method 1	287
221	Box Plot of Error Surface Sensitivity Based on Variance for BSNO _x Method 2	288
222	Box Plot of Error Surface Sensitivity Based on Variance for BSNO _x Method 3	289
223	Box Plot of Error Surface Sensitivity Based on Variance for BSNMHC Method 1	290
224	Box Plot of Error Surface Sensitivity Based on Variance for BSNMHC Method 2	291
225	Box Plot of Error Surface Sensitivity Based on Variance for BSNMHC Method 3	292
226	Box Plot of Error Surface Sensitivity Based on Variance for BSCO Method 1.	293
227	Box Plot of Error Surface Sensitivity Based on Variance for BSCO Method 2.	294
228	Box Plot of Error Surface Sensitivity Based on Variance for BSCO Method 3.	295
229	Distribution of Ideal BSNO _x for 13 Reference NTE Events	297
230	Box Plot of error Surface Sensitivity Based on Bias and Variance for BSNO _x Method 1	301
231	Box Plot of Error Surface Sensitivity Based on Bias and Variance for BSNO _x Method 2	302
232	Box Plot of Error Surface Sensitivity Based on Bias and Variance for BSNO _x Method 3	303
233	Comparison of Typical CONTINUOUS NO _x Mass Rate Data over RMC Cycle - CE-CERT versus SwRI	312
234	Engine Speed CAN Data Comparison for SwRI Laboratory Testing and CE-CERT On-Road Validation Testing (Route 2)	315

235	Fuel Rate CAN Data Comparison for SwRI Laboratory Testing and CE-CERT On-Road Validation Testing (Route 2).....	316
236	Boost Pressure CAN Data Comparison for SwRI Laboratory Testing and CE-CERT On-Road Validation Testing (Route 2).....	317
237	Injection Timing CAN Data Comparison for SwRI Laboratory Testing and CE-CERT On-Road Validation Testing (Route 2).....	318
238	Intake Manifold Temperature CAN Data Comparison for SwRI Laboratory Testing and CE-CERT On-Road Validation Testing (Route 2)	319
239	PEMS 5 Wet NO _x Comparison for SwRI Laboratory Testing and CE-CERT On-Road Validation Testing (Route 2).....	320
240	PEMS 5 Exhaust Flow Rate Comparison for SwRI Laboratory Testing and CE-CERT On-Road Validation Testing (Route 2).....	321
241	PEMS 5 NO _x Mass Flow Rate Comparison for SwRI Laboratory Testing and CE-CERT On-Road Validation Testing (Route 2).....	321
242	Brake-Specific NO _x Emission Deltas for PEMS 5 Method 1 Calculation Versus the Laboratory Reference (Laboratory Torque and BSFC)	323
243	Brake-Specific NO _x Emission Deltas for PEMS 5 Method 1 Calculation Versus the Laboratory Method 1 Calculation (ECM Torque and BSFC).....	324
244	Incremental Brake-Specific NO _x Emission Deltas Due to ECM Torque and BSFC Errors for Calculation Method 1	325
245	Incremental Brake-Specific NO _x Deltas Compared to the Incremental Torque and BSFC Errors Predicted by the Model for Calculation Method 1	326
246	Brake-Specific NO _x Emission Deltas for PEMS 5 Method 2 Calculation Versus the Laboratory Reference (Laboratory Torque and BSFC)	327
247	Brake-Specific NO _x Emission Deltas for PEMS 5 Method 2 Calculation Versus the Laboratory Method 2 Calculation (ECM Torque and BSFC).....	328
248	Incremental Brake-Specific NO _x Emission Deltas Due to ECM Torque and BSFC Errors for Calculation Method 2.....	329
249	Incremental Brake-Specific NO _x Deltas Compared to the Incremental Torque and BSFC Errors Predicted by the Model for Calculation Method 2.....	330
250	Brake-Specific NO _x Emission Deltas for PEMS 5 Method 3 Calculation Versus the Laboratory Reference (Laboratory Torque and BSFC)	331
251	Brake-Specific NO _x Emission Deltas for PEMS 5 Method 3 Calculation Versus the Laboratory Method 3 Calculation (ECM Torque and BSFC).....	332
252	Incremental Brake-Specific NO _x Emission Deltas Due to ECM Torque and BSFC Errors for Calculation Method 3	333
253	Incremental Brake-Specific NO _x Deltas Compared to the Incremental Torque and BSFC Errors Predicted by the Model for Calculation Method 3.....	334
254	ECM Broadcast Torque Errors Measured During Replay Validation Testing with a Caterpillar C15 Engine.....	335
255	ECM Broadcast Fuel Flow Rate Errors Measured During Replay Validation Testing with a Caterpillar C15 Engine.....	336
256	ECM-Based BSFC Errors Measured During Replay Validation Testing with a Caterpillar C15 Engine	337
257	ECM Broadcast Torque Errors Measured During 40-Point Map Generation with a Detroit Diesel Series 60 Engine.....	338

258	ECM Broadcast Torque Errors Measured During 40-Point Map Generation with a Caterpillar C9 Engine	339
259	ECM Broadcast Torque Errors Measured During 40-Point Map Generation with an International VT365 Engine.....	340
260	Validation On-Road and Model Generated Empirical Distribution Functions for BSNO _x Method 1	342
261	Validation On-Road and Model Generated Empirical Distribution Functions for BSNO _x Method 2	343
262	Validation On-Road and Model Generated Empirical Distribution Functions for BSNO _x Method 3	344
263	Validation On-Road and Model Generated Empirical Distribution Functions for BSNMHC Method 1	345
264	Validation On-Road and Model Generated Empirical Distribution Functions for BSNMHC Method 2	346
265	Validation On-Road and Model Generated Empirical Distribution Functions for BSNMHC Method 3	347
266	Validation On-Road and Model Generated Empirical Distribution Functions for BSCO Method 1.....	348
267	Validation On-Road and Model Generated Empirical Distribution Functions for BSCO Method 2.....	349
268	Validation On-Road and Model Generated Empirical Distribution Functions for BSCO Method 3.....	350
269	Regression Plot of 95 th Percentile Delta BSNO _x versus Ideal BSNO _x for Method 1	353
270	Regression Plot of 95 th Percentile Delta BSNO _x versus Ideal BSNO _x for Method 2	354
271	Regression Plot of 95 th Percentile Delta BSNO _x versus Ideal BSNO _x for Method 3	355
272	Regression Plot of 95 th Percentile Delta BSNMHC versus Ideal BSNMHC for Method 1	356
273	Regression Plot of 95 th Percentile Delta BSNMHC versus Ideal BSNMHC for Method 2	358
274	Regression Plot of 95 th Percentile Delta BSNMHC versus Ideal BSNMHC for Method 3	359
275	Regression Plot for 95 th Percentile Delta BSCO versus Ideal BSCO for Method 1	360
276	Regression Plot of 95 th Percentile Delta BSCO versus Ideal BSCO for Method 2	361
277	Regression Plot of 95 th Percentile Delta BSCO versus Ideal BSCO for Method 3	363
278	Variation in Zero Calibration of PEMS During On-Road Validation Testing ...	368
279	PEMS Zero Calibration Variations during Laboratory Testing.....	369

LIST OF TABLES

<u>Table</u>	<u>Page</u>
1	NTE Threshold Values Used for Measurement Allowance Program..... ii
2	Final Measurement Allowances..... ii
3	Laboratory Reference Methods..... v
4	Magnitude of Error Terms for Steady-State Error Surfaces ix
5	Magnitude of error terms for Transient Error Surfaces – gaseous analyzers and exhaust flow xi
6	Magnitude of Transient Error TERMS for ECM Variables xi
7	Magnitude of Torque and BSFC Error surfaces xii
8	Magnitude of Error Terms for Exhaust Flow Error Surfaces xiv
9	Magnitude of OEM Error Surfaces..... xiv
10	Magnitude of Time Alignment Error Surfaces xv
11	Magnitude of Error Terms for Environmental Error Surfaces..... xvi
12	Model Results and Validation..... xviii
13	NTE Thresholds for Measurement Allowance Program 12
14	Example of MEASUREMENT Allowance Determination from Test Plan 13
15	Reference NTE Events and Method 1 BS Emissions 15
16	Descriptive Statistics for BS Emissions for Reference NTE Events 18
17	Input Parameters for Reference NTE Events..... 19
18	Error Surfaces for Monte Carlo Simulation..... 21
19	Error Surfaces Used for Computing Brake-Specific Emissions by Three Calculation Methods 29
20	Example of Selection of the Measurement Error..... 37
21	1065 Audits and Performance Checks Required for the Measurement Allowance Program..... 46
22	Span Concentrations used for the SEMTECH-DS and Laboratory Analyzers..... 48
23	Dilute MEXA 7200D and Horiba CH ₄ Bench 1065 Linearity Verification Summary 49
24	Raw MEXA 7200D and Horiba CH ₄ Bench 1065 Linearity Verification Summary 49
25	PEMS 1 1065 Linearity Verification Summary..... 51
26	PEMS 2 1065 Linearity Verification Summary..... 52
27	PEMS 3 1065 Linearity Verification Summary..... 53
28	PEMS 4 1065 Linearity Verification Summary..... 54
29	PEMS 4 1065 Linearity Verification Summary Continued..... 55
30	PEMS 5 1065 Linearity Verification Summary..... 56
31	PEMS 6 1065 Linearity Verification Summary..... 57
32	PEMS 7 1065 Linearity Verification Summary..... 58
33	Horiba OBS-2200 1065 Linearity Verification Summary..... 58
34	Dilute MEXA 7200D and Horiba NMHC Bench 1065 Analyzer Verification Summary 60

35	Raw MEXA 7200D and Horiba NMHC Bench 1065 Analyzer Verification Summary	61
36	PEMS 1 1065 Analyzer Verification Summary.....	61
37	PEMS 2 1065 Analyzer Verification Summary.....	61
38	PEMS 3 1065 Analyzer Verification Summary.....	61
39	PEMS 4 1065 Analyzer Verification Summary.....	62
40	PEMS 5 1065 Analyzer Verification Summary.....	62
41	PEMS 6 1065 Analyzer Verification Summary.....	62
42	PEMS 7 1065 Analyzer Verification Summary.....	62
43	Horiba OBS-2200 1065 Analyzer Verification Summary	63
44	5-Inch Sensors Inc. EFM Linearity Results	72
45	5-Inch Horiba Exhaust Flow Meter Linearity Results	72
46	4-Inch Sensors Inc. EFM Linearity Results	75
47	3-Inch Sensors Inc. EFM Linearity Results	77
48	NTE Event Descriptions from the Test Plan.....	109
49	NTE Transition Descriptions from the Test Plan	110
50	Final Gaseous Transient Error Surface Deltas.....	129
51	nlo and nhi Speed Definitions for Engines 1, 2, and 3	133
52	Warm-Up Test Torque Errors Summary	142
53	Warm-Up Test BSFC Errors Summary	142
54	Interacting Parameters - DOE Adjustment guidance.....	144
55	Interacting Parameters - DOE Test Matrix	145
56	Test Plan DOE Engine Operating Conditions	145
57	Example of DOE Baseline Correction for Engine 1	146
58	Interacting Parameters - DOE Speed and Torque Steady-State Mode Definition for Engine 1.....	147
59	Interacting Parameters - DOE Test Matrix for Engine 1	147
60	Interacting Parameters - DOE Engine 1 Bias Corrected Torque Deltas.....	148
61	Interacting Parameters - DOE Engine 1 Bias Corrected BSFC Deltas.....	148
62	Interacting Parameters - DOE Speed and Torque Steady-State Mode Definition for Engine 3.....	149
63	Interacting Parameters - DOE Test Matrix for Engine 3	149
64	Interacting Parameters - DOE Engine 3 Bias Corrected Torque Deltas.....	150
65	Interacting Parameters -DOE Engine 3 Bias Corrected BSFC Deltas.....	150
66	Example DOE Steady-State Variance Correction using the Mean SS MAD.....	151
67	Independent Parameters adjustment guidance from the Test Plan	155
68	Independent Parameters Test Modes from the Test Plan.....	156
69	Independent Parameters Speed and Torque Steady-State Mode Definitions	156
70	Selected Fuel Properties for INDEPENDENT Parameters Testing	157
71	Independent Parameters Bias Corrected Torque Deltas	159
72	Independent Parameters Bias Corrected BSFC Deltas	159
73	Torque Interpolation Error Surface Values.....	165
74	BSFC interpolation error Surface Values	165
75	OEM Error Surface Deltas for Torque and BSFC	177
76	EFM and Vehicle Interface Adjustment and Weighting Factors Used for Time Alignment Error Generation	178

77	Brake-Specific Time Alignment Error Data for NO _x	179
78	Brake-Specific Time Alignment Error Data for CO	179
79	Reference Gases and Typical Concentrations Used During Environmental Chamber Testing	182
80	Zero, Audit, and Span Delta Recording Strategy Used During Environmental Chamber Testing	183
81	Temperature Test Profile Definition	195
82	Median Environmental Baseline NO _x Concentrations and Environmental Temperature Scaling Factors	201
83	Pressure Test Profile Definition	209
84	Hexane and Methane Contamination Combinations Used During Ambient Hydrocarbon Testing	258
85	Ambient Hydrocarbon Test Sequence	259
86	THC Measurements for Test 1 of the Ambient Hydrocarbon Test Sequence	261
87	THC Measurements for Test 2 of the Ambient Hydrocarbon Test Sequence	262
88	Summary of the Trials Deleted Due to Periodic Drift Check for BSNO _x	268
89	Summary of Trials Deleted for Each Reference NTE Event Due to Periodic Drift Check for BSNMHC Method 3	270
90	Summary of BSNO _x Convergence Interval Width as a Function of Threshold for 195 Reference NTE Events	273
91	Summary of BSNMHC Convergence Interval Width as a Function of Threshold for 195 Reference NTE Events	275
92	Summary of BSCO Convergence Interval Width as a Function of Threshold for 195 Reference NTE Events	277
93	Error Surface Sensitivity to Variance for 195 Reference NTE Events for BSNO _x Method 1	283
94	Error Surface Sensitivity to Variance for 195 Reference NTE Events for BSNO _x Method 2	283
95	Error Surface Sensitivity to Variance for 195 Reference NTE Events for BSNO _x Method 3	284
96	Error Surface Sensitivity to Variance for 195 Reference NTE Events for BSNMHC Method 1	284
97	Error Surface Sensitivity to Variance for 195 Reference NTE Events for BSNMHC Method 2	284
98	Error Surface Sensitivity to Variance for 195 Reference NTE Events for BSNMHC Method 3	285
99	Error Surface Sensitivity to Variance for 195 Reference NTE Events for BSCO Method 1	285
100	Error Surface Sensitivity to Variance for 195 Reference NTE Events for BSCO Method 2	285
101	Error Surface Sensitivity to Variance for 195 Reference NTE Events for BSCO Method 3	286
102	Ideal BSNO _x Values for 13 Reference NTE Events	296
103	Error Surface Sensitivity to Bias and Variance for 13 Reference NTE Events for BSNO _x Method 1	298

104	Error Surface Sensitivity to Bias and Variance for 13 Reference NTE Events for BSNO _x Method 2.....	298
105	Error Surface Sensitivity to Bias and Variance for 13 Reference NTE Events for BSNO _x Method 3	298
106	Error Surface Sensitivity to Bias and Variance for 13 Reference NTE Events for BSNMHC Method 1	299
107	Error Surface Sensitivity to Bias and Variance for 13 Reference NTE Events for BSNMHC Method 2	299
108	Error Surface Sensitivity to Bias and Variance for 13 Reference NTE Events for BSNMHC Method 3	299
109	Error Surface Sensitivity to Bias and Variance for 13 Reference NTE Events for BSCO Method 1.....	300
110	Error Surface Sensitivity to Bias and Variance for 13 Reference NTE Events for BSCO Method 2.....	300
111	Error Surface Sensitivity to Bias and Variance for 13 Reference NTE Events for BSCO Method 3.....	300
112	Summary of Error Surface Sensitive to Bias and Variance for BSNO _x Method 1	304
113	Summary of Error Surface Sensitive to Bias and Variance for BSNO _x Method 2	304
114	Summary of Error Surface Sensitive to Bias and Variance for BSNO _x Method 3	305
115	Summary of Error Surface Sensitive to Bias and Variance for BSNMHC Method 1.....	305
116	Summary of Error Surface Sensitive to Bias and Variance for BSNMHC Method 2.....	305
117	Summary of Error Surface Sensitive to Bias and Variance for BSNMHC Method 3.....	306
118	Summary of Error Surface Sensitive to Bias and Variance for BSCO Method 1	306
119	Summary of Error Surface Sensitive to Bias and Variance for BSCO Method 2	306
120	Summary of Error Surface Sensitive to Bias and Variance for BSCO Method 3	307
121	Correlation Test Matrix.....	308
122	Correlation Testing Results for NTE Transient Cycle.....	310
123	Correlation Test Results for RMC 13-Mode SET Cycle	311
124	Summary of Model Validation Results.....	351
125	Measurement Error at Threshold for BSNO _x Using Regression and Median Methods for Method 1	353
126	Measurement Error at Threshold for BSNO _x Using Regression and Median Methods for Method 2	354
127	Measurement Error at Threshold for BSNO _x Using Regression and Median Methods for Method 3	355
128	Measurement Error at Threshold for BSNMHC Using Regression and Median Methods for Method 1	357

129	Measurement Error at Threshold for BSNMHC Using Regression and Median Methods for Method 2	358
130	Measurement Error at Threshold for BSNMHC Using Regression and Median Methods for Method 3	359
131	Measurement Error at Threshold for BSCO Using Regression and Median Methods for Method 1	360
132	Measurement Error at Threshold for BSCO Using Regression and Median Methods for Method 2	362
133	Measurement Error at Threshold for BSCO Using Regression and Median Methods for Method 3	363
134	Measurement Error in Percent of NTE Threshold by Emissions and Calculation Method	364
135	Measurement Allowance at NTE Threshold by Emissions for Method 1	364
136	Lessons Learned During Gaseous Measurement Allowance Program.....	370

1.0 INTRODUCTION

The intent of this section of this report is to provide an overview of the program objectives, background material on the test plan, test methods, and equipment, and to briefly discuss the rationale behind each of the major components of the measurement allowance program which will be discussed in detail in later sections of the report.

This revised version of the final report contains a number of changes made following EPA's peer review of the original final report. None of the results or conclusions of the original report were affected as part of the revision. The changes made to the report primarily involved additional clarifying language in areas where the peer review process indicated that the original report was unclear or vague.

1.1 Objective

The objective of this program was to determine a set of brake-specific measurement allowances for the gaseous pollutants regulated under the Heavy-Duty In-Use Testing (HDIUT) program. These measurement allowances are intended to represent the incremental error between measuring emissions under controlled conditions in a laboratory with lab-grade equipment, and measuring emissions in the field using Portable Emissions Measurement Systems (PEMS). Measurement allowance values were generated for non-methane hydrocarbons (NMHC), carbon monoxide (CO), and oxide of nitrogen (NO_x).

The measurement allowances are fixed brake-specific values, which are intended to be added to a given NTE threshold in order to provide an additional compliance margin which accounts for the relative error between laboratory and field measurements.

The completion of this program was part of the resolution of a 2001 legal suit filed against EPA by the Engine Manufacturer's Association (EMA) and several individual engine manufacturers regarding certain portions of the Not-to-Exceed (NTE) standards. This dispute was settled on June 3, 2003. As such, this program represents a cooperative effort between EPA, EMA, and the California Air Resources Board (CARB). The program was jointly funded by all three organizations, and was conducted under the direction of a Steering Committee composed of representatives of all three organizations, as well as representatives of a number of individual engine manufacturers which are EMA members.

1.2 Background

1.2.1 *Measurement Allowance Program Test Plan*

The measurement allowance program was conducted according to procedures and guidelines which were laid out in a detailed test plan document titled *Test Plan to Determine PEMS Measurement Allowances for Gaseous Emissions Regulated under the Manufacturer-Run Heavy-Duty Diesel Engine In-Use Testing Program*. The final version of this document, which forms the basis of the program, is dated October 24, 2005. This document will be referred to as

the Test Plan throughout the remainder of the report. This final version was modified from the initial version, dated May 20, 2005, which was distributed publicly by EPA and is available via the Internet at <http://www.epa.gov/otaq/regs/hd-hwy/inuse/testplan.pdf>. The two documents are identical in terms of overall methodology and scope, and differ primarily in certain details pertaining to either test execution or data analysis.

The Test Plan was developed as a collaborative effort by the Steering Committee and all modifications made to the Test Plan were discussed and approved by the Steering Committee prior to being performed. Throughout the program, every effort was made to adhere to the procedures given in the Test Plan. However, on numerous occasions, these procedures had to be modified in response to unexpected occurrences during testing, or as a result of test data generated during the program. All such modifications that were not captured in the final Test Plan document are included in this report. When such changes are noted in the report, the original Test Plan procedure is given, along with the rationale for any changes, and the date at which these modifications were approved by the Steering Committee.

1.2.2 PEMS Steering Committee

The PEMS Steering Committee was composed primarily of representatives from EPA, EMA, CARB, and the following engine manufacturers: Cummins Engine Company, Detroit Diesel Corporation, Volvo Powertrain, Caterpillar Inc., International Engine Company, and Isuzu. Representatives of other engine manufacturers were also present for some of the Committee meetings. PEMS Steering Committee meetings were convened on an as needed basis by agreement of the Committee members. Generally, these meetings were held on a monthly basis, although bi-monthly meetings were held late in the program as key decisions were required. During the majority of the program, weekly teleconferences were held to update the group on progress and to provide feedback to SwRI. It should be noted that this required a considerable time and travel commitment on the part of Steering Committee members. SwRI would like to acknowledge this contribution, and thank the Committee members for their efforts.

In general, efforts were made to achieve unanimity among all Steering Committee members before deciding on a course of action. On the occasions that a unanimous opinion could not be formed, a majority vote of Committee members was required to decide a given issue. In such cases, which were generally rare, dissenting votes were noted for the record as desired by those in dissent.

1.2.3 Portable Emission Measurement Systems (PEMS) Description and Function

The focus of this program was the evaluation of Portable Emission Measurement Systems, which are referred to by the acronym PEMS throughout this report. A key provision of the Test Plan was that the PEMS to be evaluated had to represent commercially available hardware. The intent of this provision is captured in the following language taken from the Test Plan:

“The PEMS used in this test plan must be standard in-production makes and models that are for sale as commercially available PEMS. In addition, PEMS and any support equipment must pass a “red-face” test with respect to being consistent with acceptable practices for in-use testing. For example, use of large gas bottles that can

not be utilized by the EPA/ARB/EMA HDIU enforceable program is unacceptable. Furthermore, the equipment must meet all safety and transportation regulations for use on-board heavy-duty vehicles.”

The original intent of the program was to evaluate PEMS from two suppliers, Sensors Incorporated and Horiba Instruments. However, at the time of the start of this program, the Horiba PEMS was still in the final stages of development, therefore Horiba was not able to supply a commercially available unit. As a result, the program was conducted primarily with the Sensors Inc. SEMTECH-DS hardware. Horiba was able to supply examples of its OBS-2200 PEMS hardware in the later stages of the program, but this was evaluated only for purposes of supplemental information as time permitted. The measurement allowance values were generated using data from only the Sensors SEMTECH-DS PEMS hardware. The Test Plan called for three different PEMS units from each Manufacturer to be examined. Ultimately, due to various scheduling and hardware issues, a total of seven SEMTECH-DS units were evaluated during the program. However, all seven PEMS were not evaluated for every error source, and no more than three PEMS were used during any given error test.

The SEMTECH-DS PEMS included several major components. The first of these is the SEMTECH-DS portable gaseous emission analyzer unit. This unit housed the gaseous emission analyzers, the sampling system, and the sampling conditioning system. The unit also contained electronics for analyzer functions, interaction with the other system components, as well as for communication with the user. User interface was accomplished using a remote interface program running on a laptop computer, which was connected to the SEMTECH-DS via an Ethernet cable or using wireless communication. The front of a SEMTECH-DS PEMS is pictured in Figure 1, showing the connection points for various other components.



FIGURE 1. SENSORS INC. SEMTECH-DS PORTABLE EMISSIONS ANALYZER

The SEMTECH DS uses a variety of different analyzers to measure various gaseous emissions. Total hydrocarbons (HC) are measured using a heated flame ionization detector (HFID). Carbon monoxide (CO) and carbon dioxide (CO₂) are measured using a non-dispersive infrared (NDIR) instrument. Oxides of nitrogen (NO_x) are measured using a non-dispersive ultraviolet (NDUV) instrument, in which NO and NO₂ are measured separately and combined mathematically to produce a final NO_x value.

The SEMTECH DS units were initially supplied along with an add-on FID analyzer for methane measurement to allow for the determination of non-methane hydrocarbons (NMHC). However, only two of these units were supplied, which was not enough for all the PEMS used in the program. In addition, upon evaluation, the Steering Committee determined that these methane analyzers did not pass the red-face requirement outlined in the Test Plan and were not suitable for field use. Therefore, the methane analyzers were not used in the program, and NMHC for the PEMS was determined as 0.98 times THC, as allowed under CFR Title 40 Part 1065.

A second key component of the SEMTECH-DS PEMS is the SEMTECH EFM2 exhaust flow meter. This unit is a pitot-tube based exhaust flow measurement meter which is design to be attached to the end of a vehicle tailpipe for direct measurement of exhaust flow over a wide dynamic range. The control box contains a set of pressure transducers for differential and static pressure measurement. The EFM control unit is connected to the main SEMTECH-DS unit via a digital interface cable, and flow data is recorded along with gaseous emissions data and other parameters in a single data file. An example of the SEMTECH EFM2 flow meter is shown in Figure 2. This flow meter also incorporates the sampling probe through which the SEMTECH-DS emission analyzer samples exhaust for delivery to the gaseous analyzers. This probe is connected to the main SEMTECH-DS unit via a heated sampling line which is controlled to a temperature of 191°C, in accordance with CFR Title 40 Part 1065.

The third key component of the SEMTECH-DS is the vehicle interface. This interface is used to read engine variables broadcast from the ECM digitally via CAN. Variables are read according to either the SAE J-1939 or SAE J-1708 protocol, depending on what is available from a given engine. These ECM broadcast variables are required for estimation of torque and fuel consumption during in-use testing, as well as to determine entry into or exit from the NTE zone.

A fourth component of the SEMTECH-DS is a temperature and humidity probe. This is used by the SEMTECH-DS to monitor and record ambient temperature and humidity during in-use testing. This probe is plugged into the main SEMTECH-DS unit, which takes the raw sensor data from the probe and converts it to temperature and humidity measurement values.

Data from all of these components is generally recorded simultaneously, and stored in a single data file for each test run on a memory card in the main SEMTECH-DS unit. This data can later be retrieved via a laptop computer either over a wireless connection or via a cabled Ethernet link. The laptop software interface also provides a means of user interface for manual operations, diagnostics, and monitoring of the SEMTECH-DS during testing. The data recorded by the SEMTECH-DS is then post-processed to determine emission values and to review quality assurance parameters.



FIGURE 2. SEMTECH EFM2 EXHAUST FLOW METER AND CONTROL UNIT

1.2.4 PEMS Operations at SwRI

Once the PEMS hardware was delivered to SwRI for this program, modifications could only be conducted in accordance with strict guidelines given in the Test Plan. In general, modifications could only be conducted following approval from the Steering Committee. In addition, PEMS operations were conducted only by SwRI staff in accordance with procedures given in the standard documentation available for the PEMS. SwRI staff members were trained by PEMS manufacturer representatives prior to the start of the program. PEMS representatives were not allowed to be present during actual test operations. SwRI technicians Billy Valuk and Richard Mendez were the PEMS operators during the program.

In general, PEMS manufacturers were allowed access to the hardware during this program under only two conditions. The first was the failure of a 1065 audit performance check, in which case, the PEMS manufacturer was offered an opportunity to correct the problem. The second condition was in the event of an equipment malfunction which could not normally be repaired by an end user. In the event of such repairs, appropriate 1065 audits were repeated to validate the operation of the repaired systems before testing continued.

Throughout the course of the program, there were a variety of instances of both audit failures and equipment malfunctions. An operating log of all of these occurrences was maintained by SwRI throughout the course of the program. The complete log is included in Appendix A of this report. For each incident, the log includes the date of occurrence, observed failure symptoms, diagnostic steps, root cause analysis (if known), and corrective actions taken. This log represents the collective PEMS operation experience with seven sets of PEMS hardware over the course of roughly one year.

1.2.5 Emission Calculation Methods for In-Use Testing

Once a set of data has been recorded using PEMS hardware, calculations must be performed to determine brake-specific emission values in accordance with methods outlined in 40 CFR Part 1065 Subparts G and J. The symbolic notation given in the formulas shown later in this section is fully described in 40 CFR Part 1065 Subpart K.

40CFR Part 1065 allows for the use of any of three different calculation methods in order to determine brake-specific emission values from in-use test data. The basic calculation of brake-specific emissions requires three main inputs as follows:

$$BSEmission = \frac{Mass}{Work} = \frac{Concentration \times FlowRate}{Power}$$

The three calculation methods vary somewhat in the means used to determine either the Flow component or the Work component of this calculation. Each of the three methods is summarized below. Because each method relies on different inputs, it is possible that each method of calculation will react differently to various measurement errors. Therefore, measurement allowances must be examined independently for each method. However, according to the Test Plan methodology, only one of the three calculation methods would be selected to generate the final measurement allowances. The selection methodology is outlined later in this introduction under the Measurement Allowance Generation section.

1.2.5.1 Calculation Method 1 – “Torque” Method

Calculation Method 1 is analogous to the method used by most dynamometer laboratories, and relies on direct input of both exhaust flow and torque. In the case of exhaust flow, this is the flow rate measured by the same form of exhaust flow meter. In the case of the Sensors Inc. PEMS, this is the value measured by the SEMTECH EFM2 exhaust flow meter. Work is not measured directly, but is instead calculated using ECM broadcast engine speed and ECM broadcast engine torque. While engine speed is directly measured by the engine ECM, ECM broadcast torque is an estimate based on a variety of other parameters, therefore, torque cannot be directly verified during in-use testing. A simplified formula for this method is:

$$Method\ 1 = \frac{\sum g}{\sum Work}$$

The more complete formula used for Method 1, using NO_x as an example, is as follows:

$$e_{NO_x} (g / kW \cdot hr) = \frac{M_{NO_2} * \sum_{i=1}^N \left[(xNO_{x_i} (ppm)) * 10^{-6} * \dot{n}_i \left(\frac{mol}{s} \right) * \Delta t \right]}{\sum_{i=1}^N \left[\frac{Speed_i (rpm) * T_i (N \cdot m) * 2 * 3.14159 * \Delta t}{60 * 1000 * 3600} \right]}$$

It should be noted that calculation Method 1 is directly dependent on the accuracy of both the exhaust flow meter and the torque estimation, as well as on the measurement of gaseous concentration. This formula is applied similarly for CO and HC by replacing the measured concentration and molecular weight values for NO_x with those for the pollutant being calculated.

1.2.5.2 Calculation Method 2 – “BSFC” Method

This calculation is designated solely for in-use testing, and is designed to minimize the effect of errors related to the accuracy of the exhaust flow measurement. Calculation Method 2 relies on flow weighting of individual readings during a test event. This means that although the flow meter must be linear, it does not necessarily have to be accurate. In addition, Method 2 uses a carbon balance method to predict the fuel consumption rate, and a brake-specific fuel consumption (BSFC) value to determine a final work term for the calculation. The BSFC value is generally calculated using ECM broadcast values for fuel rate and for torque. A simplified version of this method can be expressed as:

$$Method\ 2 = \frac{\sum g}{\sum \left[\frac{CO_2\ fuel}{ECM\ fuel} \times Work \right]}$$

The more complete formula for Method 2, again using NO_x as an example, is:

$$e_{NO_x} (g / kW \cdot hr) = \frac{M_{NO_2} * \sum_{i=1}^N \left[(xNO_{x_i} (ppm)) * 10^{-6} * \dot{n}_i \left(\frac{mol}{s} \right) * \Delta t \right]}{\frac{M_C}{w_{fuel}} * \sum_{i=1}^N \left[\frac{\dot{n}_i \left(\frac{mol}{s} \right) * [xHC_i (ppm) * 10^{-6} + (xCO_i (\%) + xCO_{2_i} (\%)) * 10^{-2}] * \Delta t}{BSFC_i \left(\frac{g}{kW \cdot hr} \right)} \right]}$$

As mentioned earlier, Method 2 is not subject to accuracy errors for the exhaust flow measurement, although that measurement must still be linear for the method to function properly. Application of this formula to HC and CO is the same as what was outlined for Method 1.

1.2.5.3 Calculation Method 3 – “Fuel Specific” Method

Method 3 does not use direct measurement of exhaust flow, but relies on a carbon balance and ECM broadcast fuel rate to determine mass. The work term for Method 3 is determined identically to the work term for Method 1; using the ECM broadcast values for engine speed and torque to calculate work. Method 3 entirely circumvents the use of an exhaust flow meter, but for the HDIUT program, EPA must approve the use of Method 3 for a given test and manufacturer. A simplified version of Method 1 may be expressed as:

$$Method\ 3 = \frac{\sum \left[g \times \frac{ECM\ fuel}{CO_2\ fuel} \right]}{\sum Work}$$

The more complete formula for Method 3, using NO_x as an example is:

$$e_{NO_x} (g / kW \cdot hr) = \frac{\frac{M_{NO_2} * w_{fuel}}{M_C} * \sum_{i=1}^N \left[\frac{(xNO_{x_i} (ppm)) * 10^{-6} * \dot{m}_{fuel_i} \left(\frac{g}{s} \right)}{xHC_i (ppm) * 10^{-6} + (xCO_i (\%) + xCO_2 (\%)) * 10^{-2}} * \Delta t \right]}{\sum_{i=1}^N \left[\frac{Speed_i (rpm) * T_i (N \cdot m) * 2 * 3.14159 * \Delta t}{60 * 1000 * 3600} \right]}$$

It should be noted that Method 3 is not subject to exhaust flow measurement accuracy errors, but also that this method is wholly dependent on ECM broadcast values for both mass and work determination. Application of this formula to HC and CO is similar to that described for Method 1.

1.3 Monte Carlo Model Simulation

The desire for this program was to generate measurement allowances based on rigorous statistical methods applied to a large body of data. At the same time, it was desirable to exclude outlier data caused by extreme measurement errors which were not considered representative of normal in-use operations. A direct approach could have been to test PEMS against some kind of mobile laboratory reference (such as the CE-CERT Mobile Emission Laboratory) on a large number of vehicles, and quantify errors directly. However, such an approach would have been prohibitively expensive in terms of both time and funding. In addition, the desired laboratory reference point for error comparison was certification testing, which is normally conducted in a dynamometer laboratory facility.

Given these factors, the Steering Committee ultimately elected to use a simulation approach in order to generate the measurement allowances. In this approach, the Steering Committee would define all of the expected sources of PEMS measurement errors, based on existing in-use testing expertise and understanding of how the PEMS functioned. Each of these errors would be quantified using a series of controlled laboratory experiments, each designed to isolate errors related to a single error source. The results of each experiment would essentially be an empirical model of a given source of measurement error. In this report, these error models are referred to as error surfaces. It is important to note that each of these error surfaces represents an incremental error of PEMS measurement, as compared to an associated laboratory reference measurement.

All of these error surfaces were programmed into a computer model, which employed Monte Carlo random sampling methods to simulate the combined effects of all of these sources of error on the final measured brake-specific value. An ideal data set for a given test event was

run through the Model, and all the various errors were applied to that data set in a randomly chosen manner. Brake-specific emission values were then calculated for both the ideal and error-applied data sets, which were compared to yield a final measurement error. The process was repeated thousands of times, with many different ideal data sets, to generate a large, robust data set which was evaluated to determine a final set of combined measurement errors. These final errors, referred to in this report as deltas, were generated for each pollutant and for each calculation method, for a final set of nine deltas; three for each pollutant. A complete description of the Monte Carlo methodology and of the model is given in Section 2 of this report.

1.4 1065 PEMS and Laboratory Audit

A key provision of both certification testing and compliance testing under the HDIUT program is that manufacturers must use measurement equipment which meets the requirements outlined in 40 CFR Part 1065. In particular 40 CFR Part 1065 Subpart D outlines a set of performance checks which a measurement system must pass to insure the accuracy and reliability of the instruments.

In light of these requirements, the Test Plan outlined a process wherein both the SwRI reference laboratory and the PEMS would be audited prior to the start of testing, in accordance with the procedures outlined in 40 CFR Part 1065 Subpart D. The audit was conducted on all PEMS and laboratory instrumentation. In addition, a similar audit was also conducted on the CE-CERT Mobile Emission Laboratory (MEL), which was later used during the validation process outlined in Section 1.8. The performance checks were regularly repeated for both the PEMS and the reference laboratory, in accordance with the requirements given in Subpart D. In the event that a given PEMS failed a given Subpart D performance check during the initial audit, the PEMS manufacturer was given an opportunity to correct the issue prior to the start of actual testing, subject to the approval of the Steering Committee. The 1065 audit process and results for the SwRI laboratory and the individual PEMS are described fully in Section 3 of this report.

1.5 Engine Dynamometer Laboratory Testing

A substantial number of the individual error experiments were conducted in an engine dynamometer test cell located in the Department of Engine and Emissions Research at SwRI. The test cell used for this program was Heavy Duty Transient Test Cell 27. This particular test cell at SwRI is fully compliant with the procedures and methods of 40 CFR Part 1065. In addition, the test cell incorporates additional equipment that can be used to simulate operation at high altitudes, and also to simulate a wide range of ambient conditions in the intake air supply of the engine. These expanded test cell capabilities were required for the proper conduct of some of the experiments outlined in the Test Plan. SwRI technicians Gabriel Hernandez and Brian Moczygamba were the engine operators during the program. Billy Valuk was the Test Cell 27 emissions cart operator during the program.

In general, the tests conducted at this location involved simultaneous measurements made by both PEMS and the Laboratory on running engines. The engines were all equipped with diesel particulate filters (DPFs), in order to simulate the exhaust conditions of a 2007 or later model year engine. Because the engines that were tested were not 2007 model year engines, the

NO_x levels were roughly twice as high as those expected for such an engine. Three different test engines were supplied to SwRI by participating engine manufacturers. These engines were a heavy heavy duty (HHD) engine supplied by Daimler Chrysler, a medium heavy duty (MHD) engine supplied by Caterpillar, and a light heavy duty (LHD) engine supplied by International.

Tests conducted in the dynamometer test cell included both steady-state and transient exhaust emission measurements. In addition, a wide variety of experiments were conducted to quantify errors in ECM broadcast torque and fuel rate, as compared to Reference Laboratory measured values. Full details of all of these experiments, and their results are given in Section 4 of the report.

1.6 Environmental Chamber Testing

Another major portion of the Test Plan was devoted to characterizing PEMS measurement errors related to varying environmental conditions that might be experienced in the field during in-use testing. These tests were performed at a variety of facilities which are part of the Mechanical and Material Engineering Division at SwRI. Environmental factors included in these experiments included temperature, altitude, vibration, and electromagnetic interference. PEMS were installed in specialized test facilities designed to simulate a wide variety of conditions for each of these factors. In addition, testing was also performed to examine the effect of ambient hydrocarbon levels on the PEMS HC measurement.

No engines were involved in the environmental tests. Instead, standard reference gases were sampled by the PEMS during these tests. Therefore, the errors were determined by comparing PEMS analyzer responses to the known, and verified, concentrations of the reference gases. The exhaust flow meter was included in some of these tests, but because no exhaust was flowing through the meter during environmental testing, only zero errors were examined for exhaust flow during these tests. Full details of environmental testing and test results are given in Section 5 of this report.

1.7 Exhaust Flow Meter Testing

A small set of experiments was specified in the Test Plan to evaluate the effect of various installation and operation conditions on the exhaust flow meter. These conditions included exhaust flow pulsations, non-uniform velocity profiles (possibly caused by pipe bends location upstream of the flow meter), and the effect of wind across the open end of the exhaust flow meter. These experiments were also conducted in the dynamometer test cell described in Section 1.5. Special exhaust systems and test rigs were set up for each of these experiments. The PEMS exhaust flow meter measurements were compared to the Laboratory Reference raw exhaust flow measurement during these experiments. Exhaust flow meter experiments and the results of those tests are described in a portion of Section 4 of this report.

1.8 Model Validation

For reasons discussed earlier, the measurement allowances were generated using a Monte Carlo computer model. As with all simulations, it is vital that such a model be validated through comparison with real experimental data. In this case, the Measurement Allowance model needed to be validated against a data set generated through actual in-use field testing. Because the model generates an incremental error in comparison to a Laboratory Reference, a suitable in-use reference measurement was needed for comparison to the PEMS measurements. The Steering Committee determined that the CE-CERT Mobile Emission Laboratory, operated by the University of California-Riverside, would be an appropriate reference for validation of the model-based in-field testing.

In order to insure that the validation was not disturbed by some inherent bias between the SwRI Reference Laboratory and the CE-CERT MEL validation reference, a correlation exercise was performed between the two laboratories, prior to the start of on-road validation efforts. The CE-CERT MEL was brought to SwRI's laboratory facilities in San Antonio, Texas, and a side-by-side correlation test was run. During this test, exhaust from the same test engine was alternately routed to the measurements systems of both SwRI and CE-CERT. This was done repeatedly over the course of three days of testing. The data was then supplied to the Steering Committee, in order to allow for a determination to be made that correlation between the facilities was acceptable for the purposes of validation of the model.

After the correlation exercise was completed, a test truck was supplied to CE-CERT by Caterpillar for use in this validation exercise. In addition, one of the audited PEMS used at SwRI during the program was also delivered to CE-CERT. CE-CERT then conducted a series of on-road test runs over various driving routes in California, which were designed to take the test truck through a wide range of environmental and ambient conditions. During these tests, simultaneous measurements were made with the PEMS and the MEL in order to generate a validation data set. This formed the primary validation set for the model.

Because the CE-CERT MEL does not readily incorporate a means of direct torque measurement on a vehicle, the on-road validation data set could not be used to validate model errors associated with broadcast torque and derived BSFC. Therefore, an additional validation exercise was conducted at SwRI. This involved removal of the engine from the test truck used by CE-CERT, and installation of that engine in the SwRI dynamometer test cell. Selected portions of the CE-CERT on-road tests were then simulated in the laboratory, to the extent possible. Simultaneous laboratory and PEMS measurements were again taken during this "replay" validation exercise. However, because the laboratory incorporates actual torque measurement, it was possible to use this "replay" data set to validate the portions of the model associated with torque and BSFC measurements.

Validation of the model was assessed independently for each of the three pollutants (NMHC, CO, and NO_x), and for each of the three calculation methods. A full description of the validation efforts, including the data analysis methodology and the results of validation for each pollutant by all three calculation methods is given in Section 6, with the exception of the CE-CERT on road validation testing. This effort is described fully in a separate report, titled

Measurement Allowance On-Road Validation Project Report dated March 2007. The contents of that report are incorporated herein by reference.

1.9 Measurement Allowance Generation

The generation of a set of measurement allowances represented the final outcome of this program. The Test Plan provided a methodology by which all of the data from the millions of Model simulation runs would be collected and analyzed statistically, in order to generate a set of three potential measurement allowances for each pollutant, one for each of the three calculation methods. The Test Plan then outlined a specific method by which the final set of allowances would be chosen from among deltas generated for each of the three calculation methods. The assumption made by the Test Plan, was that the final outcome of all previous efforts would be a set of three validated potential measurement allowance values for each pollutant, NMHC, CO, and NO_x. Each potential allowance was expressed as a percentage of its associated NTE threshold.

The NTE thresholds used for this program are given in Table 13. These NTE thresholds were determined by EPA and approved by the Steering Committee during the generation of the Test Plan. The Test Plan values were supplied in g/hp-hr as shown and calculated values in g/kW-hr are also given for reference.

TABLE 13. NTE THRESHOLDS FOR MEASUREMENT ALLOWANCE PROGRAM

Pollutant	NTE Threshold	
	g/hp-hr	g/kW-hr
NMHC	0.21	0.2816
CO	19.4	26.02
NO _x	2.0	2.682

These threshold values are of critical importance to the program, as they provide the basis for the scaling of measurement allowances, the assessment of model convergence, and a variety of other calculations performed during this program. The general philosophy of the Test Plan was to determine measurement allowances based on errors at these emission levels, especially in the case of any errors that scaled with emission level.

The anticipated outcome from the model runs, analysis, and validation efforts can be represented as a table similar to the one shown in Table 14, which is repeated herein from the Test Plan. The table illustrates both the model outcome, and the process for selecting the final measurement allowance values.

TABLE 14. EXAMPLE OF MEASUREMENT ALLOWANCE DETERMINATION FROM TEST PLAN

	Measurement Errors at respective NTE threshold (%)		
Calc. Method ==>	Method 1 Torque-Speed	Method 2 BSFC	Method 3 ECM fuel specific
BSNO _x	18 %	18 %	20 %
BSNMHC	19 %	17 %	14 %
BSCO	3 %	2 %	1 %
max error ==>	19 %	18 %	20 %
min of max ==>		18%	
selected method==>	"BSFC" method		

The intent of the final selection process was to first determine the largest percentage error from among the three pollutants for each calculation method. These three largest errors would then be compared with each other, and the method which produced the smallest of these three would be chosen for calculation of the final measurement allowances. At that point, the percentages given for the chosen calculation method would be applied to the NTE threshold values given in Table 13, in order to generate the final additive, brake-specific measurement allowances for each pollutant.

An implicit assumption of the process, as described in the Test Plan, was that the values produced by the model for all three pollutants and all three calculation methods would be successfully validated. In the event that this did not occur, it would be necessary for the Steering Committee to determine a valid alternate course of action, in order to determine the final measurement allowance values.

The final model run and the selection and generation of measurement allowances are described fully in Section 7 of this report, including the final allowances approved by the Steering Committee.

2.0 MONTE CARLO MODEL

2.1 Model Background

The main objective of this portion of the project was to use Monte Carlo techniques (e.g. random sampling) in an error model to simulate the combined effects of all the agreed-upon sources of PEMS error incremental to lab error on the components of the brake-specific (BS) emissions. This was accomplished by creating “error surfaces” for the Monte Carlo simulation to sample, based upon the results of a variety of lab experiments. The constructed model was simulated for thousands of trials (i.e., iterations) using data taken from a reference data set of 195 unique NTE events. The model results were used to determine the brake-specific additive measurement allowances for NO_x, NMHC, and CO by three different calculation methods.

The error surfaces were generated from the results of each of the engine dynamometer and environmental chamber laboratory tests described in Sections 4 and 5, respectively. The engine-lab-test error surfaces covered the domain of error versus the magnitude of the signal to which the error was to be applied (i.e., 5th to 95th percentile error vs. concentration, flow, torque, etc.). The environmental-test error surfaces for shock and vibration, and electromagnetic and radio frequency interference (EMI/RFI) covered the same domain as the engine tests, but only for concentration. The environmental test for ambient hydrocarbons was similar, but the error surface did not change as a function of concentration. The environmental test error surfaces for pressure and temperature were characteristically different because they covered the domain of the environmental-test cycle time versus the magnitude of the signal to which the error was to be applied (i.e., error at a selected time vs. concentration). Details on how each surface was generated are given in Sections 4 and 5 of this report. Since these surfaces are populated with data representing the incremental errors between PEMS measurements and laboratory measurements, they were sampled directly by the model.

2.1.1 Reference NTE Events

The reference data set to which all the simulated errors were applied represented engine operations over a wide range of NTE events. This reference data set was generated from collections of real-world PEMS data sets. Parameters in the reference data set were scaled in order to exercise the model through a more appropriate range of parameters (i.e. concentrations, flows, ambient conditions, etc.). In this scaling process, care was taken to maintain the dynamic characteristics of the reference data set.

The Monte Carlo simulation model was run on a set of 195 reference NTE events collected from a number of sources. Five engine manufacturers provided a total of 97 events; 10 reference NTE events came from each of the three engines tested in the lab during the transient testing; 54 reference NTE events were created by adjusting the engine transient tests to cover a larger spread of the emissions; and 14 events came from the pre-pilot CE-CERT data. Before and after errors were applied in the Monte Carlo simulation for each of these reference NTE events.

For all the reference data that was supplied by engine manufacturers, and the CE-CERT data, it is understood that the NTE event data was based on actual field testing results. This was done to insure that the NTE reference events would be representative of in-field operation in the NTE zone. The data from the engine manufacturers was supplied directly to EPA individually. The data was reviewed at EPA and then transmitted to SwRI. No additional information regarding procedures used to generate this data was supplied to SwRI along with the reference NTE events.

NTE brake-specific emissions results were calculated for NO_x, CO and NMHC, using each of the three agreed-upon NTE calculation methods. The three different BS emissions calculation methods referred to in this test plan are:

1. Method #1: Torque-Speed Method
2. Method #2: BSFC Method
3. Method #3: Fuel Specific Method

The formulas and input constants for these three methods for each of the three emissions types are provided in Appendix B.

Table 15 lists the number of NTE events obtained from each data source and the three corresponding BS emissions calculated using Method 1. These emissions have been computed with no error values added to the input parameters. For this report, emissions with no errors added will be labeled the “ideal” emissions. In contrast, the emissions with errors added through the Monte Carlo simulation will be labeled emissions “with errors”.

TABLE 15. REFERENCE NTE EVENTS AND METHOD 1 BS EMISSIONS

Source	Number of NTE Events	BSNO _x g/kW-hr		BSCO g/kW-hr		BSNMHC g/kW-hr	
		Min	Max	Min	Max	Min	Max
International	19	1.858	5.446	0.520	1.3563	0.073	0.276
DDC	18	3.148	6.012	0.221	1.888	0.002	0.087
Caterpillar	20	0.025	5.865	0.000	1.361	0.000	0.059
Cummins	20	2.667	6.687	5.995	0.232	0.006	0.426
Volvo	20	1.396	2.457	1.159	0.266	0.004	0.014
Engine #1	28	0.844	5.799	0.145	0.496	0.000	0.000
Engine #2	28	1.815	3.397	0.150	0.511	0.000	0.004
Engine #3	28	1.586	3.467	0.261	0.530	0.000	0.004
Pre-Pilot	14	5.328	7.193	0.110	0.341	0.000	0.000

When the ideal brake-specific emission values were calculated for the various reference NTE events, it was noted that these ideal emission values were frequently different from one calculation method to another. While it was recognized that this was a realistic outcome, the Steering Committee was concerned that these discrepancies might introduce an unintended bias into the results of the Monte Carlo simulation. Therefore, the Steering Committee directed SwRI to adjust the NTE reference event data in order to align the brake-specific emission levels from all the calculation methods. In general, the values for Methods 2 and 3 tended to be very close to each other, while the Method 1 value would be farther from the other two.

The adjustment was performed by first assuming that the Method 1 result was the desired value, and that the other two calculation methods would be aligned to that result. This meant that torque, speed, and exhaust flow values were not changed. The next step of the alignment process was to adjust CO₂ values for the NTE event, in order to line up the Method 2 NO_x result with the Method 1 value. This was done by using a single multiplier on all CO₂ values for the NTE event in question. Finally the fuel rate values were adjusted slightly in order to bring Method 3 in line with Method 2. This second adjustment was generally on the order of 2 percent or less, because Methods 2 and 3 were normally fairly close to each other.

The alignment was performed in order to get the NO_x emission levels from all three methods to line up precisely. It was initially assumed that CO and NMHC would also line up, once the NO_x values were aligned. In general, that is what happened; however, selected events still demonstrated a misalignment of CO or NMHC once NO_x was aligned. The Steering Committee ultimately elected to accept small discrepancies in CO and NMHC between the calculation methods as long as the magnitude of the differences were less than 1% of the NTE threshold for CO and 2% of the NTE threshold for NMHC. Events which demonstrated larger misalignment were removed from the reference data set. This review resulted in the removal of four of the original events from the reference data set.

The distribution of the BS emissions data for the 195 reference NTE events to be simulated in the Monte Carlo model are depicted in Figure 3 through Figure 5 for NO_x, CO and NMHC, respectively. Note that each emission has data values spread above and below the corresponding NTE threshold. The NTE thresholds used in this analysis were:

- BSNO_x 2.0 g/hp-hr or 2.68204 g/kW-hr
- BSNMHC 0.21 g/hp-hr or 0.28161 g/kW-hr
- BSCO 19.4 g/hp-hr or 26.0150 g/kW-hr

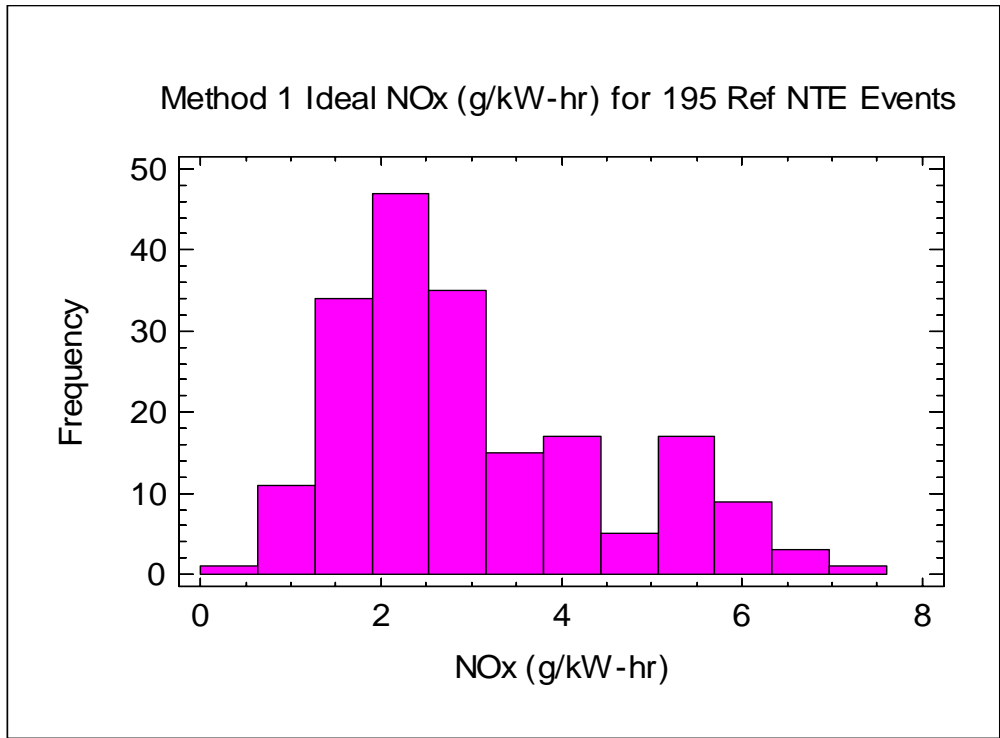


FIGURE 3. METHOD 1 BSNO_x VALUES FOR REFERENCE NTE EVENTS

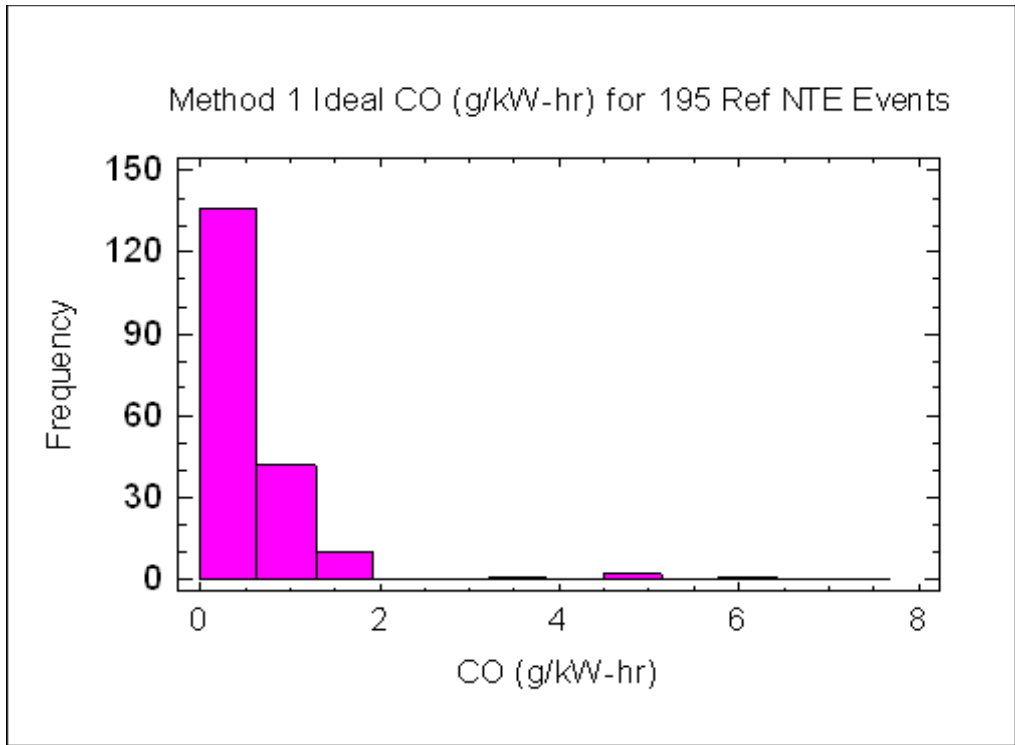


FIGURE 4. METHOD 1 BSCO VALUES FOR REFERENCE NTE EVENTS

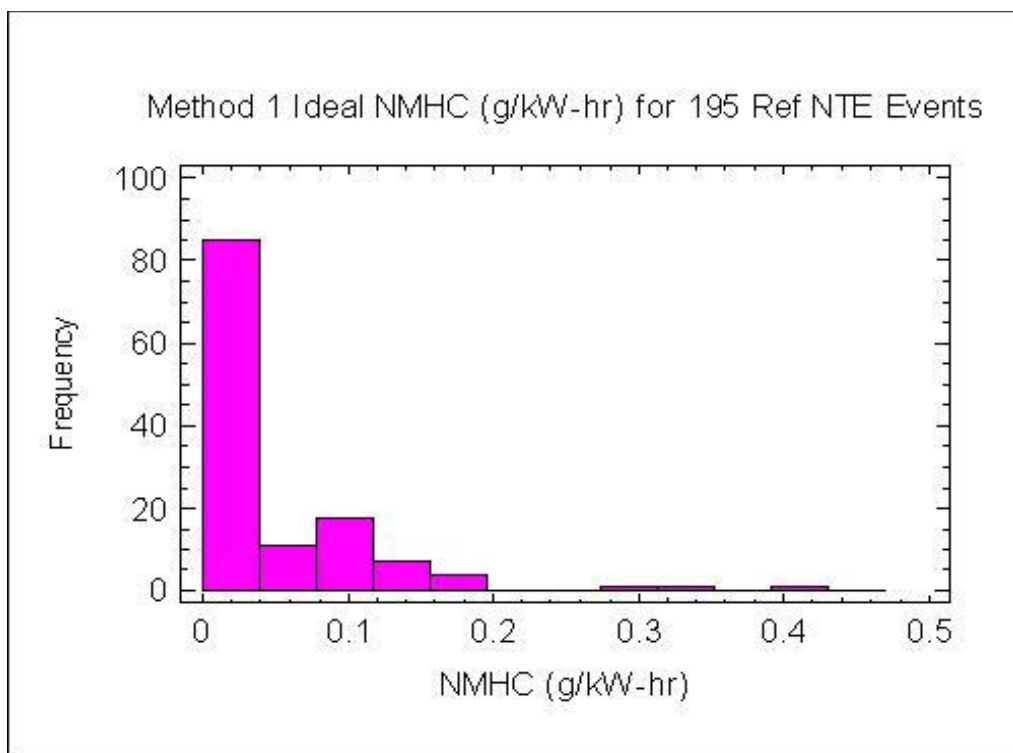


FIGURE 5. METHOD 1 BSNMHC VALUES FOR REFERENCE NTE EVENTS

Table 16 provides a summary of some descriptive statistics for the reference NTE data set for each of the three BS emissions.

TABLE 16. DESCRIPTIVE STATISTICS FOR BS EMISSIONS FOR REFERENCE NTE EVENTS

Descriptive Statistic	BSNO_x g/kW-hr	BSCO g/kW-hr	BSNMHC g/kW-hr
Minimum	0.0249	0.0000	0.0000
Maximum	7.1927	5.9949	0.4258
Mean	3.0071	0.5936	0.0287
Median	2.6033	0.3836	0.0021
Standard Deviation	1.4807	0.7129	0.0591

The parameter data provided in each reference NTE event was on a second-by-second basis with a minimum of 30 seconds and a maximum of 300 seconds. The input parameters required for the BS emissions calculation methods and the Monte Carlo simulation are listed in Table 17. An Excel file with a specific input format structure was used to standardize the format of the input files. Since the total hydrocarbons (THC) was selected as an input parameter, NMHC was computed as $THC \times 0.98$.

TABLE 17. INPUT PARAMETERS FOR REFERENCE NTE EVENTS

Variable Number	Input Variable	Units	Description
1	NTE Event Number	integer	All reference NTE events must be identified by an NTE number (e.g., 001).
2	NTE Source	alphanumeric	The source of the NTE event is the company, organization and/or lab that created the event data.
3	Engine Make	alphanumeric	Engine Make
4	Engine Model	alphanumeric	Engine Model
5	Engine Displacement	L	Engine Displacement (L)
6	Date	mm/dd/yyyy	The day the NTE event data was created (mm/dd/yyyy).
7	Time Stamp	hh:mm:ss.s	Time in seconds. Each reference NTE must contain second-by-second data only.
8	Wet CO2	%	CO2 (%)
9	Wet CO	%	CO (%)
10	Wet kNO	ppm	NO (ppm) with intake air-humidity correction
11	Wet kNO2	ppm	NO2 (ppm) with intake air-humidity correction
12	Wet THC	ppm	THC (ppm)
13	Exhaust Flow Rate	scfm	Exhaust flow rate (scfm)
14	Flowmeter Diameter	3, 4, or 5 (inches)	To compute the % of PEMS flowmeter maximum flowrate we will need to know what size flowmeter was used for each NTE event. Enter either 3, 4, or 5 to represent the following flowmeters and maximum flow rates: 3 = 3 inch EFM with maximum flow rate = 600 scfm 4 = 4 inch EFM with maximum flow rate = 1100 scfm 5 = 5 inch EFM with maximum flow rate = 1700 scfm
15	Speed	rpm	Engine speed (rpm)
16	Low Speed, nlo	rpm	To compute the % of normalized speed we will need nlo and nhi for the engine computed as follows:
17	High Speed, nhi	rpm	nlo (rpm) = lowest speed below max power at which 50% max power occurs nhi (rpm) = highest speed above max power at which 70% max power occurs
18	Fuel Rate	L/sec	Fuel rate (L/hr)
19	Max Fuel Rate	L/sec	To compute the % of maximum fuel rate we will need the max fuel rate of the engine for each NTE event. Max fuel rate (L/hr)
20	Derived Torque	N·m	Torque (N·m)
21	Peak Torque	N·m	To compute the % of maximum torque we will need the peak torque of the engine for each NTE event Peak torque (N·m)
22	BSFC	g/kW-hr	BSFC (g/kW-hr), enter this based upon interpolating your own BSFC table or use the calculation in this spreadsheet, which uses fuel rate, torque, and speed to calculate BSFC, & spgr=0.85, use appropriate conversion factors and spgr.

2.1.2 Error Surfaces

During the initial review of the Test Plan and from discussions held at several Steering Committee meetings, 52 error surfaces were initially identified and considered for inclusion in the Monte Carlo simulation model. These individual error surfaces encompassed a wide variety of error sources, and each of them was investigated in a specific experiment, as detailed later. In some cases, upon reviewing the experimental data, the Steering Committee deemed that the errors from certain sources were not significant; therefore, inclusion in the final Model was not warranted. The details regarding which errors were not included in the model are given later

under the description of the individual error experiments in Sections 4 and 5 of the report. A final total of 35 error surfaces were incorporated into the Model. Two additional errors terms were also included for time alignment as detailed later, bringing the total number of error terms incorporated in the model to 37.

Table 18 lists the error surfaces examined during the study with the surfaces excluded by the Steering Committee designated in italics. All remaining ones were implemented in the simulation model. Each error surface was assigned a number for easy identification. Additionally, two error surfaces relating to the time alignment adjustment for NO_x and CO (i.e., see Section on *Time Alignment for NO_x and CO*) were also included.

TABLE 18. ERROR SURFACES FOR MONTE CARLO SIMULATION

Measurement Error Surfaces and Deltas Used in BS Emissions Calculations				
Component	#	Test Source	Error Surface	Committee Action
1. Delta NOx	1	Engine Dyno	Delta NOx SS	
	2	Engine Dyno	Delta NOx Transient	
	3	Environ	Delta NOx EMI/RFI	Deleted by Steering Committee
	4	Environ	Delta NOx Atmospheric Pressure	Deleted by Steering Committee
	5	Environ	Delta NOx Ambient Temperature	
	6	Environ	Delta NOx Vibration	Deleted by Steering Committee
2. Delta CO	7	Engine Dyno	Delta CO SS	
	8	Engine Dyno	Delta CO Transient	Deleted by Steering Committee
	9	Environ	Delta CO EMI/RFI	Deleted by Steering Committee
	10	Environ	Delta CO Atmospheric Pressure	
	11	Environ	Delta CO Ambient Temperature	
	12	Environ	Delta CO Vibration	Deleted by Steering Committee
3. Delta NMHC NMHC = 0.98*THC	13	Engine Dyno	Delta NMHC SS	
	14	Engine Dyno	Delta NMHC Transient	
	15	Environ	Delta NMHC EMI/RFI	Deleted by Steering Committee
	16	Environ	Delta NMHC Atmospheric Pressure	
	17	Environ	Delta NMHC Ambient Temperature	
	18	Environ	Delta NMHC Vibration	Deleted by Steering Committee
4. Delta Exhaust Flow	19	Environ	Delta Ambient NMHC	
	20	Engine Dyno	Delta Exhaust Flow SS	
	21	Engine Dyno	Delta Exhaust Flow Transient	
	22	Engine Dyno	Delta Exhaust Flow Pulsation	
	23	Engine Dyno	Delta Exhaust Flow Swirl	
	24	Engine Dyno	Delta Exhaust Flow Wind	Deleted by Steering Committee
	25	Environ	Delta Exhaust EMI/RFI	
	26	Environ	Delta Exhaust Vibration	Deleted by Steering Committee
	27	Environ	Delta Exhaust Temperature	
5. Delta Torque	28	Environ	Delta Exhaust Pressure	
	29	Engine Dyno	Delta Dynamic Torque	
	30	Engine Dyno	Delta Torque DOE Testing	
	31	Engine Dyno	Delta Torque Warm-up	
	32	Engine Dyno	Delta Torque Humidity/Fuel	
	33	Engine Dyno	Delta Torque Fuel	Combined with #32
	34	Engine Dyno	Delta Torque Interpolation	
	35	Engine Manuf	Delta Torque Engine Manufacturers	
	6. Delta BSFC	36	Engine Dyno	Delta Dynamic BSFC
37		Engine Dyno	Delta BSFC DOE Testing	
38		Engine Dyno	Delta BSFC Warm-up	
39		Engine Dyno	Delta BSFC Humidity/Fuel	
40		Engine Dyno	Delta BSFC Fuel	Combined with #39
41		Engine Dyno	Delta BSFC Interpolation	
7. Delta Speed	42	Engine Manuf	Delta BSFC Engine Manufacturers	
	43	Engine Dyno	Delta Dynamic Speed	
8. Delta Fuel Rate	44	Engine Dyno	Delta Dynamic Fuel Rate	
9. Delta CO2	45	Engine Dyno	Delta CO2 SS	
	46	Engine Dyno	Delta CO2 Transient	
	47	Environ	Delta CO2 EMI/RFI	Deleted by Steering Committee
	48	Environ	Delta CO2 Atmospheric Pressure	Deleted by Steering Committee
	49	Environ	Delta CO2 Ambient Temperature	
	50	Environ	Delta CO2 Vibration	Deleted by Steering Committee

For each of the measurement errors defined in Sections 4 and 5, an error surface was created and used in the Monte Carlo simulation. Each error surface represented an additive error—or a subtractive error if the sign was negative—relative to the reference parameter value to which it was applied. Figure 6 through Figure 8 serve as a hypothetical example of how these error surfaces were created for every measurement error. Details on the construction of each

error surface used in the simulation are provided in Sections 4 and 5. The example illustrated in Figure 6 through Figure 8 represent the error surface for steady-state bias and precision NO_x concentration errors (Section on *Steady-State Concentration error Surface Generation*). The plots shown correspond to hypothetical NO_x emissions concentration data acquired in the laboratory with three PEMS and three engines, with all nine sets of PEMS data pooled together.

PEMS vs. Laboratory Nominal Results

Figure 6 was constructed from raw data acquired from steady-state engine lab tests with the PEMS at repeat testing at various concentration levels (NO_x ppm). The plot pools all bias and precision errors for all three PEMS and for all data from all three engines for all steady-state modes. Twenty repeat measurements of NO_x signals were taken for each of three PEMS yielding 60 data points at each value of the corresponding average lab NO_x values (i.e., lab nominal value). The 60 PEMS signals were plotted against the corresponding laboratory signals measured using lab equipment. Shown in Figure 6 are the 5th, 50th, and 95th percentiles corresponding to the distribution of these 60 observations using the PEMS at each average NO_x concentration level (note that the distribution of data at each NO_x level may not represent a normal distribution). Since the 50th percentiles do not lie on the dashed (diagonal) line of perfect agreement, the data suggest that there is a bias error between the PEMS and lab results. In essence this graph summarizes the statistical distribution measured by the PEMS at each concentration level sampled. The example plot in Figure 6 shows only 6 discrete average NO_x concentration levels (ranging from 100-350 ppm). However, the actual number of discrete concentration levels was determined using the total number of operating conditions actually run for all the tests on all three engines. In the section on *Steady-State Repeat Engine Testing and Error Surfaces* it is reported that 10 operating conditions from an initial number of 40 operating conditions were selected for construction of the steady-state NO_x error surface. Thus, the plot used in the Monte Carlo simulation contained 30 discrete NO_x concentration levels (10 operating conditions x 3 engines).

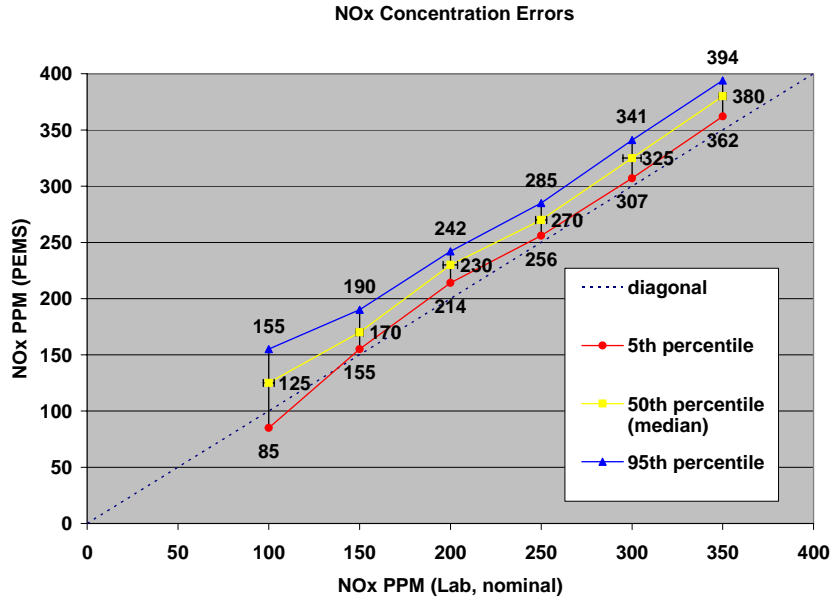


FIGURE 6. ERROR SURFACE CONSTRUCTION: PEMS VS. LABORATORY RESULTS

(PEMS – Laboratory) Deltas vs. Lab

Figure 7 illustrates the “error band” measured during testing. This plot was created by first subtracting the individual “lab nominal” NO_x value from the corresponding individual PEMS NO_x measurement for each test run. This difference was defined as the “delta” error. Second, these “PEMS - Laboratory” delta errors were pooled at each average lab nominal NO_x value to obtain the 5th, 50th, and 95th percentile values displayed in Figure 7. Therefore, the plot represents the average NO_x lab nominal at 30 discrete concentration levels versus the percentiles of the delta errors computed from the PEMS and laboratory individual test results.

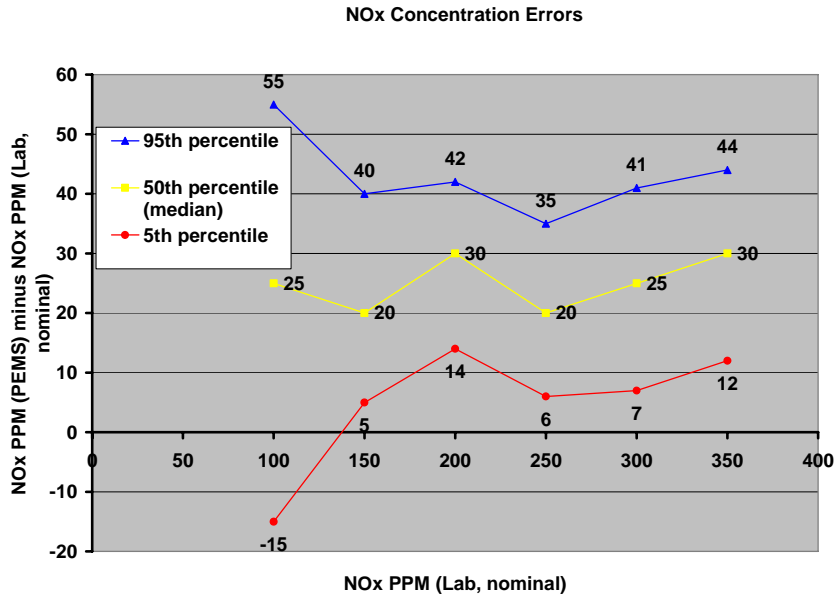


FIGURE 7. ERROR SURFACE CONSTRUCTION: (PEMS - LAB) VS. LABORATORY RESULTS

Variability Index vs. (PEMS – Laboratory) Deltas and Lab Nominal

This step normalized the plot in Figure 7 using what is called a “variability index (i_c)”. This index represented the value randomly drawn by the Monte Carlo simulation in order to select a given error level. It was allowed to vary from -1 to $+1$. The likelihood of “ i_c ” being any value between -1 through $+1$ was specified by a “probability density function (PDF)” assigned to i_c . In the case of this example, i_c was assumed to vary according to a standard normal (i.e., bell-shaped) distribution during the Monte Carlo simulations. This was because it was believed that the distribution of NO_x errors due to steady-state bias and precision would be centered about the 50th percentile of the full range of conditions measured according to the section on *Steady-State Repeat Engine Testing and Error Surfaces*. Each set of data for each lab “set point” average (i.e., lab nominal value) in Figure 7 was normalized by aligning the corresponding 5th percentile error from Figure 7 with $i_c = -1$, the 50th percentile error with $i_c = 0$, and the 95th percentile error with $i_c = +1$. These values were then plotted in Figure 8, where the y-axis is the variability index, the x-axis is the average lab nominal NO_x value, and the z-axis is the delta NO_x value. Notice that, when using this normalization approach, the 5th, 50th, and 95th percentile values remain equivalent between Figure 7 and Figure 8. Error surfaces such as the one presented in Figure 6 are the error deltas the Monte Carlo simulation program used during calculation of the BS emissions “with errors”.

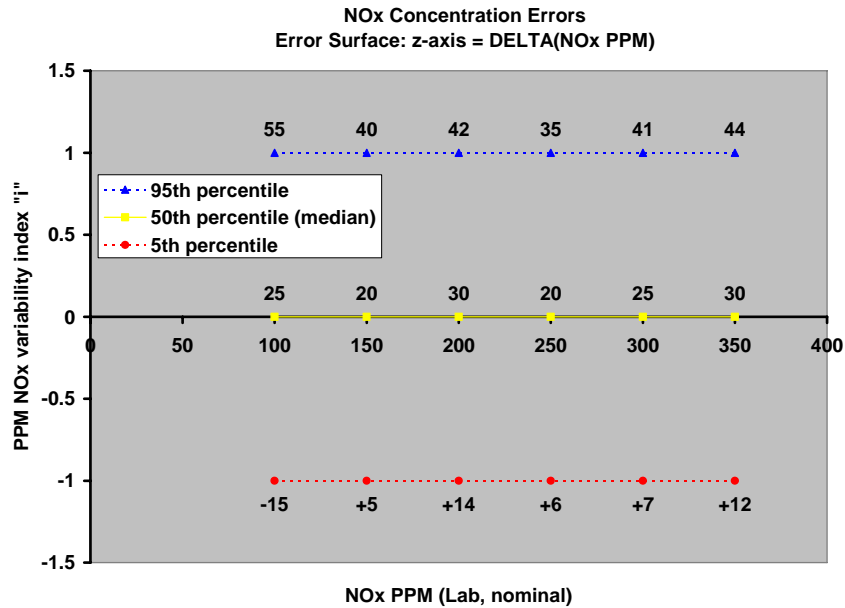


FIGURE 8. ERROR SURFACE CONSTRUCTION: ERROR AT VARIABILITY INDEX VS. LABORATORY RESULTS

2.1.3 Error Surface Sampling and Interpolation

The error model used two different probability density functions to sample the error surfaces, depending upon which experimental parameter the surface represented. To sample error surfaces that were generated from the lab test results (Section on *Engine Dynamometer Laboratory Testing*), and the environmental test results for shock and vibration, EMI/RFI, and ambient hydrocarbons, the model used a truncated standard normal PDF because these tests were designed to evenly cover the full, but finite, range of engine operation and ambient conditions. To sample error surfaces that were generated from the pressure and temperature environmental test results (Section on *Environmental Chamber Testing*), the model used a uniform PDF because these tests were already designed to cover the typical range and frequency of the respective conditions. Both of these sampling distributions are depicted in Figure 9.

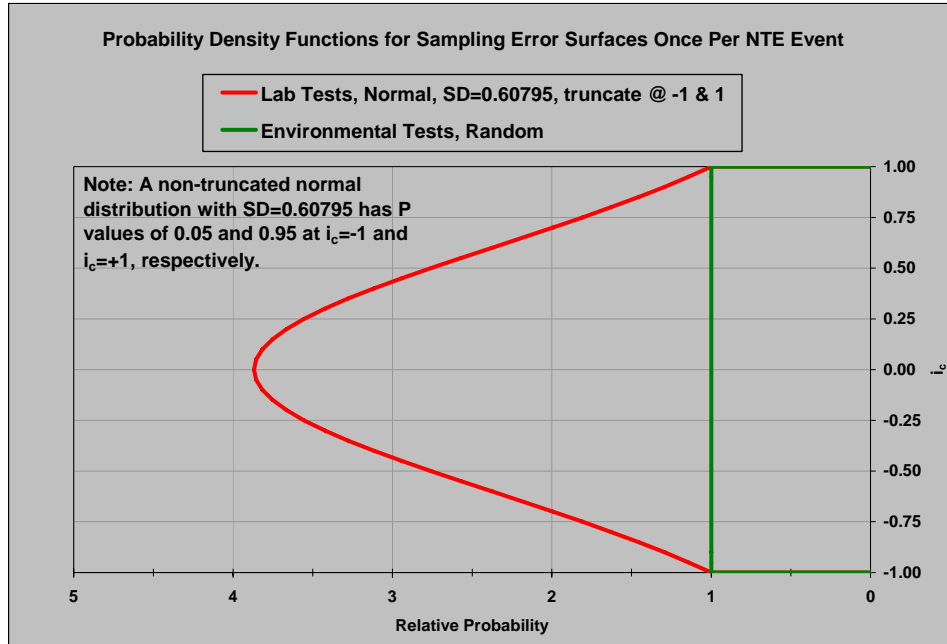


FIGURE 9. TRUNCATED STANDARD NORMAL AND UNIFORM PROBABILITY DENSITY FUNCTIONS

When using the truncated standard normal PDF (see Figure 9), the Monte Carlo model sampled normal deviates that ranged between -1 and +1. These were used as the i_c values defined in the section on *Error Surfaces*. Similarly, the pressure and temperature environmental tests used a uniform PDF to sample test time, from which calculated errors were used. All temperature error surfaces related to the four emissions were sampled uniformly from 1 to 1080 minutes while the error surfaces related to the pressure were sampled uniformly from 1 to 720 minutes. Exhaust flow error surface for temperature was sampled uniformly from 1 to 478 minutes while the exhaust flow for pressure was sampled uniformly from 1 to 360 minutes. The errors from all the other tests were aligned with the truncated standard normal PDF such that each of the 50th percentile error values at each of the tested signal magnitudes was centered at the median (i.e., 0 value) of the PDF, and the 5th and 95th percentile error values at each of the tested signal magnitudes were aligned with the extreme negative ($i_c = -1$) and positive ($i_c = +1$) edges of the PDF, respectively.

Each error surface was sampled along its i_c axis (y-axis) once per trial for a reference NTE event simulation. Hence, every error surface had a separate randomly selected i_c for each trial. Since each reference NTE event contained second-by-second parameter data, the error surface was sampled at a given i_c on the y-axis and at the several selected parameter values on the x-axis that corresponded to each second of the reference NTE event. The sampled error value was determined for the given second and parameter along the error axis (z-axis) at the intersection of the i_c value and the parameter value from the reference NTE event. This was accomplished by taking each second in the reference NTE event and finding the two adjacent x-axis values from the error surface between which to linearly interpolate to obtain the error surface x-value. Each second in the reference NTE event was linearly interpolated with the same i_c value for a particular trial at the error surface x-value. If any of the sampled lab nominal

values (NO_x, NMHC, CO, Speed, Fuel Rate, etc.) exceeded the upper or lower limits of the parameter error surface, the value of the closest endpoint of the error surface was assigned to them.

Figure 10 depicts an example of the error surface sampling using a steady-state NO_x error surface containing 30 lab nominal NO_x x-axis values. For this particular trial, the randomly selected i_c is -0.5. The example reference NTE event is noted by the symbol ‘*’ and it plotted at $i_c = -0.5$ for each second in the NTE event.

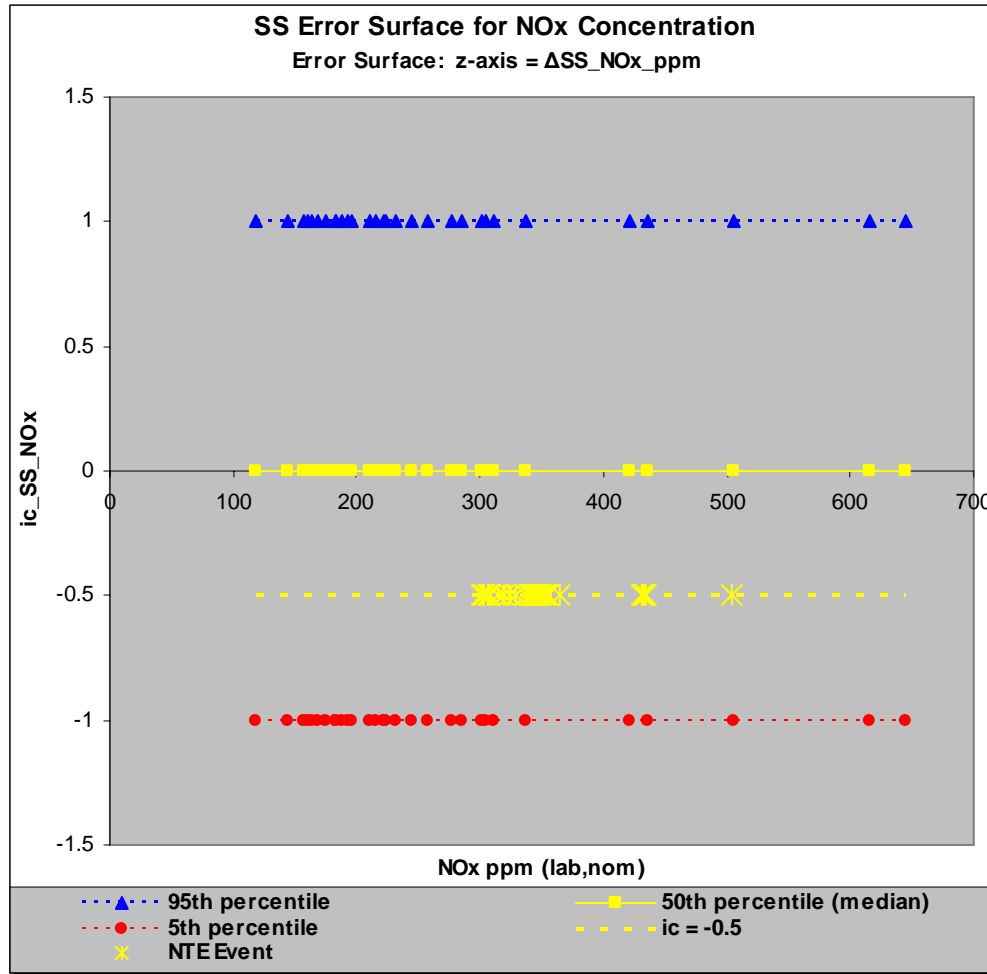


FIGURE 10. STEADY-STATE NO_x ERROR SURFACE WITH EXAMPLE SAMPLING FOR A REFERENCE NTE EVENT

2.1.4 Brake-Specific Emissions Calculations

Errors from Sections 4 and 5 were combined by adding all of the sampled errors once per trial for each reference NTE event simulation. For example, in order to assess the errors in NO_x concentration by calculation Method #1, several error surfaces were sampled and added to the corresponding parameter in the Method #1 calculation and the resulting BSNO_x “with errors”

was computed. The errors used in this calculation are the following (note that the corresponding error surface numbers are provided in the subscripts):

$$\begin{aligned} \text{NO}_x \text{ ppm 'with errors'} &= \text{NO}_x \text{ ppm}_{\text{reference}} + \Delta \text{NO}_x \text{ ppm}_1 + \\ &\quad \Delta \text{NO}_x \text{ ppm}_2 + \Delta \text{NO}_x \text{ ppm}_5 \\ \\ \text{Exhaust Flow } \% \text{ 'with errors'} &= \text{Exhaust Flow } \% \text{ reference} + \\ &\quad \Delta \text{Exhaust Flow } \%_{20} \Delta \text{Exhaust Flow } \%_{21} + \\ &\quad \Delta \text{Exhaust Flow } \%_{22} + \Delta \text{Exhaust Flow } \%_{23} + \\ &\quad \Delta \text{Exhaust Flow } \%_{25} + \Delta \text{Exhaust Flow } \%_{27} + \\ &\quad \Delta \text{Exhaust Flow } \%_{28} \\ \\ \text{Torque } \% \text{ 'with errors'} &= \text{Torque } \% \text{ reference} + \\ &\quad \Delta \text{Torque } \%_{29} + \Delta \text{Torque } \%_{30} + \\ &\quad \Delta \text{Torque } \%_{31} + \Delta \text{Torque } \%_{32} + \\ &\quad \Delta \text{Torque } \%_{34} + \Delta \text{Torque } \%_{35} \\ \\ \text{Speed } \% \text{ 'with errors'} &= \text{Speed } \% \text{ reference} + \Delta \text{Speed } \%_{43} \end{aligned}$$

where,

- $\Delta_{1,2}$ = NO_x concentration errors due to steady-state and transient errors,
- Δ_5 = NO_x concentration errors due to ambient temperature,
- $\Delta_{20,21}$ = exhaust flow errors due to steady-state and transient errors,
- $\Delta_{22,23}$ = exhaust flow errors due to pulsation and swirl,
- Δ_{25} = exhaust flow errors due to ambient temperature,
- $\Delta_{27,28}$ = exhaust flow errors due to temperature and pressure,
- Δ_{29} = torque errors due to dynamic torque,
- $\Delta_{30,31}$ = torque errors due to DOE and warm-up,
- Δ_{32} = torque errors due to interacting parameters humidity and fuel,
- $\Delta_{34,35}$ = torque errors due to interpolation and engine manufacturers,
- Δ_{43} = speed errors due to dynamic speed

Using the formulas for the calculation methods in Appendix B, the BSNO_x for Method #1 was computed without errors (“ideal”) and then with all the errors applied as outlined above. Table 19 lists all error surfaces used by each calculation method for all three emissions.

TABLE 19. ERROR SURFACES USED FOR COMPUTING BRAKE-SPECIFIC EMISSIONS BY THREE CALCULATION METHODS

Component	#	Error Surface	Method 1 Calculation			Method 2 Calculation			Method 3 Calculation		
			BSNO _x	BSCO	BSNMHC	BSNO _x	BSCO	BSNMHC	BSNO _x	BSCO	BSNMHC
1. Delta NO _x	1	Delta NO _x SS	✓			✓			✓		
	2	Delta NO _x Transient	✓			✓			✓		
	5	Delta NO _x Ambient Temperature	✓			✓			✓		
2. Delta CO	7	Delta CO SS		✓		✓	✓	✓	✓	✓	✓
	10	Delta CO Atmospheric Pressure		✓		✓	✓	✓	✓	✓	✓
	11	Delta CO Ambient Temperature		✓		✓	✓	✓	✓	✓	✓
3. Delta NMHC NMHC=0.98*THC	13	Delta NMHC SS			✓	✓	✓	✓	✓	✓	✓
	14	Delta NMHC Transient			✓	✓	✓	✓	✓	✓	✓
	16	Delta NMHC Atmospheric Pressure			✓	✓	✓	✓	✓	✓	✓
	17	Delta NMHC Ambient Temperature			✓	✓	✓	✓	✓	✓	✓
	19	Delta Ambient NMHC			✓	✓	✓	✓	✓	✓	✓
4. Delta Exhaust Flow	20	Delta Exhaust Flow SS	✓	✓	✓	✓	✓	✓			
	21	Delta Exhaust Flow Transient	✓	✓	✓	✓	✓	✓			
	22	Delta Exhaust Flow Pulsation	✓	✓	✓	✓	✓	✓			
	23	Delta Exhaust Flow Swirl	✓	✓	✓	✓	✓	✓			
	25	Delta Exhaust EM/RFI	✓	✓	✓	✓	✓	✓			
	27	Delta Exhaust Temperature	✓	✓	✓	✓	✓	✓			
	28	Delta Exhaust Pressure	✓	✓	✓	✓	✓	✓			
5. Delta Torque	29	Delta Dynamic Torque	✓	✓	✓				✓	✓	✓
	30	Delta Torque DOE Testing	✓	✓	✓				✓	✓	✓
	31	Delta Torque Warm-up	✓	✓	✓				✓	✓	✓
	32	Delta Torque Humidity/Fuel	✓	✓	✓				✓	✓	✓
	34	Delta Torque Interpolation	✓	✓	✓				✓	✓	✓
	35	Delta Torque Engine Manuf	✓	✓	✓				✓	✓	✓
6. Delta BSFC	36	Delta Dynamic BSFC				✓	✓	✓			
	37	Delta BSFC DOE Testing				✓	✓	✓			
	38	Delta BSFC Warm-up				✓	✓	✓			
	39	Delta BSFC Humidity/Fuel				✓	✓	✓			
	41	Delta BSFC Interpolation				✓	✓	✓			
	42	Delta BSFC Engine Manuf				✓	✓	✓			
7. Delta Speed	43	Delta Dynamic Speed	✓	✓	✓				✓	✓	✓
8. Delta Fuel Rate	44	Delta Dynamic Fuel Rate							✓	✓	✓
9. Delta CO ₂	45	Delta CO ₂ SS				✓	✓	✓	✓	✓	✓
	46	Delta CO ₂ Transient				✓	✓	✓	✓	✓	✓
	49	Delta CO ₂ Ambient Temperature				✓	✓	✓	✓	✓	✓

2.1.5 Periodic Drift Check

During the Monte Carlo simulation for a particular reference NTE event, the BS emissions computed during each simulation trial (with i_c selected randomly) was checked to determine whether or not a periodic drift would have invalidated the NTE event trial. The drift check results were simulated by computing the BS emissions with all the error surface errors added except those due to the environmental error surfaces. Therefore, the following error surfaces were excluded in computing the drift check: temperature error surfaces for NO_x, CO, CO₂, and NMHC; pressure error surfaces for CO and NMHC; and ambient NMHC. If the absolute difference in the BS emissions ‘with all errors’ and the BS emissions ‘with all errors except environmental’ was greater than a percentage of the emissions threshold, then periodic drift was detected and the simulation trial was eliminated from the analysis. The percentages used in this study were 4% of the NO_x and CO threshold (0.080 and 0.776 g/hp-hr, respectively) and 10% of the NMHC threshold (0.021 g/hp-hr). Figure 11 represents the periodic drift process.

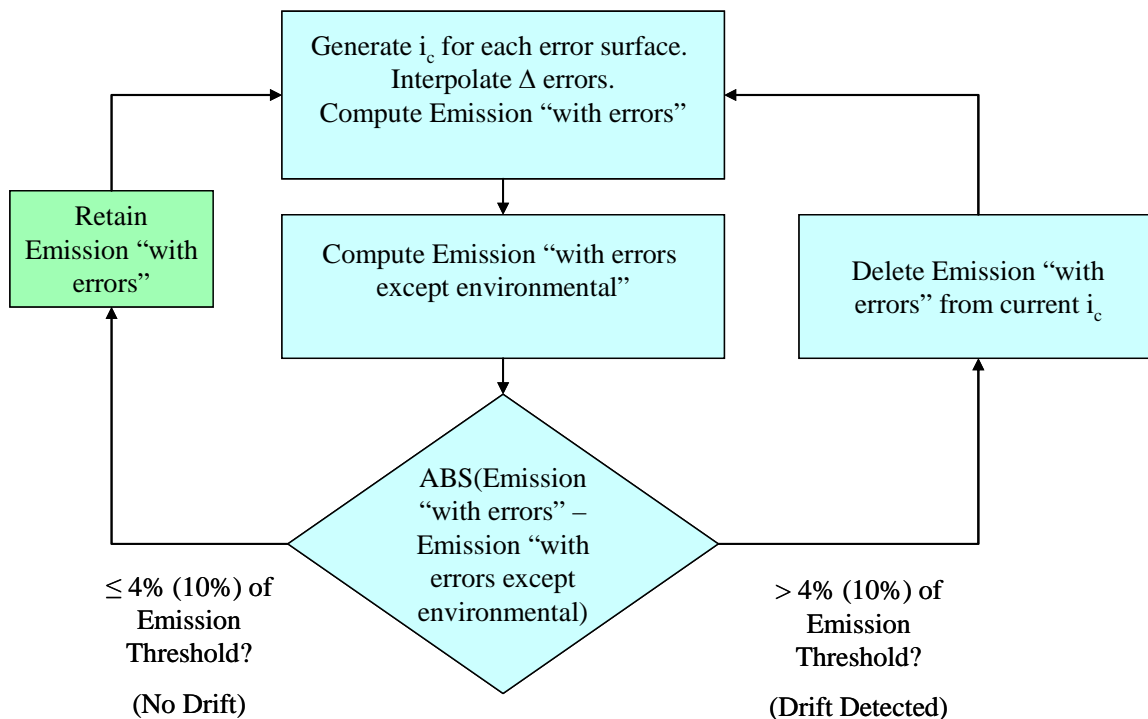


FIGURE 11. PERIODIC DRIFT CHECK FLOWCHART

2.1.6 Time Alignment for NO_x and CO

The time alignment adjustment measured the effect of errors in time alignment of the various continuous PEMS data sources on the final BS emission results. This error source was not originally included in the Test Plan, and no experiment had been designed to examine it. However, it was later decided that time alignment was a significant source of potential error, and that it should be incorporated into the Model. Time alignment values were only generated for NO_x and CO, because NMHC values were too low and too stable to see any discernible trends in NMHC due to time alignment. Details regarding the methodology used to determine the time alignment adjustment are given later in Section 4.12.

Although time alignment was not applied in the same fashion as the other error surfaces in this model, it was described as an error surface because it was sampled as a normal distribution similar to the other error surfaces. The time alignment adjustment was a multiplicative factor which was applied to the BS emission result after all other error terms had been added. The time alignment represented an adjustment up or down as a percentage of the BS emission level “with errors”. A separate time alignment factor was developed for each pollutant, and for each of the three calculation methods allowed in the HDIUT program. Thus, during the Monte Carlo simulation for each trial the brake-specific differences were computed as follows:

$$(\text{BS emissions 'with errors' * Time Alignment Adjustment}) - \text{“Ideal” BS emissions}$$

2.1.7 Convergence and Number of Trials

Since the Test Plan did not include a provision for convergence criteria, the Steering Committee was tasked to develop a convergence method. The main goal was to define how many simulation trials at a given reference NTE event were required to estimate the 95th percentile BS emission differences with a given precision. Although the Crystal Ball software contained precision control options, the method used to compute a confidence interval on percentiles was based on an analytical bootstrapping method which was not adequately documented. Thus, an independent convergence method was proposed and accepted by the Steering Committee.

A nonparametric statistical technique [Reference: Practical Nonparametric Statistics, W.J. Conover, John Wiley & Sons, 1971] was proposed which defined a 90% confidence interval for the 95th percentile of the BS emissions differences for an individual reference NTE simulation. If the width of the 90% confidence interval was less than 1% of the BS emissions threshold, then convergence was met. The following steps define the convergence method:

1. Run the Monte Carlo simulation for N trials.
2. Order the BS emissions differences from smallest to largest.
3. Identify the trial number at the lower end of the 90% confidence interval

$$n_{\text{lower}} = 0.95 * N - 1.645\sqrt{0.95 * 0.05 * N}$$
4. Identify the trial number at the upper end of the 90% confidence interval

$$n_{\text{upper}} = 0.95 * N + 1.645\sqrt{0.95 * 0.05 * N}$$
5. Compute (BS difference value at n_{upper}) – (BS difference value at n_{lower}).
6. If the result in (5) < 1% of the BS emissions NTE threshold then convergence is met.
7. 1% of Thresholds

	<u>g/hp-hr</u>	<u>g/kW-hr</u>
BSNO _x	0.0200	0.026820
BSNMHC	0.0021	0.002816
BSCO	0.1940	0.260150

The Screening Committee agreed to the proposed convergence criteria outlined above. During the initial simulation runs, all reference NTE events at an ideal BS emission level at the threshold and below appeared to converge within the 1% level in 10,000 trials. However, there were a number of reference NTE events with BS emissions levels that were as much as 3 times the NTE threshold. This presented an initial problem in terms of the stated convergence criteria since it was based on a fixed threshold value. Essentially this meant that in order to meet the criterion, some of the higher BS emission level events (>5 g/kW-hr) would have had to converge to a 90% confidence width of well below 0.5% of the threshold value, which would have required an extremely high number of trials. To correct this problem the Steering Committee chose to use the following two-step procedure in deciding the number of trials to run and the convergence criteria:

1. For all reference NTE events with NO_x values equal to or less than 2.6 g/kW-hr, a total of 10,000 trials were run and checked for convergence. It was expected that all of these would converge well within the 1% criteria at this sample size. If any individual reference NTE events did not converge at this run length, those events were run to 30,000 trials.

2. For reference NTE events with NO_x values greater than 2.6 g/kW-hr, a total of 10,000 trials were run and checked for convergence. If convergence was not achieved those same events were run to 30,000 trials. If these events still did not converge within 1% of the threshold value, the procedure was to do one of the following:

- a. If there was convergence within at least 2% of the threshold value, the reference NTE event was included as part of the simulation data set for the measurement allowance and no additional runs were made.
- b. If the reference NTE event did not converge within at least 2% of the threshold value, the event was dropped from the simulation data set considered for the measurement allowance.

In summary, the 195 reference NTE events were run at either 10,000 trials or 30,000 trials and convergence was checked. For all but four reference NTE events, the convergence criteria was met at the 1% NTE threshold value for all three emissions and all three calculations methods. Since only four reference NTE events failed the initial criteria at 1% of the NTE threshold, simulations for these four events were continued up to 50,000 trials. By that point all four NTE events met the convergence criteria.

2.1.8 Simulation Output

During the simulation of a reference NTE event, differences between the BS emissions “with errors”, including time alignment adjustment, and the ideal BS emissions were obtained by each of the three calculation methods. These differences were computed thousands of times (once per trial) until the model converged. Then the 95th percentile difference value was determined for each reference NTE event’s distributions of BS differences for each emission (NO_x, NMHC, and CO) for all three calculation methods.

The output from the Crystal Ball simulation for each reference NTE event was saved in two separate Excel files: an EXTRACT and a REPORT file. The EXTRACT file contained descriptive statistics on all differences computed for BS emissions by all three calculation methods, percentiles (0%, 5%, 10%,...95%, 100%) of the differences in BS emissions, sensitivity data for all error surfaces, and differences in BS emissions computed at each trial in the simulation.

The REPORT file contained a summary of the differences in the BS emissions for all three calculation methods including descriptive statistics, the number of trials that were not excluded due to periodic drift, a frequency histogram of the differences in BS emissions, and percentiles (0%, 5%, 10%,...95%, 100%) of the differences in BS emissions. Also included were descriptive statistics on each i_c distribution sampled for each error surface. Lastly, sensitivity charts for the differences in BS emissions for the three calculation methods were stored. These charts provided information on how much each error surface influenced the differences computed between the BS emissions “with errors” and the ideal BS emissions.

A more detailed description of the Crystal Ball output files can be found in Appendix C.

2.1.9 Step-by-Step Simulation Example

In order to clarify the simulation process the following step-by-step summary is provided. This example assumes that a single reference NTE event was simulated for the BSNO_x difference computations. Figure 12 provides an overview of the simulation process.

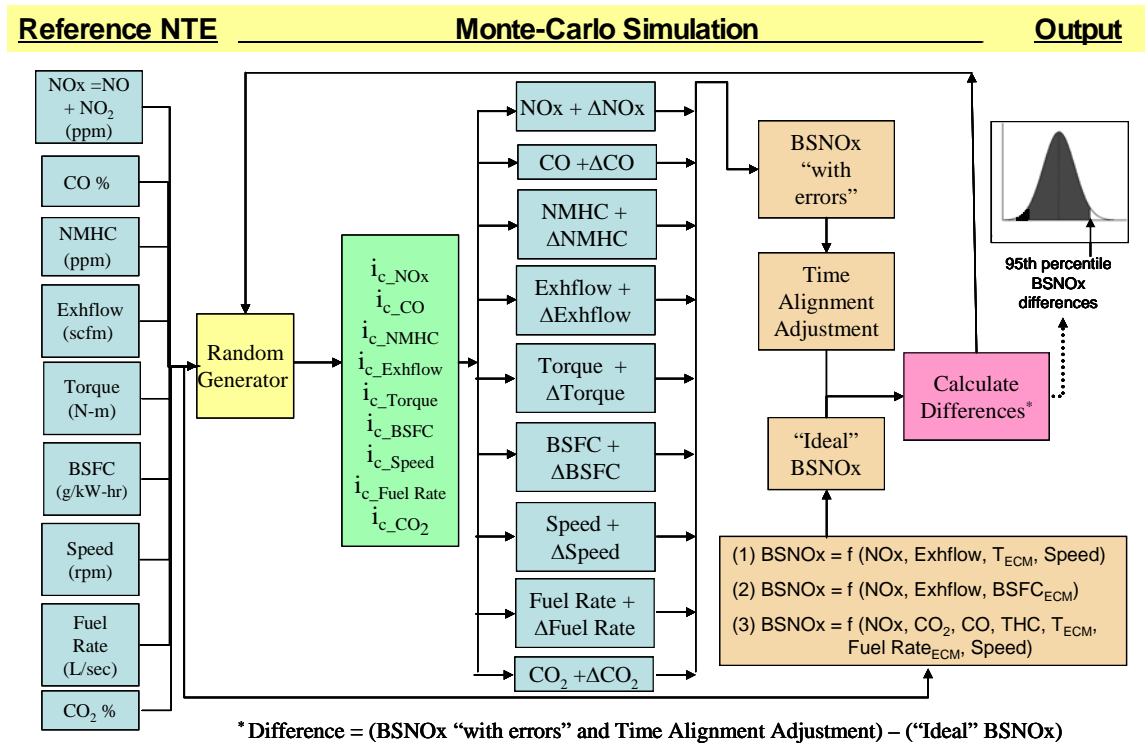


FIGURE 12. OVERVIEW OF MONTE CARLO SIMULATION FOR BSNO_x

STEP 1 Enter the reference NTE input parameters into the Monte Carlo (MC) simulation model. These include the emissions concentrations, exhaust flow, torque, BSFC, speed and fuel rate data used in all three calculation methods.

STEP 2 Compute the “ideal” BSNO_x by all three calculation methods from the reference NTE event.

STEP 3 Set-up the Monte Carlo simulation parameters in Crystal Ball. An Excel spreadsheet model was developed for use with Crystal Ball MC software for error analysis of brake-specific emissions. Crystal Ball is a graphically-oriented forecasting and simulation software that runs on Microsoft® Windows and Excel. The simulations run in this program used Crystal Ball 7.1 and 7.2.2 Academic versions and were run on PCs configured with a Pentium 4 CPU, 3.0 GHz, 2.0 GB RAM, 232 GB hard drive and Windows XP operating system. Microsoft® Excel 2003 SP was the spreadsheet software.

The options exercised in running Crystal Ball included the following:

- Number of trials = 10,000 or 30,000

- If the ideal emission < BS emission threshold then # trials = 10,000
- If the ideal emission \geq BS emission threshold then # trials = 30,000
- If convergence was not met then # trials = 50,000
- Monte Carlo sampling method with random initial seeds
- Normal speed run mode
- Suppress chart windows (fastest run time)

The Excel spreadsheet is in a modular structure following the specified model outline, and it makes provisions for the three identified calculation modules. Input cells to the model are clearly identified to facilitate any revisions that may become necessary for users who want to exercise the model with other Monte Carlo software such as @Risk or newer versions of Crystal Ball. The spreadsheet was tested with controlled test cases of simplified input distributions with the Crystal Ball add-on to confirm correct model implementation in accordance with this test plan. At least one typical analysis was run as an additional confirmation, and two independent checks were made on the ideal emissions by other SwRI staff. A complete description of the spreadsheet computations is contained in Appendix D.

STEP 4 Execute a single MC trial by randomly generating a separate i_c for each error surface used in the three calculations.

STEP 5 For each second in the reference NTE event, interpolate the Δ error for all error surfaces at the input parameter values and the randomly generated i_c . Figure 13 illustrates all the error surfaces available (in yellow) and where the corresponding Δ errors are added. Error surfaces depicted in blue were identified, discussed and eliminated by the Steering Committee.

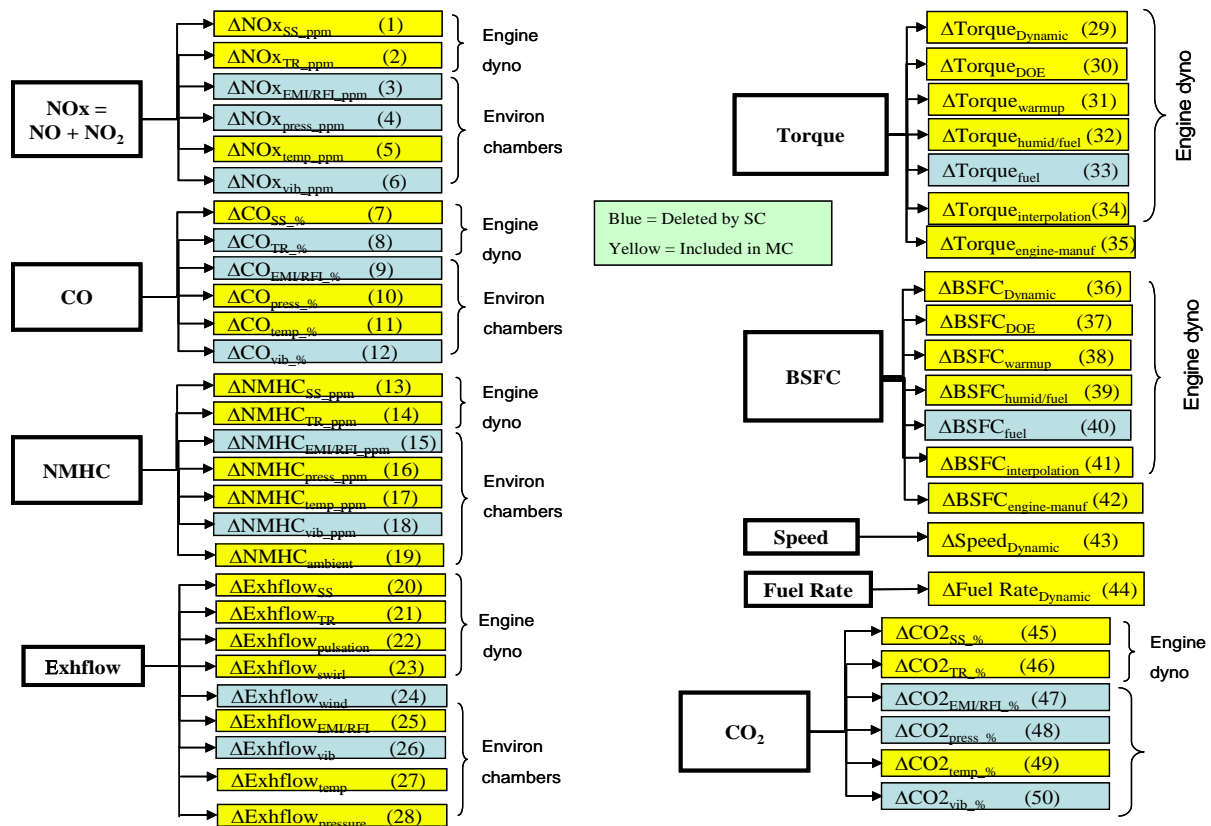


FIGURE 13. ERROR SURFACES INCLUDED IN MONTE CARLO SIMULATION

STEP 6 Compute one $BSNO_x$ “with errors” for the given MC trial by adding all the Δ error values to the reference NTE data and then calculating the $BSNO_x$ by all three calculation methods.

STEP 7 Check for periodic drift to determine if the $BSNO_x$ “with errors” for the given MC trial is valid. If it is valid then continue to Step 8. Otherwise, eliminate the data from the current trial and return to Step 4 to start a new trial.

STEP 8 Compute $BSNO_x$ difference for the current trial:

$$(\text{BS emission “with errors”} * \text{Time Alignment Adjustment}) - \text{“Ideal” BS emission}$$

STEP 9 Repeat Steps 4-8 until the number of trials is met.

STEP 10 Check the differences in $BSNO_x$ for all three calculation methods to be certain that the convergence criteria are met. If convergence is met for all three calculation methods, continue to Step 11. Otherwise, return to Step 4 and run the Monte Carlo simulation for an additional 10,000 trials until the total number of trials is 50,000.

STEP 11 Select the 95th percentile from the distribution of BSNO_x differences for each of the three calculation methods. Store the ideal BSNO_x and the 95th percentile BSNO_x differences for computing the measurement allowance.

STEP 12 Repeat Steps 1-11 for each reference NTE event.

2.1.10 Measurement Allowance

At this point in the process there were nine distributions of 95th percentile differences, where the 195 reference NTE events were pooled by the three emissions (NO_x, CO, NMHC) times three different calculation methods. Each of the 95th percentile distributions represented a range of possible measurement allowances. From each of these nine distributions of possible measurement allowances, one measurement allowance per distribution was determined. These measurement allowances were computed by a regression method or a median method as described below. Both of these calculations methods were decided by the Steering Committee prior to the start of the program, and they were specified in the Test Plan.

Regression Method

This method involved determining the correlation between the 95th percentile differences versus the ideal emission values for the reference NTE dataset. For each combination of emissions and calculation method, a least squares linear regression of the 95th percentile differences versus the ideal emissions results was computed. If the R² value from the regression model was greater than 0.90 and the SEE (standard error of the estimate or root-mean-squared-error) was less than 5% of the median ideal emission result, then the linear regression equation was used to determine the measurement allowance for that emissions and calculation method. To determine the measurement allowance the NTE threshold was used to predict the measurement allowance from the regression model. The NTE thresholds are given in Table 13. The measurement allowance was then expressed as a percentage of the NTE threshold value.

Median Method

If the linear regression did not pass the aforementioned criteria for the R² and SEE statistics, then the median value of the 95th percentile differences from the 195 reference NTE events was used as the single measurement allowance for a combination of emissions and calculation method. The measurement allowance was then expressed as a percentage of the NTE threshold value.

After all 95th percentile distributions were evaluated, there were nine measurement allowances corresponding to the nine combinations of the three emissions and the three different calculation methods.

Next the maximum allowance (in percent) among the three emissions was selected for each of the given calculation methods. The calculation method corresponding to the minimum of these three maximum values was chosen as the best method, and it provided the BS measurement allowances (in percent) for NO_x, NMHC, and CO, respectively. The final additive

BS measurement allowances were computed by multiplying each of the three measurement allowances (in percent) times their corresponding threshold values. Each of these values would be the very last value added to the actual brake-specific NTE threshold for a given engine, based on actual family emissions limit, mileage, model year, etc. Note that if any measurement allowance was determined to have a value less than zero, then that measurement allowance was set equal to zero.

Table 20 below illustrates the selection of the calculation method for all of the measurement allowances. The example is based on a hypothetical set of nine measurement allowances for the three emissions and three calculation methods. The calculation method is selected by first picking the maximum allowances of all the emissions for each of the given calculation methods. For each column the maximum value is selected (highlighted in yellow). Then the minimum of these maximums is used to select the best method (highlighted in blue). In this hypothetical case, the BSFC method would be selected. Therefore, 18%, 17%, and 2% would be selected as the best measurement allowances for NO_x, NMHC, and CO, respectively.

TABLE 20. EXAMPLE OF SELECTION OF THE MEASUREMENT ERROR

Calc. Method ==>	Measurement Errors at Respective NTE Threshold (%)		
	Method 1 Torque-Speed	Method 2 BSFC	Method 3 ECM Fuel Specific
BSNO _x	18 %	18 %	20 %
BSNMHC	19 %	17 %	14 %
BSCO	3 %	2 %	1 %
Max Error ==>	19 %	18 %	20 %
Min of Max ==>		18%	
Selected Method==>	"BSFC" Method 2		

For the data given in Table 20, the BS measurement allowances would be computed as:

- NO_x = 18 % * 2.00 g/hp-hr = 0.3600 g/hp-hr
- NMHC = 17 % * 0.21 g/hp-hr = 0.0357 g/hp-hr
- CO = 2 % * 19.4 g/hp-hr = 0.3880 g/hp-hr

2.1.11 Validation

The final validation methodology for the Monte Carlo model varied from the one that was originally proposed in the Test Plan. This occurred for several reasons.

- The method described in the Test Plan required that CE-CERT be able to measure raw emissions concentrations or determine dilution ratio accurately. However, CE-CERT's mobile laboratory was only capable of making dilute measurements; therefore a dilution

ratio needed to be established. In addition, the mobile laboratory did not include any direct method for the measurement of either exhaust flow or intake air flow. Although the CE-CERT mobile laboratory could measure dilution ratio by measuring both the total CVS flow and the dilution air flow rate, and subtracting to determine exhaust flow rate, there was some concern about the accuracy of this measurement during short NTE events involving a potentially wide dynamic range of dilution ratios. Since the success of this measurement would be critical to the model validation under the methodology given in the Test Plan, the Steering Committee decided that, due to the reliance on this dilution ratio measurement method, there was a considerable degree of risk associated with the original validation methodology, and that an alternative method might prove more robust.

- The Test Plan included an alternative methodology in the event that the CE-CERT laboratory was unable to accurately determine raw exhaust flow or dilution ratio. However, the proposed method had several potential problems, and the Steering Committee decided that this option was not a good choice due to potential bias problems.
- A third option was also mentioned briefly in the Test Plan. It involved comparing the NTE events recorded by the PEMS and the CE-CERT trailer. However, the Steering Committee decided that the proposed method of comparison was not well defined.

After several discussions the Steering Committee selected an alternative approach that was based on a robust validation method which did not rely on measurement of exhaust flow or raw gaseous concentrations. This method was initially proposed by SwRI at the June 2006 Steering Committee meeting in San Antonio. The proposed method had some similarity to the third option proposed in the Test Plan, in that the deltas (PEMS vs. Lab) generated by CE-CERT were to be compared with those generated by the Model. However, the method of comparison was different. The key assumptions in using this method are listed below.

1. It was understood that CE-CERT could not measure torque directly and that no reference torque would be available. This meant that the laboratory BS emission values provided by CE-CERT were to use the same “torque-basis” as the PEMS measurements.
2. It was assumed that CE-CERT would provide BS emission values for each on-road NTE event by all three calculation methods for both PEMS and the mobile laboratory.
3. SwRI was to calculate the “deltas” between the PEMS and the CE-CERT laboratory (i.e., PEMS – CE-CERT).
4. The CE-CERT data was to include both in-cab and on-frame mounted PEMS measurements, but these were to be pooled together to provide a single data set.
5. When the Monte Carlo Model was run through the set of 195 reference NTE events, two sets of results were to be generated. One set included BS emissions with all error surface deltas applied, and a second set which included BS emissions with some of the error surface deltas excluded (primarily those associated with torque, BSFC, speed and fuel rate). These results were to be generated simultaneously during each reference NTE model run. Essentially this yielded two Monte Carlo Model results, a “Validation” result (used for the on-road validation) and a “Full Model” result (to be used for the measurement allowance generation and for the lab replay validation).

The “Validation” result also included time alignment adjustment and checks for periodic drift.

On-Road Validation Methodology

The Measurement Error Monte Carlo Simulation Model was validated by comparing the simulation results using the data from the 195 reference NTE events to the on-road results using the data from the 100 NTE events collected using the CE-CERT trailer and PEMS unit. This was accomplished using the methodology described below.

1. Simulation Results

- The Monte Carlo Model was run using the data from the 195 reference NTE events. In order to obtain Monte Carlo Model simulations representing similar conditions to those obtained on-road, certain error surfaces needed to be suppressed in the simulations since not all of them were applicable to the conditions used in collecting the on-road data. The error surfaces excluded were all torque and BSFC error surfaces, dynamic speed and dynamic fuel rate. This is the “Validation” result described earlier.
- For each reference NTE event, various percentiles, such as the 5th and 95th, of the simulated distribution of the BS emissions differences, defined as

$\text{delta BS} = \text{BS emissions with “Validation” error} - \text{“Ideal” BS emissions},$

were obtained. In essence the model produced a “distribution of deltas” for each NTE event for all three calculation methods.

- The BS emissions included BSNMHC, BSCO, and BSNO_x using all three calculation methods. Thus, there were 9 sets of data (i.e., 3 emissions x 3 calculation methods).
- For each set of data and each percentile chosen in the study, the Monte Carlo Model produced 195 BS delta values (i.e., one from each reference NTE event). These delta BS values were ordered from smallest to largest, and then the empirical distribution function (edf) of these delta BS values was plotted. The edf is a cumulative plot of the fraction of the 195 delta BS observations that were less than or equal to x, versus each x, where x was the observed BS delta value.
- For each of the nine sets of data (3 emissions and 3 calculation methods), the edf corresponding to the 5th and 95th percentile distributions were plotted on the same plot.

Figure 14 contains an illustration of a plot of the edf for 5th and 95th percentiles. The region between these two curves was designated as the validation region for comparison of the edf obtained from the on-road data from CE-CERT.

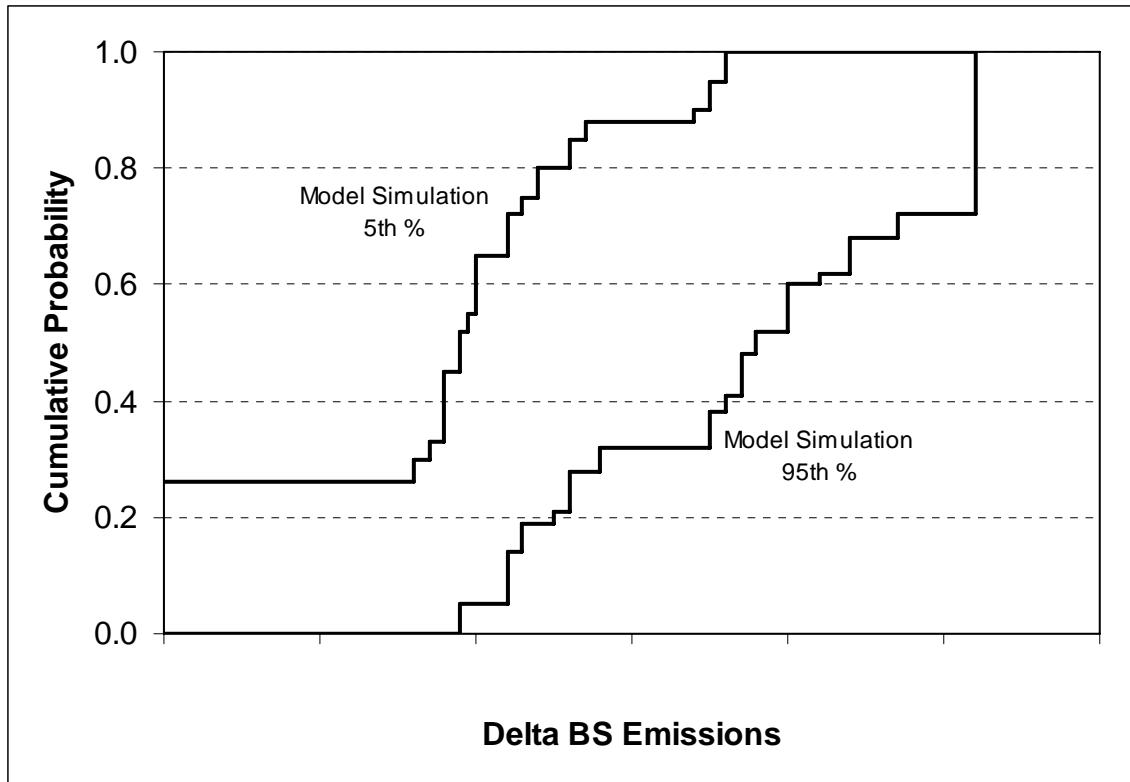


FIGURE 14. PLOT OF MODEL-GENERATED EMPIRICAL DISTRIBUTION FUNCTIONS FOR TWO PERCENTILES

2. On-Road Results

- The CE-CERT trailer was driven on selected on-road routes to collect emissions data. In addition, a PEMS installed in the tractor pulling the trailer collected emissions data. From the routes driven with the CE-CERT trailer approximately 100 NTE events were down-selected by the Steering Committee.
- For each on-road NTE event, a delta BS emissions value, defined as

$$\text{delta BS emissions} = \text{PEMS BS emissions} - \text{CE-CERT BS emissions},$$

was computed.

- As before, the BS emissions included BSNMHC, BSCO, and BSNO_x using all three calculation methods. Thus, there were 9 sets of data (i.e., 3 emissions x 3 calculation methods).
- For each set of data the delta BS values were ordered from smallest to largest and then the empirical distribution function (edf) of these delta BS values were plotted on the same plot as the matching simulation data.

The percentile edfs based on the “Validation” set of simulated data were used for comparison with the edf obtained from the on-road data. Figure 15 contains an illustration of a plot of the matching simulated and on-road edfs.

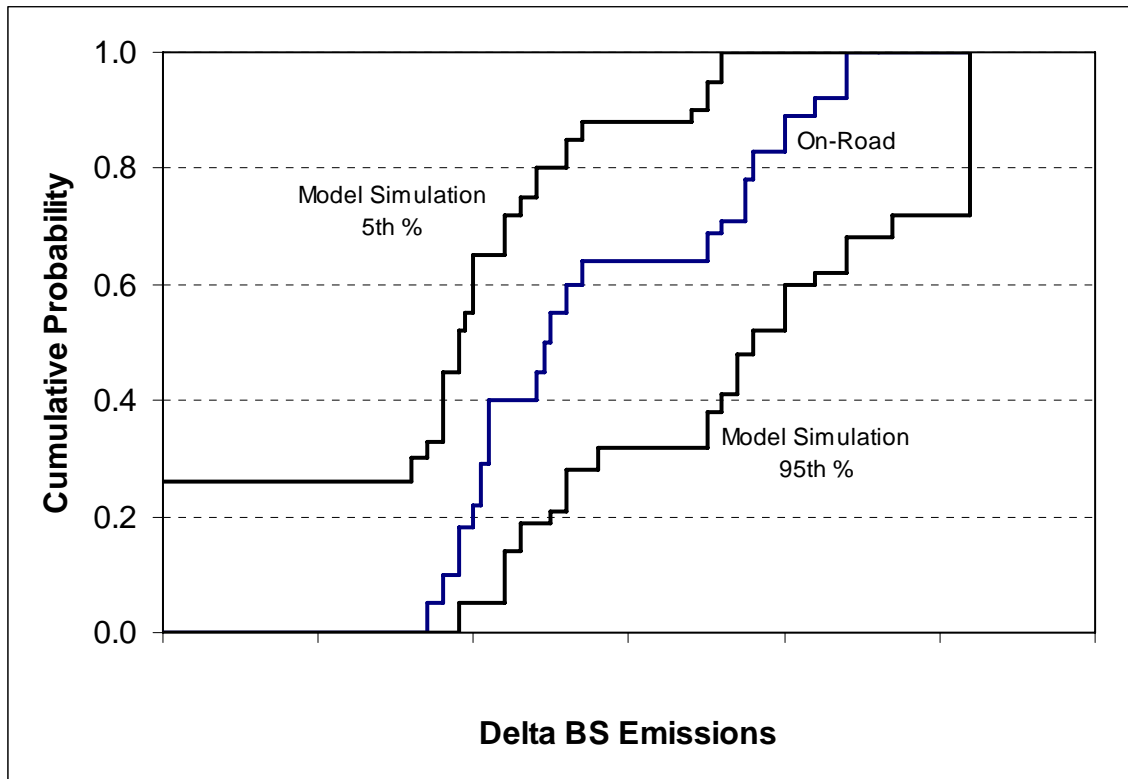


FIGURE 15. PLOT OF ON-ROAD AND MODEL-GENERATED EMPIRICAL DISTRIBUTION FUNCTIONS

3. Comparison of Results

Several methods to compare the results of the model simulation deltas and the on-road deltas for validation were presented to the Steering Committee at the June 2006 Steering Committee meeting in San Antonio. At that meeting all the validation proposals were discussed and a number of alternatives were presented.

Ultimately, the Steering Committee elected to proceed with the following method as a validation methodology. From the on-road and model-generated empirical distribution functions as shown in Figure 15, we would observe how many points of the on-road edf did not fall between the points of the boundary edfs supplied by the simulation model. The Steering Committee agreed that if at least 90% of the on-road data were within the 5th and 95th percentile differences from the model simulation the model was considered valid for a particular BS emissions and calculation method. However, if 10% of the on-road differences were outside the model edfs either on the high or the low side, then the data would be investigated to try to determine the cause. This analysis was performed independently for each pollutant and each calculation method. This decision was later confirmed at the November 2006 Steering Committee meeting in San Antonio.

It should be noted that none of these comparison methods had any effect on the final generation of the Measurement Allowances. These were still generated using the 95th percentile simulation results using the “Full Model.”

Laboratory Replay Validation Methodology

The laboratory replay validation was not as well defined as the on-road validation in the Test Plan, either in terms of testing scope or in terms of the validation methodology to be used with the resulting data. According to the Test Plan, the laboratory replay was to involve removing the engine from the test truck used by CE-CERT for the on-road validation, and using that engine to “replay” some of the on-road testing episodes in the laboratory to the extent it was possible to do so.

In the initial proposal for this program, SwRI established a planned level of effort for the laboratory replay testing involving roughly one month of effort, based on initial discussions with the Steering Committee and the limited details given in the Test Plan. This timeframe included removal of the test engine from the truck, installation in the transient cell, cycle generation, cycle tuning, and testing.

The final scope of the laboratory replay testing involved simulating one hour of operation from each of the three test routes run by CE-CERT during the on-road validation testing. During the course of the on-road validation exercise, personnel from Caterpillar were onsite with CE-CERT in order to facilitate the recording of certain proprietary engine data channels from the ECM. This was done in order to provide data to later assess the accuracy of the laboratory replay simulation. However, this data was only successfully recorded during the portion of on-road testing which was conducted with the PEMS mounted outside the truck cabin (i.e., “frame-mounted” data). As a result, only the frame-mounted on-road operations were simulated during the laboratory replay.

One hour of operation was selected from each route run by CE-CERT, with preference generally given to hours of operation containing the highest frequency of NTE events. Each hour of operation was the basis of an hour long test cycle, which was replayed in its entirety in the laboratory. The data from this hour of operation was then divided into individual NTE events via the standard entry and exit logic used throughout the program (i.e., evaluation on a 1 Hz basis). Successful replay operation was determined in close consultation with Caterpillar personnel who aided in the interpretation of proprietary engine ECM data. After successful replay operation was achieved, each cycle was repeated three times to generate a validation data set.

Brake-specific deltas were determined using two different methods, which were differentiated by the method of generating the laboratory brake-specific emissions levels for comparison to PEMS generated values. The first method was to calculate the laboratory reference values using the standard Laboratory Reference method for work calculation which involved Laboratory measured engine Speed and engine Torque (via the test cell inline torque meter). The PEMS values for each calculation method were compared to this Laboratory

Reference value to generate a delta. These are referred to as “full” deltas, since all error terms are considered.

The second method was to generate deltas using a methodology similar to that used by CE-CERT for the on-road validation data. In this method, the work term for each PEMS calculation method was used for both the Laboratory data and the PEMS data. This essentially eliminates any errors due to torque and BSFC measurement. A separate Laboratory value is generated for each calculation method under this scenario. These values were compared for each calculation method to generate another set of deltas. This second set of deltas is referred to as “mass” deltas, because effectively only errors in the determination of emission mass rates are considered.

The originally intended method for analysis of the replay data was to compare the “full” deltas for the replay validation testing to the simulation deltas generated using the “Full Model.” However, the Steering Committee later decided that this comparison was not appropriate, due to the fact that the laboratory replays were not able to test as wide a range of environmental parameters as the on-road testing. Therefore, different percentiles from the model results needed to be chosen to establish the proper validation window for the replay testing data. The validation window from the “Full Model” result, which included environmental factors, would be too wide for a proper validation.

An alternative method for the treatment of the replay data was discussed at the January 24th 2007 Steering Committee meeting. At that meeting, it was determined that the proper use for the replay data was to examine the “incremental” errors arising from torque and BSFC measurement errors which were not properly examined during the on-road validation, due to lack of a reference torque measurement. Given this direction, SwRI determined an alternate method of comparison, which was presented to the Steering Committee at the February 15th 2007 Steering Committee meeting, and is summarized below.

Monte Carlo Model Data

The model incremental deltas were determined by comparing the results of the Full Model to the results of the Validation Model. This was done on an event-by-event basis for all 195 reference NTE events. In each case, a “work” delta was generated as follows:

$$\Delta_{Model,Work} = \Delta_{Model,Full} - \Delta_{Model,Validation}$$

Replay Validation Data

As mentioned earlier, two deltas had been generated for each calculation method in comparing the PEMS brake-specific values to the Laboratory values. The “full” deltas used the Laboratory values generated using the lab measured torque as a basis for the work term. The “mass” deltas used Laboratory values generated using the same work term as the associated PEMS calculation method, essentially with any work differences cancelled out via calculation.

For each calculation method, an incremental “work” delta was generated by comparing its associated “full” delta to the appropriate “mass” delta as follows:

$$\Delta_{replay,Work} = \Delta_{replay,Full} - \Delta_{replay,Mass}$$

This calculation was performed individually for each replay NTE event and for each of the three repeat runs.

Data Comparison

Initially, the model work deltas and the replay work deltas were plotted against the brake-specific emission level for each event. For the model work deltas, the x-value was the ideal brake-specific emission level for the reference NTE event in question. For the replay validation work deltas, the x-value was the Laboratory Reference brake-specific emissions level calculated using measured torque. The plots were initially examined to see if the replay validation work deltas fell within the range of values produced by the model.

Assuming this initial assessment warranted a more rigorous comparison, the final replay validation comparison would be made in a manner similar to that used for the on-road validation data that was described above. An edf would be made using work deltas generated by the model at both the 5th and 95th percentiles to generate a validation window. This would be compared to an edf of the replay validation work deltas to determine if 90 percent or more of the replay data fell within the validation window.

3.0 1065 PEMS AND LABORATORY AUDIT

3.1 Audit Objective

An initial task of the program was to audit the PEMS and dynamometer laboratory according to 40 CFR Part 1065 Subpart D. The audit procedures were performed to insure the equipment used for the In-Use Measurement Allowance Program met the minimum performance requirements as regulated by the EPA.

3.2 Overview of 1065 Audit Activities

The list of audits to be conducted for both the laboratory and the PEMS was finalized by the Steering Committee at the August, 2005 meeting in Ann Arbor, MI. Table 21 summarizes the required audits for both the laboratory and PEMS instruments. Subsequent sections will detail the results for the individual performance checks that were conducted as part of the audits, as well as any corrective action taken as a result of those checks.

TABLE 21. 1065 AUDITS AND PERFORMANCE CHECKS REQUIRED FOR THE MEASUREMENT ALLOWANCE PROGRAM

Description	CFR Reference	Lab Raw	Lab Dilute	PEMS
Linearity	1065.307	x ¹	x ¹	x ²
Torque Meter	1065.310	x	x	
Fuel Flow	1065.320	x		
Intake Flow	1065.325	x		
Exhaust Flow	1065.330			x
CVS Verification	1065.341		x	
H2O Interference on CO2	1065.350	x	x	x
H2O and CO2 Interference on CO	1065.355	x	x	x
FID Optimization	1065.360	x ³	x ³	x ³
Non-stoichiometric raw FID O2 Interference	1065.362	x		x
Nonmethane cutter penetration fractions	1065.365	x	x	
CLD H2O and CO2 quench	1065.370	x	x	
NDUV HC and H2O Interference	1065.372			x
Chiller NO2 penetration	1065.376			x
NO2-to-NO converter check	1065.378	x	x	
1 Linearity for lab on gas analyzers, flow meters, torque meter, pressures, temperatures				
2 Linearity for PEMS on gas analyzers, exhaust flow meters				
3 Verify methane response factors only, THC instruments				

3.2.1 Laboratory Audits

The results of the laboratory audit were presented to the Steering Committee at the January, 2006 meeting in San Antonio, TX. The laboratory audit results indicated that the SwRI reference laboratory met all of the requirements given under Part 1065 Subpart D. At that time, the Steering Committee approved the laboratory audit results for both the raw and dilute sampling systems, and SwRI was not directed to take any corrective actions for the laboratory.

Regular performance checks were performed throughout the program as required by Part 1065 Subpart D. However, only the results of the initial 1065 audit are included in this report. Documentation of all regular performance checks is available at SwRI if needed.

3.2.2 PEMS Audits

The initial audits of the first four PEMS units (PEMS 1 through 4) were started in January, 2006 and completed by mid-February, 2006. These initial audits included only the 5-inch EFMs used for Engine 1 testing. Audits of the 4-inch and 3-inch EFMs were completed at a later time, closer to the testing needs for Engines 2 and 3. The PEMS units were later modified to address a 1065 NO₂ penetration check failure. PEMS 1 through 4 were audited again in June, 2006, once all modifications were completed. For these subsequent audits, only linearity and NO₂ penetration were checked.

Two additional Sensors Inc. PEMS units (PEMS 5 and 6) as well as a Horiba OBS-2200 arrived at SwRI in June, 2006. Upon arrival, PEMS 5 and 6 and the OBS-200 were given complete 1065 audits as outlined in Table 21. A final PEMS unit (PEMS 7) arrived at SwRI in October of 2006 to serve as a spare. PEMS 7 was given a complete 1065 audit at that time.

Additional PEMS linearity checks were performed as required by Part 1065 Subpart D over the course of the program. In addition, a number of additional audits were required as a result of maintenance or repairs performed on several of the PEMS units over the course of the program. This report contains the results of initial audits on all PEMS units, as well as those performed subsequent to the NO₂ penetration modifications which were completed in June of 2006. In addition, relevant audit results are also given for any major repairs or maintenance events which occurred on the PEMS equipment.

3.3 Gas Analyzer Linearity Verifications

Analyzer linearity checks were performed as specified in CFR Part 1065. The Federal Register defines linearity in terms of the maximum concentration expected during testing. Performing the PEMS and laboratory audits prior to engine testing, the maximum test concentrations were unknown. Therefore, the mono-blend linearity verification gas concentrations were used to define the 1065 linearity criteria. This interpretation of the verification resulted in the most liberal linearity criteria. Mono-blend span gases were used with a STEC Inc. Model SGD-710C 10-step gas divider, shown in Figure 16, to perform the PEMS analyzer linearity verification. Span gas concentrations for the SEMTECH-DS and laboratory analyzers were near the values listed in Table 22. Span concentrations for the PEMS were selected based on manufacturer recommendations in the SEMTECH-DS user manual. All linearity checks on the PEMS were performed using the PEMS span port.



FIGURE 16. STEC INC. MODEL SGD-710C GAS DIVIDER WITH SEMTECH-DS PEMS

TABLE 22. SPAN CONCENTRATIONS USED FOR THE SEMTECH-DS AND LABORATORY ANALYZERS

Analyzer Description	NO [ppm]	NO₂ [ppm]	NO_x [ppm]	CO₂ [%]	CO [ppm]	THC [ppmC]	CH₄ [ppmC]
Dilute MEXA 7200D and Horiba CH4 Bench	N/A	N/A	92	5.5	47	9	23
Raw MEXA 7200D and Horiba CH4 Bench	N/A	N/A	900	14.5	47	9	23
SEMTECH-DS	960	260	N/A	12	960	660	N/A

As shown in Table 23 and Table 24, the laboratory analyzers easily passed the 1065 linearity criteria. The MEXA benches use a Horiba GDC 703 gas divider and perform the linearity checks in an automated process. The STEC Inc. manual gas divider was used to check the dilute and raw CH₄ benches. Linearity checks were performed monthly for all laboratory analyzers during the program. The results of all monthly linearity checks are not included in this report beyond those associated with the initial 1065 audit of the laboratory equipment.

TABLE 23. DILUTE MEXA 7200D AND HORIBA CH₄ BENCH 1065 LINEARITY VERIFICATION SUMMARY

Verification Description	Intercept	Slope	SEE	r ²
CO NDIR				
Measured	0.00	1.00	0.03	1.00
Linearity Criteria	1.13	0.99-1.01	2.26	0.998
Pass / Fail	Pass	Pass	Pass	Pass
CO₂ NDIR				
Measured	0.00	1.00	0.00	1.00
Linearity Criteria	0.03	0.99-1.01	0.05	0.998
Pass / Fail	Pass	Pass	Pass	Pass
HC FID				
Measured	0.40	1.00	0.56	1.00
Linearity Criteria	2.21	0.99-1.01	4.43	0.998
Pass / Fail	Pass	Pass	Pass	Pass
NO_x CLD				
Measured	-0.04	1.00	0.12	1.00
Linearity Criteria	1.36	0.99-1.01	2.72	0.998
Pass / Fail	Pass	Pass	Pass	Pass
CH₄ FID with NMHC Cutter				
Measured	0.00	1.00	0.06	1.00
Linearity Criteria	0.11	0.99-1.01	0.23	0.998
Pass / Fail	Pass	Pass	Pass	Pass

TABLE 24. RAW MEXA 7200D AND HORIBA CH₄ BENCH 1065 LINEARITY VERIFICATION SUMMARY

Verification Description	Intercept	Slope	SEE	r ²
CO NDIR				
Measured	0.80	1.00	2.25	1.00
Linearity Criteria	4.52	0.99-1.01	9.04	0.998
Pass / Fail	Pass	Pass	Pass	Pass
CO₂ NDIR				
Measured	-0.01	1.01	0.03	1.00
Linearity Criteria	0.07	0.99-1.01	0.15	0.998
Pass / Fail	Pass	Pass	Pass	Pass
HC FID				
Measured	0.00	1.00	0.13	1.00
Linearity Criteria	2.34	0.99-1.01	4.68	0.998
Pass / Fail	Pass	Pass	Pass	Pass
NO_x CLD				
Measured	0.00	1.00	0.07	1.00
Linearity Criteria	1.36	0.99-1.01	2.72	0.998
Pass / Fail	Pass	Pass	Pass	Pass
CH₄ FID with NMHC Cutter				
Measured	0.00	1.00	0.06	1.00
Linearity Criteria	0.11	0.99-1.01	0.23	0.998
Pass / Fail	Pass	Pass	Pass	Pass

Table 25 summarizes the linearity verifications performed on PEMS 1. During the initial audit, PEMS 1 repeated failed the linearity check with NO and NO₂. Because PEMS 1 was the only unit to fail linearity with NO during the initial audit, the unit was returned to Sensors for correction in accordance with the Test Plan. Sensors recalibrated the NO component of the NDUV and sent PEMS 1 back to SwRI. The recalibrated unit passed the NO linearity check

PEMS 1 also failed the linearity check with NO₂, as did many of the other PEMS during the initial audit. All of these linearity failures involved the intercept being above the required level. Sensors Inc. was offered a chance to correct the problem; however they declined, indicating that they felt the units were operating correctly despite the intercept failures. Sensors Inc. indicated that they felt there were problems with the 1065 linearity requirements as written, and that widening the intercept linearity criteria should be considered. This was reported to the Steering Committee during the February 23, 2006 conference call, and the decision was made to continue testing as allowed in section 3.1.4 of the Test Plan.

During the June, 2006 linearity checks that followed the NO₂ penetration upgrades, PEMS 1 NDUV measurements became unstable and the instrument could not be zeroed or spanned properly. Following subsequent diagnostics, the NDUV analyzer was replaced by Sensors Inc. PEMS 1 passed the linearity checks for both NO and NO₂ with the new analyzer.

TABLE 25. PEMS 1 1065 LINEARITY VERIFICATION SUMMARY

Verification Description	Intercept	Slope	SEE	r ²
CO NDIR (Initial Audit)				
Measured	0.00	1.00	0.00	1.00
Linearity Criteria	4.52	0.99-1.01	9.04	0.998
Pass / Fail	Pass	Pass	Pass	Pass
CO NDIR (Check 06-05-06)				
Measured	0.00	1.00	0.00	1.00
Linearity Criteria	4.52	0.99-1.01	9.04	0.998
Pass / Fail	Pass	Pass	Pass	Pass
CO₂ NDIR (Initial Audit)				
Measured	0.02	1.00	0.02	1.00
Linearity Criteria	0.07	0.99-1.01	0.15	0.998
Pass / Fail	Pass	Pass	Pass	Pass
CO₂ NDIR (Check 06-05-06)				
Measured	0.05	1.00	0.03	1.00
Linearity Criteria	0.07	0.99-1.01	0.15	0.998
Pass / Fail	Pass	Pass	Pass	Pass
HC FID (Initial Audit)				
Measured	-0.06	1.00	0.26	1.00
Linearity Criteria	2.21	0.99-1.01	4.43	0.998
Pass / Fail	Pass	Pass	Pass	Pass
HC FID (Check 06-05-06)				
Measured	-1.68	1.00	0.53	1.00
Linearity Criteria	2.21	0.99-1.01	4.43	0.998
Pass / Fail	Pass	Pass	Pass	Pass
NO NDUV (Initial Audit)				
Measured	8.25	0.98	4.46	1.00
Linearity Criteria	4.42	0.99-1.01	8.84	0.998
Pass / Fail	Fail	Fail	Pass	Pass
NO NDUV (NO Recalibrated by Sensors Inc. 02-15-06)				
Measured	3.77	1.00	2.06	1.00
Linearity Criteria	4.42	0.99-1.01	8.84	0.998
Pass / Fail	Pass	Pass	Pass	Pass
NO NDUV (New NDUV 06-07-06)				
Measured	3.75	0.99	2.09	1.00
Linearity Criteria	4.42	0.99-1.01	8.84	0.998
Pass / Fail	Pass	Pass	Pass	Pass
NO₂ NDUV (Initial Audit)				
Measured	2.15	1.00	0.92	1.00
Linearity Criteria	1.42	0.99-1.01	2.83	0.998
Pass / Fail	Fail	Pass	Pass	Pass
NO₂ NDUV (New NDUV 06-07-06)				
Measured	-0.85	1.00	0.81	1.00
Linearity Criteria	1.29	0.99-1.01	2.58	0.998
Pass / Fail	Pass	Pass	Pass	Pass

Table 26 shows the summarized linearity verification results for PEMS 2. PEMS 2 narrowly failed linearity for NO₂ during the initial audit. Per the steering committee’s decision,

no action was taken to correct the linearity failure. During the June, 2006 audits that followed the NO₂ penetration upgrades, PEMS 2 passed the NO₂ linearity check.

TABLE 26. PEMS 2 1065 LINEARITY VERIFICATION SUMMARY

Verification Description	Intercept	Slope	SEE	r ²
CO NDIR (Initial Audit)				
Measured	-0.91	0.99	4.96	1.00
Linearity Criteria	4.52	0.99-1.01	9.04	0.998
Pass / Fail	Pass	Pass	Pass	Pass
CO NDIR (Check 06-05-06)				
Measured	-2.27	1.01	2.75	1.00
Linearity Criteria	4.52	0.99-1.01	9.04	0.998
Pass / Fail	Pass	Pass	Pass	Pass
CO₂ NDIR (Initial Audit)				
Measured	-0.02	1.00	0.02	1.00
Linearity Criteria	0.07	0.99-1.01	0.15	0.998
Pass / Fail	Pass	Pass	Pass	Pass
CO₂ NDIR (Check 06-05-06)				
Measured	0.02	1.01	0.04	1.00
Linearity Criteria	0.07	0.99-1.01	0.15	0.998
Pass / Fail	Pass	Pass	Pass	Pass
HC FID (Initial Audit)				
Measured	0.98	1.00	0.73	1.00
Linearity Criteria	2.21	0.99-1.01	4.43	0.998
Pass / Fail	Pass	Pass	Pass	Pass
HC FID (Check 06-05-06)				
Measured	0.48	1.00	0.56	1.00
Linearity Criteria	2.21	0.99-1.01	4.43	0.998
Pass / Fail	Pass	Pass	Pass	Pass
NO NDUV (Initial Audit)				
Measured	3.65	1.00	2.91	1.00
Linearity Criteria	4.42	0.99-1.01	8.84	0.998
Pass / Fail	Pass	Pass	Pass	Pass
NO NDUV (Check 06-05-06)				
Measured	3.81	1.00	3.17	1.00
Linearity Criteria	4.42	0.99-1.01	8.84	0.998
Pass / Fail	Pass	Pass	Pass	Pass
NO₂ NDUV (Initial Audit)				
Measured	2.10	1.01	1.88	1.00
Linearity Criteria	1.42	0.99-1.01	2.83	0.998
Pass / Fail	Fail	Pass	Pass	Pass
NO₂ NDUV (Check 06-05-06)				
Measured	0.46	1.00	0.59	1.00
Linearity Criteria	1.29	0.99-1.01	2.58	0.998
Pass / Fail	Pass	Pass	Pass	Pass

Table 27 summarizes the linearity verification results for PEMS 3. PEMS 3 also failed linearity for NO₂ during the initial audit. As with PEMS 1, problems developed with the NDUV

during the June, 2006 audits that followed the NO₂ penetration upgrades, and the NDUV was replaced by Sensors Inc. The new NDUV passed NO₂ linearity, but narrowly failed NO linearity. Sensors did not elect to perform any corrective action on the unit as a result of this failure. The NO linearity failure was reported to the Steering Committee during the regular conference call on June 13th, 2006, and the decision was made to continue testing despite the failure.

TABLE 27. PEMS 3 1065 LINEARITY VERIFICATION SUMMARY

Verification Description	Intercept	Slope	SEE	r ²
CO NDIR (Initial Audit)				
Measured	0.00	1.00	0.00	1.00
Linearity Criteria	4.52	0.99-1.01	9.04	0.998
Pass / Fail	Pass	Pass	Pass	Pass
CO NDIR (Check 06-05-06)				
Measured	-1.36	1.00	2.75	1.00
Linearity Criteria	4.52	0.99-1.01	9.04	0.998
Pass / Fail	Pass	Pass	Pass	Pass
CO₂ NDIR (Initial Audit)				
Measured	0.03	1.00	0.04	1.00
Linearity Criteria	0.07	0.99-1.01	0.15	0.998
Pass / Fail	Pass	Pass	Pass	Pass
CO₂ NDIR (Check 06-05-06)				
Measured	0.00	1.01	0.03	1.00
Linearity Criteria	0.07	0.99-1.01	0.15	0.998
Pass / Fail	Pass	Pass	Pass	Pass
HC FID (Initial Audit)				
Measured	0.60	1.00	0.51	1.00
Linearity Criteria	2.21	0.99-1.01	4.43	0.998
Pass / Fail	Pass	Pass	Pass	Pass
HC FID (Check 06-05-06)				
Measured	-0.96	1.00	0.27	1.00
Linearity Criteria	2.21	0.99-1.01	4.43	0.998
Pass / Fail	Pass	Pass	Pass	Pass
NO NDUV (Initial Audit)				
Measured	3.56	0.99	2.53	1.00
Linearity Criteria	4.42	0.99-1.01	8.84	0.998
Pass / Fail	Pass	Pass	Pass	Pass
NO NDUV (New NDUV 06-06-06)				
Measured	5.70	1.00	2.02	1.00
Linearity Criteria	4.42	0.99-1.01	8.84	0.998
Pass / Fail	Fail	Pass	Pass	Pass
NO₂ NDUV (Initial Audit)				
Measured	7.38	0.98	1.29	1.00
Linearity Criteria	1.42	0.99-1.01	2.83	0.998
Pass / Fail	Fail	Fail	Pass	Pass
NO₂ NDUV (New NDUV 06-06-06)				
Measured	0.73	1.01	1.17	1.00
Linearity Criteria	1.29	0.99-1.01	2.58	0.998
Pass / Fail	Pass	Pass	Pass	Pass

Table 28 shows the summarized CO₂, CO, and HC linearity verification results for PEMS 4. PEMS 4 passed the linearity check for CO₂, CO, and HC during the initial audit as well as the June 2006 checks that followed the NO₂ penetration upgrades.

TABLE 28. PEMS 4 1065 LINEARITY VERIFICATION SUMMARY

Verification Description	Intercept	Slope	SEE	r ²
CO NDIR (Initial Audit)				
Measured	0.00	1.00	0.00	1.00
Linearity Criteria	4.52	0.99-1.01	9.04	0.998
Pass / Fail	Pass	Pass	Pass	Pass
CO NDIR (Check 06-05-06)				
Measured	-1.36	1.00	3.16	1.00
Linearity Criteria	4.52	0.99-1.01	9.04	0.998
Pass / Fail	Pass	Pass	Pass	Pass
CO₂ NDIR (Initial Audit)				
Measured	-0.01	1.01	0.03	1.00
Linearity Criteria	0.07	0.99-1.01	0.15	0.998
Pass / Fail	Pass	Pass	Pass	Pass
CO₂ NDIR (Check 06-05-06)				
Measured	0.02	1.01	0.04	1.00
Linearity Criteria	0.07	0.99-1.01	0.15	0.998
Pass / Fail	Pass	Pass	Pass	Pass
HC FID (Initial Audit)				
Measured	-0.22	1.00	0.26	1.00
Linearity Criteria	2.21	0.99-1.01	4.43	0.998
Pass / Fail	Pass	Pass	Pass	Pass
HC FID (Check 06-05-06)				
Measured	-1.11	1.00	0.36	1.00
Linearity Criteria	2.21	0.99-1.01	4.43	0.998
Pass / Fail	Pass	Pass	Pass	Pass

Table 29 shows the PEMS 4 linearity check results for NO and NO₂. PEMS 4 also failed NO₂ linearity during the initial audit and June, 2006 checks. As with PEMS 3, Sensors elected to take no corrective action, and the Steering Committee elected to continue testing despite the audit failure. During Engine 2 testing, the NDUV was replaced due to measurement stability problems that eventually prevented proper zero and span operations. The new NDUV passed NO linearity, but failed NO₂ linearity. Shortly after installing the new NDUV, NO and NO₂ measurements again became noisy and erratic. The NDUV was replaced again by Sensors Inc., after which NO and NO₂ passed the linearity check.

TABLE 29. PEMS 4 1065 LINEARITY VERIFICATION SUMMARY CONTINUED

NO NDUV (Initial Audit)				
Measured	2.54	0.99	1.93	1.00
Linearity Criteria	4.42	0.99-1.01	8.84	0.998
Pass / Fail	Pass	Pass	Pass	Pass
NO NDUV (Check 06-05-06)				
Measured	0.61	1.00	2.70	1.00
Linearity Criteria	4.42	0.99-1.01	8.84	0.998
Pass / Fail	Pass	Pass	Pass	Pass
NO NDUV (New NDUV 09-14-06)				
Measured	0.36	1.00	2.81	1.00
Linearity Criteria	4.41	0.99-1.01	8.83	0.998
Pass / Fail	Pass	Pass	Pass	Pass
NO₂ NDUV (New NDUV 09-25-06)				
Measured	3.55	0.99	2.30	1.00
Linearity Criteria	4.41	0.99-1.01	8.83	0.998
Pass / Fail	Pass	Pass	Pass	Pass
NO₂ NDUV (Initial Audit)				
Measured	3.46	1.01	3.37	1.00
Linearity Criteria	1.42	0.99-1.01	2.83	0.998
Pass / Fail	Fail	Pass	Fail	Pass
NO₂ NDUV (Check 06-05-06)				
Measured	4.60	0.99	2.60	1.00
Linearity Criteria	1.29	0.99-1.01	2.58	0.998
Pass / Fail	Fail	Pass	Fail	Pass
NO₂ NDUV (New NDUV 09-14-06)				
Measured	-2.55	1.02	1.85	1.00
Linearity Criteria	1.29	0.99-1.01	2.58	0.998
Pass / Fail	Fail	Fail	Pass	Pass
NO₂ NDUV (New NDUV 09-25-06)				
Measured	0.16	1.00	1.12	1.00
Linearity Criteria	1.29	0.99-1.01	2.58	0.998
Pass / Fail	Pass	Pass	Pass	Pass

Shown in Table 30 are the linearity results for PEMS 5. No major repairs were performed on this unit during the program, subsequent to the initial audits. During the initial audit linearity checks, CO and CO₂ measurement were unstable, so valid readings could not be taken. The NDIR was replaced by Sensors Inc. PEMS 5 passed all linearity checks with the exception of NO. No action was taken to correct the NO linearity failure with PEMS 5, and the Steering Committee elected to continue testing with the unit. PEMS 5 was shipped to CE-CERT and used during the in-use validation testing. Upon return to SwRI, analyzer linearity was rechecked. Similar to the initial audit, NO failed the linearity check with high intercept. CO₂ also repeatedly failed the linearity test with low intercept. Despite the linearity check failures, PEMS 5 was used to perform the laboratory replay validation testing.

TABLE 30. PEMS 5 1065 LINEARITY VERIFICATION SUMMARY

Verification Description	Intercept	Slope	SEE	r ²
CO NDIR (Initial Audit with New NDIR 06-07-06)				
Measured	0.00	1.00	0.00	1.00
Linearity Criteria	4.52	0.99-1.01	9.04	0.998
Pass / Fail	Pass	Pass	Pass	Pass
CO NDIR (Returned from Ce-Cert 01-03-07)				
Measured	0.00	1.00	0.00	1.00
Linearity Criteria	4.52	0.99-1.01	9.04	0.998
Pass / Fail	Pass	Pass	Pass	Pass
CO₂ NDIR (Initial Audit with New NDIR 06-07-06)				
Measured	-0.06	1.01	0.05	1.00
Linearity Criteria	0.07	0.99-1.01	0.15	0.998
Pass / Fail	Pass	Pass	Pass	Pass
CO₂ NDIR (Returned from Ce-Cert 01-03-07)				
Measured	-0.11	1.01	0.06	1.00
Linearity Criteria	0.07	0.99-1.01	0.15	0.998
Pass / Fail	Fail	Pass	Pass	Pass
HC FID (Initial Audit 06-07-06)				
Measured	-0.41	1.00	0.53	1.00
Linearity Criteria	2.21	0.99-1.01	4.43	0.998
Pass / Fail	Pass	Pass	Pass	Pass
HC FID (Returned from Ce-Cert 01-03-07)				
Measured	-1.18	1.00	0.46	1.00
Linearity Criteria	2.21	0.99-1.01	4.43	0.998
Pass / Fail	Pass	Pass	Pass	Pass
NO NDUV (Initial Audit 06-07-06)				
Measured	6.65	0.99	2.50	1.00
Linearity Criteria	4.42	0.99-1.01	8.84	0.998
Pass / Fail	Fail	Pass	Pass	Pass
NO NDUV (Returned from Ce-Cert 01-03-07)				
Measured	5.00	1.00	2.63	1.00
Linearity Criteria	4.47	0.99-1.01	8.94	0.998
Pass / Fail	Fail	Pass	Pass	Pass
NO₂ NDUV (Initial Audit 06-07-06)				
Measured	0.35	1.01	0.96	1.00
Linearity Criteria	1.29	0.99-1.01	2.58	0.998
Pass / Fail	Pass	Pass	Pass	Pass
NO₂ NDUV (Returned from Ce-Cert 01-03-07)				
Measured	0.81	1.01	1.45	1.00
Linearity Criteria	1.23	0.99-1.01	2.45	0.998
Pass / Fail	Pass	Pass	Pass	Pass

Table 31 shows the summarized linearity results for PEMS 6. During the initial audit of this unit, PEMS 6 failed NO₂ linearity. As with other similar failures, no corrective action was taken by Sensors Inc., and the Steering Committee elected to proceed with testing using this unit. During Engine 3 steady-state testing, PEMS 6 NO_x measurements were biased low versus the laboratory measurements. To determine the cause of the bias, additional NO and NO₂ linearity checks were performed, with both NO and NO₂ passing the linearity tests. An addition linearity

check is also shown for the FID following a repair which was conducted following a failure during environmental baseline testing.

TABLE 31. PEMS 6 1065 LINEARITY VERIFICATION SUMMARY

Verification Description	Intercept	Slope	SEE	r ²
CO NDIR (Initial Audit 06-07-06)				
Measured	0.00	1.00	0.00	1.00
Linearity Criteria	4.52	0.99-1.01	9.04	0.998
Pass / Fail	Pass	Pass	Pass	Pass
CO₂ NDIR (Initial Audit 06-07-06)				
Measured	0.07	1.00	0.04	1.00
Linearity Criteria	0.07	0.99-1.01	0.15	0.998
Pass / Fail	Pass	Pass	Pass	Pass
HC FID (Initial Audit 06-07-06)				
Measured	-0.05	1.00	0.52	1.00
Linearity Criteria	2.21	0.99-1.01	4.43	0.998
Pass / Fail	Pass	Pass	Pass	Pass
HC FID (Repaired 08-14-06)				
Measured	-1.09	1.00	0.37	1.00
Linearity Criteria	2.21	0.99-1.01	4.43	0.998
Pass / Fail	Pass	Pass	Pass	Pass
NO NDUV (Initial Audit 06-07-06)				
Measured	1.15	1.00	1.23	1.00
Linearity Criteria	4.42	0.99-1.01	8.84	0.998
Pass / Fail	Pass	Pass	Pass	Pass
NO NDUV (Check 11-22-06)				
Measured	0.90	1.00	2.46	1.00
Linearity Criteria	4.47	0.99-1.01	8.94	0.998
Pass / Fail	Pass	Pass	Pass	Pass
NO₂ NDUV (Initial Audit 06-07-06)				
Measured	1.95	1.01	1.68	1.00
Linearity Criteria	1.29	0.99-1.01	2.58	0.998
Pass / Fail	Fail	Pass	Pass	Pass
NO₂ NDUV (Check 11-22-06)				
Measured	0.15	1.01	0.51	1.00
Linearity Criteria	1.29	0.99-1.01	2.58	0.998
Pass / Fail	Pass	Pass	Pass	Pass

Linearity results for PEMS 7 are shown in Table 32. PEMS 7 arrived at SwRI late in the project, and only initial audit results, performed in October of 2006, are shown for this unit. PEMS 7 passed the linearity checks with all analyzers. It was understood that PEMS 7 was a new unit that had been only recently received by EPA prior to shipment to SwRI.

TABLE 32. PEMS 7 1065 LINEARITY VERIFICATION SUMMARY

Verification Description	Intercept	Slope	SEE	r ²
CO NDIR (Initial Audit 10-21-06)				
Measured	0.00	1.00	0.00	1.00
Linearity Criteria	4.52	0.99-1.01	9.04	0.998
Pass / Fail	Pass	Pass	Pass	Pass
CO₂ NDIR (Initial Audit 10-21-06)				
Measured	0.02	1.00	0.05	1.00
Linearity Criteria	0.07	0.99-1.01	0.15	0.998
Pass / Fail	Pass	Pass	Pass	Pass
HC FID (Initial Audit 10-21-06)				
Measured	-0.30	1.00	0.56	1.00
Linearity Criteria	2.21	0.99-1.01	4.43	0.998
Pass / Fail	Pass	Pass	Pass	Pass
NO NDUV (Initial Audit 10-21-06)				
Measured	3.45	1.00	0.89	1.00
Linearity Criteria	4.41	0.99-1.01	8.83	0.998
Pass / Fail	Pass	Pass	Pass	Pass
NO₂ NDUV (Initial Audit 10-21-06)				
Measured	0.24	1.00	0.51	1.00
Linearity Criteria	1.29	0.99-1.01	2.58	0.998
Pass / Fail	Pass	Pass	Pass	Pass

Table 33 shows the linearity test results for the Horiba OBS-2200 PEMS unit. Mono-blend span gases were used to check linearity. The gas concentrations used for the check were 14.67 % CO₂, 904 ppm CO, 443 ppmC HC, and 892 ppm NO_x. The OBS-2200 passed the 1065 linearity criteria for all gaseous emissions.

TABLE 33. HORIBA OBS-2200 1065 LINEARITY VERIFICATION SUMMARY

Verification Description	Intercept	Slope	SEE	r ²
CO NDIR				
Measured	0.00	1.00	0.00	1.00
Linearity Criteria	4.52	0.99-1.01	9.04	0.998
Pass / Fail	Pass	Pass	Pass	Pass
CO₂ NDIR				
Measured	0.00	1.00	0.01	1.00
Linearity Criteria	0.07	0.99-1.01	0.15	0.998
Pass / Fail	Pass	Pass	Pass	Pass
HC FID				
Measured	0.05	1.00	0.49	1.00
Linearity Criteria	2.21	0.99-1.01	4.43	0.998
Pass / Fail	Pass	Pass	Pass	Pass
NO_x CLD				
Measured	-1.22	0.99	2.70	1.00
Linearity Criteria	4.49	0.99-1.01	8.98	0.998
Pass / Fail	Pass	Pass	Pass	Pass

3.4 1065 Gas Analyzer Verifications

The results of gas analyzer performance checks not related to linearity verifications are given in this section. In general, SwRI performed the analyzer audits as detailed in CFR Part 1065 Subpart D. A step-by-step description of each analyzer verification process as well as discussion of the test results are presented in the following sections. In summary, all laboratory instruments passed the verification tests. Similarly, the Horiba OBS-2200 PEMS unit passed all verifications tests. PEMS 2 and PEMS 4 failed the non-stoichiometric raw exhaust FID O₂ interference verifications. No corrective action was taken in regard to the FID O₂ interference test. All SEMTECH-DS PEMS units initially failed the chiller NO₂ penetration check. A system upgrade was implemented by Sensors Inc. after which all units passed the check. A detailed account of the chiller NO₂ penetration failure and subsequent actions are discussed in the chiller NO₂ penetration section. The PEMS units passed all other 1065 verification tests discussed below.

Generally, each of these verifications was performed once during the program, unless a major instrument repair warranted an additional check.. The major exception was the NO₂ chiller penetration check. The NO₂ penetration test was repeated after an upgrade designed to address the initial failure of all the PEMS, which is discussed in more detail below. The audit of PEMS 5, 6, and 7 occurred after the implementation of the NO₂ chiller penetration system upgrade, therefore a chiller penetration failure was not documented for these units.

Several 1065 analyzer verification tests required the use of humidified and blended gasses. SwRI therefore constructed a gas conditioning and blending cart, pictured in Figure 2, to perform the PEMS and laboratory audits. Consisting of a heated bubbler, two flow meters, an overflow system, a Vaisala dew point instrument, several thermocouples, heated rap, and various valves and stainless steel connections, the humidification rig can control the dew point of a gas blend up to 50 °C. The cart uses both a wet gas port and a dry gas port. Therefore, the cart can overflow dry gas, wet gas, or a blend of a wet gas and dry gas. The gas blending feature is useful when humidifying gases that are soluble in water, such as NO₂. Many of the performance checks involving humidified gases require that the gas be overflowed to the entry of the heated sample line of either the laboratory emission bench or PEMS unit. The overflow procedure was done to verify proper operation of sample handling and conditioning systems. Therefore, the cart was built with the capacity to overflow gas to as many as two emission benches and/or PEMS units, allowing for direct performance comparisons between units. This capability proved very useful in diagnosing problems throughout the program.

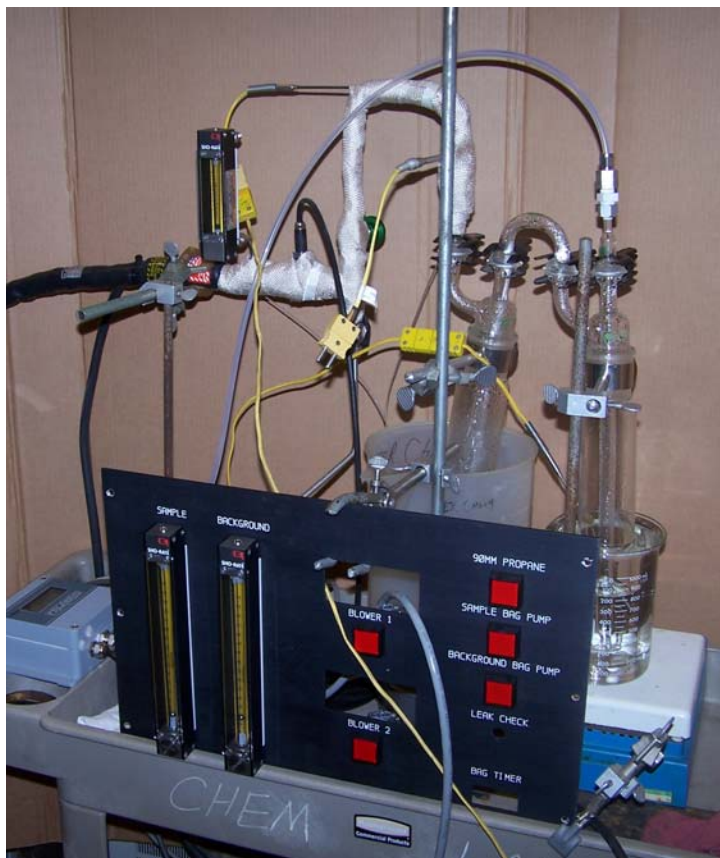


FIGURE 17. SWRI GAS HUMIDIFICATION AND BLENDING CART

The results of the various 1065 performance checks for the laboratory analyzer benches are summarize in Table 34 and Table 35. Results for the PEMS performance checks during the initial audits are given in Table 36 through Table 43.

TABLE 34. DILUTE MEXA 7200D AND HORIBA NMHC BENCH 1065 ANALYZER VERIFICATION SUMMARY

Verification Description	Meas.	Verification	P/F
1065.350 H ₂ O interference for CO ₂ NDIR [%]	0.00%	± 0.01%	Pass
1065.355 H ₂ O and CO ₂ interference for CO NDIR [ppm]	0.4	± 4.0	Pass
1065.360 FID optimization (methane response)	1.12	N/A	N/A
1065.370 CO ₂ and H ₂ O quench verification for NO _x CLD [%]	-0.21%	± 2.00%	Pass
1065.378 NO ₂ -to-NO converter conversion [%]	97.3%	> 95%	Pass
1065.365 Nonmethane cutter penetration fractions [%]	1.8%	< 2.0%	Pass

TABLE 35. RAW MEXA 7200D AND HORIBA NMHC BENCH 1065 ANALYZER VERIFICATION SUMMARY

Verification Description	Meas.	Verification	P/F
1065.350 H ₂ O interference for CO ₂ NDIR [%]	0.00%	± 0.07%	Pass
1065.355 H ₂ O and CO ₂ interference for CO NDIR [ppm]	1.4	± 48.7	Pass
1065.360 FID optimization (methane response)	1.15	N/A	N/A
1065.362 Non-stoichiometric FID O ₂ interference [%]	-0.7%	± 1.5%	Pass
1065.370 CO ₂ and H ₂ O quench verification for NO _x CLD [%]	-0.5%	± 2.0%	Pass
1065.378 NO ₂ -to-NO converter conversion [%]	96.7%	> 95%	Pass
1065.362 Non-stoichiometric CH ₄ FID O ₂ interference [%]	0.5%	± 1.5%	Pass
1065.365 Nonmethane cutter penetration fractions [%]	1.7%	< 2.0%	Pass

TABLE 36. PEMS 1 1065 ANALYZER VERIFICATION SUMMARY

Verification Description	Meas.	Verification	P/F
1065.350 H ₂ O interference for CO ₂ NDIR [%]	0.00%	± 0.07%	Pass
1065.355 H ₂ O and CO ₂ interference for CO NDIR [ppm]	21.8	± 48.7	Pass
1065.362 Non-stoichiometric FID O ₂ interference [%]	-0.8%	± 1.5%	Pass
1065.372 HC and H ₂ O interference for NO _x NDUV [ppm]	-0.6	± 4.0	Pass
1065.376 Chiller NO ₂ Penetration [%]	90.5%	> 95%	Fail
1065.376 Chiller NO ₂ Penetration [%] (Post Retrofit) (06-10-06)	100.7%	> 95%	Pass

TABLE 37. PEMS 2 1065 ANALYZER VERIFICATION SUMMARY

Verification Description	Meas.	Verification	P/F
1065.350 H ₂ O interference for CO ₂ NDIR [%]	0.00%	± 0.07%	Pass
1065.355 H ₂ O and CO ₂ interference for CO NDIR [ppm]	21.8	± 48.7	Pass
1065.362 Non-stoichiometric FID O ₂ interference [%]	4.2%	± 1.5%	Fail
1065.372 HC and H ₂ O interference for NO _x NDUV [ppm]	0.6	± 4.0	Pass
1065.376 Chiller NO ₂ Penetration [%]	89.0%	± 95%	Fail
1065.376 Chiller NO ₂ Penetration [%] (Post Retrofit) (06-10-06)	95.6%	> 95%	Pass

TABLE 38. PEMS 3 1065 ANALYZER VERIFICATION SUMMARY

Verification Description	Meas.	Verification	P/F
1065.350 H ₂ O interference for CO ₂ NDIR [%]	0.00%	± 0.07%	Pass
1065.355 H ₂ O and CO ₂ interference for CO NDIR [ppm]	10.9	± 48.7	Pass
1065.362 Non-stoichiometric FID O ₂ interference [%]	-0.1%	± 1.5%	Pass
1065.372 HC and H ₂ O interference for NO _x NDUV [ppm]	0.0	± 4.0	Pass
1065.376 Chiller NO ₂ Penetration [%]	90.1%	± 95%	Fail
1065.376 Chiller NO ₂ Penetration [%] (Post Retrofit) (06-10-06)	100.6%	> 95%	Pass

TABLE 39. PEMS 4 1065 ANALYZER VERIFICATION SUMMARY

Verification Description	Meas.	Verification	P/F
1065.350 H ₂ O interference for CO ₂ NDIR [%]	0.01%	± 0.07%	Pass
1065.355 H ₂ O and CO ₂ interference for CO NDIR [ppm]	21.8	± 48.7	Pass
1065.362 Non-stoichiometric FID O ₂ interference [%]	-0.5%	± 1.5%	Pass
1065.372 HC and H ₂ O interference for NO _x NDUV [ppm]	0.0	± 4.0	Pass
1065.376 Chiller NO ₂ Penetration [%]	89.4%	± 95%	Fail
1065.376 Chiller NO ₂ Penetration [%] (Post Retrofit) (06-10-06)	101.2%	> 95%	Pass
1065.376 Chiller NO ₂ Penetration [%] (New NDUV) (09-25-06)	100.0%	> 95%	Pass
1065.376 Chiller NO ₂ Penetration [%] (RH Sensor) (09-28-06)	98.1%	> 95%	Pass

TABLE 40. PEMS 5 1065 ANALYZER VERIFICATION SUMMARY

Verification Description	Meas.	Verification	P/F
1065.350 H ₂ O interference for CO ₂ NDIR [%]	0.00%	± 0.07%	Pass
1065.355 H ₂ O and CO ₂ interference for CO NDIR [ppm]	21.8	± 48.7	Pass
1065.362 Non-stoichiometric FID O ₂ interference [%]	-0.1%	± 1.5%	Pass
1065.372 HC and H ₂ O interference for NO _x NDUV [ppm]	0.0	± 4.0	Pass
1065.376 Chiller NO ₂ Penetration [%] (Post Retrofit) (06-10-06)	102.4%	> 95%	Pass

TABLE 41. PEMS 6 1065 ANALYZER VERIFICATION SUMMARY

Verification Description	Meas.	Verification	P/F
1065.350 H ₂ O interference for CO ₂ NDIR [%]	0.00%	± 0.07%	Pass
1065.355 H ₂ O and CO ₂ interference for CO NDIR [ppm]	27.3	± 48.7	Pass
1065.362 Non-stoichiometric FID O ₂ interference [%]	2.1%	± 1.5%	Fail
1065.372 HC and H ₂ O interference for NO _x NDUV [ppm]	0.0	± 4.0	Pass
1065.376 Chiller NO ₂ Penetration [%] (Post Retrofit) (06-10-06)	95.7%	> 95%	Pass
1065.376 Chiller NO ₂ Penetration [%] (RH Sensor) (9-15-06)	96.2%	> 95%	Pass
1065.376 Chiller NO ₂ Penetration [%] (RH Sensor) (9-21-06)	100.0%	> 95%	Pass
1065.376 Chiller NO ₂ Penetration [%] (RH Sensor) (9-28-06)	99.6%	> 95%	Pass
1065.376 Chiller NO ₂ Penetration [%] (Check) (11-27-06)	99.0%	> 95%	Pass

TABLE 42. PEMS 7 1065 ANALYZER VERIFICATION SUMMARY

Verification Description	Meas.	Verification	P/F
1065.350 H ₂ O interference for CO ₂ NDIR [%]	0.00%	± 0.07%	Pass
1065.355 H ₂ O and CO ₂ interference for CO NDIR [ppm]	11.0	± 48.7	Pass
1065.362 Non-stoichiometric FID O ₂ interference [%]	1.4%	± 1.5%	Pass
1065.372 HC and H ₂ O interference for NO _x NDUV [ppm]	1.6	± 4.0	Pass
1065.376 Chiller NO ₂ Penetration [%] (Post Retrofit) (10-24-06)	96.8%	> 95%	Pass

TABLE 43. HORIBA OBS-2200 1065 ANALYZER VERIFICATION SUMMARY

Verification Description	Meas.	Verification	P/F
1065.350 H ₂ O interference for CO ₂ NDIR [%]	0.05%	± 0.07%	Pass
1065.355 H ₂ O and CO ₂ interference for CO NDIR [ppm]	4.8	± 48.7	Pass
1065.362 Non-stoichiometric FID O ₂ interference [%]	-0.3%	± 1.5%	Pass
1065.370 CO ₂ and H ₂ O quench verification for NO _x CLD [%]	-1.4%	± 2.0%	Pass
1065.378 NO ₂ -to-NO converter conversion [%]	98.9%	± 95.0%	Pass

3.4.1 1065.350 H₂O Interference for CO₂ NDIR

The CO₂ NDIR water interference check was performed on each of the PEMS units as well as the laboratory dilute and raw analyzers. This check was performed to characterize CO₂ interference caused by water when using a NDIR analyzer. The PEMS and laboratory analyzers used sample dryers upstream of the NDIR analyzer and all passed this 1065 check.

To perform this verification, all analyzers were first zeroed and spanned as they would be prior to an emissions test. Using the humidification rig, humidified zero air was overflowed to the sample line of the analyzer. While maintaining the dew point of the zero air at 25 °C, the response of the CO₂ NDIR analyzer was recorded. This recorded value was compared to ±2 % of the lowest flow-weighted mean CO₂ concentration expected during testing. The raw verification value of ±0.07 % and dilute verification value of ±0.01 % were calculated using the Detroit Diesel Series 60 engine and FTP engine cycle. Using the lowest flow-weighted CO₂ concentration provided the most stringent test, therefore verifying the analyzer performance during all emissions tests.

3.4.2 1065.355 H₂O and CO₂ Interference for CO NDIR

The CO NDIR water and CO₂ interference check was performed on each of the PEMS units as well as the laboratory dilute and raw analyzers. This check was performed to characterize CO interference caused by water and CO₂ when using a NDIR analyzer. The PEMS and laboratory analyzers all passed this 1065 check.

To perform this verification, all analyzers were first zeroed and spanned as they would be prior to an emissions test. Using the humidification rig, humidified CO₂ span gas was overflowed to the sample line of the analyzer. While maintaining the dew point of the CO₂ span gas at 25 °C, the response of the CO NDIR analyzer was recorded. The recorded CO value was multiplied by the highest flow-weighted mean CO₂ concentration expected during testing, then divided by the CO₂ span gas concentration. For this check, the highest flow-weighted CO₂ concentration provided the most stringent test. The CO₂ value of 8 % was calculated using the Detroit Diesel Series 60 engine and RMC engine cycle. The corrected CO concentration was compared to ±2 % of the flow-weighted mean CO concentration expected at the standard. The raw CO verification value of 48.7 ppm and dilute verification value of 4 ppm were calculated using the DDC engine over a FTP heavy-duty transient cycle.

3.4.3 1065.360 FID Optimization Methane Response

The methane response factors were determined for the laboratory dilute and raw FID analyzers. The FID analyzers were first zeroed and spanned as they would be prior to an emissions test. Using a gas divider and methane span gas, the FID response to methane was characterized over 10 evenly distributed points from near zero to span concentration. The methane response factor was calculated by dividing the recorded FID response by the actual methane concentration. The mean value of the 10 methane response factors was calculated. A check was then performed to insure each of the 10 response factors was within ± 2 % of the mean.

3.4.4 1065.362 Non-stoichiometric Raw FID O₂ Interference

The O₂ raw FID interference check was performed on each of the PEMS units as well as the raw laboratory THC FID and raw laboratory NMHC FID analyzers. This check was performed to characterize O₂ interference when using a FID analyzer to measure raw exhaust from a non-stoichiometric engine. PEMS 2 and PEMS 4 failed this 1065 check.

The first step performed during this test was to zero and span the analyzers. The FID analyzers were then spanned using a propane span gas with balance nitrogen. Using a gas divider, the propane in nitrogen span gas was cut with 20 % oxygen and sampled with the FID analyzer. The FID response to the divided span gas was compared to the actual THC concentration. For all analyzers except PEMS 2 and PEMS 4, the measurement concentration was within 1.5 % of the actual concentration and therefore passed the interference check. By spanning the analyzer with propane in nitrogen, and checking the analyzer with 20 % oxygen, this verification insures the O₂ interference is acceptable during typical diesel engine operation.

Per the Steering Committee's decision, no action was taken to remedy the O₂ raw FID interference check failure of PEMS 2 and PEMS 4. The laboratory raw THC FID analyzer initially failed this check. After the FID was re-optimized, the instrument passed the verification test.

3.4.5 1065.365 Nonmethane Cutter Penetration Fractions

The nonmethane cutter (NMC) penetration verification was performed on the laboratory raw and dilute methane analyzer benches, each of which employed a NMC. Both systems passed the penetration check.

The instruments were spanned through the NMC using methane during testing and for this performance check, therefore the methane penetration fraction was set to 1.0. For the verification, the instruments were zeroed and spanned, after which ethane span gas was introduced to the bench. The concentration of ethane (in ppmC) was near the methane span value used during the check. The response of the NMC FID to ethane span gas was recorded. The recorded value was divided by the ethane span gas concentration on a ppmC basis. This fraction was less than 2 % and therefore passed the nonmethane cutter penetration check.

The dilute NMC bench initially failed the cutter penetration check. The temperature of the NMC cutter oven was increased until the bench passed the penetration verification test.

3.4.6 1065.370 CO₂ and H₂O Quench Verification for NO_x CLD

The NO_x CLD water and CO₂ quench check was performed on the laboratory raw and dilute analyzers. Both analyzers passed the quench check.

The CLD NO_x analyzers were first zeroed and spanned as they would be prior to an emissions test. The benches were then set to measure NO rather than total NO_x. The NO span gas was then sampled and the mean NO concentration was recorded. The NO span gas was then humidified and the mean dry NO concentration as well as the water content of the gas was recorded. The water quench was calculated by taking the difference between the dry and humidified span gas measurements and correcting this value using the actual water content of the span gas and the maximum water content expected during testing. The maximum water concentration expected during testing was set to 12 % for the raw analyzer and 3.5 % for the dilute analyzer. Because both raw and dilute CLD analyzers were operated in a dry mode during this program, both analyzers showed negligible water quench, indicating that the drying systems in the benches were able to successfully remove the water from the sample.

Using a gas divider, the CLD CO₂ quench was determined by measuring a blend of 50 % NO span gas and 50 % nitrogen. Next, 50 % NO span gas and 50 % CO₂ span gas was measured. The CO₂ quench was calculated by taking the difference between the 50 % nitrogen blend and the 50 % CO₂ span gas blend. The quench value was then corrected using the CO₂ concentration recorded during the test and the maximum CO₂ concentration expected during testing. The maximum CO₂ concentration expected during testing was set to 10 % for the raw analyzer and 2.2 % for the dilute analyzer. The combined water and CO₂ quench for both analyzers was less than 2 %, therefore passing the CLD quench verification test.

3.4.7 1065.372 HC and H₂O Interference for NO_x NDUV

The NO_x NDUV water and HC interference check was performed on each of the PEMS units. All PEMS devices passed this interference verification test.

The PEMS were first zeroed and spanned as they would be prior to an emissions test. Next, a blend of humidified zero air and dry propane span gas were overflowed to the sample line of the PEMS. The dew point of the gas mixture was maintained at 45 °C during these tests. Allowing time for stabilization, the NO, NO₂, and HC concentration values were recorded. The NO and NO₂ concentrations were added, and the resulting response was then adjusted to the level to the flow-weighted mean HC concentration expected at the standard. The mean HC concentration of 51 ppm was calculated using the DDC Series 60 engine over a FTP transient cycle. The verification concentration was calculated as ±2 % of the flow-weighted mean NO_x concentration expected at the standard. The mean NO_x concentration of 198 ppm was calculated using the DDC Series 60 engine over a FTP transient cycle. All PEMS showed little water and HC interference for the NO and NO₂ measurements, and easily passed the 1065 interference verification test.

3.4.8 1065.376 Chiller NO₂ Penetration

The SEMTECH-DS PEMS uses a chiller to dry the exhaust sample prior to the NDUV detector, but does not use a NO₂-to-NO converter. Therefore, the chiller NO₂ penetration check was performed. Initially, SwRI performed the chiller penetration check using a procedure similar to that performed by Sensors Inc. After the PEMS were zeroed and spanned, wet zero air with a dew point of approximately 50 °C was overflowed to the sample line and sampled for 15 to 20 minutes. Next, dry NO₂ span gas was overflowed to the sample line. Allowing time for stabilization, the NO₂ concentration was recorded and compared to the NO₂ span gas bottle concentration. The units initially read approximately 90 % of the NO₂ span concentration, and failed the verification criteria of 95 % penetration. Although this initial procedure was successful in revealing problems with NO₂ penetration, the method was less than ideal. For example, following the switch from humidified zero air to dry NO₂ span gas, the sampling system of the PEMS is continually drying. Although this drying process is slow, the NO₂ concentration does rise over time, making a stable measurement difficult to achieve.

As a result, a revised method was devised to perform the chiller NO₂ penetration check, required the use of the 1065 compliant laboratory CLD NO_x analyzer as a reference. Humidified zero air was blended with dry NO₂ span gas. The blend was adjusted to maintain a mixture dew point of approximately 45 °C with a NO₂ concentration near the span concentration. The humidified NO₂ mixture was then overflowed simultaneously to both the PEMS and the laboratory CLD NO_x analyzer. The CLD NO_x concentration was used as the reference in calculating the NO₂ penetration. It was felt that the CLD could serve as an appropriate reference value for this check, due to the fact that the laboratory CLDs did not show significant water quench (since they are run dry). In addition, the NO₂-to-NO conversion efficiency was in excess of 97% at concentrations well above those used for the chiller NO₂ penetration check.

This method more accurately simulates in-use measurement, because the sample is continuously humidified. The CLD-based penetration check method generated chiller penetration results similar to method used by Sensors Inc., but resulted in more stable and accurate values.

As discussed earlier, all of the PEMS failed the chiller NO₂ penetration check initially. Additional penetration checks were performed at varying concentrations of NO₂. These experiments revealed a trend of increasing NO₂ loss with increased NO₂ concentration. This trend is illustrated in Figure 18. It should be noted that the NO₂ span value used for testing was near 300 ppm.

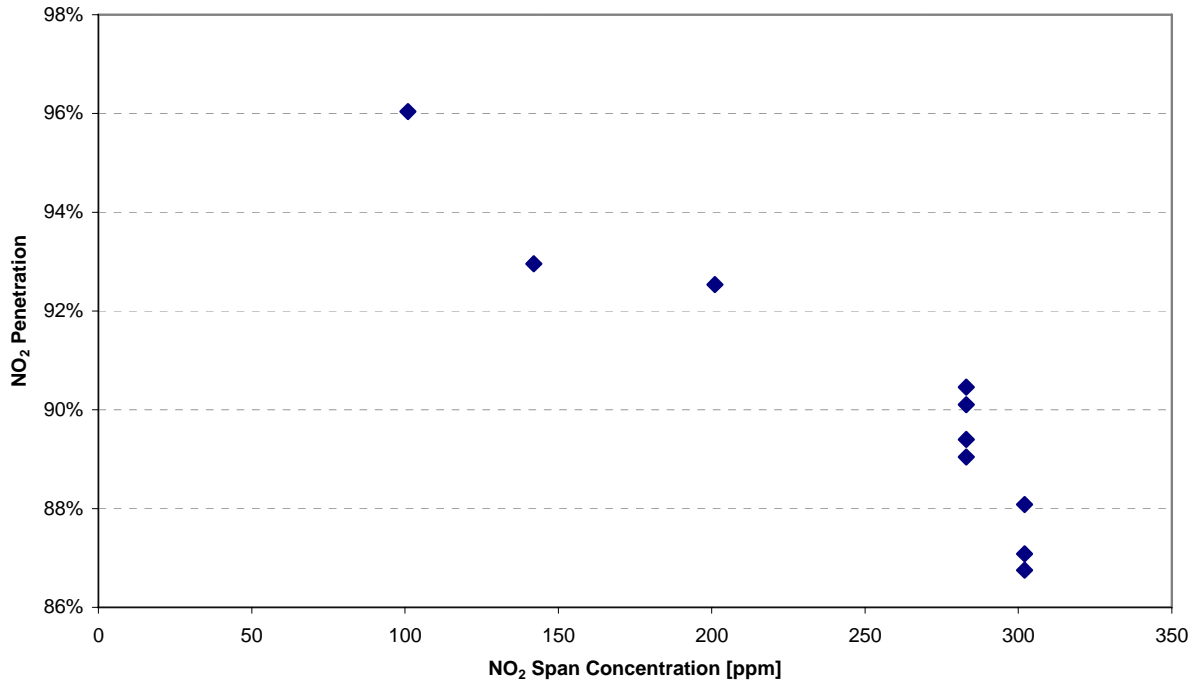


FIGURE 18. NO₂ CHILLER PENETRATION AUDIT RESULTS

These audit results were presented to the Steering Committee at the March 14th meeting in Ann Arbor, MI. Although there was concern about these results, the Steering Committee elected to run steady-state tests on Engine 1, to examine whether the performance check results would translate into an observed negative bias in the test results.

The initial steady-state results for Engine 1 were presented to the Steering Committee at the April 13, 2006 meeting in San Antonio. Figure 19 shows a summary the original steady-state NO_x concentration pooled delta data from the Detroit Diesel Series 60 engine. The data shows a definite negative NO_x bias for the PEMS at higher concentrations. This was due in part to the higher fraction of NO₂ in the overall NO_x which occur due to the use of a catalyzed DPF in the exhaust stream.

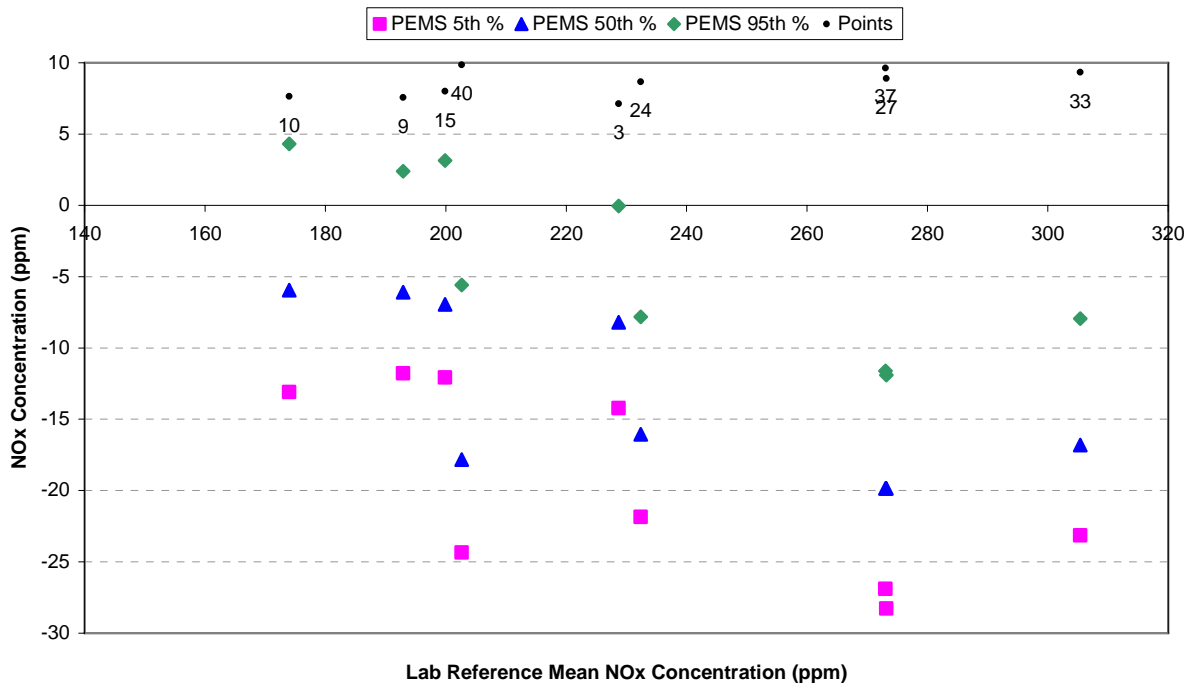


FIGURE 19. NO_x CONCENTRATION POOLED DELTA DATA FROM ENGINE 1 STEADY-STATE REPEAT TESTING PRIOR TO CHILLER NO₂ PENETRATION RETROFIT INSTALLATION

The Steering Committee deemed the low NO_x bias unacceptable for continued testing. Sensors Inc. was asked to develop an upgrade to correct the issue in as timely a manner as possible. However, it was also stipulated that the upgrade had to be acceptable as a real-world solution, and that the upgrade could be applied to all existing SEMTECH DS units.

Following the direction of the Steering Committee, Sensors Inc. developed a system upgrade to estimate the chiller NO₂ loss and numerically correct the NO₂ measurement. Upgrades were completed on all PEMS used during the measurement allowance program by the end of May, 2006. The upgrade package includes a drain manifold relative humidity sensor and software upgrade. After Sensors Inc. implemented the upgrade for the SEMTECH-DS, all units passed the NO₂ penetration check. Details of the upgrade are not included in this report for reasons of confidentiality.

After implementation of the NO₂ chiller penetration system upgrade, the Steering Committee elected to repeat the steady-state testing for Engine 1. While these results are summarized later in greater detail, a summary is given in Figure 20 to illustrate the effect of the upgrade on the data. The figure shows the pooled NO_x delta data with upgraded SEMTECH-DS units. The negative bias of the original data set was replaced with pooled errors showing a slight positive bias.

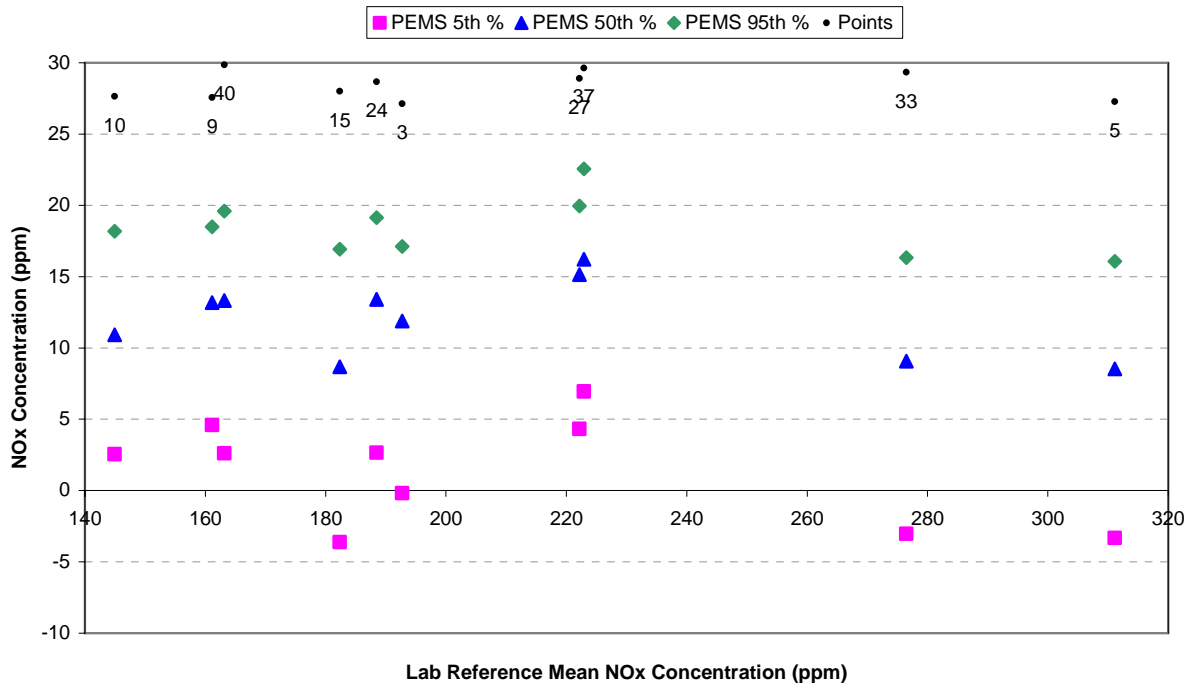


FIGURE 20. NO_x CONCENTRATION POOLED DELTA DATA FROM ENGINE 1 STEADY-STATE REPEAT TESTING AFTER CHILLER NO₂ PENETRATION RETROFIT INSTALLATION

The NO₂ penetration check failure and subsequent PEMS upgrade resulted in a schedule delay of more than two months in the execution of the program.

During dynamometer testing on Engine 2, PEMS 4 and PEMS 6 began reporting several faults stating the drain manifold relative humidity sensor was not responding. To remedy this problem, several drain manifold humidity sensors were replaced, after which the NO₂ penetration check was repeated. Sensors Inc. linked the frequent failure of the drain relative humidity sensors to drain manifolds that were allowing exhaust gas to leak past the sensor. The leaking exhaust gas carried liquid water past and onto the humidity sensors, causing the sensors to fail. A simple leak check was used to screen for properly sealed new RH sensors, which were installed in the PEMS. The PEMS passed all penetration checks after the new sensors and drain manifolds were installed.

3.4.9 1065.378 NO₂-to-NO Converter Conversion

The NO₂-to-NO converter conversion verification was performed on the laboratory raw and dilute benches. This check was performed using the automated Horiba bench software and Horiba GDC-703 gas divider, which is also capable of performing the NO_x converter check. Both raw and dilute NO₂-to-NO converters had conversion efficiencies greater than 95 %, and therefore passed this verification test.

3.5 1065 Exhaust Flow Meter Linearity Verification

The Sensors Inc. electronic flow meters (EFM) and Horiba flow meter were checked for flow linearity using a flow calibration stand at SwRI. This flow stand incorporates a set of reference laminar flow elements (LFEs), which are regularly sent for verification of NIST traceability at CEESI. The SwRI flow stand is pictured in Figure 21. The flow stand uses a positive displacement blower to pull air through the stand, therefore, the reference LFE and EFM are under a slight negative pressure during testing. The reference meters are downstream of the meter that is being calibrated. In the case of the Sensors Inc. EFMs, a length of straight pipe matching the diameter of the EFM was installed upstream of the EFM. The flow stand incorporates long lengths of straight pipe, well in excess of 10 diameters, between the two flow meters, as well as downstream of the reference meter. The stand is designed in this manner because most calibrations at SwRI focus on intake air measurement. Several manually controlled flow restriction devices, located far downstream of the reference meter, are used to set the desired flow rates during the linearity check. High precision mercury manometers are read manually to record the LFE differential and inlet pressure, while a thermocouple is used to measure the LFE inlet temperature.

The SwRI flow stand was also used to calibrate the intake air LFEs used to calculate the laboratory reference raw exhaust flow. The raw exhaust flow rate was also checked during testing by calculating a carbon balance fuel flow, using raw gaseous measurements and the raw exhaust mass rate, and comparing to the measured fuel flow mass rate. During all steady-state testing, the raw carbon balance error was generally less than 2 %.



FIGURE 21. SWRI LFE FLOW STAND MANOMETERS AND REFERENCE LFES

Sensors Inc. uses a similar LFE-based flow stand to calibrate their electronic flow meters. However, the Sensors flow stand uses a blower to push air through the reference flow meter and then through the test flow meter which is located downstream and is then vented directly to atmosphere. Therefore, the flow meters calibrated at Sensors. are under slight positive pressure. According to Sensors, the stand was designed in order to accurately simulate field conditions of an exhaust tailpipe. This discrepancy between the SwRI and Sensors Inc. flow stands may have been a factor contributing to increased exhaust flow errors during steady-state testing on Engines 2 and 3, which used the 4-inch and 3-inch flow meters respectively. However, this could not be verified, and the issue did not manifest itself with the 5-inch flow meters.

At SwRI, the Sensors Inc. and Horiba flow meters were mounted inline with the reference LFE as shown in Figure 22. A straight pipe, with length exceeding 10 diameters, was connected to the inlet of the flow meters. The EFM flow was recorded using the Sensors Inc. software. Data markers with the Sensors Inc. post processor software were used to average at least 30 seconds of data at each flow rate.

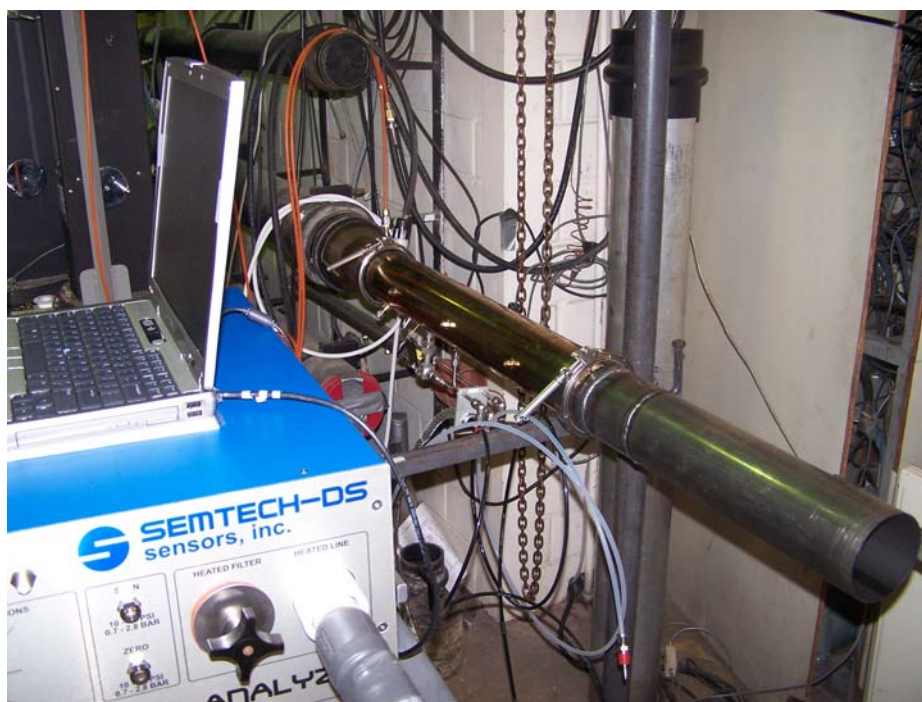


FIGURE 22. SENSORS INC. EFM MOUNTED ON THE SWRI LFE FLOW STAND

The collected flow data was processed using the 1065 linearity verifications for a raw exhaust measurement system. The sections below describe the calibration events and linearity results for the 5-inch, 4-inch, and 3-inch flow meters.

3.5.1 Five-Inch Exhaust Flow Meter Linearity

As shown in Table 44, two 5-inch Sensors Inc. flow meters passed the linearity check, while one 5-inch flow meter repeatedly failed the check. Per the Steering Committee's decision, the failed 5-inch EFM was sent to Sensors Inc. where it was recalibrated using the Sensors Inc.

flow stand. The 5-inch flow meter was then tested at SwRI where it passed the 1065 linearity check. These results appeared to indicate good agreement between the SwRI and Sensors flow stands.

TABLE 44. 5-INCH SENSORS INC. EFM LINEARITY RESULTS

Verification Description	Intercept	Slope	SEE	r ²
H05-SE05 - Initial, Test 1				
Measured	5.07	0.96	1.93	1.00
Linearity Criteria	9.42	0.98-1.02	18.85	0.99
Pass / Fail	Pass	Fail	Pass	Pass
H05-SE05 - Initial, Test 2				
Measured	6.45	0.96	4.08	1.00
Linearity Criteria	9.61	0.98-1.02	19.22	0.99
Pass / Fail	Pass	Fail	Pass	Pass
H05-SE03 - Initial				
Measured	1.60	1.00	4.50	1.00
Linearity Criteria	9.54	0.98-1.02	19.09	0.99
Pass / Fail	Pass	Pass	Pass	Pass
I05-SE05 - Initial				
Measured	4.93	1.01	4.87	1.00
Linearity Criteria	9.44	0.98-1.02	18.87	0.99
Pass / Fail	Pass	Pass	Pass	Pass
H05-SE05 - Test 1 After Recalibration at Sensors				
Measured	-1.69	1.01	1.60	1.00
Linearity Criteria	9.28	0.98-1.02	18.57	0.99
Pass / Fail	Pass	Pass	Pass	Pass

Table 45 shows the linearity results for the 5-inch Horiba exhaust flow meter. The Horiba meter, also based on pitot tube technology, showed excellent correlation with the SwRI flow stand; easily passing the 1065 linearity criteria.

TABLE 45. 5-INCH HORIBA EXHAUST FLOW METER LINEARITY RESULTS

Verification Description	Intercept	Slope	SEE	r ²
Horiba 5-Inch Exhaust Flow Meter S/N: 050702G2				
Measured	0.81	1.00	6.45	1.00
Linearity Criteria	9.58	0.98-1.02	19.17	0.99
Pass / Fail	Pass	Pass	Pass	Pass

Figure 23 shows the pooled delta data for the Sensors Inc. 5-inch flow meters versus the laboratory calculated exhaust flow for the Detroit Diesel Series 60 engine during steady-state repeat testing. Reporting median flow measurement deltas less than 2 % of point, the 5-inch flow meters showed good agreement with the laboratory exhaust flow measurement. The Sensors Inc. 5-inch EFM is rated at flows as high as 1700 scfm, therefore we were testing the meter only in its mid to lower range.

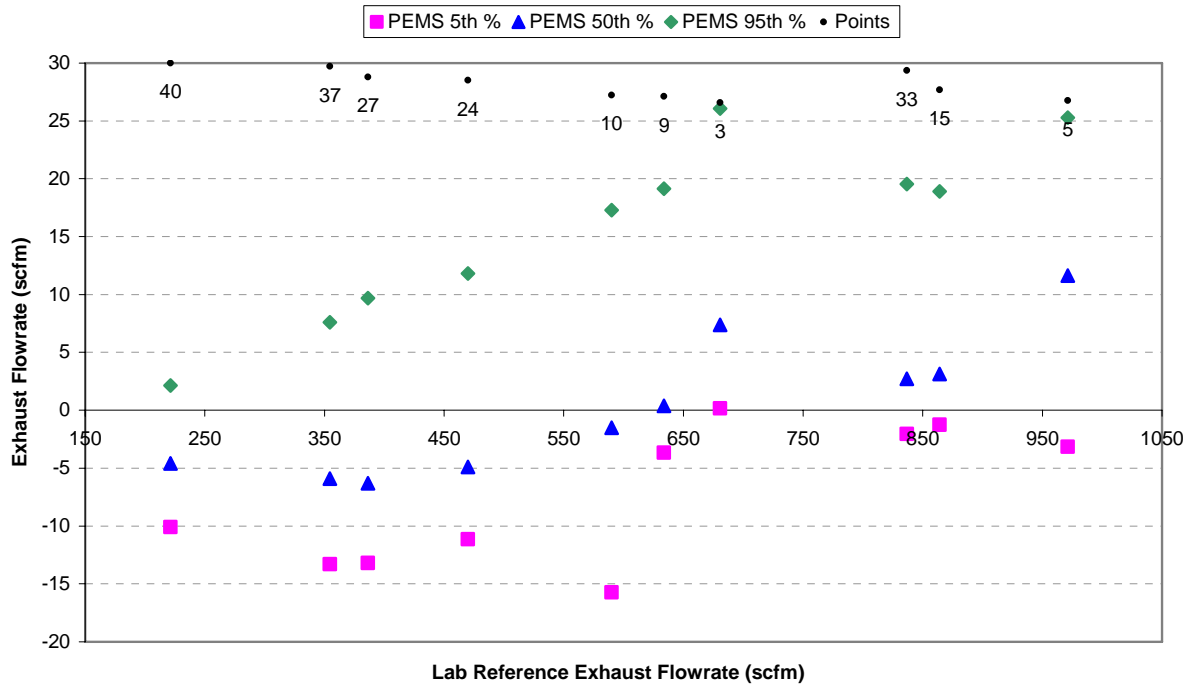


FIGURE 23. 5-INCH SENSORS EFM EXHAUST FLOW POOLED DELTA DATA FROM ENGINE 1 STEADY-STATE REPEAT TESTING

Because the Horiba OBS-2200 was delivered to SwRI late in the program, it was tested only with Engine 3. Per the recommendation of Horiba, the 5-inch flow meter was used during testing with the International VT365 engine. Figure 24 shows pooled delta data for the Horiba 5-inch flow meter versus the laboratory calculated exhaust flow during steady-state repeat testing. The Horiba flow meter showed good correlation with the SwRI calculated exhaust flows, with median deltas less than 0.5 % of point.

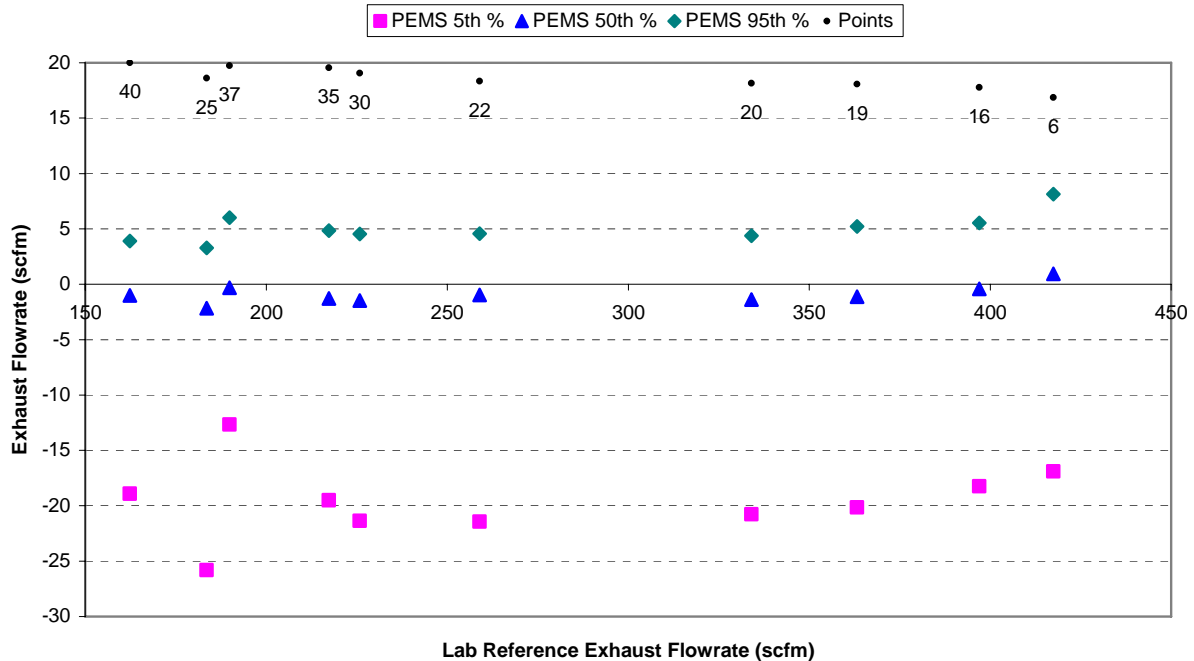


FIGURE 24. 5-INCH HORIBA EXHAUST FLOW METER POOLED DELTA DATA FROM ENGINE 3 STEADY-STATE REPEAT TESTING

3.5.2 Four-Inch Exhaust Flow Meter Linearity

Table 46 shows the linearity test results for the 4-inch flow meters in chronological order. During the initial 1065 linearity checks, all of the 4-inch flow meters failed the verification criteria with low slope values for the regression lines, with an averaging regression line slope of 0.94. As a result, the 4-inch flow meters were sent to Sensors Inc. for recalibration. After recalibration at Sensors Inc., one 4-inch flow meter, serial number H05-SE07, was returned to SwRI to re-check linearity. The flow meter again failed the linearity check with low slope, at roughly 0.97 on average. SwRI and Sensors performed a considerable number of diagnostic tests and checks in an attempt to determine the cause of the apparent discrepancy between the two flow stands. All tests with the SwRI LFE flow stand failed the linearity check with low slope.

An attempt was made to check linearity in actual engine exhaust from Engine 1 (14L DDC Series 60), using the SwRI exhaust flow measurement (from the sum of intake air and fuel flows) as the reference. It should be noted that the 4-inch flow meter was smaller than those normally used for this engine. The engine check failed linearity, but with a high slope. However, this was due in part to large negative errors at the low end of the flow range, which caused the intercept to also fail by a wide margin.

The collection of 4-inch flow meter data was presented to the Steering Committee at the July 27, 2006 meeting in Ann Arbor. The decision was made to recalibrate the 4-inch flow meters using the SwRI flow stand data. SwRI ran 15-point curves as requested by Sensors Inc.

Using the SwRI data, Sensors Inc. supplied new calibration constants for the meters. As expected, all 4-inch flow meters passed the 1065 linearity checks after they were calibrated and checked using the SwRI flow stand.

TABLE 46. 4-INCH SENSORS INC. EFM LINEARITY RESULTS

Verification Description	Intercept	Slope	SEE	r ²
H05-SE07 - Initial, Test 1				
Measured	7.28	0.95	5.99	1.00
Linearity Criteria	9.25	0.98-1.02	18.51	0.99
Pass / Fail	Pass	Fail	Pass	Pass
H05-SE07 - Initial, Test 2				
Measured	8.77	0.95	6.93	1.00
Linearity Criteria	9.18	0.98-1.02	18.36	0.99
Pass / Fail	Pass	Fail	Pass	Pass
I05-SE03 - Initial, Test 1				
Measured	4.09	0.98	6.49	1.00
Linearity Criteria	9.30	0.98-1.02	18.60	0.99
Pass / Fail	Pass	Fail	Pass	Pass
I05-SE03 - Initial, Test 2				
Measured	3.06	0.96	6.61	1.00
Linearity Criteria	9.24	0.98-1.02	18.49	0.99
Pass / Fail	Pass	Fail	Pass	Pass
I05-SE01 - Initial, Test 1				
Measured	21.47	0.92	14.56	1.00
Linearity Criteria	9.26	0.98-1.02	18.52	0.99
Pass / Fail	Fail	Fail	Pass	Pass
H05-SE07 - Test 1 After Recalibration at Sensors				
Measured	-8.11	0.98	6.42	1.00
Linearity Criteria	7.31	0.98-1.02	14.61	0.99
Pass / Fail	Fail	Fail	Pass	Pass
H05-SE07 - Test 3 After Recalibration (check on DDC Series 60 in exhaust)				
Measured	-25.74	1.03	7.26	1.00
Linearity Criteria	10.26	0.98-1.02	20.52	0.99
Pass / Fail	Fail	Fail	Pass	Pass
H05-SE07 - Test 4 After Recalibration (15-point calibration data generation)				
Measured	1.60	0.96	5.28	1.00
Linearity Criteria	7.69	0.98-1.02	15.39	0.99
Pass / Fail	Pass	Fail	Pass	Pass
H05-SE07 - Test 5 (EFM calibrated using SwRI data)				
Measured	1.87	1.00	11.70	1.00
Linearity Criteria	7.32	0.98-1.02	14.65	0.99
Pass / Fail	Pass	Pass	Pass	Pass
I05-SE03 - EFM calibrated using SwRI data				
Measured	-3.93	1.00	6.40	1.00
Linearity Criteria	7.43	0.98-1.02	14.87	0.99
Pass / Fail	Pass	Pass	Pass	Pass
I05-SE01 - EFM calibrated using SwRI data				
Measured	-3.93	1.00	6.40	1.00
Linearity Criteria	7.43	0.98-1.02	14.87	0.99
Pass / Fail	Pass	Pass	Pass	Pass

Figure 25 shows the pooled delta data for the Sensors Inc. 4-inch flow meters versus the laboratory calculated exhaust flow for the Caterpillar C9 engine during steady-state repeat testing. The 4-inch flow meter showed a trend of increasing error as exhaust flow rate increased. The median flow rate delta was near 5 % of point at the highest measured flow. Because Sensors Inc. effectively increased the slope of their EFMs when calibrating to the SwRI flow stand data, the observed engine deltas would likely have been smaller had the flow meters used the original Sensors Inc. calibration. As discussed earlier, the differences in the calibrations between Sensors Inc. and SwRI may be linked to the different designs of the two flow stands; however, the final reason for the discrepancies is not know at this time. The Sensors Inc. 4-inch EFM is rated at flows as high as 1100 scfm, therefore SwRI tested the meter over a broad range relative to the maximum flow rate.

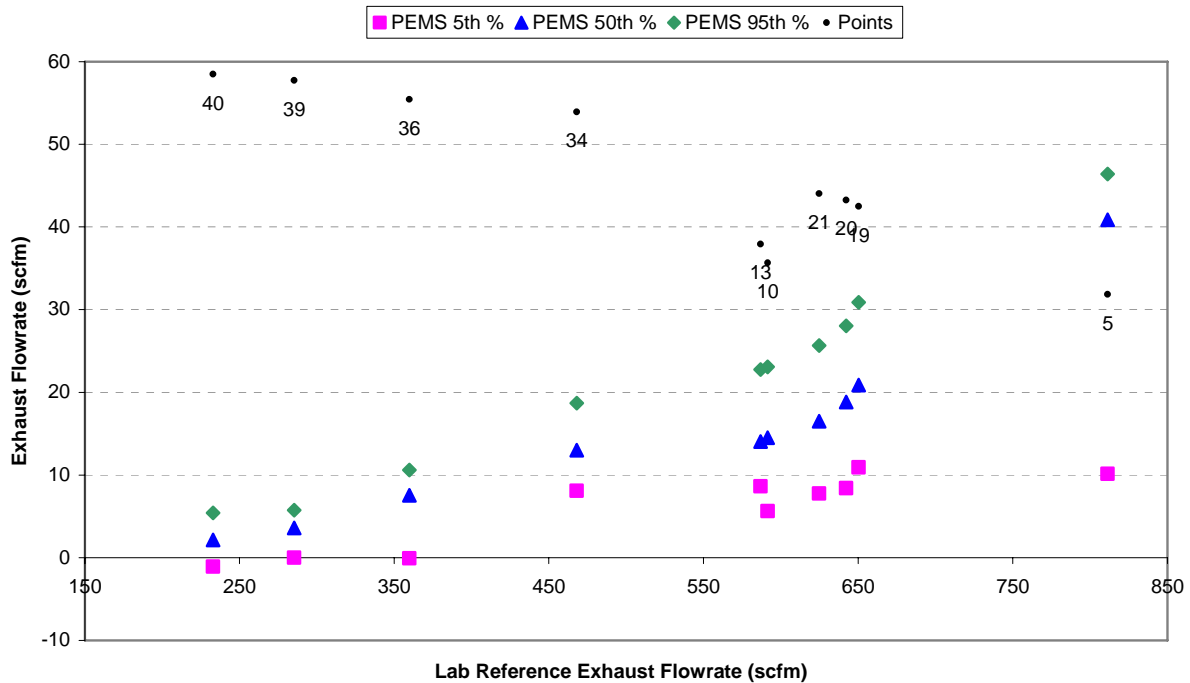


FIGURE 25. 4-INCH EFM EXHAUST FLOW POOLED DELTA DATA FROM ENGINE 2 STEADY-STATE REPEAT TESTING

3.5.3 Three-Inch Exhaust Flow Meter Linearity

The Sensors Inc. 3-inch EFM is rated at flows as high as 600 scfm, and was used on Engine 3 during the program. On an initial set of linearity checks performed in January, 2006, all of the 3-inch flow meters failed with positive slopes of 1.04 on average. The 3-inch flow meters were all returned to Sensors Inc. for recalibration. When returned to SwRI, the 3-inch EFMs failed linearity with a low slope of 0.96 on average. Table 47 summarizes the 3-inch EFM linearity data in chronological order. One 3-inch flow meter, serial number H05-SE06, was replaced by Sensors Inc. due to its outlying, low slope. Based on experiences with the 4-inch flow meters, the Steering Committee elected to recalibrate the 3-inch flow meters using data generated at SwRI. The 3-inch flow meters passed the linearity check after recalibration at SwRI. The resulting calibration increased the slope of each regression line by 4 to 5 percent. It

should be noted that the final linearity checks indicated a slight positive bias of roughly 1 percent on average, with one of the flow meters nearly failing linearity with a high slope.

TABLE 47. 3-INCH SENSORS INC. EFM LINEARITY RESULTS

Verification Description	Intercept	Slope	SEE	r ²
H05-SE04 - Initial Test 1 (Jan, 2006)				
Measured	-12.54	1.04	8.68	1.00
Linearity Criteria	5.91	0.98-1.02	11.82	0.99
Pass / Fail	Fail	Fail	Pass	Pass
H05-SE04 - Initial Test 2 (with Straight Pipe)				
Measured	-11.89	1.03	5.88	1.00
Linearity Criteria	4.73	0.98-1.02	9.47	0.99
Pass / Fail	Fail	Fail	Pass	Pass
H05-SE04 - Initial 15-point w/ Straight Pipe (Jan, 2006)				
Measured	-17.86	1.05	14.55	1.00
Linearity Criteria	6.49	0.98-1.02	12.99	0.99
Pass / Fail	Fail	Fail	Fail	Pass
H05-SE04 - Test 1 After Recalibration				
Measured	1.67	0.95	8.10	1.00
Linearity Criteria	6.37	0.98-1.02	12.74	0.99
Pass / Fail	Pass	Fail	Pass	Pass
H05-SE06 - Test 1 After Recalibration (EFM was replaced due to low slope)				
Measured	4.01	0.90	4.23	1.00
Linearity Criteria	6.77	0.98-1.02	13.54	0.99
Pass / Fail	Pass	Fail	Pass	Pass
I05-SE06 - Test 1 After Recalibration				
Measured	1.90	0.97	7.09	1.00
Linearity Criteria	6.27	0.98-1.02	12.54	0.99
Pass / Fail	Pass	Fail	Pass	Pass
H05-SE04 - EFM calibrated using SwRI data				
Measured	3.23	1.02	5.99	1.00
Linearity Criteria	5.97	0.98-1.02	11.93	0.99
Pass / Fail	Pass	Pass	Pass	Pass
I05-SE06 - EFM calibrated using SwRI data				
Measured	4.93	1.01	4.87	1.00
Linearity Criteria	9.44	0.98-1.02	18.87	0.99
Pass / Fail	Pass	Pass	Pass	Pass
I06-SE04 - EFM calibrated using SwRI data				
Measured	4.89	1.00	6.43	1.00
Linearity Criteria	6.01	0.98-1.02	12.02	0.99
Pass / Fail	Pass	Pass	Pass	Pass

Figure 26 shows the pooled delta data for the Sensors Inc. 3-inch flow meters versus the laboratory calculated exhaust flow for the International VT365 engine during steady-state repeat testing. The median flow rate delta for the 3-inch flow meters showed a nearly constant positive bias of approximately 10 % of point. The engine exhaust flow deltas would likely have been smaller had the 3-inch EFMs not been recalibrated using the SwRI LFE flow stand data. However, the recalibration only resulted in an adjustment on the order of 4 % of point, which was not large enough to explain the 10 % positive bias observed in the engine results. Because

the initial linearity check data on the SwRI flow stand indicated a positive bias, it is not clear what the final source(s) of the positive measurement bias are.

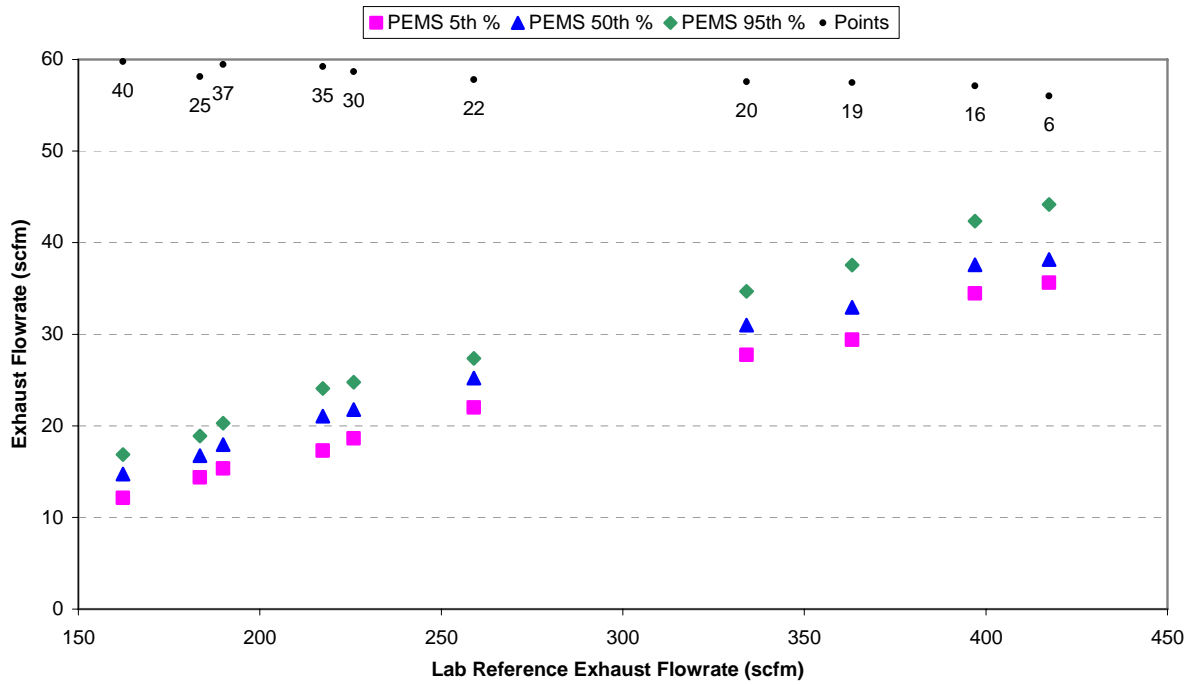


FIGURE 26. 3-INCH EFM EXHAUST FLOW POOLED DELTA DATA FROM ENGINE 3 STEADY-STATE REPEAT TESTING

4.0 ENGINE DYNAMOMETER LABORATORY TESTING

4.1 Engine Testing Objectives

Engine testing was performed to characterize bias and precision errors for the SEMTECH-DS instruments versus lab grade emission measurement equipment. Analyzer and exhaust flow rate measurements were compared over both steady-state and transient engine operation. Several engine laboratory tests were designed to evaluate errors associated with ECM-broadcast channels and subsequent interpolation errors of torque and BSFC. Finally, tests were conducted to assess the exhaust flow measurement errors due to installation related factors.

4.2 Test Engines and Dynamometer Laboratory

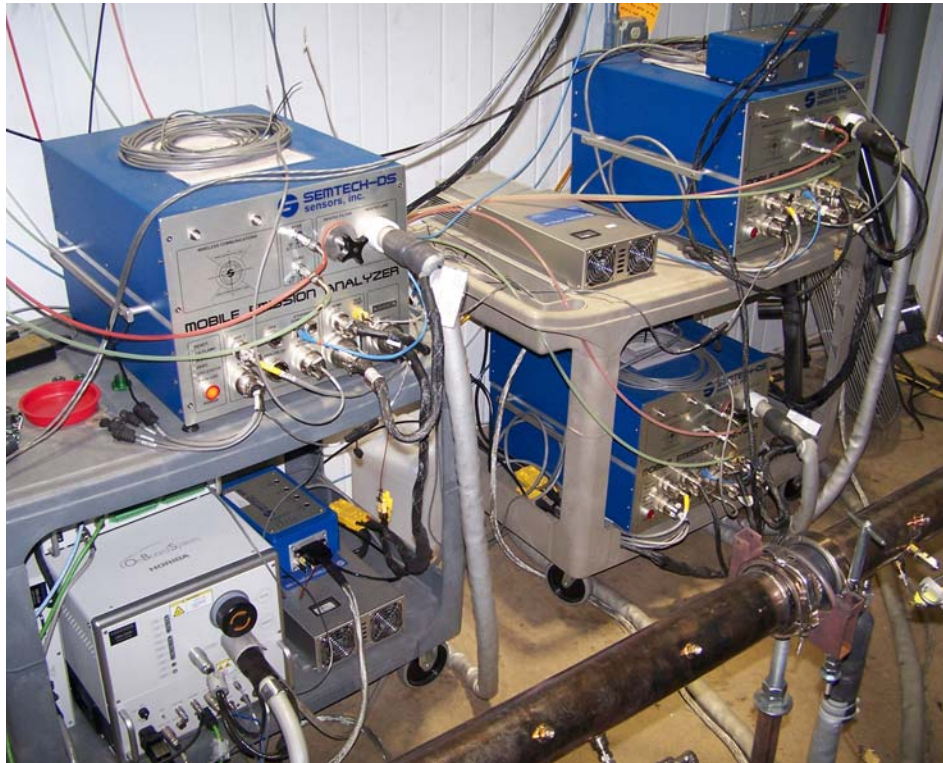


FIGURE 27 PEMS INSTRUMENTATION SETUP IN DYNAMOMETER TEST CELL



FIGURE 28 ENGINE 1 (HHD) - 14L DDC SERIES 60



FIGURE 29 ENGINE 2 (MHD) - CATERPILLAR C9



FIGURE 30 ENGINE 3 (LHD) - INTERNATIONAL VT 365



FIGURE 31 TEST CELL EXHAUST SYSTEM SHOWING PEMS FLOWMETERS AND SAMPLING POINTS

4.3 40-Point Torque and BSFC Map Generation and Error Surface

An initial task specified in the Test Plan was to generate 40-point torque and BSFC maps as well as preview laboratory and PEMS emission and flow data. The torque and BSFC maps were generated for a variety of reasons. First, the 40-point maps served as the data set used to create interpolation surfaces for the estimation of ECM Torque and ECM BSFC from ECM broadcast (CAN) speed and fuel rate signals. Second, the preview of the emission results from these points was used to aid in down-selection of the 10 test points to be used in subsequent steady-state error surface experiments. Finally, the preview data was used to determine whether multiple PEMS units could be run in parallel on a given engine during steady-state experiments, thus shortening the amount of time required for the steady-state testing.

The 40-points were chosen by the Steering Committee during the planning portions of the program, and were designed to cover the entire NTE zone as evenly as possible. Several points

were positioned slightly beyond the NTE boundary to aid in interpolation near the edges of the NTE zone.

After verifying the engines and aftertreatment systems were functioning properly, the lug curves of the engine were mapped according to the procedures in CFR Part 1065 Subpart F. An Excel spreadsheet provided by EPA, and approved by the Steering Committee, was used with the map data to generate the 40 points within the NTE zone. The lug curves and 40 NTE points are shown in Figure 32 through Figure 34 for Engine 1, Engine 2, and Engine 3, respectively. Using the laboratory raw and dilute sampling systems, as well as the PEMS, each of the 40 points was tested over 10-minute modes. The initially planned mode length was 3 minutes; however, the mode length was extended to 10 minutes following initial Engine 1 testing to insure the fuel flow measurement was stable.

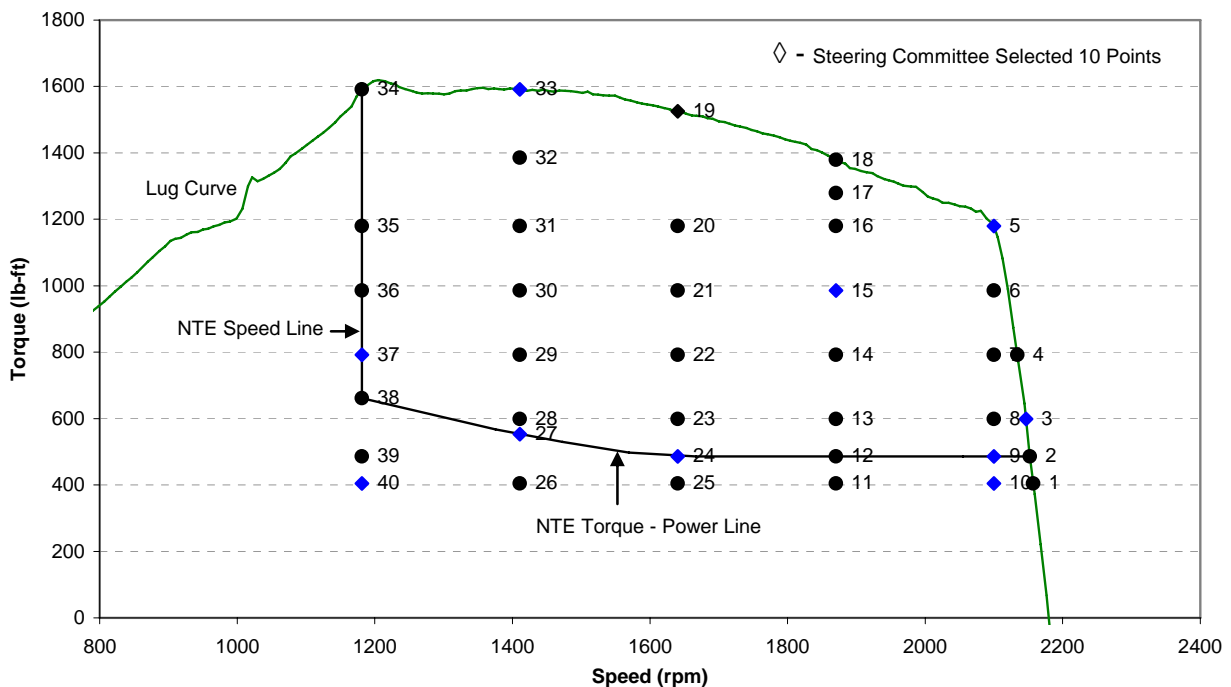


FIGURE 32. ENGINE 1 - DETROIT DIESEL SERIES 60 LUG CURVE AND 40-POINT MAP

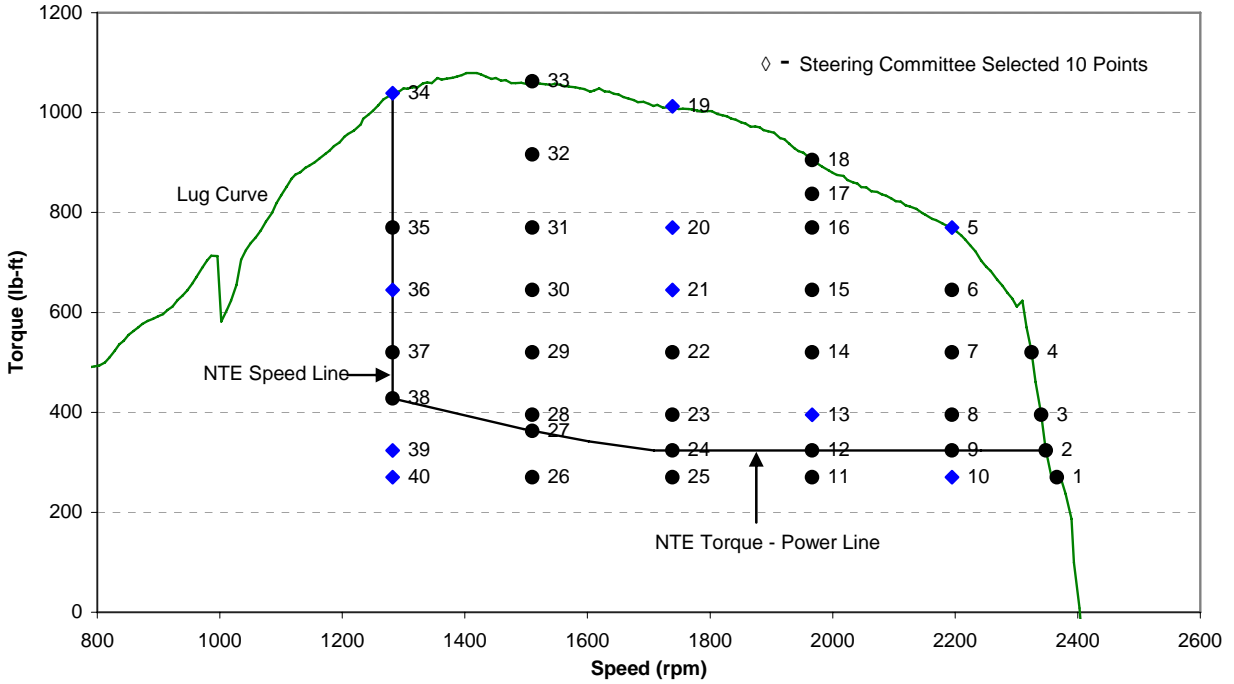


FIGURE 33. ENGINE 2 - CATERPILLAR C9 LUG CURVE AND 40-POINT MAP

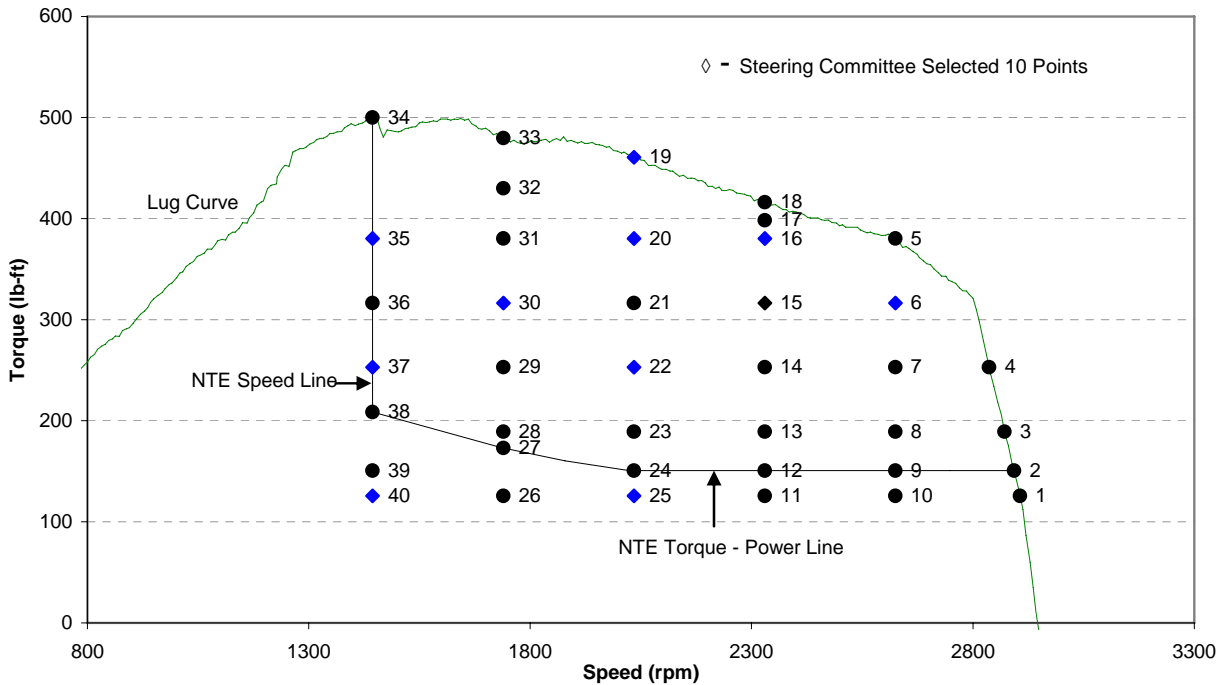


FIGURE 34. ENGINE 3 - INTERNATIONAL VT365 LUG CURVE AND 40-POINT MAP

The 40-point torque and BSFC interpolation surfaces were based on the laboratory torque measurement and the laboratory BSFC calculation from the laboratory measured fuel rate and

measured engine power. The laboratory torque and BSFC measurements were referenced to the ECM-broadcast (CAN) speed and fuel rates for each mode. Using these maps, torque and BSFC values were interpolated based off of ECM-broadcast channels. A triangular plane interpolation routine was developed by SwRI statisticians to aid in the interpolation process. The 40-point interpolation maps were used throughout dynamometer engine testing to produce ECM interpolated torque and BSFC values for comparison with the laboratory measured reference values. The torque and BSFC interpolation maps for each engine can be found in Appendix E. As requested by the Engine Manufacturers, only normalized map data is presented.

Originally, the 40-point torque and BSFC maps and interpolation routine were to be used in the Monte Carlo Error Model. The reference NTE events, supplying ECM speed and fuel rate, were to use the maps to interpolate torque and BSFC. The interpolation process in the Model was problematic because the interpolation maps were different for each engine, and engine map data was not available for the engine used to generate the reference NTE events. In addition, there were questions regarding how to choose an interpolation surface for each event, as well as the additional computational load of having to do repeated interpolations in the Model. Therefore, the final reference torque and BSFC values were supplied with each reference NTE events, and no torque and BSFC interpolations were performed in the Model.

In addition to map generation, the 40-point steady-state testing was used to preview the performance of the PEMS and laboratory. As specified in the Test Plan, the results of the 40-point testing were used to down-select the 40 points to the 10 points to be used for steady-state repeat testing. SwRI reviewed the results of 40-point testing and recommended 10 points to be used for steady-state testing. In the down-selecting process, SwRI attempted to have the selected 10 points evenly span the NO_x concentration, exhaust flow rate, and NO_x mass flow rate ranges observed during the 40-point testing. In addition, the 10-points were selected to be somewhat distributed over the NTE zone. In general, the Steering Committee approved the SwRI recommended 10-point down-selection, with only a couple points modified for the final steady-state repeat testing. The selected 10 points are shown in Figure 32 through Figure 34.

Three PEMS units were used simultaneously during the 40-point mapping process. The Test Plan called for the data to be examined to determine if running PEMS in this manner would cause measurement issues that would require subsequent testing to be conducted with one PEMS unit at a time. A particular area of concern was the use of multiple PEMS flow meters in series. Following the 40-point testing on Engine 1, the data was examined by Sensors Inc. and the Steering Committee. There was no evidence of a bias for any PEMS exhaust flow rate measurement. Sensors Inc. agreed with this assessment, and the Steering Committee elected to proceed with all further testing using the three PEMS units simultaneously. This decision was made at the April 4, 2006 conference call. Data from the 40-point maps on Engine 2 and 3 was also examined for evidence of an exhaust flow bias, but none was found.

4.4 Steady-State Repeat Engine Testing and Error Surfaces

Repeat steady-state engine testing was performed to quantify PEMS bias and precision errors versus laboratory emission measurement equipment. The measurement errors evaluated

during steady-state repeat testing included gaseous emission concentration measurements and exhaust flow rate measurements.

The steady-state test consisted of 10 modes that were selected by the Steering Committee from the 40-point mapping procedure discussed previously. The 10-mode steady-state tests were repeated 20 times. As specified in the Test Plan, the mode order of each of the steady-state tests was randomized. The mode length was 3 minutes with data averaged over the last 30 seconds of each mode. Each 10-mode test cycle was run essentially as a ramp modal cycle, although the modes were processed individually. The laboratory reference analyzers were zeroed and spanned before each cycle. The engine and laboratory sampling systems were preconditioned before each cycle as outlined in 1065.520. Following the preconditioning, the engine was brought to idle, both laboratory and PEMS sampling systems and data recording were started, and the 10-mode test cycle was started. At the end of the cycle, laboratory systems were zero and span checked. The PEMS were only spanned at the start of each test day, and were zeroed prior to the start of each cycle. This was roughly equivalent to zeroing the instrument every hour, which is the normal schedule for auto-zero maneuvers during field measurements.

Three PEMS units were tested simultaneously during steady-state testing. The SwRI dynamometer laboratory conducted both raw and dilute emission measurements. The dilute gaseous concentration measurements were converted to the equivalent raw concentrations using the CVS flow rate and the calculated exhaust flow rate. This was done by first calculating a dilute mass rate for a given pollutant, and then using the raw exhaust flow rate to back calculate a raw concentration. These the dilute-to-raw emission concentrations were used as the laboratory reference for comparison against the PEMS gaseous concentration measurements. The laboratory raw measurements were used for quality assurance purposes by providing a check on the dilute-to-raw measurements and on the raw exhaust flow measurement via carbon balance verifications. The laboratory exhaust flow rate was determined using a LFE to measure the intake air flow, a Micro-Motion fuel flow meter to measure fuel flow, and the laboratory analyzers to measure raw exhaust emission concentrations. The intake LFE measurement and the raw chemical balance were used with equation 1065.655-14 to calculate the reference exhaust flow rate. The raw exhaust flow rate was also calculated using the LFE air flow rate and measured fuel flow with the CFR Part 89 raw exhaust flow rate calculation. The two laboratory exhaust flow rate calculation methods resulted in nearly identical exhaust flow rate results.

The wet gaseous PEMS concentration data and EFM data were compared to the laboratory reference. Each PEMS measurement was compared individually to the laboratory reference. These errors, or deltas, were pooled to generate the steady-state error surfaces. For steady-state error generation, deltas were generated from paired data sets of PEMS and laboratory reference measurements. In other words, each PEMS measurements were compared directly to the associated laboratory reference measurement for that repeat.

4.4.1 Engine 1 Detroit Diesel Series 60 Steady-State

After generating the 40-point torque and BSFC maps, the Steering Committee selected 10 points to perform repeat steady-state testing. The modes selected for Engine 1 steady-state testing are shown in Figure 32. As discussed in the audit section of the report, the PEMS units

used during the initial set of steady-state measurements had all failed the 1065 NO₂ Chiller Penetration Check. The Steering Committee elected to proceed with steady-state testing to determine if the NO₂ penetration failure would affect the performance of the PEMS units during engine testing. PEMS 1, 3, and 4 were used for Engine 1 testing. PEMS 2 was not chosen initially for Engine 1 testing due to the 1065 Non-stoichiometric O₂ FID Interference audit failure.

After completion of the steady-state testing, the results were presented to the Steering Committee. The individual delta data from each PEMS was pooled. The 5th, 50th and 95th percentiles of the pooled error data was plotted against the mean laboratory reference value. As shown in Figure 19, the PEMS showed a low bias for NO_x, especially at high concentrations. The Steering Committee deemed the NO_x results unsatisfactory, and Sensors Inc. was asked to design and implement a solution to the NO₂ chiller penetration problem. A complete discussion of the NO₂ penetration solution can be found in the audit section of this report.

In June 2006, approximately two months after the initial Engine 1 steady-state testing, Sensors Inc. installed the NO₂ penetration retrofit package on the PEMS units at SwRI. The NO₂ Chiller Penetration audits were then repeated. All upgraded PEMS units passed the 1065 penetration check.

Following the PEMS upgrades and audit checks, Engine 1 steady-state testing was repeated. Again, the pooled PEMS delta data was plotted against the mean laboratory reference values. As shown in Figure 35, the low NO_x bias of the original testing was replaced with PEMS data showing a slight positive NO_x bias. The pooled gaseous concentration delta data for Engine 1 can be viewed in Appendix F. Delta data is included for both the PEMS as well as the laboratory raw measurements, with the dilute-to-raw measurements as the reference.

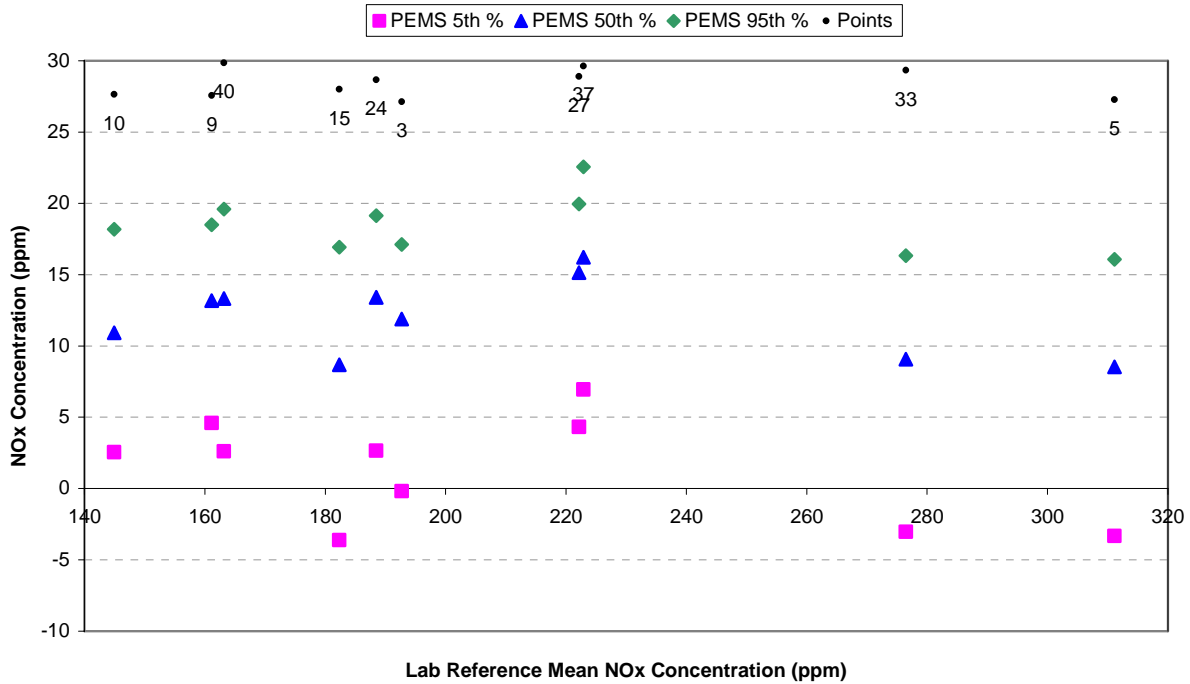


FIGURE 35. NO_x CONCENTRATION POOLED DELTAS FOR REPEAT STEADY-STATE TESTING ON ENGINE 1 AFTER NO₂ PENETRATION UPGRADE

With the Engine 1 catalyzed DPF, CO and HC emissions were very low. Although the laboratory raw and dilute analyzers reported raw CO concentration levels generally between 10 to 25 ppm, the SEMTECH-DS consistently measured CO emission levels at approximately 40 ppm. Pooled deltas for CO are given in Figure 36 for Engine 1. The high CO bias may be due in part to the low resolution of the CO detector, which has a reported resolution of 0.01% (10ppm). In addition, the CO instruments would typically read between 20 and 40 ppm when zero gas was introduced to the sample port of the SEMTECH DS using a sample probe overflow technique. The positive CO bias was apparently due in part to the sampling handling system of the unit and was observed on all three engines.

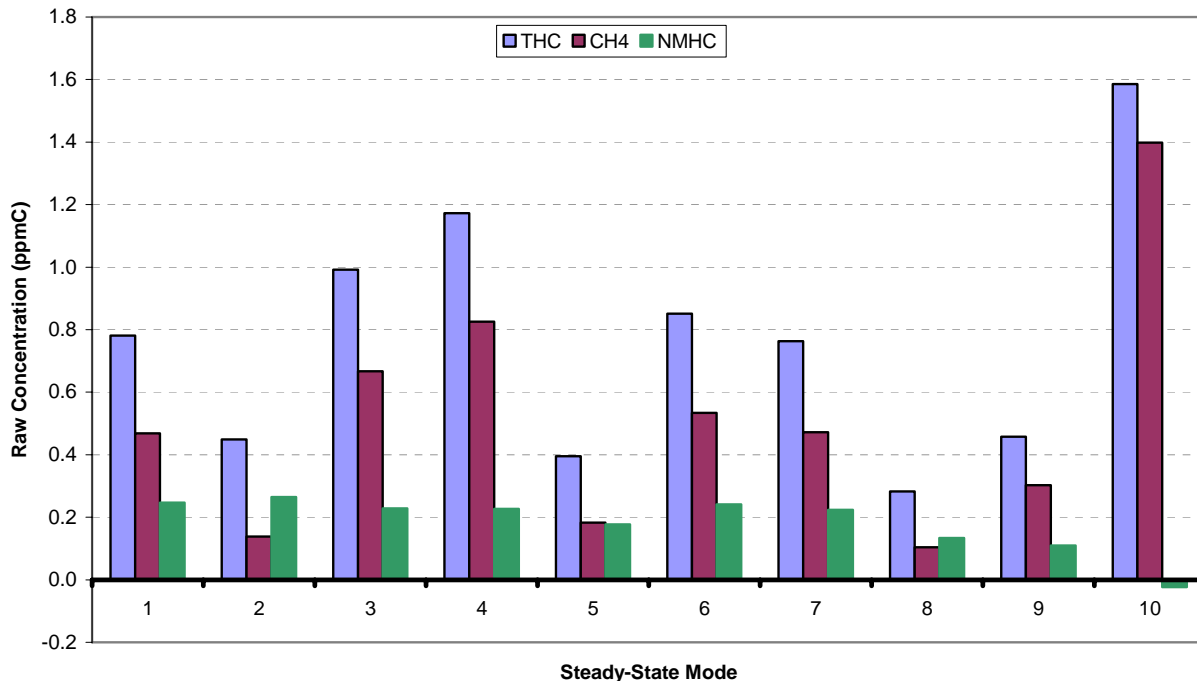


FIGURE 37. MEAN RAW HC CONCENTRATIONS FOR ENGINE 1 STEADY-STATE TESTING

The dilute NMHC measurement was further complicated because the raw exhaust concentrations were below those in the background air. Typical background levels were 3 ppmC for THC and 2.5 ppmC for NMHC. This resulted in a high occurrence of negative NMHC results. The NMHC measurement errors were further exaggerated by the dilute-to-raw scaling process. As a result, the Steering Committee elected to abandon the dilute-to-raw NMHC concentration values as the reference at the April 2006 meeting. The laboratory direct raw concentrations were chosen as the NMHC reference because the raw measurements were not complicated by background concentrations and conversion problems.

Initially, Sensors Inc. supplied two methane analyzers which could, in principal, be added to the SEMTECH-DS units. However, since these analyzers were external laboratory grade analyzers, the Steering Committee decided the methane analyzers were not suitable for field measurement. Therefore, the PEMS NMHC values were determined using only the THC measurement. The THC concentrations were multiplied by 0.98 to generate NMHC values, as given in Part 1065. Figure 38 shows PEMS NMHC concentrations for Engine 1 plotted against the associated mean raw laboratory reference values. Tailpipe HC levels for Engine 1 were below the resolution limits of the PEMS FID analyzer, which reported mostly zero THC values throughout steady-state testing. Therefore, the data from Engine 1 was not useful in producing an NMHC error surface. A final decision on how to process the NMHC data was deferred until results from Engines 2 and 3 could be reviewed.

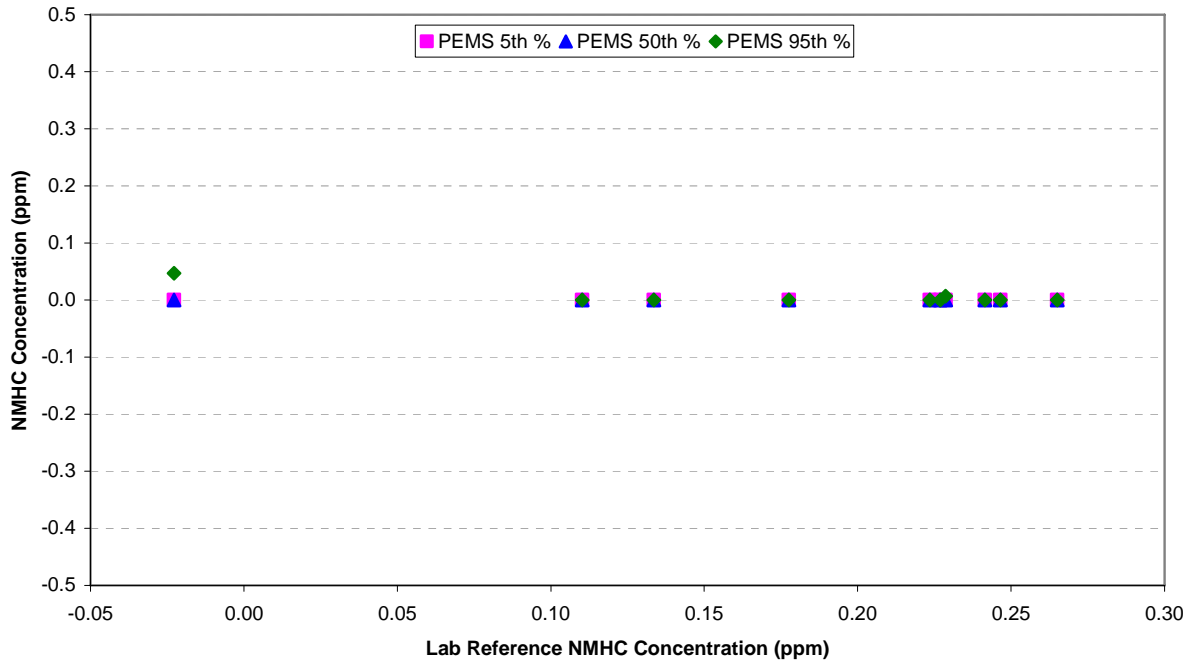


FIGURE 38. PEMS NMHC CONCENTRATIONS FOR ENGINE 1 STEADY-STATE TESTING

As shown in Figure 39, the PEMS 5-inch EFMs showed good correlation with the laboratory reference exhaust flow rate measurement, with deltas generally less than 2 to 3 percent of point. Although not used in the Model, NO_x mass flow rate errors are also shown in Appendix F. The PEMS NO_x mass flow rate measurements were biased slightly high, which is consistent with the slightly high bias observed in both NO_x concentration and the EFM measurements.

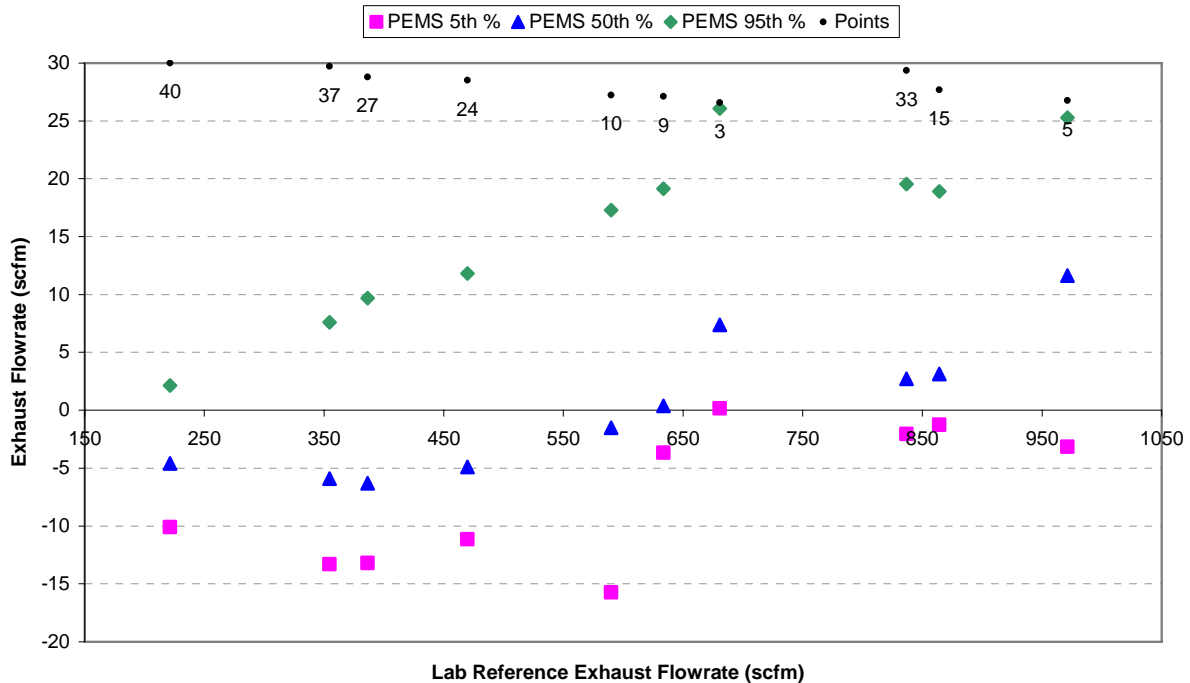


FIGURE 39. POOLED EFM DELTAS FOR ENGINE 1 STEADY-STATE TESTING – 5-INCH FLOW METER

4.4.2 Engine 2 Caterpillar C9 Steady-State

Following the generation of the 40-point torque and BSFC maps, the Steering Committee selected 10 NTE points to perform the repeat steady-state testing for Engine 2. The selected 10 points are shown in Figure 33. Prior to Engine 1 steady-state testing, PEMS 6, used in environmental testing, experienced a FID failure. Because there was an immediate need to continue environmental chamber testing, PEMS 3 was pulled from the dynamometer laboratory and used as a replacement for PEMS 6. This resulted in a schedule delay while PEMS 6 was repaired. PEMS 6 was therefore used for Engine 2 and 3 testing.

During initial Engine 2 steady-state testing, PEMS 4 NO_x values showed several outlying low points. The continuous NO and NO₂ data from PEMS 4 indicated periods when both channels were reporting zero values. Diagnostic efforts pointed to a bad NDUV lamp; therefore, Sensors Inc. replaced the NDUV. Linearity checks were performed on the new NDUV before proceeding with steady-state testing. After only a couple tests, the new NDUV in PEMS 4 began behaving erratically as well. The PEMS 4 NDUV was replaced once again. Linearity checks as well as a NO₂ penetration check were performed before continuing with Engine 2 testing.

Shortly after PEMS 4 was repaired, PEMS 6 reported a fault stating the Manifold Relative Humidity Sensor was not responding. With diagnostic support from Sensors Inc., the exhaust manifold RH sensor and sensor manifold block were removed. This assembly is part of the NO₂ penetration upgrade package which had been developed by Sensors Inc. earlier in the program. As shown in Figure 40, the sensor was found to be corroded, therefore a new sensor and sensor manifold was installed. Because the exhaust manifold relative humidity sensor was

part of the NO₂ chiller penetration retrofit kit, a 1065 NO₂ penetration check was repeated. PEMS 6 passed the penetration check with the new RH sensor. Shortly after continuing with steady-state repeat testing, PEMS 6 again reported the relative humidity sensor was not responding. The sensor was removed and found to be wet. A new sensor and sensor manifold were installed and the 1065 NO₂ Chiller Penetration check was repeated. PEMS 6 passed the audit and SwRI continued steady-state testing with Engine 2. After completing only a couple steady-state tests, PEMS 6 reported the same RH sensor fault. Again, the sensor was found to be wet.



FIGURE 40. CORRODED RH SENSOR (LEFT) COMPARED TO A NEW RH SENSOR (RIGHT)

After the third failure, Sensors Inc. recommended checking the sensor manifold block for leaks. The leak test was performed by slightly pressurizing the sensor manifold and checking for air leaking past the RH sensor. All sensor manifolds tested by SwRI had air escaping the manifold by the RH sensor. According to Sensors Inc., the escaping air likely caused liquid water to be drawn up the manifold and in contact with the relative humidity sensor, thus causing the fault. Sensors Inc. instructed SwRI to reseal the RH sensor in the sensor manifold block using silicon. A picture of a RH sensor surrounded by silicon as well as the sensor manifold block is shown in Figure 41. After resealing the RH sensor, the manifold was leak checked to insure air was not escaping from the manifold. Another 1065 NO₂ penetration check was performed after installing the new sensor. With the properly sealed sensor manifold, PEMS 6 operated without fault for the remainder of the steady-state testing.

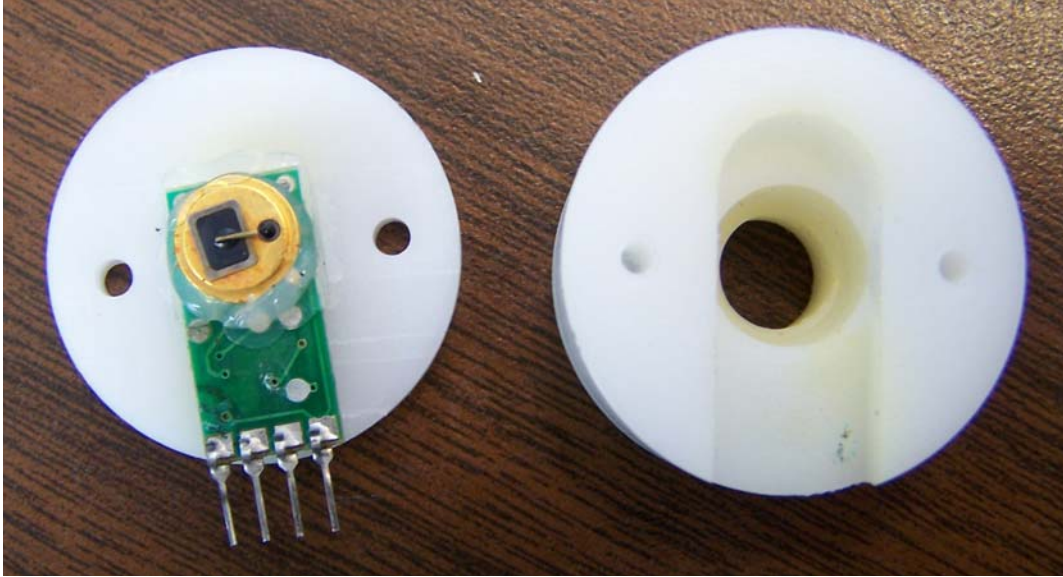


FIGURE 41. DISASSEMBLED RH SENSOR MANIFOLD WITH RH SENSOR

During this time, PEMS 4 also began to have faults pertaining to the manifold relative humidity sensor not responding. The RH sensor and manifold were replaced with a new, non-leaking manifold. After replacement of the sensor, and subsequent NO₂ penetration check, PEMS 4 reported no other problems related to the RH sensor.

Following the completion of the various repairs and diagnostic efforts, the remaining Engine 2 steady-state tests were completed. However, examination of the data following the completion of Engine 2 transient testing revealed a problem with the Caterpillar C9 steady-state data. In generating the transient error surfaces, the transient data was corrected using the variance measured during steady-state testing. The steady-state variance correction process is described in detail under the transient testing section. However, the variance of the Engine 2 steady-state data was generally larger than the variance of the transient data. After reviewing the Engine 2 steady-state data, the high variance was found to be related to the large time lapse caused by the PEMS hardware failures. Almost half of steady-state points were run prior to the PEMS hardware failures, with the remaining points run approximately 3 weeks afterward.

As seen in Figure 42, there is a definite shift in NO_x concentration for the initial steady-state points versus the points run after the PEMS repairs. Repeats 5, 9, and 12 through 20 were run 2 ½ weeks after the other steady-state repeat tests. This shift was recorded for both laboratory and PEMS analyzers. The bias error would not affect the steady-state error surfaces, as the PEMS measurements are paired with the laboratory reference and this removes variances caused by the engine. However, the variance of the pooled raw PEMS data, not the PEMS delta data, was used to generating the transient error surfaces. The high variance of the Engine 2 PEMS steady-state data would have collapsed the Engine 2 transient error surfaces due to the steady-state variance correction. Because the Engine 2 transient error surfaces would be inaccurate using the high variance steady-state data, the Steering Committee elected to repeat Engine 2 steady-state testing.

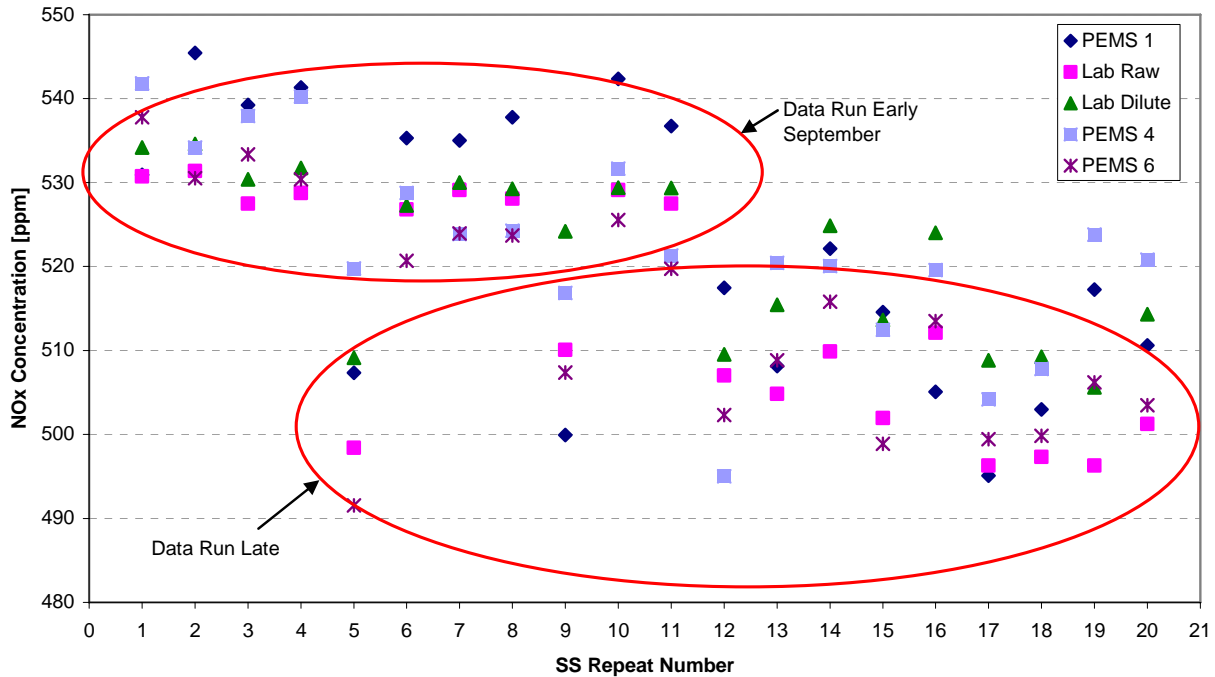


FIGURE 42. ENGINE 2 INITIAL STEADY-STATE REPEAT NO_x RESULTS SHOWING TIME DEPENDENT CONCENTRATION SHIFT

The repeated steady-state testing for Engine 2 went smoothly, with no problems from the PEMS or the laboratory. The PEMS and laboratory raw data was compared to the laboratory reference dilute-to-raw measurements. The pooled delta data was plotted versus the mean reference value. The results for the gaseous emission concentration errors are shown in Appendix F. The SEMTECH-DS median NO_x error levels for Engine 2 were generally less than 5 ppm and centered near zero.

In an attempt to address the issue of low tailpipe NMHC levels observed during Engine 1 testing, a different DPF was used for Engine 2. The Engine 2 DPF was a 2007 production DPF supplied by Caterpillar. The production DPF likely had lower precious metal loadings than the DPFs which SwRI had procured for the program. The Steering Committee hoped the production DPF would result in more useable NMHC data. Figure 43 shows raw hydrocarbon levels for Engine 2. While the NMHC concentrations were higher than Engine 1 levels, the methane and THC levels were extremely similar, resulting in reference NMHC levels still near zero. The similar THC and CH₄ levels resulted in a large occurrence of negative values for the raw laboratory reference. However, the PEMS showed measurable NMHC response for Engine 2, as seen in Figure 44.

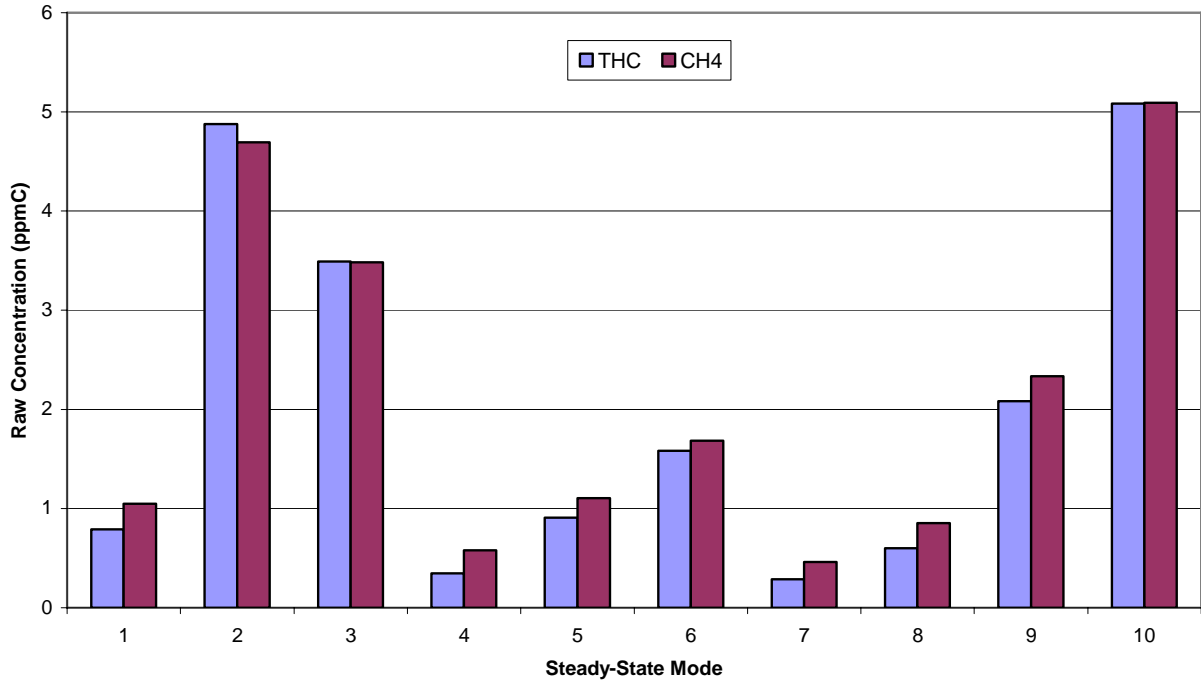


FIGURE 43. RAW HYDROCARBON LEVELS FOR ENGINE 2 STEADY-STATE TESTING

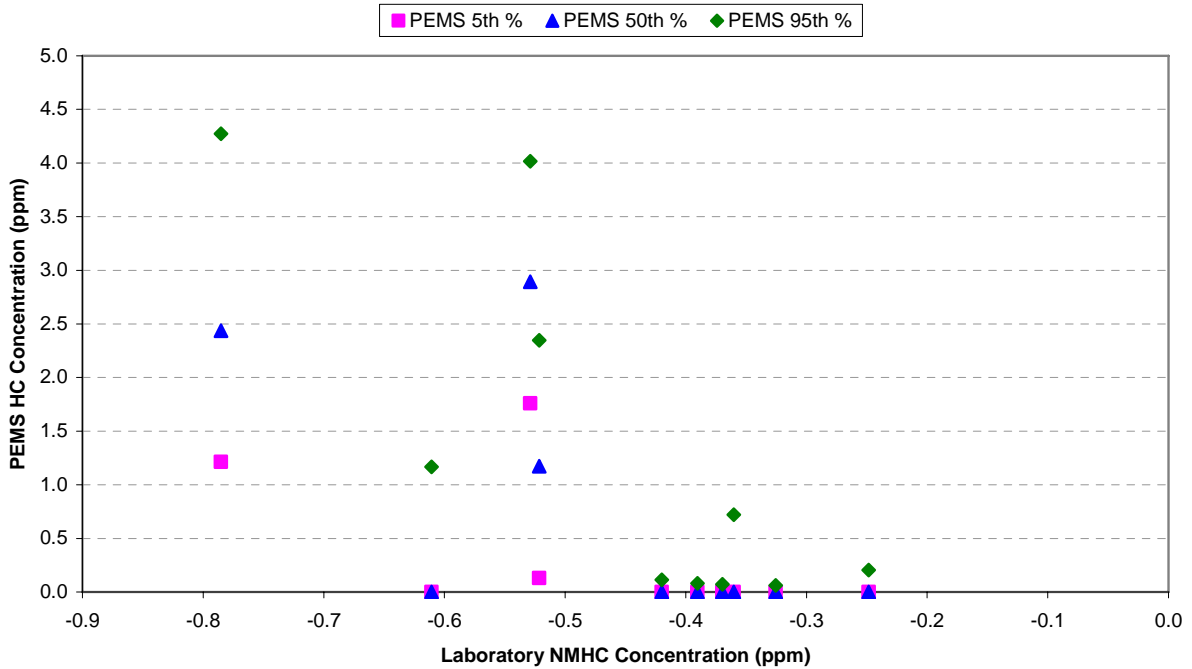


FIGURE 44. PEMS NMHC CONCENTRATIONS FOR ENGINE 2 STEADY-STATE TESTING

Over the course of several conference calls and meetings, there was considerable discussion among Steering Committee members as to how the NMHC data could be represented in the Model. Ultimately, several decisions were made regarding the NMHC error surface. First, it was determined that the laboratory reference method for NMHC was not accurate at the low NMHC levels. As a result, the NMHC error surface was collapsed to a single x-axis point, and all deltas would be generated using a reference value of zero. All of the NMHC data would be pooled together to generate a single set of 5th, 50th, and 95th percentile values. Second, the Steering Committee decided that only Engine 2 data would be used to populate the NMHC error surface, because the data from Engines 1 and 3 showed no PEMS NMHC response. These decisions were finalized at the November 2006 Steering Committee meeting in San Antonio. A similar approach was to be used for the transient error surface as well.

Although the laboratory analyzers reported CO levels under 6 ppm for all modes during Engine 2 testing, the PEMS median error was consistently near 50 ppm. Steady-state CO data for Engine 2 is found in Appendix F. This high bias was similar to the data observed for Engine 1, and was consistent for all CO measurements during this program.

The deltas measured for the PEMS 4-inch EFMs versus the laboratory reference exhaust flow rate are shown in Figure 45. Although the 4-inch flow meters passed the 1065 linearity criteria on the SwRI flow stand, the EFMs showed a positive error at high flow rates during engine testing. This error was on the order of a 5 percent positive bias. A discussion of the 4-inch EFM error results and linearization issues is included in the flow meter audit section of the report. Although not part of the measurement allowance, NO_x mass flow rate deltas for Engine 2 are also included in Appendix F. With accurate NO_x concentrations measurements, the NO_x mass flow rate error resembled the exhaust flow rate errors and had a positive bias at high NO_x mass flow rates.

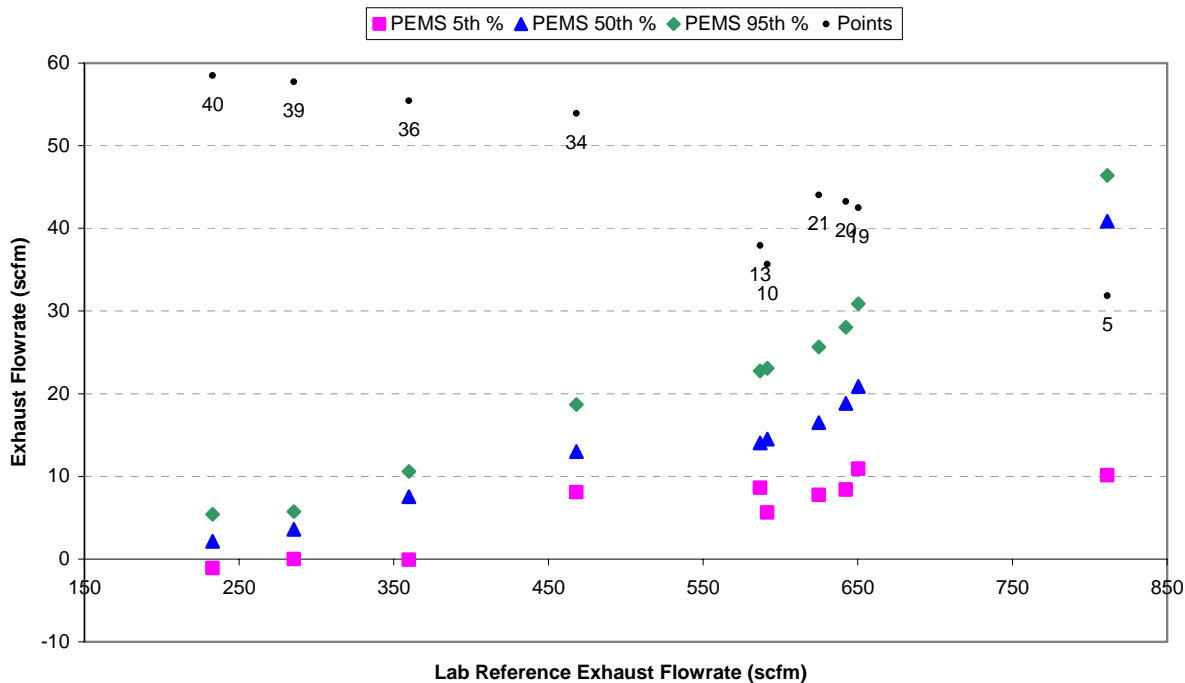


FIGURE 45. POOLED EFM DELTAS FOR ENGINE 2 STEADY-STATE TESTING – 4 INCH FLOW METER

4.4.3 Engine 3 International VT365 Steady-State

Similar to Engine 1 and 2, 10 NTE points were selected by the Steering Committee from the original 40 points tested for the torque and BSFC maps. The selected 10 points are shown in Figure 34. As with Engine 2, PEMS 1, 4, and 6 were used for Engine 3 testing. A Horiba OBS-2200 On Board Emission Measurement System was also tested during Engine 3 operation.

Engine 3 steady-state repeat testing went smoothly, with no equipment failures from the PEMS or laboratory. However, PEMS 6 consistently showed a negative NO_x bias at high concentration levels. This surfaced initially during the 40-point map testing, and was confirmed during repeat steady-state tests. Shown in Figure 46 is the PEMS 6 steady-state pooled NO_x data versus the mean laboratory reference concentrations. PEMS 1 also showed a slight negative NO_x bias at high concentrations, but not as severe as PEMS 6. Post-test span checks for all PEMS, conducted using the instrument span port, indicated no problems despite the low bias. Several diagnostic tests were performed immediately after steady-state testing with PEMS 6 to determine the cause of the bias. NO and NO_2 linearity verification results did not indicate any instrument problems. As a check, dry span gas was then overflowed to the sample line of PEMS 6. At 100 % of span value, NO read nearly 7 % below the bottle value and NO_2 read over 4 % low. At 70 % of span value, NO read approximately 2 % low while NO_2 read slightly over 1 % low. At 30 % of span value, both NO and NO_2 measurements were accurate. This confirmed the low bias problem, but only when the gas is being introduced through the sample line.

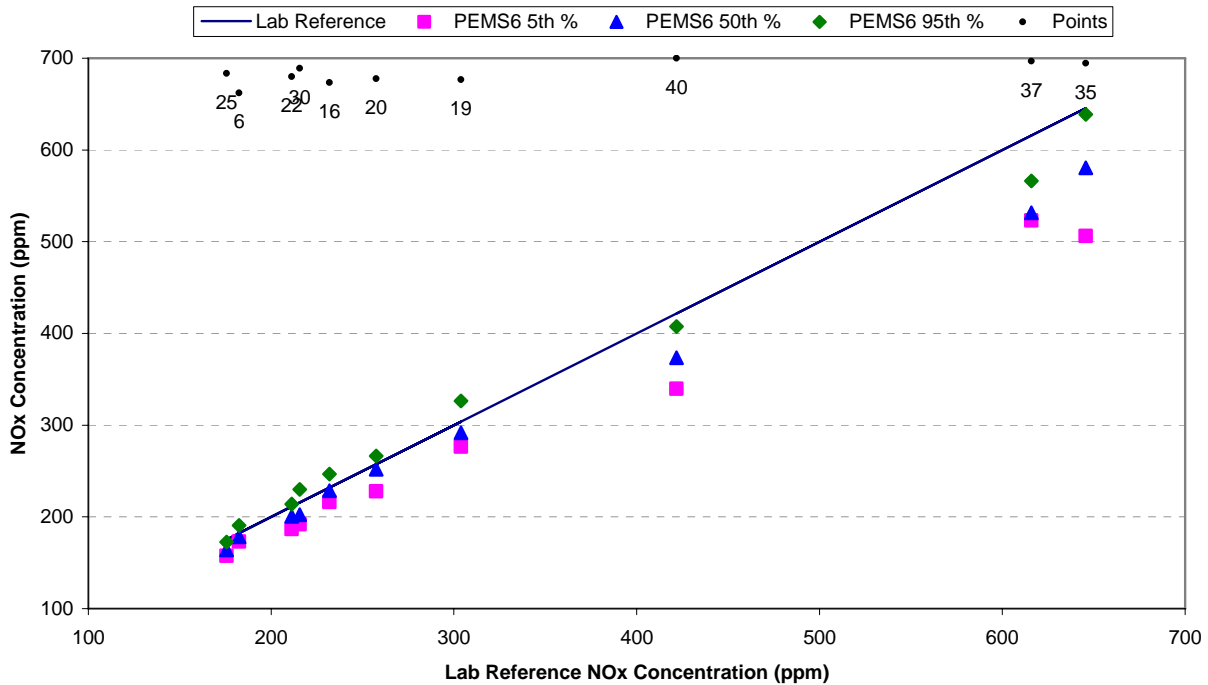


FIGURE 46. PEMS NO_x CONCENTRATION VERSUS MEAN LABORATORY REFERENCE FOR ENGINE 3 STEADY-STATE TESTING

In early December 2006, an NO₂ penetration check was performed with PEMS 6. As shown in Table 41, PEMS 6 passed a NO₂ chiller penetration check. This was unexpected, considering the low biases observed before the long weekend. Therefore, the overflow checks with dry NO and NO₂ span gas were repeated. Low biases were not observed during the repeated checks, indicating that something had changed while the PEMS were sampling ambient air over the weekend. A possible explanation for the performance difference is the drying of accumulated water in the sample handling system. It is not known at this time why some of the PEMS showed a low bias while others did not during Engine 3 steady-state testing; however, none of the analyzers failed any of the 1065 performance checks during this time. There was considerable Steering Committee discussion regarding the Engine 3 steady-state data set. The Steering Committee elected to accept the biased steady-state data because a specific cause for the low NO_x bias was not evident, and because the PEMS continued to pass all pertinent 1065 audit verifications.

Another concern with the International steady-state data was high NO_x concentration variability at high concentration levels. NTE points 35, 37, and 40 were all near peak torque speed and produced high NO_x concentrations. Although the speed and torque for these modes was consistent, the NO_x concentrations showed unexpectedly high variability, which was evident in both the lab reference data and the PEMS data. Figure 47 shows the laboratory dilute-to-raw concentrations for NTE point 35 during steady-state repeat testing. The laboratory reference NO_x concentration median absolute deviation (MAD) value calculated for point 35 was over 40 ppm. An example MAD calculation is shown below for reference. As discussed for the Caterpillar steady-state data, the high NO_x variability did not adversely affect the Engine 3

steady-state error surface data because of the individual pairing with the laboratory reference. However, the high steady-state variability does affect the transient error surfaces during the steady-state variance correction. The solution to this problem is discussed in detail in the transient engine testing section of the report.

$$MAD = \text{median}\{x_i - \text{median}(x)\}$$

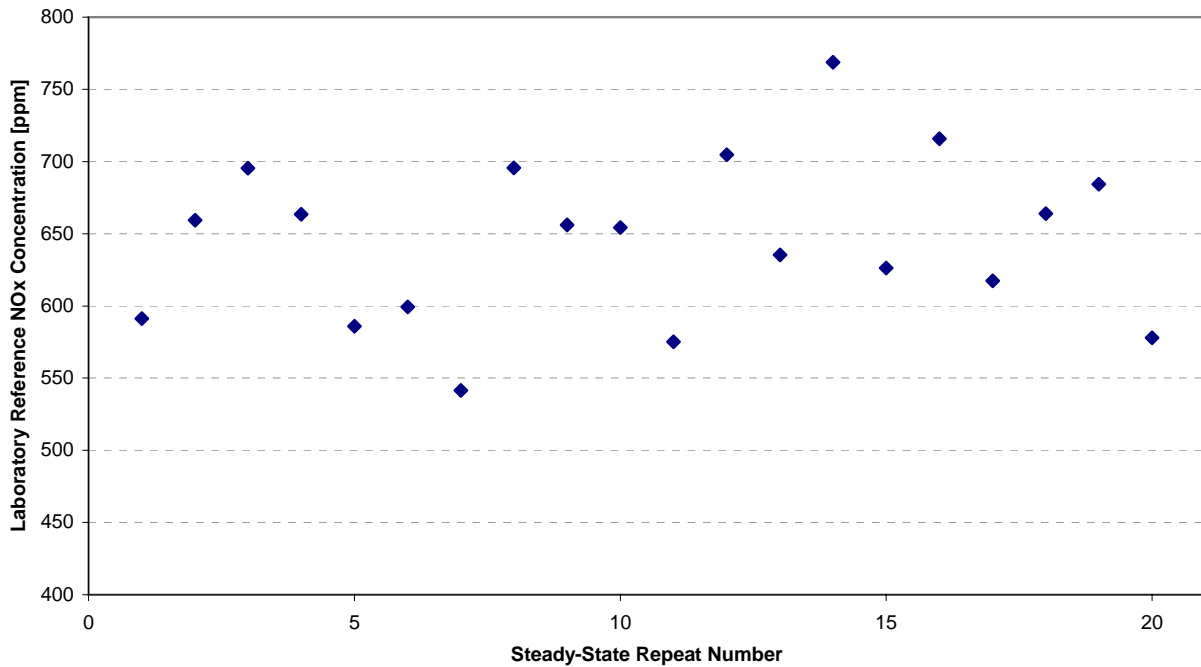


FIGURE 47. INTERNATIONAL VT365 POINT 35 NO_x CONCENTRATIONS DURING STEADY-STATE REPEAT TESTING

Another issue with the Engine 3 steady-state data was several instances of outlying data. As seen in Figure 48, NTE point 30 had 5 repeats that were significantly higher than the other 15 events. This shift was observed on all of the measurement instruments, including the laboratory dilute and raw and all of the PEMS. As a result, this instances were determined to be the result of engine variability, rather than measurement errors. Per the Steering Committee’s decision, the outlying data points were removed from steady-state data set. For NO_x concentration, events were removed from NTE points 25, 30, and 37. Outlying events were also removed from the CO, CO₂, and NO_x mass flow rate data sets.

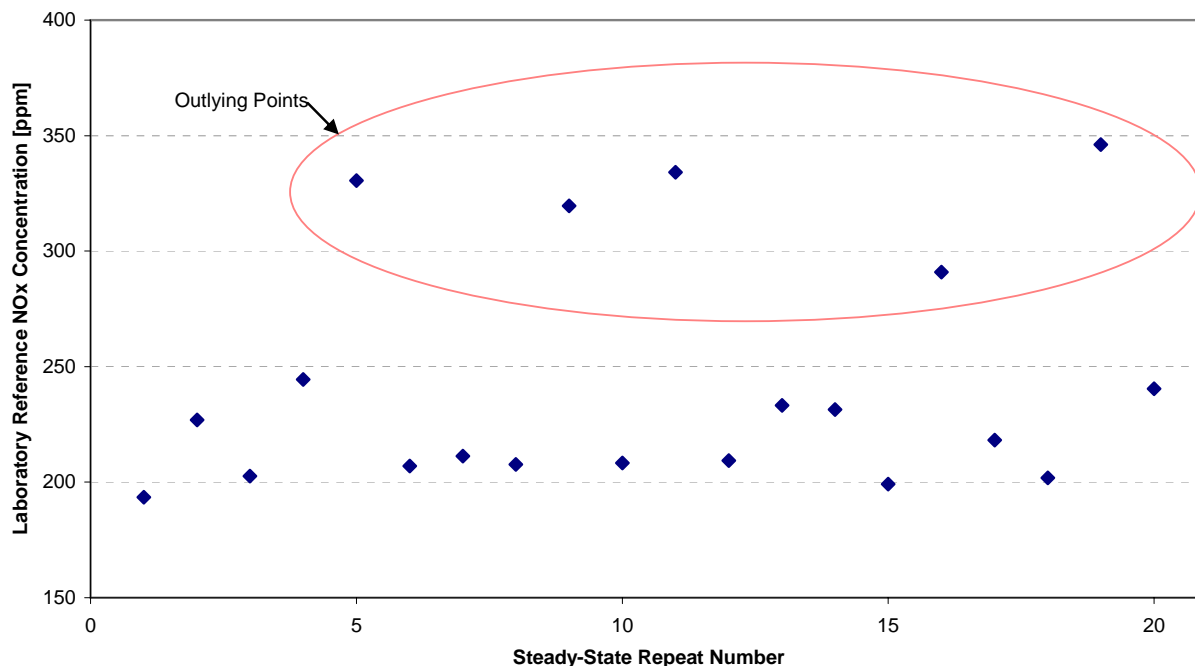


FIGURE 48. INTERNATIONAL VT365 POINT 30 NO_x CONCENTRATIONS DURING STEADY-STATE REPEAT TESTING

After removal of the outlying data, the PEMS and laboratory raw data was compared to the laboratory reference dilute-to-raw measurements. The pooled delta data was plotted versus the mean reference values. The results for the gaseous emission concentration errors are shown in Appendix F. As discussed previously, PEMS 1 and 6 showed a low bias for NO_x concentration at high levels. Similar to Engine 1 and 2, the median CO errors were near 50 ppm, with the 95th percentile values reaching 90 ppm for Engine 3. Although the PEMS showed occasional NMHC responses on Engine 3, the large body of data indicated essentially zero PEMS response to the tailpipe exhaust, similar to what was observed for Engine 1. This data ultimately reinforced the Steering Committee decision to use only Engine 2 data for NMHC error surface generation.

The deltas measured for the PEMS 3-inch EFMs versus the laboratory reference exhaust flow rate are shown in Figure 26. Although the 3-inch flow meters passed the 1065 linearity criteria on the SwRI flow stand, the EFMs showed a positive error at high flow rates during engine testing. Generally this error was on the order of 10 percent of point. A discussion of the 3-inch EFM error results and linearity is given in the flow meter audit section of the report. As shown in Figure 50, the Horiba OBS-2200 exhaust flow rate measurements showed good agreement with the laboratory reference.

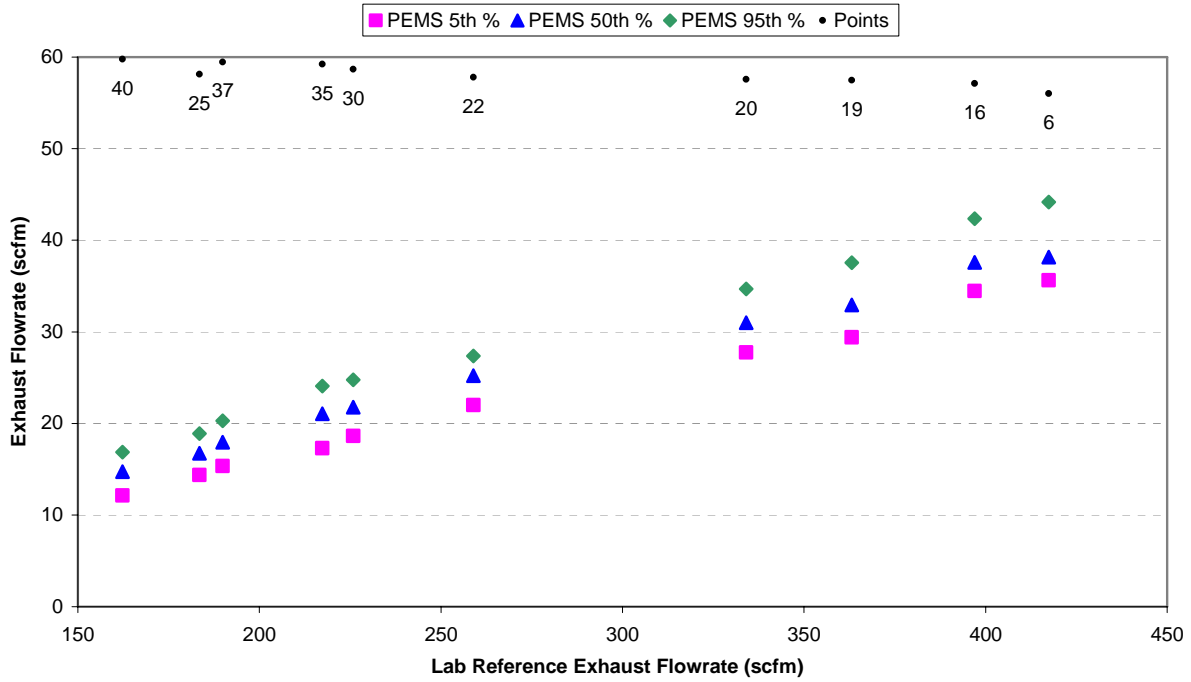


FIGURE 49. POOLED EFM DELTAS FOR ENGINE 3 STEADY-STATE TESTING – 3-INCH FLOW METER

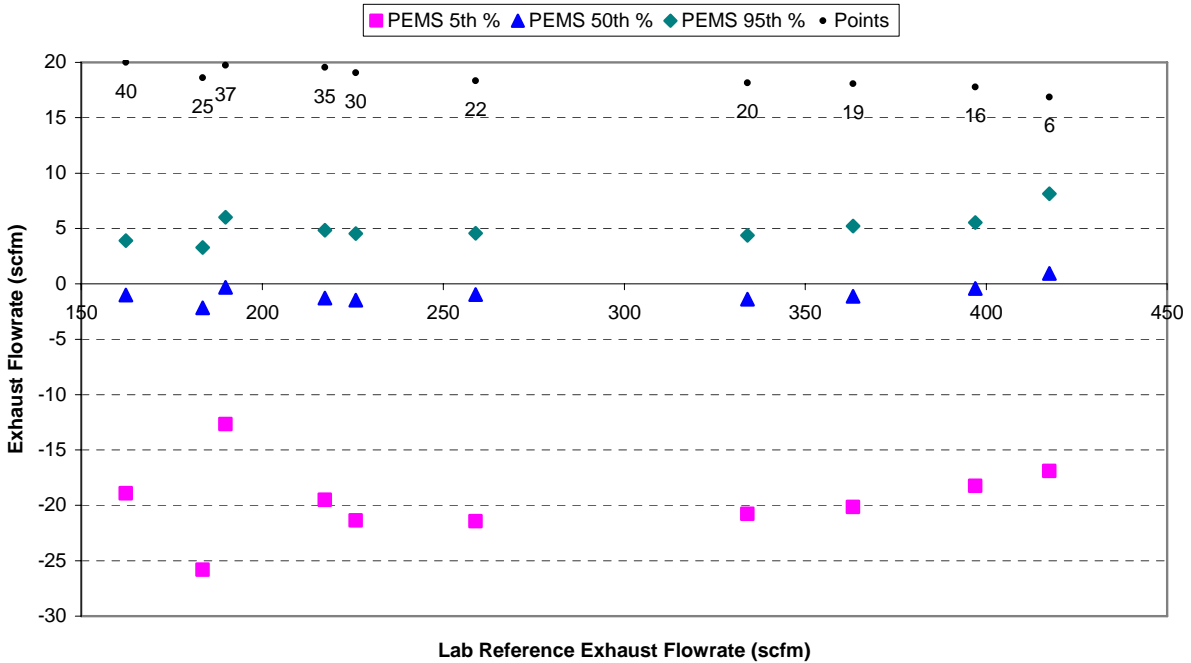


FIGURE 50. POOLED HORIBA OBS-2200 EXHAUST FLOW RATE DELTAS FOR ENGINE 3 STEADY-STATE TESTING

Although not part of the measurement allowance, NO_x mass flow rate deltas are also included in Appendix F. The NO_x mass flow rate errors were biased high in the mid-to-lower range due to the positive exhaust flow rate error. However, the negative NO_x concentration bias at high levels helped offset the NO_x mass flow rate error at the higher levels in some cases.

Figure 51 shows the pooled Horiba OBS-2200 NO_x concentration deltas measured during Engine 3 steady-state testing. Median delta values were near 10 % of point. In addition to the median bias, NO_x variability was also large, with the difference between the 95th and 5th percentile concentrations near 20% of point. The Engine 3 pooled steady-state deltas for all gaseous emissions are shown in Appendix F. As shown in Figure 52, THC measurement with the Horiba OBS-2200 showed good correlation to the SwRI raw THC concentrations, even at levels between 0.5 and 2.5 ppmC. The OBS-2200 CO₂ concentration measurements were generally higher than the laboratory reference values, with median deltas ranging from 3 to 5 % of point. With the laboratory reference CO concentrations ranging from 6 to 18 ppm, CO deltas were near -100 ppm for the 5th percentile deltas, -60 ppm for the 50th percentile, and 110 ppm for the 95th percentile error.

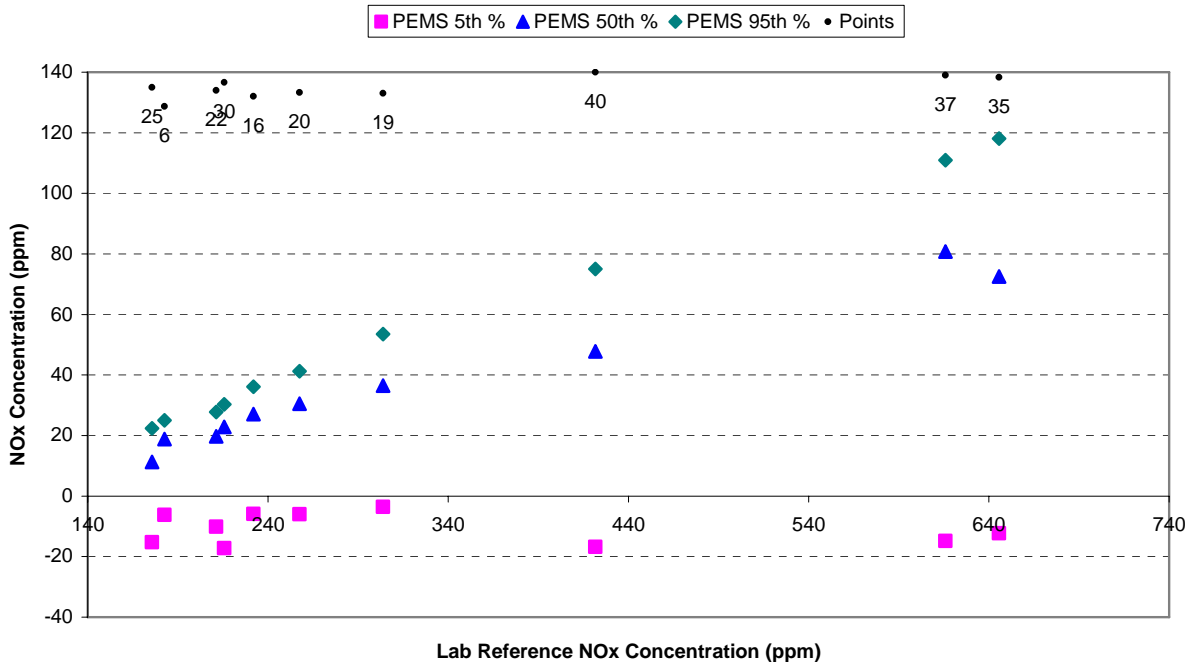


FIGURE 51. POOLED NO_x DELTAS FOR THE HORIBA OBS-2200 DURING ENGINE 3 STEADY-STATE TESTING

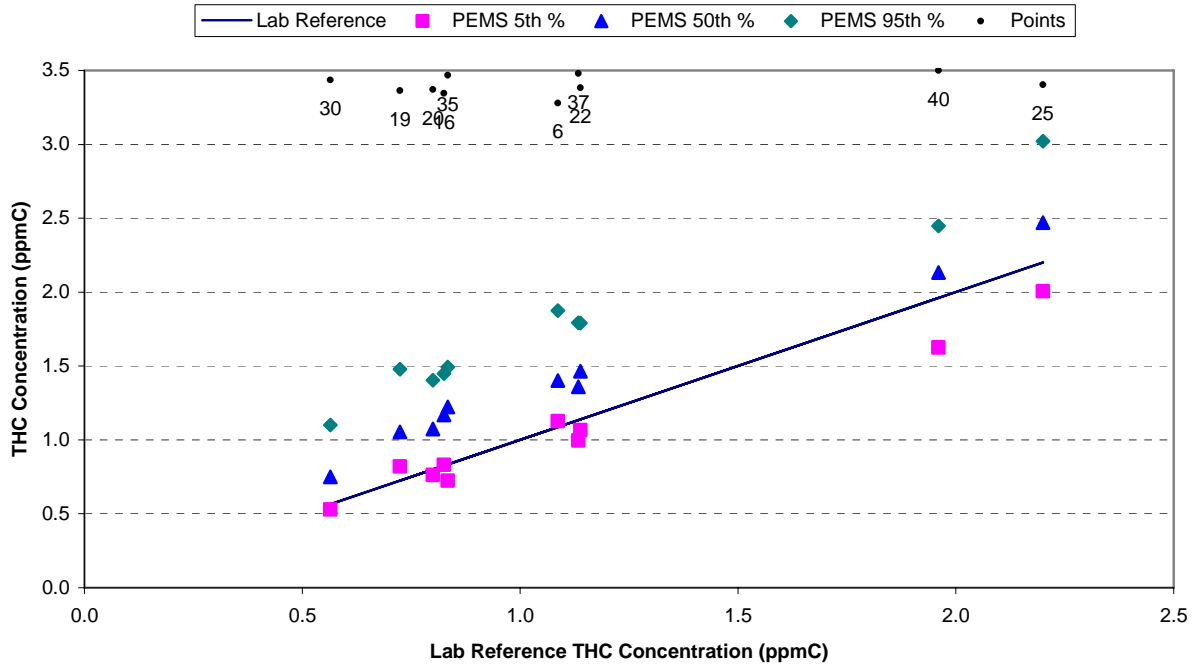


FIGURE 52. POOLED THC MEASUREMENTS FOR THE HORIBA OBS-2200 DURING ENGINE 3 STEADY-STATE TESTING

4.4.4 Steady-State Concentration Error Surface Generation

The steady-state gaseous emission concentration error surfaces were generating using the pooled PEMS EFM deltas versus the laboratory reference. The 5th, 50th, and 95th percentile values of the pooled error terms were plotted against the mean laboratory reference concentrations. Delta values were normally sampled from the steady-state gaseous concentration error surfaces for each NTE event. Because the error surfaces were level dependent, linear interpolation between points was used to determine the appropriate delta. Individual steady-state error surfaces for each engine are contained in Appendix F.

The final steady-state concentration error surfaces were generated by pooling the Engine 1, 2, and 3 error surfaces. The combined error surface is shown in Figure 53. Because the NO_x concentration error profiles for the three engines were notably different, the combined final error surface was extremely irregular, displaying sharp transitions in areas where concentration values for the three engines overlapped. The original intent of testing three engines was to generate a broad, uniform, well-distributed final error surface. The underlying assumption with this method was that the three engines would produce similar errors, and the combined error surface would therefore be relatively uniform.

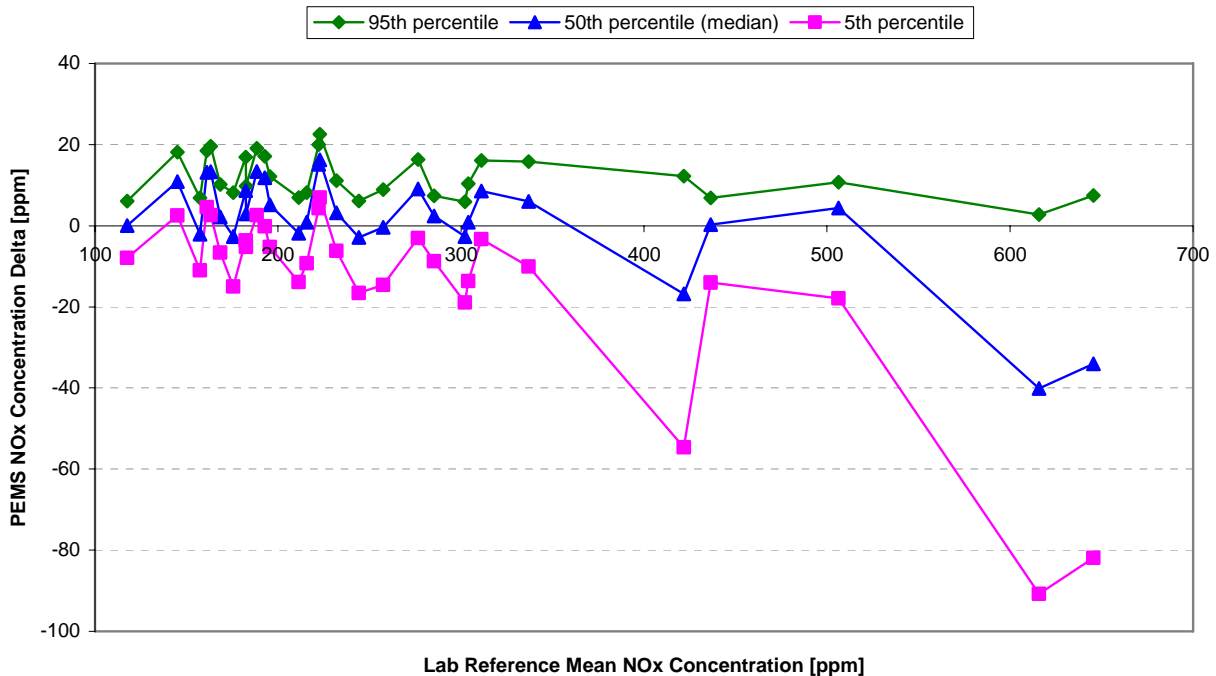


FIGURE 53. COMBINED ERROR SURFACE FOR STEADY-STATE NO_x CONCENTRATION

The combined error surface shown in Figure 53 was presented to the Steering Committee during the December 2006 meeting in San Antonio. After a lengthy discussion, the Committee elected to reprocess the final error surfaces. Because the steady-state concentration error surfaces were sampled normally, the 5th and 95th percentile deltas were to represent the largest, or worst case, delta values. Following that argument, if all engines would have generated deltas at all x-axis concentration levels, the 5th percentile value would have been generated by the engine having the lowest bias and the 95th percentile would have been generated by the engine reporting the highest bias.

The steering committee elected to reprocess the final error surfaces by linearly interpolating between each engine’s error surface data points to populate x-axis values generated by the other engines. For example, the Engine 1 deltas were used to linearly interpolate Engine 1 deltas that would have occurred at the other x-axis concentrations. This method was applied to the 5th, 50th, and 95th percentile values for each engine. For concentration values beyond the range of data actually taken for a given engine, the method for generating delta values depended on the trends observed in the measured data. If no definite trend was observed in the data for a given engine, the nearest x-axis error value was repeated to generate the extrapolated data (i.e., the first or last data point of the data set). If a trend was evident, a regression line was fit through the engine’s delta data. The regression line was then used to generate deltas for points requiring extrapolation.

Using the method described above, a 5th, 50th, and 95th percentile was generated for all three engines at each of the 30 x-axis mean laboratory reference points. Once this was done, the

final pooled error surfaces were generated. At each of the 30 x-axis points, the 5th percentile of the pooled error surface was generated by selecting the lowest 5th percentile value from the three engines at that point. In a similar manner, the 95th percentile was selected by taking the highest 95th percentile value from the three engines, and the 50th percentile was taken as the middle 50th percentile value from the three engines. The final steady-state NO_x concentration error surface used in the Model is shown in Figure 54 as an example of this process. Concentration error surfaces for each engine as well as the final combined error surfaces are shown in Appendix F for all pollutants. This process was not needed for NMHC data, because only Engine 2 data was used to generate the NMHC error surface as discussed earlier.

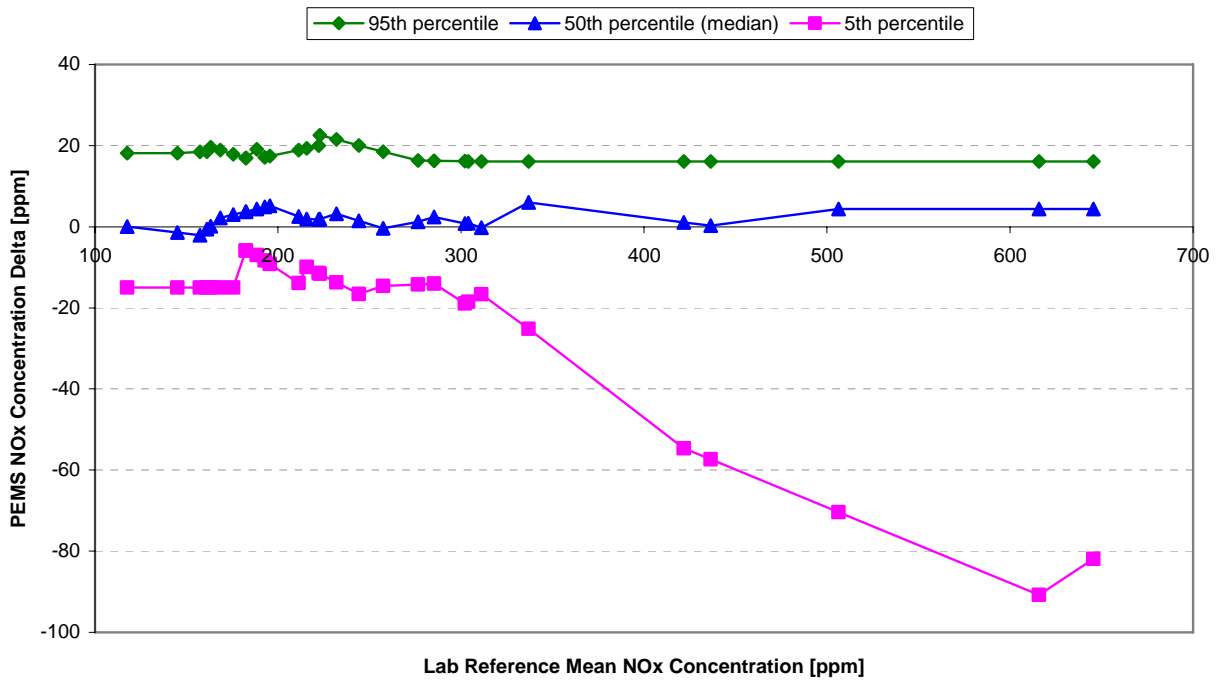


FIGURE 54. FINAL ERROR SURFACE FOR STEADY-STATE NO_x CONCENTRATION

The steady-state exhaust flow rate error surfaces were generating using the pooled PEMS EFM deltas versus the laboratory reference. The 5th, 50th, and 95th percentile values of the pooled error terms were plotted against the mean laboratory reference exhaust flow rates. The data was normalized using the maximum EFM flow rate as specified in the user manual. The maximum flow rates for the 3-inch, 4-inch, and 5-inch EFMs were 600, 1100, and 1700 scfm, respectively. The reference NTE events used in the Model supply exhaust flow rate in scfm as well as the EFM size. Using this information, the reference NTE exhaust flow rate measurement was normalized similar to the laboratory generated error surface. Using the normalized flow rate, a delta value was normally sampled from the steady-state exhaust flow error surface for each NTE event. Because the error surface was level dependent, linear interpolation was used to determine the appropriate flow rate delta. Individual steady-state error surfaces for each engine are collected in Appendix F.

The combined steady-state exhaust flow rate error surface was generated by pooling the Engine 1, 2, and 3 error surfaces. The combined error surface is shown in Figure 55. Similar to the steady-state concentration combined error surfaces, the exhaust flow rate error surface was not uniform due to error differences for each engine and EFM size.

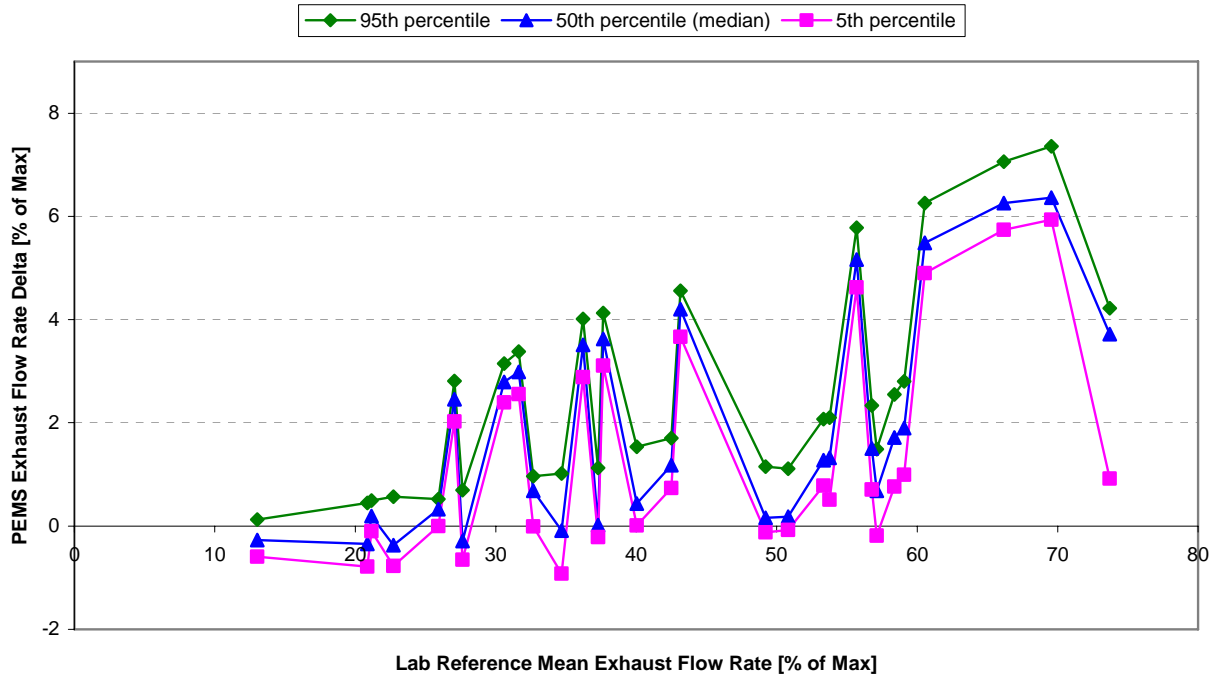


FIGURE 55. COMBINED ERROR SURFACE FOR STEADY-STATE EXHAUST FLOW RATE

The final steady-state exhaust flow rate error surface was reprocessed as described in the steady-state concentration error surface generation section. The final steady-state exhaust flow rate error surface used by the Model is shown in Figure 56.

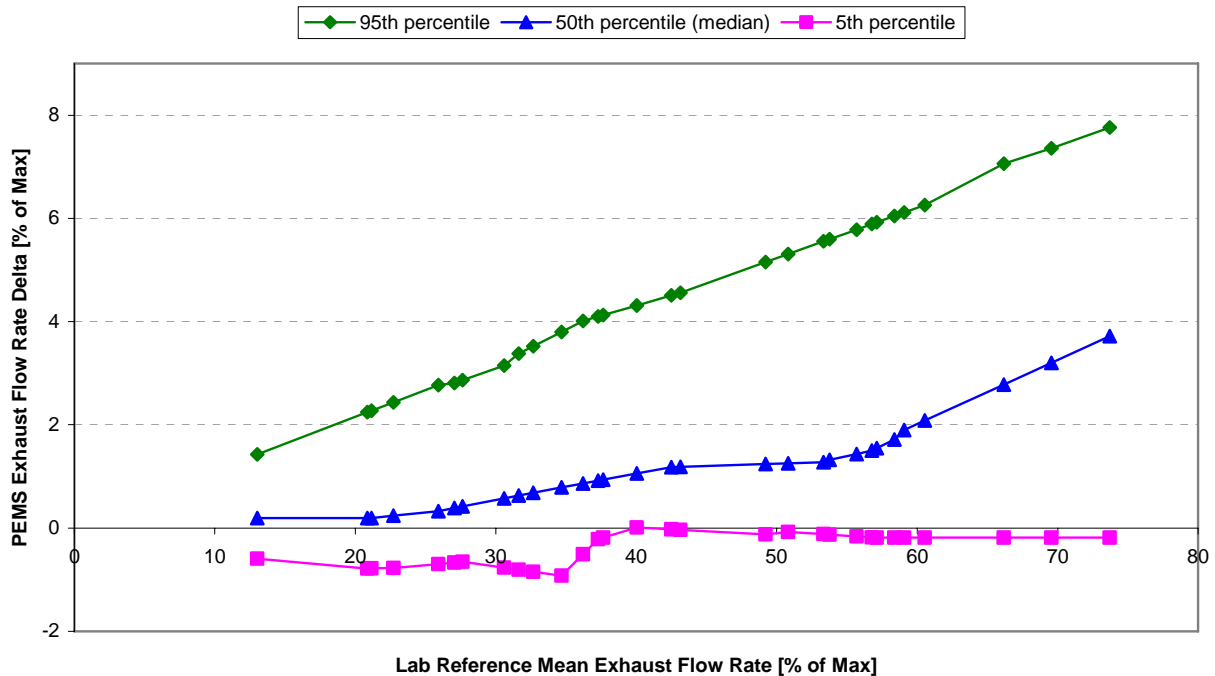


FIGURE 56. FINAL ERROR SURFACE FOR STEADY-STATE EXHAUST FLOW RATE

4.5 Transient Engine Testing and Error Surfaces

The transient engine testing was performed to evaluate the errors involved in using the SEMTECH-DS PEMS units to measure 30-second transient NTE events. It should be noted that the intent of the transient experiments was to capture errors present over and above those already observed during the steady-state experiments (i.e., errors resulting from the transient nature of the events being measured). Transient error surfaces were generated for gaseous emission concentrations, exhaust flow rate, and various ECM-related data, including ECM broadcast speed and fuel rate, and ECM interpolated torque and BSFC. In addition, the transient test data was used to generate an error surface based on time alignment errors of several key PEMS parameters.

During the development of the Test Plan, there was concern over the lack of information available regarding the accuracy and precision of the laboratory reference methods over 30-second test events. Therefore, the Steering Committee elected not to compare the laboratory and PEMS data during transient testing. Instead, the transient error surfaces account only for precision errors of the PEMS with respect to their own median measurements. There is no bias error term captured in the transient error surfaces. However, all laboratory instruments were used during transient testing for comparative purposes and to evaluate the repeatability of the lab over 32 second events. A secondary goal of the program was to assess the repeatability of the 1065-based reference laboratory methods over 30-second events of this nature.

Transient engine testing consisted of repeating 20-minute cycles containing 30 unique 32-second NTE events. An Excel spreadsheet, provided by EPA and approved by the Steering

Committee, was used to generate 30 unique NTE events for each engine, based on the engines' lug curves. In addition, 31 unique transition events were generated, allowing for varying amounts of time between NTE events during the cycle. Descriptions of the NTE and transition events were taken directly from the Test Plan and are given in Table 48 and Table 49, respectively. The NTE event order, as well as the transition order, was randomized to generate 20 different 20-minute cycles, each containing all 30 NTE events. As stated in the Test Plan, only 4 to 5 cycles were run each day, so that transient testing occurred over a span of 4 to 5 days.

TABLE 48. NTE EVENT DESCRIPTIONS FROM THE TEST PLAN

Table 3.3.3-a: Dynamic Response NTE Events			
NTE Event	¹Speed % Range	²Torque % Range	Description
NTE ₁	17%	³ 32%	Steady speed and torque; lower left of NTE
NTE ₂	59%	³ 32%	Steady speed and torque; lower center of NTE
NTE ₃	Governor line	³ 32%	Steady speed and torque; lower right of NTE
NTE ₄	17%	66%	Steady speed and torque; middle left of NTE
NTE ₅	59%	66%	Steady speed and torque; middle center of NTE
NTE ₆	Governor line	66%	Steady speed and torque; middle right of NTE
NTE ₇	17%	100%	Steady speed and torque; upper left of NTE
NTE ₈	59%	100%	Steady speed and torque; upper center of NTE
NTE ₉	100%	100%	Steady speed and torque; upper right of NTE
NTE ₁₀	Lower third	³ 32% - 100%	Highly transient torque; moderate transient speed
NTE ₁₁	Upper third	³ 32% - 100%	Highly transient torque; moderate transient speed
NTE ₁₂	Middle third	³ 32% - 100%	Highly transient torque; moderate transient speed
NTE ₁₃	17% - governed	Lower third	Highly transient speed; moderate transient torque
NTE ₁₄	17% - governed	Upper third	Highly transient speed; moderate transient torque
NTE ₁₅	17% - governed	Middle third	Highly transient speed; moderate transient torque
NTE ₁₆	Lower right diagonal		Transient; speed increases as torque increases
NTE ₁₇	Upper left diagonal		Transient; speed increases as torque increases
NTE ₁₈	Full diagonal; lower left to upper right		Transient; speed increases as torque increases
NTE ₁₉	Lower left diagonal		Transient; speed decreases as torque increases
NTE ₂₀	Upper right diagonal		Transient; speed decreases as torque increases
NTE ₂₁	Full diagonal; lower right to upper left		Transient; speed decreases as torque increases
NTE ₂₂	Third light—heavy-duty NTE event from International, Inc. data set		Sample from LHDE
NTE ₂₃	Cruise; ~ 50 mph		Sample from HDDE
NTE ₂₄	Cruise; ~ 75 mph		Sample from HDDE
NTE ₂₅	Small bulldozer		Sample from NRDE
NTE ₂₆	Large bulldozer		Sample from NRDE
NTE ₂₇	Second of three NTE events in FTP		Seconds used from FTP: 714-725, 729-743, 751-755
NTE ₂₈	Third light—heavy-duty NTE event from International, Inc. data set		Sample from LHDE
NTE ₂₉	First of two NTE events in NRTC		Seconds used from NRTC: 423-430, 444, 448-450, 462-481, increased 464 speed from 40% to 42%
NTE ₃₀	First of two NTE events in NRTC		Seconds used from NRTC: 627-629, 657-664, 685-696, 714-722
¹ Speed (rpm) = Curb Idle + (Speed % * (MTS - Curb Idle)) ² Torque (lbf-ft) = Torque % * Maximum Torque At Speed (i.e. lug curve torque at speed) ³ Torque (lbf-ft) = Maximum of (32 % * peak torque) and the torque at speed that produces (32 % * peak power)			

TABLE 49. NTE TRANSITION DESCRIPTIONS FROM THE TEST PLAN

Table 3.3.3-b: Dynamic Response Inter-NTE Events			
INT Event¹	Duration (s)	Frequency	Description
INT ₁	10	1	Initiation of cycle; INT ₁ is always first
INT ₂₋₆	2	5	Shortest and most frequent inter-NTE events
INT ₇₋₁₀	3	4	Short and frequent inter-NTE events
INT ₁₁₋₁₄	4	4	Short and frequent inter-NTE events
INT ₁₅₋₁₈	5	4	Short and frequent inter-NTE events
INT ₁₉₋₂₁	6	3	Short and frequent inter-NTE events
INT ₂₂	7	1	Medium inter-NTE event
INT ₂₃	8	1	Medium inter-NTE event
INT ₂₄	9	1	Medium inter-NTE event
INT ₂₅	11	1	Medium inter-NTE event
INT ₂₆	13	1	Long inter-NTE event
INT ₂₇	17	1	Long inter-NTE event
INT ₂₈	22	1	Long inter-NTE event
INT ₂₉	27	1	Long inter-NTE event
INT ₃₀	35	1	Longest inter-NTE event
INT ₃₁	5	1	Termination of cycle; INT _{31*} is always last

Interval speeds and torques are not identical, but they are clustered around zero torque and the speed at which 15% of peak power and 15% of peak torque are output.

These tests were all run as hot-start transient tests. The engine and aftertreatment were preconditioned before each test as recommended in 1065.520. The laboratory analyzers were zeroed and spanned prior to each test, although again, they were run for reference only. The PEMS were spanned only at the start of the day, and zeroed prior to each test. The total elapsed time for each test was near one hour, which is the recommended auto-zero frequency for the PEMS. The transient data was post-processed to extract the data associated with the 30 individual events so they could be compared across all 20 repeats.

4.5.1 Engine 1 Detroit Diesel Series 60 Transient

The transient engine testing followed the repeated Engine 1 steady-state testing with the upgraded PEMS. The initial transient task was to generate the transient cycles and tune the engine and dynamometer controls. Some of the NTE events contained highly transient speed and load changes that challenged the laboratory dynamometer as well as the test engine. Next, the lug curve from the Engine 1 was programmed into the PEMS. The PEMS used the J1939 Percent Load ECM-broadcast channel with the Engine 1 lug curve to estimate real time torque. A number of prep cycles were then run to insure the laboratory and PEMS were distinguishing the same 30 NTE events per cycle. Upon initial runs, the laboratory and PEMS missed several NTE events. Causes for the missed NTE events included engine speeds running near the governor that caused a drop in torque as well as highly transient speed and load profiles causing torque or power to drop below the 30% NTE minimum values. In addition, the PEMS estimated torque was often below the laboratory torque causing the torque or power to drop below the NTE threshold levels. A number of slight speed and torque adjustments were made to the NTE cycles before the laboratory and PEMS would consistently record 30 events per cycle.

Continuous engine speed data from the first 5 transient cycle repeats is shown in Figure 57, while torque traces are shown in Figure 58. In order to view the repeated data, the NTE events were reordered and the transition events were removed from the data set. As seen from the continuous data, many events contained highly dynamic speed and load combinations. However, the laboratory was able to achieve very good repeatability in speed and torque for the various events from cycle to cycle, even though the actual running order of events varied considerably from one cycle to the next.

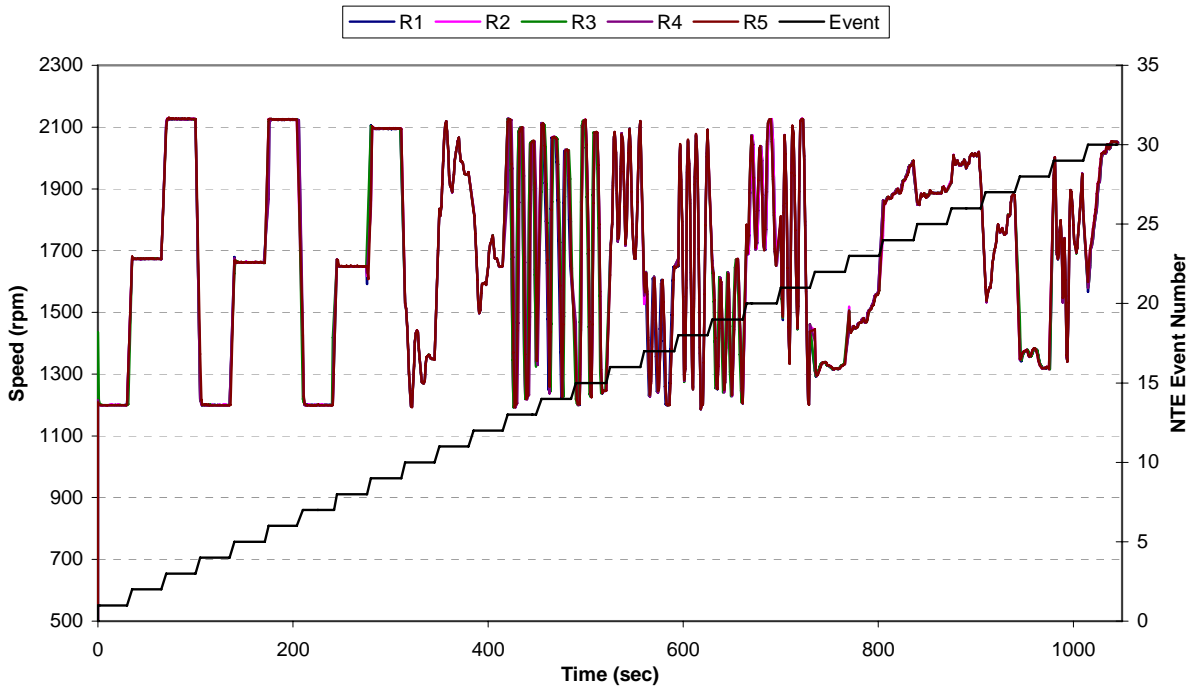


FIGURE 57. ENGINE 1 EXAMPLE SPEED TRACES DURING TRANSIENT TESTING

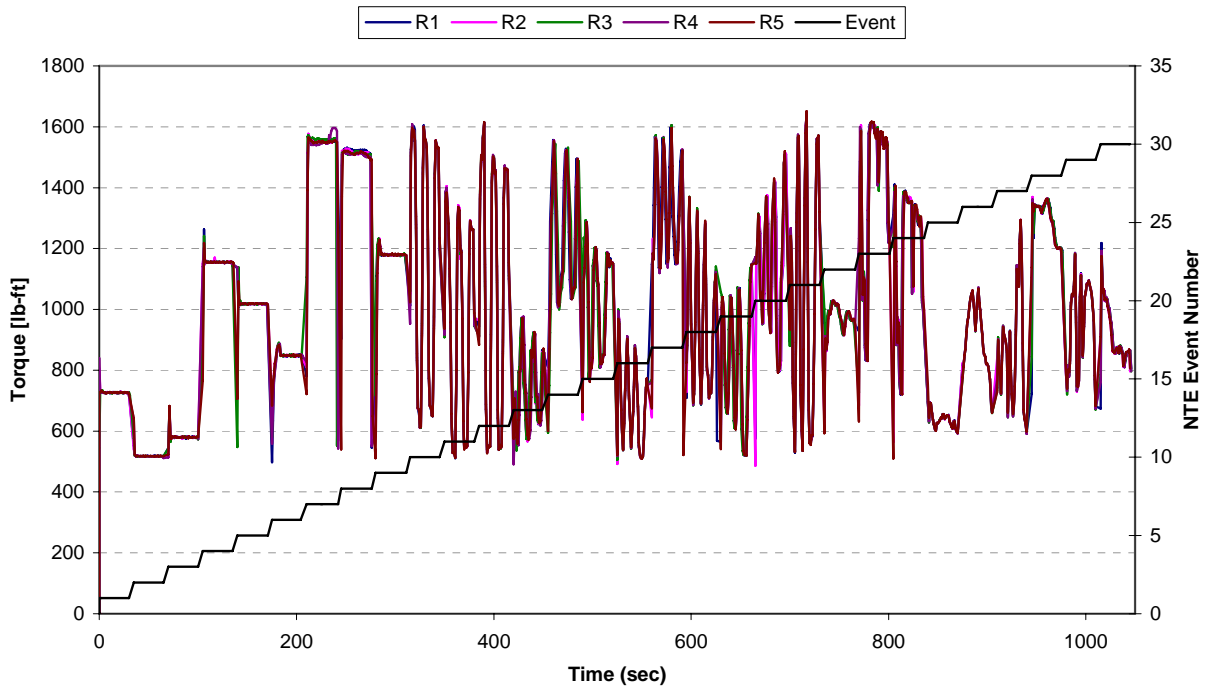


FIGURE 58. ENGINE 1 EXAMPLE TORQUE TRACES DURING TRANSIENT TESTING

At the completion of transient testing, the gaseous concentration, exhaust flow rates, and NO_x mass rates were averaged over each NTE event for all 20 repeats, and then pooled. The 5th, 50th, and 95th percentile values of the averaged data were plotted versus the mean laboratory dilute-to-raw measurements for each NTE event for reference purposes only, and to aid in data review. This data processing structure was similar to the steady-state data analysis. In reviewing the Engine 1 data, there was unexpectedly large variance for the several of the NTE events. After further investigation, a number of outlying measurements were found in the data set. The outlying points were found in both the laboratory raw and dilute measurements, as well as the PEMS data. These outlying measurements were traced to changes in engine operation during the NTE events. Shown in Figure 59, NTE Event 4 of transient cycle Repeat 2 shows a drastic drop in NO_x concentration, while the NO_x concentration of the other repeats was relatively constant. NTE Event 7 of Repeat 4 also shows a drop in NO_x concentration. These engine operation shifts may have been caused by different NTE modes orders or different transition events. The underlying data processing method for the transient surfaces assumes that engine behavior will be constant from run to run, and that any variance observed in the PEMS data is due to measurement errors. Changes in engine behavior would therefore add additional, and potentially overwhelming, variance error to the data.

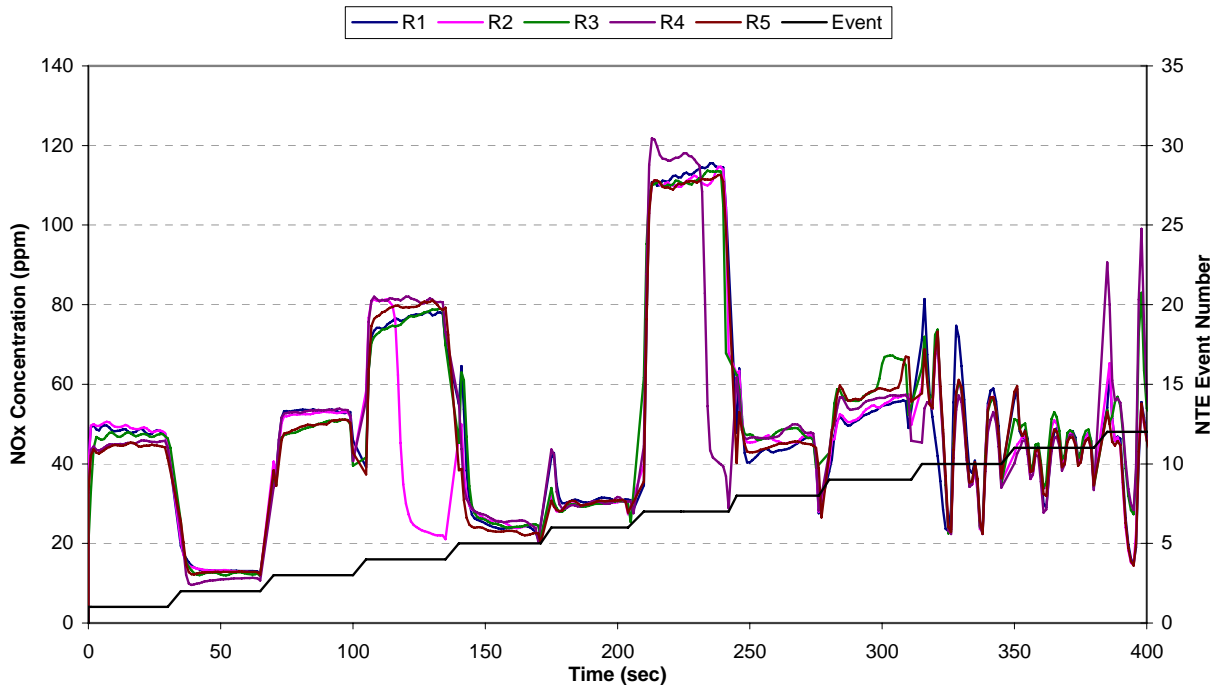


FIGURE 59. ENGINE 1 NO_x CONCENTRATION TRACES DURING TRANSIENT TESTING SHOWING OUTLYING EVENTS

In order to prevent such outliers from artificially inflating the observed transient variance, the Steering Committee decided to have SwRI remove the outlying data points at the May 2006 meeting in Ann Arbor. The removal of the outlying data was first done manually using scatter plots and eliminating obvious outlying NTE points. A more rigorous outlier test was also applied to the data set by SwRI statisticians. Outlier tests based on ASTM E 178 procedures were used to identify outlying NTE data. All tests were made at the 5% level of significance. The results from the statistical outlier tests and the scatter plot test gave similar results. Of the 600 NTE events generating during transient testing, 34 were deemed outliers and removed from the data set.

A secondary task performed by SwRI was to evaluate the repeatability of the laboratory and engine over 32-second NTE events. The laboratory brake-specific NO_x emission results for each NTE event were calculated and pooled. Figure 60 shows the 5th, 50th, and 95th percentile lab dilute BS NO_x results plotted against the mean BS NO_x for the 30 NTE events repeated 20 times. This figure was generated with the outlying NTE points removed from the Engine 1 data set. As shown in Figure 61, the median absolute deviation (MAD) was calculated for each of the 30 NTE events. Although some variation was observed, the MAD was generally in the range of 0.04 g/ (hp·hr), which is roughly 2 percent of the NTE threshold value of 2.0 g/(hp·hr) However, some NTE events showed variance over 0.08 g/(hp·hr).

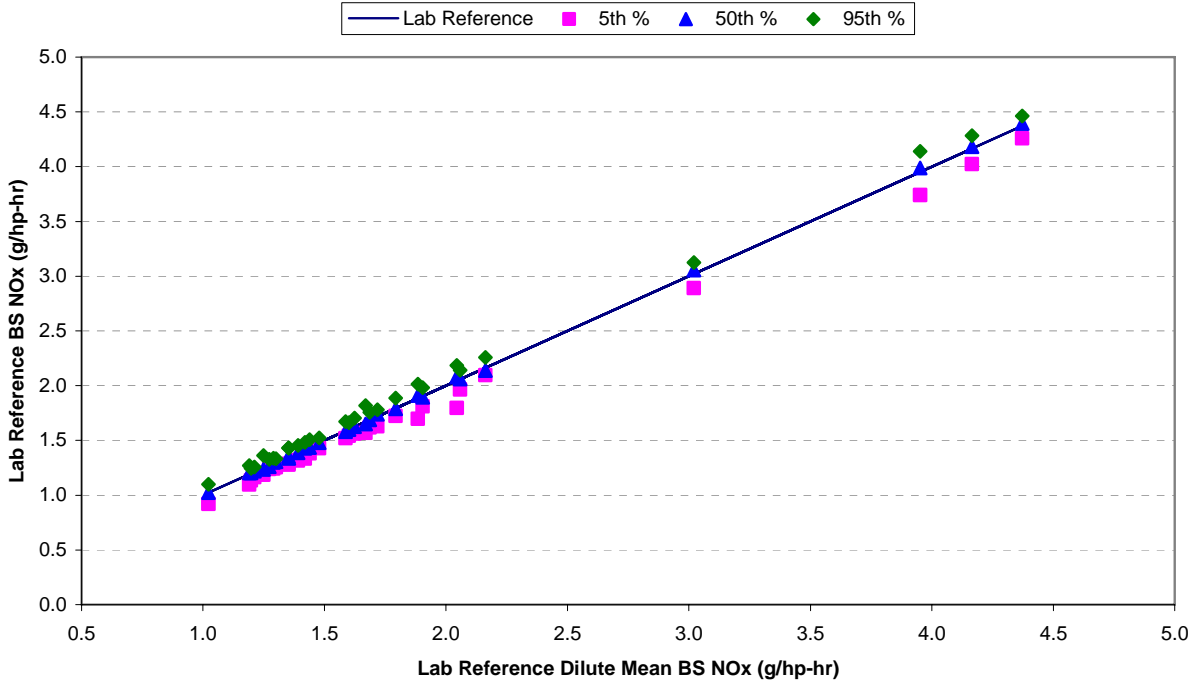


FIGURE 60. ENGINE 1 POOLED TRANSIENT TEST NTE BRAKE-SPECIFIC NO_x RESULTS

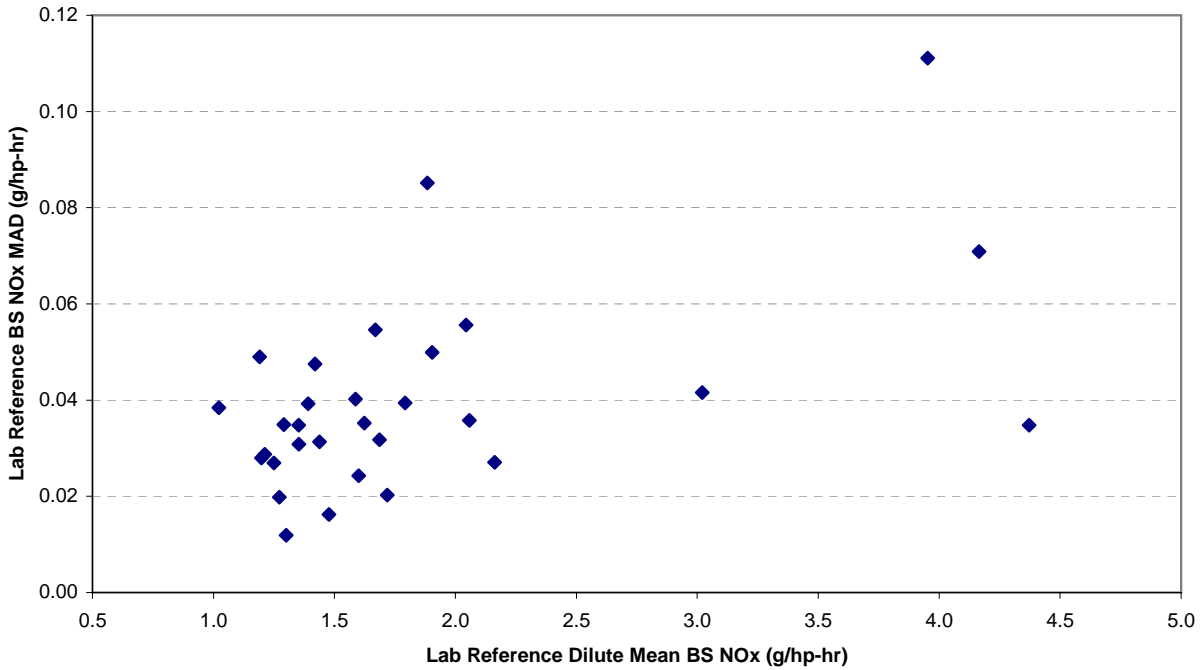


FIGURE 61. ENGINE 1 POOLED TRANSIENT TEST NTE BRAKE-SPECIFIC NO_x MAD RESULTS

Although the laboratory data was not used to generate the transient error surfaces, plots were generated to compare the PEMS performance with the laboratory measurements. As seen in Figure 62 and Figure 63, the PEMS median values during transient testing nearly matched the laboratory mean values for both NO_x concentration and exhaust flow rate, respectively.

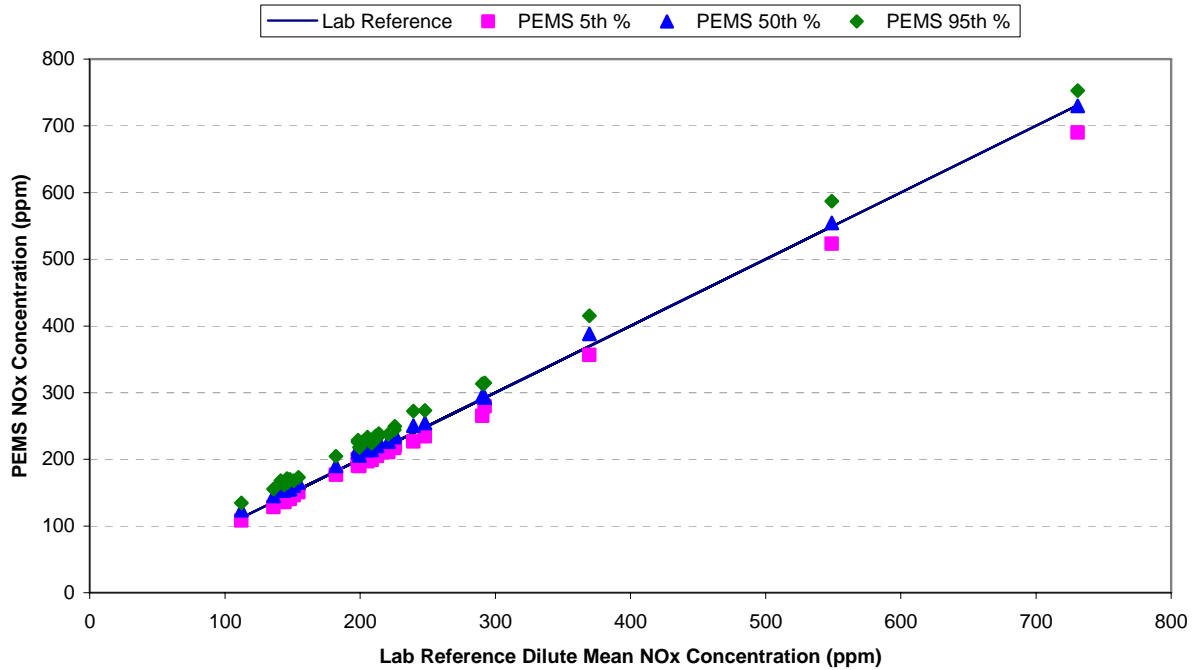


FIGURE 62. ENGINE 1 POOLED PEMS NTE NO_x CONCENTRATION DATA VERSUS THE LABORATORY MEAN

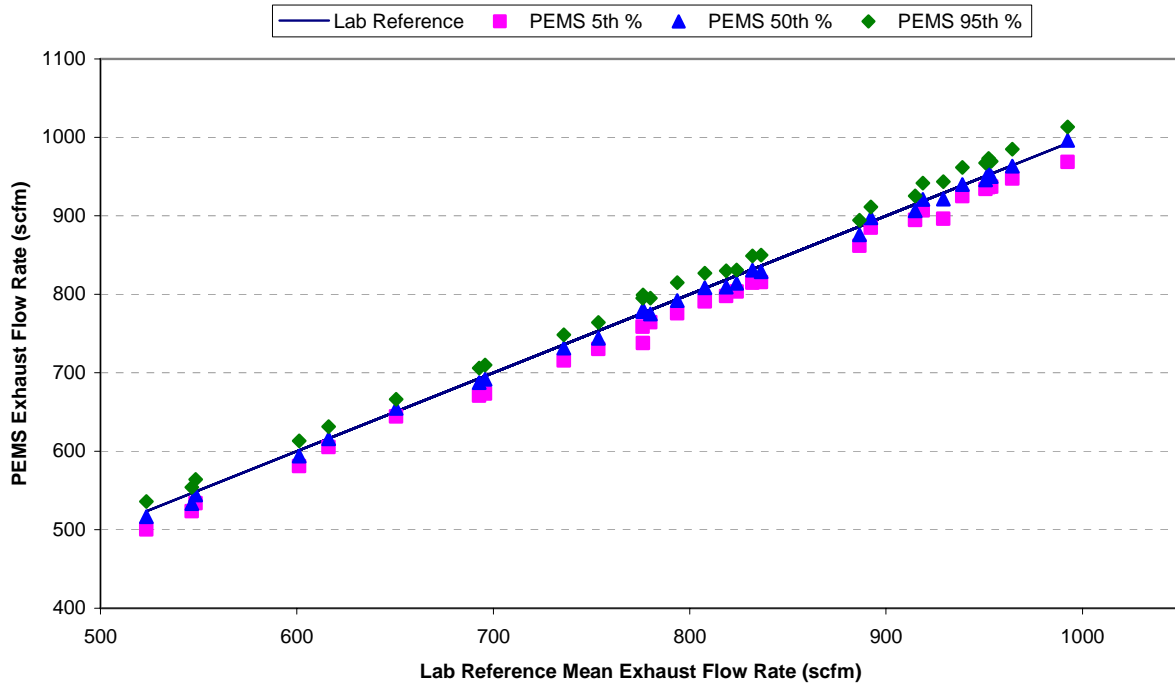


FIGURE 63. ENGINE 1 POOLED PEMS NTE EXHAUST FLOW RATE DATA VERSUS THE LABORATORY MEAN

4.5.2 Engine 2 Caterpillar C9 Transient

Engine 2 transient testing was conducted at the completion of the initial steady-state testing. A process similar to Engine 1 transient testing was followed to perform the Engine 2 repeat NTE testing. The transient data generated with the Caterpillar C9 had no outlying data due to engine operation, and the full data set was therefore used without alteration to generate the Engine 2 transient error surfaces.

Similar to Engine 1, the repeatability of the laboratory and engine was evaluated by comparing the brake-specific NO_x emission results over the 20 NTE cycle repeats. Figure 61 shows the pooled BS NO_x emission results for each of the 30 NTE events, while Figure 64 shows the BS NO_x MAD value for the 30 events. The MAD was generally around 0.04 g/(hp-hr), similar to Engine 1.

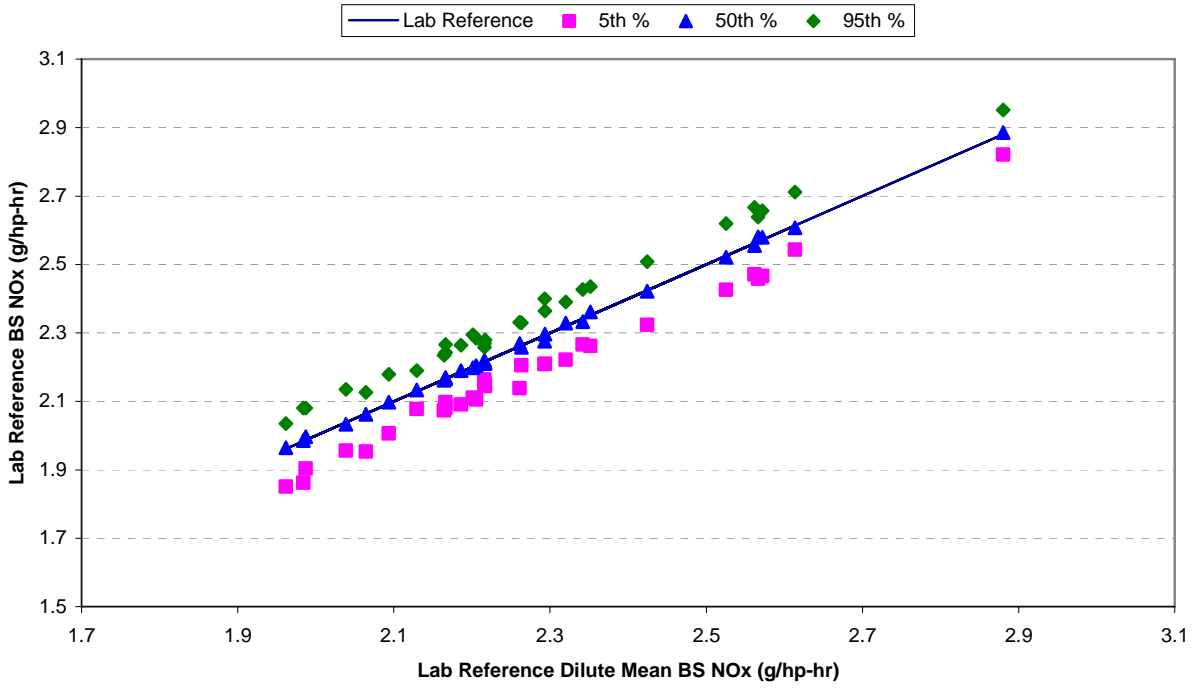


FIGURE 64. ENGINE 2 POOLED TRANSIENT TEST NTE BRAKE-SPECIFIC NO_x RESULTS

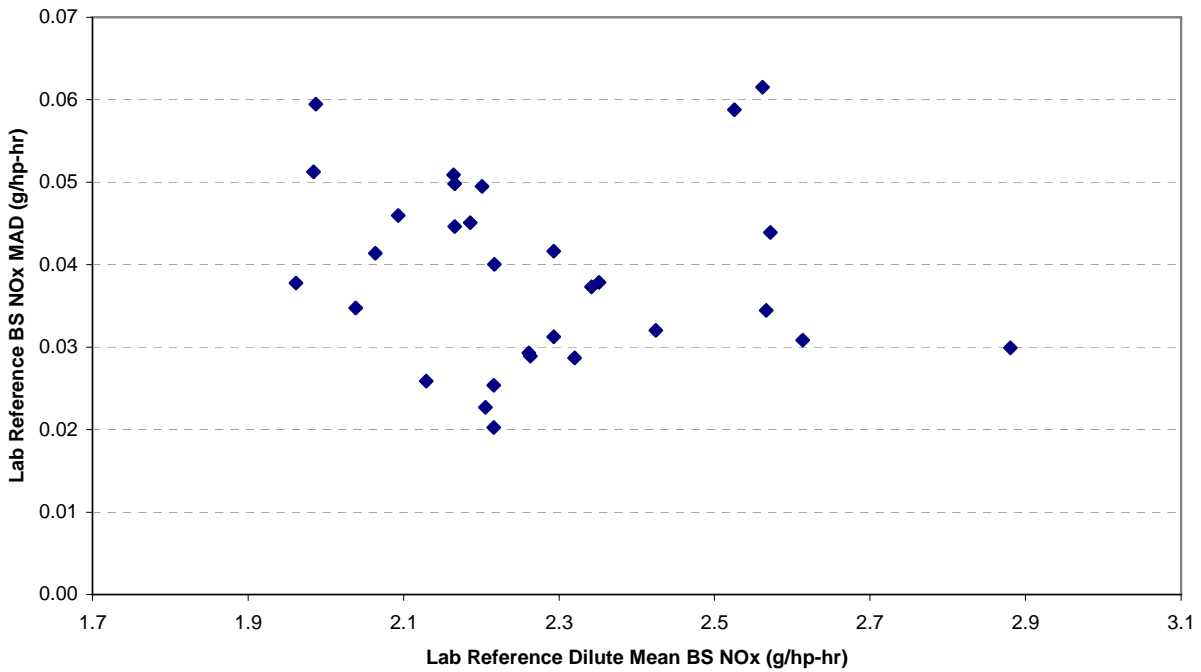


FIGURE 65. ENGINE 2 POOLED TRANSIENT TEST NTE BRAKE-SPECIFIC NO_x MAD RESULTS

Although the laboratory data was not used to generate the transient error surfaces, plots were generated to compare the PEMS performance with the laboratory measurements. As seen in Figure 66, the PEMS median NO_x concentrations during transient testing were bias slightly low. As shown in Figure 67, the positive exhaust flow rate bias observed during Engine 2 steady-state testing was also evident during transient testing.

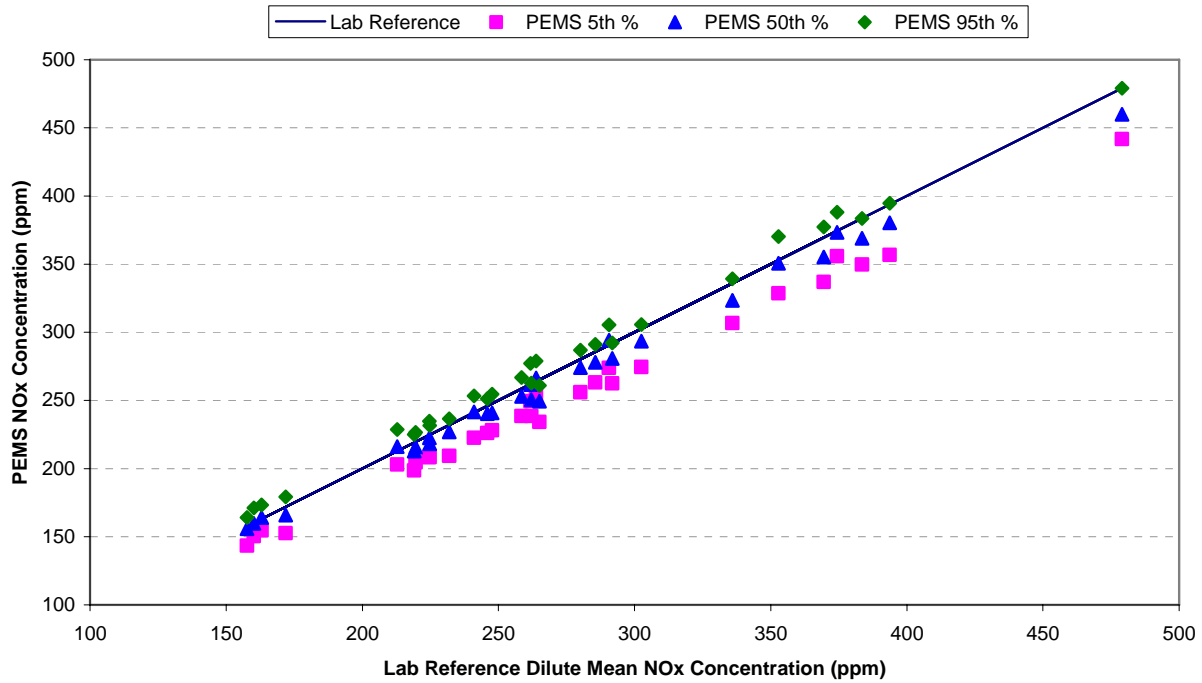


FIGURE 66. ENGINE 2 POOLED PEMS NTE NO_x CONCENTRATION DATA VERSUS THE LABORATORY MEAN

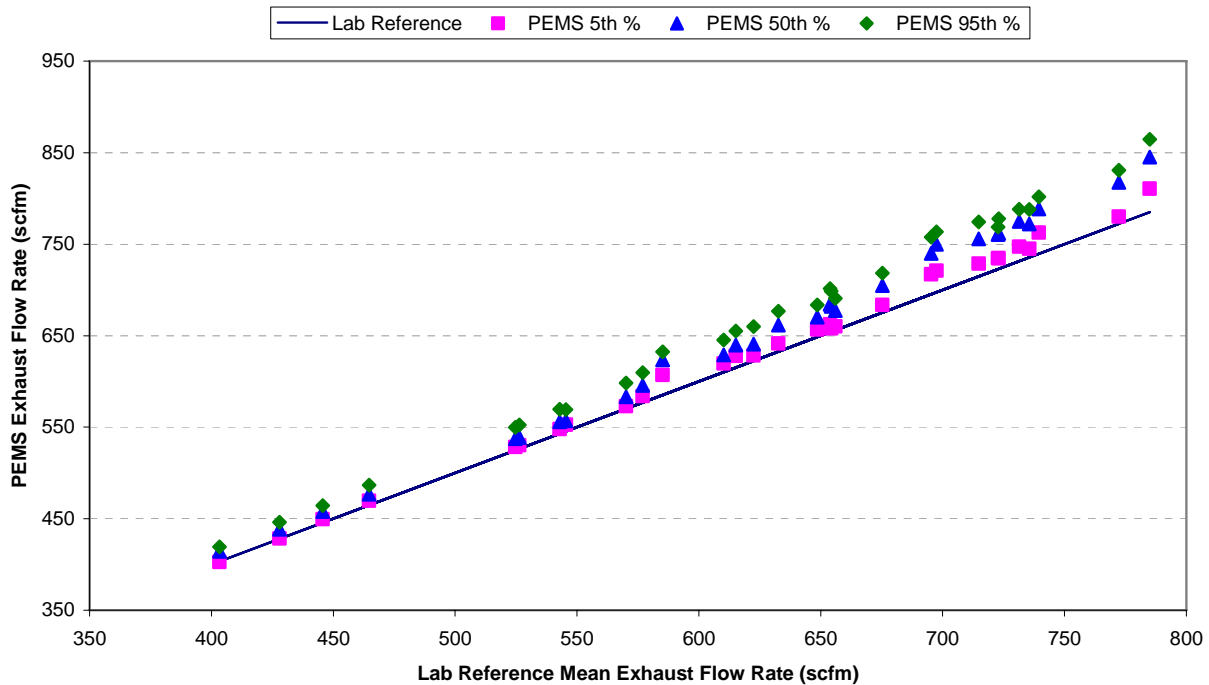


FIGURE 67. ENGINE 2 POOLED PEMS NTE EXHAUST FLOW RATE DATA VERSUS THE LABORATORY MEAN

4.5.3 Engine 3 International VT365 Transient

Engine 3 transient testing was conducted at the completion of the steady-state testing. A process similar to Engine 1 and 2 transient testing was followed to perform the Engine 3 repeat NTE testing. The transient data generated with the International VT365 had no outlying data and was used without alteration to generate the Engine 3 transient error surfaces. Engine 3 transient data showed higher variance than Engines 1 and 2. This was expected due to the higher variance observed during steady-state repeat testing. For the Engine 3 data, both laboratory and PEMS indicated a wider distribution of measurements with no obvious outlying points.

Similar to Engine 1 and 2, the repeatability of the laboratory and engine was evaluated by comparing the brake-specific NO_x emission results over the 20 NTE cycle repeats. Figure 68 shows the pooled BS NO_x emission results for each of the 30 NTE events, while Figure 69 shows the BS NO_x MAD values for the 30 events. The Engine 3 MAD was at about 0.06 g/(hp·hr), with some events over 0.1 g/(hp·hr). The higher variability of Engine 3 can be attributed to real engine-out variations in NO_x concentration. These values are roughly 3 to 5 percent of the 2.0 g/(hp·hr) threshold.

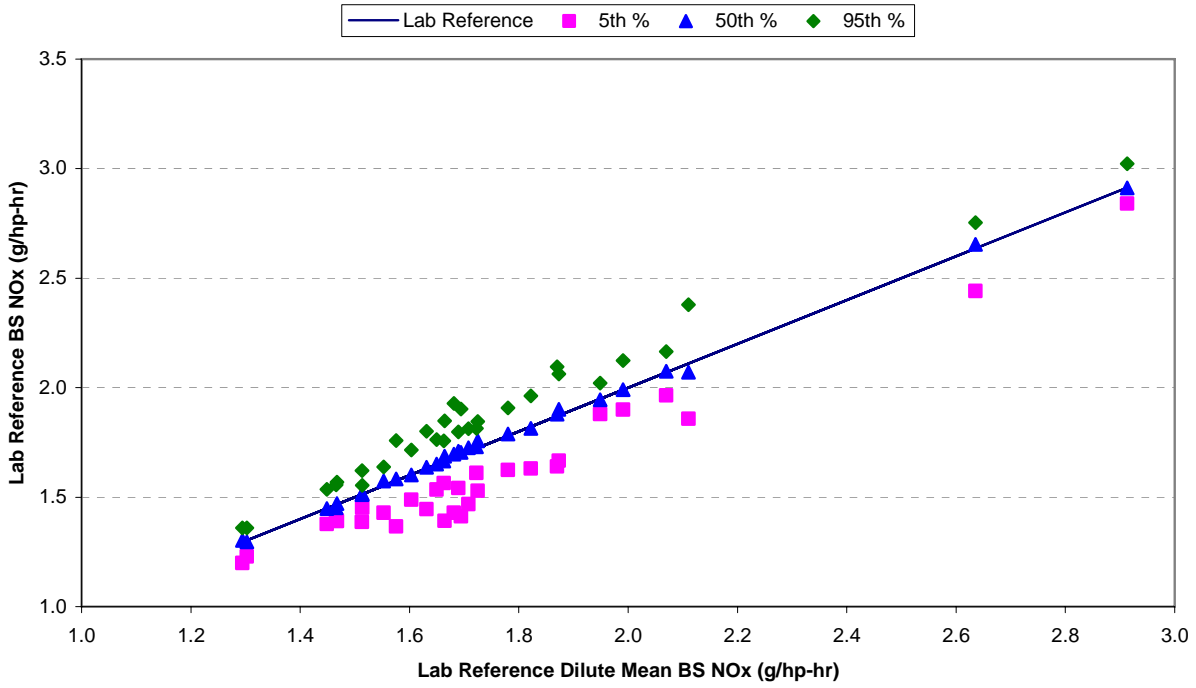


FIGURE 68. ENGINE 3 POOLED TRANSIENT TEST NTE BRAKE-SPECIFIC NO_x RESULTS

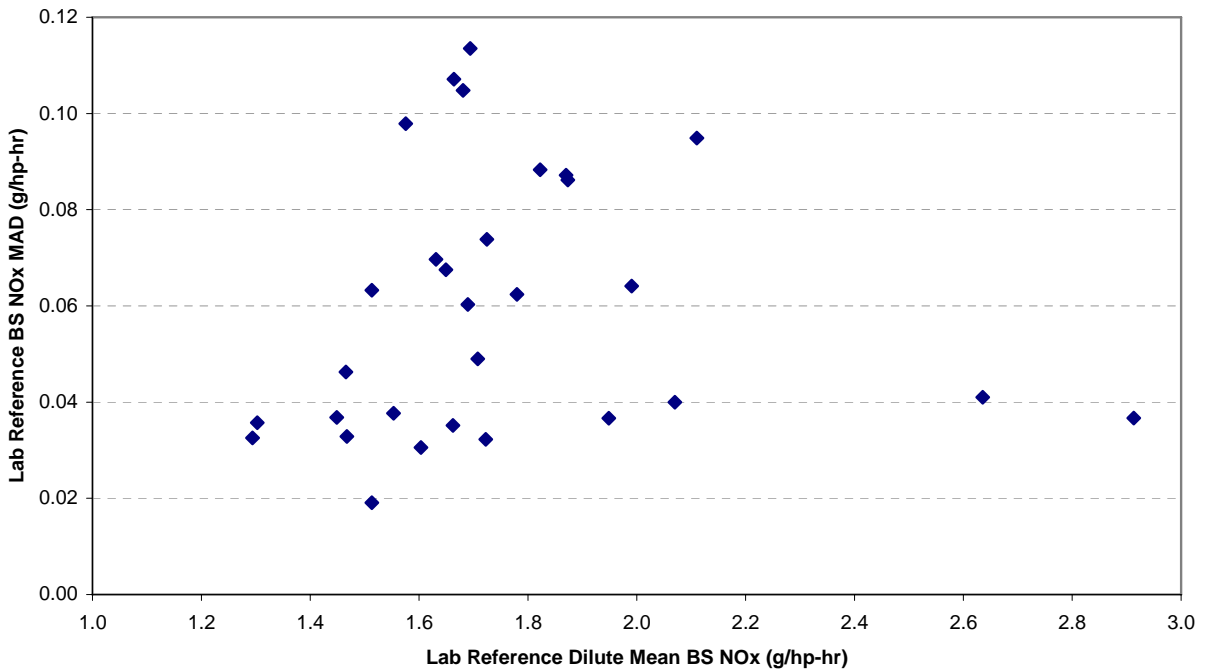


FIGURE 69. ENGINE 1 POOLED TRANSIENT TEST NTE BRAKE-SPECIFIC NO_x MAD RESULTS

Although not used for transient error surface generation, the PEMS concentration and exhaust flow rate data was plotted versus the laboratory mean values for comparative purposes. Figure 70 shows the pooled PEMS NO_x concentration data for each of the 30 repeated NTE events. Interestingly, the low NO_x concentration bias observed during Engine 3 steady-state testing did not manifest in the transient data set, with all median PEMS NO_x values near the mean laboratory concentrations. As shown in Figure 71, the positive exhaust flow bias was apparent in both the steady-state and transient testing.

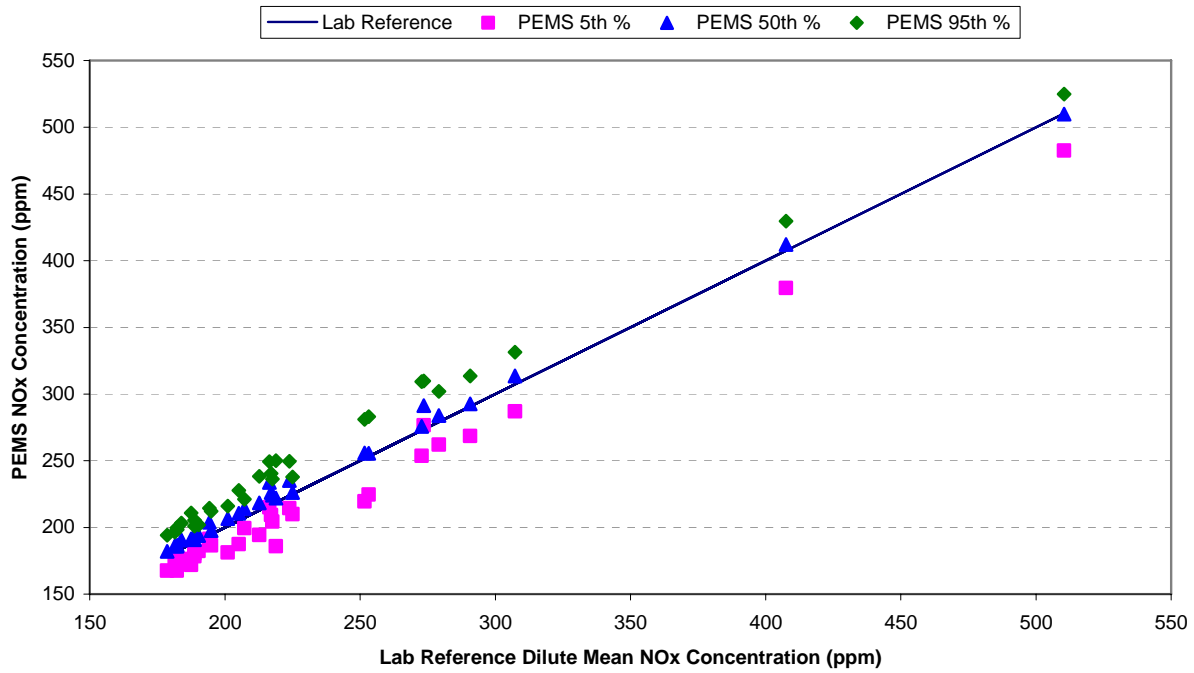


FIGURE 70. ENGINE 3 POOLED PEMS NTE NO_x CONCENTRATION DATA VERSUS THE LABORATORY MEAN

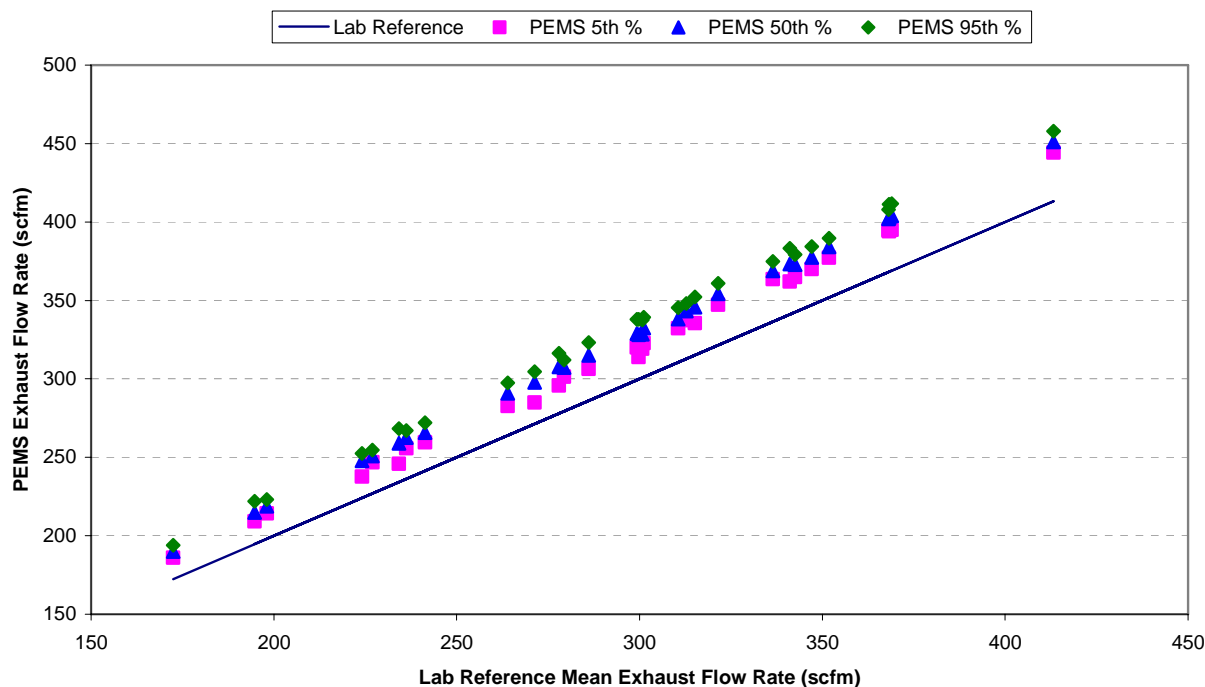


FIGURE 71. ENGINE 3 POOLED PEMS NTE EXHAUST FLOW RATE DATA VERSUS THE LABORATORY MEAN

4.5.4 Transient Concentration Error Surface Generation

A number of steps were taken to generate transient error surfaces from the raw NTE data. The concentrations used to generate the error surfaces were calculated as flow-weighted averages over each NTE event. In other words, the continuous concentration data was multiplied by the corresponding exhaust flow rate. The NTE event averaged concentration times exhaust flow rate values were then divided by the NTE event averaged exhaust flow rate. The calculation of flow-weighted concentrations was performed to capture transient variances that were pertinent to emission calculations. For example, gaseous concentrations were multiplied by the exhaust flow rate when calculating emission results, therefore, flow-weighting the concentration results captured a more representative variance measurement.

As stated previously, the data generated by the laboratory during transient testing was not used to generate the transient error surfaces. The averaged, flow-weighted PEMS concentrations were pooled. The 5th, 50th, and 95th percentile values, as well as the MAD values, were calculated for each of the 30 NTE events. To calculate the precision of the NTE testing, the 5th and 95th percentile flow-weighted PEMS concentration values were subtracted from the 50th percentile values. These delta values were then used to populate the transient error surface, with the 95th percentile minus the 50th percentile concentration values set to the 95th percentile error values and the 5th percentile minus the 50th percentile concentrating values set to the 5th percentile error values. The 50th percentile error value was set to zero for all NTE events.

Figure 72 shows the PEMS 5th and 95th percentile error values plotted against the PEMS median flow-weighted NO_x concentration for Engine 1.

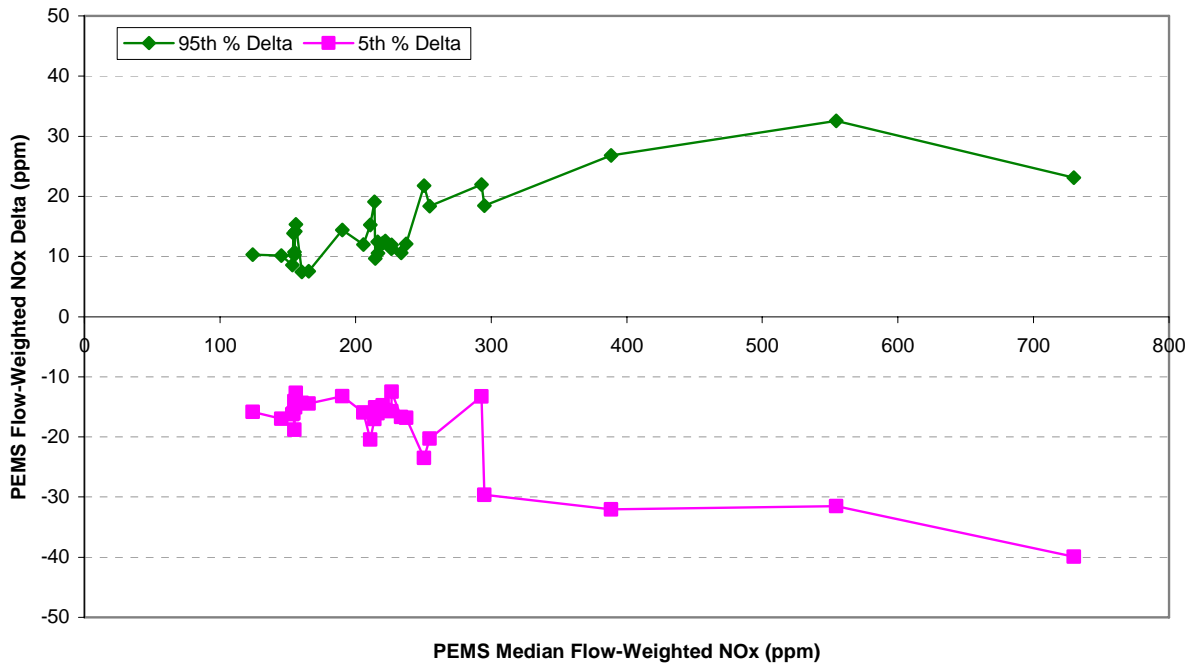


FIGURE 72. ENGINE 1 UNCORRECTED TRANSIENT FLOW-WEIGHTED NO_x CONCENTRATION ERRORS

A final task performed on the transient error surfaces was to correct the variance measured during transient testing for the variance already recorded during steady-state testing. The variance correction was performed to insure steady-state precision errors were not double-counted in the Model. The transient error surfaces would represent only the incremental precision error associated with transient operation. The PEMS concentration MAD values from both transient and steady-state testing were used to calculate a scaling factor. This scaling factor was then used to shrink or collapse the transient error surfaces to remove the steady-state variance. Figure 73 shows the transient and interpolated steady-state MAD values with the resulting scaling factor. As anticipated, the transient MAD values were generally larger than the steady-state MAD values.

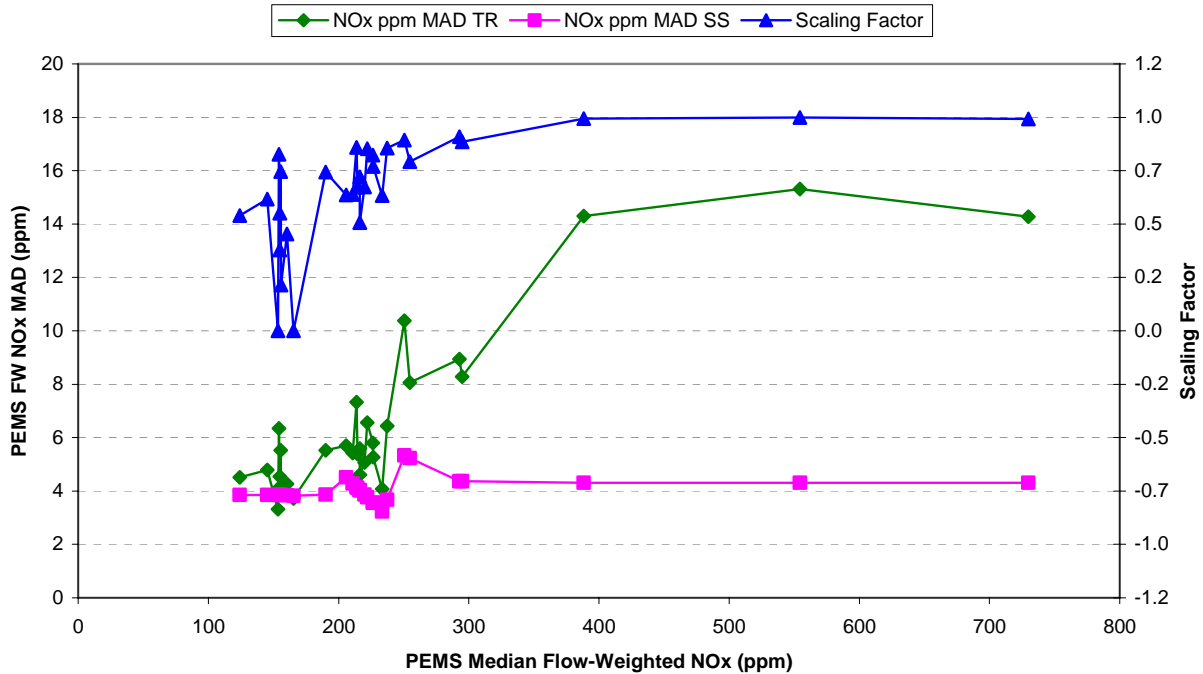


FIGURE 73. ENGINE 1 TRANSIENT AND INTERPOLATED STEADY-STATE MAD VALUES WITH RESULTING SCALING FACTOR

To calculate the scaling factor, the steady-state PEMS MAD data was linearly interpolated to generate steady-state MAD values at the 30 median PEMS concentration values measured during NTE testing. In other words, the 10 steady-state PEMS concentration median and MAD values were used with the 30 transient PEMS concentration median and MAD values to linearly interpolate steady-state MAD values at the 30 transient median values. Next, the 30 interpolated steady-state MAD values were compared to the 30 transient MAD values. If the steady-state interpolated MAD value was greater than the transient MAD value, the scaling factor was set to zero. Otherwise, the scaling factor was calculated using the following equation.

$$Scaling_Factor = \frac{\sqrt{MAD_{trans}^2 - MAD_{ss}^2}}{MAD_{trans}}$$

The final corrected NO_x concentration error surface for Engine 1 is shown in Figure 74. With most scaling factor values greater than zero, the corrected error surface looks similar to the uncorrected surface shown in Figure 72.

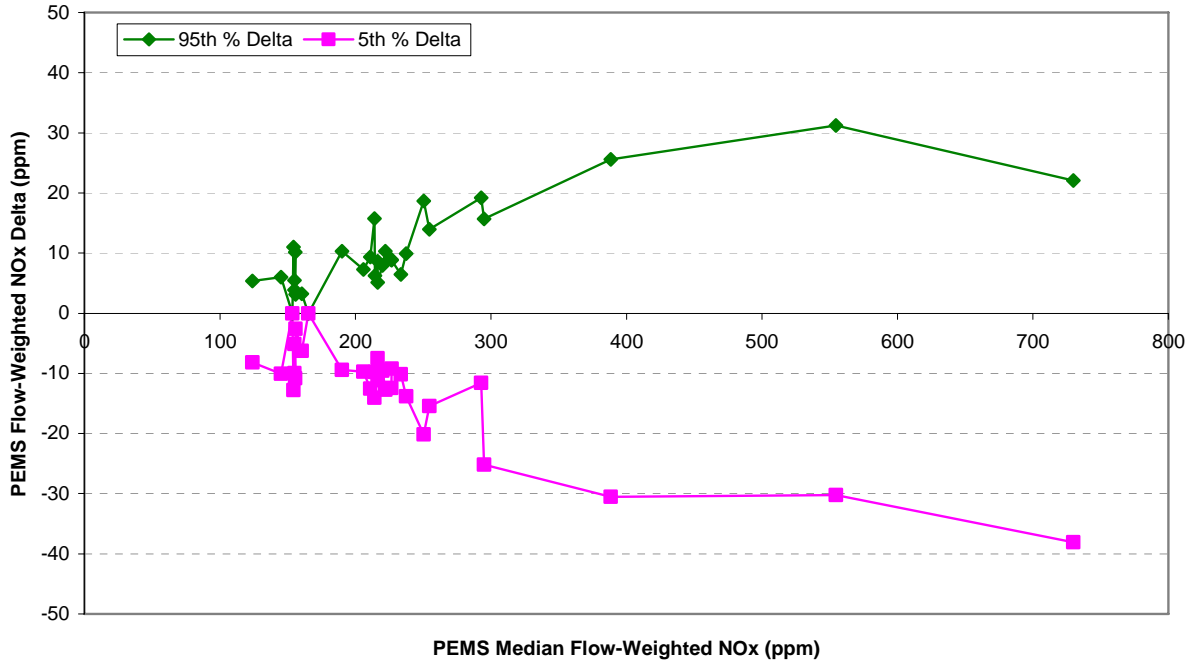


FIGURE 74. ERROR SURFACE FOR ENGINE 1 TRANSIENT FLOW-WEIGHTED NO_x CONCENTRATION

A scaling factor of zero indicated the steady-state variance was greater than the transient variance and mathematically collapsed the transient error surface value to zero. Although not anticipated when designing the experiment, the steady-state variance was sometimes larger than the transient variance, especially with Engine 3. Shown in Figure 75, the steady-state MAD values were generally larger than the transient MAD values for Engine 3, resulting in zero level scaling factors.

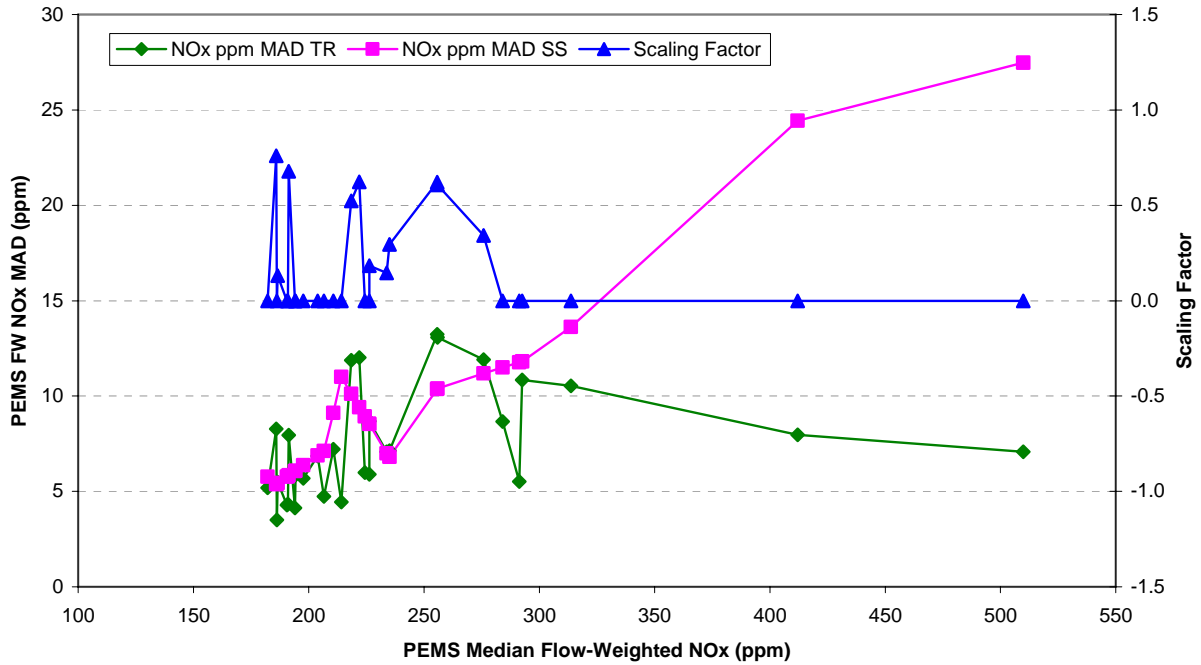


FIGURE 75. ENGINE 3 TRANSIENT AND INTERPOLATED STEADY-STATE MAD VALUES WITH RESULTING SCALING FACTOR

Figure 76 shows the final corrected NO_x concentration transient error surface for Engine 3. Due to the steady-state variance correction and zero level scaling factors, approximately two thirds of the error surface points were zero values. This was problematic, especially when the Engine 3 data was combined with data from the other two engines.

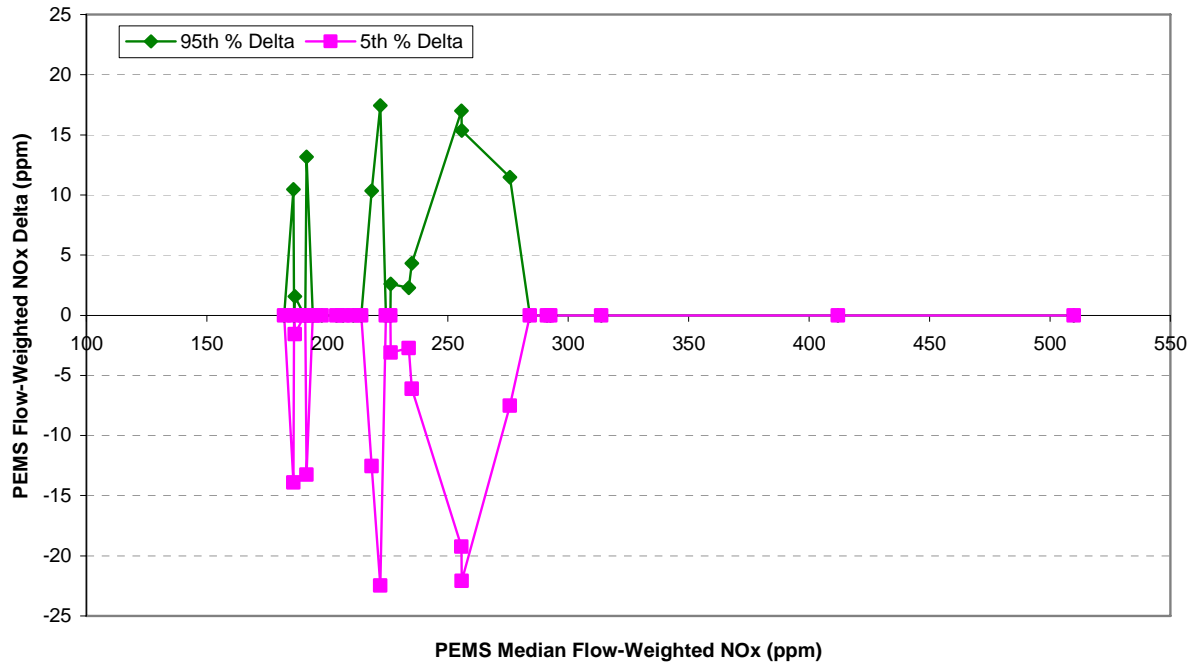


FIGURE 76. ERROR SURFACE FOR ENGINE 3 TRANSIENT FLOW-WEIGHTED NO_x CONCENTRATION

Similar to the steady-state error surfaces, the final transient error surfaces were generated by pooling the Engine 1, 2, and 3 final error surface data. Also similar to the final steady-state error surfaces, the combined transient error surfaces were highly irregular. The unevenness of the transient error surfaces was due to the variability of the transient delta data, the steady-state variance correction, and error differences between the three engines. Shown in Figure 77, the final NO_x concentration error surface for transient testing was jagged and unpredictable.

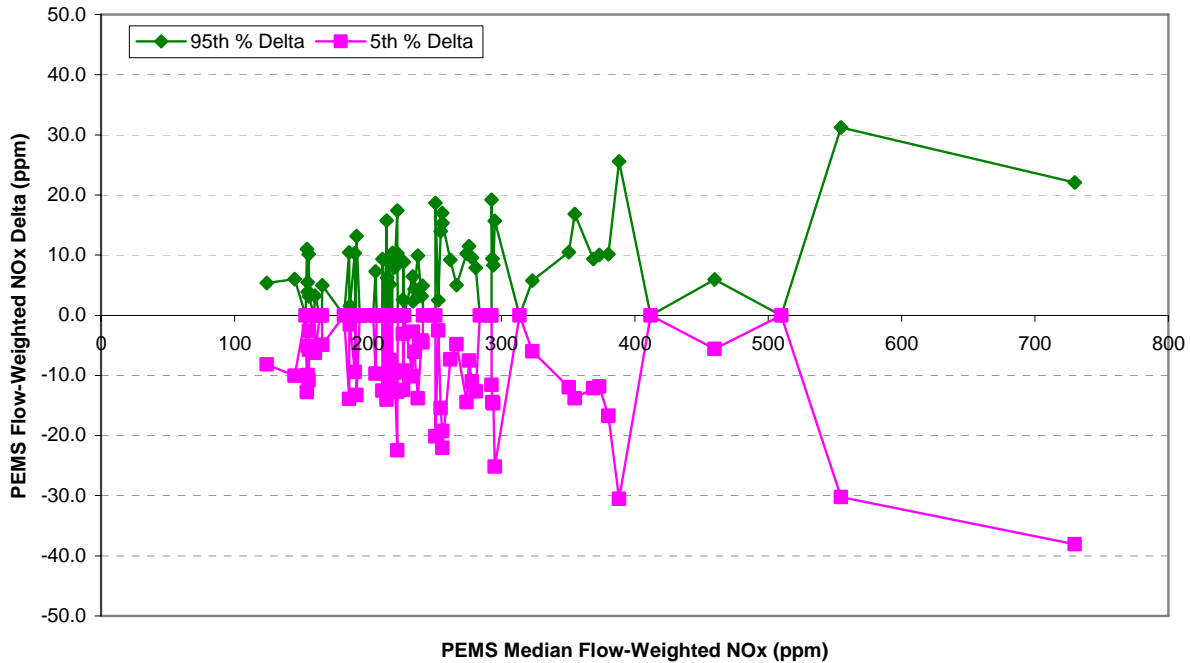


FIGURE 77. FINAL ERROR SURFACE FOR TRANSIENT FLOW-WEIGHTED NO_x CONCENTRATION

The transient error data was reviewed at the December 2006 Steering Committee meeting in San Antonio. The Steering Committee suggested removing high variability Engine 3 steady-state test points from the transient MAD correction to avoid collapsing the transient error surfaces to zero. Unfortunately, the suggested correction had little impact on the transient error surfaces, as illustrated in Figure 77. The Steering Committee decided the highly irregular error surfaces may lead to erratic Model behavior. Additional analysis was performed by Steering Committee members on the transient error data. The additional analyses confirmed that the data for Engines 1 and 2 behaved as expected with larger transient MAD values as compared to steady-state MAD values. Engine 3 generally showed a reversed trend, which was not expected. It was initially proposed that Engine 3 data be eliminated from the final transient error surfaces. The Steering Committee arrived at a solution that allowed most of the data from the three engines to be used in the error surface generation, as originally intended in the Test Plan. The solution was proposed in late December, and accepted by the Steering Committee on December 18, 2006 via email response.

Steady-state and transient MAD data for the three engines was pooled into a single data set. Selected outlier points were removed from the Engine 3 steady-state data set which showed extremely large variations, as described earlier. In addition, some of the Engine 1 data points were removed where the transient concentrations had been above all measured steady-state concentrations for the engine, thus requiring extrapolation to generate steady-state MAD values. The remaining data was pooled and root-mean-square (RMS) MAD values were generated for both steady-state and transient data sets. The MAD values were compared to generate a transient

effect MAD. The steady-state MAD was subtracted from the transient MAD, and 5th and 95th percentile values for the error surface were then generated using the following equations:

$$MAD_{te,rms} = \sqrt{MAD_{trans,rms}^2 - MAD_{ss,rms}^2}$$

$$Delta_{5thPercentile_i} = Concentration_i * (-1.65 * MAD_{te,rms})$$

$$Delta_{95thPercentile_i} = Concentration_i * (+1.65 * MAD_{te,rms})$$

The 1.65 term in the equations above is the factor from a normal distribution which covers 90 percent of the distribution around the median. This data analysis method essentially produces an error surface which is a line, and makes the assumption that the transient errors are dominated by span errors. This assumption is generally supported by the data.

The error surfaces for CO, NO_x, and CO₂ were all processed in this manner. In the case of CO, the MAD_{trans,rms} was actually less than the MAD_{ss,rms}, indicating that steady-state errors were still larger than transient errors. Therefore, the CO transient error surface was set to zero for all values. The final error surface values are given in Table 50 below. These values each describe a pair of lines, with values at any given emission concentration determined via linear interpolation.

TABLE 50. FINAL GASEOUS TRANSIENT ERROR SURFACE DELTAS

Pollutant / Concentration	Percentiles ¹		
	5 th	50 th	95 th
NO _x	delta, ppm		
0	0.00	0.00	0.00
3000	-72.03	0.00	72.03
CO ₂	delta, %		
0	0.0000	0.0000	0.0000
20	-0.1904	0.0000	0.1904
¹ Based on sampling with normal distribution			

The transient concentration error surfaces are sampled normally in the Model, once per NTE event. Concentration errors are linearly interpolated between x-axis points on the error surface based on the reference NTE event concentrations and the error surface median x-axis concentration levels. Transient error surface data can be found in Appendix G for all transient testing.

4.5.5 Transient Flow Meter Error Surface Generation

Transient flow meter error surfaces were generated as described in the Transient Concentration Error Surface Generation section of the report. Weighting was not performed with the PEMS EFM data. The PEMS exhaust flow data was pooled and the 5th, 50th, and 95th

percentile values were calculated for each of the 30 repeated NTE events. Variance errors were calculated by taking the difference between the 95th and 50th percentiles and the 5th and 50th percentiles of the pooled PEMS exhaust flow rate data. Finally, the steady-state variance was removed from the transient data set by calculating and applying a scaling factor based on the interpolated steady-state MAD calculation and the transient MAD values.

The exhaust flow rate error surfaces were normalized as a percent of the maximum EFM flow rate. Engine 1, 2, and 3 used the 5, 4, and 3-inch diameter EFMs, respectively. As specified in the Sensors Inc. EFM user manual, the maximum flow rates for the 3-inch, 4-inch, and 5-inch EFMs were 600, 1100, and 1700 scfm, respectively. Shown in Figure 78 through Figure 80 are the transient exhaust flow error surfaces for engine 1, 2, and 3, respectively. Zero values indicated the steady-state variability was larger than the transient variance at that exhaust flow rate level.

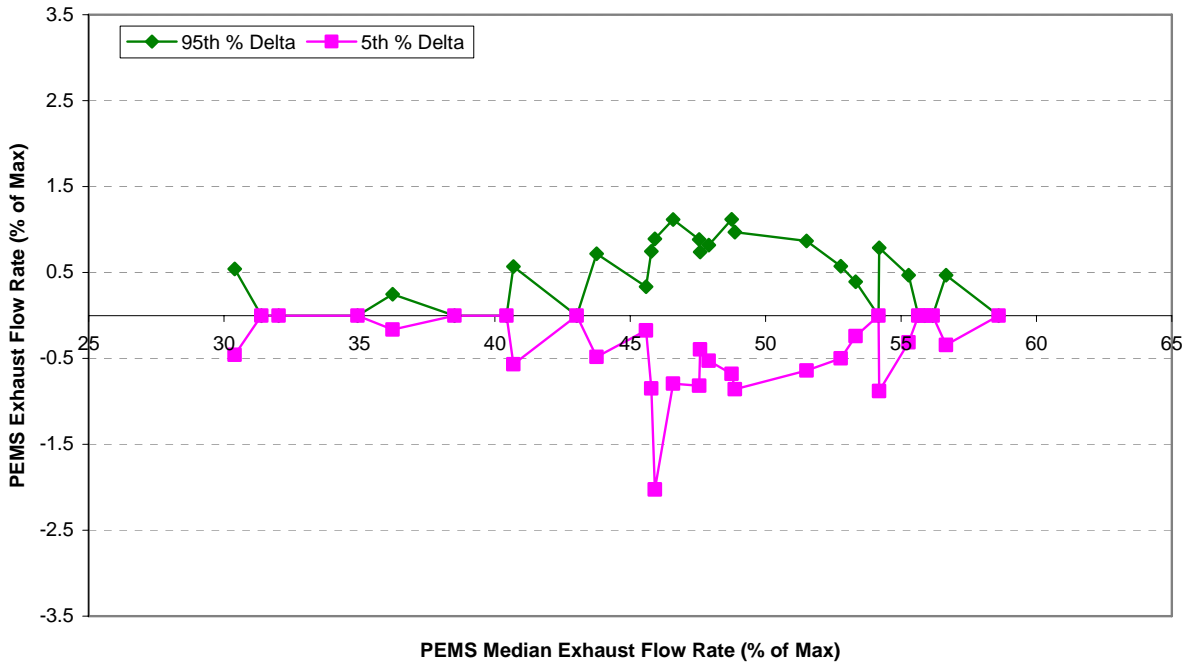


FIGURE 78. ERROR SURFACE FOR ENGINE 1 TRANSIENT EXHAUST FLOW RATE

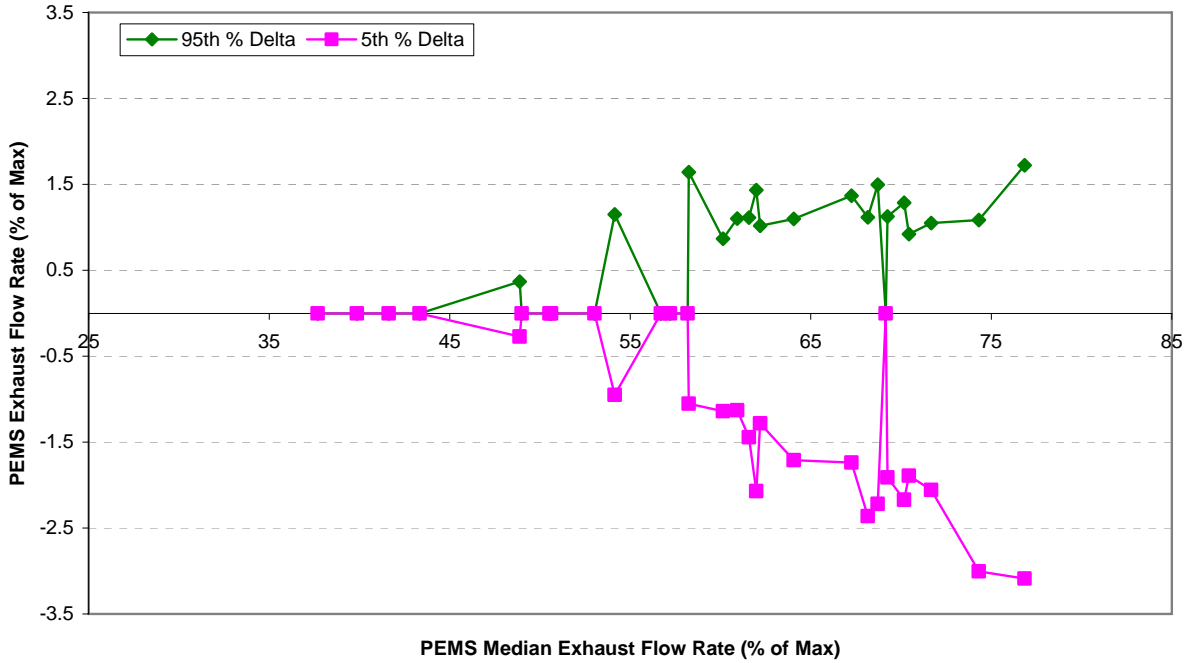


FIGURE 79. ERROR SURFACE FOR ENGINE 2 TRANSIENT EXHAUST FLOW RATE

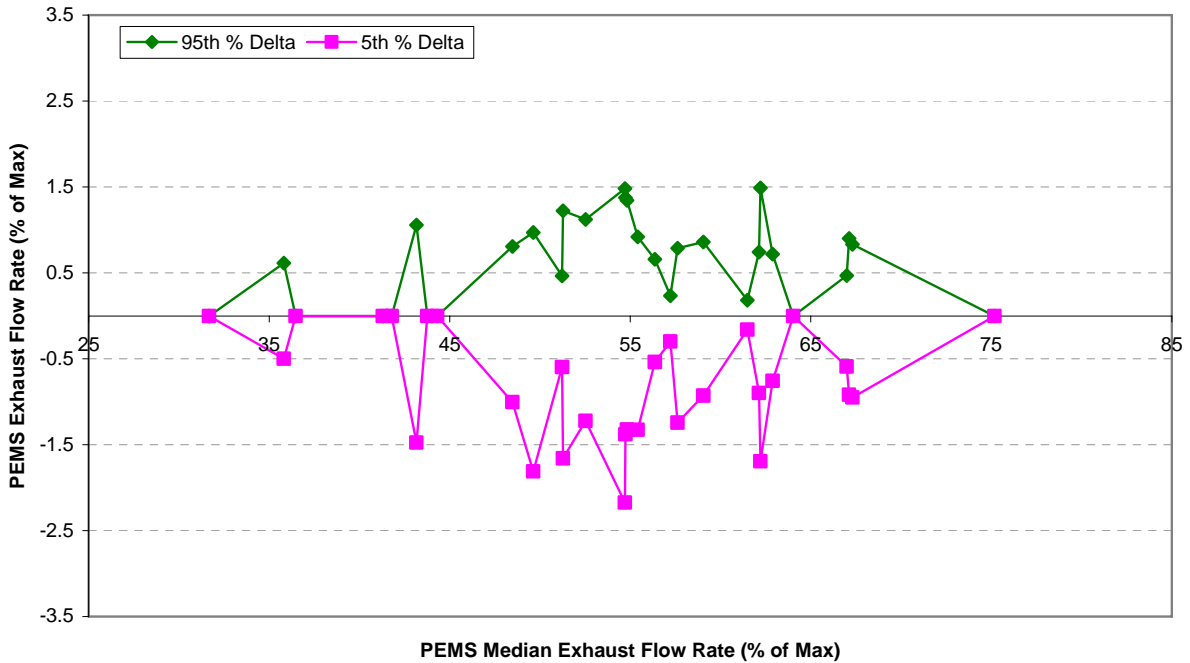


FIGURE 80. ERROR SURFACE FOR ENGINE 3 TRANSIENT EXHAUST FLOW RATE

The combined, final exhaust flow rate error surface is shown in Figure 81. As with the other final transient error surfaces, the final exhaust flow rate error was jagged. The unevenness of the transient error surface was due to the variability of the transient delta data, the steady-state variance correction, and error differences between the three engines.

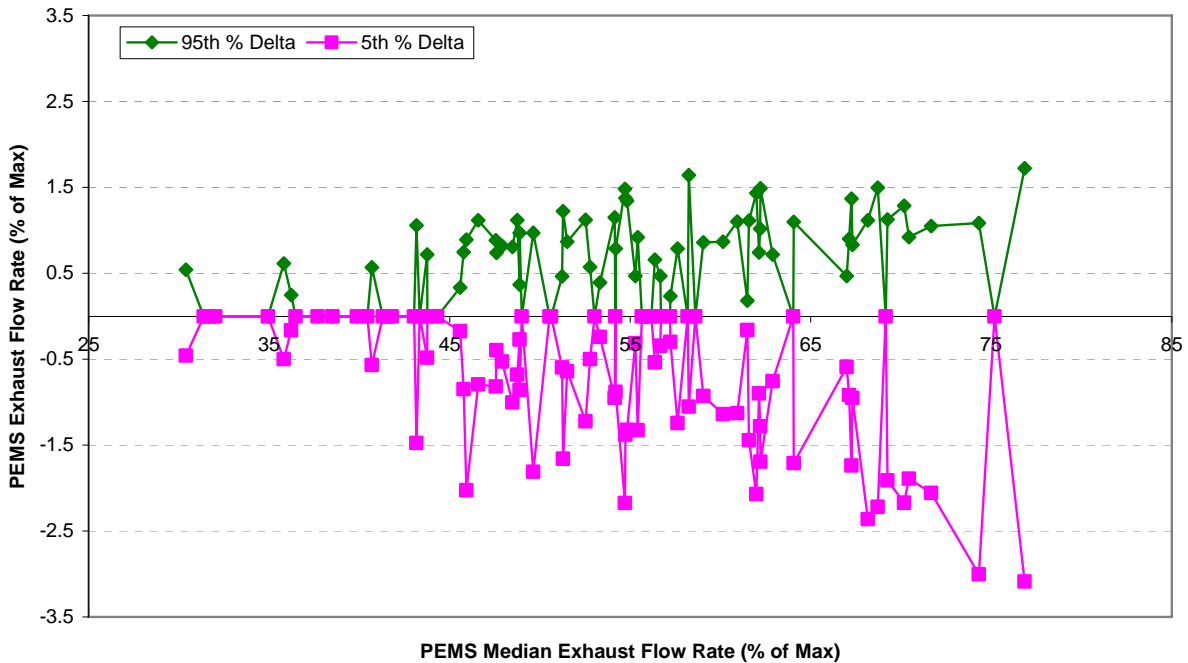


FIGURE 81. FINAL ERROR SURFACE FOR TRANSIENT EXHAUST FLOW RATE

The Steering Committee did not elect to re-analyze the transient EFM error surface data, and therefore this error surface was used in the Model as shown in Figure 81.

4.5.6 Transient Dynamic Error Surface Generation

The dynamic error surfaces were generated to capture the variance of ECM-broadcast speed and fuel rate measurements over the repeated 32-second NTE events. In addition, the variance of the interpolated torque and BSFC from the 40-point maps was evaluated. The generation of the dynamic error surfaces followed the procedure described in the Transient Concentration Error Surface Generation section of the report and summarized in the Transient Flow Meter Error Surface Generation section of the report. The dynamic error surface generation process, however, did not include a steady-state variance correction. A steady-state variance correction was not needed because the parameters evaluated for the dynamic error surfaces did not have error surfaces for steady-state testing. Therefore, there was no concern of double counting dynamic errors.

ECM-broadcast fuel rate was calculated as an average over the NTE event and received no weighting. The dynamic fuel rate error surface was normalized using the engine’s maximum fuel rate, which was taken as the highest fuel rate recorded during the 40-point mapping

procedure. The Detroit Diesel Series 60 recorded a maximum fuel rate of 98 L/h, the Caterpillar C9 measured 75 L/h, and the International VT365 delivered a maximum fuel rate of 46 L/h. The final dynamic fuel rate error surface is shown in Figure 82. The fuel rate variance errors were generally less than 1.0 % of the engine’s maximum fuel rate.

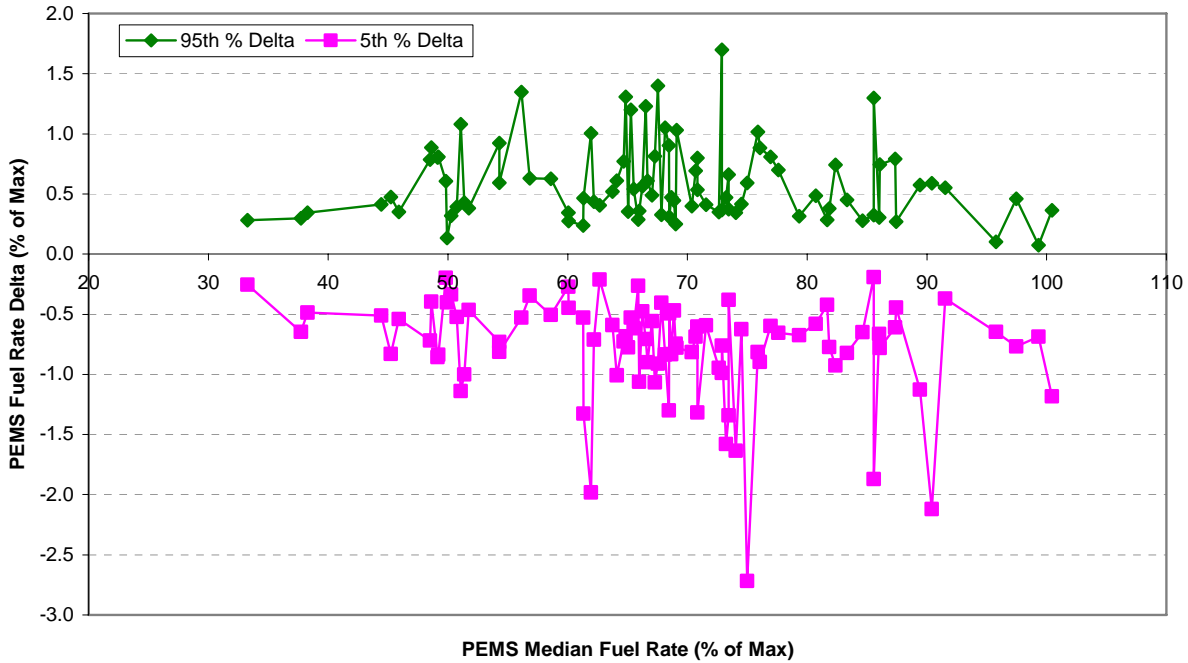


FIGURE 82. FINAL ERROR SURFACE FOR DYNAMIC ECM FUEL RATE

ECM-broadcast speed was weighted using the interpolated torque from the 40-point maps. The interpolated torque weighted ECM speed was calculated as an average over each NTE event. The ECM speed error surface was normalized with n_{lo} speed equal to 0.0 % and n_{hi} speed equal to 100 %. Table 51 shows the n_{lo} and n_{hi} speed definitions for each engine.

TABLE 51. NLO AND NHI SPEED DEFINITIONS FOR ENGINES 1, 2, AND 3

	nlo Speed (rpm)	nhi Speed (rpm)
Engine 1 DDC	1014	2129
Engine 2 CAT	1099	2320
Engine 3 INT	1198	2839

The final combined dynamic ECM speed error surface is shown in Figure 83. The ECM-broadcast speed showed little variation over the 20 repeated transient tests. The majority of the 5th and 95th percentile error terms were less than 0.2 % of normalized speed.

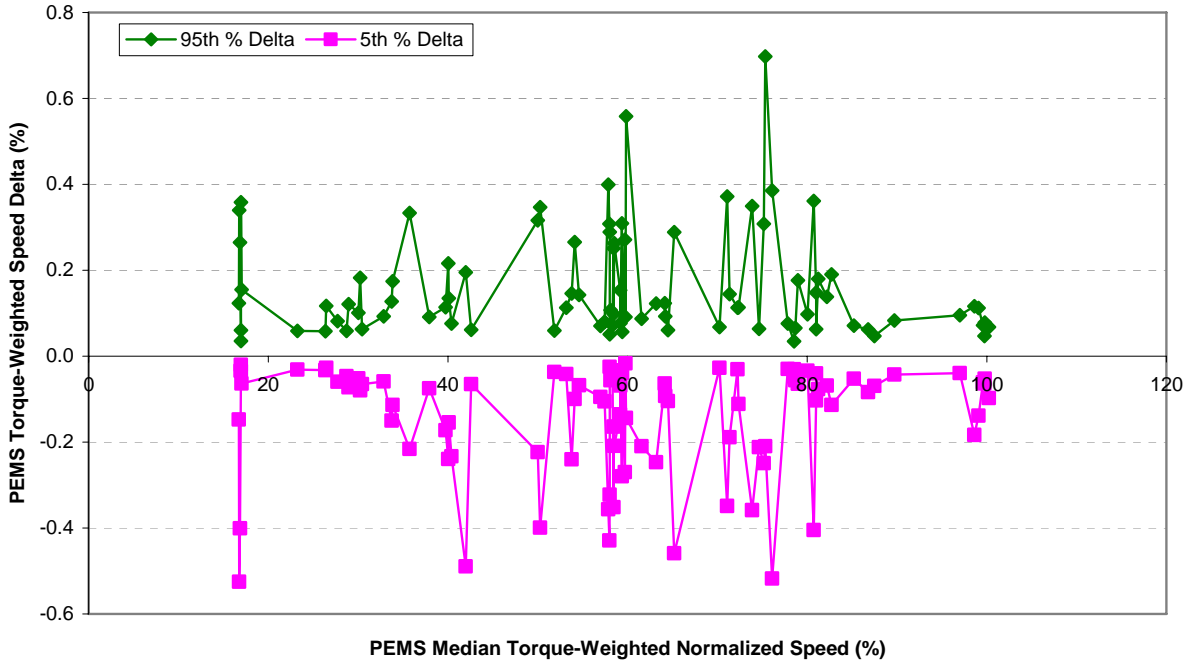


FIGURE 83. FINAL ERROR SURFACE FOR DYNAMIC ECM SPEED

Interpolated torque from the 40-point map was weighted using ECM-broadcast speed. The ECM speed-weighted interpolated torque was calculated as an average over each NTE event. The interpolated torque error surface was normalized as a percent of peak torque. Peak torque measured during the lug curve tests at SwRI was 2195 N·m for Engine 1, 1464 N·m for Engine 2, and 681 N·m for Engine 3. The final ECM speed-weighted interpolated torque error surface is shown in Figure 84. Most variance errors were less than 1.0 % of peak torque for all engines.

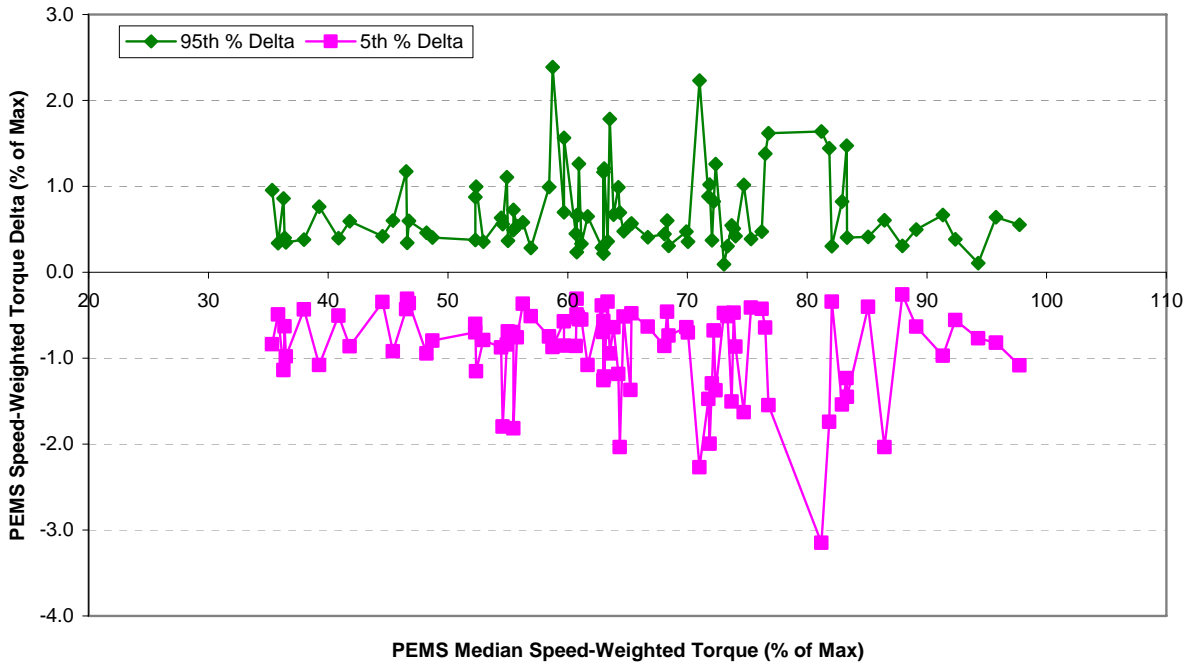


FIGURE 84. FINAL ERROR SURFACE FOR DYNAMIC INTERPOLATED TORQUE

Interpolated BSFC from the 40-point map was weighted using ECM-broadcast fuel rate. ECM fuel rate-weighted interpolated BSFC was calculated as an average over each NTE event. Figure 85 shows the final dynamic interpolated BSFC error surface. Similar to the other dynamic error surfaces, BSFC variability over the repeated NTE events was low, with most variance errors less than 1.0 g/(kW·hr).

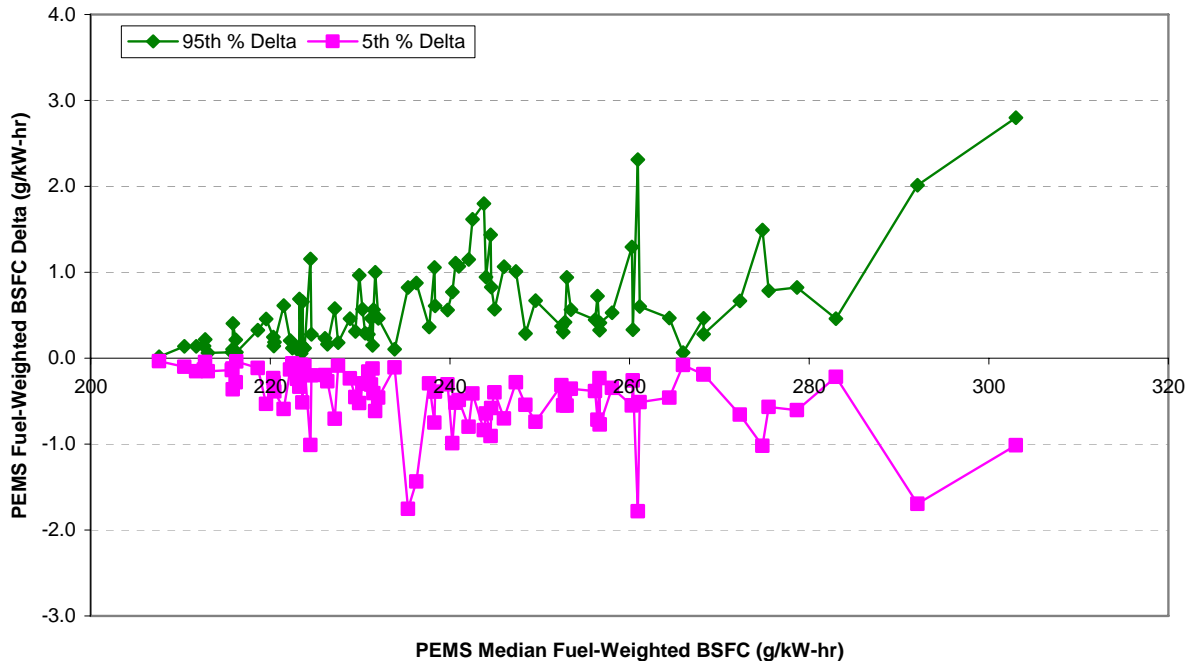


FIGURE 85. FINAL ERROR SURFACE FOR DYNAMIC INTERPOLATED BSFC

4.6 Interacting Parameters - Warm-Up Test Error Surface

The warm-up tests were conducted to evaluate ECM-broadcast torque and map errors due to variations in oil viscosity, fuel temperature, oil temperature, and coolant temperature. Because independently controlling these parameters was difficult, cold start tests were performed to cumulatively estimate these ECM errors as the engine passed from cold to stable operating temperatures. The errors associated with ECM fuel rate and ECM speed translated into torque and BSFC errors through the 40-point map interpolation process. Warm-up tests were performed on each of the three engines. The Detroit Diesel Series 60 and International VT365, both EGR engines, were cooled to ambient temperature, approximately 18 °C, prior to the warm-up test. The Caterpillar C9 was cooled to 0 °C for the warm-up test.

4.6.1 Interacting Parameters - Warm-Up Test Procedure

The original experimental design given in the Test Plan called for a single warm-up test on each engine with the speed and load condition specified by the Steering Committee. The initial choice was a high speed (Speed C), light load condition. However, when the first cycle was run with the DDC engine, the intake manifold temperature never reached the NTE threshold value. This data was decidedly unsatisfactory for the measurement allowance.

Following a discussion of the warm-up test results at the May 24, 2006 meeting in Ann Arbor, the target speed and load was changed by the Steering Committee to Speed C and WOT to insure the event would enter the NTE zone. Because the engine was at maximum operator

demand, actual torque varied throughout the warm-up test. The original intent of the warm-up test was to hold torque constant throughout the cycle, therefore another test was run using Speed C and a lower torque target (although still a high load point). Ultimately, the Steering Committee elected to pool the data from both WOT and part-load tests. This decision was made at the July 27, 2006 meeting in Ann Arbor after reviewing the results from both tests. Similar tests were run for engines 2 and 3.

According to the finalized procedure, two 30-minute warm-up tests were run with each engine. One test was run at C-speed and WOT, while the other test was performed at C-speed and part load. The target torque values during the part load tests were set just low enough to achieve constant torque control throughout the 30-minute warm-up cycle. The part load tests were conducted by starting the engine and promptly ramping to the target speed and load, which was held constant for the remainder of the cycle. The WOT tests were similar to the part load tests, but the engines were ramped to the target speed and WOT. Using the recorded ECM speed and fuel rate with the 40-point torque and BSFC maps, the interpolated torque and BSFC were compared to the laboratory reference values. Although the 40-point BSFC map used fuel consumption measurements from the laboratory fuel flow meter, BSFC calculated from the dilute emission measurements was used as the lab reference for the warm-up tests. The laboratory fuel flow meter system has an inherent time lag that would have resulted in incorrect reference BSFC measurements during the transient warm-up test. In addition, there was also concern with the fuel flow measurement accuracy due to the density change of the fuel during the warm-up process.

In order to achieve cold start temperatures of 0° C, an insulating box was built to enclose the Caterpillar engine. The partially built enclosure is shown in Figure 86, while the completed insulating box is shown in Figure 87. The enclosure surrounded both the Caterpillar engine as well the exhaust after treatment system. A re-circulating alcohol refrigeration system was used with dry ice to achieve a heat sink with temperature below 0° C.



FIGURE 86. CATERPILLAR C9 ENGINE PARTIALLY ENCLOSED IN THE INSULATING BOX PRIOR TO THE WARM-UP TEST



FIGURE 87. CATERPILLAR C9 ENGINE FULLY ENCLOSED IN THE INSULATING BOX PRIOR TO THE WARM-UP TEST

4.6.2 Interacting Parameters - Warm-Up Data Analysis

The Test Plan did not initially include a method for how the data from the Interacting Parameters Warm-up test would be used to generate an error surface. There was considerable Steering Committee discussion of the course of several months regarding the appropriate

analysis of the data. The methodology was tentatively established following the completion of Engine 1 testing, and was later adjusted with the completion of Engine 2 testing.

A number of concerns had to be balanced in the treatment of the warm-up data. On the one hand, it was necessary to attempt to use the warm-up data to capture a wide range of possible variations in engine fluid temperatures and viscosities. This was complicated by the fact that the test was designed to explore cold temperatures and therefore only elevated viscosity levels. On the other hand, there was a desire not to include any data that was not representative of operation in the NTE zone.

An additional complicating factor was due to the interpolation of torque and BSFC from the 40-point maps using ECM-broadcast speed and fuel rate. Because the warm-up cycle target speed and load set points did not match a mode from the 40-point maps, a certain amount of interpolation bias error was included in the data. This error was accounted for elsewhere in the Model; therefore it was necessary to remove the bias due to the interpolation process prior to generating error surfaces.

The data analysis method finally approved by the Steering Committee is described below. Torque is used in the example, but the same methodology is also applied to BSFC. First, the continuous data for the warm-up test was assembled, including the interpolated torque which was generated via post processing. To remove the interpolation bias, data near the end of the warm-up test, where all of the engine parameters had stabilized, was examined to generate an average stabilized value for both the reference torque (from the laboratory torque-meter) and the interpolated torque (based on ECM-broadcast speed and fuel rate). These two values were compared in order to evaluate the interpolation bias error. This offset was then applied to the continuous interpolated torque data set, shifting the data set to equalize the stabilized interpolated torque values with the reference torque-meter values. An example of this bias correction is illustrated in Figure 88.

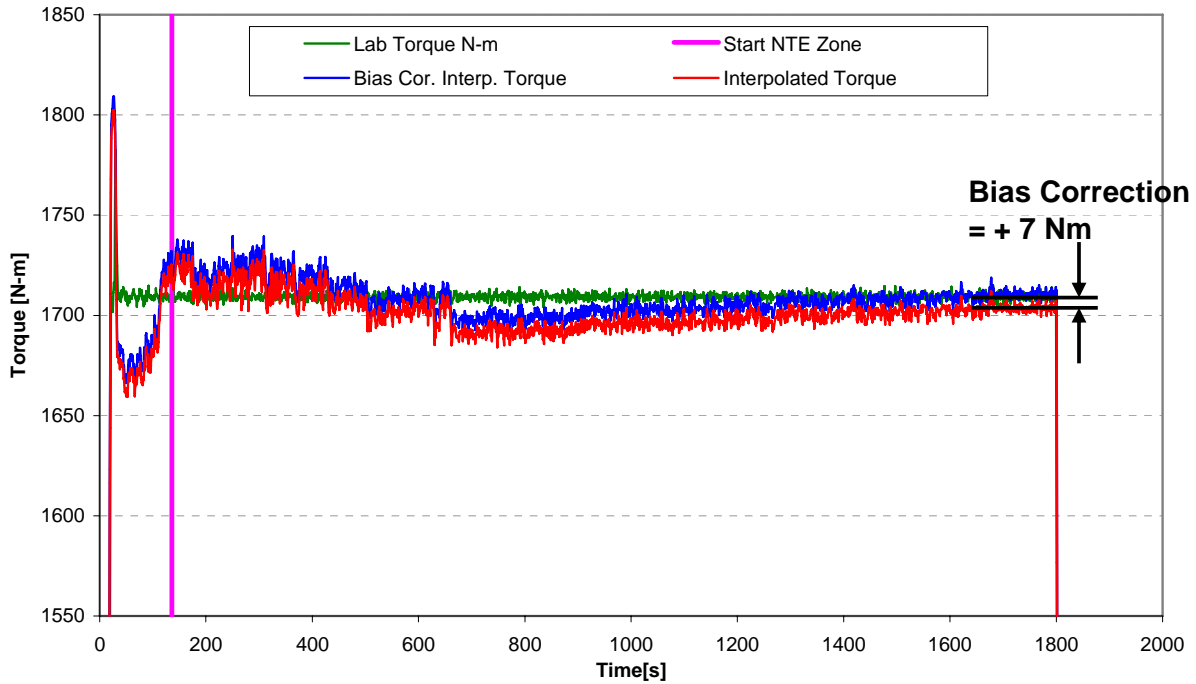


FIGURE 88 EXAMPLE OF WARM-UP TEST BIAS CORRECTION, DDC ENGINE PART LOAD TEST

Once the interpolation bias correction was complete, the temperature data was examined to determine when the NTE zone was entered. These entry points were based on the NTE zone criteria given in CFR 40 Part 86.1370-2007. The primary trigger common to all three engines was the aftertreatment outlet temperature, which must be 250 °C or higher. For Engines 1 and 3, which were EGR equipped, additional trigger points are defined for engine coolant temperature (ECT) and intake manifold temperature (IMT), as given in CFR 40 Part 86.1370-2007. An example of the determination of NTE zone entry for Engine 1 is shown in Figure 89.

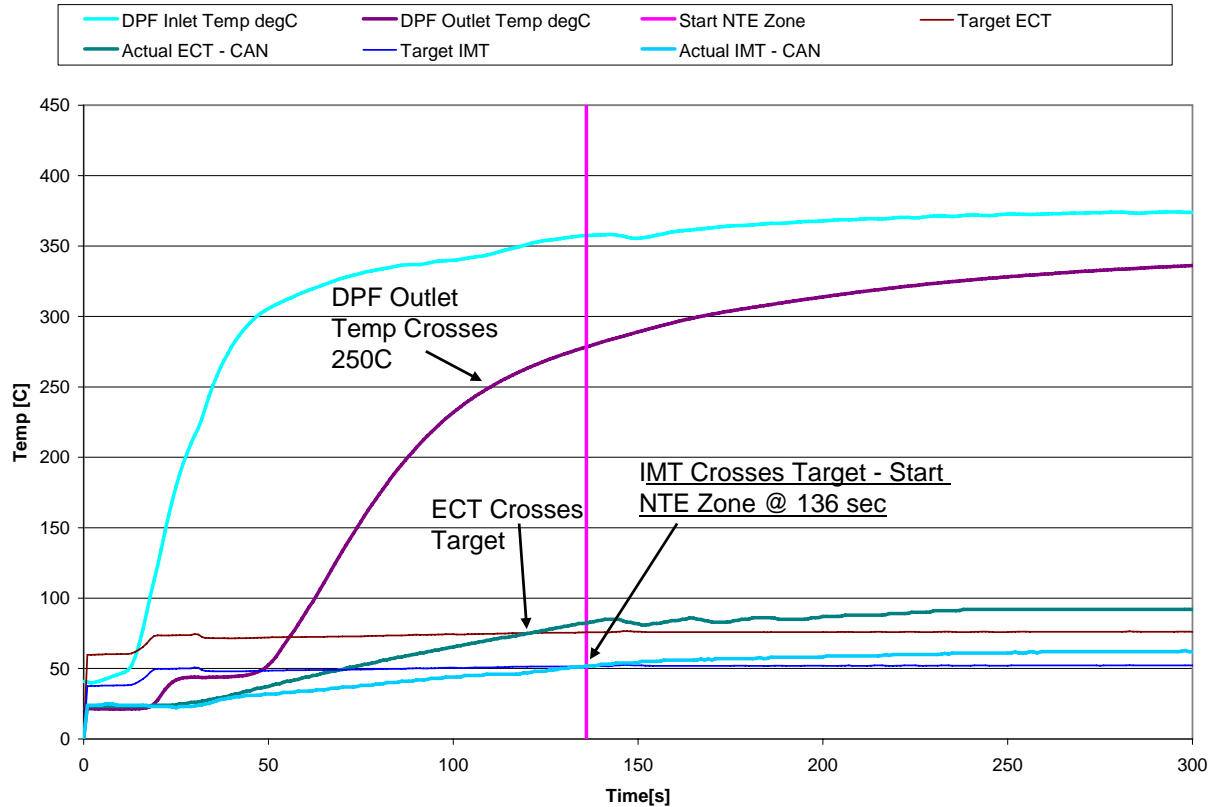


FIGURE 89 EXAMPLE OF DETERMINATION OF NTE ZONE ENTRY FOR WARMUP TEST, DDC ENGINE PART LOAD POINT

The continuous data was then examined to determine the maximum difference between the bias-corrected interpolated torque and the reference torque after entry into the NTE zone. If the difference resulted in a positive delta (interpolated minus reference), the value was set to the 95th percentile delta torque error value. The negative of the same value was set to the 5th percentile error value for that test. If the delta from the data was negative, the value became the 5th percentile for the test, while it's positive, or mirror-image, became the 95th percentile delta. The 50th percentile error values for all warm-up tests were set to zero. Torque was processed as percent of maximum torque, while BSFC was calculated directly in engineering units.

Temperature, torque, and BSFC data is shown for each warm-up test in Appendix H. These plots show temperature profiles related to the NTE zone, bias corrected interpolated torque with laboratory reference torque, as well as bias corrected interpolated BSFC with laboratory reference BSFC.

4.6.3 Interacting Parameters – Warm-Up Error Surface Generation

Using the process outlined above, torque and BSFC errors were calculated for each warm-up test. Table 52 shows the torque deltas, while Table 53 summarizes the BSFC errors. Torque errors for the Detroit Diesel Series 60 and International VT 365 engines were similar.

The Caterpillar C9 engine, with a cold-start temperature near 0 °C, had significantly larger torque deltas. BSFC errors were similar among all engines with the exception of the Caterpillar C9 part load test. The Engine 2 BSFC error was over three times as large as the deltas from the Engine 1 and 3 part load tests.

TABLE 52. WARM-UP TEST TORQUE ERRORS SUMMARY

Engine	Operating Point C-Speed	5th % Torque Error [% Peak Torque]	50th % Torque Error [% Peak Torque]	95th % Torque Error [% Peak Torque]
DDC HHD	WOT	-3.4	0.0	3.4
	78% Peak Torque	-1.2	0.0	1.2
CAT MHD	WOT	-14.2	0.0	14.2
	65% Peak Torque	-11.3	0.0	11.3
INT LHD	WOT	-3.5	0.0	3.5
	73% Peak Torque	-1.7	0.0	1.7
MEAN		-5.9	0.0	5.9

TABLE 53. WARM-UP TEST BSFC ERRORS SUMMARY

Engine	Operating Point C-Speed	5th % BSFC Error [g/kW-hr]	50th % BSFC Error [g/kW-hr]	95th % BSFC Error [g/kW-hr]
DDC HHD	WOT	-4	0	4
	78% Peak Torque	-7	0	7
CAT MHD	WOT	-5	0	5
	65% Peak Torque	-24	0	24
INT LHD	WOT	-6	0	6
	73% Peak Torque	-7	0	7
MEAN		-9	0	9

As decided by the Steering Committee, the mean values of the pooled torque and BSFC deltas were used to create the final interacting parameters error surfaces. Figure 90 shows the final warm-up torque error surface, while the BSFC error surface is shown in Figure 91. The interacting parameters error surfaces are sampled normally and have a single x-axis point. The warm-up deltas will be applied to each torque and BSFC value from the reference NTE events, independent of level.

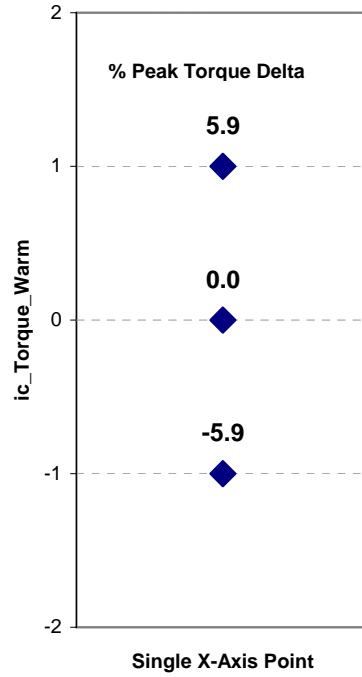


FIGURE 90. ERROR SURFACE FOR INTERACTING PARAMETERS - WARM-UP DELTA TORQUE

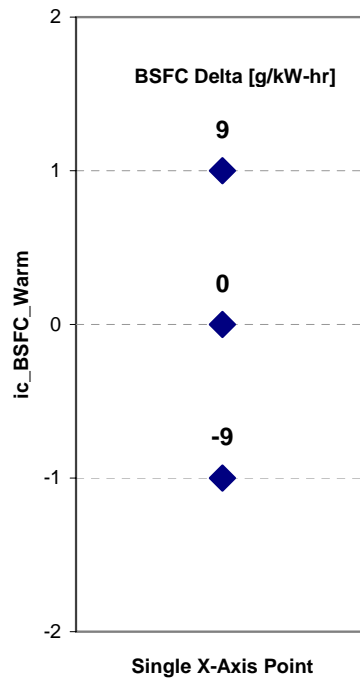


FIGURE 91. ERROR SURFACE FOR INTERACTING PARAMETERS WARM-UP DELTA BSFC

4.7 Torque and BSFC Interacting Parameters - Design of Experiment

The objective of the interacting parameters DOE experiment was to evaluate torque and BSFC map errors due to a number of variable engine parameters. The list of parameters included intake restriction, exhaust restriction, barometric pressure, and charge air cooler outlet temperature. Because the 40-point maps were generated using nominal set points for the parameters listed above, torque and BSFC values from the ECM interpolation would be inaccurate due to engine parameter variations. The purpose of the interacting parameters DOE was to compare the laboratory reference torque and BSFC with the interpolated values under a broad range of engine operation. Ranges of adjustment for each parameter were defined according to Table 54, which was copied from the Test Plan.

TABLE 54. INTERACTING PARAMETERS - DOE ADJUSTMENT GUIDANCE

Parameter	Minimum	Maximum
Intake air restriction	Minimum capable*	Max. allowed by manufacturer*
Exhaust gas restriction	Minimum capable*	Max. allowed by manufacturer*
Barometric pressure	82.7 kPa	105 kPa
Charge air cooler out temperature	Minimum per manufacturer specifications and ambient conditions**	Maximum per manufacturer specifications and ambient conditions**

*Consider removing after treatment to extend range of restrictions

** Assume that a 1 deg. change in ambient temperature corresponds to a 1 deg. change in charge air cooler out temperature

Although the program was run in a test cell capable of simulated high altitudes, the cell could not simulate altitudes lower than approximately 689 feet. Therefore, the maximum achievable barometric pressure was near 99 kPa, the typical atmospheric pressure for San Antonio.

There was considerable Steering Committee discussion about exhaust backpressure set points, because DPFs will be used on all 2007 engines. A final decision was reached on the March 27, 2006 conference call. The Steering Committee agreed that the backpressure set points should represent the minimum backpressure with a clean DPF installed, and the maximum backpressure with a dirty DPF. That maximum was defined as the highest level of backpressure the engine control system would allow before triggering an active regeneration based on DPF differential pressure. SwRI was directed to obtain these values from the engine manufacturers for each test engine.

The interacting parameter DOE test was performed on Engine 1 and Engine 3 only. For each engine, SwRI worked with the engine manufacturers and the Steering Committee to define appropriate adjustment ranges according to the guidance given in Table 54. A Design of Experiment (DOE) test matrix (half factorial with resolution IV, 4 factors and 1 center point) was used, resulting in nine test points. In addition, a tenth point was added by SwRI representing the standard laboratory conditions used for steady-state and transient testing. In some cases, the

standard conditions were not at the center point of the adjustment range. The additional tenth point was not originally intended as part of the error surface generation, but was to be used for diagnostic and information purposes. The generic DOE test matrix is given in Table 55, while specific set points used for each engine are given later in this section.

TABLE 55. INTERACTING PARAMETERS - DOE TEST MATRIX

Run #	Intake Air Restriction	Exhaust Restriction	Barometer [kPa]	Inlet Air Temp [degC]
1 - BL	Center	Center	99.0	24
2	Center	Center	90.7	24
3	Min Possible	Max Dirty DPF	82.6	29
4	Max Allowed	Min Clean DPF	82.6	29
5	Min Possible	Min Clean DPF	99.0	37
6	Max Allowed	Max Dirty DPF	99.0	37
7	Max Allowed	Min Clean DPF	99.0	Min Possible
8	Min Possible	Max Dirty DPF	99.0	Min Possible
9	Min Possible	Min Clean DPF	82.6	Min Possible
10	Max Allowed	Max Dirty DPF	82.6	Min Possible
1 - Min Possible Inlet Air Temp = 9°C to 10°C 2 - Charge Air Cooler set point is Inlet Air Temp + Manufacturers' allowed temperature rise 3 - Barometer of 99.0 kPa is estimated, actual max value varied slightly due to ambient conditions				

In order to allow for a larger range of adjustment of various parameters, the DPFs were removed from the exhaust, and the LFEs used for intake air flow measurement were removed from the intake air ducting.

Each DOE test matrix point was evaluated at five different steady-state load points. The original mode definitions were given in the Test Plan as shown in Table 56.

TABLE 56. TEST PLAN DOE ENGINE OPERATING CONDITIONS

DOE Engine Operating Conditions (%speed, and %torque respectively)				
17%, 32%	100%, 100%	59%, 49%	100%, 32%	100%, 100%

During the course of initial DOE testing on Engine 1, it was observed that the 100 % load points were not repeatable because engine performance at WOT was not consistent across all of the DOE test conditions. Therefore, the WOT points were adjusted to a lower level where the torque set points could be maintained for all DOE tests. The 100 % speed points were also

lowered slightly to 97 % to insure repeatable load points. In addition, the modes were lengthened to 10 minutes to allow for complete stabilization of the fuel flow measurement system. These adjustments were approved by the Steering Committee during the May 23, 2006 meeting in Ann Arbor.

4.7.1 Interacting Parameters - DOE Data Analysis

During the evaluation of the Engine 1 DOE data, a consistent bias was evident in the DOE torque and BSFC deltas for each test mode. Even the DOE test run with nominal engine parameter set points showed a significant bias. It was found that the bias was the result of the interpolation process which was used to generate the ECM torque and BSFC values. Because interpolation error was already included in the error Model, the Steering Committee felt it was necessary to remove the interpolation bias from the DOE error surface data. To address this problem, SwRI proposed that the data from the additional baseline DOE test be used to generate a bias correction for the nine DOE conditions. The correction was applied independently for each of the five test modes. The Steering Committee approved this approach at the May 23, 2006 meeting in Ann Arbor. An example of this bias correction for Engine 1 torque data is given in Table 57. In this example, the bias correction results in an upward shift of 1.1% to all DOE data for Mode 1.

TABLE 57 EXAMPLE OF DOE BASELINE CORRECTION FOR ENGINE 1

DOE Number	Delta Torque (% of Peak Torque)					Baseline Corrected Delta Torque (% of Peak Torque)				
	Mode 1	Mode 2	Mode 3	Mode 4	Mode 5	Mode 1	Mode 2	Mode 3	Mode 4	Mode 5
1-Baseline	-1.1%	-1.8%	-0.3%	0.2%	0.2%	N/A	N/A	N/A	N/A	N/A
2	-1.0%	-1.9%	-0.2%	0.3%	0.9%	0.1%	-0.1%	0.0%	0.1%	0.7%
3	-0.2%	2.1%	0.4%	1.3%	5.0%	0.9%	3.8%	0.6%	1.2%	4.8%
4	-0.6%	-1.1%	-0.1%	0.8%	2.6%	0.5%	0.7%	0.1%	0.6%	2.4%
5	-0.9%	-1.0%	0.2%	0.6%	0.7%	0.2%	0.8%	0.5%	0.4%	0.5%
6	-0.1%	2.4%	1.0%	1.3%	3.9%	1.0%	4.2%	1.2%	1.2%	3.7%
7	-1.2%	-2.4%	-0.3%	-0.2%	-0.6%	-0.1%	-0.6%	-0.1%	-0.4%	-0.8%
8	-1.2%	-1.6%	-0.3%	0.3%	0.4%	-0.1%	0.2%	0.0%	0.1%	0.2%
9	-1.3%	-2.6%	-0.5%	0.0%	0.4%	-0.2%	-0.8%	-0.3%	-0.2%	0.2%
10	-0.4%	1.1%	0.0%	1.1%	3.9%	0.7%	2.9%	0.3%	1.0%	3.7%

4.7.2 Engine 1 Detroit Diesel Series 60 DOE

The DOE matrix was run several times on the Detroit Diesel Series 60 engine as adjustments were made to the test methodology. These changes were in response to the test results and subsequent Steering Committee decisions. The final speed and torque set points used for Engine 1 are given in Table 58. As noted above, these final points were different from those used during the initial DOE run on this engine, due to the need to maintain the same torque level for all DOE test conditions.

TABLE 58. INTERACTING PARAMETERS - DOE SPEED AND TORQUE STEADY-STATE MODE DEFINITION FOR ENGINE 1

	Speed [% NTE]	Torque [% Peak]
Mode 1	17%	43%
Mode 2	17%	94%
Mode 3	59%	49%
Mode 4	97%	32%
Mode 5	97%	71%

The actual engine parameter set points used for the Engine 1 DOE test matrix are given in Table 59. The charge air cooler set point temperatures were based on a specification of 28 °C temperature rise from ambient (inlet air) temperature. For inlet air temperatures at 10 °C, the inlet air dew point temperature was lowered to 7 °C, rather than the standard set point of 15 °C, in order to prevent condensation in the intake air stream.

TABLE 59. INTERACTING PARAMETERS - DOE TEST MATRIX FOR ENGINE 1

DOE Number	Intake Air Restriction ¹ [kPa]	Exhaust Restriction ² [kPa]	CVS Pressure ³ [kPa]	Boost After Temp ⁴ [°C]	Inlet Air Temp ⁵ [°C]	Dew Point Temperature [°C]
1- BL	4.0	17	99	52	24	15
2	4.0	17	91	52	24	15
3	1.5	30	83	57	29	15
4	5.0	12	83	57	29	15
5	1.5	12	99	64	37	15
6	5.0	30	99	64	37	15
7	5.0	12	99	38	10	7
8	1.5	30	99	38	10	7
9	1.5	12	83	38	10	7
10	5.0	30	83	38	10	7

Notes:

1. Minimum achievable intake air restriction was 1.5 kPa
2. Maximum dirty DPF restriction was 30 kPa - Minimum clean DPF restriction was 12 kPa
3. Maximum achievable CVS pressure was 99 kPa
4. Temperature was set based on a fixed offset from the inlet air temperature
5. Minimum achievable inlet air temperature was 10 °C

The final baseline corrected errors for Engine 1 are given in Table 60 and Table 61 for Torque and BSFC, respectively.

TABLE 60. INTERACTING PARAMETERS - DOE ENGINE 1 BIAS CORRECTED TORQUE DELTAS

DOE Number	Baseline Corrected Delta Torque (% of Peak Torque)				
	Mode 1	Mode 2	Mode 3	Mode 4	Mode 5
1-Baseline	N/A	N/A	N/A	N/A	N/A
2	0.1%	-0.1%	0.0%	0.1%	0.7%
3	0.9%	3.8%	0.6%	1.2%	4.8%
4	0.5%	0.7%	0.1%	0.6%	2.4%
5	0.2%	0.8%	0.5%	0.4%	0.5%
6	1.0%	4.2%	1.2%	1.2%	3.7%
7	-0.1%	-0.6%	-0.1%	-0.4%	-0.8%
8	-0.1%	0.2%	0.0%	0.1%	0.2%
9	-0.2%	-0.8%	-0.3%	-0.2%	0.2%
10	0.7%	2.9%	0.3%	1.0%	3.7%

TABLE 61. INTERACTING PARAMETERS - DOE ENGINE 1 BIAS CORRECTED BSFC DELTAS

DOE Number	Baseline Corrected Delta BSFC Fuel Flow (g/kW-h)				
	Mode 1	Mode 2	Mode 3	Mode 4	Mode 5
1-Baseline	N/A	N/A	N/A	N/A	N/A
2	-2	-1	-1	-1	-3
3	-8	-11	-6	-9	-13
4	-5	-3	-3	-3	-8
5	-2	-2	-2	-2	0
6	-7	-14	-8	-9	-10
7	2	3	2	3	3
8	1	-1	0	-1	0
9	1	2	1	1	-1
10	-6	-7	-5	-6	-10

4.7.3 Engine 3 International VT365 DOE

The torque and speed set points used for Engine 3 are given in Table 62. Following the direction of the Steering Committee, the points were selected to be identical to those used for Engine 1. However, due to the shape of the torque curve for Engine 3, Mode 5 could not be run at the desired combination of 97 % NTE speed and 71 % of maximum torque. In order to maintain a consistent load point for use in the error surface, the speed set point was adjusted down to the highest speed at which 71 % percent of maximum torque could be reliably maintained at all DOE conditions. The mode 5 target speed was therefore adjusted from 97 % NTE speed to 85 % NTE speed.

TABLE 62. INTERACTING PARAMETERS - DOE SPEED AND TORQUE STEADY-STATE MODE DEFINITION FOR ENGINE 3

	Speed [% NTE]	Torque [% Peak]
Mode 1	17%	43%
Mode 2	17%	94%
Mode 3	59%	49%
Mode 4	97%	32%
Mode 5	85%	71%

The engine parameter set points used for the Engine 3 DOE testing are given in Table 59. Similar to Engine 1 testing, the engine manufacturer of Engine 3 was consulted to determine appropriate set points for the DOE test matrix.

TABLE 63. INTERACTING PARAMETERS - DOE TEST MATRIX FOR ENGINE 3

DOE Number	Intake Air Restriction¹ [kPa]	Exhaust Restriction² [kPa]	CVS Pressure³ [kPa]	Boost After Temp⁴ [°C]	Inlet Air Temp⁵ [°C]	Dew Point Temperature [°C]
1- BL	3.5	17	99	39	24	15
2	3.5	17	91	39	24	15
3	0.7	24	83	45	29	15
4	3.7	12	83	45	29	15
5	0.7	12	99	52	37	15
6	3.7	24	99	52	37	15
7	3.7	12	99	31	10	7
8	0.7	24	99	31	10	7
9	0.7	12	83	31	10	7
10	3.7	24	83	31	10	7

Notes:

1. Minimum achievable intake air restriction was 0.7 kPa
2. Maximum dirty DPF restriction was 24 kPa - Minimum clean DPF restriction was 12 kPa
3. Maximum achievable CVS pressure was 99 kPa
4. Temperature was set based on a fixed offset from the inlet air temperature
5. Minimum achievable inlet air temperature was 10 °C

The final baseline corrected data for Engine 3 is given in Table 64 and Table 65 for Torque and BSFC, respectively.

TABLE 64. INTERACTING PARAMETERS - DOE ENGINE 3 BIAS CORRECTED TORQUE DELTAS

DOE Number	Baseline Corrected Delta Torque (% of Peak Torque)				
	Mode 1	Mode 2	Mode 3	Mode 4	Mode 5
1-Baseline	N/A	N/A	N/A	N/A	N/A
2	0.5%	2.4%	0.1%	0.3%	0.9%
3	1.9%	4.3%	-0.1%	1.5%	1.2%
4	1.1%	3.7%	-1.1%	1.1%	0.9%
5	0.7%	1.8%	0.4%	0.7%	0.2%
6	1.0%	3.8%	1.4%	1.5%	2.4%
7	0.4%	-1.5%	-0.8%	0.4%	-0.6%
8	1.0%	0.0%	0.6%	0.9%	0.4%
9	1.6%	0.9%	-1.5%	1.0%	-1.2%
10	1.8%	3.9%	-0.8%	1.8%	1.7%

TABLE 65. INTERACTING PARAMETERS -DOE ENGINE 3 BIAS CORRECTED BSFC DELTAS

DOE Number	Baseline Corrected Delta BSFC Fuel Flow (g/kW-h)				
	Mode 1	Mode 2	Mode 3	Mode 4	Mode 5
1-Baseline	N/A	N/A	N/A	N/A	N/A
2	-3	-5	-2	-3	-3
3	-6	-9	-4	-12	-7
4	-3	-7	0	-9	-5
5	-6	-4	-3	-7	-2
6	-8	-9	-10	-14	-11
7	-1	3	2	-3	3
8	-4	0	-4	-8	-2
9	-3	0	3	-7	2
10	-6	-7	-2	-15	-8

4.7.4 Interacting Parameters - DOE Error Surface Generation

To generate the interacting parameters DOE error surfaces, the baseline corrected error data for each mode was evaluated to generate a 5th, 50th, and 95th percentile delta across all nine DOE conditions. The errors captured during this experiment included bias errors as well as precision errors. However, the dynamic torque and BSFC error surfaces generated during transient engine testing captured the precision errors associated with the interpolation process of torque and BSFC. Not wanting to double count error sources in the Model, the variability of the interpolation process was removed from the interacting parameters DOE error surfaces. This was accomplished by shrinking the 5th, 50th, and 95th percentile delta values by the interpolated torque and BSFC variance experienced during steady-state testing. The steady-state variance was calculated as the mean of the 10 steady-state interpolated torque and BSFC MAD values over the 20 repeats. The mean of the 10 MAD values was then used to collapse the raw DOE error data. After the variance correction, the delta percentiles were then plotted with the x-axis values calculated as the mean modal value.

The error correction due to the removal of the steady-state variance was minimal due to the relatively small steady-state torque and BSFC MAD values. The mean interpolated torque MAD values were 0.1 % of peak torque for Engine 1 and 0.3 % of peak torque for Engine 3. The mean BSFC MAD values were 0.2 g/(kW·hr) for both Engine 1 and Engine 3. An example of the MAD correction is show in Table 66. The bias corrected deltas, shown on the left, are collapsed using the mean MAD value to generate the final MAD corrected deltas.

TABLE 66. EXAMPLE DOE STEADY-STATE VARIANCE CORRECTION USING THE MEAN SS MAD

Bias Corrected PEMS vs Lab Delta	Bias Corrected PEMS vs Lab Delta	Bias Corrected PEMS vs Lab Delta	SS BSFC Mean of 10 MADs [g/kW-hr]	MAD Corrected PEMS vs Lab Delta	MAD Corrected PEMS vs Lab Delta	MAD Corrected PEMS vs Lab Delta
5th percentile [g/kW-hr]	50th percentile [g/kW-hr]	95th percentile [g/kW-hr]		5th percentile [g/kW-hr]	50th percentile [g/kW-hr]	95th percentile [g/kW-hr]
-13.1	-2.4	2.8	0.2	-12.9	-2.2	2.6
-7.6	-1.7	1.8	0.2	-7.4	-1.5	1.6
-7.1	-2.1	1.5	0.2	-6.9	-1.9	1.3
-11.9	-2.7	1.8	0.2	-11.7	-2.5	1.6
-9.3	-2.3	2.0	0.2	-9.1	-2.1	1.8

Figure 92 and Figure 93 show the corrected DOE torque and BSFC error surface data for Engine 1.

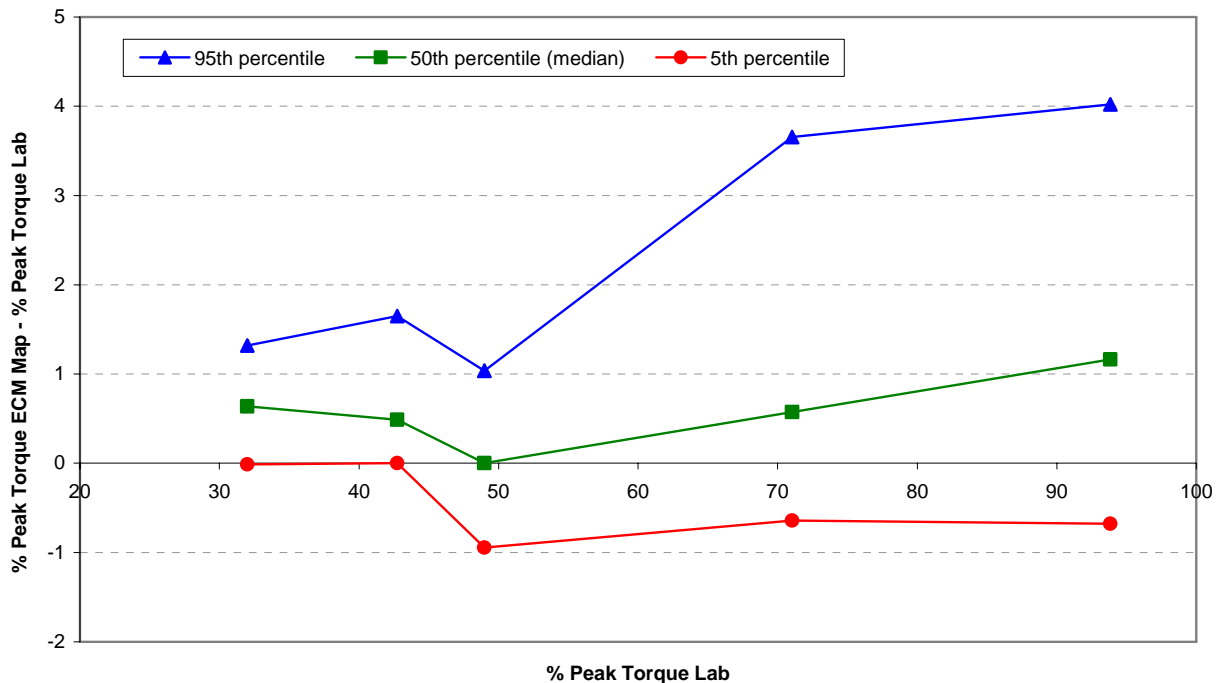


FIGURE 92. ERROR SURFACE FOR INTERACTING PARAMETERS - DOE ENGINE 1 DELTA TORQUE

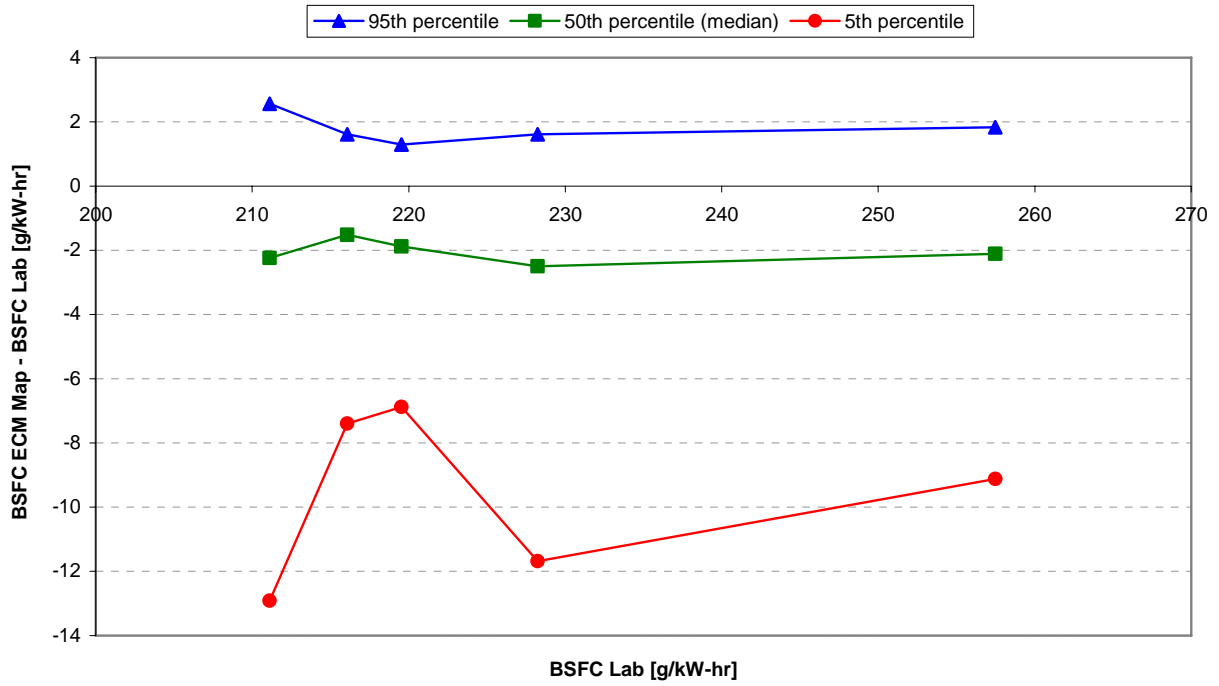


FIGURE 93. ERROR SURFACE FOR INTERACTING PARAMETERS - DOE ENGINE 1 DELTA BSFC

Figure 94 and Figure 95 show the corrected interacting parameters DOE torque and BSFC error surface data for Engine 3.

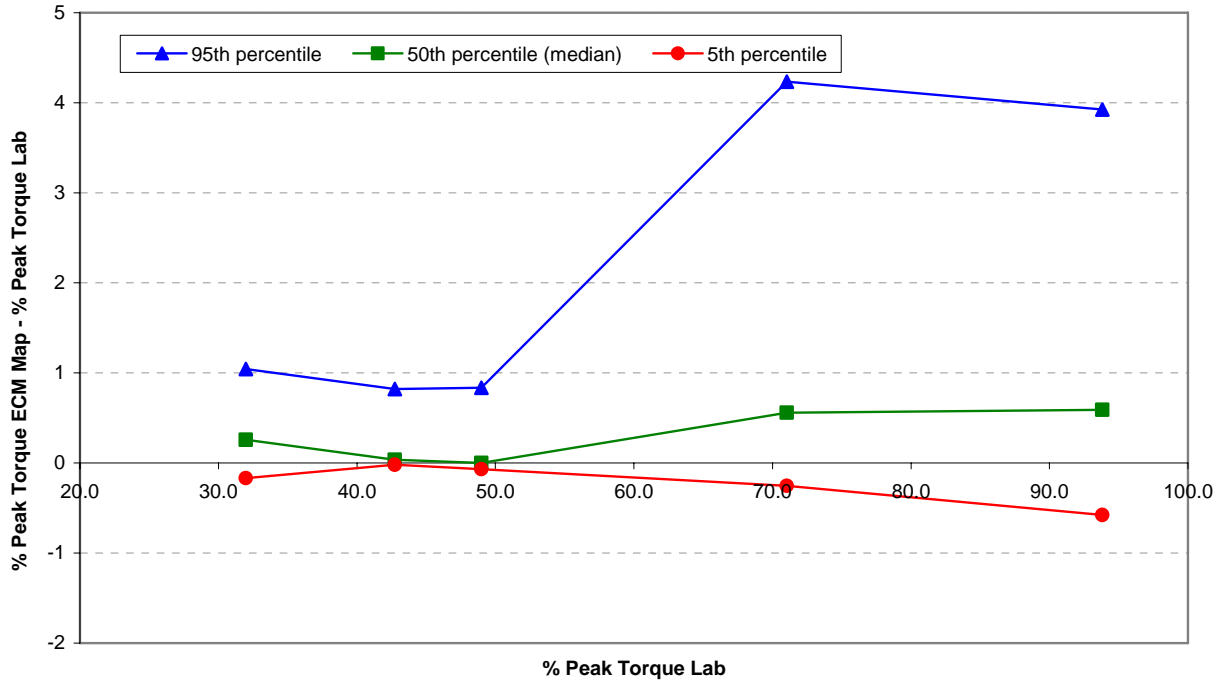


FIGURE 94. ERROR SURFACE FOR INTERACTING PARAMETERS - DOE ENGINE 3 DELTA TORQUE

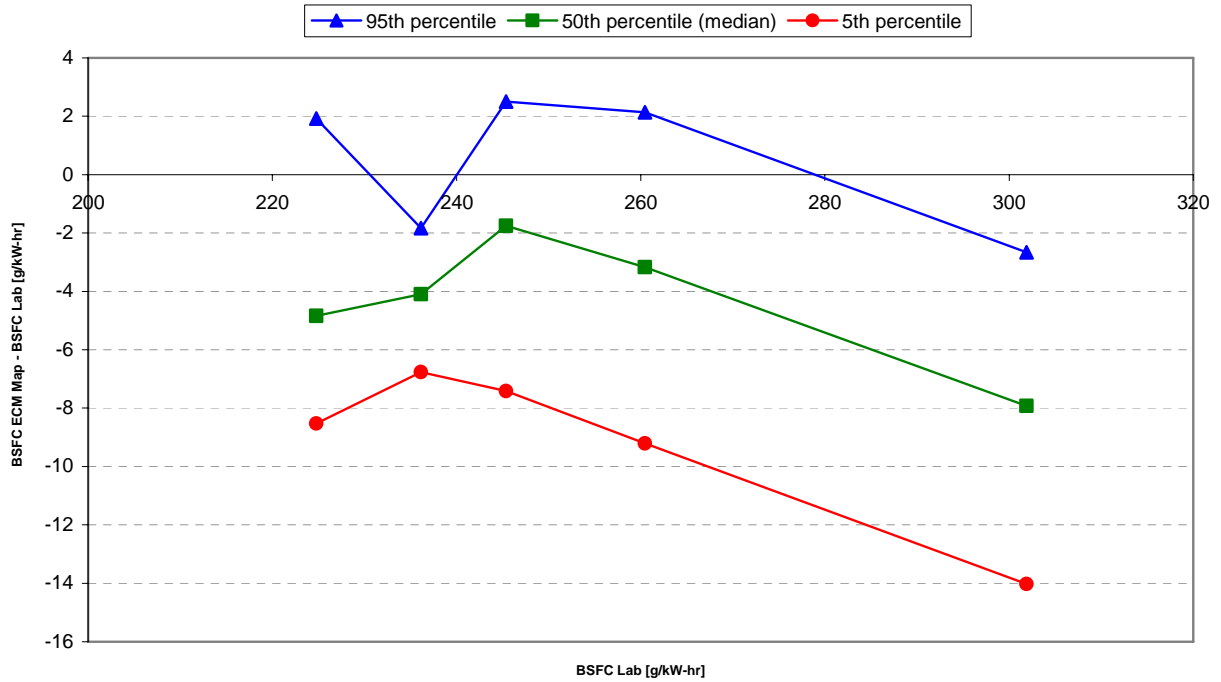


FIGURE 95. ERROR SURFACE FOR INTERACTING PARAMETERS - DOE ENGINE 3 DELTA BSFC

To generate the final DOE error surfaces, the torque and BSFC errors from the Engine 1 and Engine 2 DOE matrix were pooled. The 5th, 50th, and 95th percentile deltas were then calculated from the pooled data set. The variance correction was accomplished by calculating the mean of the pooled steady-state interpolated torque and BSFC MAD values from Engine 1 and Engine 3. The mean MAD values for the pooled data were 0.2 % of peak torque and 0.5 g/(kW·hr) for BSFC. The final torque and BSFC error surfaces for the interacting parameters DOE testing are shown in Figure 96 and Figure 97. The DOE error surfaces are sampled normally. Having a broad range of x-axis torque and BSFC values, errors are linearly interpolated from these error surfaces based on level.

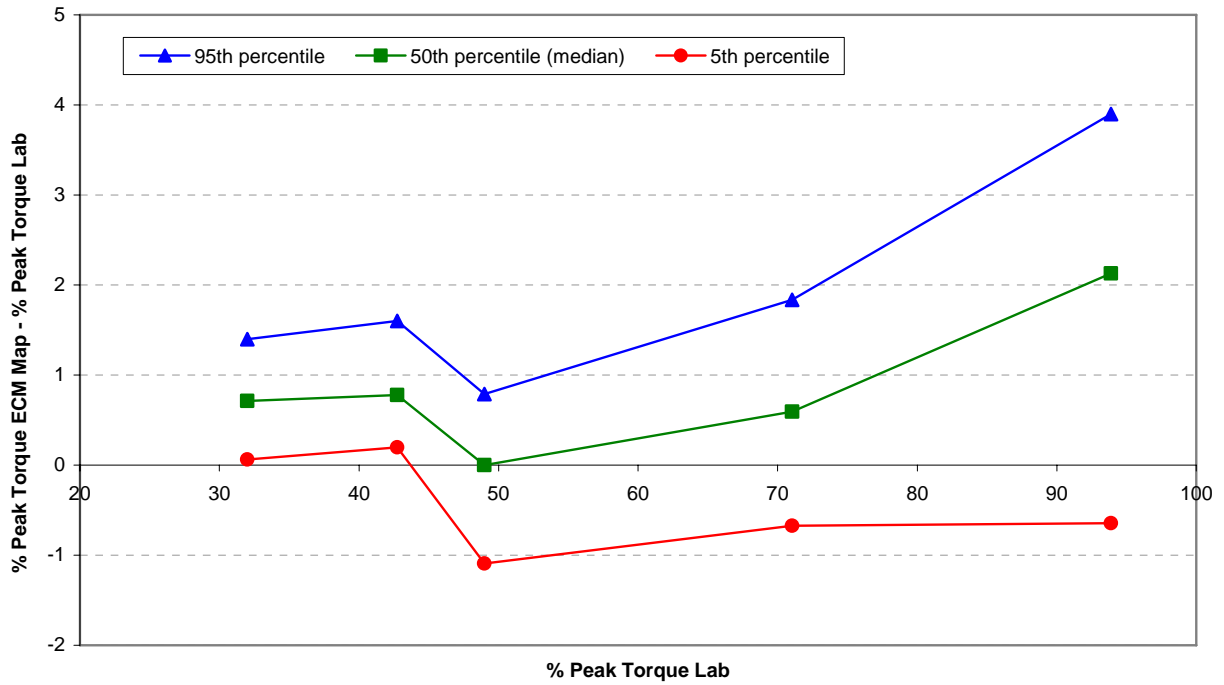


FIGURE 96. ERROR SURFACE FOR INTERACTING PARAMETERS - DOE DELTA TORQUE FINAL

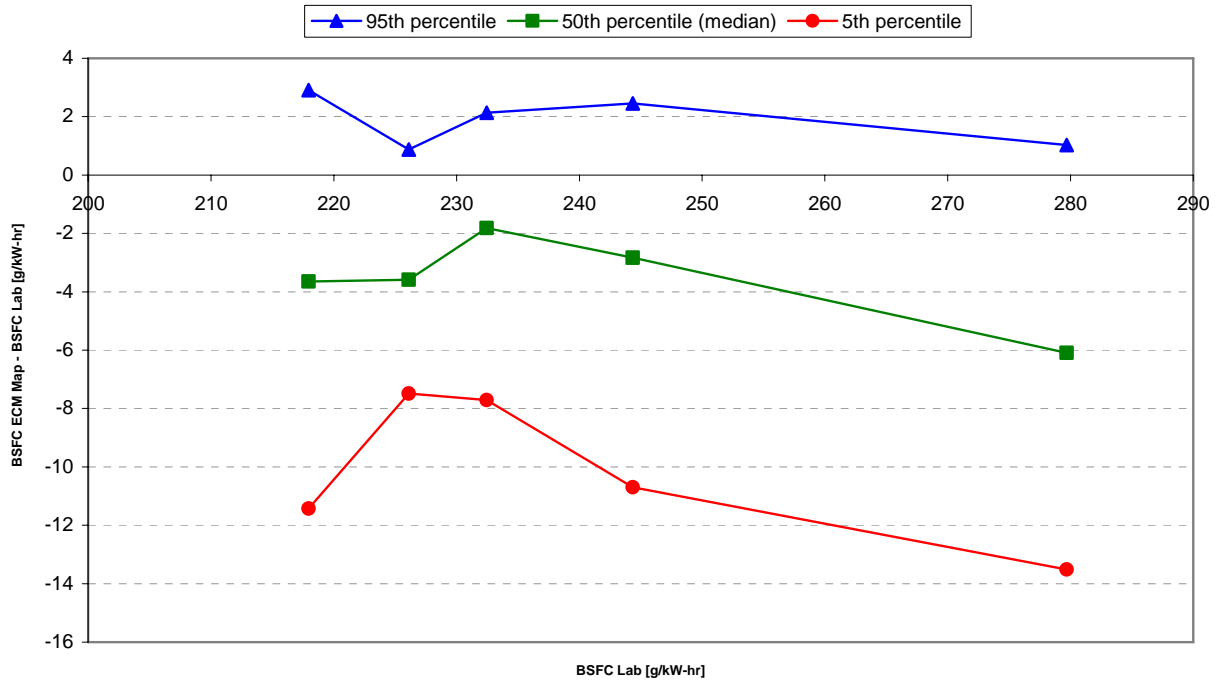


FIGURE 97. ERROR SURFACE FOR INTERACTING PARAMETERS - DOE DELTA BSFC FINAL

4.8 Torque and BSFC Independent Parameters Sensitivity Analysis

The independent parameters test was conducted to evaluate torque and BSFC map errors due to variations in intake air humidity and fuel properties. The Steering Committee had an option to add additional parameters into this matrix, but other parameters were not added. This test was performed only using Engine 2. The Test Plan called for SwRI to run a sensitivity analysis using the parameters given in Table 67.

TABLE 67. INDEPENDENT PARAMETERS ADJUSTMENT GUIDANCE FROM THE TEST PLAN

Sensitivity Parameter Set Points			
Parameter	Minimum (#1)	Mid. (#2)	Maximum (#3)
Intake air humidity	Minimum possible (@30 deg. C); 0 grains/lb dry air	50% RH (@30 deg. C); 95 grains/lb dry air	95% RH (@30 deg. C)*; 180 grains/lb dry air
Fuel properties	Fuel used in program	Fuel selection #2	California ULSD

*Run charge air cooler water inlet temperature of 30 deg. C

At each test condition, three steady-state modes were run according to the direction given in the Test Plan and as shown in Table 68. Note that original mode definitions are given as NTE percent speed and percent torque at speed.

TABLE 68. INDEPENDENT PARAMETERS TEST MODES FROM THE TEST PLAN

Sensitivity Engine Operating Conditions (%speed, and %torque respectively)		
17%, 32%	59%, 49%	100%, 100%

Although the original Test Plan called for only running selected conditions across the three modes, SwRI determined that there was little difficulty in changing test conditions once the test apparatus was set up and the fuels were procured. Therefore, SwRI elected to run a complete test matrix for a total of nine test conditions.

As with the Interacting Parameters DOE, it was necessary to adjust the final test modes slightly from those given in the Test Plan to position the points in the NTE zone and to insure the target torque values could be maintained at all of the test conditions. The torque value for mode 1 was increased to insure the mode 1 power was always above the NTE limit of 30 % maximum power. The speed and torque set points for mode 3 were decreased to pull the point away from the governor line, thus insuring the mode was repeatable throughout the independent parameters testing. Table 69 shows the final three modes of the steady-state test cycle run for the independent parameters testing. The mode length was set to 10-minutes to insure stable fuel flow measurement for the BSFC error surfaces.

TABLE 69. INDEPENDENT PARAMETERS SPEED AND TORQUE STEADY-STATE MODE DEFINITIONS

	Speed [% NTE]	Torque [% Peak]
Mode 1	17%	43%
Mode 2	59%	49%
Mode 3	97%	56%

It was not possible to perform testing using an exhaustive matrix of fuel properties during this program. Therefore, the Test Plan called for three fuels to represent a range of potential fuel properties that might be available in the field. The first two fuels were specified in the Test Plan. The first was the base ULSD 2-D certification grade fuel used during the program, while the second was to be a representative California ULSD fuel. SwRI procured several drums of BP ECD-1 ULSD fuel from California to meet this requirement. The third test fuel was to be selected by the Steering Committee. Initially, SwRI proposed a very low aromatic (less than 10% by volume) fuel, but the Steering Committee felt that a high aromatic fuel would be more representative of fuels available in the northern and eastern parts of the U.S. Therefore, SwRI located a low API gravity ULSD test fuel from Chevron Phillips, which was selected as the third test fuel by the Steering Committee. A summary of selected fuel properties for the three Independent Parameters test fuels is given in Table 70.

TABLE 70. SELECTED FUEL PROPERTIES FOR INDEPENDENT PARAMETERS TESTING

Property	Units	Test Fuels		
		Base Fuel	CARB ULSD	Third Fuel
Aromatics	% vol	29.5	24.5	35.0
Cetane Number		44.4	54.3	40.4
Viscosity	cSt @ 40C	2.5	2.4	2.6
API Gravity		35.2	38.8	33.1
Sulfur	ppm	10	3	6.2
Distillation				
	10% deg F	214	206	207
	90% deg F	311	321	344
Description		Haltermann EPA 2-D Cert fuel	BP EC Diesel-1	Chevron Phillips Low API ULSD

The mean intake air humidity levels recorded during testing were 4 gr/lb for the low humidity points, 90 gr/lb for the middle humidity points, and 192 gr/lb for the high humidity points. In order to reach the near zero humidity levels requested in the Test Plan, a specialized humidity control system had to be used to condition the engine intake air. This custom-designed system is incorporated into the intake air stream of the test cell at SwRI on an as needed basis in order to achieve very low humidity levels, while imposing a very low additional restriction on the intake air system. Shown in Figure 98, the humidity control system employs a large bed of desiccant that is used to remove water from the intake air, and incorporates bypass legs and post-bed cooling heat exchangers to maintain the desired intake air temperature and humidity conditions.



FIGURE 98. INTAKE AIR LOW HUMIDITY CONTROL SYSTEM

4.8.1 Independent Parameters Data Analysis

For the interacting parameters testing, ECM speed and ECM fuel rate were used with the 40-point maps to interpolate modal torque and BSFC values. These values were compared to the laboratory reference measurements. As with the 40-point BSFC map, the reference BSFC was calculated using the laboratory fuel flow meter. As expected, there were errors inherent in the interpolation process using the 40-point maps. Because the interpolation errors were accounted for in the Model, the Steering Committee elected to remove the interpolation bias errors. A process was used similar that used for the Interacting Parameters DOE, wherein all data values were bias corrected using the error values from a baseline condition. The baseline condition chosen for the Independent Parameters test was Test Fuel 1 with normal 95 gr/lb humidity level. Corrections were performed on a mode-by-mode basis.

Shown in Table 71 are the bias corrected interpolated torques versus laboratory torque delta values for the Independent Parameters testing. Table 72 contains the bias corrected interpolated BSFC versus laboratory BSFC delta values.

TABLE 71. INDEPENDENT PARAMETERS BIAS CORRECTED TORQUE DELTAS

Intake Humidity	Fuel	Delta Torque Bias Corrected (% of Peak Torque)		
		Mode 1	Mode 2	Mode 3
Min	1	-0.5%	-0.3%	-0.4%
	2	0.8%	1.1%	1.2%
	3	-1.1%	-0.9%	-0.9%
Norm	1	0.0%	0.0%	0.0%
	2	1.0%	1.2%	1.7%
	3	-1.0%	-0.9%	-1.1%
High	1	-0.2%	0.0%	-0.3%
	2	1.9%	2.3%	1.7%
	3	0.0%	0.1%	-0.7%

TABLE 72. INDEPENDENT PARAMETERS BIAS CORRECTED BSFC DELTAS

Intake Humidity	Fuel	Delta BSFC Bias Corrected (g/kW-h)		
		Mode 1	Mode 2	Mode 3
Min	1	3.5	2.3	3.0
	2	2.3	2.2	1.8
	3	0.5	0.9	2.1
Norm	1	0.0	0.0	0.0
	2	2.8	0.9	0.3
	3	0.6	1.9	2.7
High	1	-0.7	-0.7	0.8
	2	-4.1	-4.7	-2.3
	3	-5.0	-4.0	-0.5

4.8.2 Independent Parameters Error Surface Generation

The Test Plan originally called for separate error surfaces to be generated for fuel and humidity. However, while a clear trend was apparent with test fuel, no trends could be observed related to humidity. Therefore, SwRI proposed that all the data be pooled into a single Independent Parameters error surface each for torque and BSFC. Furthermore, the final torque values for the three modes actually represented a relatively narrow range of torque, therefore no trend in the data based on torque level could be determine. As a result, SwRI suggested that the data for all three modes be pooled, and further that no x-axis be used on the final error surface. The Steering Committee approved these changes during the November 21, 2006 conference call. As a result, the overall 5th, 50th, and 95th percentiles were calculated from the pooled data sets shown in Table 71 and Table 72.

Figure 99 shows the delta torque error surface for the independent parameters testing. With only one x-axis point, the normally sampled delta torque values were applied to each torque value in the reference NTE events in the Model.

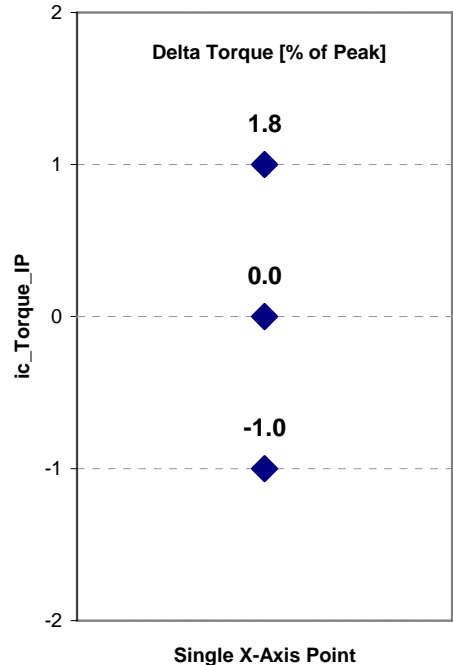


FIGURE 99. ERROR SURFACE FOR INDEPENDENT PARAMETERS DELTA TORQUE

Shown in Figure 100 is the delta BSFC error surface for the independent parameters testing. Similar to the delta torque error surface, the BSFC surface was collapsed to a single x-axis point. The pooled 5th, 50th, and 95th percentile values will be normally sampled and applied to each reference NTE event BSFC value.

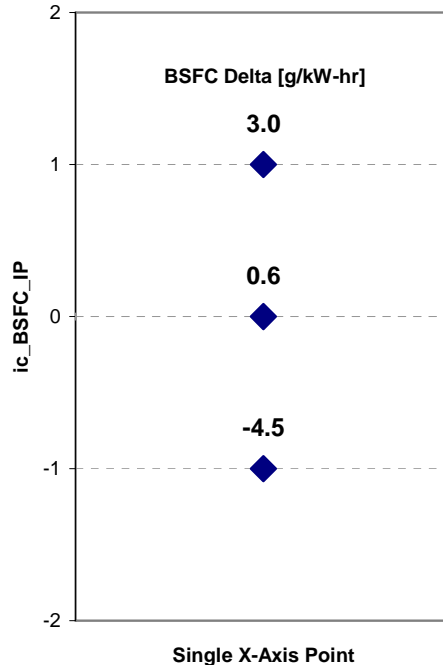


FIGURE 100. ERROR SURFACE FOR INDEPENDENT PARAMETERS DELTA BSFC

4.9 Torque and BSFC Interpolation Errors

During the design of the Test Plan, it was determined that a 40-point speed and fuel rate matrix would be used to define an interpolation surface to predict Torque and BSFC from CAN Speed and CAN Fuel Rate. While the 40-point matrix was used throughout the program, the Steering Committee decided the 40-point matrix was too dense, placing an excessive mapping burden on engine manufacturers. The Steering Committee determined that a 20-point matrix would be more typical of actual field testing. However, the smaller matrix would lead to increased interpolation errors.

The interpolation error surfaces were designed to capture the incremental error involved in dropping from an interpolation surface based on a 40-point test matrix to one based on a 20-point test matrix. The generation of these error surfaces was a computational exercise carried out using the initial 40-point steady-state map data. For each engine, the Steering Committee down-selected 20 points from the original 40 to generate the coarser grid. The 20-point maps selected by the Steering Committee are shown in Figure 101 through Figure 103 for Engine 1, Engine 2, and Engine 3, respectively.

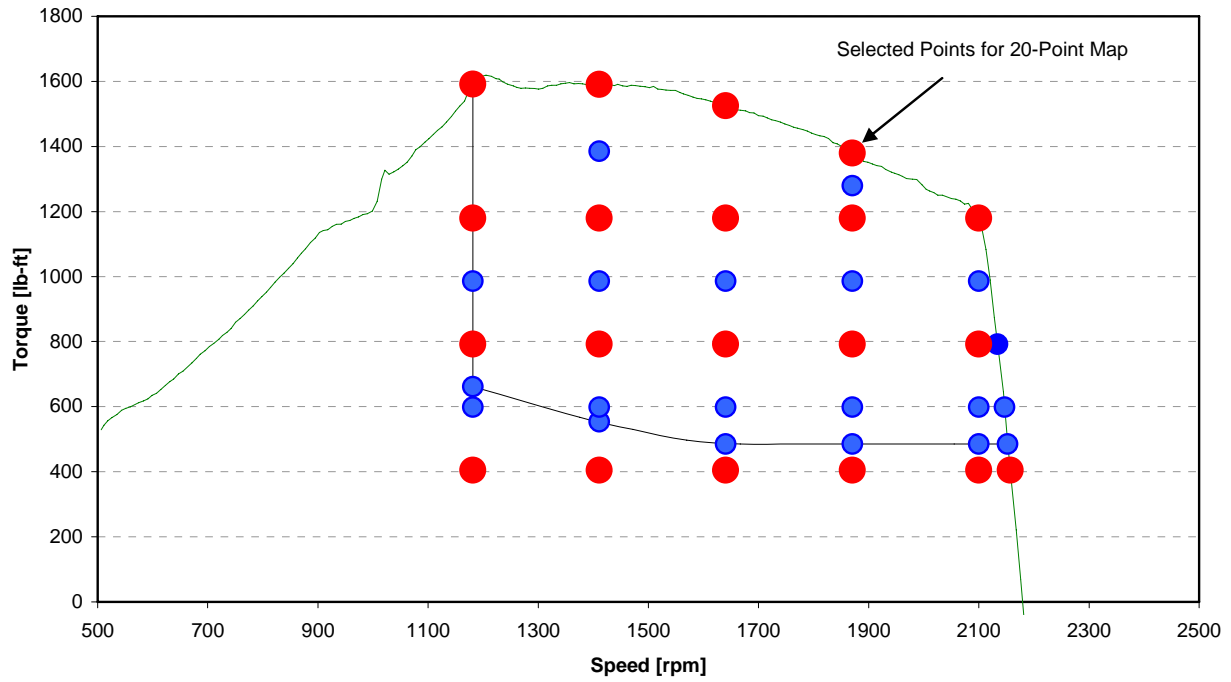


FIGURE 101. DETROIT DIESEL SERIES 60 DOWN SELECTED 20-POINT MAP

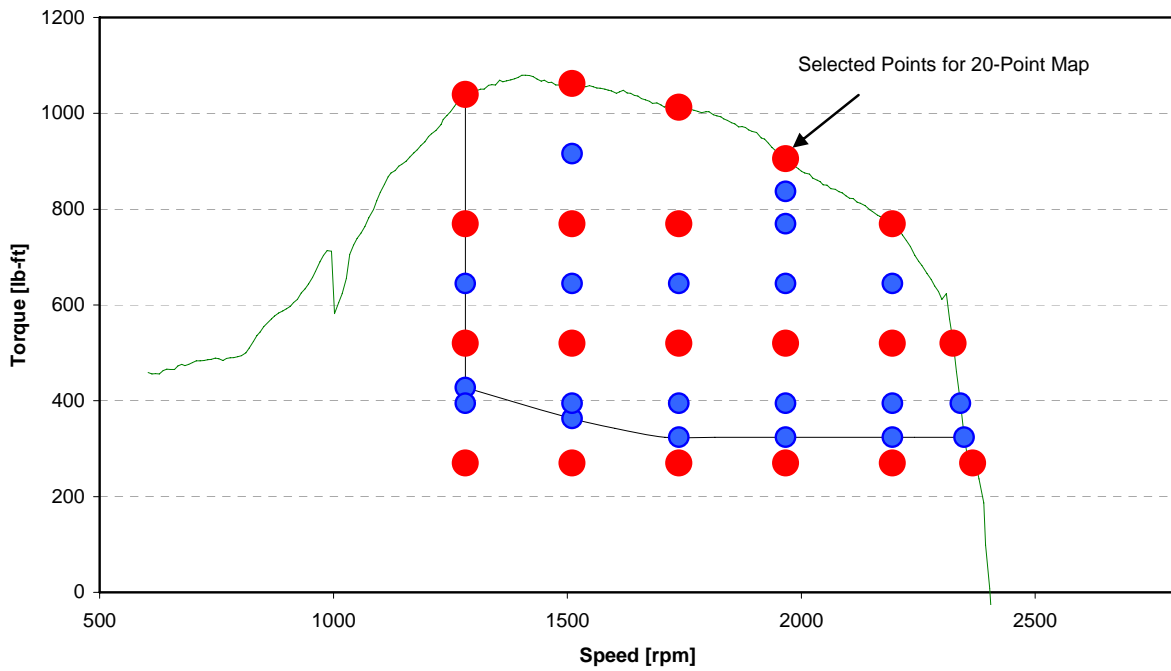


FIGURE 102. CATERPILLAR C9 DOWN SELECTED 20-POINT MAP

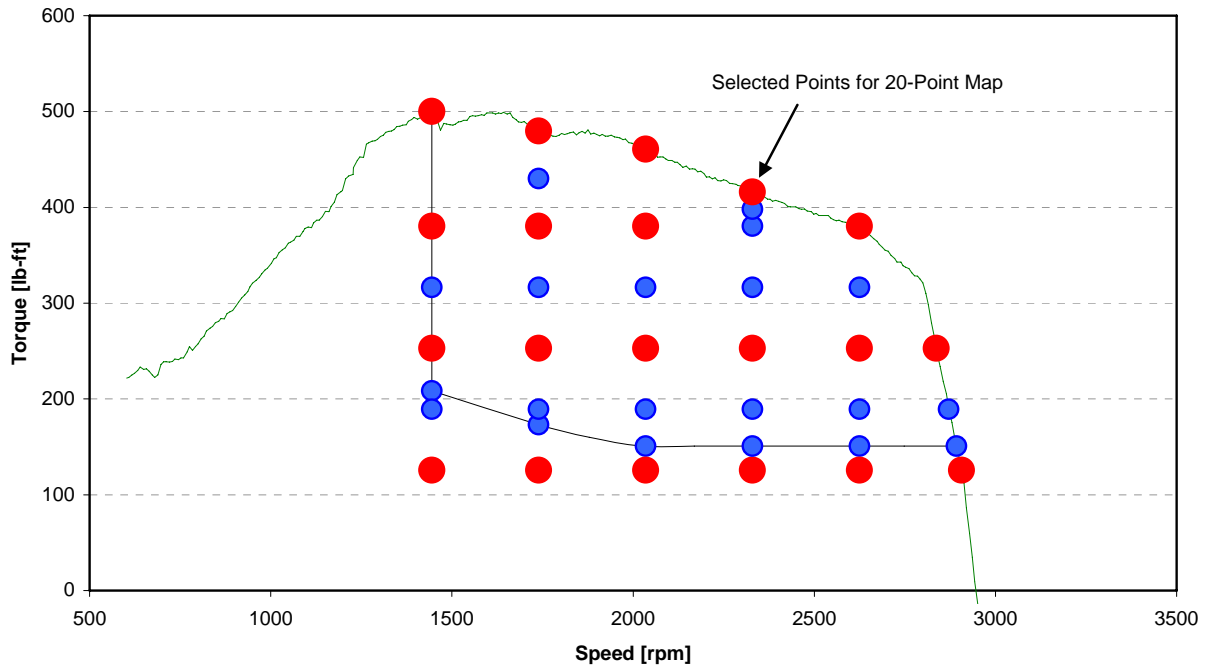


FIGURE 103. INTERNATIONAL VT365 DOWN SELECTED 20-POINT MAP

For each engine a matrix of several thousand CAN-Speed and CAN-Fuel Rate combinations was run using both 40-point and 20-point interpolation surfaces. The interpolated torque and BSFC values were compared to generate the final deltas, with the 20-point values subtracted from the 40-point values. An example of the results from this computational exercise is shown in Figure 104 for Engine 1 interpolated torque. The results for all three engines are given in Appendix I.

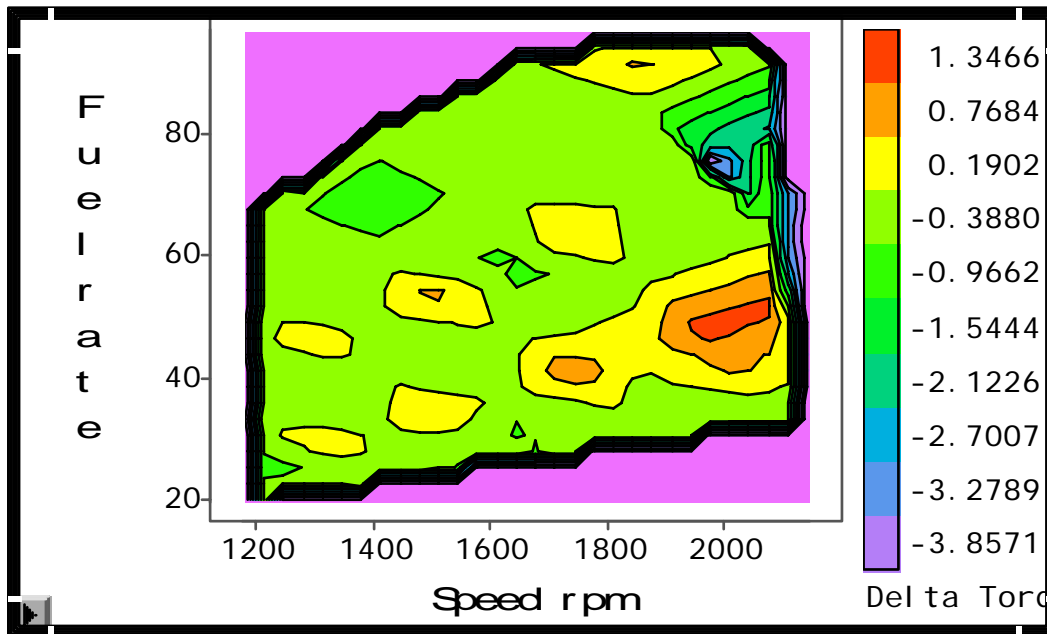


FIGURE 104. INTERPOLATED TORQUE ERROR (% PEAK TORQUE) BY SPEED (RPM) AND FUEL RATE (G/S) FOR ENGINE #1

4.9.1 Interpolation Error Surface Generation

To generate the final error surfaces, the interpolated torque and BSFC 20-point versus 40-point delta data was pooled for each engine, and 5th, 50th, and 95th percentile values were generated. The percentile values for each engine were then averaged to generate the final deltas for interpolation error surfaces. The error surfaces do not have an x-axis, as the interpolation error was not found to scale with either speed or fuel rate, but remained relatively constant across the entire performance map for each engine.

For torque the error surfaces are expressed as percent of maximum engine torque, while BSFC errors are given in engineering units of g/(kW·hr). Each of these surfaces is sampled normally, once per NTE event. The final error surface values are given in Table 73 and Table 74 for torque and BSFC, respectively. The error surfaces are depicted in Figure 105 and Figure 106 for torque and BSFC, respectively.

TABLE 73. TORQUE INTERPOLATION ERROR SURFACE VALUES

Engine	Number of Points	Percentiles		
		5 th	50 th	95 th
1	8944	-0.82 %	0.00 %	0.80 %
2	5741	-0.84 %	0.16 %	2.55 %
3	5197	-1.00%	0.01 %	1.34 %
Averaged		-0.89 %	0.06 %	1.57 %

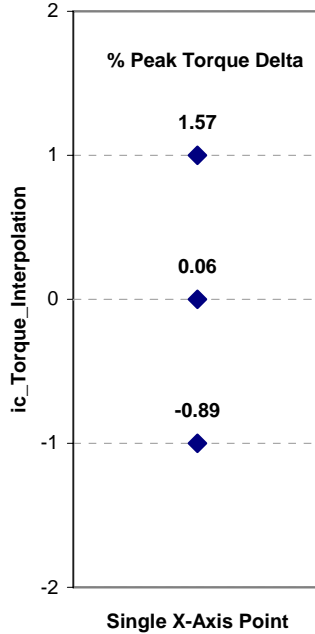


FIGURE 105. TORQUE INTERPOLATION ERROR SURFACE

TABLE 74. BSFC INTERPOLATION ERROR SURFACE VALUES

Engine	Number of Points	Percentiles		
		5 th	50 th	95 th
1	8944	-3.96	0.49	8.60
2	5741	-3.27	0.05	7.89
3	5197	-0.12	1.98	10.94
Averaged		-2.45	0.84	9.14

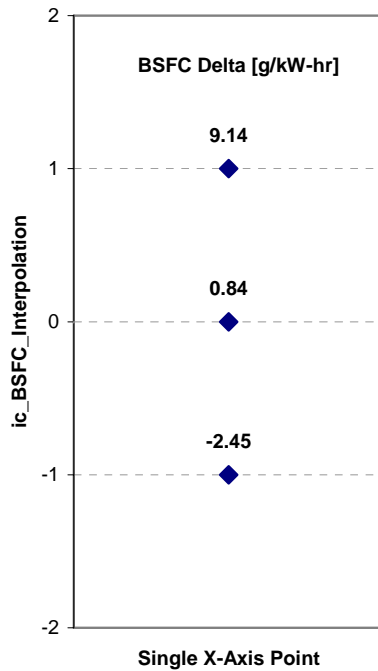


FIGURE 106. BSFC INTERPOLATION ERROR SURFACE

4.10 Exhaust Flow Meter Testing

Exhaust flow meter testing was performed to evaluate potential bias errors due to installation related factors. Flow meter testing included an exhaust pulsation test, an exhaust swirl testing, and an exhaust tailpipe wind test. Using the Detroit Diesel Series 60 and 5-inch EFM, steady-state tests were conducted to compare the SEMTECH-DS EFM flow rate to the laboratory flow rate.

The ten steady-state points tested during the flow meter testing were identical to the modes selected for Engine 1 steady-state repeat testing. The laboratory flow rate was determined using a LFE to measure the intake air flow, a Micro-Motion fuel flow meter to measure fuel flow, and the laboratory analyzers to measure raw exhaust emission concentrations. The intake LFE measurement and the raw chemical balance were used with equation 1065.655-14 to calculate the reference exhaust flow rate. As a check, the LFE air flow rate and measured fuel flow were also used to calculate the exhaust flow rate using the CFR Part 89 raw exhaust flow rate calculation. The two laboratory exhaust flow rate calculation methods gave nearly identical exhaust flow rate results. The raw carbon balance error was modally calculated to insure the laboratory reference exhaust flow rate was accurate to within two percent.

4.10.1 Pulsation Test

The pulsation test was performed to evaluate the bias and precision of the PEMS flow meters when subjected to large pressure pulsations in the exhaust system. To conduct this test,

the DPFs were removed from the exhaust system, so that pulsations in the exhaust would not be damped by its presence. The EFM was mounted 2 to 3 meters downstream of the turbocharger outlet. Exhaust pipes, with lengths exceeding 10-diameters, were mounted before and after the EFM. The exhaust was routed out the large overhead door of the laboratory, and was therefore vented directly to the atmosphere.

The 10-mode steady-state test was repeated 5 times. The pooled SEMTECH-DS EFM flow rate deltas versus the laboratory reference flows are shown in Figure 107. The PEMS flow meters were biased high during the pulsation testing.

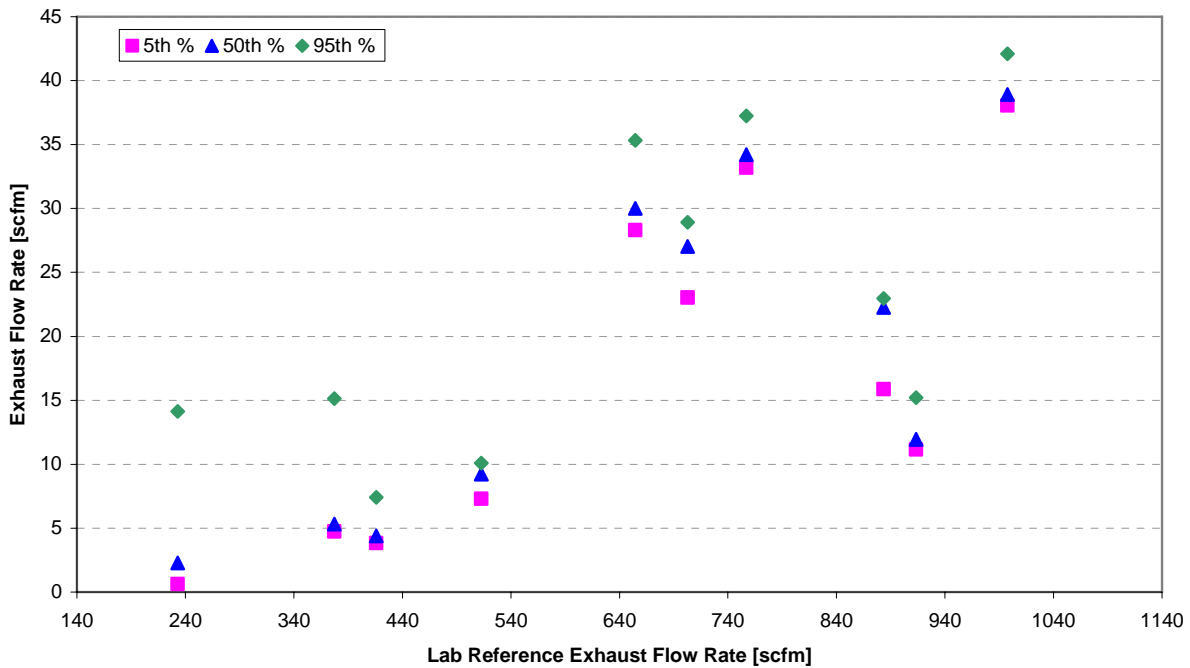


FIGURE 107. PULSATION TEST SEMTECH-DS EXHAUST FLOW RATE DELTAS – RAW DATA

In order to avoid double counting exhaust flow errors, the bias recorded during steady-state testing was subtracted from the pulsation test data. Figure 108 shows the EFM errors after the mean steady-state exhaust flow rate bias was removed from the flow rate deltas. The steady-state bias correction yielded a more uniform, positive exhaust flow rate bias. It should be noted that, because this experiment was conducted using the 5-inch EFM, this steady-state bias correction was small, because only a small amount of bias was observed during steady-state tests involving the 5-inch flow meters (see Section 4.4.1 above).

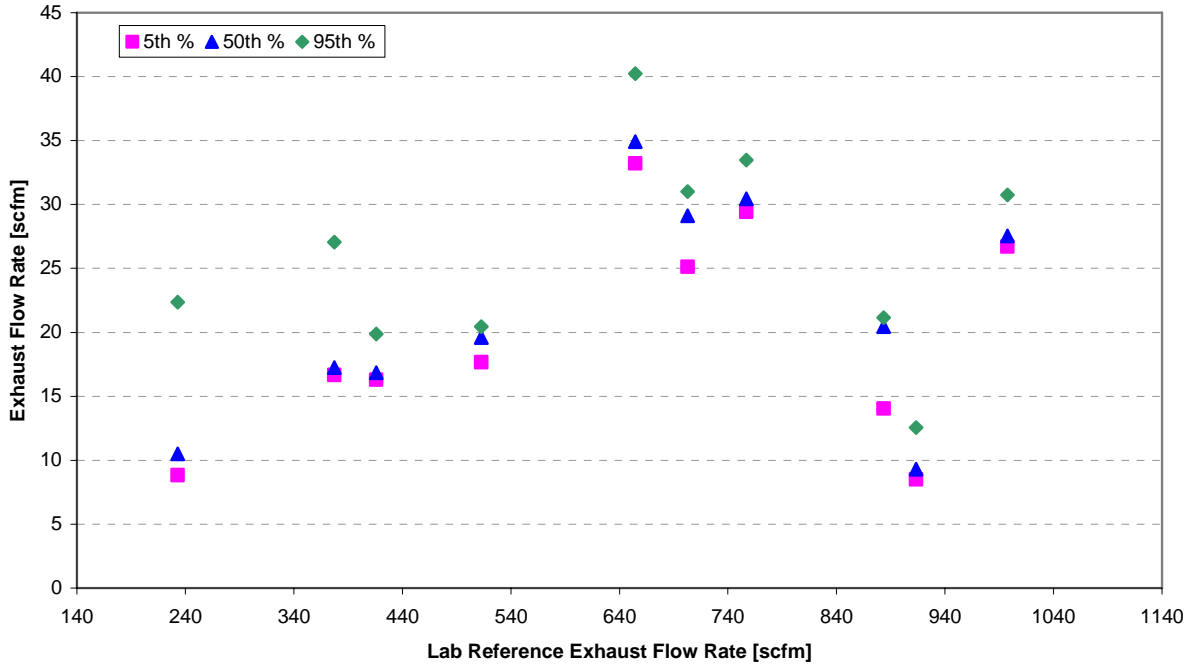


FIGURE 108. PULSATION TEST SEMTECH-DS EXHAUST FLOW RATE DELTA - CORRECTED FOR STEADY-STATE BIAS

4.10.2 Pulsation Error Surface Generation

Using the bias corrected EFM data, an exhaust flow rate pulsation error surface was constructed for use in the Monte Carlo Model. The exhaust flow rate data was normalized using the EFM maximum flow rate specification. In the case of the 5-inch EFM, the maximum flow rate was 1700 scfm. Shown in Figure 109 are the flow rate delta values that were used in the Model. Using normalized flow rate data from the reference NTE events, a flow rate delta was normally sampled from the error surface. Linear interpolation was used for NTE reference points within the data set. Points outside the data set were determined using the data set maximum or minimum values, with no extrapolation beyond the values generated during testing. The pulsation error surface generated positive exhaust flow errors when used in the Model.

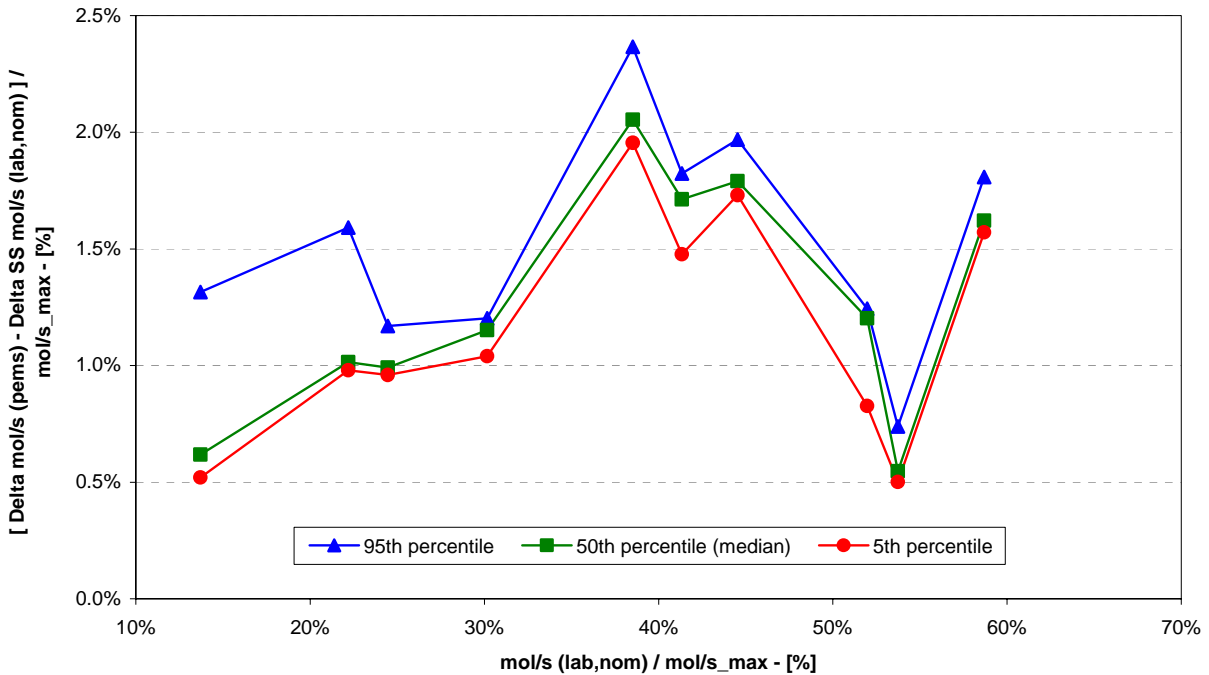


FIGURE 109. ERROR SURFACE FOR PULSATION EXHAUST FLOW RATE

4.10.3 Non-Uniform Velocity Profile Swirl Test

The swirl test was conducted to evaluate PEMS flow meter errors when the EFM was subjected to non-uniform flow velocity profiles upstream of the EFM. Two short radius 90° elbows were connected in perpendicular planes to introduce exhaust swirl before the inlet of the PEMS flow meter. The engine after-treatment system was installed during the swirl test. The swirl exhaust system was also vented out the overhead door of the laboratory, directly to atmosphere following the EFM.

Five repeats of the 10-mode steady-state test were run to characterize the EFM error due to swirl. The pooled SEMTECH-DS EFM flow rate deltas versus the laboratory reference flows for the swirl test are shown in Figure 110. The PEMS flow meter errors appeared to show a level dependence, with increasing errors as flow rate increased.

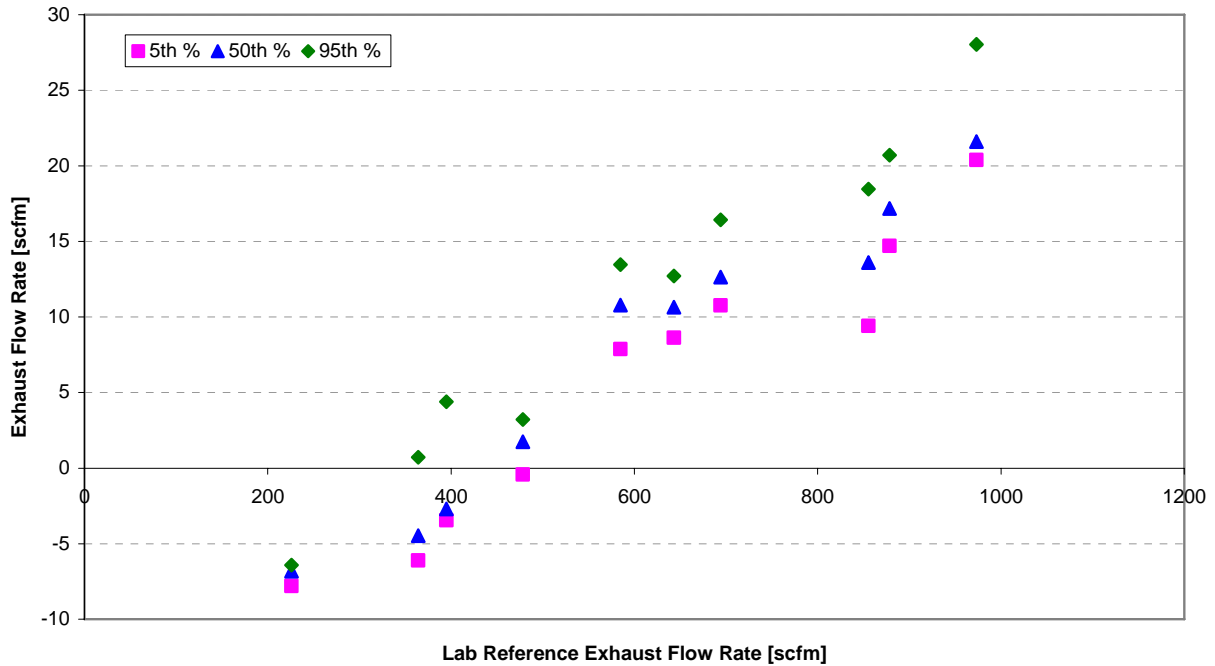


FIGURE 110. SWIRL TEST SEMTECH-DS EXHAUST FLOW RATE DELTAS – RAW DATA

In order to avoid double counting exhaust flow errors, the bias recorded during steady-state testing was subtracted from the swirl test data. Figure 111 shows the swirl test EFM errors after the mean steady-state exhaust flow rate bias was removed from the flow rate deltas. The steady-state bias correction eliminated much of the level dependency, resulting in a more uniform, positive exhaust flow rate bias. . Again, it should be noted that, because this experiment was conducted using the 5-inch EFM, this steady-state bias correction was small, because only a small amount of bias was observed during steady-state tests involving the 5-inch flow meters (see Section 4.4.1 above).

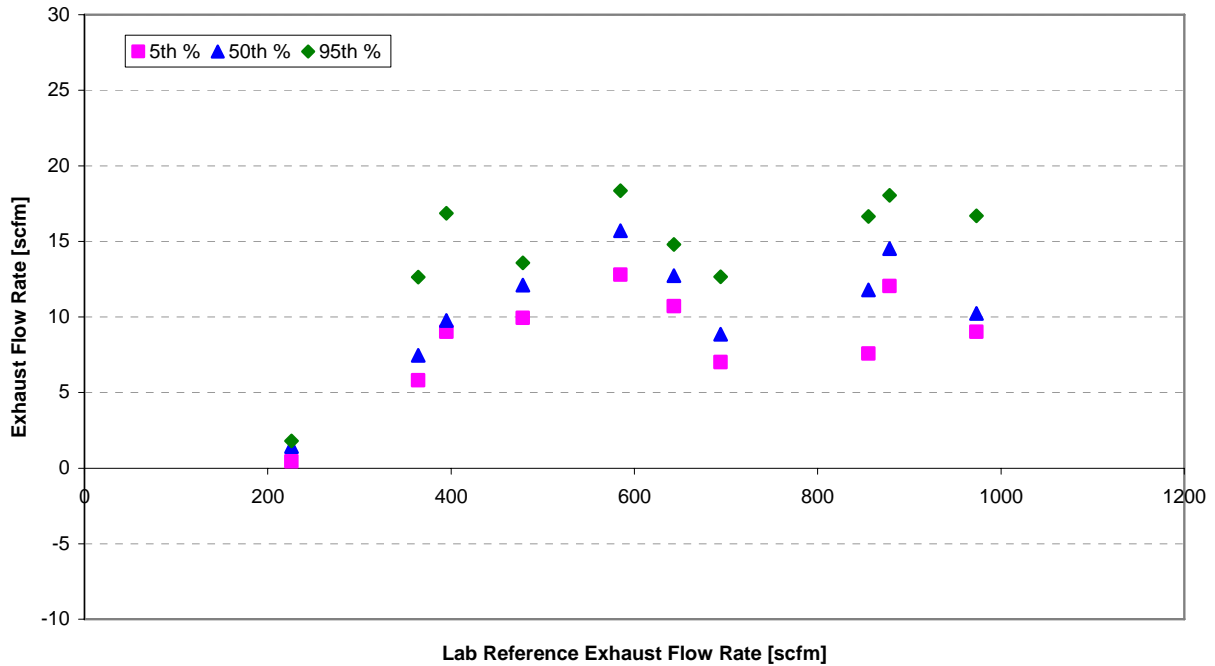


FIGURE 111. SWIRL TEST SEMTECH-DS EXHAUST FLOW RATE DELTAS - CORRECTED FOR STEADY-STATE BIAS

4.10.4 Swirl Error Surface Generation

Using the bias corrected EFM data, an exhaust flow rate swirl error surface was constructed for use in the Monte Carlo Model. The exhaust flow rate data was normalized using the EFM maximum flow rate specification. In the case of the 5-inch EFM, the maximum flow rate was 1700 scfm. Shown in Figure 112 are the flow rate delta values that were used in the Model. Using normalized flow rate data from the reference NTE events, a flow rate delta was normally sampled from the error surface. Linear interpolation was used for NTE reference points within the data set. Points outside the data set were determined using the data set maximum or minimum values. The swirl error surface generated positive exhaust flow errors when used in the Model.

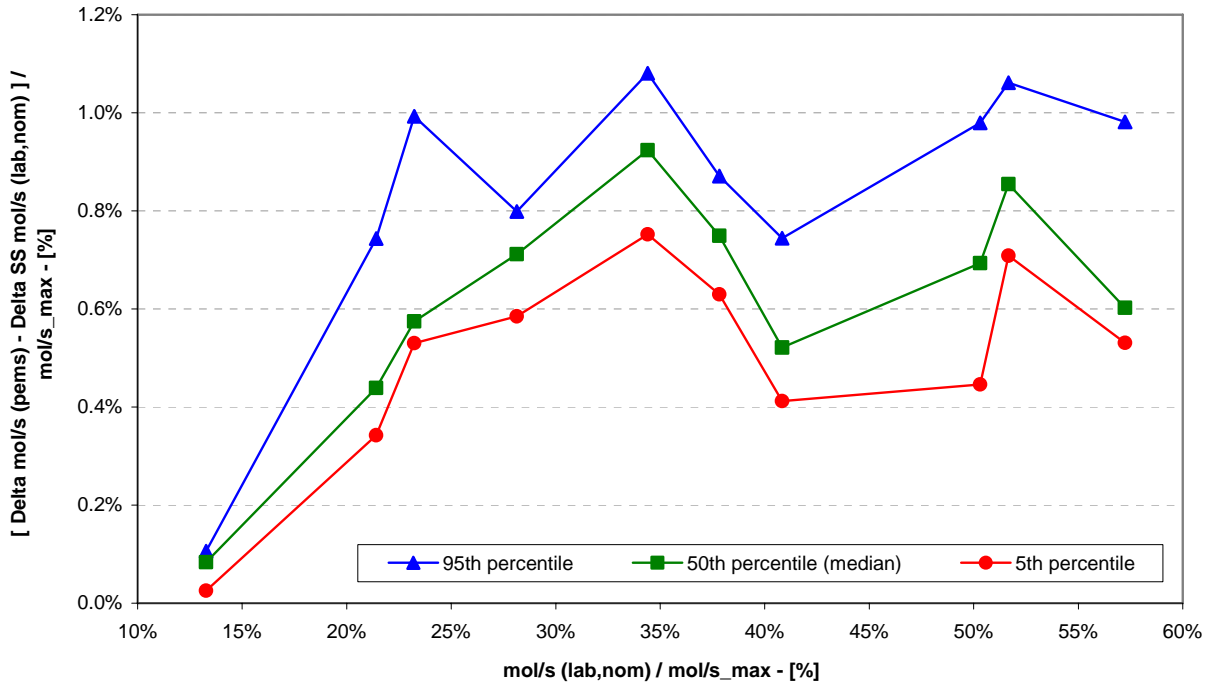


FIGURE 112. ERROR SURFACE FOR SWIRL EXHAUST FLOW RATE

4.10.5 Tailpipe Wind Test

The tailpipe wind test was performed to determine EFM errors when the outlet of the flow meter was subjected to high velocity air currents. The Steering Committee was initially unsure if this experiment would result in significant errors, and how those errors would be processed if they were found to be significant. Therefore, the Test Plan called for an initial experiment to be run in order to determine the possible magnitude of this potential exhaust flow error source. According to the Test Plan, if the initial experiment showed an error of less than 1 percent, no further experimentation would be performed, and the error surface would be dropped from the Model. The experiment called for a high velocity air stream to be directed at the outlet of the EFM at a variety of angles while the engine was operating at the 5 test modes. The flow was to be designed to simulate a 60 mph wind velocity.

Figure 113 shows the experimental setup used for the initial test. A high velocity blower system was used to direct air across the outlet of the EFM. A pitot tube device was used to measure the air velocity at the outlet of the blower system. The air velocity was within the Test Plan specification of 60 to 65 mph. Three steady-state tests, each consisting of the 5 steady-state modes for EFM testing, were run with the blower system. One test was run with the high velocity air stream perpendicular to the EFM, one with the air stream directed 45° into the EFM, and one test with the air stream directed 45° out of the EFM. Figure 114 shows the three blower orientations during the wind testing. A fourth steady-state test was run without the blower as a baseline reference.

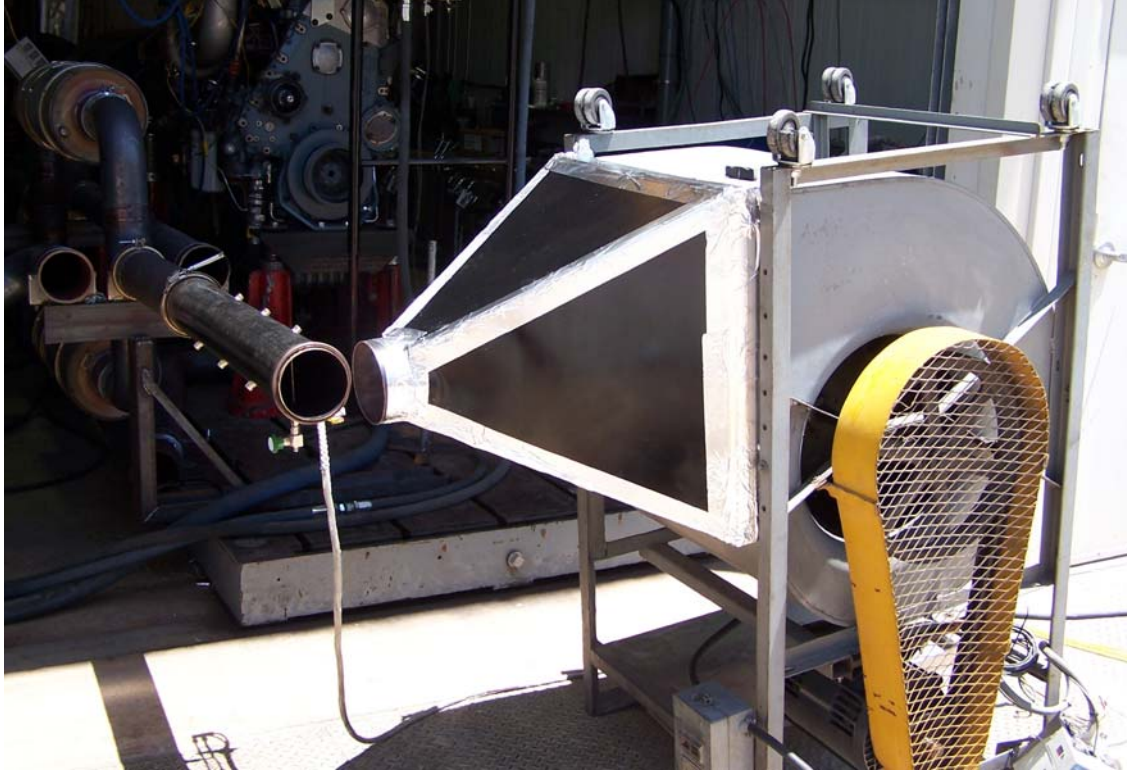


FIGURE 113. HIGH VELOCITY BLOWER SYSTEM

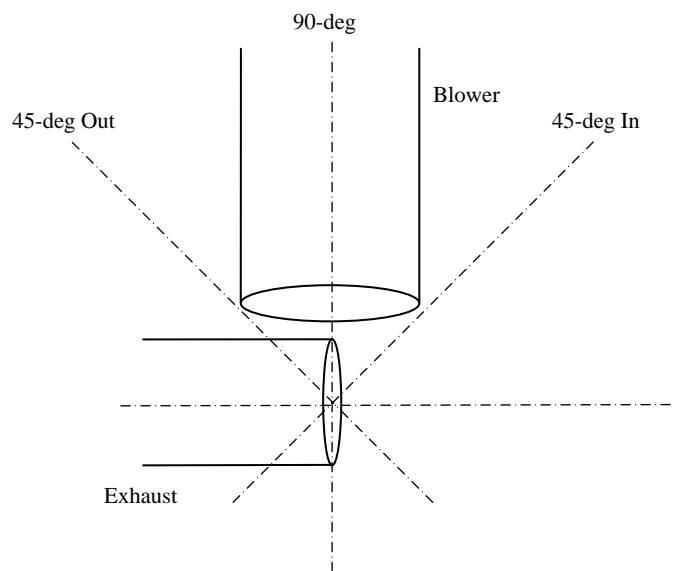


FIGURE 114. EFM WIND TEST FLOW SCHEMATIC

Figure 115 shows the exhaust deltas for the three steady-state tests with the blower and the one baseline test without the blower. The errors recorded during the blower tests were similar to the baseline errors. When corrected for the baseline error, the blower deltas collapse to

near zero errors. Figure 116 shows the baseline corrected blower deltas. One outlying exhaust flow delta was measured during the 45° out testing.

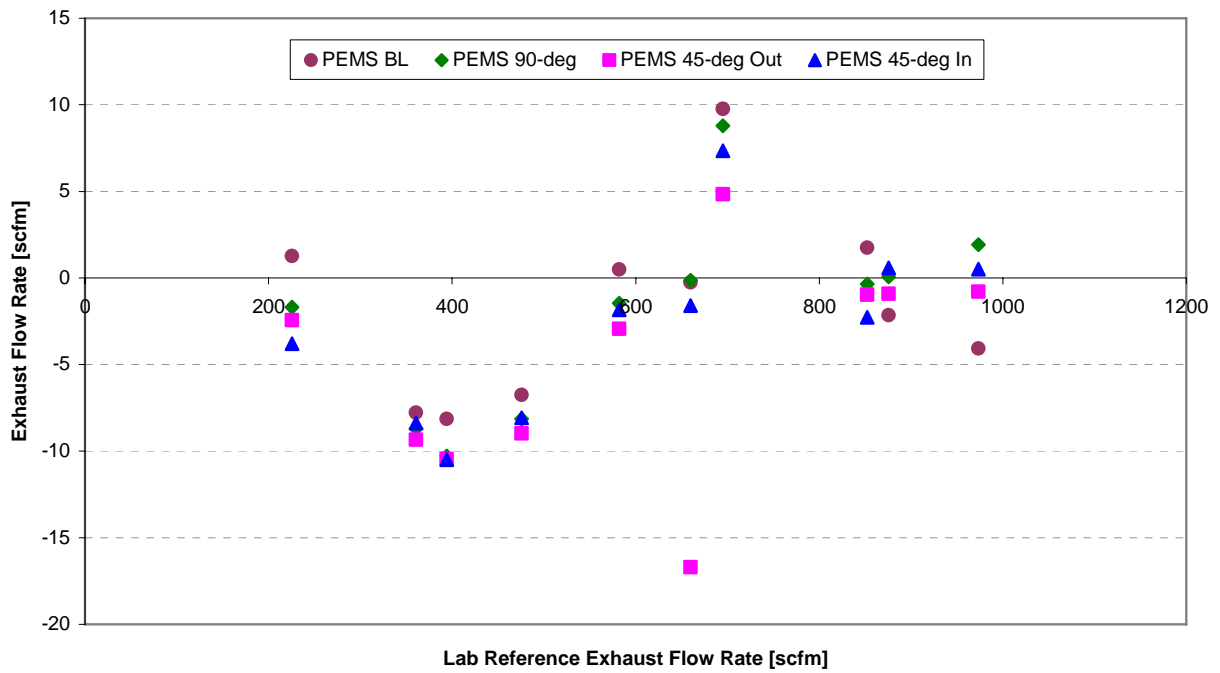


FIGURE 115. SWIRL TEST SEMTECH-DS EXHAUST FLOW RATE DELTAS – RAW DATA

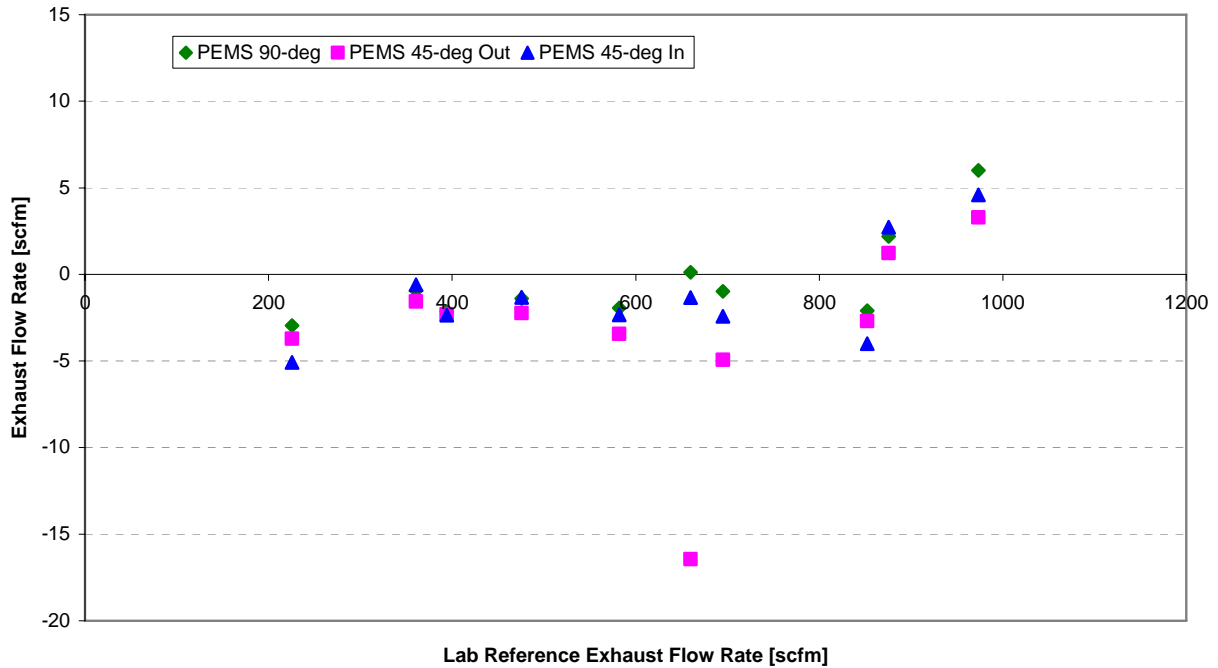


FIGURE 116. WIND TEST SEMTECH-DS EXHAUST FLOW RATE DELTAS - CORRECTED FOR STEADY-STATE BIAS

As specified in the Test Plan, the results from the blower tests were reviewed by the Steering Committee to determine if further testing and development of an error surface would be needed for the tailpipe wind test. Figure 117 shows the mean baseline corrected exhaust flow delta with 95 % confidence level error bars. This calculation was performed with and without the one outlying flow rate delta. Because the 95 % confidence level bars nearly crossed zero error, it was likely the errors generated from further tailpipe wind testing would be negligible. In addition, the magnitude of all of the errors observed was considerably smaller than one percent of the maximum flow for the flow meter. The Steering Committee therefore elected to not perform further tailpipe wind testing and eliminated the wind exhaust flow rate error surface. This decision was finalized at the June, 2006 Steering Committee meeting in San Antonio.

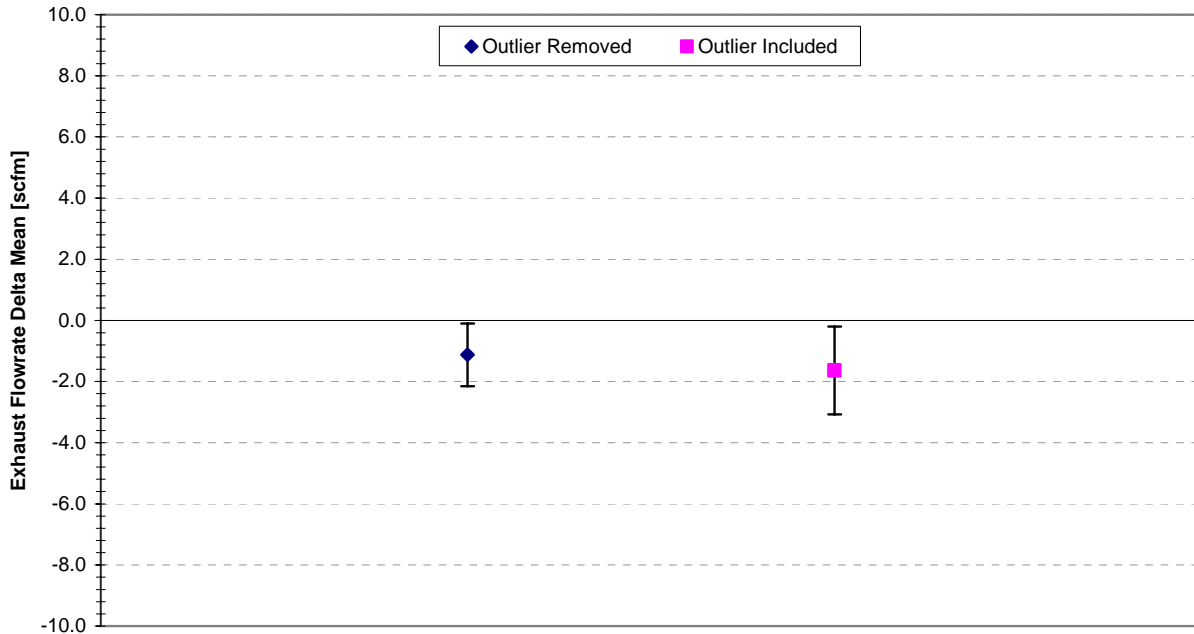


FIGURE 117. WIND TEST MEAN DELTA VALUES WITH 95 % CONFIDENCE LEVEL BARS

4.11 Torque and BSFC - OEM Supplied Error Surfaces

The purpose of the OEM supplied error surfaces was to capture ECM torque and BSFC errors that could result from factors not characterized during this program. The additional error sources included engine-to-engine production variability and the operation of non-deficiency AECDs. As part of the Test Plan, participating engine manufacturers were asked to submit data regarding these potential error sources to EPA. EPA was then tasked with analyzing the data and developing a single error surface each for torque and BSFC which would combine the various error sources.

Data was submitted by five engine manufacturers prior to the final deadline of August 1, 2006. EPA conducted an initial analysis, the results of which were reported to the Steering Committee in a memo from EPA dated August 28, 2006. As part of the analysis, EPA held private discussions with each manufacturer that submitted data, due to the confidential nature of the information being submitted. Following the initial analysis, additional information was requested regarding BSFC errors due to AECD operation, to resolve discrepancies in the data set. Additional data was supplied by two manufacturers regarding this topic, after which EPA completed a final analysis. The results of the final analysis were submitted to the Steering Committee in a second memo dated November 2, 2006, and included a final proposal for the error surface values. The Steering Committee approved the final form of the OEM error surfaces at the November 2, 2006 meeting in San Antonio, as they appeared in the second memo. Copies of both memos are included in Appendix J.

The final error surface values are summarized in Table 75 below. These surfaces are sampled once per NTE event using a normal distribution. The error levels were determined to scale with level, therefore the error surface values are defined as percent of point adjustments.

TABLE 75. OEM ERROR SURFACE DELTAS FOR TORQUE AND BSFC

Parameter	Percentiles ¹		
	5 th , % point	50 th , % point	95 th , % point
Torque	-6.5%	0 %	+6.5%
BSFC	-5.9%	0 %	+5.9%
¹ Based on sampling with normal distribution			

4.12 Time Alignment Error Surfaces

When processing the PEMS data recorded during transient dynamometer testing, the question of time alignment was brought up by the Steering Committee. When using the PEMS software to process test data, delay times for several variables can be used to time align the data recorded from different sources. The variables that can be time aligned include gaseous emission concentration data, the exhaust flow meter measurement, and the data recorded using the vehicle interface. SwRI used the procedures detailed in Sensors Inc. Application Note #06-001 titled *Time Alignment of Raw Data* to time align the data recorded during transient testing. Transient data was also sent to Sensors to insure the data was time aligned correctly. Time alignment of the SwRI transient data was relatively straightforward due to the sharp NTE event entry and exit transitions, which were a deliberate part of the experimental design. Several engine manufacturers indicated aligning data generated during field testing was often difficult due to the difficulty of finding such clear transitions on many real-world field data sets. Several examples of such difficult data sets were shared by Committee members during the course of the discussions to illustrate the issue. With events as short as 30 seconds, small time alignment errors result in significant differences in brake-specific emission results. Therefore, the Steering Committee elected to account for time alignment errors in the Measurement Allowance Error Model.

The first step in this analysis was to decide the level of typical alignment errors. Based on input from the Engine Manufacturers, time alignment errors up to 1 second are possible, however, errors near 0.5 seconds are more likely. Shown in Table 76, a matrix of time alignment errors was generated. The gaseous emission delay times were left unchanged, while the EFM and vehicle interface delay times were adjusted. To account for the relative likelihood of occurrence, weighting factors were applied to each matrix point. Points with delay time errors equal to or less than 0.5 were assumed to occur most often and received a relative weighting factor of 8. Points with one variable at a 1 second delay time error and the other parameter at no error received a weighting factor of 2. The diagonal points with the EFM and the vehicle interface both having a delay time error of 1 second were assumed least likely to occur and therefore received a relative weighting factor of 1.

TABLE 76. EFM AND VEHICLE INTERFACE ADJUSTMENT AND WEIGHTING FACTORS USED FOR TIME ALIGNMENT ERROR GENERATION

Time Alignment Adjustment Number	EFM Adjustment [sec]	Vehicle Interface Adjustment [sec]	Relative Weighting Factor
1	-0.5	-0.5	8
2	-0.5	0.0	8
3	-0.5	0.5	8
4	0.0	-0.5	8
5	0.0	0.0	8
6	0.0	0.5	8
7	0.5	-0.5	8
8	0.5	0.0	8
9	0.5	0.5	8
10	-1.0	-1.0	1
11	-1.0	0.0	2
12	-1.0	1.0	1
13	0.0	-1.0	2
14	0.0	1.0	2
15	1.0	-1.0	1
16	1.0	0.0	2
17	1.0	1.0	1

One transient NTE test from each test engine was reprocessed using each of the time alignment adjustment combinations shown in Table 76. Recall that each transient test was comprised of 30 different 32-second NTE events. For each NTE event, brake-specific emissions were calculated using each of the 3 calculations methods. The differences between the brake-specific results calculated with the time alignment adjustments and the brake-specific results calculated with the nominal time alignment were calculated as a percent of point for each NTE event. With 30 NTE events per cycle and 17 time alignment combinations, 510 time alignment errors were calculated for each engine. Once the time alignment error data was pooled for the 3 engines, a statistical routine was run to apply the specified relative weighting. The routine essentially duplicated each error measurement as specified by the weighting factor, generating a significantly larger pooled error data set. Finally, the 5th, 50th, and 95th percentile error values were calculated for the pooled and weighted error data. The brake-specific time alignment error data is shown in Table 77 for NO_x, and Table 78 for CO. Time alignment data was not generated for NMHC as nearly all PEMS THC measurements were zero.

TABLE 77. BRAKE-SPECIFIC TIME ALIGNMENT ERROR DATA FOR NO_x

Engine	Calculation Method	NO _x 5th Percentile [% of Point]	NO _x 50th Percentile [% of Point]	NO _x 95th Percentile [% of Point]
1	1	-3.3	0.0	1.6
	2	-2.3	0.0	1.8
	3	-1.6	0.0	4.5
2	1	-3.7	-0.5	0.4
	2	-0.9	0.0	0.0
	3	-0.8	0.0	1.6
3	1	-2.0	0.0	1.9
	2	-1.0	0.0	1.8
	3	-1.6	0.0	3.3
Pooled & Weighted	1	-3.2	-0.1	1.5
	2	-1.3	0.0	1.5
	3	-1.4	0.0	2.9

TABLE 78. BRAKE-SPECIFIC TIME ALIGNMENT ERROR DATA FOR CO

Engine	Calculation Method	CO 5th Percentile [% of Point]	CO 50th Percentile [% of Point]	CO 95th Percentile [% of Point]
1	1	-6.6	-0.1	5.2
	2	-5.9	0.0	5.1
	3	-5.7	0.0	12.3
2	1	-8.4	-0.1	5.8
	2	-6.0	0.0	6.1
	3	-5.6	0.0	12.7
3	1	-2.8	0.0	2.2
	2	-3.0	0.0	3.6
	3	-4.8	0.0	12.5
Pooled & Weighted	1	-7.5	0.0	4.6
	2	-5.4	0.0	5.1
	3	-5.2	0.0	12.3

Figure 118 graphically depicts the pooled and weighted brake-specific time alignment errors for NO_x and CO. In the Model, the time alignment errors were applied to the NTE BS result with all errors applied just prior to the subtraction of the reference NTE brake-specific result. The time alignment errors were sampled normally and were dependent on the calculation method. An example of the time alignment error application is shown below.

Method 1 BSNO_x (with full errors) = 3.8 g/kW-hr
 Method 1 BSNO_x (ideal) = 3.5 g/kW-hr
 Method 1 BSNO_x Time Alignment Error = 0.78197%
 Delta BS NO_x = (3.8 + (3.8*0.0078197)) - 3.5 = 0.329714 g/kW-hr

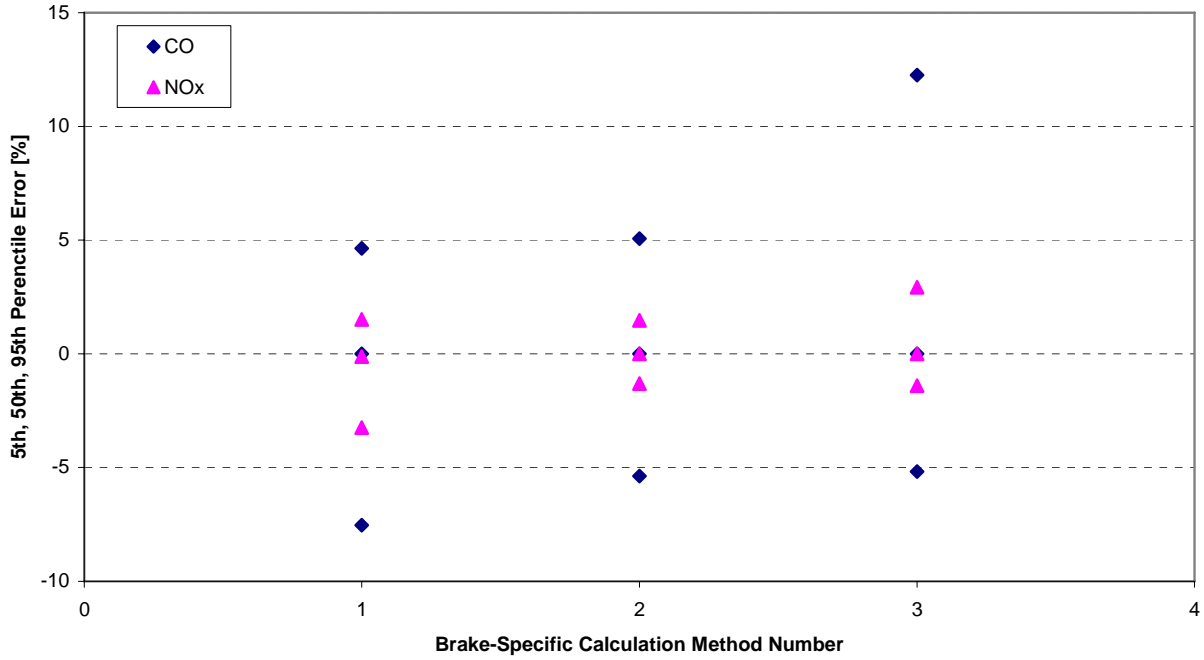


FIGURE 118. POOLED AND WEIGHTED BRAKE-SPECIFIC TIME ALIGNMENT ERROR DATA FOR NO_x AND CO

5.0 ENVIRONMENTAL CHAMBER TESTING

5.1 Environmental Testing Objective

Environmental testing was performed with the SEMTECH-DS devices to quantify gaseous emission concentration and exhaust flow measurement errors when the PEMS were subjected to a variety of environmental disturbances. Environmental conditions evaluated during the program included ambient temperature, ambient pressure, electromagnetic interference, and ambient hydrocarbons. Each environmental test was designed to simulate environmental disturbances that would likely be encountered during in-use field testing.

SwRI's Mechanical and Material Engineering Division (Division 18) performed the environmental testing on site, as specified in the Test Plan and determined by the Steering Committee. Eric Dornes was the managerial Division 18 contact prior to and during the environmental testing. Rick Pitman performed temperature, pressure, and vibration testing, while David Smith and Herbert Walker performed the electromagnetic radiation testing.

5.2 Environmental Testing Procedure

During the various environmental tests, the performance of the PEMS was evaluated by sampling and measuring reference gases. Bottled gases were selected to challenge each PEMS gas analyzer at zero, audit, and span levels. The concentrations of the bottled gases were used as the reference to evaluate the PEMS response to the various environmental disturbances. The PEMS measured responses were compared to the reference concentrations to determine errors or deltas during the environmental testing. The bottled reference gases and corresponding concentrations are shown in Table 79. Reference gas concentrations were chosen based on recommended audit and span levels in the Sensors Inc. user manual. AL size compressed gas cylinders were procured from Scott Specialty Gases. During the program, the Scott gas bottle concentration values were used as the reference. However, each Scott concentration was verified by SwRI before being used for testing. The Test Plan originally specified the use of methane audit and span bottles during environmental testing to challenge the PEMS methane analyzers. However, the SEMTECH-DS methane analyzers were not accepted by the Steering Committee as in-use field instruments and were not used in the Measurement Allowance Program. The Steering Committee therefore elected to eliminate the methane reference gases from the environmental testing procedure.

TABLE 79. REFERENCE GASES AND TYPICAL CONCENTRATIONS USED DURING ENVIRONMENTAL CHAMBER TESTING

Bottle Description	THC [ppm]	CO [ppm]	CO₂ [%]	NO [ppm]	NO₂ [ppm]	Balance
Zero Air	0	0	0	0	0	N/A
NO₂ Audit	0	0	0	0	73	Air
NO₂ Span	0	0	0	0	243	Air
Quad Audit	159.9	178	6.04	257	0	N ₂
Quad Span	663	960	12	980	0	N ₂

The reference gases were overflowed to the inlet of the PEMS sample lines during environmental testing. Using an automated solenoid manifold, the reference gases were sampled at a specific frequency and in a predetermined order. The Test Plan recommended sampling each reference gas for 60 seconds. The first 30 seconds was intended to purge the system and allow the analyzer responses to stabilize, with the final 30 seconds used to record a stable mean measurement. Preliminary data indicated the NDUV NO₂ analyzers had not stabilized after the 30 second purge, therefore the purge duration was lengthened to 45 seconds for each reference gas. With a 45-second purge time and 30-second sample length, each reference gas was sampled for 75 seconds before switching to the next gas. Even after the 45-second purge, initial data indicated the NO₂ concentration was still increasing after switching from the quad blend span gas to the NO₂ span gas. The sample order of the reference gases was therefore set to minimize the stabilization problem of the system, with audit gases preceding the corresponding span gases. The reference gas sequence below decreased the stabilization times of the span gases and was used throughout environmental testing.

1. Purified zero air reference gas
2. NO₂ audit reference gas
3. NO₂ span reference gas
4. Quad blend audit reference gas
5. Quad blend span reference gas

During environmental testing, zero, audit, and span errors were recorded by comparing the 30-second mean concentrations of the recorded PEMS measurements to the reference gas concentrations. Although audit and span deltas could only be recorded when the corresponding audit and span reference gases were being sampled, zero deltas were recorded whenever the analyzer's audit or span gas was not flowing. For example, a zero delta was recorded for NO₂ during the zero air measurement as well as during the quad blend audit and quad blend span gas measurements. Recording a zero delta for NO₂ during the quad blend gas measurements was possible because the quad blend gases contained negligible levels of NO₂. Likewise, zero deltas were recorded for NO, CO, CO₂, and THC during the NO₂ audit and span measurements due to the absence of the quad blend gases in the NO₂ reference gases. The recording strategy used during environmental testing is shown in Table 80. Again, it should be noted that the delta recorded was always the actual analyzer reading minus the reference gas concentration.

TABLE 80. ZERO, AUDIT, AND SPAN DELTA RECORDING STRATEGY USED DURING ENVIRONMENTAL CHAMBER TESTING

Bottle Sequence	Bottle Description	THC [ppm]	CO [ppm]	CO₂ [%]	NO [ppm]	NO₂ [ppm]
1	Zero Air	zero	zero	See Note	zero	zero
2	NO₂ Audit	zero	zero	zero	zero	audit
3	NO₂ Span	zero	zero	zero	zero	span
4	Quad Audit	audit	audit	audit	audit	zero
5	Quad Span	span	span	span	span	zero

Note:
 Slow decay of CO₂ following the quad span gas caused high zero measurements during the zero air test.
 CO₂ zero measurements after the quad span gas were not included in the delta data set.

After reviewing initial environmental data, it was evident CO₂ zero deltas showed a systematic trend. CO₂ zero errors recorded during zero air measurements were higher than zero deltas recorded for NO₂ audit and NO₂ span gas measurements. Figure 119 shows the repeated CO₂ zero delta behavior. The continuous PEMS concentration data indicated the high bias of the zero air CO₂ zero deltas were caused by the continuing decay of the CO₂ measurement after switching from the quad blend span gas to zero air. Figure 120 shows the response and slow decay of a PEMS CO₂ analyzer when zero air is sampled after the quad span gas. After reviewing the initial environmental delta data, the Steering Committee elected to remove the biased CO₂ zero delta recorded during the zero air measurement from the CO₂ zero error population.

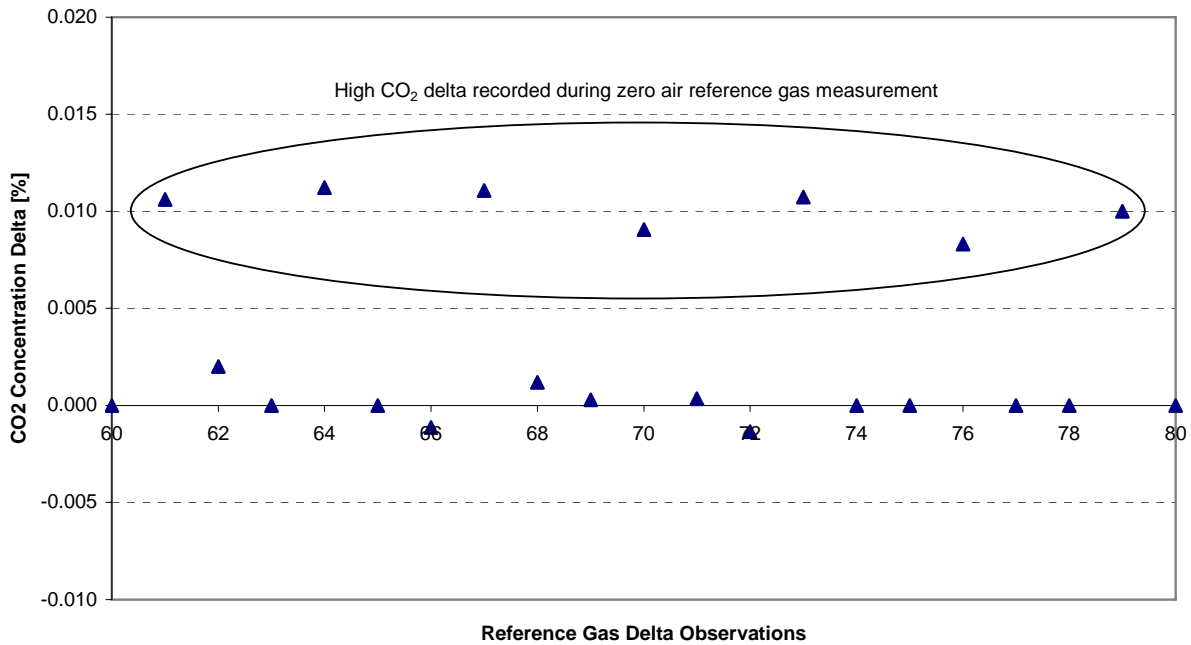


FIGURE 119. SYSTEMATIC HIGH CO₂ BIAS DURING ZERO AIR REFERENCE GAS MEASUREMENT

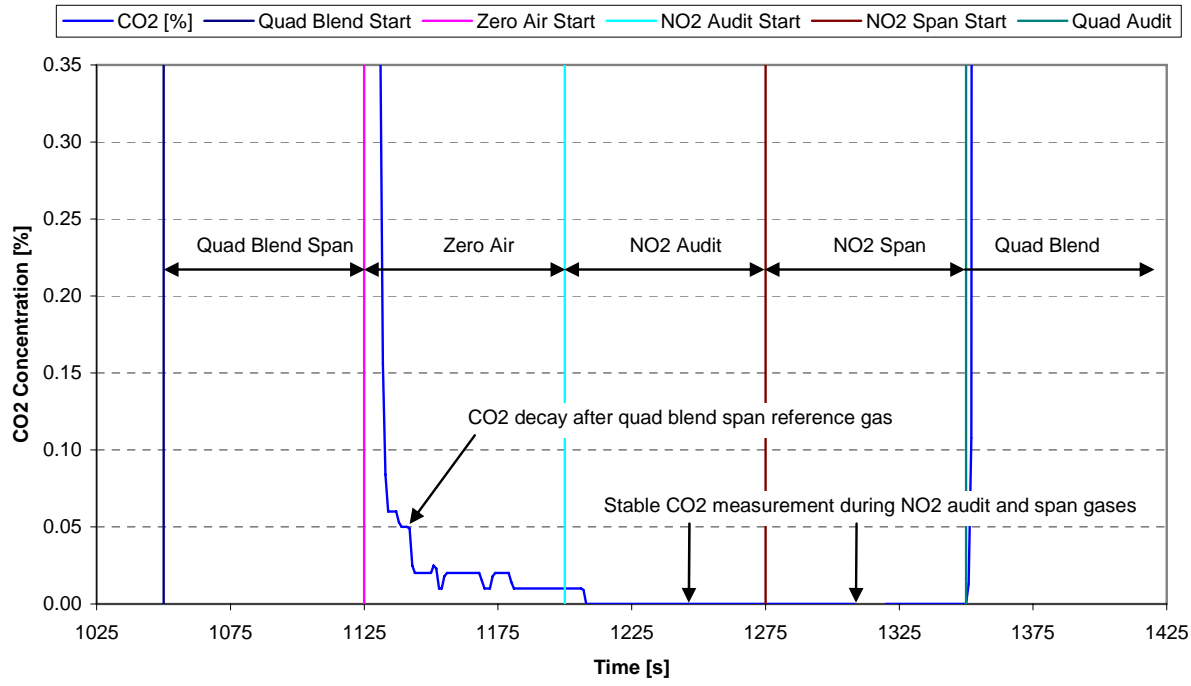


FIGURE 120. CO₂ CONCENTRATION DECAY DURING ZERO AIR MEASUREMENT FOLLOWING THE QUAD BLEND SPAN REFERENCE GAS

During environmental testing, the PEMS were operated in a manner representative of in-use field testing. Each SEMTECH-DS was started and allowed to thermally equilibrate while sampling ambient air for 60 to 90 minutes prior to testing. The PEMS were then zeroed and spanned as specified in the SEMTECH-DS user's manual. The PEMS were spanned with the quad blend reference span gases measured during environmental testing. During testing, the auto-zero feature of the PEMS was used to zero the devices hourly. At the completion of the environmental chamber test, the PEMS were again zeroed and spanned. Span maneuvers were therefore performed only at the beginning and end of each environmental test.

Zero air was used to zero the PEMS instruments throughout the environmental testing program. Also, the PEMS were modified to use zero air as the SEMTECH-DS FID air source rather than ambient air. The use of zero air eliminated potential hydrocarbon measurement errors due to contaminated ambient air. The removal of ambient air hydrocarbon variability during engine and environmental testing was essential because the Ambient Hydrocarbon environmental test was specifically designed to capture FID measurement errors due to varying levels and different species of ambient hydrocarbons. Therefore, zero air was used throughout the program to avoid double counting measurement errors due to ambient hydrocarbons.

A Sensors Inc. 5-inch exhaust flow meter accompanied the SEMTECH-DS units during environmental testing to evaluate the response of the PEMS EFM to various environmental perturbations. One end of the EFM was capped to prevent air flow through the flow meter during testing. Therefore, EFM measurements were recorded as 30-second mean zero errors throughout each environmental test.

The SEMTECH-DS chassis is designed to house a small, high pressure FID fuel bottle. Sensors Inc. recommends using the Scotty 104 aluminum gas cylinder from Scott Gas Company. A full Scotty 104 FID fuel bottle can operate the FID for approximately 7 hours, which was not sufficient for the 8-hour environmental chamber tests. Therefore, midway through each environmental chamber test, the FID fuel bottle was replaced and the FID was re-zeroed and spanned. During the 8-hour pressure test, the PEMS was enclosed in a sealed chamber, making FID fuel bottle replacements impossible. Therefore, two FID bottles were plumbed in parallel during the pressure test. Since the environmental chamber testing, Sensors Inc. has procured FID fuel bottles with a higher pressure rating, allowing FID operation for over 8 hours.

5.3 Baseline Testing

Baseline testing was performed with three SEMTECH-DS devices to determine bias and precision measurement errors for the PEMS with environmental conditions maintained at a nominal level. It was assumed that each subsequent environmental chamber test would inherently include the bias and precision errors recorded during baseline testing. Therefore, the bias and variability errors measured during baseline testing were used to correct the measurement errors generated during each environmental test.

Originally, PEMS 2, 5, and 6 were scheduled to be used for environmental testing. However, during preliminary baseline tests, the PEMS 6 FID would not reach operating temperature and would therefore not zero or span properly. Due to the environmental

temperature chamber schedule, it was necessary to complete the baseline testing as soon as possible. In order to expedite baseline and temperature testing, PEMS 6 was replaced with PEMS 3 from the dynamometer test lab. The use of PEMS 6 in the dynamometer laboratory was deemed acceptable because Engine 1 testing was complete and Engine 2 testing had not started. Therefore, all of Engine 2 and 3 testing was performed with PEMS 1, 4, and 6.

Baseline testing was performed in the Thermotron Walk-In temperature control chamber. Although not used to control the ambient temperature, the chamber provided an environment that was well ventilated, shielded from EMI and RFI, and maintained at relatively constant pressure and temperature. The Walk-In chamber was also large enough to test 3 PEMS devices simultaneously.

After the SEMTECH-DS devices and EFM had warmed and equilibrated, the PEMS were zeroed and spanned. Next, the PEMS were set to sample the reference gases which were controlled by the automated solenoid manifold and overflowed to the inlet of the SEMTECH-DS sample lines. The PEMS measured the indexing reference gases for approximately 60 minutes, after which the PEMS would perform an automated zero maneuver. Baseline testing was conducted for 8 hours, generating 72 independent measurements for each gas. At the completion of the 8-hour baseline test, the PEMS were zeroed and spanned.

The initial baseline testing indicated PEMS 2 and 3 had a NO₂ loss problem. Figure 121 shows the PEMS NO₂ delta data during the first 4 hours of baseline testing. As discussed in the Environmental Test Procedure section, the NO₂ delta values were calculated by subtracting the 30-second mean PEMS NO₂ measurement from the NO₂ span bottle concentration. The initial NO₂ delta values for all PEMS were accurate. However, as the test progressed, PEMS 2 and PEMS 3 showed a decrease in NO₂ concentration measurements which resulted in large negative deltas. Curiously, PEMS 2 and PEMS 3 biased NO₂ measurements recovered during the second and third hours of the 8-hour baseline test.

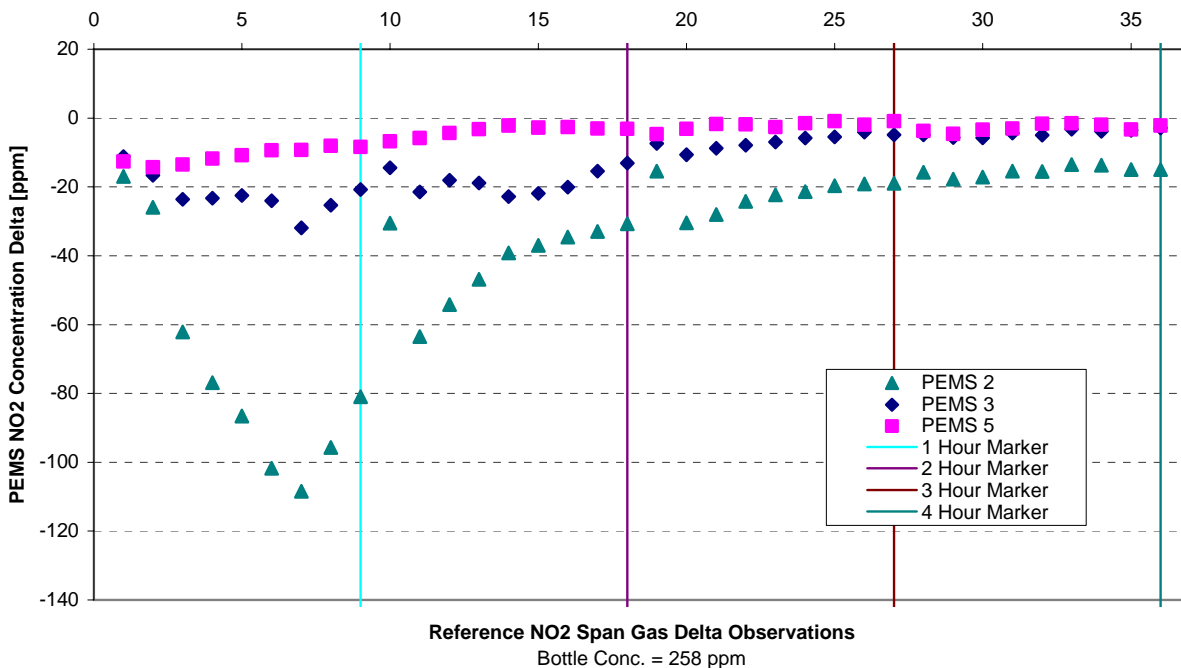


FIGURE 121. PEMS NO₂ DELTA DATA DURING INITIAL ENVIRONMENTAL BASELINE TESTING

The drastic loss of NO₂ during baseline testing prompted an investigation by SwRI and Sensors Inc. Figure 122 shows the NO and NO₂ response of PEMS 2 during the first hour of baseline testing. During the first measurement of the NO₂ span bottle, PEMS 2 reported a concentration near the bottle concentration, yielding a relatively small delta measurement. As expected, PEMS 2 reported near zero concentration levels of NO during the first measurement of the NO₂ span bottle. As the test progressed, the NO₂ concentration measurement of PEMS 2 decreased significantly. As the measured NO₂ concentration decreased, PEMS 2 reported increased levels of NO during measurement the NO₂ span gas. Because the NO₂ span bottle contained negligible levels of NO, measuring over 40 ppm of NO with PEMS 2 during the NO₂ span gas measurement was unexpected. With reduced levels of NO₂ and increased levels of NO, it was apparent a NO₂ to NO conversion was taking place. However, the sum of NO₂ and NO during the NO₂ span gas measurement was still less than the NO₂ span bottle concentration, indicating NO₂ was not only being converted to NO, but also lost.

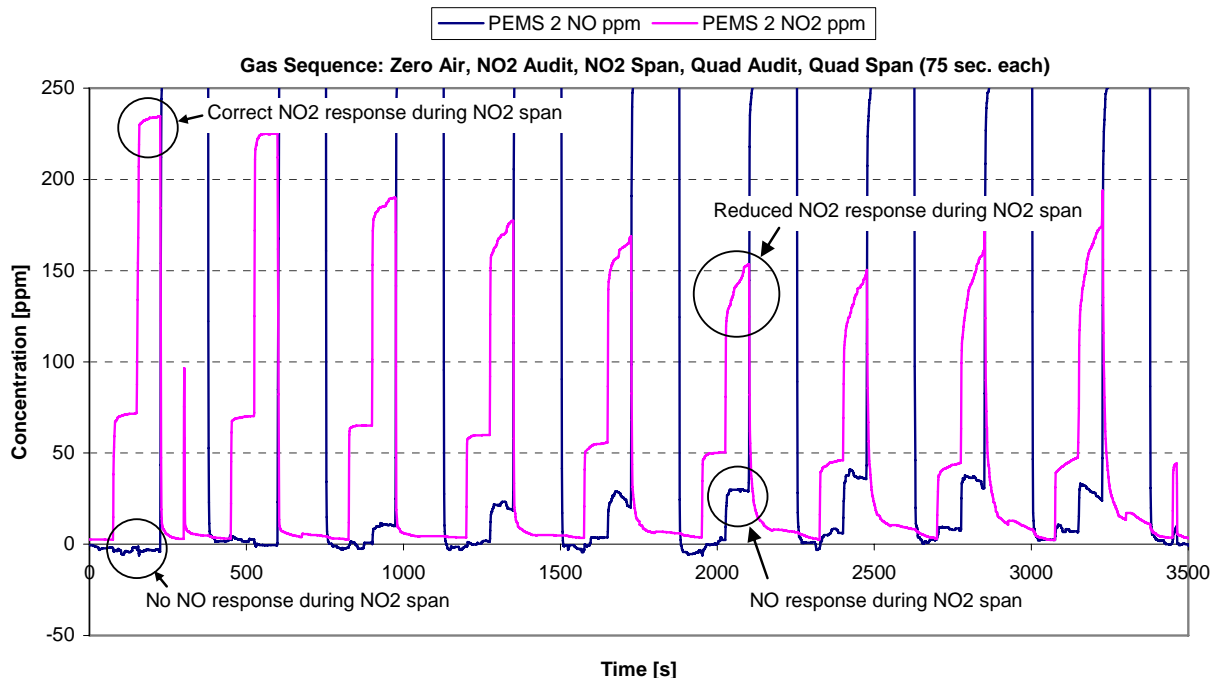


FIGURE 122. PEMS 2 NO AND NO₂ RESPONSE DURING HOUR 1 OF INITIAL ENVIRONMENTAL BASELINE TESTING

In trying to repeat the NO₂ loss problem, it was discovered that the PEMS units had to be turned off or left idle for several hours before the NO₂ loss phenomena could be repeated. PEMS 2 had to be left idle overnight to reproduce the results shown in Figure 121. To insure the SwRI overflow gas delivery system was not causing the NO₂ loss/conversion problem observed with PEMS 2 and 3, the Horiba OBS-2200 was fed gas from the SwRI supply manifold and operated in NO mode during a repeated baseline type test. Similar to the initial baseline test, PEMS 2 and 3 showed a loss in NO₂ and an increase in NO. The Horiba OBS-2200 showed no NO concentration increase during the NO₂ span gas measurement, indicating the NO₂ loss and conversion was not caused by the SwRI gas delivery hardware. Next, a test was run with the sample time for zero air increased to 300 seconds to observe the effect of a lengthened zero air purge. The sample times for the audit and span gases were left at 75 seconds. The NO₂ loss with extended zero air sample time was similar to the initial baseline test results.

Another test was performed with the quad blend audit and span gases removed from the gas cycle sequence to determine if the presence of HC, CO, CO₂, or NO was causing the NO₂ loss problem. Although a slight NO₂ loss was observed, the magnitude of the loss was greatly reduced with the quad blend gases removed from the gas sampling sequence. A question then surfaced about whether the reduction in NO₂ loss was caused by the removal of HC, CO, CO₂, and NO, or the absence of sampling gases that contained no oxygen. Because the NO₂ audit and span gases are balanced with air, removing the quad blend audit and span gases (balance N₂), eliminated the sampling of gases with no oxygen. A test was therefore performed with N₂ gas in place of the quad blend audit and span gases. The gas sequence for this experiment was zero air, NO₂ audit gas, NO₂ span gas, N₂ and N₂ again. All gases were sampled for 75 seconds. With

quad blend gases replaced with N₂, the NO₂ loss was similar to the initial baseline test results. Therefore, the NO₂ loss problem appeared to be dependant on the PEMS sampling oxygen-free gases.

The next NO₂ conversion/loss test was performed with the PEMS filters and heated sample line removed from the system. Again, results were similar to the initial baseline testing, showing significant NO₂ loss. A test was then performed with the SEMTECH-DS thermoelectric chiller bypassed in the sample handling system. With the chiller bypassed in the system, the NO₂ measure was nearly perfect and showed no loss or conversion issues. Figure 123 shows the NO₂ and NO response for PEMS 2 with the thermoelectric chiller bypassed and then reconnected. With the chiller bypassed, the NO₂ measurement was near the span bottle concentration of 248 ppm. Once the chiller was reconnected in the sample handling system, the NO₂ loss/conversion problem became immediately apparent.

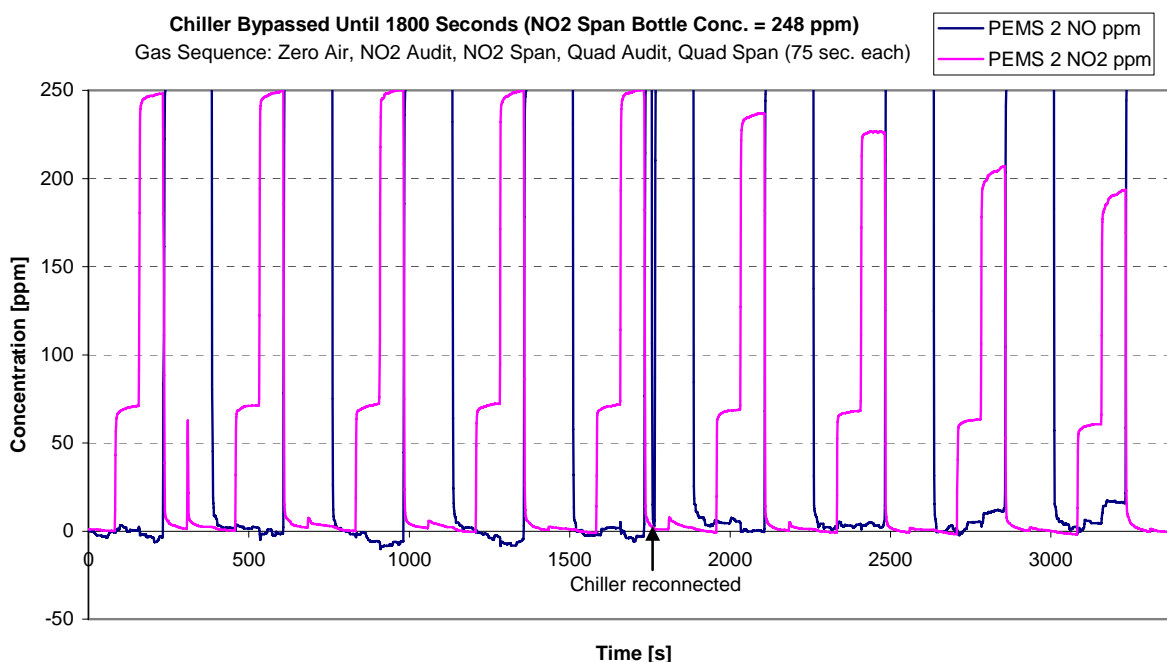


FIGURE 123. PEMS 2 NO₂ AND NO RESPONSE WITH THERMOELECTRIC CHILLER BYPASSED AND RECONNECTED

PEMS 2 and 3 received new thermoelectric chillers. After installation of the replacement chillers, no NO₂ loss or conversion was evident. A possible explanation for the NO₂ loss problem is that the chillers' internal passivated coating may have been compromised. All PEMS units, with the exception of PEMS 7, were used for emission testing prior to being sent to SwRI for use in the Measurement Allowance Program. Not knowing the history of each PEMS, use or misuse of the PEMS before arrival at SwRI may have caused the chiller NO₂ loss/conversion problem.

Environmental baseline testing was repeated with PEMS 2 and 3 after installation of the new thermoelectric chillers. PEMS 5, showing no NO₂ loss or conversion during the initial baseline test, did not undergo repeated baseline testing. Rather, PEMS 5 performed temperature chamber testing shortly after the initial environmental baseline test. Immediately after temperature testing, PEMS 5 was shipped to CE-CERT to avoid delaying the on-road model validation testing.

The compiled zero delta data for the 8-hour environmental baseline test is shown in Figure 124 for PEMS 2. During the test, 216 zero delta observations were recorded for each gaseous emission with the exception of CO₂. Due to the elimination of the biased CO₂ zero deltas measured while sampling zero air, 144 CO₂ zero deltas were recorded during the baseline test. With the replacement chiller, PEMS 2 showed NO₂ and NO zero deltas within ± 5 ppm. The NO₂ and NO deltas were added to produce the NO_x zero delta measurement. Hydrocarbon zero measurements were also accurate, with zero deltas less than 2 ppm. As discussed in the Environmental Testing Procedure section of the report, the FID fuel bottle was replaced midway through the baseline test; after which the FID was re-zeroed and spanned. Considering the 10 ppm resolution of the CO analyzer and past experience measuring positive CO biases through the PEMS sample line, the 70 ppm range of CO zero deltas was not unexpected. The CO₂ analyzer provided accurate zero measurements with zero deltas within ± 0.01 %. The environmental chamber test results for PEMS 2, 3, and 5 are included in Appendix K.

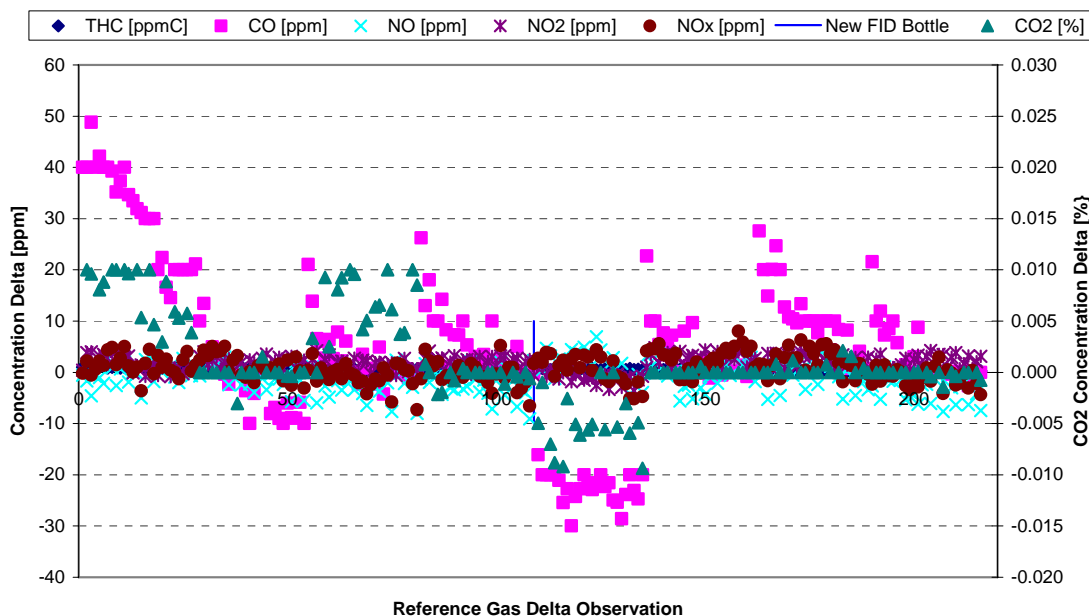


FIGURE 124. PEMS 2 ENVIRONMENTAL BASELINE ZERO DELTA MEASUREMENTS

The audit delta observations for PEMS 2 are shown in Figure 125. During the 8-hour baseline test, 72 audit deltas were recorded for each gaseous emission. As listed in Table 79, the quad blend reference audit bottle concentrations were near 160 ppmC THC, 178 ppm CO, 6 % CO₂, and 247 ppm NO. The NO₂ audit bottle concentration was near 73 ppm. The PEMS mean

gaseous measurements were compared to the reference audit bottle concentrations to generate the audit delta values. NO audit deltas were centered around zero and generally within ± 5 ppm. NO₂ audit deltas showed a negative bias of approximately 8 ppm. A noticeable positive shift in the NO₂ audit deltas is evident after observation number 45. The shift in the NO₂ delta measurement was due a zero calibration adjustment at the end of one of the 8 hour long segments of testing. The zero adjust can also be seen in the zero delta data at observation number 45 in Figure 124. Although the THC zero delta data was accurate, a positive bias of approximately 10 ppmC was evident with the THC audit measurement, indicating a possible span error. After replacing the FID fuel bottle and re-zeroing and spanning the FID, the audit delta measurement shifted to approximately 8 ppmC. CO₂ showed a slight negative audit delta bias, with deltas between -0.05 and 0.0 %. CO showed a slight positive audit delta bias, with deltas between 0 and 50 ppm. Bottle naming errors are included in the audit delta data set because the SEMTECH-DS instruments were not spanned with the audit reference gases. However, the reference gas concentrations were named by Scott Specialty Gas Company and checked by SwRI. In general, the Scott and SwRI bottle measurements were within ± 1.0 %. Baseline audit deltas for PEMS 3 and 5 can be found in Appendix K.

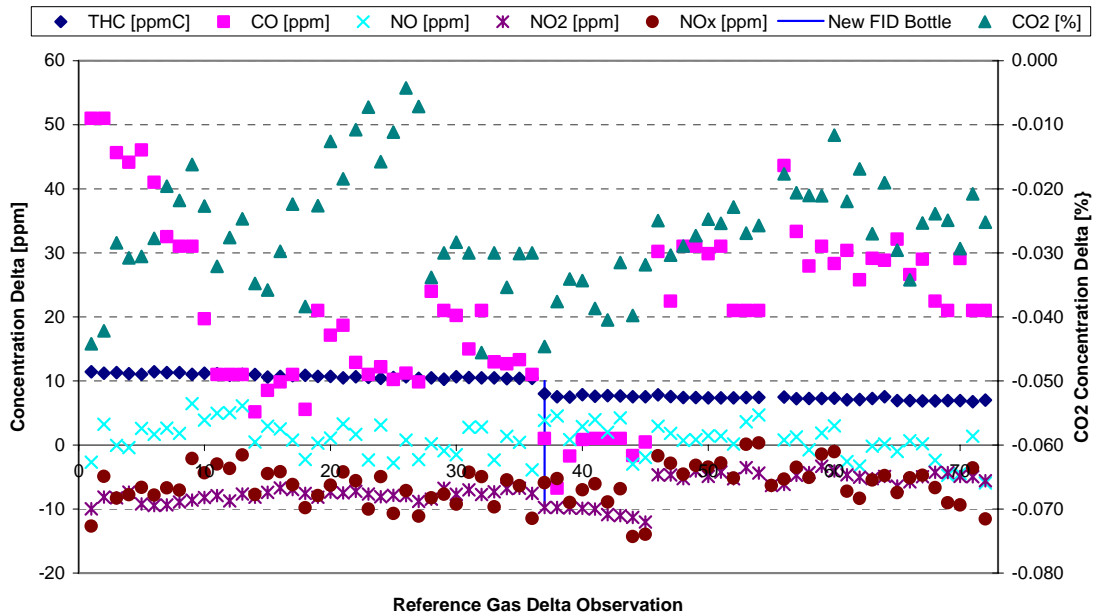


FIGURE 125. PEMS 2 ENVIRONMENTAL BASELINE AUDIT DELTA MEASUREMENTS

The span delta measurements for PEMS 2 are shown in Figure 126. During the 8-hour baseline test, 72 span deltas were recorded for each gaseous emission. As listed in Table 79, the quad blend reference span bottle concentrations were near 663 ppmC THC, 960 ppm CO, 12 % CO₂, and 980 ppm NO. The NO₂ audit bottle concentration was near 243 ppm. The PEMS 30-second mean gaseous measurements were compared to the reference span bottle concentrations to generate the span delta values. With the replacement thermoelectric chiller, PEMS 2 NO₂ measurements showed no significant negative bias and no conversion of NO₂ to NO. NO₂ span deltas were generally within ± 5 ppm. During the first half of the baseline test, NO span deltas

were center around zero error. During the second half of the test, PEMS 2 NO measurements drifted slightly negative, with NO deltas reaching -15 ppm. The THC span deltas were biased 10 ppmC high during the first half of the 8-hour baseline test. After replacing the FID fuel bottle the FID was re-zeroed and spanned. After the THC zero and span maneuvers, the THC span deltas were near zero. CO₂ span deltas were between -0.02 and 0.04, while CO span deltas were typically between -20 and 40 ppm. Because the PEMS were spanned with the reference span gases used during baseline testing, bottle naming errors are not included span delta data set.

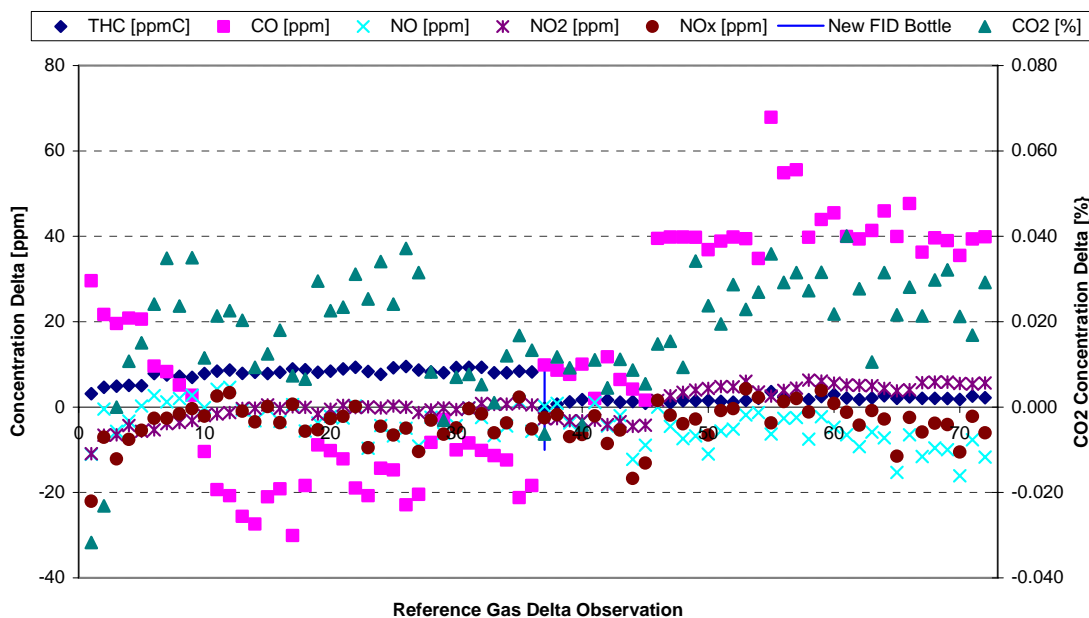


FIGURE 126. PEMS 2 ENVIRONMENTAL BASELINE SPAN DELTA MEASUREMENTS

Deltas observed during environmental baseline testing were likely caused by a number of factors. For example, the PEMS analyzers were zeroed and spanned through the zero and span ports on the front of the SEMTECH-DS instruments. When using the zero and span ports, the reference gases bypassed the majority of the sample handling system, including the stainless steel cooler, the coalescing filter, and the thermoelectric chiller. Using a pneumatic path to zero and span the analyzers that was different than the path used during sampling may have caused environmental baseline errors.

Zero and span maneuver errors were also captured during the baseline test. The ability of the PEMS to zero and span accurately was captured during environmental baseline testing. Although 8 zero events occurred for each PEMS during baseline testing, only one span event was performed for NO, NO₂, CO, and CO₂. THC was spanned twice during baseline testing. As discussed in the environmental error surface sections of the report, having only one span event for each environmental test complicated the extraction of PEMS measurement errors caused by environmental factors. Deltas caused by span errors were often larger than the delta data for an environmental test, thus resulting in biases that were not related to the environmental condition

being tested. The data for each environmental test and for each PEMS was therefore reviewed before environmental error surfaces were calculated.

As discussed in the Environmental Test Procedure section of the report, a Sensors Inc. 5-inch EFM was used to capture possible flow measurement errors due to environmental disturbances. One end of the flow meter was capped to prevent air flow through the meter. Throughout baseline testing, 30-second EFM flow rate averages were taken with each reference gas observation. Shown in Figure 127, the observations were calculated as zero deltas for the flow measurement system. Most 30-second mean measurements were below 0.6 scfm. Rated at 1700 scfm, the maximum observed flow meter error was less than 0.1 % of full scale. The baseline EFM data was compared to the EFM data from other environmental tests to determine flow measurement errors due to changes in environmental conditions.

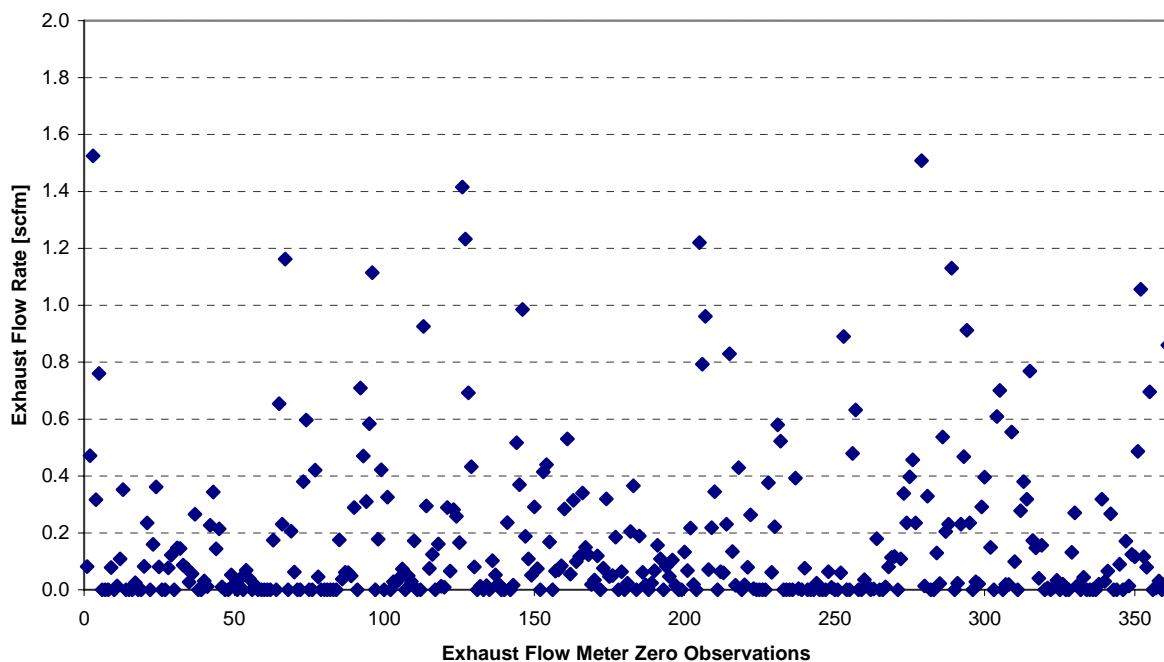


FIGURE 127. 5-INCH EFM ENVIRONMENTAL BASELINE ZERO DELTA MEASUREMENTS

5.4 Temperature Chamber Testing

Temperature chamber testing was performed with three SEMTECH-DS devices to quantify PEMS gaseous concentration and exhaust flow measurement errors due to changes in ambient temperature. The temperature test was designed to simulate real-world temperatures and changes in temperature. Therefore, the temperature profile used during testing nearly matched the atmospheric temperature distribution of EPA's 2002 National Emissions Inventory (NEI) model. Taken from the Test Plan, Figure 128 shows the NEI temperature distribution as well as the test cycle temperature distribution.

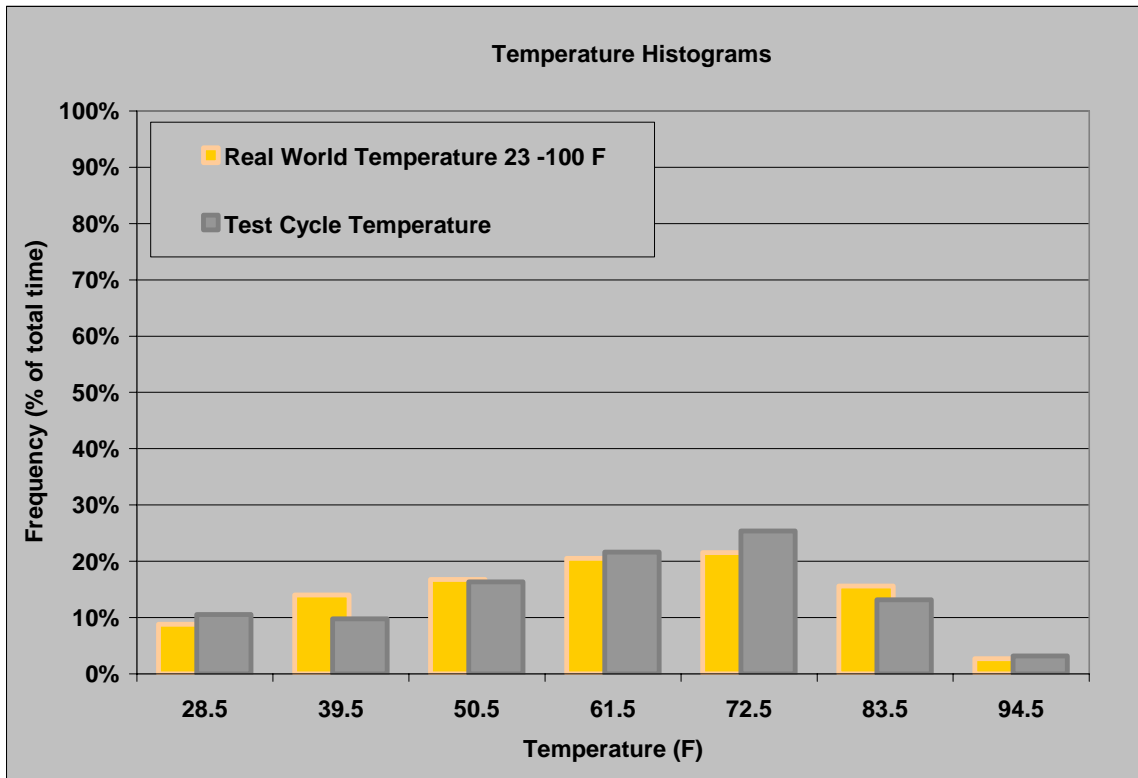


FIGURE 128. TEMPERATURE HISTOGRAMS FOR NEI MODEL AND TEST PROFILE

The ambient temperature profile used for chamber testing was defined by a series of temperature ramps with soaking periods between each transition. As written in the Test Plan, Table 81 and Figure 129 define the 8-hour ambient temperature profile used during the program.

TABLE 81. TEMPERATURE TEST PROFILE DEFINITION

Ambient Temperature Test Sequence					
Phase	Temperature		Time	Rate	Comments
	°C	°F	min	°C/min	
1 Soak	13.89	57	10	0.00	Cool in-garage pre-test PEMS operations
2 Ramp	13.89-5.00	57-23	5	-3.78	Leaving cool garage into cold ambient
3 Soak	-5.00	23	5	0.00	Operating at cold temperature outside of vehicle
4 Ramp	-5.00-12.78	23-55	145	0.12	Diurnal warming during cool day
5 Soak	12.78	55	40	0.00	Steady cool temperature during testing
6 Ramp	12.78-28.33	55-83	5	3.11	Return to hot garage on a cool day
7 Soak	28.33	83	52	0.00	Hot in-garage pre- post- test PEMS operations
8 Ramp	28.33-37.78	83-100	5	1.89	Leaving ho garage into hot ambient
9 Soak	37.78	100	8	0.00	Operating at hot temperature outside of vehicle
10 Ramp	37.78-22.22	100-72	100	-0.16	Diurnal cooling during hot day
11 Soak	22.22	72	60	0.00	Steady moderate temperature during testing
12 Ramp	22.22-13.89	72-57	5	-1.67	Return to cool garage on a moderate day
13 Soak	13.89	57	40	0.00	Cool in-garage post-test PEMS operations

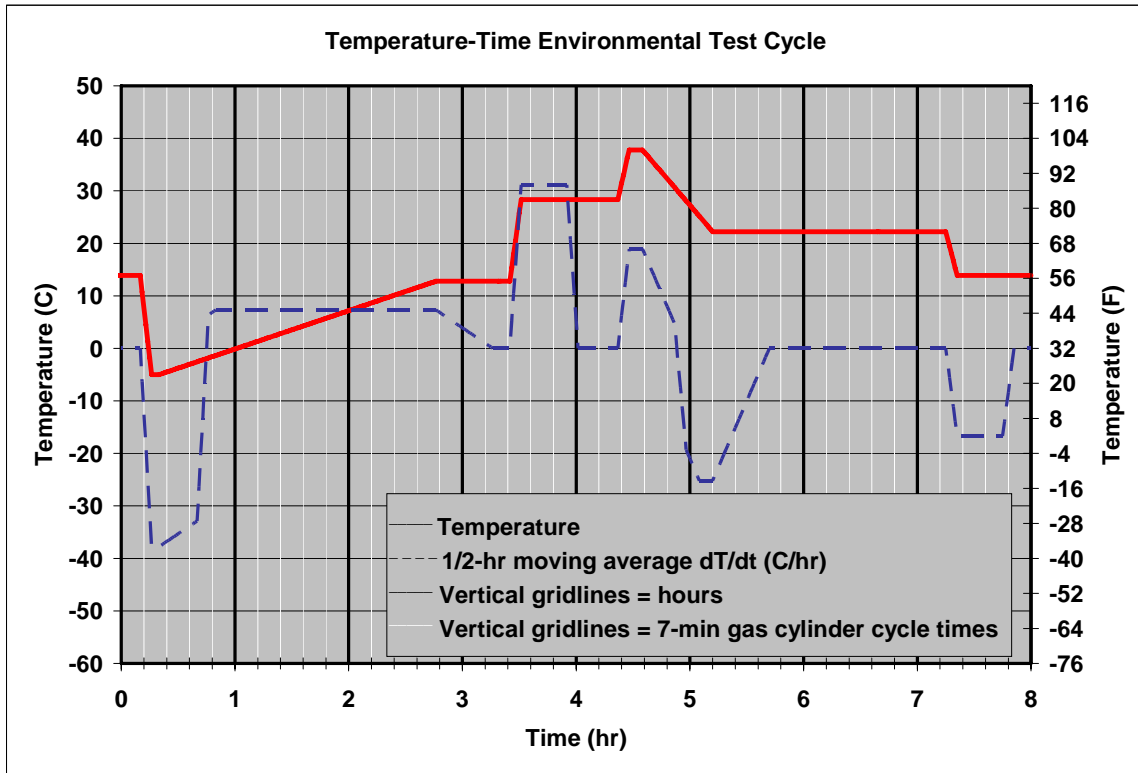


FIGURE 129. TEMPERATURE TEST PROFILE AND MOVING AVERAGE

Temperature testing was originally scheduled to be performed with a Thermotron Walk-In temperature enclosure. The Walk-In chamber could easily house three PEMS devices, therefore, temperature testing could be completed in one day. However, with the PEMS and auxiliary hardware, it was unlikely the large Thermotron Walk-In would achieve the steepest cooling ramps as defined in the Test Plan. Therefore, each PEMS was tested individually with a smaller Thermotron SM-32 temperature control chamber, shown in Figure 130. The Thermotron

SM-32 used liquid nitrogen for supplemental cooling, and achieved all target temperatures and ramp rates. The Thermotron SM-32 chamber housed the PEMS unit, EFM, and temperature/relative humidity probe. The SEMTECH-DS heated sample lines, zero and span gas lines, drain lines, and Ethernet cables were routed out of the chamber through ports on the chamber sides.



FIGURE 130. THERMOTRON SM-32 TEMPERATURE CONTROL CHAMBER WITH SUPPLEMENTAL LIQUID NITROGEN CYLINDER

Prior to executing the environmental temperature test, the PEMS were allowed to thermally equilibrate while sampling ambient air for over one hour. The PEMS were then zeroed and spanned at ambient temperature, approximately 23°C. The environmental temperature test was then started by ramping to the initial temperature soak point as specified in the Test Plan. During the 8-hour temperature test, the PEMS were automatically zeroed every hour. The temperature control chamber was not paused during the test, therefore, zero events occurred at the temperatures defined by the Test Plan's temperature profile definition. Zero events occurred near the hour markers shown in Figure 129. Similar to environmental baseline testing, zero, audit, and span deltas were recorded by comparing the 30-second PEMS mean concentration measurements to the reference gas concentrations. PEMS 3 performed temperature testing in a Sensors Inc. environmental enclosure.

The zero deltas measured during the 8-hour temperature test are shown in Figure 131 for PEMS 2. Mean temperature measurements from the PEMS temperature/relative humidity probe are also shown in Figure 131. Analyzer zero drift caused by temperature variation was evident throughout the temperature test. For example, during the steep temperature ramp at the

beginning of the cycle, NO, NO₂, and CO drifted downward. The zero maneuver at the end of the first hour of operation corrected the negative zero drift. Positive zero drift was evident during the 4th and 5th hours of testing when the temperature was increasing aggressively. Again, the hourly zero maneuvers continually corrected the zero drift. Slight negative drift occurred during the last 3 hours of the 8-hour test, when the chamber temperature was decreasing. CO₂ and THC measurements were largely unaffected by the temperature fluctuations experienced during the environmental temperature test. Temperature data is included for all PEMS in Appendix K. NO, NO₂, CO, and CO₂ behaved similarly with the three PEMS units during the temperature tests. THC measurements with PEMS 3 and 5 showed slightly more susceptibility to temperature induced zero drift than PEMS 2.

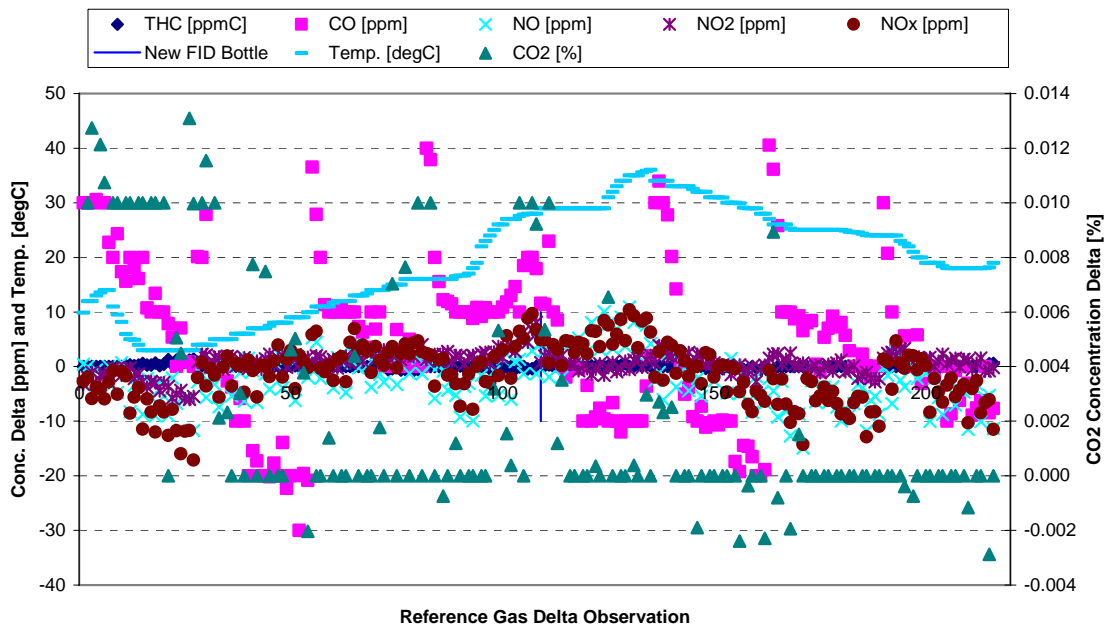


FIGURE 131. PEMS 2 ENVIRONMENTAL TEMPERATURE ZERO DELTA MEASUREMENTS

Figure 132 shows the audit deltas measured during environmental temperature testing for PEMS 2. For reference, the PEMS temperature probe mean measurement is plotted with the audit delta values. During the first hour of the temperature cycle, the NO₂ audit measurement drifted negative, similar to the zero measurement. The zero maneuver at the end of the first hour of testing not only corrected the zero drift, but also corrected the negative audit drift. The NO₂ audit delta remained between -5 and -10 ppm for the last 7 hours of the 8-hour test. NO audit deltas were between -10 and 10 ppm throughout the test. The THC audit deltas appeared unaffected by temperature variation; however, the THC audit delta was near 20 ppm for the first half of the test. After replacing the FID fuel bottle and zeroing and spanning the FID, the audit deltas were below 10 ppm. CO and CO₂ temperature audit deltas were similar to the audit deltas observed during baseline testing. As seen in Appendix K, the audit delta behavior was similar between the PEMS, with PEMS 3 and 5 showing slightly more THC temperature drift.

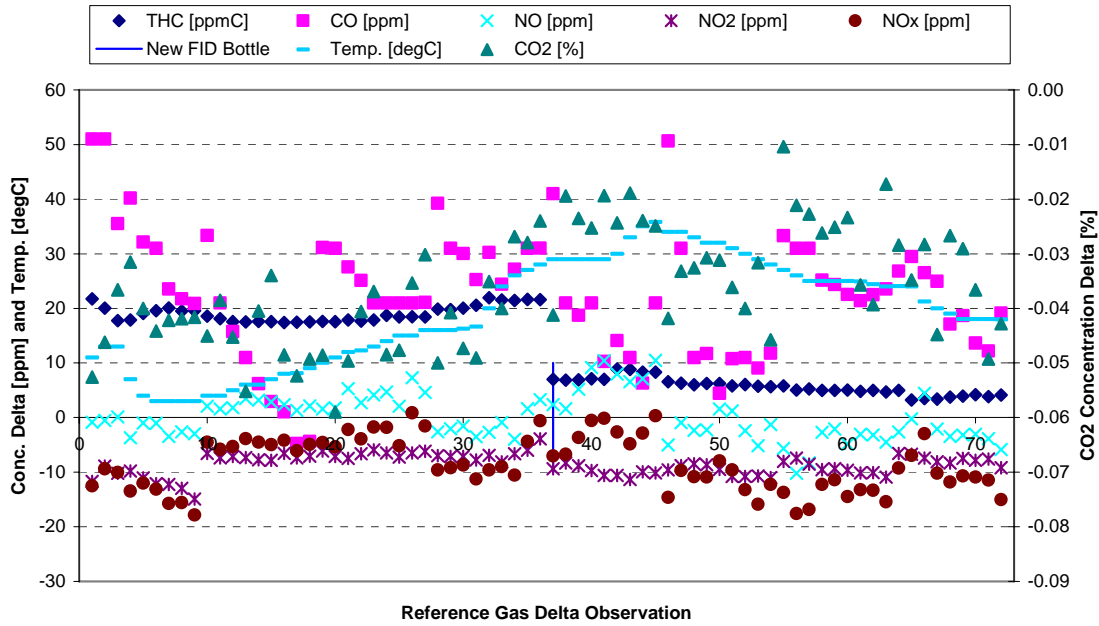


FIGURE 132. PEMS 2 ENVIRONMENTAL TEMPERATURE AUDIT DELTA MEASUREMENTS

Figure 133 shows the span deltas for PEMS 2 during the temperature test. NO₂ span deltas were minimal, generally within ± 5 ppm. NO, CO, and CO₂ span deltas were similar or slightly more variable than the span deltas observed during baseline testing. PEMS 2 THC span deltas showed large perturbations that followed a trend similar to the temperature profile. PEMS 3 and 5 also showed THC span deltas that were larger than the baseline test span deltas. An explanation offered by Sensor Inc. in regard to the large PEMS 2 THC span delta measurements was that the FID drain pressure may have been slightly elevated. The FID is sensitive to drain backpressure, which may have been slightly elevated due to the extended length of the drain lines during temperature testing. The Steering Committee elected to accept the temperature data although the THC span delta data may have been influenced by the test setup. Due to the low THC levels of the reference NTE events used in the Model, the THC span deltas would never be used in the Model calculations. Because the NO, NO₂, CO, and CO₂ temperature delta data was sound, and the THC span delta would not influence the Model, it was decided not to repeat the temperature testing.

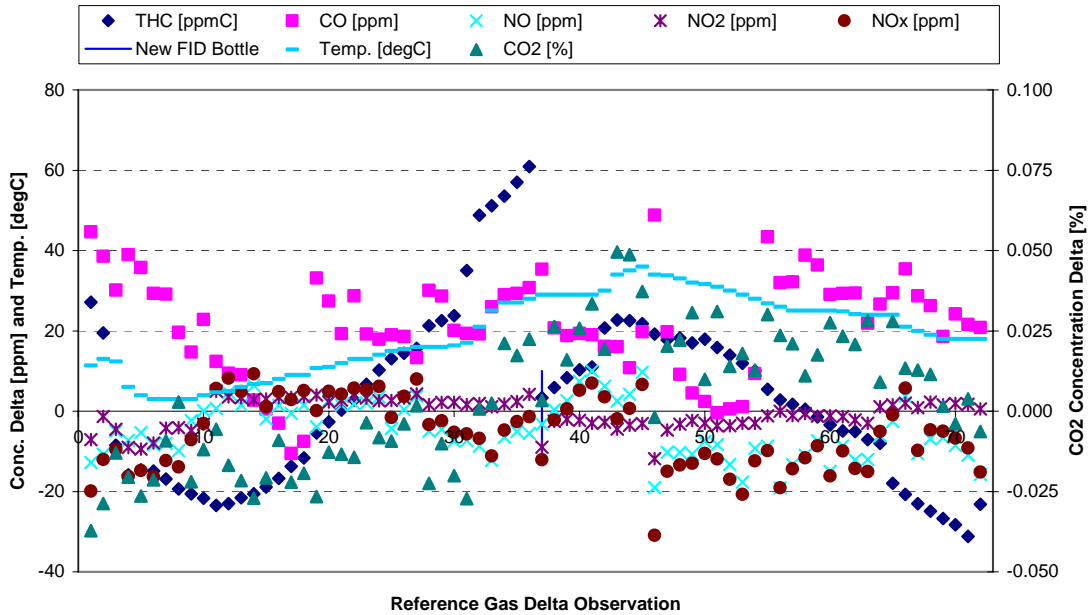


FIGURE 133. PEMS 2 ENVIRONMENTAL TEMPERATURE SPAN DELTA MEASUREMENTS

A Sensors Inc. 5-inch EFM also underwent environmental temperature testing. The flow meter with pressure transducer enclosure was placed in the temperature chamber during the 8-hour test. Similar to baseline testing, one end of the EFM was capped to prevent air flow through the meter. Figure 134 shows the 30-second mean flow meter measurements during the temperature test. The zero deltas observed during temperature testing largely resembled the EFM deltas recorded during baseline testing. Two periods midway through the temperature test showed slightly increase EFM measurements. One perturbation occurred after the 150th mean delta measurement, while the other occurred between observation number 200 and 250. The deviations from zero were small, with the maximum zero error under 0.3 % of the EFM’s rated flow range of 1700 scfm.

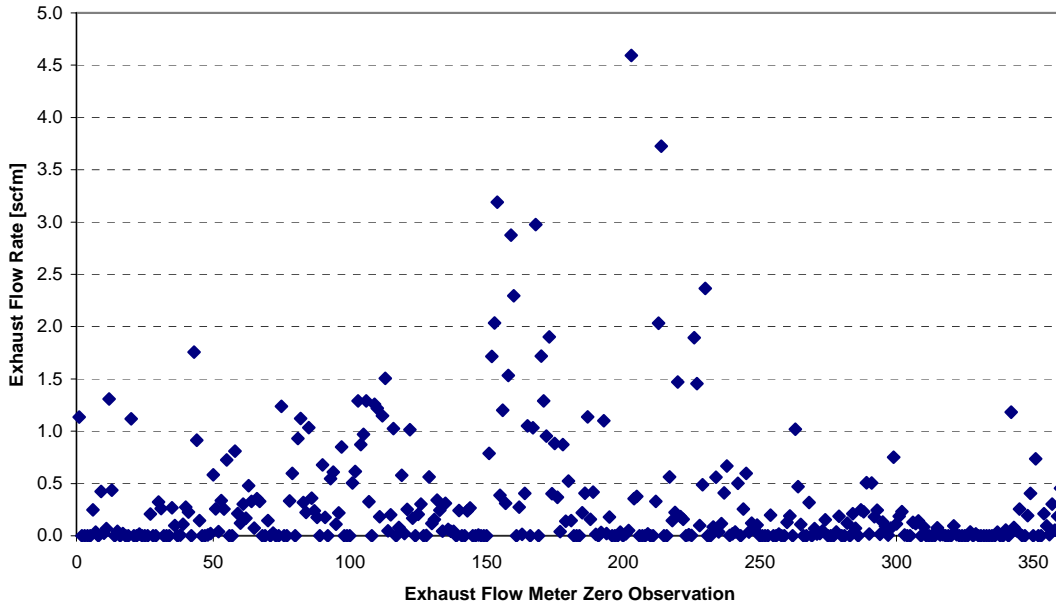


FIGURE 134. 5-INCH EFM ENVIRONMENTAL TEMPERATURE ZERO DELTA MEASUREMENTS

5.4.1 Temperature Error Surface Generation

Because the temperature test was designed to simulate real-world temperatures and changes in temperature, the deltas measured during temperature testing were randomly sampled in the Model. However, it was assumed that temperature chamber testing would inherently include the bias and precision errors recorded during baseline testing. Therefore, the bias and variability errors measured during baseline testing were used to correct the measurement errors generated during each environmental test.

The initial step in generating the temperature error surfaces was to correct each temperature measurement error for any bias measured during baseline testing. This discussion focuses on NO_x concentration, however, the same process was applied to each gaseous emission. The median baseline NO_x delta was calculated for each PEMS at the zero, audit, and span levels. The median baseline deltas were subtracted from each delta measured during temperature testing. For example, the PEMS 2 median baseline zero delta was subtracted from each PEMS 2 delta recorded during temperature testing. A similar procedure was performed for the audit and span deltas. The median environmental baseline NO_x concentrations for PEMS 2, 3, and 5 are shown in Table 83. To remove the baseline variability from the temperature test data, multiplicative scaling factors were calculated. The median absolute deviation (MAD) was calculated for each baseline delta data set as well as the bias corrected temperature delta data set. Scaling factors were calculated using the equation below. The scaling factors, shown in Table 82, were multiplied to each bias corrected temperature delta to reduce the variability of the data. Similar to the bias correction, the variability correction was performed for each PEMS and at the zero, audit, and span levels.

$$\text{Scaling_Factor} = \frac{\sqrt{MAD_{Rad}^2 - MAD_{BL}^2}}{MAD_{Rad}}$$

TABLE 82. MEDIAN ENVIRONMENTAL BASELINE NO_x CONCENTRATIONS AND ENVIRONMENTAL TEMPERATURE SCALING FACTORS

		Median Baseline NO_x Delta [ppm]	NO_x Temperature Scaling Factor
Zero	PEMS 2	0.9	0.85
	PEMS 3	2.3	0.66
	PEMS 5	3.2	0.77
Audit	PEMS 2	-6.1	0.90
	PEMS 3	-6.3	0.93
	PEMS 5	-10.5	0.88
Span	PEMS 2	-2.9	0.94
	PEMS 3	-4.7	0.91
	PEMS 5	-7.5	0.97

Figure 135 through Figure 137 show the corrected zero, audit, and span NO_x temperature deltas for each PEMS. The corrected temperature deltas for all gaseous emission can be found in Appendix K. The trends of the NO_x deltas measured during temperature testing could be linked to changes in temperature by comparing the deltas with the chamber temperature profile. Also, the 3 PEMS showed similar NO_x delta patterns, indicating a susceptibility to ambient temperature. Therefore, inclusion of the NO_x temperature error surface was justified. CO, CO₂, and NMHC delta trends were not as easily linked to changes in temperature. Also, the CO, CO₂, and NMHC delta patterns for the 3 PEMS were not as tightly matched as for NO_x. Therefore, it was not clear whether the CO, CO₂, and NMHC deltas were caused by the ambient temperature test or by some other factors. This problem was presented to the Steering Committee. After review of the data and recommendations by SwRI, a decision was reached to include temperature error surfaces for all of the gaseous emissions. Justification for the inclusion of all pollutants included the following.

1. The variance of the temperature data was generally larger than the baseline data, indicating an ambient temperature susceptibility.
2. The deltas from one or more PEMS showed a subtle correlation to the chamber temperature profile.
3. There was slight agreement of the delta patterns between PEMS, indicating a common error source.

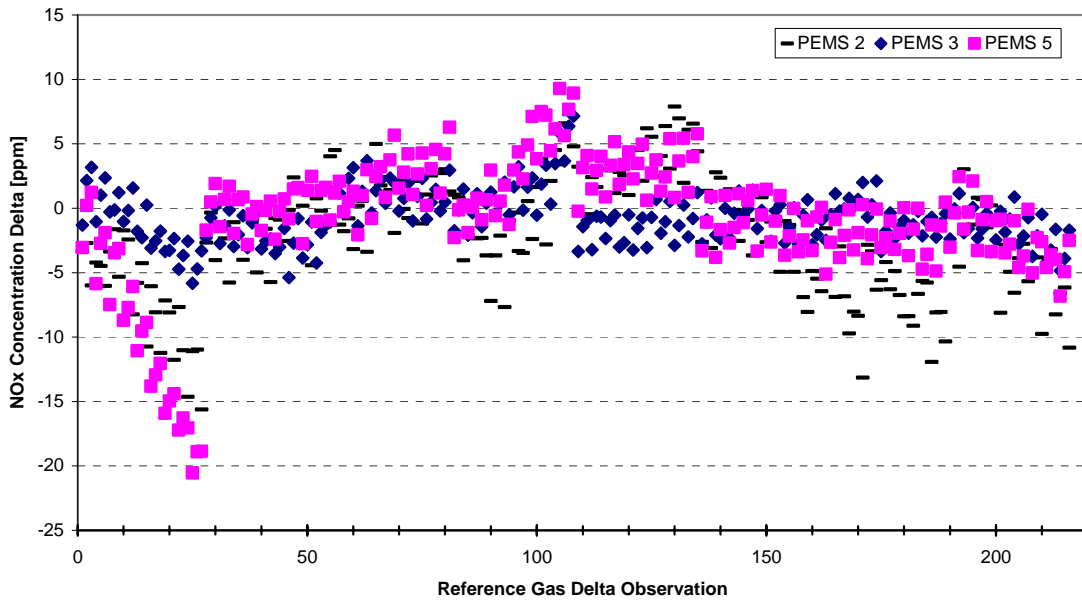


FIGURE 135. ERROR SURFACE FOR ENVIRONMENTAL TEMPERATURE NO_x CONCENTRATION ZERO DELTA MEASUREMENTS

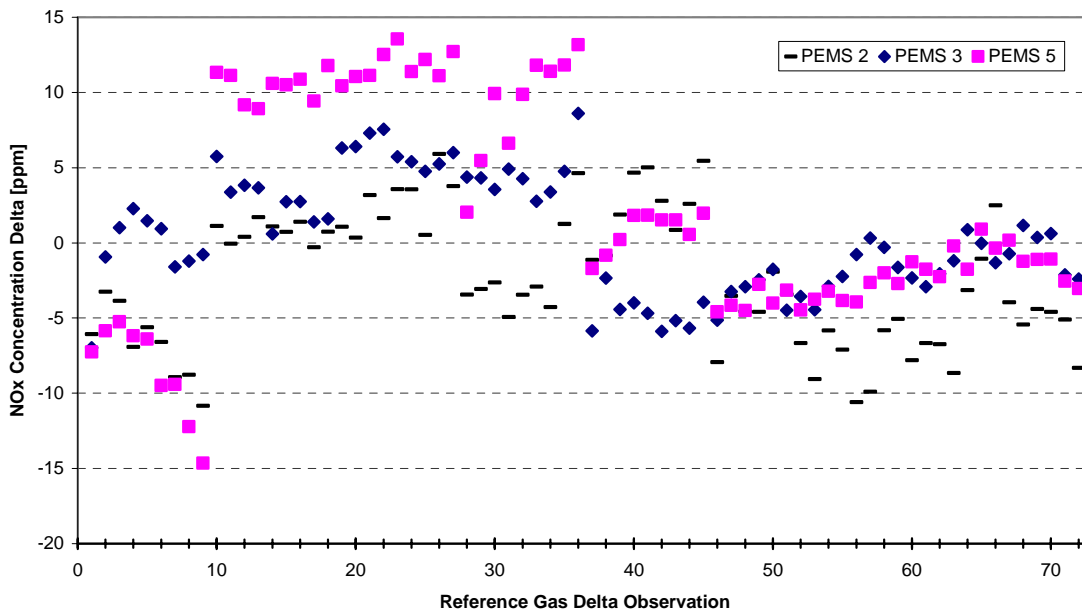


FIGURE 136. ERROR SURFACE FOR ENVIRONMENTAL TEMPERATURE NO_x CONCENTRATION AUDIT DELTA MEASUREMENTS

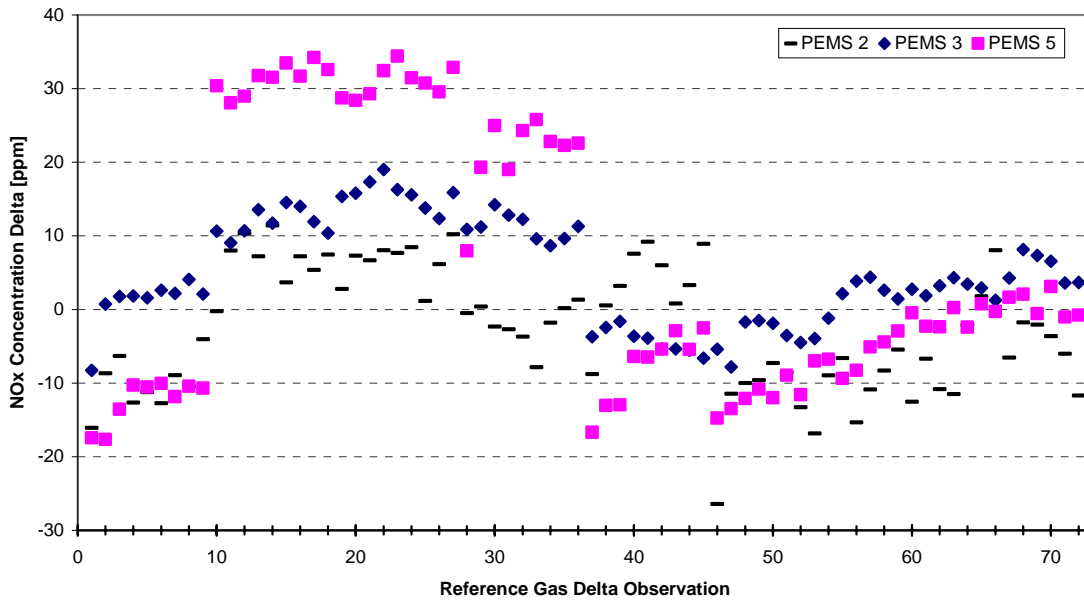


FIGURE 137. ERROR SURFACE FOR ENVIRONMENTAL TEMPERATURE NO_x CONCENTRATION SPAN DELTA MEASUREMENTS

The baseline corrected deltas were sampled randomly in the Model. The Model was initially programmed to randomly sample 360 zero, audit, and span observations for each PEMS. With temperature data for 3 PEMS, the Model was programmed to use 1080 zero, audit, and span deltas. PEMS 2 data was used for observation 1 to 360, PEMS 3 data was used for observation 361 to 720, and PEMS 5 data was used for observation 721 to 1080. However, during temperature testing, only 216 zero observations, 72 audit observations, and 72 span observations were recorded for each PEMS. The data for each PEMS was expanded by repeating delta observations to generate 360 zero, audit, and span observations for each PEMS. The final NO_x error surface for environmental temperature testing is shown in Figure 138. Final temperature error surfaces for CO, CO₂, and NMHC can be found in Appendix K.

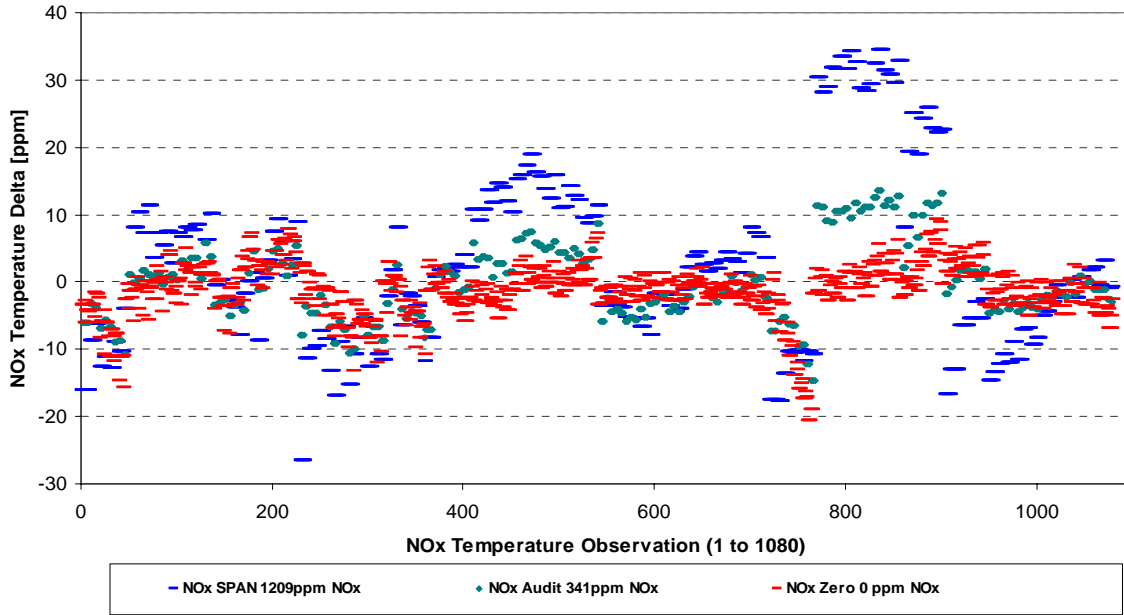


FIGURE 138. FINAL ERROR SURFACE FOR ENVIRONMENTAL TEMPERATURE NO_x CONCENTRATION

For each cycle of the Model, a number from 1 to 1080 was randomly selected. At the selected observation, zero, audit, and span delta values were sampled. Based on the concentrations of the reference NTE events, delta values were linearly interpolated from the zero, audit, and span delta data.

On occasion, the variance measured during environmental baseline testing was greater than the variance measured during temperature testing. During these instances, a scaling factor could not mathematically be calculated. Therefore, each delta observation was set to the difference between the median delta value measured during temperature testing and the median delta value measured during the environmental baseline testing. An example of this correction is shown in Figure 139 for CO span deltas.

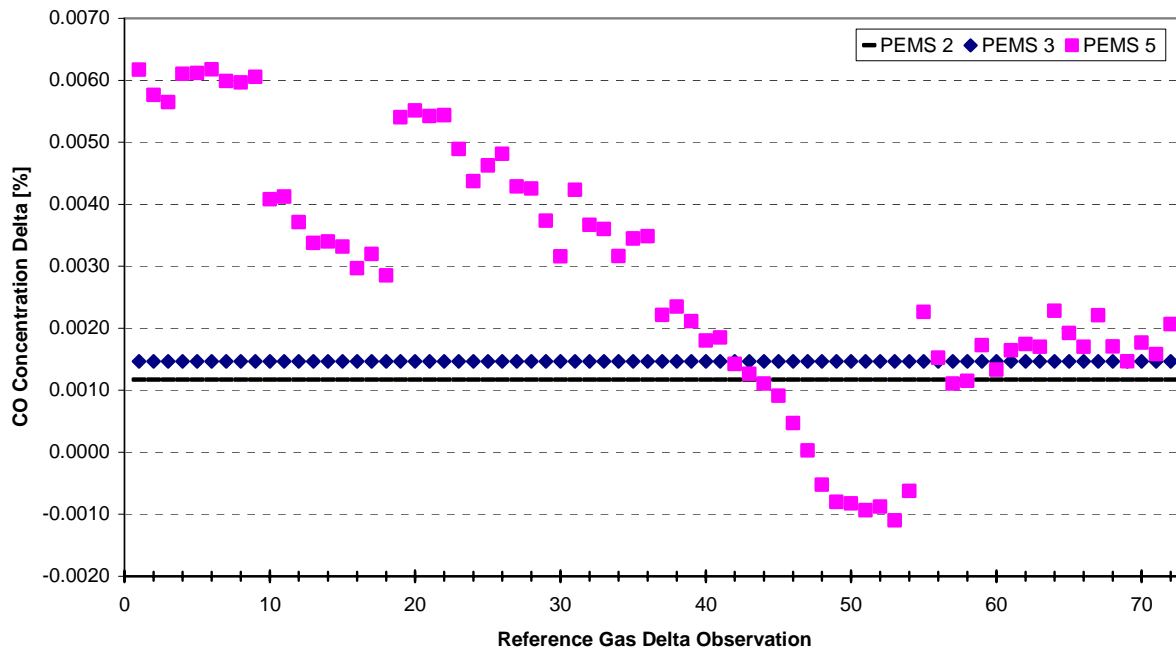


FIGURE 139. CORRECTED CO DELTAS MEASURED DURING ENVIRONMENTAL TEMPERATURE TESTING

It was later decided that if the variance of the baseline test exceeded the variance of the temperature test, it was unlikely the changes in ambient temperature adversely affected the performance of the PEMS. Therefore, the bias differences captured by the subtraction of the temperature and baseline median deltas are not likely due to changes in ambient temperature. Following this argument, all delta observations in the final errors surfaces were set to zero if the baseline MAD exceeded the temperature test MAD. An example of this correction is shown in Figure 140 for CO.

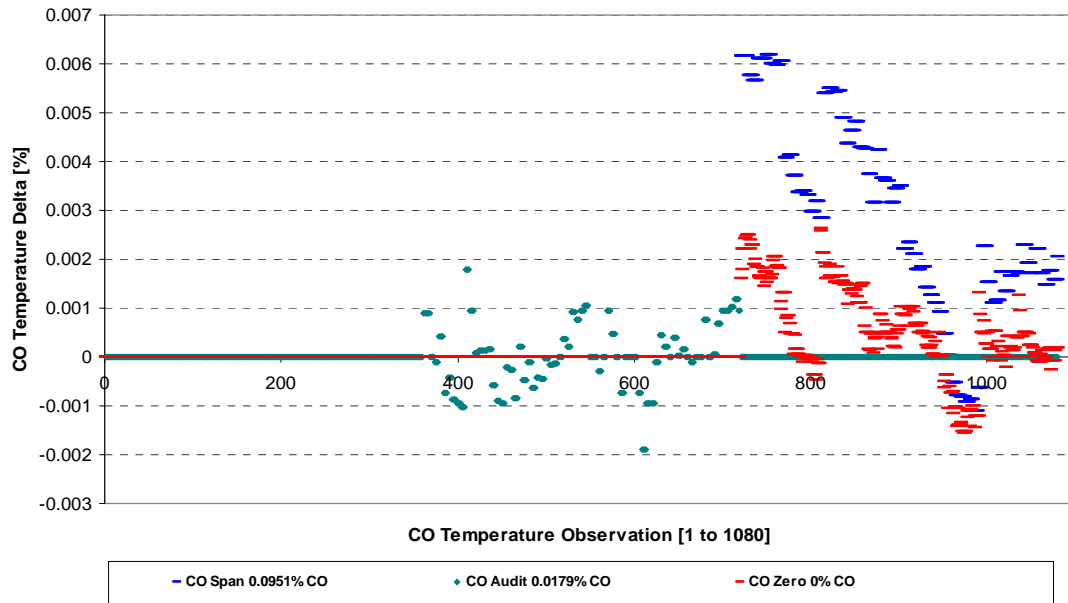


FIGURE 140. FINAL ERROR SURFACE FOR ENVIRONMENTAL TEMPERATURE CO CONCENTRATION

A temperature error surface was also generated for exhaust flow rate. Similar to the gaseous concentration error surfaces, the temperature exhaust flow rate data was corrected for the bias error and variance recorded during baseline testing. The baseline correction process was slightly modified for the exhaust flow rate because the PEMS automatically set all negative flow rate measurements to zero. With all negative measurements set to zero, the distribution of the flow rate data was inaccurate.

To generate the exhaust flow rate error surface for temperature, all zero flow rate measurements were removed from both the temperature and baseline tests; thus generating a more accurate variance comparison between the two data sets. With zero deltas removed, the median exhaust flow rate measurement from the baseline test was subtracted from each temperature exhaust flow rate delta. This process was inconsequential because the median baseline delta was less than 0.01 % of the flow meter’s maximum flow rating. Next the MAD of the baseline data was compared to the MAD of the bias corrected temperature data. Using the equation below, the MAD values were used to calculate a scaling factor. Each temperature exhaust flow measurement was multiplied by the scaling factor to shrink the variance of the temperature data by the variance measured during environmental baseline testing.

$$Scaling_Factor = \frac{\sqrt{MAD_{Rad}^2 - MAD_{BL}^2}}{MAD_{Rad}}$$

All negative corrected temperature deltas were set to zero. The data was then mirrored about the zero axis, generating twice the number of zero observations as well as negative deltas. Negative deltas were generated to restore the negative data lost during the zero clipping process and because exhaust measurements performed during engine operation in the NTE zone would

be subjected to both positive and negative exhaust flow rate errors. The final exhaust flow rate error surface for temperature testing is shown in Figure 141. Temperature exhaust flow rate deltas were sampled randomly in the Model and applied to each reference NTE event exhaust flow rate independent of level.

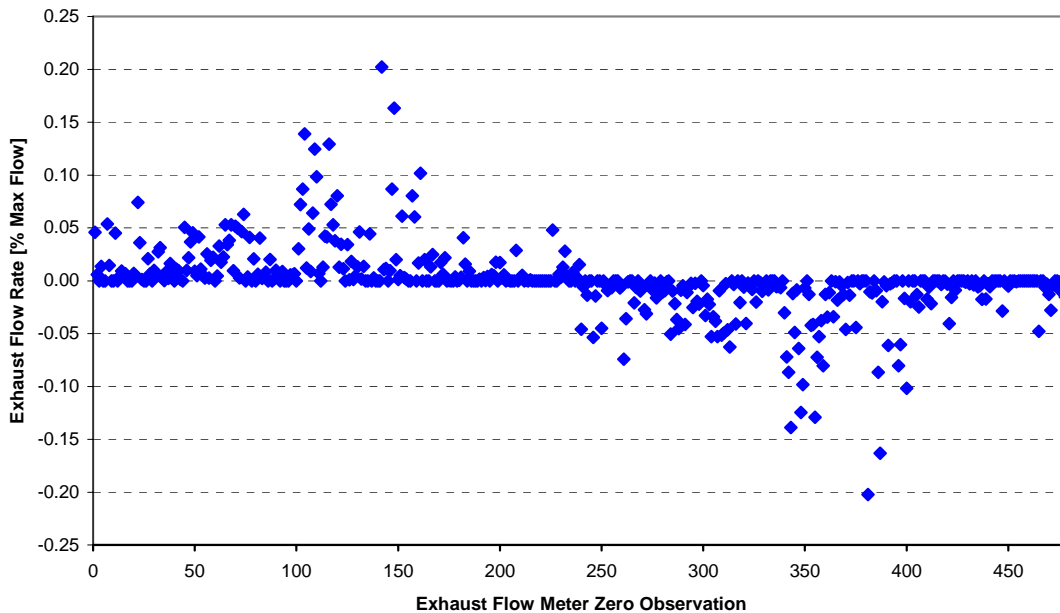


FIGURE 141. ERROR SURFACE FOR ENVIRONMENTAL TEMPERATURE EXHAUST FLOW RATE DELTA MEASUREMENTS

5.5 Pressure Chamber Testing

Pressure chamber testing was performed with two SEMTECH-DS devices to quantify PEMS gaseous concentration and exhaust flow measurement errors due to changes in ambient pressure. The pressure test was designed to simulate real-world pressures and changes in pressure. Therefore, the pressure profile used during testing nearly matched the atmospheric pressure distribution of EPA's 2002 National Emissions Inventory (NEI) model. Taken from the Test Plan, Figure 142 shows the NEI pressure distribution as well as the test cycle pressure distribution.

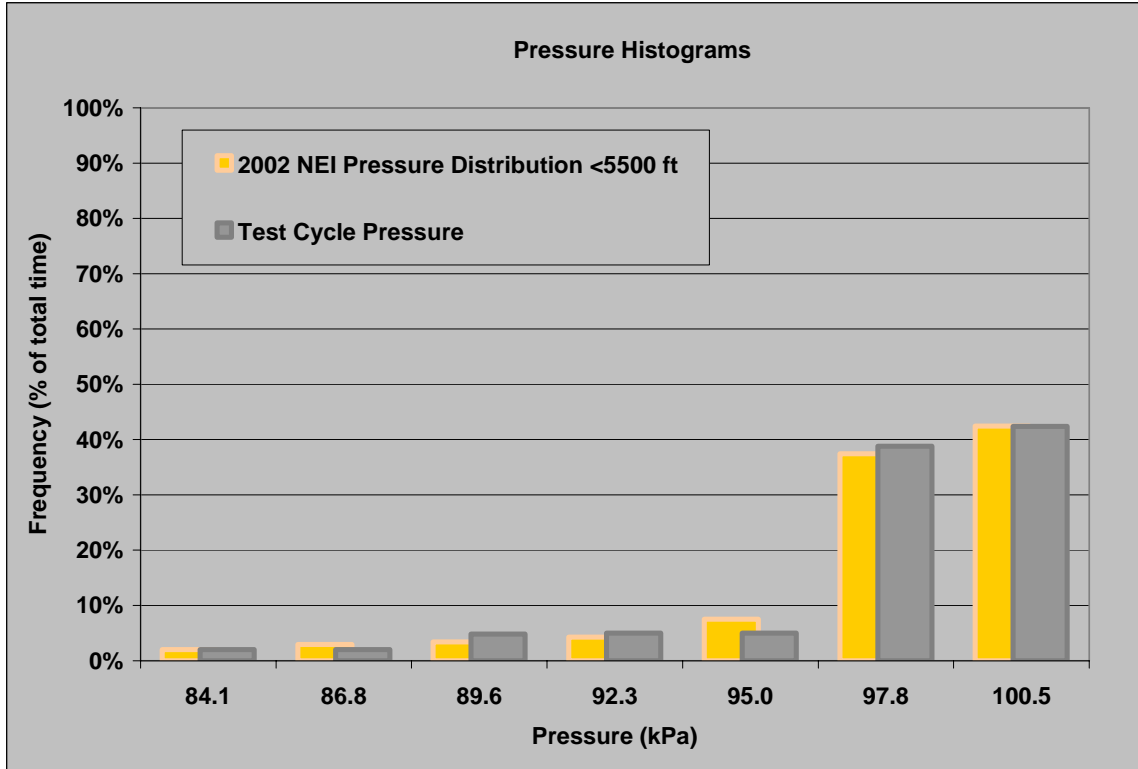


FIGURE 142. PRESSURE HISTOGRAMS FOR NEI MODEL AND TEST PROFILE

The ambient pressure profile used for chamber testing was defined by a series of pressure ramps with soaking periods between each transition. As written in the Test Plan, Table 83 and Figure 143 define the 8-hour ambient pressure profile used during the program.

TABLE 83. PRESSURE TEST PROFILE DEFINITION

Atmospheric Pressure Test Sequence					
Phase	Pressure		Time	Rate	Comments
	kPa	Alt. ft.	min	ft/min	
1 Soak	101	89	10	0	Flat near sea-level
2 Ramp	101-97	89-1203	20	56	Moderate hill climb from sea level
3 Soak	97	1203	20	0	Flat at moderate elevation
4 Ramp	97-101.87	1203- -148	60	-23	Moderate descent to below sea level
5 Soak	101.87	-148	20	0	Flat at extreme low elevation
6 Ramp	101.87-101	-148-89	20	12	Moderate hill climb to near sea level
7 Soak	101	89	20	0	Flat near sea level
8 Ramp	101-97	89-1203	20	56	Moderate hill climb from sea level
9 Soak	97	1203	25	0	Flat at moderate elevation
10 Ramp	97-96.6	1203-1316	20	6	Slow climb from moderate elevation
11 Soak	96.6	1316	20	0	Flat at moderate elevation
12 Ramp	96.6-82.74	1316-5501	20	209	Rapid climb to NTE limit
13 Soak	82.74	5501	20	0	Flat at NTE limit
14 Ramp	82.74-96.8	5501-1259	30	-141	Rapid descent from NTE limit
15 Soak	96.8	1259	20	0	Flat at moderate elevation
16 Ramp	96.8-90	1259-3244	15	132	Rapid hill climb to mid elevation
17 Soak	90	3244	10	0	Flat at mid elevation
18 Ramp	90-96.8	3244-1259	20	-99	Rapid descent within middle of NTE
19 Soak	96.8	1259	20	0	Flat at moderate elevation
20 Ramp	96.8-99.2	1259-586	20	-34	Moderate descent to lower elevation
21 Soak	99.2	586	20	0	Flat at lower elevation
22 Ramp	99.2-101	586-89	10	-50	Moderate decent to near sea-level
23 Soak	101	89	20	0	Flat near sea-level

Pressure-Time Environmental Test Cycle

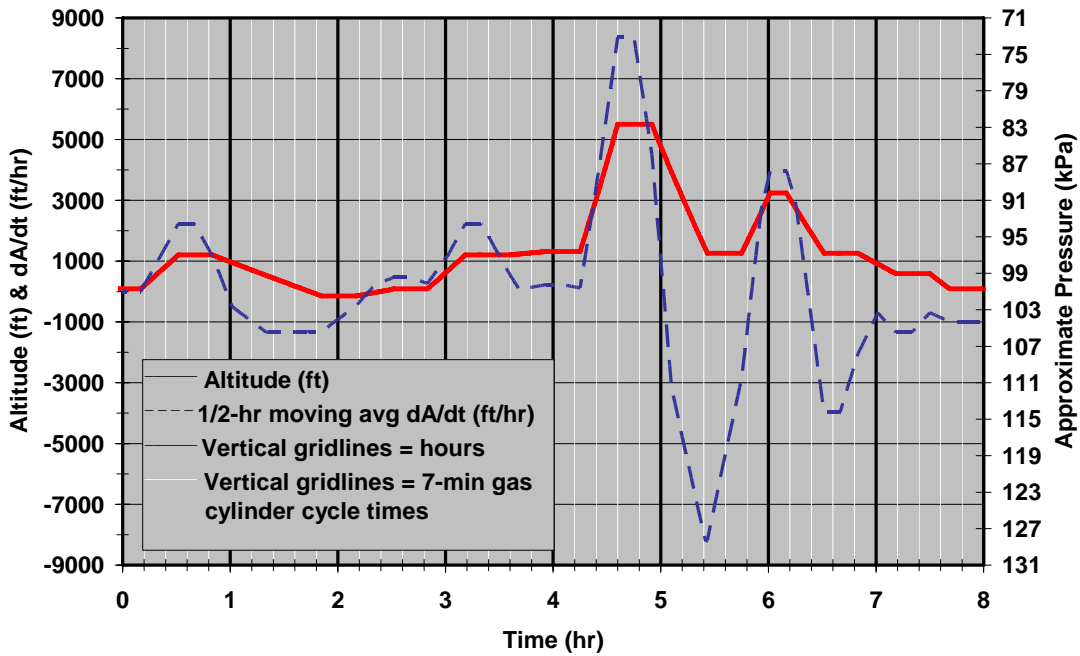


FIGURE 143. PRESSURE TEST PROFILE AND MOVING AVERAGE

The environmental pressure test was conducted in the altitude chamber shown in Figure 144. The chamber consisted of a cylindrical top that rested on a flat, circular base. The chamber was specifically designed to simulate elevated altitudes and can attain pressure levels representative of 65,000 feet of elevation. As the chamber pressure is lowered below ambient pressure, the chamber top is pulled downward, creating a tight seal between the chamber base and top. However, the Test Plan specified pressure levels up to 101.87 kPa or 148 feet below sea level. Attaining positive pressure in the altitude chamber was problematic because the o-ring sealing mechanism between the chamber top and base would shift and leak. Using weather stripping, clay, and duct tape, a revised sealing mechanism was implemented that allowed the chamber to achieve all pressures and pressure ramp rates as specified in the Test Plan.



FIGURE 144. ALTITUDE CHAMBER TOP – REMOVED FROM BASE

As shown in Figure 145, PEMS 2 and 3 were tested simultaneously in the altitude chamber. PEMS 3 was tested in a Sensors Inc. environmental enclosure. A 5-inch EFM was also tested in the chamber. In order to accurately simulate elevation changes, the PEMS sample line overflow system, overflow FID zero air system, and PEMS drain lines were vented inside the altitude chamber. Figure 145 shows a preliminary and incorrect setup with venting occurring outside the chamber. Low restriction, electronic flow meters were installed in the sample line overflow stream and FID zero air overflow stream to insure adequate bypass flow was maintained during the 8-hour pressure test. Gas lines and Ethernet cables were routed out of the chamber through a hole in the base plate. Clay and expanding foam insulation spray was used to seal the lines and cables exiting the chamber base. With no access to the PEMS once the chamber top was sealed to the base, replacing the FID fuel bottles during the 8-hour test was not possible. Therefore, two Scotty 104 FID fuel bottles were plumbed together in parallel for each PEMS unit. With two FID fuel bottles, the PEMS operated without FID fuel bottle replacement during the altitude simulation test.

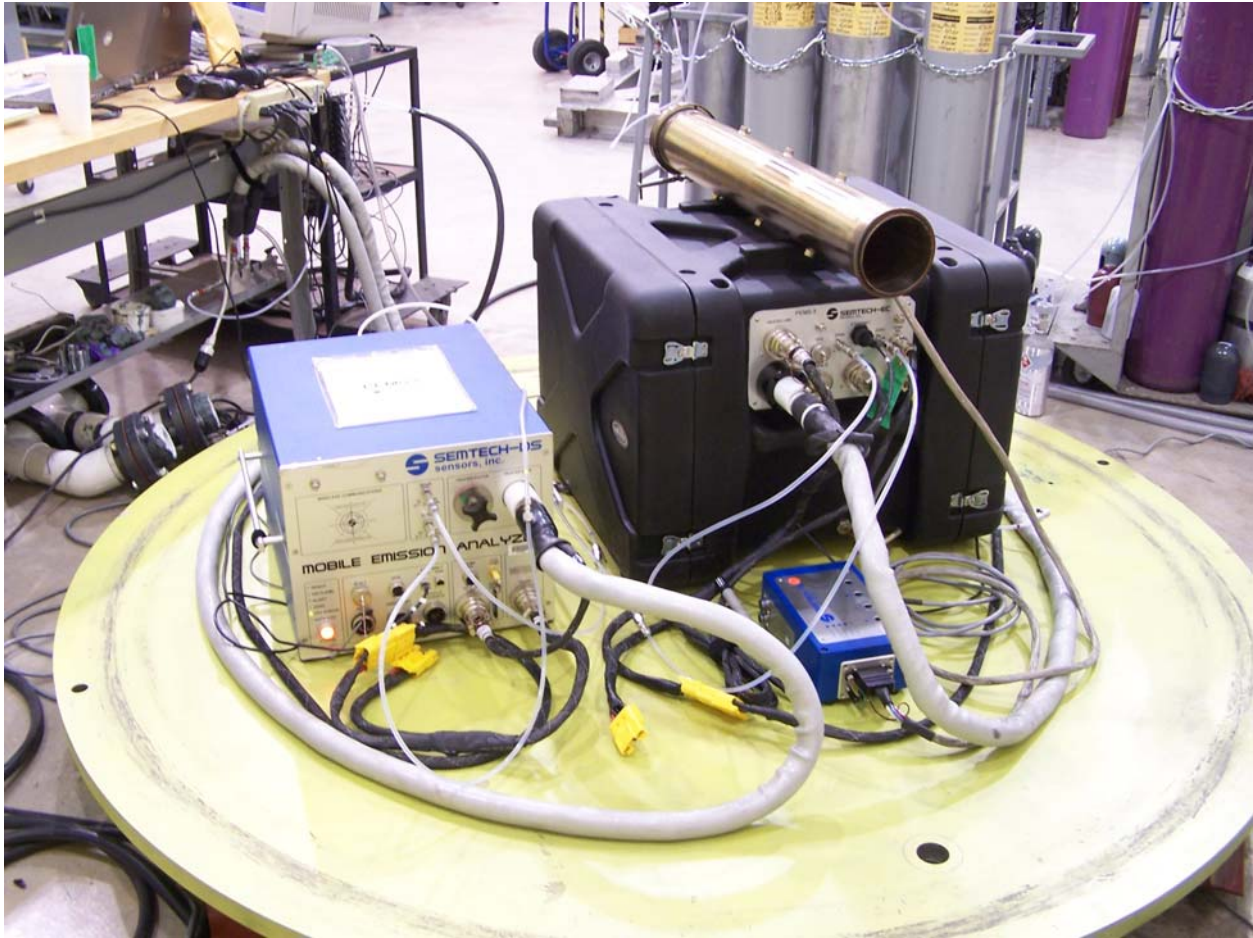


FIGURE 145. PEMS EQUIPMENT ON ALTITUDE CHAMBER BASE

Prior to executing the environmental pressure test, the PEMS were allowed to thermally equilibrate while sampling ambient air for over one hour. The altitude chamber top was then sealed to the chamber base. Figure 146 shows the assembled altitude chamber with pressure control equipment. Next, the PEMS were zeroed and spanned at ambient pressure, approximately 98 kPa. The environmental pressure test was then started by ramping to the initial pressure soak point as specified in the Test Plan. During the 8-hour pressure test, the PEMS were automatically zeroed every hour. The pressure control chamber was not paused during the test, therefore, zero events occurred at the pressures defined by the Test Plan's pressure profile definition. Zero events occurred near the hour markers shown in Figure 143. Similar to environmental baseline and temperature testing, zero, audit, and span deltas were recorded by comparing the 30-second PEMS mean concentration measurements to the reference gas concentrations.



FIGURE 146. ALTITUDE CHAMBER AND PRESSURE CONTROL EQUIPMENT DURING TESTING

The zero deltas measured during the 8-hour pressure test are shown in Figure 147 for PEMS 2. Mean pressure measurements from the PEMS ambient pressure transducer are also shown in Figure 147. Environmental pressure results for PEMS 3 are included in Appendix K. In general, the PEMS zero errors showed little variation during environmental pressure test. NO₂ measurements were relatively stable throughout the pressure test. PEMS 2 NO zero measurements drifted upward during the first hour of pressure testing. However, the pressure change was not significant during the first hour of testing and PEMS 3 showed no NO drift during the initial hour of the test. Therefore, the PEMS 2 NO drift during the first hour of testing was not likely caused by changes in pressure, but perhaps thermal equilibration of the NDUV. PEMS 2 and 3 both showed slight negative NO drift during the steep negative pressure ramp to the soak pressure of 82.74 kPa. The NO measurements drifted back in a positive direction during the positive pressure ramp from the 82.74 kPa soak pressure. THC zero measurements were relatively stable during the pressure test. Similar to NO, THC zero deltas showed slight negative drift during negative pressure ramps, and slight positive drift during positive pressure ramps. CO and CO₂ zero deltas did not show significant deviations due to changes in pressure.

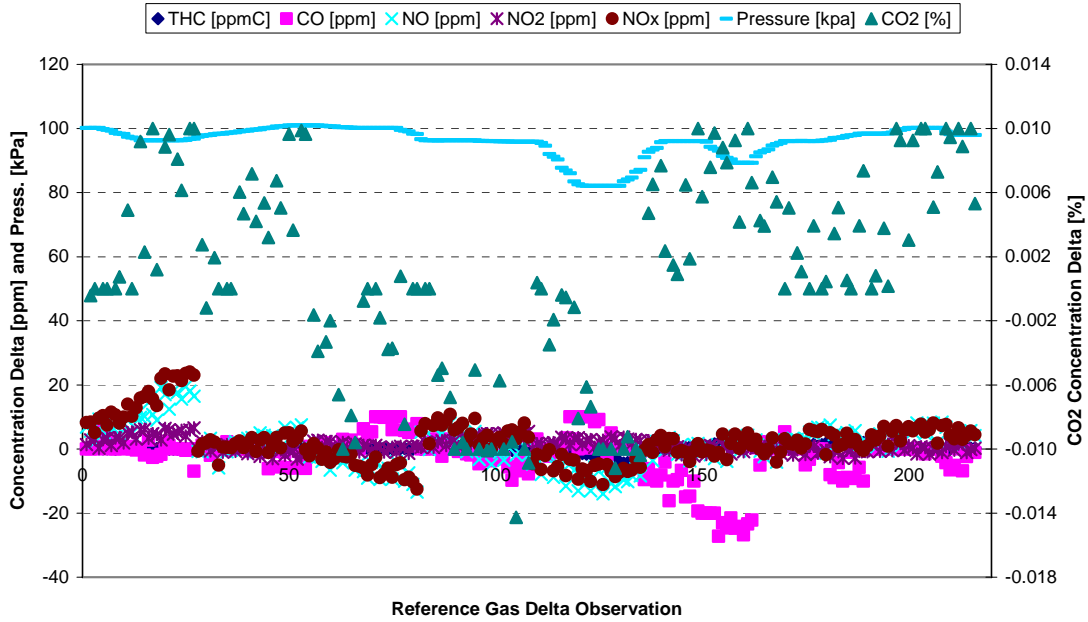


FIGURE 147. PEMS 2 ENVIRONMENTAL PRESSURE ZERO DELTA MEASUREMENTS

PEMS 2 audit level deltas measured during the environmental pressure test are shown in Figure 148. NO₂, THC, and CO₂ deltas were relatively stable and showed no trends with pressure. Similar to the zero deltas, PEMS 2 showed positive NO audit level drift during the first hour of testing. Because PEMS 3 showed no NO drift during the first hour of pressure testing and the pressure was relatively constant during this period, the PEMS 2 NO drift was likely caused by a factor other than pressure change. CO audit measurements showed positive response when the pressure in the altitude chamber was reduced. PEMS 2 CO audit deltas reached 70 ppm during the pressure soak at 82.74 kPa.

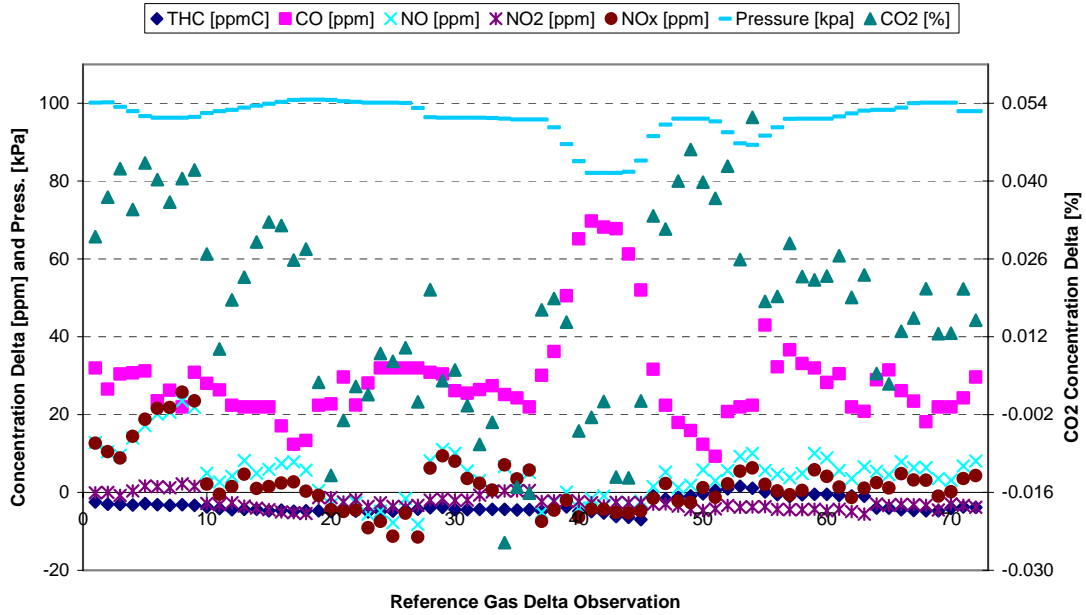


FIGURE 148. PEMS 2 ENVIRONMENTAL PRESSURE AUDIT DELTA MEASUREMENTS

The environmental pressure test span deltas are shown in Figure 149 for PEMS 2. NO₂ measurements were steady and unaffected by changes in pressure. NO span measurements were more variable; however, it was difficult to determine a link between the NO deltas and the chamber pressure. THC span measurements showed slight positive response with lower chamber pressures. CO and CO₂ span measurements were both affected by chamber pressure. CO span deltas reached 140 ppm during the pressure soak at 82.74 kPa and 50 ppm during the 90 kPa soak. CO₂ span measurements had a negative response to lowered chamber pressure, with CO₂ span deltas reaching -0.13 % during the 82.74 kPa soak. PEMS 3 pressure test span deltas, which were similar to PEMS 2, can be found in Appendix K.

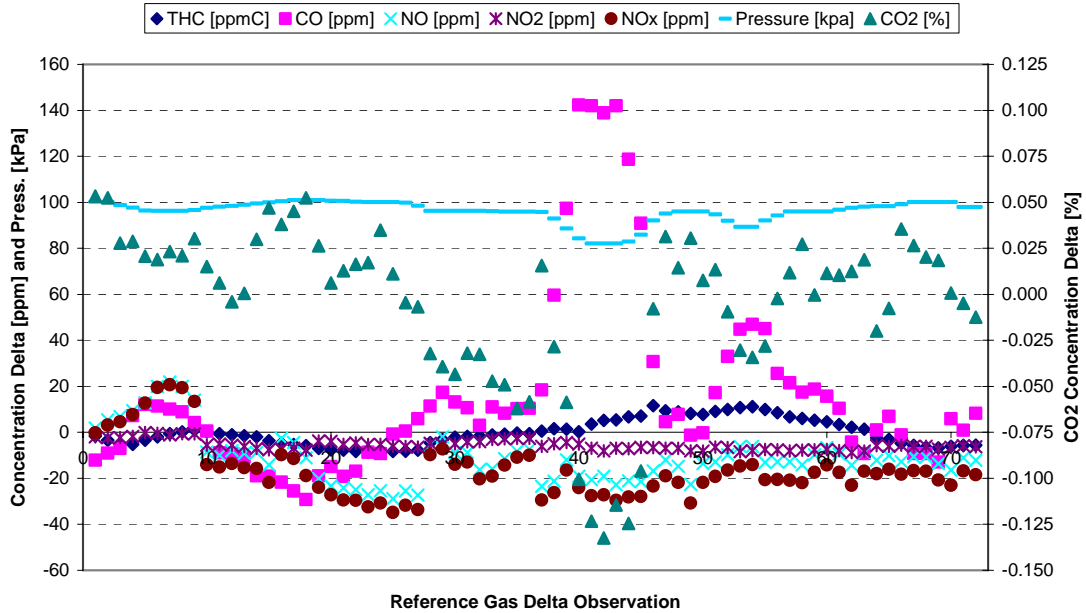


FIGURE 149. PEMS 2 ENVIRONMENTAL PRESSURE SPAN DELTA MEASUREMENTS

The response of a 5-inch Sensors Inc. flow meter was also measured during the environmental pressure test. With one end capped to prevent air flow through the meter, the 30-second mean measurements were recorded at zero deltas. Figure 150 shows the EFM deltas observed during pressure testing. Unlike baseline and temperature testing, most EFM measurements were above zero during pressure testing. Although the EFM measurement errors were small compared to the 1700 scfm flow rating of the meter, the PEMS EFM showed positive interference during the environmental pressure test. When the chamber pressure was below approximately 990 mbar, the EFM zero deltas were between 5 and 8 scfm. When the chamber pressure was above 990 mbar, the EFM deltas were between 0 and 4 scfm.

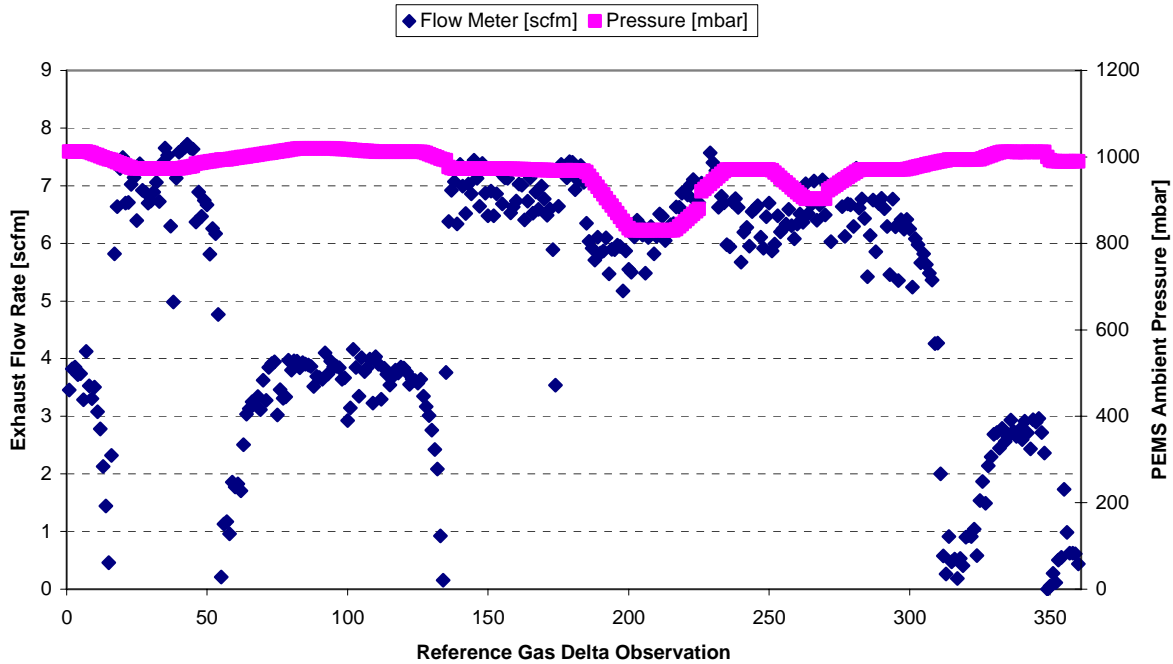


FIGURE 150. 5-INCH EFM ENVIRONMENTAL PRESSURE ZERO DELTA MEASUREMENTS

5.5.1 Pressure Error Surface Generation

The process used to generate the pressure error surfaces was similar to the environmental temperature error surface calculation method. The pressure delta data for each PEMS was corrected for baseline bias and variance. As with the temperature error surfaces, it was difficult to determine which gaseous emissions showed a susceptibility to the ambient pressure disturbances. Criteria similar to the temperature error surfaces were used to decide which pressure error surfaces should be included in the Model. As shown in Figure 151, the trends of the NMHC span deltas followed the ambient pressure traces recorded in the pressure chamber. Also, the two PEMS showed similar NMHC span delta behavior, indicating a common source of error. CO also showed definite ties between the delta behavior and the pressure traces. Therefore, NMHC and CO pressure error surfaces were included in the model. For NO_x and CO₂, no correlation could be made between the delta data and the pressure profile or between the two PEMS. Therefore, the NO_x and CO₂ deltas were not likely affected by the changes in ambient pressure. NO_x and CO₂ pressure error surfaces were not included in the Model. The environmental pressure error surfaces can be found in Appendix K.

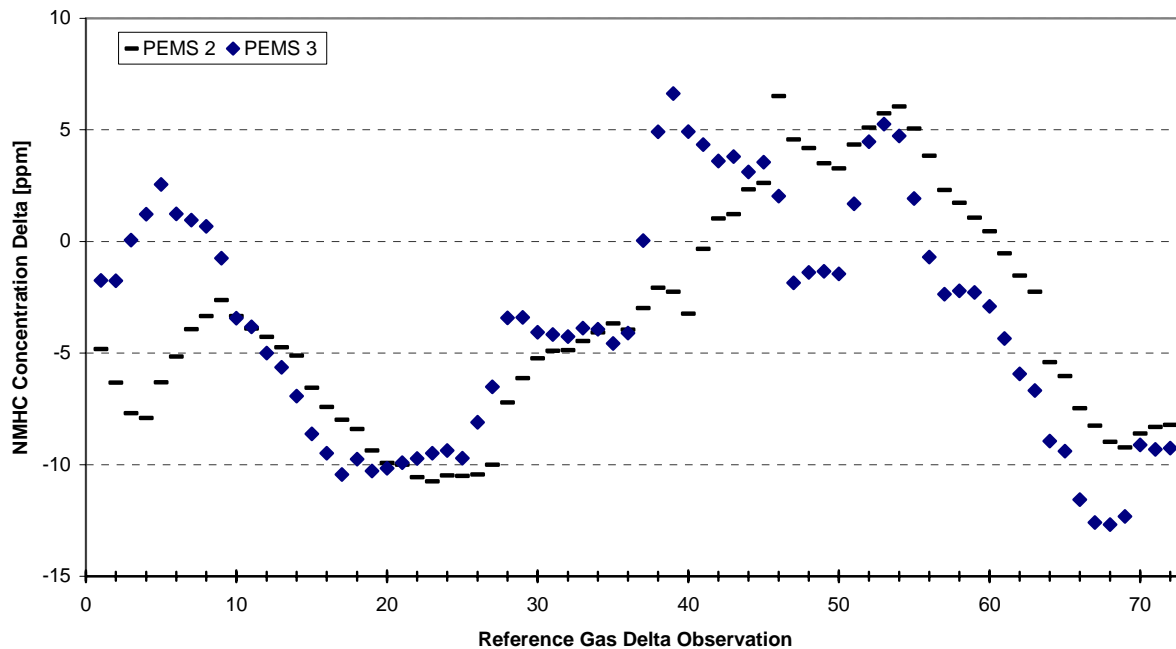


FIGURE 151. NMHC CORRECTED DELTA DATA FOR THE ENVIRONMENTAL PRESSURE TESTING

Similar to the temperature error surfaces, pressure delta data was spread to cover 360 observations for each PEMS at the zero, audit, and span levels. With only 2 PEMS evaluated during pressure testing, the final NMHC and CO error surfaces were randomly sampled using 720 observations. Figure 152 shows the final NMHC error surface generated during pressure testing. Delta data was linearly interpolated between the zero, audit, and span deltas at a given observation based on the concentrations in the reference NTE events.

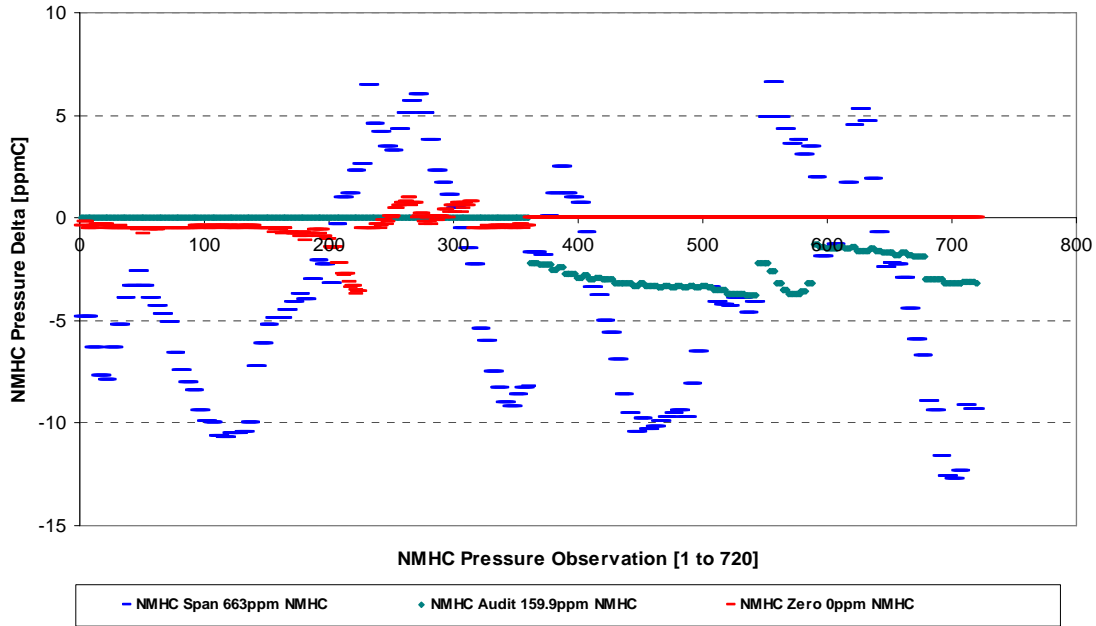


FIGURE 152. FINAL ERROR SURFACE FOR ENVIRONMENTAL PRESSURE NMHC CONCENTRATION

A process similar to the temperature exhaust flow rate error surface calculation method was used to generate the pressure exhaust flow rate error surface. The pressure exhaust flow data was corrected for baseline bias and variance. The zero deltas were removed from the baseline flow meter data. Interesting, all exhaust flow rate deltas were greater than zero during pressure testing, therefore removal of zero data was not necessary. Although minor, the pressure flow rate data was corrected for the baseline bias. After the bias correction, the variance correction was applied using the scaling factor calculation. Due to excessive variability of the pressure flow rate data, the scaling factor was calculated to be 0.995, and therefore had little effect on the pressure flow rate data. The final pressure exhaust flow rate error surface is shown in Figure 153. The pressure flow rate error surface was sampled randomly and without level dependence.

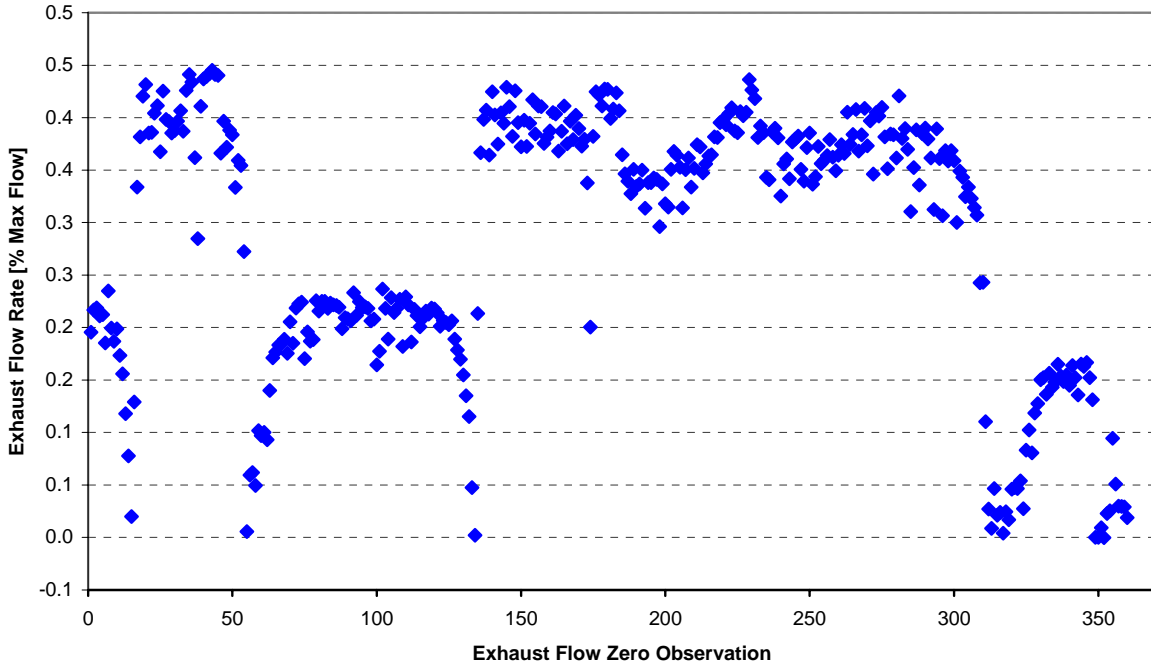


FIGURE 153. ERROR SURFACE FOR ENVIRONMENTAL PRESSURE EXHAUST FLOW RATE

5.6 Radiation Chamber Testing

Radiation chamber testing was performed with one SEMTECH-DS to quantify PEMS gaseous concentration and exhaust flow measurement errors due to Electromagnetic Interference (EMI) and Radio Frequency Interference (RFI). The four Society of Automotive Engineers (SAE) tests selected for radiation chamber testing were Bulk Current Injection, Radiated Immunity, Electrostatic Discharge, and Conducted Transients.

5.6.1 Bulk Current Injection

SAE test J1113/4 titled *Immunity to Radiated Electromagnetic Fields-Bulk Current Injection (BCI) Method* was performed to evaluate the PEMS response to radiated electromagnetic fields on the PEMS cabling. Based on the SAE Standard test descriptions and recommendations from SwRI specialists, the Steering Committee elected to test the PEMS using the specifications detailed in Region 2, Class B of the J1113/4 test protocol. As shown in Figure 154, a calibrated current probe was used to inject RF current into the PEMS cables. For each test, the probe was positioned 120 mm, 450 mm, and 750 mm from the cable connector. In other words, a complete test was performed with the probe located 120 mm from the cable connector. Another complete test was performed with the probe located 450 mm from the cable connector, and another test at 750 mm. Each test consisted of stepping the current probe frequency from 1 MHz to 400 MHz. Listed below, SwRI used the maximum frequency step size as stated in the SAE test protocol.

- 1 MHz to 10 MHz – 1 MHz step size
- 10 MHz to 200 MHz – 10 MHz step size
- 200 MHz to 400 MHz – 20 MHz step size

The SAE standard called for a minimum dwell time of 2 seconds at each frequency. However, SwRI used a dwell time of 5 seconds to insure the electromagnetic field had stabilized. As specified by the SAE Standard, the current probe was calibrated to deliver 60 milliamps of current. Figure 155 shows the device used to calibrate the bulk current injection probe.



FIGURE 154. BULK CURRENT INJECTION PROBE



FIGURE 155. CALIBRATION DEVICE FOR THE BULK CURRENT INJECTION PROBE

During Bulk Current Injection testing, the PEMS was powered with the Sensors Inc. inverter as well as a 12-volt automotive battery. The battery was used during radiation testing to simulate PEMS field testing. Figure 156 shows PEMS 7 setup in a radiation chamber during Bulk Current Injection testing. Similar to baseline testing, the PEMS was zeroed and spanned after warming for over one hour. The PEMS was zeroed approximately every hour during testing. Unlike temperature and pressure testing, which were continuous 8-hours tests, several BCI tests were completed each hour. The Steering Committee elected to take advantage of the segmented radiation testing and add short periods of baseline or zero stimulation testing during each hour of testing. As observed with temperature and pressure testing, it was often difficult to determine if the cause of increased delta measurements was due to changes in the environmental condition being tested, or some other factor. Adding periods of baseline testing throughout the BCI test offered direct comparison of PEMS measurement deltas with and without radiation stimulation. The baseline comparisons aided in determining if PEMS deltas were caused by BCI or some other factor.

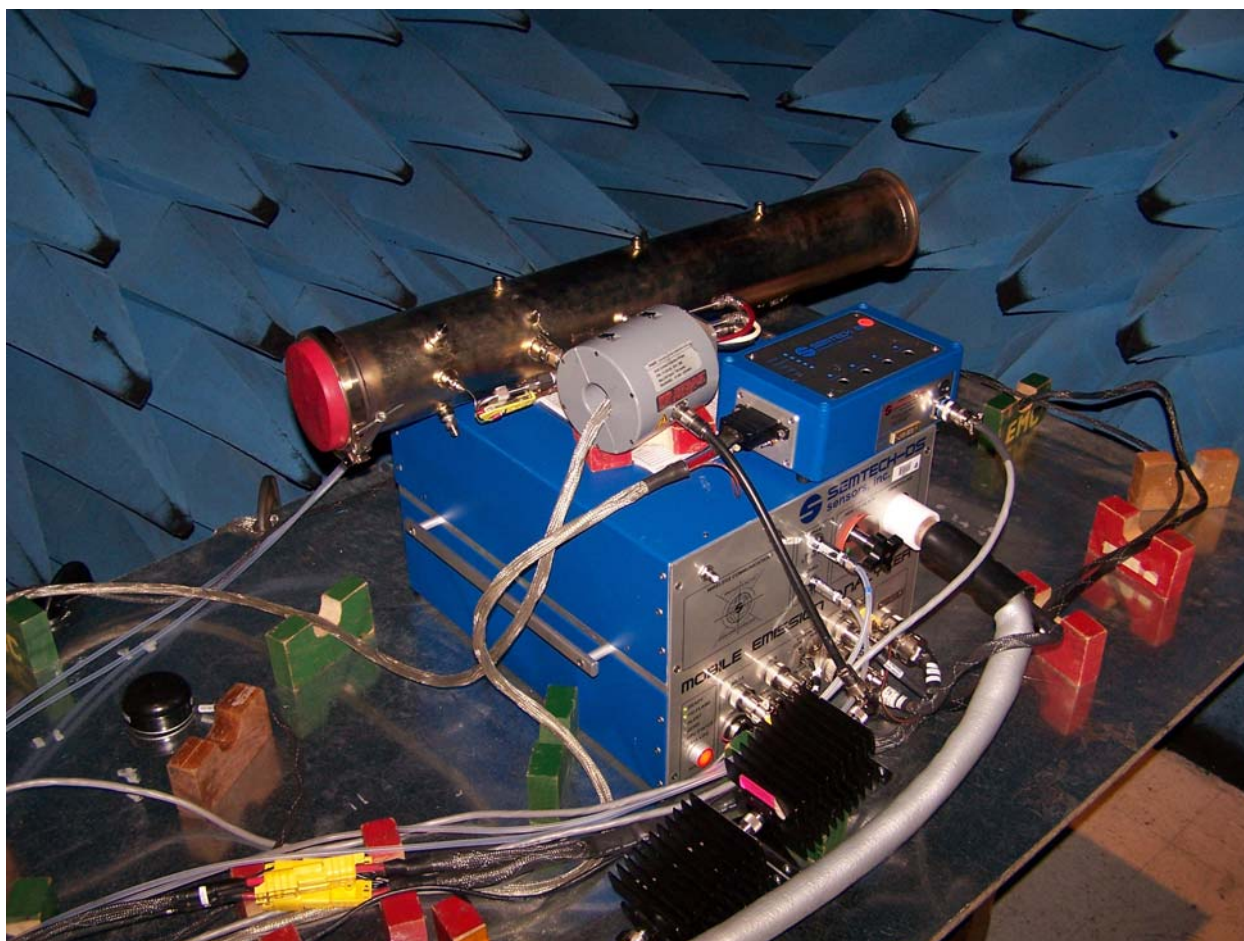


FIGURE 156. PEMS 7 IN THE RADIATION CHAMBER UNDERGOING BULK CURRENT INJECTION TESTING

The cables evaluated during BCI testing included the 12-volt power supply cables, the auxiliary 1 cable, the Ethernet cable, the temperature/relative humidity probe cable, the heated line power cable, and the EFM cables. Initially, PEMS 3 was used for BCI testing. However, while testing the power cable, the PEMS reported several FID faults and eventually shut down the FID due to high FID temperature. The probe current was reduced from 60 milliamps to 40 milliamps, but the FID still shutdown between 26 and 46 MHz. Fearing a problem with PEMS 3, PEMS 7 was used for BCI testing. Although similar FID faults and problems existed with PEMS 7, the issues occurred less frequently. When testing the power cable, the probe current was reduced to 40 milliamps due to FID shutdown problems at 60 milliamps. All other cables were tested at 60 milliamps. Throughout testing, a number of faults and problems occurred. Most faults were related to the FID. According to Sensors Inc., the FID faults and shutdowns may have been related to problems with the FID DC to AC board. Communication between the laptop and PEMS unit was disrupted several times. Communication between the PEMS and EFM was also disrupted, requiring the PEMS to be restarted to restore communication. After the PEMS was restarted, the analyzers were zeroed and spanned before continuing the BCI test.

Figure 157 shows the PEMS 7 gaseous emission concentration zero deltas measured during Bulk Current Injection testing. PEMS zero events as well as the periods of baseline testing are marked in Figure 157. Although difficult to see in the chart, NO zero deltas were within a range of ± 5 ppm and showed no noticeable difference between BCI testing and the baseline portions of the test. In general, NO₂ zero deltas during BCI and baseline testing were between 0 and 5 ppm. One NO₂ measurement showed an outlying positive delta of 7.6 ppm while another outlying NO₂ delta was at -15.5 ppm. With the exception of the two outlying NO₂ zero measurements, NO₂ deltas showed no difference between BCI and baseline testing. With the exception of the first hour of testing, THC zero deltas were typically within ± 1 ppmC. Although the THC zero measurement drifted downward during the first hour of testing, the baseline testing at the beginning and end of the hour test segment showed similar drift behavior; indicating the drift was not caused by current injection. In general, CO and CO₂ zero measurements showed similar deltas during baseline and BCI testing. However, 4 CO zero observations and 1 CO₂ observation were outlying, low deltas that indicated a possible susceptibility to the BCI test. With the exception of a few outlying points, there was no noticeable difference between the measurements taken during BCI testing and those taken during baseline testing. Therefore, the effect of the electromagnetic radiation on the PEMS cabling was minor.

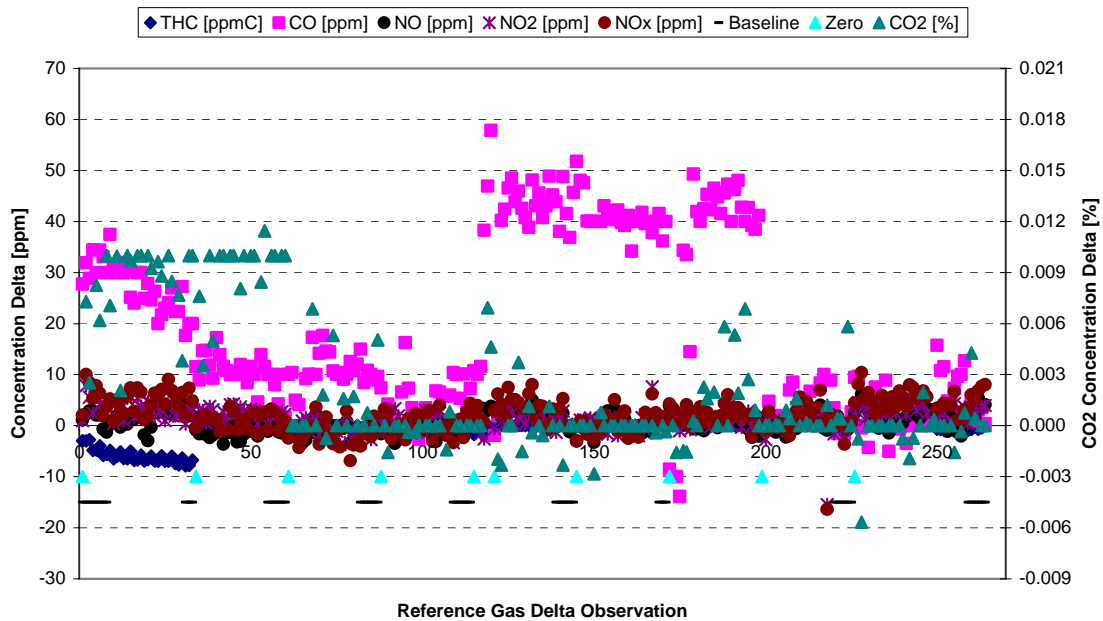


FIGURE 157. PEMS 7 ENVIRONMENTAL RADIATION BCI ZERO DELTA MEASUREMENTS

Figure 158 shows the PEMS 7 audit delta measurements during BCI testing. The shift in audit delta levels after the PEMS was restarted was due to a zero and span event for all analyzers. Similar to the BCI zero deltas, almost all of the BCI audit deltas were similar to the baseline audit deltas, indicating BCI testing had little effect on the PEMS gaseous measurement systems. The only exceptions were 1 low CO audit measurement and 5 high CO₂ measurements.

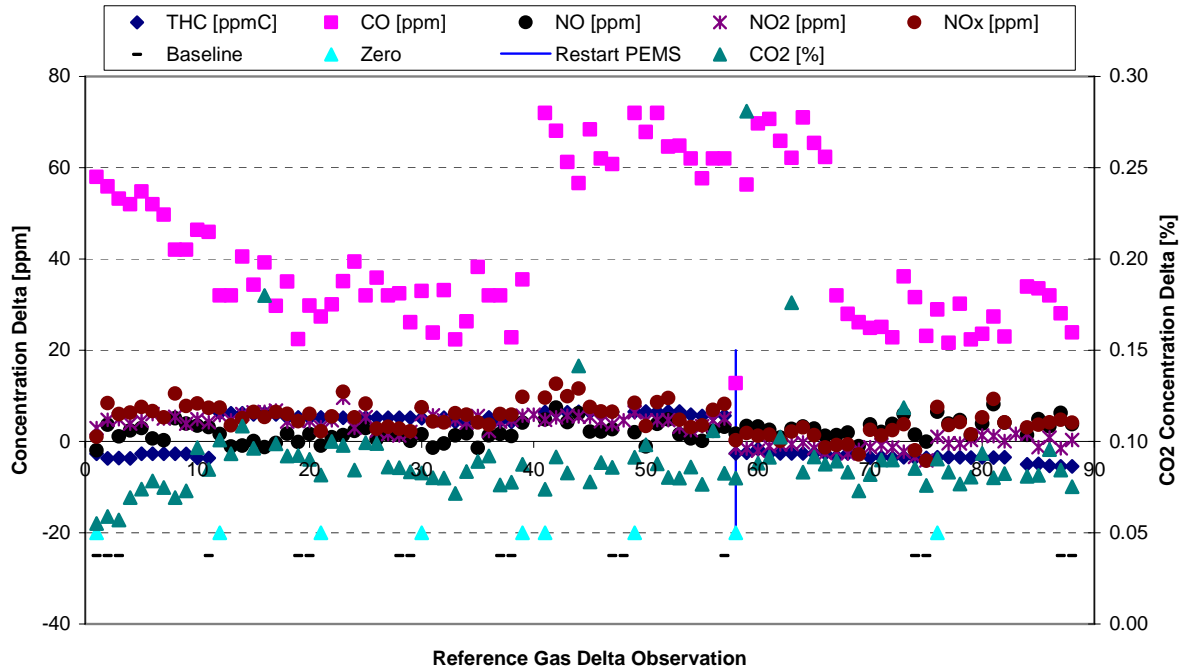


FIGURE 158. PEMS 7 ENVIRONMENTAL RADIATION BCI AUDIT DELTA MEASUREMENTS

The span deltas measured during BCI testing are shown in Figure 159. The PEMS was restarted during the BCI test to restore communication with the EFM. The PEMS was zeroed and spanned after being restarted, resulting in a shift in span delta measurements. Similar to the BCI zero and audit deltas, the BCI span deltas nearly all matched the baseline deltas through the environmental test. However, 1 CO span delta observation was outlying and low, 5 CO₂ span deltas were high, and 1 NO₂ span delta was high. Because of the vast similarity between BCI deltas and baseline deltas, the effect of the Bulk Current Inject testing on the PEMS span measurements was minor.

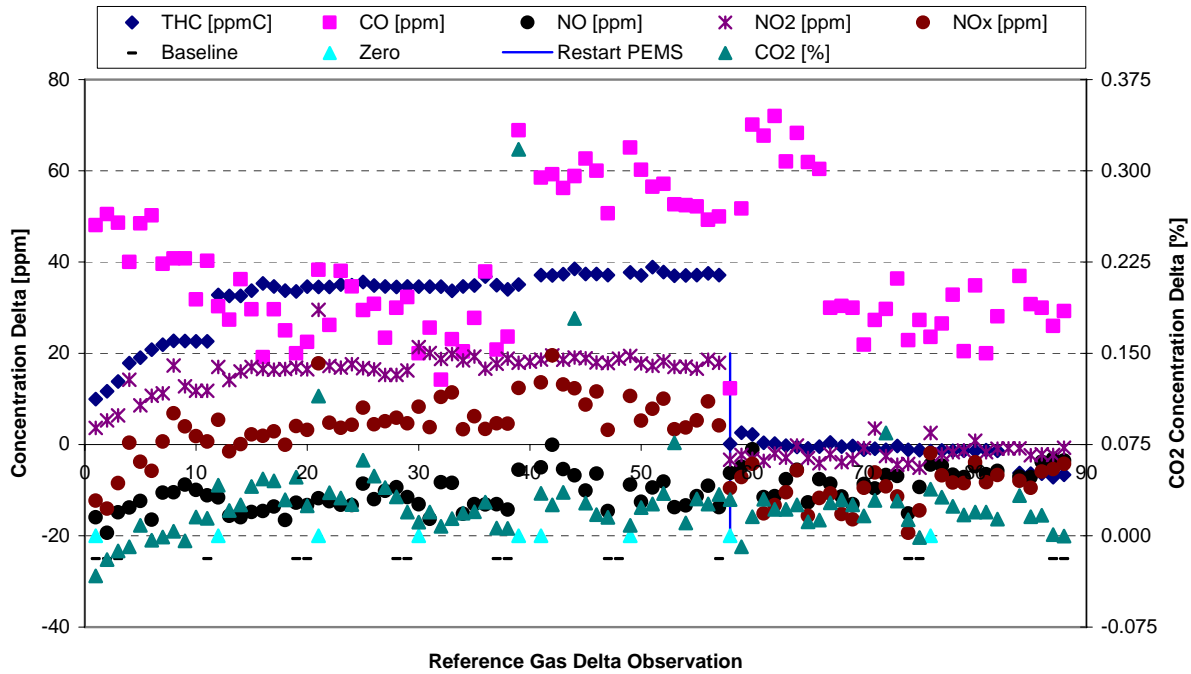


FIGURE 159. PEMS 7 ENVIRONMENTAL RADIATION BCI SPAN DELTA MEASUREMENTS

As shown in Figure 160, the 5-inch EFM was susceptible to the BCI test. The EFM reported several elevated measurements throughout BCI testing. EFM zero deltas were near zero during baseline test segments, indicating the positive EFM measurements were most likely caused by the BCI tests.

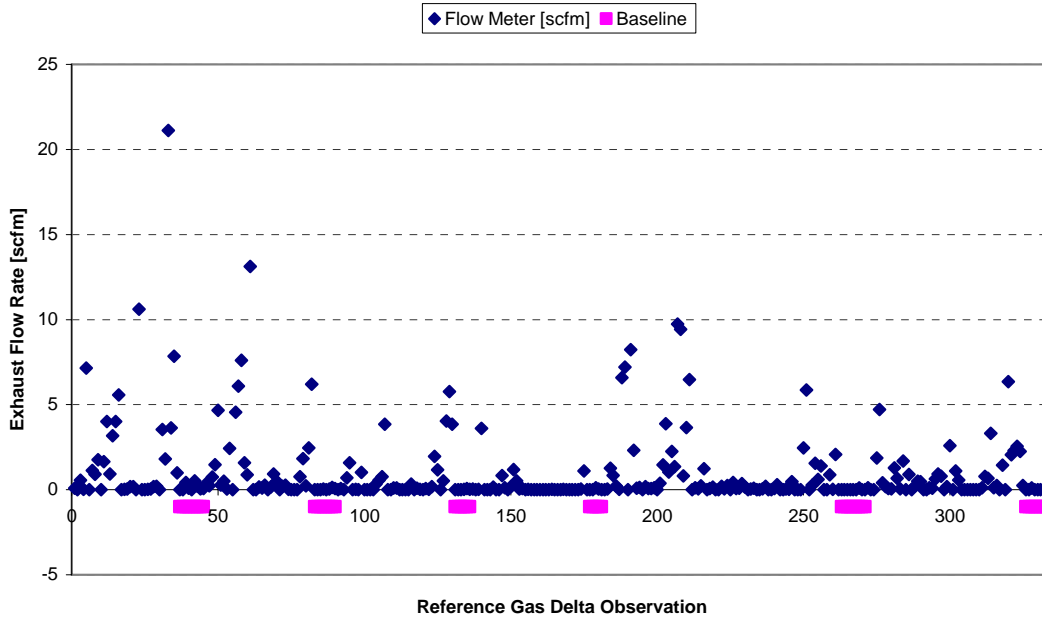


FIGURE 160. 5-INCH EFM ENVIRONMENTAL RADIATION BCI ZERO DELTA MEASUREMENTS

5.6.2 Radiated Immunity

SAE test J1113/21 titled *Electromagnetic Compatibility Measurement Procedure for Vehicle Components - Part 21: Immunity to Electromagnetic Fields, 10 kHz to 18 GHz, Absorber-Lined Chamber* was performed to evaluate the PEMS response to continuous narrowband electromagnetic fields on the PEMS and PEMS cabling. Based on the SAE Standard test descriptions and recommendations from SwRI specialists, the Steering committee elected to test the PEMS using the specifications detailed in Region 2, Class B of the J1113/21 test protocol. As shown in Figure 161, the Radiated Immunity test was performed in an absorber-lined radiation test room. The absorber medium was carbon-impregnated foam. A series of antennas and a host of power electronics, shown in Figure 162, were used to generate the RF fields specified in the SAE test protocol.

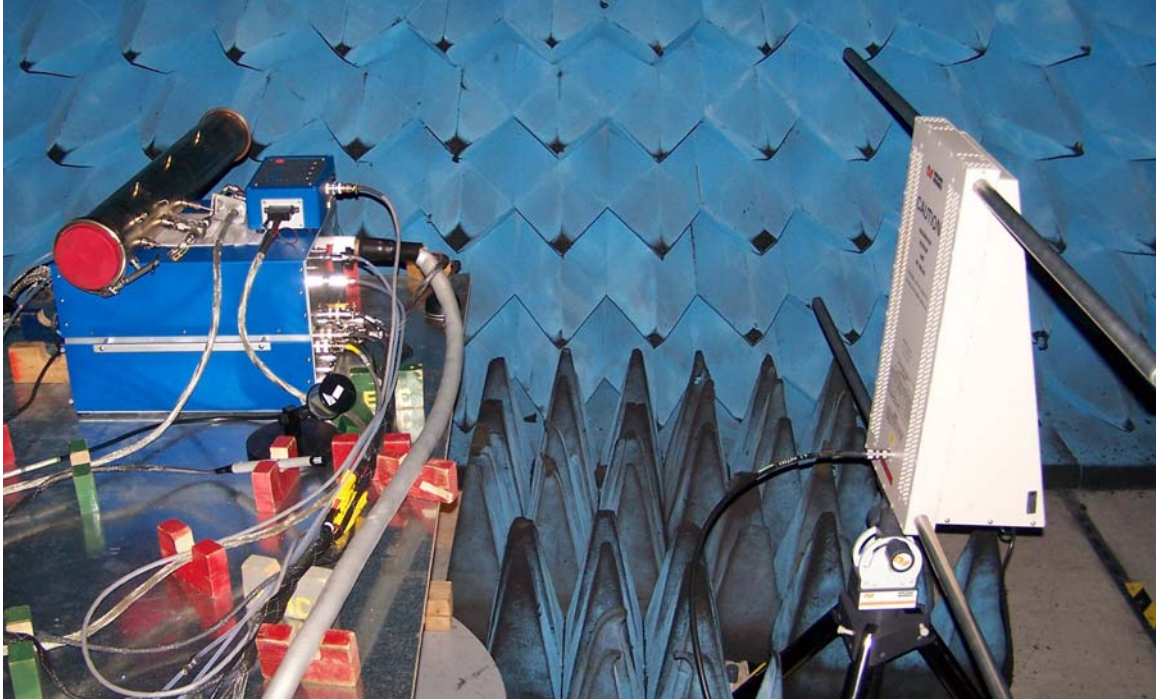


FIGURE 161. PEMS 7 AND RADIATION ANTENNA IN THE ABSORBER-LINED RADIATION CHAMBER DURING RADIATED IMMUNITY TESTING



FIGURE 162. SIGNAL GENERATORS, AMPLIFIERS, OSCILLOSCOPES AND OTHER ELECTRONICS USED TO PERFORM RADIATION TESTING

The Radiated Immunity tests consisted of stepping the electromagnetic field frequency from 10 kHz to 1 GHz. Experts at SwRI recommended ending the Radiated Immunity testing at 1 GHz rather than 18 GHz as specified by the standard. Because the maximum oscillator speed of the PEMS was relatively low, testing at higher frequencies would have likely shown no measurement or operational susceptibilities. Listed below, SwRI used the maximum frequency step size as stated in the SAE test protocol. The SAE standard called for a minimum dwell time of 2 seconds at each frequency. However, SwRI used a dwell time of 5 seconds to insure the electromagnetic field had stabilized. Although the SAE Standard specified using a field intensity of 50 volts/meter, the intensity was reduced during testing to prevent the PEMS FID from shutting down.

- 10 kHz to 100 kHz – 10 kHz step size
- 100 kHz to 1 MHz – 100 kHz step size
- 1 MHz to 10 MHz – 1 MHz step size
- 10 MHz to 200 MHz – 2 MHz step size
- 200 MHz to 1 GHz – 20 MHz step size

During Radiated Immunity testing, PEMS 7 was operated in a manner similar to Bulk Current Injection Testing. The PEMS was powered with the Sensors Inc. inverter as well as a 12-volt automotive battery. Similar to baseline testing, the PEMS was zeroed and spanned after warming for over one hour. The PEMS was zeroed approximately every hour during Radiated

Immunity testing. Also, short periods of baseline or zero stimulation testing were included during each hour of testing to determine if the PEMS deltas were caused by electromagnetic radiation or some other factor.

During initial Radiated Immunity testing, the field intensity was set to the SAE Standard specification of 50 volts/meter. At 50 volts/meter, PEMS 7 produced numerous faults and warnings pertain to the FID, and eventually shutdown the FID. Testing was then repeated with a field intensity of 25 volts/meter. PEMS 7 displayed several FID faults and warnings, and shutdown the FID at an electromagnetic frequency of 164 MHz. The Radiated Immunity test was repeated a third time, this time at the CE Standard field intensity specification of 10 volts/meter. At 10 volts/meter PEMS 7 performed similarly to the 25 volts/meter test, and shutdown the FID at 164 MHz. After further testing, it was determined that the PEMS FID would not operate with a field intensity of 10 volts/meter between the frequency range of 164 to 178 MHz. Therefore, testing was performed until the FID shutdown at 164 MHz. After the FID was restarted, testing was continued from 178 MHz. Throughout Radiated Immunity testing, the field intensity was set as high as possible without causing functional PEMS failures. If a large number faults occurred, or if the PEMS FID shutdown, the radiation test was often repeated at a lower field intensity.

Figure 163 shows the PEMS 7 zero deltas measured during Radiated Immunity testing. Following the initial baseline testing, the electromagnetic frequency was ramped from 30 to 164 MHz at 25 volts/meter in a horizontal direction. At observation number 36 with a frequency of 164 MHz, the PEMS FID shutdown. The PEMS was then restarted. After baseline observations 37 through 45, the electromagnetic frequency was ramped from 30 to 164 MHz at 10 volts/meter, observation number 46 through 60. Even at 10 volts/meter, the FID shutdown at 164 MHz. Testing was then continued with the radiation frequency ramped from 178 to 260 MHz at 10 volts/meter during reference gas observations 61 through 72. The FID shutdown again at 260 MHz and 10 volts/meter. During measurement 73 through 99, the electromagnetic radiation was ramped from 260 to 300 MHz at 10 volts/meter, 300 MHz to 1000 MHz at 25 volts/meter, and after changing antennas, from 200 to 1000 MHz at 25 volts/meter in a vertical direction. A short baseline segment was included from observation 91 through 96. Radiated Immunity testing continued by ramping vertically from 30 to 50 MHz at 10 volts/meter and 50 to 200 volts/meter at 25 volts/meter. Using a bipolar antenna, the electromagnetic frequency was ramped from 10 kHz to 6 MHz at 25 volts/meter and from 7 to 30 MHz at 10 volts/meter. Testing was concluded by recording deltas with no radiation to generate a final baseline test segment.

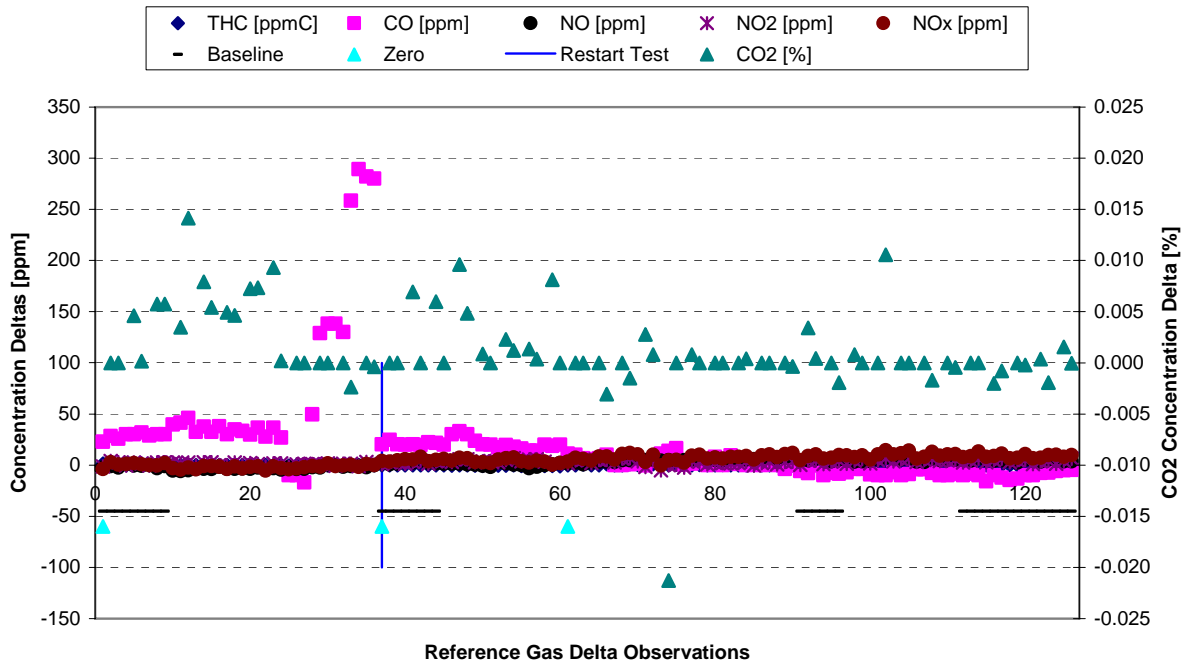


FIGURE 163. PEMS 7 ENVIRONMENTAL RADIATION RADIATED IMMUNITY ZERO DELTA MEASUREMENTS

Throughout Radiated Immunity testing, the only zero deltas that showed notable perturbations due to electromagnetic radiation were for CO when ramped from 120 to 164 MHz at 25 volts/meter. One low CO₂ concentration delta was recorded during radiation testing. All other deltas resembled baseline measurements, indicating measurement errors were not caused by electromagnetic radiation.

Figure 164 and Figure 165 show the PEMS 7 audit and span deltas recorded during Radiated Immunity testing. Similar to the zero deltas, the electromagnetic radiation affected the CO audit and span measurements from 120 to 164 MHz at 25 volts/meter. One high CO₂ audit and span delta was observed near 120 MHz at 25 volts/meter. All other audit and span measurements appeared unaffected by the electromagnetic radiation.

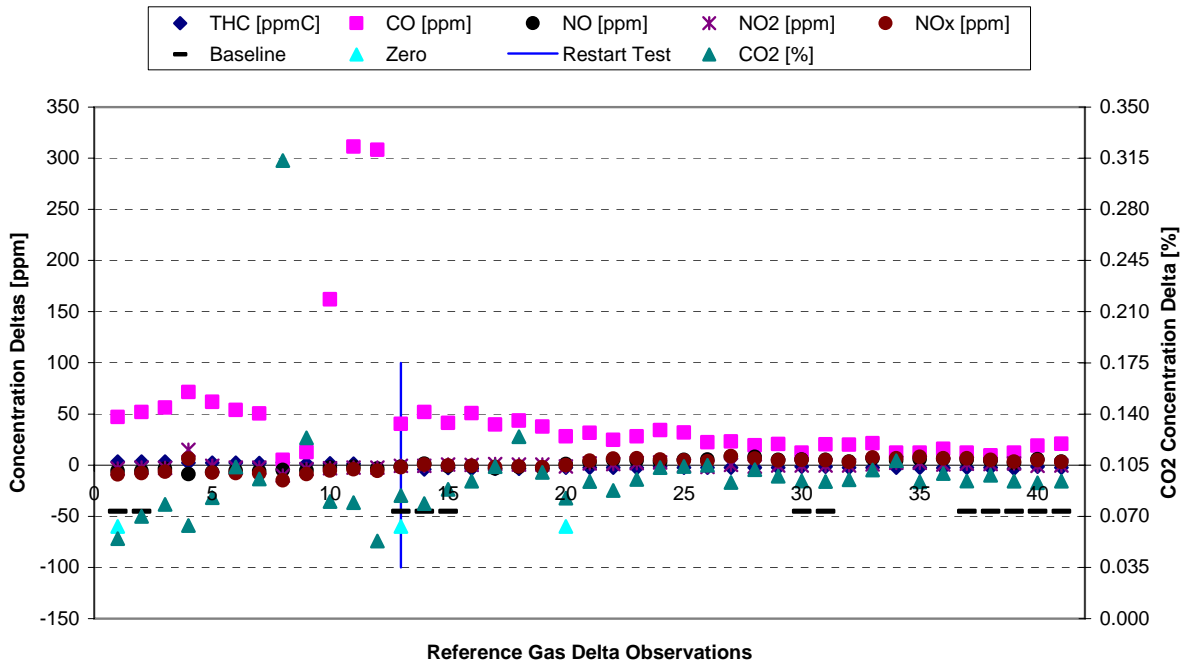


FIGURE 164. PEMS 7 ENVIRONMENTAL RADIATION RADIATED IMMUNITY AUDIT DELTA MEASUREMENTS

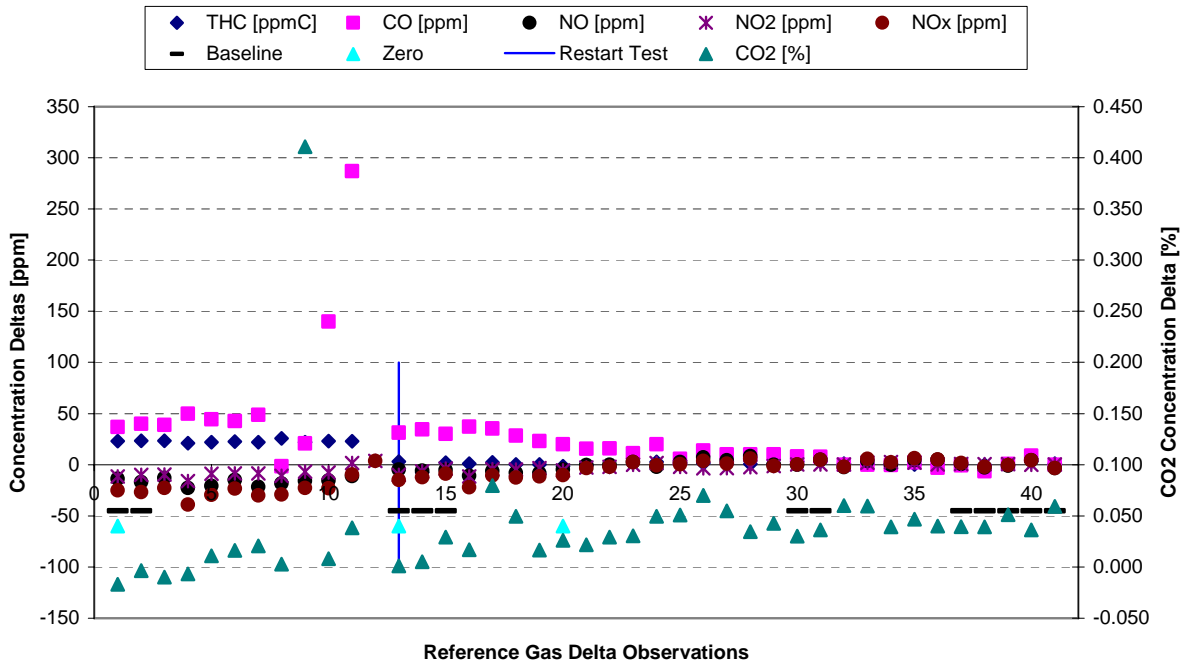


FIGURE 165. PEMS 7 ENVIRONMENTAL RADIATION RADIATED IMMUNITY SPAN DELTA MEASUREMENTS

Figure 166 shows the exhaust flow meter zero deltas recorded during Radiated Immunity testing. Although most measurements were near zero, several segments of radiation testing showed elevated EFM readings. EFM susceptibility was recorded at a field intensity of 25 volts/meter and electromagnetic frequencies ranging from 120 to 164 MHz (horizontal polarity), 300 to 1000 MHz (horizontal polarity), and 200 to 1000 MHz (vertical polarity).

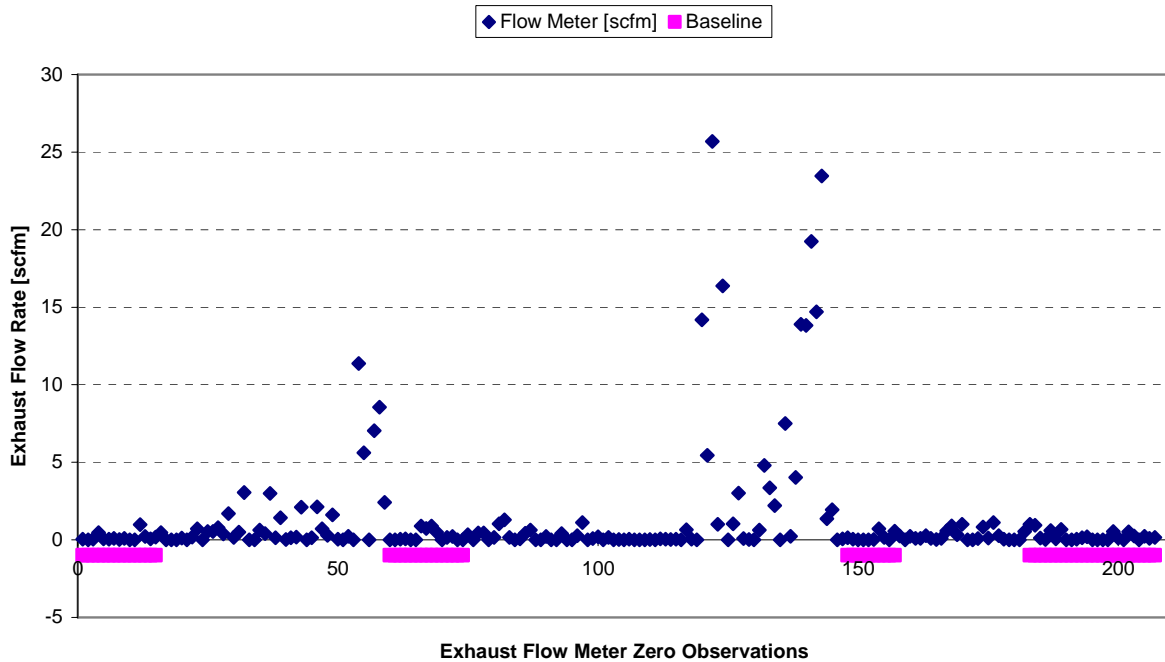


FIGURE 166. 5-INCH EFM ENVIRONMENTAL RADIATION RADIATED IMMUNITY ZERO DELTA MEASUREMENTS

5.6.3 Electrostatic Discharge

SAE test J1113/13 titled *Electromagnetic Compatibility Measurement Procedure for Vehicle Components--Part 13: Immunity to Electrostatic Discharge* was performed to evaluate the PEMS response to Electrostatic Discharges (ESDs) on the PEMS and auxiliary equipment. Based on the SAE Standard test descriptions and recommendations from SwRI specialists, the Steering committee elected to test the PEMS using the specifications detailed in Region 2, Class B of the J1113/13 test protocol. ESDs were delivered at over 80 locations on the PEMS, the EFM, the EFM pressure transducer enclosure, the humidity probe, and PEMS connectors. Using the Electrostatic Discharge Simulator shown in Figure 167, the discharge was delivered directly, or with the simulator tip touching the discharge surface; as well as indirectly, or with the simulator tip not touching the discharge surface. The direct discharge was performed by placing the simulator tip on the discharge surface and energizing the discharge gun. The indirect discharge was performed by energizing the discharge gun away from the discharge surface. The energized gun tip was then moved towards the discharge surface until the voltage potential

caused an arc and the discharge was released. Both direct and indirect ESDs were performed at each of the discharge locations.



FIGURE 167. ELECTROSTATIC DISCHARGE SIMULATOR USED DURING ELECTROSTATIC DISCHARGE TESTING

As specified by the SAE Standard test procedure, the Electrostatic Discharge Simulator was calibrated to deliver 4000 volts. An Electrostatic Voltmeter, shown in Figure 168, was used to calibrate the Electrostatic Discharge Simulator.



FIGURE 168. ELECTROSTATIC VOLTMETER USED TO CALIBRATE THE ELECTROSTATIC DISCHARGE SIMULATOR

During Electrostatic Discharge testing, PEMS 7 was operated in a manner similar to Bulk Current Injection and Radiated Immunity testing. The PEMS was powered with the Sensors Inc. inverter as well as a 12-volt automotive battery. Similar to baseline testing, the PEMS was zeroed and spanned after warming for over one hour. Due to the reduced length of the ESD testing, and the inclusion of baseline test segments, PEMS 7 was only zeroed once during the Electrostatic Discharge test. Periods of baseline or zero stimulation testing were included at the beginning and end of the ESD test to determine if the electrostatic discharge had any effect on the PEMS measurements. To capture potential measurement errors, the discharge events, being extremely brief, were timed to occur during the 30-second recorded measurements. Several discharge locations were tested during each 30-second measurement.

Figure 169 shows the PEMS 7 zero delta measurements during Electrostatic Discharge testing. Baseline test segments were included at the beginning and end of the test, with one zero event occurring at observation number 28. In general, the zero deltas during testing resembled the deltas measured during baseline testing, indicating the ESD testing had little effect on the PEMS measurement. Two CO₂ zero measurements were outlying and high. With the ESDs being extremely brief, short perturbations in the PEMS measurements may not have been revealed in a 30-second average measurement. Therefore, the continuous data was reviewed for each PEMS measurement to insure a short duration measurement error was not overlooked. The continuous data showed no evidence of susceptibility to the ESDs.

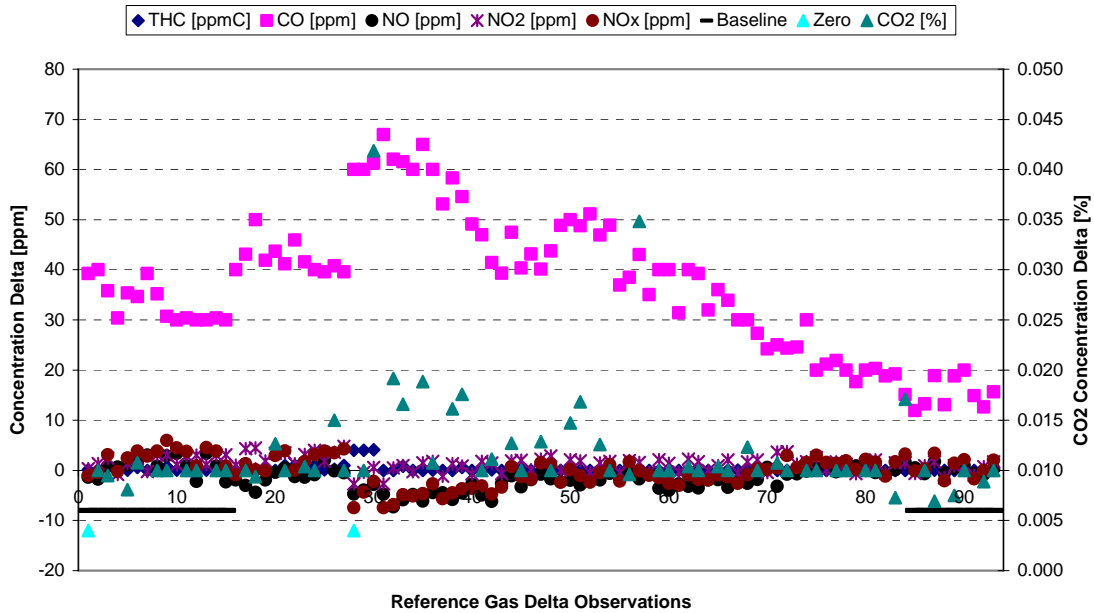


FIGURE 169. PEMS 7 ENVIRONMENTAL RADIATION ELECTROSTATIC DISCHARGE ZERO DELTA MEASUREMENTS

Figure 170 and Figure 171 show the PEMS 7 audit and span deltas measured during Electrostatic Discharge testing. After the zero event at observation number 10, the delta measurements for NO, NO₂, and CO₂ had a noticeable shift. Although stable prior to the zero calibration, the NO, NO₂, and CO₂ delta measurements showed noticeable positive drift after being re-zeroed. The baseline test segment at the end of the test showed no shift in delta measurements compared to those during ESD testing. Therefore, the deltas observed during ESD testing were not likely caused by the Electrostatic Discharge. Furthermore, the continuous data for each PEMS measurement was reviewed to insure short duration measurement perturbations were not overlooked using the 30-second mean measurement. The continuous data showed no evidence of short term measurement errors.

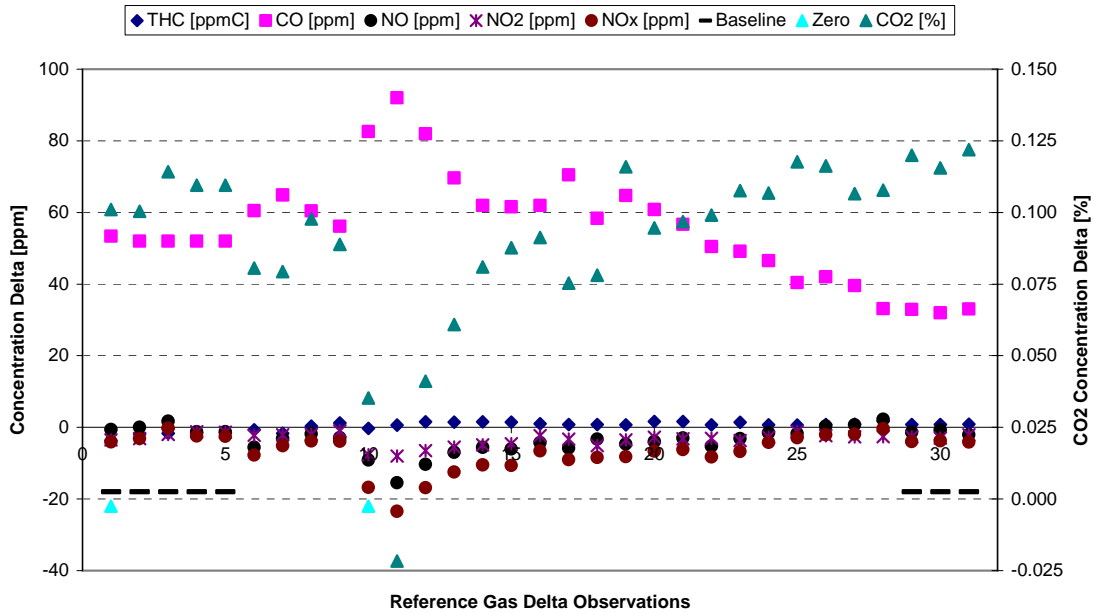


FIGURE 170. PEMS 7 ENVIRONMENTAL RADIATION ELECTROSTATIC DISCHARGE AUDIT DELTA MEASUREMENTS

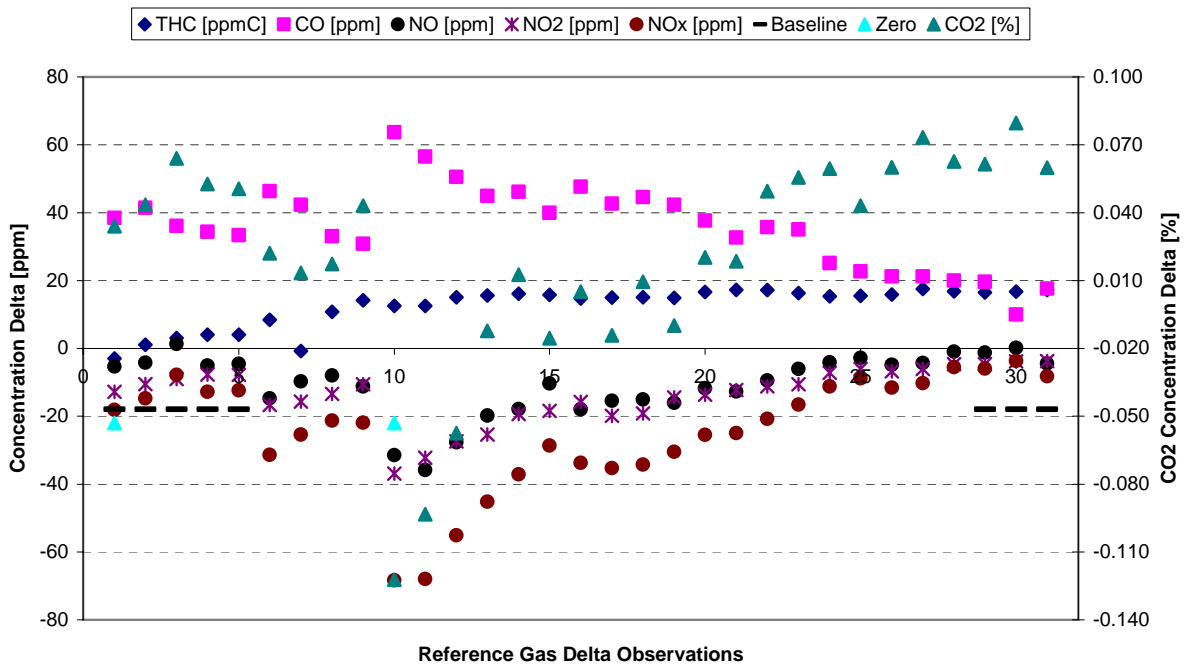


FIGURE 171. PEMS 7 ENVIRONMENTAL RADIATION ELECTROSTATIC DISCHARGE SPAN DELTA MEASUREMENTS

Figure 172 shows the EFM measurements during ESD testing. Nearly all of the EFM zero deltas recorded during ESD testing were below 0.2 scfm. Curiously, the largest zero deltas

were measured at the end of the test during baseline testing. The 30-second mean delta data suggests ESD testing had little affect on the exhaust flow measurements. Similar to gaseous concentration measurements, the continuous EFM data was examined and found to show no evidence of short duration measurement errors.

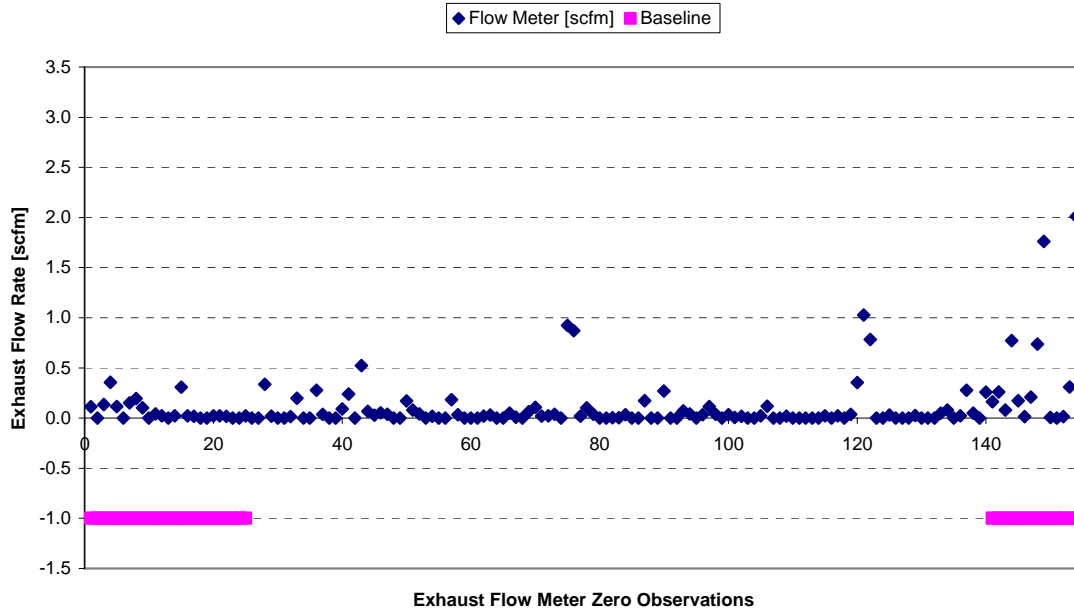


FIGURE 172. 5-INCH EFM ENVIRONMENTAL RADIATION ELECTROSTATIC DISCHARGE ZERO DELTA MEASUREMENTS

5.6.4 Conducted Transients

SAE test J1113/11 titled *Immunity to Conducted Transients on Power Leads* was performed to evaluate the PEMS response to transient voltage disturbances on the PEMS 12-volt power supply cable. Based on the SAE Standard test descriptions and recommendations from SwRI specialists, the Steering committee elected to test the PEMS using the specifications detailed in Region 2, Class B of the J1113/11 test protocol. Due to the high current draw of the PEMS, a Schaffner NSG 5200 Automotive Electronics Test System was rented to perform the Conducted Transients testing. A Schaffner test system is shown in Figure 173. The test system included a Burst Generator Module, a Load Dump Module, a Pulse Generator Module, and an Automotive ECM Test System with PC. The Schaffner system included all of the hardware and software necessary to perform each of the Conducted Transients as specified in the SAE Standard.



FIGURE 173. SCHAFFNER NSG 5200 AUTOMOTIVE ELECTRONICS TEST SYSTEM

During Conducted Transients testing, the power cable to the PEMS heated sample line was disconnected to keep the PEMS current draw below 30 amps, which was the limit of the Schaffner test system. The Schaffner NSG 5200 was connected in series between the PEMS and 12-volt power supply. With the test system installed, the PEMS supply voltage dropped to 8 volts using the Sensors Inc. power supply. Therefore, a SwRI 12-volt power supply was used to power the PEMS during Conducted Transients testing. Similar to the other radiation tests, a 12-volt automotive battery was connected in parallel with the power supply. The PEMS supply voltage was maintained at approximately 13 volts during testing. Using the Schaffner test system, a number of voltage disturbances were introduced through the PEMS power supply cable. The voltage perturbations ranged from -200 to 100 volts with bursts as short as 250 ns and voltage spikes lasting up to 2, 4, or 200 ms. The tests consisted of voltage spikes with slow recovery, voltage spikes with quick recovery, repeated voltage bursts, and a load dump. All 200 ms voltage spikes with slow recovery would cause the PEMS to shut down. The 200 ms duration tests were repeated at a quarter of the voltage disturbance amplitude, however, the PEMS continued to shutdown. Therefore, the response of the PEMS to 200 ms voltage disturbances was not characterized in this experiment. Similarly, the load dump experiment caused the PEMS to shutdown, therefore, no PEMS response data was gathered for that portion of the Conducted Transient testing.

Figure 174 shows an example voltage trace of a voltage spike with slow recovery during Conducted Transient testing. The voltage disturbance had an amplitude of -100 volts and recovery time of 4 ms.

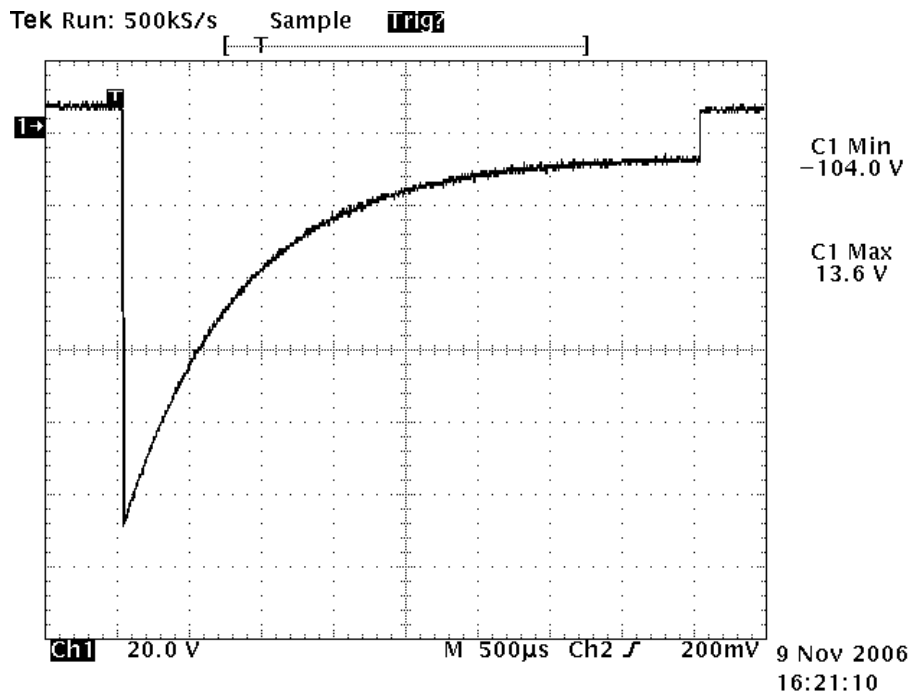


FIGURE 174. EXAMPLE VOLTAGE TRACE DURING A VOLTAGE SPIKE WITH SLOW RECOVERY

Figure 175 shows an example voltage trace of a voltage spike with quick recovery during Conducted Transient testing. The voltage disturbance had an amplitude of 50 volts and recovery time of 0.05 ms.

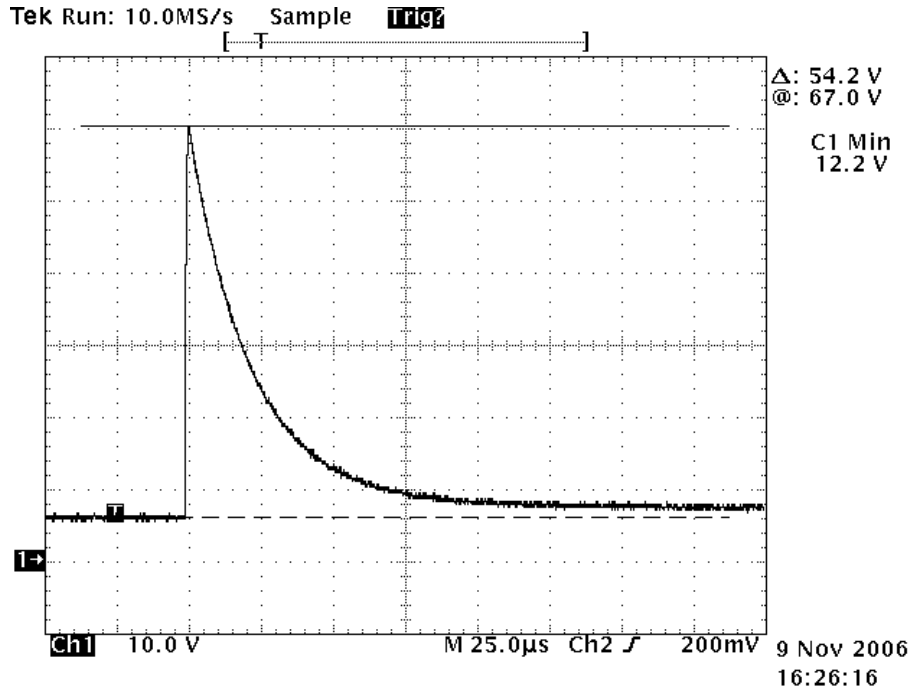


FIGURE 175. EXAMPLE VOLTAGE TRACE DURING A VOLTAGE SPIKE WITH QUICK RECOVERY

Figure 176 shows a voltage trace for a short duration voltage burst. The voltage burst had an amplitude of -150 volts, a rise time of 2 ns, and a recovery time of 100 ns. Voltage burst tests consisted of repeating a series of 10 voltage bursts.

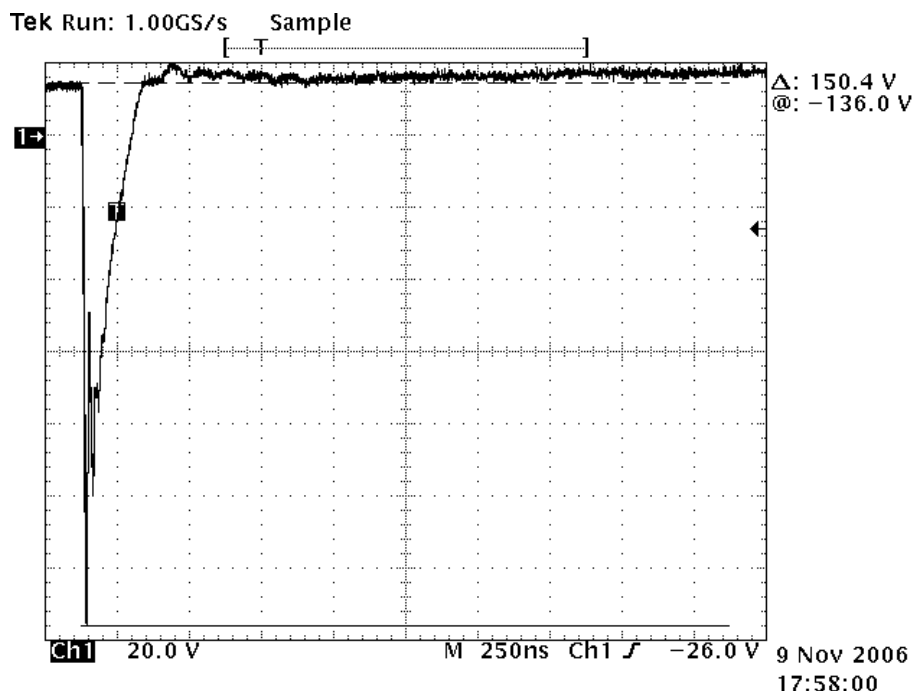


FIGURE 176. EXAMPLE VOLTAGE TRACE DURING A VOLTAGE BURST

Prior to testing, PEMS 7 was zeroed and spanned after warming for over one hour. Periods of baseline or zero stimulation testing were included throughout the Conducted Transient test to determine if the voltage disturbances had any effect on the PEMS measurements. To capture potential measurement errors, the voltage perturbations, being extremely brief, were timed to occur during the 30-second recorded measurements. Typically, one Conducted Transient test was performed during each 30-second measurement.

Figure 177 shows the PEMS 7 zero delta measurements during Conducted Transient testing. Zero events occurred at zero observation number 16 and 77, while a day break occurred at observation number 92; requiring the PEMS to be zeroed and spanned. Due to the extended length of time required to setup each Conducted Transient test, a large portion of the data collected was zero stimulation baseline testing. Differentiating between the test deltas and baseline deltas for each gaseous measurement is difficult, therefore, the voltage disturbances delivered to the PEMS during Conducted Transient testing had little to no affect on the PEMS measurements.

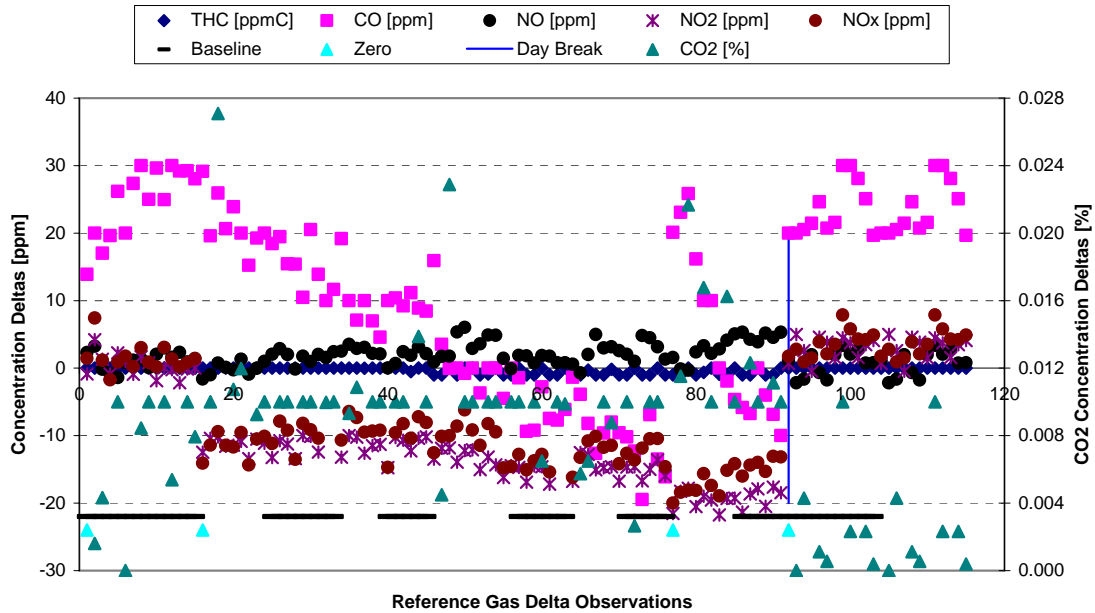


FIGURE 177. PEMS 7 ENVIRONMENTAL RADIATION CONDUCTED TRANSIENT ZERO DELTA MEASUREMENTS

Figure 178 and Figure 179 show the audit and span deltas for PEMS 7 during Conducted Transient testing. Zero events occurred at observation number 6 and 26. The PEMS was zeroed and spanned following the day break at observation number 31. Although each gaseous pollutant exhibited audit and span deltas, the baseline deltas transitioned smoothly with the test deltas, indicating the Conducted Transient testing had little affect on the PEMS measurement systems.

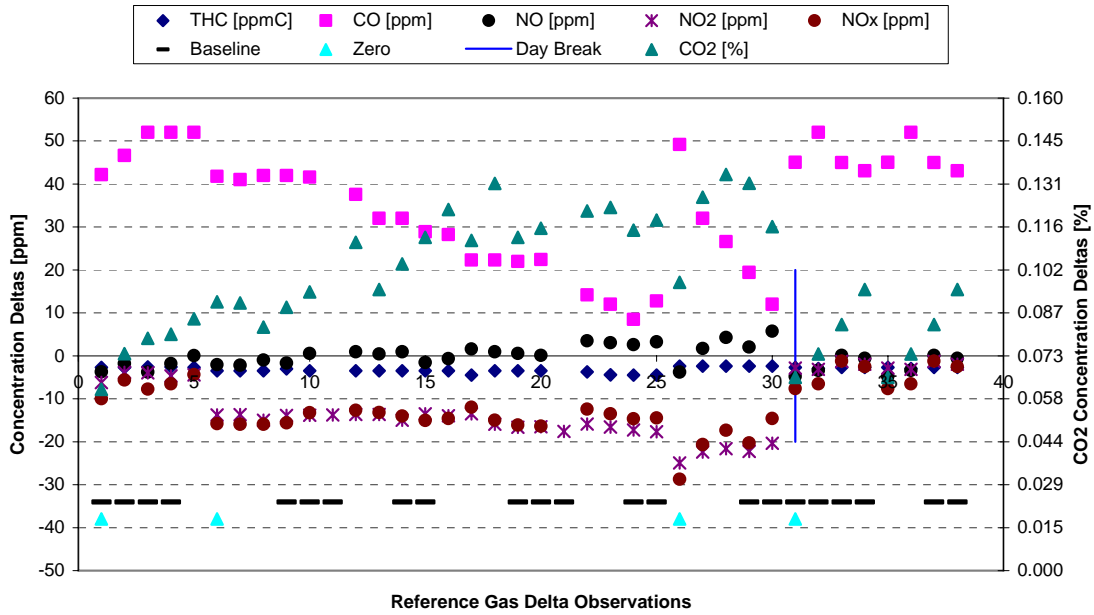


FIGURE 178. PEMS 7 ENVIRONMENTAL RADIATION CONDUCTED TRANSIENT AUDIT DELTA MEASUREMENTS

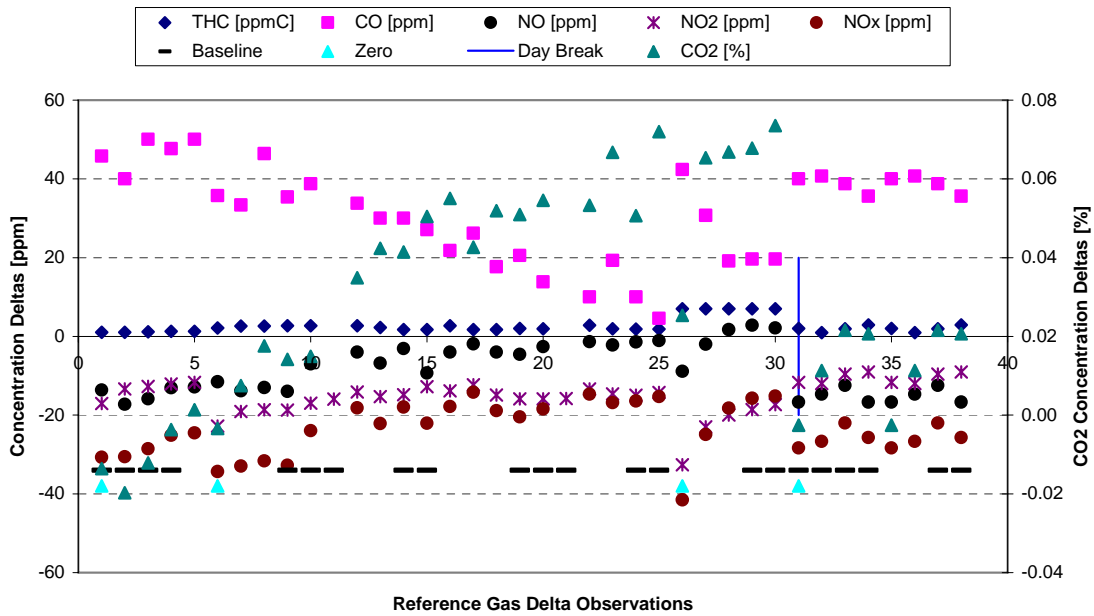


FIGURE 179. PEMS 7 ENVIRONMENTAL RADIATION CONDUCTED TRANSIENT SPAN DELTA MEASUREMENTS

Figure 180 shows the EFM zero measurements during Conducted Transient testing. Most of the exhaust flow meter 30-second average measurements were less than 0.2 scfm.

Occasional measurements were recorded above 0.5 scfm, however, several of these measurements occurred during baseline testing. The maximum observed delta of 1.5 scfm is less than 0.1% of the meter's 1700 scfm full scale flow rating.

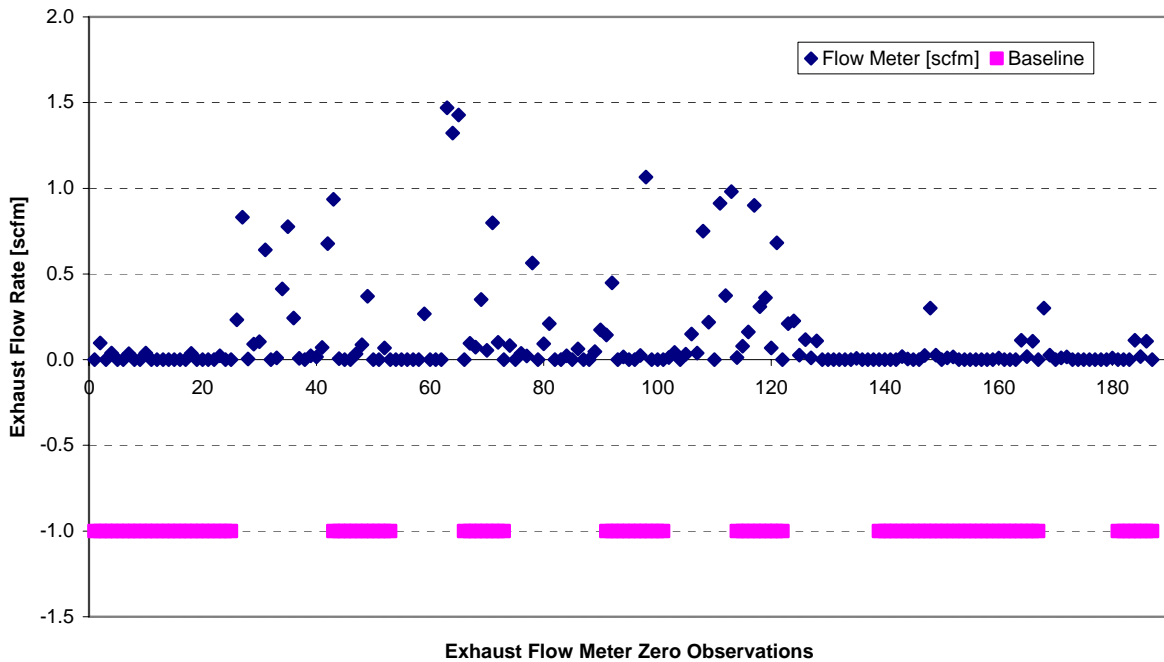


FIGURE 180. 5-INCH EFM ENVIRONMENTAL RADIATION CONDUCTED TRANSIENT ZERO DELTA MEASUREMENTS

5.6.5 Radiation Error Surface Generation

As described in the Test Plan, the measurement error data gathered during the Bulk Current Injection, Radiated Immunity, Electrostatic Discharge, and Conducted Transients testing was to be pooled to generate a radiation error surface. Because the radiation tests challenged the PEMS at the most extreme radiation levels the equipment would likely be subjected to during in-use testing, the radiation error surface was to be processed differently than the Temperature and Pressure error surfaces. The pooled radiation data was to be corrected for the environmental baseline bias and variation. The 5th, 50th, and 95th percentile values of the pooled, corrected radiation data was to be used to generate error surfaces at the zero, audit and span levels. These radiation error surfaces were to be sampled normally.

As described in the previous radiation test sections, nearly all of the radiation delta data resembled the corresponding baseline deltas; indicating the PEMS showed very little susceptibility to the radiation tests. The only notable radiation susceptibility was for a few high biased CO and CO₂ measurements. Because the radiation error surface would use the 95th percentile deltas, the Steering Committee elected to calculate the 95th percentile deltas for zero, audit, and span to determine if the high CO and CO₂ deltas caused by the radiation testing were

outside the 95th percentile delta. Shown in Figure 181 through Figure 183 are the pooled zero, audit, and span delta measurements for all of the radiation testing. The baseline test segments were extracted from the pooled radiation delta data set. The 95th percentile values are shown as a line for each gaseous emission. The high CO and CO₂ deltas were greater than the 95th percentile; therefore, the radiation error surfaces would not include any measurement error data caused by radiation effects. Based on this data, radiation error surfaces were not generated for use in the Model.

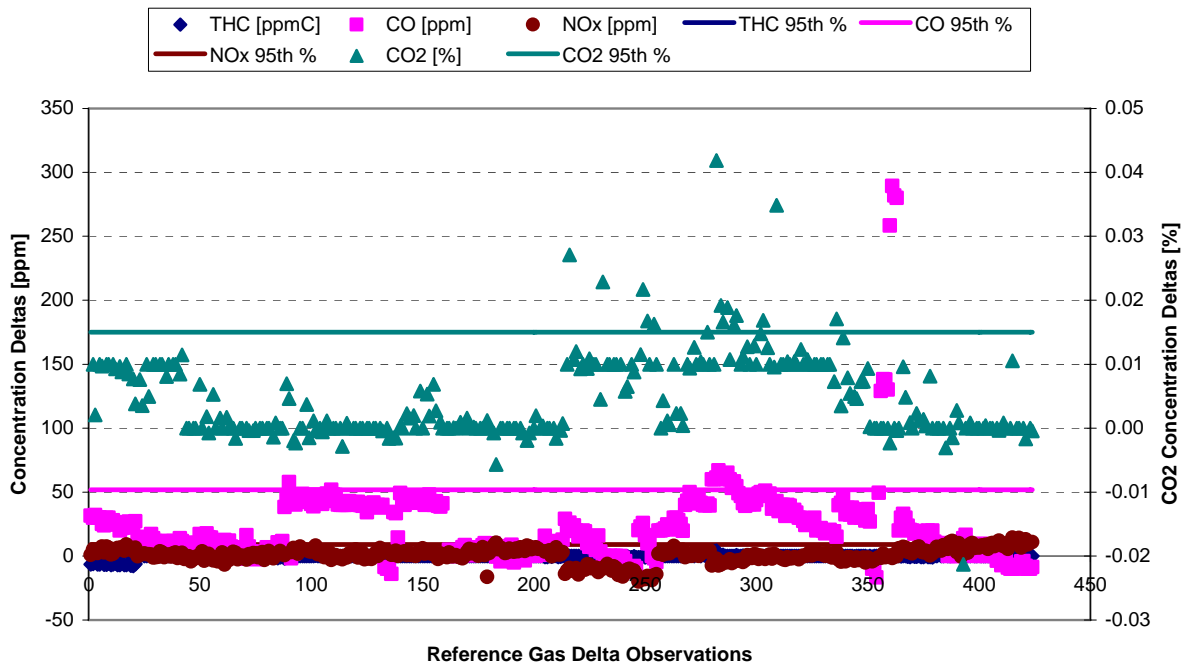


FIGURE 181. COMBINED RADIATION CHAMBER ZERO DELTA TEST RESULTS

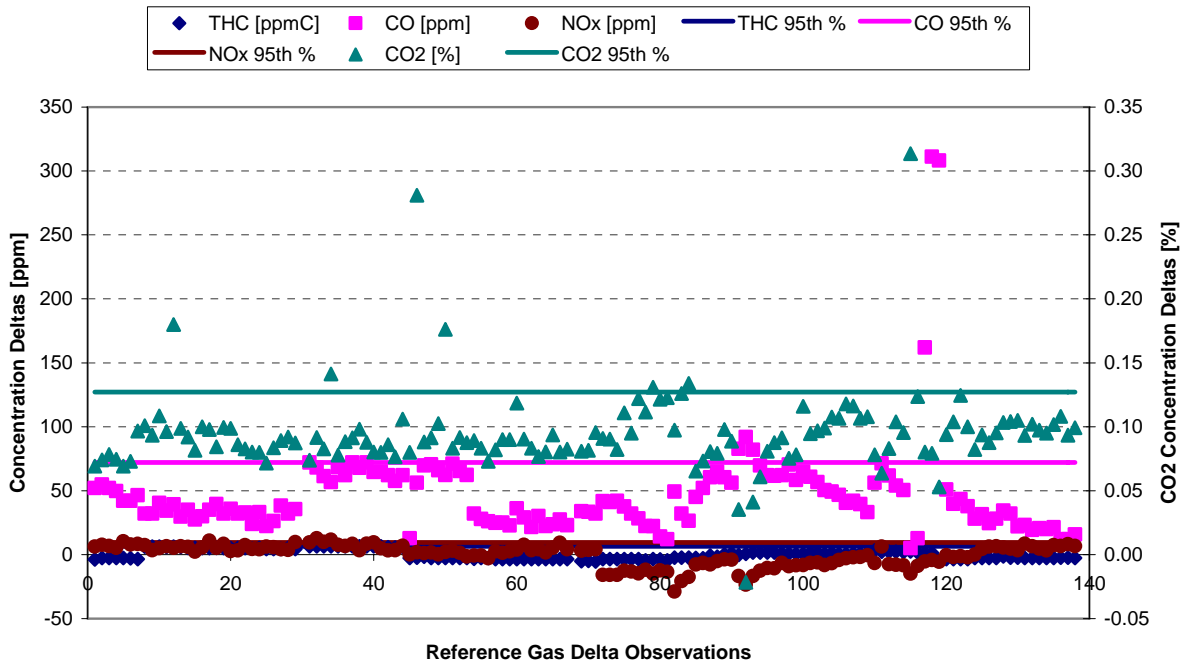


FIGURE 182. COMBINED RADIATION CHAMBER AUDIT DELTA TEST RESULTS

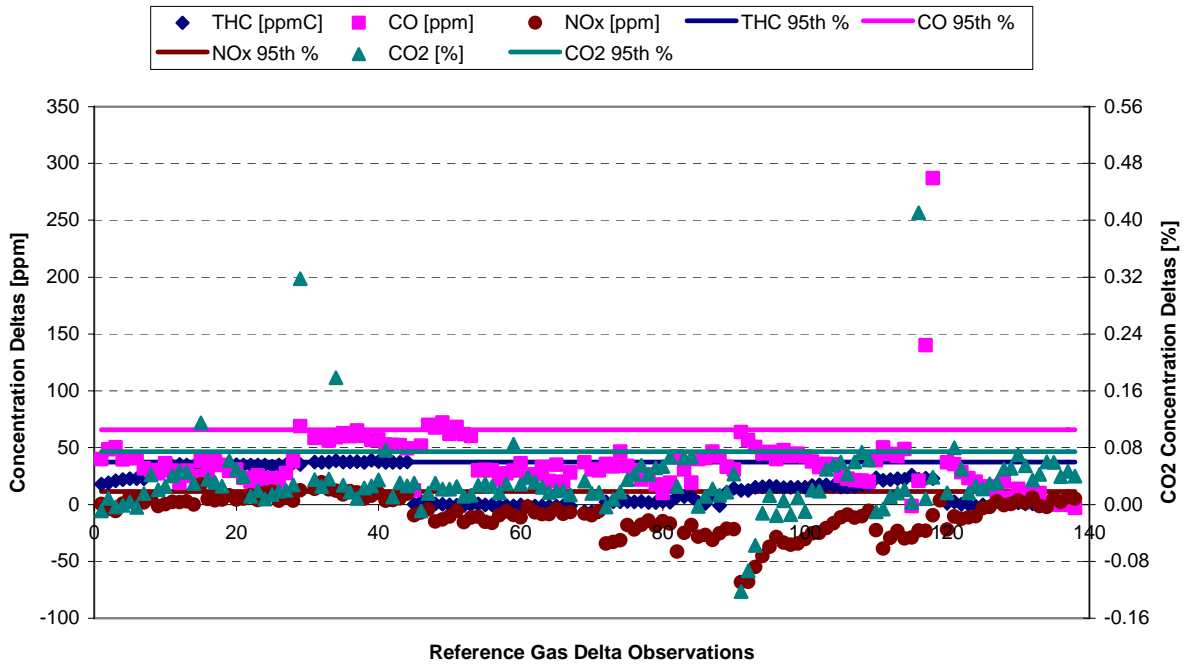


FIGURE 183. COMBINED RADIATION CHAMBER SPAN DELTA TEST RESULTS

Shown in Figure 184, the radiation exhaust flow rate zero measurements were pooled after the baseline test segments were removed from each test. As directed in the Test Plan, the radiation error surfaces were to be generated using the 5th, 50th, and 95th percentile delta observations from the pooled measurement errors. However, the PEMS set all negative flow rate measurements to zero. With an incomplete distribution of negative flow rate delta measurements, an alternate error surface generation method was developed. All zero measurements were removed from the pooled radiation exhaust flow measurements as well as the environmental baseline exhaust flow measurement data set. Approximately one third of the data was removed from the both the radiation and baseline exhaust flow data sets. Removal of the zero level exhaust flow rate measurements was necessary to more accurately compare the variance of the radiation and baseline error data.

To avoid over counting exhaust flow rate measurement errors, it was necessary to remove the bias and variance measured during environmental baseline testing from the radiation exhaust flow rate data. With zero deltas removed, the median exhaust flow rate measurement from the baseline test was subtracted from each radiation exhaust flow rate delta. This process was inconsequential because the median baseline delta was less than 0.01 % of the flow meter's maximum flow rating. Next the MAD of the baseline data was compared to the MAD of the bias corrected radiation data. Using the equation below, the MAD values were used to calculate a scaling factor. Each radiation exhaust flow measurement was multiplied by the scaling factor to shrink the variance of the radiation data by the variance measured during environmental baseline testing.

$$Scaling_Factor = \frac{\sqrt{MAD_{Rad}^2 - MAD_{BL}^2}}{MAD_{Rad}}$$

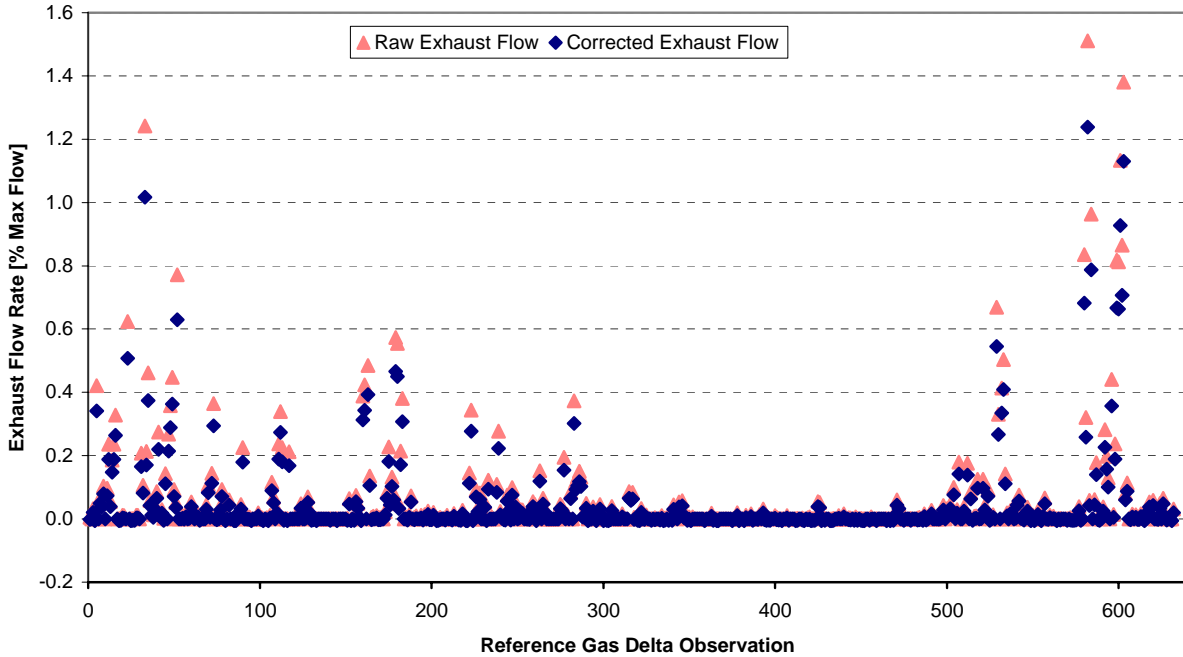


FIGURE 184. POOLED EXHAUST FLOW RATE ZERO DELTAS MEASURED DURING ENVIRONMENTAL RADIATION TESTING

After the radiation exhaust flow rate data was corrected for the baseline bias and variance, the 5th, 50th, and 95th percentile deltas were generated for use in the radiation exhaust flow rate error surface. With an incomplete delta distribution, the Steering Committee elected to calculate the 95th percentile of the corrected radiation delta data. The negative of the 95th percentile delta value was set to the 5th percentile and the 50th percentile was set to zero. The final error surface for radiation exhaust flow rate is shown in Figure 185.

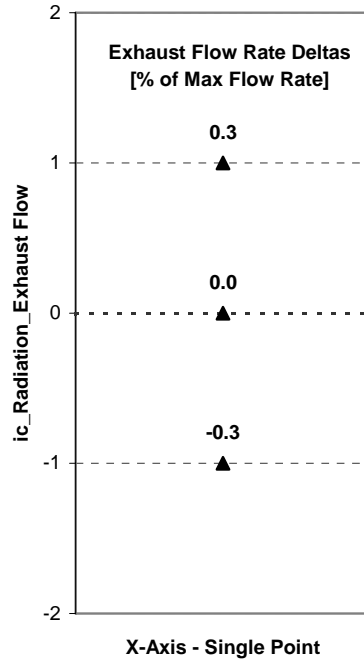


FIGURE 185. ERROR SURFACE FOR ENVIRONMENTAL RADIATION EXHAUST FLOW RATE DELTA MEASUREMENTS

5.7 Vibration Table Testing

Vibration testing was performed to determine PEMS gaseous concentration measurement errors due to vehicle vibrations. Due to mounting issues, the PEMS EFM was not used during vibration testing. Shown in Figure 186, an Unholtz-Dickie Corporation electro-dynamic shaker system was used to perform vibration testing with PEMS 3 in a Sensors Inc. environmental enclosure. The shaker system used random movement to reproduce vibration defined by the desired Power Spectral Density (PSD).



FIGURE 186. PEMS 3 IN AN ENVIRONMENTAL ENCLOSURE DURING VIBRATION TESTING USING AN UNHOLTZ-DICKIE SHAKER SYSTEM

The vibration test was intended to simulate vibration typically experienced by the PEMS during in-use on-road testing. As stated in the Test Plan, the Steering Committee originally decided to test the PEMS using the PSD from the Mil Standard 810, US Highway Truck Vibration Exposure. However, Sensors Inc. independently performed the Mil Standard 810 and observed functional failures shortly after commencing the vibration test. After Sensors Inc. reported the failures to the Steering Committee, SwRI was asked to generate vibration spectra representative of an on-road truck. Vibration data collected with an Army M915A2 Semi-Tractor, shown in Figure 187, was used to generate vibration spectra. The vibration data collected with the M915A2 Tractor was comprised of accelerometer data at 8 locations on the truck. The accelerometers were located on the truck frame as well as the cab.



FIGURE 187. ARMY M915A2 SEMI-TRACTOR USED TO GENERATE VIBRATION SPECTRA FOR VIBRATION TESTING

After reducing the raw vibration data, SwRI proposed a revised PSD. However, the M915A2 Tractor was limited to 55 mph during testing. With the speed of most on-road trucks exceeding 55 mph, the Steering Committee elected to have SwRI generate a PSD at 70 mph. The 55 mph, 70 mph, and Mil Standard 810 are shown in Figure 188. The 70 mph PSD resulted in a vibration energy increase factor of 2.69 over the 55 mph PSD. SwRI also performed a comparison of the lateral acceleration data and vertical acceleration data. Overall, the lateral and vertical accelerations were nearly equal, therefore, one PSD was used for vibration testing in each PEMS axis. Over 86 % of the M915A2 Tractor vibration energy was below 500 Hz.

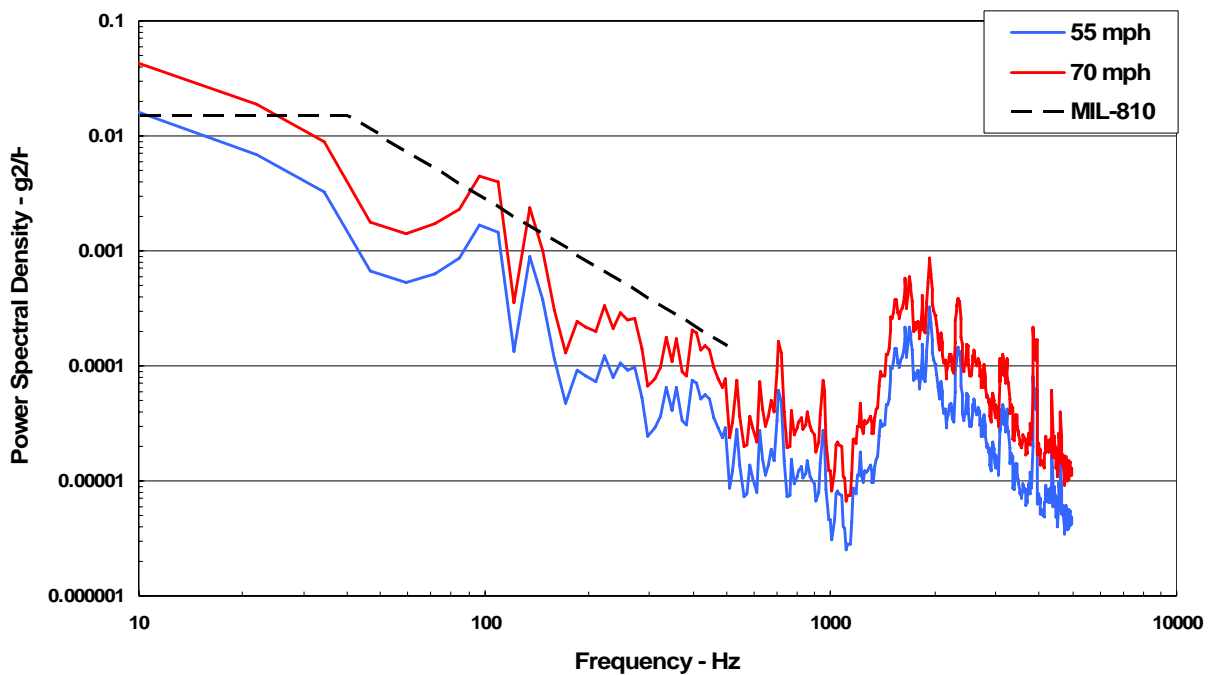


FIGURE 188. POWER SPECTRAL DENSITIES EVALUATED FOR VIBRATION TESTING

After warming for over one hour, PEMS 3 was zeroed and spanned with no stimulus prior to vibration testing. Similar to temperature and pressure testing, the PEMS was zeroed hourly, during which the shaker table was turned off. Using the 70 mph PSD, PEMS 3 was first tested for lateral, side-to-side vibration. During the first hour of testing, the PEMS reported a warning that the environmental enclosure heated line temperature was low. Also, the enclosure cooling fans were not operational. The cause of the aforementioned problems was due to a failure of the 12-volt power connector from the PEMS to the environmental enclosure. After repairing the broken connector, PEMS 3 was tested for 3 more hours of side-to-side vibration. Next, the PEMS was turned and tested for lateral, front-to-back vibration. After only 10-minutes of vibration testing, the PEMS reported a high temperature fault for the FID and automatically shutdown the FID. The PEMS was shutdown and restarted, however, the PEMS could not communicate with the compact flashcard during the restart procedure. Without flashcard communication, the user cannot log onto the PEMS. After trying several different flash cards and numerous diagnostic measures, PEMS 3 was shipped to Sensors Inc. for repair. Sensors Inc. diagnosed the problem as a failed ribbon cable and returned PEMS 3 to SwRI for further testing. Unfortunately, most of the PEMS data was lost due to the cable failure.

After considering the PEMS failures using the 70 mph PSD, the Steering Committee elected to proceed with vibration testing using the 55 mph PSD. With the possibility of another functional failure, vibration testing was initially performed for only two hours in each direction to generate vibration deltas for each axis. Also, the shaker table was turned off for a segment of each hour of vibration testing to generate baseline data. The table was also turned off during zero and span operations.

Figure 189 shows the PEMS 3 zero deltas measured during environmental vibration testing. Zero events were performed hourly, with baseline test segments included during each hour of vibration testing. The first two hours of testing were lateral, side-to-side vibration, hours 3 and 4 were lateral, front-to-back vibration, hours 5 through 7 were vertical vibration, hour 8 was lateral, side-to-side vibration, and hour 9 was lateral, front-to-back vibration. NO, NO₂, CO, and CO₂ zero deltas showed no evidence of vibration susceptibility when compared to the baseline test segments.

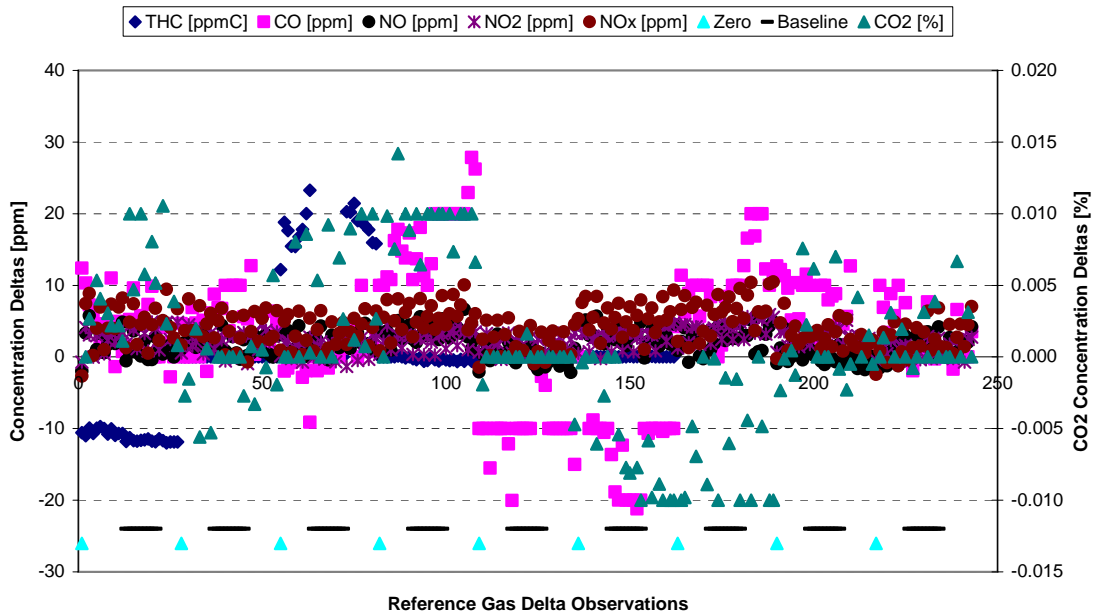


FIGURE 189. PEMS 3 ENVIRONMENTAL VIBRATION ZERO DELTA MEASUREMENTS

Figure 190 shows the PEMS 3 THC zero delta measurements during vibration testing. During test hour 3, which was lateral, front-to-back vibration, the PEMS showed elevated zero deltas during vibration testing. During the baseline segment of hour 3, the THC zero deltas returned to near zero levels. At the end of test hour number 3, the PEMS reported a fault indicating the FID internal reference pressure was out of its limits. Curiously, the FID fuel bottle was nearly empty at the end of test hour number 3. When replacing FID fuel bottle, the quick-connect device used to connect the FID bottle to the PEMS was found to be broken. With a functional quick-connect, the THC zero deltas showed no evidence of susceptibility to vibration in any axis. The elevated THC zero measurements and low FID fuel bottle pressure were likely caused by the failure of the FID fuel bottle connection device.

At the end of test hour 6, the PEMS reported a fault indicating the FID gas flow was too high or too low. After test 6, the FID would not zero or span, although the FID interface indicated the FID was operating at the correct temperature and the FID flame was lit. The PEMS was restarted several times in attempt to restore FID operation, however, the FID would not zero or span. Therefore, testing was continued without THC measurements after test hour 6. During test hour number 9, a loud pop was heard from the PEMS and the THC measurement returned.

According to Sensors Inc., the pop noise was likely the FID lighting during vibration testing. When the FID fuel bottle was removed after test 9, the quick-connect was again found to be broken. The connection failures were most likely due to the lateral, front-to-back vibration causing the FID fuel bottle to slide forward and backward in the PEMS case and stress the connection.

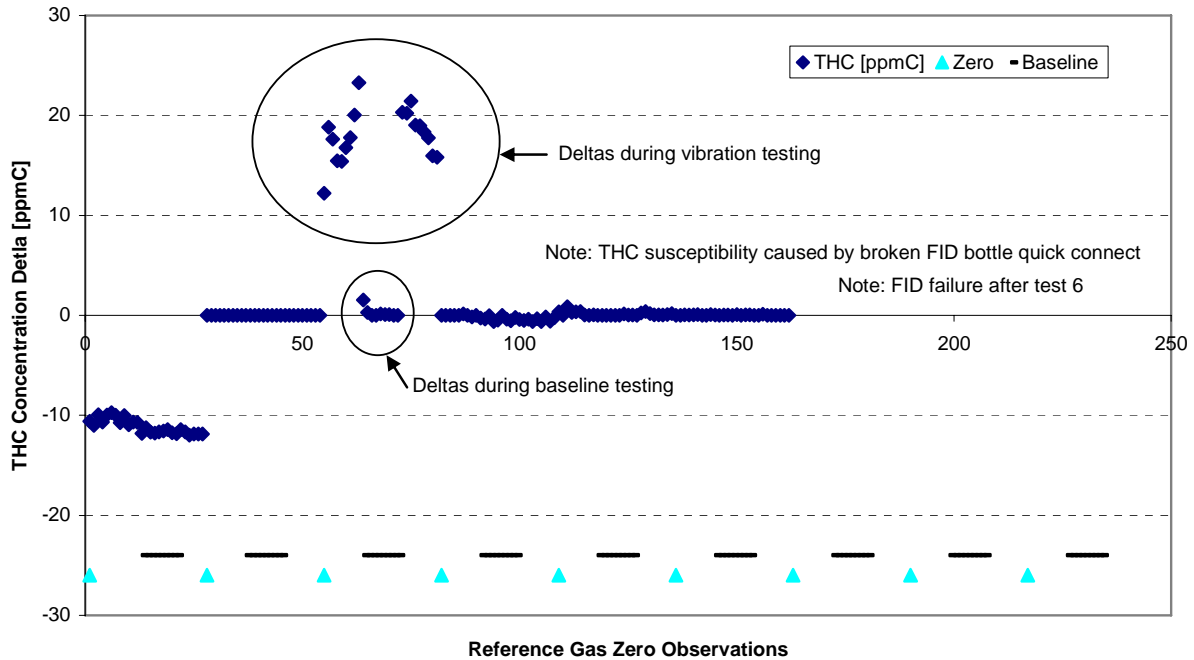


FIGURE 190. PEMS 3 ENVIRONMENTAL VIBRATION THC ZERO DELTA MEASUREMENTS

Figure 191 and Figure 192 show the audit and span deltas for PEMS 3 during environmental vibration testing. CO and CO₂ audit and span deltas showed no differences between the vibration test data and baseline test data, indicating CO and CO₂ measurements were not susceptible to vibration. THC audit and span deltas were similar to the THC zero deltas and showed elevated measurements during test hour number 3. As discussed previously, the elevated THC deltas during hour 3 were likely caused by a broken FID fuel bottle connector. With a functional FID bottle connector, the THC audit and span deltas were similar for vibration and baseline testing. As discussed below, NO_x deltas showed slightly elevated measurements during lateral, side-to-side vibration when compared to the baseline testing. Most of the shift between vibration and baseline testing was caused by the NO₂ measurement, with NO measurements being unaffected by the vibration tests.

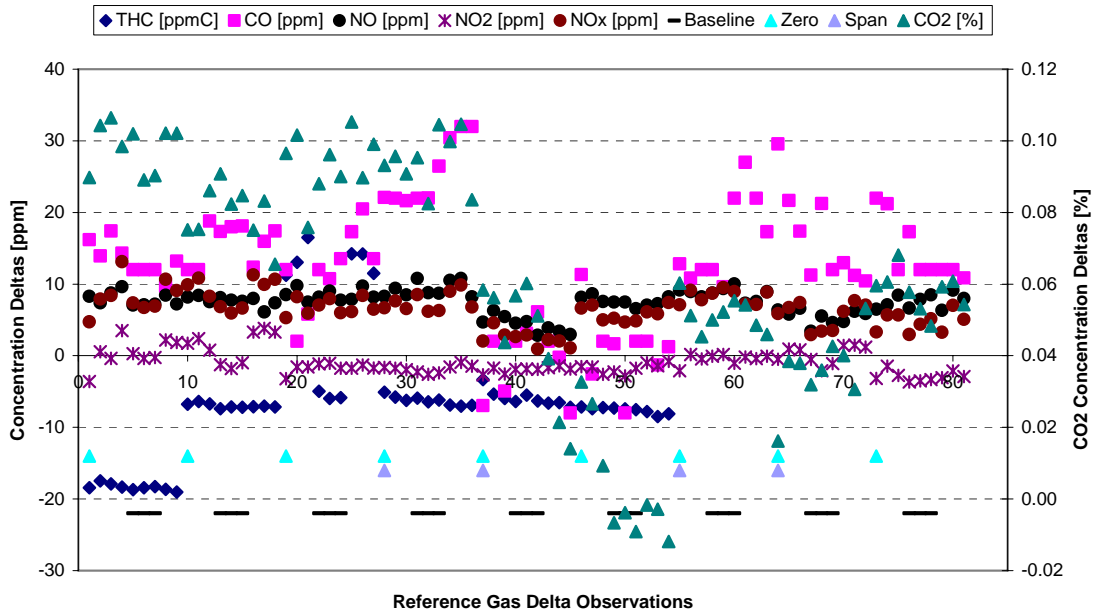


FIGURE 191. PEMS 3 ENVIRONMENTAL VIBRATION AUDIT DELTA MEASUREMENTS

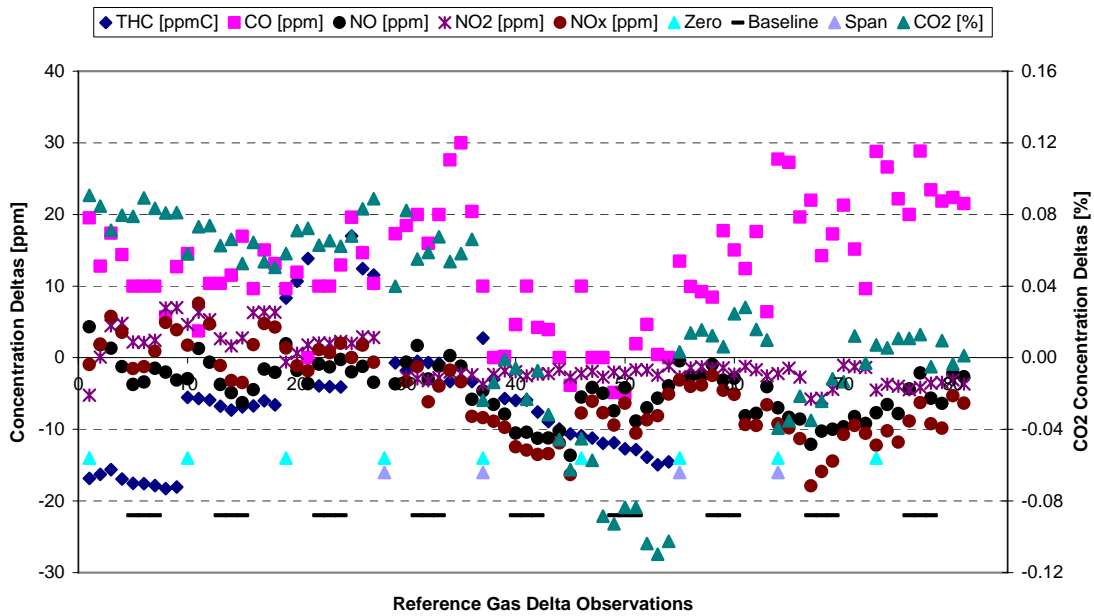


FIGURE 192. PEMS 3 ENVIRONMENTAL VIBRATION SPAN DELTA MEASUREMENTS

Figure 193 shows the NO_x span deltas for PEMS 3 during vibration testing. During lateral side-to-side vibration, test hours 1,2, and 8, there was a noticeable difference between the

deltas observed during vibration testing and the deltas observed during baseline testing. All baseline deltas showed a definite negative shift compared to the vibration deltas directly prior to and after the baseline segment. The slight NO_x susceptibility to lateral, side-to-side vibration was driven by the NO₂ measurement deltas.

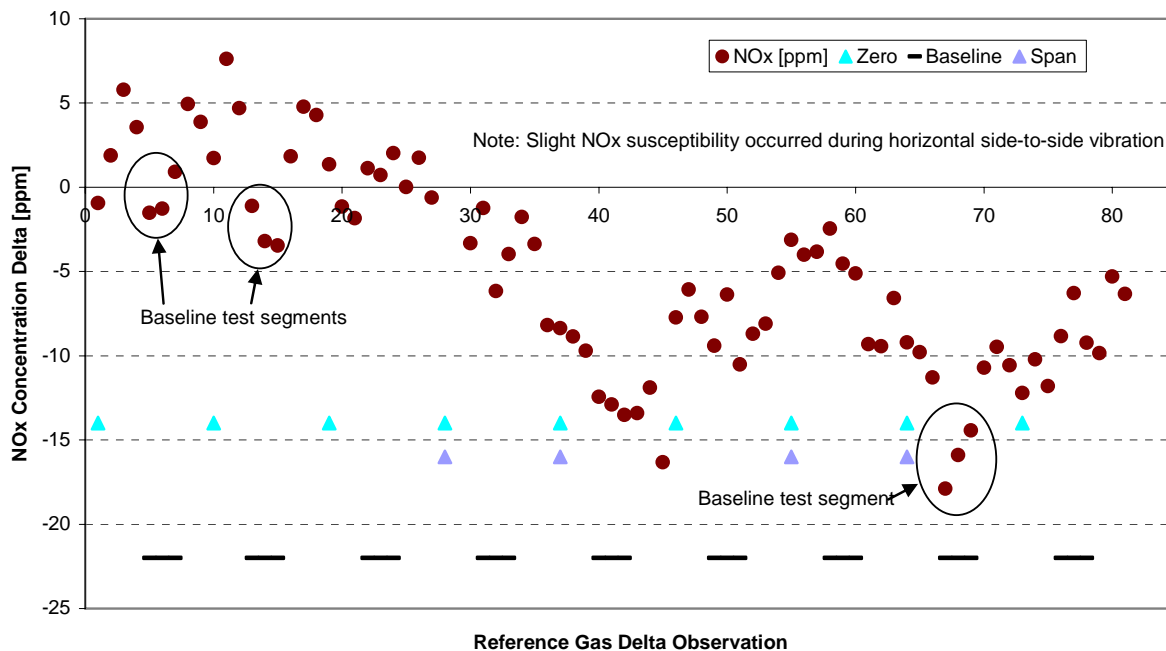


FIGURE 193. PEMS 3 ENVIRONMENTAL VIBRATION NO_x SPAN DELTA MEASUREMENTS

Nearly all of the deltas measured during vibration matched the deltas measured during the baseline test segments. Furthermore, the NO_x susceptibility to lateral vibration was minor and only evident during span measurements. Therefore, the Steering Committee elected not to generate an environmental vibration error surface for use in the Monte Carlo Model.

5.8 Ambient Hydrocarbon Testing

The Ambient Hydrocarbon test was performed to determine the PEMS FID response to varying levels and compositions of hydrocarbon in the ambient air. One source of potential FID measurement errors included the use of ambient air as the FID burner air source. Hydrocarbon in the ambient air would enter the FID reaction chamber as burner air, causing measurement inaccuracy. Ambient air is also used to zero the FID, therefore, ambient hydrocarbons will also affect the FID zero calibration. During laboratory engine testing and environmental testing, the PEMS was zeroed using bottled zero air. Zero air was also overflowed to the FID burner air inlet throughout the program. It was necessary to eliminate ambient hydrocarbon contamination during engine and environmental testing to insure errors due to ambient hydrocarbons were only capture during the Ambient Hydrocarbon test.

Ambient Hydrocarbon testing was performed with PEMS 2. Throughout testing, zero air was overflowed to the inlet of the PEMS sample line. Instead of overflowing zero air to the FID burner air inlet as was done during engine and environmental testing, air mixtures with varying levels and compositions of hydrocarbons were introduced to the FID burner during Ambient Hydrocarbon testing. Shown in Table 84, 9 combinations of Hexane and Methane were used to contaminate the FID burner air. According to EPA, the Hexane and Methane concentrations selected for Ambient Hydrocarbon testing were deliberately chosen to exceed typical ambient hydrocarbon variation to insure the test capture the full range of possible THC measurement errors. The hydrocarbon gas mixtures were generated using a 4 ppmC Hexane gas bottle, a 4 ppmC Methane gas bottle, a 16 ppmC Hexane bottle, and a 16 ppmC Methane bottle, all balance air. A gas divider was used to blend the hydrocarbon gases 50/50 to achieve the desired concentration levels. Two computer controlled electronic solenoid manifolds were used to automatically control the hydrocarbon combinations.

TABLE 84. HEXANE AND METHANE CONTAMINATION COMBINATIONS USED DURING AMBIENT HYDROCARBON TESTING

Hydrocarbon Combination	Hexane [ppmC]	Methane [ppmC]
1	0	0
2	2	2
3	8	8
4	0	2
5	2	8
6	8	0
7	0	8
8	2	0
9	8	2

As specified in the Test Plan, the FID was stabilized using one of 7 different combinations of FID air hydrocarbon contamination. After the FID had stabilized with a given hydrocarbon combination, the FID was zeroed using zero air and spanned. The PEMS was then set to sample zero air which was overflowed to the inlet of the heated sample line. Next, the FID burner air was automatically cycled through the hydrocarbon combinations shown in Table 84. Each hydrocarbon combination was sampled for 90 seconds; 60 seconds to purge and stabilize and 30 seconds to record an averaged measurement. Taken from the Test Plan, Table 85 shows the test sequence used for Ambient Hydrocarbon testing. The FID was first zeroed while using the FID burner air hydrocarbon concentrations shown in the merged cells. After the FID was zeroed, the PEMS was set to sample zero air and the FID burner air was cycled through the 10 hydrocarbon combinations levels to the right of the merged cells. Although only 9 hydrocarbon combinations were possible, the first combination was repeated at the end of each test. The test sequence was repeated one time.

TABLE 85. AMBIENT HYDROCARBON TEST SEQUENCE

Ambienet Hydrocarbons Test Sequence					Ambienet Hydrocarbons Test Sequence				
Phase	Burner air hydrocarbons during		Burner air hydrocarbons during		Phase	Burner air hydrocarbons during		Burner air hydrocarbons during	
	Hexane, ppm	Methane, ppm	Hexane, ppm	Methane, ppm		Hexane, ppm	Methane, ppm	Hexane, ppm	Methane, ppm
1			0	0	51			8	8
2			2	2	52			0	0
3			8	8	53			2	2
4			0	2	54			8	0
5	0	0	2	8	55	8	0	0	2
6			8	0	56			2	8
7			0	8	57			8	2
8			2	0	58			0	8
9			8	2	59			2	0
10			0	0	60			8	8
11			2	2	61			0	0
12			8	8	62			2	2
13			0	0	63			8	8
14			2	8	64			0	2
15	2	2	8	0	65	0	8	2	8
16			0	2	66			8	0
17			2	0	67			0	8
18			8	2	68			2	0
19			0	8	69			8	2
20			2	2	70			0	0
21			8	8	71			2	2
22			2	2	72			8	8
23			0	0	73			0	0
24			8	2	74			2	8
25	8	8	2	0	75	2	2	8	0
26			0	8	76			0	2
27			8	0	77			2	0
28			2	8	78			8	2
29			0	2	79			0	8
30			8	8	80			2	2
31			0	0	81			8	8
32			2	2	82			0	0
33			8	8	83			2	2
34			0	2	84			8	0
35	0	2	2	8	85	8	0	0	2
36			8	0	86			2	8
37			0	8	87			8	2
38			2	0	88			0	8
39			8	2	89			2	0
40			0	0	90			8	8
41			2	2					
42			8	8					
43			0	0					
44			2	8					
45	2	8	8	0					
46			0	2					
47			2	0					
48			8	2					
49			0	8					
50			2	2					

Figure 194 and Table 86 show the THC measurements for the first test as specified in the Ambient Hydrocarbon test sequence. As specified in the Test Plan, each test sequence was repeated one time. The FID was zeroed with no FID burner air hydrocarbon contamination. The FID burner air was then cycled through the hydrocarbon combinations shown in Table 86. Having zeroed the FID with no Hexane or Methane FID air contamination, the initial and final THC measurements, both with no FID air contamination, were near zero. With 2 ppmC Methane

contamination in the FID burner air, the PEMS measured approximately 18 ppmC THC while sampling zero air. With 8 ppmC Methane contamination, the PEMS reported approximately 58 ppmC THC while sampling zero air. Hexane contamination introduced to the FID burner air had little effect on the PEMS THC measurement. The PEMS use a charcoal filter in the FID burner air line to absorb ambient hydrocarbon prior to reaching the FID. The charcoal filter apparently absorbed nearly all of the Hexane, but had little effect on the Methane contamination.

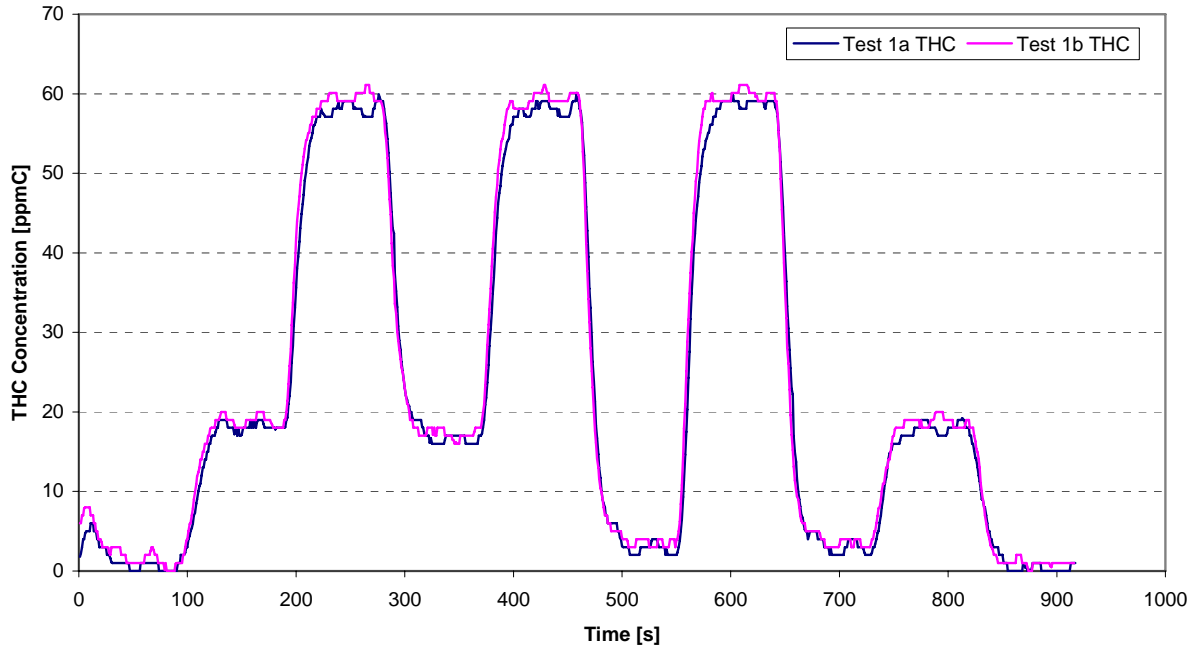


FIGURE 194. THC MEASUREMENTS FOR TEST 1 OF THE AMBIENT HYDROCARBON TEST SEQUENCE

TABLE 86. THC MEASUREMENTS FOR TEST 1 OF THE AMBIENT HYDROCARBON TEST SEQUENCE

FID Air Hexane [ppmC]	FID Air Methane [ppmC]	Gas Switch Time [s]	Test 1a THC [ppmC]	Test 1b THC [ppmC]
0	0	90	0.5	1.2
2	2	180	18.3	19.0
8	8	270	58.1	59.7
0	2	360	16.6	17.0
2	8	450	58.1	59.6
8	0	540	2.9	3.5
0	8	630	58.9	60.1
2	0	720	2.9	3.5
8	2	810	17.8	18.9
0	0	900	0.3	0.8
Pretest zero was performed with 0 ppmC Hexane and 0 ppmC Methane				

Figure 195 and Table 87 show the THC measurements for the second test as specified in the Ambient Hydrocarbon test sequence. Prior to performing the second test, the FID was stabilized and zeroed with 2 ppmC Hexane and 2 ppmC Methane FID burner air contamination. The FID air contamination was varied according to the concentrations specified in Table 87. The first and last measurements occurred with FID air hydrocarbon contamination levels similar to the hydrocarbon combination used to zero the FID. Therefore, the initial and final THC measurements were near zero. With 8 ppmC Methane contamination, the PEMS reported approximately 39 ppmC THC while sampling zero air. At 0 ppmC Methane contamination, the PEMS reported approximately -15 ppmC THC while sampling zero air. As observed during test number 1, Hexane contamination had little effect on the PEMS THC measurement.

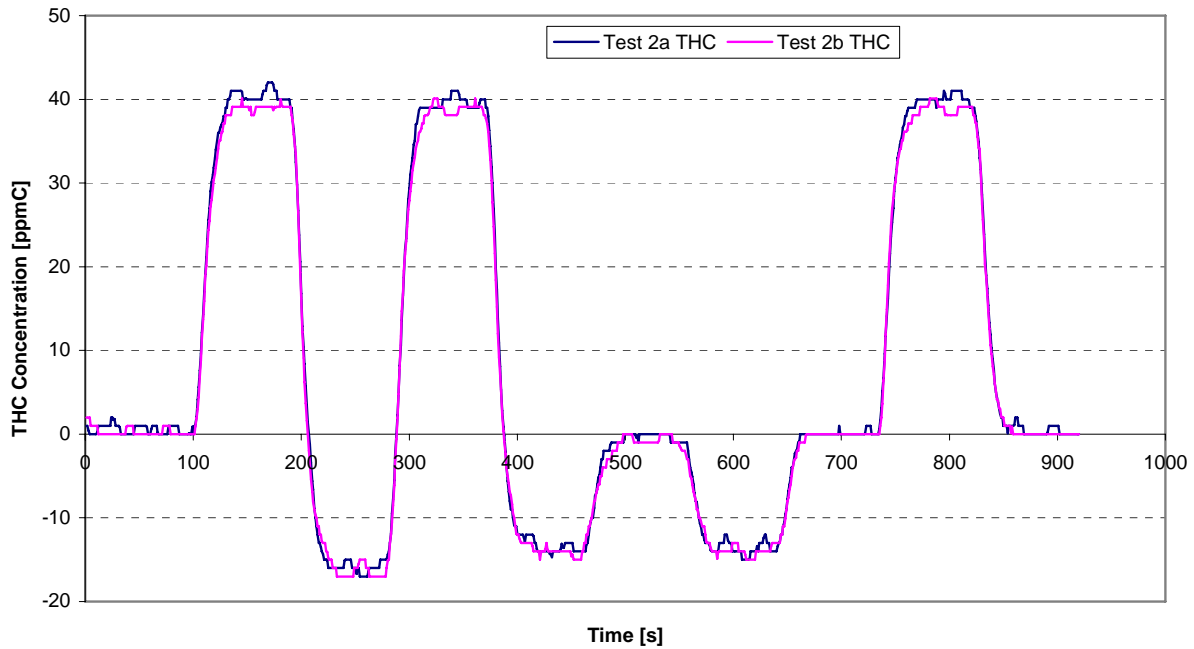


FIGURE 195. THC MEASUREMENTS FOR TEST 2 OF THE AMBIENT HYDROCARBON TEST SEQUENCE

TABLE 87. THC MEASUREMENTS FOR TEST 2 OF THE AMBIENT HYDROCARBON TEST SEQUENCE

FID Air Hexane [ppmC]	FID Air Methane [ppmC]	Gas Switch Time [s]	Test 2a THC [ppmC]	Test 2b THC [ppmC]
2	2	90	0.5	0.2
8	8	180	40.6	39.0
0	0	270	-16.1	-16.3
2	8	360	40.0	38.7
8	0	450	-13.8	-14.0
0	2	540	-0.1	-0.7
2	0	630	-13.9	-14.1
8	2	720	0.0	0.0
0	8	810	40.3	39.0
2	2	900	0.3	0.0

Pretest zero was performed with 2 ppmC Hexane and 2 ppmC Methane

PEMS 2 would not zero with 8 ppmC Methane contamination in the FID burner air. The PEMS would not perform an electronic zero with the high Methane FID air contamination because the measured THC zero concentration was outside the zero limits of the PEMS. Therefore, test 3, 5, and 7, each requiring the FID to be zeroed with 8 ppmC Methane contamination, were eliminated from test sequence. Each test repeat resulted in similar zero

measurements with the exception of test 6. Shown in Figure 196, the test 6a THC trace appeared normal, but the test 6b THC measurement was lower than expected. The test was repeated, however, the test 6c THC trace appeared normal, and the test 6d trace appeared low. No explanation for the variation in the test 6 results was evident. Also, test 9, which was identical to test 6, had both repeats similar to test 6a and test 6c. The results from test 6 were not used in the final data analysis due to the measurement variation and because test 9 was a duplicate of test 6.

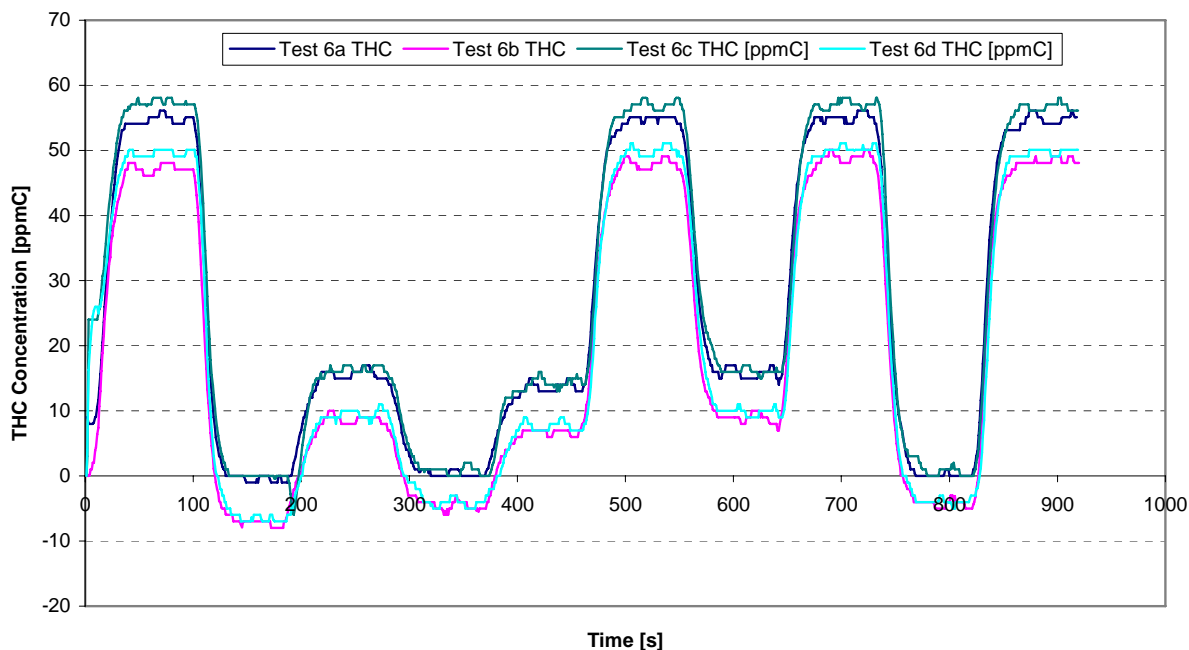


FIGURE 196. THC MEASUREMENTS FOR TEST 6 OF THE AMBIENT HYDROCARBON TEST SEQUENCE

5.8.1 Ambient Hydrocarbon Error Surface Generation

The 30-second mean zero air THC measurements were pooled from test 1, 2, 4, 8, and 9 of the Ambient Hydrocarbon test sequence. The THC measurements were multiplied by 0.98 to generate NMHC zero measurement errors. As discussed previously, Hexane had little effect on the PEMS THC measurement due to the use of a charcoal filter. Therefore, the PEMS THC measurement errors were driven by the Methane contamination in the FID burner air. Shown in Figure 197, the pooled PEMS NMHC errors generated a nearly linear relationship with respect to the FID air Methane contamination concentration.

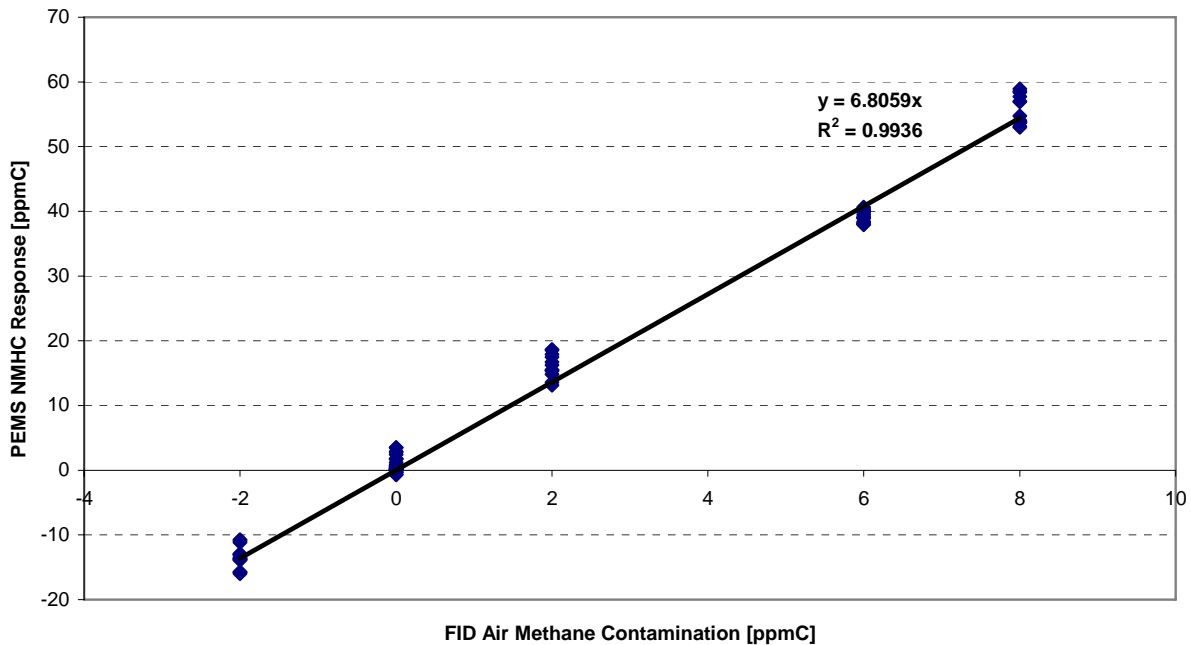


FIGURE 197. PEMS 3 NMHC RESPONSE VERSUS FID AIR METHANE CONTAMINATION MEASURED DURING AMBIENT HYDROCARBON TESTING

The linear relationship between the PEMS NMHC zero measurement error and the FID air Methane contamination concentration was used to calculate the 5th and 95th percentile values for the Ambient Hydrocarbon error surface. With the calculated NMHC response to ambient Methane, the only task remaining was to determine appropriate 5th and 95th percentile values for the real world ambient Methane levels. A great deal of deliberation was exercised by the Steering Committee to determine appropriate levels of variation for ambient Methane. As written in the test plan, Methane levels recorded by CE-CERT during the on-road validation were used as a reference. During CE-CERT’s testing, the maximum change in Methane concentration was 1.8 ppmC. However, the objective of the Ambient Hydrocarbon test was to capture the worst case Methane variation. Therefore, CE-CERT’s Methane data could only be used the minimum Methane variation. Historical Methane data was then examined from EPA, SwRI and engine manufacturer test labs. The difference between the 5th and 95th percentile values for each lab was considered the worst case Methane variation. Using the pool of Methane data, the Steering Committee ultimately agreed to use a Methane variation of 2.2 ppmC.

With no justification to bias the error surface, the 5th percentile Methane concentration was set to -1.1 ppmC, while the 95th percentile Methane concentration was set to 1.1 ppmC. Using the linear relationship between the PEMS NMHC response and ambient Methane variation, the 5th and 95th percentile Methane concentrations were used to calculate the 5th and 95th percentile PEMS NMHC deltas for the final Ambient Hydrocarbon error surface. Shown in Figure 198, the 5th and 95th percentile NMHC deltas were -7.5 and 7.5 ppmC respectively. The Ambient Hydrocarbon error surface was sampled normally and applied to each reference NTE event NMHC concentration regardless of level.

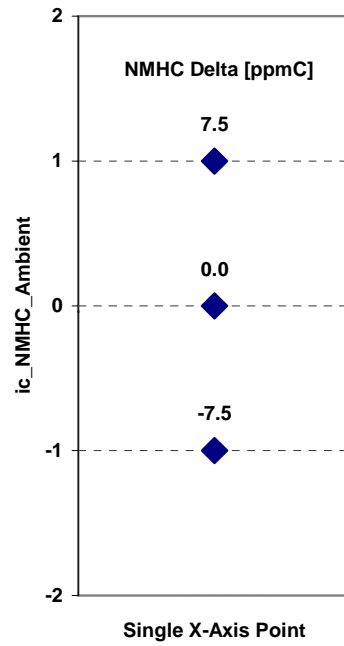


FIGURE 198. ERROR SURFACE FOR AMBIENT HYDROCARBON TESTING

6.0 MODEL RESULTS AND VALIDATION

6.1 Model Results

The objective of this section is to present the results from the Monte Carlo simulation runs, the post-processing computations of the measurement allowances, and the model validation analyses. Useful background information is contained in Section 2.0 of this report where the Monte Carlo error model is described along with the techniques and methods used in the model simulation runs and the validation process. A total of 10,000 to 30,000 simulation trials (with four NTE events running to 50,000 trials) were run for each of the reference 195 NTE events, and approximately four million simulation trials were run for all the combination of settings for these 195 reference events.

6.2 Results of Drift Correction

This section contains a summary of the number and percent of the simulation trials that were deleted due to periodic drift. Section 2.1.5 on *Periodic Drift Check* contains a detailed description and a flowchart of the procedure used to check whether or not a periodic drift invalidated any of the reference NTE event trials. This procedure was applied to the simulation data obtained for each of the three emissions for each of the three calculation methods.

No periodic drift was detected for the BSCO emissions for any of the three calculation methods. Thus, no simulation trials were deleted in any of the drift correction checks for BSCO for all 195 reference NTE events. However, for BSNO_x and BSNMHC, periodic drift was detected.

Figure 199 through Figure 201 display relative frequency (in percent) histograms for the percent of simulation trials for BSNO_x, using each of the three calculation methods, that were deleted for each of the 195 reference NTE events due to periodic drift. A summary of the results is given in Table 88. For the three calculation methods, the average percent of the simulation trials that was deleted across the 195 reference NTE events ranged from 2.09% for Method 2 to 3.45% for Method 1. The maximum percent that was deleted ranged from 11.27% for Method 2 to 15.41% for Method 1.

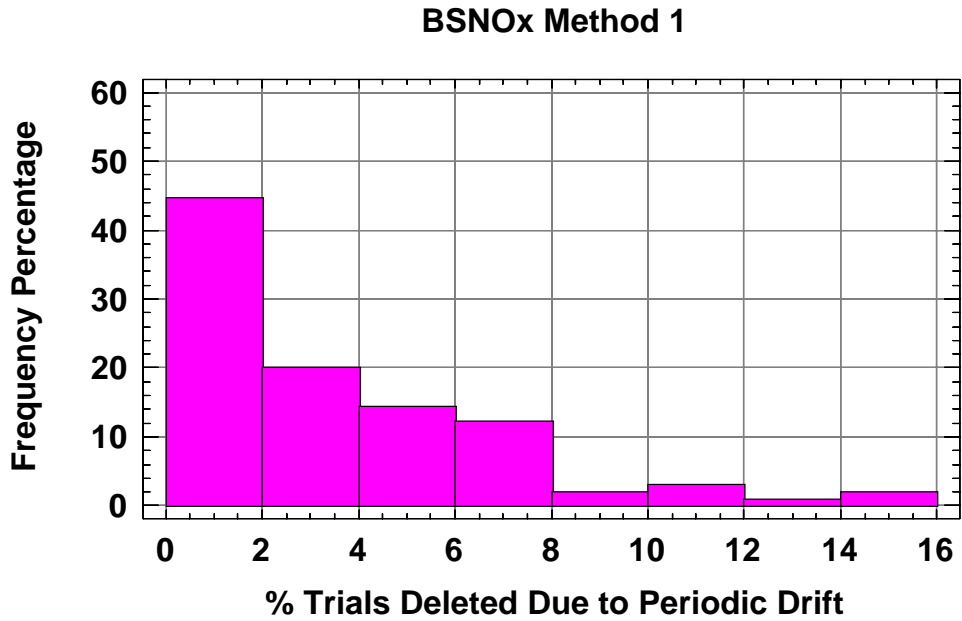


FIGURE 199. PERCENT OF TRIALS DELETED FOR EACH REFERENCE NTE EVENT DUE TO PERIODIC DRIFT CHECK FOR BSNO_x METHOD 1

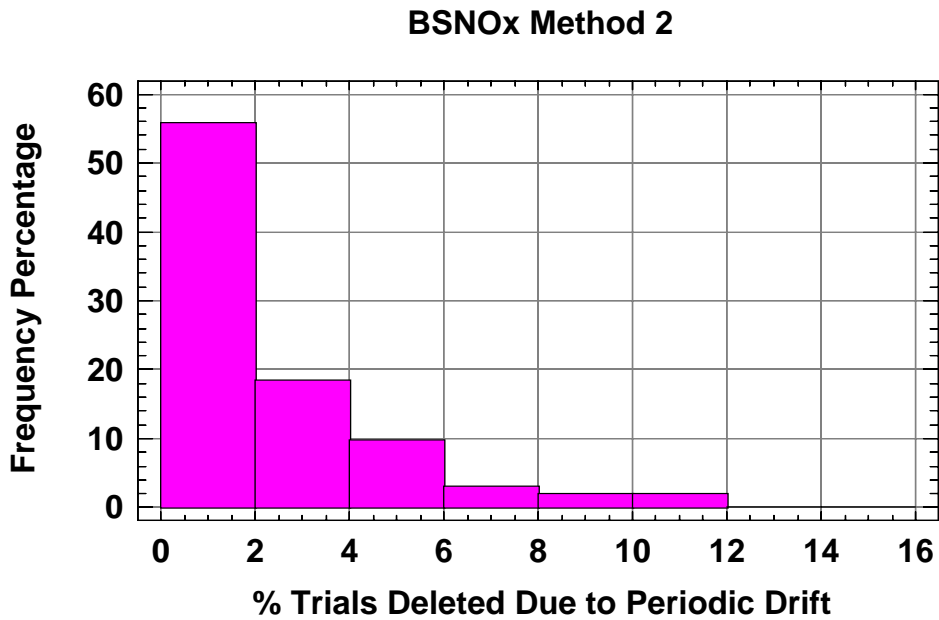


FIGURE 200. PERCENT OF TRIALS DELETED FOR EACH REFERENCE NTE EVENT DUE TO PERIODIC DRIFT CHECK FOR BSNO_x METHOD 2

BSNO_x Method 3

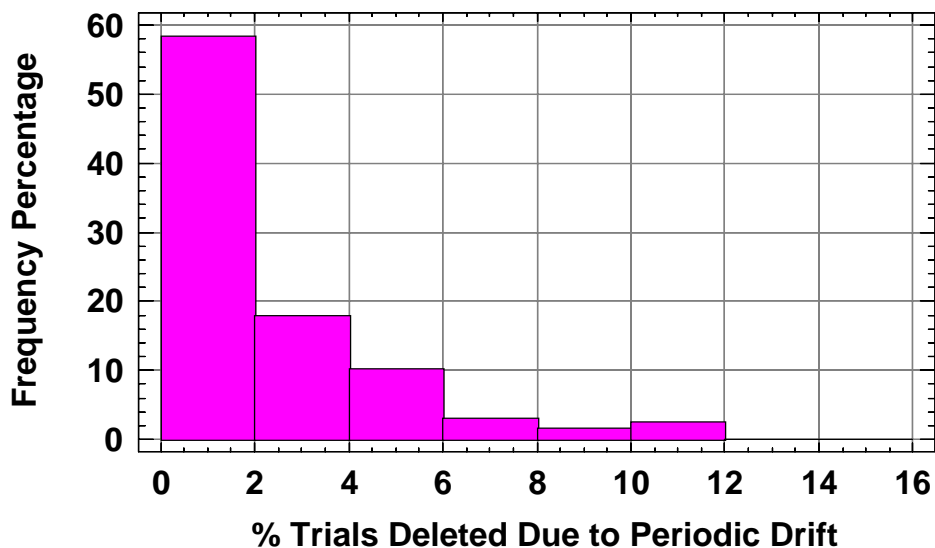


FIGURE 201. PERCENT OF TRIALS DELETED FOR EACH REFERENCE NTE EVENT DUE TO PERIODIC DRIFT CHECK FOR BSNO_x METHOD 3

TABLE 88. SUMMARY OF THE TRIALS DELETED DUE TO PERIODIC DRIFT CHECK FOR BSNO_x

Method	# Reference NTE Events	Mean %	Min %	Max %
1	195	3.45	0	15.41
2	195	2.09	0	11.27
3	195	2.11	0	11.32

Figure 202 through Figure 204 display relative frequency (in percent) histograms for the percent of simulation trials for BSNMHC, using each of the three calculation methods, that were deleted for each of the 195 reference NTE events due to periodic drift. A summary of the results is given in Table 89. For the three calculation methods, the average percent of the simulation trials that was deleted across the 195 reference NTE events ranged from 1.89% for Method 2 to 4.01% for Method 1. The maximum percent that was deleted ranged from 14.33% for Method 2 to 21.21% for Method 1.

BSNMHC Method 1

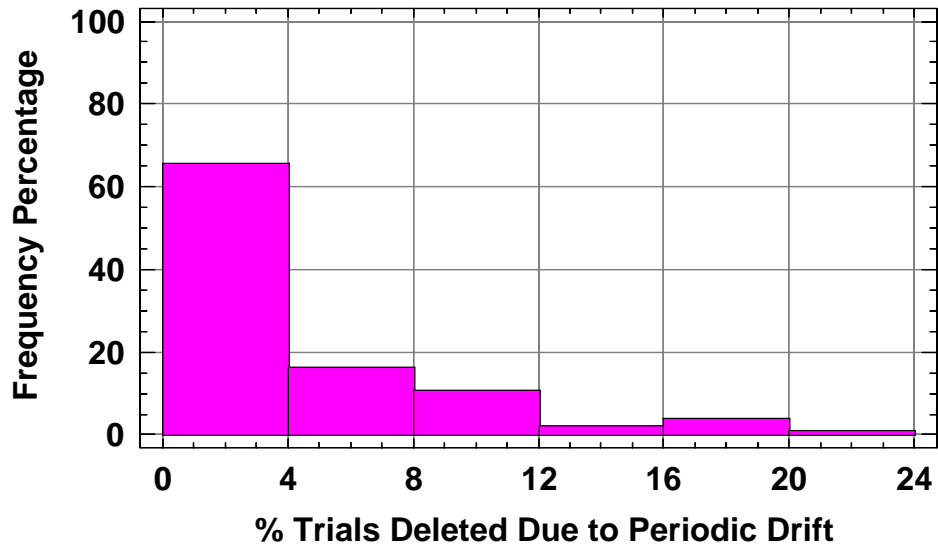


FIGURE 202. PERCENT OF TRIALS DELETED FOR EACH REFERENCE NTE EVENT DUE TO PERIODIC DRIFT CHECK FOR BSNMHC METHOD 1

BSNMHC Method 2

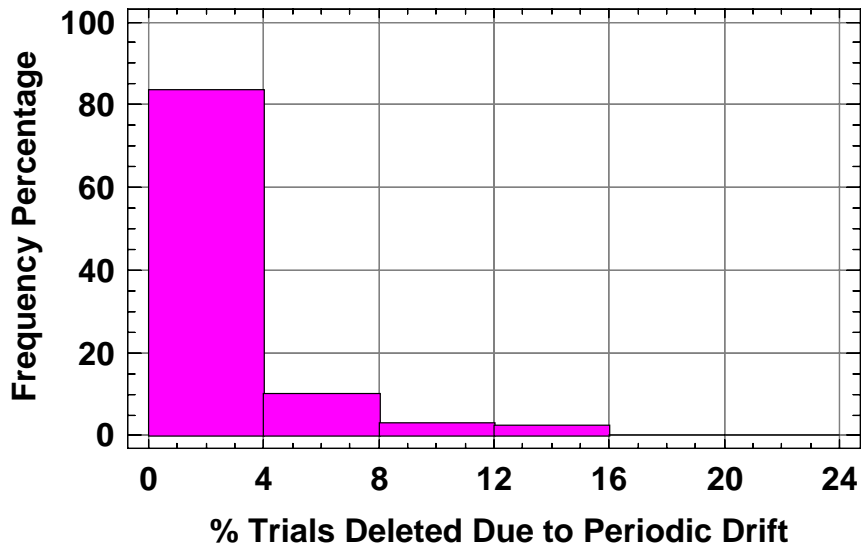


FIGURE 203. PERCENT OF TRIALS DELETED FOR EACH REFERENCE NTE EVENT DUE TO PERIODIC DRIFT CHECK FOR BSNMHC METHOD 2

BSNMHC Method 3

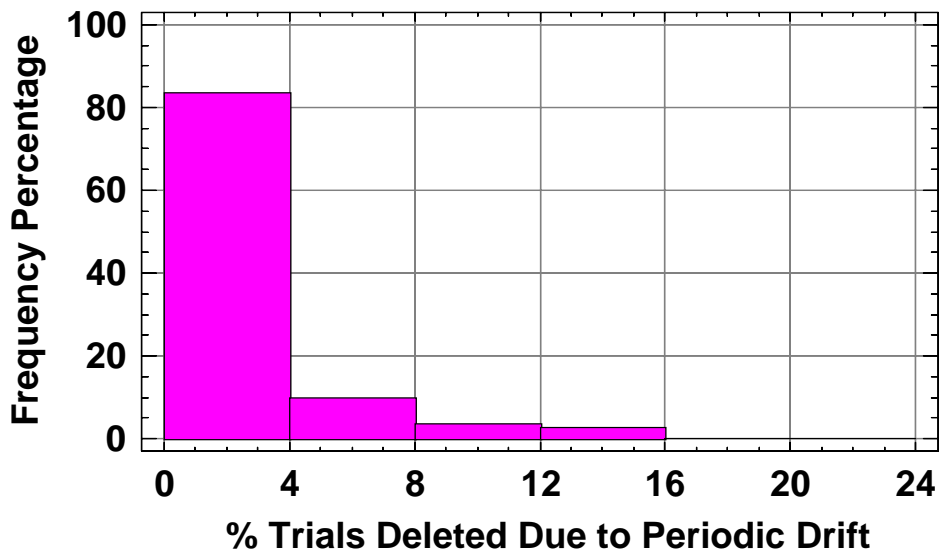


FIGURE 204. PERCENT OF TRIALS DELETED FOR EACH REFERENCE NTE EVENT DUE TO PERIODIC DRIFT CHECK FOR BSNMHC METHOD 3

TABLE 89. SUMMARY OF TRIALS DELETED FOR EACH REFERENCE NTE EVENT DUE TO PERIODIC DRIFT CHECK FOR BSNMHC METHOD 3

Method	#Ref NTE Events	Mean %	Min %	Max %
1	195	4.01	0.05	21.21
2	195	1.89	0.00	14.33
3	195	1.93	0.00	14.35

6.3 Convergence Results from MC Runs

This section contains a summary of the checks to determine if the convergence criteria were met for the simulation runs. Section 2.1.7 on *Convergence and Number of Trials* contains a detailed description of the convergence methodology and the procedures followed to check for convergence for the reference NTE event trials. This procedure was applied to the simulation data obtained for each of the three emissions and all three calculation methods.

Figure 205 through Figure 207 contain relative frequency (in percent) histograms for the widths of the 90% confidence intervals for the 95th percentiles of the corresponding BSNO_x differences for the 195 individual reference NTE events where the confidence interval widths are expressed as a percent of the BSNO_x emissions NTE threshold. This is done for each of the three calculation methods. A summary of the results is given in Table 90. Of interest was whether or

not the simulations converged within 1% of the threshold value. For the three calculation methods, the maximum percent of the confidence interval widths that were within 1% of the threshold value across the 195 reference NTE events ranged from 0.481% for Method 2 to 0.984% for Method 1. Thus, all 195 reference events met the convergence criteria.

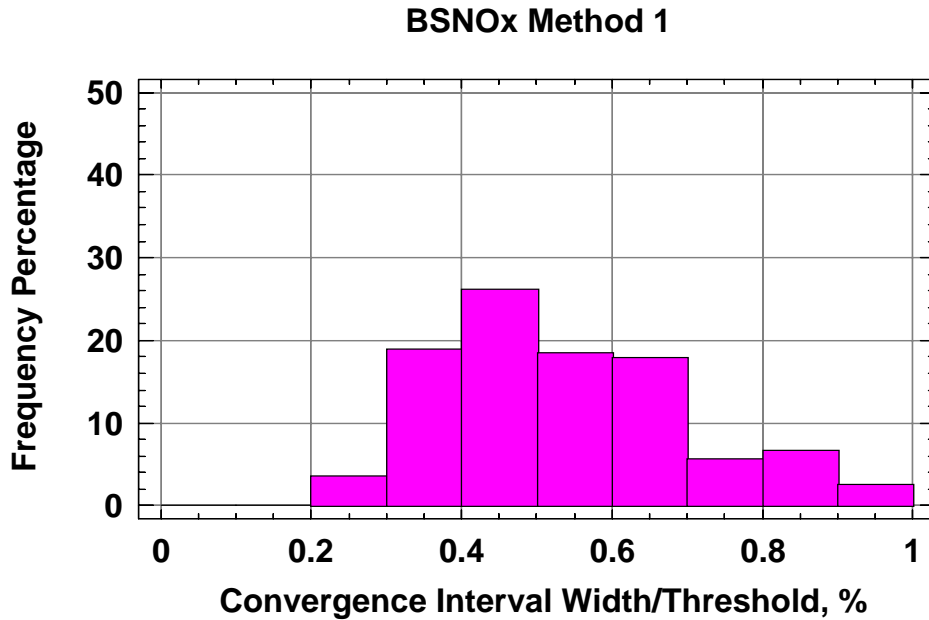


FIGURE 205. CONVERGENCE INTERVAL WIDTH AS A PERCENT OF THRESHOLD FOR BSNO_x METHOD 1

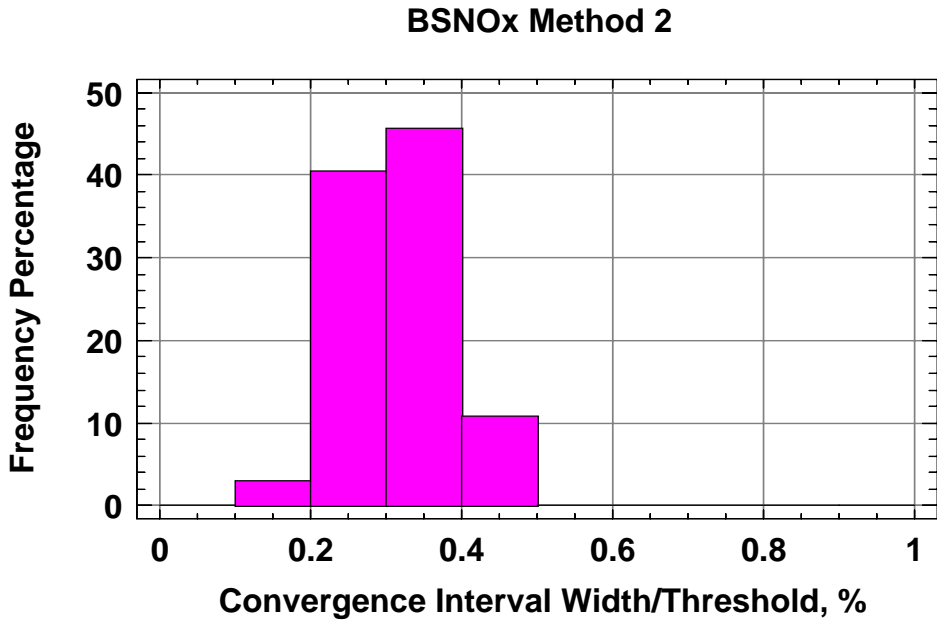


FIGURE 206. CONVERGENCE INTERVAL WIDTH AS A PERCENT OF THRESHOLD FOR BSNO_x METHOD 2

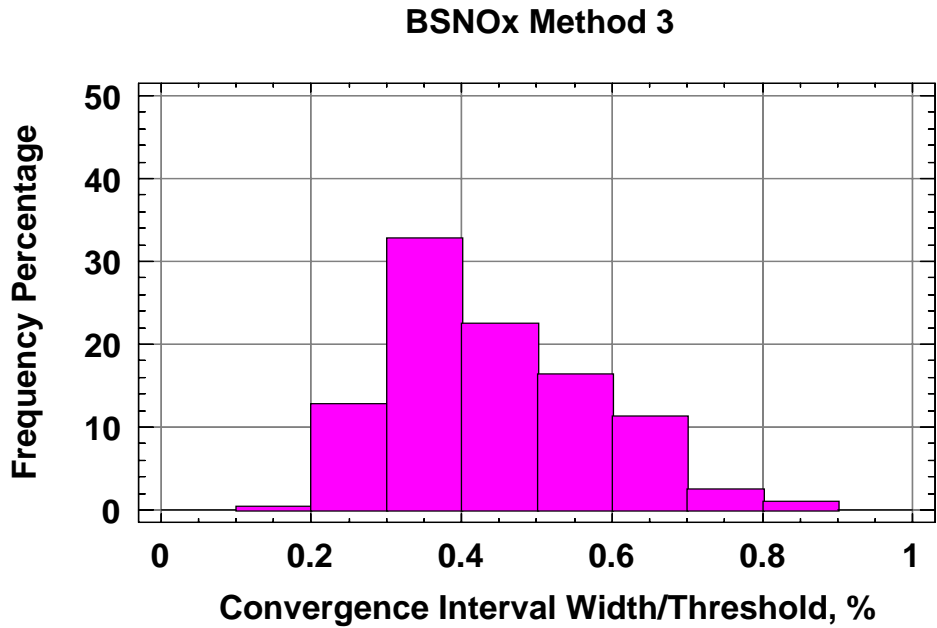


FIGURE 207. CONVERGENCE INTERVAL WIDTH AS A PERCENT OF THRESHOLD FOR BSNO_x METHOD 3

TABLE 90. SUMMARY OF BSNO_x CONVERGENCE INTERVAL WIDTH AS A FUNCTION OF THRESHOLD FOR 195 REFERENCE NTE EVENTS

Method	# Ref NTE Events	Mean %	Min %	Max %
1	195	0.534	0.236	0.984
2	195	0.313	0.157	0.481
3	195	0.444	0.190	0.889

Figure 208 through Figure 210 contain relative frequency (in percent) histograms for the widths of the 90% confidence intervals for the 95th percentiles of the corresponding BSNMHC differences for the 195 individual reference NTE events where the confidence interval widths are expressed as a percent of the BSNMHC emissions NTE threshold. This is done for each of the three calculation methods. A summary of the results is given in Table 91. Of interest was whether or not the simulations converged within 1% of the threshold value. For the three calculation methods, the maximum percent of the confidence interval widths that were within 1% of the threshold value across the 195 NTE events ranged from 0.429% for Method 2 to 0.604% for Method 1. Thus, all 195 events met the convergence criteria.

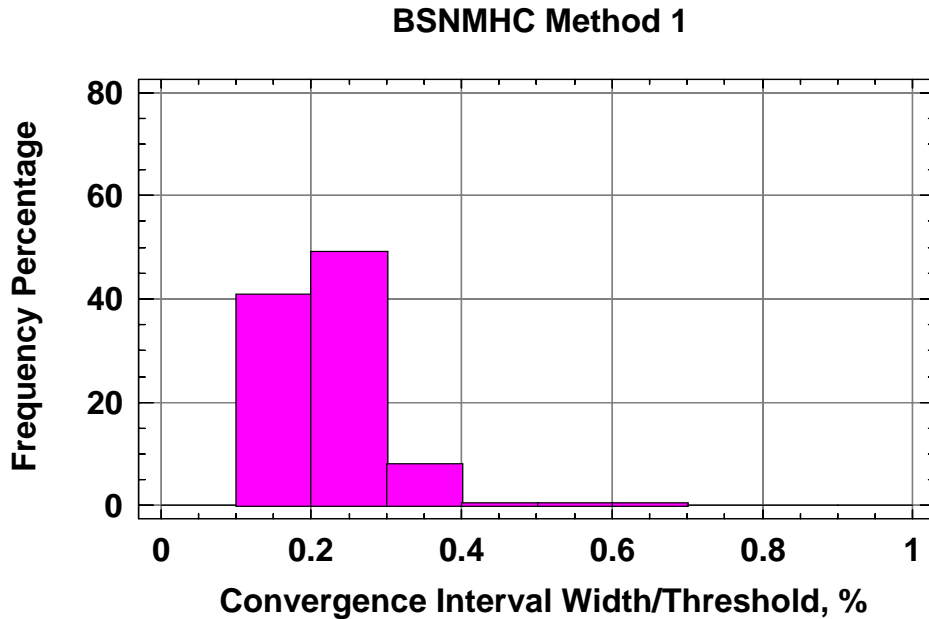


FIGURE 208. CONVERGENCE INTERVAL WIDTH AS A PERCENT OF THRESHOLD FOR BSNMHC METHOD 1

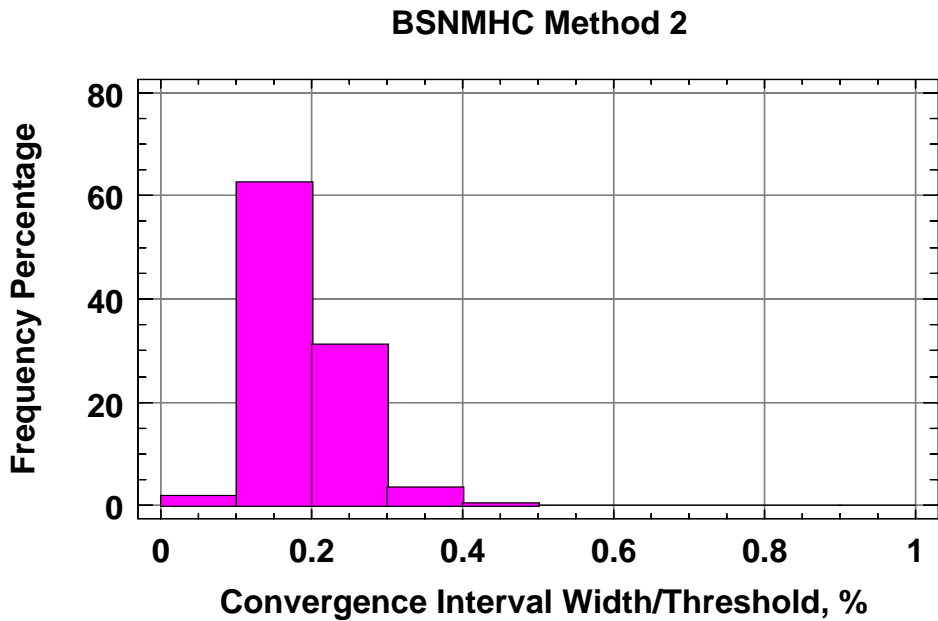


FIGURE 209. CONVERGENCE INTERVAL WIDTH AS A PERCENT OF THRESHOLD FOR BSNMHC METHOD 1

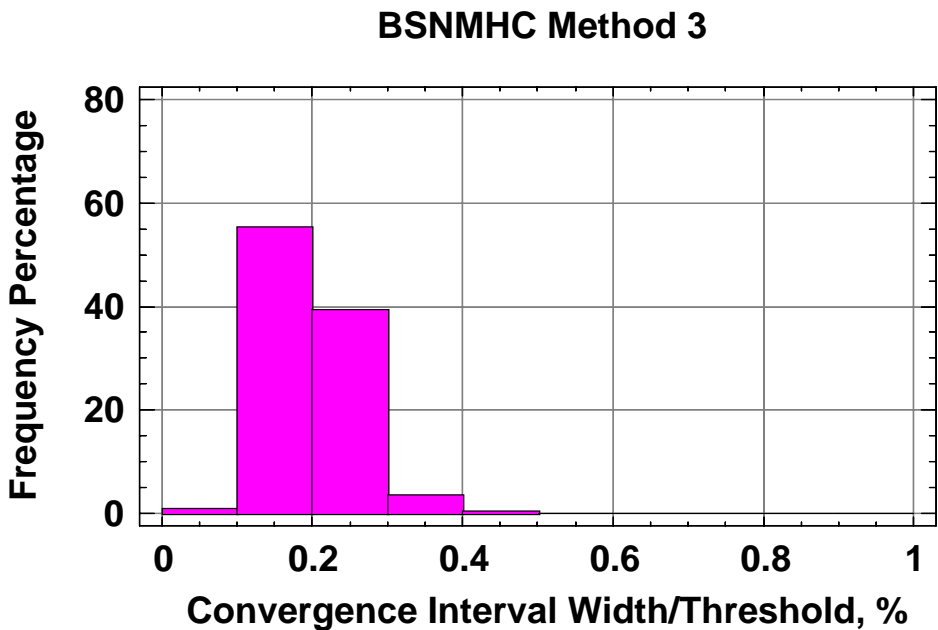


FIGURE 210. CONVERGENCE INTERVAL WIDTH AS A PERCENT OF THRESHOLD FOR BSNMHC METHOD 3

TABLE 91. SUMMARY OF BSNMHC CONVERGENCE INTERVAL WIDTH AS A FUNCTION OF THRESHOLD FOR 195 REFERENCE NTE EVENTS

Method	# Ref NTE Events	Mean %	Min %	Max %
1	195	0.222	0.113	0.604
2	195	0.188	0.090	0.429
3	195	0.197	0.005	0.480

Figure 211 through Figure 213 contain relative frequency (in percent) histograms for the widths of the 90% confidence intervals for the 95th percentiles of the corresponding BSCO differences for the 195 individual reference NTE events where the confidence interval widths are expressed as a percent of the BSCO emissions NTE threshold. This is done for each of the three calculation methods. A summary of the results is given in Table 92. Of interest was whether or not the simulations converged within 1% of the threshold value. For the three calculation methods, the maximum percent of the confidence interval widths that were within 1% of the threshold value across the 195 NTE events ranged from 0.076% for Method 2 to 0.202% for Method 3. Thus, all 195 events met the convergence criteria.

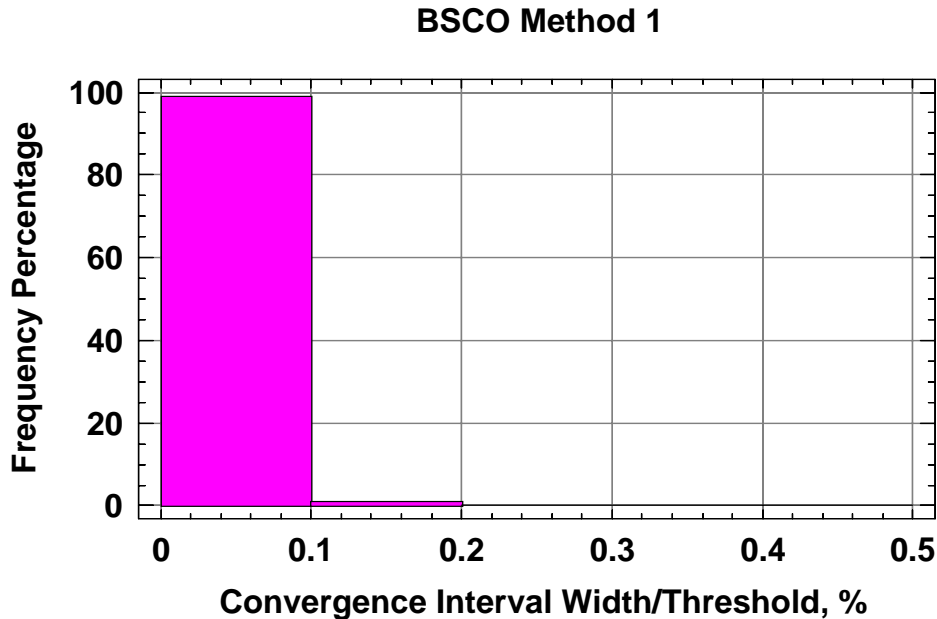


FIGURE 211. CONVERGENCE INTERVAL WIDTH AS A PERCENT OF THRESHOLD FOR BSCO METHOD 1

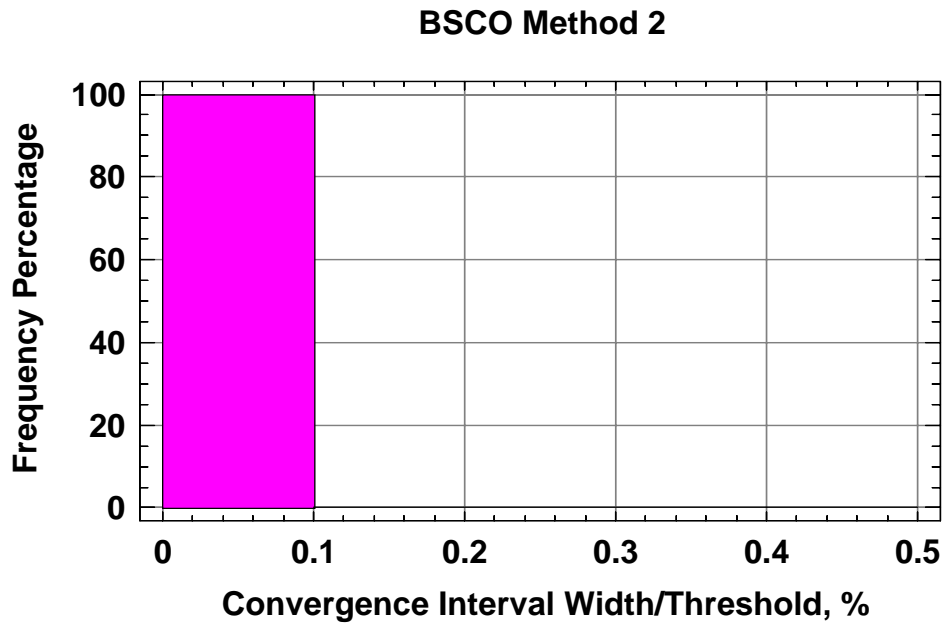


FIGURE 212. CONVERGENCE INTERVAL WIDTH AS A PERCENT OF THRESHOLD FOR BSCO METHOD 2

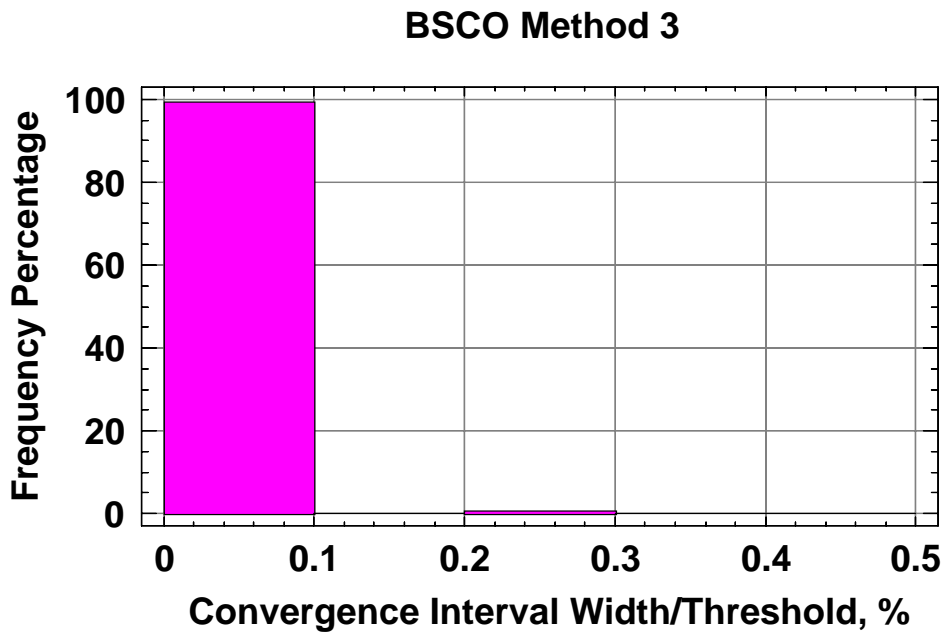


FIGURE 213. CONVERGENCE INTERVAL WIDTH AS A PERCENT OF THRESHOLD FOR BSCO METHOD 3

TABLE 92. SUMMARY OF BSCO CONVERGENCE INTERVAL WIDTH AS A FUNCTION OF THRESHOLD FOR 195 REFERENCE NTE EVENTS

Method	# Ref NTE Events	Mean %	Min %	Max %
1	195	0.034	0.013	0.102
2	195	0.025	0.009	0.076
3	195	0.032	0.013	0.202

6.4 Delta BS Emissions Plots for 95th Percentiles

This section contains plots of the 95th percentile delta emissions values obtained by simulation for each reference NTE event distribution of BS differences for each emissions for all three calculation methods. Section 2.1.8 on *Simulation Output* contains more details on the simulation output and the methodology used to compute the delta values.

Figure 214 through Figure 216 display box plots of the 95th percentile delta emissions for all three methods. The ends of the boxes mark the location of the 25th and 75th percentiles of the delta emissions while the horizontal line inside the box indicates the location of the median, or 50th percentile, of the data. The plus sign inside the box denotes the location of the mean of the data. The two vertical lines (i.e., whiskers) extending above and below the box denote the distance to the farthest observation that does not exceed the endpoint $\pm 1.5 \times (\text{height of the box})$. Observations outside these vertical lines are individually noted on the graph as square symbols.

Viewing Figure 214, it can be observed that the 95th percentile delta BSNO_x values based on Method 1 had larger values and more spread in the data than did the corresponding values computed using Methods 2 and 3. Further, the delta values based on Method 2 had the smallest variation and the lowest values of all three methods.

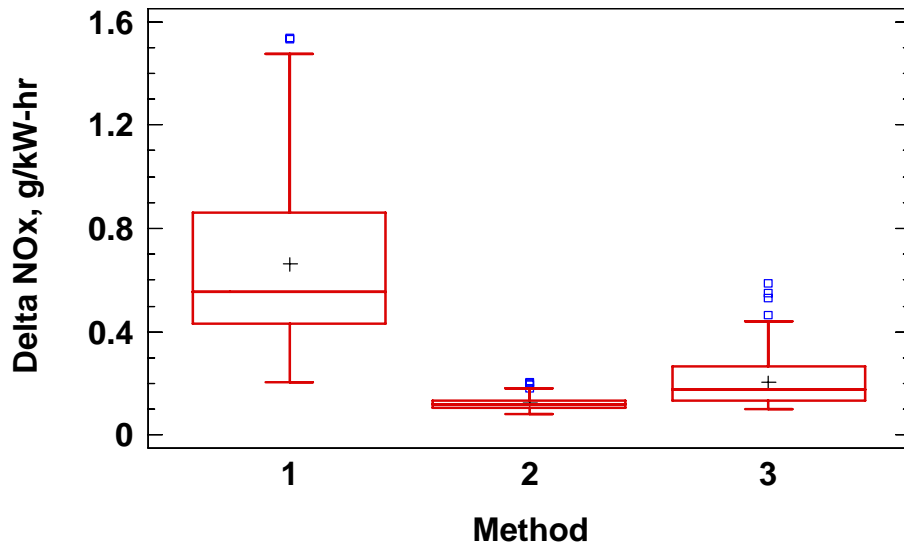


FIGURE 214. BOX PLOT OF 95TH PERCENTILE DELTA BSNO_x FOR THREE METHODS FROM 195 REFERENCE NTE EVENTS

Viewing Figure 215, the 95th percentile delta BSNMHC values are not as different for the three methods as the delta BSNO_x values. The delta values based on Method 1 are slightly higher than similar values based on the other two methods, and the data is more skewed to the right than the data for the other two methods. Again, the delta values based on Method 2 had the lowest values of all three methods.

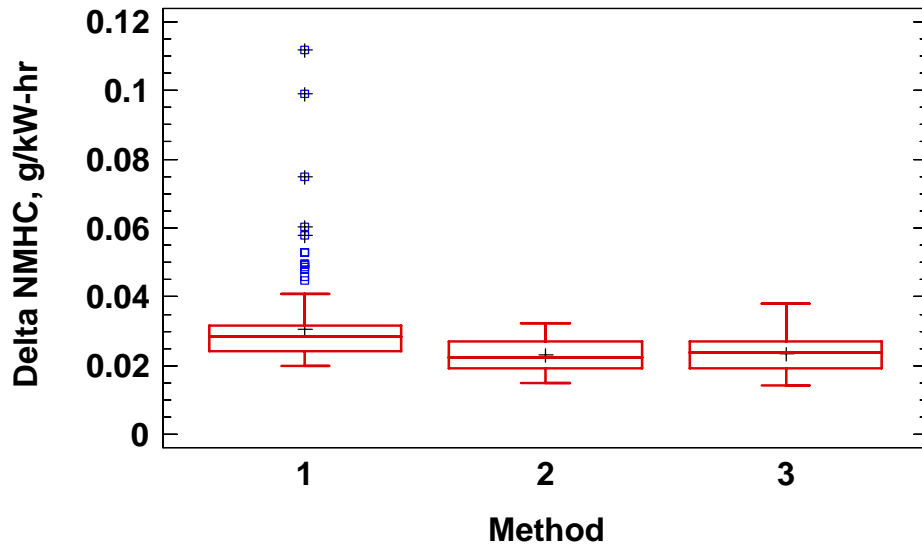


FIGURE 215. BOX PLOT FOR 95TH PERCENTILE DELTA BSCO FOR THREE METHODS FROM 195 REFERENCE NTE EVENTS

Viewing Figure 216, the 95th percentile delta BSCO values are similar in spread to the data for the delta BSNMHC values. The delta values based on Method 1 are again slightly higher than similar values based on the other two methods, and the data is more skewed to the right than the data for the other two methods. The delta values based on Method 2 had the lowest values of all three methods, and there is some skewness to the right for the data based on all three methods.

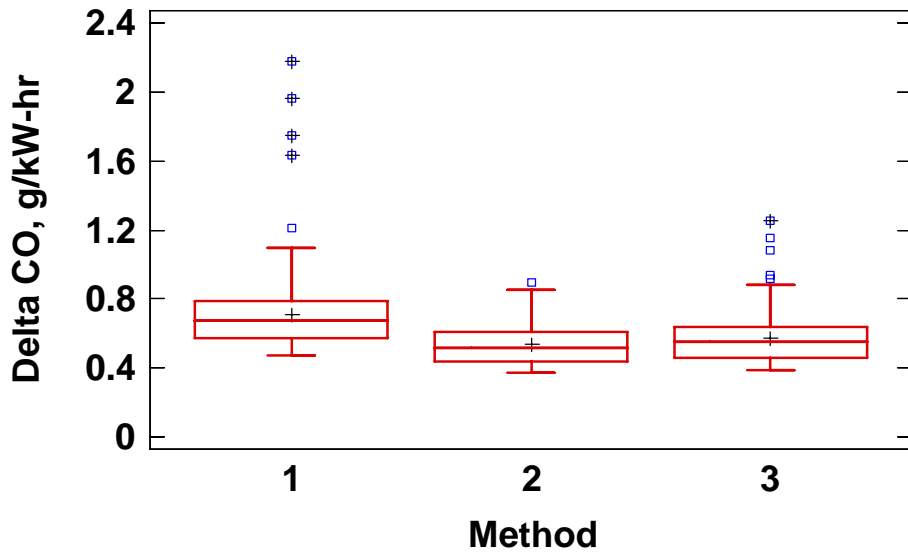


FIGURE 216. BOX PLOT FOR 95TH PERCENTILE DELTA BSCO FOR THREE METHODS FOR 195 REFERENCE NTE EVENTS

An alternative way to compare the 95th percentile deltas across the three calculation methods is to plot the deltas for the same reference NTE event on a scatter plot, as illustrated in Figure 217 through Figure 219. As seen in Figure 217, the ideal BSNO_x for each reference NTE event is plotted against its 95th percentile deltas for calculation methods 1, 2, and 3. This plot depicts the large range in 95th percentile deltas for Method 1 as compared to Methods 2 and 3. Similar inferences can be made for BSNMHC (Figure 218) and BSCO (Figure 219).

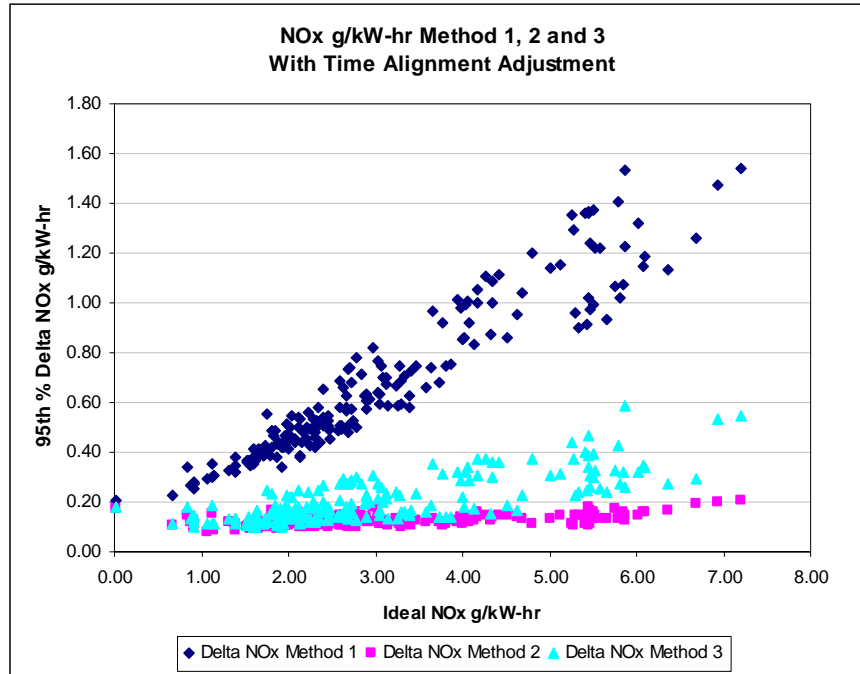


FIGURE 217. COMPARISON OF 95TH PERCENTILE DELTA BSNO_x FOR METHODS 1, 2, AND 3 FOR 195 REFERENCE NTE EVENTS

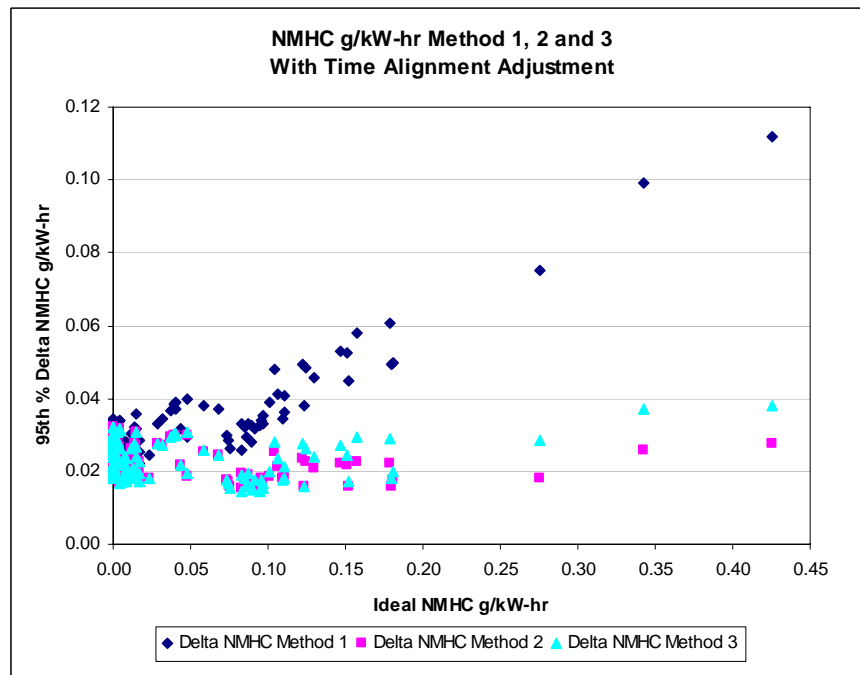


FIGURE 218. COMPARISON OF 95TH PERCENTILE DELTA BSNMHC FOR METHODS 1, 2, AND 3 FROM 195 REFERENCE NTE EVENTS

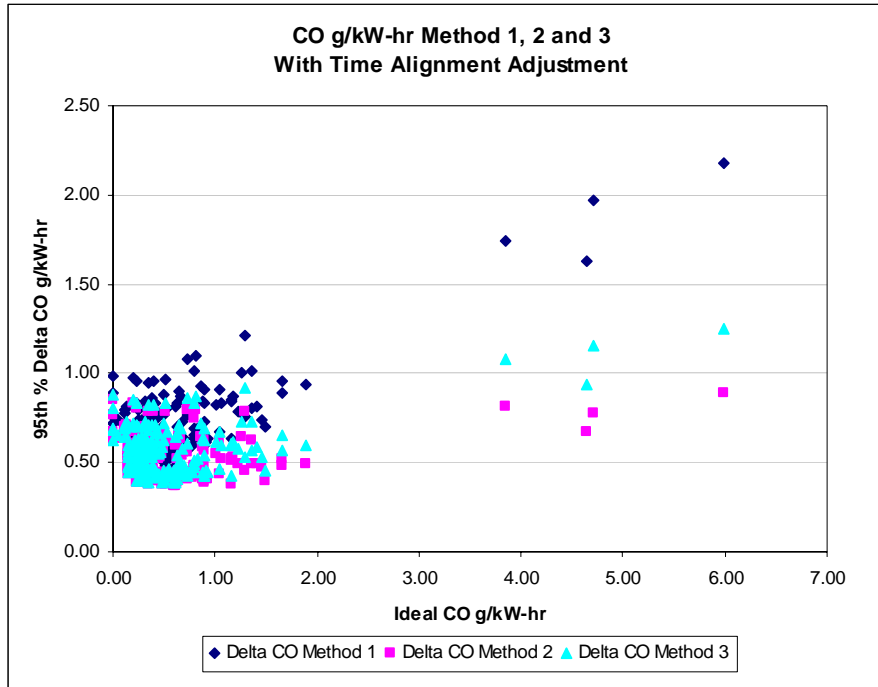


FIGURE 219. COMPARISON OF 95TH PERCENTILE DELTA BSCO FOR METHODS 1, 2, AND 3 FROM 195 REFERENCE NTE EVENTS

6.5 Sensitivity Based on Variance

This section contains a summary of the error surfaces that contributed the most to the variance of the generated BS emissions. During the MC simulation for each reference NTE event, sensitivity charts produced by Crystal Ball were generated and stored in the REPORT files. Crystal Ball calculates sensitivity by computing the rank correlation coefficient between every assumption (error surface) and forecast value (delta BS emissions) while the simulation is running. Positive rank correlations indicate that an increase in the assumption is associated with an increase in the forecast. The larger the absolute value of the rank correlation the stronger the relationship.

Sensitivity charts in Crystal Ball provide a means by which the variance of the error surfaces affects the variance in the forecast values. Hence, the sensitivity charts developed during a MC simulation are displayed as “Contribution to Variance” charts which are calculated by squaring the rank correlation coefficients for all assumptions used in a particular forecast and then normalizing them to 100%. The assumption (error surface) with the highest contribution to variance (in absolute value of the percent) is listed first in the sensitivity chart.

Simulation results from all 195 reference NTE events produced sensitivity values for all three 95th percentile delta emissions by all three calculation methods. Table 93 through Table 101 summarize the error surfaces in which the contribution to the variance sensitivity value was at least 5% in magnitude compared to all the other error surfaces. Note that the number of error

surfaces whose sensitivity values were greater than 5% ranged from 3 to 6 for all three delta emissions and three calculation methods. Also note that while some error surfaces were sensitive for most of the 195 reference NTE events (e.g., 195 events for 1_NO_x_SS BSNO_x Method 2 in Table 94), others were sensitive for a small fraction of the reference NTE events (e.g., only 17 events for 2_NO_x_Transient for BSNO_x Method 2 in Table 94).

Table 93 through Table 95 list the sensitivity descriptive statistics for the delta BSNO_x emissions for Methods 1, 2 and 3, respectively. In the first column of these tables the error surfaces with at least a 5% contribution to variance are listed followed by the number of reference NTE events in which this occurred. The mean contribution-to-variance normalized percentage is also given along with the minimum and maximum values. For Methods 1 and 3, the largest mean normalized variance was from error surface #31, torque warm-up, followed closely by error surface #1, NO_x steady state. For Method 2, the largest mean normalized variance was from error surface #1, NO_x steady-state, followed by error surface #42 due to BSFC from the engine manufacturers' data.

TABLE 93. ERROR SURFACE SENSITIVITY TO VARIANCE FOR 195 REFERENCE NTE EVENTS FOR BSNO_x METHOD 1

Error Surface	# Ref NTE Events	Mean, %	Minimum, %	Maximum, %
1_NO _x SS	195	27.90	9.40	99.60
20_Exhaust Flow_SS	185	10.34	5.30	15.70
31_Torque Warm-up	193	-34.65	-61.40	-11.40
35_Torque Engine Manufacturers	192	-15.96	-25.40	-1.10

TABLE 94. ERROR SURFACE SENSITIVITY TO VARIANCE FOR 195 REFERENCE NTE EVENTS FOR BSNO_x METHOD 2

Error Surface	# Ref NTE Events	Mean, %	Minimum, %	Maximum, %
1_NO _x SS	195	47.23	29.30	99.70
2_NO _x Transient	17	5.26	5.00	5.70
37_BSFC DOE	93	6.48	5.00	9.80
38_BSFC Warm-up	182	10.29	5.10	15.20
41_BSFC Interpolation	56	5.42	5.00	6.40
42_BSFC Engine Manufacturers	193	24.43	5.20	38.20

TABLE 95. ERROR SURFACE SENSITIVITY TO VARIANCE FOR 195 REFERENCE NTE EVENTS FOR BSNO_x METHOD 3

Error Surface	# Ref NTE Events	Mean, %	Minimum, %	Maximum, %
1_NO _x SS	195	30.59	10.10	99.70
31_Torque Warm-up	194	-38.37	-65.80	-12.00
35_Torque Engine Manufacturers	193	-17.89	-29.50	-5.20

Table 96 through Table 98 list the sensitivity descriptive statistics for the delta BSNMHC emissions for Methods 1, 2 and 3, respectively. For all three methods, the largest mean normalized variance was from the error surface #19, NMHC ambient effect.

TABLE 96. ERROR SURFACE SENSITIVITY TO VARIANCE FOR 195 REFERENCE NTE EVENTS FOR BSNMHC METHOD 1

Error Surface	# Ref NTE Events	Mean, %	Minimum, %	Maximum, %
13_NMHC SS	134	6.01	5.00	9.60
19_NMHC Ambient	195	85.70	18.20	93.30
20_Exhaust Flow SS	14	7.63	5.10	10.30
31_Torque Warm-up	38	-16.78	-48.20	-5.20
35_Torque Engine Manufacturers	30	-8.48	-16.60	-5.00

TABLE 97. ERROR SURFACE SENSITIVITY TO VARIANCE FOR 195 REFERENCE NTE EVENTS FOR BSNMHC METHOD 2

Error Surface	# Ref NTE Events	Mean, %	Minimum, %	Maximum, %
13_NMHC SS	122	5.65	5.00	8.10
19_NMHC Ambient	195	89.34	40.90	93.50
37_BSFC DOE	1	5.00	5.00	5.00
38_BSFC Warm-up	7	7.84	5.40	10.90
42_BSFC Engine Manufacturers	30	9.86	5.00	27.90

TABLE 98. ERROR SURFACE SENSITIVITY TO VARIANCE FOR 195 REFERENCE NTE EVENTS FOR BSNMHC METHOD 3

Error Surface	# Ref NTE Events	Mean, %	Minimum, %	Maximum, %
13_NMHC SS	114	5.64	5.00	8.20
19_NMHC Ambient	195	86.98	22.30	93.30
31_Torque Warm-up	38	-16.97	-50.90	-5.00
35_Torque Engine Manufacturers	28	-8.86	-16.70	-5.10

Table 99 through Table 101 list the sensitivity descriptive statistics for the delta BSCO emissions for Methods 1, 2 and 3, respectively. For all three methods, the largest mean normalized variance was from the error surface #7, CO steady-state.

TABLE 99. ERROR SURFACE SENSITIVITY TO VARIANCE FOR 195 REFERENCE NTE EVENTS FOR BSCO METHOD 1

Error Surface	# Ref NTE Events	Mean, %	Minimum, %	Maximum, %
7_CO SS	195	76.20	9.30	96.30
20_Exhaust Flow SS	32	7.48	5.00	11.60
31_Torque Warm-up	122	-13.29	-44.60	-5.00
35_Torque Engine Manufacturers	63	-7.77	-17.60	-5.00
52_CO Time Alignment	56	7.40	5.00	15.80

TABLE 100. ERROR SURFACE SENSITIVITY TO VARIANCE FOR 195 REFERENCE NTE EVENTS FOR BSCO METHOD 2

Error Surface	# Ref NTE Events	Mean, %	Minimum, %	Maximum, %
7_CO SS	195	85.82	20.10	98.10
37_BSFC DOE	2	5.35	5.00	5.70
38_BSFC Warm-up	14	7.07	5.00	10.90
42_BSFC Engine Manufacturers	65	9.12	5.00	28.10
52_CO Time Alignment	41	8.61	5.00	21.70

**TABLE 101. ERROR SURFACE SENSITIVITY TO VARIANCE FOR 195
REFERENCE NTE EVENTS FOR BSCO METHOD 3**

Error Surface	# Ref NTE Events	Mean, %	Minimum, %	Maximum, %
7_CO SS	195	75.49	8.40	96.20
31_Torque Warm-up	120	-13.40	-43.20	-5.10
35_Torque Engine Manufacturers	62	-7.79	-16.40	-5.00
52_CO Time Alignment	97	11.29	5.00	29.40

The contribution to normalized variance sensitivities from Table 93 through Table 95 are illustrated pictorially as box plots in Figure 220 through Figure 222 for BSNO_x Methods 1, 2 and 3, respectively. Only the error surfaces with at least 65 of the 195 reference NTE events (1/3 of the events) are included as box plots. The mean normalized variance for each of the plotted error surfaces is noted by a “+” symbol in the boxes. The error surface with the largest mean normalized variance is plotted at the left of the chart. The error surface with the second largest mean normalized variance is plotted second from the left, and so on. Figure 221 and Figure 223 demonstrate the high sensitivity to the error surface #31, torque warm-up. Figure 222 as well as Figure 221 and Figure 223 illustrate the high sensitivity to the error surface #1, NO_x steady-state.

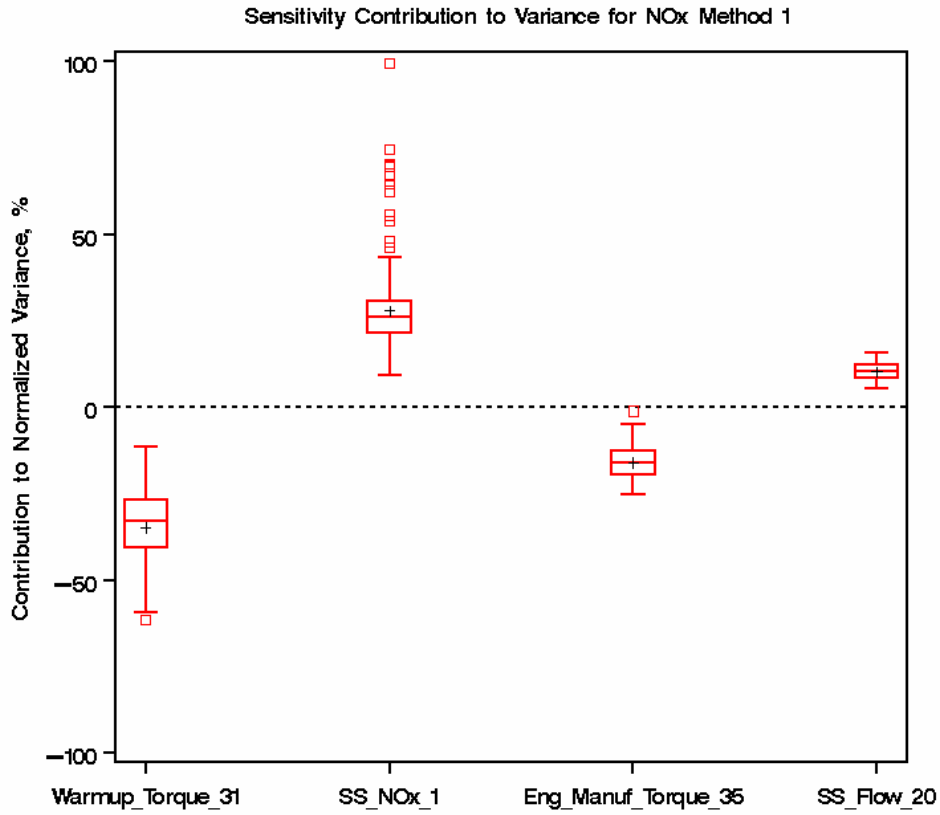


FIGURE 220. BOX PLOT OF ERROR SURFACE SENSITIVITY BASED ON VARIANCE FOR BSNO_x METHOD 1

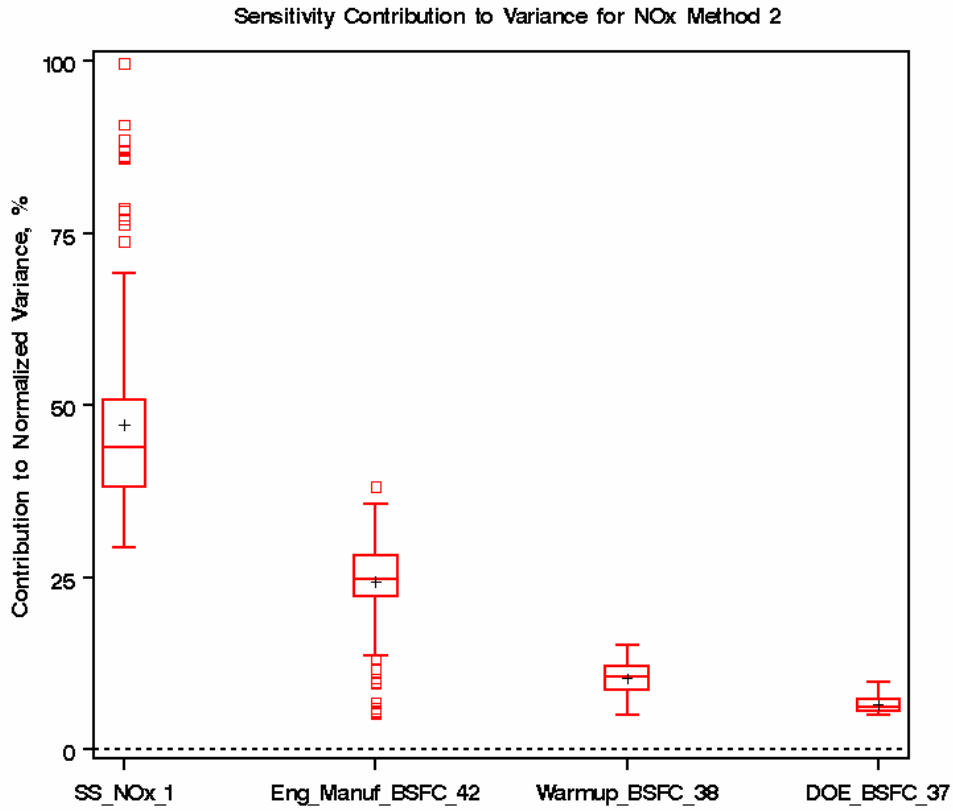


FIGURE 221. BOX PLOT OF ERROR SURFACE SENSITIVITY BASED ON VARIANCE FOR BSNO_x METHOD 2

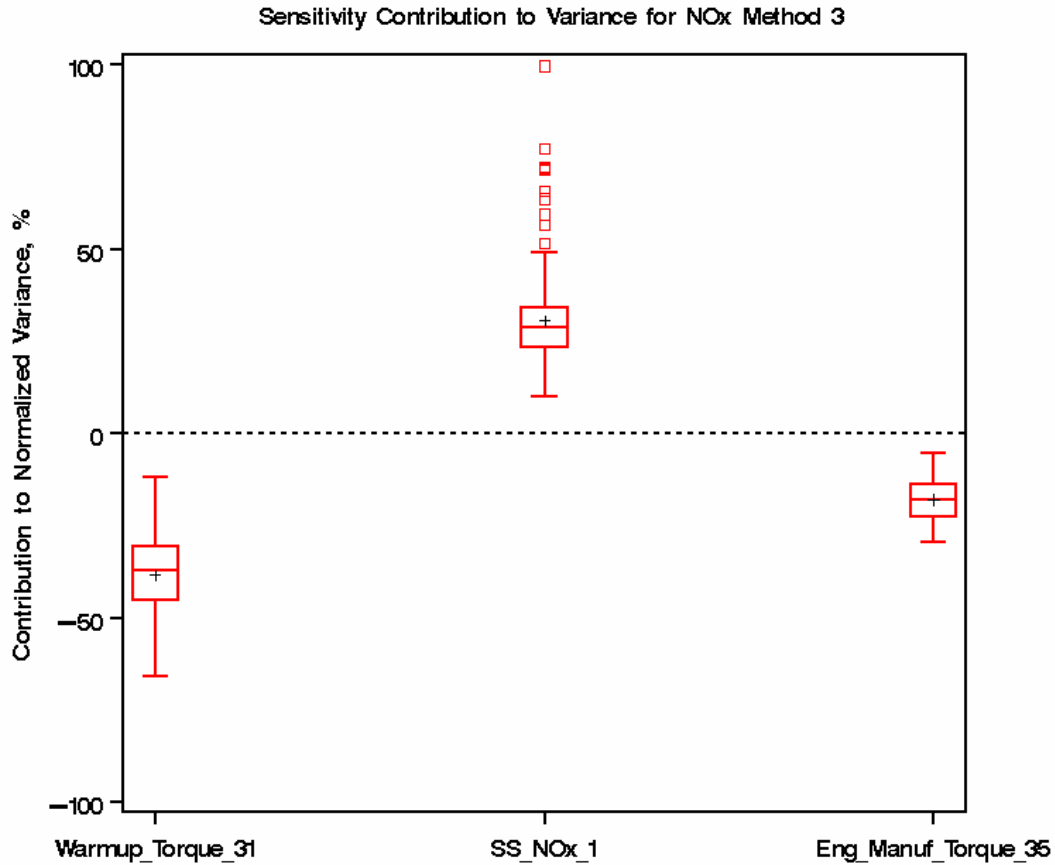


FIGURE 222. BOX PLOT OF ERROR SURFACE SENSITIVITY BASED ON VARIANCE FOR BSNO_x METHOD 3

The contribution to normalized variance sensitivities from Table 96 through Table 98 are illustrated pictorially as box plots in Figure 223 through Figure 225 for BSNMHC Methods 1,2 and 3, respectively. Each of these figures demonstrates the high sensitivity to the error surface #19, NMHC ambient effect.

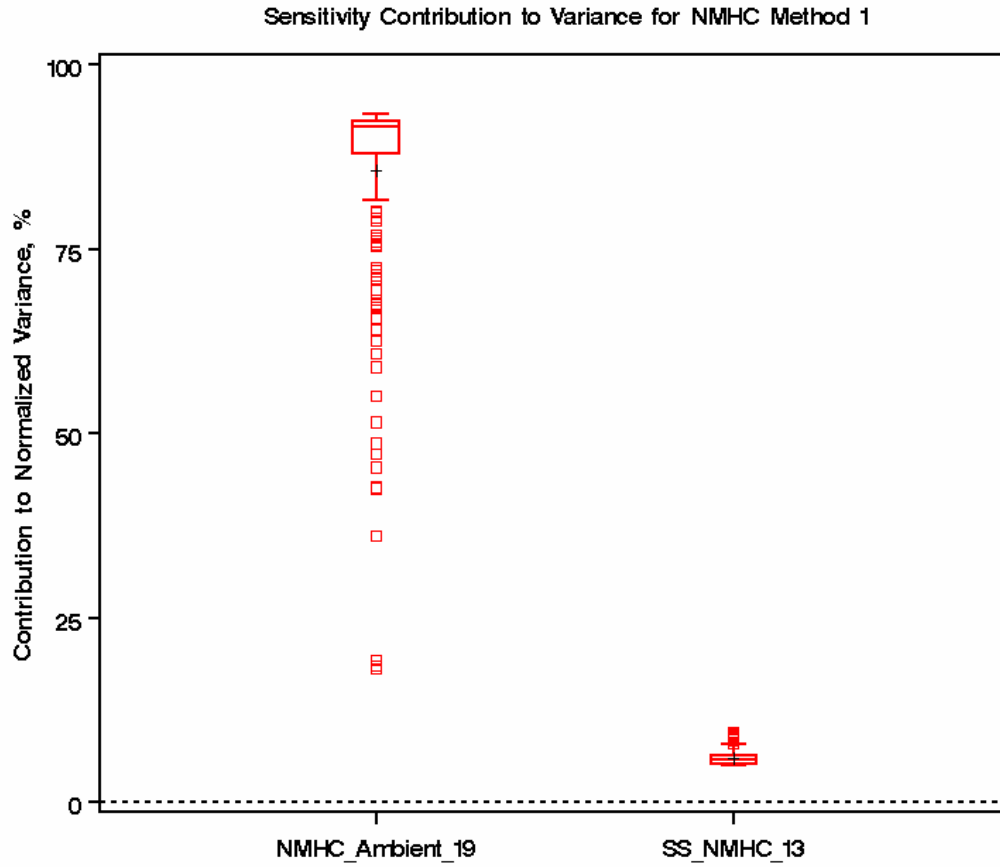


FIGURE 223. BOX PLOT OF ERROR SURFACE SENSITIVITY BASED ON VARIANCE FOR BSNMHC METHOD 1

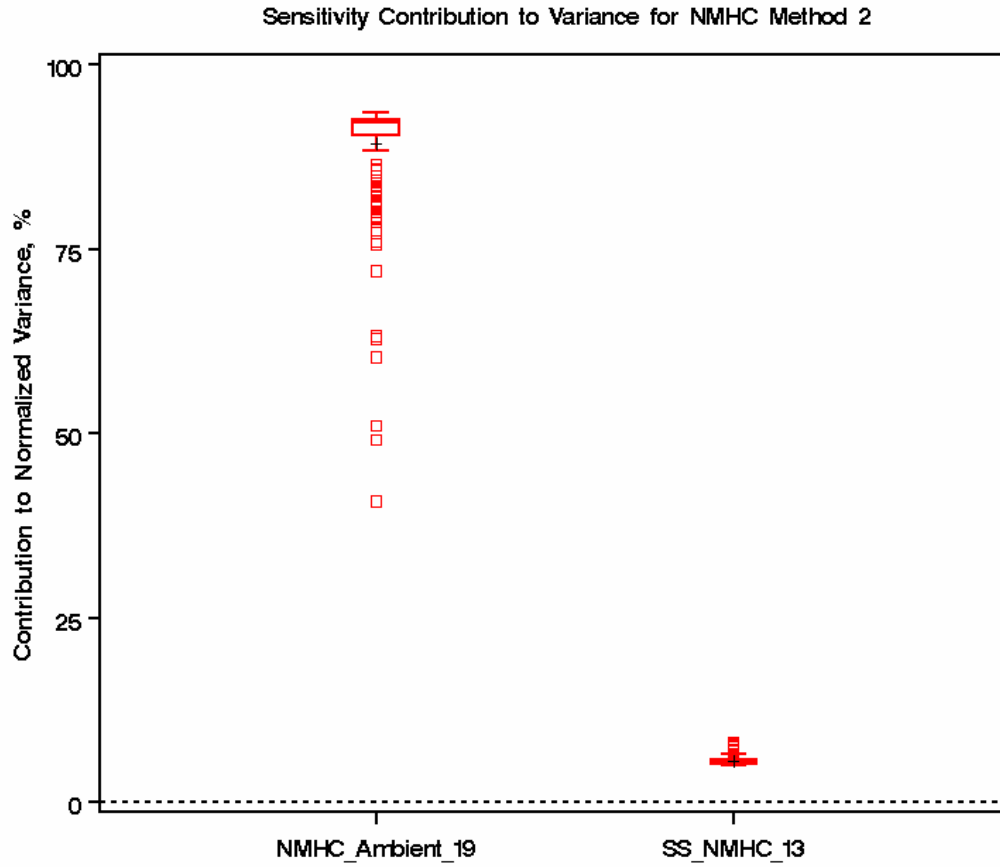


FIGURE 224. BOX PLOT OF ERROR SURFACE SENSITIVITY BASED ON VARIANCE FOR BSNMHC METHOD 2

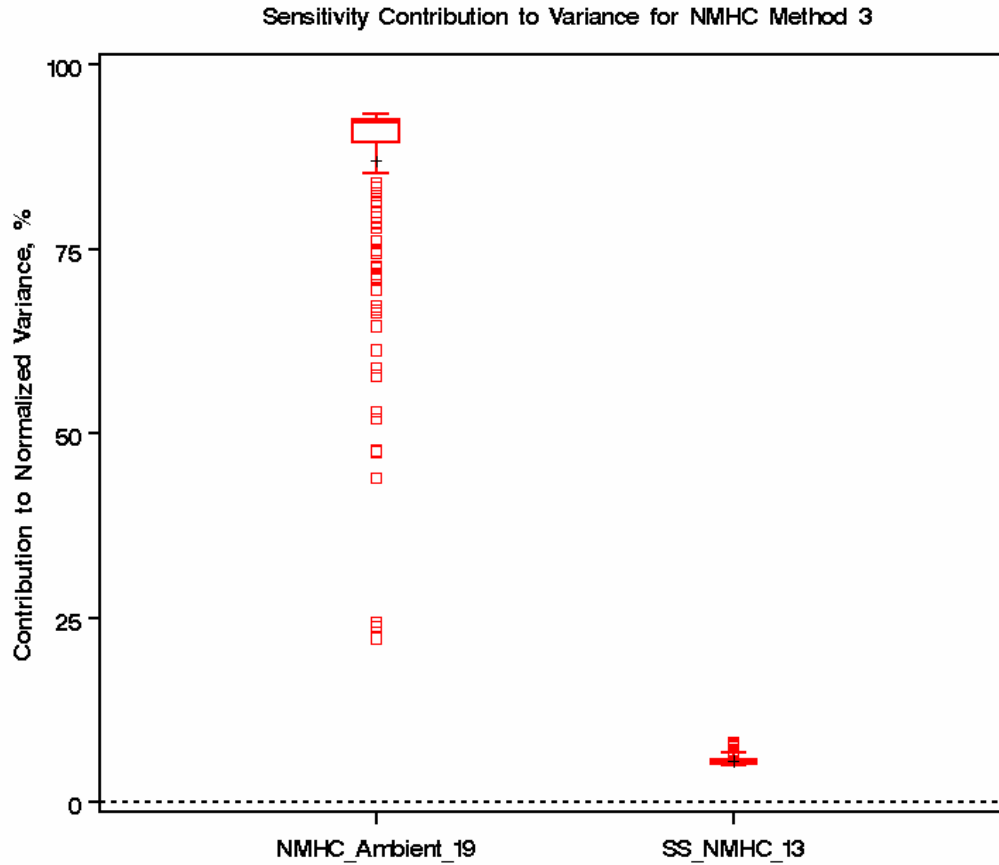


FIGURE 225. BOX PLOT OF ERROR SURFACE SENSITIVITY BASED ON VARIANCE FOR BSNMHC METHOD 3

The contribution to normalized variance sensitivities from Table 99 through Table 101 are illustrated pictorially as box plots in Figure 226 through Figure 228 for BSCO Methods 1,2 and 3, respectively. Each of these figures demonstrates the high sensitivity to error surface #7, CO steady-state.

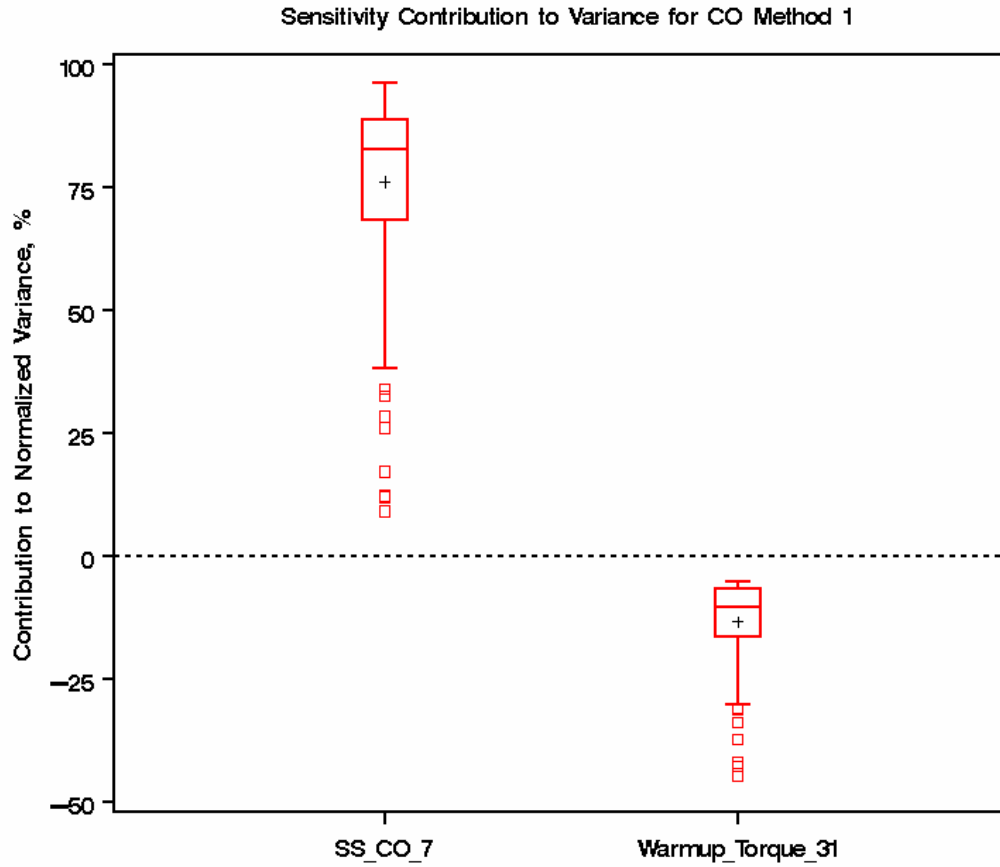


FIGURE 226. BOX PLOT OF ERROR SURFACE SENSITIVITY BASED ON VARIANCE FOR BSCO METHOD 1

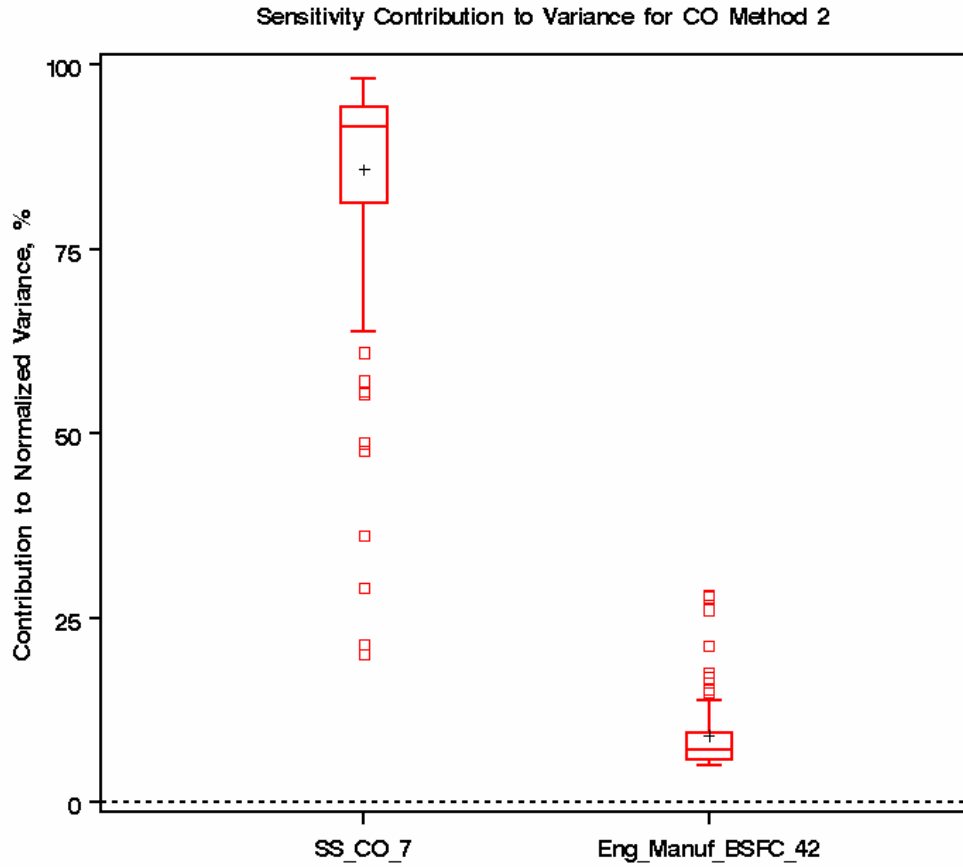


FIGURE 227. BOX PLOT OF ERROR SURFACE SENSITIVITY BASED ON VARIANCE FOR BSCO METHOD 2

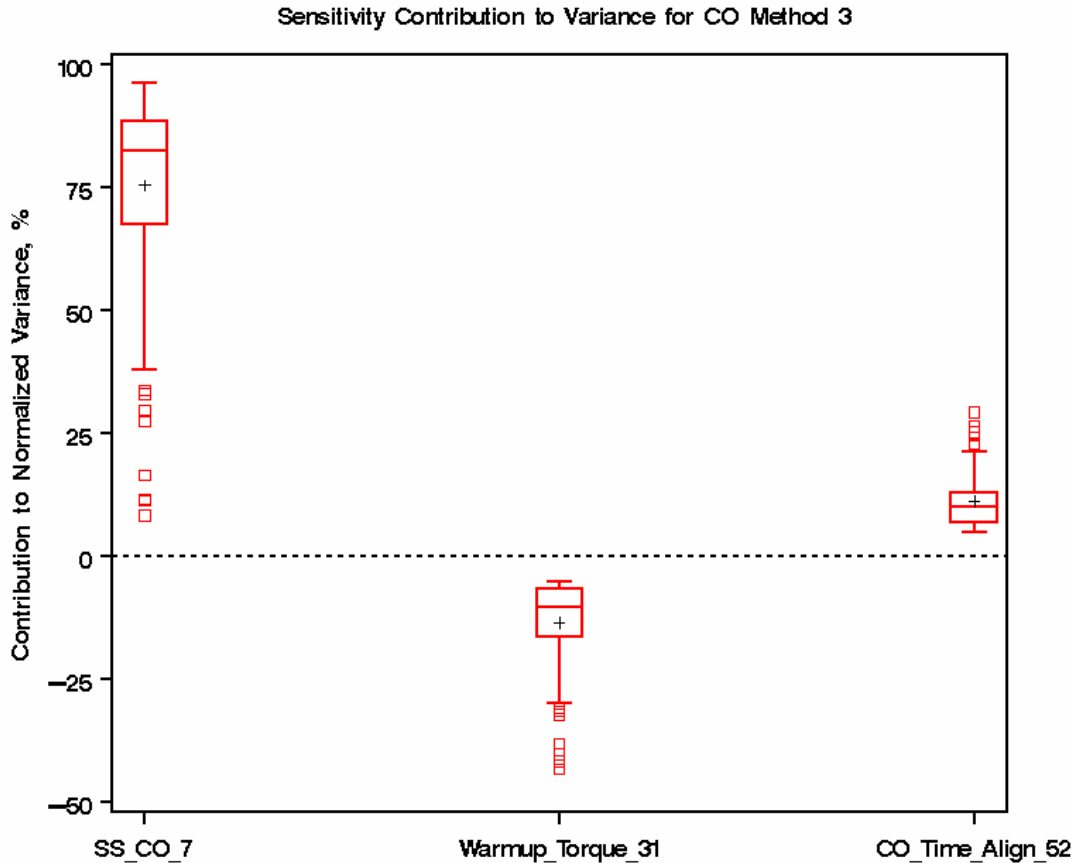


FIGURE 228. BOX PLOT OF ERROR SURFACE SENSITIVITY BASED ON VARIANCE FOR BSCO METHOD 3

6.6 Sensitivity Based on Bias and Variance

This section contains a summary of the error surfaces that contributed the most to the bias of the generated BS emissions. The sensitivity charts developed in Crystal Ball help identify the error surfaces (assumptions) that are sensitive to changes in variation with respect to their effect on the three delta BS emissions. Another type of sensitivity examined in this study was concerned with the effects of potential “bias” in error surfaces and their effects on the forecast values. In order to study these effects a new error surface assumption was added to the MS simulation model for each of the original 35 error surfaces (excluding the two error surfaces for time alignment).

This assumption was sampled as a discrete binary distribution (i.e., on or off) during the simulation. For each trial of the simulation, 35 original error surfaces and 35 ‘on/off’ error surfaces were sampled according to their defined sample distribution. If the ‘on/off’ error surface produced an ‘off’ condition, the delta emissions from that particular error surface were not added to the BS emissions computations for the BS emissions ‘with errors’. Similarly, if the

‘on/off’ error surface produced an ‘on’ condition, the delta emissions from that particular error surface were added to the BS emissions calculations.

During every trial of the simulation, the exclusions due to the ‘off’ conditions resulted in various combinations of the error surface delta emissions being added to the BS emissions ‘with errors’ computations. Over the course of a MC simulation with thousands of trials, the sensitivity of a particular error either ‘on’ or ‘off’ was assessed by examining the change in the forecast delta emission. Therefore, in a single MC simulation of a reference NTE event sensitivities due to variance and/or bias were explored.

During this phase of the simulation, thirteen reference NTE events were selected to be re-run with the additional ‘on/off’ error surface assumptions included in the MC model. These events were selected to bound the NTE BSNO_x threshold of 2.6820 g/kW-hr and are listed in Table 102 along with their ideal BSNO_x values. Also included in Table 102 is the number of trials run for each of the MC simulations. Figure 229 illustrates the distribution of the ideal BSNO_x values for the thirteen reference NTE events as a frequency histogram.

TABLE 102. IDEAL BSNO_x VALUES FOR 13 REFERENCE NTE EVENTS

Reference NTE Event #	Ideal BSNO_x g/kW-hr	Trials Run During MC Simulation
38	0.0249	10,000
44	1.0730	10,000
87	1.5207	10,000
148	1.9985	10,000
82	2.4568	10,000
163	2.5907	10,000
63	2.6670	10,000
46	2.6957	30,000
51	2.8298	10,000
69	3.0257	30,000
157	3.4666	30,000
1	1.0713	30,000
25	5.4061	30,000

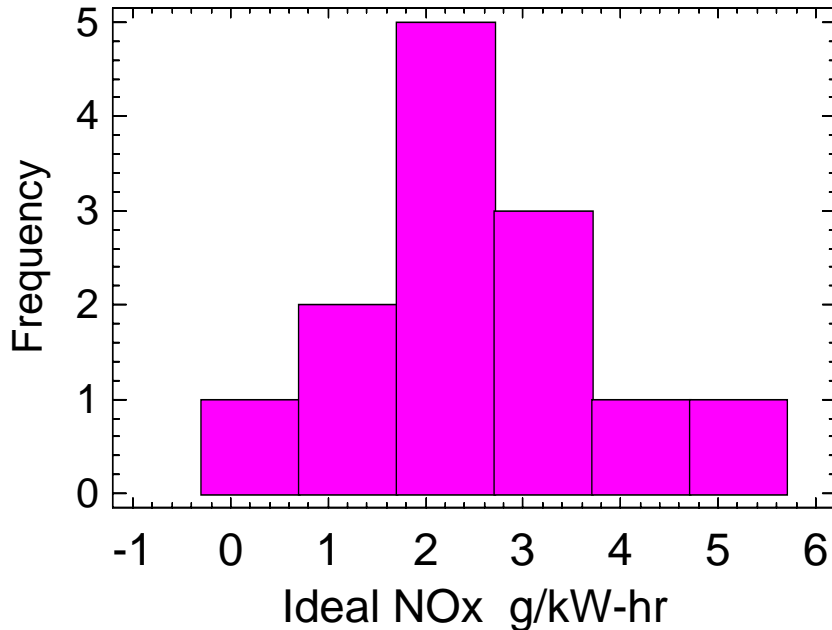


FIGURE 229. DISTRIBUTION OF IDEAL BSNO_x FOR 13 REFERENCE NTE EVENTS

Monte Carlo simulations, including the additional 35 ‘on/off’ error surfaces, were run on all thirteen reference NTE events for 10,000 or 30,000 trials each. EXTRACT data files and REPORT files were generated for all three emissions and three calculation methods. All reference NTE events converged within 1% of the NTE emissions threshold.

Simulation results from these reference NTE events produced sensitivity values for all three 95th percentile delta emissions by all three calculation methods. Table 103 through Table 111 summarize the error surfaces in which either the contribution-to-variance normalized sensitivity value or the ‘on/off’ bias check for the error surface was at least 5% in magnitude compared to all the other error surfaces. If the label in the error surface contains the words ‘OnOff’ then it represents a check for bias; otherwise, the error surface indicates a check for variance. Note that the number of error surfaces whose sensitivity values due to variance were greater than 5% ranged from 3 to 5 for all three delta emissions and all three calculation methods. Also note that all three emissions by all three calculation methods identified at least one ‘on/off’ error surface in which a bias effect was noted.

Table 103 through Table 105 list the sensitivity due to variance and bias descriptive statistics for the delta BSNO_x emissions for Methods 1, 2 and 3, respectively. In the first column of these tables the error surfaces with at least a 5% contribution-to-variance are listed followed by the number of reference NTE events in which this occurred. The mean contribution-to-variance normalized percentage is also given along with the minimum and maximum values. For Methods 1 and 3, the largest mean normalized variance was from error surface #31, torque warm-up, which was the same result obtained in the previous analysis in Section 6.6. For Method 2, the largest mean normalized variance was from the ‘on/off’ error surface for CO₂ steady-state followed by error surface #1 due to NO_x steady-state.

TABLE 103. ERROR SURFACE SENSITIVITY TO BIAS AND VARIANCE FOR 13 REFERENCE NTE EVENTS FOR BSNO_x METHOD 1

Error Surface	# Ref NTE Events	Mean, %	Minimum, %	Maximum, %
1_NO _x SS	13	21.02	8.40	92.70
20_Exhaust Flow_SS	11	6.33	5.40	8.10
31_Torque Warm-up	12	-23.21	-34.40	-12.80
35_Torque Engine Manufacturers	12	-9.78	-12.20	-7.40
51_NO _x Time Alignment	8	6.05	5.40	7.10
OnOff_Exhaust Flow Pulsation	12	14.70	5.60	19.00
OnOff_Exhaust Flow Swirl	1	5.70	5.70	5.70
OnOff_Exhaust Flow SS	10	14.58	8.70	21.30

TABLE 104. ERROR SURFACE SENSITIVITY TO BIAS AND VARIANCE FOR 13 REFERENCE NTE EVENTS FOR BSNO_x METHOD 2

Error Surface	# Ref NTE Events	Mean, %	Minimum, %	Maximum, %
1_NO _x SS	13	29.46	14.30	92.30
37_BSFC DOE	1	5.00	5.00	5.00
38_BSFC Warm-up	6	6.33	5.20	8.30
42_BSFC Engine Manufacturers	12	13.55	10.80	17.10
OnOff_CO ₂ SS	12	-34.93	-39.40	-20.80
OnOff_BSFC DOE	8	-6.46	-8.30	-5.10

TABLE 105. ERROR SURFACE SENSITIVITY TO BIAS AND VARIANCE FOR 13 REFERENCE NTE EVENTS FOR BSNO_x METHOD 3

Error Surface	# Ref NTE Events	Mean, %	Minimum, %	Maximum, %
1_NO _x SS	13	23.62	11.20	92.90
31_Torque Warm-up	12	-27.83	-38.20	-15.90
35_Torque Engine Manufacturers	12	-11.69	-15.00	-8.60
51_NO _x Time Alignment	7	5.96	5.00	7.80
OnOff_CO ₂ SS	12	-25.22	-32.90	-15.90

Table 106 through Table 108 list the sensitivity and bias descriptive statistics for the delta BSNMHC emissions for Methods 1, 2 and 3, respectively. For all three methods, the largest mean normalized variance was from the error surface #19, NMHC ambient effect.

TABLE 106. ERROR SURFACE SENSITIVITY TO BIAS AND VARIANCE FOR 13 REFERENCE NTE EVENTS FOR BSNMHC METHOD 1

Error Surface	# Ref NTE Events	Mean, %	Minimum, %	Maximum, %
13_NMHC SS	10	7.05	6.10	8.70
19_NMHC Ambient	13	58.33	11.90	73.80
20_Exhaust Flow SS	1	6.40	6.40	6.40
31_Torque Warm-up	4	-15.60	-25.60	-5.70
35_Torque Engine Manufacturers	3	-8.37	-9.80	-5.90
OnOff_Exhaust Flow Pulsation	3	14.80	9.20	19.30
OnOff_Exhaust Flow SS	3	11.00	8.20	12.40
OnOff_NMHC SS	11	13.89	5.00	18.80

TABLE 107. ERROR SURFACE SENSITIVITY TO BIAS AND VARIANCE FOR 13 REFERENCE NTE EVENTS FOR BSNMHC METHOD 2

Error Surface	# Ref NTE Events	Mean, %	Minimum, %	Maximum, %
13_NMHC SS	10	6.78	6.00	8.2
19_NMHC Ambient	13	62.33	21.60	74.20
38_BSFC Warm-up	2	5.60	5.50	5.70
42_BSFC Engine Manufacturers	3	10.67	7.40	14.20
OnOff_CO2 SS	3	-24.67	-36.90	-12.60
OnOff_NMHC SS	11	13.95	6.80	19.30

TABLE 108. ERROR SURFACE SENSITIVITY TO BIAS AND VARIANCE FOR 13 REFERENCE NTE EVENTS FOR BSNMHC METHOD 3

Error Surface	# Ref NTE Events	Mean, %	Minimum, %	Maximum, %
13_NMHC SS	10	6.84	6.00	7.90
19_NMHC Ambient	13	60.51	14.90	74.10
31_Torque Warm-up	4	-18.68	-32.20	-5.40
35_Torque Engine Manufacturers	3	-9.87	-11.80	-6.40
OnOff_CO2 SS	3	-18.63	-26.20	-11.00
OnOff_NMHC SS	11	13.64	5.50	17.50

Table 109 through Table 111 list the sensitivity and bias descriptive statistics for the delta BSCO emissions for Methods 1, 2 and 3, respectively. For all three methods, the largest mean normalized variance was from the ‘on/off’ error surface for CO steady-state (average near 80% for all three methods).

TABLE 109. ERROR SURFACE SENSITIVITY TO BIAS AND VARIANCE FOR 13 REFERENCE NTE EVENTS FOR BSCO METHOD 1

Error Surface	# Ref NTE Events	Mean, %	Minimum, %	Maximum, %
7_CO SS	10	6.06	5.00	7.30
31_Torque Warm-up	1	-13.50	-13.50	-13.50
35_Torque Engine Manufacturers	1	-5.20	-5.20	-5.20
52_CO Time Alignment	1	20.00	20.00	20.00
OnOff_Exhaust Flow Pulsation	1	10.80	10.80	10.80
OnOff_Exhaust Flow SS	1	6.20	6.20	6.20
OnOff SS CO	13	80.63	31.30	91.30

TABLE 110. ERROR SURFACE SENSITIVITY TO BIAS AND VARIANCE FOR 13 REFERENCE NTE EVENTS FOR BSCO METHOD 2

Error Surface	# Ref NTE Events	Mean, %	Minimum, %	Maximum, %
7_CO SS	12	6.31	5.30	7.40
42_BSFC Engine Manufacturers	1	5.80	5.80	5.80
52_CO Time Alignment	1	20.00	20.00	20.00
OnOff_CO2 SS	1	-16.20	-16.20	-16.20
OnOff_CO SS	13	82.82	43.80	91.20

TABLE 111. ERROR SURFACE SENSITIVITY TO BIAS AND VARIANCE FOR 13 REFERENCE NTE EVENTS FOR BSCO METHOD 3

Error Surface	# Ref NTE Events	Mean, %	Minimum, %	Maximum, %
7_CO SS	9	6.14	5.50	7.30
31_Torque Warm-up	1	-13.10	-13.10	-13.10
52_CO Time Alignment	6	12.10	5.50	36.00
OnOff_CO2 SS	1	-10.40	-10.40	-10.40
OnOff_CO SS	13	79.75	28.00	91.20

The contribution to normalized variance and bias sensitivities from Table 103 through Table 105 are illustrated pictorially as box plots in Figure 230 through Figure 232 for BSNO_x Methods 1, 2 and 3, respectively. Only the error surfaces with at least 5 of the thirteen reference NTE events (1/3 of the events) are included as box plots. The mean normalized variance for each of the plotted error surfaces is noted by a “+” symbol in the boxes. The error surface with the largest mean normalized variance is plotted at the left of the chart. The error surface with the second largest mean normalized variance is plotted second from the left, and so on. Similar plots could also be generated for BSNMHC and BSCO. Figure 230 and Figure 232 demonstrate the high sensitivity to the error surface #31, torque warm-up. This was also seen in the analyses using the 195 reference NTE events. Also note in Figure 230 that bias effects due to exhaust

flow pulsation and steady-state were important. Figure 231 and Figure 232 also show a bias effect due to CO₂ steady-state.

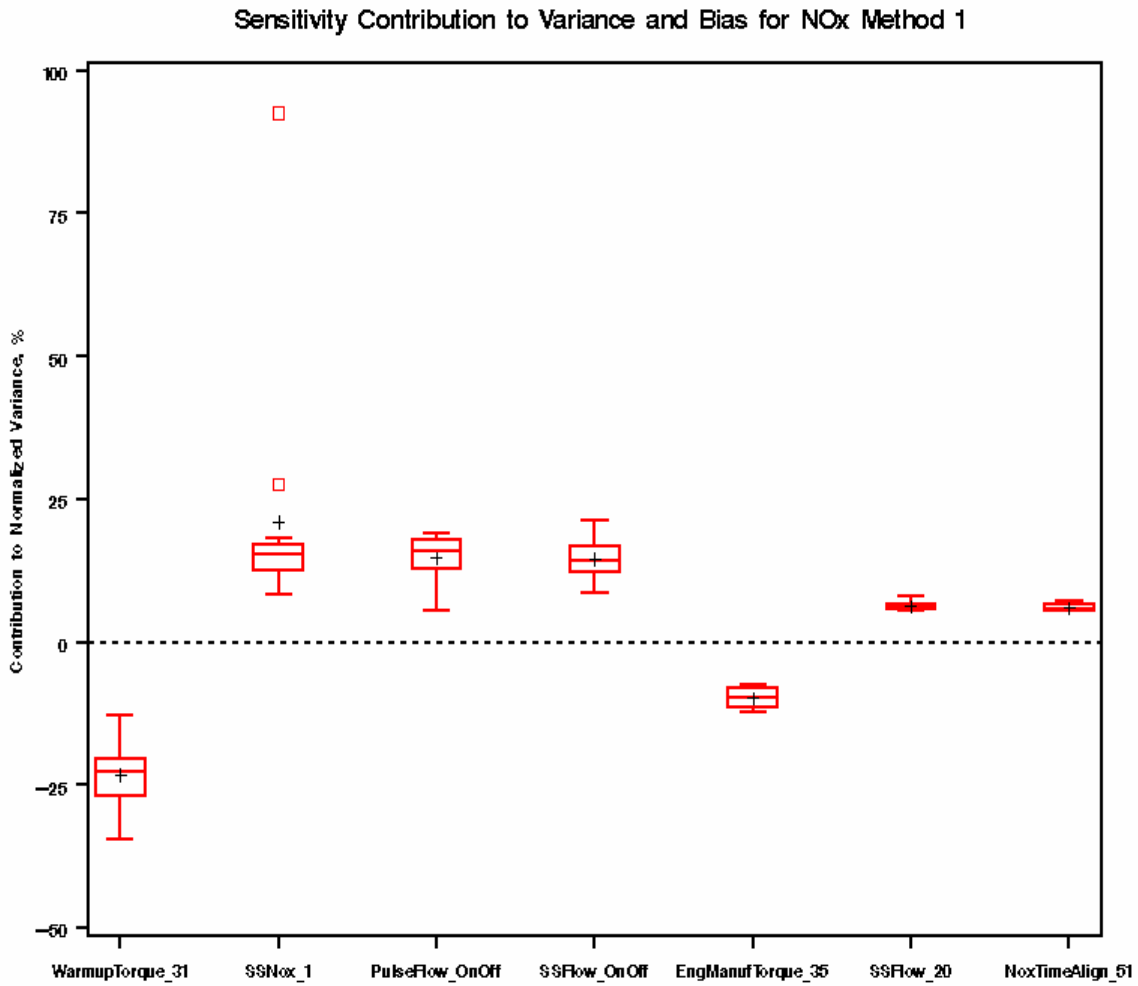


FIGURE 230. BOX PLOT OF ERROR SURFACE SENSITIVITY BASED ON BIAS AND VARIANCE FOR BSNO_x METHOD 1

Sensitivity Contribution to Variance and Bias for NOx Method 2

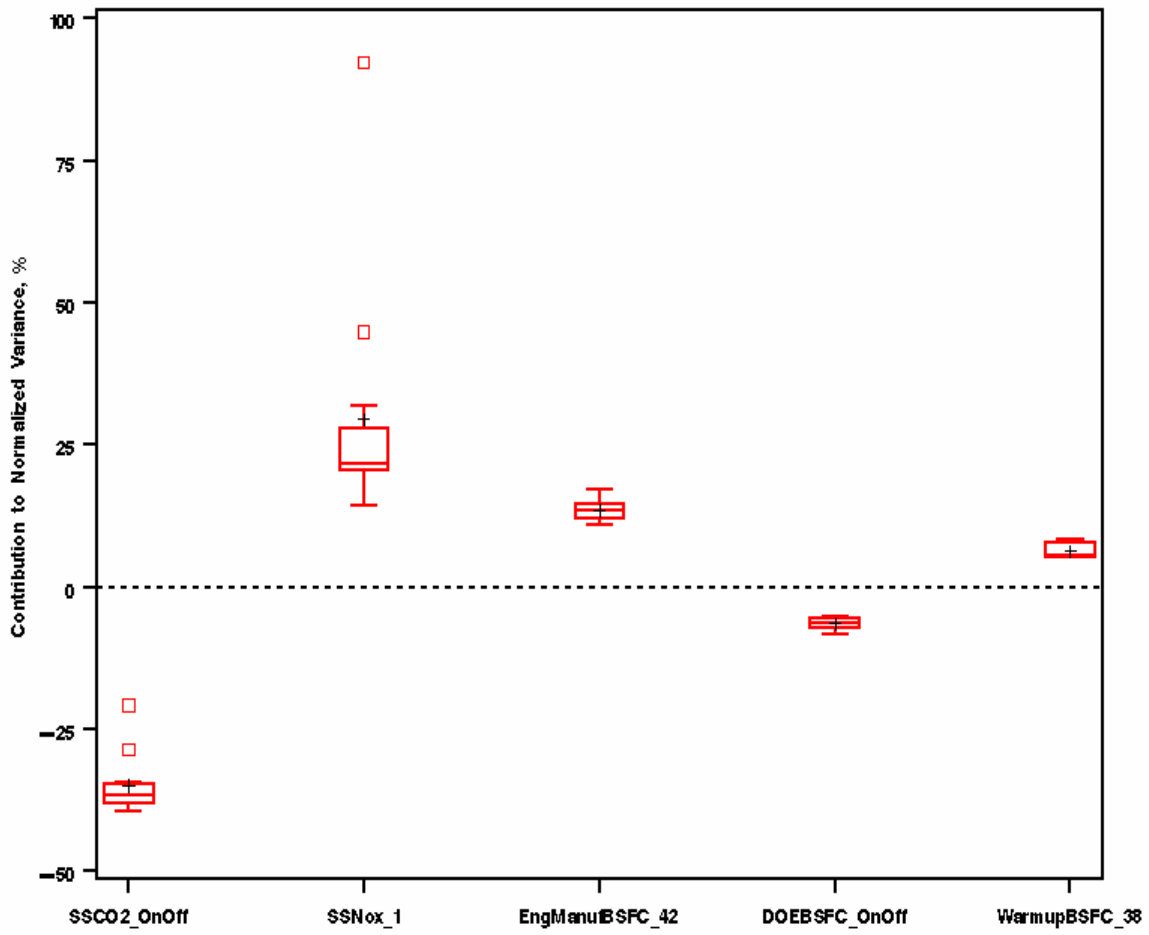


FIGURE 231. BOX PLOT OF ERROR SURFACE SENSITIVITY BASED ON BIAS AND VARIANCE FOR BSNO_x METHOD 2

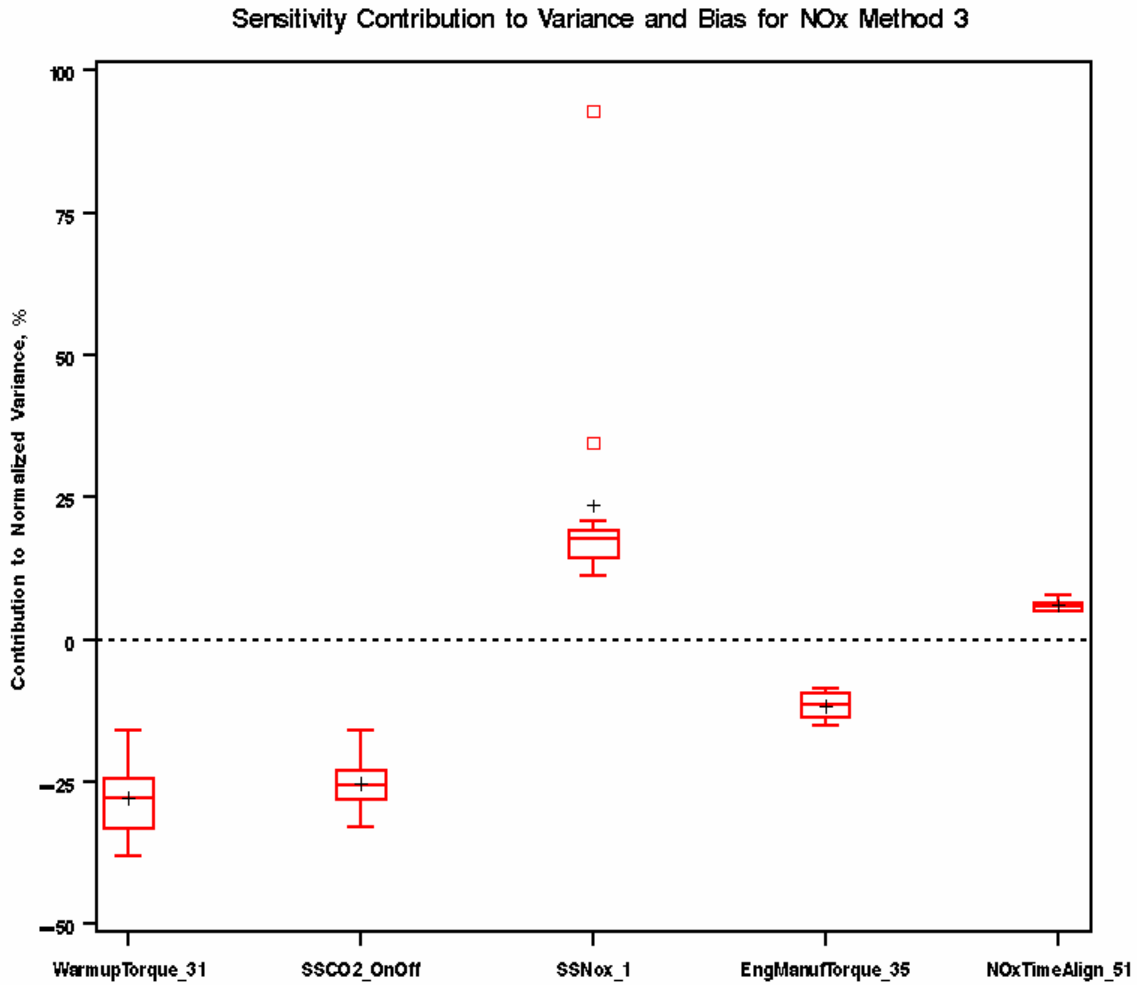


FIGURE 232. BOX PLOT OF ERROR SURFACE SENSITIVITY BASED ON BIAS AND VARIANCE FOR BSNO_x METHOD 3

A summary of the sensitivity results due to variance only and both variance and bias MC simulations are provided in Table 112 through Table 120 for all three emissions and all three calculation methods.

TABLE 112. SUMMARY OF ERROR SURFACE SENSITIVE TO BIAS AND VARIANCE FOR BSNO_x METHOD 1

Sensitivity to Variance			Sensitivity to Bias and Variance		
195 Ref NTE Events			13 Ref NTE Events		
#	Error Surface	Avg Contribution to Normalized Variance, %	#	Error Surface	Avg Contribution to Normalized Variance, %
1	SS_NOx	27.90	1	SS_NOx	21.02
20	SS_Flow	10.34	20	SS_Flow	6.33
31	Warmup_Torque	-34.65	31	Warmup_Torque	-23.21
35	Eng_Manuf_Torque	-15.96	35	Eng_Manuf_Torque	-9.78
			51	NOx_Time_Align	6.05
				Pulse_Flow_OnOff	14.70
				SS_Flow_OnOff	14.58

TABLE 113. SUMMARY OF ERROR SURFACE SENSITIVE TO BIAS AND VARIANCE FOR BSNO_x METHOD 2

Sensitivity to Variance			Sensitivity to Bias and Variance		
195 Ref NTE Events			13 Ref NTE Events		
#	Error Surface	Avg Contribution to Normalized Variance, %	#	Error Surface	Avg Contribution to Normalized Variance, %
1	SS_NOx	47.22	1	SS_NOx	29.46
37	DOE_BSFC	6.48			
38	Warmup_BSFC	10.29	38	Warmup_BSFC	6.33
42	Eng_Manuf_BSFC	24.43	42	Eng_Manuf_BSFC	13.55
			51	NOx_Time_Align	6.05
				SS_CO2_OnOff	-34.93
				DOE_BSFC_OnOff	-6.46

TABLE 114. SUMMARY OF ERROR SURFACE SENSITIVE TO BIAS AND VARIANCE FOR BSNO_x METHOD 3

Sensitivity to Variance			Sensitivity to Bias and Variance		
195 Ref NTE Events			13 Ref NTE Events		
#	Error Surface	Avg Contribution to Normalized Variance, %	#	Error Surface	Avg Contribution to Normalized Variance, %
1	SS_NO _x	30.59	1	SS_NO _x	23.62
31	Warmup_Torque	-38.37	31	Warmup_Torque	-27.83
35	Eng_Manuf_Torque	-17.89	35	Eng_Manuf_Torque	-11.69
			51	NO _x _Time_Align	5.96
				SS_CO ₂ _OnOff	-25.22

TABLE 115. SUMMARY OF ERROR SURFACE SENSITIVE TO BIAS AND VARIANCE FOR BSNMHC METHOD 1

Sensitivity to Variance			Sensitivity to Bias and Variance		
195 Ref NTE Events			13 Ref NTE Events		
#	Error Surface	Avg Contribution to Normalized Variance, %	#	Error Surface	Avg Contribution to Normalized Variance, %
13	SS_NMHC	6.01	13	SS_NMHC	7.05
19	NMHC_Ambient	85.70	19	NMHC_Ambient	58.33
				SS_NMHC_OnOff	13.86

TABLE 116. SUMMARY OF ERROR SURFACE SENSITIVE TO BIAS AND VARIANCE FOR BSNMHC METHOD 2

Sensitivity to Variance			Sensitivity to Bias and Variance		
195 Ref NTE Events			13 Ref NTE Events		
#	Error Surface	Avg Contribution to Normalized Variance, %	#	Error Surface	Avg Contribution to Normalized Variance, %
13	SS_NMHC	5.65	13	SS_NMHC	6.78
19	NMHC_Ambient	89.34	19	NMHC_Ambient	62.33
				SS_NMHC_OnOff	13.95

TABLE 117. SUMMARY OF ERROR SURFACE SENSITIVE TO BIAS AND VARIANCE FOR BSNMHC METHOD 3

Sensitivity to Variance			Sensitivity to Bias and Variance		
195 Ref NTE Events			13 Ref NTE Events		
#	Error Surface	Avg Contribution to Normalized Variance, %	#	Error Surface	Avg Contribution to Normalized Variance, %
13	SS_NMHC	5.64	13	SS_NMHC	6.84
19	NMHC_Ambient	86.98	19	NMHC_Ambient	60.51
				SS_NMHC_OnOff	13.64

TABLE 118. SUMMARY OF ERROR SURFACE SENSITIVE TO BIAS AND VARIANCE FOR BSCO METHOD 1

Sensitivity to Variance			Sensitivity to Bias and Variance		
195 Ref NTE Events			13 Ref NTE Events		
#	Error Surface	Avg Contribution to Normalized Variance, %	#	Error Surface	Avg Contribution to Normalized Variance, %
7	SS_CO	76.20	7	SS_CO	6.06
31	Warmup_Torque	-13.29			
				SS_CO_OnOff	80.63

TABLE 119. SUMMARY OF ERROR SURFACE SENSITIVE TO BIAS AND VARIANCE FOR BSCO METHOD 2

Sensitivity to Variance			Sensitivity to Bias and Variance		
195 Ref NTE Events			13 Ref NTE Events		
#	Error Surface	Avg Contribution to Normalized Variance, %	#	Error Surface	Avg Contribution to Normalized Variance, %
7	SS_CO	85.82	7	SS_CO	6.31
42	Eng_Manuf_BSFC	9.12			
				SS_CO_OnOff	82.82

TABLE 120. SUMMARY OF ERROR SURFACE SENSITIVE TO BIAS AND VARIANCE FOR BSCO METHOD 3

Sensitivity to Variance			Sensitivity to Bias and Variance		
195 Ref NTE Events			13 Ref NTE Events		
#	Error Surface	Avg Contribution to Normalized Variance, %	#	Error Surface	Avg Contribution to Normalized Variance, %
7	SS_CO	75.49	7	SS_CO	6.14
31	Warmup_Torque	-13.40			
52	CO_Time_Align	11.29	52	CO_Time_Align	12.10
				SS_CO_OnOff	79.74

6.7 CE-CERT Mobil Emission Laboratory Correlation

As mentioned previously, the primary means of validation for the Monte Carlo Model was through the use of a comparison set of measurement deltas generated through in-field testing. This was accomplished using the CE-CERT Mobile Emission Laboratory (MEL), which is operating by staff from the University of California-Riverside. In order to insure that the validation was not disturbed by some inherent bias between the SwRI Reference Laboratory and the CE-CERT MEL Validation Reference, the Test Plan included a correlation exercise that was to be performed between the two laboratories, prior to the start of on-road validation efforts. The CE-CERT MEL was brought to SwRI’s laboratory facilities in San Antonio, Texas, and a side-by-side correlation test was run. This correlation testing was performed during June of 2006.

At this point in the program, SwRI had just recently completed dynamometer testing of Engine 1, which was the DDC Series 60 heavy-heavy duty engine. This engine was still installed in the test cell at that time, and therefore it was the engine that was used for the correlation exercise.

The trailer housing the CE-CERT MEL was positioned directly behind the SwRI laboratory facilities, in such a manner that the test cell could be readily accessed via a high-bay access door. This position allowed for the easy connection of the MEL dilution tunnel exhaust inlet to the test cell exhaust system. The exhaust system was constructed in such a manner that it could be easily disconnected at a downstream of the DPFs, and an exhaust pipe extension was fabricated and positioned in order to allow for relatively quick connect to the CE-CERT exhaust inlet.

This arrangement allowed for easy switching of the exhaust between the two test facilities, allowing for tests to be conducted on both facilities during a single day with minimum interruption. The Test Plan did not initially include a test matrix for the correlation, and therefore a correlation test matrix was developed by SwRI and proposed to the Steering Committee for approval. Following approval, the correlation testing was conducted essentially as proposed over the course of three days of testing.

The primary test cycle used during the correlation test was termed the “NTE Cycle.” This cycle was in fact one of the 20 NTE transient cycles which had been previously used to generate data for the Transient Error Surface, which was described earlier in Section 4.5 of the report. It was felt that a cycle which included a number of NTE events would be appropriate for basis for correlation, because the CE-CERT MEL would later be used to generate validation data during NTE operation. However, the basis for comparison between the labs was the overall cycle average brake-specific emissions. The correlation was not assessed on an event-by-event basis, although this data was available for comparison. This NTE cycle was run in triplicate each day by both labs in succession.

In addition to the NTE cycle, the test matrix also included duplicate runs of the RMC 13-mode SET test by each lab every day. This cycle was included in the test matrix in order to provide some steady-state measurements that would hopefully aid in determining the cause of any discrepancies between the two laboratories, if any such differences were found during NTE cycle testing.

The test matrix is illustrated in Table 121. In total, nine NTE cycles were run for each laboratory and six RMC cycles were run for each laboratory. On each day, one laboratory would run in the morning, and then the exhaust would be switched for the afternoon runs on the other laboratory.

TABLE 121. CORRELATION TEST MATRIX

Test Day	Test Laboratory	Test Cycles
1	SwRI	3 x NTE Cycle
		2 x RMC Cycle
	CE-CERT	3 x NTE Cycle
		2 x RMC Cycle
2	CE-CERT	3 x NTE Cycle
		2 x RMC Cycle
	SwRI	3 x NTE Cycle
		2 x RMC Cycle
3	SwRI	3 x NTE Cycle
		2 x RMC Cycle
	CE-CERT	3 x NTE Cycle
		2 x RMC Cycle

Prior to the start of the correlation exercise, any periodic QA checks which were due according to the schedule outlined in 40 CFR Part 1065 Subpart D were conducted. In addition, CVS propane recovery checks were performed by both laboratories prior to the start of testing. The start of testing was delayed several days by an electronic hardware failure with the MEL CVS, but this was repaired once a replacement part was procured, and further test operations proceeded without any major incident. The MEL CVS propane recovery check was repeated following this repair, to insure that flow measurements were still correct.

As an additional QA measure, span bottles from each facility were read using the instruments from the other facility. In all cases, span concentrations were within 1 percent of expected values.

The brake-specific emission results from the correlation testing for all three days are summarized in Table 122 for the NTE Transient Cycle and in Table 123 for the RMC cycle. The results of greatest interest to the Steering Committee were the NO_x results. On the NTE Transient Cycle, the test labs showed a difference of 2.1 percent, with CE-CERT being higher than SwRI. This difference was matched closely by a 2.7 percent difference in CO₂ measurements in the same direction. The close match between these numbers may have indicated that the primary discrepancy between the two labs was related to measurement of total CVS flow.

TABLE 122. CORRELATION TESTING RESULTS FOR NTE TRANSIENT CYCLE

Test Day	Test Date	Test Number	Transient Emissions, g/hp-hr					
			THC	CH4	NMHC	CO	NOx	CO2
1	6/29/2006	SwRI-NTE-1	0.003	-0.005	0.008	0.057	1.99	540.4
	6/29/2006	SwRI-NTE-2	0.003	0.001	0.002	0.057	1.97	540.9
	6/29/2006	SwRI-NTE-3	0.004	0.003	0.001	0.057	1.99	542.0
			0.003	0.000	0.004	0.057	1.98	541.1
	6/29/2006	CE-CERT-NTE-1	0.001	0.001	-0.001	0.044	2.03	557.6
	6/29/2006	CE-CERT-NTE-2	0.001	0.002	-0.001	0.044	2.03	558.0
	6/29/2006	CE-CERT-NTE-3	0.001	0.002	-0.001	0.042	2.04	557.8
			0.001	0.002	-0.001	0.043	2.03	557.8
Day 1 Difference			-287.6%	119.7%	546.0%	-31.7%	2.4%	3.0%
2	6/30/2006	SwRI-NTE-1	0.004	0.001	0.003	0.058	2.04	541.5
	6/30/2006	SwRI-NTE-2	0.003	0.002	0.001	0.054	2.01	543.0
	6/30/2006	SwRI-NTE-3	0.003	0.002	0.001	0.057	2.02	542.4
			0.003	0.002	0.002	0.056	2.02	542.3
	6/30/2006	CE-CERT-NTE-1	0.002	0.001	0.000	0.041	2.04	554.2
	6/30/2006	CE-CERT-NTE-2	0.001	0.002	-0.001	0.040	2.05	551.7
	6/30/2006	CE-CERT-NTE-3	0.001	0.002	-0.001	0.041	2.04	551.1
			0.001	0.002	0.000	0.041	2.04	552.3
Day 2 Difference			-148.3%	8.2%	556.3%	-38.2%	1.0%	1.8%
3	7/5/2006	SwRI-NTE-1	0.005	-0.007	0.012	0.055	2.01	539.5
	7/5/2006	SwRI-NTE-2	0.003	0.002	0.001	0.052	1.99	540.4
	7/5/2006	SwRI-NTE-3	0.003	0.002	0.001	0.053	2.00	541.2
			0.004	-0.001	0.005	0.053	2.00	540.4
	7/5/2006	CE-CERT-NTE-1	0.001	0.002	-0.001	0.042	2.06	558.5
	7/5/2006	CE-CERT-NTE-2	0.001	0.002	-0.001	0.043	2.05	558.0
	7/5/2006	CE-CERT-NTE-3	0.002	0.002	0.000	0.042	2.07	554.8
			0.001	0.002	-0.001	0.042	2.06	557.1
Day 3 Difference			-159.4%	152.1%	960.2%	-26.2%	2.9%	3.0%
Standard for 2005 Series 60 Engine			0.14	0.14	0.14	15.5	2.2	
Overall Results - NTE Cycle								
SwRI	Mean		0.004	0.0001	0.004	0.056	2.001	541.3
	Stdev		0.001	0.0036	0.004	0.002	0.020	1.1
	Cvar-1SD				108.9%	3.8%	1.0%	0.2%
CE-CERT	Mean		0.001	0.002	-0.001	0.042	2.044	555.7
	Stdev		0.0003	0.0003	0.0004	0.001	0.014	2.9
	Cvar-1SD				59.0%	3.3%	0.7%	0.5%
	%point		-65.1%	2336.2%	-117.4%	-24.2%	2.1%	2.7%
	%standard		-1.6%	1.3%	-2.9%	-0.1%	1.9%	n/a

TABLE 123. CORRELATION TEST RESULTS FOR RMC 13-MODE SET CYCLE

Test Day	Test Date	Test Number	Transient Emissions, g/hp-hr					
			THC	CH4	NMHC	CO	NOx	CO2
1	6/29/2006	SwRI-RMC-1	0.004	0.000	0.004	0.054	1.79	499.8
	6/29/2006	SwRI-RMC-2	0.003	0.002	0.001	0.057	1.80	499.8
			0.004	0.001	0.003	0.055	1.80	499.8
	6/29/2006	CE-CERT-RMC-1	0.000	0.001	-0.002	0.048	1.88	511.7
	6/29/2006	CE-CERT-RMC-2	0.000	0.001	-0.001	0.052	1.88	510.5
			0.000	0.001	-0.002	0.050	1.88	511.1
Day 1 Difference			-109%	23%	-160%	-9.5%	4.6%	2.3%
2	6/30/2006	SwRI-RMC-1	0.002	0.000	0.002	0.054	1.83	500.6
	6/30/2006	SwRI-RMC-2	0.002	0.000	0.002	0.053	1.84	501.1
			0.002	0.000	0.002	0.053	1.84	500.8
	6/30/2006	CE-CERT-RMC-1	0.001	0.002	-0.001	0.043	1.90	508.1
	6/30/2006	CE-CERT-RMC-2	0.000	0.002	-0.001	0.041	1.91	509.0
			0.001	0.002	-0.001	0.042	1.90	508.5
Day 2 Difference			-72%	1586%	-161%	-21.4%	3.6%	1.5%
3	7/5/2006	SwRI-RMC-1	0.002	0.002	0.000	0.052	1.84	498.9
	7/5/2006	SwRI-RMC-2	0.002	0.002	0.001	0.052	1.85	499.0
			0.002	0.002	0.000	0.052	1.85	499.0
	7/5/2006	CE-CERT-RMC-1	0.000	0.002	-0.002	0.041	1.92	514.2
	7/5/2006	CE-CERT-RMC-2	0.000	0.001	0.000	0.045	1.89	514.6
			0.000	0.001	-0.001	0.043	1.91	514.4
Day 3 Difference			-84%	-35%	-314%	-17.4%	3.2%	3.1%
Standard for 2005 Series 60 Engine			0.14	0.14	0.14	15.5	2.2	
Overall Results for RMC Cycle								
SwRI	Mean		0.003	0.001	0.002	0.053	1.827	499.9
	Stdev		0.001	0.001	0.001	0.002	0.024	0.9
	Cvar-1SD				80.0%	3.4%	1.3%	0.2%
CE-CERT	Mean		0.0002	0.002	-0.001	0.045	1.897	511.3
	Stdev		0.0005	0.001	0.001	0.004	0.015	2.7
	Cvar-1SD				48.5%	9.7%	0.8%	0.5%
	%point		-92.6%	42.9%	-171.9%	-16.0%	3.8%	2.3%
	%standard		-1.8%	0.3%	-2.1%	-0.1%	3.1%	

The RMC cycle showed a larger NO_x difference of 3.8 percent, with CE-CERT again being higher than SwRI. However, the CO₂ difference for this cycle was similar to that observed during the NTE cycle at 2.3 percent. In this case it is unlikely that all of the NO_x differences are related to CVS flow discrepancies alone.

Continuous data for the RMC was examined in order to attempt to determine the reasons for the larger discrepancies observed on that cycle. An example of continuous NO_x mass rate comparison is given in Figure 233. It was noted that NO_x mass rates were closer together at higher levels, associated with high load modes of operation during the RMC. The facilities diverged more at lower load modes, which had correspondingly lower NO_x levels. These

differences cannot be related entirely to flow rate measurements, because CO₂ correlated more closely between the two laboratories than NO_x. Examination of linearity data for both NO_x analyzers did not reveal any obvious reasons why the two systems should have diverged more at lower concentration levels.

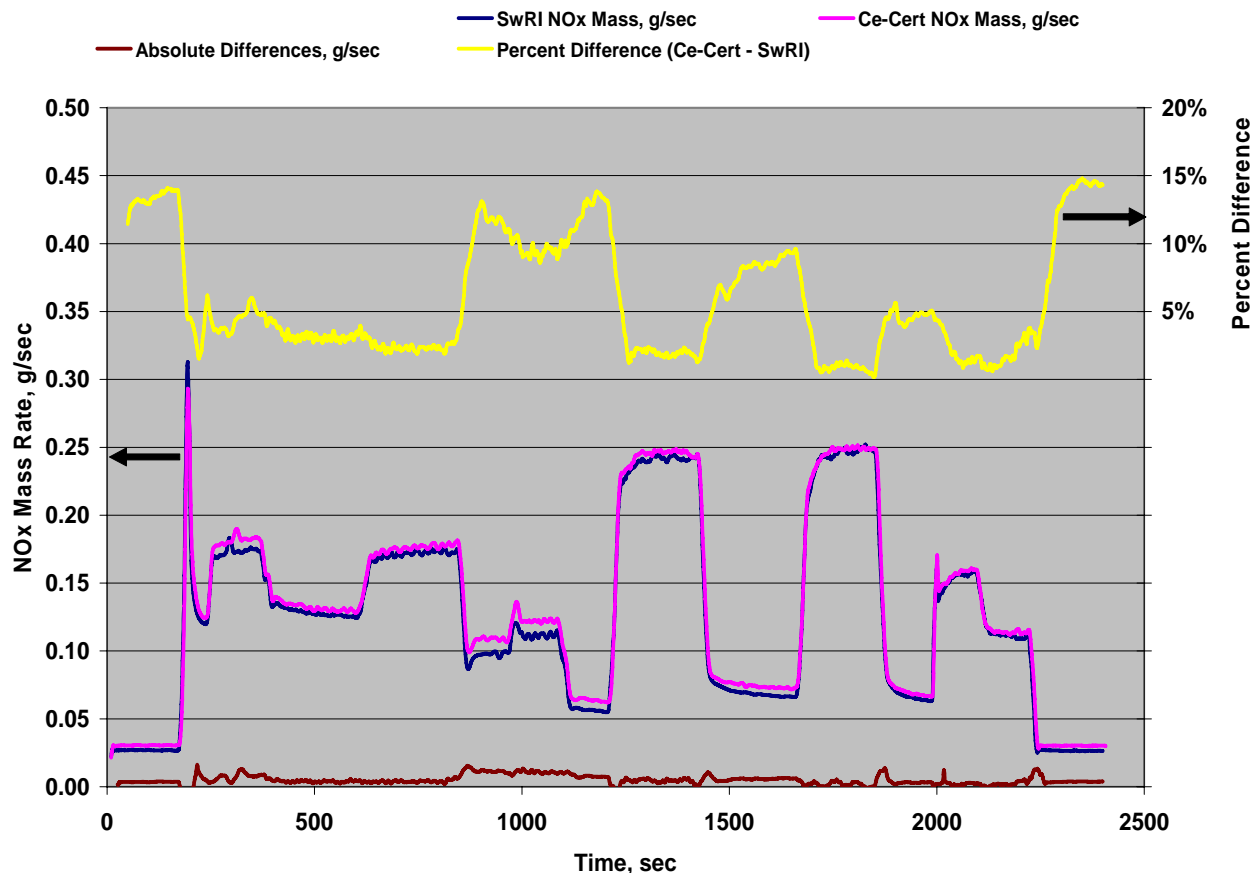


FIGURE 233. COMPARISON OF TYPICAL CONTINUOUS NOX MASS RATE DATA OVER RMC CYCLE - CE-CERT VERSUS SWRI

One area of difference noted between the two laboratories was in terms of CVS flow rate. The SwRI test cell ran at an average flow rate of 4350 scfm, while the CE-CERT tunnel ran at an average flow rate of 2775 scfm. These flow rates translate to an average dilution ratio during the RMC of 7.3 versus 4.6 for SwRI and CE-CERT respectively. It is not known if this difference is related to any of the measurement differences observed between the two laboratories.

The Steering Committee examined these results during the July 7, 2006 conference call. The primary area of interest was the NO_x correlation between the two facilities. The NTE cycle correlation of 2 percent was generally considered good by the Steering Committee; however, there was some concern expressed over the larger discrepancy that was observed during the RMC cycle.

The Test Plan did not include any guidance on assessing correlation. The initial proposal was to use an analysis similar to that given in 40 CFR Part 1065.12 for alternative method approvals. If this proved unsuccessful, the Steering Committee would assess the absolute differences observed to determine if an acceptable level of correlation was achieved.

An initial data analysis was performed using the methodology laid out in that part of the CFR. As outlined in that procedure, both a F-test and a t-test were performed to compare the two sets of NO_x data, using appropriate F_{crit} and t_{crit} values given in the tables in Part 1065, and a 90 % confidence interval. This was done using the NTE cycle data, as that cycle was the primary cycle of comparison. The result of this analysis indicated a failure of the t-test for NO_x, meaning that the 2 percent difference in NO_x observed was statistically significant. However, it was noted that this was due in part to the high degree of test-to-test repeatability observed for both laboratories over the three days of testing.

The Steering Committee examined all of these results along with the F-test and t-test results. Ultimately, the Steering Committee determined at the July 7, 2006 conference call that the level of correlation achieved between the two facilities was acceptable for the performance of the validation testing. This determination was based primarily on the fact that the NTE cycle was deemed more likely to be the kind of operation observed by CE-CERT during on-road testing, and the correlation results for that cycle at 2 percent difference between the labs was considered sufficient to proceed with testing.

It should be noted that this correlation exercise did represent a unique opportunity to compare two 1065 compliant measurement systems using the same test engine and dynamometer installation. In this comparison, any correlation issues related to test cell installation or cycle operation were eliminated by the fact that the same test article was used for both comparisons.

6.8 CE-CERT On Road Validation Testing

The generation of the On-Road Validation data set was performed by CE-CERT using their MEL. This on-road effort was conducted under a separate contract which was funded by the California Air Resources Board (ARB), as part of their contribution to the Measurement Allowance program. The test truck was supplied by Caterpillar, and it incorporated a C-15 heavy heavy duty diesel engine in it. Initially, the truck was configured only with diesel oxidation catalysts (DOCs), rather than DPFs. A pair of DPFs was supplied for use during validation testing by International. These DPFs were shipped to CE-CERT, and were installed on the truck by a local Caterpillar dealer in Riverside, California.

The MEL was used as the reference laboratory measurement during the on-road testing. The PEMS unit used during the on-road testing was PEMS 5, which had previously been audited by SwRI, and was used during selected Environmental Chamber testing described earlier in Section 5 of this report. In addition, one of the 5-inch EFM2 exhaust flow meters was also used for the on-road testing. This flow meter had been previously audited by SwRI, and was also used during Environmental Chamber testing. In addition, it had also been used for Engine 1 dynamometer tests at SwRI. The 5-inch flow meter was selected due to the size of the test engine in the truck.

The actual performance and results of the CE-CERT on-road validation testing are not included in this report. Full details on this part of the program are given in a separate report, titled "Measurement Allowance On-Road Validation Project Report," dated March 2007. The contents of that report are incorporated herein by reference.

SwRI had only a very limited role in the performance of the on-road testing itself, generally limited to arranging for the delivery of the test truck and PEMS hardware both to and from CE-CERT. Caterpillar representatives were onsite with CE-CERT staff during the replay testing, but were there only in order to assist in the recording of proprietary engine ECM data channels, which would later be used to aid in the Laboratory Replay Validation described later in this report. All validation testing was conducted solely by CE-CERT staff.

Sensors staff was onsite briefly at CE-CERT prior to testing, but only to assist in the installation of a purge option which was designed to keep the pressure sensing lines of the EFM2 exhaust flow meter free from condensation during on-road testing. The installation of this option was approved by the Steering Committee prior to the start of on-road testing.

6.9 Laboratory Replay Testing

Because the CE-CERT MEL does not readily incorporate a means of direct torque measurement on a vehicle, the on-road validation data set could not be used to validate model errors associated with broadcast torque and derived BSFC. Therefore, an additional validation exercise was conducted at SwRI. This involved removal of the Caterpillar C15 engine from the test truck used by CE-CERT, and installation of the engine in the SwRI dynamometer test cell. The dual DPFs used during the CE-CERT validation were also removed from the truck and installed in the laboratory exhaust system. The SwRI test cell used for the laboratory replay validation was the same dynamometer test cell used throughout the program. PEMS 5 with 5-inch EFM, which was used for the CE-CERT validation exercise, was shipped back to SwRI for use in the replay validation testing. Selected portions of the CE-CERT on-road tests were then simulated in the laboratory, to the extent possible. Simultaneous laboratory and PEMS measurements were again taken during this replay validation exercise. However, because the laboratory incorporates actual torque measurement, it was possible to use this replay data set to validate the portions of the model associated with torque and BSFC measurements.

After the replay engine installation was complete, the CAT C15 was power validated and a lug curve was generated. Next, one hour test segments from the CE-CERT on-road validation were extracted from the test data to be replayed in the SwRI test cell. During the CE-CERT model validation exercise, CAN engine data was recorded with proprietary Caterpillar software. Using the CAT engine data as well as the PEMS NTE event data, one 1-hour test segment was extracted from each of the 3 routes tested during the CE-CERT validation exercise. The 1-hour test segments were chosen to include a large number of NTE events while also offering diverse engine operation. Each 1-hour cycle was repeated a minimum of 3 times.

The Caterpillar CAN engine data was used to insure the laboratory testing reproduced the engine operation experience during the CE-CERT testing. With assistance from Caterpillar, the

CAN engine data recorded during SwRI laboratory testing was compared to the CAN data recorded during the CE-CERT on-road validation. Upon initial replay attempts, it was apparent the engine was producing significantly more boost at SwRI than it did during the on-road testing. After reviewing the engine data, Caterpillar concluded that the truck likely had a boost leak during the CE-CERT testing, causing the unexpectedly low boost pressure. To accurately simulate the CE-CERT replay, SwRI implemented an adjustable boost leak in the intercooler system. With the boost pressure similar between SwRI and CE-CERT testing, the correlation of most of the engine parameters improved. After several iterations of testing at SwRI and subsequent recommendations by Caterpillar, the accuracy of the engine replay was deemed acceptable by Caterpillar and SwRI.

The first replay test cycle was taken from Route 1, which was the San Diego trip. Because the average elevation during Route 1 nearly matched the elevation of San Antonio, no altitude simulation was necessary. Cycle 2 was taken from Route 2, which was the trip to Mammoth Mountain. The test cell simulated the average barometric pressure calculated for the hour test segment used for the replay. Cycle 3 was extracted from Route 3, which was the return trip from Mammoth Mountain back to Riverside. Similar to cycle 2, the test cell simulated the average elevation calculated for the hour-long test segment of Route 3. For cycle 2 the elevation simulation was 4500 feet, while for cycle 3 the average elevation was 3500 feet.

Figure 234 shows the average NTE event engine speed recorded with the Caterpillar software for cycle 2 in the laboratory and for the CE-CERT on-road validation test. The SwRI and CE-CERT speed traces showed excellent correlation for all replay tests.

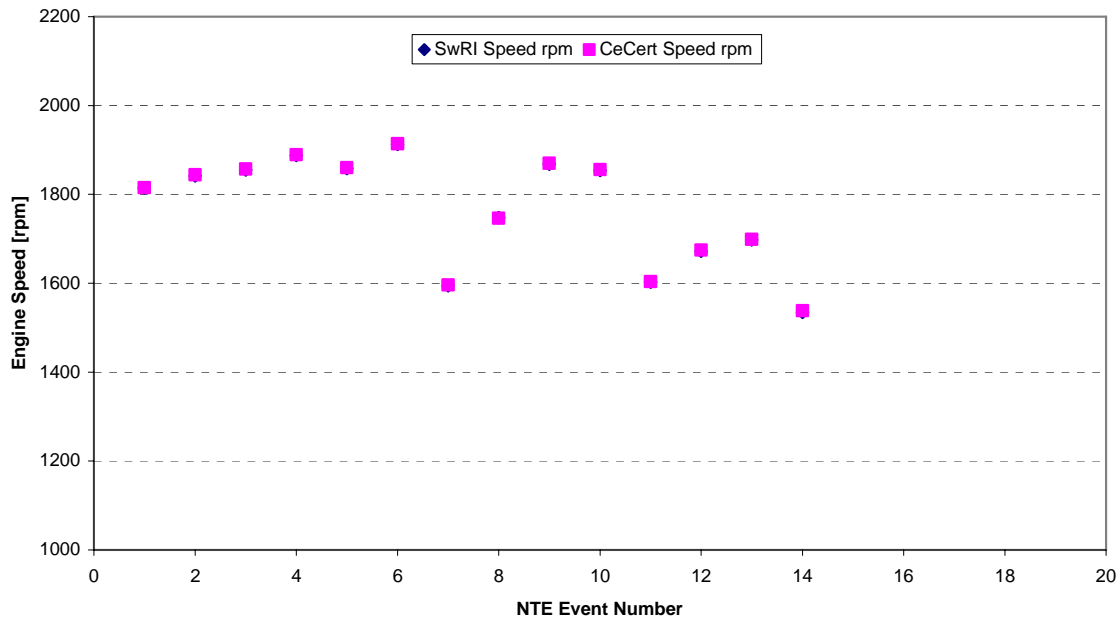


FIGURE 234. ENGINE SPEED CAN DATA COMPARISON FOR SWRI LABORATORY TESTING AND CE-CERT ON-ROAD VALIDATION TESTING (ROUTE 2)

The SwRI and CE-CERT average NTE CAN fuel rate is shown in Figure 235 for cycle 2. Cycle 2 and 3 showed tight fuel rate correlation. Cycle 1 showed good agreement with the exception of a couple NTE events where the delta between SwRI and CE-CERT CAN fuel rate data was near 3 gal/h.

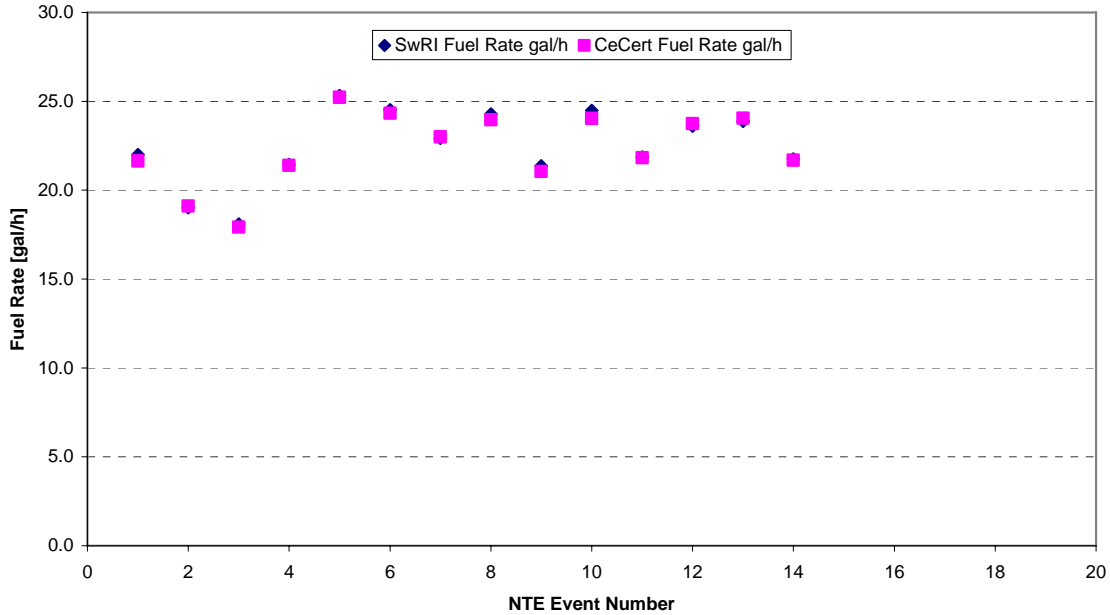


FIGURE 235. FUEL RATE CAN DATA COMPARISON FOR SWRI LABORATORY TESTING AND CE-CERT ON-ROAD VALIDATION TESTING (ROUTE 2)

Figure 236 shows the boost pressure recorded during the SwRI replay and the CE-CERT on-road test. With the laboratory intercooler system, it was impossible to match the boost pressure for each NTE event. Therefore, SwRI attempted to center the NTE errors so that the test average error was near zero.

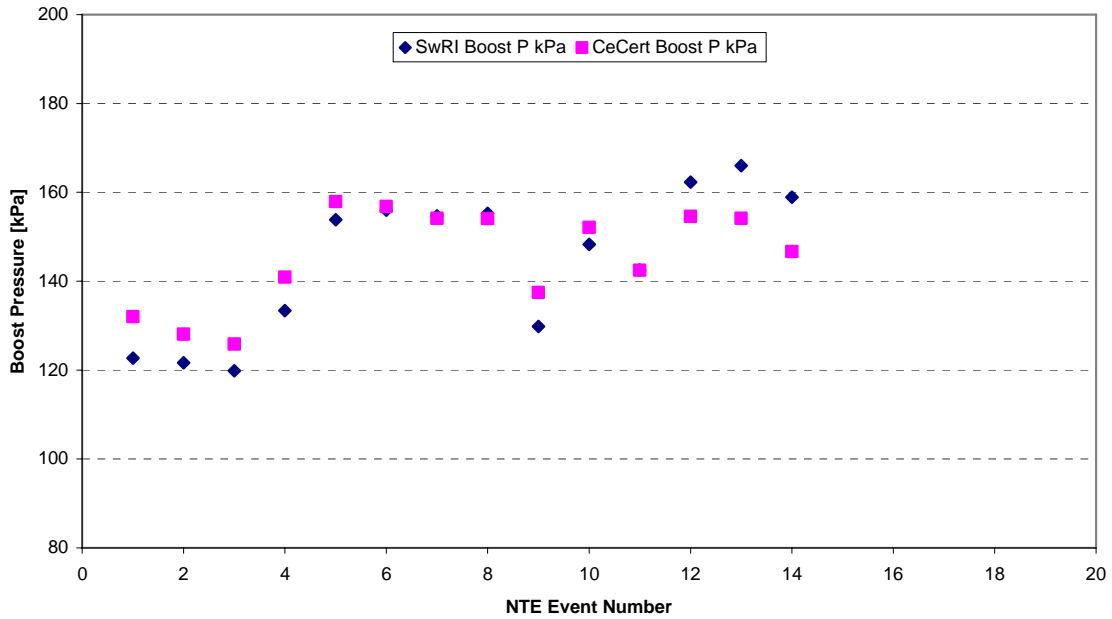


FIGURE 236. BOOST PRESSURE CAN DATA COMPARISON FOR SWRI LABORATORY TESTING AND CE-CERT ON-ROAD VALIDATION TESTING (ROUTE 2)

The timing discrepancies between the SwRI and CE-CERT testing are shown in Figure 237 for cycle 2. Nearly all timing differences for all cycles were within 1 degree of engine rotation.

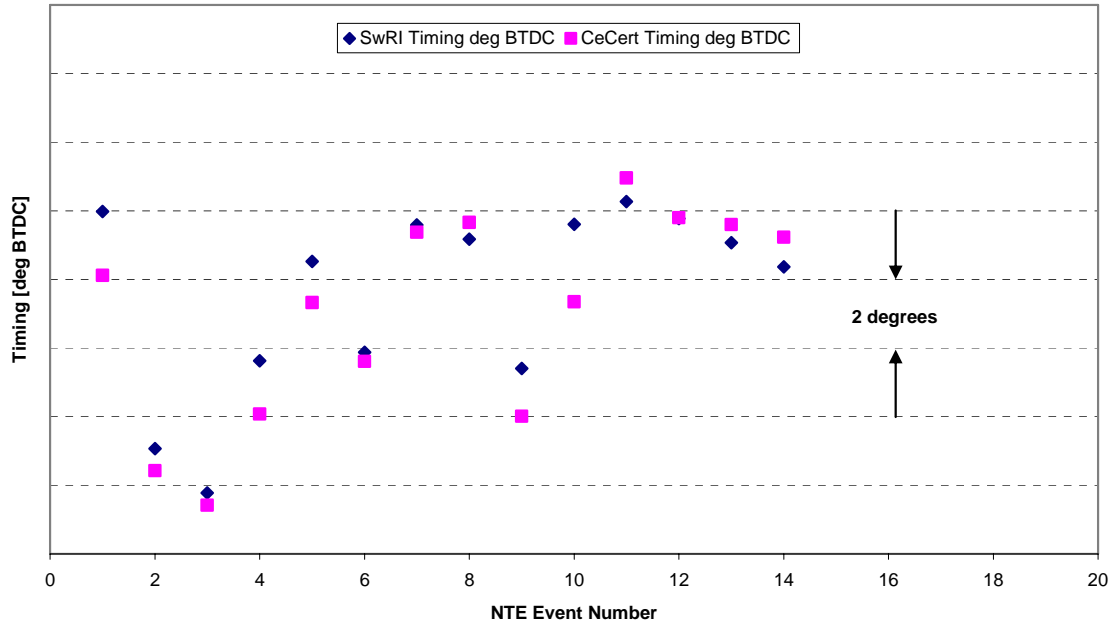


FIGURE 237. INJECTION TIMING CAN DATA COMPARISON FOR SWRI LABORATORY TESTING AND CE-CERT ON-ROAD VALIDATION TESTING (ROUTE 2)

Figure 238 shows the intake manifold temperature comparison between SwRI and CE-CERT. Similar to the boost pressure, an exact match between SwRI and CE-CERT could not be achieved for all NTE events. The intake manifold temperature was set to achieve a balance between positive and negative NTE event differences. The exhaust backpressure was likely similar between the SwRI laboratory and CE-CERT tests because identical DPFs were used during both validation efforts. The intake restriction was set per the manufacturers' specification during laboratory testing. Different fuels were used during testing at SwRI and during CE-CERT's on-road testing. Also, no effort was taken to reproduce the intake air humidity levels observed during the CE-CERT testing.

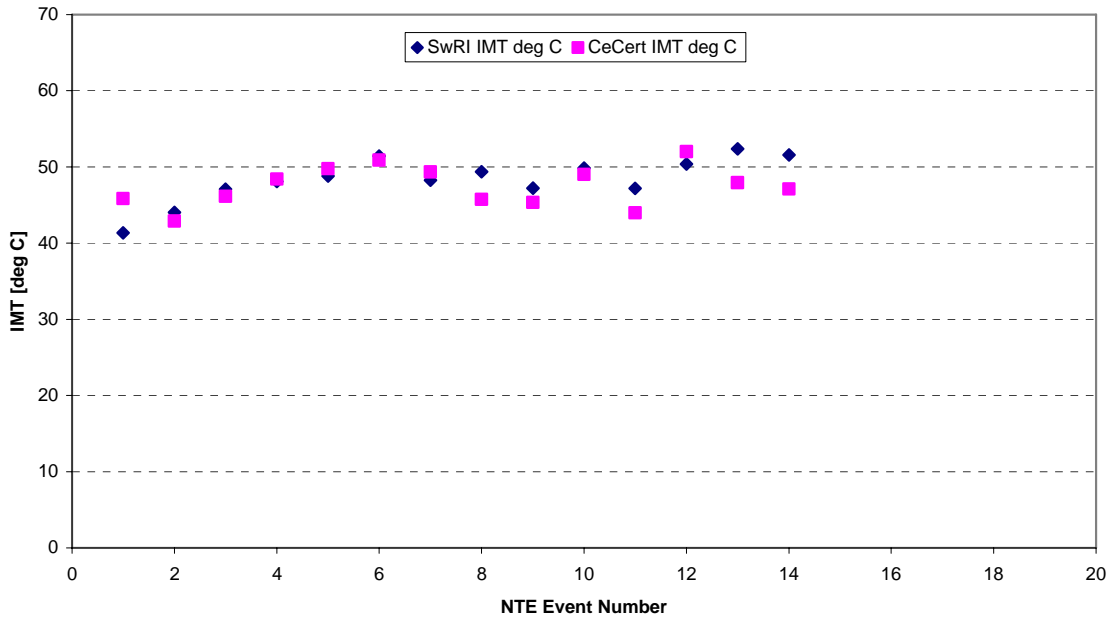


FIGURE 238. INTAKE MANIFOLD TEMPERATURE CAN DATA COMPARISON FOR SWRI LABORATORY TESTING AND CE-CERT ON-ROAD VALIDATION TESTING (ROUTE 2)

Figure 239 shows the average NTE wet NO_x concentrations measured using PEMS 5 in the SwRI Laboratory and during the CE-CERT testing. PEMS 5 measured slightly lower wet NO_x concentrations at SwRI compared to during the CE-CERT validation. A possible explanation for the difference in wet NO_x concentration may have been a difference in intake air humidity, as no effort was taken to match this parameter. Cycle 1 and 3 wet NO_x concentration correlations were tighter than those measured for cycle 2. Cycle 1 wet NO_x deltas were centered, with some positive and negative differences. Cycle 3 SwRI NO_x deltas were biased slightly negative.

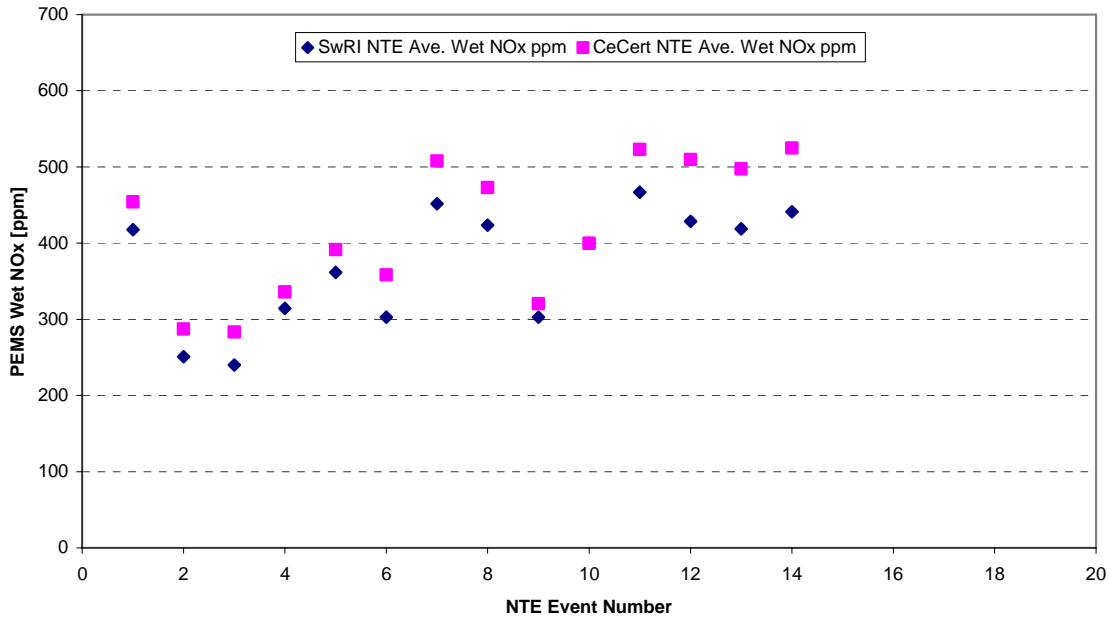


FIGURE 239. PEMS 5 WET NO_x COMPARISON FOR SWRI LABORATORY TESTING AND CE-CERT ON-ROAD VALIDATION TESTING (ROUTE 2)

Figure 240 and Figure 241 show the PEMS 5 exhaust flow rate and wet NO_x mass rate for SwRI and CE-CERT validation tests. The exhaust flow rates showed good correlation for the three cycles. Therefore, the wet NO_x mass flow rates showed trends similar to wet NO_x concentration.

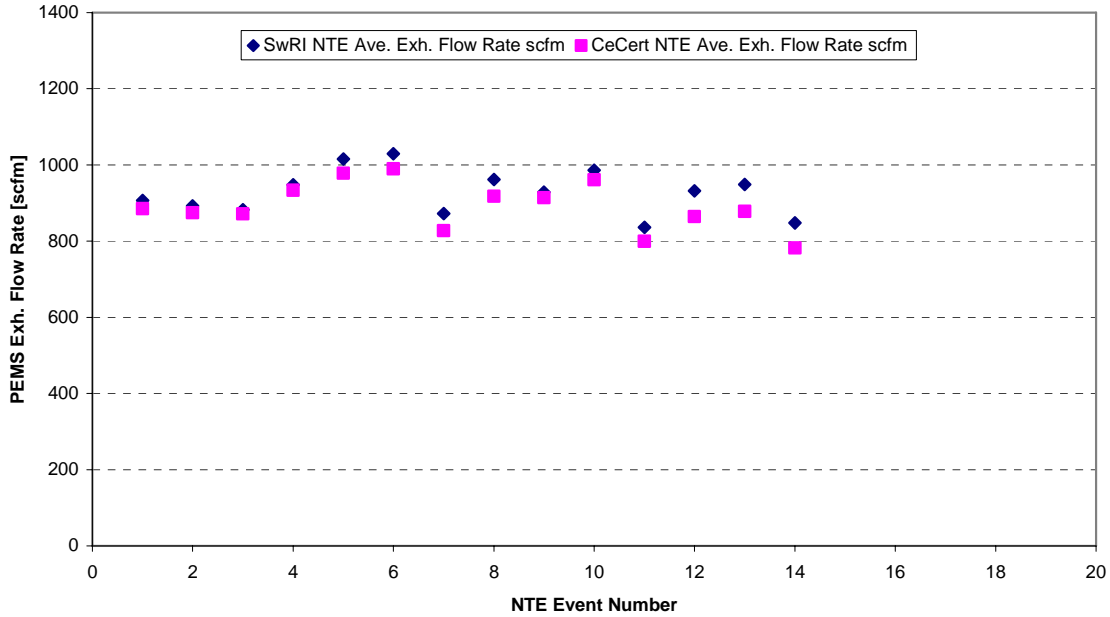


FIGURE 240. PEMS 5 EXHAUST FLOW RATE COMPARISON FOR SWRI LABORATORY TESTING AND CE-CERT ON-ROAD VALIDATION TESTING (ROUTE 2)

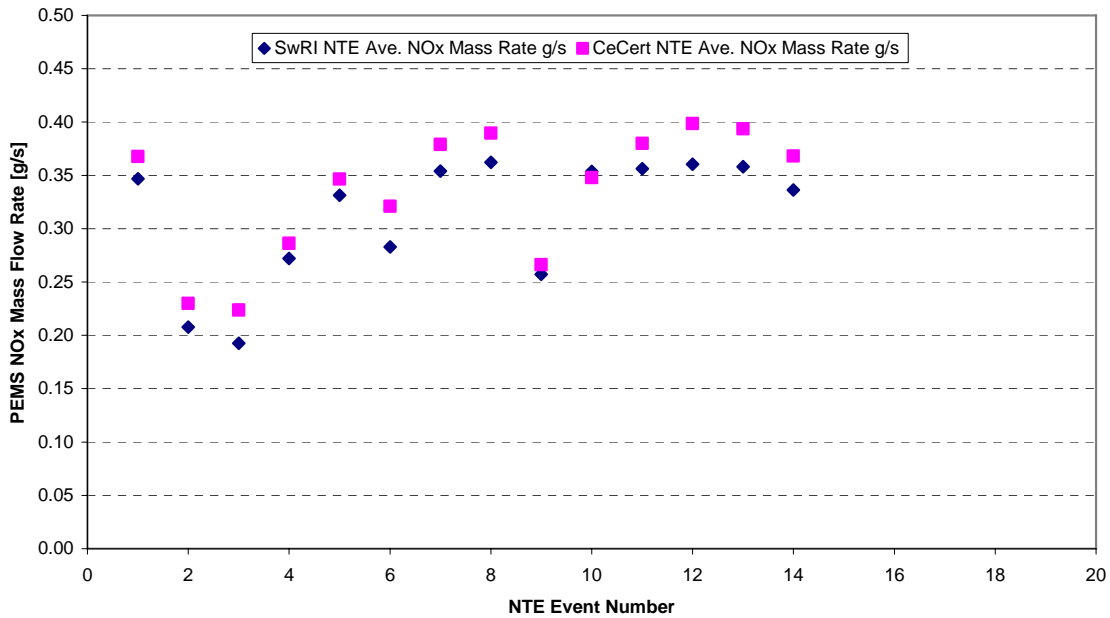


FIGURE 241. PEMS 5 NO_x MASS FLOW RATE COMPARISON FOR SWRI LABORATORY TESTING AND CE-CERT ON-ROAD VALIDATION TESTING (ROUTE 2)

Brake-specific emission results for each NTE event were calculated with data from PEMS 5 using the three different calculation methods for each cycle repeat. The PEMS relied on ECM broadcast parameters to calculate the work term of each calculation method. Based on Caterpillar's recommendation, the percent torque, percent friction torque, and reference torque J1939 CAN broadcast channels were used to estimate torque. ECM broadcast fuel rate was used with the ECM torque estimation to calculate BSFC. The PEMS brake-specific emission results were compared to the laboratory dilute reference brake-specific emission results. The laboratory reference calculation method used torque from the inline torque meter to determine work.

The NO_x emission deltas for PEMS 5 using calculation Method 1 are shown in Figure 242. Cycle 1 deltas were relatively small, with most NO_x deltas between -0.05 and 0.1 g/(hp·hr). Cycle 2 and 3 deltas, however, were unexpected large, with deltas ranging from 0.0 to 0.6 g/(hp·hr) for NO_x. To insure the large deltas were not caused by a problem with PEMS 5, cycle 1 and 2 data was compared for PEMS 4. The PEMS 4 and 5 delta results were similar, indicating PEMS 5 was functioning properly. There was also concern that the altitude simulation was causing PEMS measurement errors or errors with the ECM broadcast torque and fuel rate parameters. Due to the experimental setup, the PEMS sample line and EFM were the only components of the measurement system subjected to the reduced pressure during the cycle 2 and 3 altitude simulation. With all other PEMS ports referenced to ambient pressure, the PEMS was near the fault limit for sample vacuum. To insure the altitude simulation was not the cause of the increased brake-specific deltas, cycle 3 was repeated with no altitude simulation, as was done with cycle 1. PEMS 5 cycle 3 deltas were similar with and without altitude simulation, indicating the altitude simulation did not affect the PEMS measurements or the ECM broadcast torque information. Similarly, the PEMS concentration data, as compared to the laboratory raw concentration measurements, showed no susceptibility to the reduced pressure at the sample line inlet.

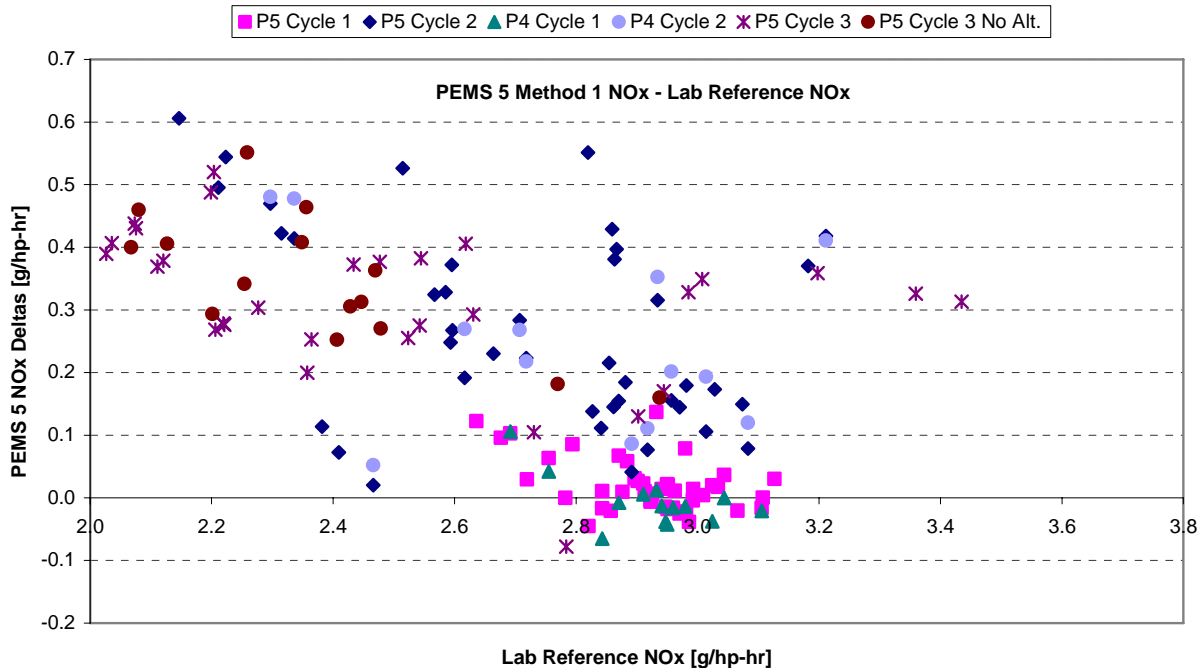


FIGURE 242. BRAKE-SPECIFIC NO_x EMISSION DELTAS FOR PEMS 5 METHOD 1 CALCULATION VERSUS THE LABORATORY REFERENCE (LABORATORY TORQUE AND BSFC)

With the cause of the substantial brake-specific deltas unknown, SwRI performed another comparison between the PEMS and the laboratory NTE emission results. During the second comparison, the laboratory used the ECM broadcast parameters used by the PEMS to perform calculation by Method 1, 2, and 3. With similar torque, fuel rate, and BSFC values, as well as similar calculation techniques, this second computational exercise was a comparison of emission mass. The second SwRI correlation was similar to the comparison process used during the CE-CERT on-road validation testing. The reprocessed Method 1 brake-specific deltas for the PEMS versus the laboratory are shown in Figure 234. The large deltas observed during the PEMS comparison to the laboratory reference are significantly diminished when similar torque and BSFC terms are used for the PEMS and laboratory.

During altitude simulation, the PEMS EFM was subjected to pressures lower than ambient pressure. According to Sensors Inc., the EFM static pressure measurement system was not designed to operate with the EFM below the ambient pressure recorded by the barometric pressure sensor in the PEMS. Therefore, operation with the EFM at reduced pressure and the PEMS at ambient pressure caused inaccurate flow measurement. Cycle 3, at 3500 feet of elevation simulation, showed similar brake-specific results with and without altitude simulation. Therefore, the EFM was not likely affected by the 3500 elevation simulation. However, cycle 2, at 4500 feet of elevation simulation, showed brake-specific deltas nearly double those measured during cycle 2 testing. The EFM static pressure measurement problem may have caused the increased deltas observed for cycle 2.

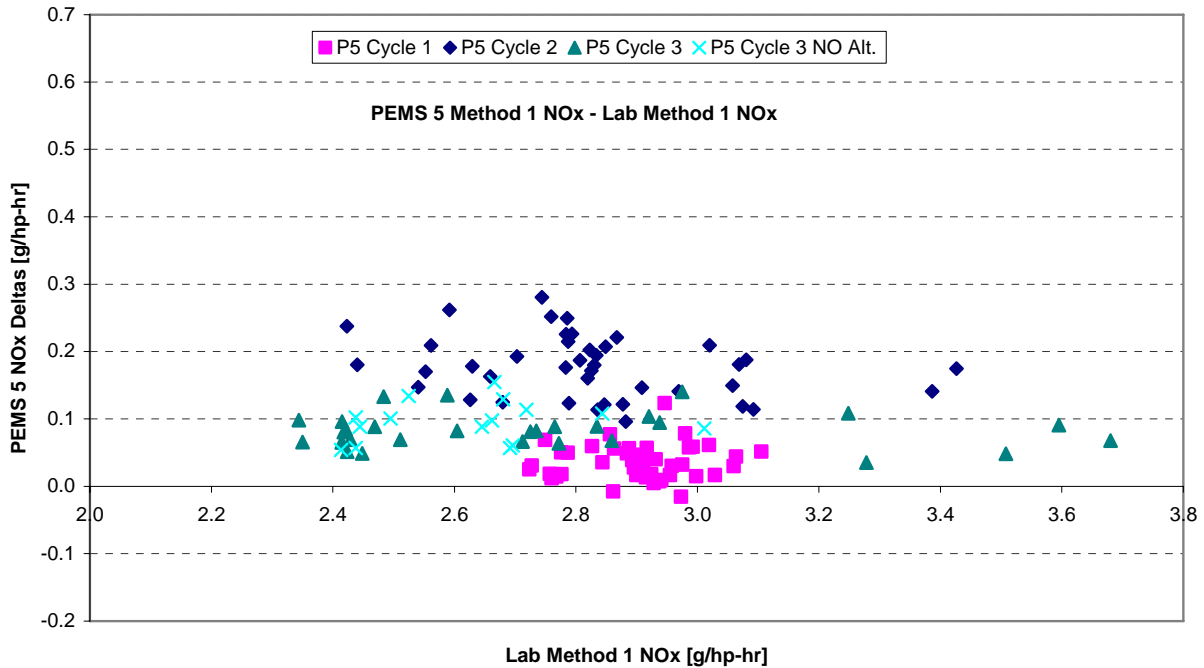


FIGURE 243. BRAKE-SPECIFIC NO_x EMISSION DELTAS FOR PEMS 5 METHOD 1 CALCULATION VERSUS THE LABORATORY METHOD 1 CALCULATION (ECM TORQUE AND BSFC)

The purpose of the replay testing was to compare the ECM torque and BSFC errors measured with the Caterpillar C15 engine to the incremental torque and BSFC errors predicted by the Model. As mentioned earlier, two deltas had been generated for each calculation method in comparing the PEMS brake-specific values to the Laboratory values. The “full” deltas, shown in Figure 242, were calculated using the lab measured torque as the basis for the work term. The “mass” deltas, shown in Figure 243, were calculated using ECM torque, fuel rate, and BSFC for the laboratory as well as the PEMS. For each calculation method, an incremental “work” delta was generated by comparing the associated “full” delta to the appropriate “mass” delta. As shown in the equation below, this calculation was performed individually for each replay NTE event.

$$\Delta_{replay,Work} = \Delta_{replay,Full} - \Delta_{replay,Mass}$$

The Caterpillar C15 Method 1 work deltas generated using the equation above are shown in Figure 244. The work deltas are cycle dependant and showed errors as large as those calculated for the full replay. Therefore, the ECM torque and fuel rate errors were a key cause of the brake-specific deltas observed in Figure 242.

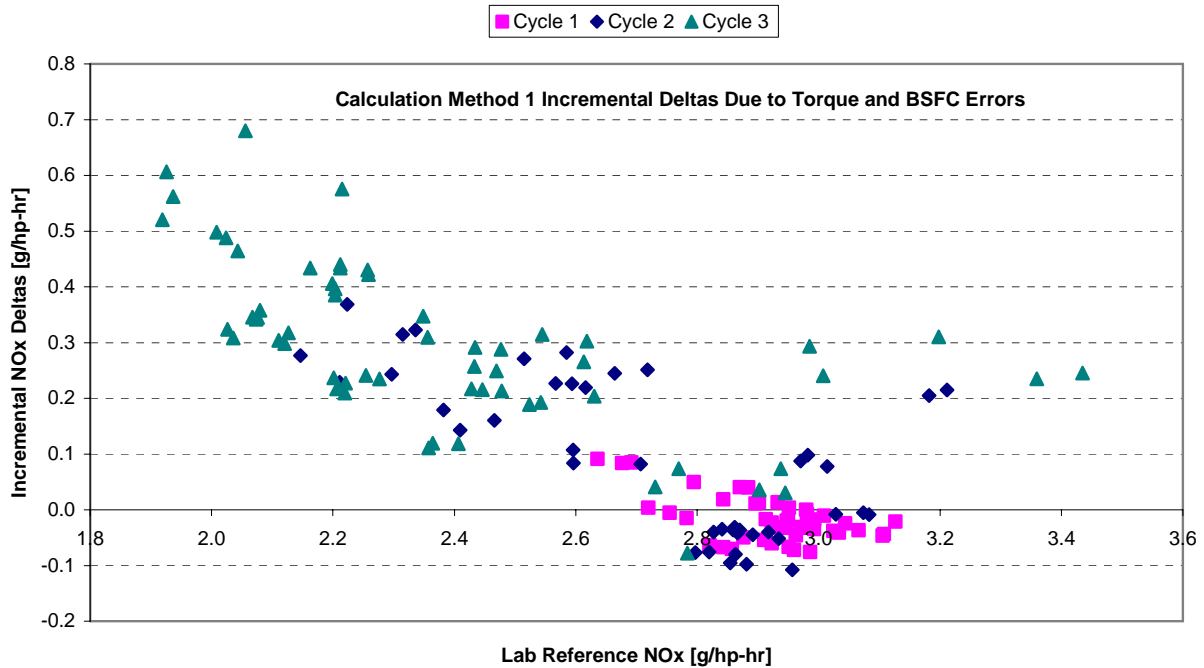


FIGURE 244. INCREMENTAL BRAKE-SPECIFIC NO_x EMISSION DELTAS DUE TO ECM TORQUE AND BSFC ERRORS FOR CALCULATION METHOD 1

The incremental torque and BSFC deltas predicted by the Model were determined by comparing the results of the Full Model to the results of the Validation Model. The distinction between these two sets of model results was described earlier in Section 2.1.11. The Full Model results were calculated with all error surfaces active, including the torque and BSFC error surfaces. The Validation Model deltas were calculated with error surfaces related to torque and BSFC inactive. The difference between the Full Model deltas and the Validation Model deltas yield deltas solely due to torque and BSFC error terms in the Model. The calculation shown below was performed on an event-by-event basis for all reference NTE events, generating 195 Model predicted ECM torque and BSFC deltas.

$$\Delta_{Model,Work} = \Delta_{Model,Full} - \Delta_{Model,Validation}$$

The comparison between the ECM torque and BSFC errors measured with the Caterpillar C15 engine to the incremental torque and BSFC errors predicted by the Model are shown in Figure 245 for calculation method number 1. Ideally, the replay torque and BSFC errors would have been less than the incremental torque and BSFC deltas predicted by the model. However, it should be noted that some of the replay error data exceeded the predicted values, with some of the replay data work deltas being several times larger than the work deltas predicted by the Model using the calculation given above. As described above, the predicted “work deltas” are the difference between the Full Model and the Validation Model for a given NTE event.

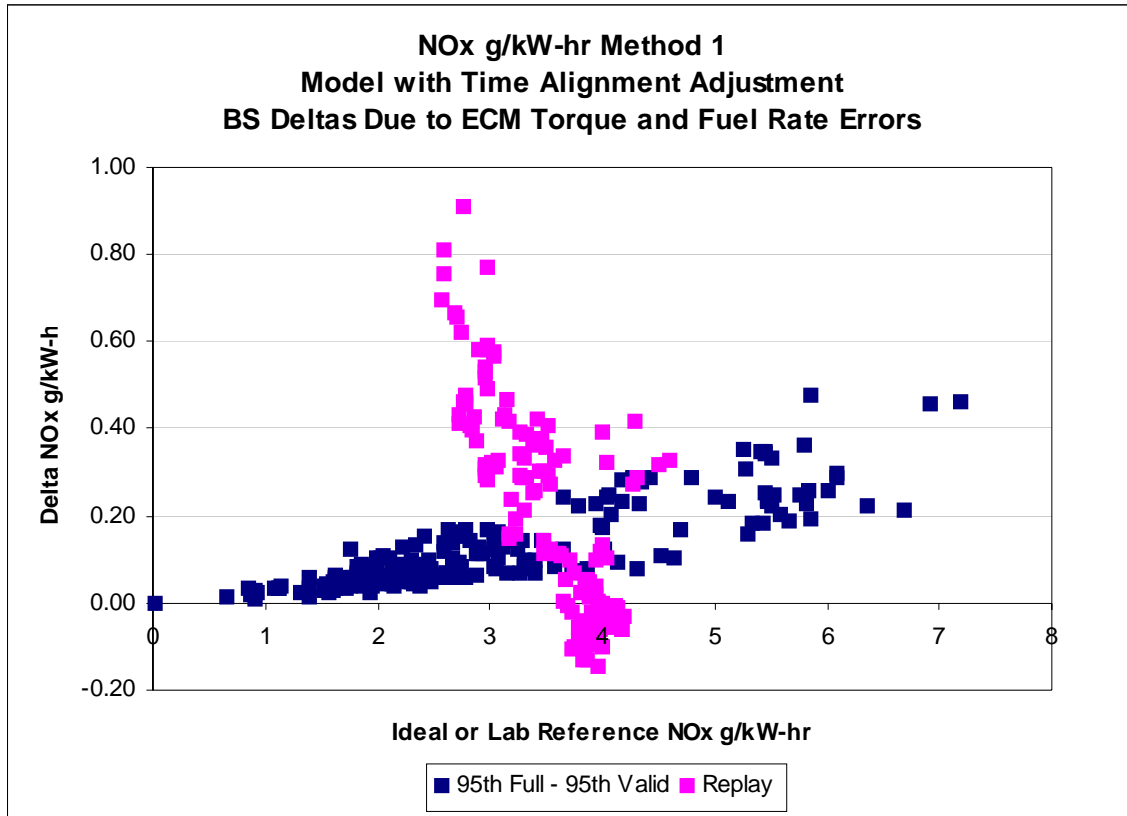


FIGURE 245. INCREMENTAL BRAKE-SPECIFIC NO_x DELTAS COMPARED TO THE INCREMENTAL TORQUE AND BSFC ERRORS PREDICTED BY THE MODEL FOR CALCULATION METHOD 1

Figure 246 shows the brake-specific NO_x emission results for PEMS 5 Method 1 calculations versus the laboratory reference emission results for each replay NTE event. The laboratory reference results were calculated using torque measured with the inline torque meter. Similar to the Method 1 calculations, Method 1 calculations with cycle 1 resulted in relatively small deltas, while cycle 2 and 3 had substantially larger brake-specific emission errors.

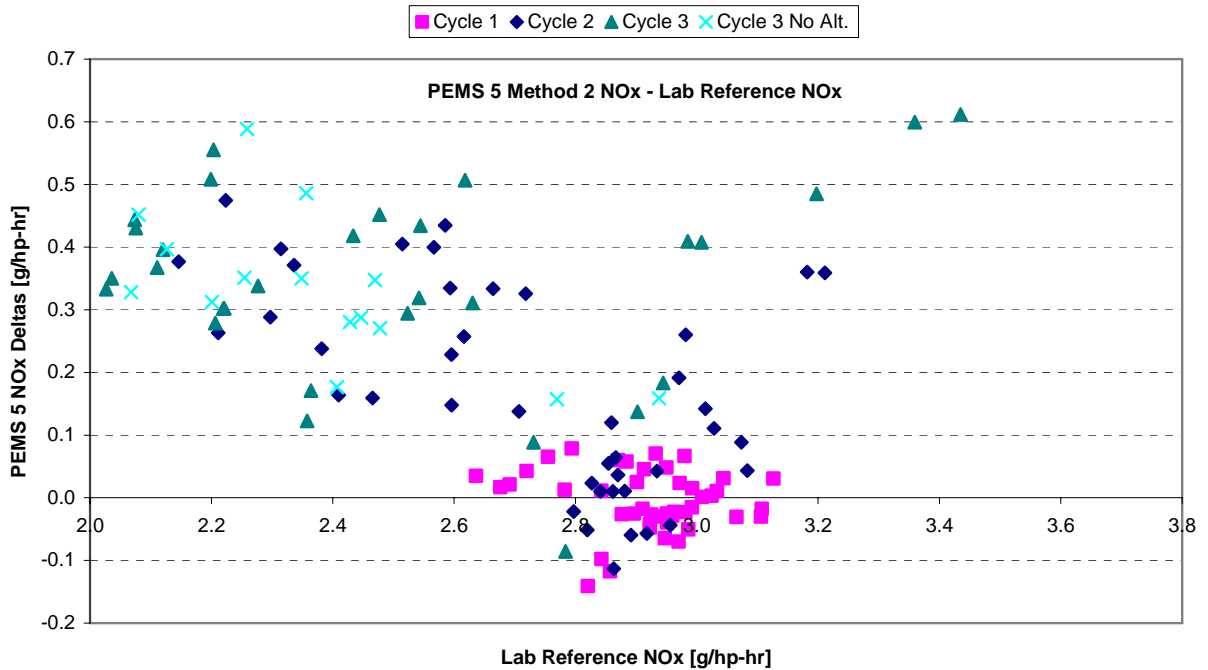


FIGURE 246. BRAKE-SPECIFIC NO_x EMISSION DELTAS FOR PEMS 5 METHOD 2 CALCULATION VERSUS THE LABORATORY REFERENCE (LABORATORY TORQUE AND BSFC)

As described previously for calculation Method 1, Method 1 brake-specific deltas were also calculated with the laboratory using ECM torque and fuel rate as well as the Method 1 emission calculation procedure. Using similar torque, fuel rate, and BSFC terms, PEMS 5 brake-specific NO_x results were similar to the laboratory dilute results. Essentially a comparison of NTE mass, the results indicate the large brake-specific errors observed in Figure 246 were due to torque and BSFC errors.

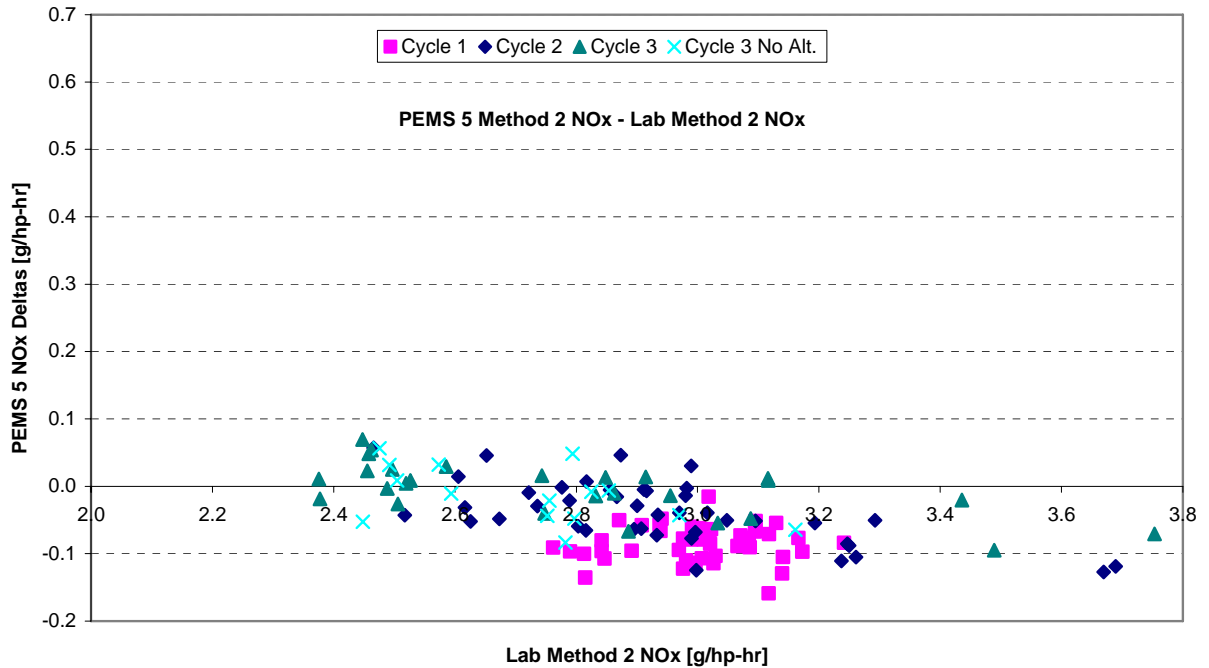


FIGURE 247. BRAKE-SPECIFIC NO_x EMISSION DELTAS FOR PEMS 5 METHOD 2 CALCULATION VERSUS THE LABORATORY METHOD 2 CALCULATION (ECM TORQUE AND BSFC)

The Method 1 incremental torque and BSFC errors measured during replay testing were calculated by subtracting the full deltas, shown in Figure 246, from the mass deltas shown in Figure 247. Shown in Figure 248, Method 1 torque and BSFC errors accounted for the majority of the error observed when the PEMS brake-specific NO_x results were compared to the laboratory reference results.

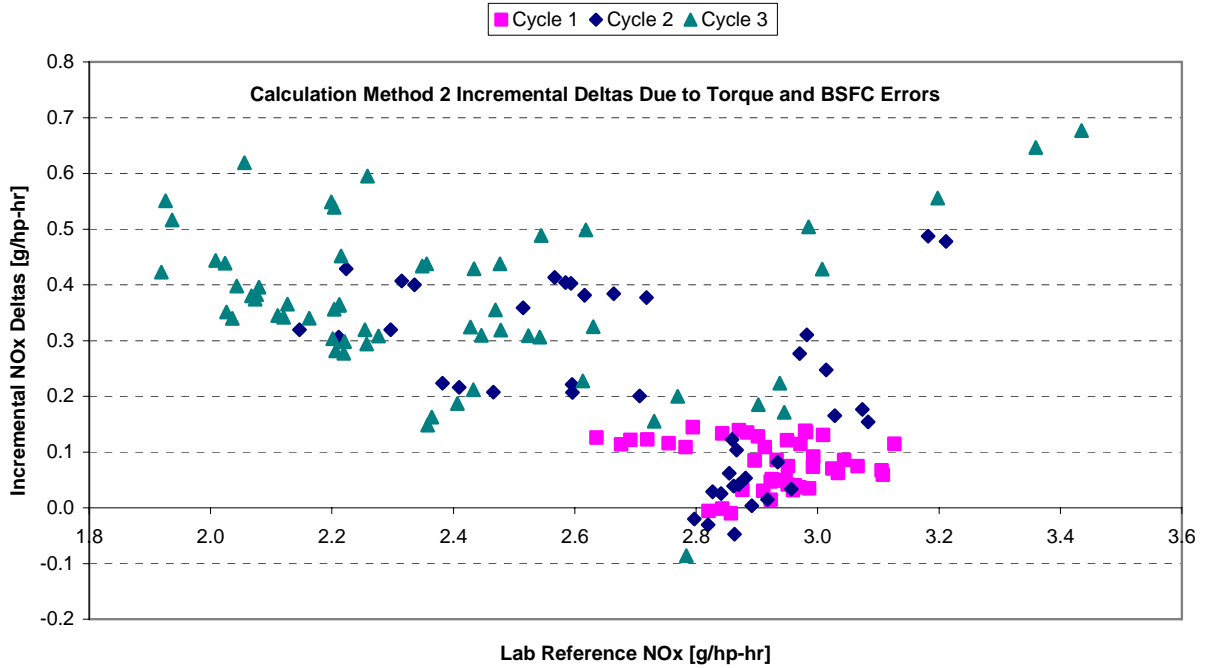


FIGURE 248. INCREMENTAL BRAKE-SPECIFIC NO_x EMISSION DELTAS DUE TO ECM TORQUE AND BSFC ERRORS FOR CALCULATION METHOD 2

Similar to calculation Method 1, the torque and fuel rate errors measured with PEMS 5 using calculation Method 1 were compared to the incremental torque and BSFC errors predicted by the Model. Shown in Figure 249, the Method 1 torque and fuel rate errors measured during replay testing with the Caterpillar C15 engine were considerably larger than the Model prediction.

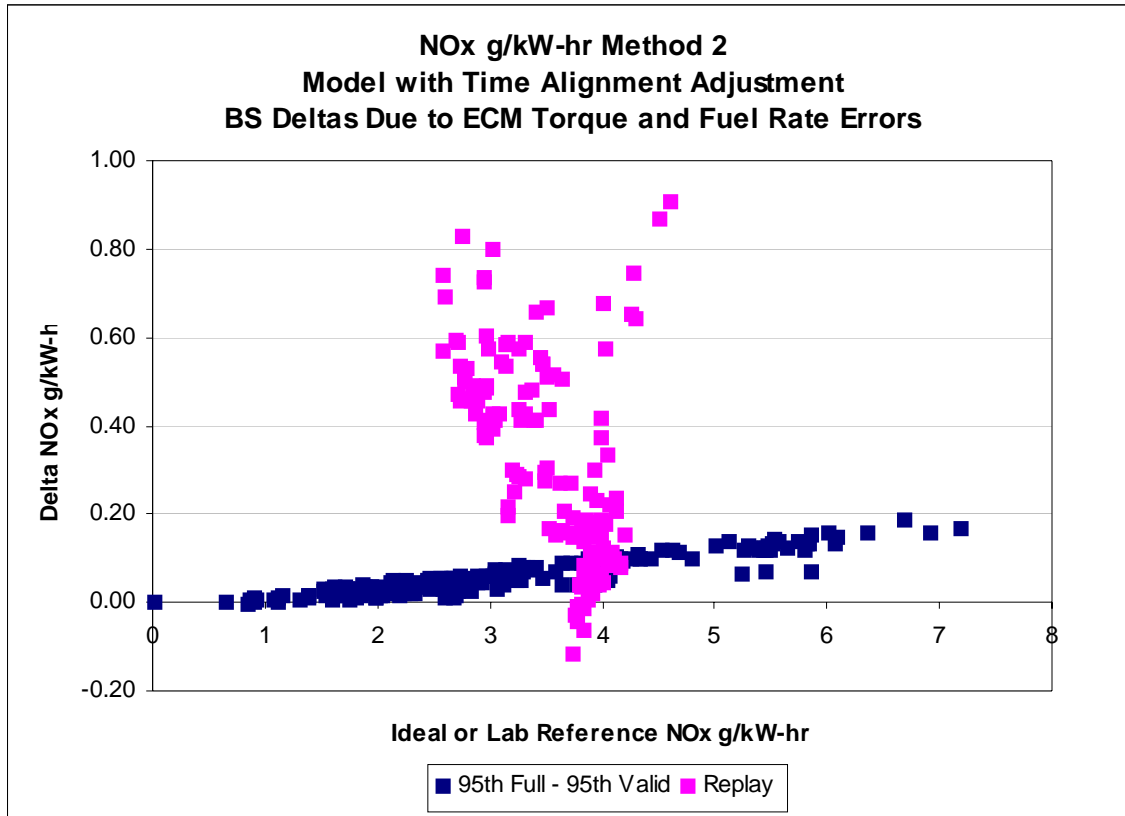


FIGURE 249. INCREMENTAL BRAKE-SPECIFIC NO_x DELTAS COMPARED TO THE INCREMENTAL TORQUE AND BSFC ERRORS PREDICTED BY THE MODEL FOR CALCULATION METHOD 2

Because it was decided to calculate BSFC for the PEMS using ECM broadcast torque and fuel rate, Method 1 and 3 calculations were nearly identical. Therefore, the Method 1 brake-specific emission results and conclusions were similar to calculation Method 1. Figure 250 shows the PEMS 5 Method 1 brake-specific NO_x deltas when compared to the laboratory reference emission calculation method. Similar to Method 1 and 2, Method 1 cycle 2 and 3 deltas were unexpectedly large, while cycle 1 deltas were notably reduced.

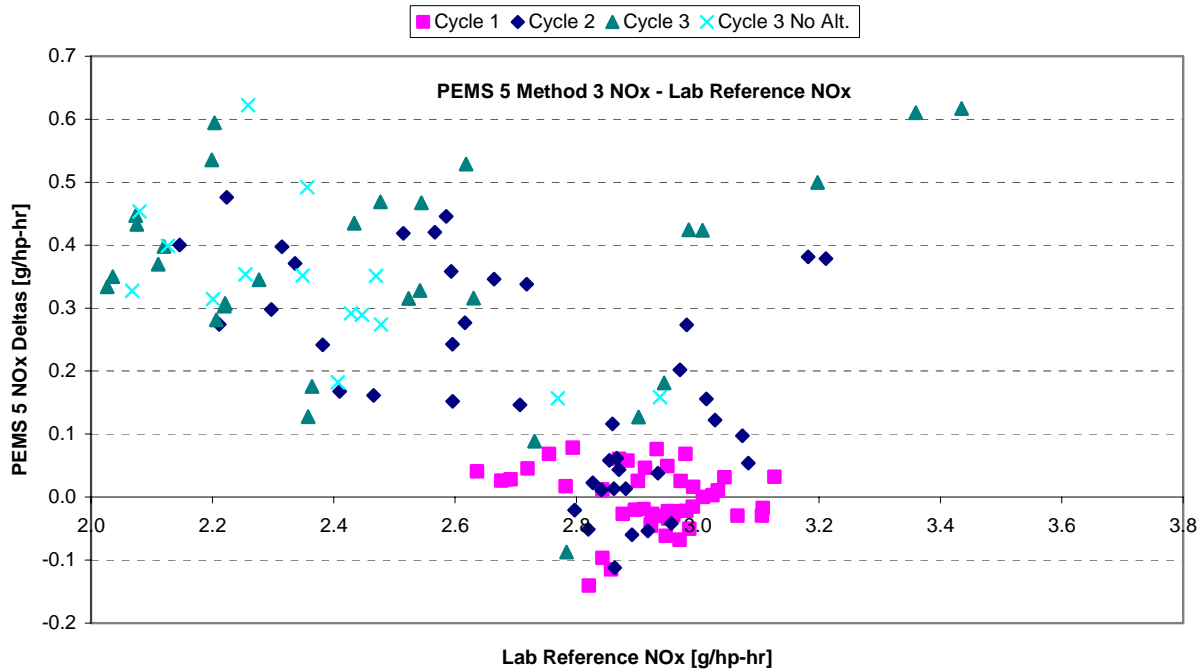


FIGURE 250. BRAKE-SPECIFIC NO_x EMISSION DELTAS FOR PEMS 5 METHOD 3 CALCULATION VERSUS THE LABORATORY REFERENCE (LABORATORY TORQUE AND BSFC)

Figure 251 shows the brake-specific PEMS 5 deltas when the laboratory used the ECM torque, fuel rate, and BSFC values to calculation brake-specific emissions. When torque and BSFC errors were removed from the PEMS and laboratory comparison, thus yielding a mass comparison, the deltas for the three cycles collapsed, with most errors between -0.1 and 0.1 g/(hp·hr). Therefore, ECM torque and fuel rate errors were the key factors driving the large cycle 2 and 3 deltas shown in Figure 250.

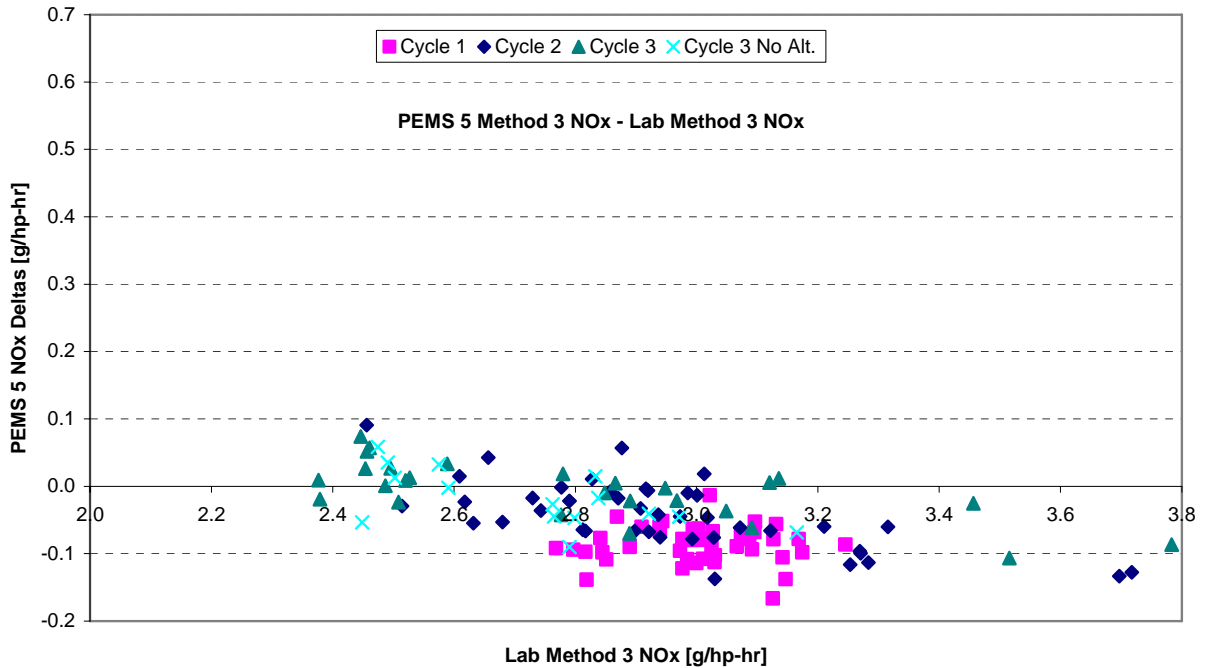


FIGURE 251. BRAKE-SPECIFIC NO_x EMISSION DELTAS FOR PEMS 5 METHOD 3 CALCULATION VERSUS THE LABORATORY METHOD 3 CALCULATION (ECM TORQUE AND BSFC)

Figure 252 shows the incremental ECM torque and BSFC errors measured during replay testing. These deltas were determined by taking the difference between the PEMS errors calculated against the laboratory reference results and the PEMS errors calculated against the laboratory results using ECM torque and BSFC. Similar to the other calculation methods, Method 1 ECM torque and fuel rate errors were large in comparison to the mass emission deltas shown in Figure 251.

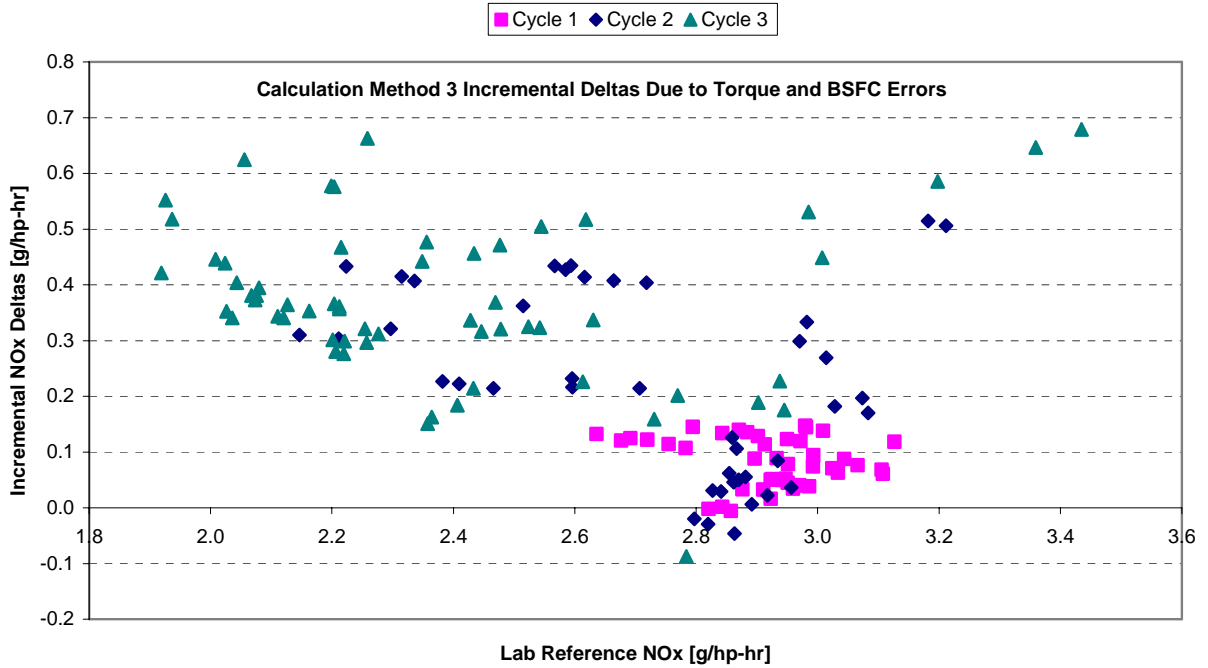


FIGURE 252. INCREMENTAL BRAKE-SPECIFIC NO_x EMISSION DELTAS DUE TO ECM TORQUE AND BSFC ERRORS FOR CALCULATION METHOD 3

Similar to calculation Method 1 and 2, the torque and fuel rate errors measured with PEMS 5 using calculation Method 1 were compared to the incremental Method 1 torque and BSFC errors predicted by the Model. Shown in Figure 253, the Method 1 torque and fuel rate errors measured during replay testing with the Caterpillar C15 engine were considerably larger than the Model prediction.

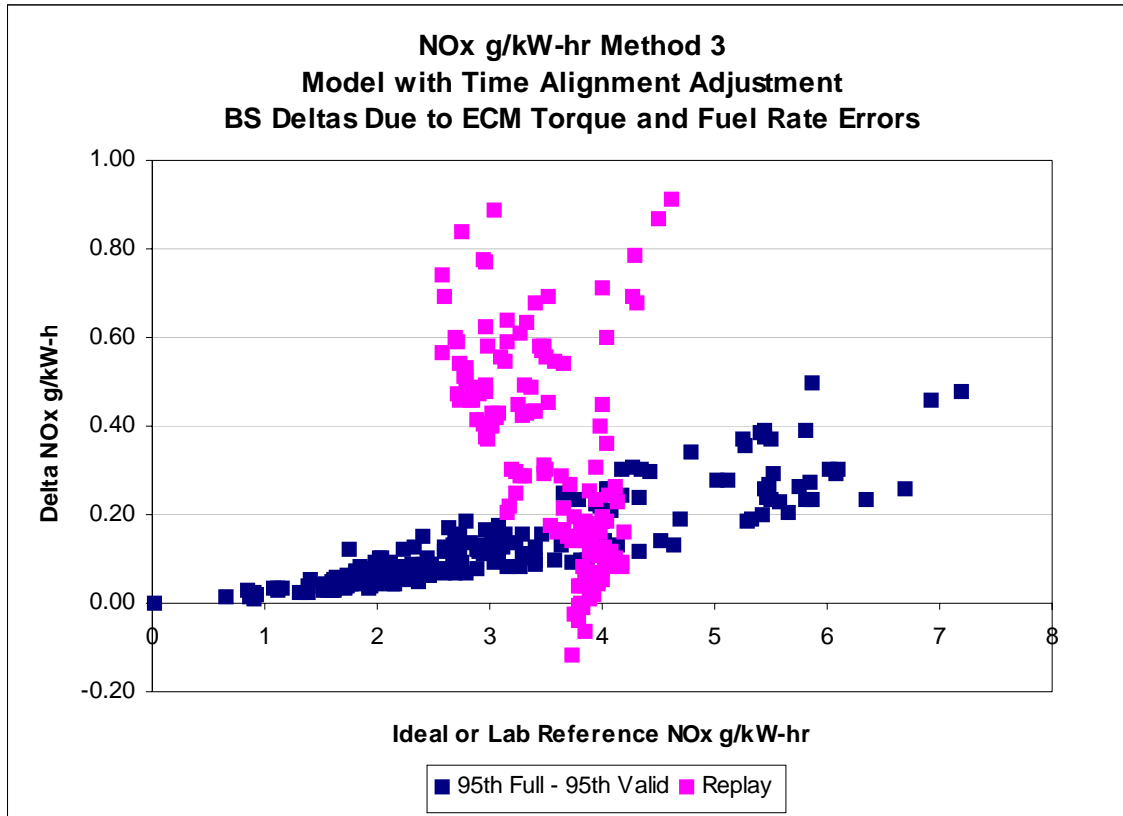


FIGURE 253. INCREMENTAL BRAKE-SPECIFIC NO_x DELTAS COMPARED TO THE INCREMENTAL TORQUE AND BSFC ERRORS PREDICTED BY THE MODEL FOR CALCULATION METHOD 3

A number of additional comparisons were calculated to determine the cause of the large work deltas observed between the ECM broadcast parameters and the laboratory reference methods. As shown in Figure 254, the NTE average ECM torque was compared to the laboratory inline torque meter. As discussed previously, the brake-specific deltas were calculated using the percent torque, percent friction torque, and reference torque J1939 CAN broadcast channels. Cycle 1 torque deltas were well within $\pm 5\%$ of point. However, cycle 2 and 3 deltas showed deltas ranging from -10 to -15 % at lower levels. Torque deltas appeared to be a function of torque level, with high torque level deltas having significantly less error than at lower torque levels. Cycle 3 torque deltas were also examined with no altitude simulation as well as with no boost leak. The additional tests showed torque errors similar to the original altitude test, indicating the altitude simulation and boost leak had little effect on the ECM's torque prediction. Per Caterpillar's request, PEMS torque deltas were also calculated using the percent load at current speed CAN broadcast channel with the engine's lug curve. Using the lug curve generated at SwRI, the torque deltas were within $\pm 5\%$ of point. However, during in-use testing, engine manufacturers would likely use the certification lug curve for the ECM torque estimation. With the certification lug, the ECM torque deltas were also within $\pm 5\%$ of point.

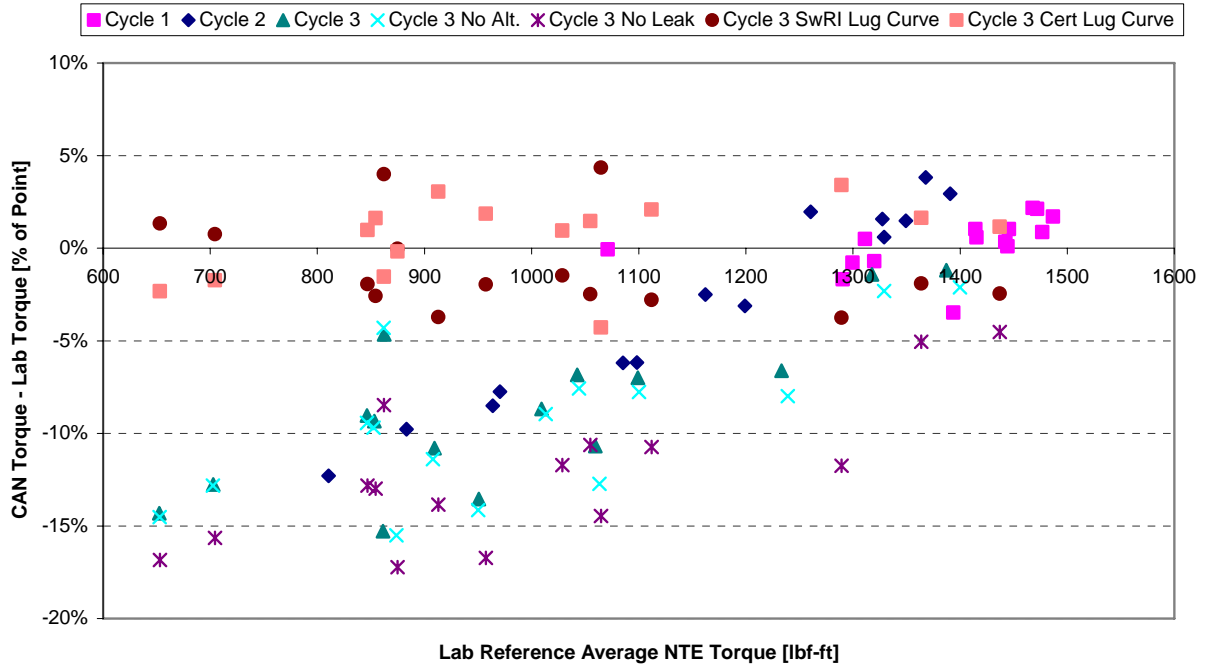


FIGURE 254. ECM BROADCAST TORQUE ERRORS MEASURED DURING REPLAY VALIDATION TESTING WITH A CATERPILLAR C15 ENGINE

NTE event average deltas between the ECM fuel rate and the laboratory dilute carbon balance fuel rate are shown in Figure 255 for the 3 cycles. Most fuel rate errors were between 0 and 6 % of point. The dilute carbon balance error versus the laboratory fuel flow meter was approximately -1.0 to -1.5 %, therefore, the deltas shown in Figure 255 may be approximately 1.0 % high.

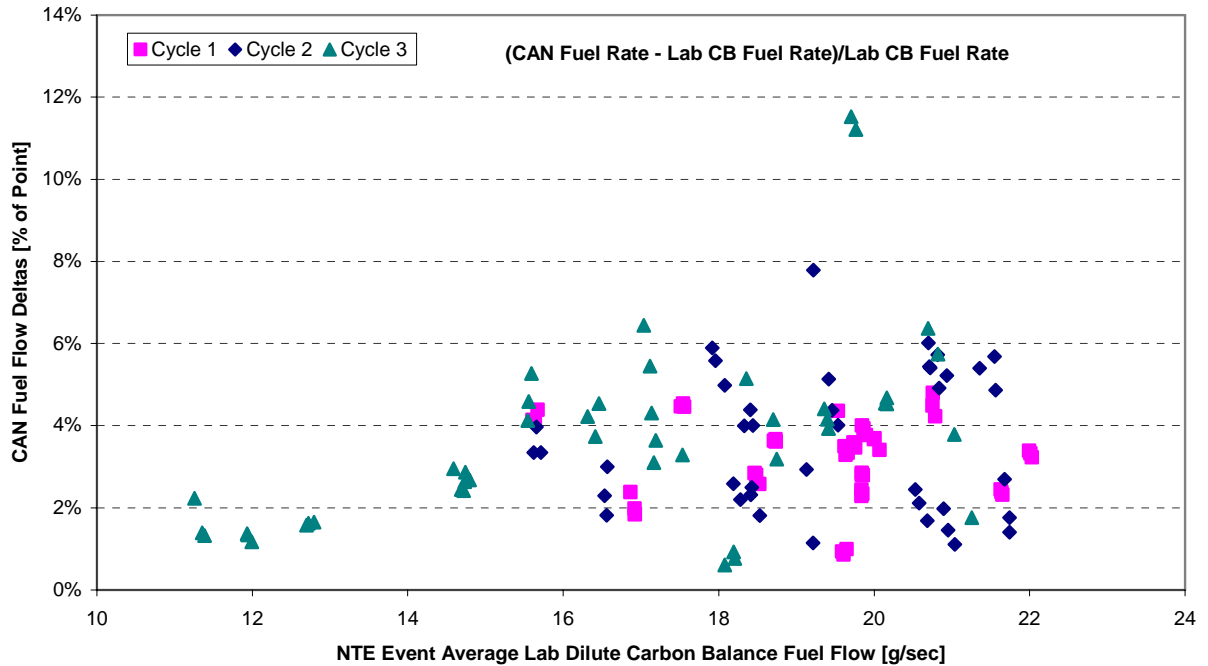


FIGURE 255. ECM BROADCAST FUEL FLOW RATE ERRORS MEASURED DURING REPLAY VALIDATION TESTING WITH A CATERPILLAR C15 ENGINE

The BSFC values used for the PEMS brake-specific emission calculations were calculated using the ECM broadcast torque and fuel rate parameters. The ECM-based BSFC values were compared to the laboratory BSFC results which were calculated using the dilute carbon balance fuel flow and the inline torque meter. The deltas between the ECM and laboratory BSFC are shown in Figure 256. For cycle 1, BSFC deltas were between 0 and 5 % of point. Cycle 2 and 3, however, had significantly higher BSFC deltas, with peak values near 20 %.

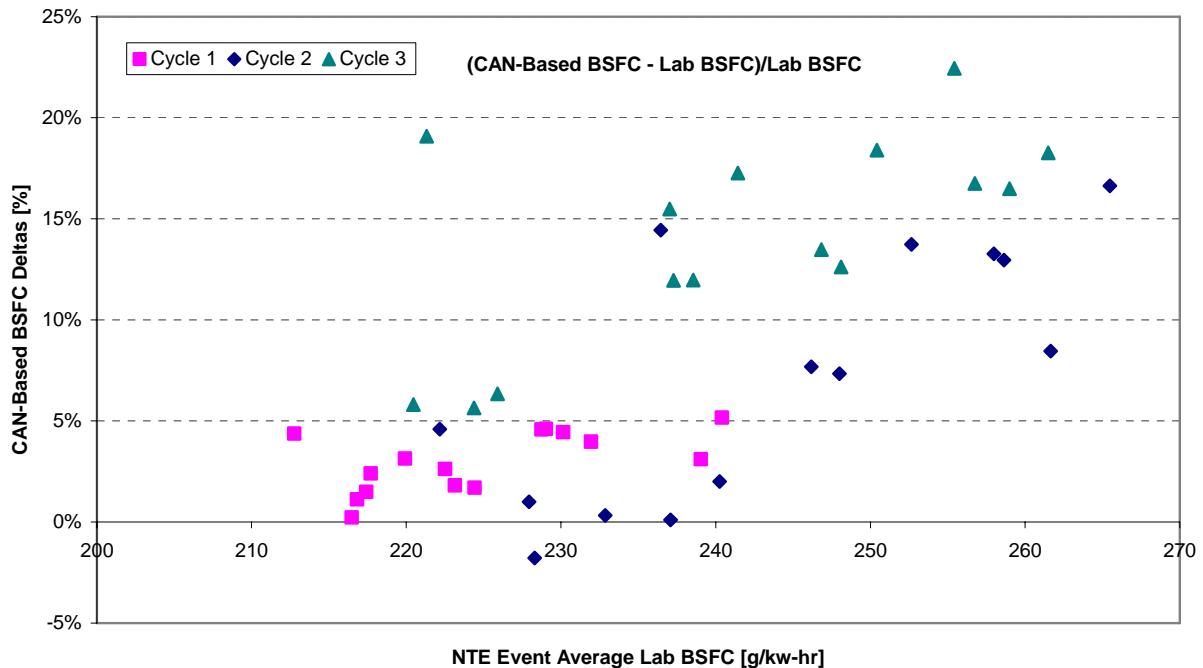


FIGURE 256. ECM-BASED BSFC ERRORS MEASURED DURING REPLAY VALIDATION TESTING WITH A CATERPILLAR C15 ENGINE

After reviewing the ECM torque and BSFC errors measured with the Caterpillar C15 replay engine, the Steering Committee instructed SwRI to calculate ECM torque errors for the other test engines used during the program. Using the 40-point engine map data, the ECM broadcast torque estimates were compared to the laboratory inline torque meter. Figure 257 shows the ECM torque deltas for the Detroit Diesel Series 60 engine. The ECM torque errors were calculated using two methods. One method used the percent torque, percent friction torque, and reference torque J1939 CAN broadcast channels, while the other method used the percent load at current speed CAN broadcast channel with the engine’s certification lug curve. For the DDC engine, the ECM broadcast torque errors were within $\pm 10\%$ of point. Using the DDC certification lug curve, the high level torque errors were similar to the ECM J1939 broadcast torque errors. However, the lug curve method torque errors increased as the steady-state torque level decreased.

According to the J1939 protocol, the percent load at current speed J1939 parameter represents indicated engine torque, not brake torque. Therefore, the lug curve method most likely neglected friction torque, and overestimated brake torque. At high loads, the friction torque error is a small percentage of the total torque, therefore, the difference between indicated torque and brake torque is inconsequential. However, at lighter loads, the friction torque errors become significant, and most likely caused the large lug curve torque deltas shown in Figure 257. The SEMTECH-DS software allows the user to input a curb idle % load value that is used to calculate brake torque from indicated torque. The equation was developed at the University of West Virginia and is shown below. This calculation assumes friction torque is constant during all engine operation.

$$\% _ Load_{Brake} = \frac{ECM _ \% _ Load_{Indicated} - \% _ Load_{Friction}}{100\% - \% _ Load_{Friction}}$$

SwRI did not use the curb idle % load correction when processing the lug curve error data.

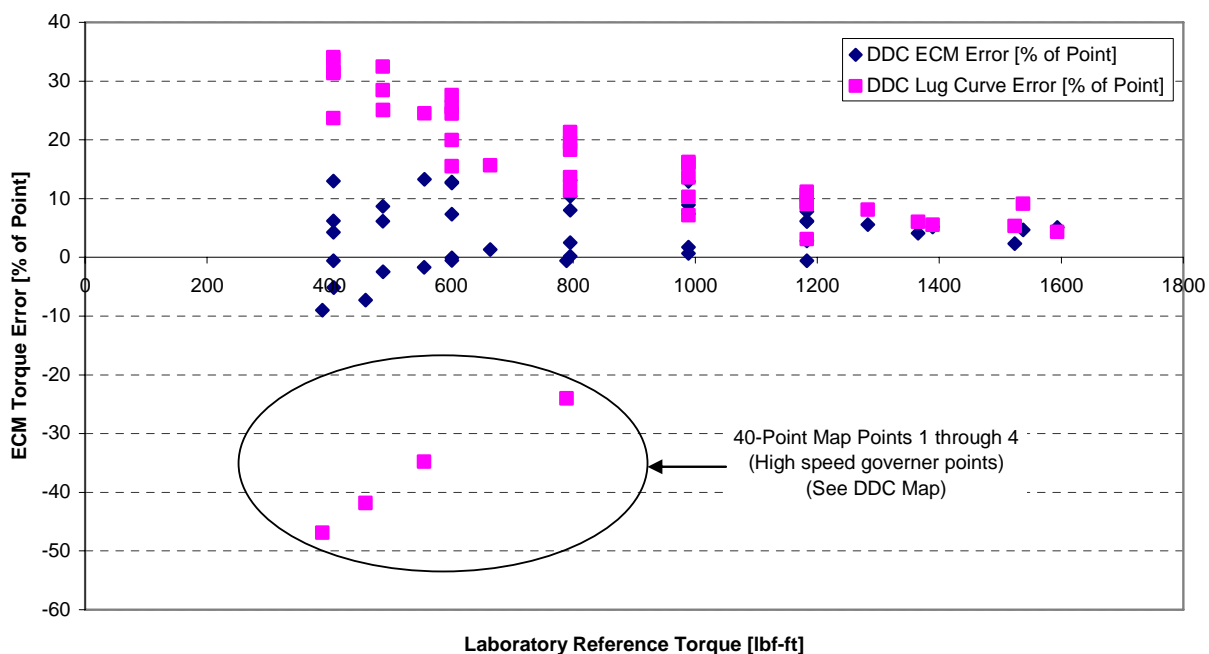


FIGURE 257. ECM BROADCAST TORQUE ERRORS MEASURED DURING 40-POINT MAP GENERATION WITH A DETROIT DIESEL SERIES 60 ENGINE

Figure 258 shows the ECM torque errors for the Caterpillar C9 test engine. The ECM broadcast torque errors were similar to the errors generated using the certification lug curve torque estimation technique. Similar to the DDC engine, torque errors were minimal at high load points, but increased as the load level decreased. Engine 2 had torque errors near 50 % of point at low load points.

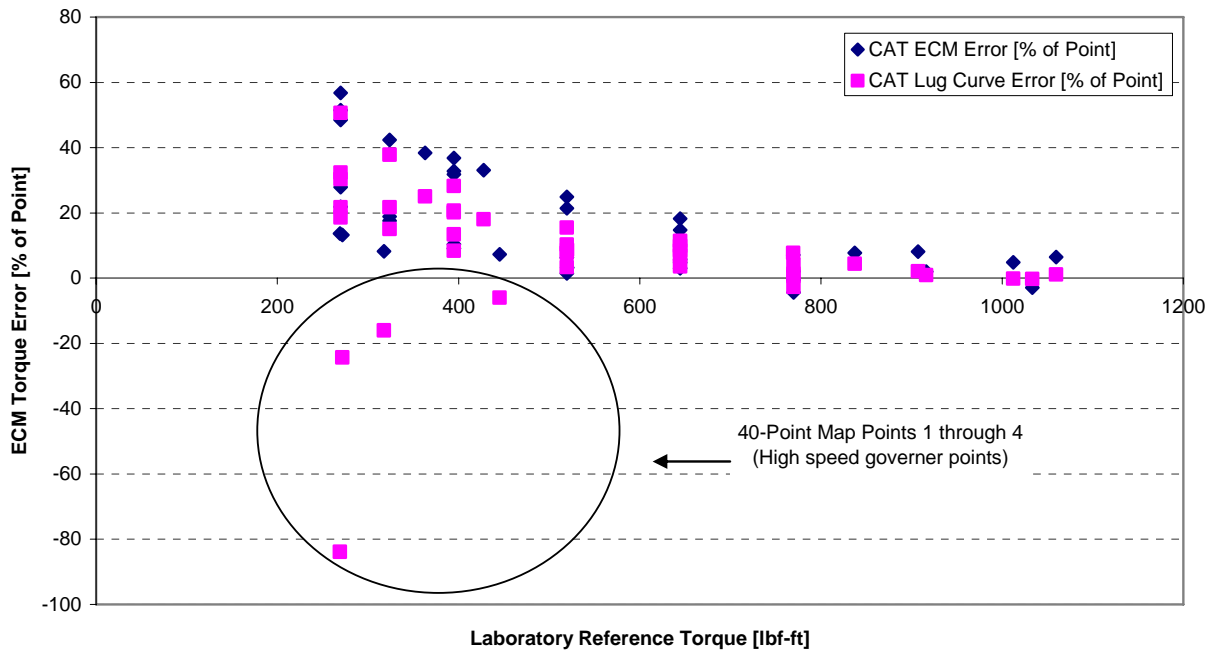


FIGURE 258. ECM BROADCAST TORQUE ERRORS MEASURED DURING 40-POINT MAP GENERATION WITH A CATERPILLAR C9 ENGINE

Figure 259 shows the ECM torque errors for the International VT365 testing engine. The International engine did not broadcast J1939 torque parameters, therefore, J1708 percent load at current speed was used with a certification lug curve to calculate torque. At high torque levels, the ECM torque error was almost 8 % low. Similar to engines 1 and 2, engine 3 torque errors increased as the load level decreased. At the lowest load levels, the torque error was approximately 20 %. For all lug curve torque analysis, the curb idle % load correction was not used.

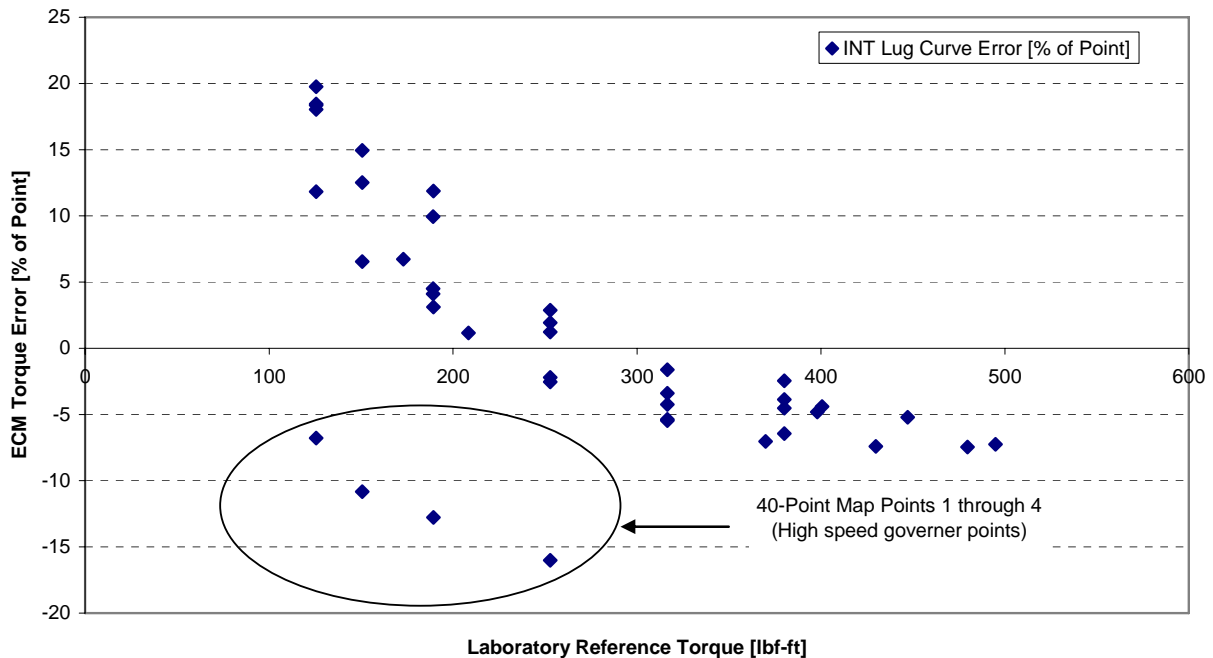


FIGURE 259. ECM BROADCAST TORQUE ERRORS MEASURED DURING 40-POINT MAP GENERATION WITH AN INTERNATIONAL VT365 ENGINE

The ECM torque and BSFC errors measured during replay testing were substantially larger than the incremental torque and BSFC errors predicted by the model, indicating the torque and BSFC portion of the Model did not validate. One potential cause for the Model invalidation was that the deltas of the manufacturer supplied error surfaces for torque and BSFC were far less than the ECM torque and BSFC deltas measured with the replay engine. In fact, the torque deltas for all of the engine exceeded the OEM supplied torque and BSFC errors. A complete discussion of the manufacturer supplied error surfaces can be found in the Torque and BSFC OEMs Supplied Error Surfaces section of the report.

Although the replay engine testing showed torque and BSFC deltas that exceeded the Model prediction, the Steering Committee decided to take no action in regard to the replay validation testing results.

6.10 Validation Results

This section contains a summary of the model validation results, Section 2.1.11 on *Validation* contains a more detailed description of the validation methodology utilized both in the simulation and in the on-road data collection efforts.

During the Monte Carlo simulation of the 195 reference NTE events some of the error surfaces were excluded in the computation of the BS emissions ‘with errors’ so that the simulation represented conditions used in collecting the on-road data. The error surfaces excluded were torque errors (# 29-32, 34, 35), BSFC errors (#36-39, 41, 42), dynamic speed

(#43) and dynamic fuel rate (#44). As described earlier in Section 2.1.11, this was necessary due to the fact that there was no reference torque or reference fuel flow measurement during on-road data collection. Therefore it would not be appropriate to use these error terms from the simulation when comparing to the on-road data set, as the on-road data set would not include any errors generated from those measurements. For each reference NTE event, the differences in BS emissions were computed as:

$$\text{delta BS emissions} = \text{BS emissions with "Validation error"} - \text{"Ideal" BS emissions.}$$

These delta emissions were computed for each of the three emissions and all three calculation methods. The validation results also included time alignment and checks for periodic drift.

The on-road results were gathered from selected routes driven to collect emissions data with a CE-CERT trailer and a PEMS installed in the tractor pulling the trailer (see Section 2.1.11 on *Validation*). For each on-road NTE event, a delta BS emissions value was computed as

$$\text{delta BS emissions} = \text{PEMS BS emissions} - \text{CE-CERT BS emissions.}$$

These differences were computed for all three emissions and three calculation methods. The on-road delta BS emissions were calculated from 81 NTE events for BSNO_x and 87 NTE events for BSNMHC and BSCO selected by the Steering Committee from the original set of data collected on-road. All of the NTE events selected from the on-road data were drift corrected.

From the MC simulations, the 5th and 95th percentile delta BS emissions were extracted from the output files for each reference NTE event. These percentiles were then plotted as empirical distribution functions (edf) to form a validation interval for the on-road data. Also plotted was the edf computed from the on-road NTE events. Figure 260 represents the validation plot for the BSNO_x Method 1 analyses. Since all of the on-road delta BSNO_x emissions fell within the 5th and 95th percentiles of the simulation results the model was validated for this method and emissions.

Validation Analysis 5th and 95th Percentile Deltas
 Compared Ref NTE #1-195 to Corrected 81 CE-CERT Deltas
 NO_x (g/kW-hr) Method 1

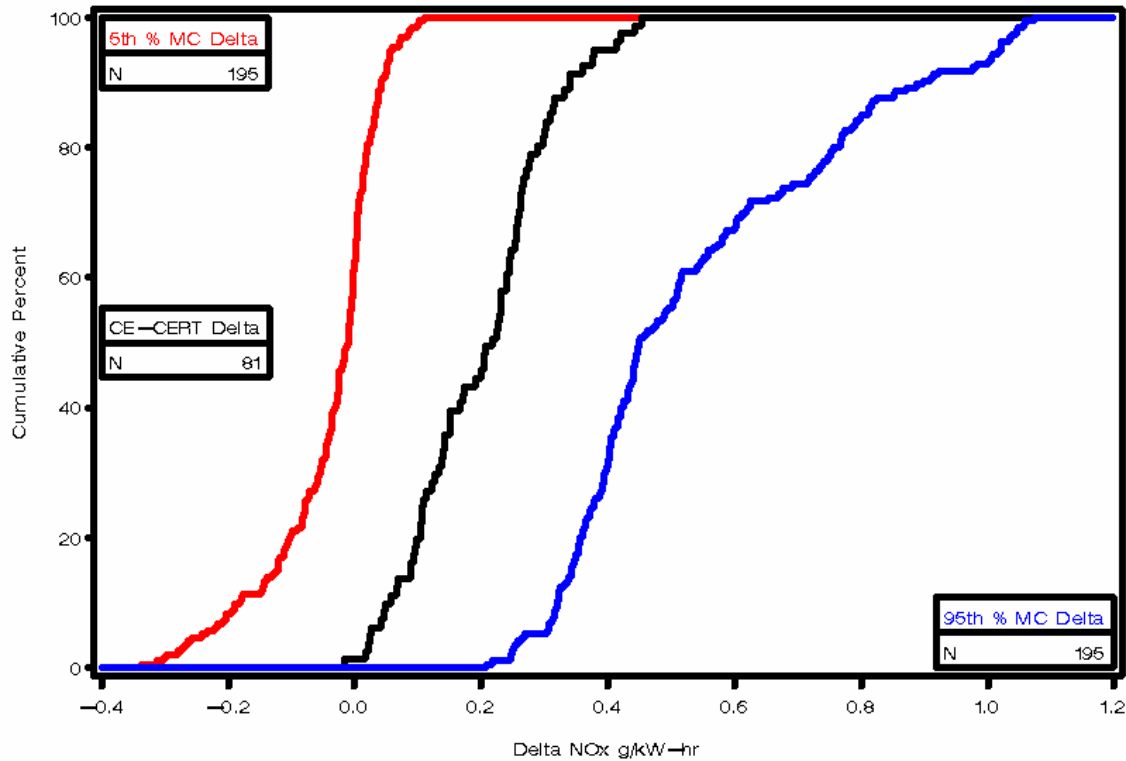


FIGURE 260. VALIDATION ON-ROAD AND MODEL GENERATED EMPIRICAL DISTRIBUTION FUNCTIONS FOR BSNO_x METHOD 1

The validation edf plot for the BSNO_x Method 2 results is shown in Figure 261. Note that approximately 45% of the on-road delta BSNO_x emissions fell above the 95th percentile deltas from the simulation model. Thus, the model was not considered valid for the BSNO_x Method 2 results.

Validation Analysis 5th and 95th Percentile Deltas
 Compared Ref NTE #1-195 to Corrected 81 CE-CERT Deltas
 NO_x (g/kW-hr) Method 2

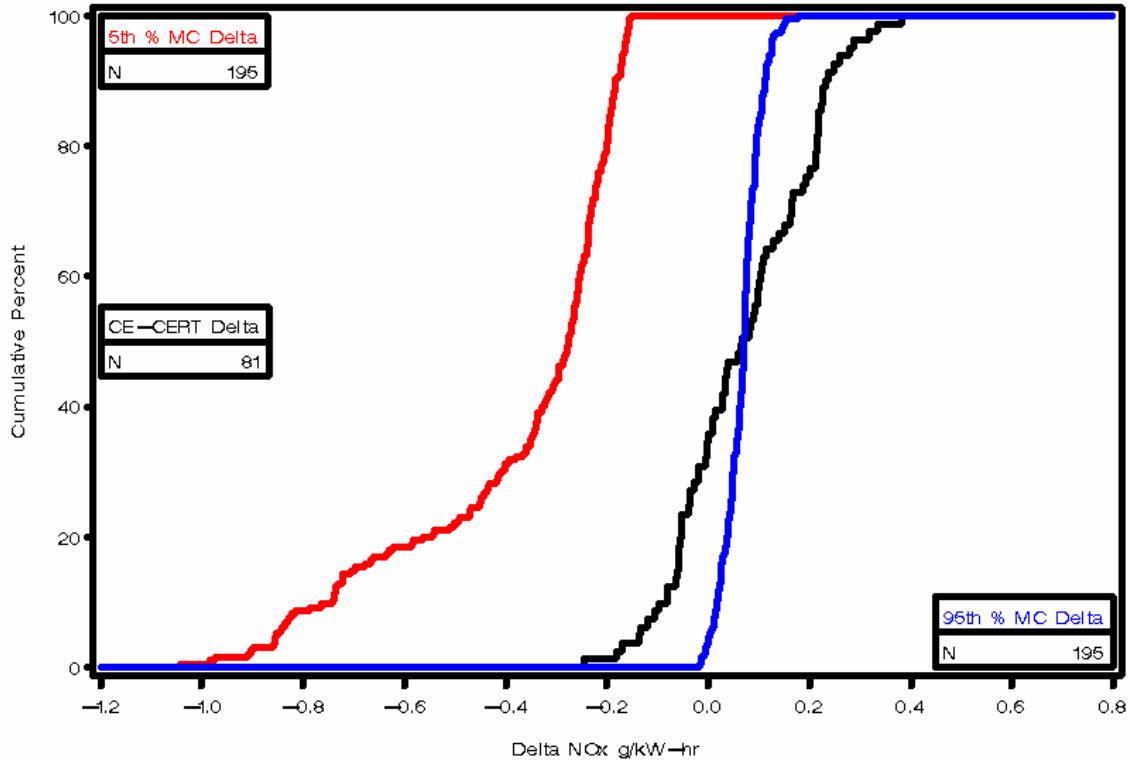


FIGURE 261. VALIDATION ON-ROAD AND MODEL GENERATED EMPIRICAL DISTRIBUTION FUNCTIONS FOR BSNO_x METHOD 2

The validation edf plot for the BSNO_x Method 3 results is shown in Figure 262. Note that approximately 55% of the on-road delta BSNO_x emissions fell above the 95th percentile deltas from the simulation model. Thus, the model was not considered valid for the BSNO_x Method 3 results.

Validation Analysis 5th and 95th Percentile Deltas
 Compared Ref NTE #1-195 to Corrected 81 CE-CERT Deltas
 NO_x (g/kW-hr) Method 3

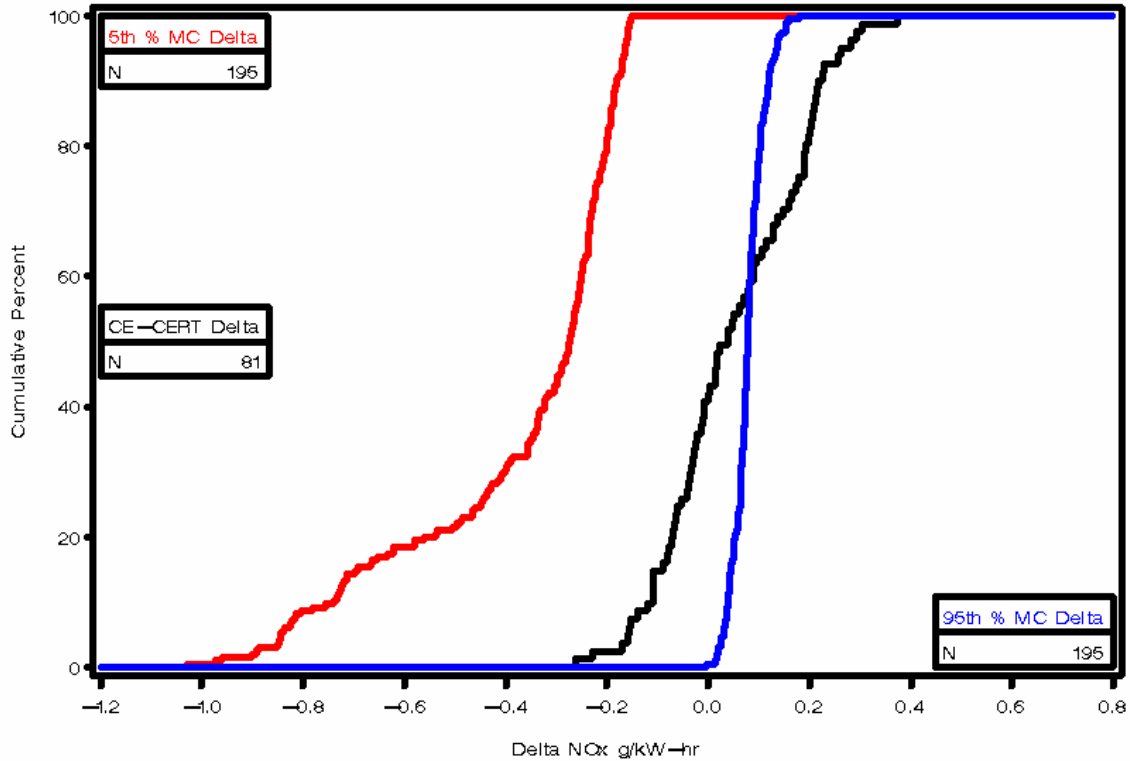


FIGURE 262. VALIDATION ON-ROAD AND MODEL GENERATED EMPIRICAL DISTRIBUTION FUNCTIONS FOR BSNO_x METHOD 3

Figure 263 through Figure 265 represent the validation plots for the BSNMHC analyses for Methods 1, 2 and 3, respectively. Since the entire on-road delta BSNMHC emissions fell within the 5th and 95th percentiles of the simulation results the model was validated for all three methods for BSNMHC emissions.

Validation Analysis 5th and 95th Percentile Deltas
Compared Ref NTE #1-196 to Corrected 87 CE-CERT Deltas
NMHC (g/kW-hr) Method 1

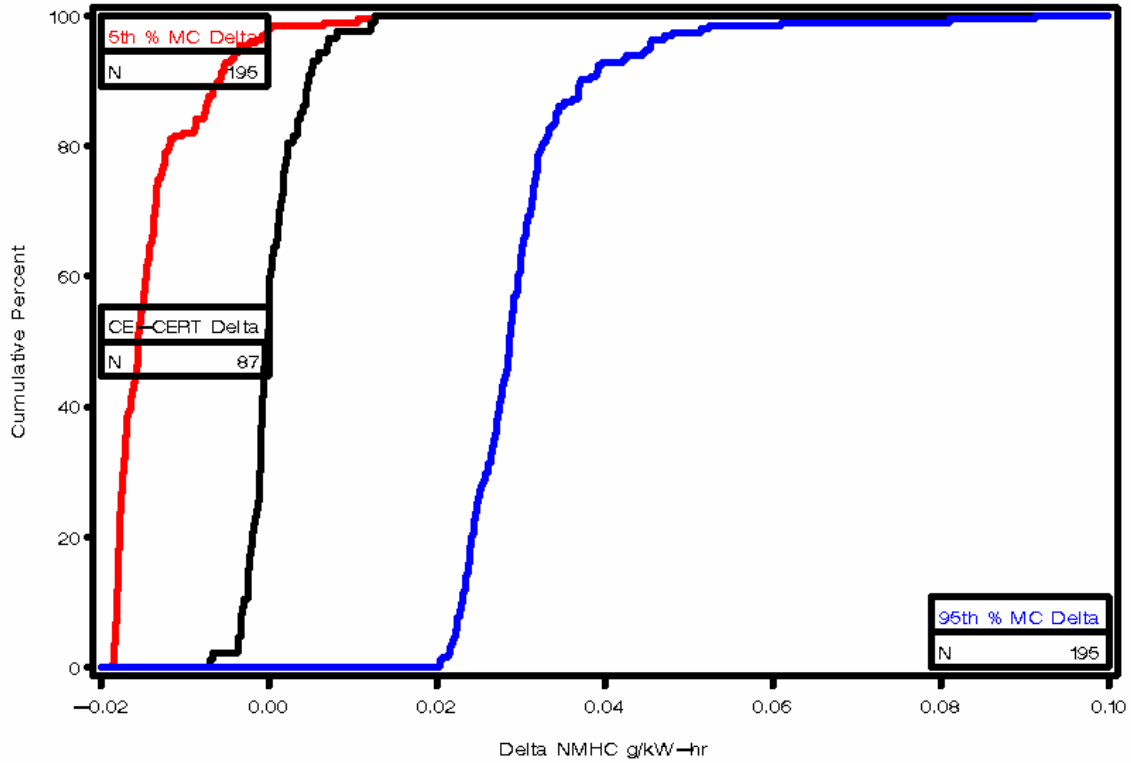


FIGURE 263. VALIDATION ON-ROAD AND MODEL GENERATED EMPIRICAL DISTRIBUTION FUNCTIONS FOR BSNMHC METHOD 1

Validation Analysis 5th and 95th Percentile Deltas
Compared Ref NTE #1-195 to Corrected 87 CE-CERT Deltas
NMHC (g/kW-hr) Method 2

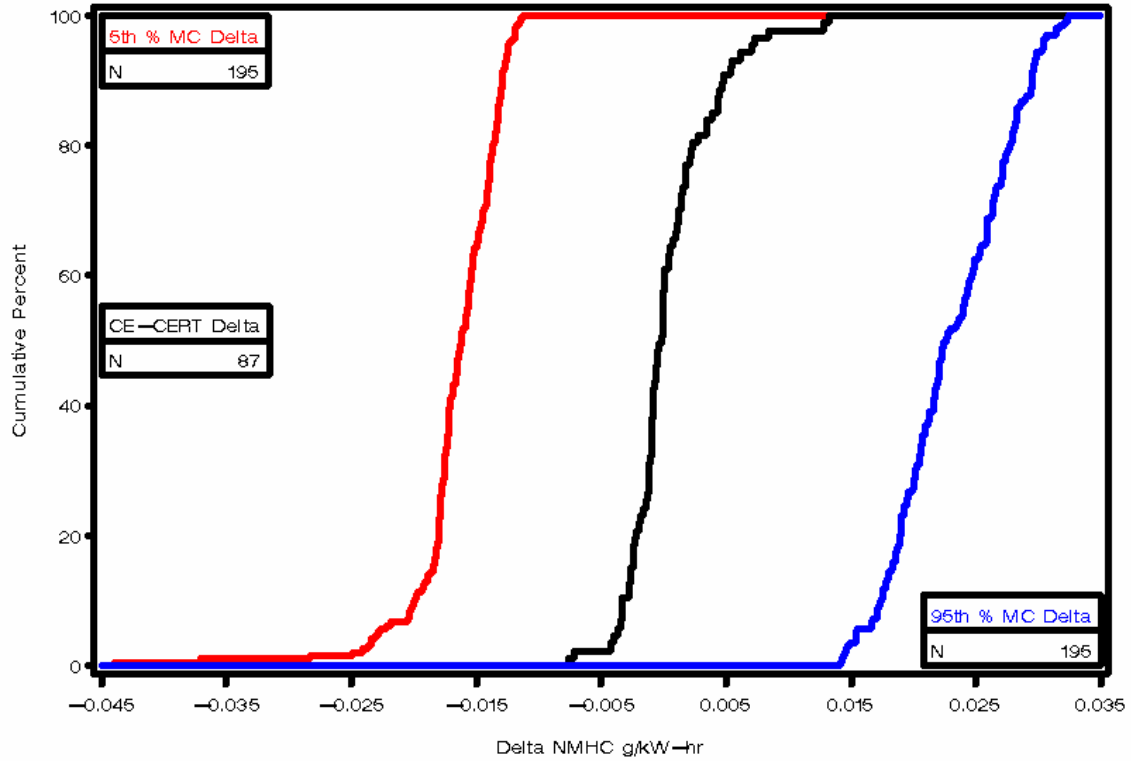


FIGURE 264. VALIDATION ON-ROAD AND MODEL GENERATED EMPIRICAL DISTRIBUTION FUNCTIONS FOR BSNMHC METHOD 2

Validation Analysis 5th and 95th Percentile Deltas
 Compared Ref NTE #1-196 to Corrected 87 CE-CERT Deltas
 NMHC (g/kW-hr) Method 3

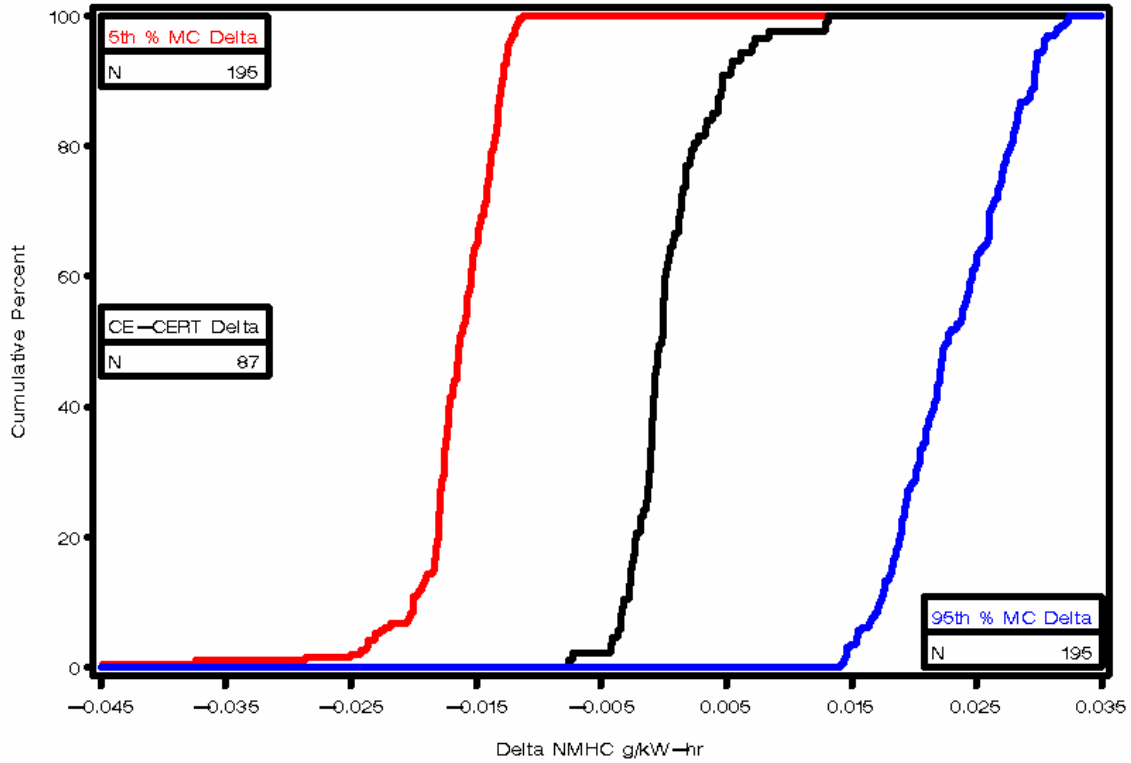


FIGURE 265. VALIDATION ON-ROAD AND MODEL GENERATED EMPIRICAL DISTRIBUTION FUNCTIONS FOR BSNMHC METHOD 3

The validation edf plot for the BSCO Method 1 results is shown in Figure 266. Note that all of the of the on-road delta BSCO emissions fell below the 5th percentile deltas from the simulation model. Thus, the model was not considered valid for the BSCO Method 1 results.

Validation Analysis 5th and 95th Percentile Deltas
 Compared Ref NTE #1-196 to Corrected 87 CE-CERT Deltas
 CO (g/kW-hr) Method 1

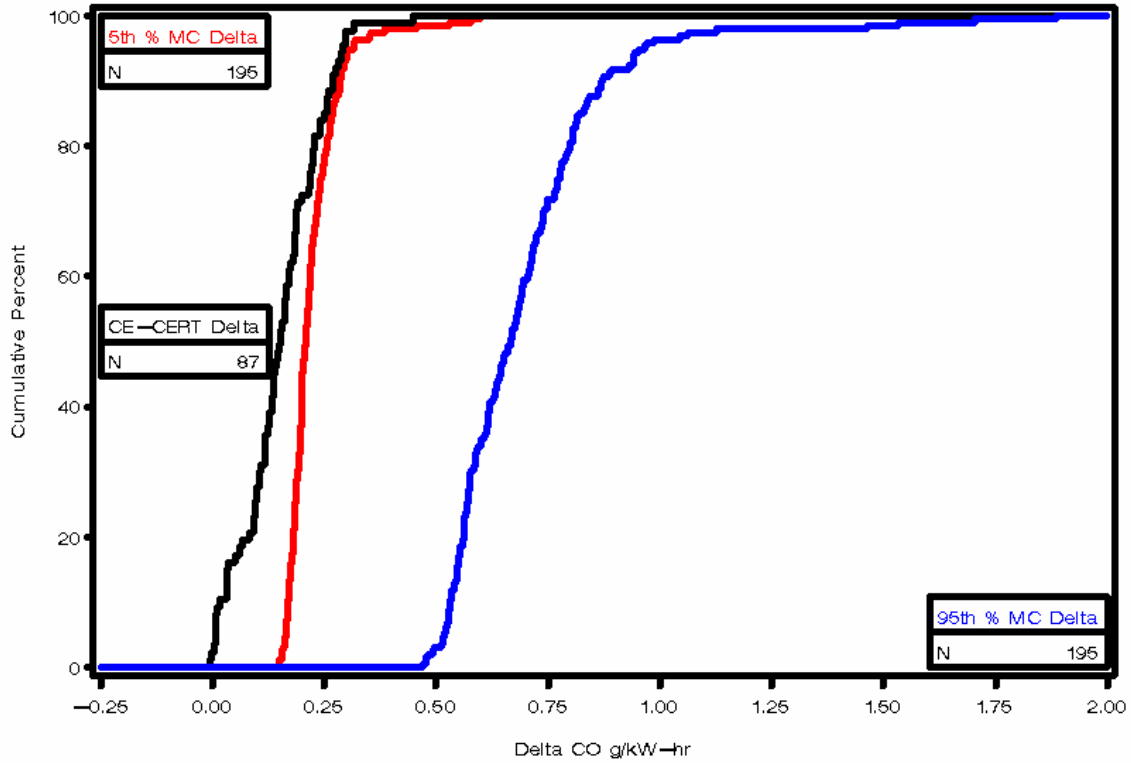


FIGURE 266. VALIDATION ON-ROAD AND MODEL GENERATED EMPIRICAL DISTRIBUTION FUNCTIONS FOR BSCO METHOD 1

The validation edf plots for the BSCO Methods 2 and 3 results are shown in Figure 267 and Figure 268, respectively. Note that approximately 20% of the on-road delta BSCO emissions fell below the 5th percentile deltas from the simulation model for both methods. Thus, the model was not considered valid for the BSCO Method 2 or Method 3 results.

Validation Analysis 5th and 95th Percentile Deltas
Compared Ref NTE #1-195 to Corrected 87 CE-CERT Deltas
CO (g/kW-hr) Method 2

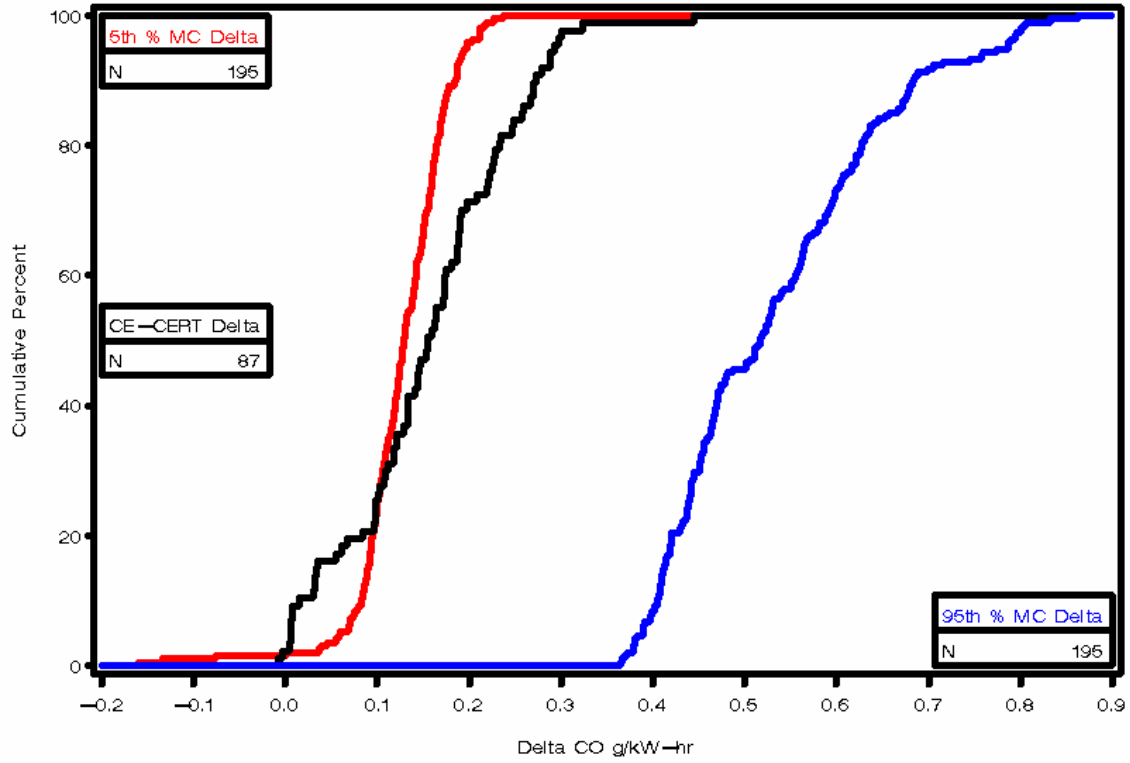


FIGURE 267. VALIDATION ON-ROAD AND MODEL GENERATED EMPIRICAL DISTRIBUTION FUNCTIONS FOR BSCO METHOD 2

Validation Analysis 5th and 95th Percentile Deltas
 Compared Ref NTE #1-195 to Corrected 87 CE-CERT Deltas
 CO (g/kW-hr) Method 3

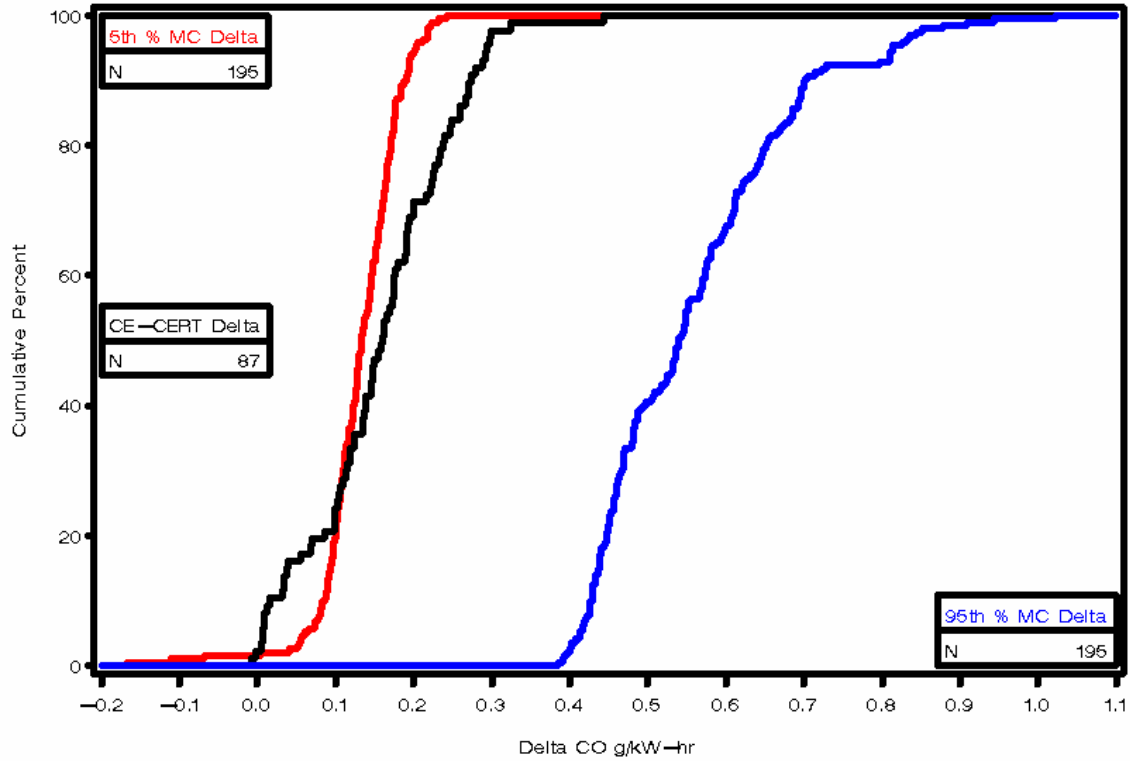


FIGURE 268. VALIDATION ON-ROAD AND MODEL GENERATED EMPIRICAL DISTRIBUTION FUNCTIONS FOR BSCO METHOD 3

Table 124 summarizes the results of the model validation for each of the three emissions and all the methods.

TABLE 124. SUMMARY OF MODEL VALIDATION RESULTS

CE-CERT Deltas < 95th Percentile Deltas from Validation-MC Model			
Emission	Method 1 Torque-Speed	Method 2 BSFC	Method 3 ECM Fuel Specific
BSNOx	Yes	No	No
BSNMHC	Yes	Yes	Yes
BSCO	Yes	Yes	Yes
CE-CERT Deltas > 5th Percentile Deltas from Validation-MC Model			
BSNOx	Yes	Yes	Yes
BSNMHC	Yes	Yes	Yes
BSCO	No	No	No

7.0 MEASUREMENT ALLOWANCE GENERATION AND CONCLUSIONS

This section of the report contains a description of the final generation of the Measurement Allowances, as well as a summary of some of the major conclusions derived from this program.

7.1 Measurement Error Allowance Results

This section contains a summary of the measurement error allowance results using both a regression method and a median method to determine the measurement allowance. Section 2.1.10 on *Measurement Allowance* contains a detailed description of the methodology followed in determining these values. This procedure was applied to the simulation data for all 195 reference NTE events obtained for each of the three emissions and all three calculation methods.

Figure 269 contains a regression plot of the 95th percentile delta BSNO_x values (using Method 1 and with time alignment adjustment) versus the Ideal BSNO_x values for the 195 reference NTE events. Included in the right-hand corner of the plot is the equation for the fitted regression line, and the R-square (R²) value and root mean square error (RMSE) value for the regression fit. The R-square value of 90.56% met the criteria given in the Test Plan for use of the regression line for generation of a potential measurement allowance, and indicates that the magnitude of the 95th percentile BSNO_x delta was linear with respect to the ideal BSNO_x level. The RMSE value of 0.0955 displays the size of the estimated standard deviation of the predicted 95th percentile BSNO_x values.

Table 125 includes a comparison of the results of the regression method based on Figure 269 and the median method as described in the Section 2.1.10 on *Measurement Allowance*. Under the heading of “Regression Method” in the table, it is shown that the R-square and RMSE criteria are met by the data and that the measurement error at the BSNO_x threshold, based on using the regression line to predict the value, is 22.2981% when expressed as a percent of the threshold value of 2.68204. Since the Regression Method is applicable, the Median Method, though shown in the table for comparison purposes, is not applicable.

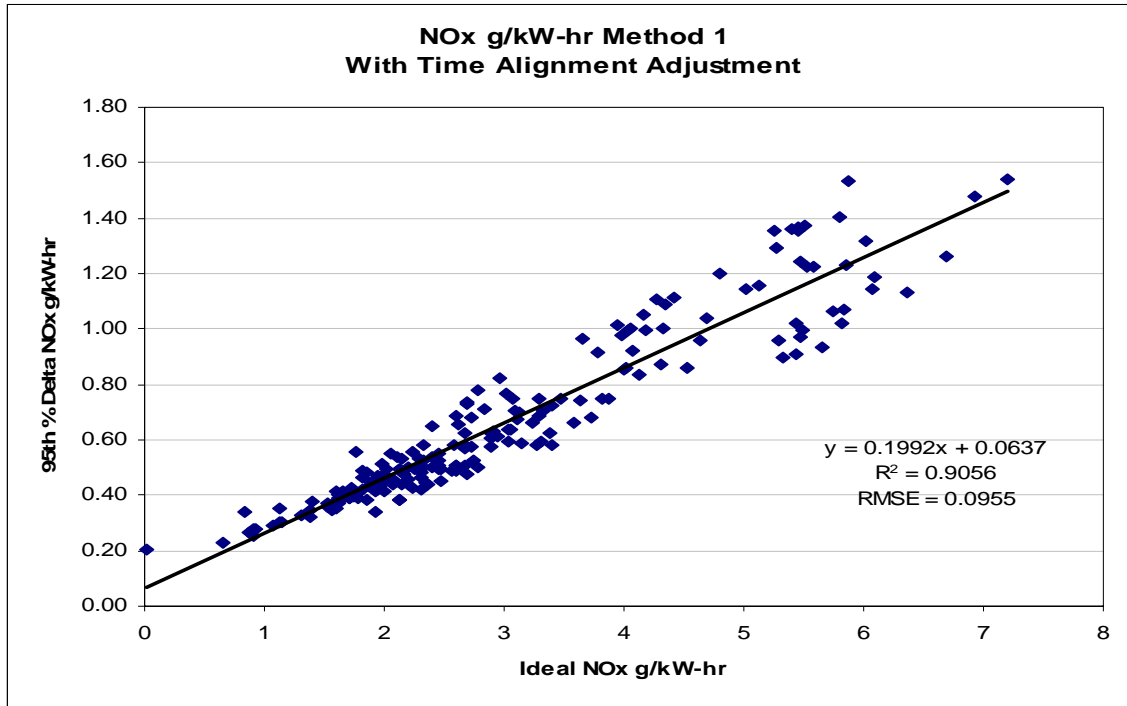


FIGURE 269. REGRESSION PLOT OF 95TH PERCENTILE DELTA BSNO_x VERSUS IDEAL BSNO_x FOR METHOD 1

TABLE 125. MEASUREMENT ERROR AT THRESHOLD FOR BSNO_x USING REGRESSION AND MEDIAN METHODS FOR METHOD 1

Regression Method			Median Method	
R ²	0.9065	Met Criteria		
RMSE(SEE)	0.0955	Met Criteria		
5% Median Ideal	0.1302			
Predicted 95 th % Delta at Threshold	0.5980		Median 95 th % Delta	0.5558
Measurement Error @ Threshold=2.68204	22.2981%		Measurement Error @ Threshold=2.68204	20.7215%

Figure 270 contains a regression plot of the 95th percentile delta BSNO_x values (using Method 2 and with time alignment adjustment) versus the Ideal BSNO_x values for the 195 reference NTE events. The R-square value indicates that 33.64% of the variation in the 95th percentile BSNO_x values is explained by the Ideal BSNO_x values for the Method 2 data. The RMSE value is 0.0181.

Table 126 includes a comparison of the results of the regression method based on Figure 270 and the median method. Under the heading of “Regression Method” in the table, it is shown that the R-square criterion for using this method is not met by the data. Thus, the Median Method must be used. Under the heading “Median Method” in the table, the measurement error

at the BSNO_x threshold, based on using the median of the 195 95th percentile delta BSNO_x values, is 4.4507% when expressed as a percent of the threshold value of 2.68204.

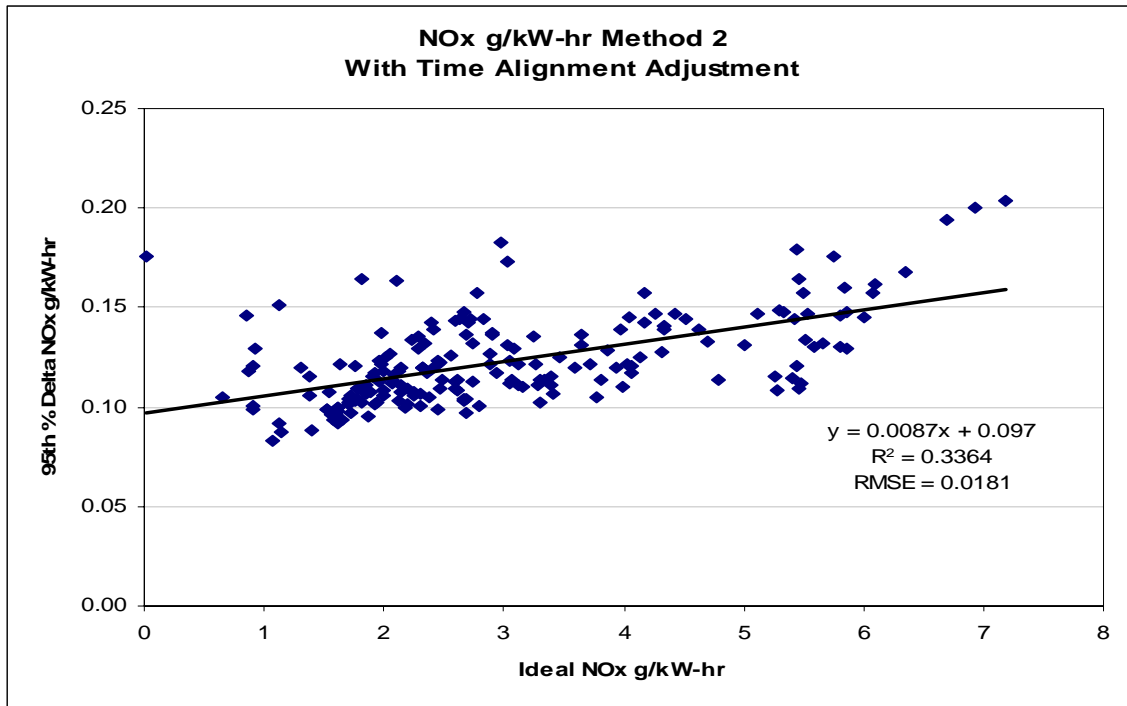


FIGURE 270. REGRESSION PLOT OF 95TH PERCENTILE DELTA BSNO_x VERSUS IDEAL BSNO_x FOR METHOD 2

TABLE 126. MEASUREMENT ERROR AT THRESHOLD FOR BSNO_x USING REGRESSION AND MEDIAN METHODS FOR METHOD 2

Regression Method			Median Method	
R ²	0.3364	Did Not Meet Criteria		
RMSE(SEE)	0.0181	Met Criteria		
5% Median Ideal	0.1302			
Predicted 95 th % Delta at Threshold	0.1203		Median 95 th % Delta	0.1194
Measurement Error @ Threshold=2.68204	4.1853%		Measurement Error @ Threshold=2.68204	4.4507%

Figure 271 contains a regression plot of the 95th percentile delta BSNO_x values (using Method 3 and with time alignment adjustment) versus the Ideal BSNO_x values for the 195 reference NTE events. The R-square value indicates that 58.28% of the variation in the 95th percentile BSNO_x values is explained by the Ideal BSNO_x values for the Method 3 data. The RMSE value is 0.0603.

Table 127 includes a comparison of the results of the regression method based on Figure 271 and the median method. Under the heading of “Regression Method” in the table, it is shown that the R-square criterion for using this method is not met by the data. Thus, the Median Method must be used. Under the heading “Median Method” in the table, the measurement error at the BSNO_x threshold, based on using the median of the 195 95th percentile delta BSNO_x values, is 6.6088% when expressed as a percent of the threshold value of 2.68204.

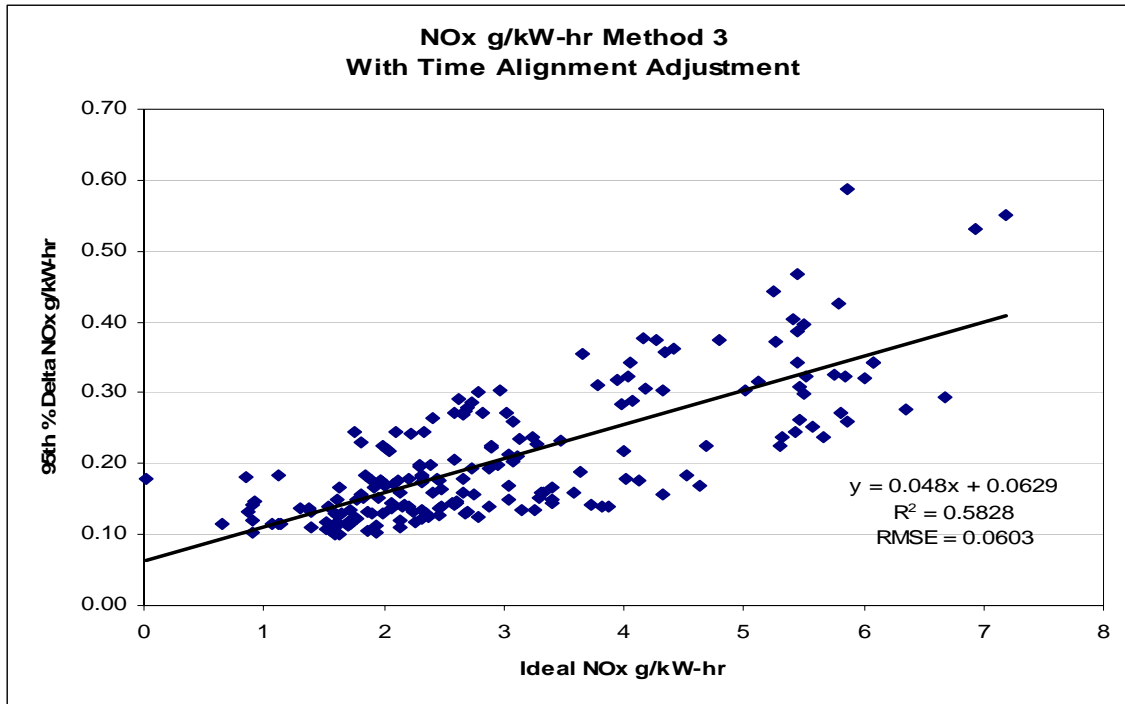


FIGURE 271. REGRESSION PLOT OF 95TH PERCENTILE DELTA BSNO_x VERSUS IDEAL BSNO_x FOR METHOD 3

TABLE 127. MEASUREMENT ERROR AT THRESHOLD FOR BSNO_x USING REGRESSION AND MEDIAN METHODS FOR METHOD 3

Regression Method			Median Method	
R ²	0.5828	Did Not Meet Criteria		
RMSE(SEE)	0.0603	Met Criteria		
5% Median Ideal	0.1302			
Predicted 95 th % Delta at Threshold	0.1916		Median 95 th % Delta	0.1773
Measurement Error @ Threshold=2.68204	7.1455%		Measurement Error @ Threshold=2.68204	6.6088%

Figure 272 contains a regression plot of the 95th percentile delta BSNMHC values (using Method 1 and with time alignment adjustment) versus the Ideal BSNMHC values for the 195 reference NTE events. The R-square value indicates that 79.73% of the variation in the 95th

percentile BSN_{OX} values is explained by the Ideal BSNMHC values for the Method 1 data. The RMSE value is 0.0049.

Table 128 includes a comparison of the results of the regression method based on Figure 272 and the median method. Under the heading of “Regression Method” in the table, it is shown that both the R-square and RMSE criteria for using this method are not met by the data. Thus, the Median Method must be used. Under the heading “Median Method” in the table, the measurement error at the BSNMHC threshold, based on using the median of the 195 95th percentile delta BSNMHC values, is 10.0778% when expressed as a percent of the threshold value of 0.28161.

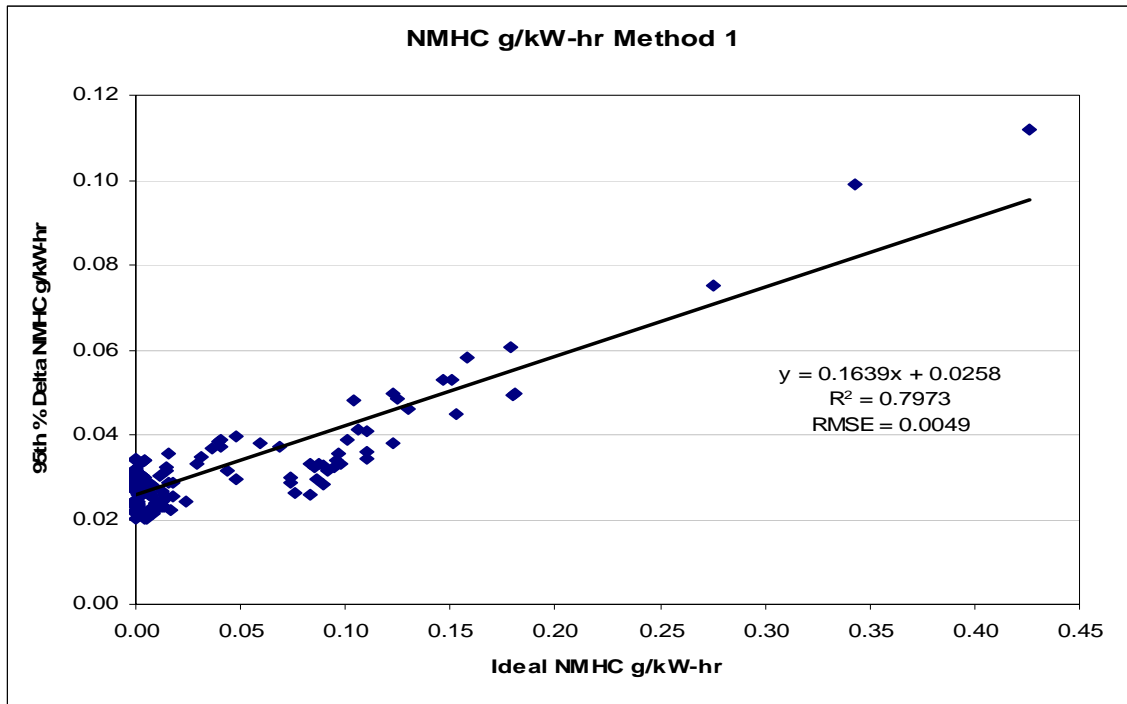


FIGURE 272. REGRESSION PLOT OF 95TH PERCENTILE DELTA BSNMHC VERSUS IDEAL BSNMHC FOR METHOD 1

TABLE 128. MEASUREMENT ERROR AT THRESHOLD FOR BSNMHC USING REGRESSION AND MEDIAN METHODS FOR METHOD 1

Regression Method			Median Method	
R ²	0.7973	Did Not Meet Criteria		
RMSE(SEE)	0.0049	Did Not Meet Criteria		
5% Median Ideal	0.0001			
Predicted 95 th % Delta at Threshold	0.0719		Median 95 th % Delta	0.0284
Measurement Error @ Threshold=0.28161	25.5339%		Measurement Error @ Threshold=0.28161	10.0778%

Figure 273 contains a regression plot of the 95th percentile delta BSNMHC values (using Method 2 and with time alignment adjustment) versus the Ideal BSNMHC values for the 195 reference NTE events. The R-square value indicates that 7.07% of the variation in the 95th percentile BSNO_x values is explained by the Ideal BSNMHC values for the Method 2 data. The RMSE value is 0.0042.

Table 129 includes a comparison of the results of the regression method based on Figure 273 and the median method. Under the heading of “Regression Method” in the table, it is shown that both the R-square and RMSE criteria for using this method are not met by the data. Thus, the Median Method must be used. Under the heading “Median Method” in the table, the measurement error at the BSNMHC threshold, based on using the median of the 195 95th percentile delta BSNMHC values, is 8.0310% when expressed as a percent of the threshold value of 0.28161.

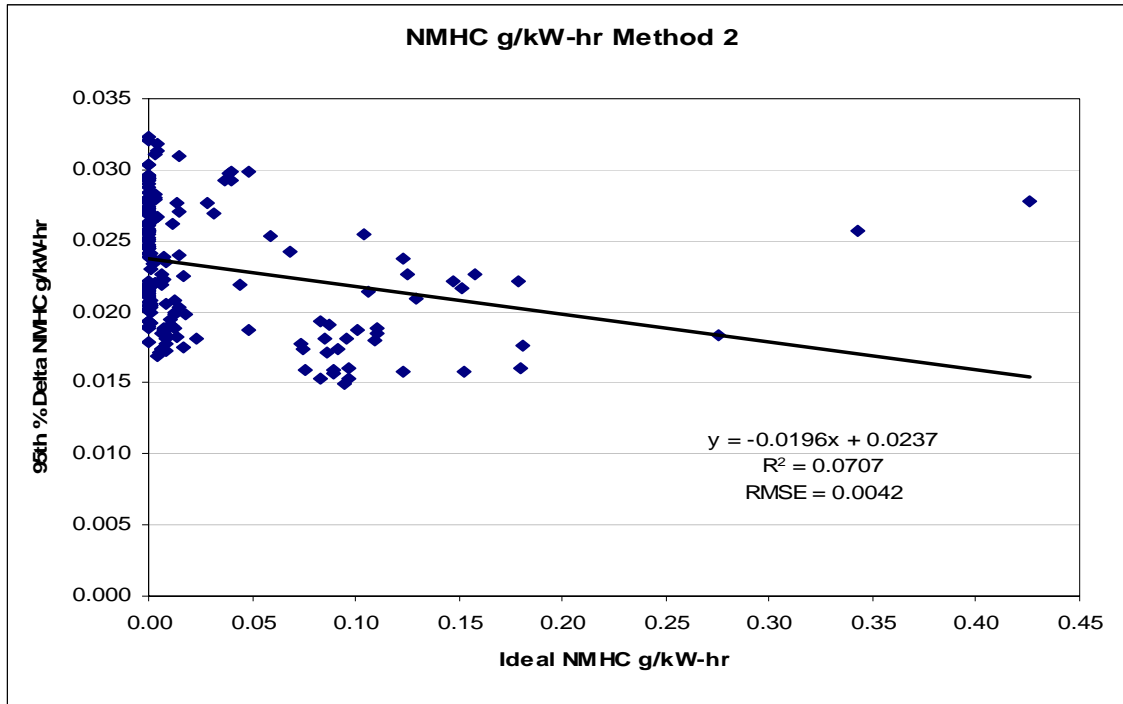


FIGURE 273. REGRESSION PLOT OF 95TH PERCENTILE DELTA BSNMHC VERSUS IDEAL BSNMHC FOR METHOD 2

TABLE 129. MEASUREMENT ERROR AT THRESHOLD FOR BSNMHC USING REGRESSION AND MEDIAN METHODS FOR METHOD 2

Regression Method			Median Method	
R ²	0.0707	Did Not Meet Criteria		
RMSE(SEE)	0.0042	Did Not Meet Criteria		
5% Median Ideal	0.0001			
Predicted 95 th % Delta at Threshold	0.0182		Median 95 th % Delta	0.0226
Measurement Error @ Threshold=0.28161	6.4671%		Measurement Error @ Threshold=0.28161	8.0310%

Figure 274 contains a regression plot of the 95th percentile delta BSNMHC values (using Method 3 and with time alignment adjustment) versus the Ideal BSNMHC values for the 195 reference NTE events. The R-square value indicates that 0.21% of the variation in the 95th percentile BSNO_x values is explained by the Ideal BSNMHC values for the Method 3 data. The RMSE value is 0.0047.

Table 130 includes a comparison of the results of the regression method based on Figure 274 and the median method. Under the heading of “Regression Method” in the table, it is shown that both the R-square and RMSE criteria for using this method are not met by the data. Thus, the Median Method must be used. Under the heading “Median Method” in the table, the

measurement error at the BSNMHC threshold, based on using the median of the 195 95th percentile delta BSNMHC values, is 8.4436% when expressed as a percent of the threshold value of 0.28161.

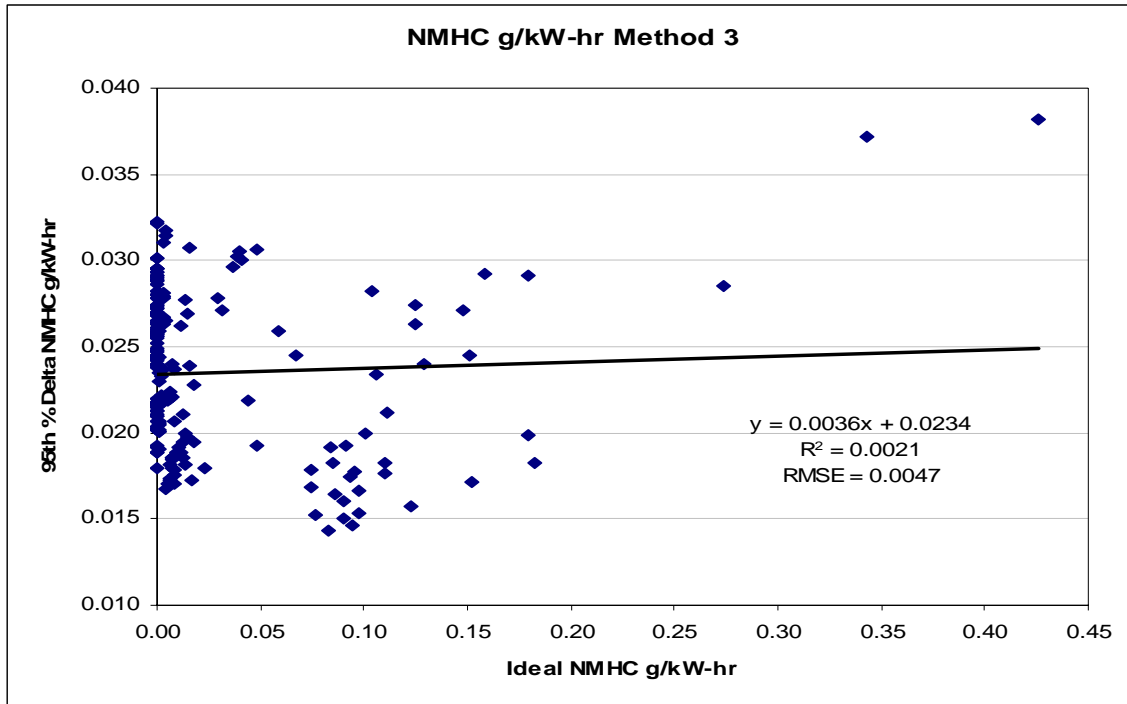


FIGURE 274. REGRESSION PLOT OF 95TH PERCENTILE DELTA BSNMHC VERSUS IDEAL BSNMHC FOR METHOD 3

TABLE 130. MEASUREMENT ERROR AT THRESHOLD FOR BSNMHC USING REGRESSION AND MEDIAN METHODS FOR METHOD 3

Regression Method			Median Method	
R ²	0.0021	Did Not Meet Criteria		
RMSE(SEE)	0.0047	Did Not Meet Criteria		
5% Median Ideal	0.0001			
Predicted 95 th % Delta at Threshold	0.0244		Median 95 th % Delta	0.0238
Measurement Error @ Threshold=0.28161	8.6739%		Measurement Error @ Threshold=0.28161	8.4436%

Figure 275 contains a regression plot of the 95th percentile delta BSCO values (using Method 1 and with time alignment adjustment) versus the Ideal BSCO values for the 195 reference NTE events. The R-square value indicates that 60.48% of the variation in the 95th percentile BSCO values is explained by the Ideal BSCO values for the Method 1 data. The RMSE value is 0.1403.

Table 131 includes a comparison of the results of the regression method based on Figure 275 and the median method. Under the heading of “Regression Method” in the table, it is shown that both the R-square and RMSE criteria for using this method are not met by the data. Thus, the Median Method must be used. Under the heading “Median Method” in the table, the measurement error at the BSCO threshold, based on using the median of the 195 95th percentile delta BSNMHC values, is 2.5775% when expressed as a percent of the threshold value of 26.015.

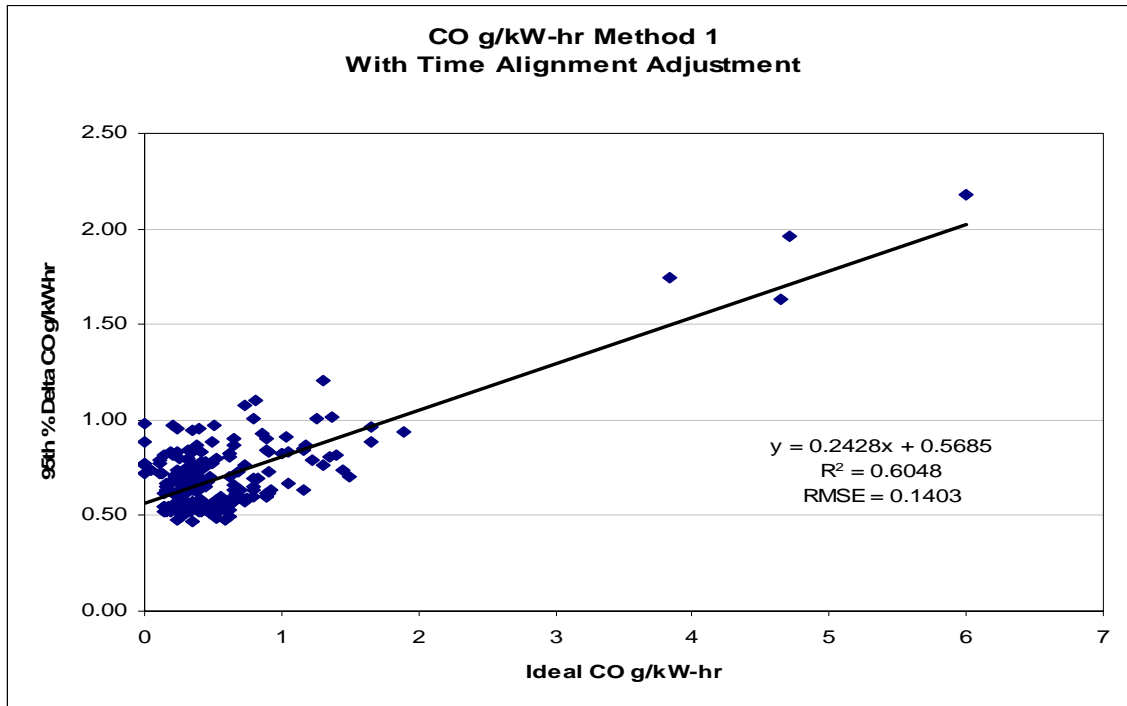


FIGURE 275. REGRESSION PLOT FOR 95TH PERCENTILE DELTA BSCO VERSUS IDEAL BSCO FOR METHOD 1

TABLE 131. MEASUREMENT ERROR AT THRESHOLD FOR BSCO USING REGRESSION AND MEDIAN METHODS FOR METHOD 1

Regression Method			Median Method	
R ²	0.6048	Did Not Meet Criteria		
RMSE(SEE)	0.1403	Did Not Meet Criteria		
5% Median Ideal	0.0192			
Predicted 95 th % Delta at Threshold	2.0242		Median 95 th % Delta	0.6705
Measurement Error @ Threshold=26.015	7.7808%		Measurement Error @ Threshold=26.015	2.5775%

Figure 276 contains a regression plot of the 95th percentile delta BSCO values (using Method 2 and with time alignment adjustment) versus the Ideal BSCO values for the 195

reference NTE events. The R-square value indicates that 3.67% of the variation in the 95th percentile BSCO values is explained by the Ideal BSCO values for the Method 2 data. The RMSE value is 0.1139.

Table 132 includes a comparison of the results of the regression method based on Figure 276 and the median method. Under the heading of “Regression Method” in the table, it is shown that both the R-square and RMSE criteria for using this method are not met by the data. Thus, the Median Method must be used. Under the heading “Median Method” in the table, the measurement error at the BSCO threshold, based on using the median of the 195 95th percentile delta BSNMHC values, is 1.9924% when expressed as a percent of the threshold value of 26.015.

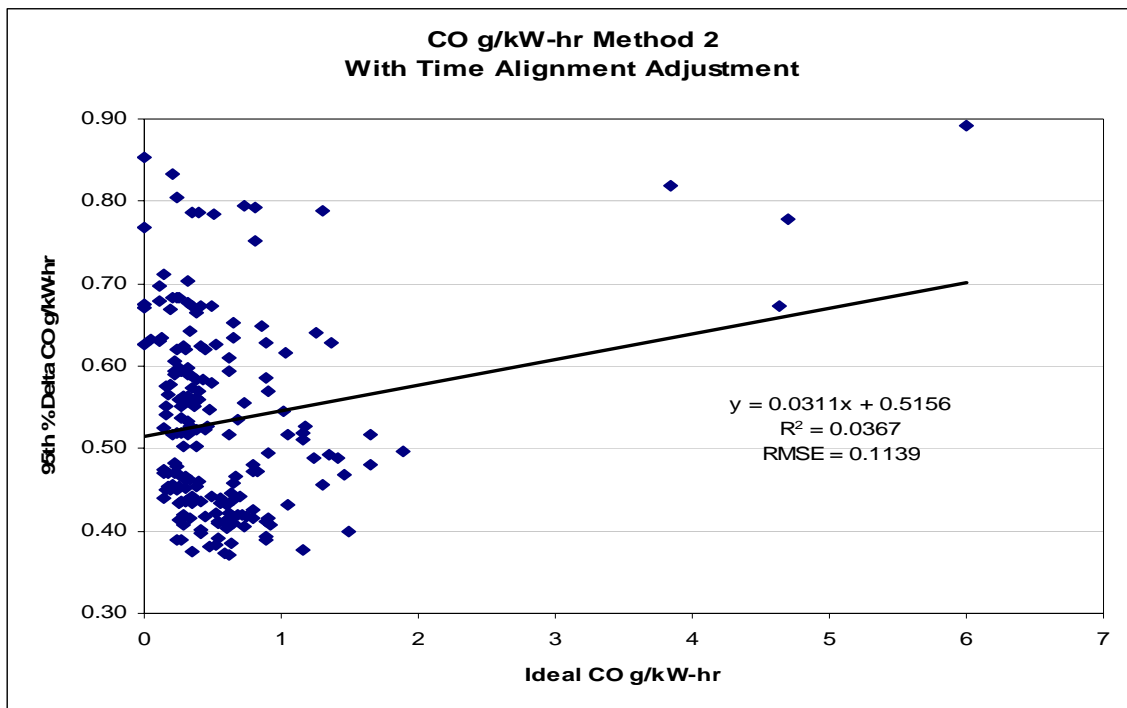


FIGURE 276. REGRESSION PLOT OF 95TH PERCENTILE DELTA BSCO VERSUS IDEAL BSCO FOR METHOD 2

TABLE 132. MEASUREMENT ERROR AT THRESHOLD FOR BSCO USING REGRESSION AND MEDIAN METHODS FOR METHOD 2

Regression Method			Median Method	
R ²	0.0367	Did Not Meet Criteria		
RMSE(SEE)	0.1139	Did Not Meet Criteria		
5% Median Ideal	0.0192			
Predicted 95 th % Delta at Threshold	0.7020		Median 95 th % Delta	0.5183
Measurement Error @ Threshold=26.015	2.6986%		Measurement Error @ Threshold=26.015	1.9924%

Figure 277 contains a regression plot of the 95th percentile delta BSCO values (using Method 3 and with time alignment adjustment) versus the Ideal BSCO values for the 195 reference NTE events. The R-square value indicates that only 22.09% of the variation in the 95th percentile BSCO values is explained by the Ideal BSCO values for the Method 3 data. The RMSE value is 0.1254.

Table 133 includes a comparison of the results of the regression method based on Figure 277 and the median method. Under the heading of “Regression Method” in the table, it is shown that both the R-square and RMSE criteria for using this method are not met by the data. Thus, the Median Method must be used. Under the heading “Median Method” in the table, the measurement error at the BSCO threshold, based on using the median of the 195 95th percentile delta BSNMHC values, is 2.1117% when expressed as a percent of the threshold value of 26.015.

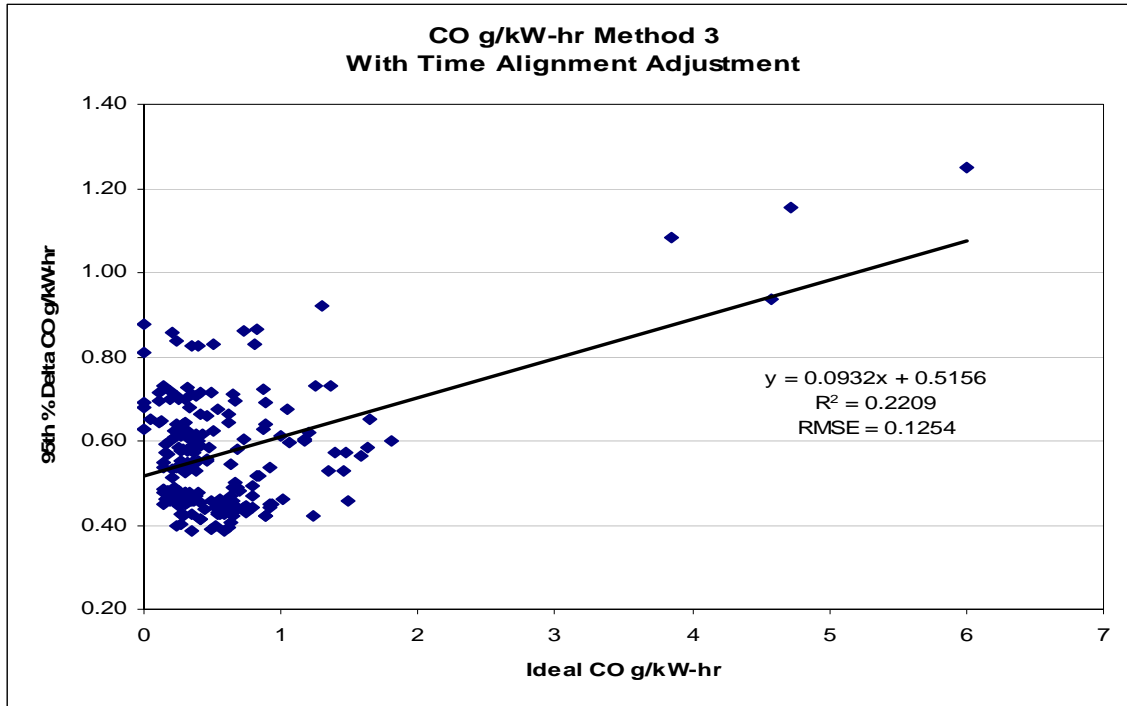


FIGURE 277. REGRESSION PLOT OF 95TH PERCENTILE DELTA BSCO VERSUS IDEAL BSCO FOR METHOD 3

TABLE 133. MEASUREMENT ERROR AT THRESHOLD FOR BSCO USING REGRESSION AND MEDIAN METHODS FOR METHOD 3

Regression Method			Median Method	
R ²	0.2209	Did Not Meet Criteria		
RMSE(SEE)	0.1254	Did Not Meet Criteria		
5% Median Ideal	0.0192			
Predicted 95 th % Delta at Threshold	1.0744		Median 95 th % Delta	0.5494
Measurement Error @ Threshold=26.015	4.1299%		Measurement Error @ Threshold=26.015	2.1117%

Table 134 contains a summary of the measurement error values contained in Table 125 through Table 133. The values are categorized by emissions and by calculation method. The maximum error by method is listed in the last row of the table. Although the Test Plan methodology (i.e., see Section 2.1.10 on *Measurement Allowance*) initially indicated that the minimum of these values was to be used to select the best method, the actual choice is dependent on the ability to validate the model runs using the on-road CE-CERT data. After reviewing the validation results given in Table 124 and noting that only Method 1 validated for BSNO_x, the Steering Committee decided at a meeting held on February 26, 2007 to use Method 1 to determine the measurement error allowance.

TABLE 134. MEASUREMENT ERROR IN PERCENT OF NTE THRESHOLD BY EMISSIONS AND CALCULATION METHOD

Measurement Errors (%) at Respective NTE Threshold			
Emission	Method 1 Torque-Speed	Method 2 BSFC	Method 3 ECM Fuel Specific
BSNO _x	22.30	4.45	6.61
BSNMHC	10.08	8.03	8.44
BSCO	2.58	1.99	2.11
Max Error	22.30	8.03	8.44

Note: Values in table cells shaded white were successfully validation, while values in cells shaded grey were not validated.

Table 135 includes in the last column of the table the measurement error allowances by emissions for Method 1. The values are 0.44596 g/hp-hr for BSNO_x, 0.02116 g/hp-hr for BSNMHC, and 0.50002 g/hp-hr for BSCO.

TABLE 135. MEASUREMENT ALLOWANCE AT NTE THRESHOLD BY EMISSIONS FOR METHOD 1

Emission	Method 1 Measurement Error %	NTE Threshold g/kW-hr	Measurement Allowance, g/kW-hr	Measurement Allowance, g/hp-hr
BSNO _x	22.30	2.68204	0.59804	0.44596
BSNMHC	10.08	0.28161	0.02838	0.02116
BSCO	2.58	26.015	0.67054	0.50002

7.2 Conclusions

The primary result of this program is the set of Measurement Allowances given in the previous section. However, a number of other observations and conclusions may be drawn from the experiences and data generated over the course of the program. This section of the report details some of these observations, as well as recommendations arising from them.

7.2.1 Engine-Installation-PEMS Variability

During the course of this program, a variety of PEMS were used to measure emissions from three different engines. It became apparent that the measurement errors observed were not consistent from installation to installation. In some cases the use of different equipment contributed to the changes, for example the use of different size flow-meters. In other cases, selected PEMS did not behave in the same fashion from engine to engine, as was the case for PEMS 6 which experienced large negative errors during steady-state testing for Engine 3, but not for Engine 2. At other times, PEMS equipment was repaired or replaced, after which different behavior was observed, as was the case with PEMS 4 which demonstrated different NO_x measurement errors on Engine 2 after the NDUV instrument was replaced.

The steady-state error surface data reflected these variations in the fact that the original errors surfaces were not very smooth in nature, and showed abrupt changes in error magnitudes for many key parameters at similar reference levels. In many cases, these abrupt changes took place because data at similar reference levels was generated on different test engines and test installations. This behavior underscores the fact that there is considerable variability arising from PEMS to PEMS and installation to installation.

The Test Plan was designed to use multiple engines in order to get some sense of this variability. However, with only three examples or “samples” of different installations in the plan, many on the Steering Committee felt in hindsight that this source of variation was not very well characterized from a statistical point of view. It is suggested that any future efforts to assess PEMS variation should somehow include a better means of assessing this source of error.

7.2.2 PEMS 1065 Audit Failures

In general, the PEMS passed most of the performance checks required under 40 CFR Part 1065 Subpart D. However, as was noted in Section 3 of the report, there were numerous linearity failures associated with the SEMTECH-DS instruments, particularly in the case of the NDUV analyzer which measures NO and NO₂. Although the Steering Committee approved the continuation of the program despite these problems, this was an issue of concern to many on the Committee. It has been noted earlier that, due to the manner in which the Test Plan was laid out, the linearity requirements used to audit the PEMS represented a relatively liberal interpretation of the regulations given in Subpart D, as a result of use of the span values for the instruments as the “maximum concentration expected during testing” for scaling of the requirements. Despite this interpretation, numerous intercept deviations were still observed. Due to the requirement that testing under the HDIUT program must be conducted using instruments meeting all requirements of 40 CFR Part 1065, such deviations could be problematic.

There was considerable Steering Committee debate regarding this issue. It is suggested that in any future programs of this type, a complete set of audit data should be supplied by any participating instrument manufacturers prior to the start of the program, in order to demonstrate that all 1065 requirements can be met. However, Part 1065 audits should still be conducted as part of any such program to verify compliance.

7.2.3 Method 2 and Method 3 Validation for NO_x

There was considerable discussion among the Steering Committee regarding the reasons that the Model results for Methods 2 and 3 did not validate with respect to NO_x emissions. A significant amount of effort was also directed at determining the cause for the lack of validation of these two methods. These efforts were directed both at examining the Model results, and at scrutinizing the CE-CERT on-road validation test results.

Examination of the CE-CERT results did uncover several relatively minor issues, which were corrected by CE-CERT or dealt with by the Steering Committee. However, no significant procedural issues were found either with the operation of the PEMS or of the MEL. The Steering Committee found no major faults with the CE-CERT data which would have changed the conclusions of the validation process. Ultimately the CE-CERT results were judged by all Steering Committee members to be a valid data set, and this opinion is shared by SwRI staff as well.

In a similar manner, the Steering Committee did not find that the lack of validation arose from any deficiencies in the manner with which SwRI conducted the experiments that supplied data to the Model. In addition, extensive quality assurance and checking were performed on the Model itself in order to insure that it performed in the manner intended by the Test Plan.

As a result of these investigations, therefore, it must be assumed that the reason for the lack of validation of Methods 2 and 3 for NO_x arose from a real difference in PEMS behavior between the laboratory tests at SwRI and the field tests conducted by CE-CERT. This would seem to indicate that some source of variation that occurred during the field tests was not captured by the various experiments which supplied data for the model. This difference could not be related to any Torque or BSFC errors, as those were not relevant to the on-road validation results, as explained earlier in Section 6. In addition, the difference could not be related to the exhaust flow measurement, because this would have also affected the Method 1 results.

Given these observations, the only likely causes for the lack of validation are related either to the measurement of CO₂ or of NO_x itself. In the case of CO₂, the lower deltas would have to be caused by a positive bias in the CO₂ errors predicted by the model as compared to those observed during on-road testing. The Model does in fact incorporate a positive bias in CO₂ errors, as reflected in the steady-state CO₂ error surface. This in turn reflects the fact that negative PEMS CO₂ measurement errors were not observed during laboratory testing. However, examination of the CO₂ data from on-road testing indicates that negative errors were also not observed during the on-road validation. Therefore, it is unlikely that a CO₂ bias was the cause of the lack of validation.

As a result, the root cause for the lack of validation is likely to lie with the NO_x measurement itself. This could be the result either of a bias between the two data sets, or the result of variation. Both reference facilities had been correlated earlier in the program, and no procedural errors were found either for SwRI or for CE-CERT. In addition, the PEMS used for on-road validation testing was one of the units used at SwRI, and was later used again by SwRI for laboratory validation and found to be in good working order. For these reasons, and following a certain amount of engineering analysis, the Steering Committee could not determine

a reason that a bias should exist between the two data sets which would result in lack of validation for Methods 2 and 3.

Another possibility which was raised during Steering Committee discussions was that the level of variance predicted by the Model was not wide enough to encompass the results observed during the CE-CERT validation testing. The steady-state NO_x error surface generally predicts an error of ± 20 ppm at the concentrations observed during on-road validation testing. The sensitivity analysis given in Section 6 earlier indicates that this surface is a dominant driver of NO_x errors for Methods 2 and 3 in the Model. It is possible that the deltas observed during on-road validation testing fell outside this range. Unfortunately, it is not possible to determine concentration deltas directly from the CE-CERT data as no raw reference concentrations are available for comparison with PEMS values.

An analysis of PEMS instrument QA data was conducted for both the CE-CERT data and some of the steady-state experiments used to generate data for the Model at SwRI. Figure 278 shows zero calibration data observed during on-road testing, while Figure 279 shows similar data for Engine 3 tests at SwRI. A comparison of these two data sets indicates much larger amounts of variation in PEMS zero calibration adjustments during on-road testing, as compared to similar adjustments in the laboratory. It should be noted that the range of these variations observed during on-road testing is actually larger than the spread predicted by the steady-state NO_x error surface in the Model. The cause of these larger variations is not known, but they do indicate that some source of error is present in the on-road data that was not apparent during laboratory tests.

A possible explanation for this difference in behavior is that it could be the result of the installation and equipment variations described earlier. A concern of several Steering Committee members was that there were essentially only three observations of this potential error source, and that the on-road validation experiment may have represented a data point outside that range of errors observed during these three cases. If this was the case, it would suggest that the spread of the actual steady-state NO_x error from 5th to 95th percentile is in fact wider than what was given in the steady-state NO_x error surface. This does not suggest that the observations made during the Measurement Allowance program were incorrect, but rather that not enough observations were made to fully characterize the error. Unfortunately, there was not way to test this hypothesis within the scope of the program, and therefore there is no way of knowing if this explanation is valid.

PEMs Total NO+NO₂ Zero Calibrations

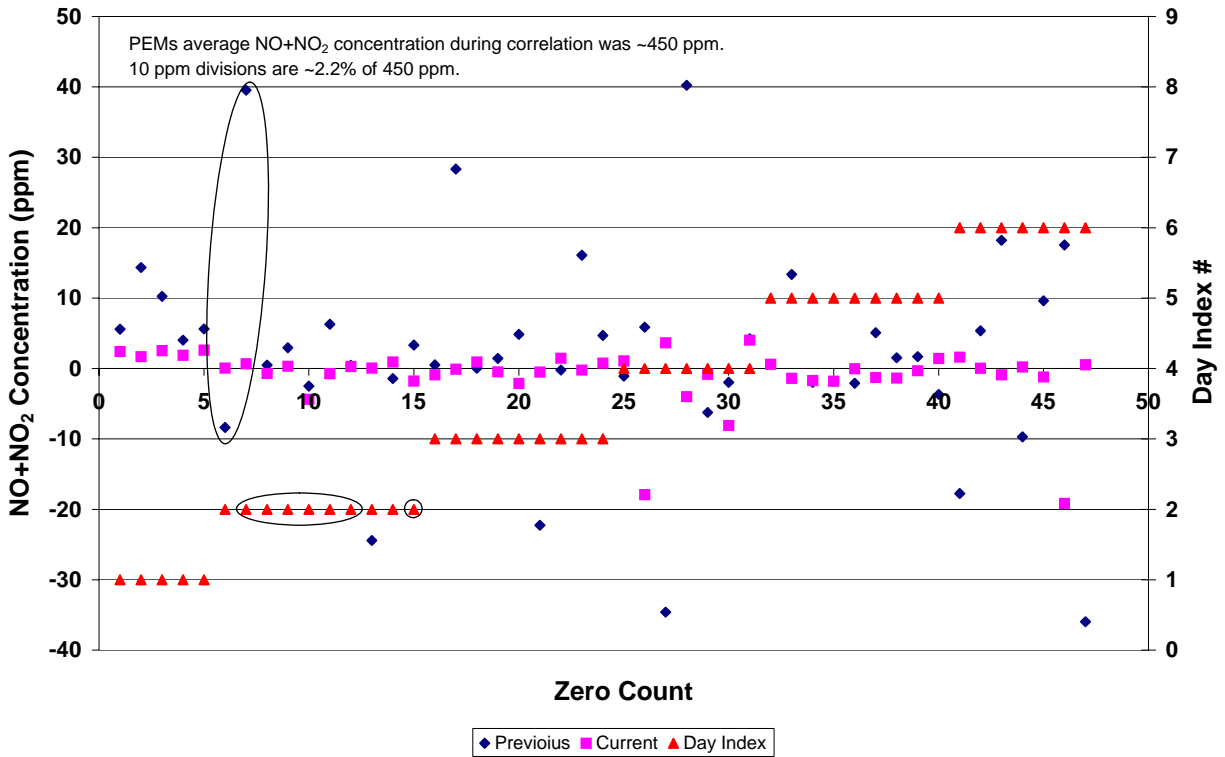


FIGURE 278. VARIATION IN ZERO CALIBRATION OF PEMs DURING ON-ROAD VALIDATION TESTING

PEMs 1 and 4 Total NO+NO₂ Zero Calibrations Engine 3 Testing @ SwRI

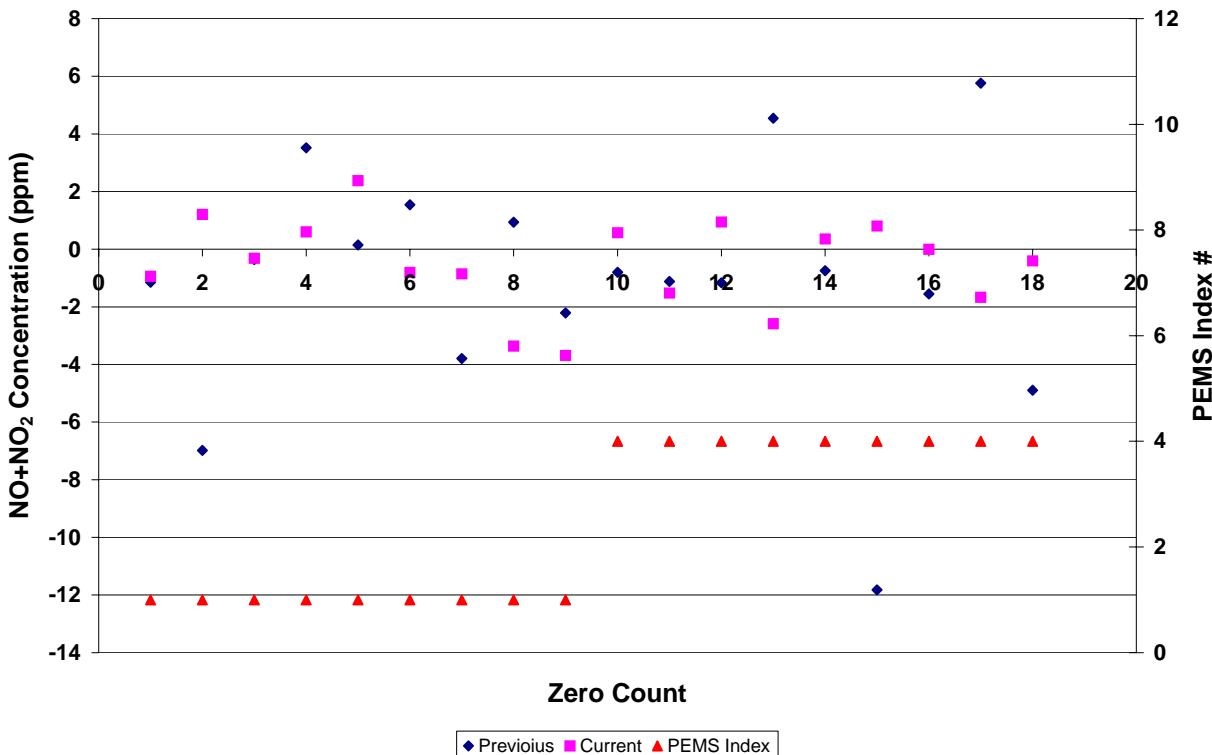


FIGURE 279. PEMS ZERO CALIBRATION VARIATIONS DURING LABORATORY TESTING

Ultimately, the Steering Committee decision was to accept the measurement allowances predicted by the model for Method 1, as these were the only validated numbers. However, EPA indicated that they would continue investigations into the possible causes for the lack of validation of Methods 2 and 3, as well as look into modifications that might result in achieving validation of those methods. It was agreed that any potential revision of the measurement allowances that might arise from such investigations would be reviewed by the Steering Committee and pursued as a cooperative effort between EPA, EMA and CARB. Further it was determined that such changes would not apply before the 2010 model year.

7.2.4 PEMS Sampling Handling System Issues and Overflow Checks

As described throughout this report, and related in Appendix A, there were numerous issues observed with the PEMS over the course of the program. Many of these issues were ultimately traced to problems of deficiencies within the sample handling system of the SEMTECH-DS. In many cases, an overflow span check proved to be the diagnostic exercise which helped to isolate the source of the issue. In such a check, the instrument is zero and span calibrated using the calibration port, and then the same span gas is overflowed to the sample probe such that it enters the instrument through the sample line and passes through the sample

handling system. Although such a check is not required by 1065, SwRI found this to be an invaluable tool for assessing PEMS and for diagnosing problems.

Therefore based on its experiences with these devices, SwRI would recommend the inclusion of such an overflow check in the regular operations of a PEMS. Such a check could be performed on installation of the PEMS on a vehicle, and again at the conclusion of testing. While such a check is not strictly required under Part 1065, it is felt that performance of such a check would help to identify many potential problems which could otherwise compromise PEMS data.

7.2.5 *Lessons Learned for Future Programs*

Near the conclusion of this program, the Steering Committee engaged in several discussions regarding various issues that arose during the program, and how they might be addressed in any future work of this kind. This was particularly relevant given the fact that a subsequent effort is about to be undertaken involving in-use PM measurement.

The result of these discussions was a list of issues, findings, and observations which were collectively termed as “lessons learned.” This list is not necessarily exhaustive, but it does represent a group of observations that the Steering Committee collectively felt were the most important in terms of how any future program of this kind might be conducted. These observations are summarized in Table 136 below. It is hoped that this information will be useful in planning for future efforts of this kind.

TABLE 136. LESSONS LEARNED DURING GASEOUS MEASUREMENT ALLOWANCE PROGRAM

1.	The Steering Committee felt that a number of the biases observed on several error surfaces were likely the results of the limited number of engines and installations tested, rather than a true systematic bias. Therefore, it was recommended that error surfaces should be centered around zero unless there is a technical reason not to do so. Observed biases during program could not always be explained from a technical standpoint.
2.	Broadcast torque needs to be revisited as an error term. The following ideas were suggested on this topic: a. Try to build an exception within the test program (extended data could still be added in as before) b. Variability c. Hardware/Software changes d. Check manufacturer supplied data vs. test data
3.	Check engine to engine variability/differences. Try to structure the program to account for this error source in a more robust manner.
4.	Some error surfaces displayed highly irregular and erratic that were often the result of different PEMS system behavior from on test engine to another. (ex, exhaust flow delta varied between different sized flow meters for different engines). Test Plan anticipate more consistent behavior from engine to

	engine, and experimental design likely missed capturing sources of error beyond the errors expected in Test Plan development (reproducibility are larger than expected). Consider longer time frames.
5.	CE-CERT validation was key to selecting Measurement Allowance.
6.	Environmental errors were generally small compared to baseline variability study. Limited number of exceptions. Environmental test generally caused functional failures rather than measurement errors.
7.	Vibration test was a frequency and direction spectrum of wide range of frequencies to directly assess errors due to in-use vibration. It did not sweep frequencies to identify susceptibility. This was out of scope. Limited field vibration data. Consider adding 3-axis accelerometers on PEMS.
8.	Errors in measurement of ambient temperature and humidity were not included.
9.	PEMS OEM manuals need to be available at start of test plan to better follow manufacturer's recommendations. Any gray areas or multiple methods need to be clarified before start of testing.
10.	Incremental errors due to transient operation were smaller than expected.
11.	Test engines emissions levels were much lower than threshold values for NMHC and CO, data values primarily demonstrated PEMS performance near zero levels, rather than at emission threshold values. Therefore, Measurement Allowances may not entirely represent performance at threshold. Recommended that future work try to use test articles near thresholds, even if systems need to be modified to produce them.
12.	Document control of Test Plan was weak.
13.	Steering Committee decisions were not well documented during the course of the program in an easily referenced manner. Improvement ideas include meeting and conference call minutes, monthly reports, change history of test plan.
14.	Time alignment errors were larger than expected. Improvement idea is to include phase errors in the model.
15.	Test plan was not clear on the decision process if model did not validate.
16.	Test plan did not specify how to use replay validation data.
17.	Drift check in the model was weak.
18.	PEMS issues burned up nearly all the contingency in the schedule. Back-up PEMS was key to staying on schedule.
19.	Method of pooling data into a single error surfaces changed based on actual results.
20.	PEMS vehicle installation process as a source of error was included in the program only at the CE-CERT on road validation stage. Improvement idea is to run the on-road validation earlier to provide input in developing the model.
21.	Documents were shared via SwRI FTP website. Improvement idea is to use a more standardized website layout. Need better data organization for online data storage area.
22.	1065 has some gray areas with respect to PEMS performance checks. In the process 1065 checks were prototyped and revisions were adapted.
23.	Open issue on how to get PEMS to eventually PASS ALL 1065 checks.

Example: linearity check failures.

24. 1065 was not complete prior to start of gaseous programs. Improvement idea is to expect PEMS supplier to have run and passed 1065 checks before starting next program.

APPENDIX A
SEMTECH-DS OPERATION LOG

SwRI Semtech PEMS Log

Date	PEMS #	Summary	Problem Occurred During	Description	
1/4/2006	1,2,3,4	High CO reading	Audit	Symptoms	* CO reads 20-40 ppm when zero air is sampled after a zero/span procedure
				Problem	* Possibly caused by change in sample pressure
					* Different sample path for zero/span and sample
				Solution	* None
1/9/06 - 1/27/06	5" EFM	1065 flow measurement	Audit	Symptoms	* 5-inch EFM repeatedly failed 1065 linearity criteria
				Problem	* Incorrect or outdated curve constants
		linearity failure		Solution	* Sent flow meter to Sensors for recalibration
					* Performed linearity check - passed
1/12/06 - 2/15/06	1	1065 NO linearity failure	Audit	Symptoms	* NO repeatedly failed 1065 linearity - high intercept, low slope
				Problem	* Incorrect or outdated curve constants
				Solution	* Sent PEMS 1 to Sensors for recalibration of the NDUV
					* Performed linearity check - passed
1/15/2006	1,2,3,4	1065 NO2 linearity failure	Audit	Symptoms	* NO2 repeatedly failed 1065 linearity - high intercept, low slope
				Problem	* Incorrect or outdated curve constants
				Solution	* None taken
2/7/2006	2	1065 FID O2 interference failure	Audit	Symptoms	* FID repeatedly failed 1065.362 non-stoichiometric FID O2 interference
				Problem	* FID not tuned/optimized
				Solution	* None taken
2/15/06 - 5/24/06	1,2,3,4	1065 NO2 penetration failure	Audit	Symptoms	* PEMS repeatedly failed 1065.376 Chiller NO2 Penetration
				Problem	* Loss of NO2 in sample conditioning system
				Solution	* Sensors filter bowl and chiller drain manifold retrofit with RH/Temp sensor
					* Correction Factor implemented by Sensors using RH sensor
3/30/2006	4	Spikes in EFM data	Test	Symptoms	* EFM data had short spikes of excessive flow
				Problem	* Unknown, may be linked to inverter problem below (4/3/06)
				Solution	* None
4/3/2006	4	Unstable NO2 PEMS would not power-up	Test	Symptoms	* Unstable and erratic NO2 readings
					* Unit eventually would not turn on
				Problem	* Inverter was supplying only 6 volts to the PEMS
				Solution	* Replaced inverter

6/5/2006	3	NDUV failure	Test	Symptoms	* NO and NO2 readings unstable and noisy
					* NO and NO2 gains high or saturated
				Problem	* NDUV lamp malfunction (Carl Ensfield)
				Solution	* Replaced NDUV
					* Performed linearity and NO2 penetration check (NO linearity failed)
6/5/2006	3	1065 NO linearity failure	Audit	Symptoms	* NO repeatedly failed 1065 linearity (high intercept)
				Problem	* Incorrect or outdated curve constants
				Solution	* None taken
6/6/2006	5	NDIR failure	Test	Symptoms	* CO and CO2 readings erratic and noisy
				Problem	* NDIR failure
				Solution	* Sensors replaced NDIR
					* Performed linearity checks - passed
6/6/2006	1	NDUV failure	Test	Symptoms	* Fault - NDUV not responding
				Problem	* NDUV communication error
				Solution	* Replaced NDUV
					* Performed linearity and NO2 penetration check - passed
6/7/2006	5	1065 NO linearity failure	Audit	Symptoms	* NO repeatedly failed 1065 linearity (high intercept)
				Problem	* Incorrect or outdated curve constants
				Solution	* None taken
6/7/2006	6	1065 NO2 linearity failure	Audit	Symptoms	* NO2 repeatedly failed 1065 linearity (high intercept)
				Problem	* Incorrect or outdated curve constants
				Solution	* None taken
6/8/2006	6	1065 FID O2 interference failure	Audit	Symptoms	* FID repeatedly failed 1065.362 non-stoichiometric FID O2 interference
				Problem	* FID not tuned/optimized
				Solution	* None taken
6/9/2006	4	NO and NO2	Test	Symptoms	* NO and NO2 were unstable/noisy when attempting to zero/span
		Unstable		Problem	* Unknown - possible NDUV lamp malfunction
				Solution	* Restarted unit
6/19/2006	1	Vehicle Interface	Test	Symptoms	* Fault - "Vehicle Interface not responding"
		not responding			* Could not link to CAN bus
				Problem	* Dearborn Group adapter not functioning
				Solution	* Replaced Dearborn Group adapter
7/12/06 - 8/2/06	4" EFM's	4" EFM's failed 1065 linearity	Audit	Symptoms	* 4-inch EFM's failed 1065 linearity check compared to SwRI flow stand
					* EFM's failed slope - low
					* 4-inch EFM's showed similar biases compared to SwRI engine exh. data
				Problem	* Incorrect or outdated curve data
				Solution	* Formulated new curve data based on SwRI flow stand measurements
					* Entered new linearization data for the flow meters
					* Performed linearity checks - passed

7/14/2006	2,5	24-volts delivered to digital input	Setup	Notes	* SwRI connection error - 24 volts delivered to digital input 1
					* Aux 2 connector, pin 14 - digital input 1 was delivered 24 volts
				Symptoms	* Units shut down and would not restart
				Problem	* Damaged I/O board in one unit, damaged several boards in other unit
				Solution	* Units sent to Sensors for repair - board replacement
7/20/2006	6	FID failure	Test	Symptoms	* FID temperature increases slowly
					* FID does not reach operating temperature
					* FID does not zero/span
					* FID fault - "No zero/span performed, basic data installed"
					* FID fault - "FID Battery Backed Ram Corrupt"
				Problem	* FID block heater not functioning
				Solution	* Sensors rebuilt FID at SwRI
					* Replaced block heater
					* FID appeared dirty and well used (Louciano)
					* Performed linearity check - passed
8/8/2006	2,3,5	Low THC span	Test	Symptoms	* FIDs would not span to correct value (FIDs would span low)
					* FID digital gains saturated
					* Adjustment of FID gain potentiometers did not solve problem
				Problem	* Excessive backpressure on FID drain
					* Backpressure due to test setup - long/restrictive drain lines
					* FID drains and main drains were combined
				Solution	* Rerouted drain lines, keeping FID and main drains separate
					* Used large 3" flexible hose to decrease drain backpressure
8/10/2006	6	FID failure	Test	Symptoms	* FID would not span to correct value (FID would span low)
					* FID digital gain saturated
					* Adjustment of FID gain potentiometer did not solve problem
				Problem	* FID capillary tube obstructed
				Solution	* Sensors rebuilt FID at SwRI
					* Replaced FID capillary tube
					* Problem likely caused by prior FID rebuild (7/20/06)
					* Performed linearity check - passed

8/15/2006	2,3,5	CO span error	Test	Symptoms	* CO unstable and noisy during zero and span operation
					* CO readings from zero to several thousand ppm during span
				Problem	* CO digital gains saturated
					* Likely caused from zeroing with span gas or spanning with zero air
				Solution	* Repeatedly zeroed and spanned CO analyzers
					* Instability subsided after first zero/span operation, reading higher than span
					* CO readings were correct after second zero/span operation
8/22/2006	2,3	NO2 conversion/losses	Test	Symptoms	* NO2 showed a significant drop during environmental baseline testing
					* NO2 span decreased during first hour of testing, then began to recover
					* When NO2 decreased, NO increased - possible conversion of NO2 to NO
				Problem	* Problem with PEMS chillers - possible deterioration of passivated coating
				Solution	* Replaced chillers in PEMS 2 and 3
					* Tested PEMS, PEMS 2 - no NO2 loss, PEMS 3 - NO2 loss still prevalent
8/28/2006	5	Temperature probe failure	Test	Symptoms	* Ambient temperature probe generating unrealistic temperature data
					* PEMS temperature data 11 degC below SwRI measurement
				Problem	* Temperature/humidity probe failure
				Solution	* Replace temperature/humidity probe
9/6/2006	3	NO2 conversion/losses	Test	Symptoms	* NO2 loss still prevalent with replacement chiller from Sensors (8/22/06)
					* NO2 span decreased during first hour of testing, then began to recover
					* When NO2 decreased, NO increased - possible conversion of NO2 to NO
				Problem	* Problem with PEMS chillers - possible deterioration of passivated coating
				Solution	* Replaced chiller in PEMS 3 (replacement #2)
					* Tested PEMS, PEMS 3 - no NO2 loss
					* Repeated baseline environmental testing on PEMS 2 and 3
					* Repeated temperature testing on PEMS 3
9/8/2006	3	Enclosure wiring problem	Test	Symptoms	* Unit turned on and shut off after several seconds when in the enclosure
					* Unit eventually would not turn on when in the enclosure
				Problem	* 12-volt power cable in the enclosure had a bad connection
				Solution	* Repaired cable connection

9/11/2006	4	Manifold RH/Temp failure	Test	Symptoms	* Fault - "Manifold RH/Temp sensor not responding"
					* Manifold RH reading absent
					* Fault cleared, then RH reading was erratic, jumping between 60 and 100%
				Problem	* Manifold RH/Temp sensor corroded
				Solution	* Replaced manifold RH/Temp sensor
					* Performed NO2 penetration check - passed
9/14/2006	6	Manifold RH/Temp failure and communication error	Test	Symptoms	* Fault - "Manifold RH/Temp sensor not responding"
					* Manifold RH reading absent
				Problem	* Manifold RH/Temp sensor wet
				Solution	* Replaced manifold RH/Temp sensor
					* New sensor would not respond/communicate
					* Reloaded firmware to reinitialize settings
9/14/2006	4	NDUV failure	Test	Symptoms	* NO and NO2 readings lower than expected, often zero
					* NO and NO2 readings higher than expected
					* NO and NO2 readings erratic and noisy
					* NO and NO2 measurements have excessive drift
					* NO and NO2 gains high or saturated
				Problem	* NDUV lamp malfunction (Carl Ensfield)
					* NDUV gains were saturated (Louie Moret)
				Solution	* Replaced NDUV
					* Performed linearity and NO2 penetration check - NO2 failed
9/15/2006	4	1065 NO2 linearity failure	Audit	Symptoms	* NO2 repeatedly failed 1065 linearity (low intercept, high slope)
				Problem	* Incorrect or outdated curve constants
				Solution	* None taken
9/19/2006	6	Manifold RH/Temp failure	Test	Symptoms	* Fault - "Manifold RH/Temp sensor not responding"
					* Manifold RH reading absent
				Problem	* Manifold RH/Temp sensor wet
				Solution	* Replaced manifold RH/Temp sensor
9/20/2006	2	Drain pump failure	Test	Symptoms	* Warning - "Low vacuum drain 2"
					* Pressure #3 (Filter bowl drain) vacuum low (near ambient pressure)
					* Pressure #3 would not draw vacuum when sample line disconnected
					* Unit would not pass a leak check
				Problem	* Drain pump not operating when checked
					* Drain pump started to rotate, but would stop under vacuum
				Solution	* Replaced drain pump with PEMS 6 drain pump

9/20/2006	2	Drain pump mounting	Test	Symptoms	* Aluminum drain pump mounting bracket broken
		bracket broken		Problem	* Mounting bracket cracked
				Solution	* Welded bracket and reinstalled in PEMS
9/20/2006	6	EFM data not reported in post-processed file	Test	Symptoms	* EFM flow data was not reported in 4 SS post-processed files
					* EFM flow data was in data section of the .xml files
				Problem	* EFM description data missing from header section of the .xml files
				Solution	* Added EFM description data to the header section of the .xml file
					* Reprocessed the data files
9/21/2006	6	(completion of Fix from 9/20)	Audit	Notes	* Installed new drain pump in PEMS 6
					* Performed leak check
					* Performed NO2 penetration check (new RH sensor and drain pump)
		Vehicle Interface	Test	Symptoms	* Fault - "Vehicle Interface not responding"
		not responding			* Could not link to CAN bus
				Problem	* Dearborn Group adapter not functioning
				Solution	* Replaced Dearborn Group adapter
9/25/2006	4	NDUV failure	Test	Symptoms	* NO and NO2 readings lower than expected, often zero
					* NO and NO2 readings higher than expected
					* NO and NO2 readings erratic and noisy
					* NO and NO2 measurements have excessive drift
					* NO and NO2 gains high or saturated
				Problem	* NDUV lamp malfunction (Carl Ensfield)
				Solution	* Replaced NDUV
					* Performed linearity and NO2 penetration check - passed
9/27/2006	4, 6	Manifold RH/Temp failure	Test	Symptoms	* Fault - "Manifold RH/Temp sensor not responding"
					* Manifold RH reading absent, not updating, or erratic
				Problem	* Manifold RH/Temp sensor wet
					* Manifold not sealed properly - air/water leaking past sensor
				Solution	* Disassembled new drain manifolds
					* Resealed manifolds with Silicon
					* Sealed manifolds around sensor connectors
					* Performed leak checks on the manifolds - passed
					* Performed NO2 penetration checks - passed

9/28/06 - 10/3/06	3" EFMs	3" EFMs failed 1065 linearity	Audit	Symptoms	* 2 3-inch EFMs failed 1065 linearity check compared to SwRI flow stand * EFMs failed slope * One EFM close (0.95), one bad (.90)
				Problem	* Incorrect or outdated curve data
				Solution	* Replaced one bad EFM * Entered new linearization data for both flow meters * Performed linearity checks - both EFMs passed
10/5/2006	3	Vibration failures	Test	Notes	* PEMS operated for 4 hours of side-to-side horizontal vibration * PEMS operated for 10 minutes of front-to-back horizontal vibration
		Problem 1		Symptoms	* During first hour of vib. testing, enclosure heated line warning, low temp * During first hour of vib. testing, enclosure fans stopped operating
				Problem	* 12-volt power connection to enclosure failed on PEMS (soldered wires broke)
				Solution	* Temporary solution - external 12-volt power supply to enclosure
		Problem 2		Symptoms	* During first 10-min. of side-to-side vib., FID high temp fault * FID fault - FID temperature exceeded limits - reading 219 degF * Unit was shut down - took approximately 3 minutes to restart * Could not communicate with the compact flash card * Can not log onto unit without flash card communication * Some data from previous tests were lost
				Problem	* Flash card ribbon cable failure (not known prior to sending unit to Sensors)
				Solution	* Unit sent to Sensors for repair * Installed new flash card ribbon cable
10/11/2006	2	EFM data not reported in post-processed file	Test	Symptoms	* EFM flow data was not reported in EFM linearity test * EFM flow data was in data section of the .xml files
				Problem	* EFM description data missing from header section of the .xml files
				Solution	* Added EFM description data to the header section of the .xml file * Reprocessed the data files
10/18/2006	2	FID battery backed ram corrupt	Test	Symptoms	* FID fault - "FID battery backed ram corrupt" * Fault would not clear
				Problem	* Unknown
				Solution	* Restarting unit has cleared this fault in the past * After restart, lost communication with the unit (see Communication error 10/18/06)

10/18/2006	2	Communication and/or processor failure	Test	Symptoms	* Could not log onto PEMS - "Connection Failed"
					* CPU Status LED on, but not blinking
					* Could not turn unit off with the power button on the PEMS (had to unplug unit)
					* Restarted unit several times, still no communication
					* Installed new flash card, still no communication
				Problem	* Corrupt flash card (Sensors Inc.)
				Solution	* Sent PEMS 2 to Sensors Inc. for repair
					* Sensors Inc. replaced flash card, communication restored
10/19/2006	3	Bulk Current Injection (BCI) FID Failure	Test	Symptoms	* BCI to the 12-volt PEMS power cable (Standard J1113-4 Class B, Region 2)
					* 60 milliamps, 26-46 MHz
					* Caused erratic readings for the FID oven temperature, FID fuel pressure, and FID internal reference pressure
					* Fault - "FID oven temperature out of limits"
					* Fault - "FID internal reference pressure out of limits"
					* Warning - "Warming Up"
					* High FID oven temperature reading caused the FID to shut down
				Problem	* PEMS susceptibility to BCI, FID susceptibility to BCI
				Solution	* Replaced PEMS 3 with PEMS 7
					* Sent PEMS 3 to Sensors for repair
					* PEMS 7 did not turn off the FID when tested over similar conditions
					* PEMS 7 reported similar faults and warnings, but to a lesser extent than PEMS 3

10/23/2006	7	Bulk Current Injection (BCI) Failures	Test	Test 1	* BCI to power supply cable
					* Lost communication with EFM
				Solution	* Turned EFM off and back on, communication restored
				Test 2	* BCI to power supply cable
					* Fault - "FID internal ref pressure out of limits" (96 MHz)
				Solution	* Cleared fault
				Test 3	* BCI to Aux 1 cable
					* Fault - "FID oven temp out of range" (91 MHz)
					* Warning - "Warming Up" (on briefly)
				Solution	* Cleared fault
				Test 5a	* BCI to Ethernet cable
					* Fault - "FID internal ref pressure out of limits" (80 MHz)
					* Lost communication with the PEMS (96 MHz)
				Solution	* Cleared fault
					* Log back onto PEMS, continued test
				Test 7	* Fault - "FID internal ref pressure out of limits" (96 MHz)
					* Fault - "FID oven temp out of range" (360 MHz)
				Solution	* Faults would not clear while BCI was active
					* Stopped BCI, cleared faults and proceeded with testing
				Test 9	* BCI to EFM cable at EFM box
					* EFM not responding (prior to 170 MHz)
				Solution	* Restarted PEMS and software to restore communication with the EFM
10/23/2006	7	EFM data not reported in post-processed file	Test	Symptoms	* EFM flow data was not reported in BCI test
					* EFM flow data was in data section of the .xml files
				Problem	* EFM description data missing from header section of the .xml files
				Solution	* Added EFM description data to the header section of the .xml file
					* Reprocessed the data files

10/25/2006	7	Radiated Immunity	Test	Test 1	* Warning - "Warming Up" (on briefly) (42 MHz, 25 V/m)
		(RI) Failures			* Warning - "Warming Up" (on briefly) (74 MHz, 25 V/m)
					* FID oven temp reading 203 (74 MHz, 25 V/m)
					* Fault - "FID oven temp out of range" (76 MHz, 25 V/m) - cleared fault
					* Fault - "FID oven temp out of range" (78 MHz, 20 V/m) - cleared fault
					* Fault - "FID oven temp out of range" (82 MHz, 15 V/m) - cleared fault
					* Fault - "FID internal ref pressure out of limits" (86 MHz, 15 V/m) - cleared fault
					* Fault - "FID oven temp out of range" (128 MHz, ? V/m) - cleared fault
					* Fault - "FID internal ref pressure out of limits" (128 MHz, V/m) - cleared fault
					* Warning - "Warming Up" (on briefly) (128 MHz, ? V/m)
					* Lost communication with the PEMS (148 MHz, ? V/m) - logged back onto PEMS
					* FID shut down, oven temp reading 213 (164 MHz, ? V/m)
				Solution	* Restart test using lower intensity (10 V/m)
				Test 3	* FID oven temp reading 205 (164 MHz, 10 V/m)
					* FID shut down, oven temp reading 215 (168 MHz, 10 V/m) - restarted FID
				Solution	* Can not operate FID between 168 and 178 MHz at 10 V/m
					* Continued testing at 178 MHz and 10 V/m
				Test 4	* FID shut down, oven temp reading 232 (260 MHz, 10 V/m) - restarted PEMS
					* Chiller reading 20 degC when PEMS was restarted - restarted PEMS
				Solution	* Restarted PEMS and continued testing
11/9/2006	6	Manifold RH/Temp failure	CAT SS Testing	Symptoms	* Fault - "Manifold RH/Temp sensor not responding"
				Problem	* Manifold RH/Temp sensor wet
					* Manifold not sealed properly - air/water leaking past sensor
				Solution	* Fault cleared
					* Checked RH reading - OK
					* Continued testing

11/16/2006	6	Manifold RH/Temp	INT 40-Point Testing	Symptoms	* Fault - "Manifold RH/Temp sensor not responding"
		failure			* Manifold RH reading absent, not updating, or erratic
				Problem	* Manifold RH/Temp sensor wet
					* Manifold not sealed properly - air/water leaking past sensor
				Solution	* Removed drain manifold with RH sensor
					* Performed leak check on new replacement manifold - Passed
					* Performed NO2 penetration checks - Passed
11/16/2006	3	Vibration Failures	Vibration Testing	Test 3	* Fault - "FID internal ref pressure out of limits"
					* FID bottle low - broken FID bottle quick connect
				Solution	* Replaced FID bottle and quick connect
				Test 6	* Fault - "FID gas flow is too high or too low"
					* Lost control of the FID
				Solution	* Turned FID off overnight
				Test 7	* FID slow to come up to operating temperature
					* FID would not span - FID oven at 191 degC
				Solution	* None taken, continued testing with no THC measurement
				Test 9	* Heard a "pop" from the PEMS - FID responding and reporting THC values
					* Fault - "FID internal ref pressure out of limits"
					* FID bottle low - broken FID bottle quick connect
				Solution	* Replaced FID bottle and quick connect
1/30/2006	5	Sample Line Failure	CAT C15 40-Point	Symptoms	* Fault - "High vacuum on drains 1 and 2"
					* Fault occurred after PEMS 5 was set to sample ambient air after being in standby overnight
			Testing	Problem	* Heated sample line blocked
					* Cause of blockage unknown
				Solution	* Replaced sample line
1/31/2006	5	Sample Line Failure	CAT C15 40-Point	Symptoms	* Fault - "High vacuum on drains 1 and 2"
					* Fault occurred after PEMS 5 was set to sample ambient air after being in standby overnight
			Testing	Problem	* Heated sample line blocked
					* Cause of blockage unknown
				Solution	* Replaced sample line

APPENDIX B
BRAKE-SPECIFIC EMISSION CALCULATIONS FOR NO_x, CO, AND NMHC

The following sections detail the calculation formulas and the required input constants. For Methods #1 and #2 the conversion of *exhaust flow rate* from SCFM to mol/s is:

$$\dot{n}_i \left(\frac{\text{mol}}{\text{s}} \right) = \frac{\dot{n}_i (\text{SCFM}) * \frac{1}{35.31467} \left(\frac{\text{m}^3}{\text{ft}^3} \right) * \frac{1}{60} \left(\frac{\text{min}}{\text{s}} \right) * 101325 (\text{Pa})}{293.15 (\text{K}) * 8.314472 \left(\frac{\text{J}}{\text{mol} * \text{K}} \right)}$$

Brake-Specific NO_x Concentration for Method #1

Input constants:

$$\Delta t = 1 (\text{sec})$$

$$M_{NO_2} = 46.0055 \left(\frac{\text{g}}{\text{mol}} \right)$$

$$e_{NO_x} (g / kW \cdot hr) = \frac{M_{NO_2} * \sum_{i=1}^N \left[(xNO_{2_i} (\text{ppm}) + xNO_i (\text{ppm})) * 10^{-6} * \dot{n}_i \left(\frac{\text{mol}}{\text{s}} \right) * \Delta t \right]}{\sum_{i=1}^N \left[\frac{Speed_i (\text{rpm}) * T_i (N \cdot m) * 2 * 3.14159 * \Delta t}{60 * 1000 * 3600} \right]}$$

Brake-Specific CO Concentration for Method #1

Input constants:

$$\Delta t = 1 (\text{sec})$$

$$M_{CO} = 28.0101 \left(\frac{\text{g}}{\text{mol}} \right)$$

$$e_{CO} (g / kW \cdot hr) = \frac{M_{CO} * \sum_{i=1}^N \left[(xCO_i (\%)) * 10^{-2} * \dot{n}_i \left(\frac{\text{mol}}{\text{s}} \right) * \Delta t \right]}{\sum_{i=1}^N \left[\frac{Speed_i (\text{rpm}) * T_i (N \cdot m) * 2 * 3.14159 * \Delta t}{60 * 1000 * 3600} \right]}$$

Brake-Specific NMHC Concentration for Method #1

Input constants:

$$\Delta t = 1 \text{ (sec)}$$

$$M_{NMHC} = 13.875389 \left(\frac{g}{mol} \right)$$

$$e_{NMHC} (g / kW \cdot hr) = \frac{M_{NMHC} * \sum_{i=1}^N \left[(x_{NMHC_i} (ppm)) * 10^{-6} * \dot{n}_i \left(\frac{mol}{s} \right) * \Delta t \right]}{\sum_{i=1}^N \left[\frac{Speed_i (rpm) * T_i (N \cdot m) * 2 * 3.14159 * \Delta t}{60 * 1000 * 3600} \right]}$$

Brake-Specific NO_x Concentration for Method #2

Input constants:

$$w_{fuel} = 0.869 \quad \text{Mass fraction of carbon in the fuel.}$$

$$\Delta t = 1 \text{ (sec)}$$

$$M_C = 12.0107 \left(\frac{g}{mol} \right)$$

$$M_{NO_2} = 46.0055 \left(\frac{g}{mol} \right)$$

$$e_{NO_x} (g / kW \cdot hr) = \frac{M_{NO_2} * \sum_{i=1}^N \left[(x_{NO_2_i} (ppm) + x_{NO_i} (ppm)) * 10^{-6} * \dot{n}_i \left(\frac{mol}{s} \right) * \Delta t \right]}{\frac{M_C}{w_{fuel}} * \sum_{i=1}^N \left[\frac{\dot{n}_i \left(\frac{mol}{s} \right) * [x_{NMHC_i} (ppm) * 10^{-6} + (x_{CO_i} (\%) + x_{CO_2_i} (\%)) * 10^{-2}] * \Delta t}{BSFC_i \left(\frac{g}{kW \cdot hr} \right)} \right]}$$

Brake-Specific CO Concentration for Method #2

Input constants:

$$w_{fuel} = 0.869 \quad \text{Mass fraction of carbon in the fuel.}$$

$$\Delta t = 1 \text{ (sec)}$$

$$M_C = 12.0107 \left(\frac{g}{mol} \right)$$

$$M_{CO} = 28.0101 \left(\frac{g}{mol} \right)$$

$$e_{CO}(g/kW \cdot hr) = \frac{M_{CO} * \sum_{i=1}^N \left[(xCO_i(\%)) * 10^{-2} * \dot{n}_i \left(\frac{mol}{s} \right) * \Delta t \right]}{\frac{M_C}{w_{fuel}} * \sum_{i=1}^N \left[\frac{\dot{n}_i \left(\frac{mol}{s} \right) * [xNMHC_i(ppm) * 10^{-6} + (xCO_i(\%) + xCO_{2_i}(\%)) * 10^{-2}] * \Delta t}{BSFC_i \left(\frac{g}{kW \cdot hr} \right)} \right]}$$

Brake-Specific NMHC Concentration for Method #2

Input constants:

$$w_{fuel} = 0.869 \quad \text{Mass fraction of carbon in the fuel.}$$

$$\Delta t = 1 \text{ (sec)}$$

$$M_C = 12.0107 \left(\frac{g}{mol} \right)$$

$$M_{NMHC} = 13.875389 \left(\frac{g}{mol} \right)$$

$$e_{NMHC}(g/kW \cdot hr) = \frac{M_{NMHC} * \sum_{i=1}^N \left[(xNMHC_i(ppm)) * 10^{-6} * \dot{n}_i \left(\frac{mol}{s} \right) * \Delta t \right]}{\frac{M_C}{w_{fuel}} * \sum_{i=1}^N \left[\frac{\dot{n}_i \left(\frac{mol}{s} \right) * [xNMHC_i(ppm) * 10^{-6} + (xCO_i(\%) + xCO_{2_i}(\%)) * 10^{-2}] * \Delta t}{BSFC_i \left(\frac{g}{kW \cdot hr} \right)} \right]}$$

Brake-Specific NO_x Concentration for Method #3

Input constants:

$w_{fuel} = 0.869$ Mass fraction of carbon in the fuel.

$$M_C = 12.0107 \left(\frac{g}{mol} \right)$$

$$M_{NO_2} = 46.0055 \left(\frac{g}{mol} \right)$$

$$\Delta t = 1 \text{ (sec)}$$

Example mass fuel mass rate calculation :

$$\dot{m}_{fuel_i} \left(\frac{g}{s} \right) = Fuelrate_i \left(\frac{L}{sec} \right) * 851.0 \left(\frac{g}{L} \right)$$

$$e_{NO_x} (g / kW \cdot hr) = \frac{\frac{M_{NO_2} * w_{fuel}}{M_C} * \sum_{i=1}^N \left[\frac{(xNO_{2_i} (ppm) + xNO_i (ppm)) * 10^{-6} * \dot{m}_{fuel_i} \left(\frac{g}{s} \right)}{xNMHC_i (ppm) * 10^{-6} + (xCO_i (\%) + xCO_{2_i} (\%)) * 10^{-2}} * \Delta t \right]}{\sum_{i=1}^N \left[\frac{Speed_i (rpm) * T_i (N \cdot m) * 2 * 3.14159 * \Delta t}{60 * 1000 * 3600} \right]}$$

Brake-Specific CO Concentration for Method #3

Input constants:

$w_{fuel} = 0.869$ Mass fraction of carbon in the fuel.

$$M_C = 12.0107 \left(\frac{g}{mol} \right)$$

$$M_{CO} = 28.0101 \left(\frac{g}{mol} \right)$$

$$\Delta t = 1 \text{ (sec)}$$

Example mass fuel mass rate calculation :

$$\dot{m}_{fuel_i} \left(\frac{g}{s} \right) = Fuelrate_i \left(\frac{L}{sec} \right) * 851.0 \left(\frac{g}{L} \right)$$

$$e_{CO} (g / kW \cdot hr) = \frac{\frac{M_{CO} * w_{fuel}}{M_C} * \sum_{i=1}^N \left[\frac{(xCO_i (\%)) * 10^{-2} * \dot{m}_{fuel_i} \left(\frac{g}{s} \right)}{xNMHC_i (ppm) * 10^{-6} + (xCO_i (\%) + xCO_{2_i} (\%)) * 10^{-2}} * \Delta t \right]}{\sum_{i=1}^N \left[\frac{Speed_i (rpm) * T_i (N \cdot m) * 2 * 3.14159 * \Delta t}{60 * 1000 * 3600} \right]}$$

Brake-Specific NMHC Concentration for Method #3

Input constants:

$$w_{fuel} = 0.869 \quad \text{Mass fraction of carbon in the fuel.}$$

$$M_C = 12.0107 \left(\frac{g}{mol} \right)$$

$$M_{NMHC} = 13.875389 \left(\frac{g}{mol} \right)$$

$$\Delta t = 1 \text{ (sec)}$$

Example mass fuel mass rate calculation :

$$\dot{m}_{fuel_i} \left(\frac{g}{s} \right) = Fuelrate_i \left(\frac{L}{sec} \right) * 851.0 \left(\frac{g}{L} \right)$$

$$e_{NMHC} (g / kW \cdot hr) = \frac{\frac{M_{NMHC} * w_{fuel}}{M_C} * \sum_{i=1}^N \left[\frac{(x_{NMHC_i} (ppm)) * 10^{-6} * \dot{m}_{fuel_i} \left(\frac{g}{s} \right)}{x_{NMHC_i} (ppm) * 10^{-6} + (x_{CO_i} (\%) + x_{CO_2_i} (\%)) * 10^{-2}} * \Delta t \right]}{\sum_{i=1}^N \left[\frac{Speed_i (rpm) * T_i (N \cdot m) * 2 * 3.14159 * \Delta t}{60 * 1000 * 3600} \right]}$$

APPENDIX C
CRYSTAL BALL OUTPUT FILE DESCRIPTIONS

EXTRACT DATA FILES

1.0 Simulation Variables

The simulation variables listed in Table 1 were extracted at the completion of the Monte Carlo simulation run for each reference NTE event. Crystal Ball classifies variables into two categories: assumptions and forecasts. Assumptions are the estimated inputs into the simulation model such as the variability indices used to sample each error surface. All assumption variables in this study are identified by an “i_c” at the beginning of the variable name. Forecasts are values calculated by a forecast formula in the spreadsheet cells. Examples of forecast variables used in this study are “Full MC Delta NO_x Method 1” and “Validation MC Delta CO Method 2”.

TABLE 1. SIMULATION VARIABLES

Variable Name	Description
001_DeNO _x (g/kW-hr), Method 1_TA_DC	Full MC Delta NO _x Method 1 Time Alignment and Periodic Drift Check
002_Valid DeNO _x (g/kW-hr), Method 1_TA_DC	Validation MC Delta NO _x Method 1 Time Alignment and Periodic Drift Check
003_DeNO _x (g/kW-hr), Method 2_TA_DC	Full MC Delta NO _x Method 2 Time Alignment and Periodic Drift Check
004_Valid DeNO _x (g/kW-hr), Method 2_TA_DC	Validation MC Delta NO _x Method 2 Time Alignment and Periodic Drift Check
005_DeNO _x (g/kW-hr), Method 3_TA_DC	Full MC Delta NO _x Method 3 Time Alignment and Periodic Drift Check
006_Valid DeNO _x (g/kW-hr), Method 3_TA_DC	Validation MC Delta NO _x Method 3 Time Alignment and Periodic Drift Check
007_DeCO (g/kW-hr), Method 1_TA_DC	Full MC Delta CO Method 1 Time Alignment and Periodic Drift Check
008_Valid DeCO (g/kW-hr), Method 1_TA_DC	Validation MC Delta CO Method 1 Time Alignment and Periodic Drift Check
009_DeCO (g/kW-hr), Method 2_TA_DC	Full MC Delta CO Method 2 Time Alignment and Periodic Drift Check
010_Valid DeCO (g/kW-hr), Method 2_TA_DC	Validation MC Delta CO Method 2 Time Alignment and Periodic Drift Check
011_DeCO (g/kW-hr), Method 3_TA_DC	Full MC Delta CO Method 3 Time

	Alignment and Periodic Drift Check
012_Valid DeCO (g/kW-hr), Method 3_TA_DC	Validation MC Delta CO Method 3 Time Alignment and Periodic Drift Check
013_DeNMHC (g/kW-hr), Method 1_DC	Full MC Delta NMHC Method 1 Periodic Drift Check
014_Valid DeNMHC (g/kW-hr), Method 1_DC	Validation MC Delta NMHC Method 1 Periodic Drift Check
015_DeNMHC (g/kW-hr), Method 2_DC	Full MC Delta NMHC Method 2 Periodic Drift Check
016_Valid DeNMHC (g/kW-hr), Method 2_DC	Validation MC Delta NMHC Method 2 Periodic Drift Check
017_DeNMHC (g/kW-hr), Method 3_DC	Full MC Delta NMHC Method 3 Periodic Drift Check
018_Valid DeNMHC (g/kW-hr), Method 3_DC	Validation MC Delta NMHC Method 3 Periodic Drift Check
019_DeNOx (g/kW-hr), Method 1_DC	Full MC Delta NOx Method 1 Periodic Drift Check
020_Valid DeNOx (g/kW-hr), Method 1_DC	Validation MC Delta NOx Method 1 Periodic Drift Check
021_DeNOx (g/kW-hr), Method 2_DC	Full MC Delta NOx Method 2 Periodic Drift Check
022_Valid DeNOx (g/kW-hr), Method 2_DC	Validation MC Delta NOx Method 2 Periodic Drift Check
023_DeNOx (g/kW-hr), Method 3_DC	Full MC Delta NOx Method 3 Periodic Drift Check
024_Valid DeNOx (g/kW-hr), Method 3_DC	Validation MC Delta NOx Method 3 Periodic Drift Check
025_DeCO (g/kW-hr), Method 1_DC	Full MC Delta CO Method 1 Periodic Drift Check
026_Valid DeCO (g/kW-hr), Method 1_DC	Validation MC Delta CO Method 1 Periodic Drift Check
027_DeCO (g/kW-hr), Method 2_DC	Full MC Delta CO Method 2 Periodic Drift Check
028_Valid DeCO (g/kW-hr), Method 2_DC	Validation MC Delta CO Method 2 Periodic Drift Check
029_DeCO (g/kW-hr), Method 3_DC	Full MC Delta CO Method 3 Periodic Drift Check
030_Valid DeCO (g/kW-hr), Method 3_DC	Validation MC Delta CO Method 3 Periodic Drift Check
031_DeNOx (g/hp-hr), Method 1_TA_DC	Full MC Delta NOx Method 1 Time Alignment and Periodic Drift Check
032_Valid DeNOx (g/hp-hr), Method 1_TA_DC	Validation MC Delta NOx Method 1 Time Alignment and Periodic

	Drift Check
033_DeNOx (g/hp-hr), Method 2_TA_DC	Full MC Delta NOx Method 2 Time Alignment and Periodic Drift Check
034_Valid DeNOx (g/hp-hr), Method 2_TA_DC	Validation MC Delta NOx Method 2 Time Alignment and Periodic Drift Check
035_DeNOx (g/hp-hr), Method 3_TA_DC	Full MC Delta NOx Method 3 Time Alignment and Periodic Drift Check
036_Valid DeNOx (g/hp-hr), Method 3_TA_DC	Validation MC Delta NOx Method 3 Time Alignment and Periodic Drift Check
037_DeCO (g/hp-hr), Method 1_TA_DC	Full MC Delta CO Method 1 Time Alignment and Periodic Drift Check
038_Valid DeCO (g/hp-hr), Method 1_TA_DC	Validation MC Delta CO Method 1 Time Alignment and Periodic Drift Check
039_DeCO (g/hp-hr), Method 2_TA_DC	Full MC Delta CO Method 2 Time Alignment and Periodic Drift Check
040_Valid DeCO (g/hp-hr), Method 2_TA_DC	Validation MC Delta CO Method 2 Time Alignment and Periodic Drift Check
041_DeCO (g/hp-hr), Method 3_TA_DC	Full MC Delta CO Method 3 Time Alignment and Periodic Drift Check
042_Valid DeCO (g/hp-hr), Method 3_TA_DC	Validation MC Delta CO Method 3 Time Alignment and Periodic Drift Check
043_DeNMHC (g/hp-hr), Method 1_DC	Full MC Delta NMHC Method 1 Periodic Drift Check
044_Valid DeNMHC (g/hp-hr), Method 1_DC	Validation MC Delta NMHC Method 1 Periodic Drift Check
045_DeNMHC (g/hp-hr), Method 2_DC	Full MC Delta NMHC Method 2 Periodic Drift Check
046_Valid DeNMHC (g/hp-hr), Method 2_DC	Validation MC Delta NMHC Method 2 Periodic Drift Check
047_DeNMHC (g/hp-hr), Method 3_DC	Full MC Delta NMHC Method 3 Periodic Drift Check
048_Valid DeNMHC (g/hp-hr), Method 3_DC	Validation MC Delta NMHC Method 3 Periodic Drift Check
049_DeNOx (g/hp-hr), Method 1_DC	Full MC Delta NOx Method 1 Periodic Drift Check
050_Valid DeNOx (g/hp-hr), Method 1_DC	Validation MC Delta NOx Method

	1 Periodic Drift Check
051_DeNOx (g/hp-hr), Method 2_DC	Full MC Delta NOx Method 2 Periodic Drift Check
052_Valid DeNOx (g/hp-hr), Method 2_DC	Validation MC Delta NOx Method 2 Periodic Drift Check
053_DeNOx (g/hp-hr), Method 3_DC	Full MC Delta NOx Method 3 Periodic Drift Check
054_Valid DeNOx (g/hp-hr), Method 3_DC	Validation MC Delta NOx Method 3 Periodic Drift Check
055_DeCO (g/hp-hr), Method 1_DC	Full MC Delta CO Method 1 Periodic Drift Check
056_Valid DeCO (g/hp-hr), Method 1_DC	Validation MC Delta CO Method 1 Periodic Drift Check
057_DeCO (g/hp-hr), Method 2_DC	Full MC Delta CO Method 2 Periodic Drift Check
058_Valid DeCO (g/hp-hr), Method 2_DC	Validation MC Delta CO Method 2 Periodic Drift Check
059_DeCO (g/hp-hr), Method 3_DC	Full MC Delta CO Method 3 Periodic Drift Check
060_Valid DeCO (g/hp-hr), Method 3_DC	Validation MC Delta CO Method 3 Periodic Drift Check
061_DeNOx (g/kW-hr), Method 1_TA	Full MC Delta NOx Method 1 Time Alignment
062_DeCO (g/kW-hr), Method 1_TA	Full MC Delta CO Method 1 Time Alignment
063_DeNMHC (g/kW-hr), Method 1	Full MC Delta NMHC Method 1
064_DeNOx (g/kW-hr), Method 2_TA	Full MC Delta NOx Method 2 Time Alignment
065_DeCO (g/kW-hr), Method 2_TA	Full MC Delta CO Method 2 Time Alignment
066_DeNMHC (g/kW-hr), Method 2	Full MC Delta NMHC Method 2 Time Alignment
067_DeNOx (g/kW-hr), Method 3_TA	Full MC Delta NOx Method 3 Time Alignment
068_DeCO (g/kW-hr), Method 3_TA	Full MC Delta CO Method 3 Time Alignment
069_DeNMHC (g/kW-hr), Method 3	Full MC Delta NMHC Method 3
070_DeNOx (g/kW-hr), Method 1	Full MC Delta NOx Method 1
071_DeCO (g/kW-hr), Method 1	Full MC Delta CO Method 1
072_DeNOx (g/kW-hr), Method 2	Full MC Delta NOx Method 2
073_DeCO (g/kW-hr), Method 2	Full MC Delta CO Method 2
074_DeNOx (g/kW-hr), Method 3	Full MC Delta NOx Method 3
075_DeCO (g/kW-hr), Method 3	Full MC Delta CO Method 3
076_DeNOx (g/hp-hr), Method 1_TA	Full MC Delta NOx Method 1 Time Alignment

077_DeCO (g/hp-hr), Method 1_TA	Full MC Delta CO Method 1 Time Alignment
078_DeNMHC (g/hp-hr), Method 1	Full MC Delta NMHC Method 1
079_DeNOx (g/hp-hr), Method 2_TA	Full MC Delta NOx Method 2 Time Alignment
080_DeCO (g/hp-hr), Method 2_TA	Full MC Delta CO Method 2 Time Alignment
081_DeNMHC (g/hp-hr), Method 2	Full MC Delta NMHC Method 2
082_DeNOx (g/hp-hr), Method 3_TA	Full MC Delta NOx Method 3 Time Alignment
083_DeCO (g/hp-hr), Method 3_TA	Full MC Delta CO Method 3 Time Alignment
084_DeNMHC (g/hp-hr), Method 3	Full MC Delta NMHC Method 3
085_DeNOx (g/hp-hr), Method 1	Full MC Delta NOx Method 1
086_DeCO (g/hp-hr), Method 1	Full MC Delta CO Method 1
087_DeNOx (g/hp-hr), Method 2	Full MC Delta NOx Method 2
088_DeCO (g/hp-hr), Method 2	Full MC Delta CO Method 2
089_DeNOx (g/hp-hr), Method 3	Full MC Delta NOx Method 3
090_DeCO (g/hp-hr), Method 3	Full MC Delta CO Method 3
091_Valid DeNOx (g/kW-hr), Method 1_TA	Validation MC Delta NOx Method 1 Time Alignment
092_Valid DeCO (g/kW-hr), Method 1_TA	Validation MC Delta CO Method 1 Time Alignment
093_Valid DeNMHC (g/kW-hr), Method 1	Validation MC Delta NMHC Method 1
094_Valid DeNOx (g/kW-hr), Method 2_TA	Validation MC Delta NOx Method 2 Time Alignment
095_Valid DeCO (g/kW-hr), Method 2_TA	Validation MC Delta CO Method 2 Time Alignment
096_Valid DeNMHC (g/kW-hr), Method 2	Validation MC Delta NMHC Method 2
097_Valid DeNOx (g/kW-hr), Method 3_TA	Validation MC Delta NOx Method 3 Time Alignment
098_Valid DeCO (g/kW-hr), Method 3_TA	Validation MC Delta CO Method 3 Time Alignment
099_Valid DeNMHC (g/kW-hr), Method 3	Validation MC Delta NMHC Method 3
100_Valid DeNOx (g/kW-hr), Method 1	Validation MC Delta NOx Method 1
101_Valid DeCO (g/kW-hr), Method 1	Validation MC Delta CO Method 1
102_Valid DeNOx (g/kW-hr), Method 2	Validation MC Delta NOx Method 2
103_Valid DeCO (g/kW-hr), Method 2	Validation MC Delta CO Method 2
104_Valid DeNOx (g/kW-hr), Method 3	Validation MC Delta NOx Method 3

105_Valid DeCO (g/kW-hr), Method 3	Validation MC Delta CO Method 3
106_Valid DeNOx (g/hp-hr), Method 1_TA	Validation MC Delta NOx Method 1 Time Alignment
107_Valid DeCO (g/hp-hr), Method 1_TA	Validation MC Delta CO Method 1 Time Alignment
108_Valid DeNMHC (g/hp-hr), Method 1	Validation MC Delta NMHC Method 1
109_Valid DeNOx (g/hp-hr), Method 2_TA	Validation MC Delta NOx Method 2 Time Alignment
110_Valid DeCO (g/hp-hr), Method 2_TA	Validation MC Delta CO Method 2 Time Alignment
111_Valid DeNMHC (g/hp-hr), Method 2	Validation MC Delta NMHC Method 2 Time Alignment
112_Valid DeNOx (g/hp-hr), Method 3_TA	Validation MC Delta NOx Method 3 Time Alignment
113_Valid DeCO (g/hp-hr), Method 3_TA	Validation MC Delta CO Method 3 Time Alignment
114_Valid DeNMHC (g/hp-hr), Method 3	Validation MC Delta NMHC Method 3
115_Valid DeNOx (g/hp-hr), Method 1	Validation MC Delta NOx Method 1
116_Valid DeCO (g/hp-hr), Method 1	Validation MC Delta CO Method 1
117_Valid DeNOx (g/hp-hr), Method 2	Validation MC Delta NOx Method 2
118_Valid DeCO (g/hp-hr), Method 2	Validation MC Delta CO Method 2
119_Valid DeNOx (g/hp-hr), Method 3	Validation MC Delta NOx Method 3
120_Valid DeCO (g/hp-hr), Method 3	Validation MC Delta CO Method 3
121_eNOx (g/kW-hr), Method 1 Mode 2_TA	Full MC BSNOx “with errors” Method 1 and Time Alignment
122_eCO (g/kW-hr), Method 1 Mode 2_TA	Full MC BSCO “with errors” Method 1 and Time Alignment
123_eNMHC (g/kW-hr), Method 1 Mode 2	Full MC BSNMHC “with errors” Method 1
124_eNOx (g/kW-hr), Method 2 Mode 2_TA	Full MC BSNOx “with errors” Method 2 and Time Alignment
125_eCO (g/kW-hr), Method 2 Mode 2_TA	Full MC BSCO “with errors” Method 2 and Time Alignment
126_eNMHC (g/kW-hr), Method 2 Mode 2	Full MC BSNMHC “with errors” Method 2
127_eNOx (g/kW-hr), Method 3 Mode 2_TA	Full MC BSNOx “with errors” Method 3 and Time Alignment
128_eCO (g/kW-hr), Method 3 Mode 2_TA	Full MC BSCO “with errors” Method 3 and Time Alignment
129_eNMHC (g/kW-hr), Method 3 Mode 2	Full MC BSNMHC “with errors” Method 3

130_eNOx (g/kW-hr), Method 1 Mode 2	Full MC BSNOx “with errors” Method 1
131_eCO (g/kW-hr), Method 1 Mode 2	Full MC BSCO “with errors” Method 1
132_eNOx (g/kW-hr), Method 2 Mode 2	Full MC BSNOx “with errors” Method 2
133_eCO (g/kW-hr), Method 2 Mode 2	Full MC BSCO “with errors” Method 2
134_eNOx (g/kW-hr), Method 3 Mode 2	Full MC BSNOx “with errors” Method 3
135_eCO (g/kW-hr), Method 3 Mode 2	Full MC BSCO “with errors” Method 3
136_eNOx (g/kW-hr), Method 1 Mode 1	Full MC BSNOx “with errors except environmental” Method 1
137_eCO (g/kW-hr), Method 1 Mode 1	Full MC BSCO “with errors except environmental” Method 1
138_eNMHC (g/kW-hr), Method 1 Mode 1	Full MC BSNMHC “with errors except environmental” Method 1
139_eNOx (g/kW-hr), Method 2 Mode 1	Full MC BSNOx “with errors except environmental” Method 2
140_eCO (g/kW-hr), Method 2 Mode 1	Full MC BSCO “with errors except environmental” Method 2
141_eNMHC (g/kW-hr), Method 2 Mode 1	Full MC BSNMHC “with errors except environmental” Method 2
142_eNOx (g/kW-hr), Method 3 Mode 1	Full MC BSNOx “with errors except environmental” Method 3
143_eCO (g/kW-hr), Method 3 Mode 1	Full MC BSCO “with errors except environmental” Method 3
144_eNMHC (g/kW-hr), Method 3 Mode 1	Full MC BSNMHC “with errors except environmental” Method 3
145_eNOx (g/kW-hr), Method 1 Mode 0	Full MC BSNOx “ideal” Method 1
146_eCO (g/kW-hr), Method 1 Mode 0	Full MC BSCO “ideal” Method 1
147_eNMHC (g/kW-hr), Method 1 Mode 0	Full MC BSNMHC “ideal” Method 1
148_eNOx (g/kW-hr), Method 2 Mode 0	Full MC BSNOx “ideal” Method 2
149_eCO (g/kW-hr), Method 2 Mode 0	Full MC BSCO “ideal” Method 2
150_eNMHC (g/kW-hr), Method 2 Mode 0	Full MC BSNMHC “ideal” Method 2
151_eNOx (g/kW-hr), Method 3 Mode 0	Full MC BSNOx “ideal” Method 3
152_eCO (g/kW-hr), Method 3 Mode 0	Full MC BSCO “ideal” Method 3
153_eNMHC (g/kW-hr), Method 3 Mode 0	Full MC BSNMHC “ideal” Method 3
154_eNOx (g/kW-hr), Method 1 Reject Flag	Full MC BSNOx Periodic Drift Check Flag Method 1
155_eCO (g/kW-hr), Method 1 Reject Flag	Full MC BSCO Periodic Drift

	Check Flag Method 1
156_eNMHC (g/kW-hr), Method 1 Reject Flag	Full MC BSNMHC Periodic Drift Check Flag Method 1
157_eNOx (g/kW-hr), Method 2 Reject Flag	Full MC BSNOx Periodic Drift Check Flag Method 2
158_eCO (g/kW-hr), Method 2 Reject Flag	Full MC BSCO Periodic Drift Check Flag Method 2
159_eNMHC (g/kW-hr), Method 2 Reject Flag	Full MC BSNMHC Periodic Drift Check Flag Method 2
160_eNOx (g/kW-hr), Method 3 Reject Flag	Full MC BSNOx Periodic Drift Check Flag Method 3
161_eCO (g/kW-hr), Method 3 Reject Flag	Full MC BSCO Periodic Drift Check Flag Method 3
162_eNMHC (g/kW-hr), Method 3 Reject Flag	Full MC BSNMHC Periodic Drift Check Flag Method 3
163_Valid eNOx (g/kW-hr), Method 1 Mode 2_TA	Validation MC BSNOx “with errors” Method 1 and Time Alignment
164_Valid eCO (g/kW-hr), Method 1 Mode 2_TA	Validation MC BSCO “with errors” Method 1 and Time Alignment
165_Valid eNMHC (g/kW-hr), Method 1 Mode 2	Validation MC BSNMHC “with errors” Method 1
166_Valid eNOx (g/kW-hr), Method 2 Mode 2_TA	Validation MC BSNOx “with errors” Method 2 and Time Alignment
167_Valid eCO (g/kW-hr), Method 2 Mode 2_TA	Validation MC BSCO “with errors” Method 2 and Time Alignment
168_Valid eNMHC (g/kW-hr), Method 2 Mode 2	Validation MC BSNMHC “with errors” Method 2
169_Valid eNOx (g/kW-hr), Method 3 Mode 2_TA	Validation MC BSNOx “with errors” Method 3 and Time Alignment
170_Valid eCO (g/kW-hr), Method 3 Mode 2_TA	Validation MC BSCO “with errors” Method 3 and Time Alignment
171_Valid eNMHC (g/kW-hr), Method 3 Mode 2	Validation MC BSNMHC “with errors” Method 3
172_Valid eNOx (g/kW-hr), Method 1 Mode 2	Validation MC BSNOx “with errors” Method 1
173_Valid eCO (g/kW-hr), Method 1 Mode 2	Validation MC BSCO “with errors” Method 1
174_Valid eNOx (g/kW-hr), Method 2 Mode 2	Validation MC BSNOx “with errors” Method 2
175_Valid eCO (g/kW-hr), Method 2 Mode 2	Validation MC BSCO “with errors” Method 2
176_Valid eNOx (g/kW-hr), Method 3 Mode 2	Validation MC BSNOx “with errors” Method 3

177_Valid eCO (g/kW-hr), Method 3 Mode 2	Validation MC BSCO “with errors” Method 3
178_Valid eNOx (g/kW-hr), Method 1 Mode 1	Validation MC BSNOx “with errors except environmental” Method 1
179_Valid eCO (g/kW-hr), Method 1 Mode 1	Validation MC BSCO “with errors except environmental” Method 1
180_Valid eNMHC (g/kW-hr), Method 1 Mode 1	Validation MC BSNMHC “with errors except environmental” Method 1
181_Valid eNOx (g/kW-hr), Method 2 Mode 1	Validation MC BSNOx “with errors except environmental” Method 2
182_Valid eCO (g/kW-hr), Method 2 Mode 1	Validation MC BSCO “with errors except environmental” Method 2
183_Valid eNMHC (g/kW-hr), Method 2 Mode 1	Validation MC BSNMHC “with errors except environmental” Method 2
184_Valid eNOx (g/kW-hr), Method 3 Mode 1	Validation MC BSNOx “with errors except environmental” Method 3
185_Valid eCO (g/kW-hr), Method 3 Mode 1	Validation MC BSCO “with errors except environmental” Method 3
186_Valid eNMHC (g/kW-hr), Method 3 Mode 1	Validation MC BSNMHC “with errors except environmental” Method 3
187_Valid eNOx (g/kW-hr), Method 1 Reject Flag	Validation MC BSNOx Periodic Drift Check Flag Method 1
188_Valid eCO (g/kW-hr), Method 1 Reject Flag	Validation MC BSCO Periodic Drift Check Flag Method 1
189_Valid eNMHC (g/kW-hr), Method 1 Reject Flag	Validation MC BSNMHC Periodic Drift Check Flag Method 1
190_Valid eNOx (g/kW-hr), Method 2 Reject Flag	Validation MC BSNOx Periodic Drift Check Flag Method 2
191_Valid eCO (g/kW-hr), Method 2 Reject Flag	Validation MC BSCO Periodic Drift Check Flag Method 2
192_Valid eNMHC (g/kW-hr), Method 2 Reject Flag	Validation MC BSNMHC Periodic Drift Check Flag Method 2
193_Valid eNOx (g/kW-hr), Method 3 Reject Flag	Validation MC BSNOx Periodic Drift Check Flag Method 3
194_Valid eCO (g/kW-hr), Method 3 Reject Flag	Validation MC BSCO Periodic Drift Check Flag Method 3
195_Valid eNMHC (g/kW-hr), Method 3 Reject Flag	Validation MC BSNMHC Periodic Drift Check Flag Method 3
196_eNOx (g/hp-hr), Method 1 Mode 2_TA	Full MC BSNOx “with errors” Method 1 and Time Alignment

197_eCO (g/hp-hr), Method 1 Mode 2_TA	Full MC BSCO “with errors” Method 1 and Time Alignment
198_eNMHC (g/hp-hr), Method 1 Mode 2	Full MC BSNMHC “with errors” Method 1
199_eNOx (g/hp-hr), Method 2 Mode 2_TA	Full MC BSNOx “with errors” Method 2 and Time Alignment
200_eCO (g/hp-hr), Method 2 Mode 2_TA	Full MC BSCO “with errors” Method 2 and Time Alignment
201_eNMHC (g/hp-hr), Method 2 Mode 2	Full MC BSNMHC “with errors” Method 2
202_eNOx (g/hp-hr), Method 3 Mode 2_TA	Full MC BSNOx “with errors” Method 3 and Time Alignment
203_eCO (g/hp-hr), Method 3 Mode 2_TA	Full MC BSCO “with errors” Method 3 and Time Alignment
204_eNMHC (g/hp-hr), Method 3 Mode 2	Full MC BSNMHC “with errors” Method 3
205_Valid eNOx (g/hp-hr), Method 1 Mode 2_TA	Validation MC BSNOx “with errors” Method 1 and Time Alignment
206_Valid eCO (g/hp-hr), Method 1 Mode 2_TA	Validation MC BSCO “with errors” Method 1 and Time Alignment
207_Valid eNMHC (g/hp-hr), Method 1 Mode 2	Validation MC BSNMHC “with errors” Method 1
208_Valid eNOx (g/hp-hr), Method 2 Mode 2_TA	Validation MC BSNOx “with errors” Method 2 and Time Alignment
209_Valid eCO (g/hp-hr), Method 2 Mode 2_TA	Validation MC BSCO “with errors” Method 2 and Time Alignment
210_Valid eNMHC (g/hp-hr), Method 2 Mode 2	Validation MC BSNMHC “with errors” Method 2
211_Valid eNOx (g/hp-hr), Method 3 Mode 2_TA	Validation MC BSNOx “with errors” Method 3 and Time Alignment
212_Valid eCO (g/hp-hr), Method 3 Mode 2_TA	Validation MC BSCO “with errors” Method 3 and Time Alignment
213_Valid eNMHC (g/hp-hr), Method 3 Mode 2	Validation MC BSNMHC “with errors” Method 3 and Time Alignment
01_ic_SS_NOx	Random Sampling Variability Index for SS NOx Error Surface
02_ic_TR_NOx	Random Sampling Variability Index for Transient NOx Error Surface
05_ic_Temperature_NOx	Random Sampling Variability Index for NOx Temperature Error Surface

07_ic_SS_CO	Random Sampling Variability Index for SS CO
10_ic_Pressure_CO	Random Sampling Variability Index for CO Pressure
11_ic_Temperature_CO	Random Sampling Variability Index for CO Temperature
13_ic_SS_NMHC	Random Sampling Variability Index for SS NMHC
14_ic_TR_NMHC	Random Sampling Variability Index for Transient NMHC
16_ic_Pressure_NMHC	Random Sampling Variability Index for NMHC Pressure
17_ic_Temperature_NMHC	Random Sampling Variability Index for NMHC Temperature
19_ic_NMHC_Ambient	Random Sampling Variability Index for Ambient NMHC
20_ic_SS_flow	Random Sampling Variability Index for SS Exhaust Flow
21_ic_TR_Flowrate	Random Sampling Variability Index for Transient Exhaust Flow
22_ic_Pulsation_flow	Random Sampling Variability Index for Exhaust Flow Pulsation
23_ic_Swirl_flow	Random Sampling Variability Index for Exhaust Flow Swirl
25_ic_Radiation_Exhaust Flow	Random Sampling Variability Index for Exhaust Flow EMI/RFI Radiation
27_ic_Temperature_Exhaust Flow	Random Sampling Variability Index for Exhaust Flow Temperature
28_ic_Pressure_Exhaust Flow	Random Sampling Variability Index for Exhaust Flow Pressure
29_ic_TR_Torque	Random Sampling Variability Index for Dynamic Torque
30_ic_Torque_DOE	Random Sampling Variability Index for Torque Design of Experiments Testing
31_ic_Torque_Warm	Random Sampling Variability Index for Torque Warm-up
32_ic_Torque_IP	Random Sampling Variability Index for Torque Independent Parameters Humidity and Fuel
34_ic_Torque_Interpolation	Random Sampling Variability Index for Torque Interpolation
35_ic_Torque_Engine Manufacturers	Random Sampling Variability Index for Torque Engine

	Manufacturers
36_ic_TR_BSFC	Random Sampling Variability Index for Dynamic BSFC
37_ic_BSFC_DOE	Random Sampling Variability Index for BSFC Design of Experiments
38_ic_BSFC_Warm	Random Sampling Variability Index for BSFC Warm-up
39_ic_BSFC_IP	Random Sampling Variability Index for BSFC Independent Parameters Humidity and Fuel
41_ic_BSFC_Interpolation	Random Sampling Variability Index for BSFC Interpolation
42_ic_BSFC_Engine Manufacturers	Random Sampling Variability Index for BSFC Engine Manufacturers
43_ic_TR_Speed	Random Sampling Variability Index for Dynamic Speed
44_ic_TR_Fuel Rate	Random Sampling Variability Index for Dynamic Fuel Rate
45_ic_SS_CO2	Random Sampling Variability Index for SS CO2
46_ic_TR_CO2	Random Sampling Variability Index for Transient CO2
49_ic_Temperature_CO2	Random Sampling Variability Index for CO2 Temperature
51_ic_NOx_Time Alignment	Random Sampling Variability Index for NOx Time Alignment
52_ic_CO_Time Alignment	Random Sampling Variability Index for CO Time Alignment

2.0 Statistics

Descriptive statistics summarizing the values obtained during a single reference NTE event simulation are provided in Table 2.

TABLE 2. DESCRIPTIVE STATISTICS FOR SIMULATION VARIABLES

Statistic	Definition
Trials	Number of times the simulation was repeated and not discarded due to periodic drift
Mean	Arithmetic average
Median	The value midway between the smallest value and the largest value

Mode	Value that occurs most often
Standard Deviation	Measurement of variability of a distribution. The square root of the variance
Variance	The average of the squares of the deviations of a number of values from their mean
Skewness	A measure of the degree of deviation of a distribution from the norm of a symmetric distribution
Kurtosis	A measure of the degree of peakedness of a distribution
Coefficient of Variability	Standard deviation/Mean
Minimum	Smallest value
Maximum	Largest value
Range Width	Largest value – smallest value
Mean Standard Error	Standard deviation of the distribution of possible sample means
Filtered Values	Number of trial discarded due to periodic drift

3.0 Percentiles

Percentiles are the probability of achieving values below a particular percentage in the following increments: 0, 5, 10, 15, 20, 25, 30, 35, 40, 45, 50, 55, 60, 65, 70, 75, 80, 85, 90, 95, and 100%. Percentiles are computed for each of the simulations variables described in Section 1.1.

4.0 Sensitivity Data

Sensitivity data are provided by computing the rank correlation coefficient for all error surfaces and all simulation variables. The EXTRACT data file contains the absolute value of the rank correlation.

5.0 Trial Values

The value for all simulation variables is provided at each trial of the simulation.

REPORT FILES

1.0 Report Summary

This section includes the simulation start date and time, stop date and time, number of trials run, sampling type (Monte Carlo), random seed used, and run statistics.

2.0 Forecasts

Descriptive statistics, percentiles, and a frequency histogram are provided for forecast variables 001_DeNO_x (g/kW-hr), Method 1_TA_DC through 030_Valid DeCO (g/kW-hr), Method 3_DC (see Table 1).

3.0 Assumptions

Descriptive statistics, percentiles, distribution parameters, and a distribution chart are provided for assumption variables 01_ic_SS_NO_x through 52_ic_CO_Time Alignment (see Table 1).

4.0 Sensitivity Charts

Sensitivity charts are provided for forecast variables 001_DeNO_x (g/kW-hr), Method 1_TA_DC through 030_Valid DeCO (g/kW-hr), Method 3_DC (see Table 1). Crystal Ball calculates sensitivity by computing rank correlation coefficients between every assumption (error surface) and forecast (BS emissions and delta BS emissions) while the simulation is running. Positive rank correlations indicate that an increase in the assumption is associated with an increase in the forecast. The larger the absolute value of the rank correlation the stronger the relationship.

The sensitivity charts developed during the MC simulation are displayed as ‘Contribution to Variance’ charts which are calculated by squaring the rank correlation coefficients for all assumptions used in a particular forecast and then normalizing them to 100%. Figure 1 displays a sensitivity chart for the delta NO_x Method #1 with time alignment and periodic drift check forecast. The assumption with the highest contribution to variance (in absolute value) is plotted at the top of the chart. In this example, as you increase the torque warm-up there is a decrease in the delta NO_x Method #1 values. Only the top nine assumptions are plotted in the sensitivity charts.

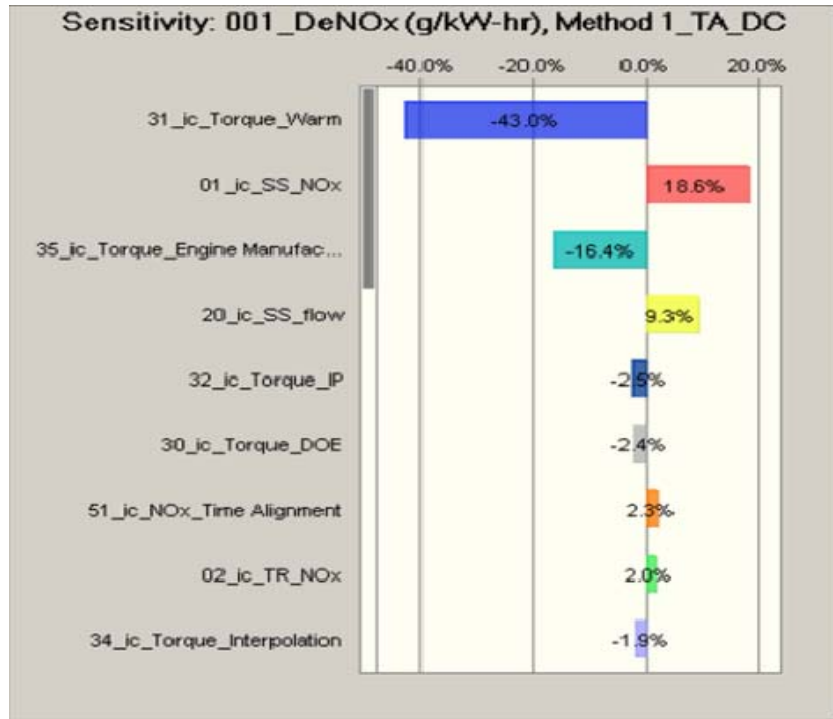


FIGURE 1. SENSITIVITY CHART FOR DELTA NO_x METHOD 1

APPENDIX D
MONTE CARLO SPREADSHEET COMPUTATIONS

1.0 DESCRIPTION OF ASSUMPTIONS

The following assumptions were made in running the Monte Carlo model:

- Only one reference NTE event can be run at a time through the Monte Carlo simulation workbook.
- Uniform (1 second in duration) time steps are used in the reference NTE events.
- Standard format and engineering units for reference NTE data established for the project are observed, and applied to the reference NTE event before the NTE event is entered in the Error Model workbook for Monte Carlo simulation.
- Any wet – dry matter conversions, if not negligible, have been performed on the appropriate reference NTE event values before the reference NTE event was entered in the Error Model workbook for Monte Carlo simulation. No wet – dry conversions are performed in the workbook.
- Any reference NTE event normalizations to produce similar emissions brake-specific results from the three emissions calculation methods have been appropriately performed before the reference NTE event was entered in the Error Model workbook for Monte Carlo simulation. No normalizations among the three methods are performed in the workbook.
- Emissions models for three calculation methods and three emissions are computed during one MC simulation run.
- Error surface models and supporting data were approved by the Steering Committee.
- The error model spreadsheet has been correctly implemented, and its interaction with Monte Carlo tools like Crystal Ball is correctly understood.
- Random number generation by a Monte Carlo tool like Crystal Ball is correct.
- Convergence of the completed MC simulation was processed and checked outside of this workbook using a SAS[®] computer program.

2.0 WORKSHEET DESCRIPTIONS

2.1 Macro Description

The Macro can be viewed in the Excel spreadsheet with the menu selections Tools>Macros>Macro1>Edit. The purpose of Macro1 is to expedite clearing extra cells below the reference NTE event in the Methods worksheet and to delete extra rows in the Delta error worksheets. The macro also performs Mode 0 calculations and stores resultant 'ideal emissions' values for application in subsequent Monte Carlo simulation.

The user must begin with the starter version of the Excel file which has 300 rows of equations in columns X - CF and in rows 52 - 351 in the Methods worksheet. The starter spreadsheet also has 300 rows of equations below charts in columns B - F, or B - L, in applicable Delta worksheets. The user copies the reference NTE event into columns A - V, row 52 and down, in the Methods worksheet. It is then necessary to confirm that cell J45 in the Methods worksheet displays the correct number of rows of the reference NTE event.

Macro execution can be accomplished through the menu selections Tools>Macros>Macro1>Run. Note that this macro clears cells without deleting rows in the Methods worksheet, and deletes rows in the Delta worksheets. This macro will not work if the reference NTE event has only one row. For a reference NTE event with exactly two rows, this macro will corrupt the second "check" values in columns B-F type Delta worksheets. Check values are not used in the simulation, but are provided as a diagnostic aid. Apply the macro for reference NTE events with no more than 300 rows.

The reader can follow the description of execution that follows by viewing the macro and observing the comment rows provided throughout the macro text. In execution, the macro first reads the contents of J45 in the Methods worksheet. It uses the number of rows in the reference NTE event defined by J45 to determine how many rows to clear and delete in the spreadsheet. It checks that the number of rows is between 2 and 299, inclusive. It will also execute correctly for 300 rows.

Next, the macro clears cell contents in columns X - CF below the reference NTE event in the Methods worksheet. Note the macro, as written, will not execute properly if the starter spreadsheet has been revised with row insertion or deletion in certain areas of the spreadsheet. As written, the macro initiates in cell X52, counts down through the NTE Event rows, and clears contents in the range from there in column X through cell CF351.

Next, the macro deletes extra rows below the reference NTE event in Delta worksheet 1. For Delta worksheet 1 it initiates in cell B79 and counts down through the rows of the reference NTE event to the first row to be deleted. It selects the range of rows from there down through row 378, deletes the rows, copies some equations and a value to the last row in the range the charts use, and returns the cursor to cell F68 leaving the display more or less centered on the charts in the worksheet.

Subsequently, the macro performs similar operations in other Delta worksheets; however, the initiating cell and final row differ among the worksheets. The Delta worksheets processed in this way are 1, 2, 5, 7, 8, 10, 11, 16, 17, 20, 21, 22, 23, 29, 30, 36, 37, 43, 44, 45, 46 and 49.

Following the row deletion operations in the Delta worksheets, or directly when the reference NTE event has 300 rows, the macro prepares for the Mode 0 (ideal emissions) calculation. First, in the Methods worksheet it copies the equations in row 52, columns X through CF, to the last row in the reference NTE event. This clears any errors introduced in the last row; however, it assumes that row 52 is correct. The last cell in column AC (Δt) is cleared for aesthetics, since the Δt values are not applied in the model calculations.

The Mode 0 calculation is performed by the macro by changing the value in cell A6 of the Summary worksheet to 0. Then in the Methods worksheet, the values from cells CU22 through CU32 are pasted (values only) to cells O22 through O32 where they are referenced by formulas during Monte Carlo simulation. The macro changes the value of A6 in the Summary worksheet to 2 in preparation for the Monte Carlo simulation, and moves the cursor to cell CT18 of the Methods worksheet.

Additional comments regarding the macro operation are presented in the following section descriptions of the model spreadsheet.

2.2 Worksheet 1: ErrorControl

The ErrorControl worksheet of the Error Model workbook implements 52 logic switch functions. The user enters a numerical “1” in column D in each row corresponding to error surfaces to be included in the calculation. A numerical “0” is applied to error surfaces to be excluded in the calculation.

Error surfaces are numbered sequentially 1 through 50, and Time Alignment error surfaces are designated 51 and 52. The numbered error surfaces are defined in columns A – C, and information pertinent to their usage is presented in columns E – V of the worksheet. Column E displays warning messages when an unusual value is entered in column D.

The control switch elements in the worksheet are deliberately placed on rows in the worksheet corresponding to the error surfaces to expedite equation checking in the Methods worksheet where the control switch variables are applied in conjunction with error surfaces from the correspondingly numbered “Delta” worksheets

The numbered error surfaces and time alignment controls that have been implemented are defined in the following Table 1.

TABLE 1. ERROR SURFACES USED IN SIMULATION

Component	No.	Error Surface
Delta NO _x	1	Delta NO _x SS
	2	Delta NO _x Transient
	5	Delta NO _x Ambient Temperature
Delta CO	7	Delta CO SS
	10	Delta CO Atmospheric Pressure
	11	Delta CO Ambient Temperature
Delta NMHC NMHC = 0.98*THC	13	Delta NMHC SS
	14	Delta NMHC Transient
	16	Delta NMHC Atmospheric Pressure
	17	Delta NMHC Ambient Temperature
	19	Delta Ambient NMHC
Delta Exhaust Flow	20	Delta Exhaust Flow SS
	21	Delta Exhaust Flow Transient
	22	Delta Exhaust Flow Pulsation
	23	Delta Exhaust Flow Swirl
	25	Delta Exhaust EMI/RFI
	27	Delta Exhaust Temperature
	28	Delta Exhaust Pressure
Delta Torque	29	Delta Dynamic Torque
	30	Delta Torque DOE Testing (Interacting Parameters Test)
	31	Delta Torque Warm-up (Interacting Parameters Test)
	32	Delta Torque Humidity / Fuel (Independent Parameters Test)
	34	Delta Torque Interpolation
	35	Delta Torque Engine Manufacturers
Delta BSFC	36	Delta Dynamic BSFC
	37	Delta BSFC DOE Testing (Interacting Parameters Test)
	38	Delta BSFC Warm-up (Interacting Parameters Test)
	39	Delta BSFC Humidity / Fuel (Independent Parameters Test)
	41	Delta BSFC Interpolation
	42	Delta BSFC Engine Manufacturers
Delta Speed	43	Delta Dynamic Speed
Delta Fuel Rate	44	Delta Dynamic Fuel Rate
Delta CO ₂	45	Delta CO ₂ SS
	46	Delta CO ₂ Transient
	49	Delta CO ₂ Ambient Temperature
Time Alignment	51	Delta NO _x Time Alignment
	52	Delta CO Time Alignment

The thirty-five (35) error surfaces that have been implemented are included or excluded by the controls numbered 1 – 49 identified in Table 1. Three NO_x time alignment errors are controlled by number 51 and three CO time alignment errors are controlled by number 52. When all 35 error controls and both time alignment controls are on (included in calculation), the sum of column D in the worksheet ErrorControl is 37.

2.3 Worksheet 2: Summary

The Summary worksheet in the Error Model workbook comprises input mode control in rows 4 – 10 and output summary in rows 12 – 142.

The calculation mode control is accomplished with cell A6 where the user normally confirms that a numerical value of “2” is designated. Mode 2 designates emissions calculation with all errors applied. Mode 1 corresponds to a calculation of emissions with all errors applied except environmental errors and time alignment. Mode 0 designates an “ideal” emissions calculation with no errors applied. In Monte Carlo error model simulation performed in this study Mode 2 was used.

Mode 0 is used off-line prior to Monte Carlo simulation to generate the “ideal” emissions for a given reference NTE event. The Mode 0 values are calculated by entering a value of “0” in cell A6. The Mode 0 calculation and subsequent storing of the “ideal” emissions results may be accomplished manually (as described above) or by exercising a provided macro. The macro automatically sets the value in cell A6 to zero, calculates and saves the “ideal” emissions values, and returns the value in A6 to “2” in preparation for the Monte Carlo simulation. The locations where the reference NTE event must be entered manually, and the locations where the “ideal” emissions must be saved (done automatically if the macro is used) are described in the Methods worksheet section.

Mode 1 calculations are fully implemented in the Error Model spreadsheet and used for drift correction calculations. Mode 1 in cell A6 is not typically used but can be applied for diagnostic purposes.

The output summary section of the Summary worksheet in rows 12 – 142 presents numerically and descriptively labeled outputs of the emissions and emissions error calculations. The suffix ‘_TA’ indicates that time alignment has been applied to the result, and the suffix ‘_DC’ indicates that periodic drift correction has been applied to the result. Both time alignment and periodic drift correction are applied in the Methods worksheet. However, a result in the Summary worksheet with designation ‘_TA’ has been calculated with an emissions value plus errors all modified by the applicable time alignment percentage just prior to subtracting the “ideal” emissions to produce the emissions difference. Time alignment was applied only to NO_x and CO emissions. Similarly, a result in the Summary worksheet with designation ‘_DC’ has been calculated by a drift correction formulation. A periodic drift rejection flag was checked by logic.

Consider the logic in cell C19 for the output 001_DeNO_x (g/kW-hr), Method 1_TA_DC. The logic checks the drift rejection flag in cell C43. If the flag is 1, a huge negative number

(typically -9999999, from cell D13) is returned in cell C19. Otherwise, the time aligned value from the Methods worksheet is returned in cell C19 of the Summary worksheet.

In the output summary, the cells that are highlighted in turquoise color are designated by Crystal Ball as “Forecast” (or output) random variables. When running the Monte Carlo simulation with Crystal Ball, a filter is designated for the ‘_DC’ (drift corrected) “Forecasts” such that a value less than -9999 (or similar huge negative number, but greater than the value typically -9999999 returned when drift flag is 1) will be rejected. The filter on the “Forecast” rejects the values meeting the filter criterion (drift correction). Thus, when data is “Extracted” from a Crystal Ball Monte Carlo simulation, drift corrected (rejected) values are omitted (cells are empty) in the Excel spreadsheet of simulation output values. It is expected that other Monte Carlo software comparable to Crystal Ball, such as @Risk, will have similar rejection provisions with which periodic drift correction based on the calculated flag can be accomplished.

A total of 213 outputs (“Forecasts”) are designated in the Summary worksheet covering the number of output values from three emissions (NO_x, CO and NMHC), three calculation methods (Methods 1, 2 and 3), with and without time alignment, and with and without drift correction, for the full error model and for the validation model (designated Valid in Summary worksheet variable labels). All of these “Forecasts” are provided in both units of grams/kW-hr and (for selected outputs) in grams/hp-hr. This variety of calculations was accomplished in the Methods worksheet.

2.4 Worksheet 3: Methods

The Methods worksheet of the Error Model workbook comprises the following areas:

- Notes and diagnostic guides are located principally in rows 1 – 22 in columns A – CF, continuing on row 5 through column DD.
- Reference NTE event data are located in rows 35 - 351 of columns A – W. Actual reference NTE event data must be entered manually starting on row 52 in columns A – V. One to 300 rows of reference NTE event data are allowed. Uniform (one second interval) time steps are assumed represented by the reference NTE data.
- Parameters calculated are located in rows 35 – 351 of columns X – CF. The number of rows of these parameter equations must match the number of rows in the reference NTE event. Excess cells in these columns may be cleared manually or automatically during execution of the macro.
- Mode 0, Ideal Emissions for this reference NTE event are stored in column O rows 22 – 32 (either manually or automatically by the macro). Related data on the same rows are located in columns CT – DD.
- Input i_c random variable distributions (Crystal Ball uses the terminology “Assumptions” for these inputs) are located in rows 26 – 32 of columns AG - CF.

- Emissions calculations by three methods are located in rows 6 - 101 of columns CG – CJ (Method 1), CK – CN (Method 2) and CO – CR (Method 3). This part of the worksheet calculates full model, validation model, time alignment and drift correction.

2.5 Methods Worksheet: Notes and Diagnostic Guide

In rows 1 – 22 for columns A – CF, several descriptive labels and references are defined for use in navigating through the worksheet. Row 5, columns A-DD, contains column identification numbers referenced in rows 7 through 22 (depending on the column). For example, in column H the values 65 and 66 in rows 8 and 9, respectively, indicate that the values in column H (rows 52 and following rows) are applied in columns 65 (BM) and 66 (BN) labeled on row 5. If the user scrolls to cells BM52 or BN52 it is observed that the spreadsheet formulas in these cells refer to values from column H. Also, column H, rows 10, 11 and 12 indicate that the values in column H (rows 52 down) are also applied in the Delta (emissions error surface) tabs ‘45 Delta CO2 SS’, ‘46 Delta CO2 Transient’ and ‘49 Delta CO2 Ambient Temperature’. The information in the notes and diagnostic guide was not applied by the spreadsheet in any of the emissions calculations. It was included with the intent to simplify diagnostics by providing information on locations where spreadsheet values were applied elsewhere in the spreadsheet. Outside the areas indicated above, some other notes, comments and diagnostic guides may be found in other areas of the spreadsheet.

2.5.1 Methods Worksheet: Reference NTE Event

The reference NTE event used in the simulation was entered in rows 35-351 of columns A – W. Actual reference NTE event data must be entered manually starting on row 52 in columns A – V. A minimum of one and a maximum of 300 rows of reference NTE event data are allowed. Equal time steps (1 second intervals) are assumed in the reference NTE data rows. The standard format and engineering units of reference NTE event data established for this project must be observed. These are described in the column headings on rows 47 – 51, columns A – V.

2.5.2 Methods Worksheet: Parameters

Parameters applied in the three emissions methods are calculated in rows 35 – 351 of columns X – CF. The number of rows of these parameter equations must match the number of rows in the reference NTE event. Excess cells in these columns may be cleared manually or automatically during execution of the macro.

The formulas applied in rows 52 and down in columns X – CF have been produced by normal edit-copy (typically of row 52 in these columns) and edit-paste to rows 53 and following rows in these columns. The Δt values displayed in column AC are not used in any calculation, but are displayed so a user can confirm uniform reference NTE event time sampling. The last cell in column AC can be cleared (done automatically by the macro). Note that excess cells in these columns must be cleared, and row deletion operations should not be applied since this would affect other areas in the Methods worksheet.

Certain sums are performed in several columns over the Parameter rows (range of the reference NTE event). These are accomplished in row 46 in columns AU – AX, BC, BD, BI, BJ, BO – BR and BU – CF. Certain constants applied in the calculation are stored in cells AW42, BC42, BI42, BP40 and BP42. Other constants or conversion factors are incorporated numerically in spreadsheet formulas. Typical of these is “0.01” to convert a percentage to a fraction.

Specific parameters or variables are calculated in the various columns for application in all three methods, full model and validation model, and for drift correction. Time alignment distinctions are not generated in this area of the spreadsheet. Table 2 lists the parameters used in the Methods worksheet, the columns where they are computed and a brief description of the parameters.

TABLE 2. METHODS WORKSHEET PARAMETER COLUMN DESCRIPTIONS

Methods Worksheet Parameters Column Descriptions		
Subject	Column	Description
Engine operating state percentages	X – AB	Convert NTE Event variables to percentages: speed, torque, fuel rate, exhaust flow
Δ Time	AC	Displays Δt between NTE Event rows
NMHC	AD	Calculate NMHC ppm as 0.98 of THC ppm
Fuel Rate	AE	Calculate fuel rate g/s based on fuel density of 851 g/L
Exhaust Flow Calculations	AF	Convert exhaust flow SCFM to mol/s
	AG	Sum exhaust flow errors from Delta tabs 20, 21, 22, 23, 25 27 and 28 expressed in % of mol/s maximum. Respective ErrorControl tab switches are applied.
	AH	Convert the total exhaust flow error in % of maximum mol/s to mol/s
	AI	Add the mol/s exhaust flow error to the exhaust flow in mol/s. Mode control logic is applied.
Speed with error	AJ	Add engine speed error from Delta tab 43 expressed as % of engine range converted to rpm to engine speed in rpm. Mode control logic and ErrorControl switch are applied.
Fuel rate with error	AK	Add fuel rate from Delta tab 44 expressed as % of maximum fuel rate converted to g/s to engine fuel rate in g/s. Mode control logic and ErrorControl switch are applied.
Torque	AL	Sum torque errors from Delta tabs 29, 30, 31, 32, 34 expressed as % of peak torque, and from Delta tab 35 expressed as % of NTE point torque converted to % of peak torque. ErrorControl switches are applied.
	AM	Add the total torque error expressed as % of peak torque converted to N·m to engine torque in N·m. Mode control logic is applied.
BSFC	AN	Sum BSFC errors from Delta tabs 36, 37, 38, 39, 41 expressed as g/kW-hr, and from Delta tab 42 expressed as % of NTE point BSFC converted to g/kW-hr. ErrorControl switches are applied.
	AO	Add the total BSFC error expressed as g/kW-hr to engine BSFC in g/kW-hr. Mode control logic is applied.
NOx and Δ NOx, ppm	AP	Sum engine NO ppm and NO ₂ ppm.
	AQ	Sum environmental NOx errors. Error from Delta tab 5 is the only one developed.
	AR	Sum other NOx errors including errors from Delta tabs 1 and 2.

	AS	Add the total NO _x errors expressed as ppm to engine ideal NO _x in ppm. Mode control logic is applied.
	AT	Add the NO _x errors except environmental expressed as ppm to engine ideal NO _x in ppm for drift correction calculation. Mode control logic is applied.
NO _x · Exhaust Flow	AU	Form product of NO _x fraction (all errors case, column AS) and exhaust flow (mol/s, column AI) for application in Methods 1 and 2.
	AV	Form product of NO _x fraction (all errors except environmental, column AT) and exhaust flow (mol/s, column AI) for application in Methods 1 and 2 drift correction.
Speed · Torque	AW	Form product of Speed (rpm, all errors case, column AJ) and Torque (N·m, all errors case, column AM) for application in Methods 1 and 3. Convert rpm to radians/sec with 2π radians/revolution, minutes to seconds with 60sec/min, N·m/sec to watt hr with 3600Joules/watt hr, and watt to kW with 1000w/kW.
	AX	Form product of Speed (rpm, no errors for validation case, column O) and Torque (N·m, no errors for validation case, column T) for application in Methods 1 and 3. Convert rpm to radians/sec with 2π radians/revolution, minutes to seconds with 60sec/min, N·m/sec to watt hr with 3600Joules/watt hr, and watt to kW with 1000w/kW.
CO and Δ CO, %	AY	Sum environmental CO errors including errors from Delta tabs 10 and 11.
	AZ	Sum other CO errors. Error from Delta tab 7 is the only one developed.
	BA	Add the total CO errors expressed as % to engine CO in %. Mode control logic is applied.
	BB	Add the CO errors except environmental expressed as % to engine CO in % for drift correction calculation. Mode control logic is applied.
CO · Exhaust Flow	BC	Form product of CO fraction (all errors case, column BA) and exhaust flow (mol/s, column AI) for application in Methods 1 and 2.
	BD	Form product of CO fraction (all errors except environmental, column BB) and exhaust flow (mol/s, column AI) for application in Methods 1 and 2 drift correction.
NMHC and Δ NMHC, ppm	BE	Sum environmental NMHC errors including errors from Delta tabs 16, 17 and 19.
	BF	Sum other NMHC errors including errors from Delta tabs 13 and 14.
	BG	Add the total NMHC errors expressed as ppm to engine NMHC in PPM. Mode control logic is applied.
	BH	Add the NMHC errors except environmental expressed as ppm to engine NMHC in ppm for drift correction calculation. Mode control logic is applied.
NMHC · Exhaust Flow	BI	Form product of NMHC fraction (all errors case, column BG) and exhaust flow (mol/s, column AI) for application in Methods 1 and 2.
	BJ	Form product of NMHC fraction (all errors except environmental, column BH) and exhaust flow (mol/s, column AI) for application in Methods 1 and 2 drift correction.
CO ₂ and Δ CO ₂ , %	BK	Sum environmental CO ₂ errors. Error from Delta tab 49 is the only one developed.
	BL	Sum other CO ₂ errors including errors from Delta tabs 45 and 46.
	BM	Add the total CO ₂ errors expressed as % to engine CO ₂ in %. Mode control logic is applied.
	BN	Add the CO ₂ errors except environmental expressed as % to engine CO ₂ in % for drift correction calculation. Mode control logic is applied.

Exhaust Flow · [NMHC + (CO+CO ₂)] / BSFC	BO	Form product of NMHC fraction plus CO and CO ₂ fractions (all errors case, columns BG, BA and BM) and exhaust flow (mol/s, column AI) divided by BSFC (g/kW-hr, all errors case, column AO) for application in Method 2.
	BP	Form product of NMHC fraction plus CO and CO ₂ fractions (all errors except environmental, columns BH, BB and BN) and exhaust flow (mol/s, column AI) divided by BSFC (g/kW-hr, with errors, column AO) for application in Method 2 drift correction.
	BQ	Form product of NMHC fraction plus CO and CO ₂ fractions (all errors case, columns BG, BA and BM) and exhaust flow (mol/s, column AI) divided by BSFC (g/kW-hr, no errors case, column V) for application in Method 2 validation.
	BR	Form product of NMHC fraction plus CO and CO ₂ fractions (all errors except environmental, columns BH, BB and BN) and exhaust flow (mol/s, column AI) divided by BSFC (g/kW-hr, no errors, column V) for application in Method 2 validation drift correction.
NMHC + (CO+CO ₂)	BS	Form sum of NMHC fraction plus CO and CO ₂ fractions (all errors case, columns BG, BA and BM) for application in Method 3.
	BT	Form sum of NMHC fraction plus CO and CO ₂ fractions (all errors except environmental, columns BH, BB and BN) for application in Method 3.
NOx · Fuel Rate / [NMHC + (CO+CO ₂)]	BU	Form product of NOx fraction (all errors case, using column AS) and Fuel Rate (g/s, all errors case, column AK) divided by sum of NMHC fraction plus CO and CO ₂ fractions (all errors case, column BS) for application in Method 3.
	BV	Form product of NOx fraction (all errors except environmental, using column AT) and Fuel Rate (g/s, with error, column AK) divided by sum of NMHC fraction plus CO and CO ₂ fractions (all errors except environmental, column BT) for application in Method 3 drift correction.
CO · Fuel Rate / [NMHC + (CO+CO ₂)]	BW	Form product of CO fraction (all errors case, using column BA) and Fuel Rate (g/s, all errors case, column AK) divided by sum of NMHC fraction plus CO and CO ₂ fractions (all errors case, column BS) for application in Method 3.
	BX	Form product of CO fraction (all errors except environmental, using column BB) and Fuel Rate (g/s, with error, column AK) divided by sum of NMHC fraction plus CO and CO ₂ fractions (all errors except environmental, column BT) for application in Method 3 drift correction.
NMHC · Fuel Rate / [NMHC + (CO+CO ₂)]	BY	Form product of NMHC fraction (all errors case, using column BG) and Fuel Rate (g/s, all errors case, column AK) divided by sum of NMHC fraction plus CO and CO ₂ fractions (all errors case, column BS) for application in Method 3.
	BZ	Form product of NMHC fraction (all errors except environmental, using column BH) and Fuel Rate (g/s, with error, column AK) divided by sum of NMHC fraction plus CO and CO ₂ fractions (all errors except environmental, column BT) for application in Method 3 drift correction.
NOx · Fuel Rate / [NMHC + (CO+CO ₂)]	CA	Form product of NOx fraction (all errors case, using column AS) and Fuel Rate (g/s, selected errors case, column AE) divided by sum of NMHC fraction plus CO and CO ₂ fractions (all errors case, column BS) for application in Method 3 validation.
	CB	Form product of NOx fraction (all errors except environmental, using column AT) and Fuel Rate (g/s, selected errors case, column AE) divided by sum of NMHC fraction plus CO and CO ₂ fractions (all errors except environmental, column BT) for application in Method 3 validation drift correction.

CO · Fuel Rate / [NMHC + (CO+CO ₂)]	CC	Form product of CO fraction (all errors case, using column BA) and Fuel Rate (g/s, selected errors case, column AE) divided by sum of NMHC fraction plus CO and CO ₂ fractions (all errors case, column BS) for application in Method 3 validation.
	CD	Form product of CO fraction (all errors except environmental, using column BB) and Fuel Rate (g/s, selected errors case, column AE) divided by sum of NMHC fraction plus CO and CO ₂ fractions (all errors except environmental, column BT) for application in Method 3 validation drift correction.
NMHC · Fuel Rate / [NMHC + (CO+CO ₂)]	CE	Form product of NMHC fraction (all errors case, using column BG) and Fuel Rate (g/s, selected errors case, column AE) divided by sum of NMHC fraction plus CO and CO ₂ fractions (all errors case, column BS) for application in Method 3 validation.
	CF	Form product of NMHC fraction (all errors except environmental, using column BH) and Fuel Rate (g/s, selected errors case, column AE) divided by sum of NMHC fraction plus CO and CO ₂ fractions (all errors except environmental, column BT) for application in Method 3 validation drift correction.

2.5.3 Methods Worksheet: Mode 0 Ideal Emissions

For the reference NTE event in rows 52 and down in columns A – V, an ideal emissions value must be calculated and stored for application in the emissions difference calculations. The ideal case can be calculated either manually or automatically by the macro. Following the calculation, the ideal values are stored by edit-copy edit-paste-special-values operation to the cells in column O, rows 22 – 32. The manual operations described below are performed automatically by the macro, if executed, after manually entering the reference NTE event.

After manually entering the reference NTE event to be simulated and checking that the number of rows of equations in the Parameters section matches the rows in the reference NTE event, a numerical “0” can be entered in cell A6 of the Summary worksheet. The Methods worksheet should have calculated Mode 0 results using the reference NTE event. If error messages like “#VALUE or #DIV/0!” are displayed, there is probably still a mismatch between the rows of the reference NTE event and Parameter equations. When calculated properly (with 0 in Summary A6), the values displayed in the Methods worksheet columns CU, CV, CW, DB and DD will be equal on each of the rows 22 – 32. The values in column CX are not yet equal (unless previously calculated and stored for this reference NTE event) because they reflect the values stored in Methods worksheet column O, rows 22 – 32. The next manual step is to edit-copy column CU, rows 22 -32, and store the values by edit-paste-special-values in column O, rows 22 -32. Now in rows 22 -32 the columns CU - DD should be equal. The final step is to return to Summary worksheet cell A6 and change the value from 0 to 2. At this point the spreadsheet could be run in Monte Carlo simulation to produce properly sampled values. However, if the user desires to monitor charts provided in the Delta worksheets during the simulation, further row-matching to the reference NTE event is required in most of the Delta worksheets.

The manual operations described in the previous paragraph are intended to explain how the Mode 0 ideal emissions are calculated and stored for use in the Monte Carlo simulation when Δemissions values are calculated using the ideal emissions results stored in O22 – O32. The reference NTE event must be entered with an operation such as a manual edit-copy and edit-paste or edit-paste-special-values operation. At this point the macro can be executed with tools-

macro-macros-(macro1)-run operation. The macro automatically performs the mode 0 calculation, stores the mode 0 results in O22 – O32, and changes Summary A6 back to mode 2.

The macro also deletes extraneous rows from all the appropriate Delta worksheets so the charts therein display properly. It is important to copy the reference NTE event into a fully ‘loaded’ starter file with equations filled on 300 rows in the Parameters area, and with full 300 row complement of equation-rows in each of the appropriate Delta worksheets for the macro to modify the spreadsheet properly.

2.5.4 Methods Worksheet: Input i_c Random Variable Distributions

Probability distribution parameters are applied, and simulation trial values of the inputs are generated in rows 26 – 32 of columns AG - CF. Rows 26 and 27 are used to input distribution parameters. Rows 28 and 29 contain descriptive labels brought from the appropriate Delta worksheet. Row 30 is an information-only number, row 31 contains the name label applied in Monte Carlo simulation to the input i_c , and row 32 is where the Monte Carlo simulation tool places generated randomly-sampled values during simulation. The values in row 31 are referenced by formula in the respective Delta worksheets where they are used for interpolation on the error surfaces.

The Monte Carlo tool in Crystal Ball uses the terminology “Assumptions” for these inputs. Two distribution forms are applied: truncated normal (Gaussian), and discrete uniform. For the normal distribution, the applied standard deviation is in row 27. In Crystal Ball, the standard deviation cell on row 27 and the label cell on row 31 were referenced by equation in the Crystal Ball assumption setup window, the mean was input as 0, and the distribution was truncated at -1 and at +1. Since all the truncated normal i_c distributions are identical (although the sampled trial values from each will be random in the Monte Carlo simulation), the Crystal Ball define-copy data and define-paste data operations were applied to define the truncated normal distributions for other i_c variables once the first one had been defined.

For the discrete uniform distributions, the minimum discrete value (1 in all cases) was applied in row 26, the maximum discrete value was applied in row 27 and the other row descriptions are the same as before. Again, one of these inputs was setup with Crystal Ball “define assumption” and then applied with Crystal Ball define-copy data and define-paste data operations to other i_c cells on row 32 where a discrete uniform distribution was applied. When Crystal Ball “Assumptions” were defined, Crystal Ball colored each input cell bright green. It is expected that @Risk has similar input definition procedures.

During a Monte Carlo simulation, the Monte Carlo tool (e.g. Crystal Ball) placed a numerical value in each of the i_c cells on row 32. Then the spreadsheet was exercised to perform interpolations in all the Delta worksheets. The resulting error sample values for the entire reference NTE event were returned to the Methods worksheet Parameters area, and then the Methods worksheet Emission Calculations section computes Δ emissions using three methods, full model and validation, drift correction, time alignment and not, etc. to generate one set of the 213 output values described in the Summary section. The simulation tool stores the set of 37 random input values from row 32 as well as the 213 output values in an Excel data base from

which the corresponding sets of values can later be extracted. Once each trial was completed, the simulation tool randomly sampled a second set of input values from the respective probability distributions, placed the values in the cells on row 32, exercised the spreadsheet again, stored the input and output values, and went to a third trial, etc. Typically 10,000 and 30,000 trials, depending on the reference NTE event, were used in this project with this Error Model workbook.

Note that there are three ways the user can control the effect of the i_c values in the emissions calculations:

1. Mode control in Summary A6,
2. Include / exclude switches in ErrorControl column D, and
3. Specification of input random variables (“Assumptions”) and their probability distributions in the Methods worksheet row 32.

These three ways of controlling the i_c values are independent, but the effects are interdependent as follows. Mode control determines what categories of errors are added into the calculations. Mode controls categories of errors are classified as:

1. Mode 0 - no errors included
2. Mode 1 - “all” but ‘environmental’ errors included
3. Mode 2 - “all” errors added into the calculations.

“All” in this context represents those error surfaces turned on by the switches in the ErrorControl worksheet. The input random variable distribution controls the distribution of the sampled i_c values applied during Monte Carlo simulation for the several Delta error surfaces. Mode and ErrorControl switches must be appropriately turned on for the effects of the sampled i_c values to be included in the emissions difference results. These controls affect the calculations in the Methods worksheet Parameters and Emission Calculations sections.

2.5.5 Methods Worksheet: Emission Calculations

In the area of rows 6 - 101 of columns CG – CR the brake-specific emissions and Δ emissions calculations are performed using the variables and parameters generated in the Parameters section. Three sets of columns, structured similarly, calculate the full model, validation model, time alignment and drift correction for the following methods:

1. Method 1 calculations are applied in columns CG – CJ,
2. Method 2 calculations are applied in columns CK – CN, and
3. Method 3 calculations are in columns CO – CR.

Columns CG - CJ for Method 1 are typical of the methods where the structure is the same, but the formulas are a little different. Column CG is an information-only column that displays Method 1 formulas implemented by equations in columns CH – CJ. Column CH performs the

NO_x emission calculations, while column CI performs the CO emissions and column CJ performs the NMHC calculations. The structure of the three columns is the same. Formulas implemented in the three columns are the same, but the equations implementing the formulas apply variables and parameters appropriate to the respective emissions.

As an example of the calculation for NO_x Method 1 we will examine column CH in detail. The full model calculation was accomplished in cells CH48 – CH74. The ideal emissions result was brought into the area by equation in CH51. Full model NO_x emissions (eNO_x) in g/kW-hr were calculated in CH54. Cells CH55 – CH59 are information-only diagnostic aids. The full model Method 1 result in CH54 is calculated by the formula in Figure 1.

$$e_{NO_x} (g / kW \cdot hr) = \frac{M_{NO_2} * \sum_{i=1}^N \left[(xNO_{2_i} (ppm) + xNO_{i_i} (ppm)) * 10^{-6} * \dot{n}_i \left(\frac{mol}{s} \right) * \Delta t \right]}{\sum_{i=1}^N \left[\frac{Speed_i (rpm) * T_i (N \cdot m) * 2 * 3.14159 * \Delta t}{60 * 1000 * 3600} \right]}$$

FIGURE 1. BRAKE-SPECIFIC NOX BY METHOD 1

In the formula for the full model mode 2, delta error values sampled from the Delta worksheets 1, 2 and 5 have been added to xNO_2 , xNO . Similarly, delta error values sampled from Delta worksheets 20-23 and 25-28 have been added to the exhaust flow, delta errors sampled from worksheets 29-32 and 34-35 were added to torque, and worksheet 43 deltas were added to speed. The Δt values are equal (1 second) and therefore cancel out of the equation.

‘Full’ model Mode 1 (with all errors except environmental errors from Delta worksheet 5) is calculated in CH64. Cells CH65 – CH69 are for information-only.

The full model rejection flag is calculated in CH74. A rejection flag is computed as shown in Figure 2. For reference NTE events with ideal NO_x emissions below the threshold of 2.682 g/kW-hr (2.0 g/hp-hr), the allowable band is defined by full model emissions |mode 1 – mode 2| ≤ 4% of threshold. For reference NTE events with ideal NO_x emissions above the threshold, the allowable band is defined by full model emissions |mode 1 – mode 2| ≤ 4% of ideal emissions.

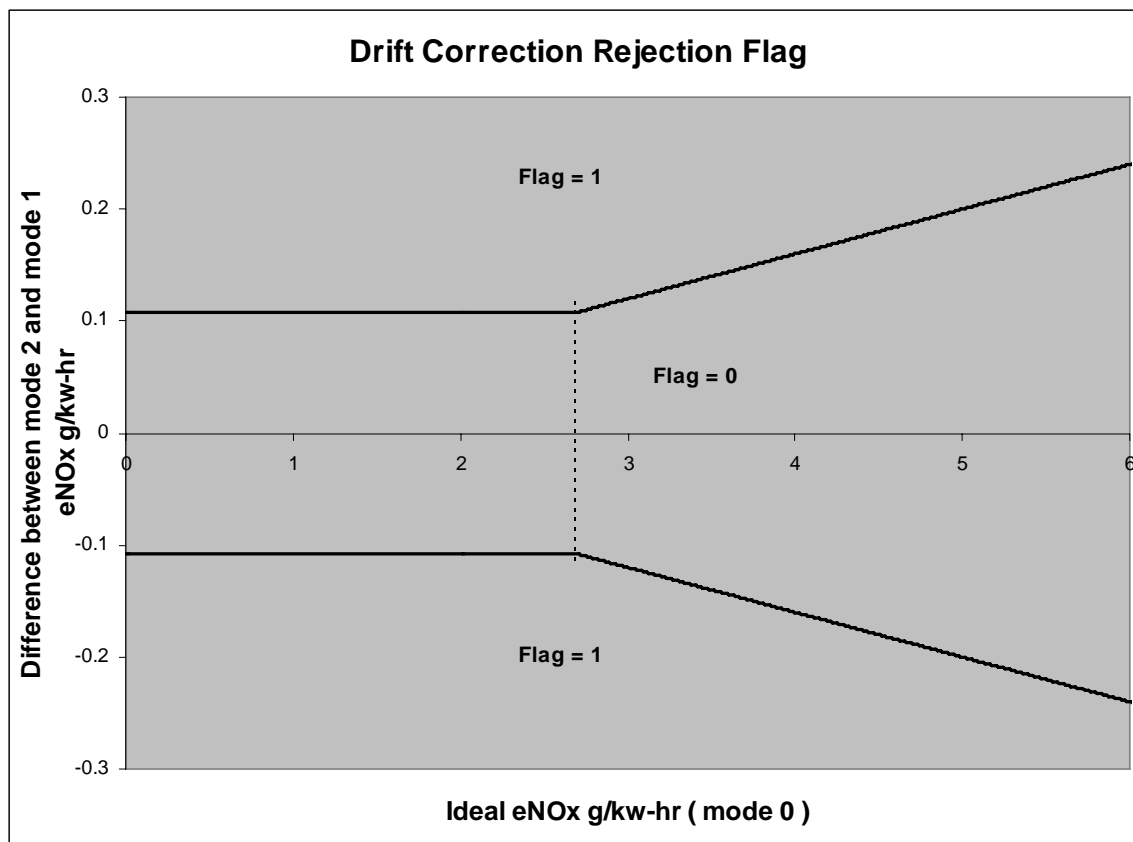


FIGURE 2. PLOT ILLUSTRATING PERIODIC DRIFT CORRECTION FLAG

The validation model calculation was accomplished in the cells CH79 – CH101. Validation model NO_x emissions (g/kW-hr) was calculated in cell CH81. Cells CH82 – CH86 are information-only. Validation model Mode 1 (with ‘all’ errors except certain environmental errors) was calculated in CH91. Cells CH92 – CH96 are information-only. The validation model rejection flag was calculated in CH101. For reference NTE events with ideal NO_x emissions below the threshold of 2.682 g/kW-hr (2.0 g/hp-hr), the allowable band was defined by validation model emissions $|\text{mode 1} - \text{mode 2}| \leq 4\%$ of threshold. For reference NTE events with ideal NO_x emissions above the threshold, the allowable band was defined by validation model emissions $|\text{mode 1} - \text{mode 2}| \leq 4\%$ of ideal emissions.

The drift correction flag was computed similarly for CO and NMHC emissions with different thresholds and allowable bands. For CO the threshold was 26.016 g/kW-hr (19.4 g/hp-hr) and the allowable band was again defined at 4%. For NMHC the threshold was 0.282 g/kW-hr (0.21 g/hp-hr) and the allowable band was defined at 10%.

Continuing with column CH for NO_x, the time alignment indicated by the suffix ‘_TA’ in the label in CH24 was calculated for the full model in CH25. The Time Alignment was applied as a modification by a percentage of the full model NO_x emissions result from CH54. The time alignment for NO_x expressed as a percentage from Delta worksheet 51 was converted to a fraction, and the fractional increment g/kW-hr was added to the NO_x expressed in g/kW-hr. The

mode control logic and ErrorControl switch are applied. The same calculation of time alignment for the validation result from CH81 was done in CH42 again with mode control and ErrorControl.

In CH14 the full model ΔNO_x value in g/kW-hr was calculated for the time alignment case by subtracting the ideal emissions in g/kW-hr from the result in CH25 described in the previous paragraph. The full model ΔNO_x value in g/kW-hr was converted to g/hp-hr in CH11. Similar results for the validation model are in CH15 and CH12.

Rejection flags are taken to the Summary worksheet where drift correction explained in the Summary worksheet section has been described. Additional result combinations are calculated and presented for NO_x Method 1 in column C of the Summary worksheet using results described above from column CH of the Methods worksheet.

Calculations for NO_x by Method 1 described above for column CH are similar for CO and NMHC by Method 1 in columns CI and CJ, respectively. Similar calculations for NO_x , CO and NMHC by Method 2 are presented in columns CL – CN, and by Method 3 in columns CP – CR.

2.6 Worksheet 4: Constants and Equations

The Constants&Eqns tab was strictly a snapshot of the equations used in the brake-specific emissions calculations. It displayed the equations and constants implemented in spreadsheet formulas of the Methods worksheet. The various parts all shown together in this worksheet are redisplayed at appropriate locations in the Methods worksheet.

2.7 Worksheet 5: SS NO_x Error Surface

The 1 Delta NO_x SS worksheet was the first Delta worksheet. Its functional structure, formulas, charts and operation are similar to the following worksheets:

- 7 Delta CO SS
- 20 Delta Exhaust Flow SS
- 22 Delta Exhaust Flow Pulsation
- 23 Delta Exhaust Flow Swirl
- 30 Delta Torque DOE Testing
- 37 Delta BSFC DOE Testing
- 45 Delta CO_2 SS

With only minor changes in charts and structure, its function, formulas and operation are also similar to the following worksheets:

- 2 Delta NO_x Transient
- 21 Delta Exhaust Flow Transient
- 29 Delta Dynamic Torque
- 36 Delta Dynamic BSFC

- 43 Delta Dynamic Speed
- 44 Delta Dynamic Fuel Rate
- 46 Delta CO2 Transient

The following provides a brief summary of the 1 Delta NO_x SS worksheet:

- Rows 1 – 7 contain descriptive information about the error surface implemented in the worksheet.
- Rows 8 - 42 present the error surface in columns A – L. Other columns, M – W, on these rows generate a lookup table used with an interpolation routine.
- Figures A, B and C follow.
- Rows 76 – 379 calculate the ΔNO_x SS error values for each row of the reference NTE event. These values were returned to the Methods tab Parameters section.

The following paragraphs describe in further detail functions in the 1 Delta NO_x SS worksheet:

Data from the error surface (rows 13 – 42, columns A – L, in this Delta worksheet) must be entered in sorted order (sorted on Lab Nominal column C in ascending order) for proper operation of the x-lookup-interpolation function. The three figures chart the error function. Figure A plots several data sets versus the x-value, Lab Nominal (column C). Figure A y-values are NO_x ppm (PEMS) including Lab Nominal (column C), 95th percentile (column F), 50th percentile (median) (column E) and 5th percentile (column D).

Related error surface data are plotted in Figure B. Figure B plots several data sets versus the same x-value, Lab Nominal (column C). Figure B y-values are the difference, NO_x ppm (PEMS) – NO_x ppm (lab, nom). The differences plotted may not correspond exactly to the values shown in Figure A because of the statistical procedure applied in calculating the differences shown in Figure B. This procedure is described in Sections 4.0 and 5.0 of this report. Figure B plots the 95th percentile (column I), the 50th percentile (median) (column H) and the 5th percentile (column G). In addition to the error surface data, Figure B also shows the interpolation line designated $i_c = xx$ (column V), and the reference NTE event values on the interpolation line (column F rows 80 through end of the reference NTE event versus Lab Nominal x-values in column B rows 80 through end of the reference NTE event). When $i_c = +1$, the interpolation line plots on the 95th percentile. When $i_c = 0$, the interpolation line plots on the 50th percentile. When $i_c = -1$, the interpolation line plots on the 5th percentile. The reference NTE event always plots on the interpolation line, with points at the x-values in the reference NTE event.

The error surface data were also plotted in the format of Figure C. Again the x-axis was the same Lab nominal (column C). This time the y-axis data are the i_c values. Thus, the 95th percentile plots at +1, the 50th percentile plots at 0 and the 5th percentile plots at -1. The interpolation line plots at the value of i_c , and the reference NTE event plots on the interpolation line at the x-values in the reference NTE event. If appropriate value labels were displayed in Figure C, the values would represent the error surface plotted on a z-axis above the two-dimensional x-y plane. These error surface values are displayed graphically in Figure B.

Now consider inner rows 13 – 41 in the look-up table in columns T – W. Column T is a repetition of the x-value from column C. Column U calculates a row-to-row Δ for the x-values in column T for use in interpolation. Column V computes the interpolation line linearly interpolated according to the value of i_c between the median and the 95th percentile if $i_c > 0$ (on median if $i_c = 0$ and on 95th percentile if $i_c = +1$); and between the median and the 5th percentile if $i_c < 0$ (on median if $i_c = 0$ and on 5th percentile if $i_c = -1$). Only one i_c value (from cell E80) is applied in this calculation of the interpolation line. The Microsoft Excel vertical lookup function VLOOKUP is applied to the table in rows 12 – 42 in columns T – W. This is done in rows 80 and down in column F. Because of the way the VLOOKUP function operates, the first row cells T12 and V12, and the last row cell W42 (all three cells distinguished by darker line borders) contain formulas or values different from the formulas of the inner rows. The formula in cell T12 assures that the lookup function can always find an x-value in its table. The formula in V12 and the value in W12 assure that the interpolation in cells F80 to the end of the reference NTE event data returns the nearest Δ NO_x SS value on the interpolation line if the x-value is outside the range of the error surface lab nominal values.

Before going to the interpolation accomplished in F80 and down, consider briefly the formulation on rows 12 – 43 in columns O – R. This formulation considers one x-value from the reference NTE event, the first one, in cell B80 and selects the two adjacent rows in the error surface between which to interpolate on the B80 x-value. The result is formed on row 43 in these columns and then the “check” cell G80 accomplishes the i_c controlled interpolation. This provides an alternative calculation check on one row in the reference NTE event.

Now consider the interpolation for each point in the reference NTE event. Column B, row 80 and down, brings the lab nominal x-value from the Methods worksheet reference NTE event. For this Delta worksheet, that x-value is $x_{NO}(\text{ppm}) + x_{NO_2}(\text{ppm})$. The out-of-range flags are information-only indicating points in the reference NTE event with x-value out of the range of the error surface lab nominal. The i_c value for this Delta worksheet was brought into cell E80 from the Methods worksheet i_c area. Each point in the reference NTE event was interpolated with the same i_c value, but with its own x-value. Recalling that the interpolation line in column V was computed with this one i_c value, the x-interpolation between the appropriate two adjacent rows in the error surface can now be accomplished. This requires using the x-value on each row in column B, B80 and down, in the VLOOKUP function, and performing the required calculation using the looked-up values and deltas from the look-up table. The calculation is done with the formulas in cell F80 and down. The values computed in column F, cell F80 and down through the reference NTE event, could be considered elements of a column matrix or vector, and are returned to the Methods worksheet Parameters section.

In the Monte Carlo simulation, the Methods worksheet combines this reference NTE event result vector from the 1 Delta NO_x SS worksheet with similar results from other error surfaces, calculates Δ emissions by three methods, full model and validation, drift reject flags, time alignment, etc. to produce a set of 213 output values (“Forecasts” in Crystal Ball terminology) described in the Summary worksheet section. This was done having input 35 i_c values (including 1 i_c value for this Delta NO_x SS) and two time alignment values all chosen by random sample from the appropriate truncated normal or uniform distribution as explained in the Methods worksheet section. Then another sample set of 35 plus two randomly sampled values

was input (only one i_c value coming to this Delta function again). The reference NTE event NO_x SS vector was recomputed with the one new i_c value, returned to Methods worksheet and another set of 213 output values was produced. This process was repeated many times until a statistical convergence criterion, described in Section 2, was satisfied. Typically, 10,000 to 30,000 sets of 37 input values and 213 output values were produced to satisfy the convergence criterion with this Error Model spreadsheet.

The number of rows in the Delta worksheet reference NTE event area (rows 80 and down) should match the number of rows in the reference NTE event applied in the Methods worksheet for proper function of Figures B and C. The starter spreadsheet has been set up with the range of charted reference NTE event series extending through row 379 in this Delta worksheet. The balance of the spreadsheet should calculate correctly when a reference NTE event is properly entered in the Methods tab and Parameters formulas properly aligned, although figures like B and C will not display properly until the last row of the reference NTE event is coincident with the end of the range of the charted reference NTE event series. This could be done manually in each Delta worksheet where needed, however, the macro was designed to convert the fully 'loaded' starter workbook after the reference NTE event was entered in the Methods worksheet. The macro uses the row count in the reference NTE event, aligns formulas in the Methods worksheet Parameters area, and eliminates extra rows in the reference NTE event area of each appropriate Delta worksheet. Again, the macro will do the operations correctly only on a fully 'loaded' starter workbook set up with 300 rows of formulas in the Methods worksheet Parameter area, and in each of the Delta worksheets using the reference NTE event.

One further detail in 1 Delta NO_x SS is the value computed in cell E75 and its label in E74. Each Delta worksheet has such a cell where the i_c value is reflected. The intent is to provide the user a further diagnostic capability through the user's designation of such cells as outputs ("Forecasts") in Monte Carlo simulation. This would allow the user to statistically process the input data with the same Crystal Ball (@Risk, etc.) tools used to process the outputs. Crystal Ball allows extraction of all the input (Crystal Ball applies the term "Assumptions" to the inputs) trial values without reflecting them as outputs ("Forecasts").

APPENDIX E
40-POINT TORQUE AND BSFC MAP DATA

Table Type Torque
 Engine Manufacturer DDC
 Engine Model Series 60
 Model Year 2005
 Serial Number 06R0767368
 Fuel Density 851 [g/L]
 Peak Torque 2195 [N-m]
 nlo 1014 [rpm]
 nhi 2129 [rpm]

Point	Raw Data		Normalized Data		
	ECM Speed rpm	Lab Torque N-m	ECM Speed nlo = 0% nhi = 100%	ECM Fuel Rate % of Maximum Fuel Rate	Lab Torque % of Peak Torque
1	2152	541	102%	34%	25%
2	2148	632	102%	39%	29%
3	2142	764	101%	46%	35%
4	2131	1074	100%	60%	49%
5	2095	1599	97%	97%	73%
6	2095	1336	97%	81%	61%
7	2095	1074	97%	66%	49%
8	2095	811	97%	53%	37%
9	2095	658	97%	44%	30%
10	2094	548	97%	38%	25%
11	1866	548	76%	33%	25%
12	1866	658	76%	38%	30%
13	1867	811	76%	46%	37%
14	1867	1074	76%	58%	49%
15	1867	1336	76%	73%	61%
16	1867	1599	76%	87%	73%
17	1867	1735	76%	95%	79%
18	1867	1858	76%	100%	85%
19	1636	2052	56%	94%	93%
20	1636	1599	56%	72%	73%
21	1636	1336	56%	60%	61%
22	1636	1074	56%	49%	49%
23	1636	811	56%	38%	37%
24	1636	658	56%	32%	30%
25	1636	548	56%	28%	25%
26	1407	548	35%	23%	25%
27	1407	750	35%	30%	34%
28	1407	811	35%	32%	37%
29	1407	1074	35%	42%	49%
30	1407	1336	35%	51%	61%
31	1407	1599	35%	60%	73%
32	1407	1878	35%	71%	86%
33	1407	2136	35%	84%	97%
34	1179	2058	15%	68%	94%
35	1179	1599	15%	53%	73%
36	1179	1336	15%	44%	61%
37	1178	1074	15%	36%	49%
38	1178	896	15%	30%	41%
39	1178	811	15%	27%	37%
40	1179	548	15%	20%	25%

Table Type BSFC
 Engine Manufacturer DDC
 Engine Model Series 60
 Model Year 2005
 Serial Number 06R0767368
 Fuel Density 851 [g/L]
 Peak Torque 2195 [N-m]
 nlo 1014 [rpm]
 nhi 2129 [rpm]

Point	Raw Data	Normalized Data		
	ECM Speed rpm	ECM Speed nlo = 0% nhi = 100%	ECM Fuel Rate % of Maximum Fuel Rate	BSFC % of Max
1	2152	102%	34%	100
2	2148	102%	39%	96
3	2142	101%	46%	92
4	2131	100%	60%	85
5	2095	97%	97%	81
6	2095	97%	81%	82
7	2095	97%	66%	85
8	2095	97%	53%	90
9	2095	97%	44%	96
10	2094	97%	38%	106
11	1866	76%	33%	95
12	1866	76%	38%	91
13	1867	76%	46%	88
14	1867	76%	58%	84
15	1867	76%	73%	83
16	1867	76%	87%	82
17	1867	76%	95%	81
18	1867	76%	100%	81
19	1636	56%	94%	79
20	1636	56%	72%	81
21	1636	56%	60%	77
22	1636	56%	49%	79
23	1636	56%	38%	82
24	1636	56%	32%	86
25	1636	56%	28%	89
26	1407	35%	23%	85
27	1407	35%	30%	81
28	1407	35%	32%	80
29	1407	35%	42%	77
30	1407	35%	51%	80
31	1407	35%	60%	75
32	1407	35%	71%	76
33	1407	35%	84%	77
34	1179	15%	68%	77
35	1179	15%	53%	77
36	1179	15%	44%	78
37	1178	15%	36%	78
38	1178	15%	30%	79
39	1178	15%	27%	80
40	1179	15%	20%	86

Table Type Torque
 Engine Manufacturer CAT
 Engine Model C9
 Model Year 2005
 Serial Number 9DG05784
 Fuel Density 851 [g/L]
 Peak Torque 1464 [N-m]
 nlo 1099 [rpm]
 nhi 2320 [rpm]

Point	Raw Data		Normalized Data		
	ECM Speed rpm	Lab Torque N-m	ECM Speed nlo = 0% nhi = 100%	ECM Fuel Rate % of Maximum Fuel Rate	Lab Torque % of Peak Torque
1	2366	365	104%	55%	25%
2	2348	369	102%	55%	25%
3	2340	431	102%	59%	29%
4	2325	604	100%	72%	41%
5	2195	1043	90%	100%	71%
6	2195	874	90%	91%	60%
7	2195	705	90%	74%	48%
8	2194	535	90%	63%	37%
9	2194	439	90%	57%	30%
10	2194	366	90%	53%	25%
11	1966	366	71%	41%	25%
12	1966	439	71%	46%	30%
13	1966	535	71%	52%	37%
14	1966	705	71%	62%	48%
15	1966	874	71%	74%	60%
16	1966	1043	71%	84%	71%
17	1965	1135	71%	93%	78%
18	1966	1230	71%	98%	84%
19	1738	1372	52%	88%	94%
20	1738	1043	52%	70%	71%
21	1738	874	52%	63%	60%
22	1738	705	52%	53%	48%
23	1738	535	52%	48%	37%
24	1738	439	52%	44%	30%
25	1738	366	52%	41%	25%
26	1510	366	34%	31%	25%
27	1510	492	34%	37%	34%
28	1510	535	34%	39%	37%
29	1510	705	34%	47%	48%
30	1510	874	34%	53%	60%
31	1510	1043	34%	57%	71%
32	1510	1242	34%	68%	85%
33	1510	1436	34%	78%	98%
34	1281	1401	15%	62%	96%
35	1281	1043	15%	51%	71%
36	1281	874	15%	44%	60%
37	1281	705	15%	37%	48%
38	1281	580	15%	33%	40%
39	1281	535	15%	32%	37%
40	1281	366	15%	24%	25%

Table Type BSFC
 Engine Manufacturer CAT
 Engine Model C9
 Model Year 2005
 Serial Number 9DG05784
 Fuel Density 851 [g/L]
 Peak Torque 1464 [N-m]
 nlo 1099 [rpm]
 nhi 2320 [rpm]

Point	Raw Data	Normalized Data		
	ECM Speed rpm	ECM Speed nlo = 0% nhi = 100%	ECM Fuel Rate % of Maximum Fuel Rate	BSFC % of Max
1	2366	104%	55%	100
2	2348	102%	55%	99
3	2340	102%	59%	95
4	2325	100%	72%	87
5	2195	90%	100%	77
6	2195	90%	91%	82
7	2195	90%	74%	83
8	2194	90%	63%	87
9	2194	90%	57%	93
10	2194	90%	53%	98
11	1966	71%	41%	90
12	1966	71%	46%	86
13	1966	71%	52%	81
14	1966	71%	62%	78
15	1966	71%	74%	76
16	1966	71%	84%	73
17	1965	71%	93%	74
18	1966	71%	98%	72
19	1738	52%	88%	69
20	1738	52%	70%	71
21	1738	52%	63%	74
22	1738	52%	53%	76
23	1738	52%	48%	81
24	1738	52%	44%	84
25	1738	52%	41%	89
26	1510	34%	31%	85
27	1510	34%	37%	80
28	1510	34%	39%	79
29	1510	34%	47%	75
30	1510	34%	53%	73
31	1510	34%	57%	69
32	1510	34%	68%	69
33	1510	34%	78%	68
34	1281	15%	62%	67
35	1281	15%	51%	70
36	1281	15%	44%	71
37	1281	15%	37%	74
38	1281	15%	33%	77
39	1281	15%	32%	79
40	1281	15%	24%	80

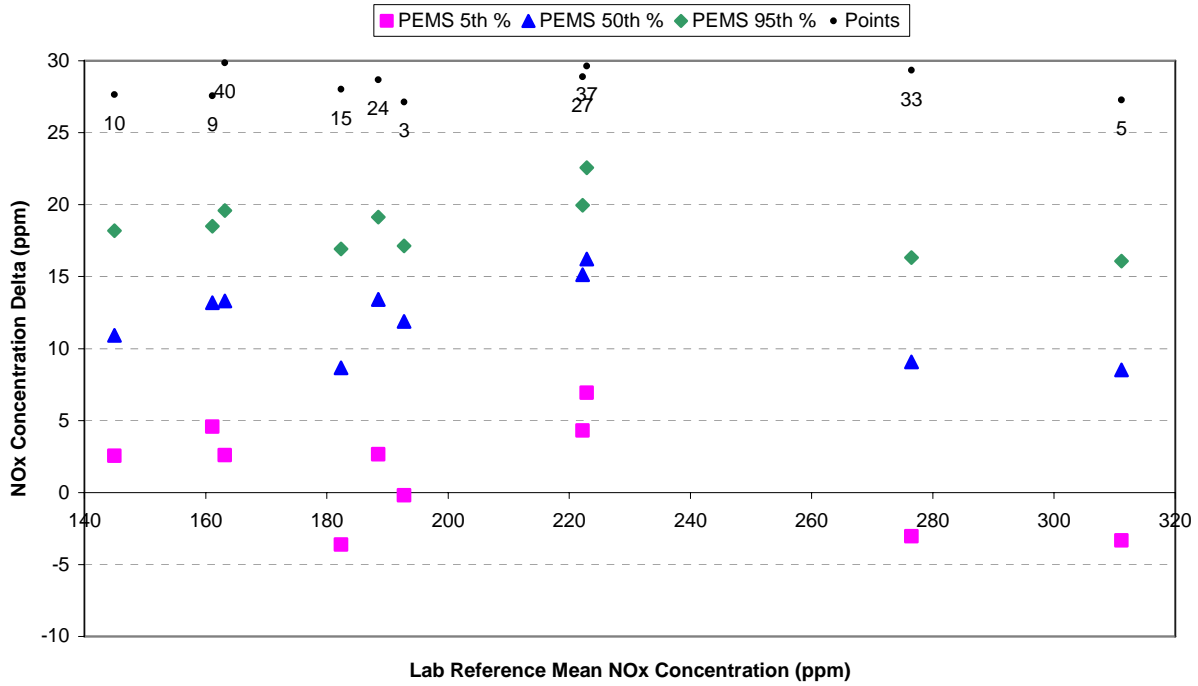
Table Type Torque
 Engine Manufacturer INT
 Engine Model VT365
 Model Year 2006
 Serial Number 332259
 Fuel Density 851 [g/L]
 Peak Torque 681 [N-m]
 nlo 1198 [rpm]
 nhi 2839 [rpm]

Point	Raw Data		Normalized Data		
	ECM Speed rpm	Lab Torque N-m	ECM Speed nlo = 0% nhi = 100%	ECM Fuel Rate % of Maximum Fuel Rate	Lab Torque % of Peak Torque
1	2903	170	104%	47%	25%
2	2890	204	103%	53%	30%
3	2868	257	102%	64%	38%
4	2832	343	100%	81%	50%
5	2622	502	87%	100%	74%
6	2621	429	87%	88%	63%
7	2621	343	87%	72%	50%
8	2621	257	87%	58%	38%
9	2621	204	87%	47%	30%
10	2620	170	87%	41%	25%
11	2328	170	69%	36%	25%
12	2328	204	69%	41%	30%
13	2328	257	69%	51%	38%
14	2328	343	69%	63%	50%
15	2328	429	69%	75%	63%
16	2328	516	69%	87%	76%
17	2328	540	69%	91%	79%
18	2328	543	69%	92%	80%
19	2033	607	51%	86%	89%
20	2033	516	51%	74%	76%
21	2033	429	51%	62%	63%
22	2032	343	51%	52%	50%
23	2032	257	51%	43%	38%
24	2032	204	51%	36%	30%
25	2032	170	51%	31%	25%
26	1739	170	33%	26%	25%
27	1739	234	33%	32%	34%
28	1739	257	33%	34%	38%
29	1739	343	33%	44%	50%
30	1739	429	33%	52%	63%
31	1739	515	33%	63%	76%
32	1739	583	33%	68%	86%
33	1739	650	33%	76%	96%
34	1444	671	15%	64%	99%
35	1444	515	15%	50%	76%
36	1443	429	15%	42%	63%
37	1444	343	15%	35%	50%
38	1444	283	15%	30%	41%
39	1444	257	15%	28%	38%
40	1444	170	15%	21%	25%

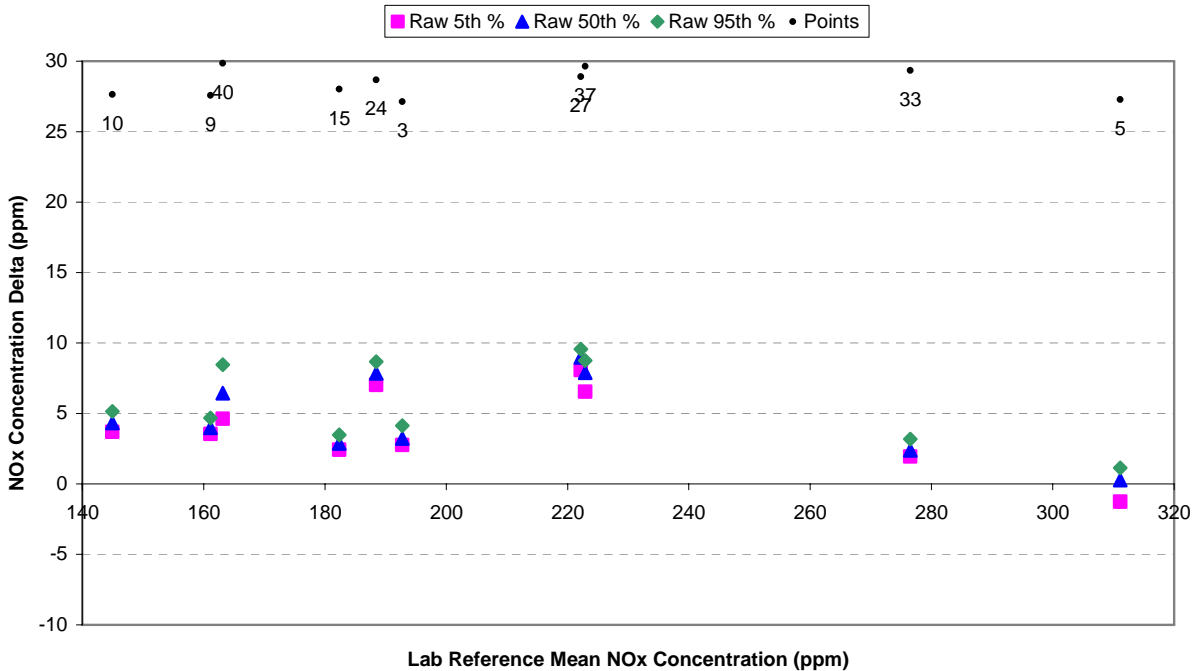
Table Type BSFC
 Engine Manufacturer INT
 Engine Model VT365
 Model Year 2006
 Serial Number 332259
 Fuel Density 851 [g/L]
 Peak Torque 681 [N-m]
 nlo 1198 [rpm]
 nhi 2839 [rpm]

Point	Raw Data	Normalized Data		
	ECM Speed rpm	ECM Speed nlo = 0% nhi = 100%	ECM Fuel Rate % of Maximum Fuel Rate	BSFC % of Max
1	2903	104%	47%	100
2	2890	103%	53%	94
3	2868	102%	64%	87
4	2832	100%	81%	82
5	2622	87%	100%	77
6	2621	87%	88%	78
7	2621	87%	72%	80
8	2621	87%	58%	85
9	2621	87%	47%	91
10	2620	87%	41%	98
11	2328	69%	36%	91
12	2328	69%	41%	86
13	2328	69%	51%	80
14	2328	69%	63%	76
15	2328	69%	75%	74
16	2328	69%	87%	73
17	2328	69%	91%	73
18	2328	69%	92%	73
19	2033	51%	86%	68
20	2033	51%	74%	69
21	2033	51%	62%	70
22	2032	51%	52%	72
23	2032	51%	43%	77
24	2032	51%	36%	82
25	2032	51%	31%	88
26	1739	33%	26%	84
27	1739	33%	32%	75
28	1739	33%	34%	73
29	1739	33%	44%	71
30	1739	33%	52%	68
31	1739	33%	63%	68
32	1739	33%	68%	66
33	1739	33%	76%	66
34	1444	15%	64%	64
35	1444	15%	50%	65
36	1443	15%	42%	65
37	1444	15%	35%	68
38	1444	15%	30%	71
39	1444	15%	28%	72
40	1444	15%	21%	82

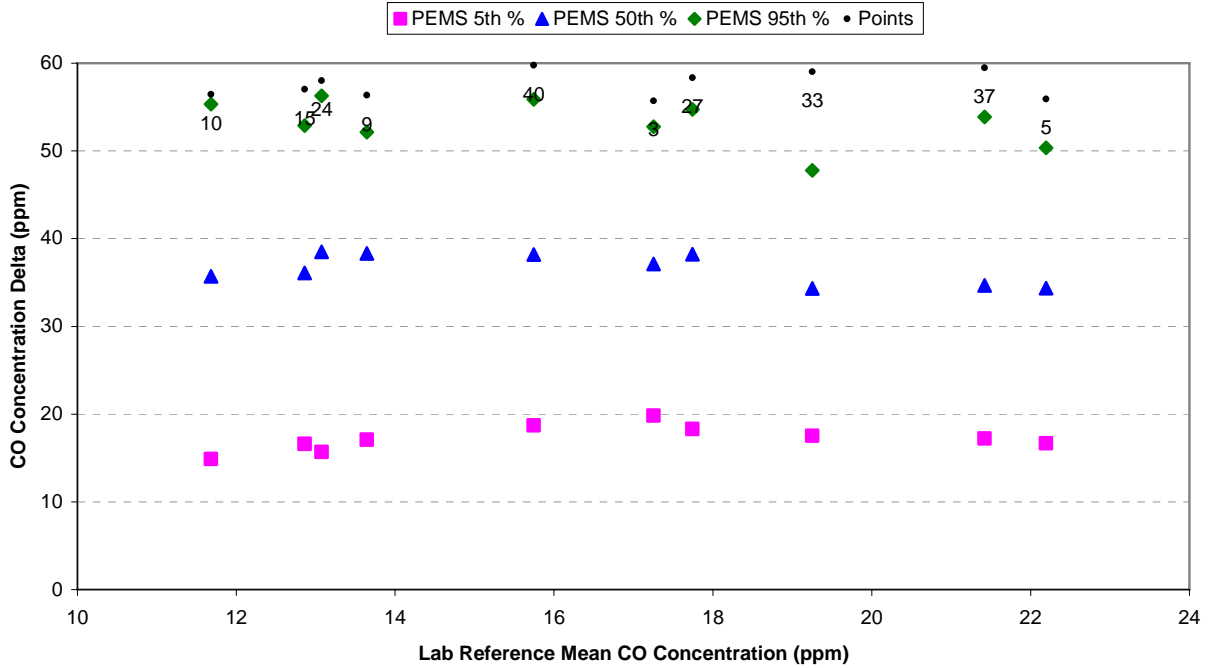
APPENDIX F
STEADY-STATE ERROR SURFACE DATA



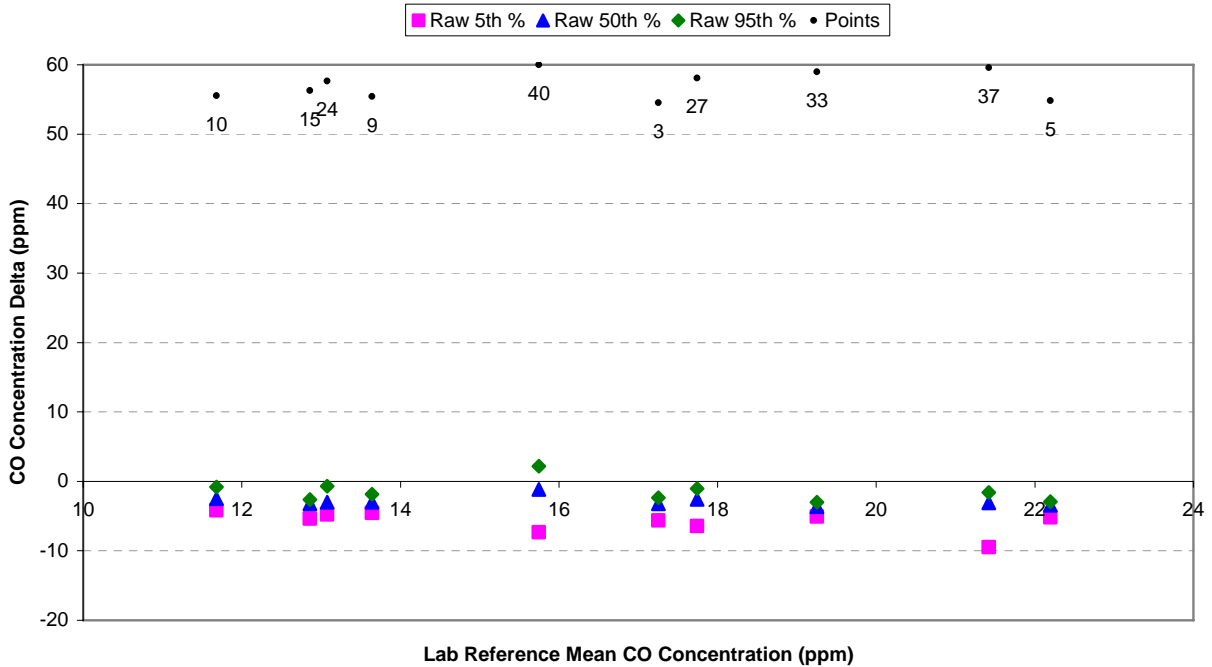
PEMS NO_x CONCENTRATION DELTA VERSUS THE LABORATORY REFERENCE FOR ENGINE 1 STEADY-STATE TESTING



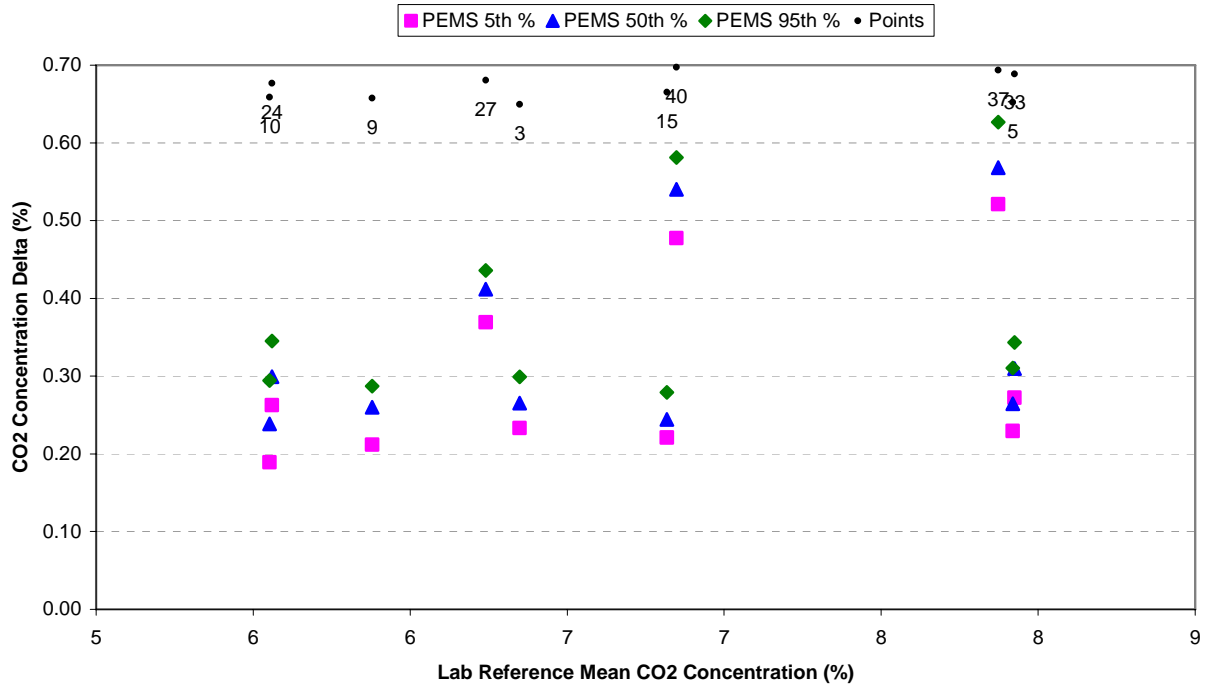
LAB RAW NO_x CONCENTRATION DELTA VERSUS THE LABORATORY REFERENCE FOR ENGINE 1 STEADY-STATE TESTING



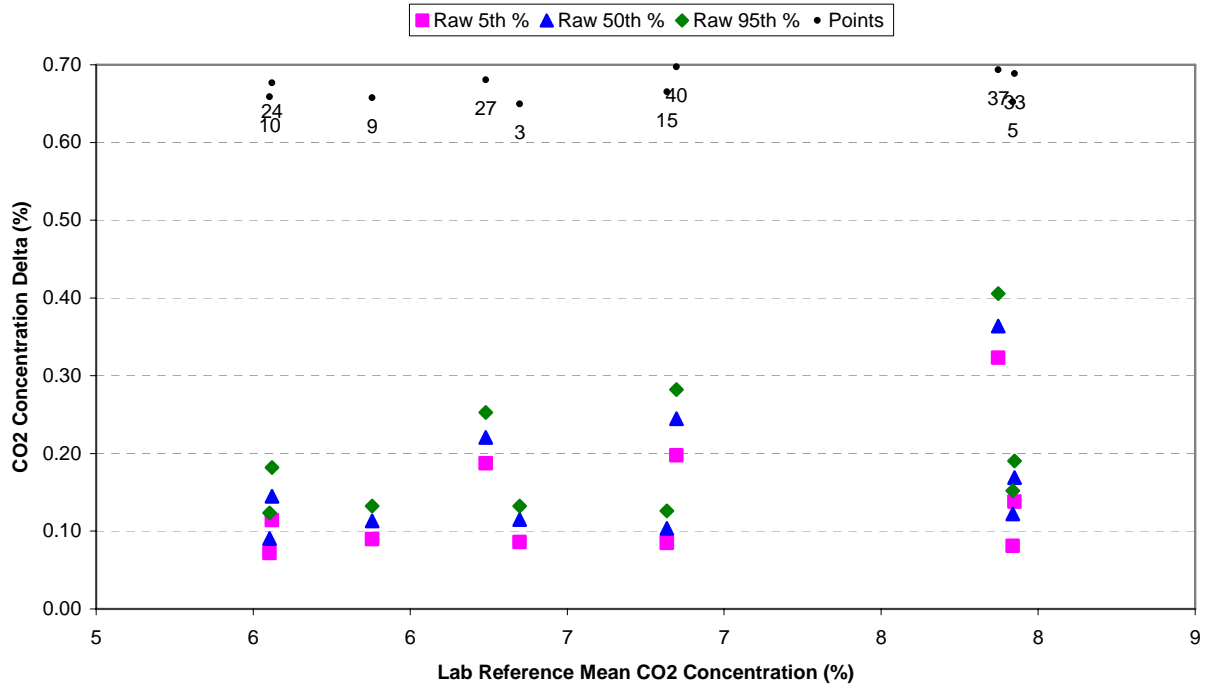
PEMS CO CONCENTRATION DELTA VERSUS THE LABORATORY REFERENCE FOR ENGINE 1 STEADY-STATE TESTING



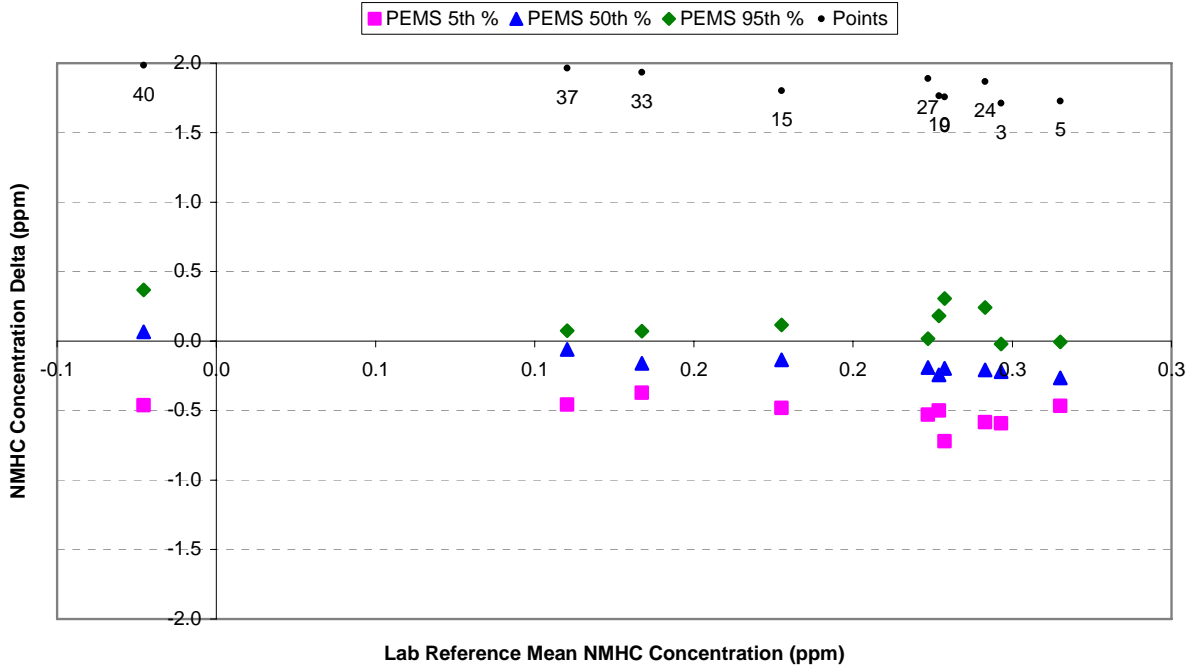
LAB RAW CO CONCENTRATION DELTA VERSUS THE LABORATORY REFERENCE FOR ENGINE 1 STEADY-STATE TESTING



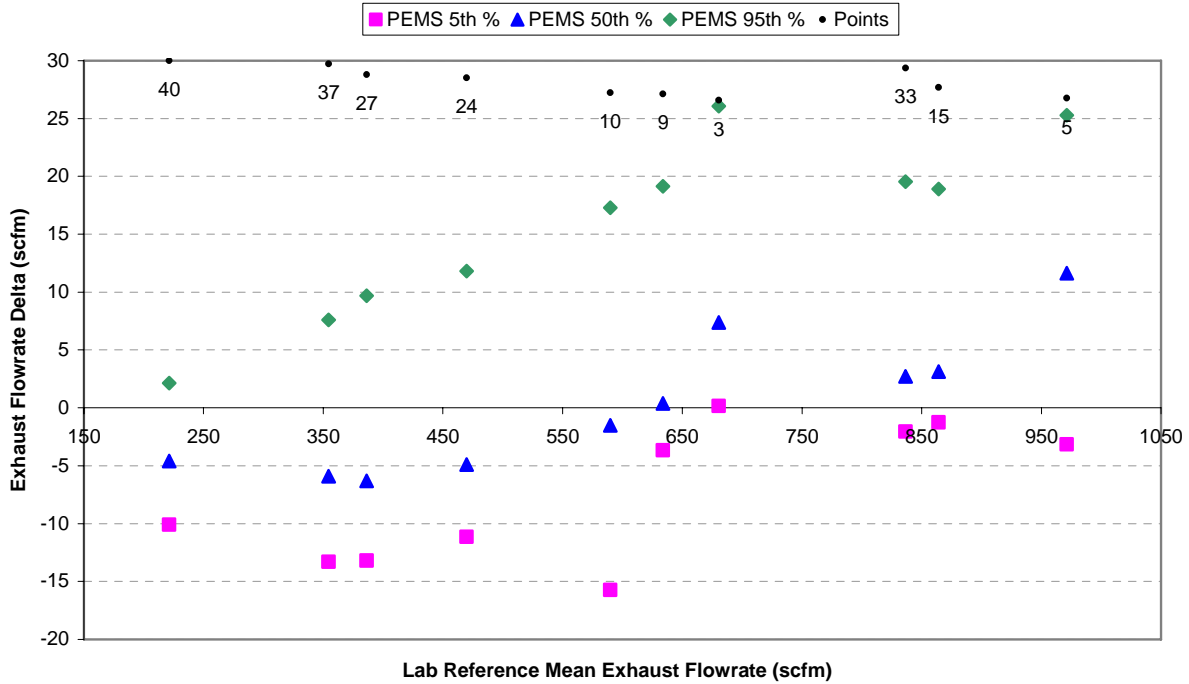
PEMS CO₂ CONCENTRATION DELTA VERSUS THE LABORATORY REFERENCE FOR ENGINE 1 STEADY-STATE TESTING



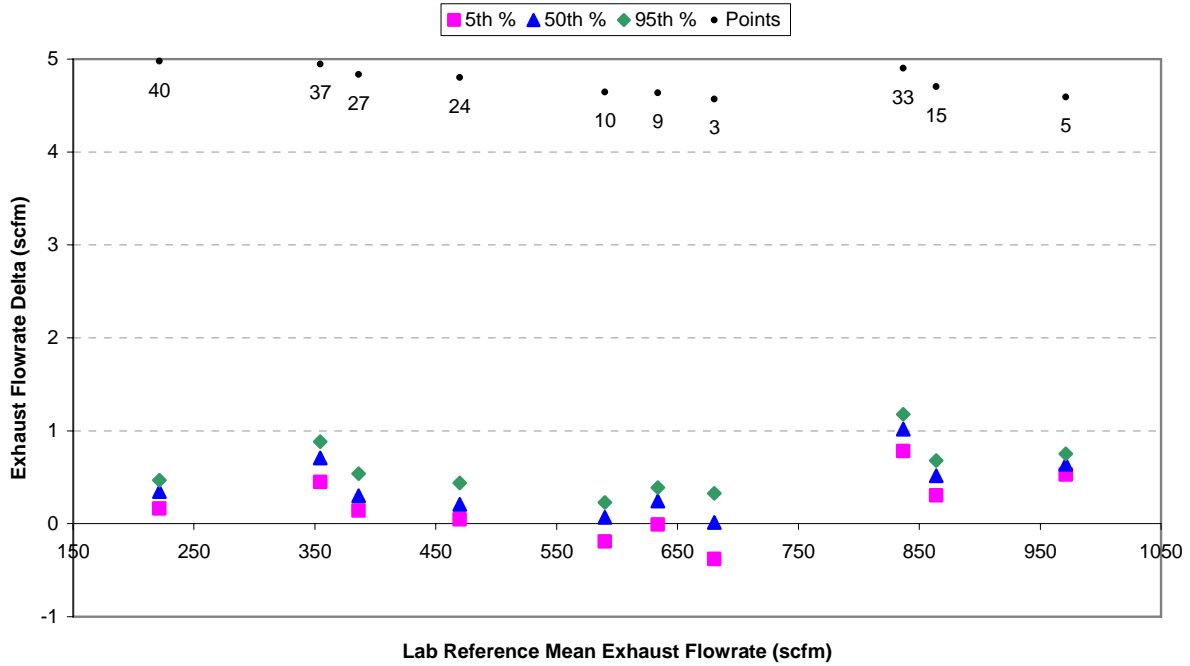
LAB RAW CO₂ CONCENTRATION DELTA VERSUS THE LABORATORY REFERENCE FOR ENGINE 1 STEADY-STATE TESTING



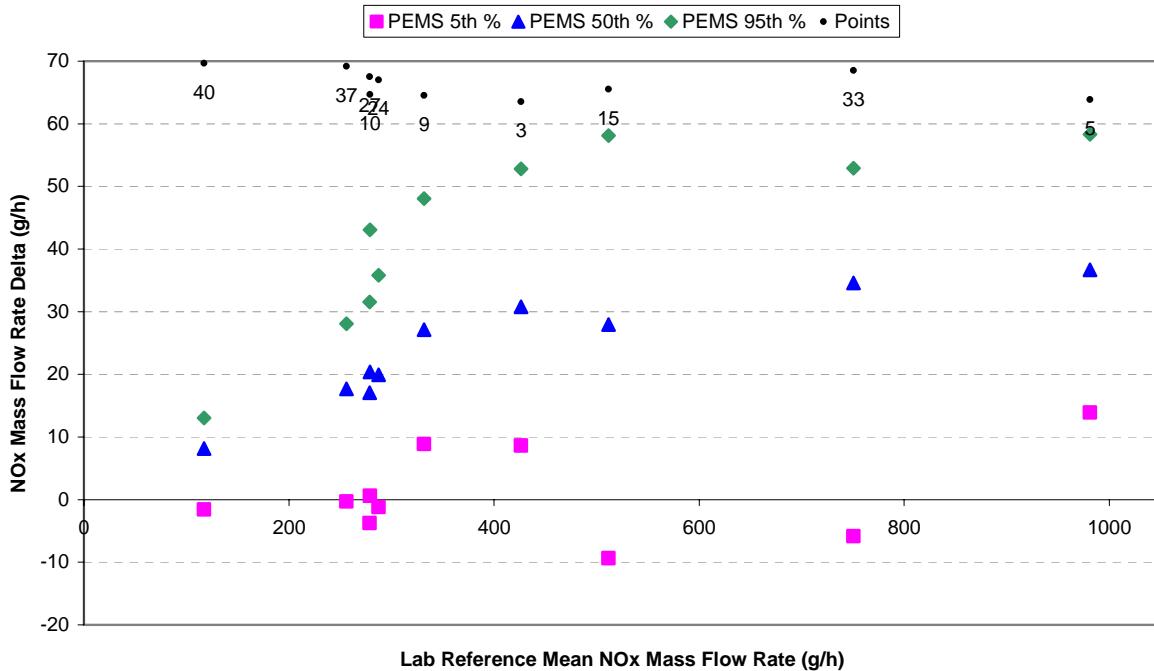
PEMS NMHC CONCENTRATION DELTA VERSUS THE LABORATORY REFERENCE FOR ENGINE 1 STEADY-STATE TESTING



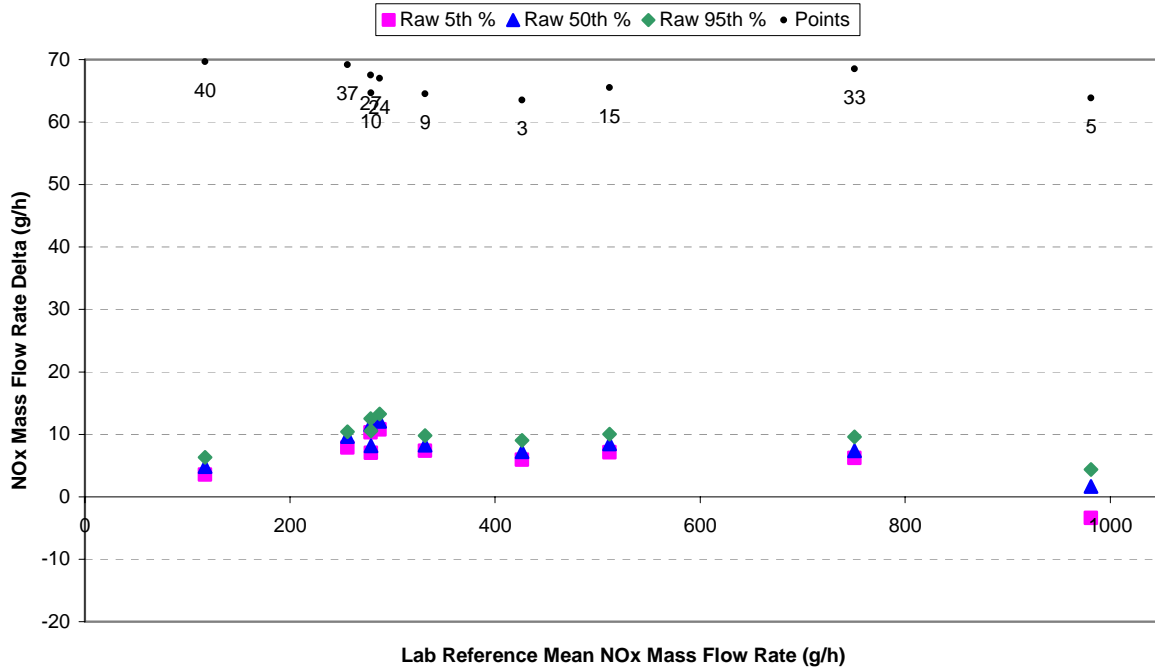
PEMS EXHAUST FLOW RATE DELTA VERSUS THE LABORATORY REFERENCE FOR ENGINE 1 STEADY-STATE TESTING



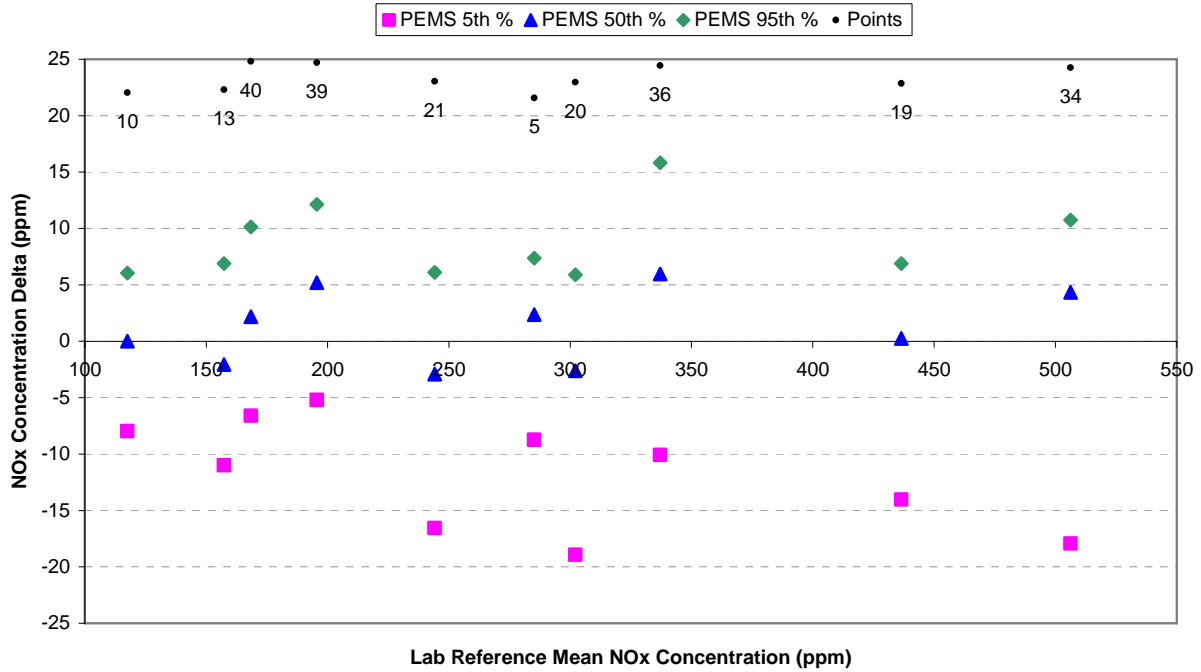
LAB RAW EXHAUST FLOW RATE DELTA VERSUS THE LABORATORY REFERENCE FOR ENGINE 1 STEADY-STATE TESTING



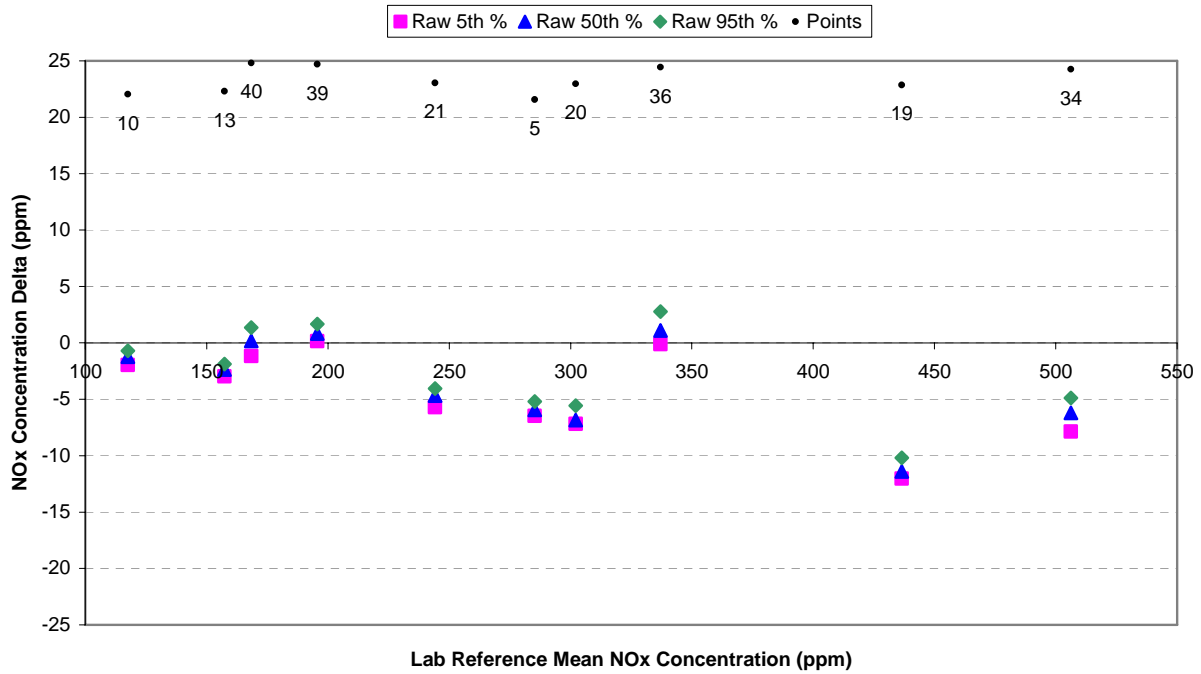
PEMS NO_x MASS FLOW RATE DELTA VERSUS THE LABORATORY REFERENCE FOR ENGINE 1 STEADY-STATE TESTING



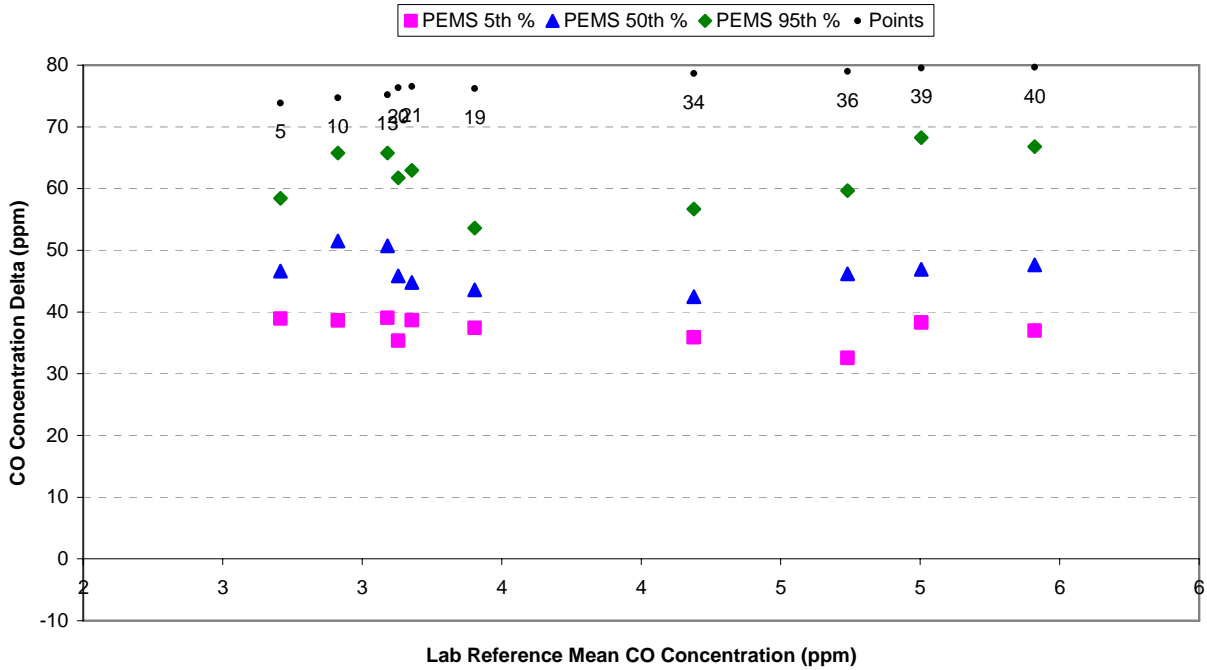
LAB RAW NO_x MASS FLOW RATE DELTA VERSUS THE LABORATORY REFERENCE FOR ENGINE 1 STEADY-STATE TESTING



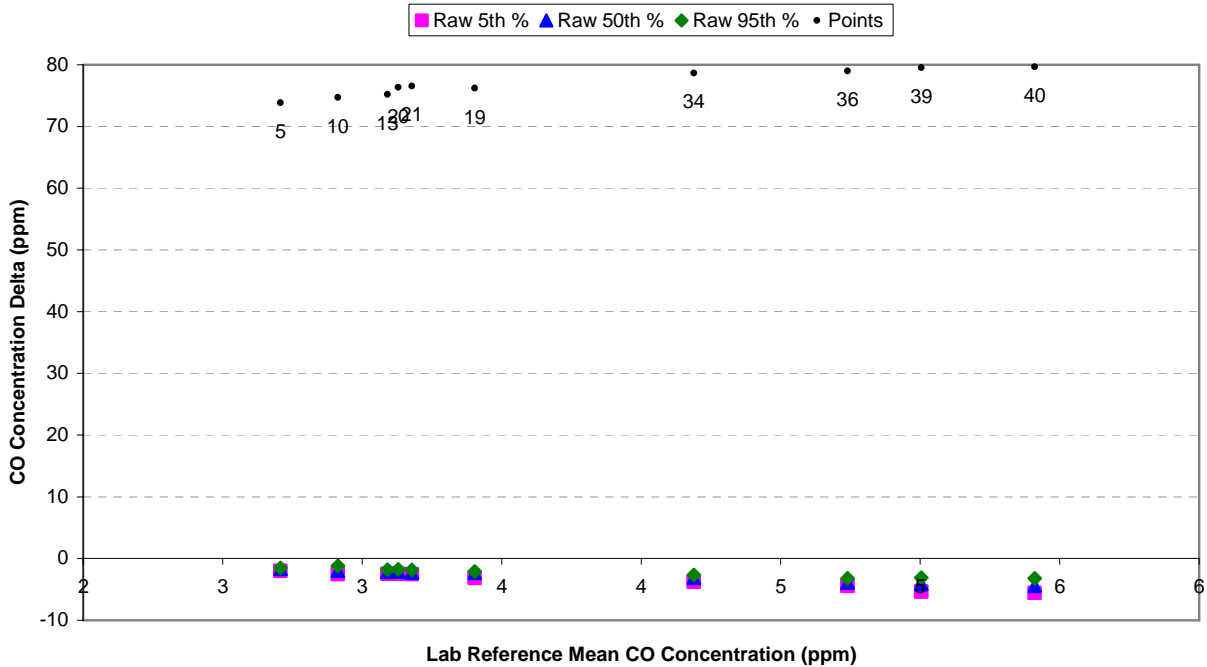
PEMS NO_x CONCENTRATION DELTA VERSUS THE LABORATORY REFERENCE FOR ENGINE 2 STEADY-STATE TESTING



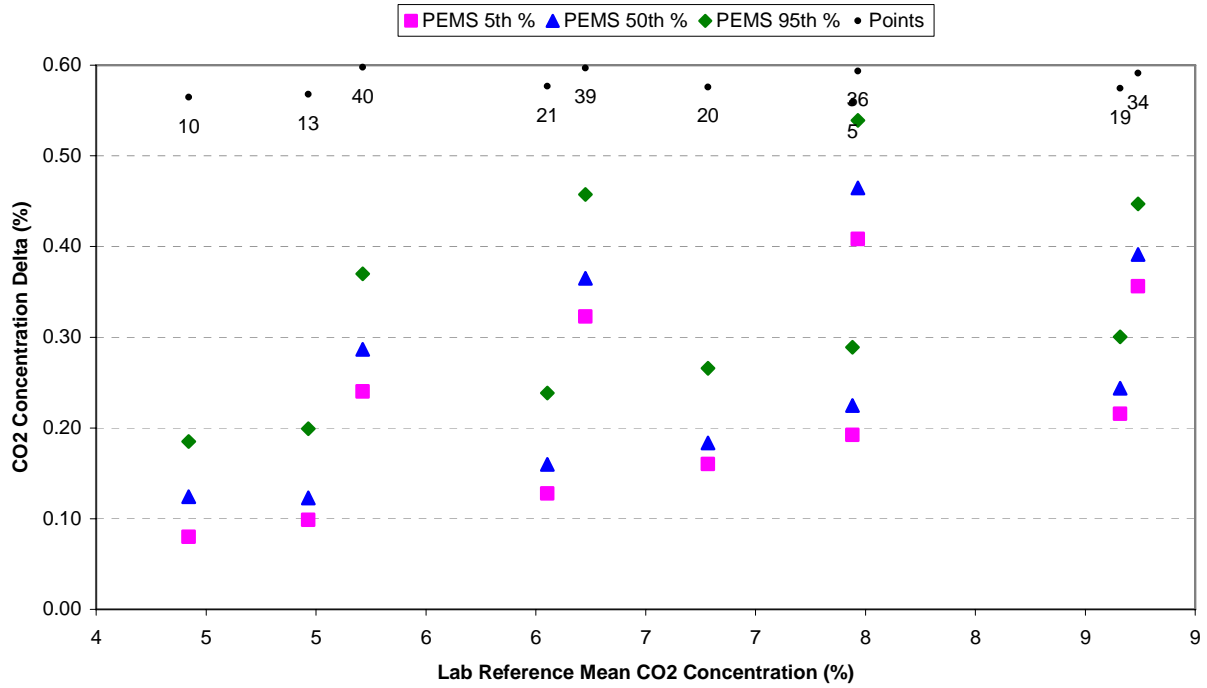
LAB RAW NO_x CONCENTRATION DELTA VERSUS THE LABORATORY REFERENCE FOR ENGINE 2 STEADY-STATE TESTING



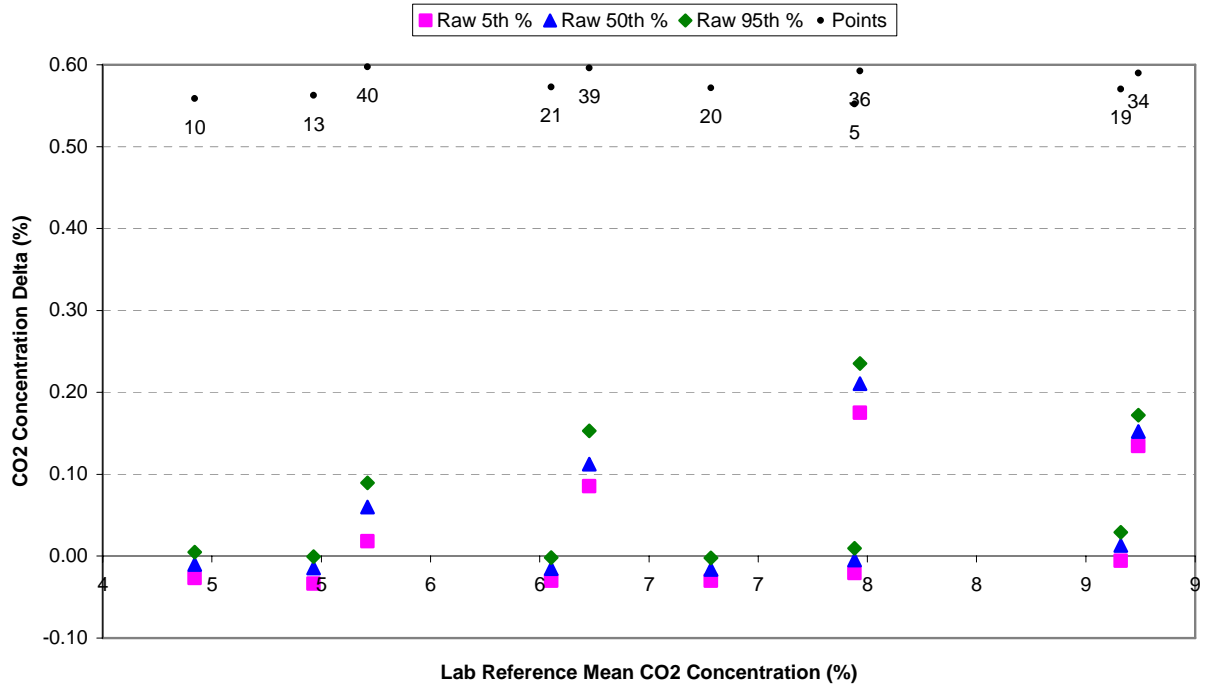
PEMS CO CONCENTRATION DELTA VERSUS THE LABORATORY REFERENCE FOR ENGINE 2 STEADY-STATE TESTING



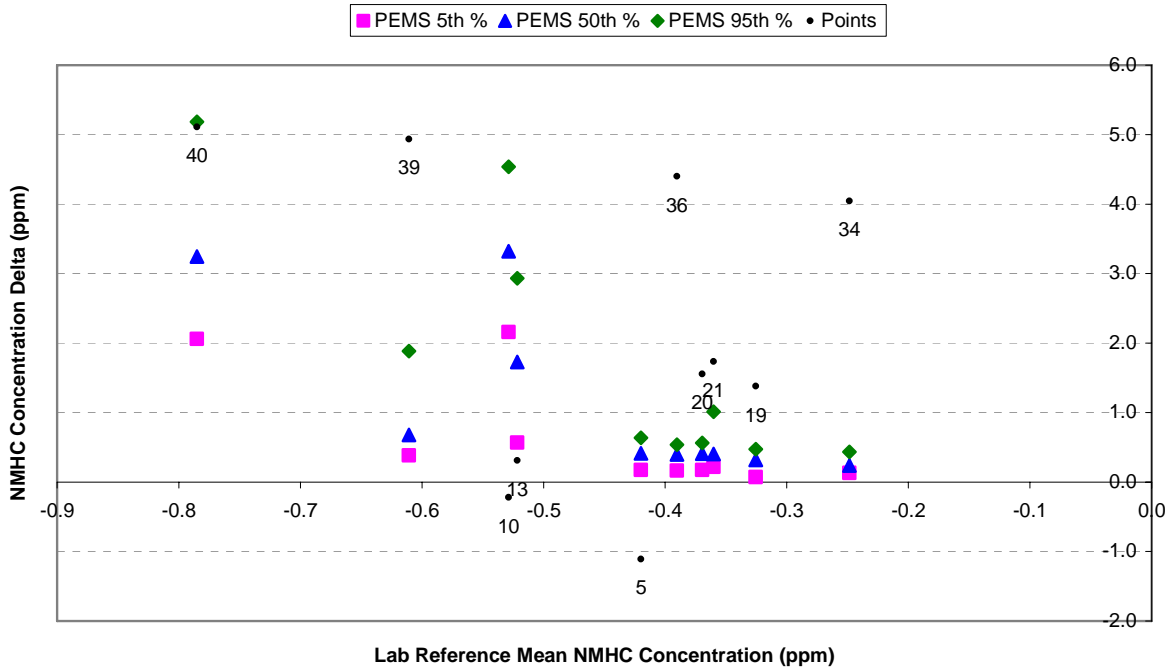
LAB RAW CO CONCENTRATION DELTA VERSUS THE LABORATORY REFERENCE FOR ENGINE 2 STEADY-STATE TESTING



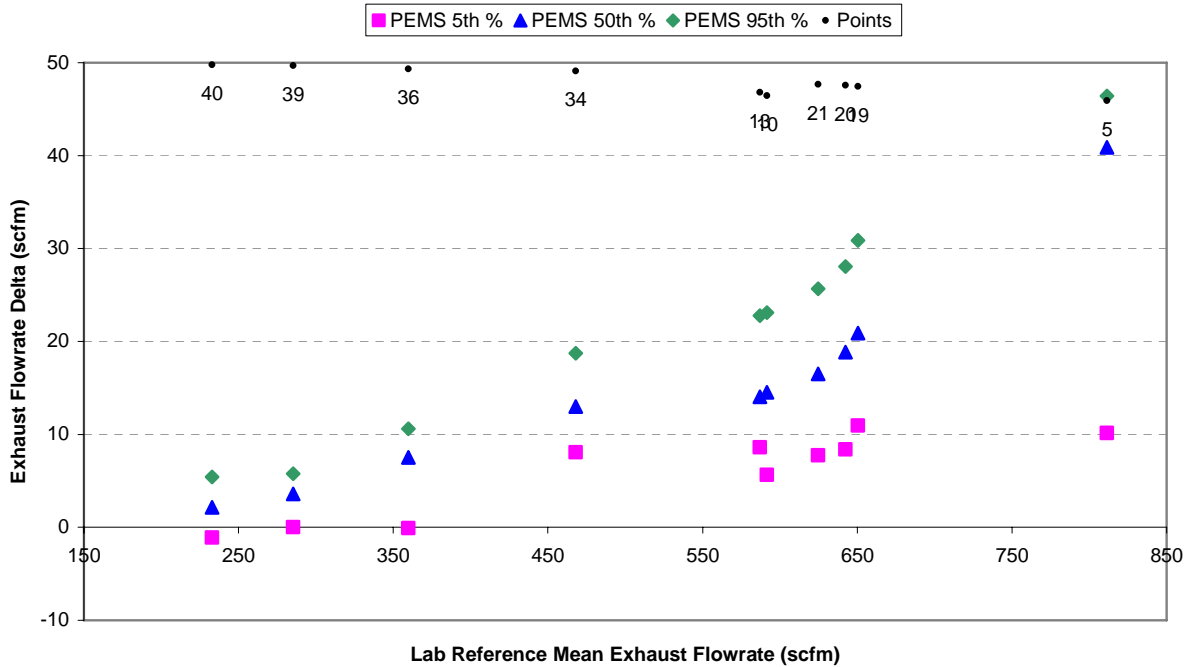
PEMS CO₂ CONCENTRATION DELTA VERSUS THE LABORATORY REFERENCE FOR ENGINE 2 STEADY-STATE TESTING



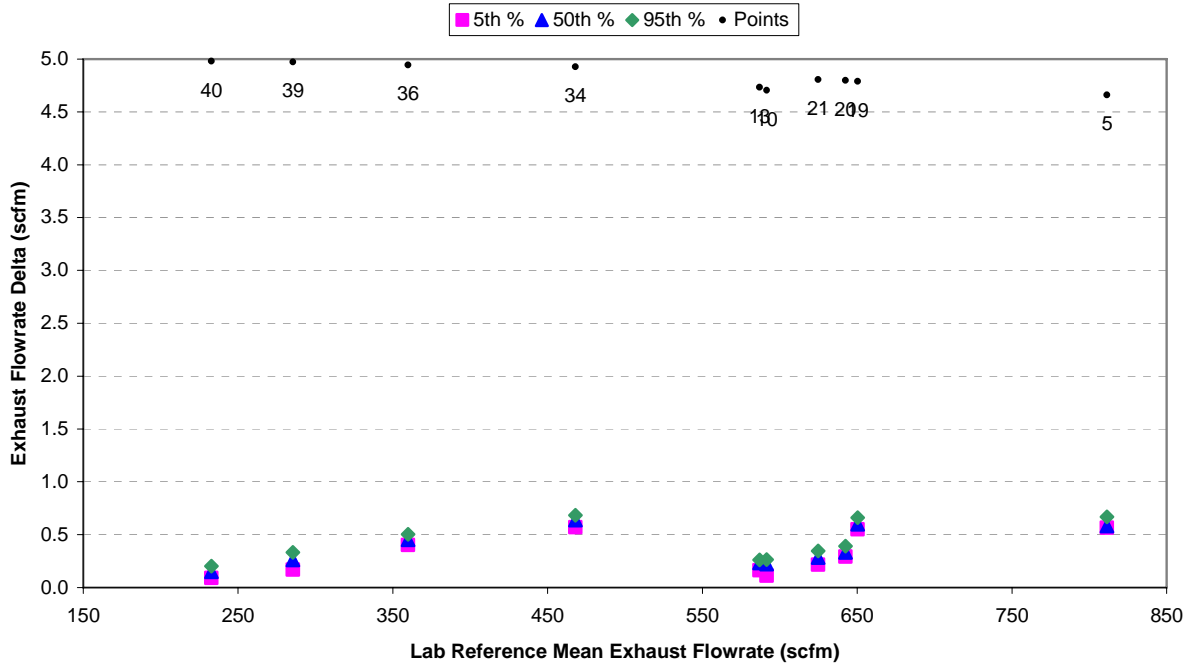
LAB RAW CO₂ CONCENTRATION DELTA VERSUS THE LABORATORY REFERENCE FOR ENGINE 2 STEADY-STATE TESTING



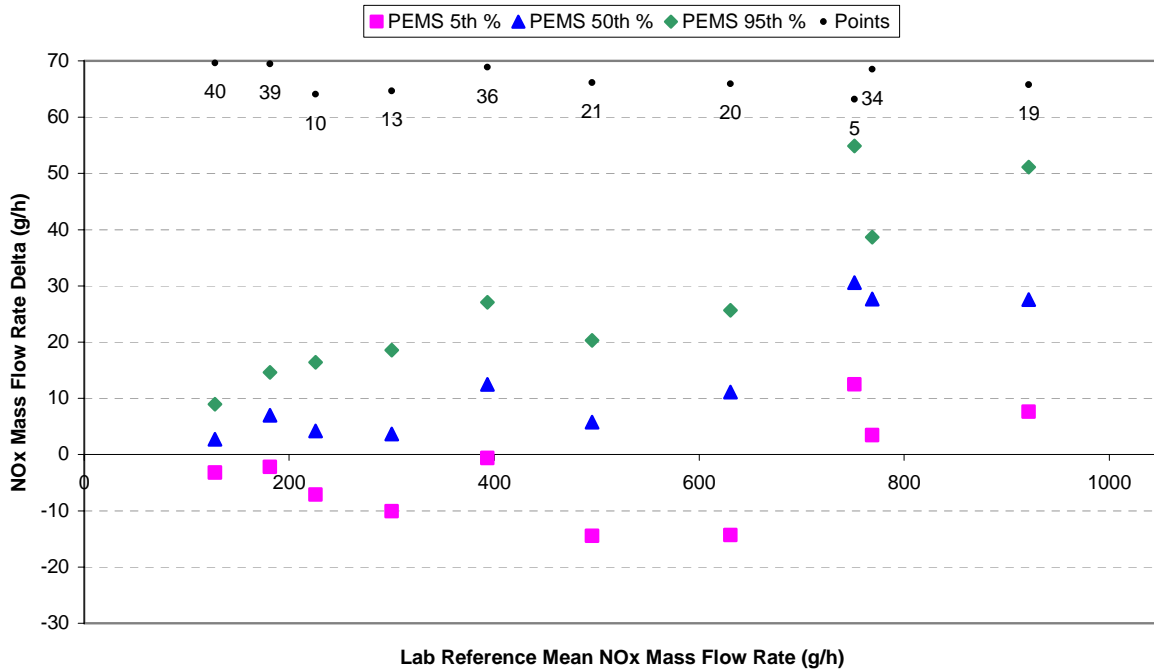
PEMS NMHC CONCENTRATION DELTA VERSUS THE LABORATORY REFERENCE FOR ENGINE 2 STEADY-STATE TESTING



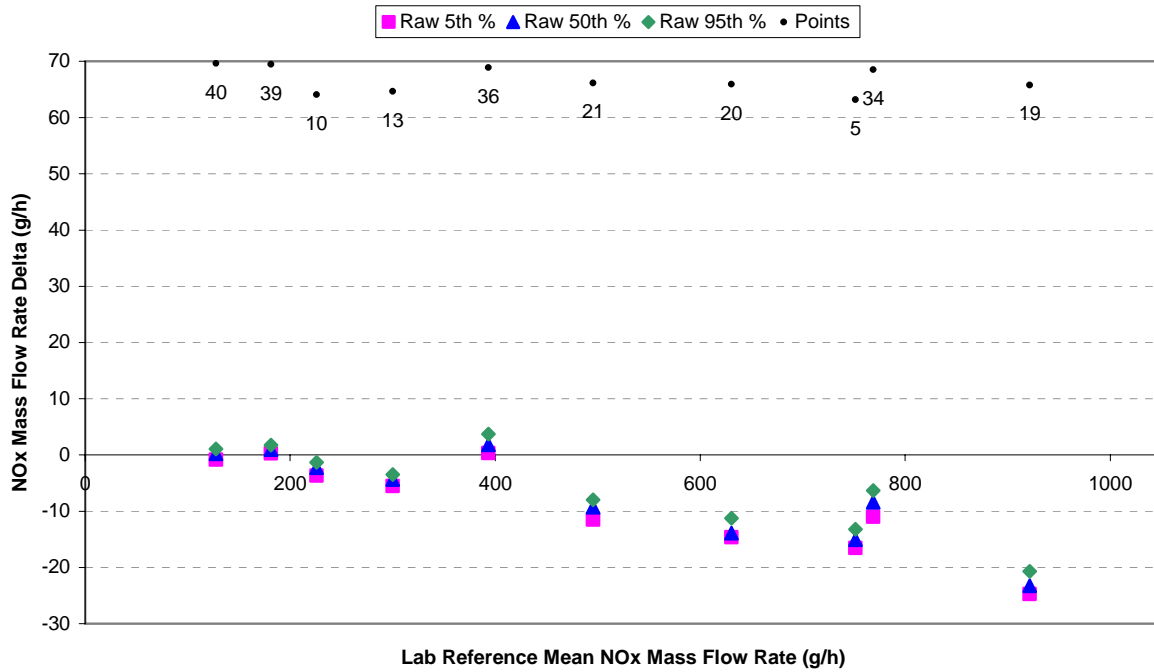
PEMS EXHAUST FLOW RATE DELTA VERSUS THE LABORATORY REFERENCE FOR ENGINE 2 STEADY-STATE TESTING



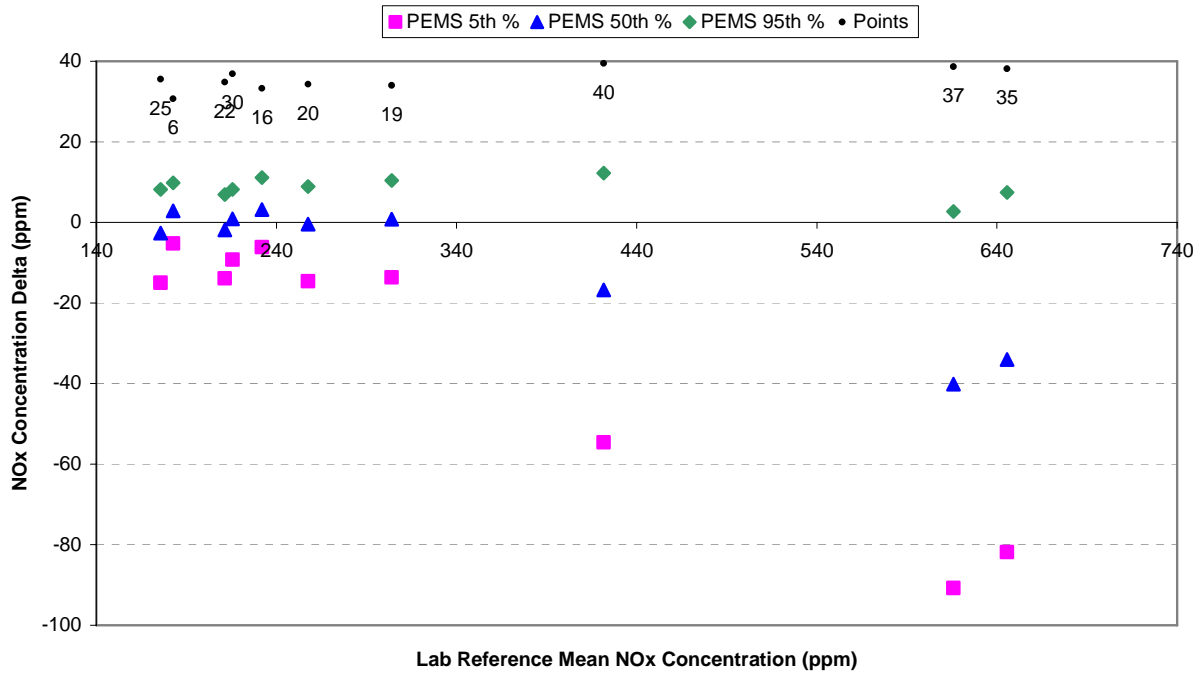
LAB RAW EXHAUST FLOW RATE DELTA VERSUS THE LABORATORY REFERENCE FOR ENGINE 2 STEADY-STATE TESTING



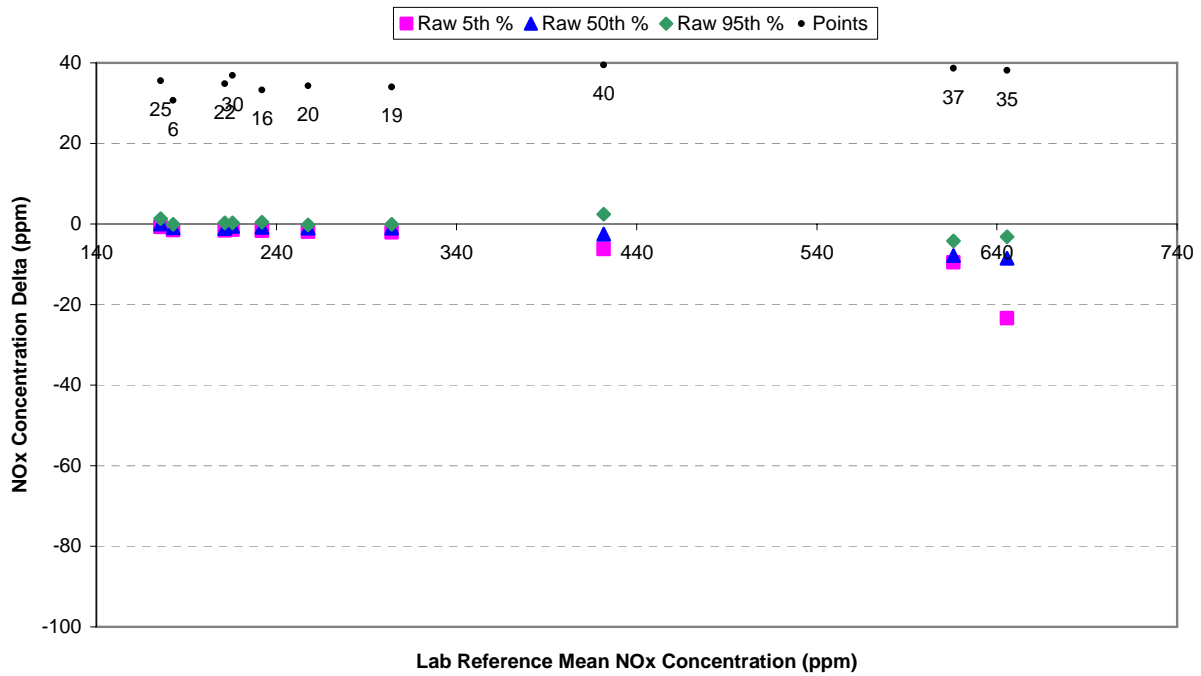
PEMS NO_x MASS FLOW RATE DELTA VERSUS THE LABORATORY REFERENCE FOR ENGINE 2 STEADY-STATE TESTING



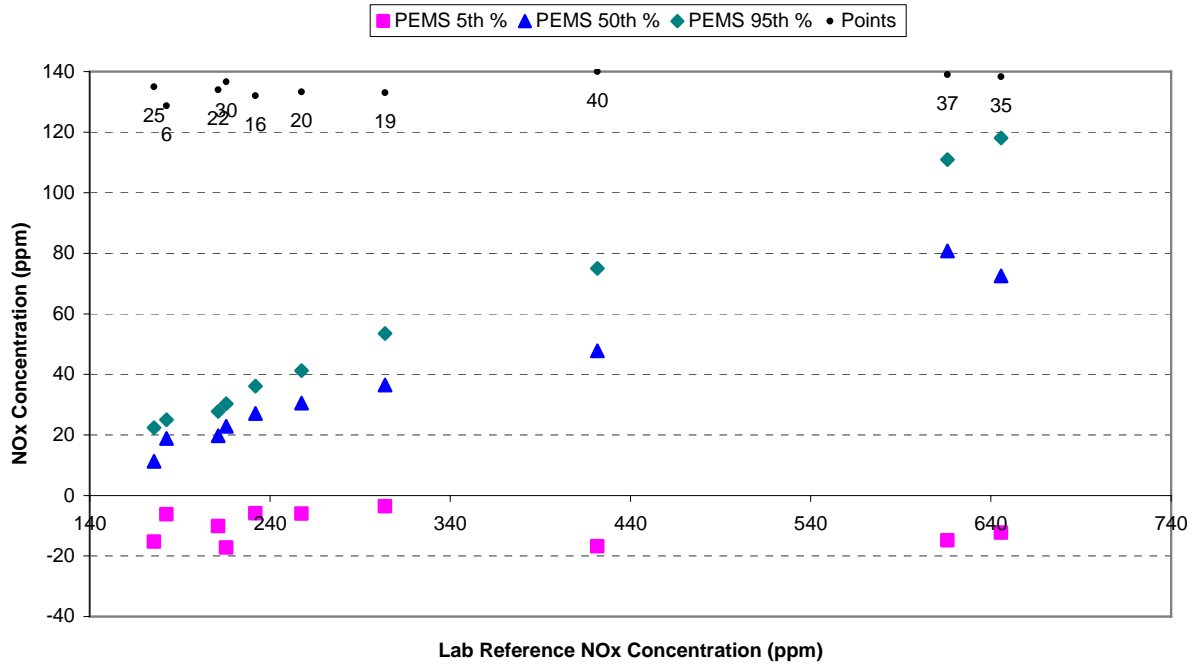
LAB RAW NO_x MASS FLOW RATE DELTA VERSUS THE LABORATORY REFERENCE FOR ENGINE 2 STEADY-STATE TESTING



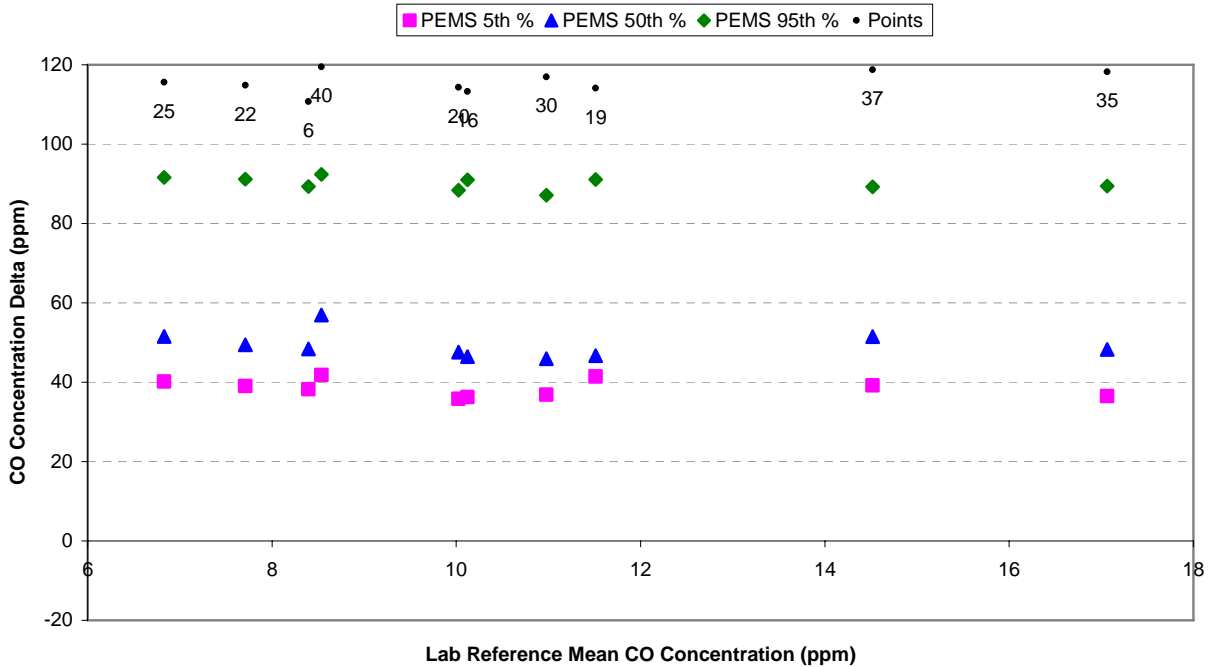
PEMS NO_x CONCENTRATION DELTA VERSUS THE LABORATORY REFERENCE FOR ENGINE 3 STEADY-STATE TESTING



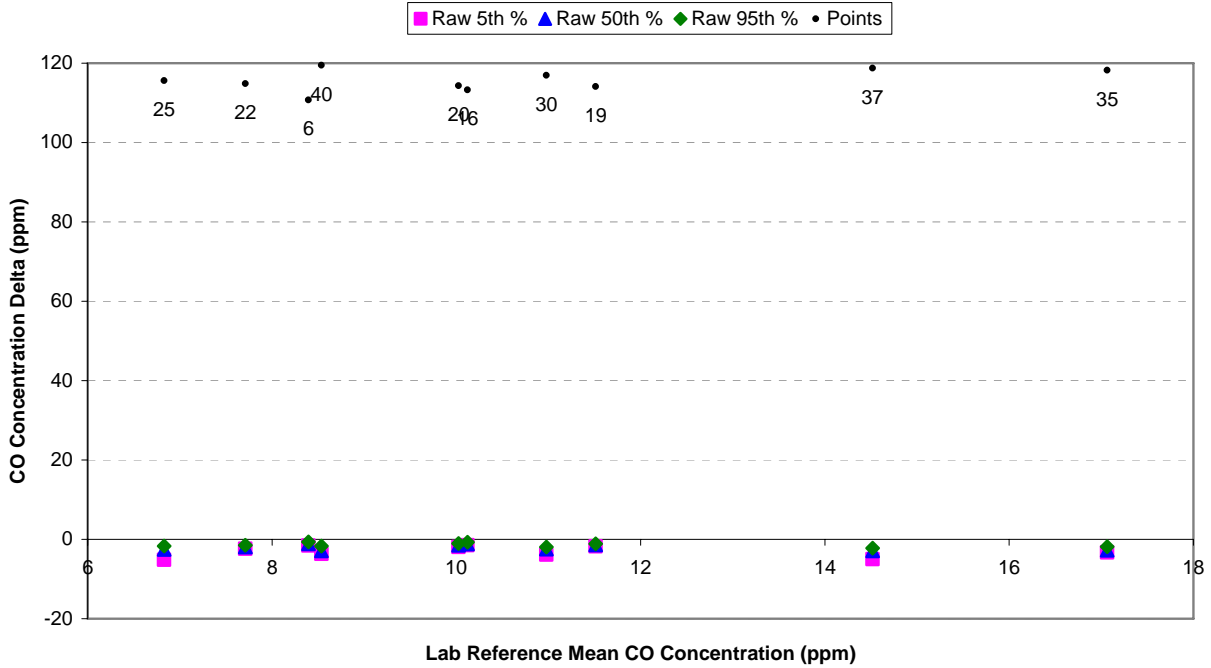
LAB RAW NO_x CONCENTRATION DELTA VERSUS THE LABORATORY REFERENCE FOR ENGINE 3 STEADY-STATE TESTING



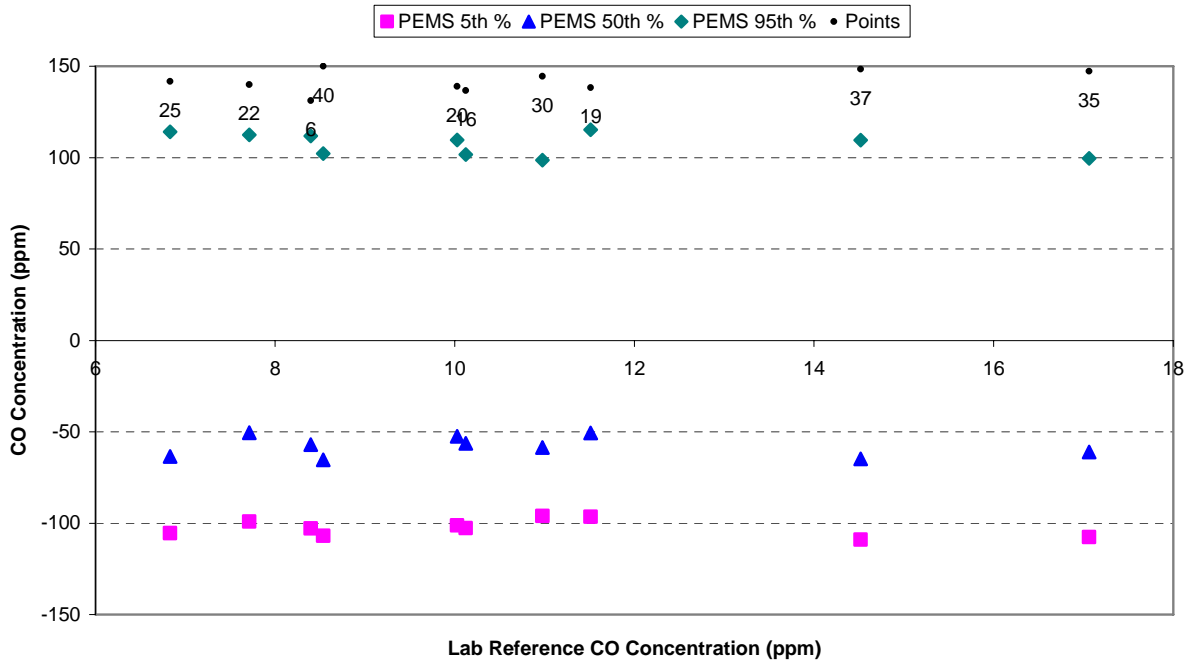
HORIBA OBS-2200 NO_x CONCENTRATION DELTA VERSUS THE LABORATORY REFERENCE FOR ENGINE 3 STEADY-STATE TESTING



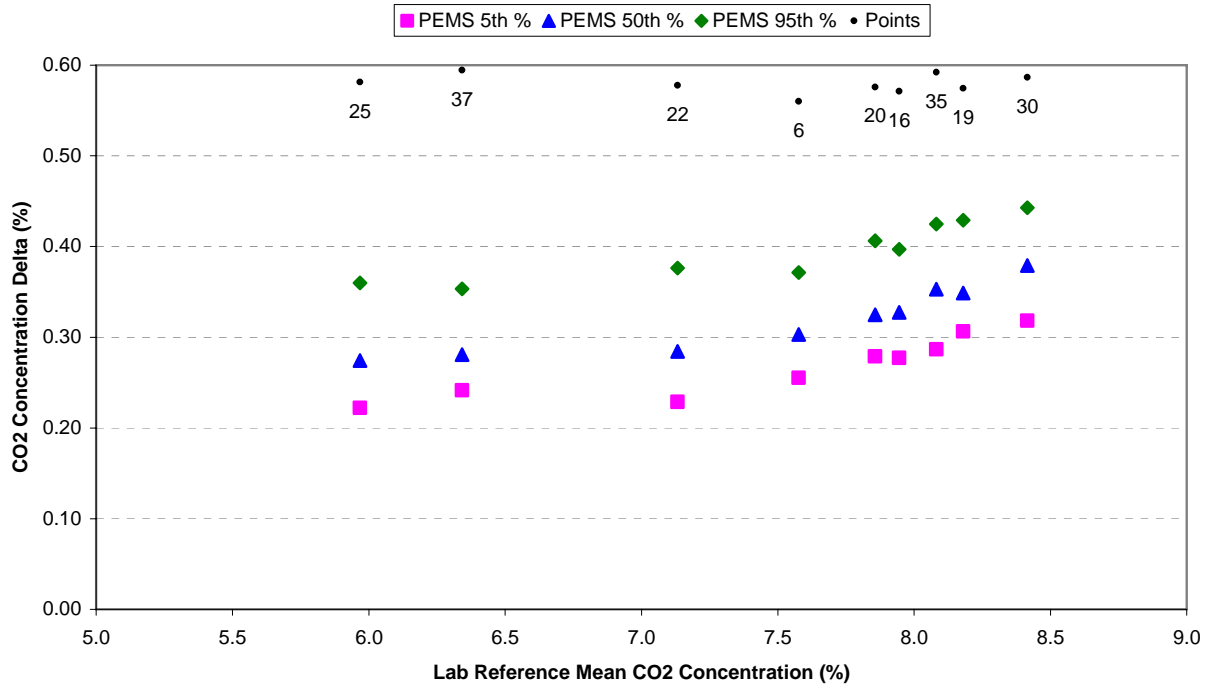
PEMS CO CONCENTRATION DELTA VERSUS THE LABORATORY REFERENCE FOR ENGINE 3 STEADY-STATE TESTING



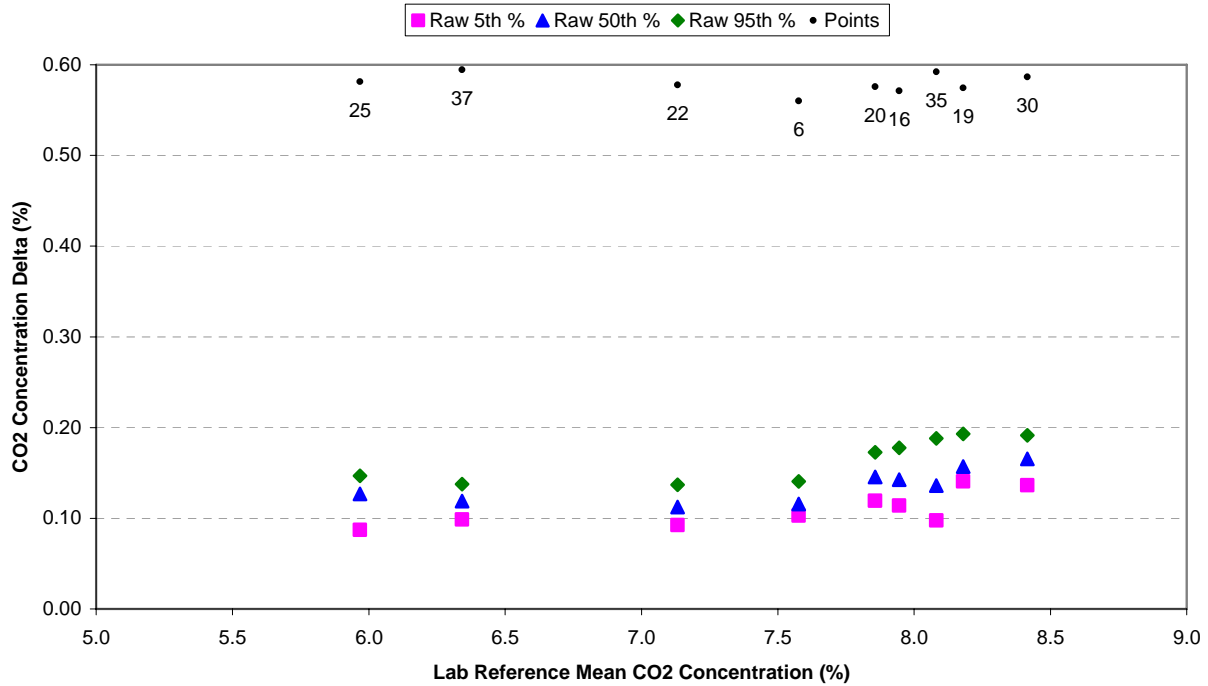
LAB RAW CO CONCENTRATION DELTA VERSUS THE LABORATORY REFERENCE FOR ENGINE 3 STEADY-STATE TESTING



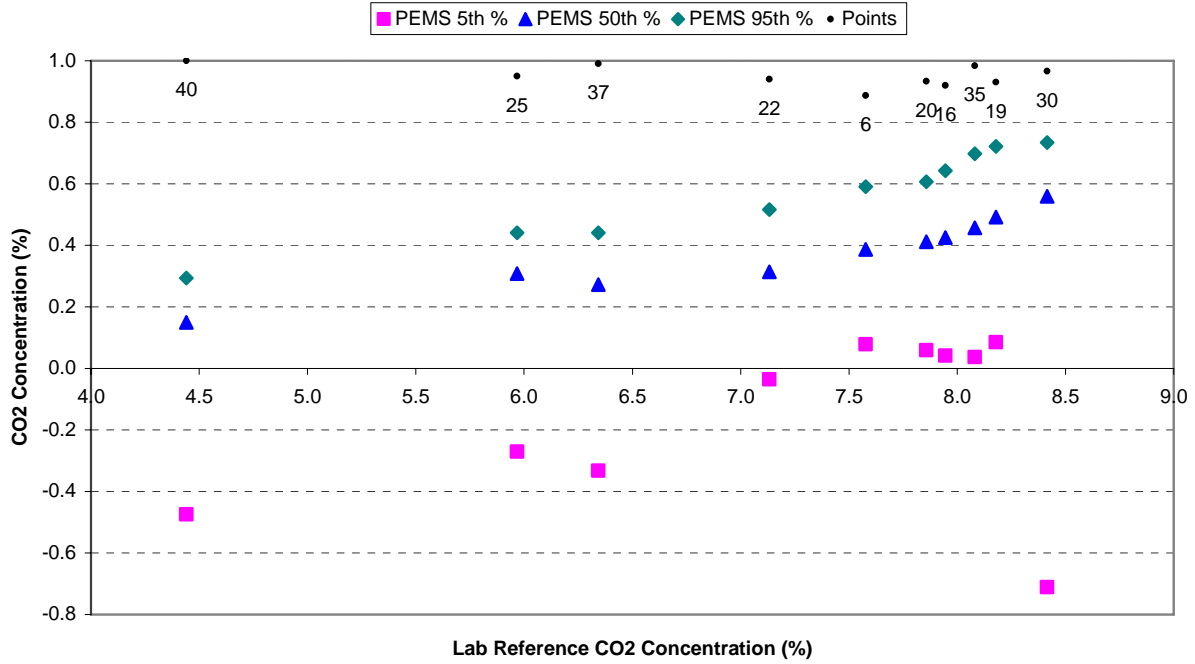
HORIBA OBS-2200 CO CONCENTRATION DELTA VERSUS THE LABORATORY REFERENCE FOR ENGINE 3 STEADY-STATE TESTING



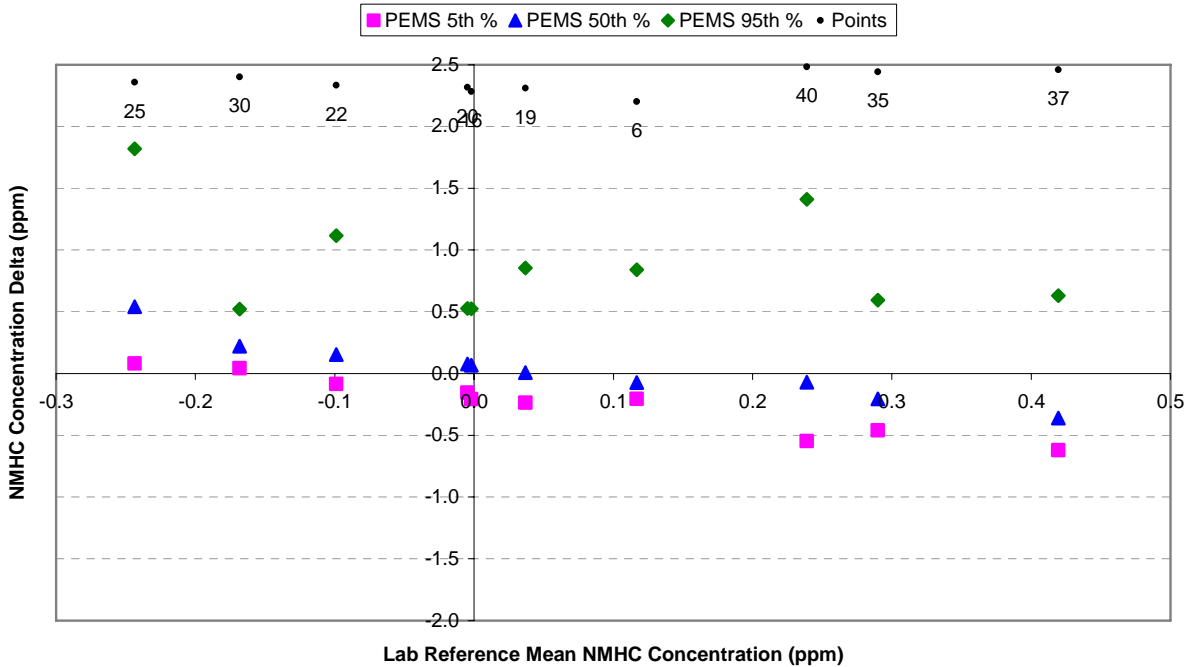
PEMS CO₂ CONCENTRATION DELTA VERSUS THE LABORATORY REFERENCE FOR ENGINE 3 STEADY-STATE TESTING



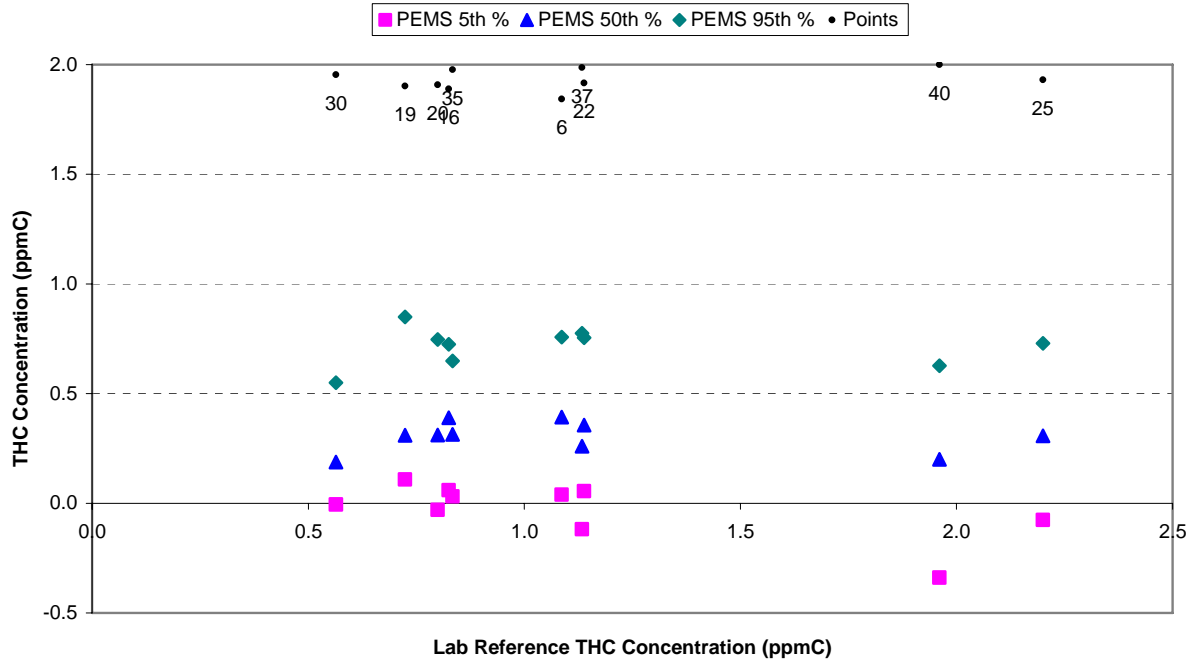
LAB RAW CO₂ CONCENTRATION DELTA VERSUS THE LABORATORY REFERENCE FOR ENGINE 3 STEADY-STATE TESTING



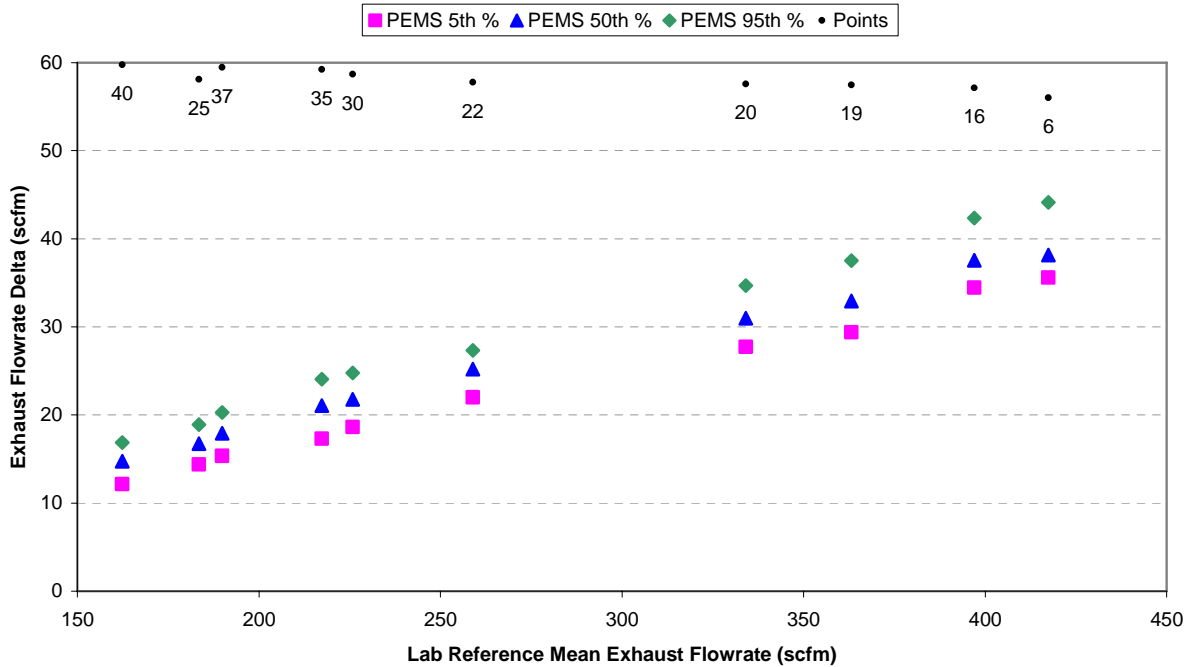
HORIBA OBS-2200 CO₂ CONCENTRATION DELTA VERSUS THE LABORATORY REFERENCE FOR ENGINE 3 STEADY-STATE TESTING



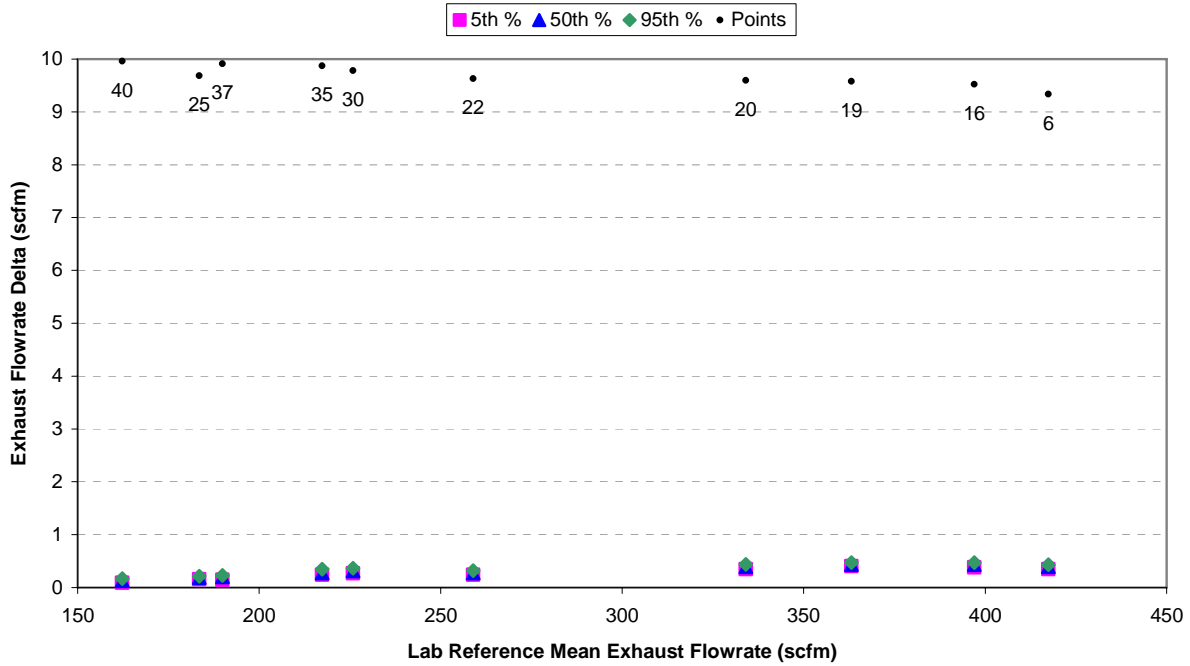
PEMS NMHC CONCENTRATION DELTA VERSUS THE LABORATORY REFERENCE FOR ENGINE 3 STEADY-STATE TESTING



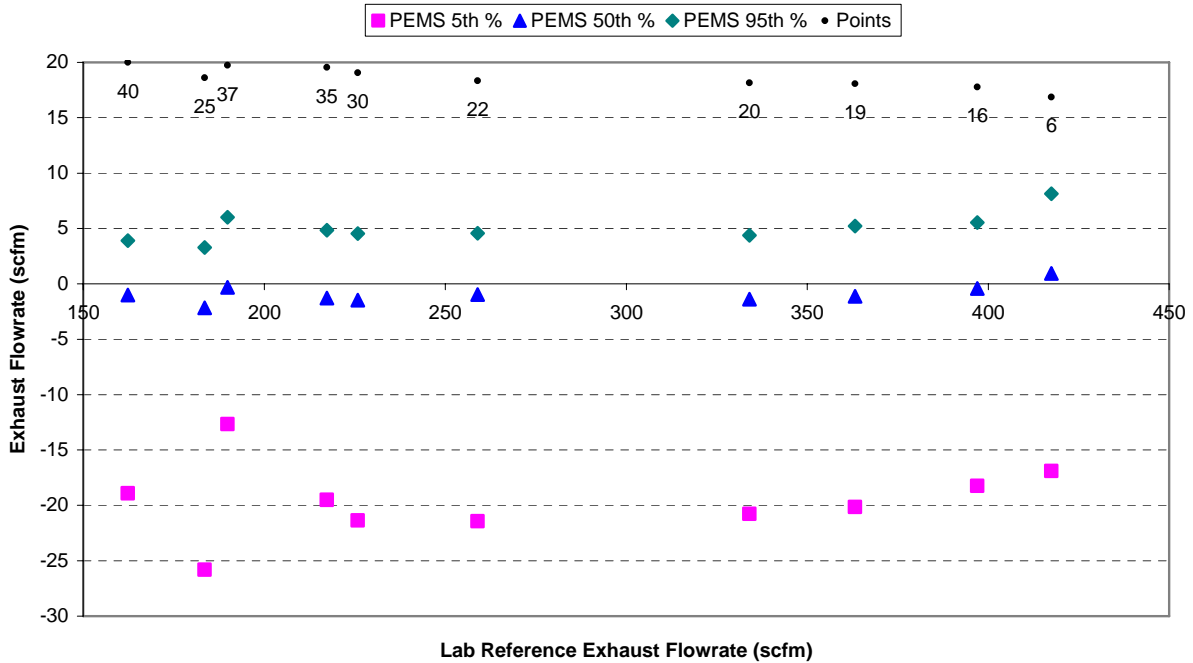
HORIBA OBS-2200 THC CONCENTRATION DELTA VERSUS THE LABORATORY REFERENCE FOR ENGINE 3 STEADY-STATE TESTING



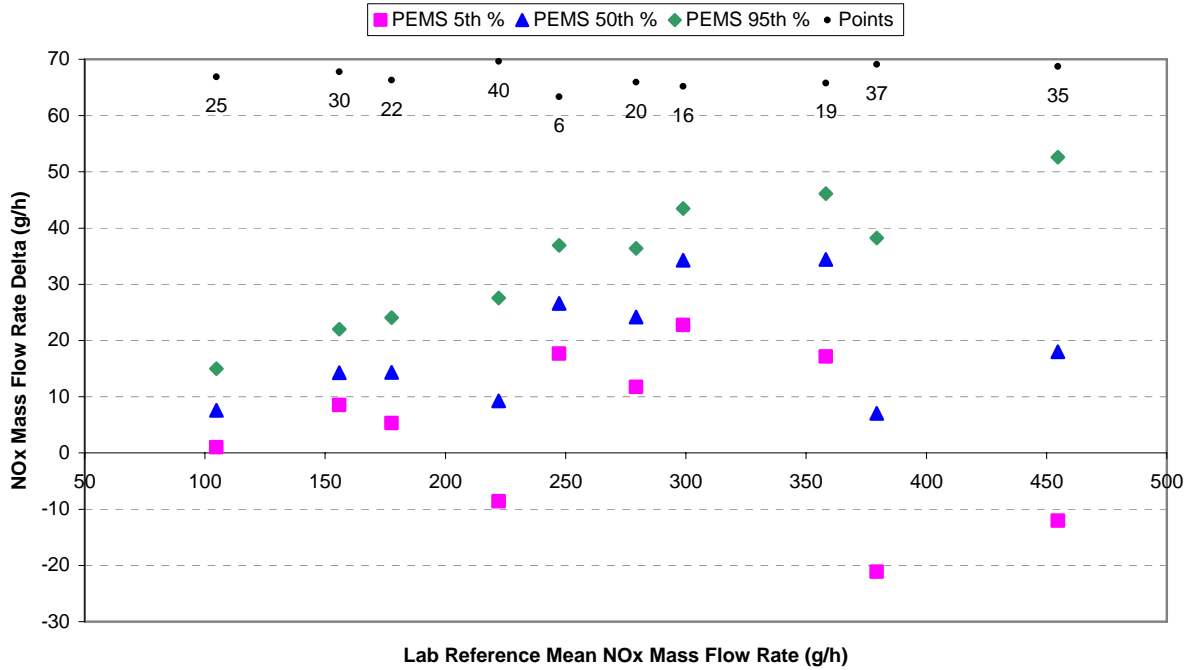
PEMS EXHAUST FLOW RATE DELTA VERSUS THE LABORATORY REFERENCE FOR ENGINE 3 STEADY-STATE TESTING



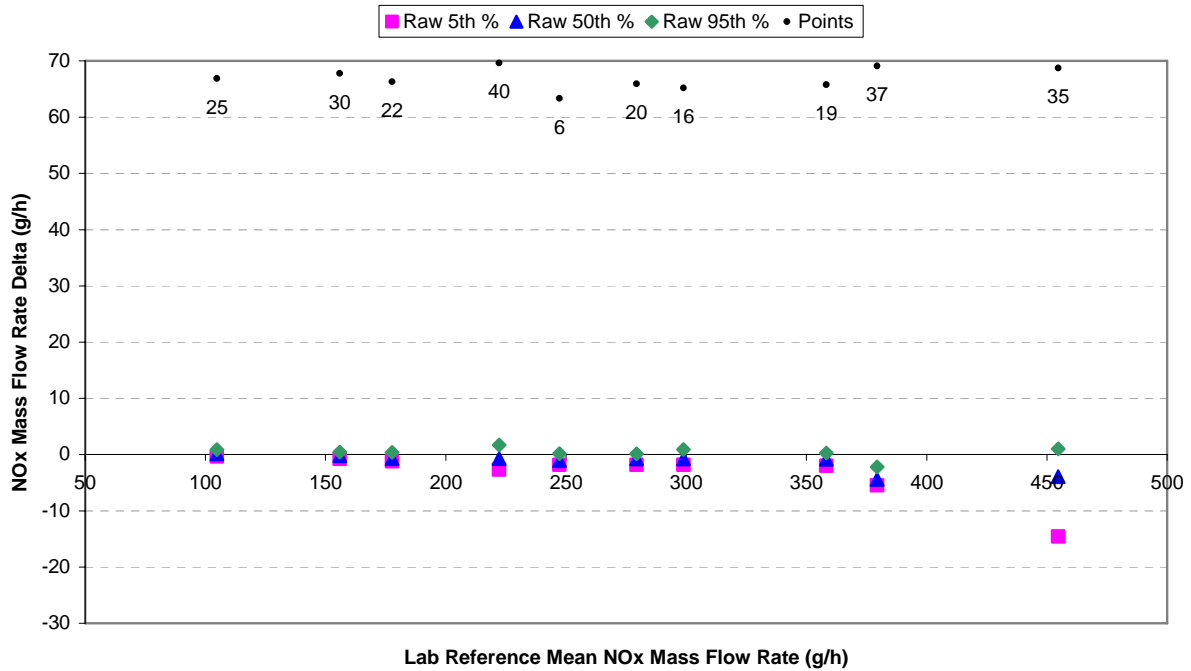
LAB RAW EXHAUST FLOW RATE DELTA VERSUS THE LABORATORY REFERENCE FOR ENGINE 3 STEADY-STATE TESTING



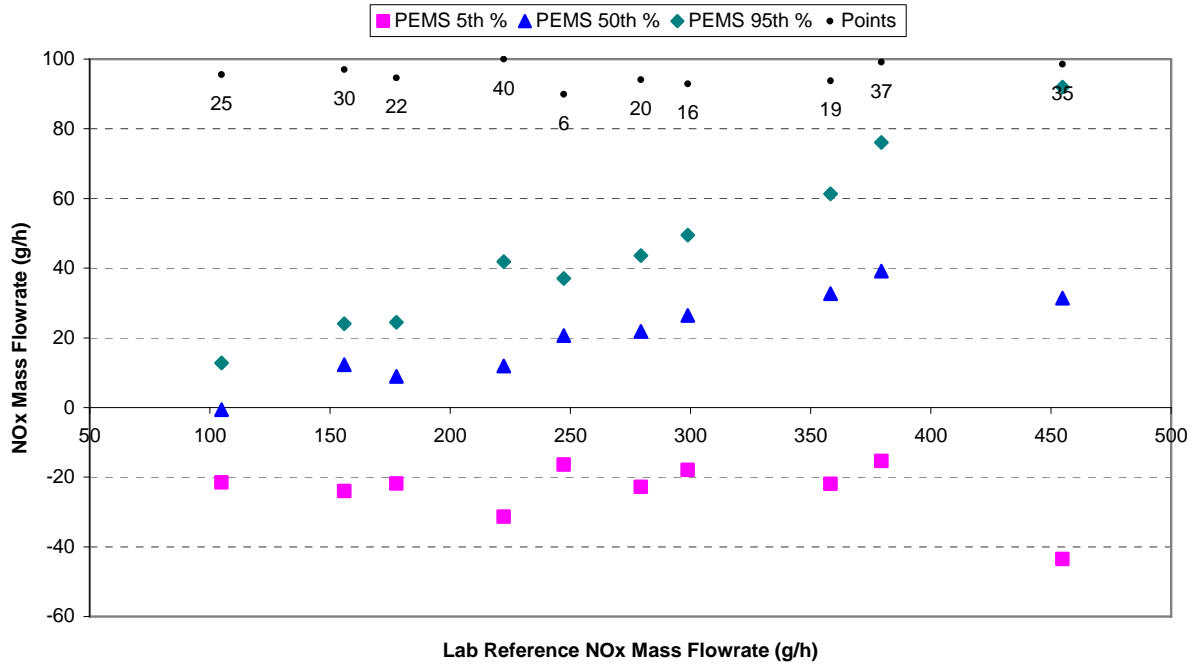
HORIBA OBS-2200 EXHAUST FLOW RATE DELTA VERSUS THE LABORATORY REFERENCE FOR ENGINE 3 STEADY-STATE TESTING



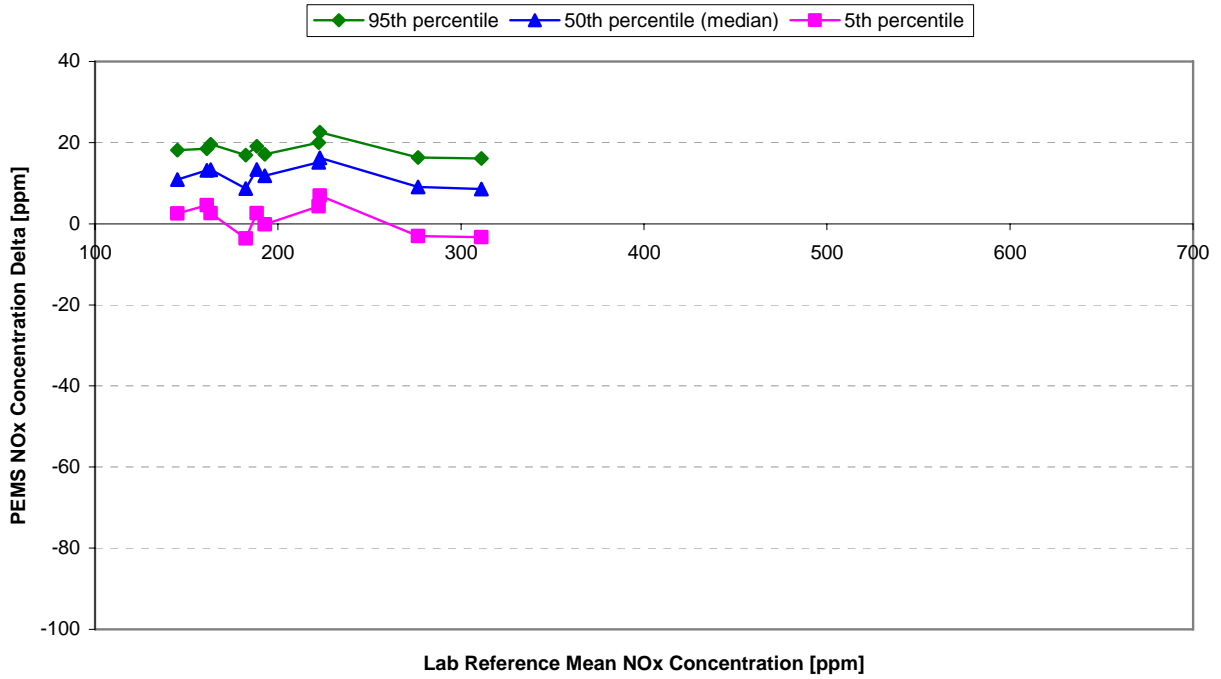
PEMS NO_x MASS FLOW RATE DELTA VERSUS THE LABORATORY REFERENCE FOR ENGINE 3 STEADY-STATE TESTING



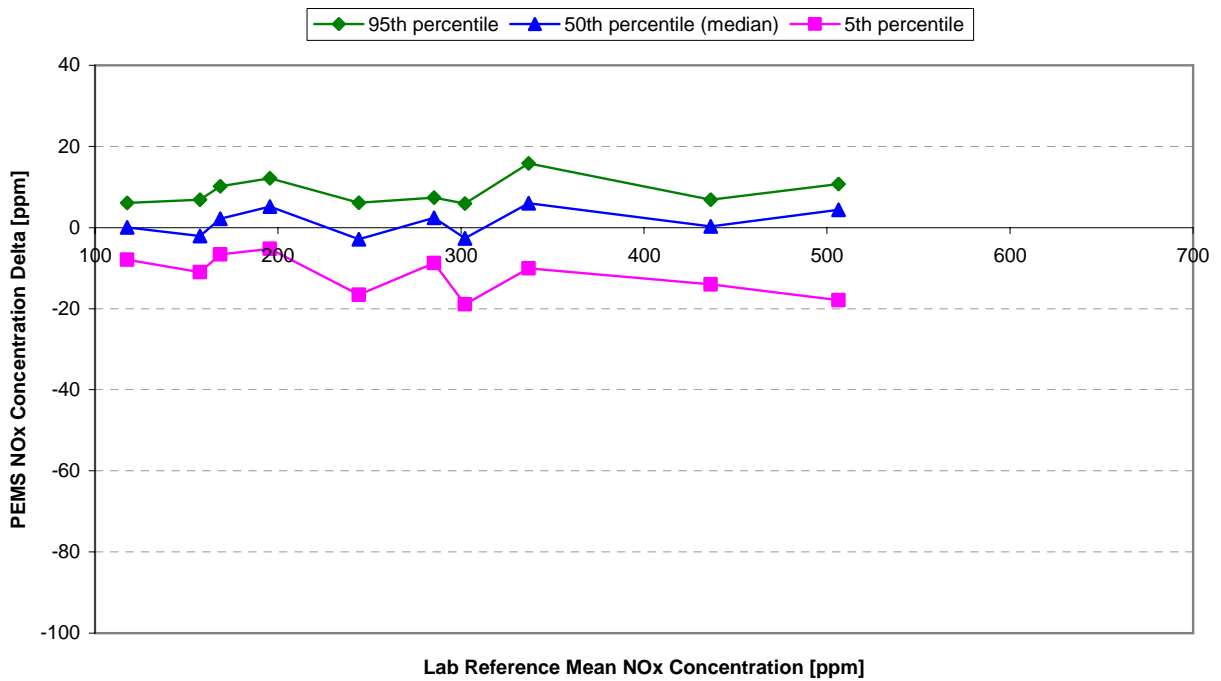
LAB RAW NO_x MASS FLOW RATE DELTA VERSUS THE LABORATORY REFERENCE FOR ENGINE 3 STEADY-STATE TESTING



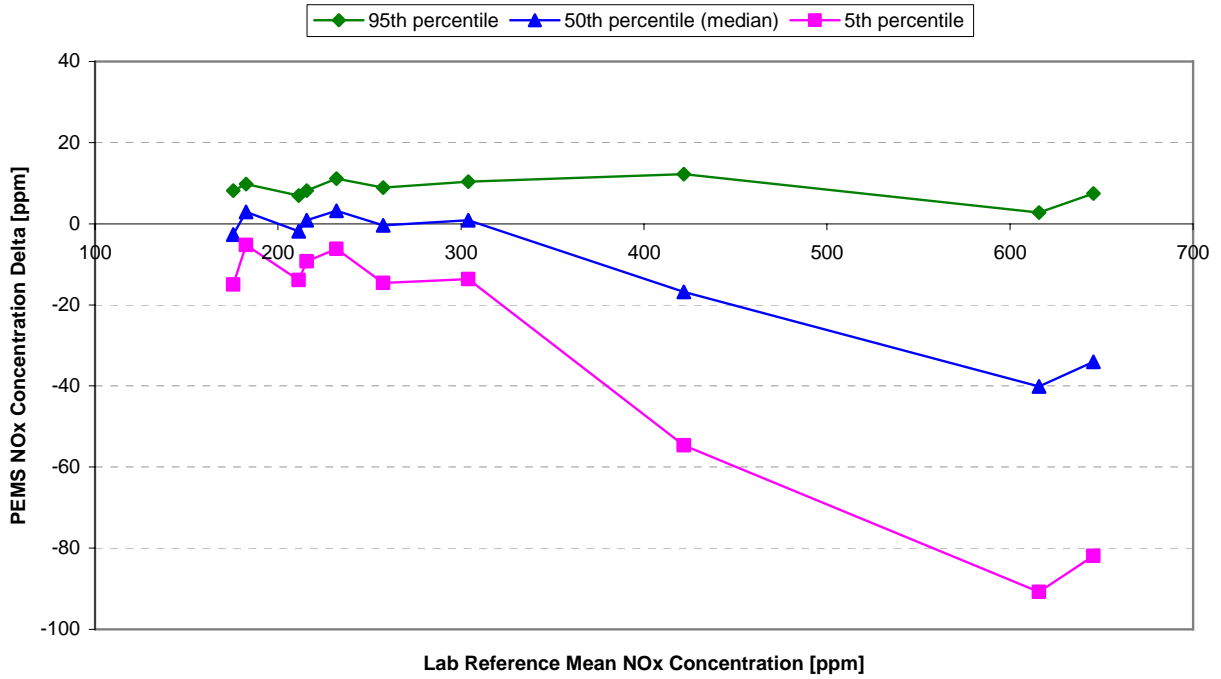
HORIBA OBS-2200 NO_x MASS FLOW RATE DELTA VERSUS THE LABORATORY REFERENCE FOR ENGINE 3 STEADY-STATE TESTING



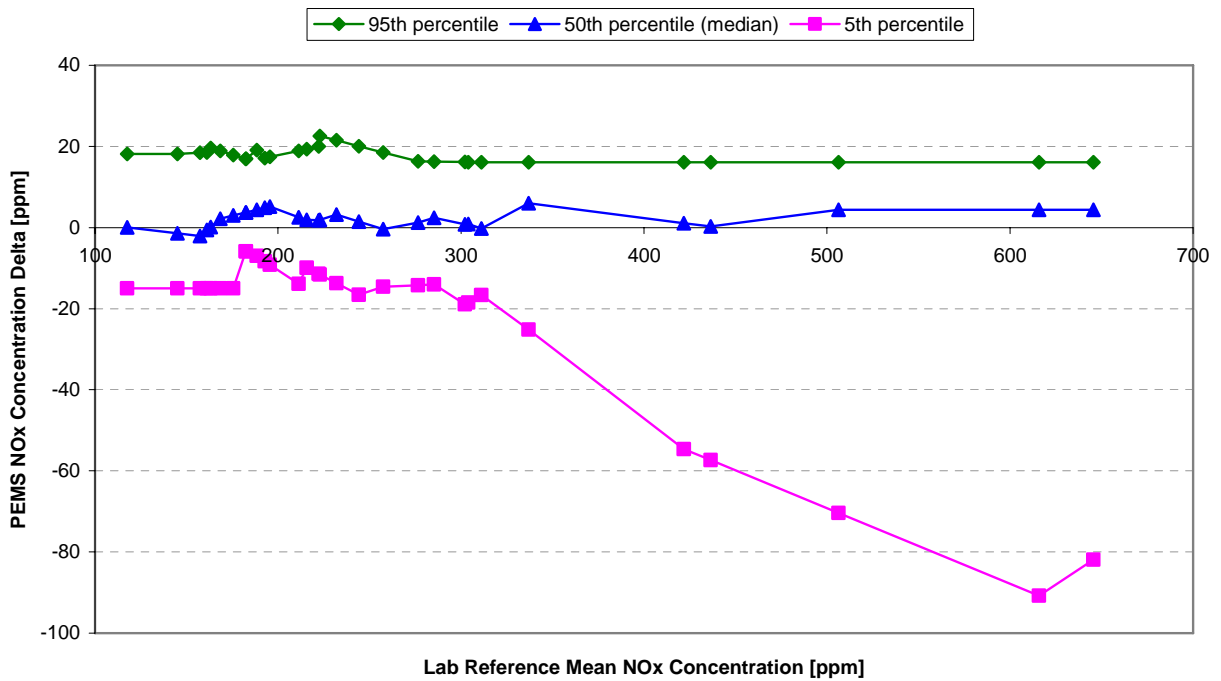
ENGINE 1 ERROR SURFACE FOR STEADY-STATE NO_x CONCENTRATION



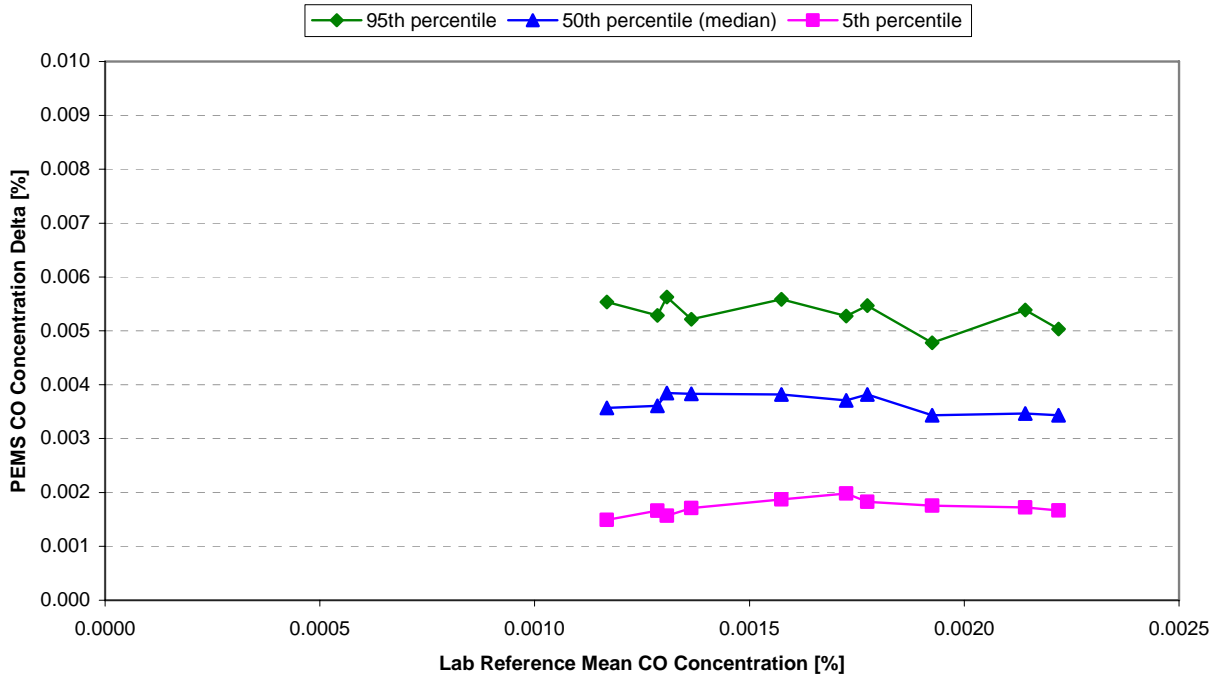
ENGINE 2 ERROR SURFACE FOR STEADY-STATE NO_x CONCENTRATION



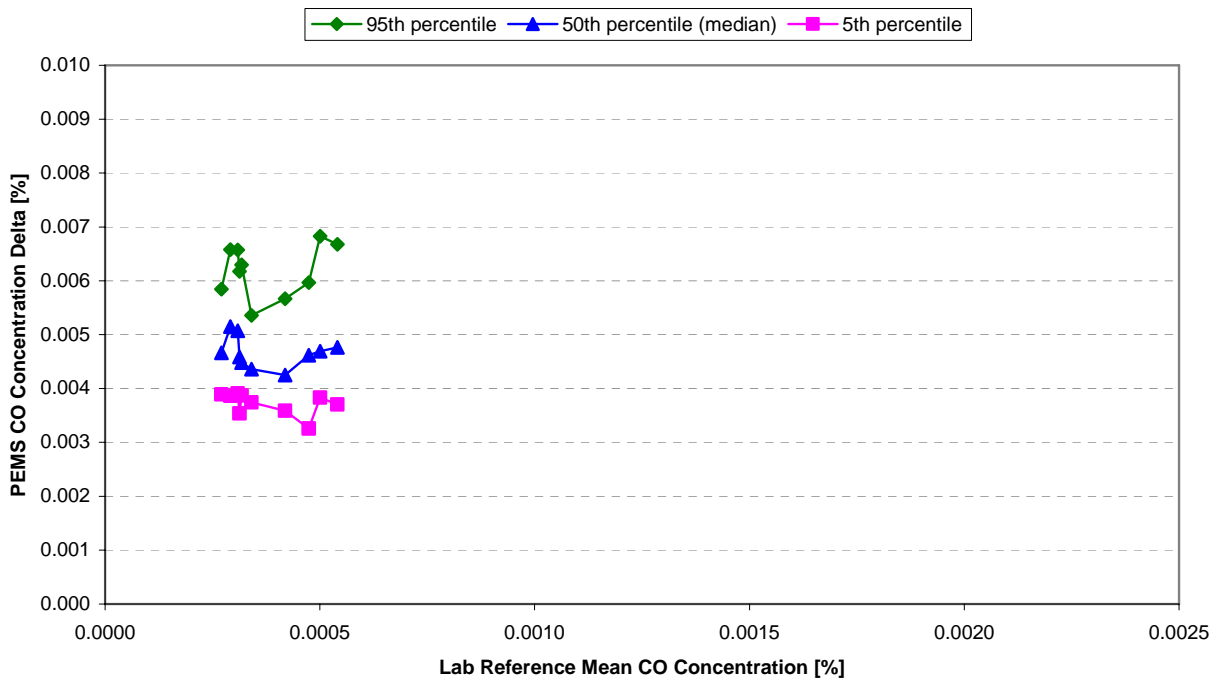
ENGINE 3 ERROR SURFACE FOR STEADY-STATE NO_x CONCENTRATION



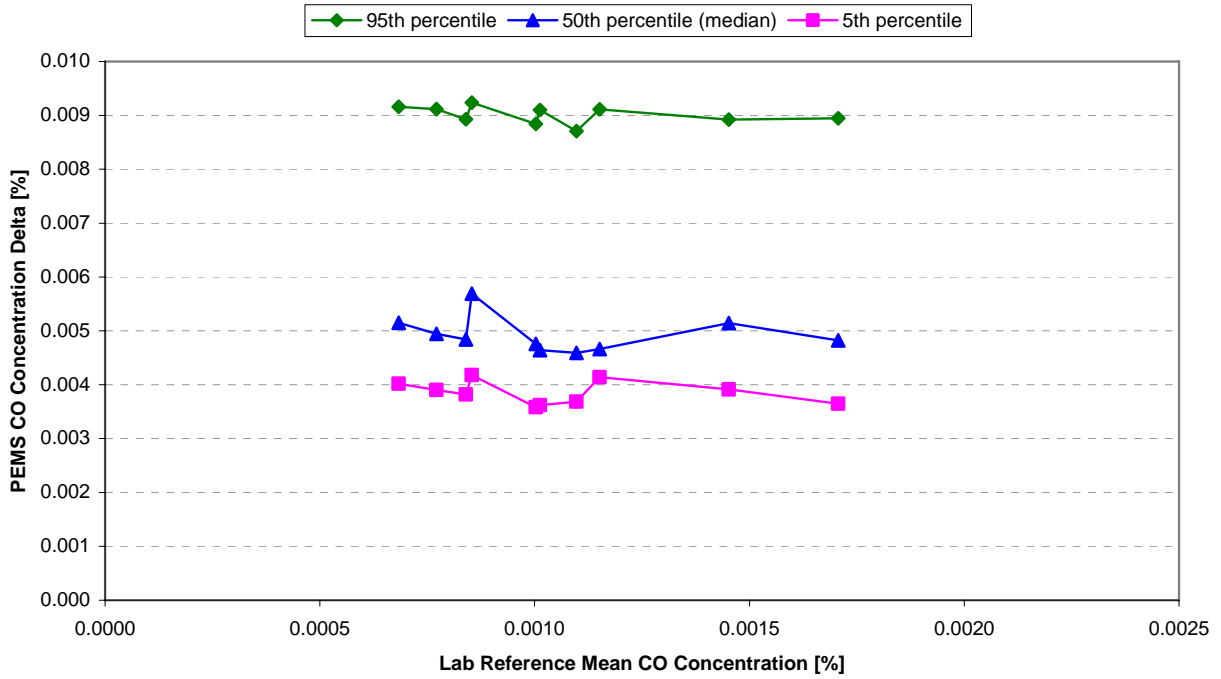
FINAL ERROR SURFACE FOR STEADY-STATE NO_x CONCENTRATION



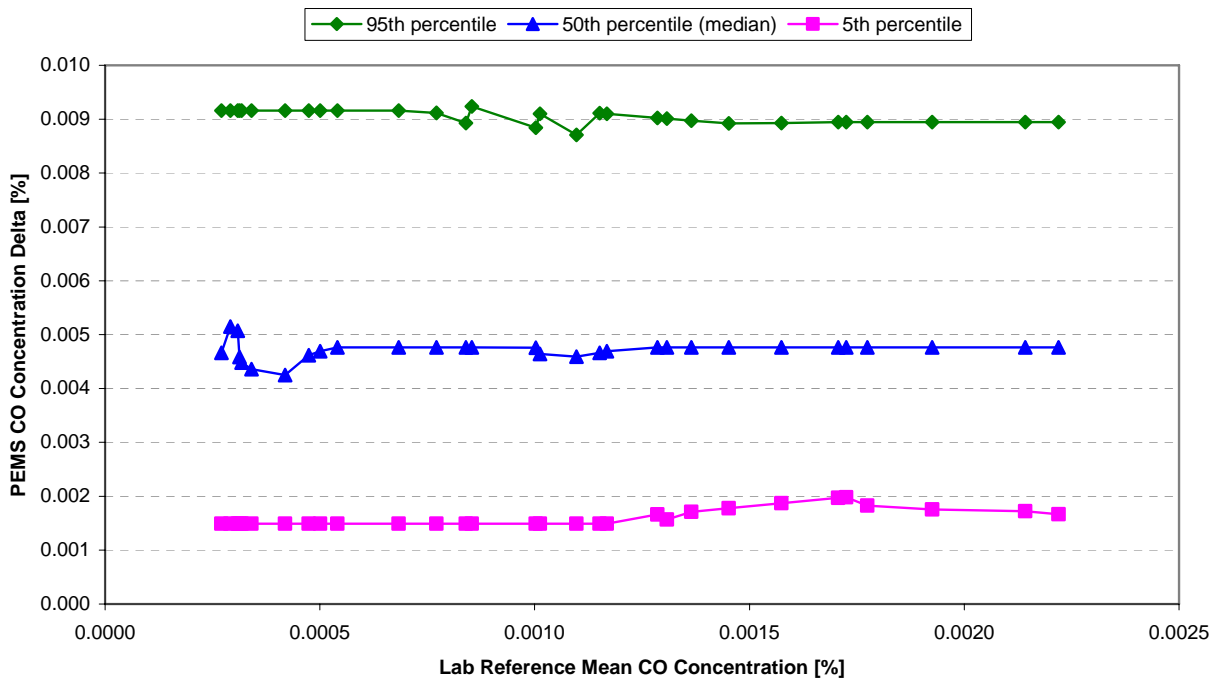
ENGINE 1 ERROR SURFACE FOR STEADY-STATE CO CONCENTRATION



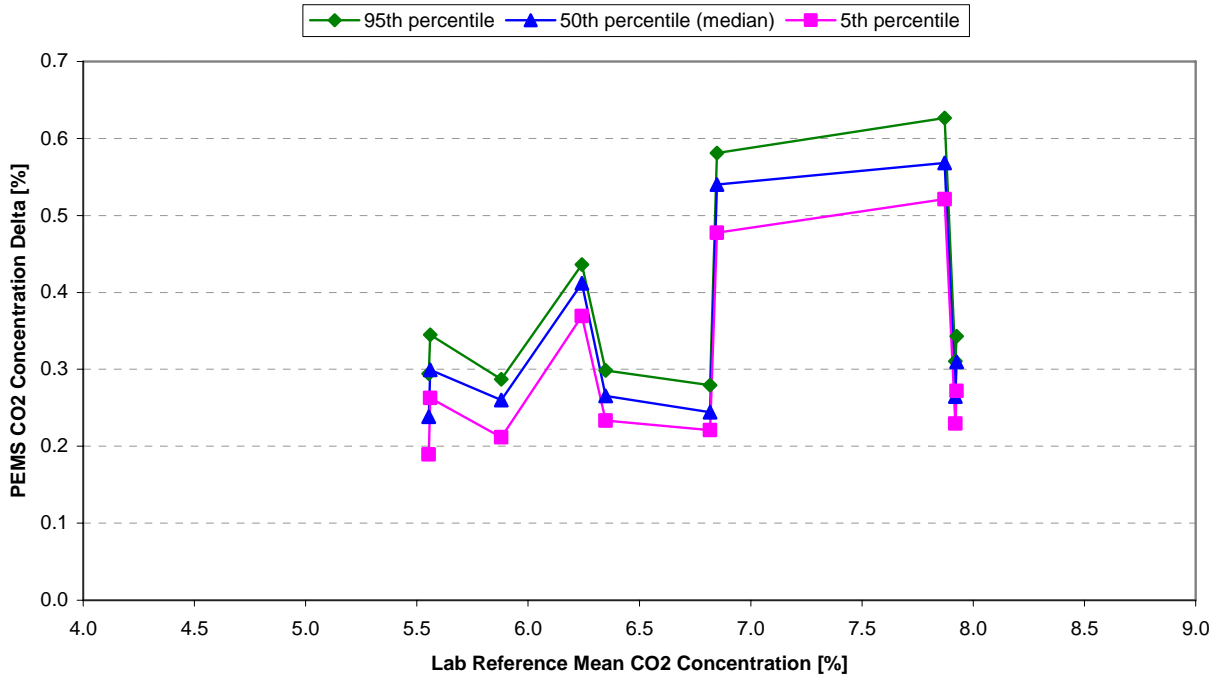
ENGINE 2 ERROR SURFACE FOR STEADY-STATE CO CONCENTRATION



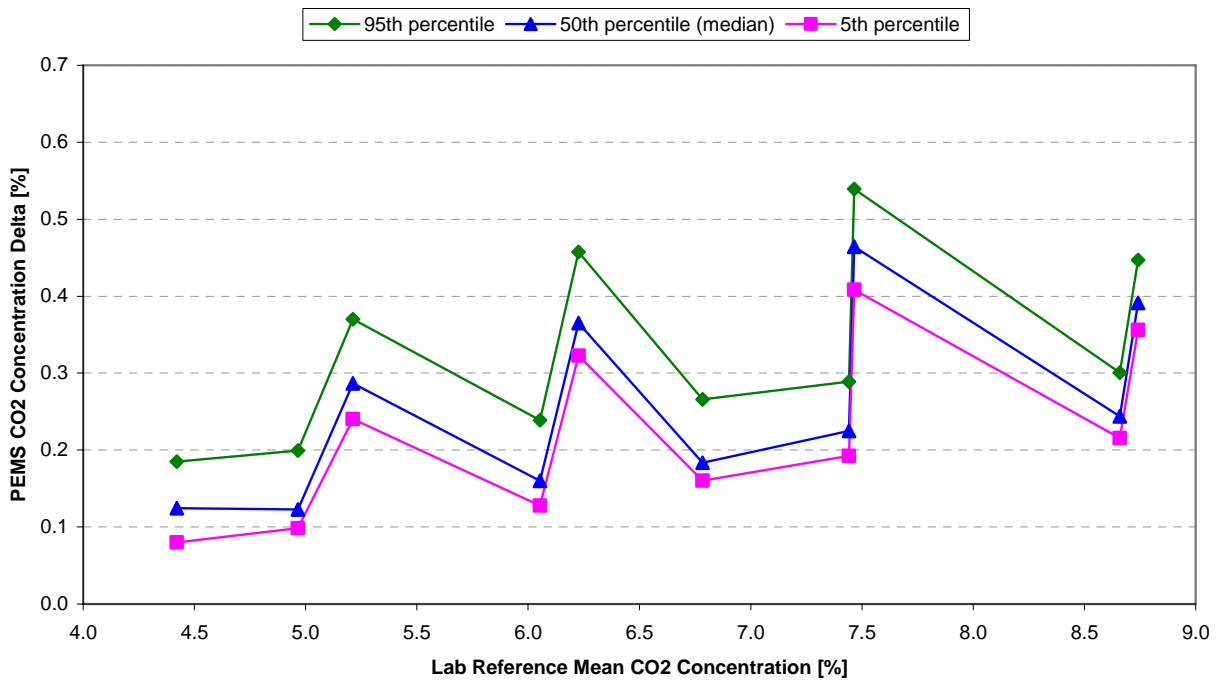
ENGINE 3 ERROR SURFACE FOR STEADY-STATE CO CONCENTRATION



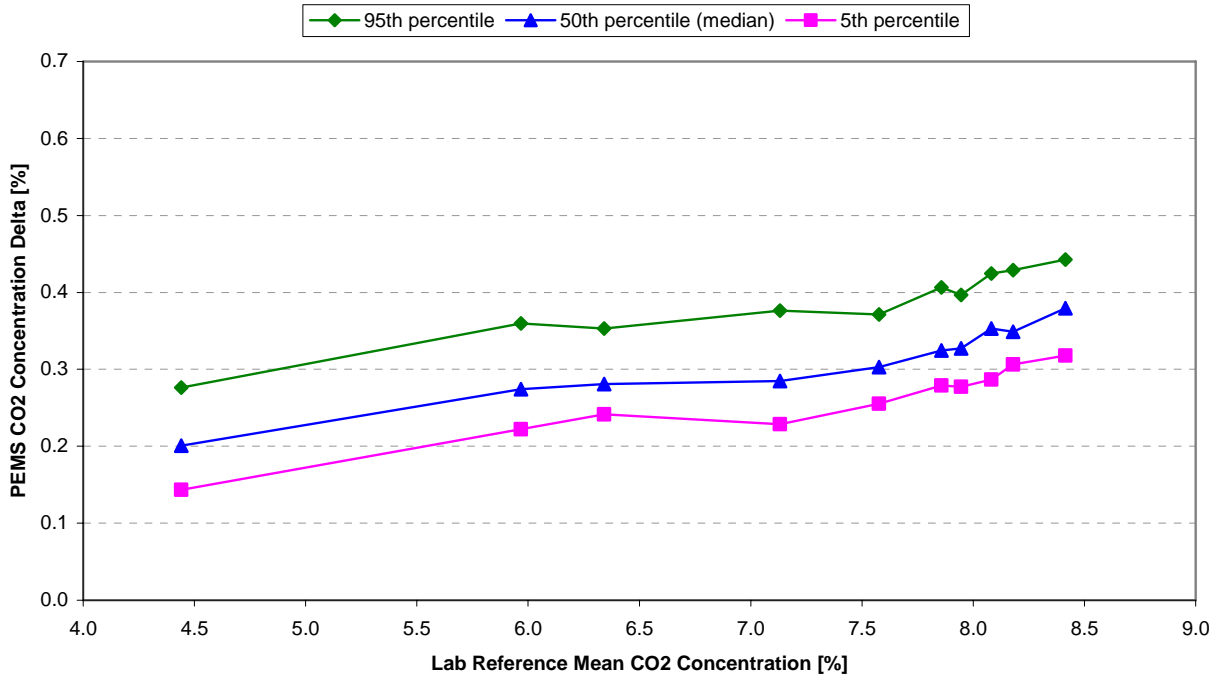
FINAL ERROR SURFACE FOR STEADY-STATE CO CONCENTRATION



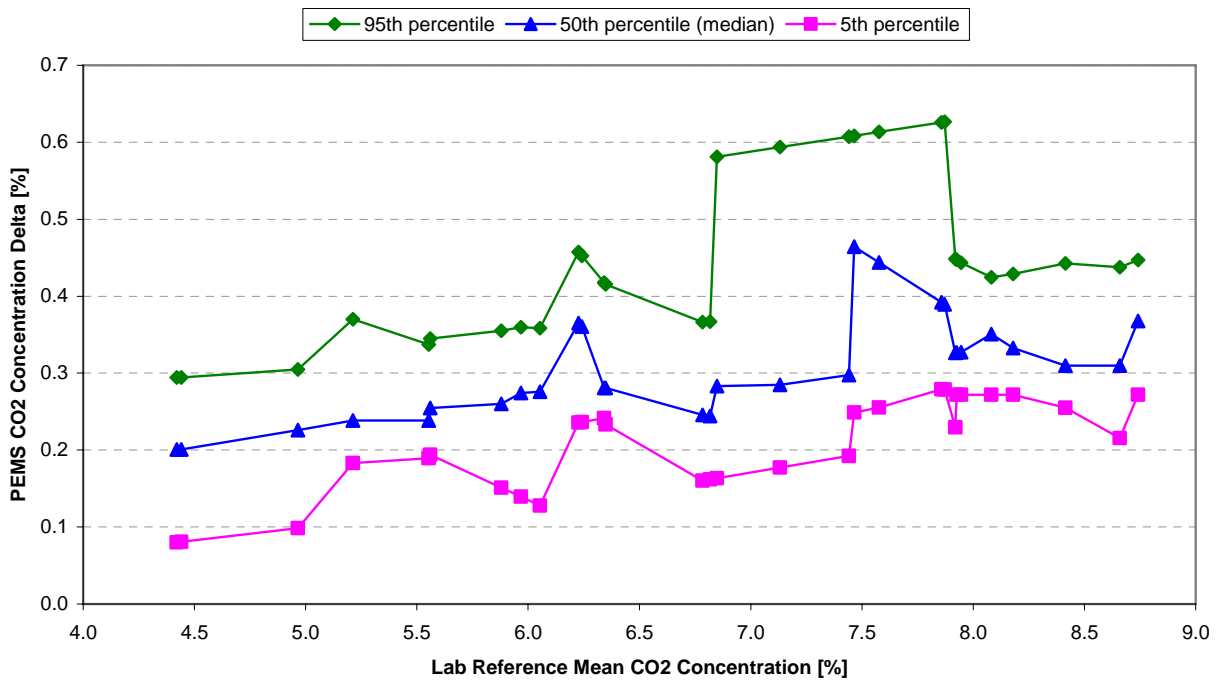
ENGINE 1 ERROR SURFACE FOR STEADY-STATE CO₂ CONCENTRATION



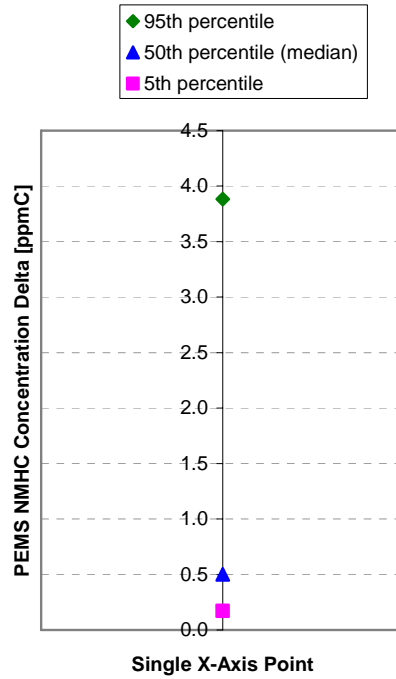
ENGINE 2 ERROR SURFACE FOR STEADY-STATE CO₂ CONCENTRATION



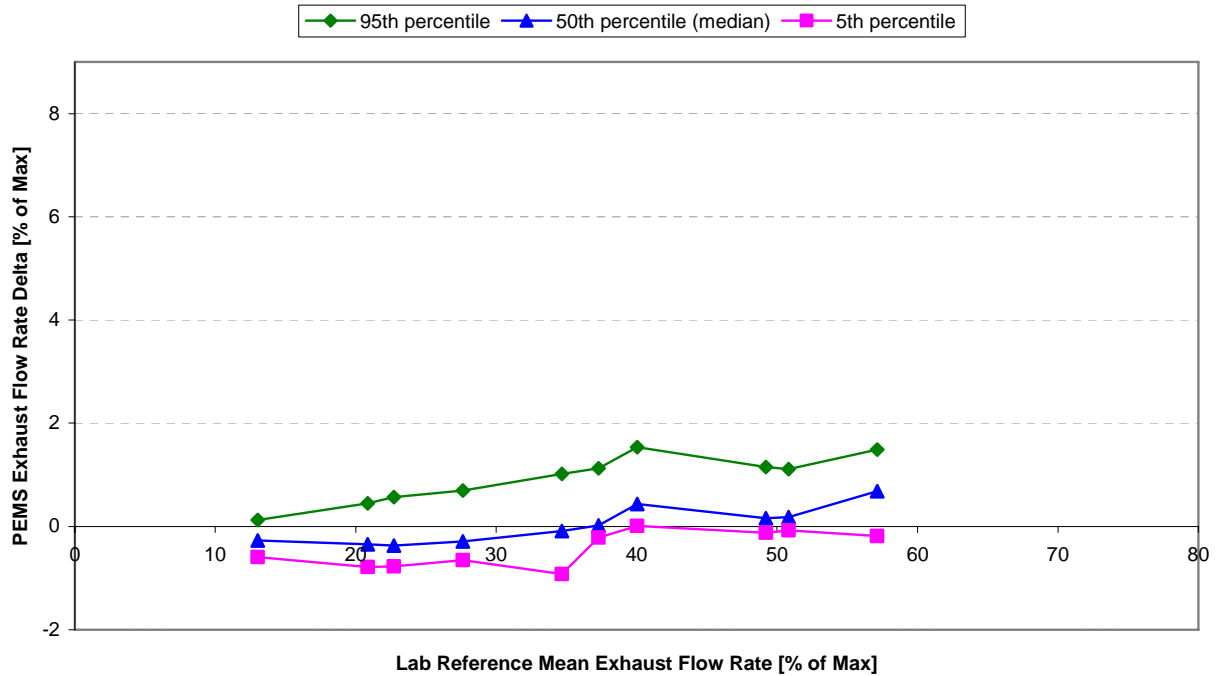
ENGINE 3 ERROR SURFACE FOR STEADY-STATE CO₂ CONCENTRATION



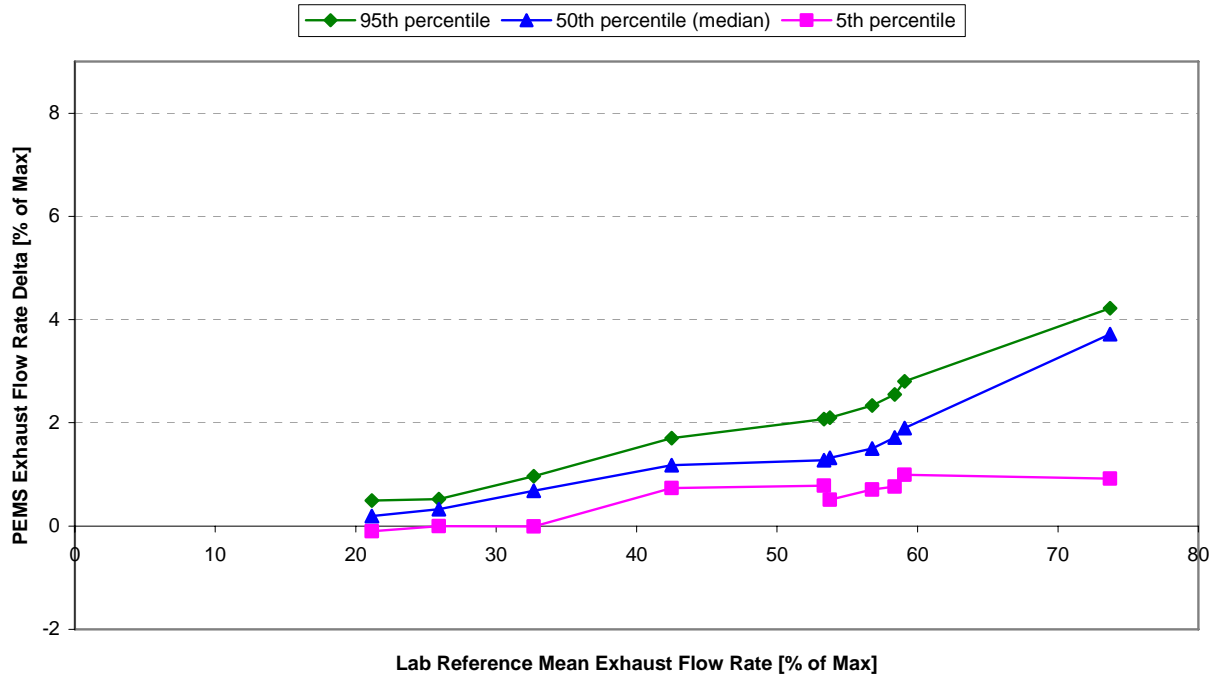
FINAL ERROR SURFACE FOR STEADY-STATE CO₂ CONCENTRATION



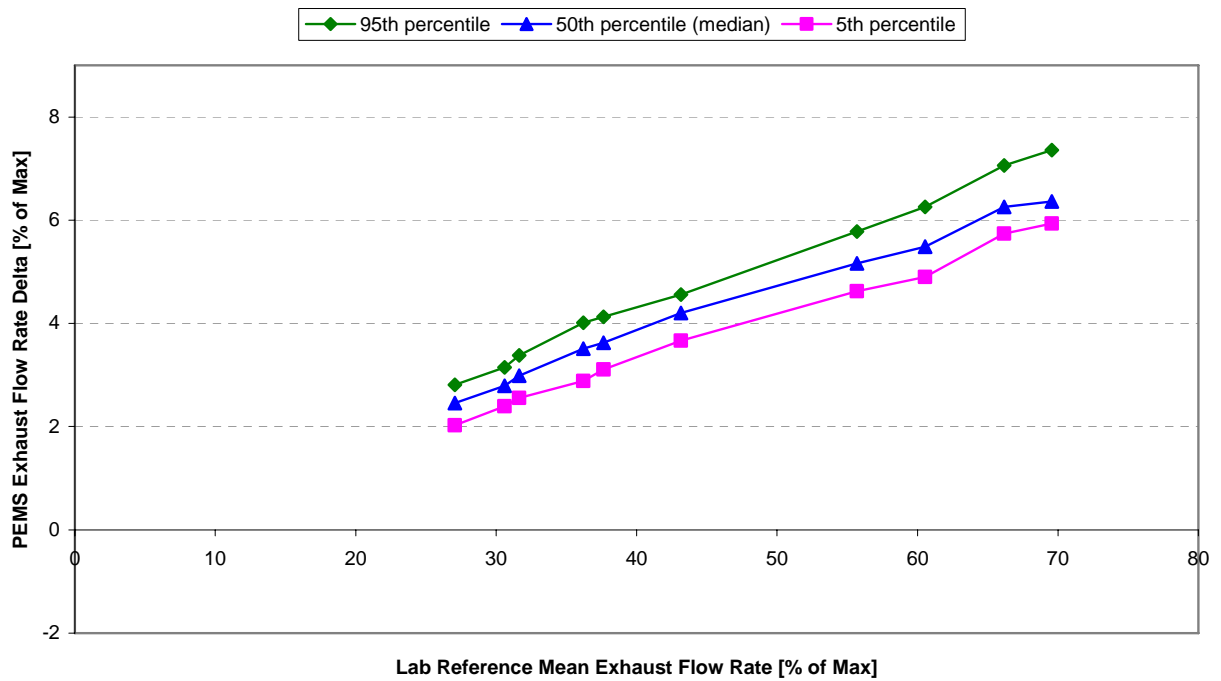
**FINAL ERROR SURFACE FOR STEADY-STATE NMHC CONCENTRATION
(ENGINE 2 DATA ONLY)**



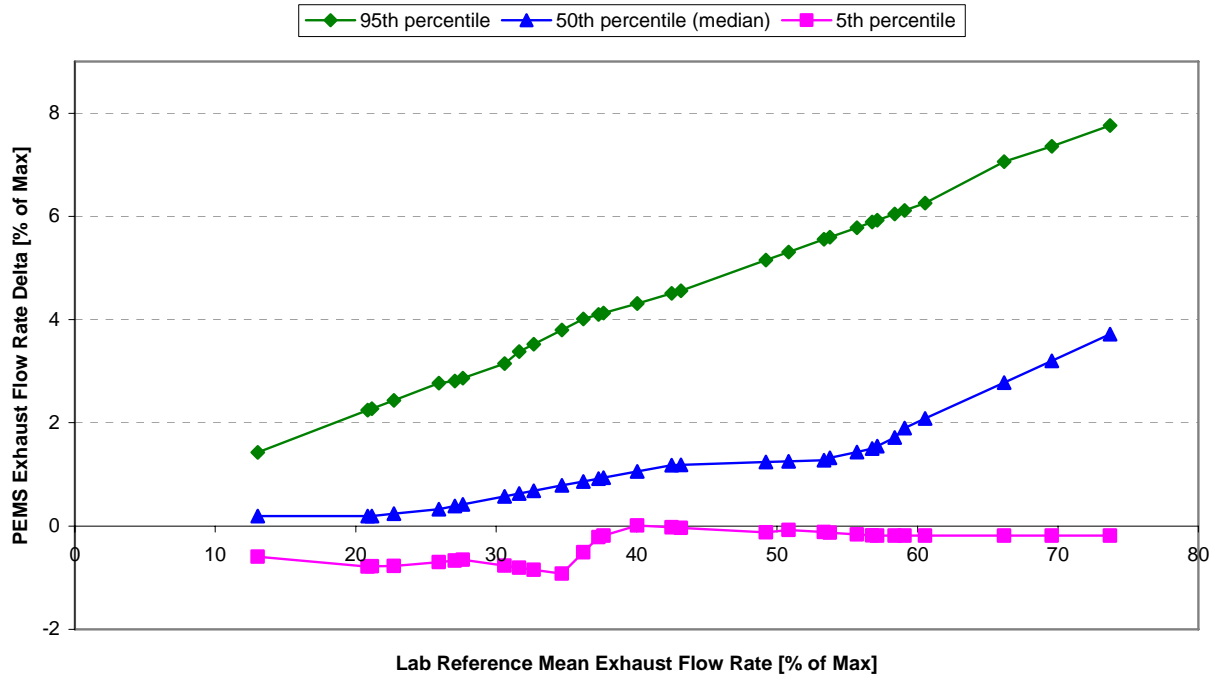
ENGINE 1 ERROR SURFACE FOR STEADY-STATE EXHAUST FLOW RATE



ENGINE 2 ERROR SURFACE FOR STEADY-STATE EXHAUST FLOW RATE

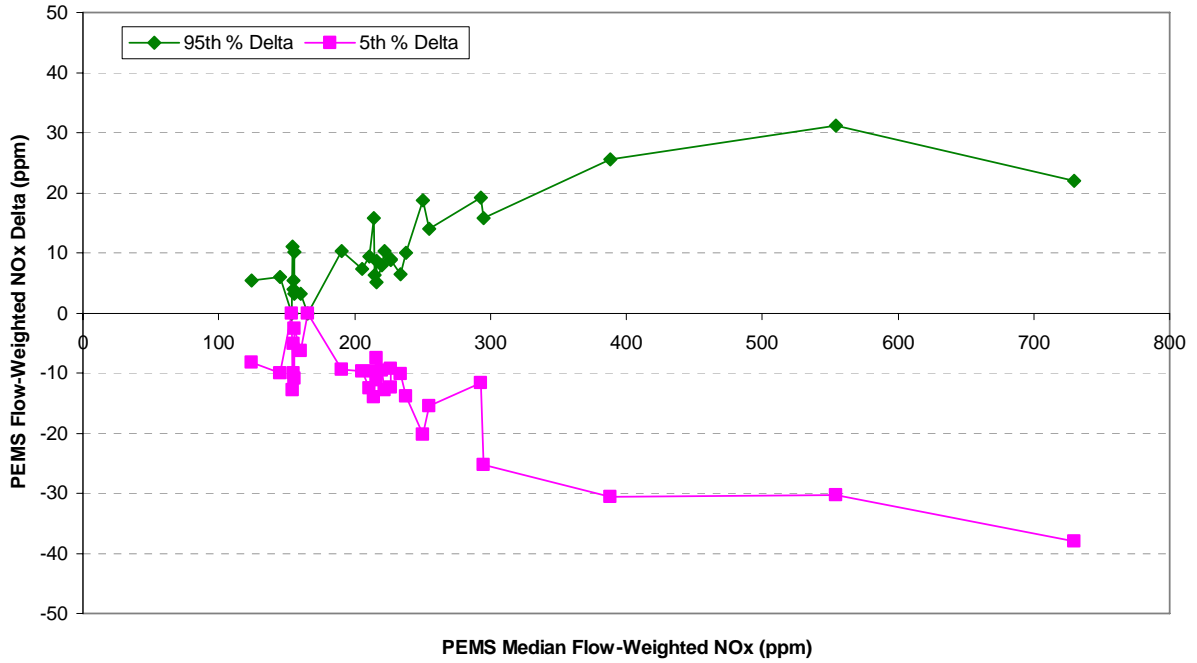


ENGINE 3 ERROR SURFACE FOR STEADY-STATE EXHAUST FLOW RATE

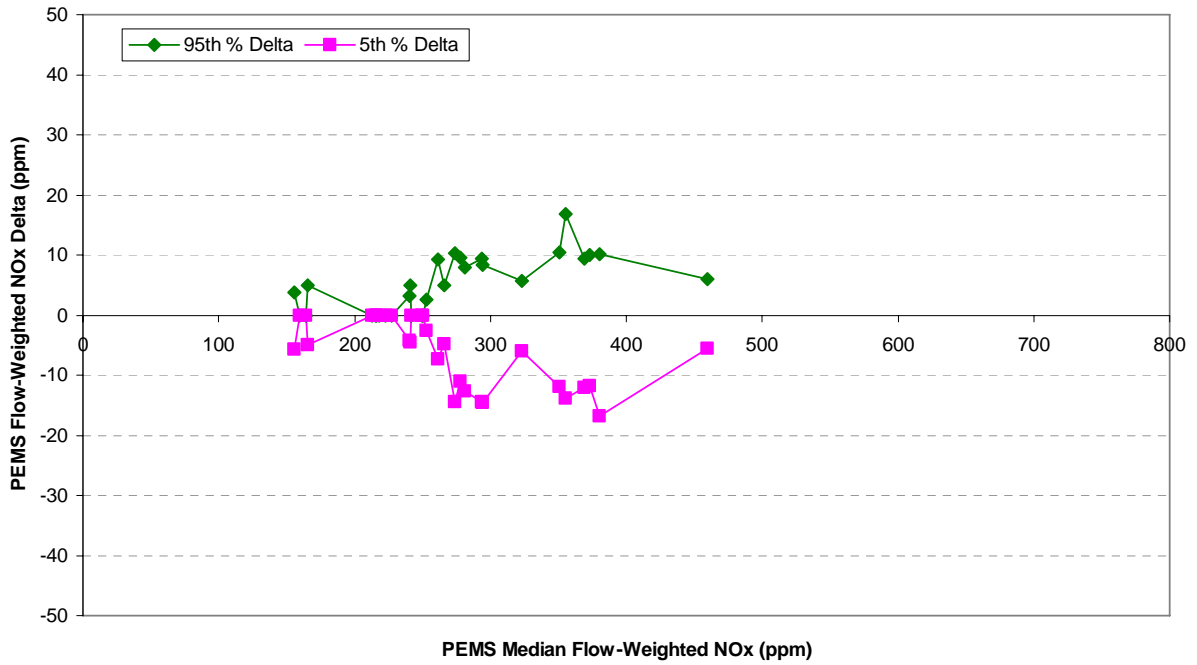


FINAL ERROR SURFACE FOR STEADY-STATE EXHAUST FLOW RATE

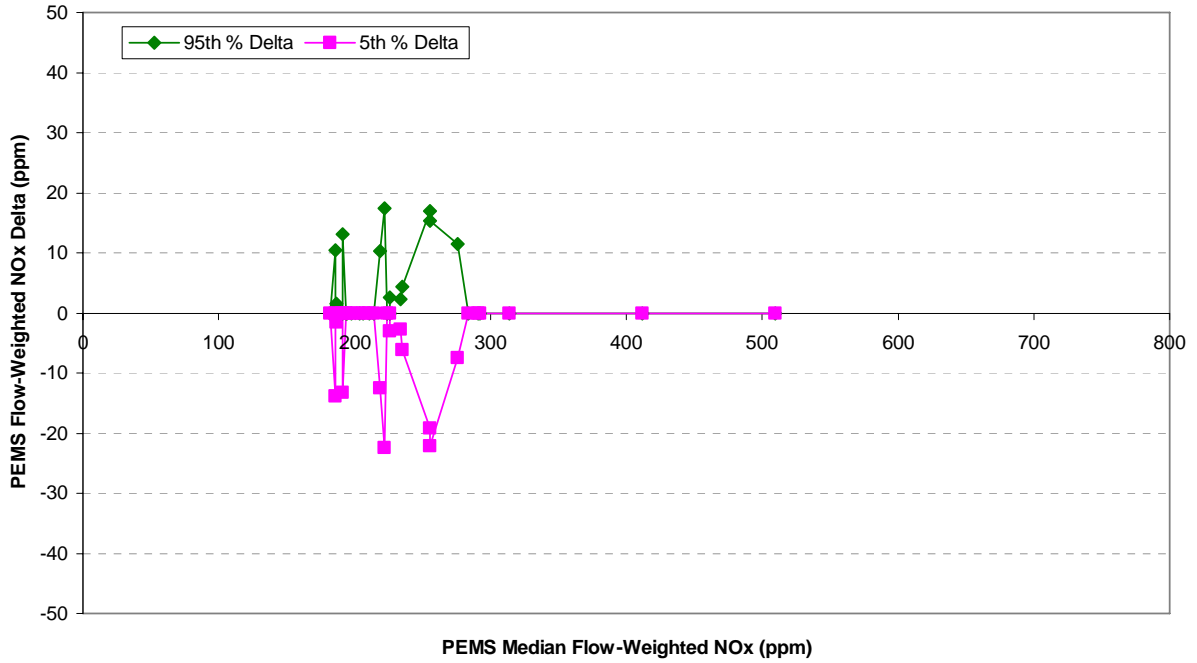
APPENDIX G
TRANSIENT ERROR SURFACE DATA



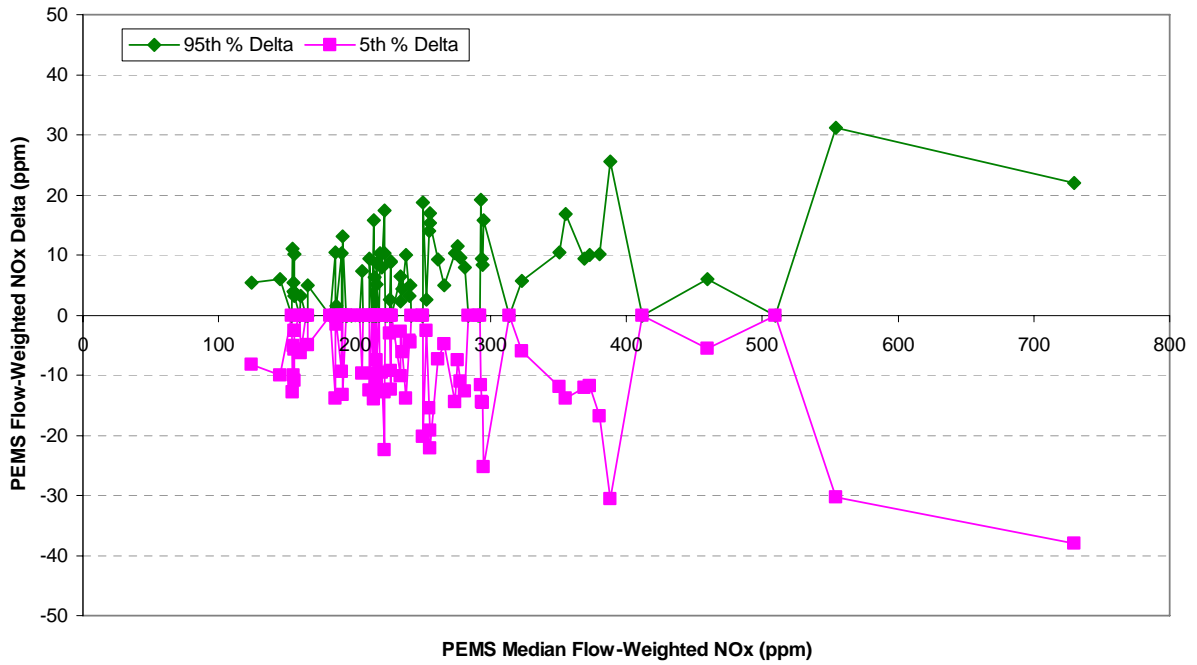
ENGINE 1 ERROR SURFACE FOR TRANSIENT NO_x CONCENTRATION



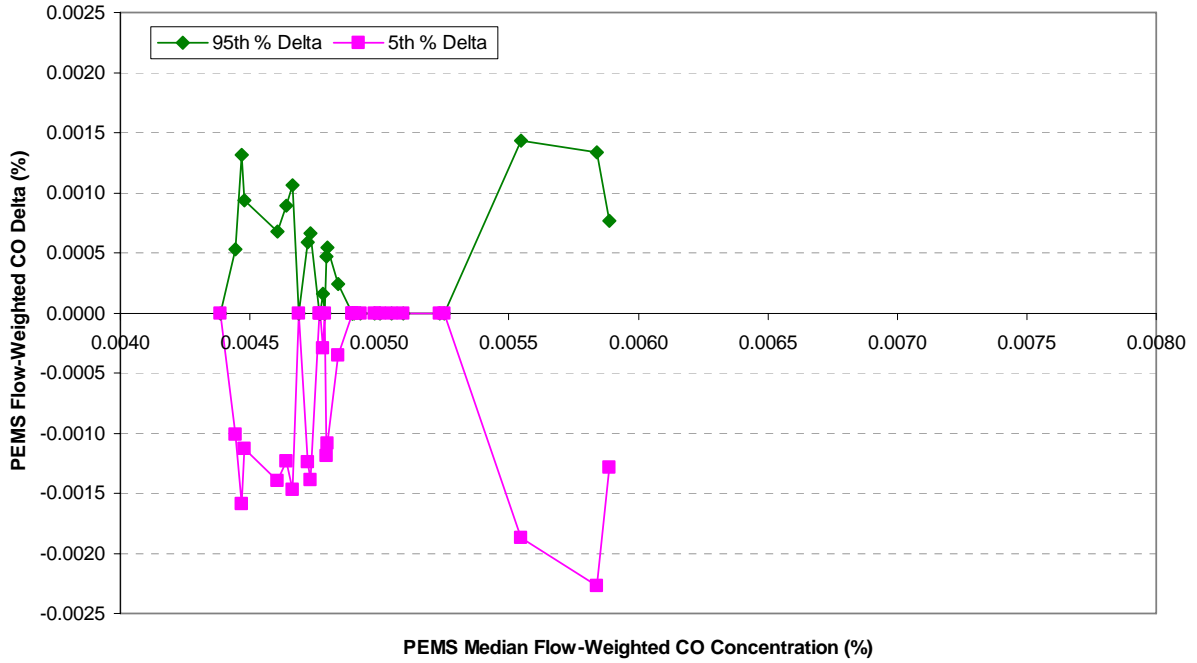
ENGINE 2 ERROR SURFACE FOR TRANSIENT NO_x CONCENTRATION



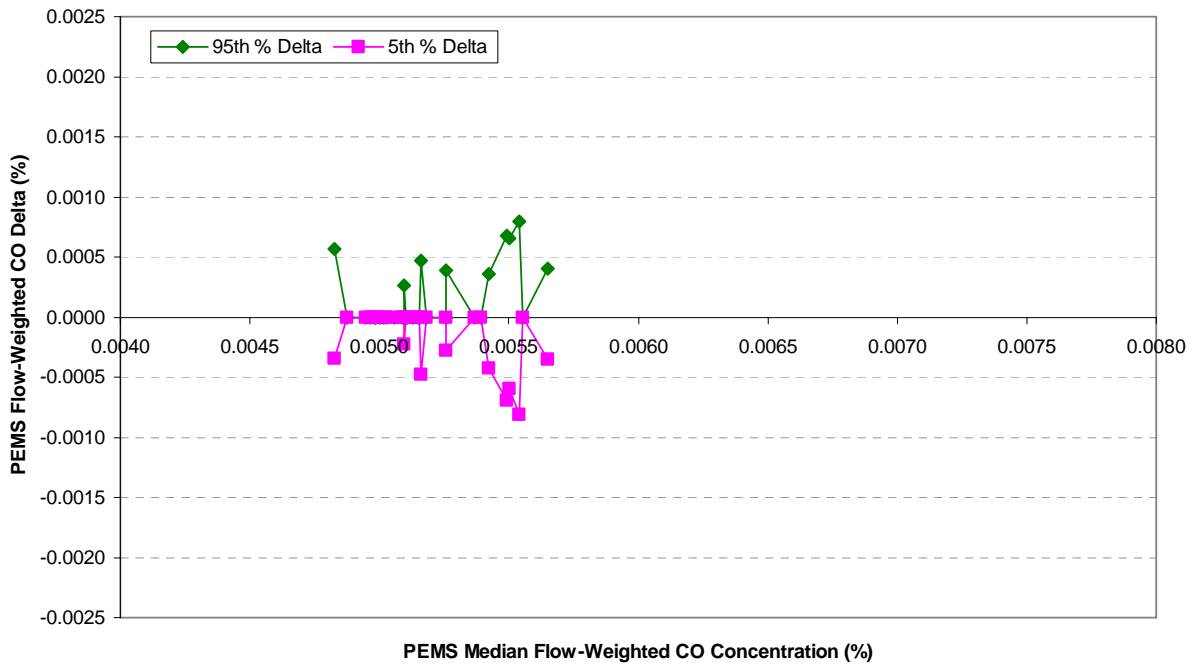
ENGINE 3 ERROR SURFACE FOR TRANSIENT NO_x CONCENTRATION



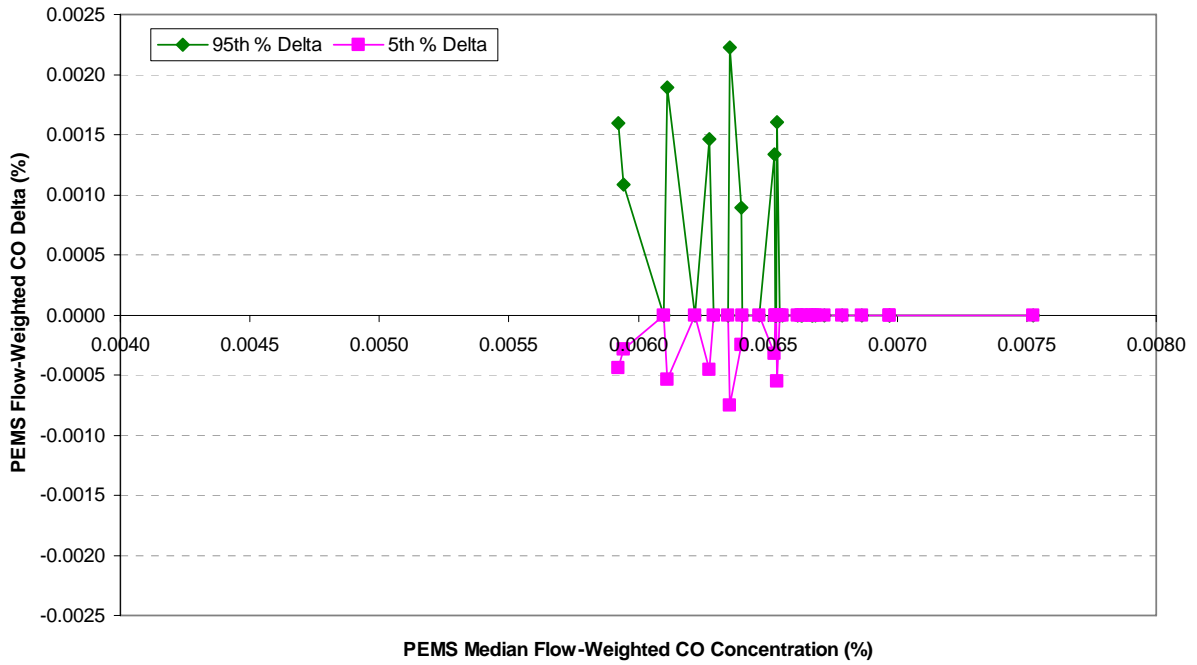
FINAL ERROR SURFACE FOR TRANSIENT NO_x CONCENTRATION



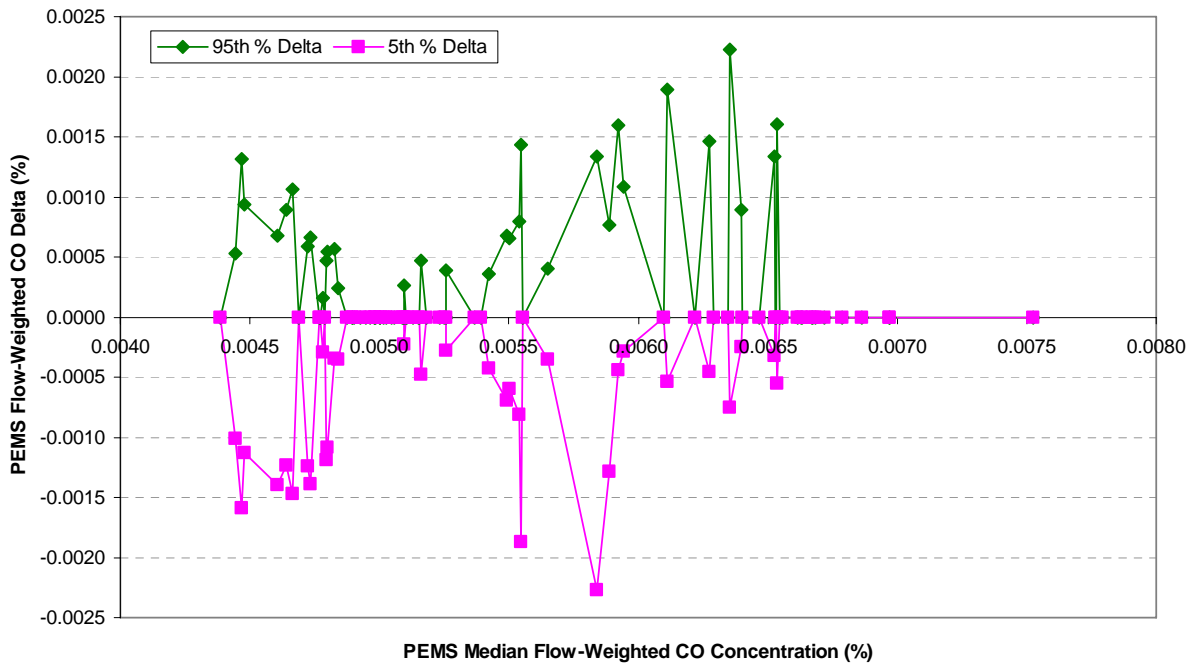
ENGINE 1 ERROR SURFACE FOR TRANSIENT CO CONCENTRATION



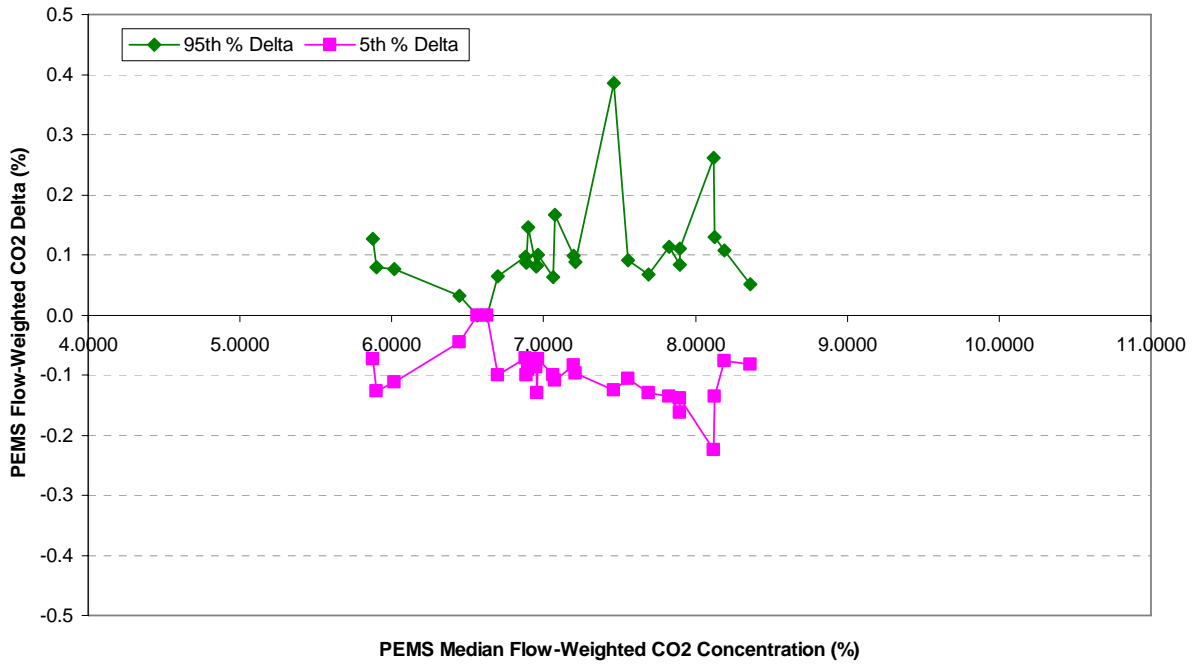
ENGINE 2 ERROR SURFACE FOR TRANSIENT CO CONCENTRATION



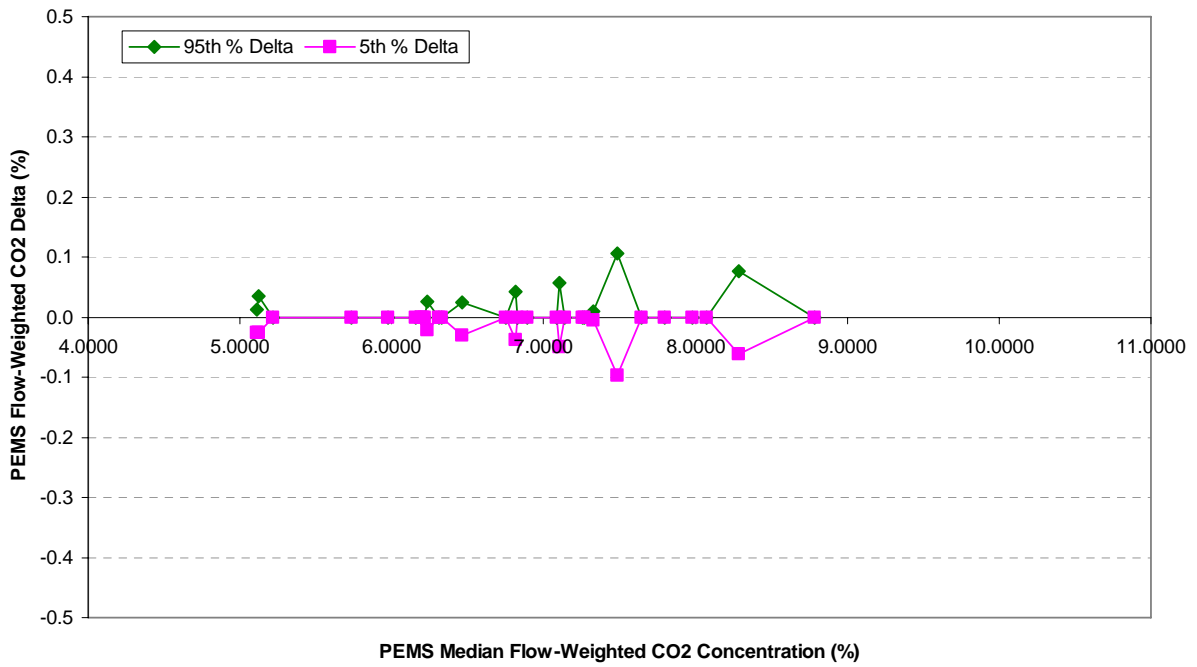
ENGINE 3 ERROR SURFACE FOR TRANSIENT CO CONCENTRATION



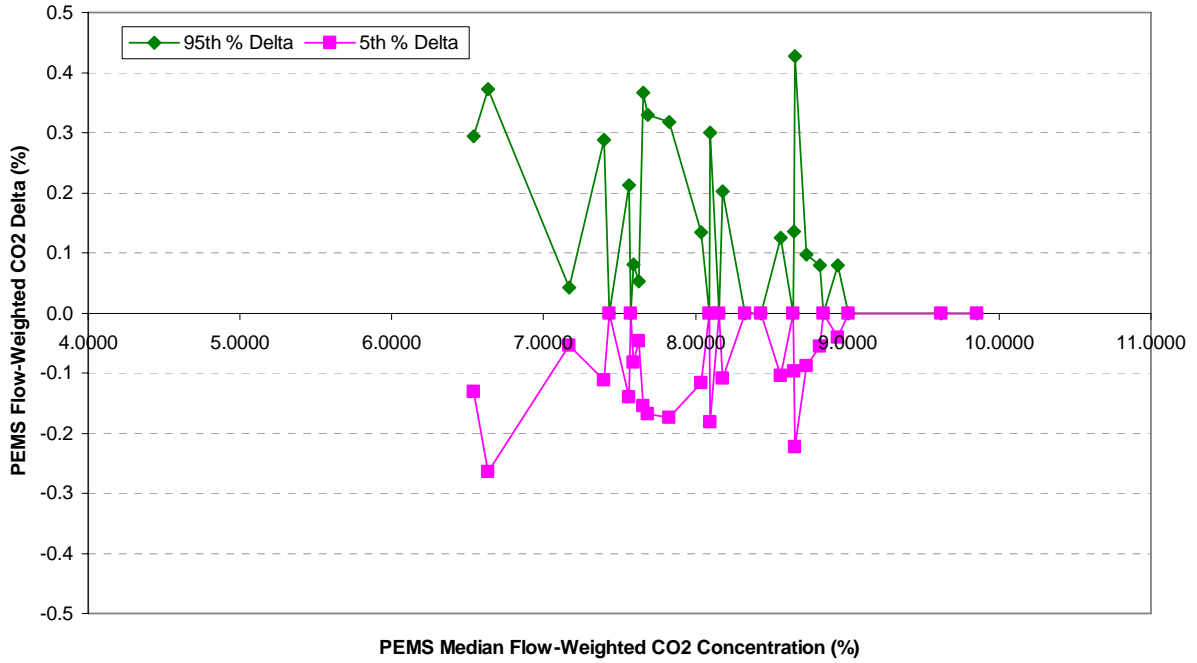
FINAL ERROR SURFACE FOR TRANSIENT CO CONCENTRATION



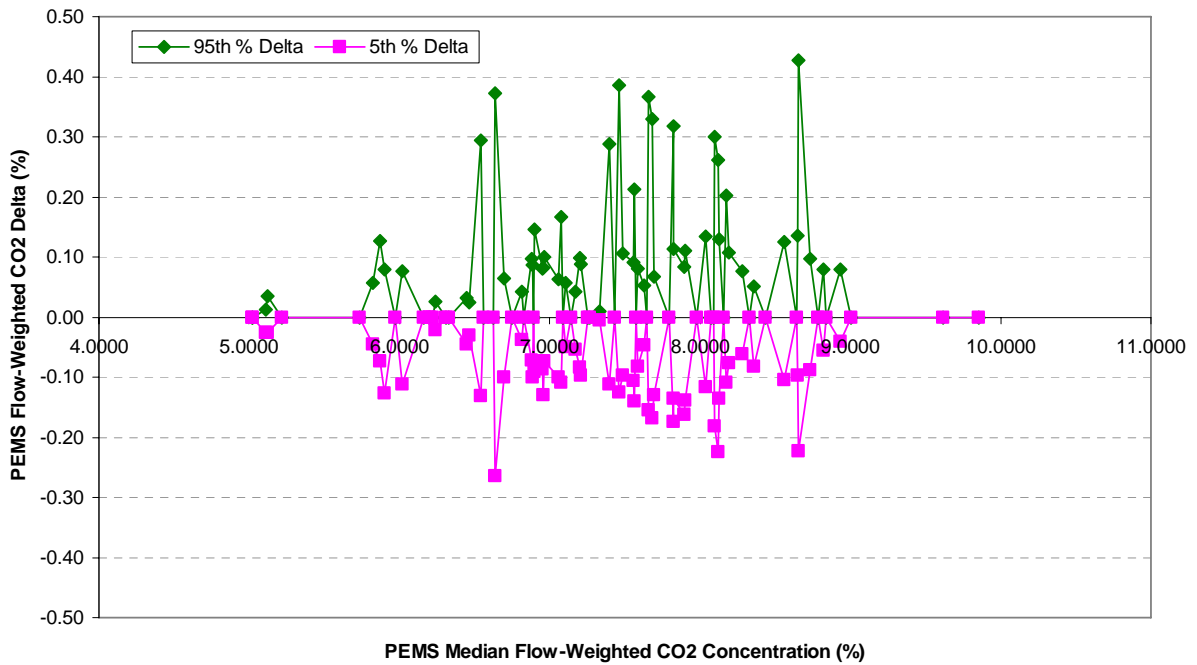
ENGINE 1 ERROR SURFACE FOR TRANSIENT CO₂ CONCENTRATION



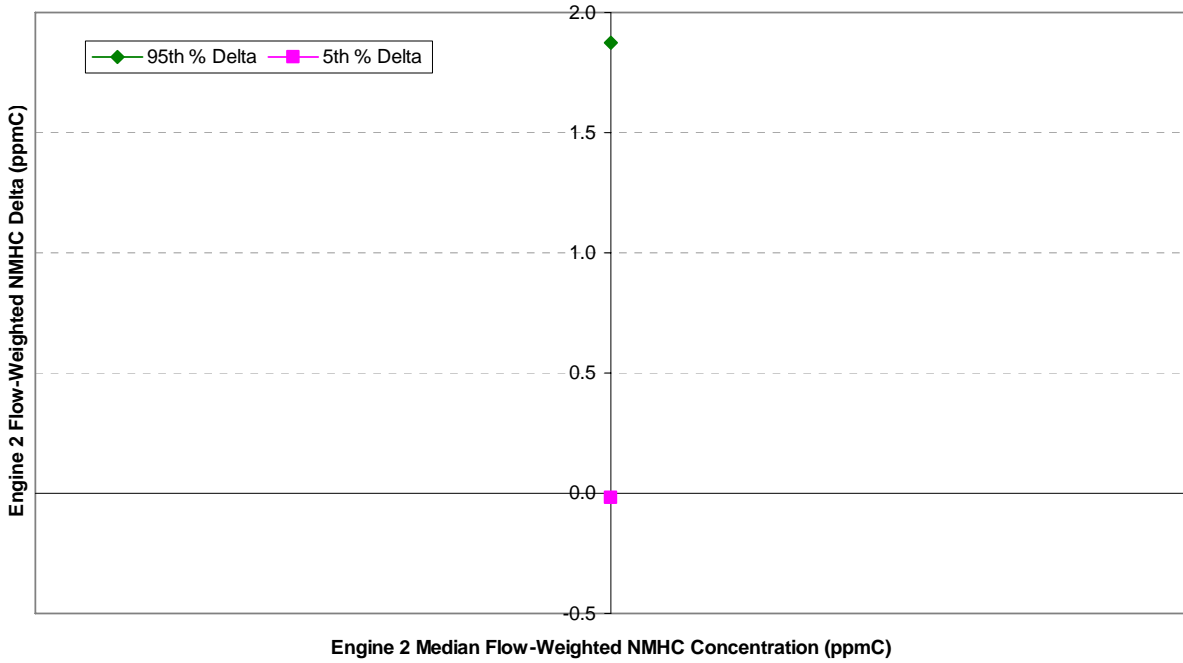
ENGINE 2 ERROR SURFACE FOR TRANSIENT CO₂ CONCENTRATION



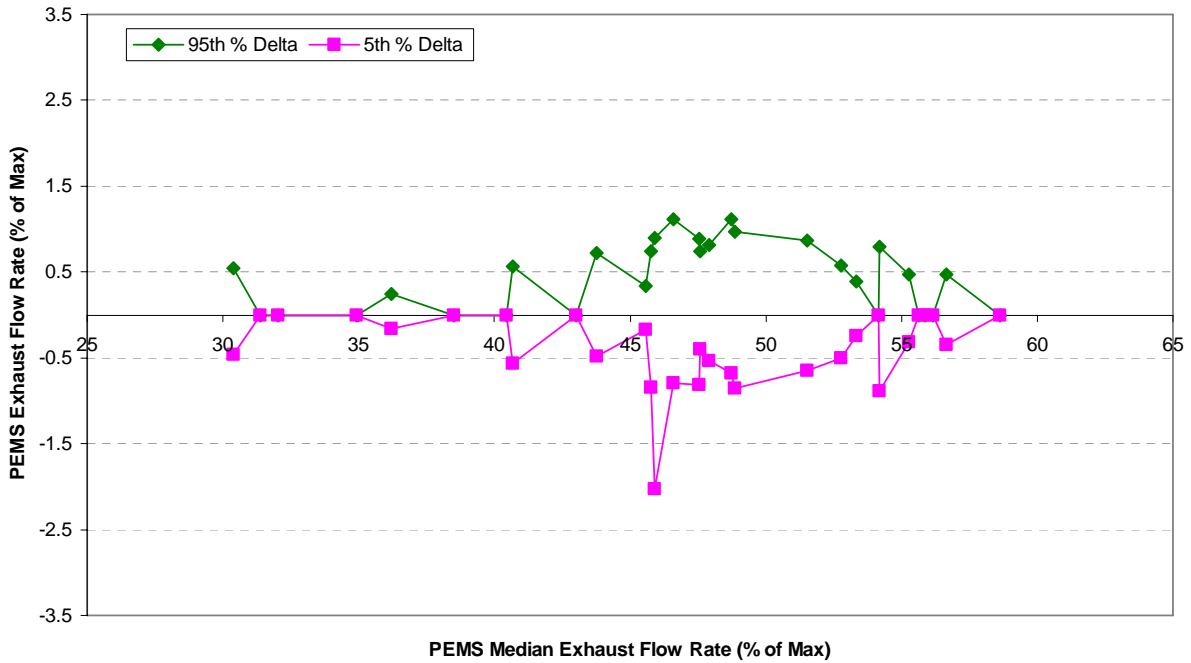
ENGINE 3 ERROR SURFACE FOR TRANSIENT CO₂ CONCENTRATION



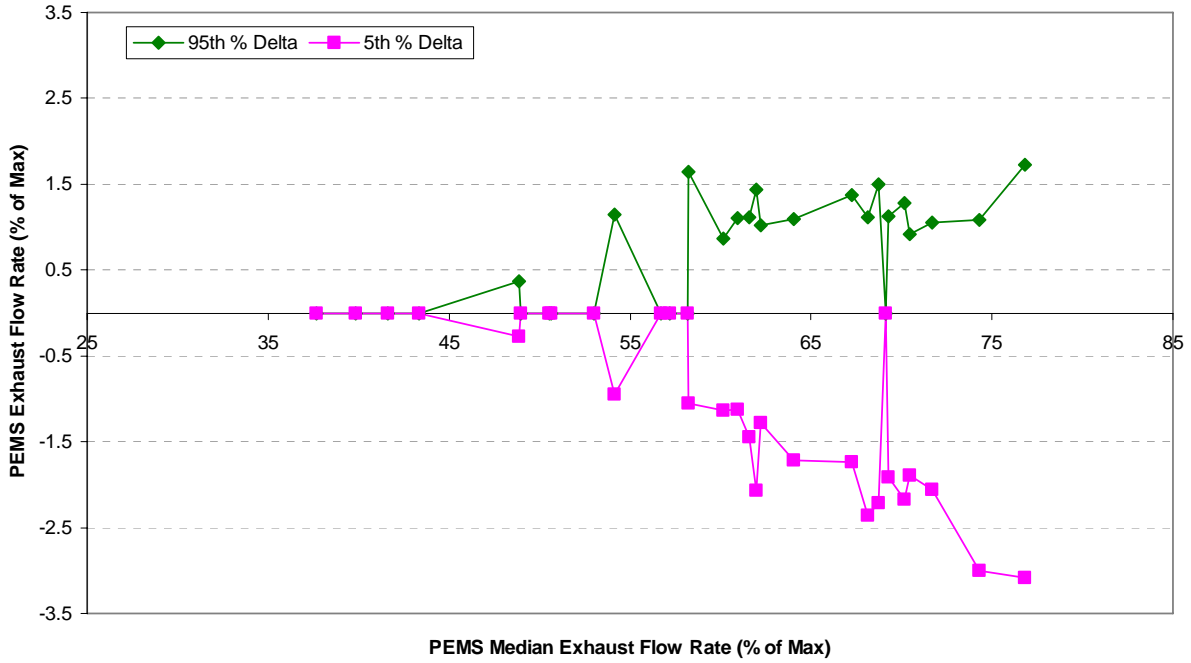
FINAL ERROR SURFACE FOR TRANSIENT CO₂ CONCENTRATION



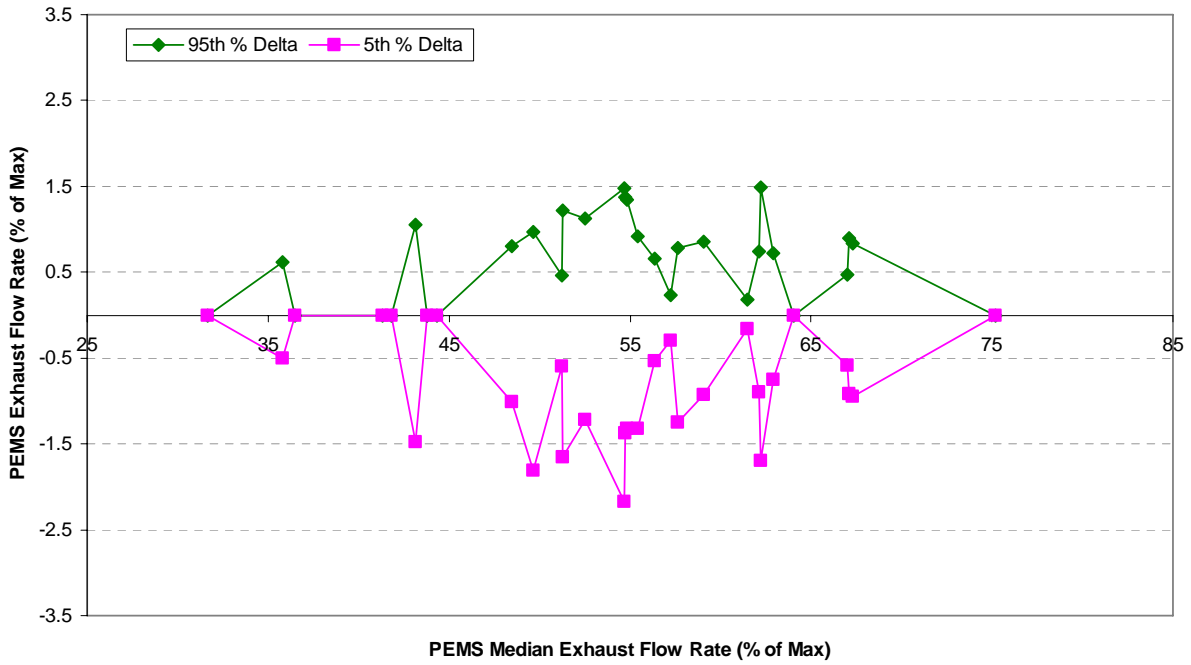
FINAL ERROR SURFACE FOR TRANSIENT NMHC CONCENTRATION (ENGINE 2 DATA ONLY)



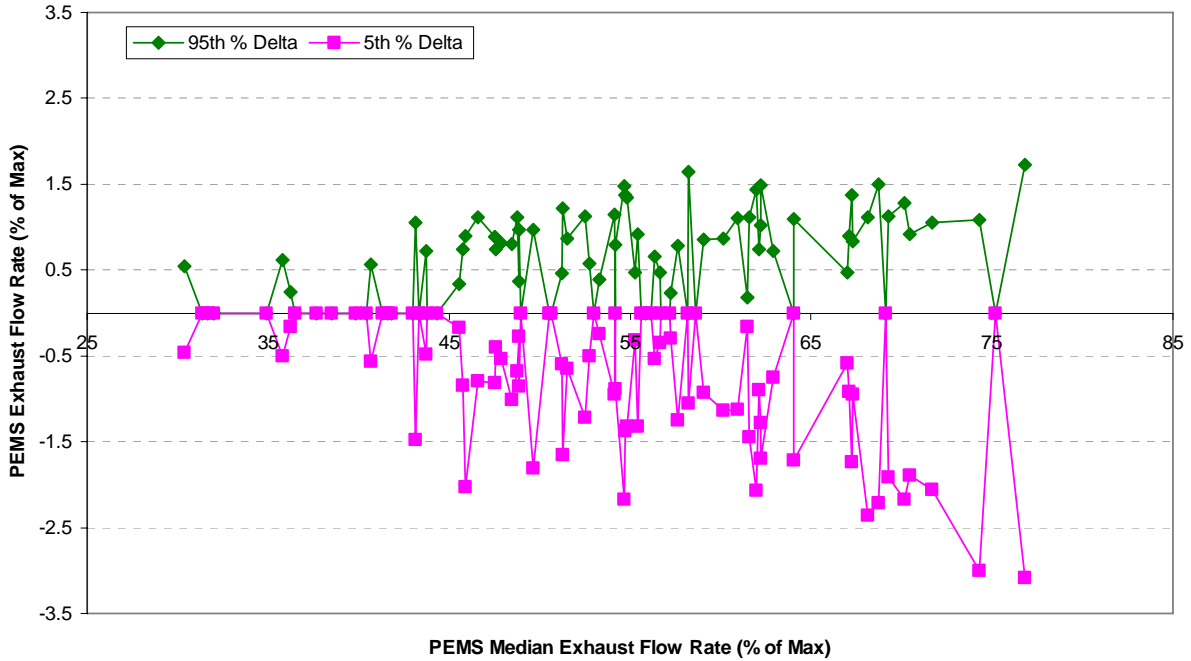
ENGINE 1 ERROR SURFACE FOR TRANSIENT EXHAUST FLOW RATE



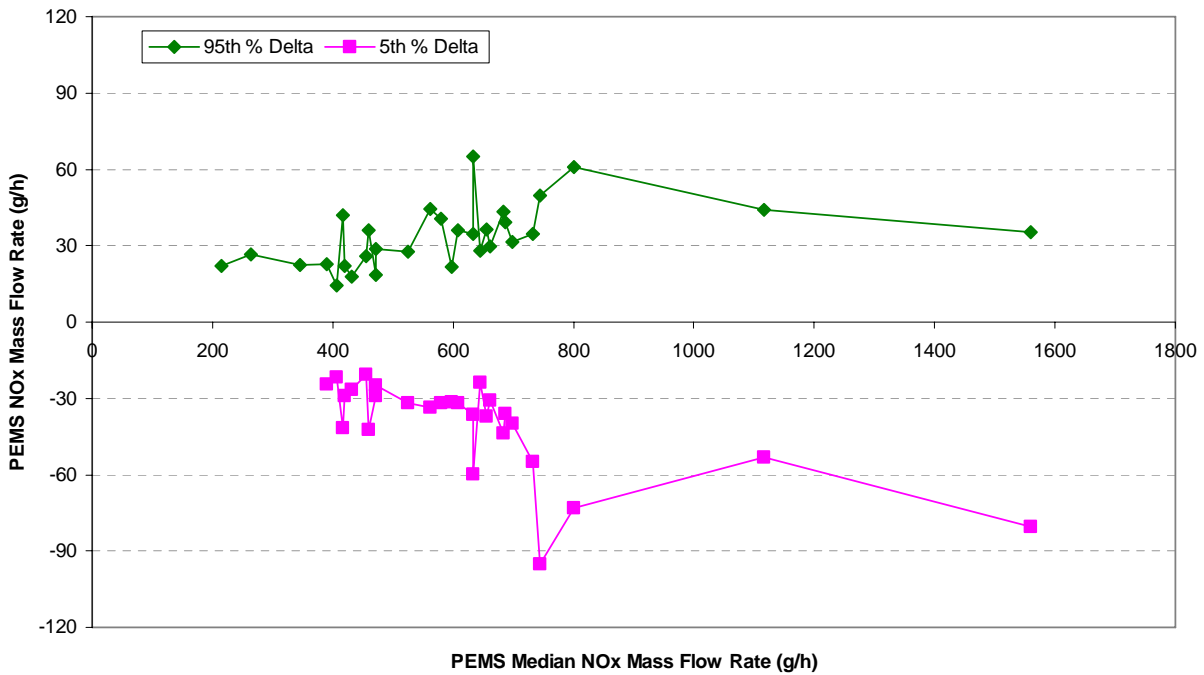
ENGINE 2 ERROR SURFACE FOR TRANSIENT EXHAUST FLOW RATE



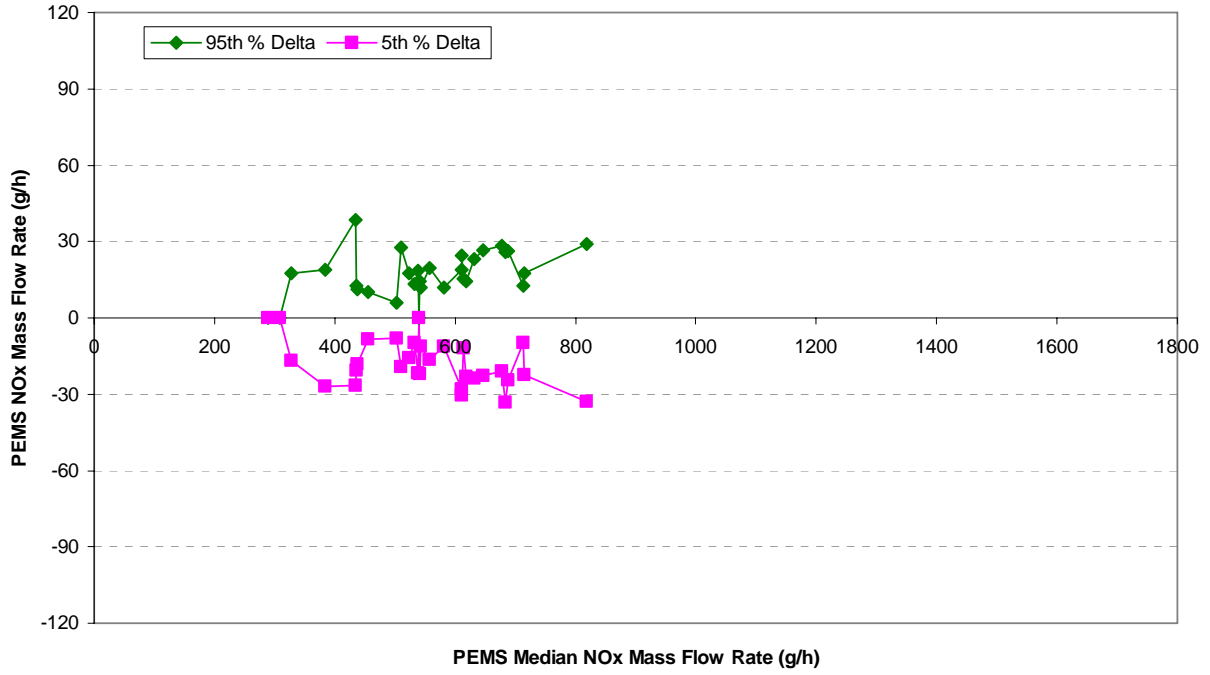
ENGINE 3 ERROR SURFACE FOR TRANSIENT EXHAUST FLOW RATE



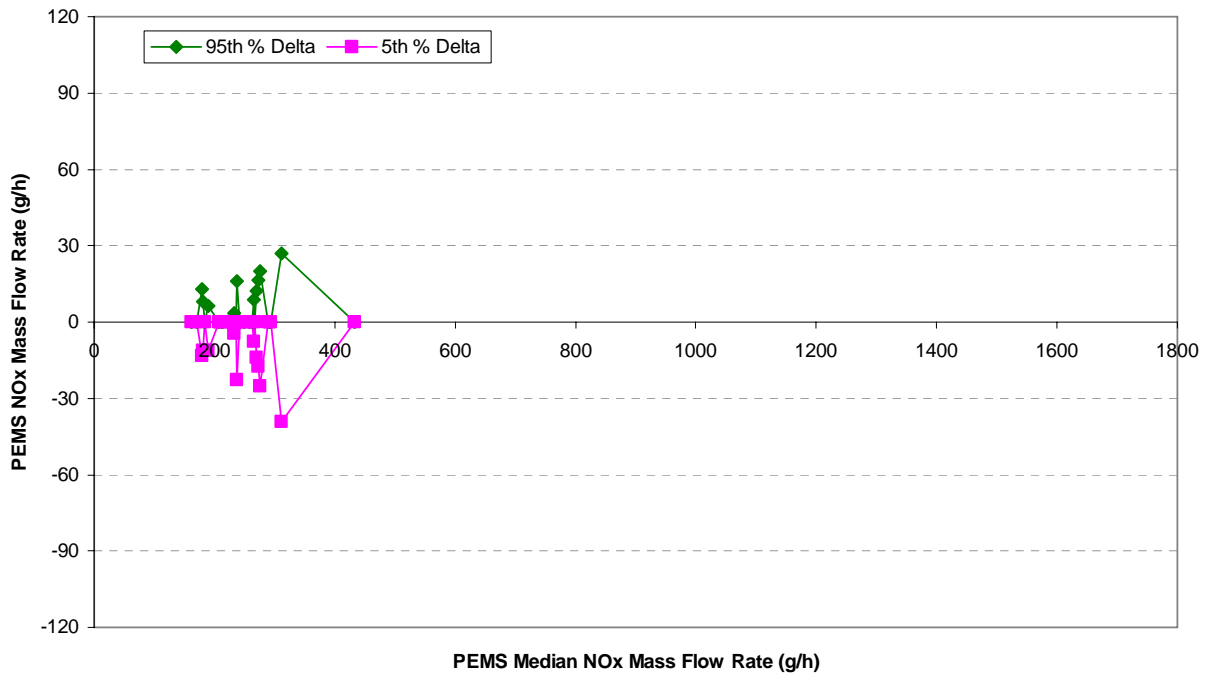
FINAL ERROR SURFACE FOR TRANSIENT EXHAUST FLOW RATE



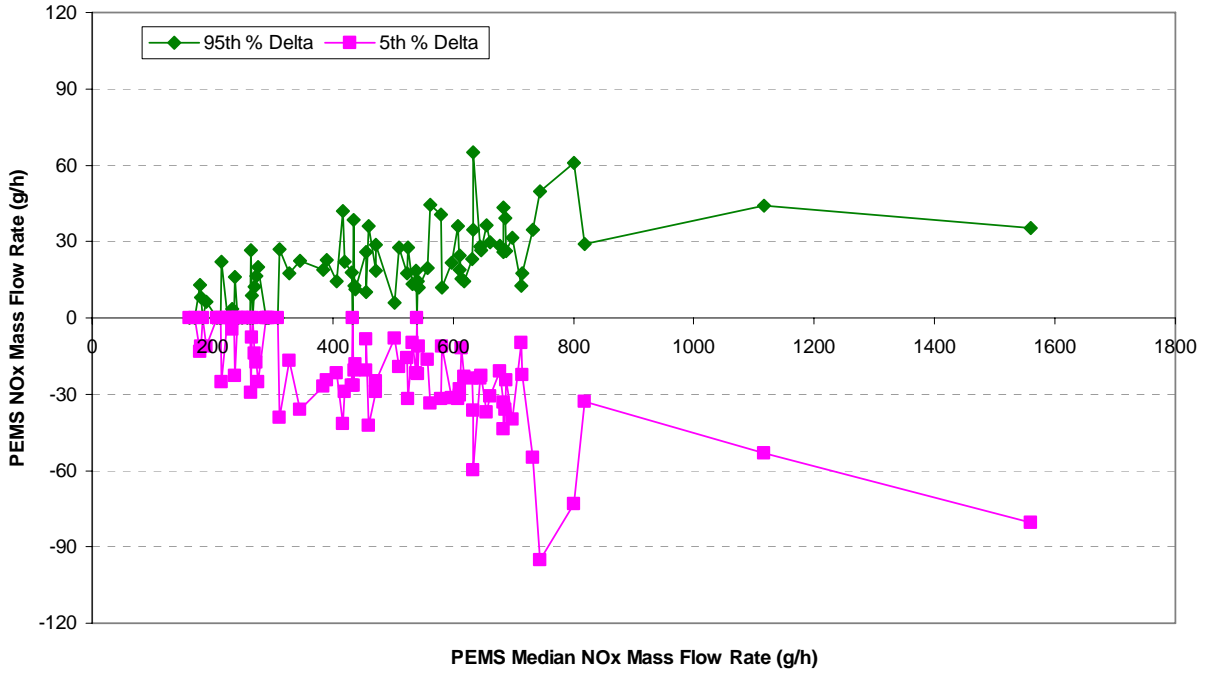
ENGINE 1 ERROR SURFACE FOR TRANSIENT NO_x MASS FLOW RATE



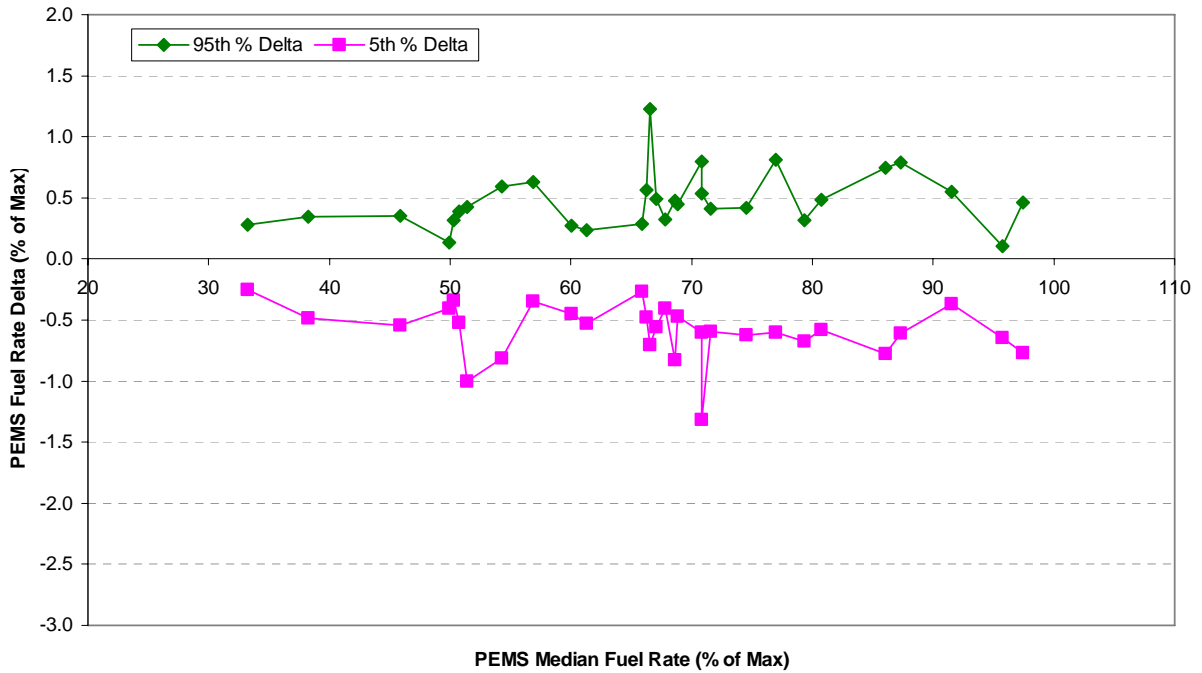
ENGINE 2 ERROR SURFACE FOR TRANSIENT NO_x MASS FLOW RATE



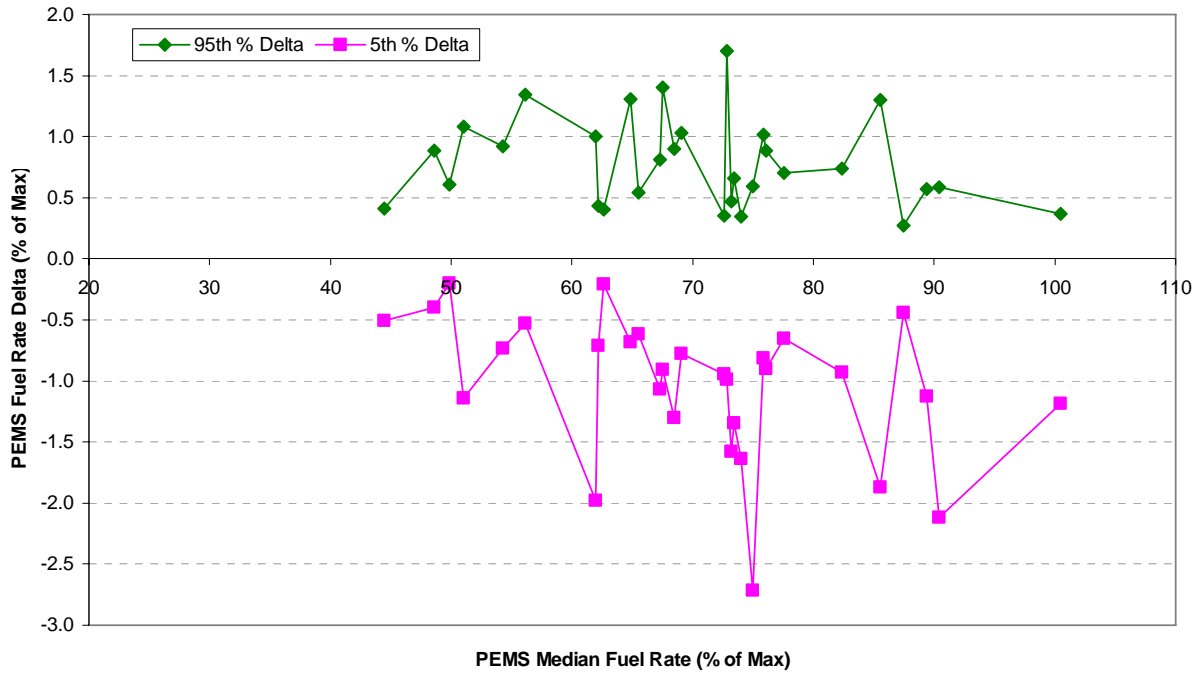
ENGINE 3 ERROR SURFACE FOR TRANSIENT NO_x MASS FLOW RATE



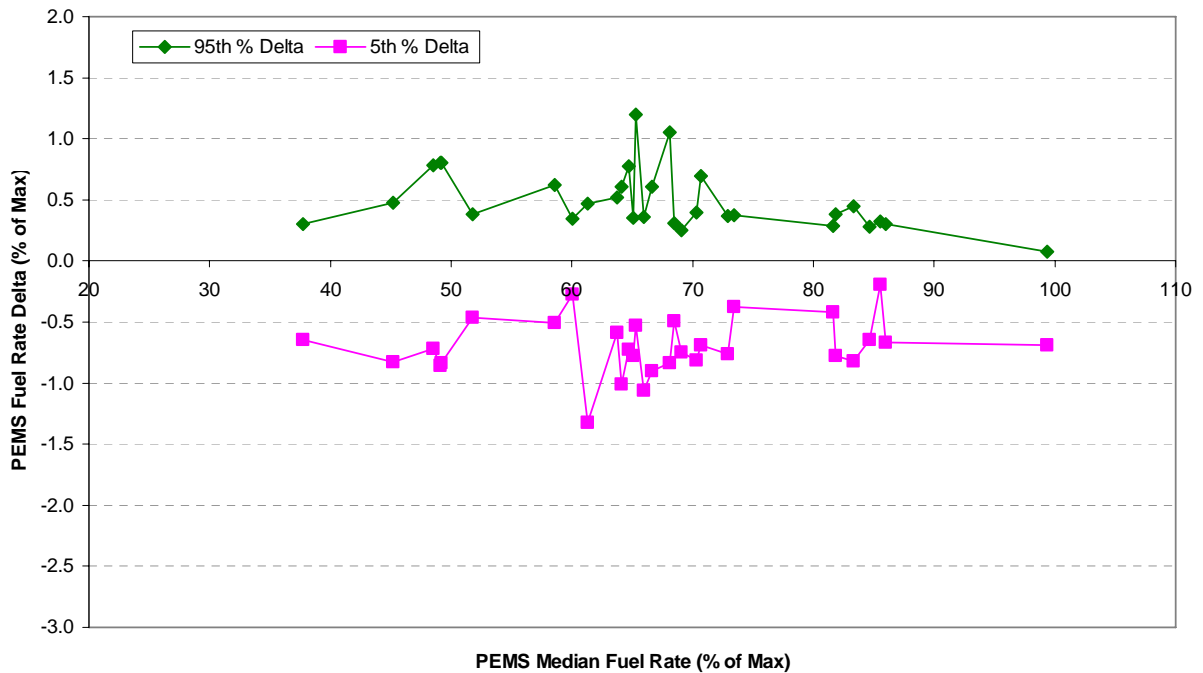
FINAL ERROR SURFACE FOR TRANSIENT NO_x MASS FLOW RATE



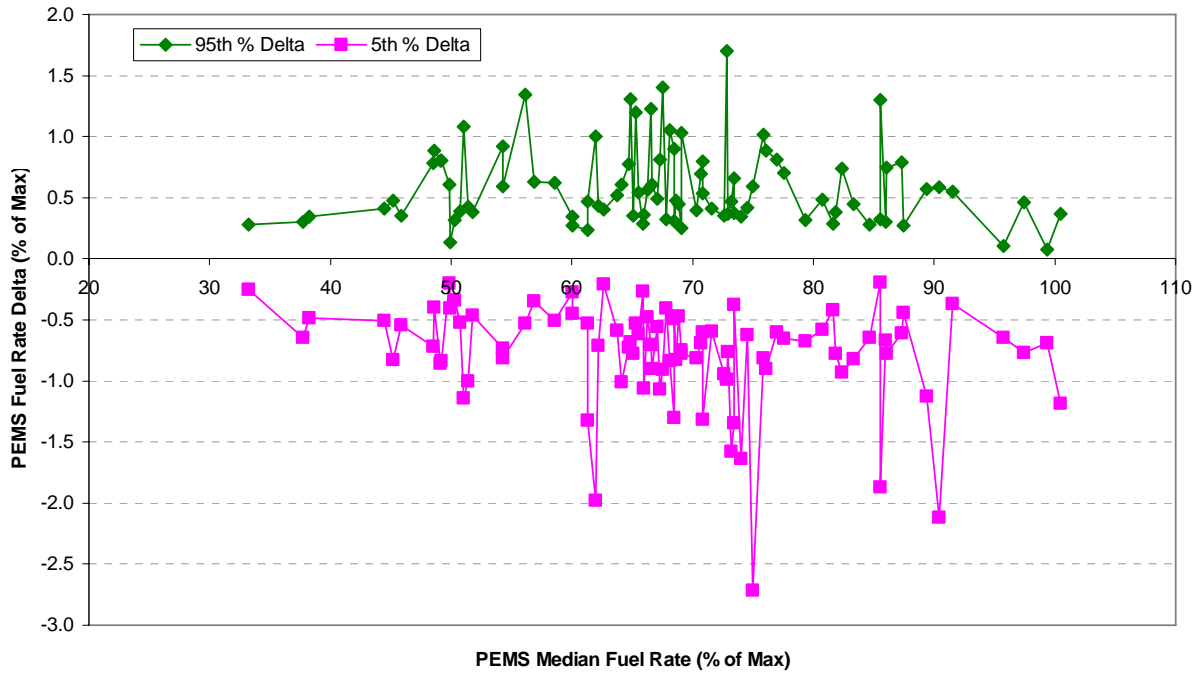
ENGINE 1 ERROR SURFACE FOR TRANSIENT ECM FUEL RATE



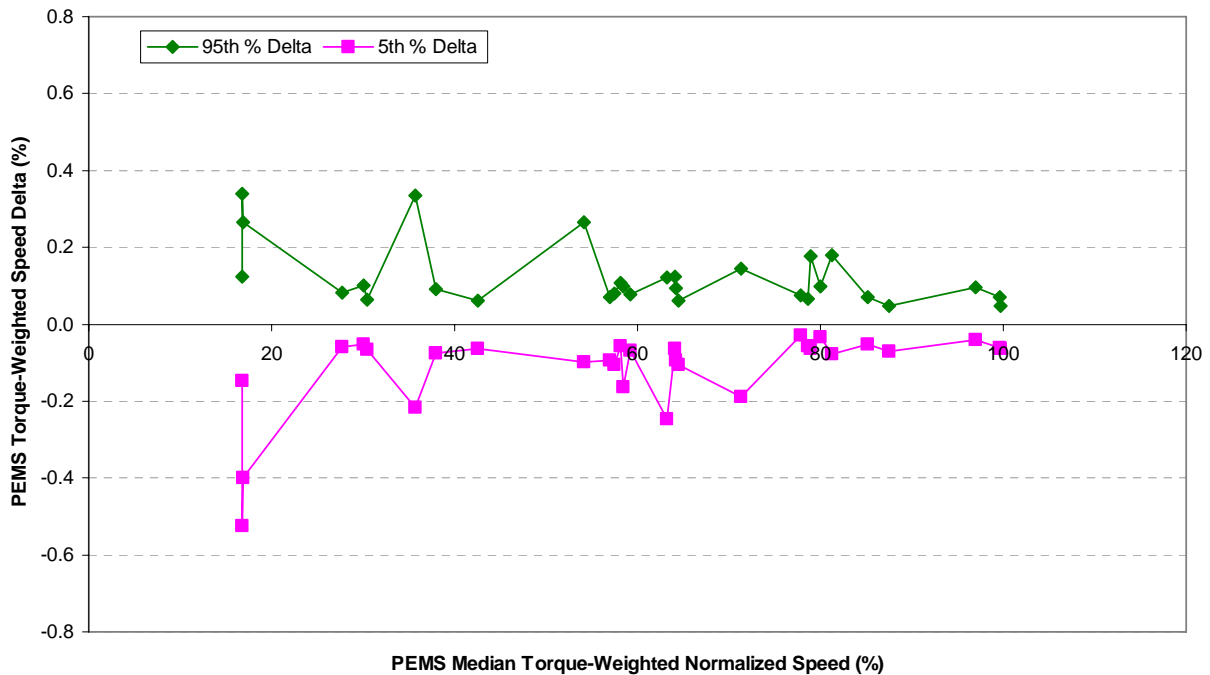
ENGINE 2 ERROR SURFACE FOR TRANSIENT ECM FUEL RATE



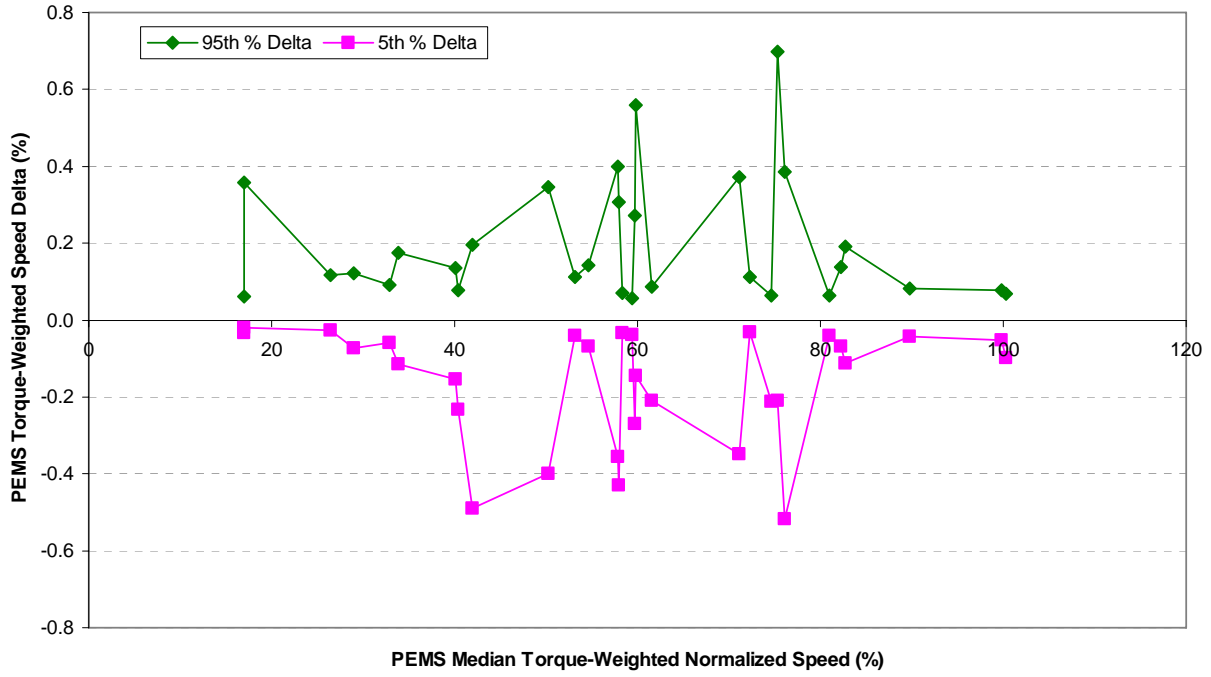
ENGINE 3 ERROR SURFACE FOR TRANSIENT ECM FUEL RATE



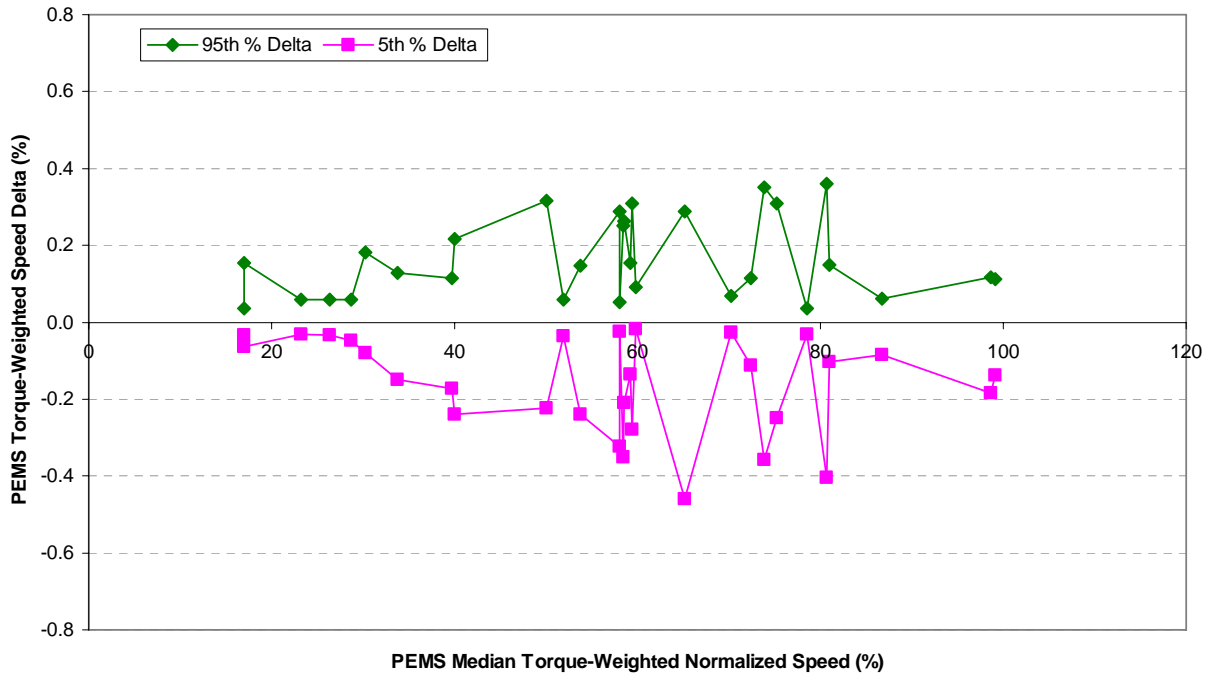
FINAL ERROR SURFACE FOR TRANSIENT ECM FUEL RATE



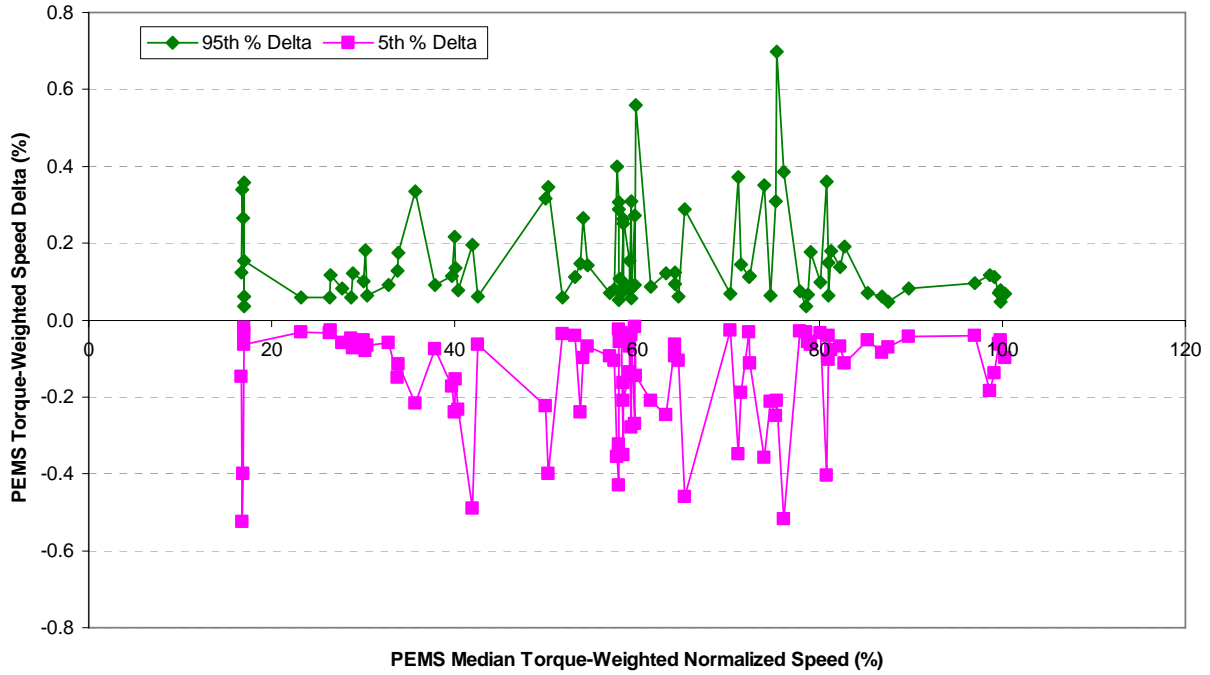
ENGINE 1 ERROR SURFACE FOR TRANSIENT ECM SPEED



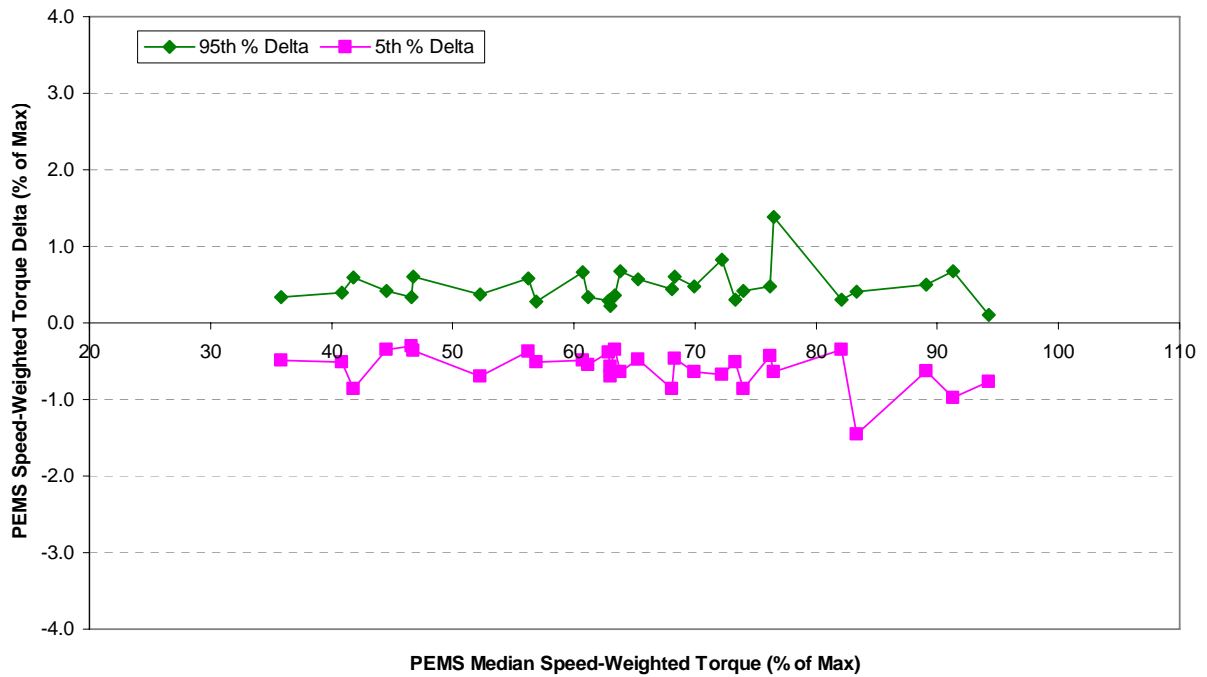
ENGINE 2 ERROR SURFACE FOR TRANSIENT ECM SPEED



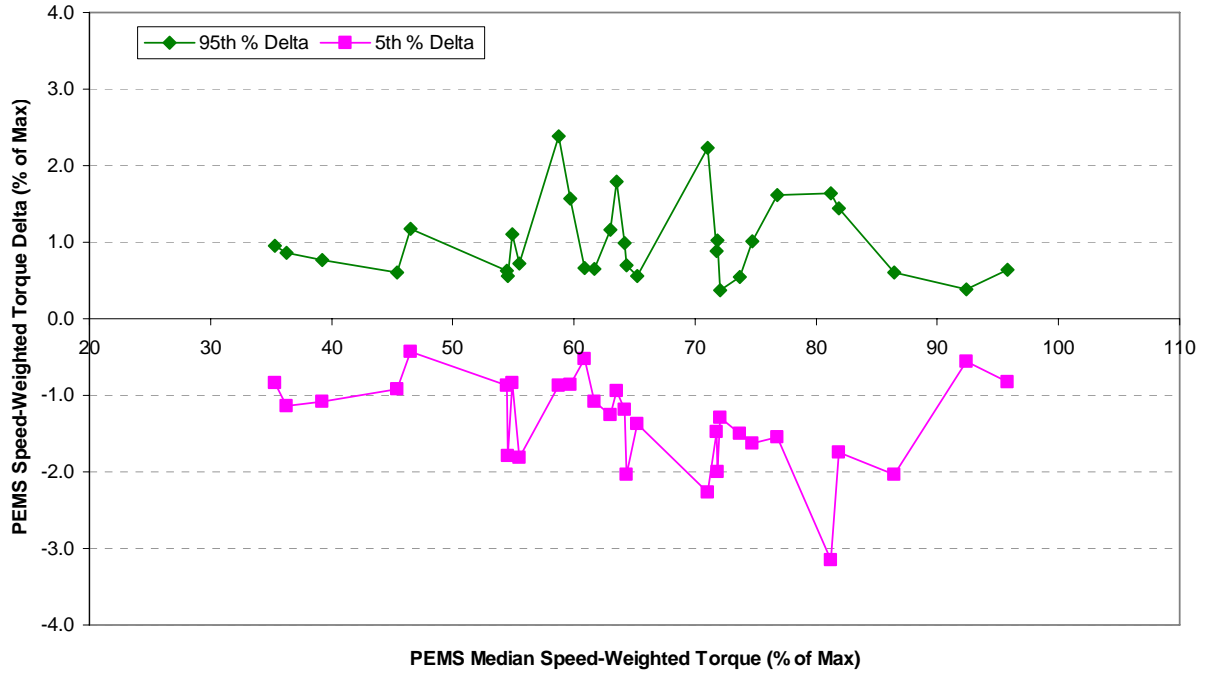
ENGINE 3 ERROR SURFACE FOR TRANSIENT ECM SPEED



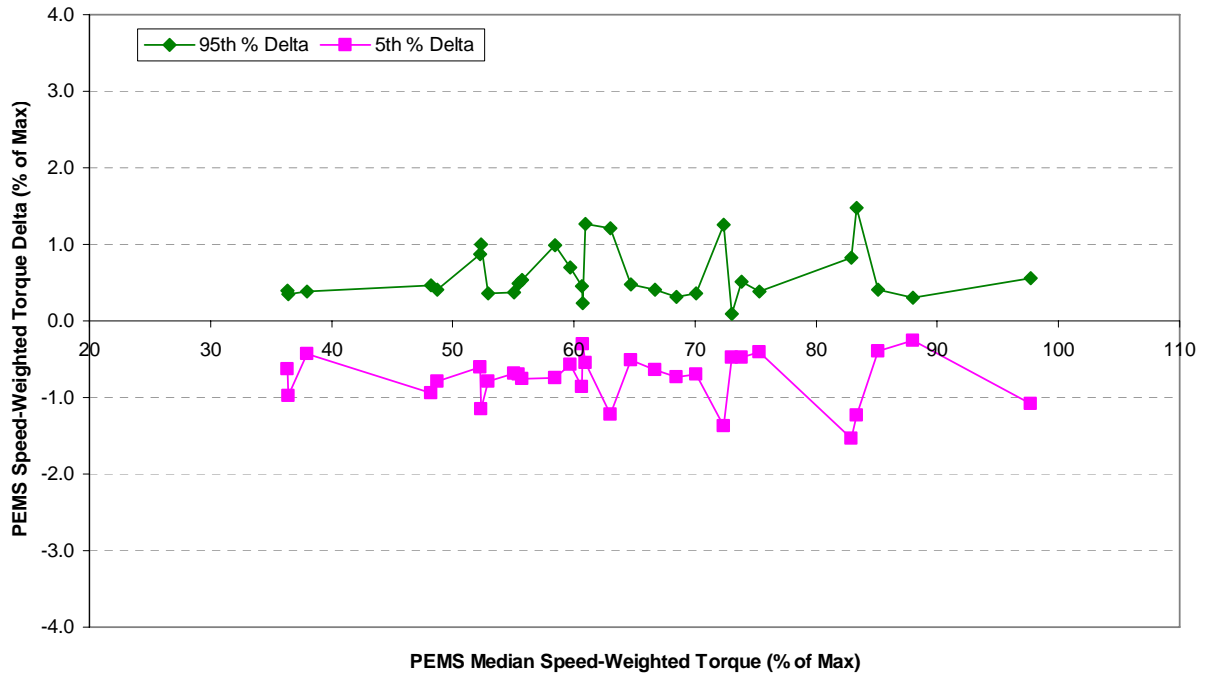
FINAL ERROR SURFACE FOR TRANSIENT ECM SPEED



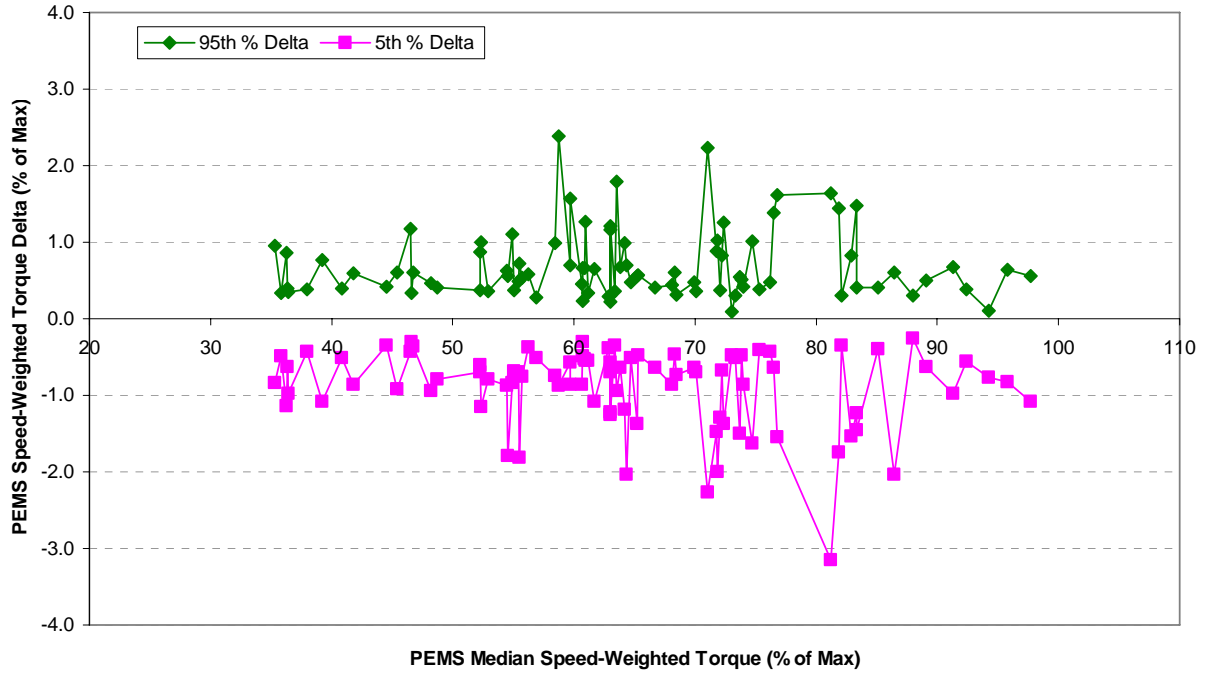
ENGINE 1 ERROR SURFACE FOR TRANSIENT INTERPOLATED TORQUE



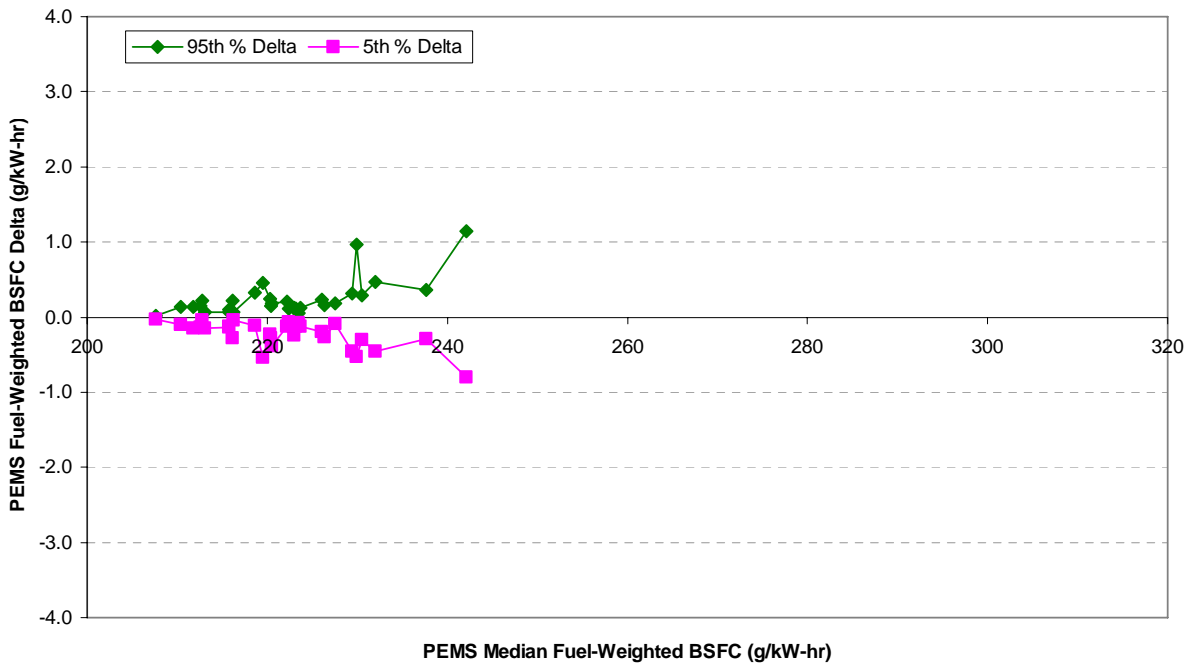
ENGINE 2 ERROR SURFACE FOR TRANSIENT INTERPOLATED TORQUE



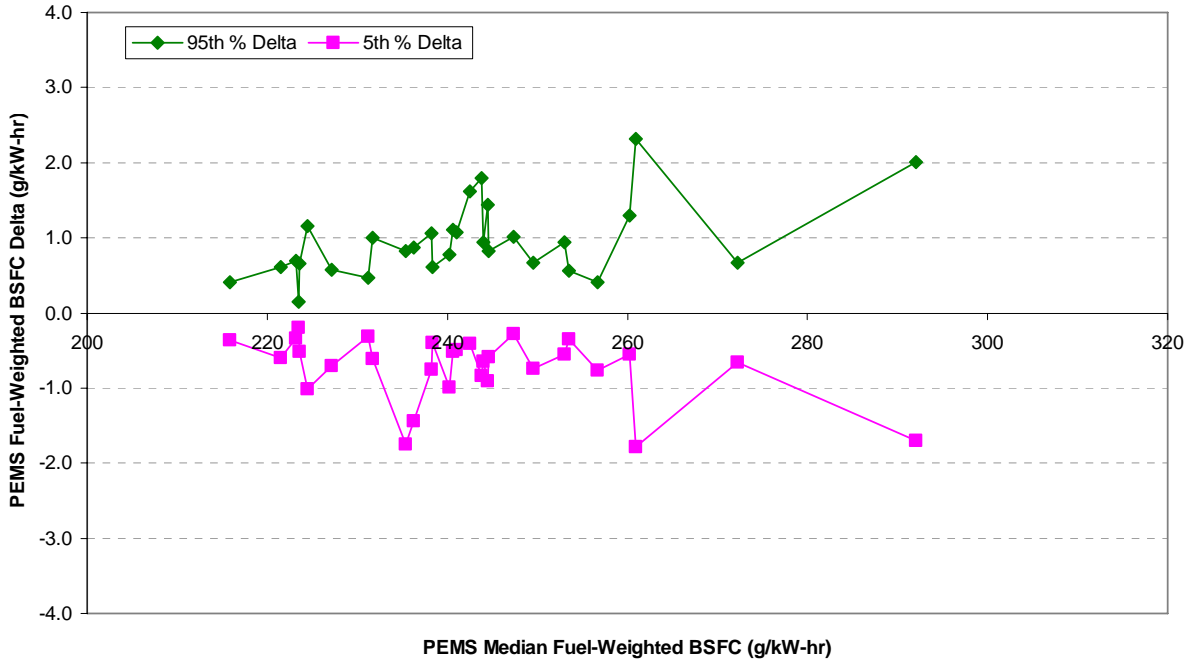
ENGINE 3 ERROR SURFACE FOR TRANSIENT INTERPOLATED TORQUE



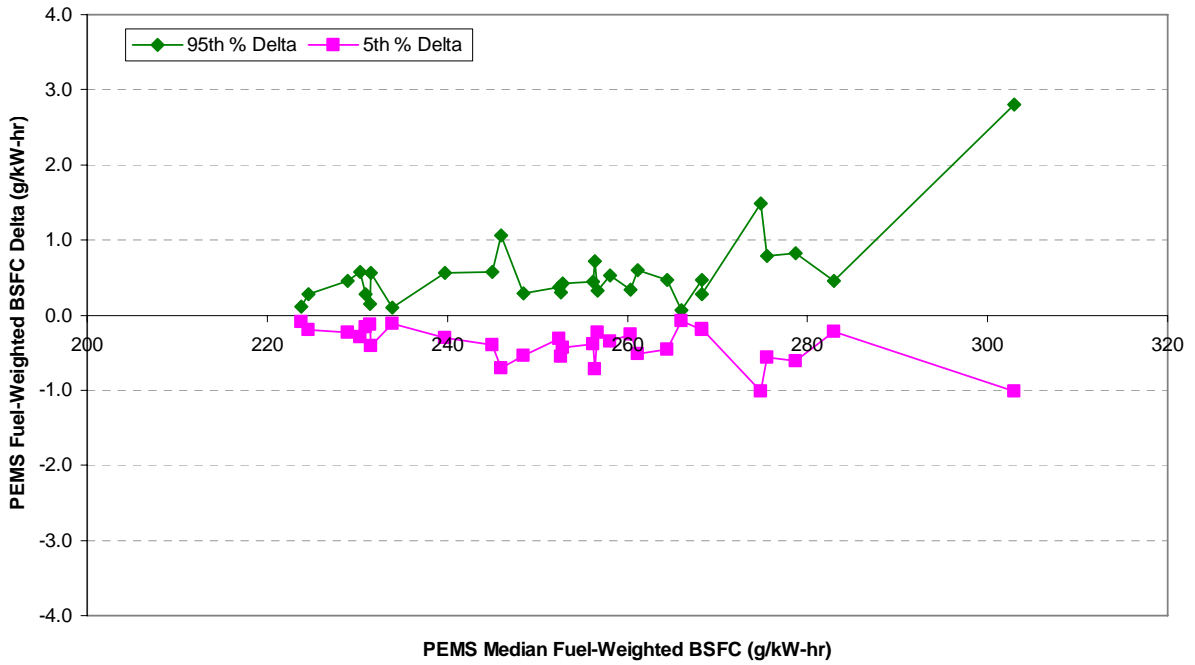
FINAL ERROR SURFACE FOR TRANSIENT INTERPOLATED TORQUE



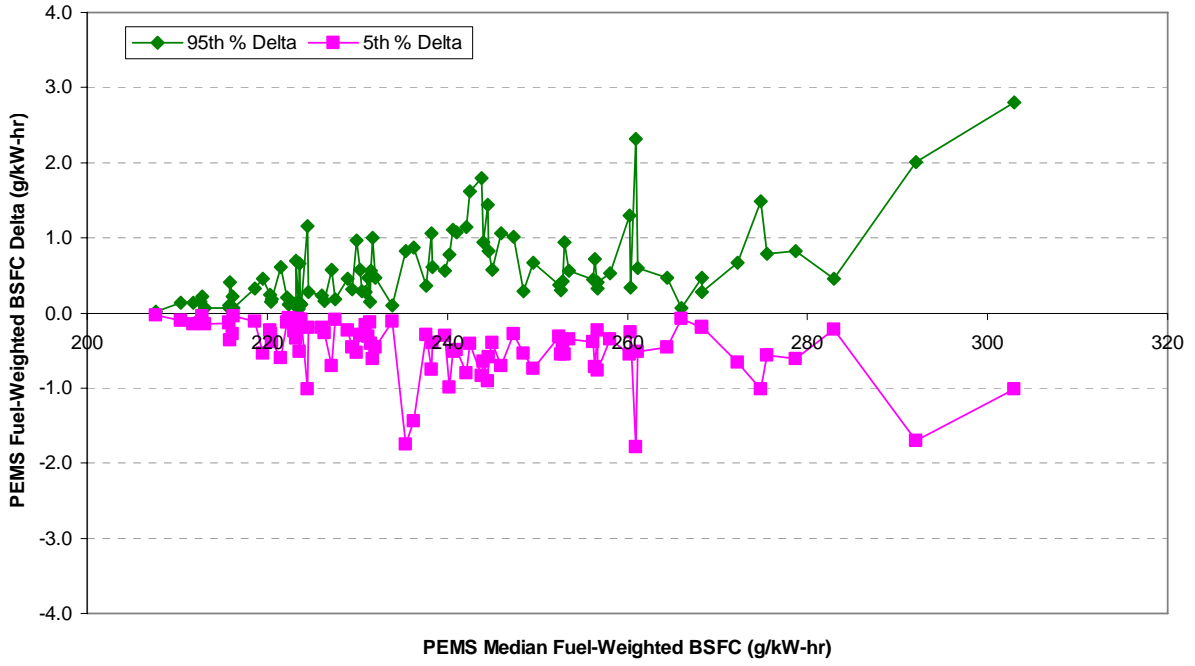
ENGINE 1 ERROR SURFACE FOR TRANSIENT INTERPOLATED BSFC



ENGINE 2 ERROR SURFACE FOR TRANSIENT INTERPOLATED BSFC

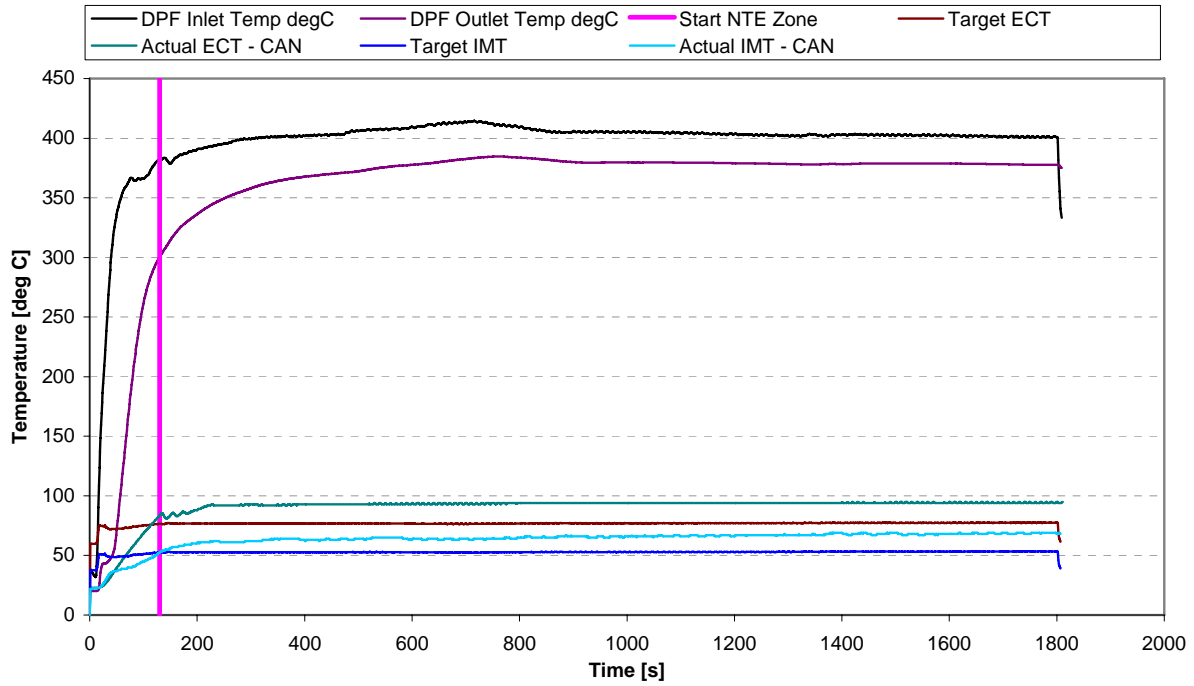


ENGINE 3 ERROR SURFACE FOR TRANSIENT INTERPOLATED BSFC

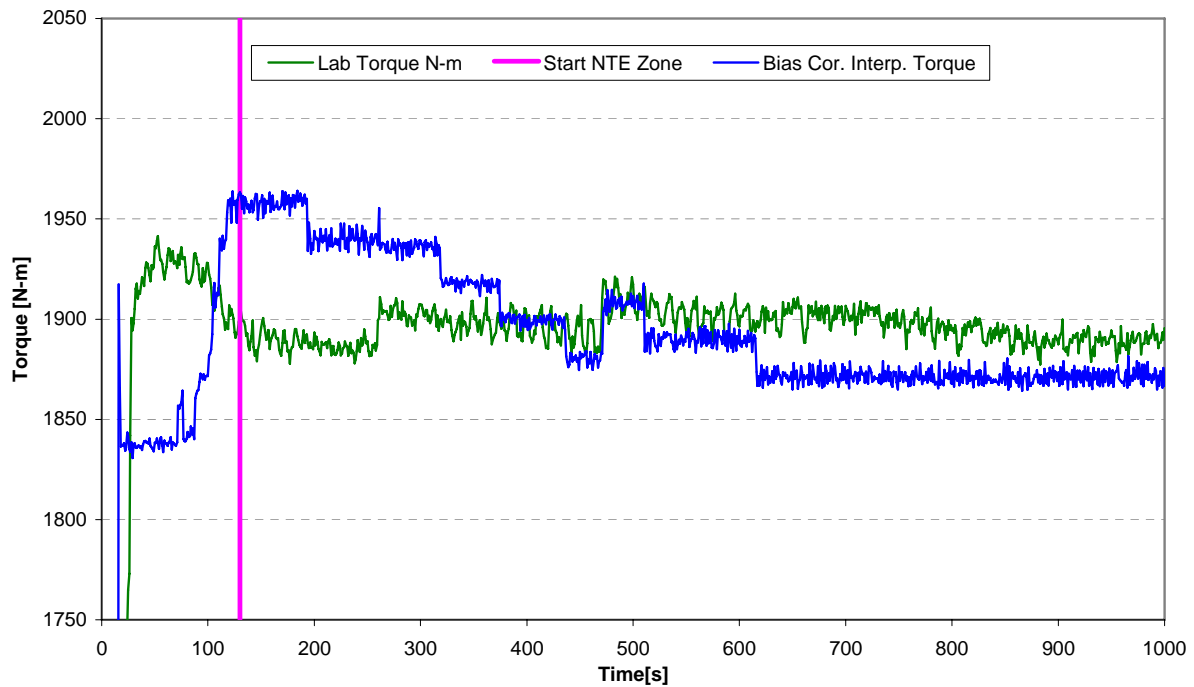


FINAL ERROR SURFACE FOR TRANSIENT INTERPOLATED BSFC

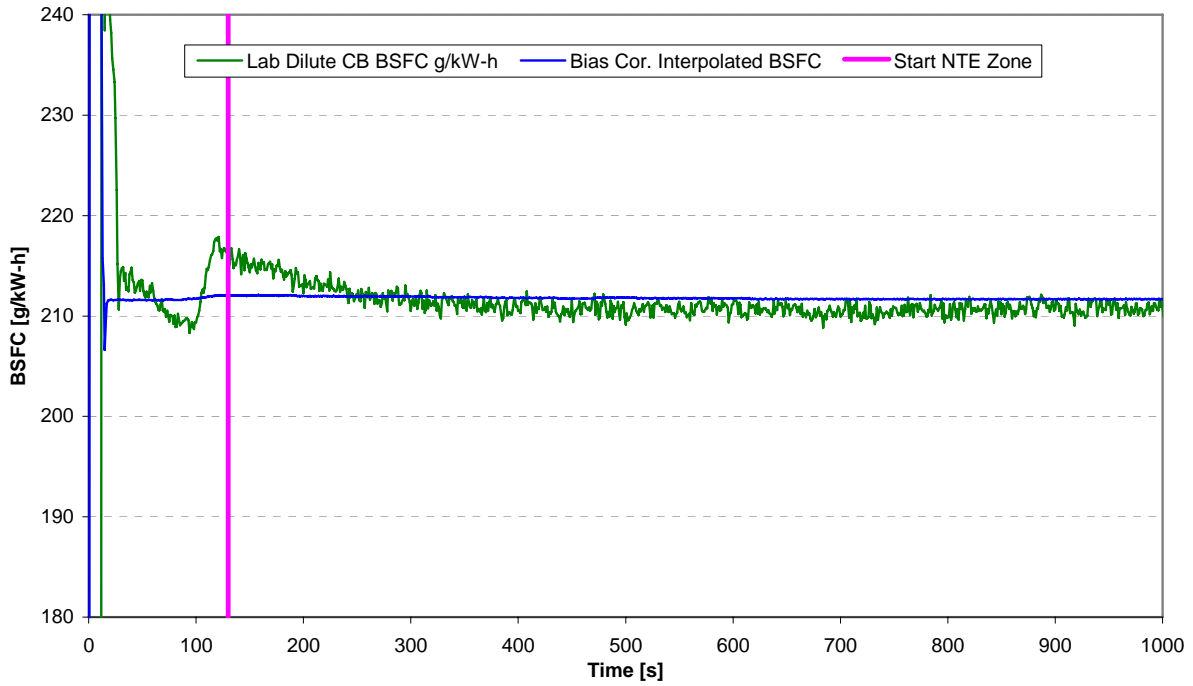
APPENDIX H
INTERACTING PARAMETERS – DOE ERROR SURFACE DATA



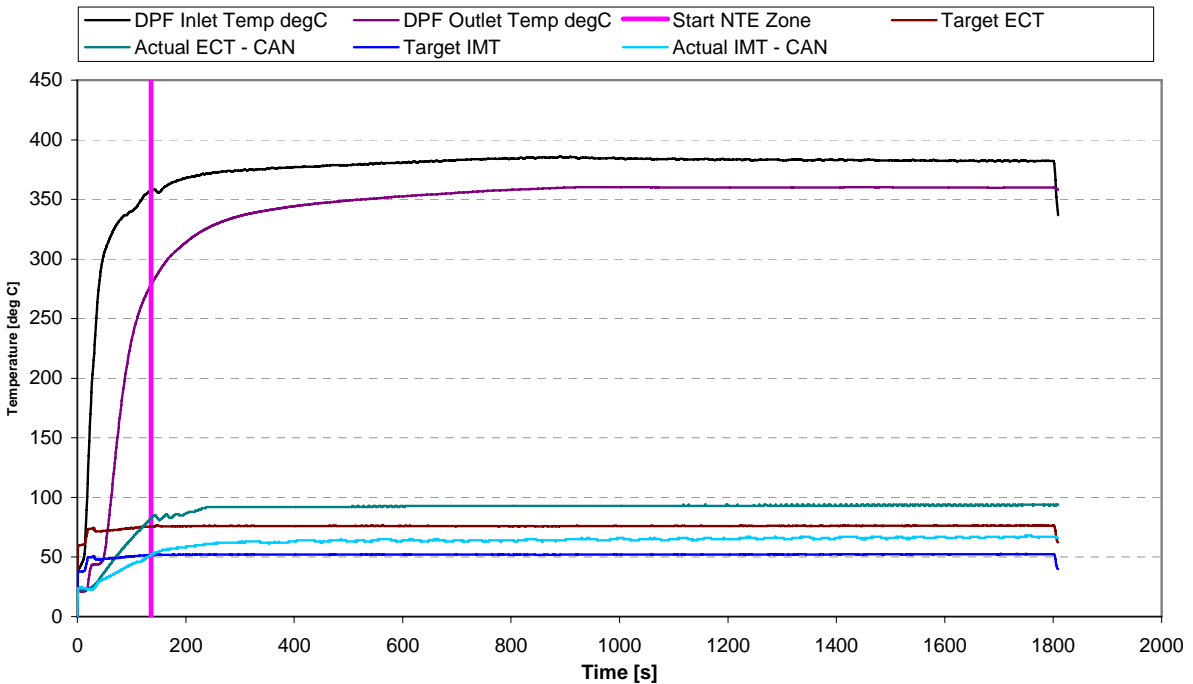
WARM-UP TEST TEMPERATURE PROFILES FOR ENGINE 1 AT WOT



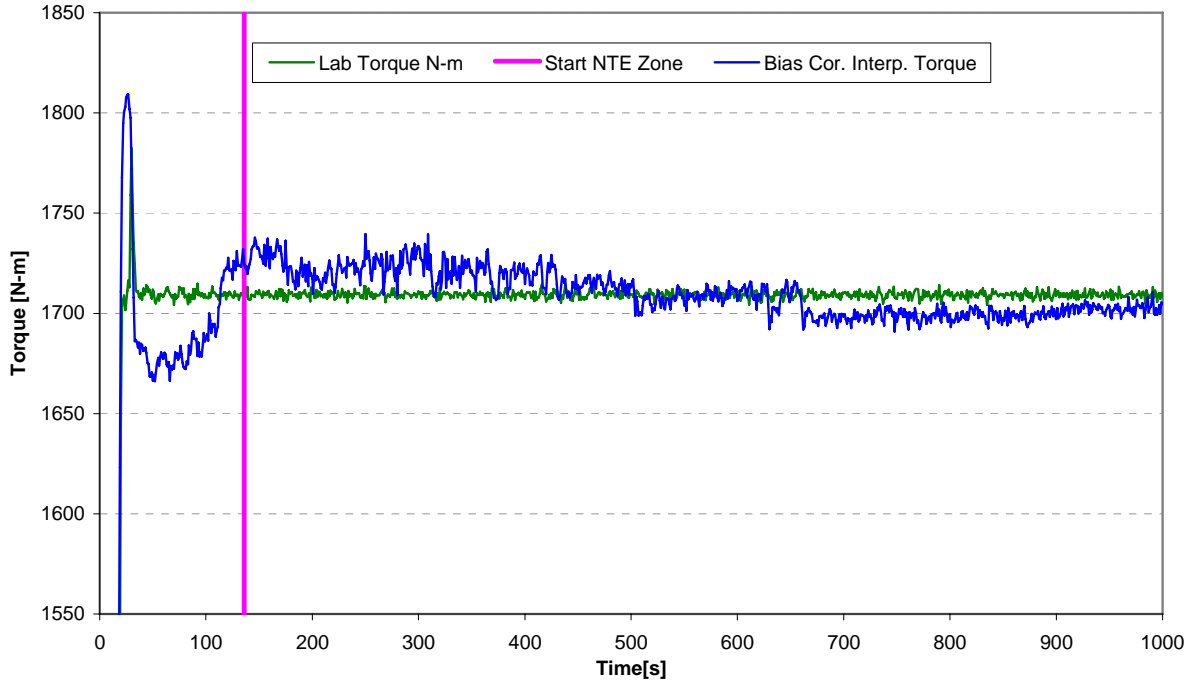
WARM-UP TEST LABORATORY AND INTERPOLATED TORQUE TRACES FOR ENGINE 1 AT WOT



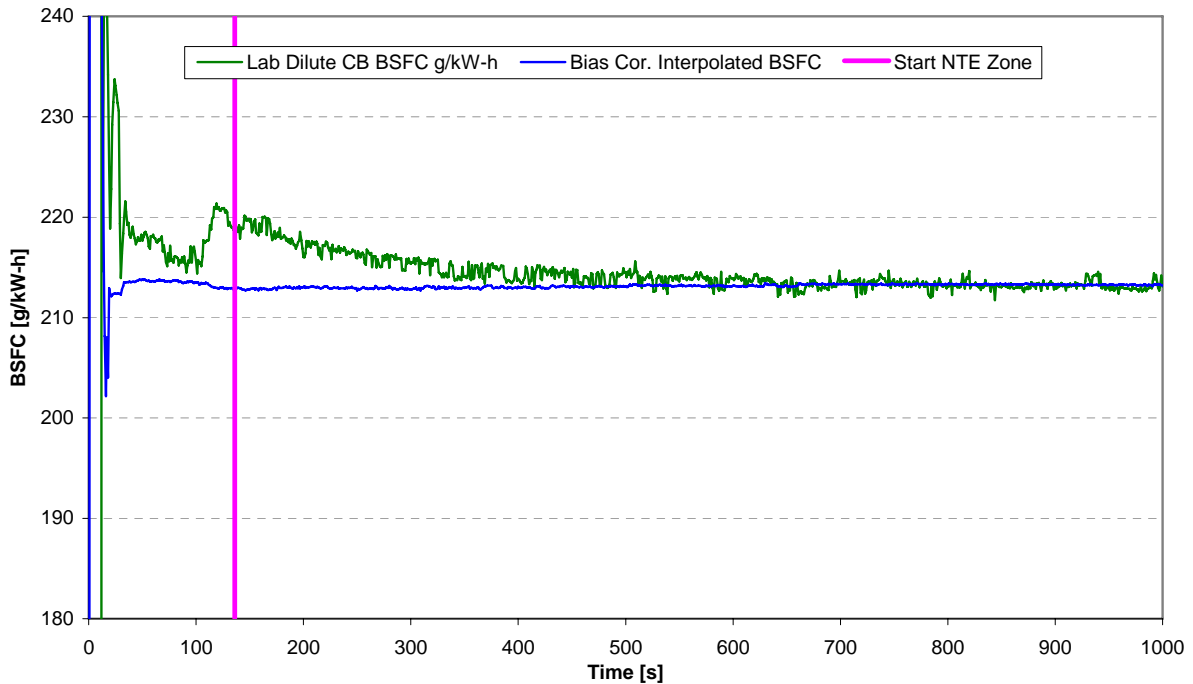
WARM-UP TEST LABORATORY AND INTERPOLATED BSFC TRACES FOR ENGINE 1 AT WOT



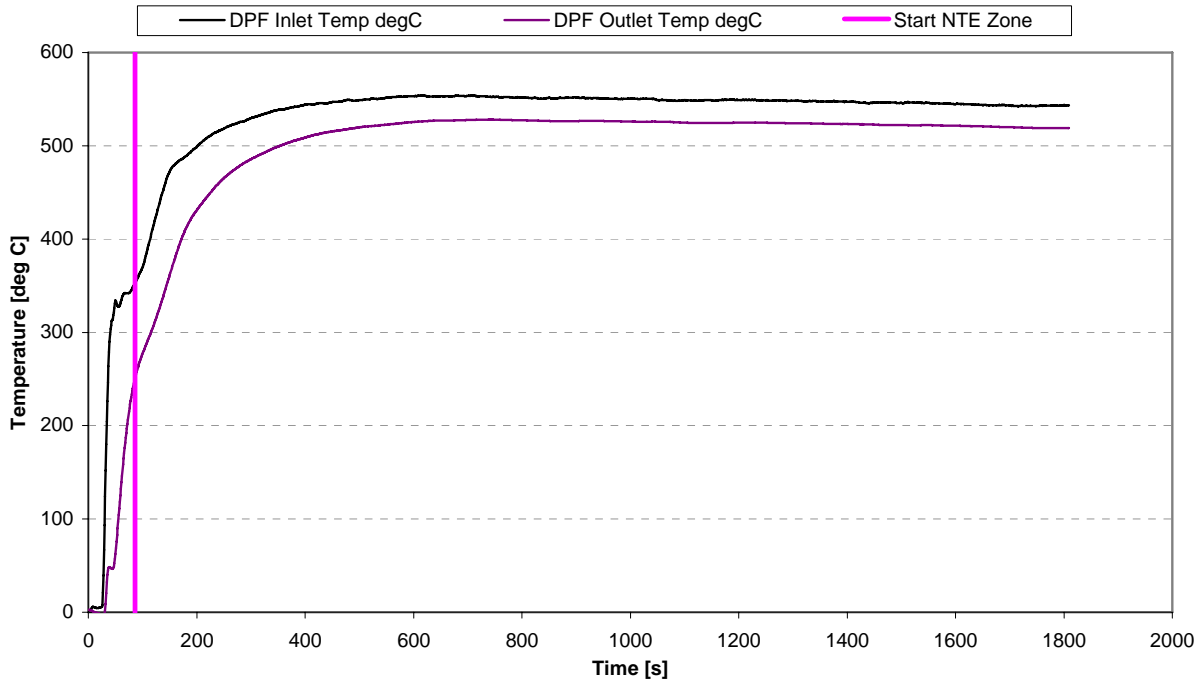
WARM-UP TEST TEMPERATURE PROFILES FOR ENGINE 1 AT PART LOAD



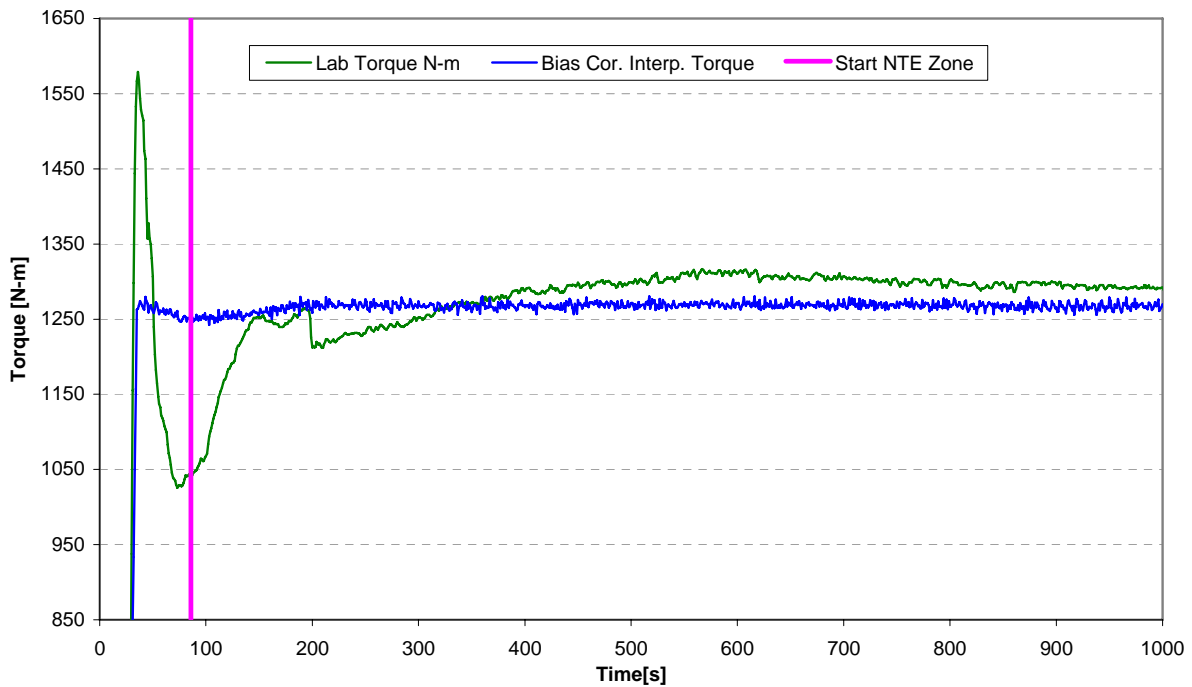
WARM-UP TEST LABORATORY AND INTERPOLATED TORQUE TRACES FOR ENGINE 1 AT PART LOAD



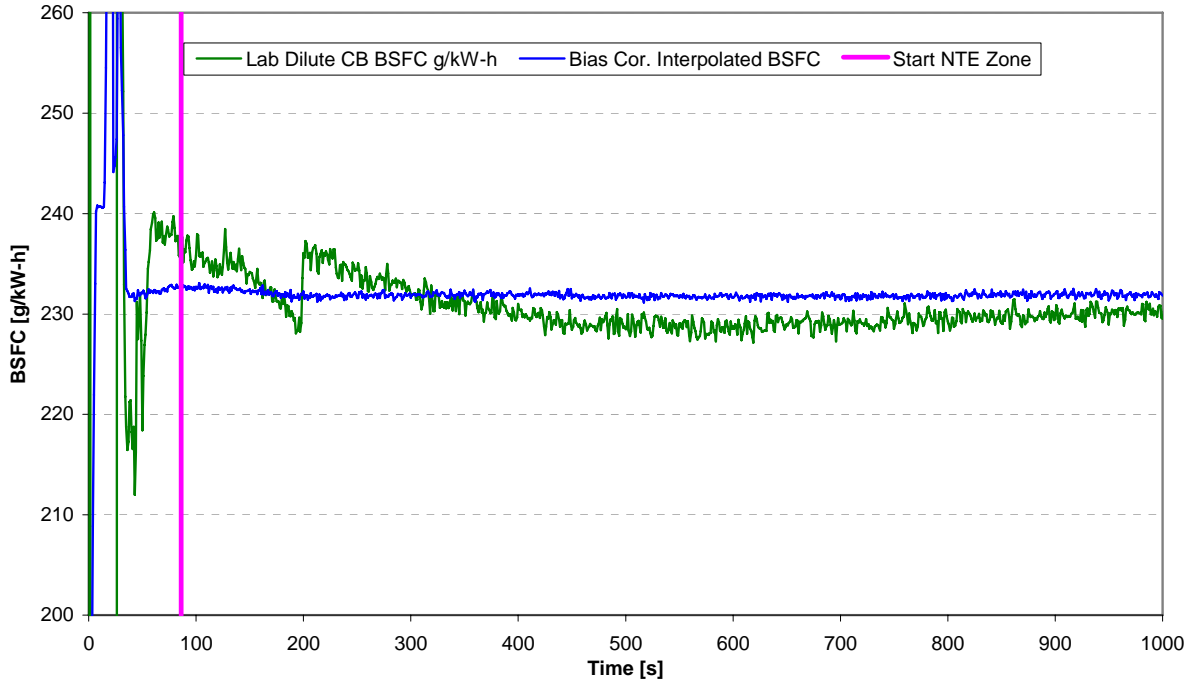
WARM-UP TEST LABORATORY AND INTERPOLATED BSFC TRACES FOR ENGINE 1 AT PART LOAD



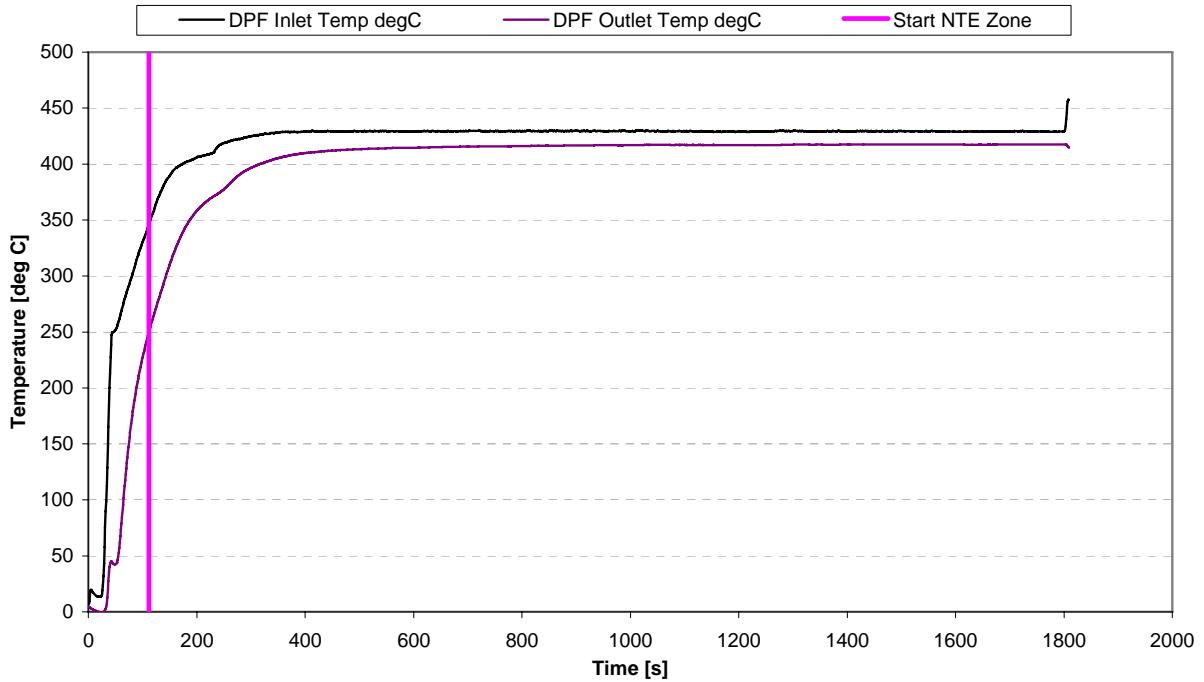
WARM-UP TEST TEMPERATURE PROFILES FOR ENGINE 2 AT WOT



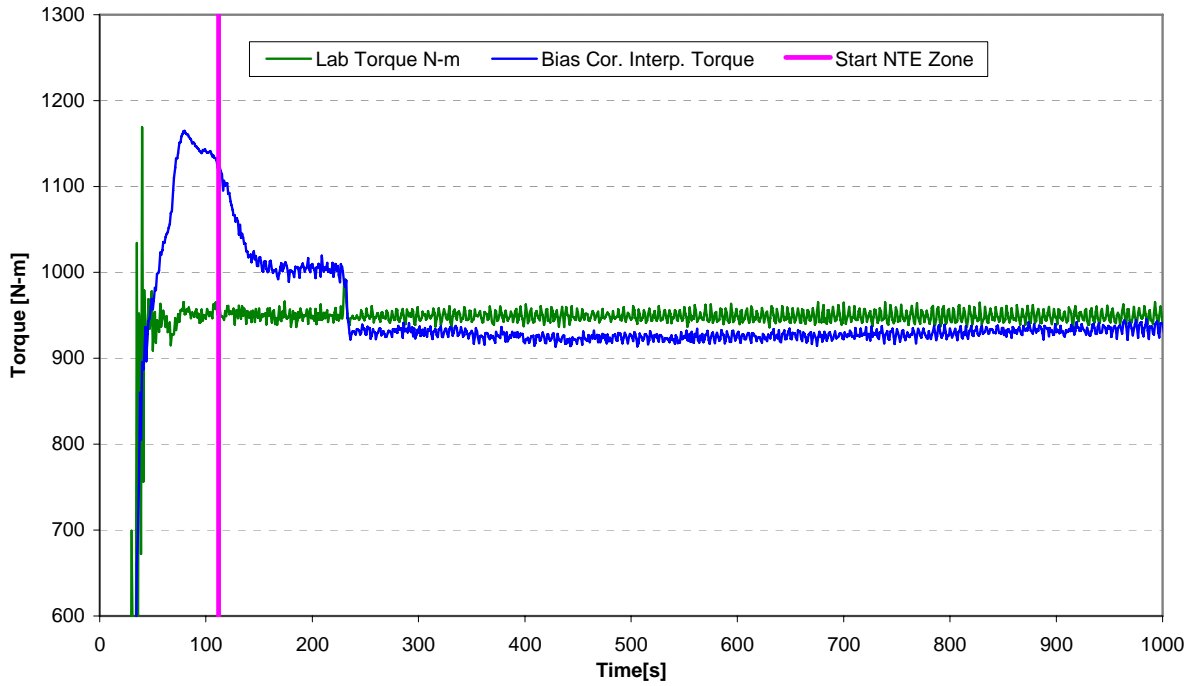
WARM-UP TEST LABORATORY AND INTERPOLATED TORQUE TRACES FOR ENGINE 2 AT WOT



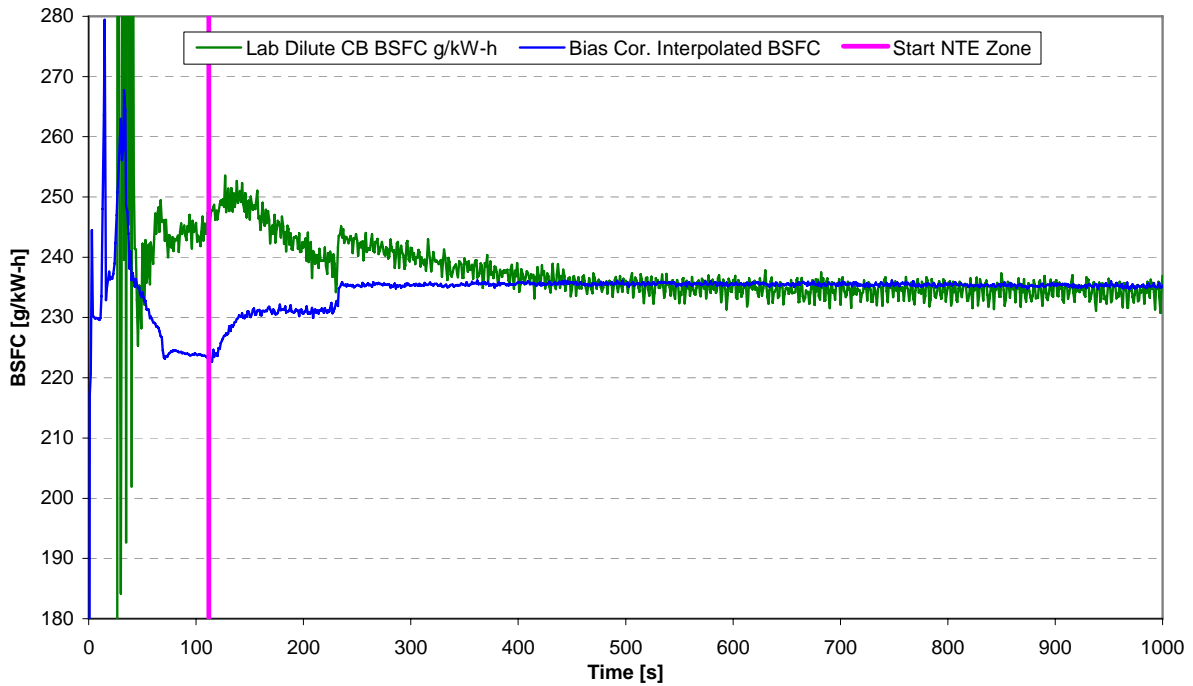
WARM-UP TEST LABORATORY AND INTERPOLATED BSFC TRACES FOR ENGINE 2 AT WOT



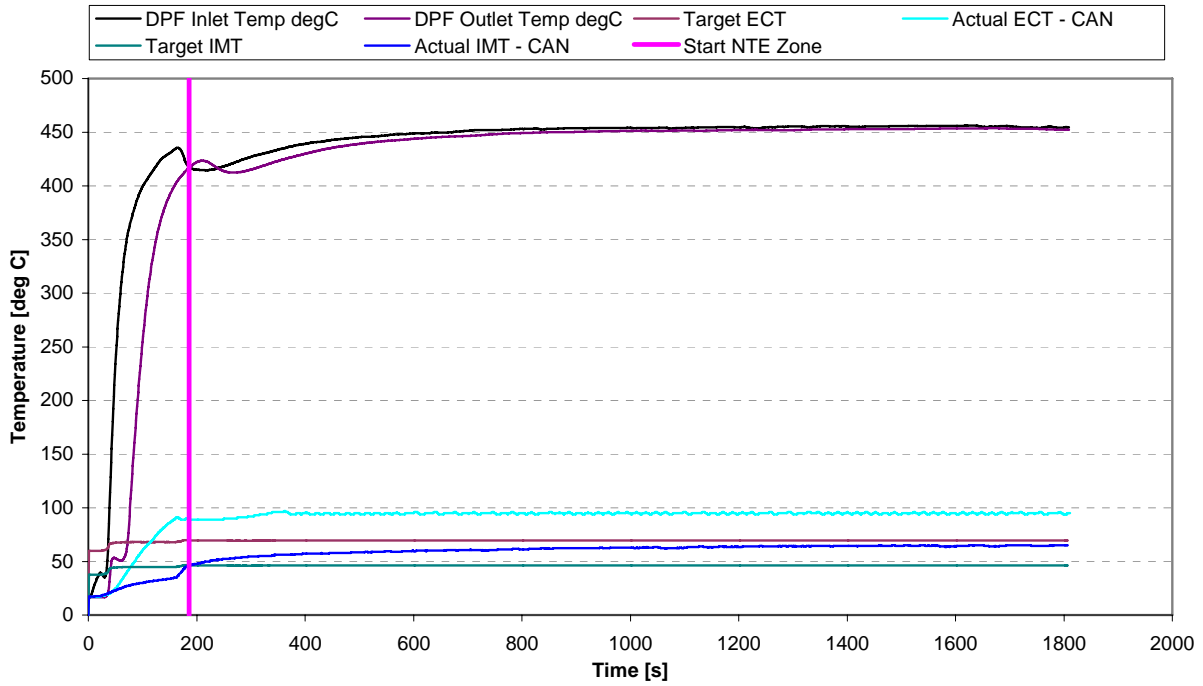
WARM-UP TEST TEMPERATURE PROFILES FOR ENGINE 2 AT PART LOAD



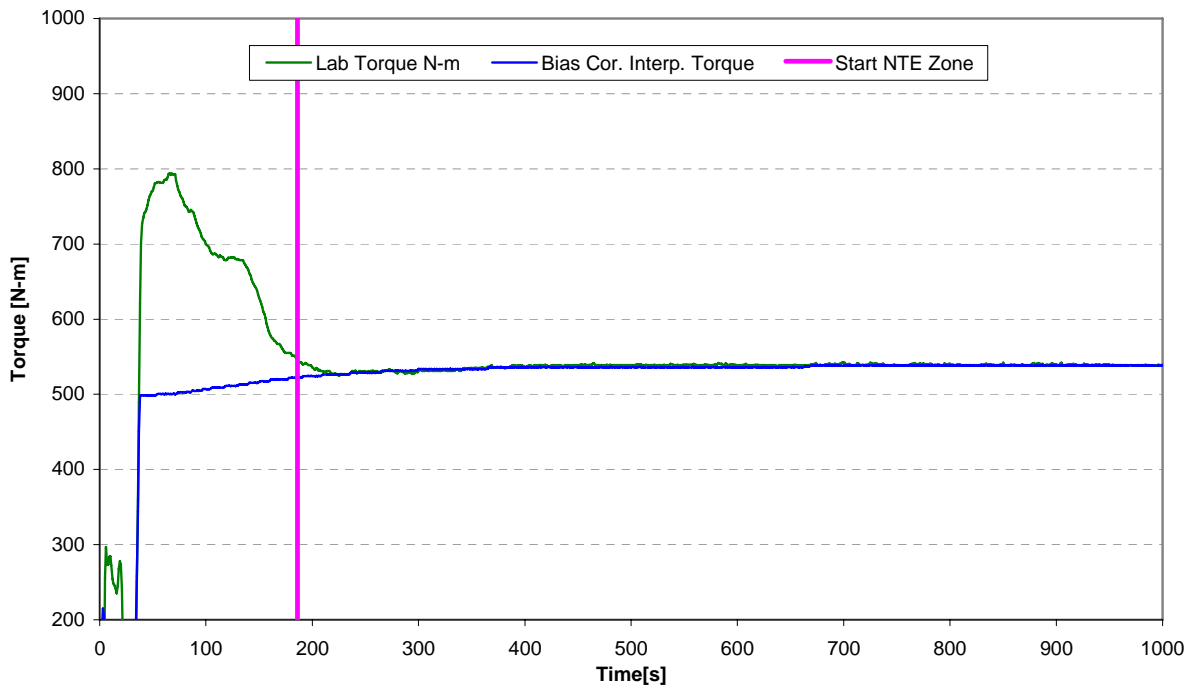
WARM-UP TEST LABORATORY AND INTERPOLATED TORQUE TRACES FOR ENGINE 2 AT PART LOAD



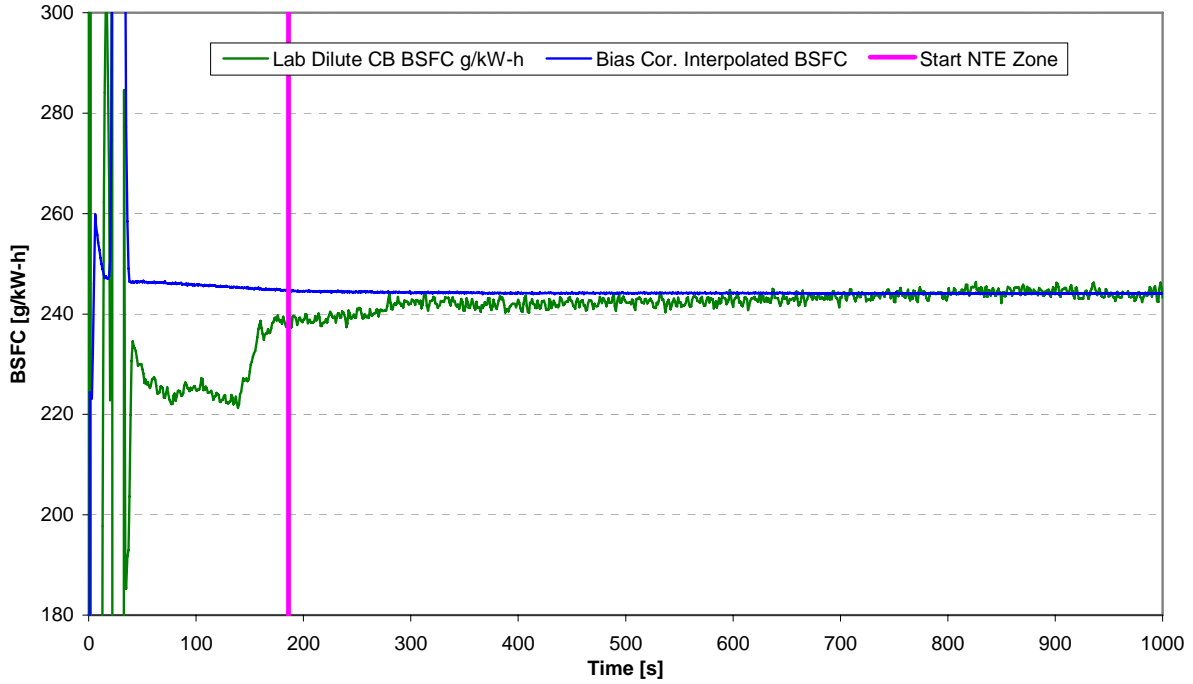
WARM-UP TEST LABORATORY AND INTERPOLATED BSFC TRACES FOR ENGINE 2 AT PART LOAD



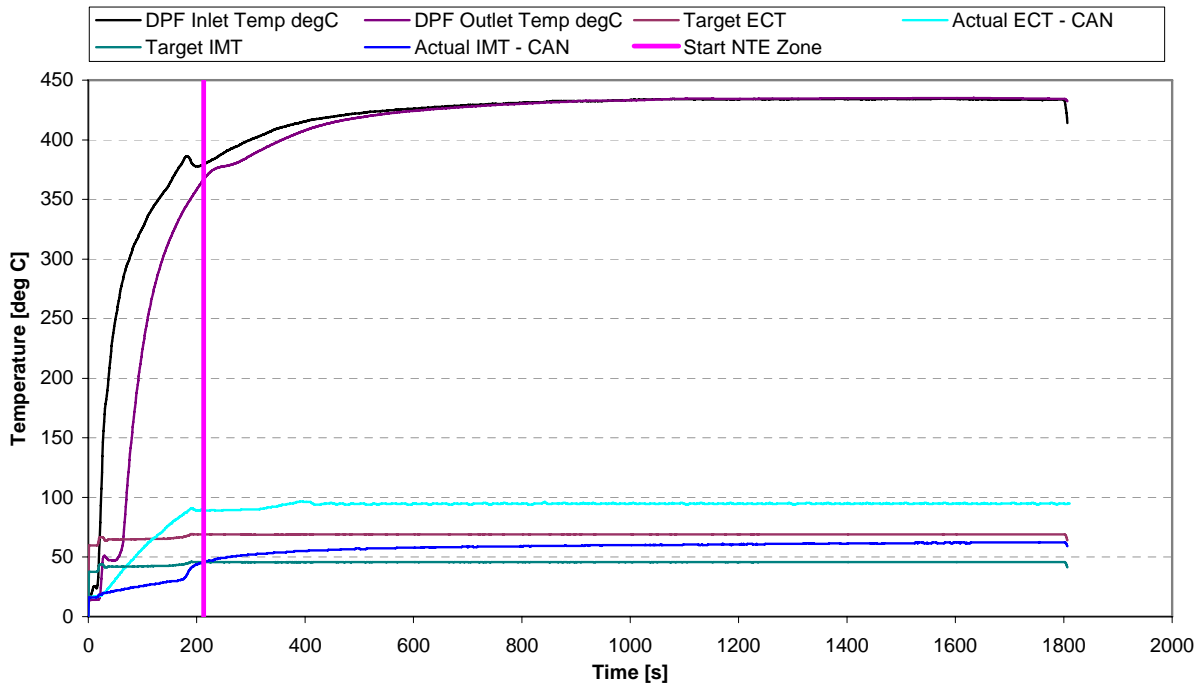
WARM-UP TEST TEMPERATURE PROFILES FOR ENGINE 3 AT WOT



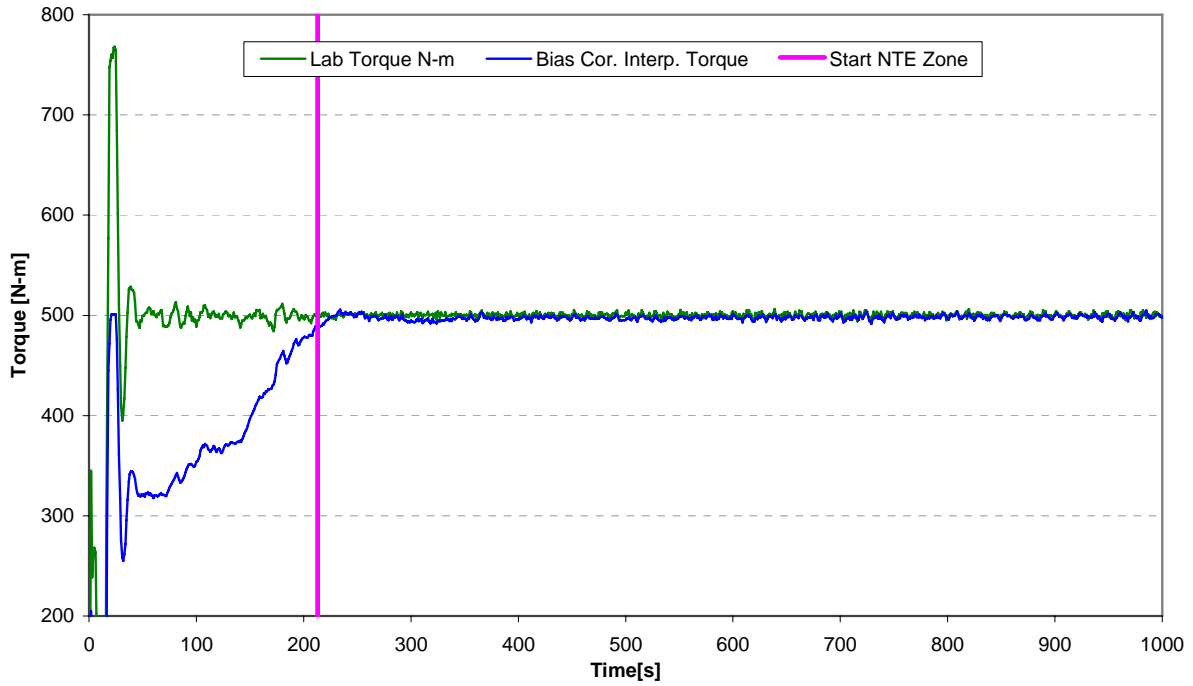
WARM-UP TEST LABORATORY AND INTERPOLATED TORQUE TRACES FOR ENGINE 3 AT WOT



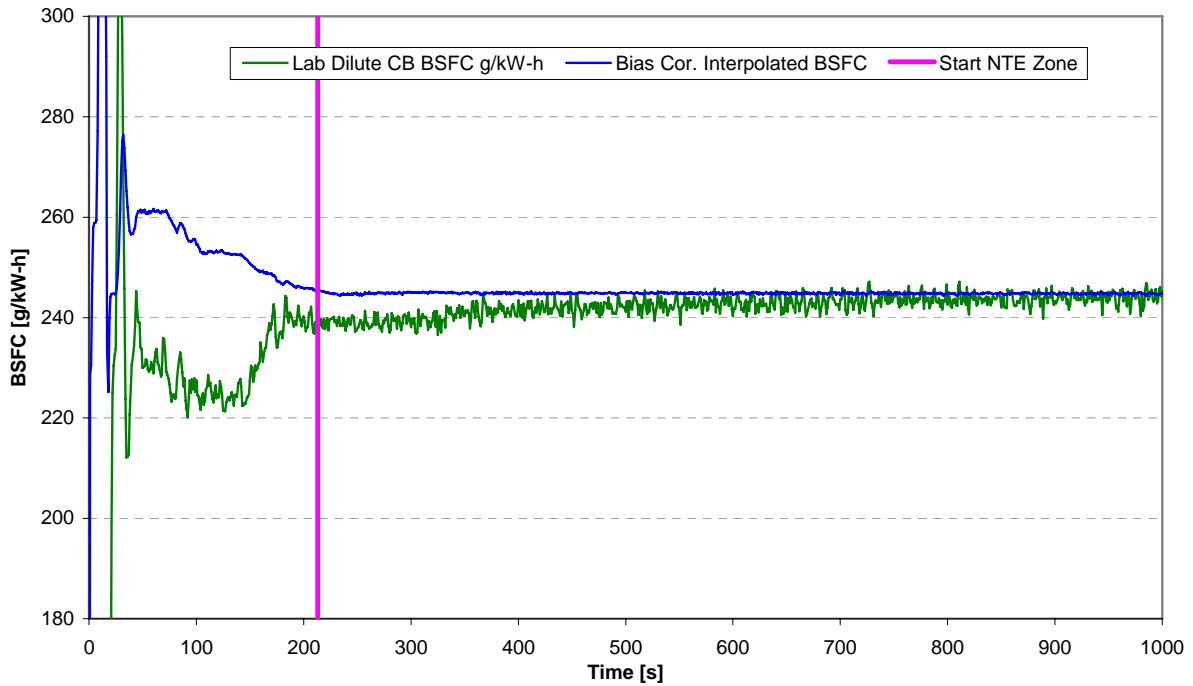
WARM-UP TEST LABORATORY AND INTERPOLATED BSFC TRACES FOR ENGINE 3 AT WOT



WARM-UP TEST TEMPERATURE PROFILES FOR ENGINE 3 AT PART LOAD

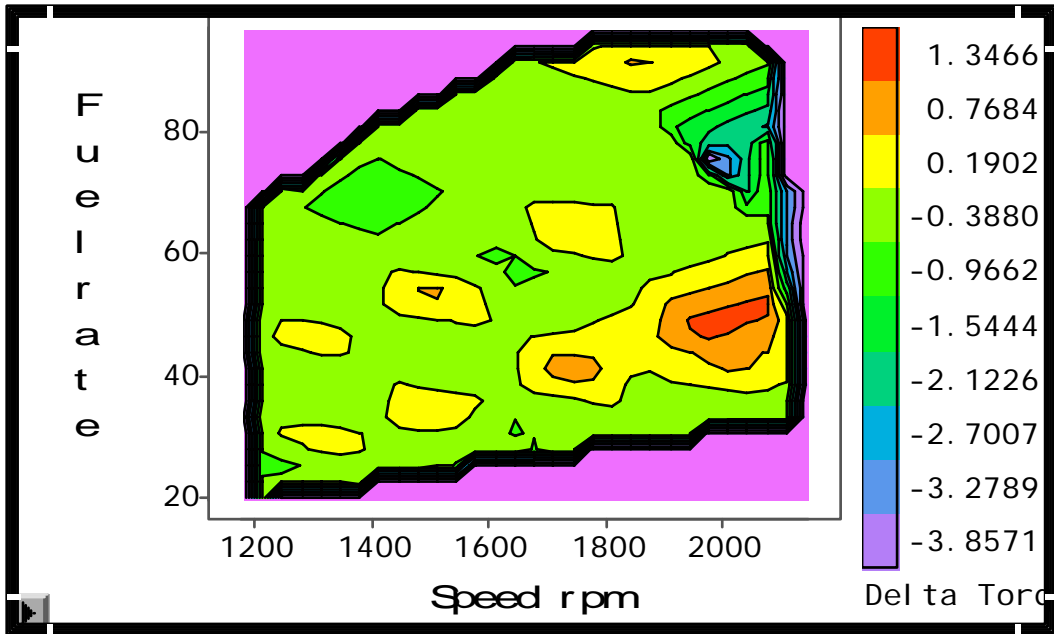


WARM-UP TEST LABORATORY AND INTERPOLATED TORQUE TRACES FOR ENGINE 3 AT PART LOAD

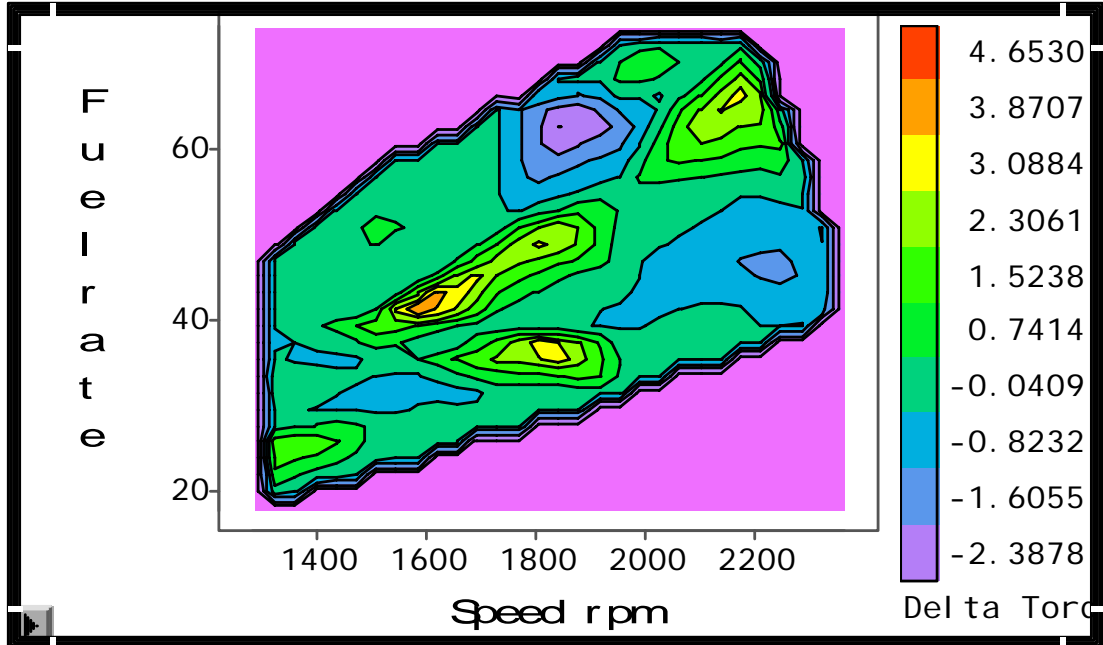


WARM-UP TEST LABORATORY AND INTERPOLATED BSFC TRACES FOR ENGINE 3 AT PART LOAD

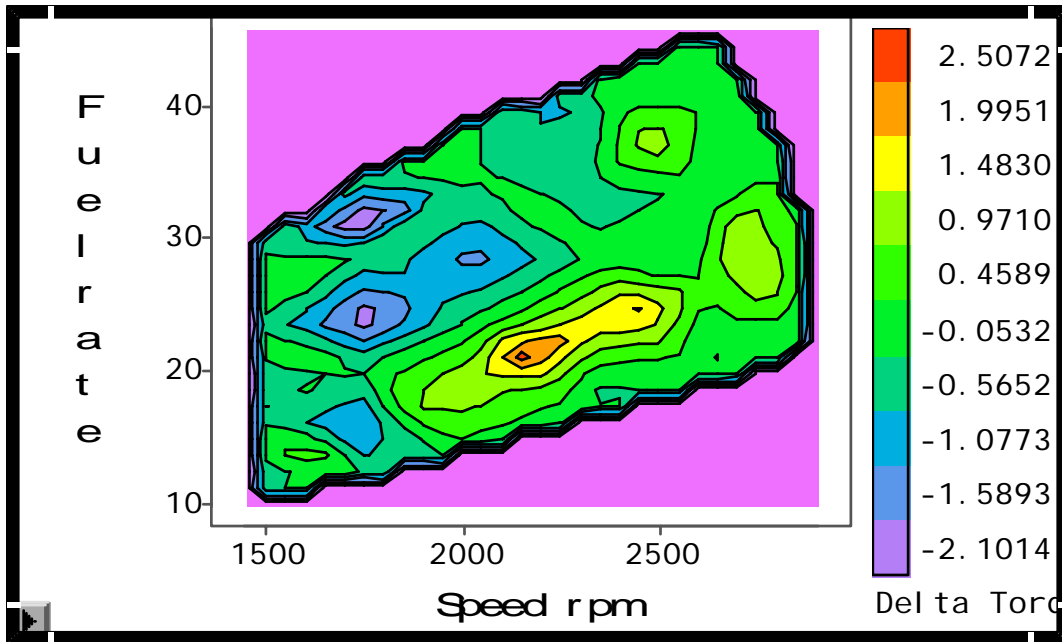
APPENDIX I
INTERPOLATION TORQUE AND BSFC ERROR MAPS



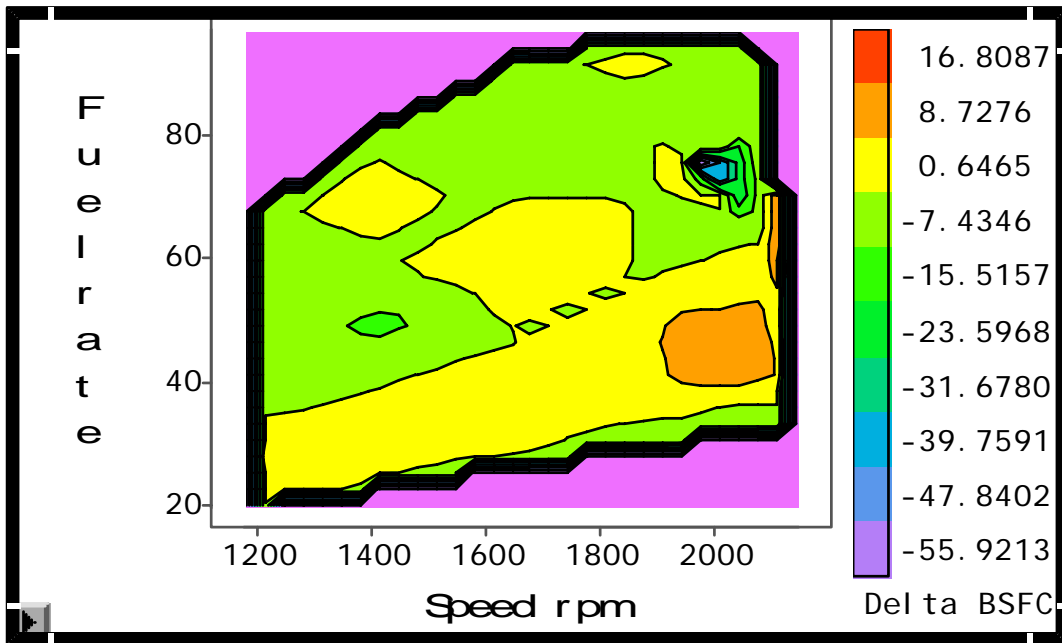
INTERPOLATED TORQUE ERROR (% PEAK TORQUE) BY SPEED (RPM) AND FUEL RATE (G/S) FOR ENGINE #1



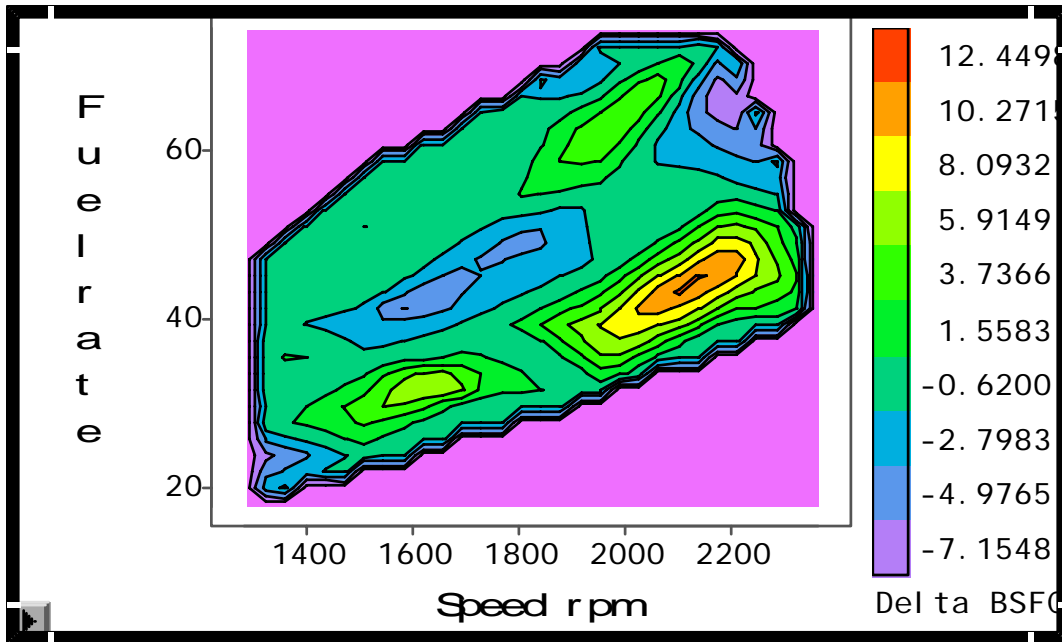
INTERPOLATED TORQUE ERROR (% PEAK TORQUE) BY SPEED (RPM) AND FUEL RATE (G/S) FOR ENGINE #2



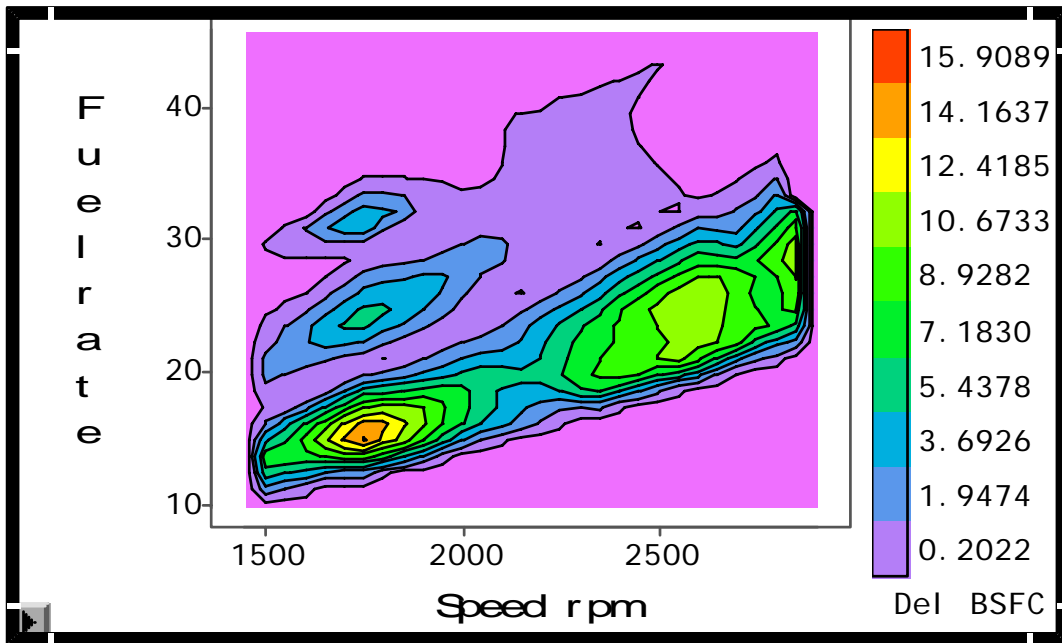
INTERPOLATED TORQUE ERROR (% PEAK TORQUE) BY SPEED (RPM) AND FUEL RATE (G/S) FOR ENGINE #3



INTERPOLATED BSFC ERROR (G/KW-HR) BY SPEED (RPM) AND FUEL RATE (G/S) FOR ENGINE #1



INTERPOLATED BSFC ERROR (G/KW-HR) BY SPEED (RPM) AND FUEL RATE (G/S) FOR ENGINE #2



INTERPOLATED BSFC ERROR (G/KW-HR) BY SPEED (RPM) AND FUEL RATE (G/S) FOR ENGINE #3

APPENDIX J
EVALUATION OF MANUFACTURER SUPPLIED ERROR SURFACES

August 28, 2006

From: Matt Spears, US EPA
To: Measurement Allowance Steering Committee
Subject: Evaluation of Manufacturer-Submitted Error Surfaces

Background

In May 2005 EPA, CARB, and EMA signed a Memorandum of Agreement (MOA), which among other things, described how to evaluate manufacturer voluntary submissions of data that demonstrated non-deficiency AECD effects or production variability effects on the ability to estimate NTE torque/BSFC values from ECM parameters, using prescribed mapping procedures. In the Agreement it stated that, “EPA and CARB, in consultation with HDOH engine manufacturers, will utilize this information, if reasonably common among manufacturers, to determine and include a margin component in the error model that accounts for the variability in the torque/BSFC values used in the NTE brake-specific emission calculations. For example, EPA/CARB would consider information for an additional allowance if variability due to non-deficiency AECDs is consistent across manufacturers. If variability is inconsistent and infrequent across the submissions or if there is a consistent bias, EPA and CARB would expect manufacturers to account for these errors by creating more sophisticated algorithms that decrease the infrequent large deviations or account for the consistent bias that exists across manufacturers.”

Methods

Five engine manufacturers submitted data to EPA and CARB for both torque and BSFC. Three of the five manufacturers submitted error surface data that summarized their total error of all of the component errors that they considered. The other two manufacturers submitted data that depicted various sources of error, such as production variability, deterioration, and ECM algorithm accuracy. For these two manufacturers who did not send actual error surface data, I constructed or approximated error surfaces so that the error surfaces from all manufacturers could be compared. For error types (e.g. production variability) where I received data from several engines from a given manufacturer, I determined the 5th, 50th, and 95th percentile errors from each engine’s data set, and then I averaged the percentile results across multiple engines because there was almost no scatter of percentile errors between engines. Once I had single 5th, 50th and 95th percentile errors for each type of error, I added the 5th, 50th and 95th percentiles for each type of error, respectively, to arrive at “worst case” composite errors. I used these results to create error surfaces for torque and BSFC. Note that I did not take an RSS approach to summing these error types.

To analyze the consistency of the various submitted error surfaces across manufacturers, according to the MOA, I examined the error surfaces for bias (50th percentile values), skew (symmetry of 5th and 95th percentile values), dependency of error

magnitude as a function of level (torque, BSFC), and the magnitude of individual manufacturer’s error surfaces versus the average of the remaining manufacturer error surfaces (outliers).

Observations

1. There was no consistent evidence of bias. Nearly all of the 50th percentile errors were zero or near zero for both torque and BSFC from all manufacturers.
2. There was no consistent evidence of skew. Most of the manufacturers reported symmetrical values (but opposite sign) for the 5th and 95th percentile values for both torque and BSFC.
3. There was no consistent evidence of %-error being a function of level. One individual manufacturer reported significant BSFC %-error changes as a function of level. However, the magnitudes of the BSFC errors from that manufacturer were also very inconsistent (an order of magnitude higher) compared to the other four manufacturers’ BSFC error data. When data from all five manufacturers was aggregated, there was no correlation of torque %-error versus torque or—for the four consistent manufacturers’ error surfaces—BSFC %-error versus BSFC.
4. Because there was no consistent bias, skew, or dependency of %-error as a function of level, I examined the average values of the manufacturers’ 5th and 95th percentile values. For torque the average value for all five manufacturers was -5.68% for the 5th percentile value and +5.68% for the 95th percentile value. For BSFC, I discarded one manufacturer’s data based upon good engineering judgment and based upon the terms of the MOA because every data point on the error surface was over ten times the magnitude of any other manufacturer’s corresponding BSFC error. This manufacturer’s BSFC data was deemed inconsistent with the four other manufacturer’s data. For BSFC the average value for the four remaining manufacturers was -1.35% for the 5th percentile value and +1.35% for the 95th percentile value.

Conclusions

Based upon my analysis, and in accordance with the terms of the Memorandum of Agreement and associated Test Plan, I conclude that the following error surfaces should be added to the error model to account for the consistent torque and BSFC error depicted in the manufacturer-submitted data:

Parameter	Sampling Distribution	5th percentile	50th percentile	95th percentile
Torque	Normal, once per NTE	-5.7% of point	0	+5.7% of point
BSFC	Normal, once per NTE	-1.4% of point	0	+1.4% of point

Respectfully Submitted,



Matthew W Spears

November 2, 2006

From: Matt Spears, US EPA
To: Measurement Allowance Steering Committee
Subject: Re-Evaluation of Manufacturer-Submitted Error Surfaces

Background

On August 28, 2006 I submitted a memo to the steering committee indicating the results of my analysis of the manufacturer-submitted error surface data. This original memo is attached for reference. Subsequently, we (the steering committee) had a discussion of my original memo, and as a follow-up, the EMA members of the steering committee requested an opportunity to submit to EPA/CARB some additional data. Specifically, they requested to submit data that included the torque and BSFC ECM errors due to non-deficiency AECD operation. I agreed to contact those engine manufacturers that had not originally submitted such information. Ultimately, two of those engine manufacturers submitted additional information.

Methods and Observations

One company, Cummins, Inc., submitted a comprehensive analysis of all the errors that affect ECM torque and BSFC prediction. The Cummins submission was the only data that I received, either originally or in this second round of data submission, that contained a direct comparison of ECM-derived BSFC versus lab-determined BSFC. Furthermore, the Cummins submission included a thorough statistical analysis of all of the sources of error, including data previously submitted.

The other company submitted SET data for ECM torque and measured torque at two different modes of engine operation. Based upon a discussion with that company, I determined that one of the modes of operation was the mode from which ECM torque is derived. Since the other mode of operation was of lower engine efficiency, ECM torque and ECM derived BSFC reported during the less efficient mode of operation would result in a consistent and significant low bias of reported emissions. Because this approach to ECM torque programming might not be consistent among manufacturers, I was reluctant to include the low bias indicated from this data. After correcting for the low bias, the resulting torque error differed from the Cummins data by less than one percentage point.

I also reanalyzed the data from the one company that originally submitted non-deficiency AECD data. This company's BSFC data was initially discarded as part of my original analysis, which I explained in my original memo. This dataset only presented data indicating deviations of torque/BSFC between modes of engine operation, and did not identify which mode(s) of operation were used to determine ECM torque or BSFC. This dataset also included several non-NTE data points. After filtering the non NTE data from this data set, the resulting BSFC 5th and 95th percentage points were roughly reduced by half. Because I could not identify which mode(s) of engine operation were

used for ECM calibration, I could not subtract any bias from this spread. Even without subtracting any bias, the resulting BSFC errors differed from the Cummins analysis by less than two percentage points.

Conclusion

Based upon all of the data submitted, and in accordance with the terms of the Memorandum of Agreement and associated Test Plan, I conclude that the error surfaces proposed by Cummins should be included in the error model to account for the consistent torque and BSFC error depicted in the manufacturer-submitted data. The Cummins dataset and analysis is comprehensive and it imposes no bias on the error surface. Furthermore, other less complete datasets indicate errors very close to those reported by Cummins. Below are the revised values for the error surfaces:

Parameter	Sampling Distribution	5 th percentile	50 th percentile	95 th percentile
Torque	Normal, once per NTE	-6.5% of point	0	+6.5% of point
BSFC	Normal, once per NTE	-5.9% of point	0	+5.9% of point

For a comparison of these values based upon the original data submission, please refer to my original memo, attached.

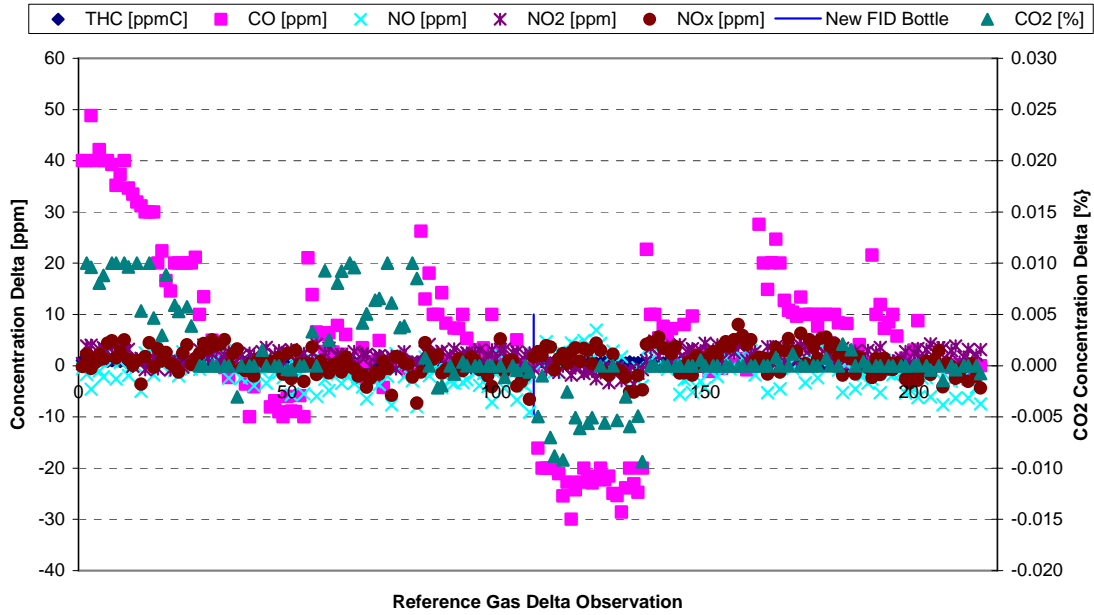
Respectfully Submitted,



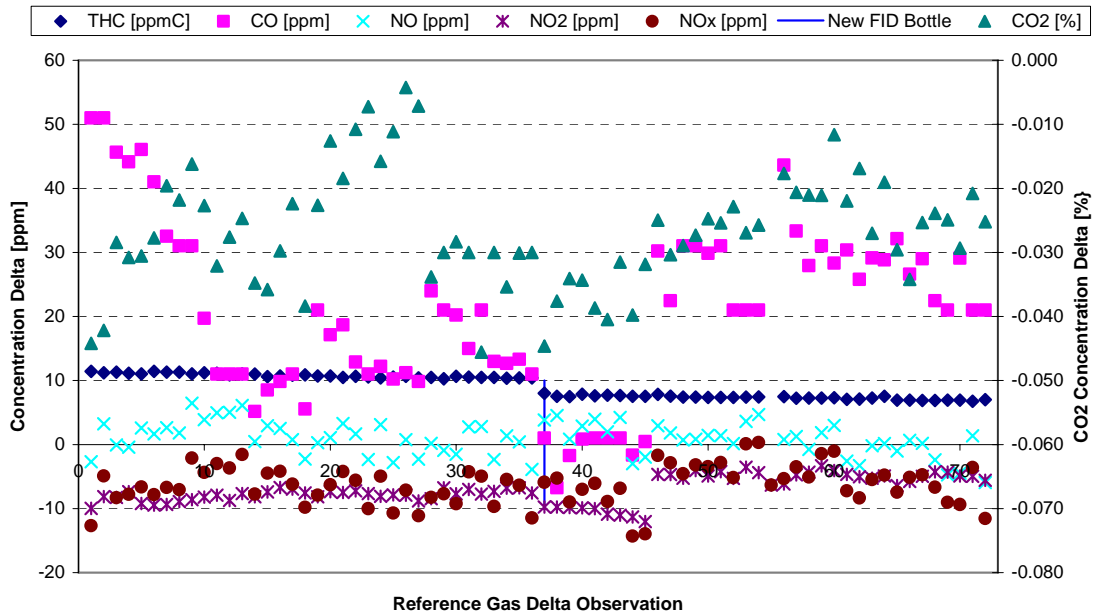
Matthew W Spears

Encl.

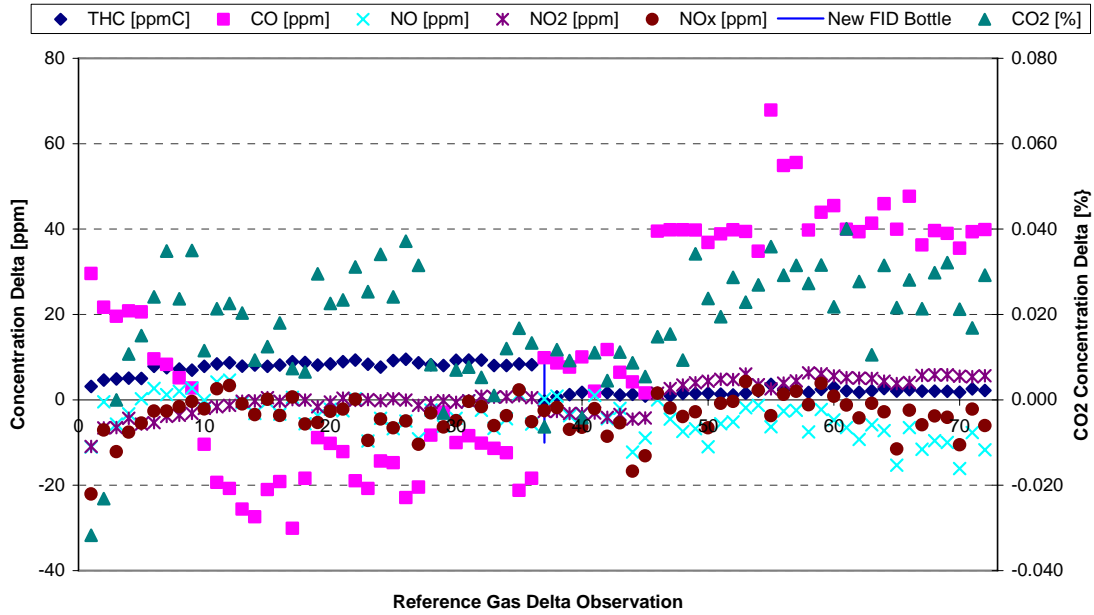
APPENDIX K
ENVIRONMENTAL CHAMBER TESTING RESULTS AND ERROR SURFACES



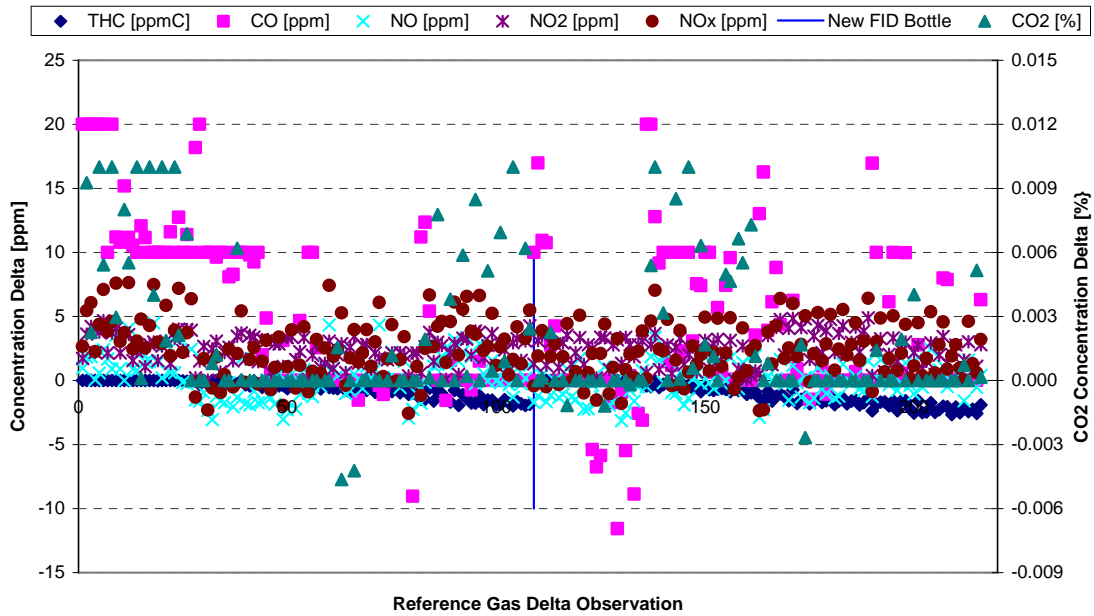
PEMS 2 ENVIRONMENTAL BASELINE ZERO DELTA MEASUREMENTS



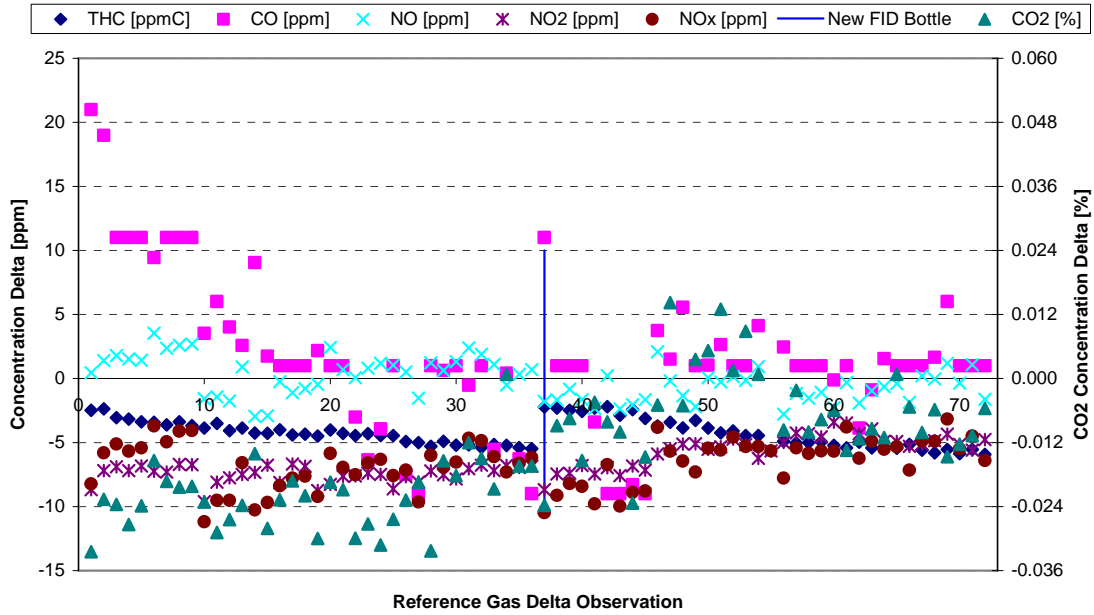
PEMS 2 ENVIRONMENTAL BASELINE AUDIT DELTA MEASUREMENTS



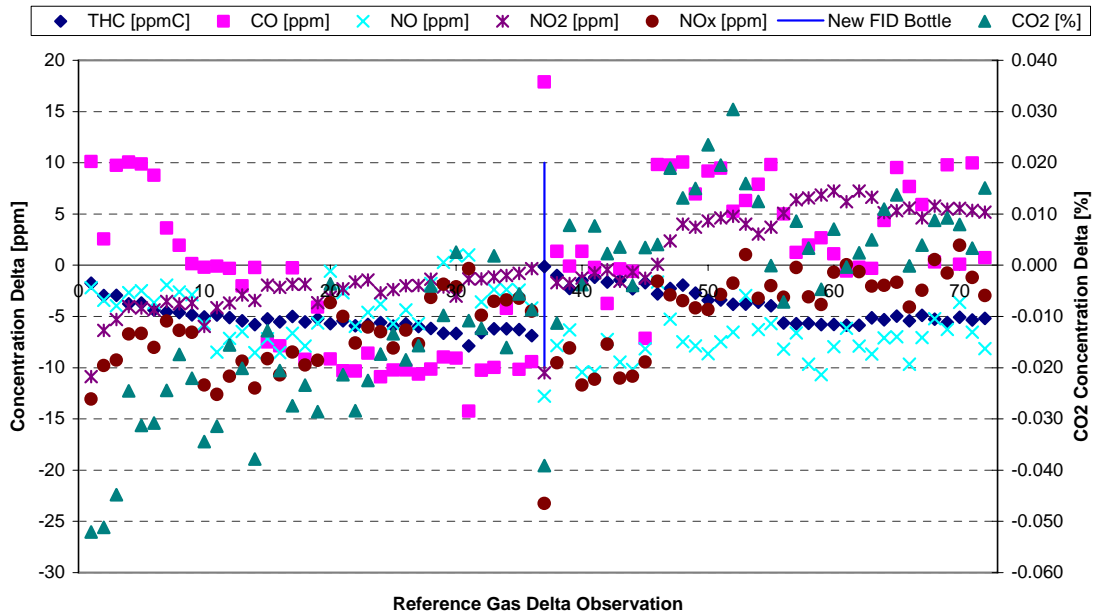
PEMS 2 ENVIRONMENTAL BASELINE SPAN DELTA MEASUREMENTS



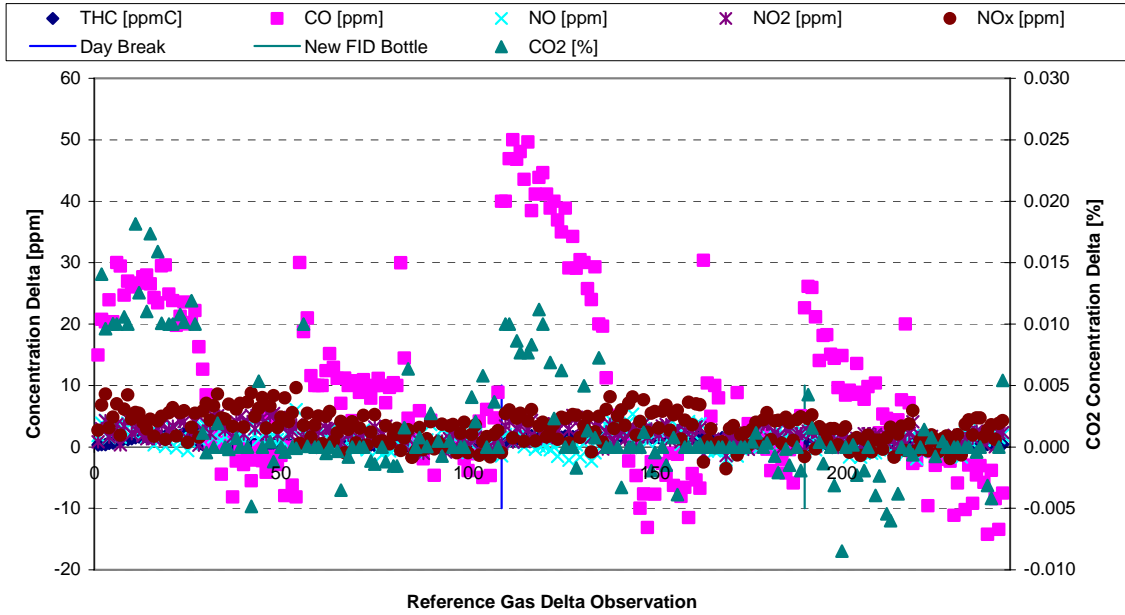
PEMS 3 ENVIRONMENTAL BASELINE ZERO DELTA MEASUREMENTS



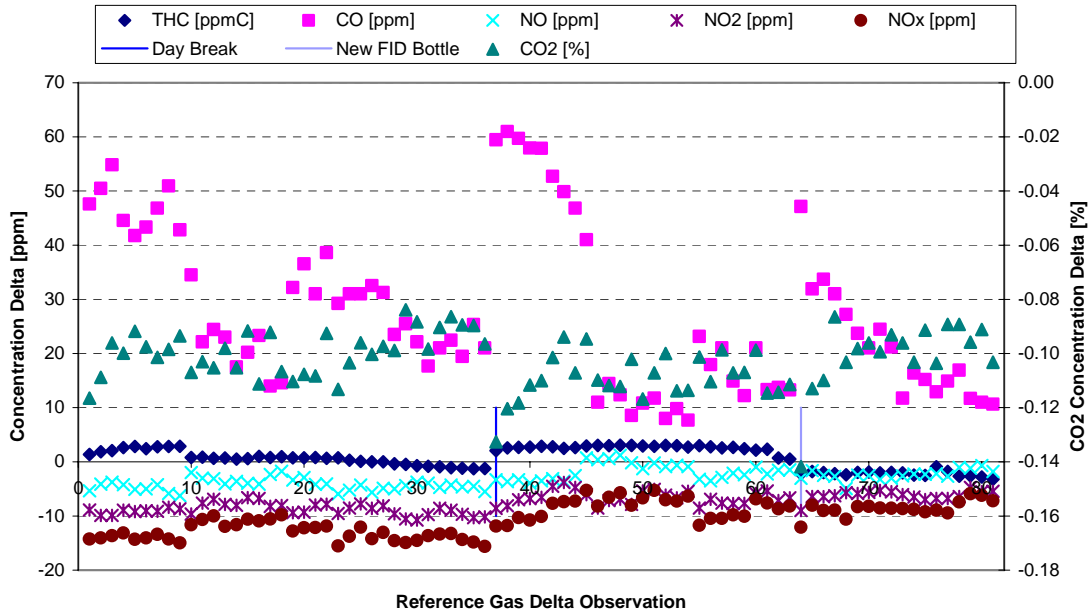
PEMS 3 ENVIRONMENTAL BASELINE AUDIT DELTA MEASUREMENTS



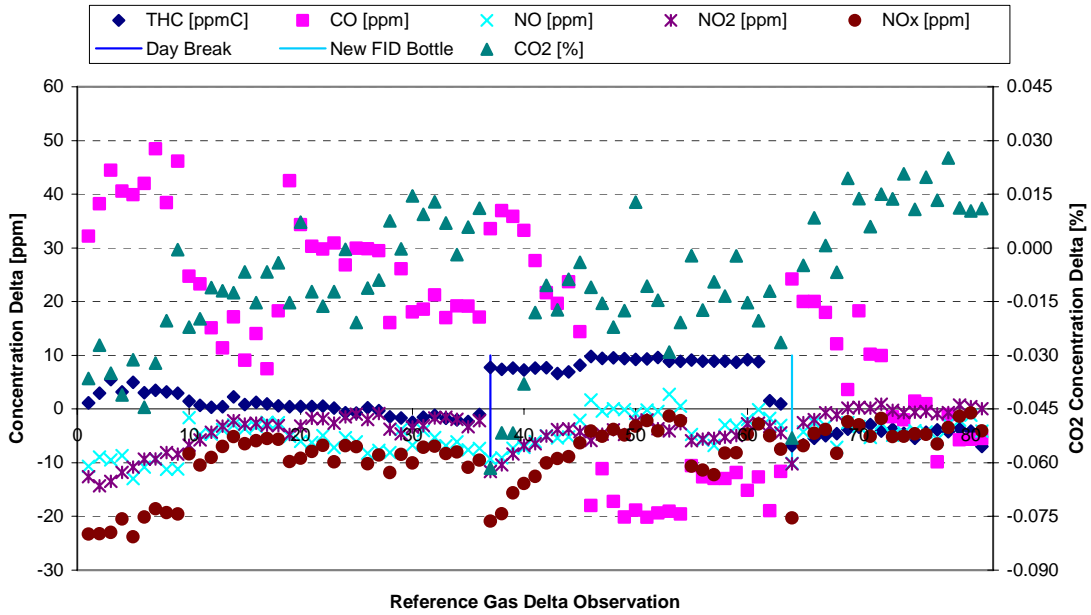
PEMS 3 ENVIRONMENTAL BASELINE SPAN DELTA MEASUREMENTS



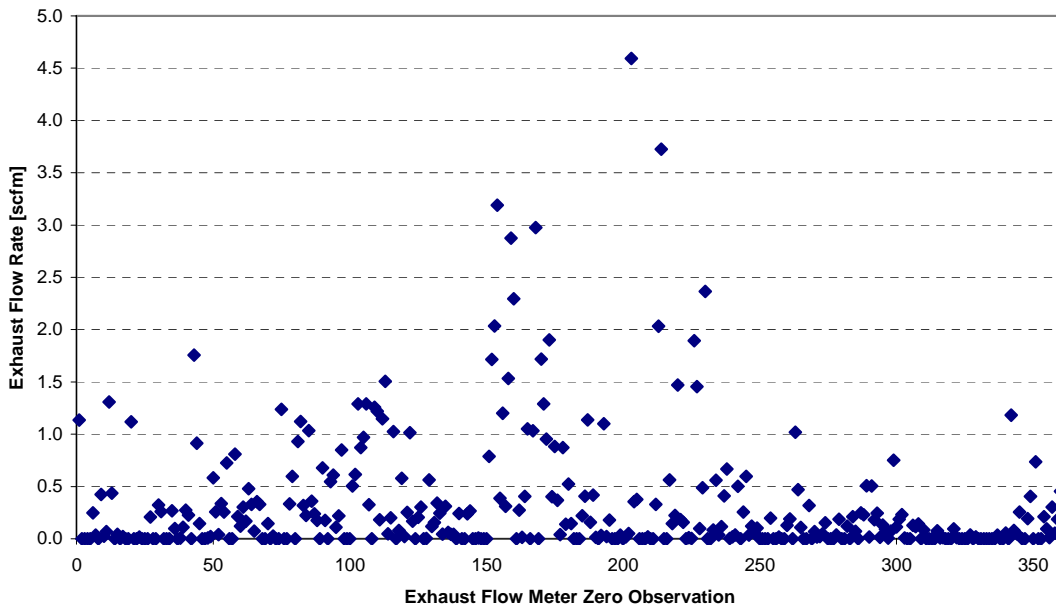
PEMS 5 ENVIRONMENTAL BASELINE ZERO DELTA MEASUREMENTS



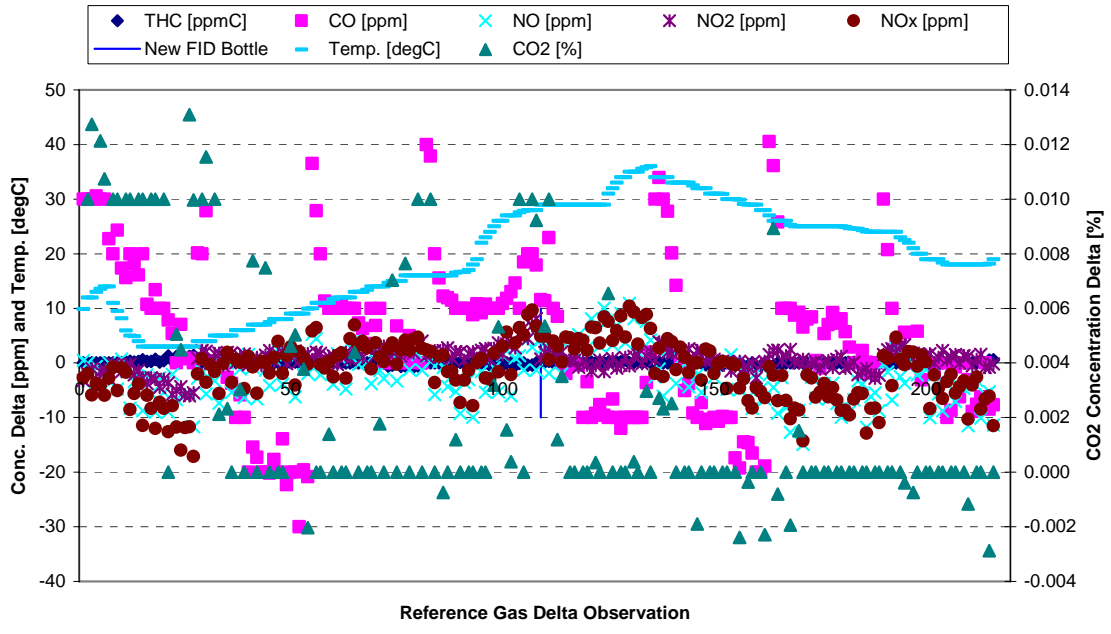
PEMS 5 ENVIRONMENTAL BASELINE AUDIT DELTA MEASUREMENTS



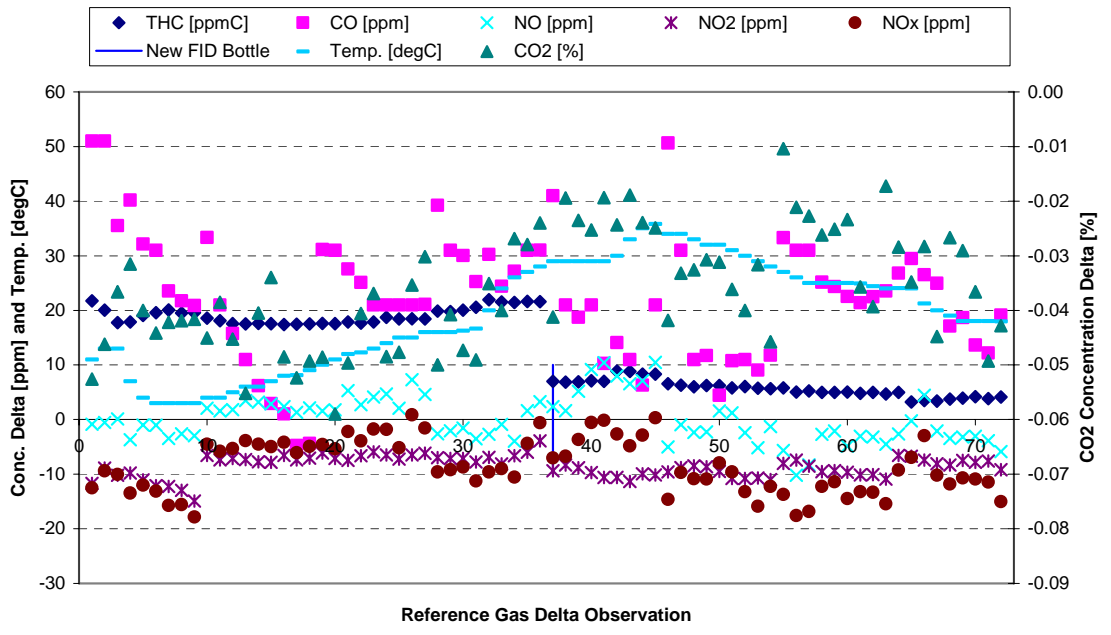
PEMS 5 ENVIRONMENTAL BASELINE SPAN DELTA MEASUREMENTS



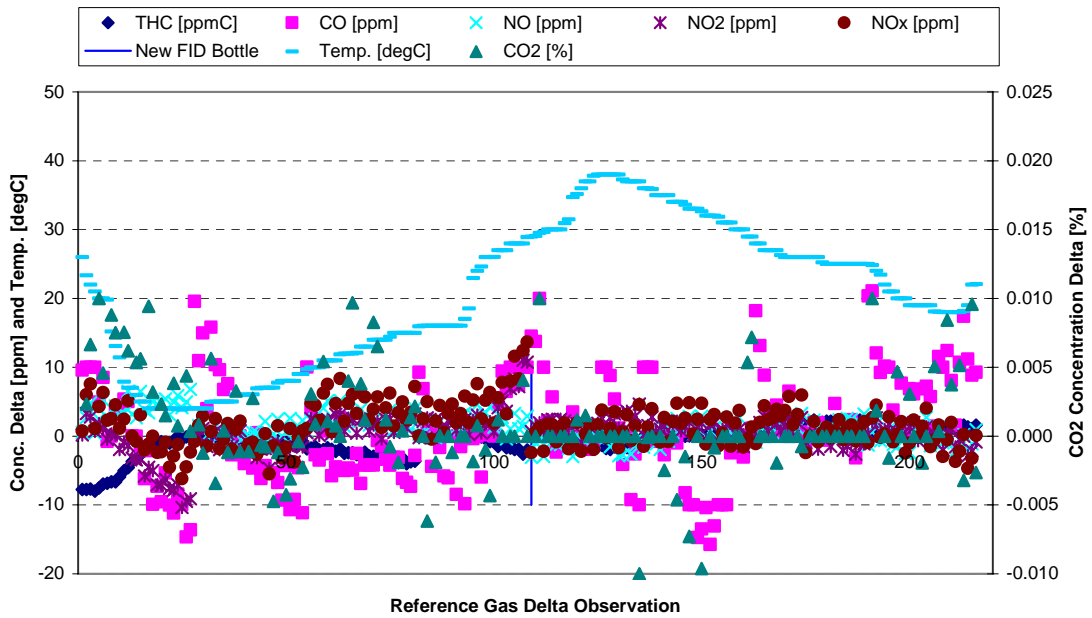
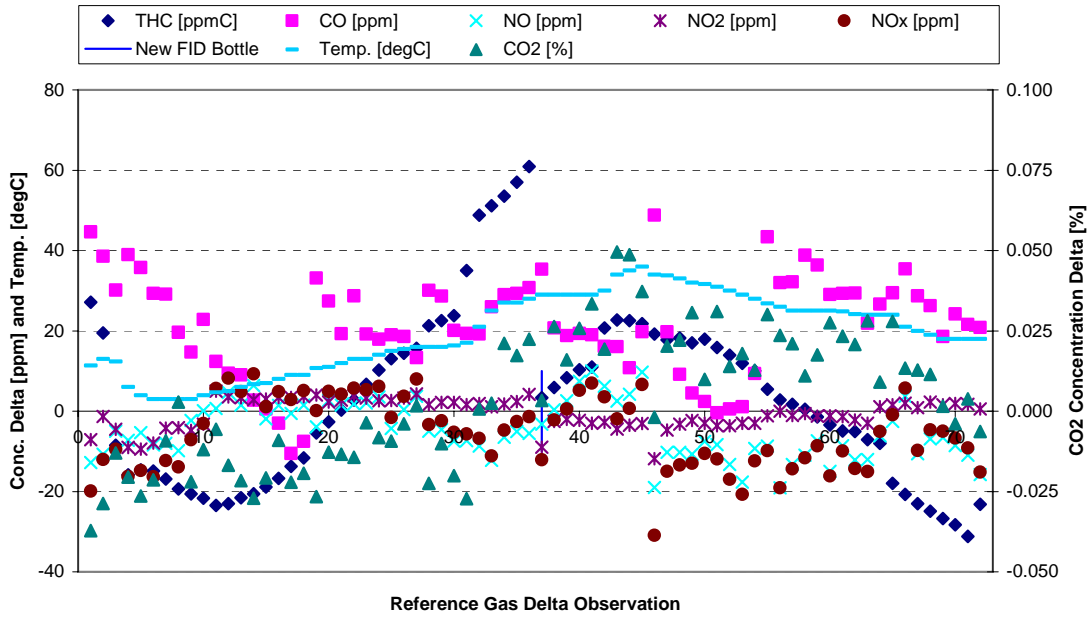
5-INCH EFM ENVIRONMENTAL BASELINE ZERO DELTA MEASUREMENTS

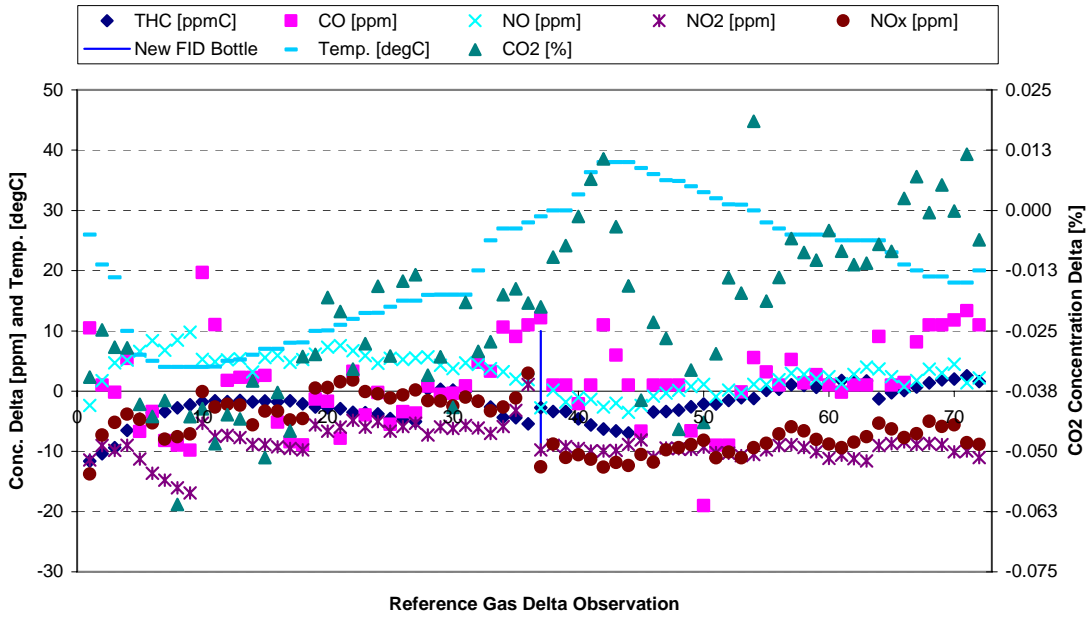


PEMS 2 ENVIRONMENTAL TEMPERATURE ZERO DELTA MEASUREMENTS

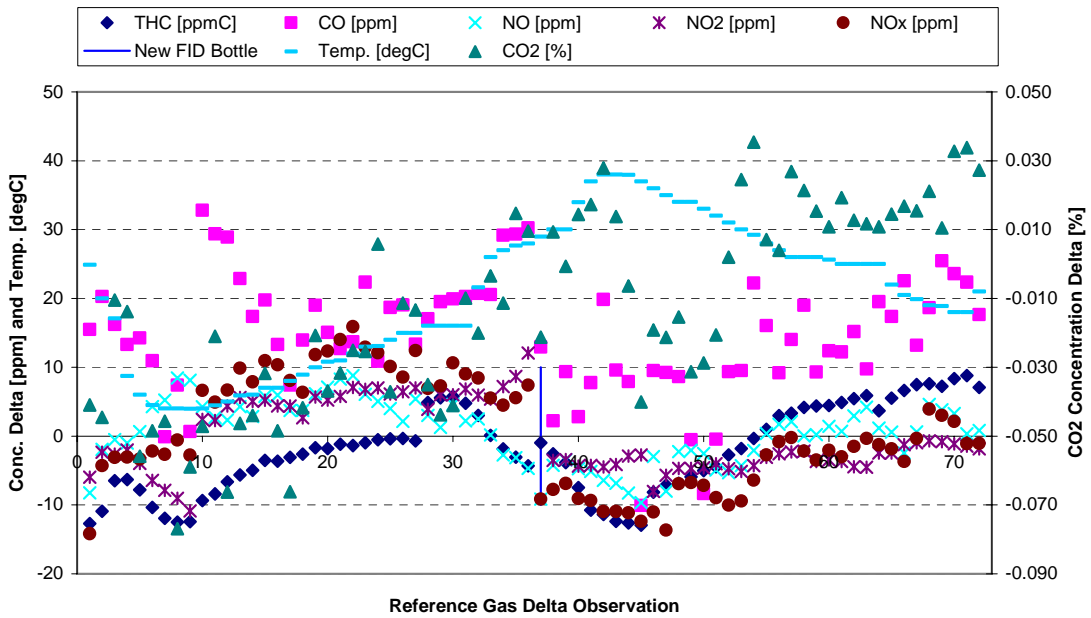


PEMS 2 ENVIRONMENTAL TEMPERATURE AUDIT DELTA MEASUREMENTS

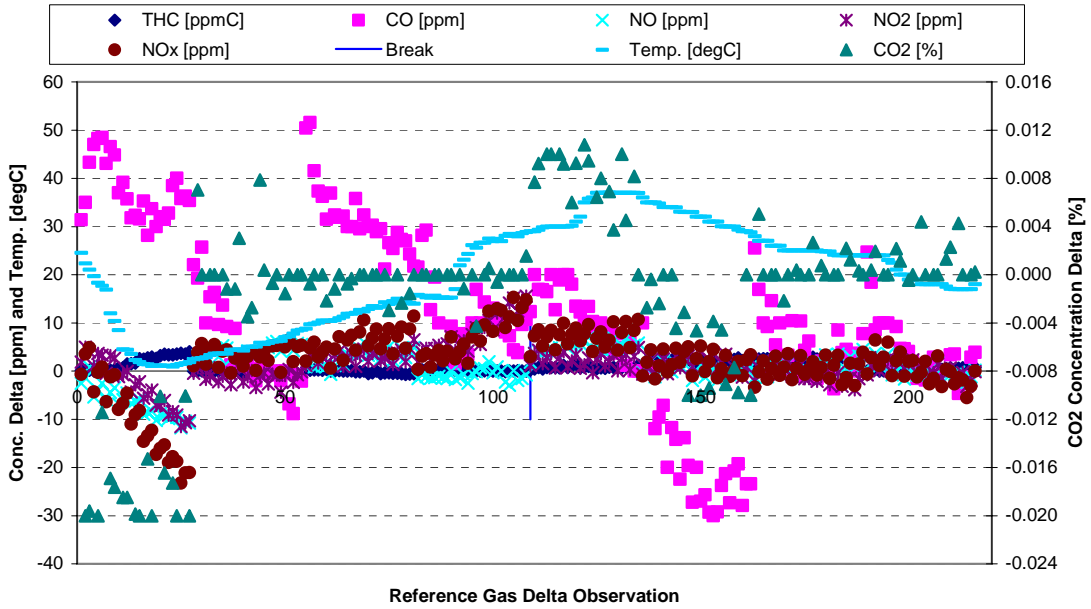




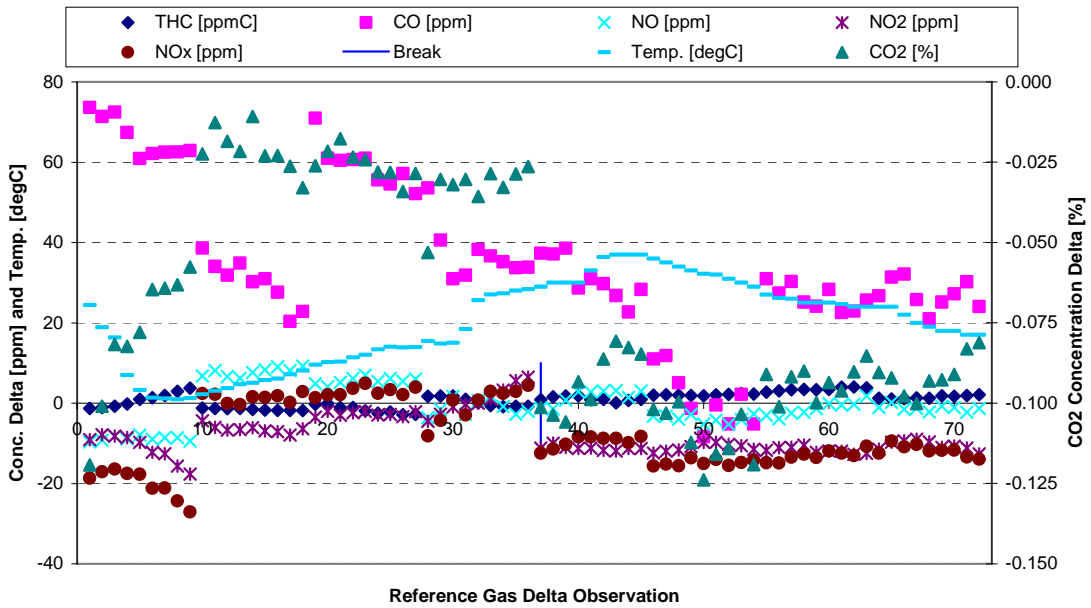
PEMS 3 ENVIRONMENTAL TEMPERATURE AUDIT DELTA MEASUREMENTS



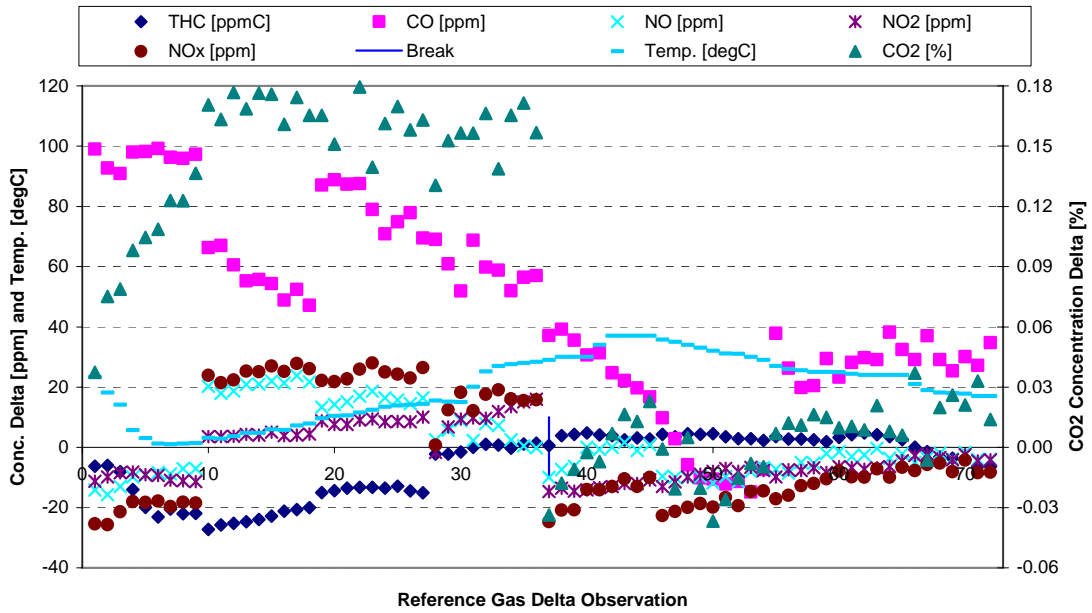
PEMS 3 ENVIRONMENTAL TEMPERATURE SPAN DELTA MEASUREMENTS



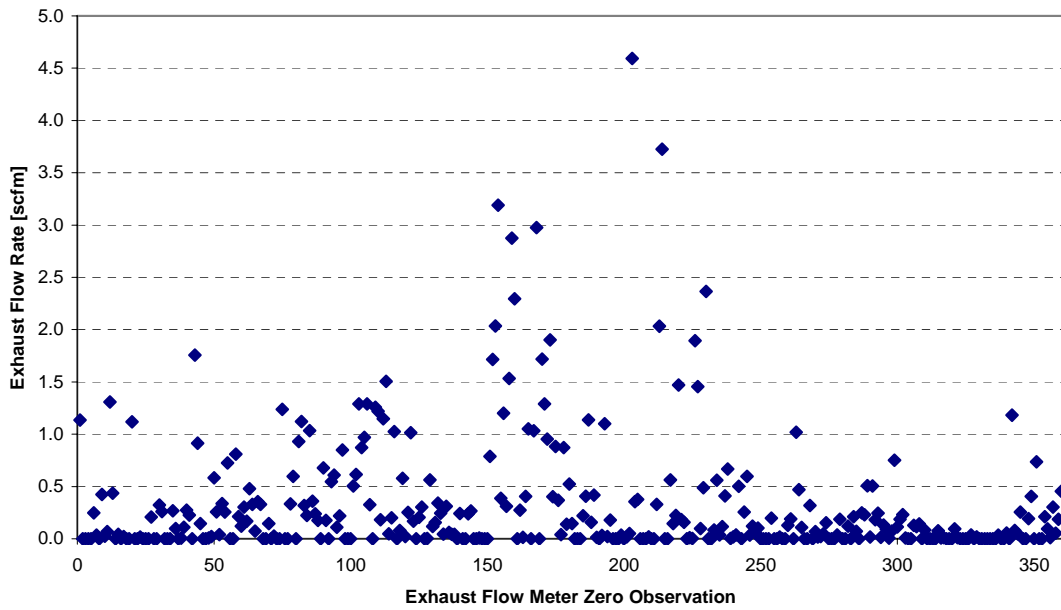
PEMS 5 ENVIRONMENTAL TEMPERATURE ZERO DELTA MEASUREMENTS



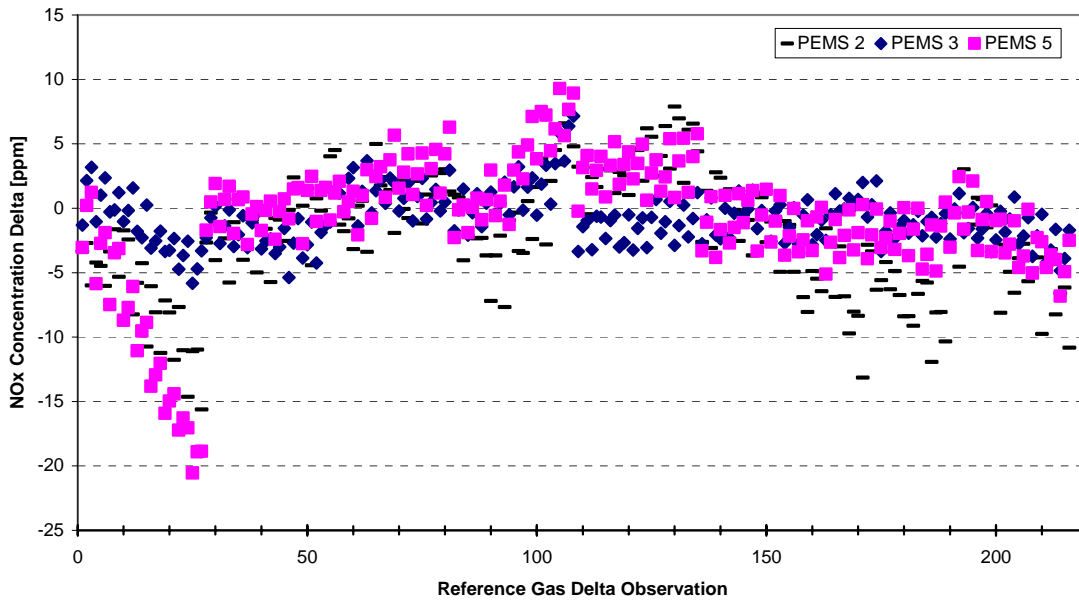
PEMS 5 ENVIRONMENTAL TEMPERATURE AUDIT DELTA MEASUREMENTS



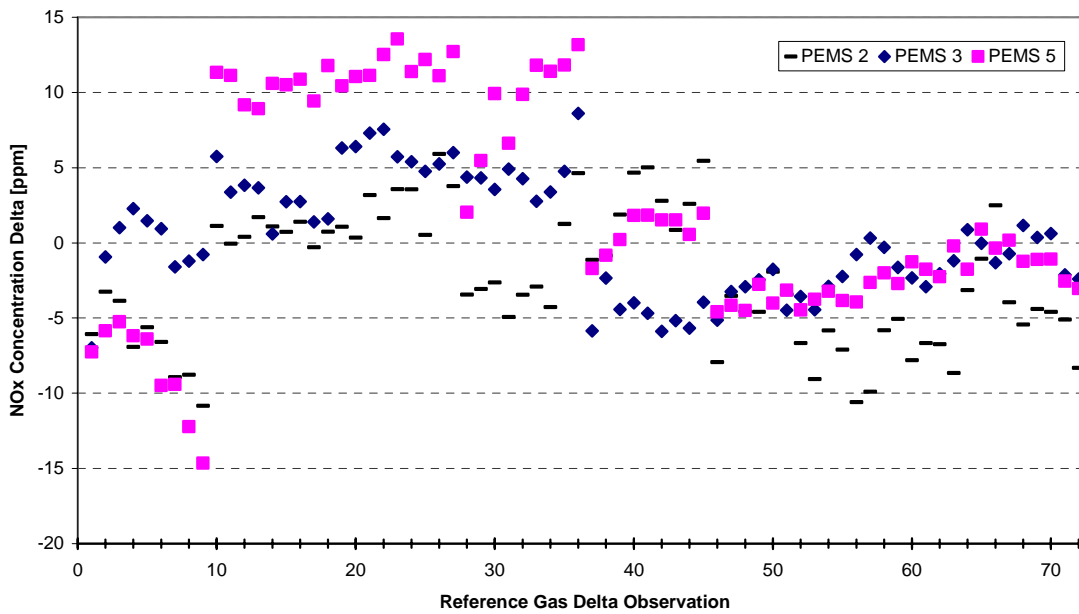
PEMS 5 ENVIRONMENTAL TEMPERATURE SPAN DELTA MEASUREMENTS



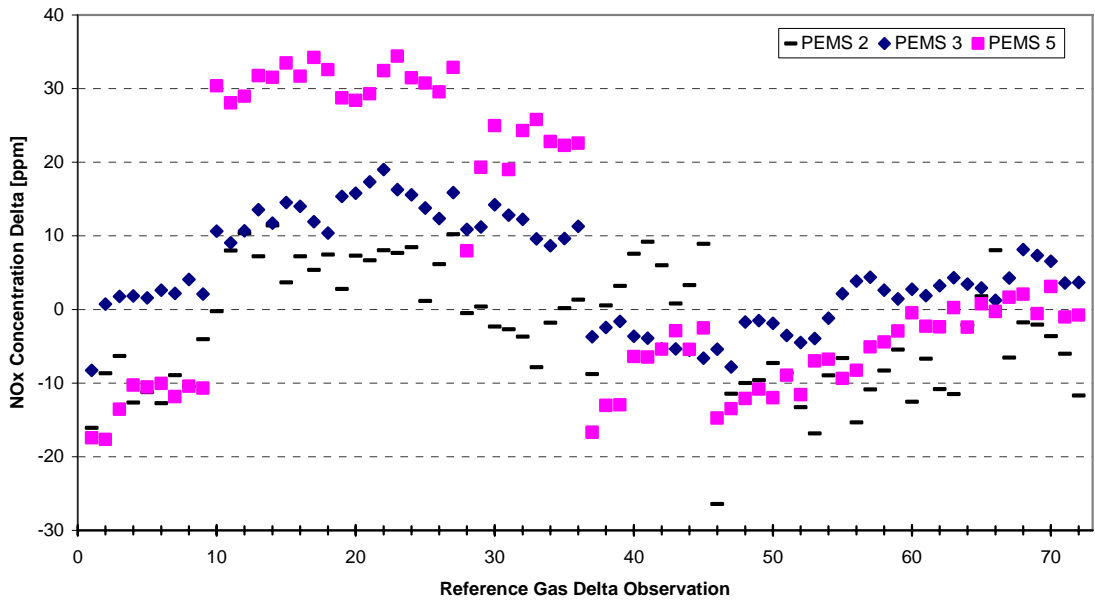
5-INCH EFM ENVIRONMENTAL TEMPERATURE ZERO DELTA MEASUREMENTS



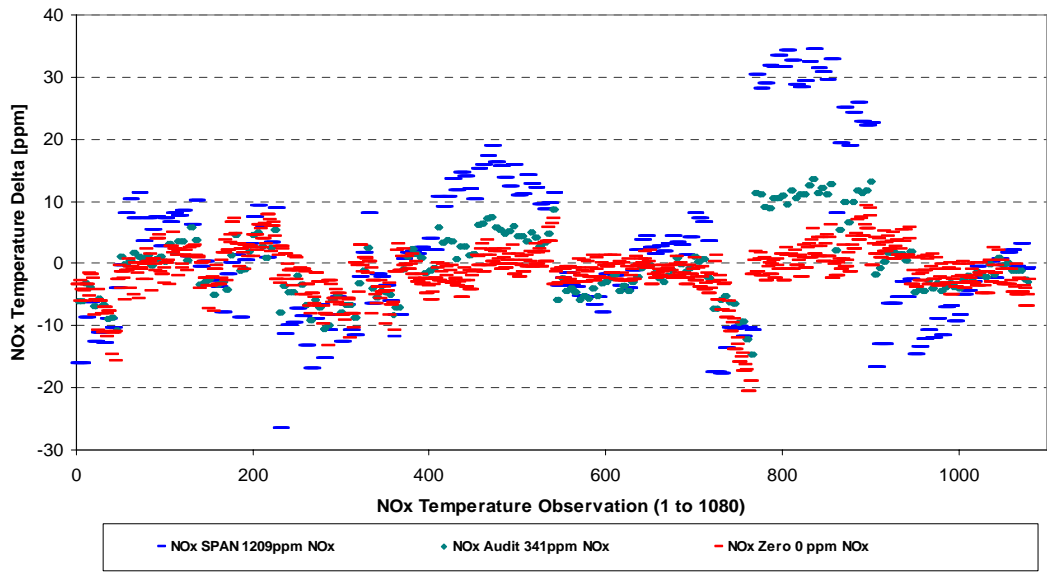
ERROR SURFACE FOR ENVIRONMENTAL TEMPERATURE NO_x CONCENTRATION ZERO DELTA MEASUREMENTS



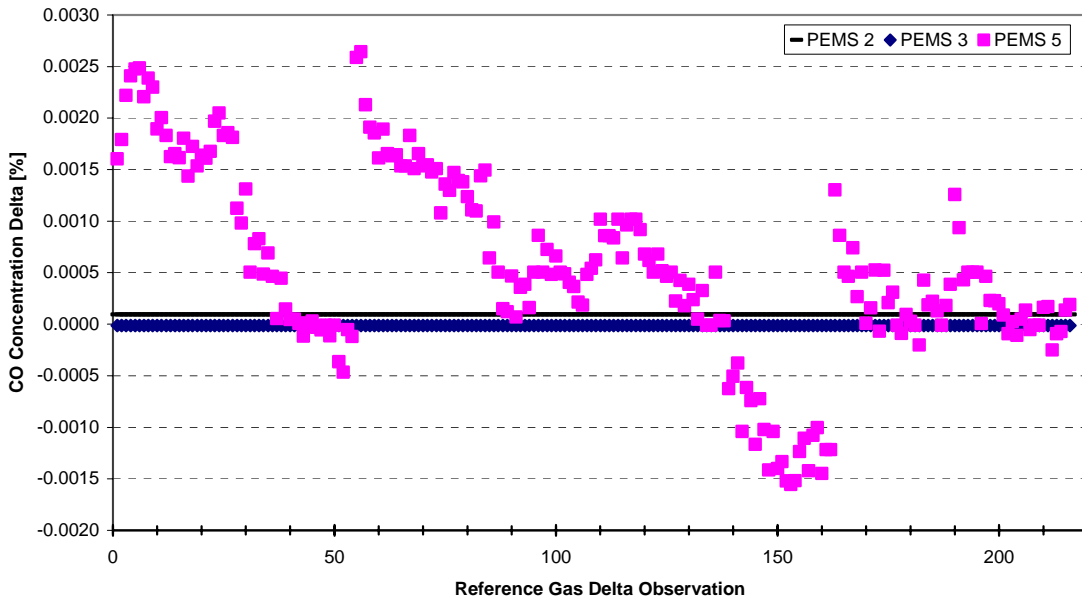
ERROR SURFACE FOR ENVIRONMENTAL TEMPERATURE NO_x CONCENTRATION AUDIT DELTA MEASUREMENTS



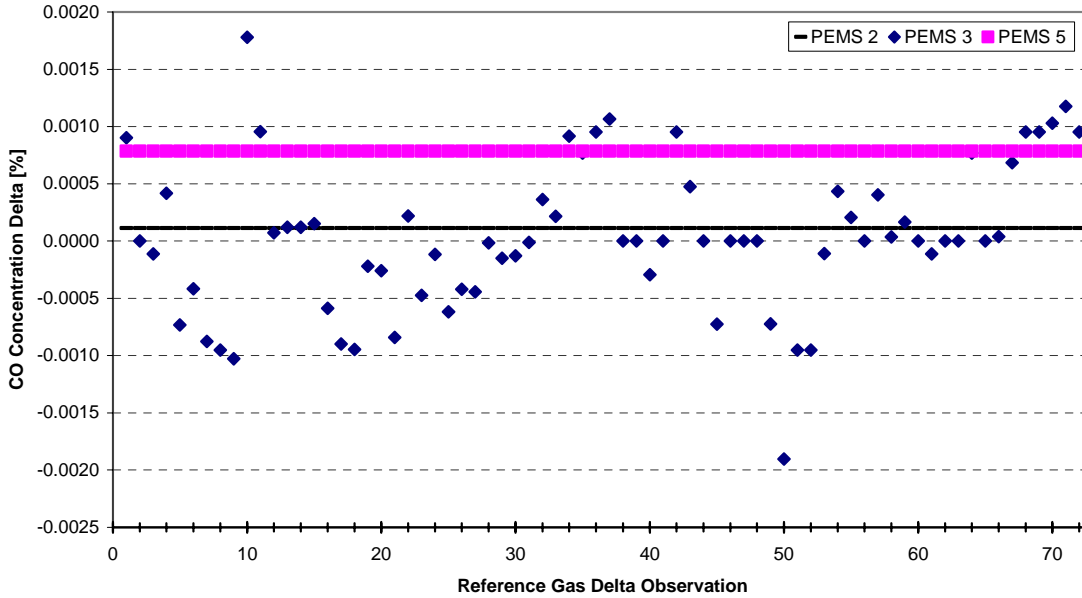
ERROR SURFACE FOR ENVIRONMENTAL TEMPERATURE NO_x CONCENTRATION SPAN DELTA MEASUREMENTS



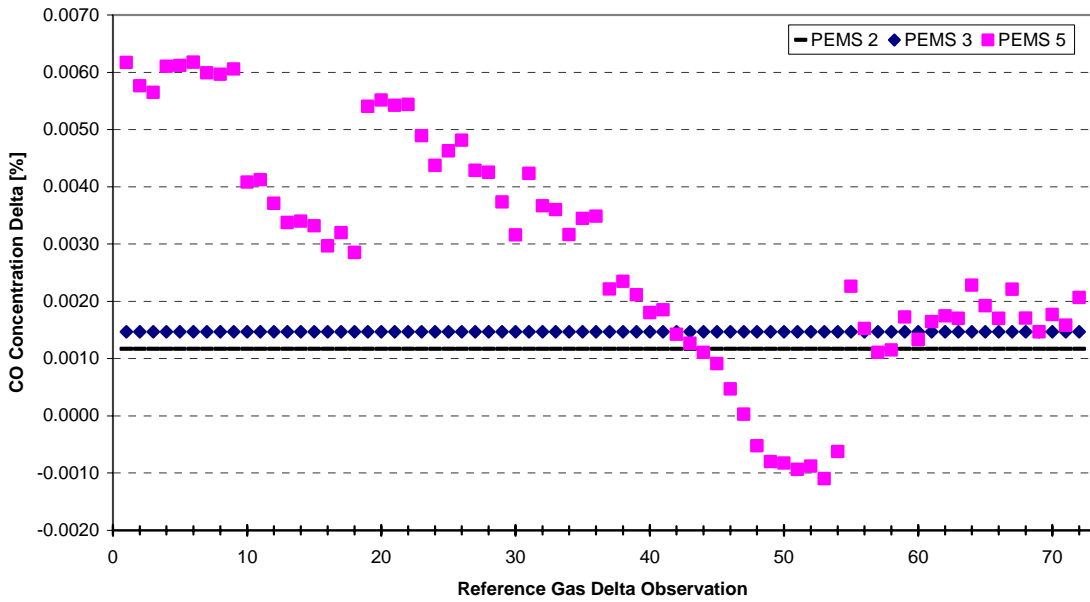
FINAL ERROR SURFACE FOR ENVIRONMENTAL TEMPERATURE NO_x CONCENTRATION



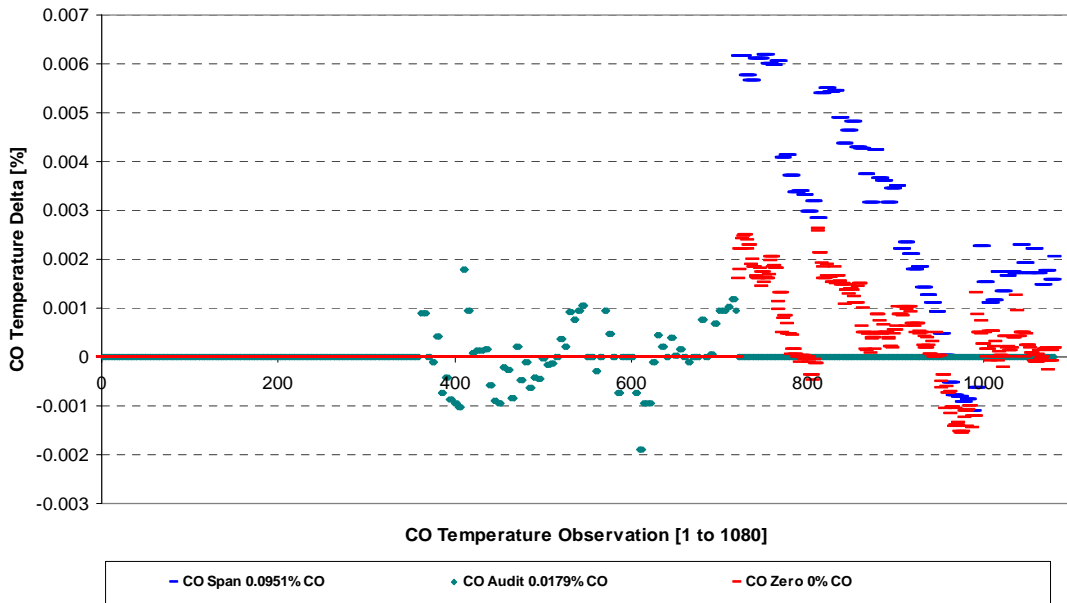
ERROR SURFACE FOR ENVIRONMENTAL TEMPERATURE CO CONCENTRATION ZERO DELTA MEASUREMENTS



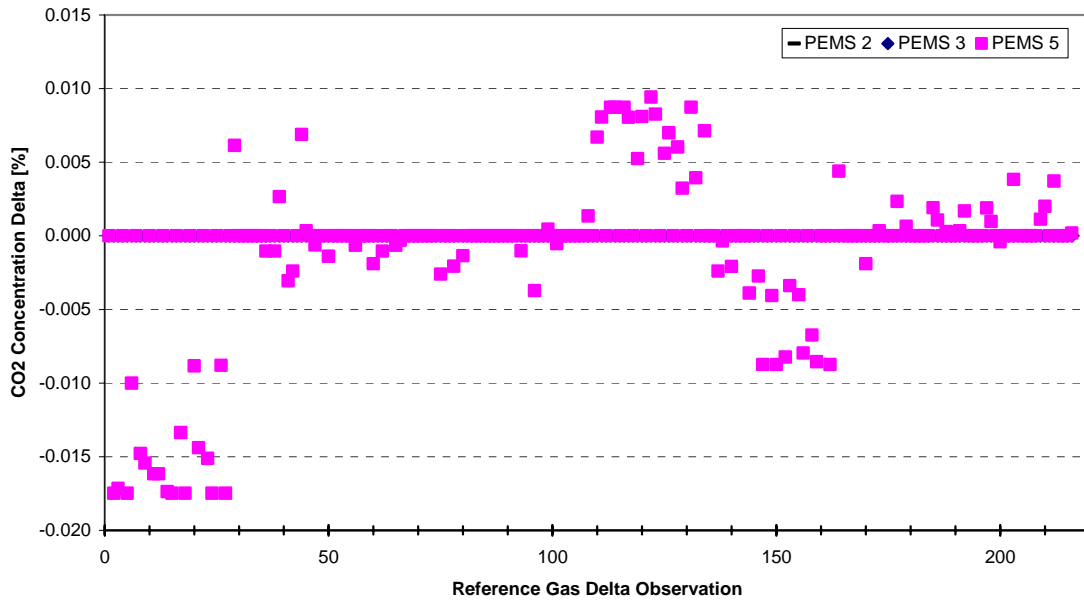
ERROR SURFACE FOR ENVIRONMENTAL TEMPERATURE CO CONCENTRATION AUDIT DELTA MEASUREMENTS



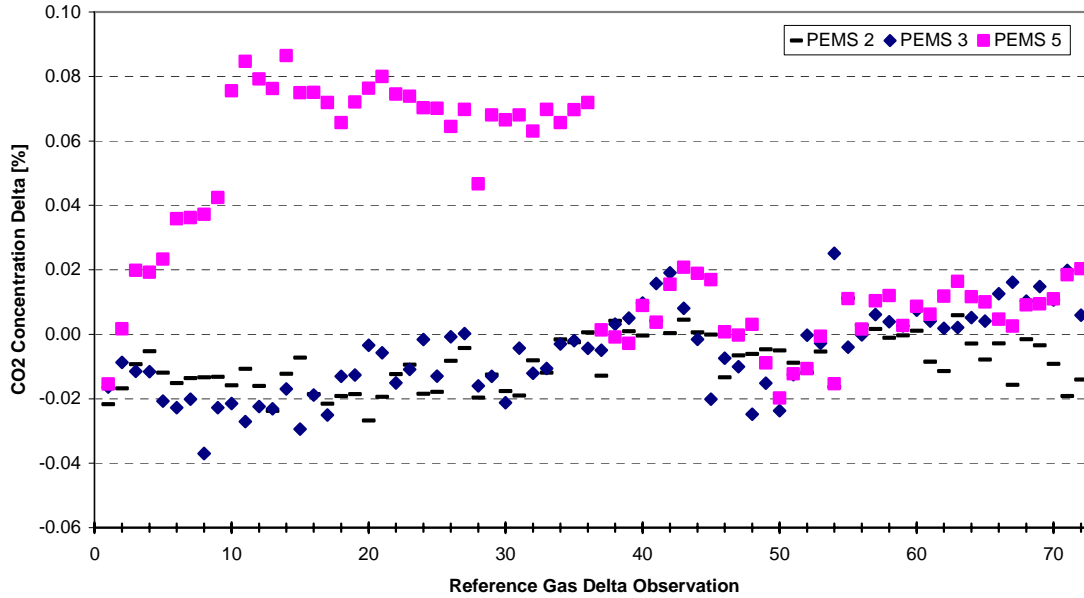
ERROR SURFACE FOR ENVIRONMENTAL TEMPERATURE CO CONCENTRATION SPAN DELTA MEASUREMENTS



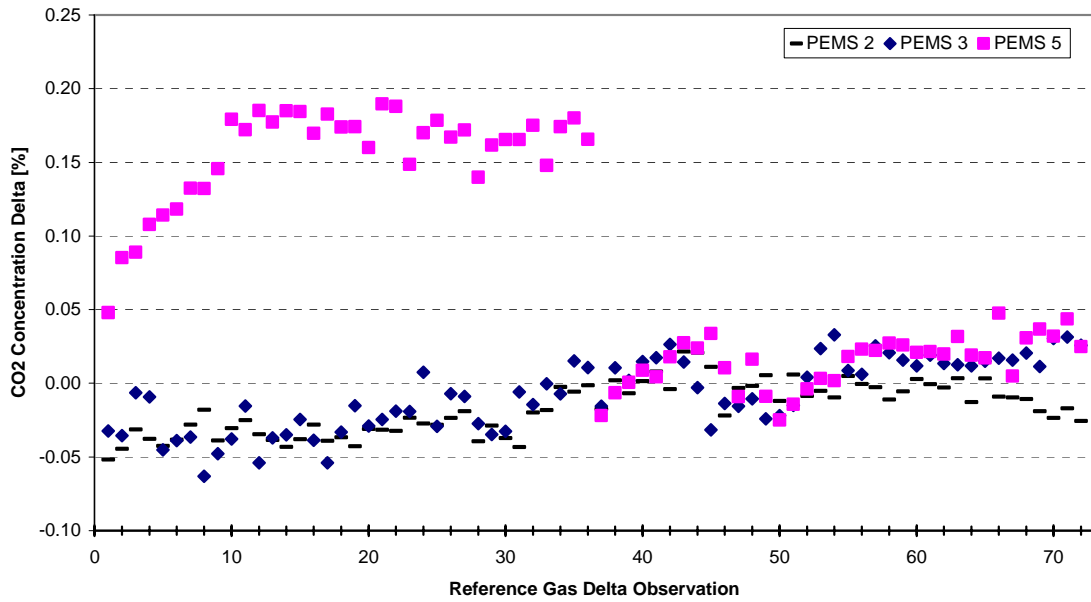
FINAL ERROR SURFACE FOR ENVIRONMENTAL TEMPERATURE CO CONCENTRATION



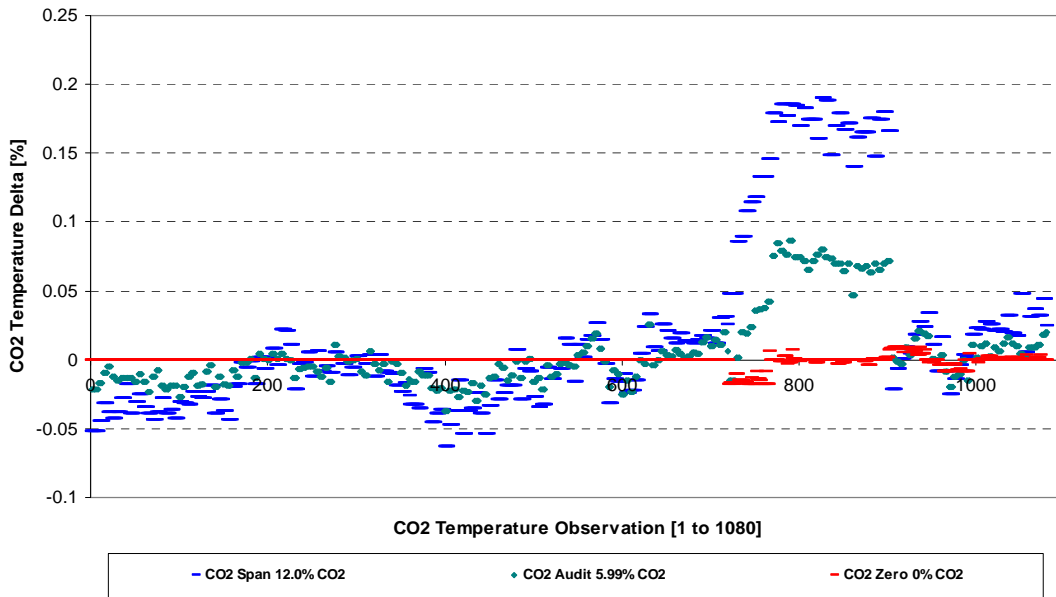
ERROR SURFACE FOR ENVIRONMENTAL TEMPERATURE CO₂ CONCENTRATION ZERO DELTA MEASUREMENTS



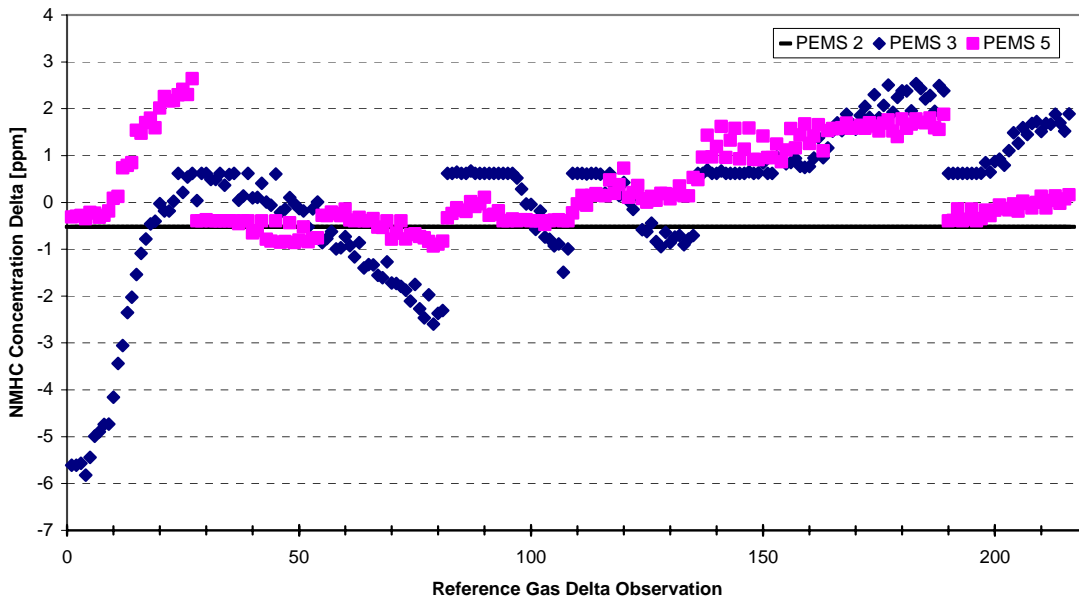
ERROR SURFACE FOR ENVIRONMENTAL TEMPERATURE CO₂ CONCENTRATION AUDIT DELTA MEASUREMENTS



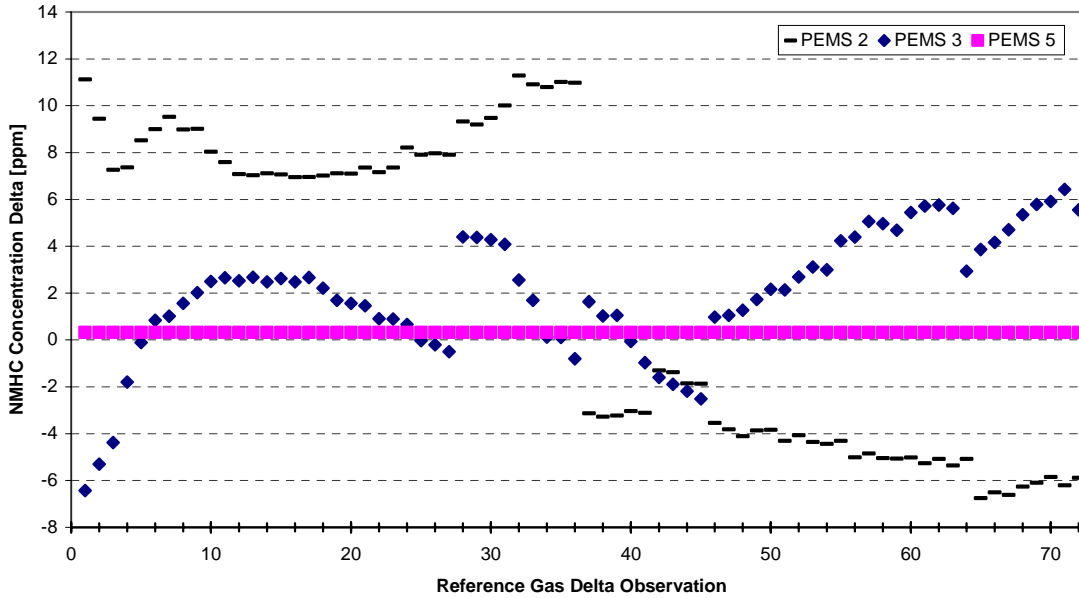
ERROR SURFACE FOR ENVIRONMENTAL TEMPERATURE CO₂ CONCENTRATION SPAN DELTA MEASUREMENTS



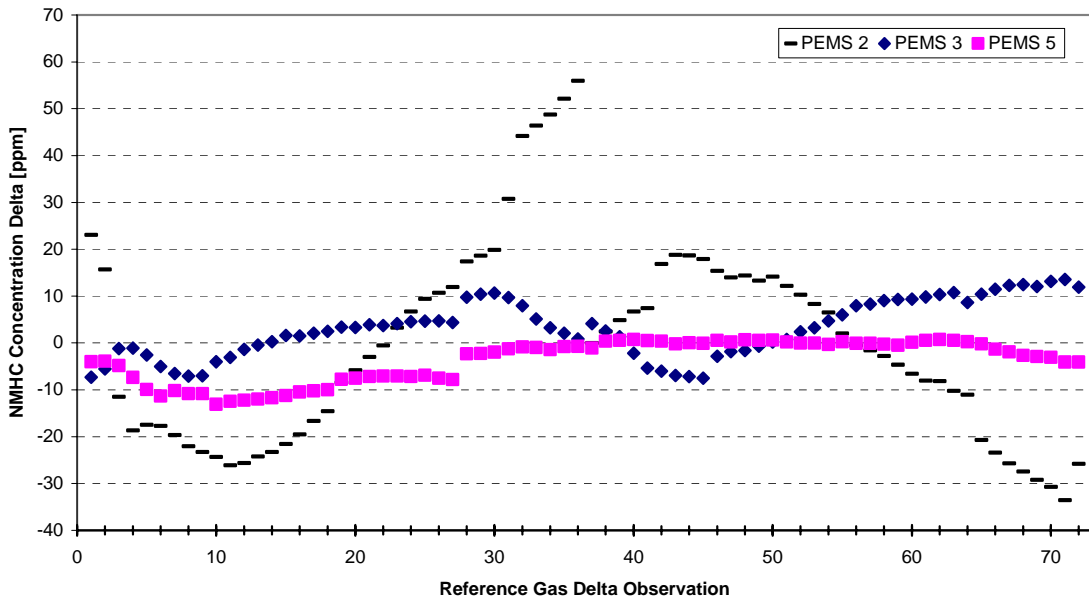
FINAL ERROR SURFACE FOR ENVIRONMENTAL TEMPERATURE CO₂ CONCENTRATION



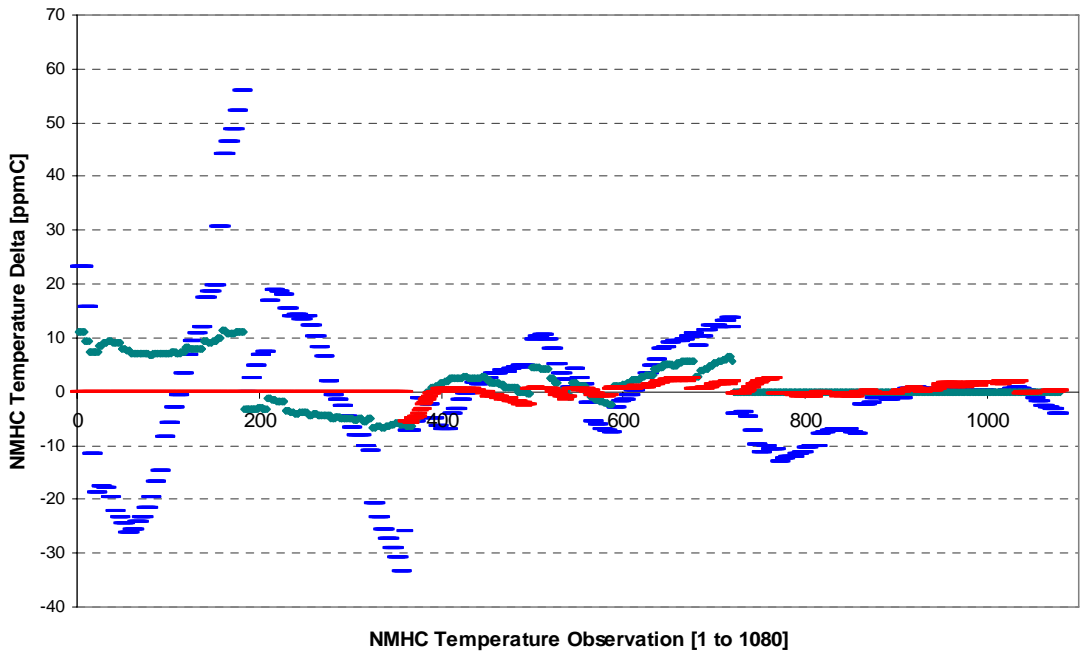
ERROR SURFACE FOR ENVIRONMENTAL TEMPERATURE NMHC CONCENTRATION ZERO DELTA MEASUREMENTS



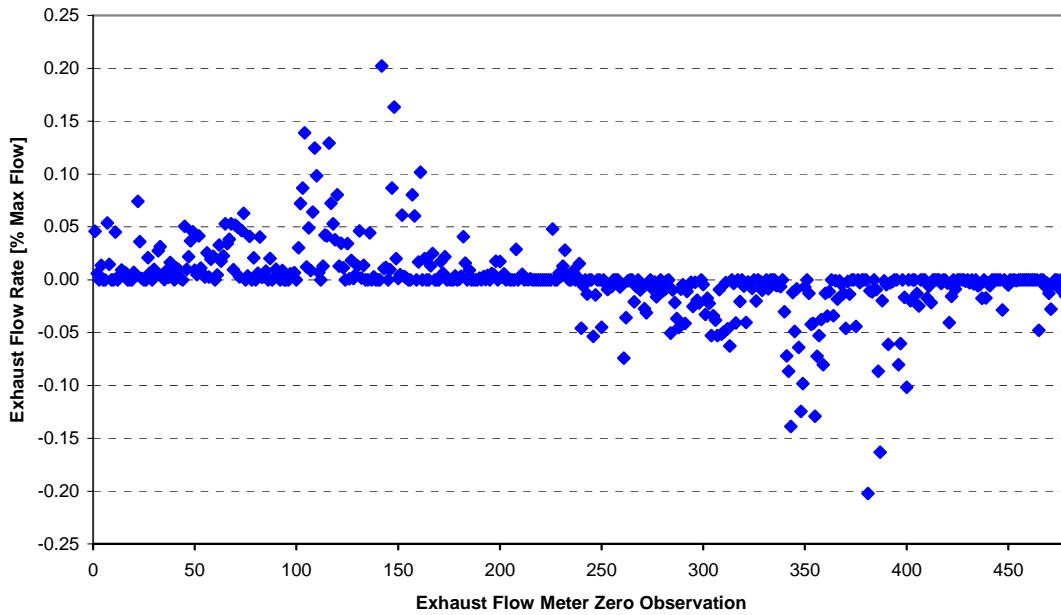
ERROR SURFACE FOR ENVIRONMENTAL TEMPERATURE NMHC CONCENTRATION AUDIT DELTA MEASUREMENTS



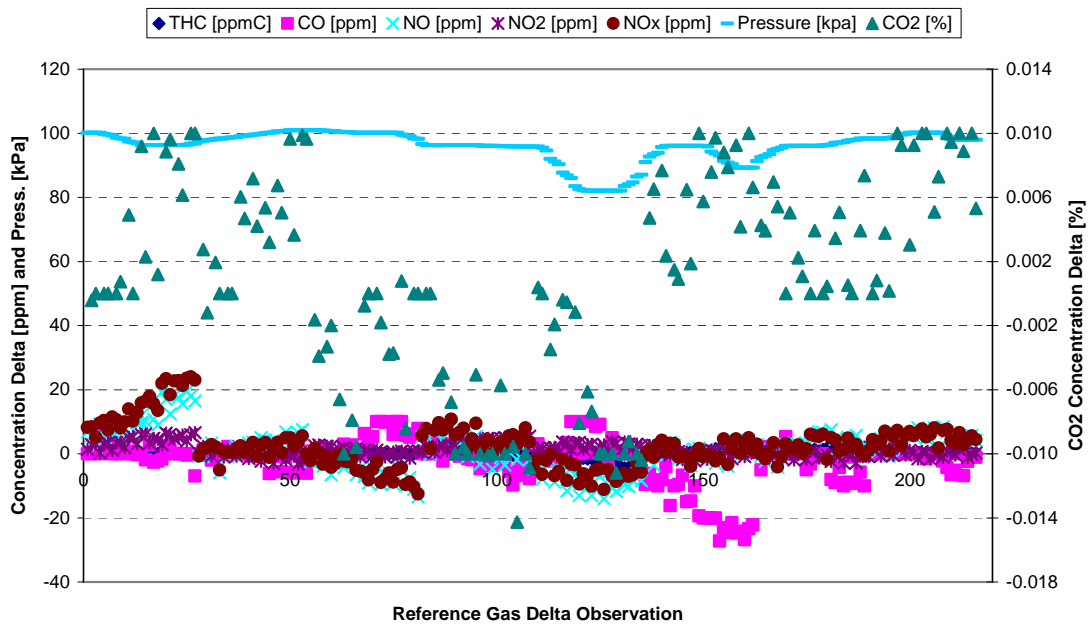
ERROR SURFACE FOR ENVIRONMENTAL TEMPERATURE NMHC CONCENTRATION SPAN DELTA MEASUREMENTS



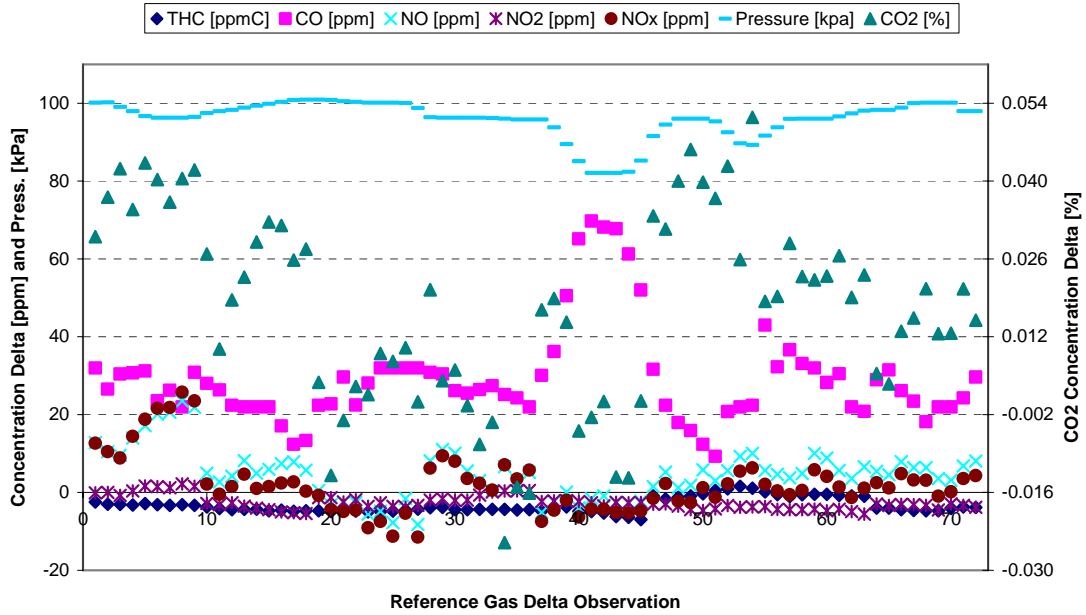
FINAL ERROR SURFACE FOR ENVIRONMENTAL TEMPERATURE NMHC CONCENTRATION



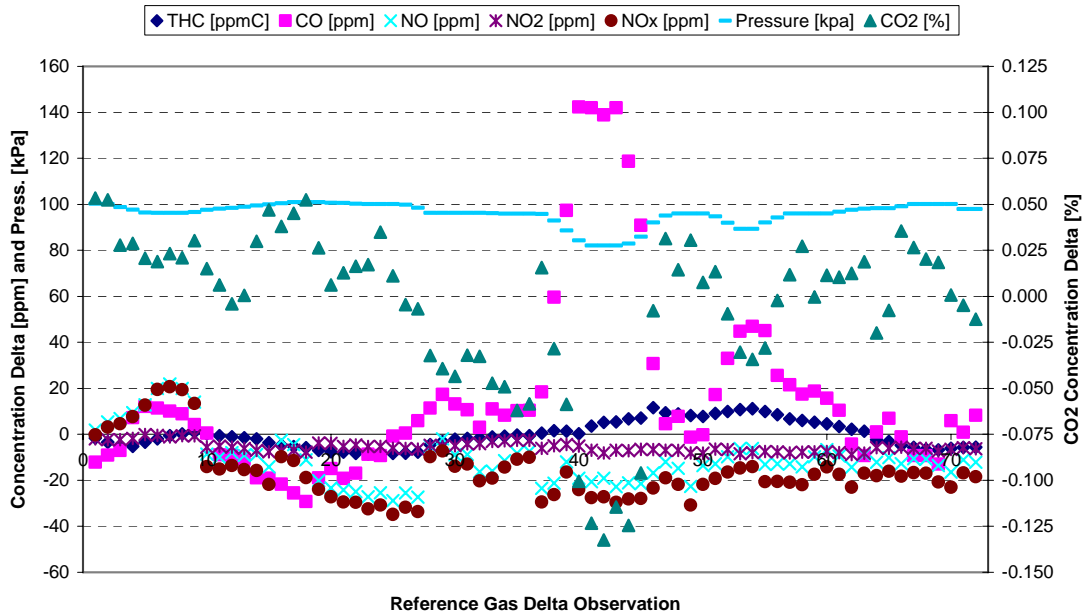
ERROR SURFACE FOR ENVIRONMENTAL TEMPERATURE EXHAUST FLOW RATE DELTA MEASUREMENTS



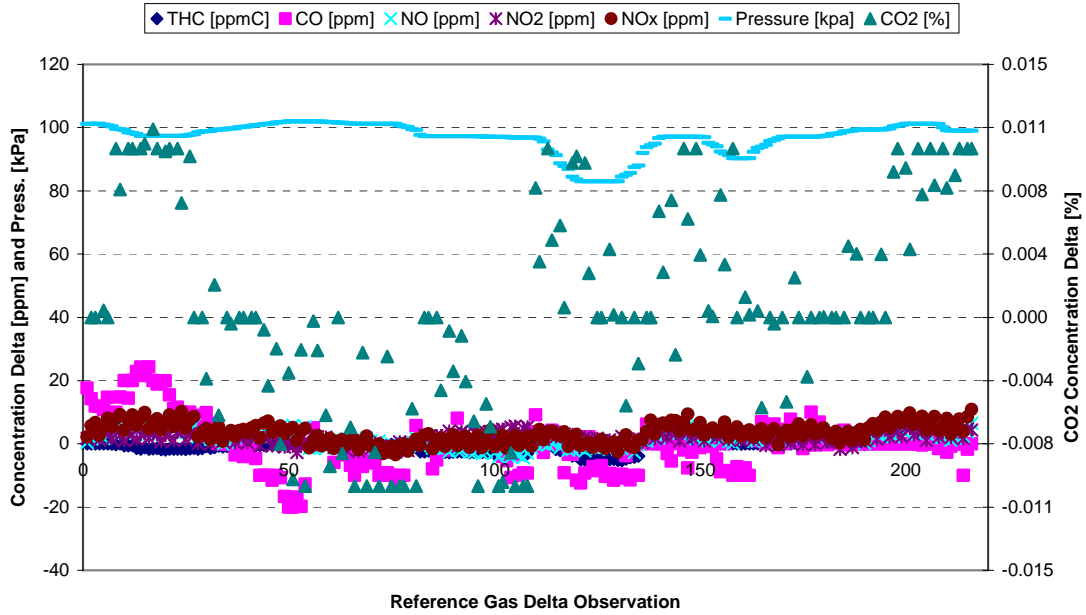
PEMS 2 ENVIRONMENTAL PRESSURE ZERO DELTA MEASUREMENTS



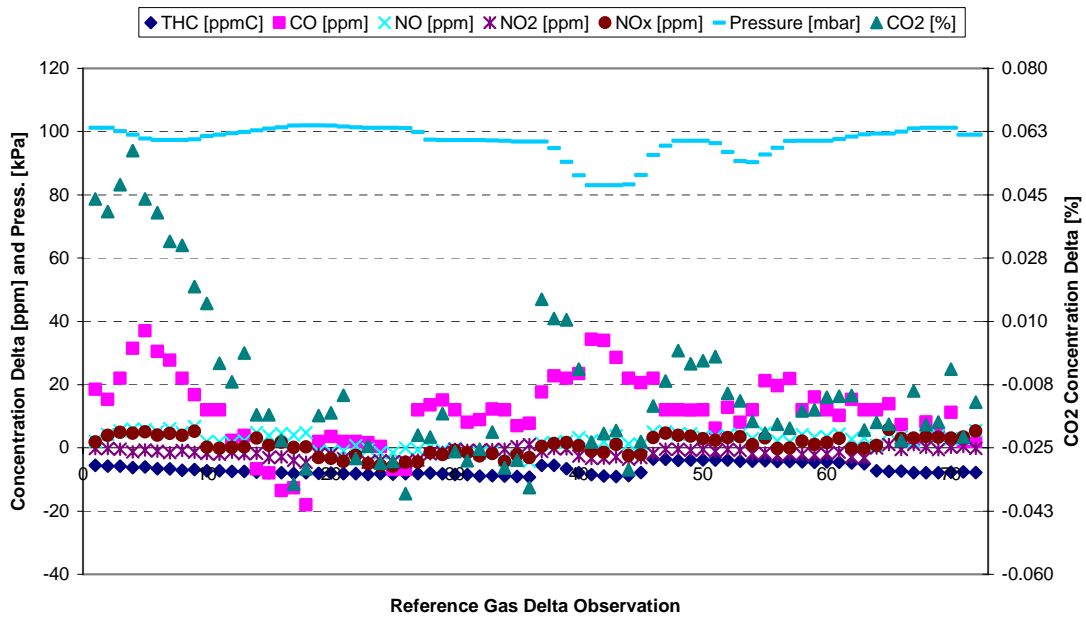
PEMS 2 ENVIRONMENTAL PRESSURE AUDIT DELTA MEASUREMENTS



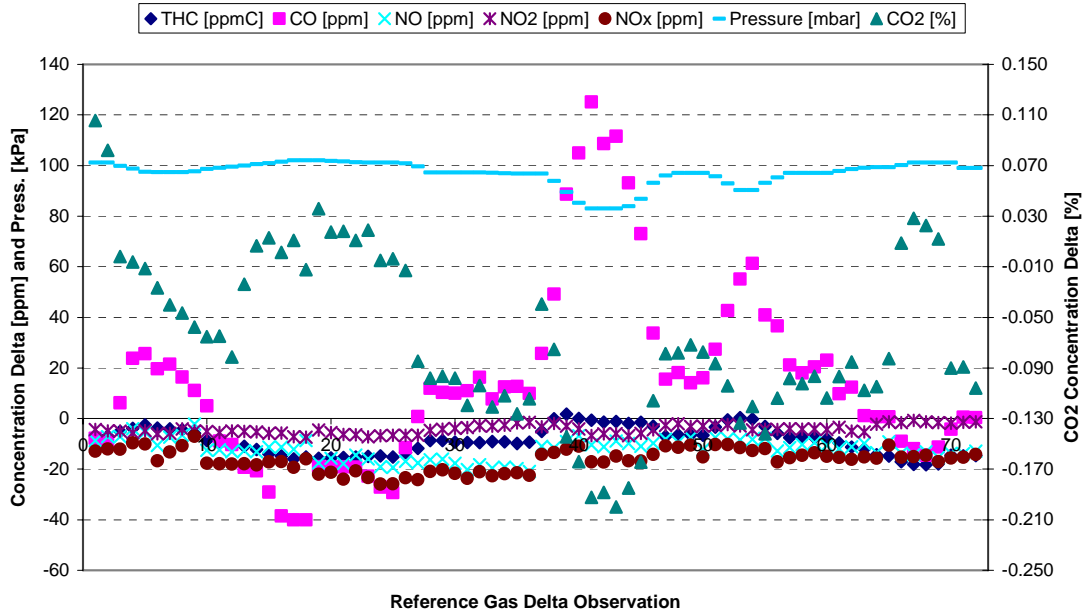
PEMS 2 ENVIRONMENTAL PRESSURE SPAN DELTA MEASUREMENTS



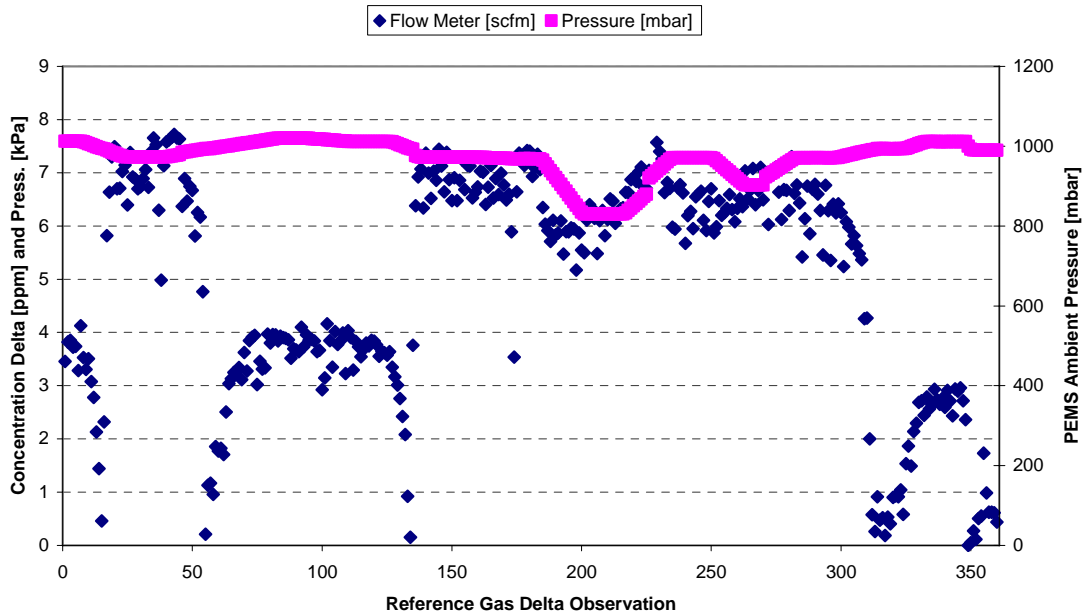
PEMS 3 ENVIRONMENTAL PRESSURE ZERO DELTA MEASUREMENTS



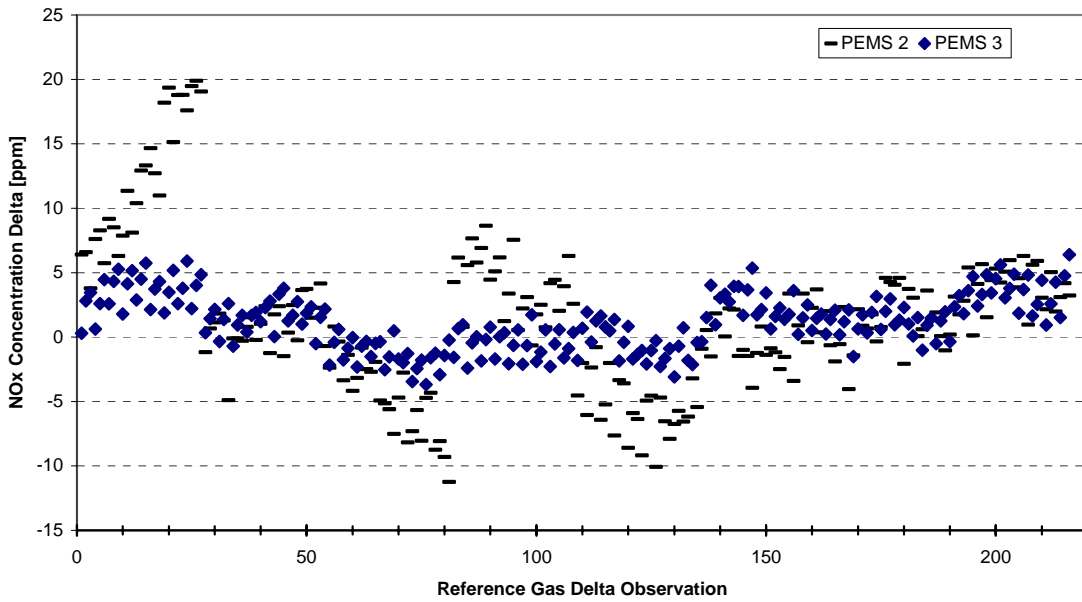
PEMS 3 ENVIRONMENTAL PRESSURE AUDIT DELTA MEASUREMENTS



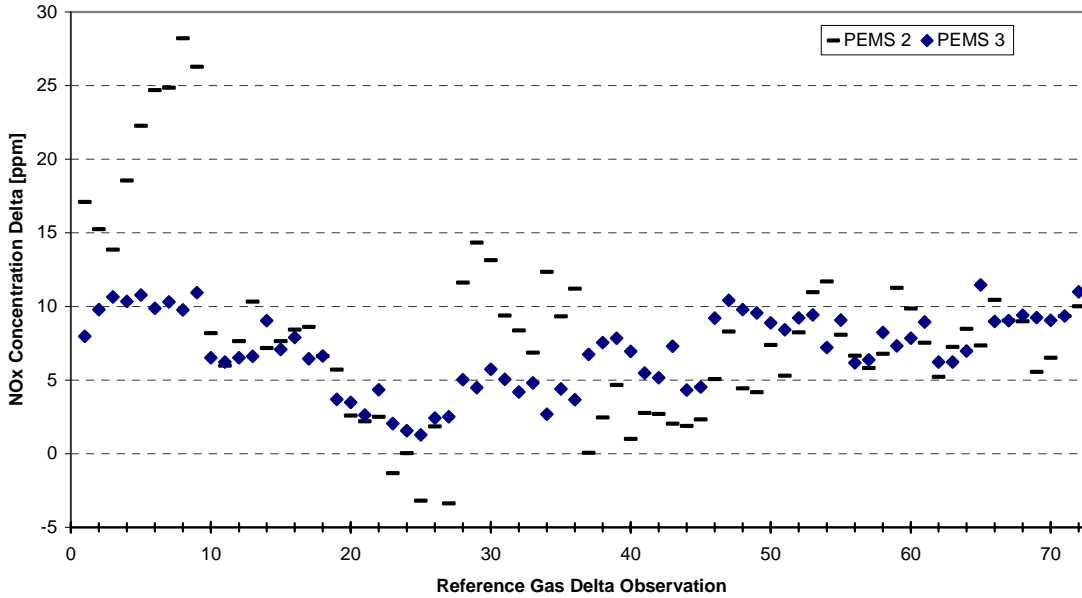
PEMS 3 ENVIRONMENTAL PRESSURE SPAN DELTA MEASUREMENTS



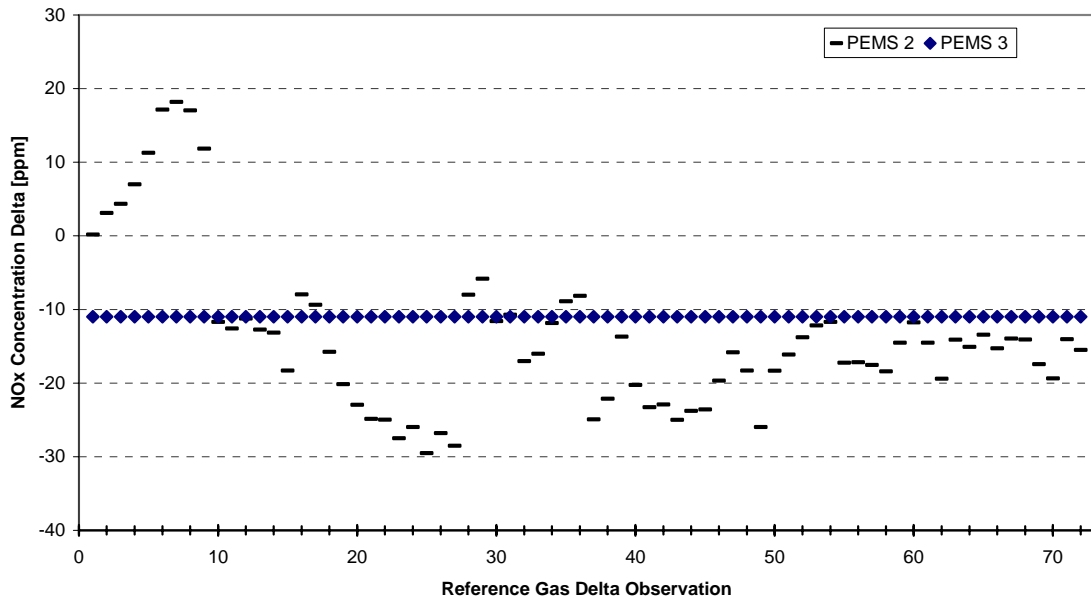
5-INCH EFM ENVIRONMENTAL PRESSURE ZERO DELTA MEASUREMENTS



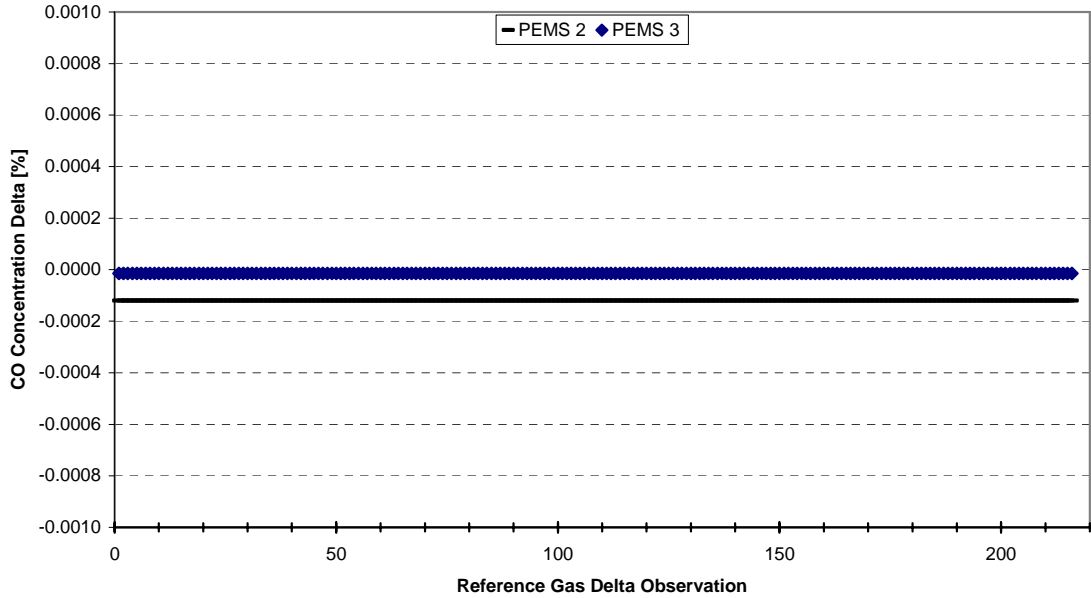
ERROR SURFACE (NOT USED IN THE MODEL) FOR ENVIRONMENTAL PRESSURE NO_x CONCENTRATION ZERO DELTA MEASUREMENTS



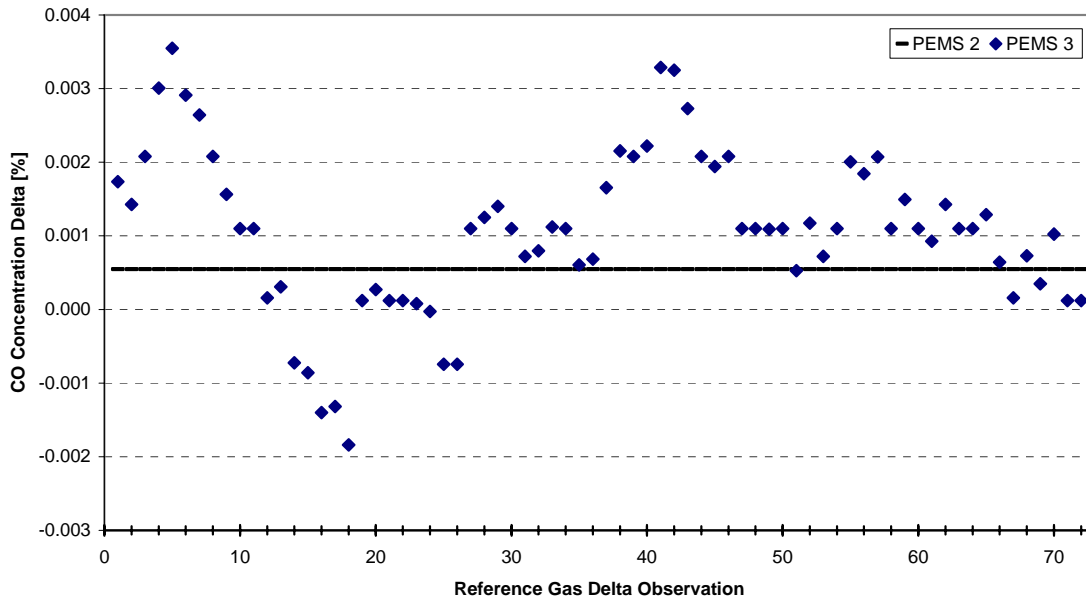
ERROR SURFACE (NOT USED IN THE MODEL) FOR ENVIRONMENTAL PRESSURE NO_x CONCENTRATION AUDIT DELTA MEASUREMENTS



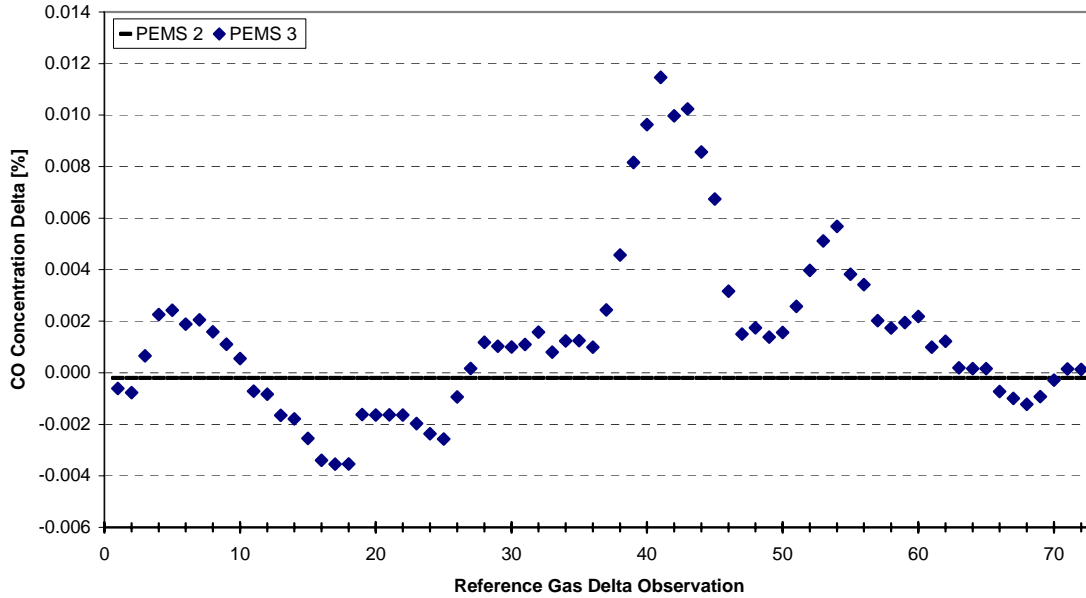
ERROR SURFACE (NOT USED IN THE MODEL) FOR ENVIRONMENTAL PRESSURE NO_x CONCENTRATION SPAN DELTA MEASUREMENTS



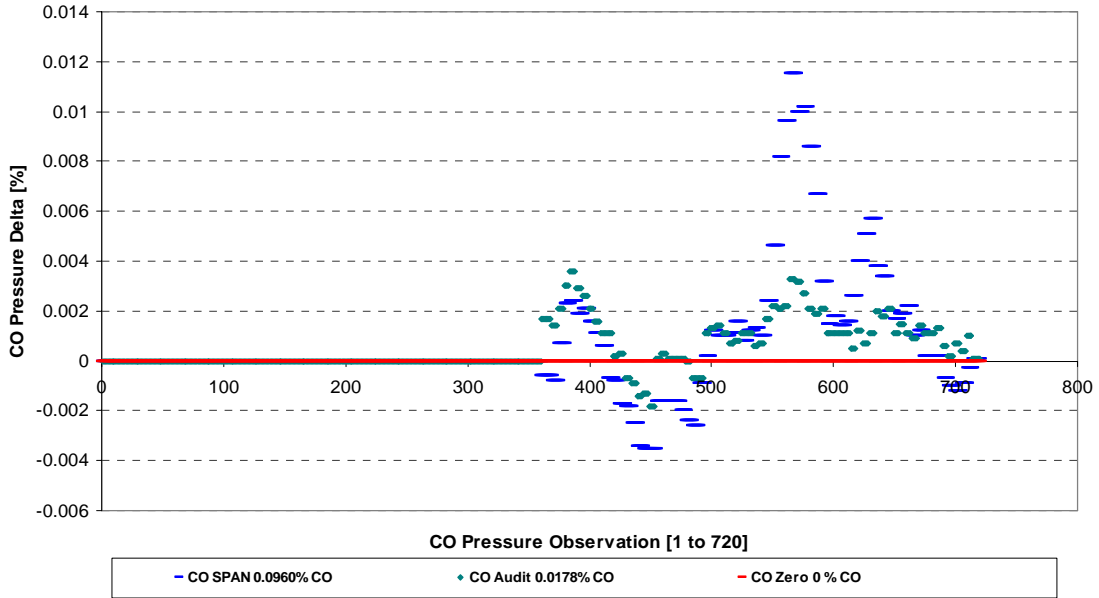
ERROR SURFACE FOR ENVIRONMENTAL PRESSURE CO CONCENTRATION ZERO DELTA MEASUREMENTS



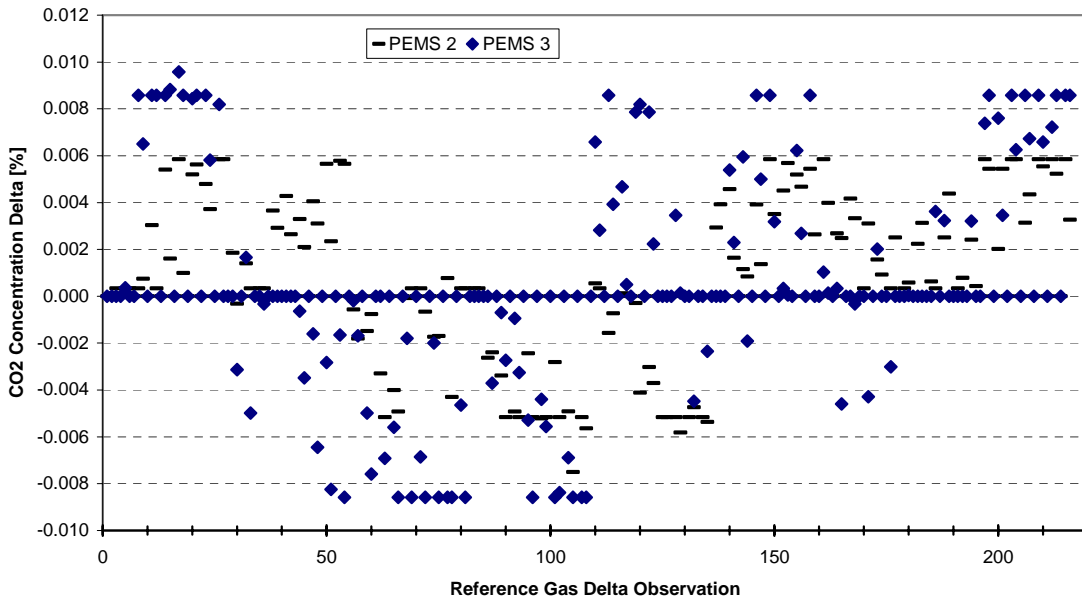
ERROR SURFACE FOR ENVIRONMENTAL PRESSURE CO CONCENTRATION AUDIT DELTA MEASUREMENTS



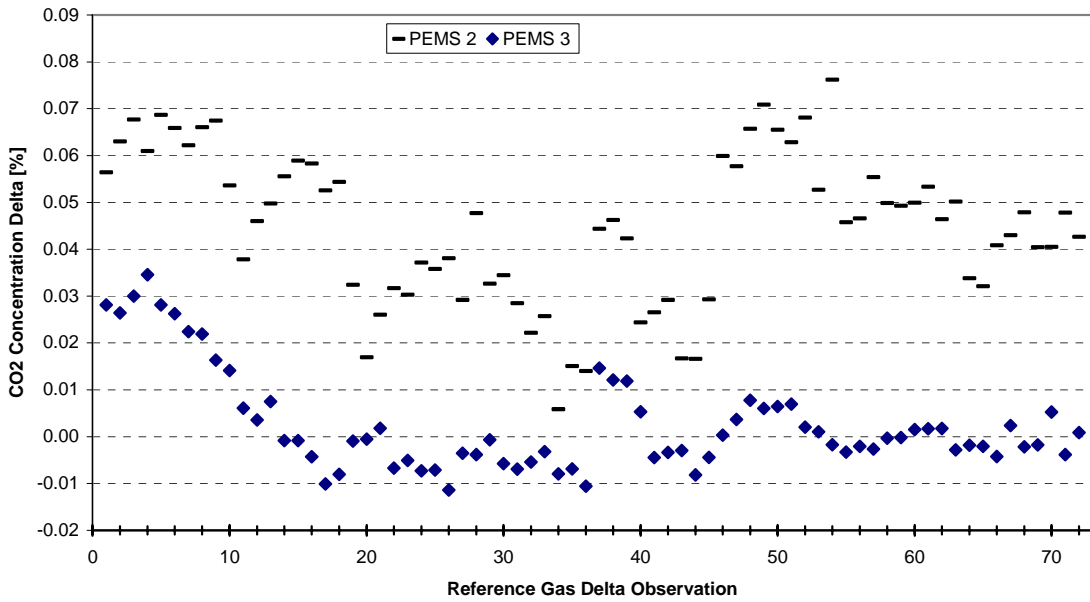
ERROR SURFACE FOR ENVIRONMENTAL PRESSURE CO CONCENTRATION SPAN DELTA MEASUREMENTS



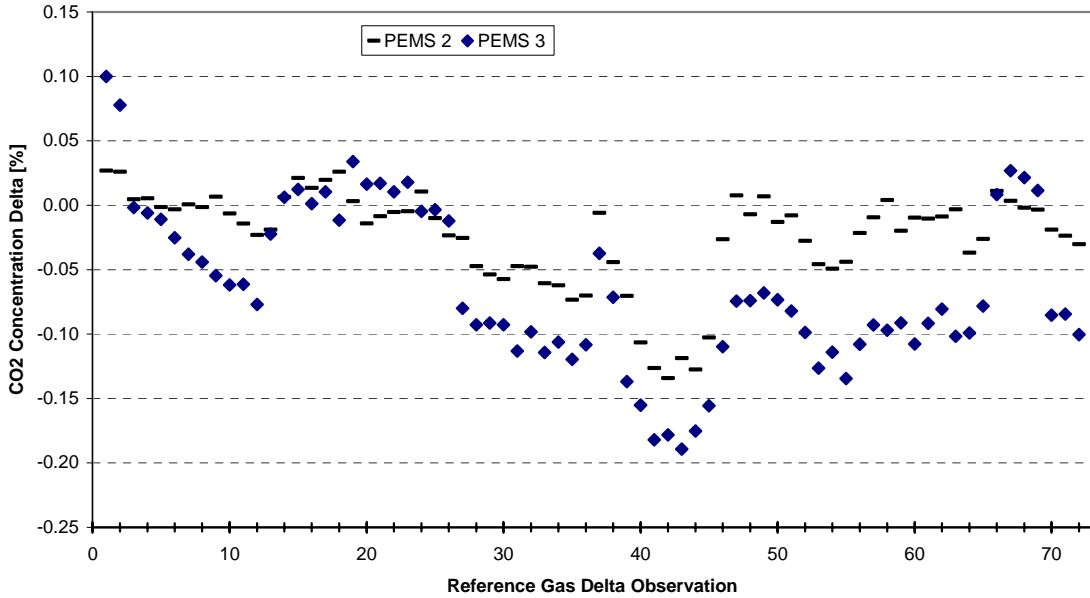
FINAL ERROR SURFACE FOR ENVIRONMENTAL PRESSURE CO CONCENTRATION



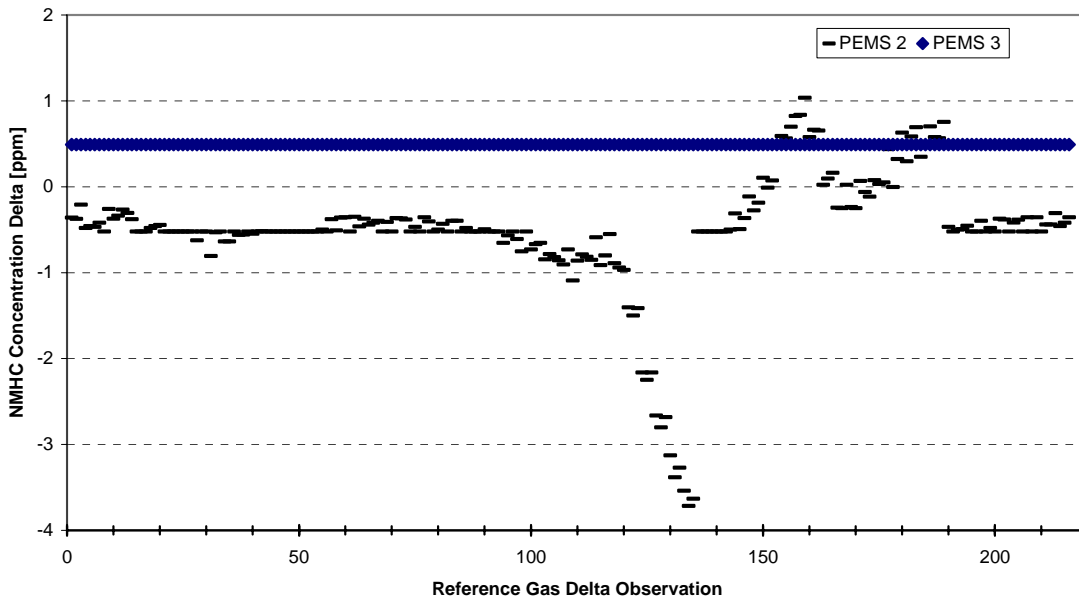
ERROR SURFACE (NOT USED IN THE MODEL) FOR ENVIRONMENTAL PRESSURE CO₂ CONCENTRATION ZERO DELTA MEASUREMENTS



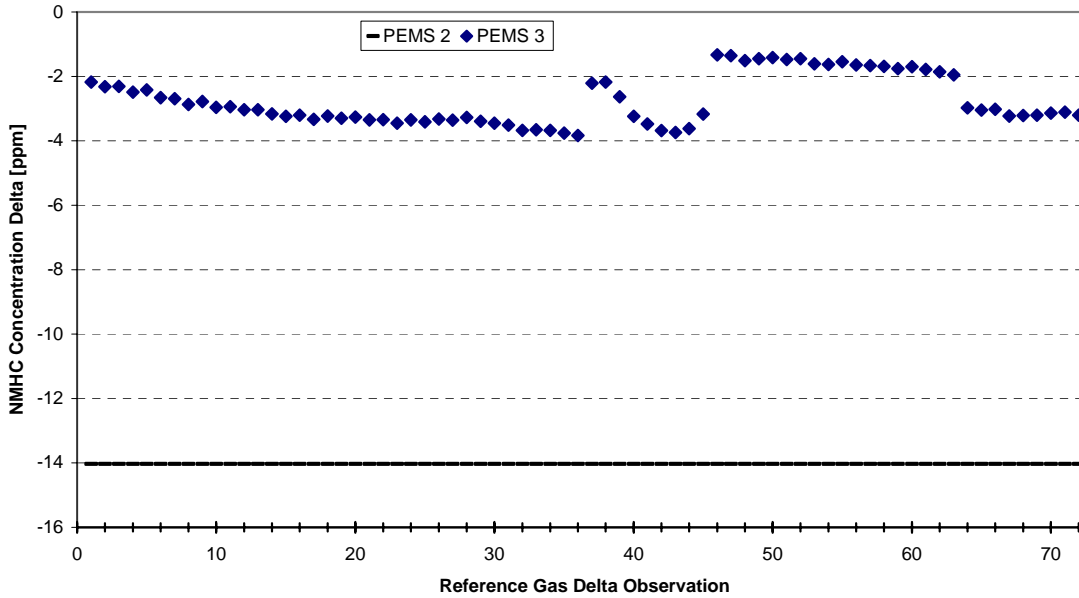
ERROR SURFACE (NOT USED IN THE MODEL) FOR ENVIRONMENTAL PRESSURE CO₂ CONCENTRATION AUDIT DELTA MEASUREMENTS



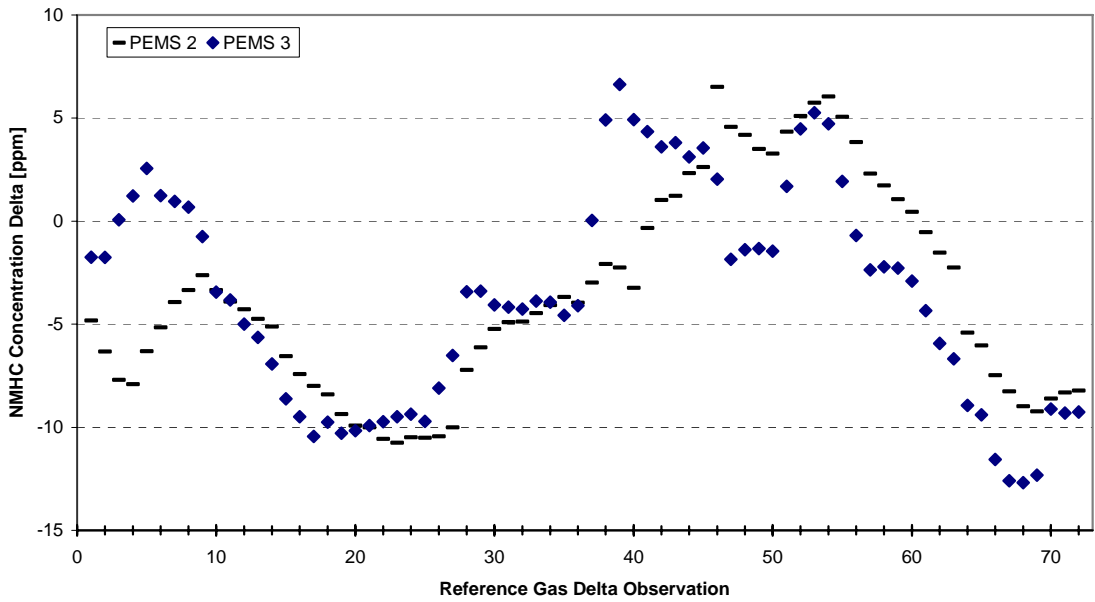
ERROR SURFACE (NOT USED IN THE MODEL) FOR ENVIRONMENTAL PRESSURE CO₂ CONCENTRATION SPAN DELTA MEASUREMENTS



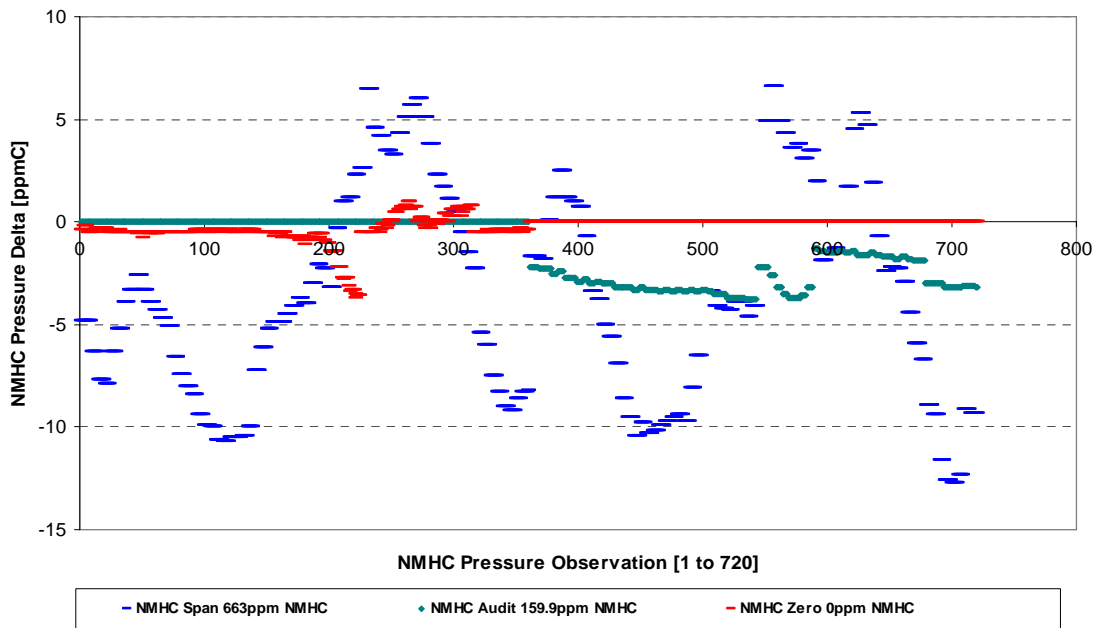
ERROR SURFACE FOR ENVIRONMENTAL PRESSURE NMHC CONCENTRATION ZERO DELTA MEASUREMENTS



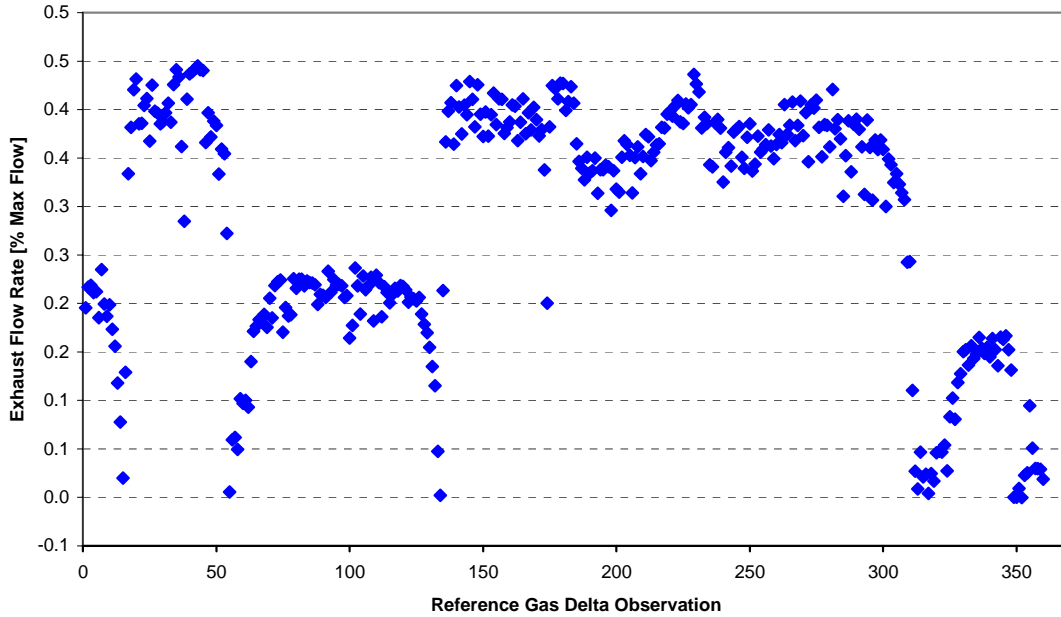
ERROR SURFACE FOR ENVIRONMENTAL PRESSURE NMHC CONCENTRATION AUDIT DELTA MEASUREMENTS



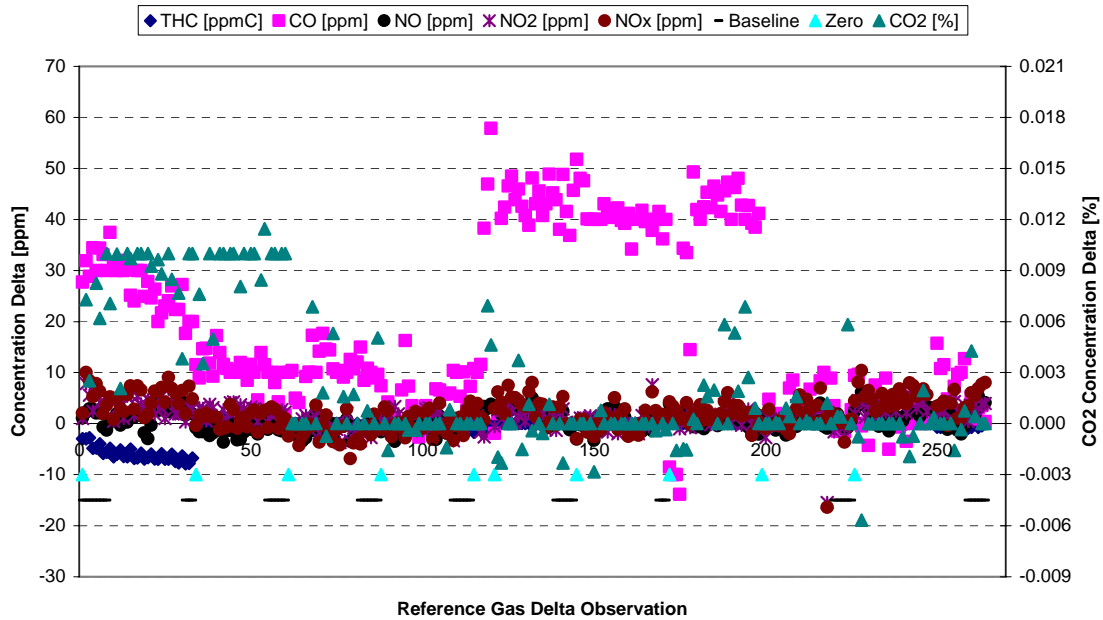
ERROR SURFACE FOR ENVIRONMENTAL PRESSURE NMHC CONCENTRATION SPAN DELTA MEASUREMENTS



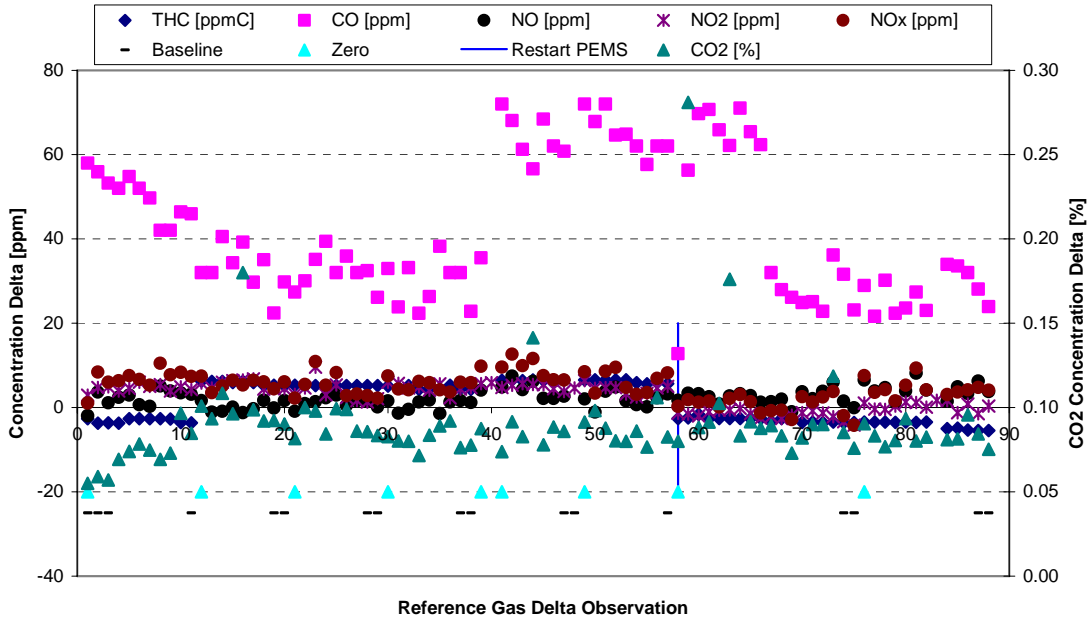
FINAL ERROR SURFACE FOR ENVIRONMENTAL PRESSURE NMHC CONCENTRATION



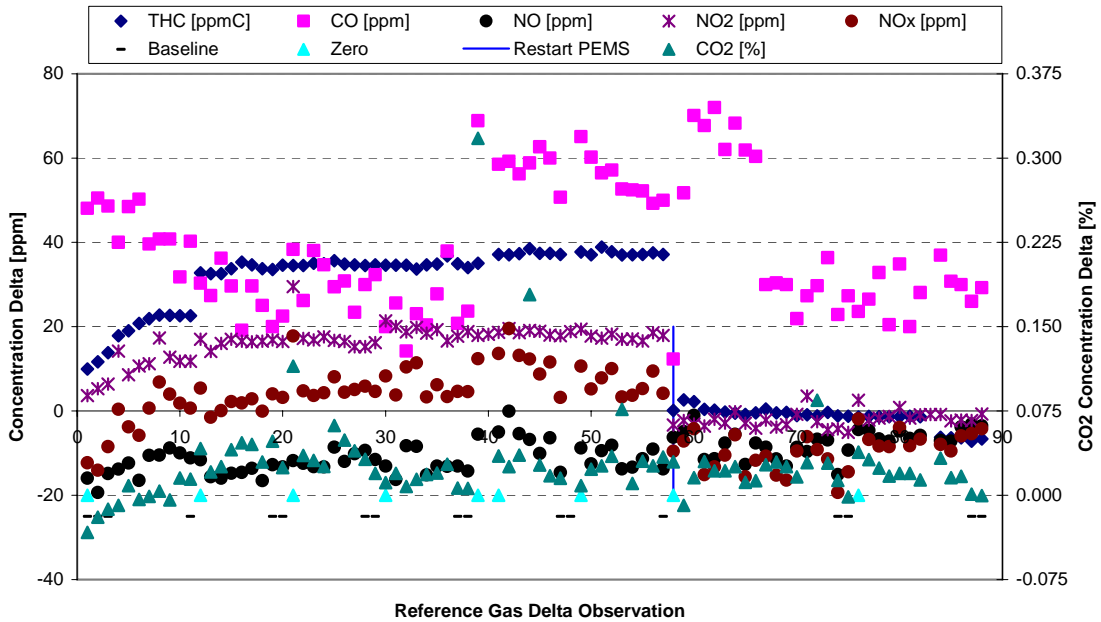
ERROR SURFACE FOR ENVIRONMENTAL TEMPERATURE EXHAUST FLOW RATE DELTA MEASUREMENTS



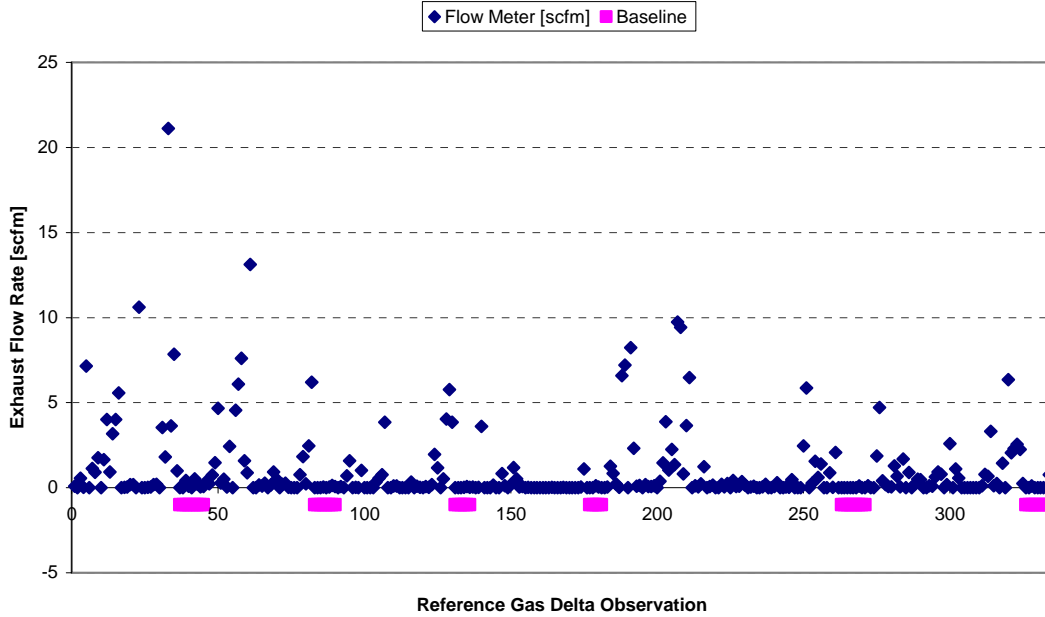
PEMS 7 ENVIRONMENTAL RADIATION BCI ZERO DELTA MEASUREMENTS



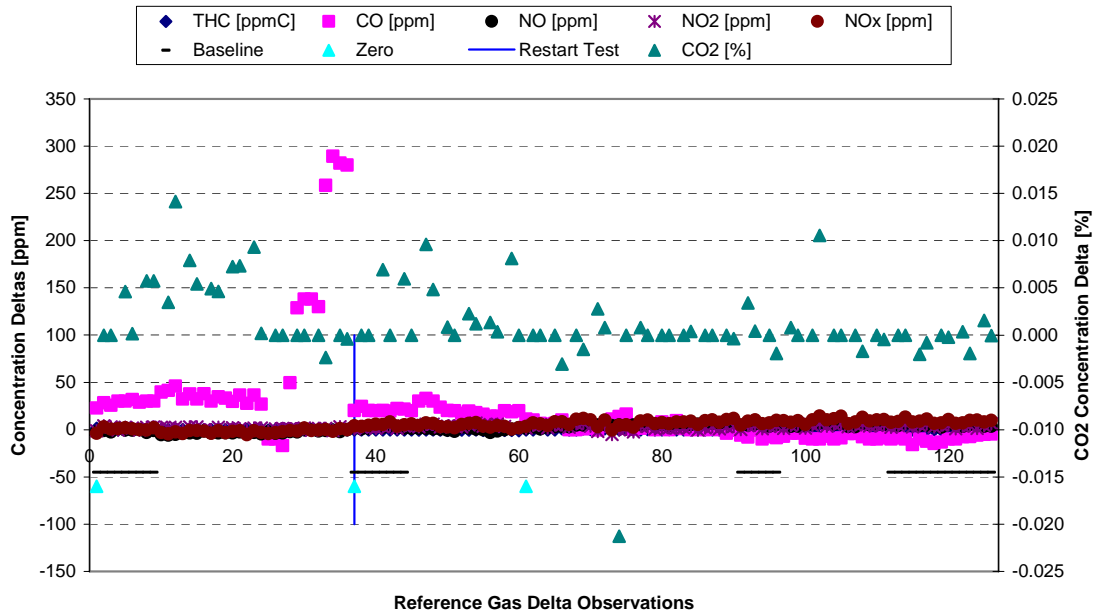
PEMS 7 ENVIRONMENTAL RADIATION BCI AUDIT DELTA MEASUREMENTS



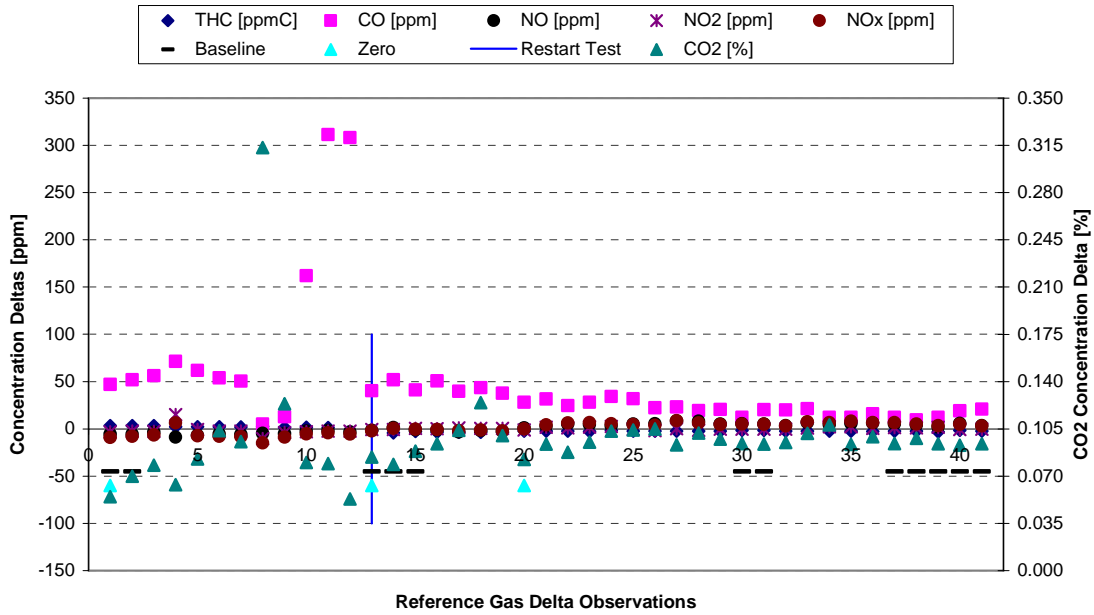
PEMS 7 ENVIRONMENTAL RADIATION BCI SPAN DELTA MEASUREMENTS



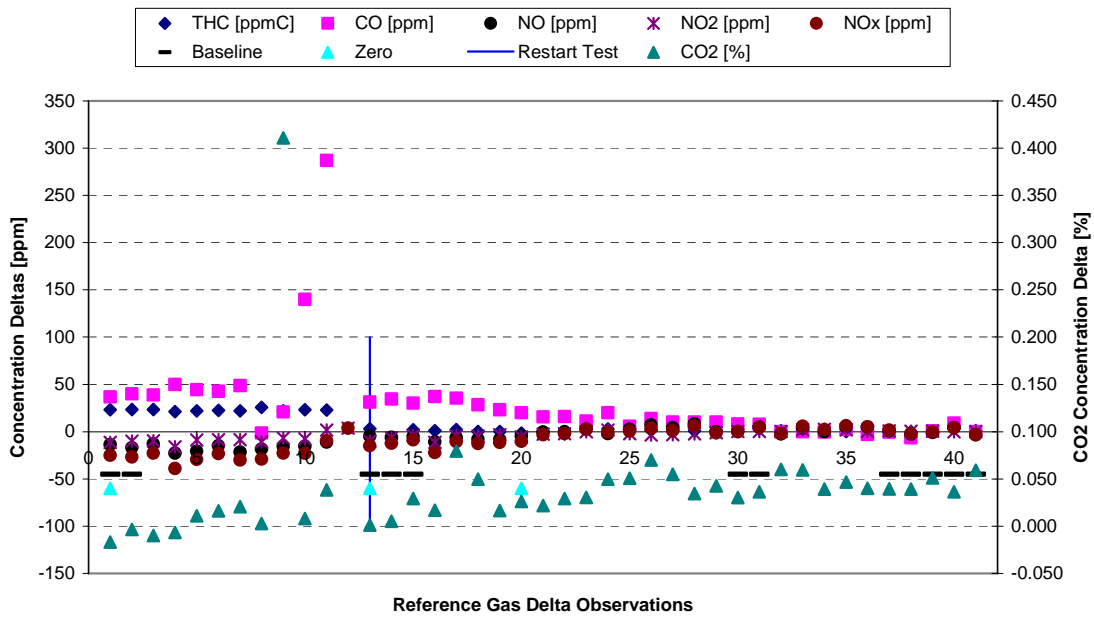
5-INCH EFM ENVIRONMENTAL RADIATION BCI ZERO DELTA MEASUREMENTS



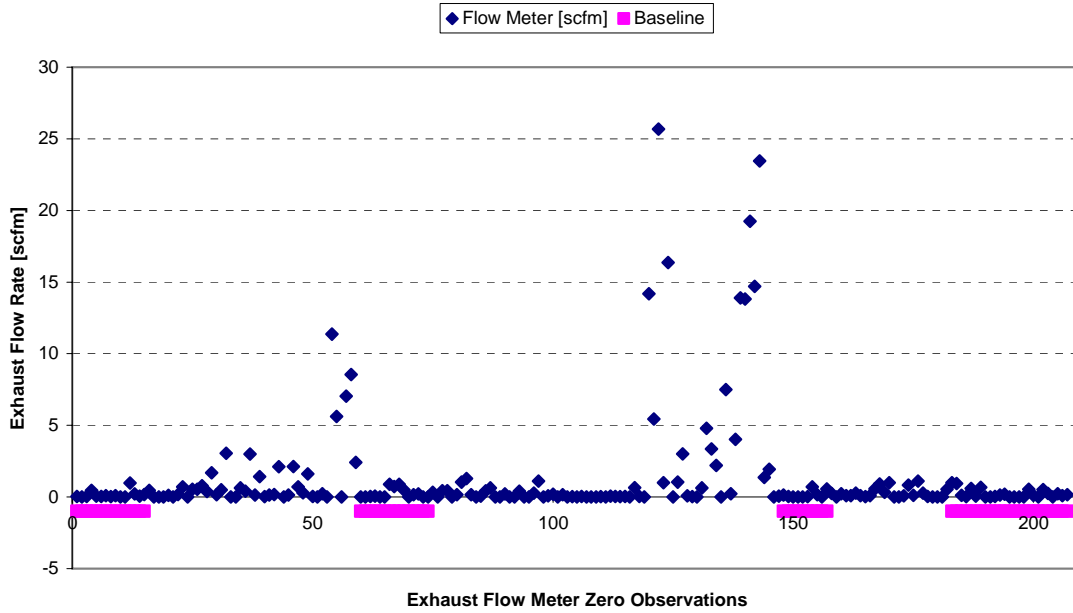
PEMS 7 ENVIRONMENTAL RADIATION RADIATED IMMUNITY ZERO DELTA MEASUREMENTS



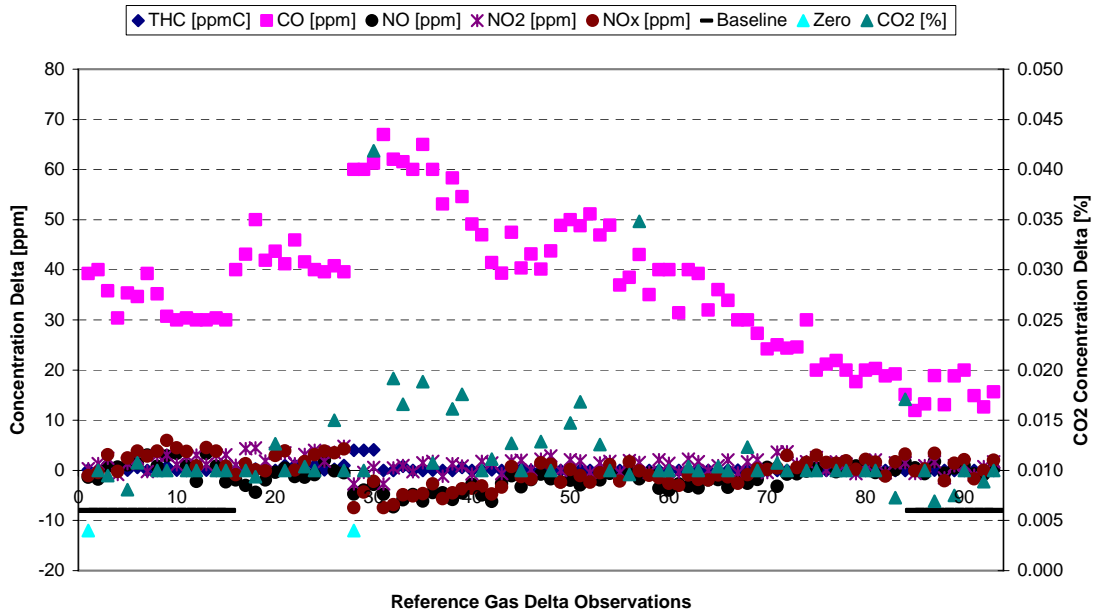
**PEMS 7 ENVIRONMENTAL RADIATION RADIATED IMMUNITY AUDIT
DELTA MEASUREMENTS**



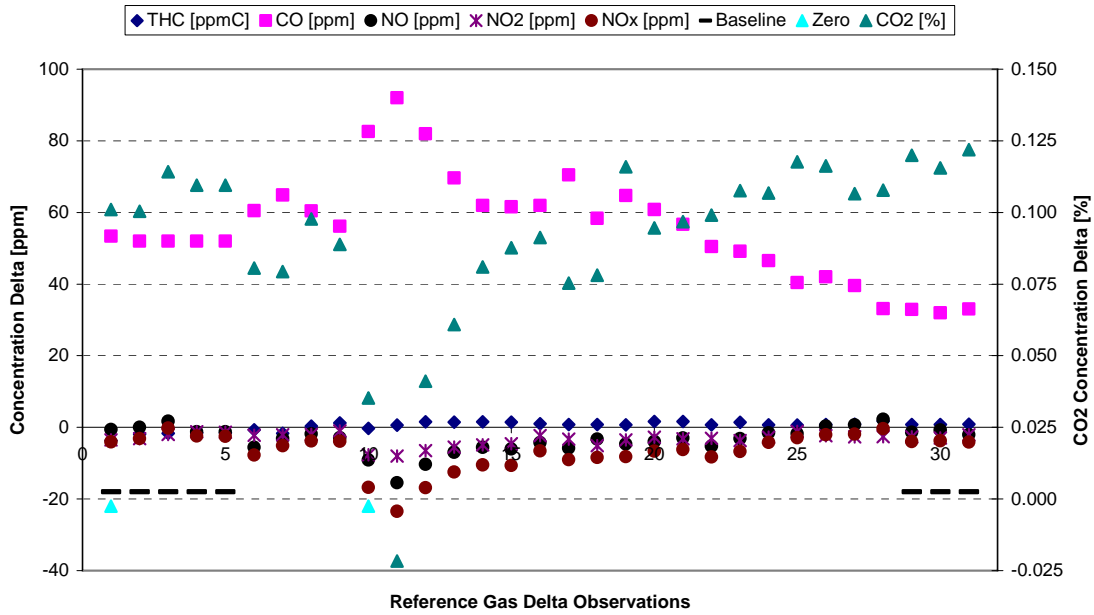
**PEMS 7 ENVIRONMENTAL RADIATION RADIATED IMMUNITY SPAN
DELTA MEASUREMENTS**



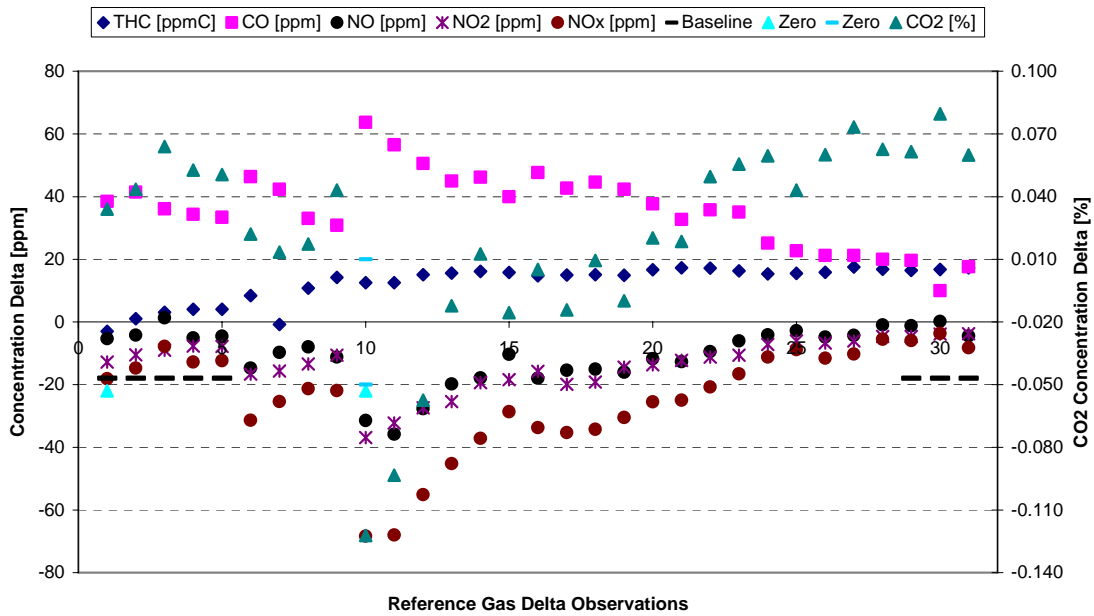
5-INCH EFM ENVIRONMENTAL RADIATION RADIATED IMMUNITY ZERO DELTA MEASUREMENTS



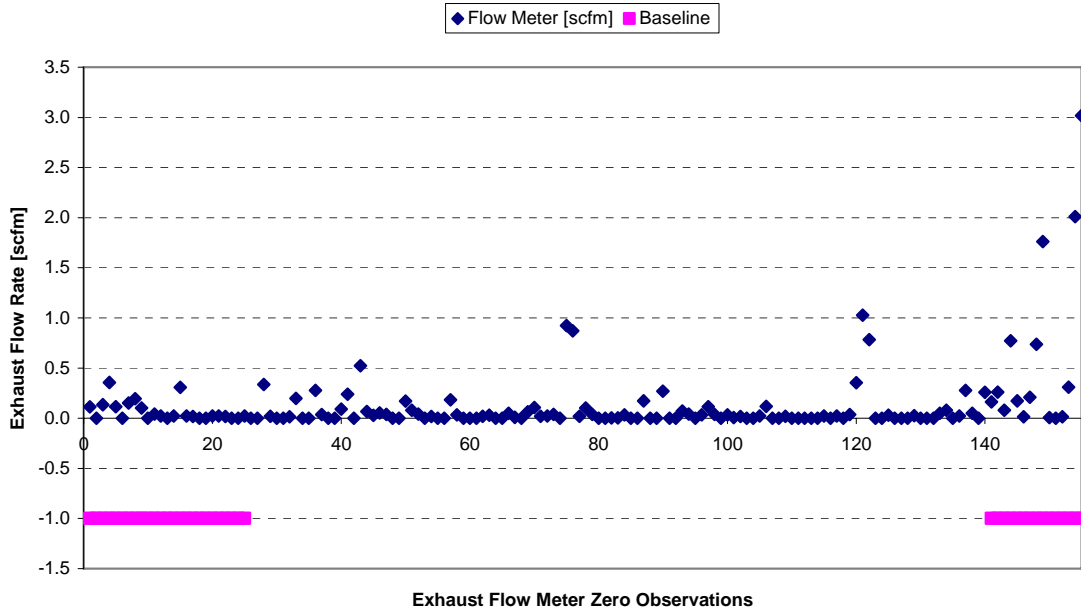
PEMS 7 ENVIRONMENTAL RADIATION ELECTROSTATIC DISCHARGE ZERO DELTA MEASUREMENTS



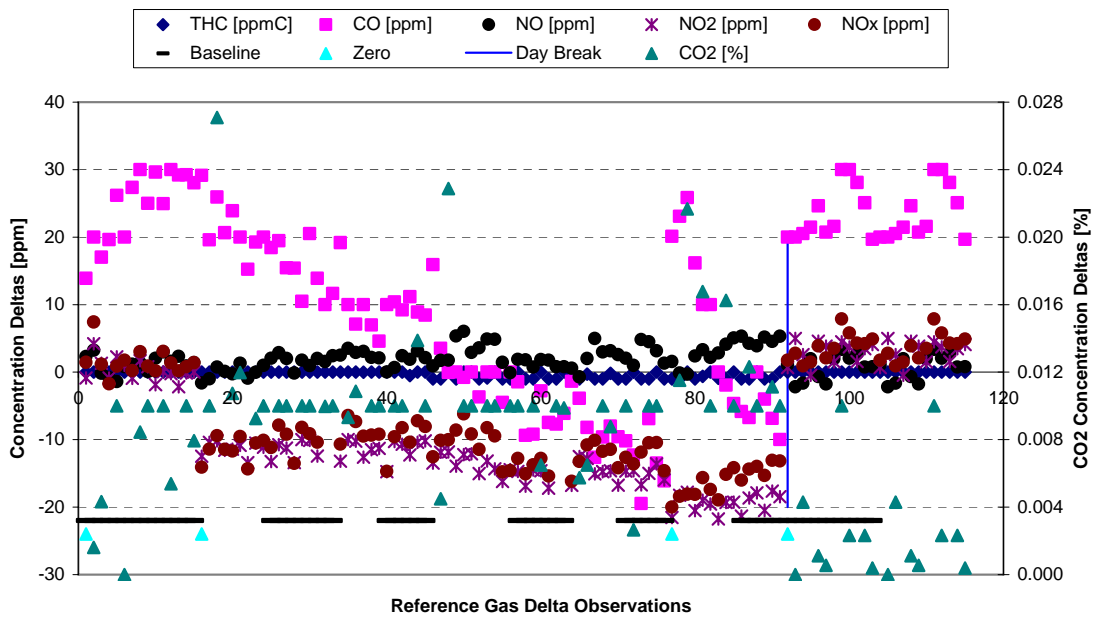
**PEMS 7 ENVIRONMENTAL RADIATION ELECTROSTATIC DISCHARGE
AUDIT DELTA MEASUREMENTS**



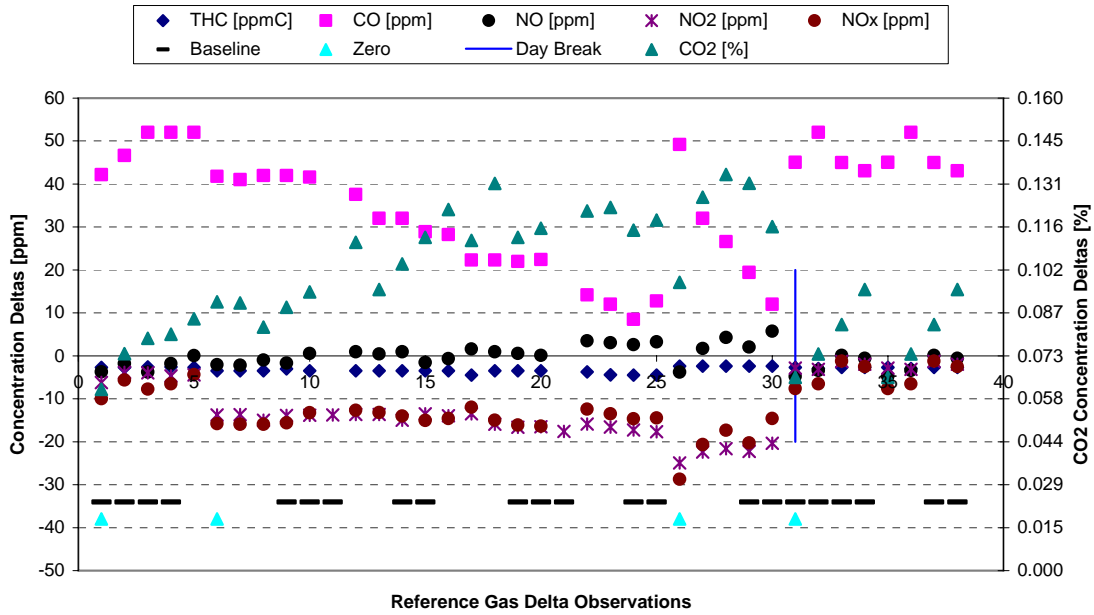
**PEMS 7 ENVIRONMENTAL RADIATION ELECTROSTATIC DISCHARGE
SPAN DELTA MEASUREMENTS**



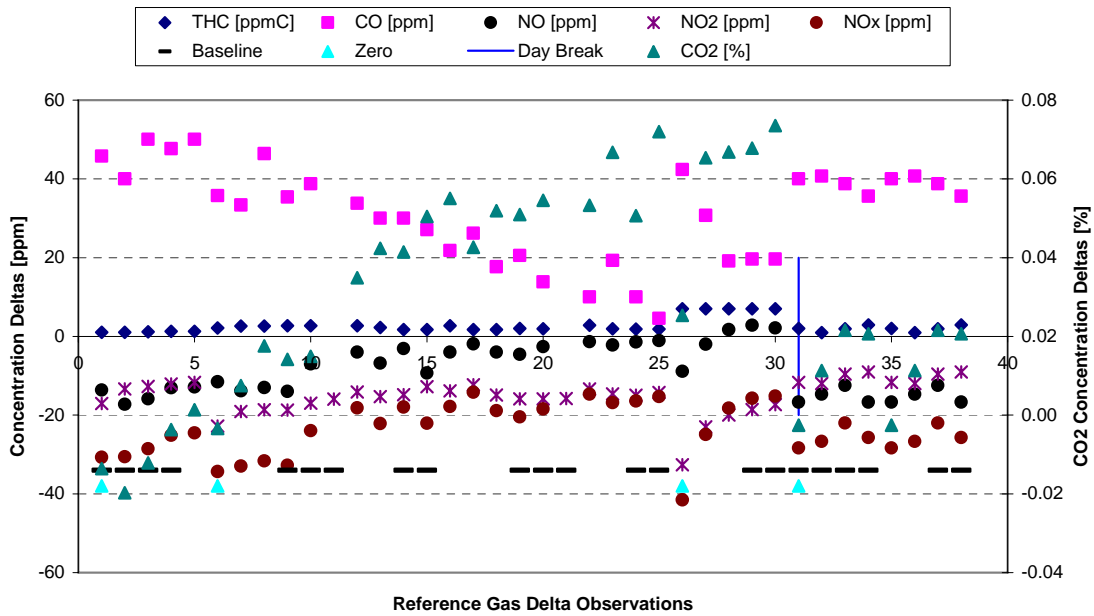
5-INCH EFM ENVIRONMENTAL RADIATION ELECTROSTATIC DISCHARGE ZERO DELTA MEASUREMENTS



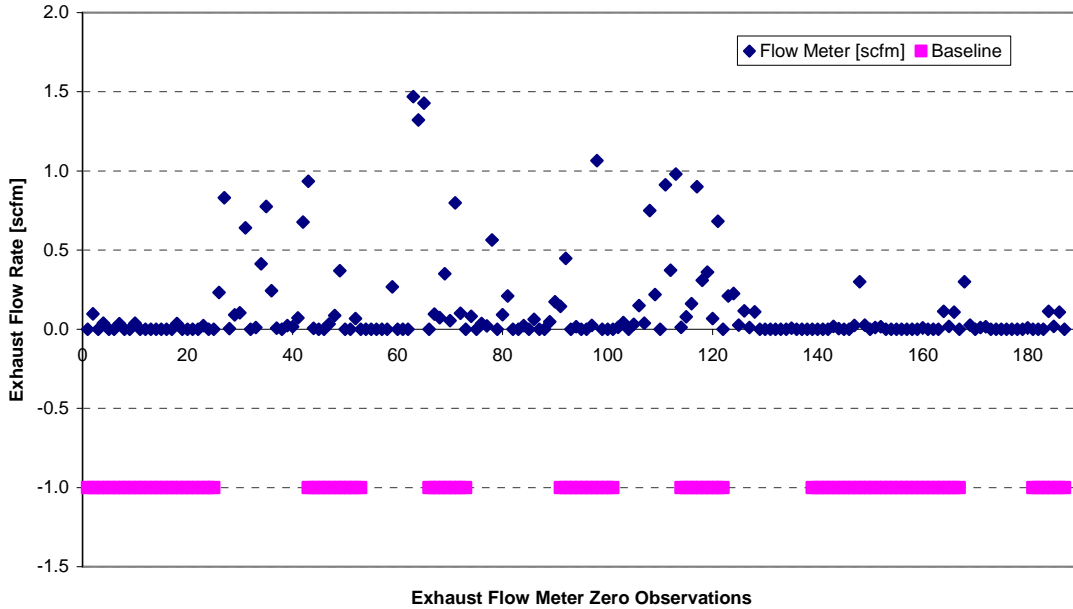
PEMS 7 ENVIRONMENTAL RADIATION CONDUCTED TRANSIENT ZERO DELTA MEASUREMENTS



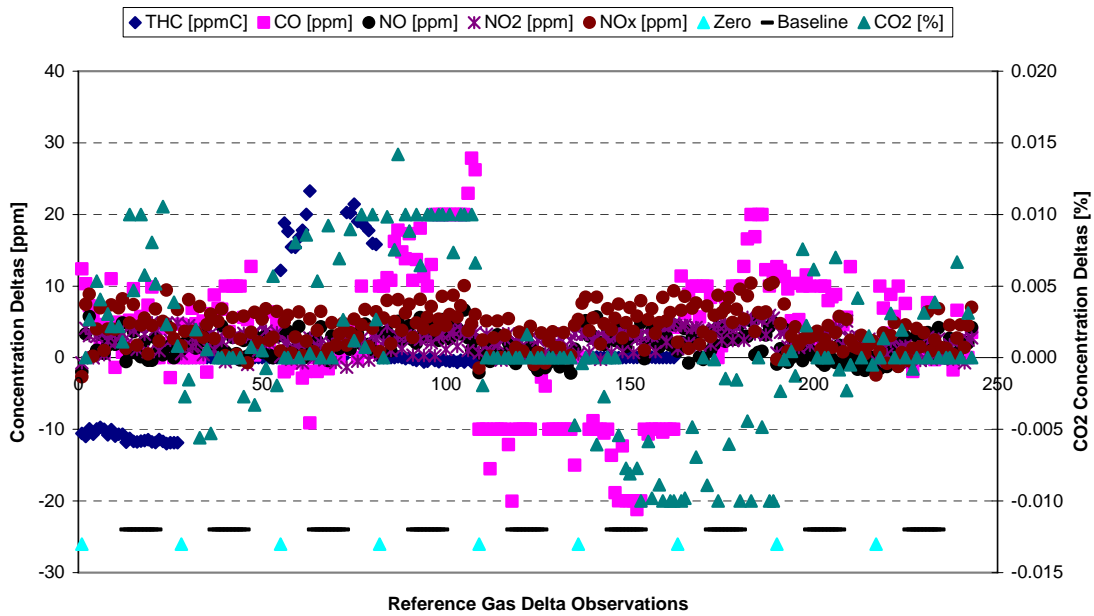
**PEMS 7 ENVIRONMENTAL RADIATION CONDUCTED TRANSIENT AUDIT
DELTA MEASUREMENTS**



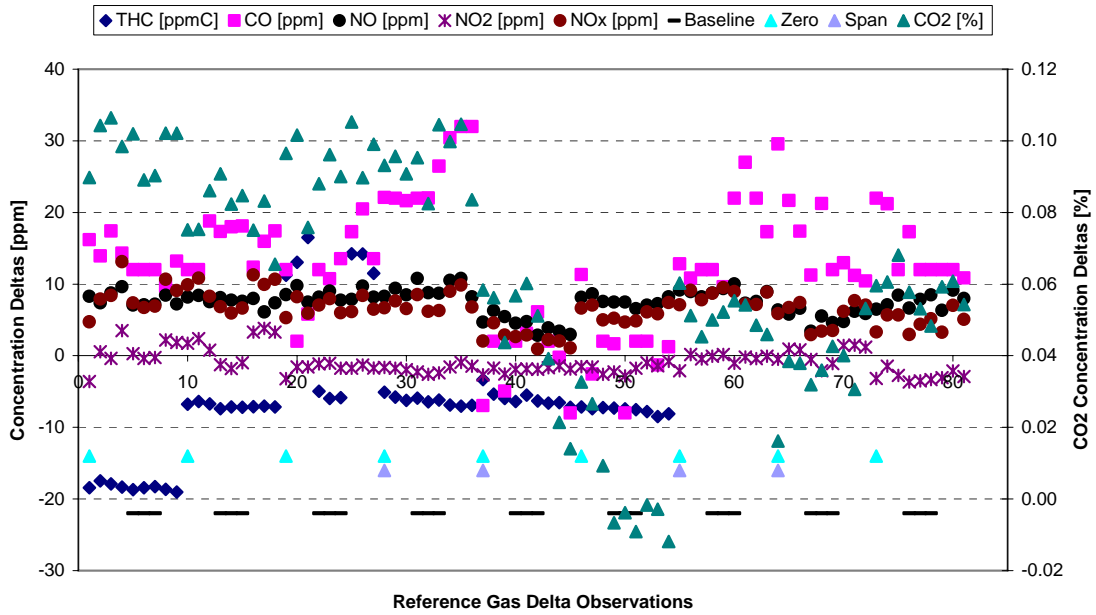
**PEMS 7 ENVIRONMENTAL RADIATION CONDUCTED TRANSIENT SPAN
DELTA MEASUREMENTS**



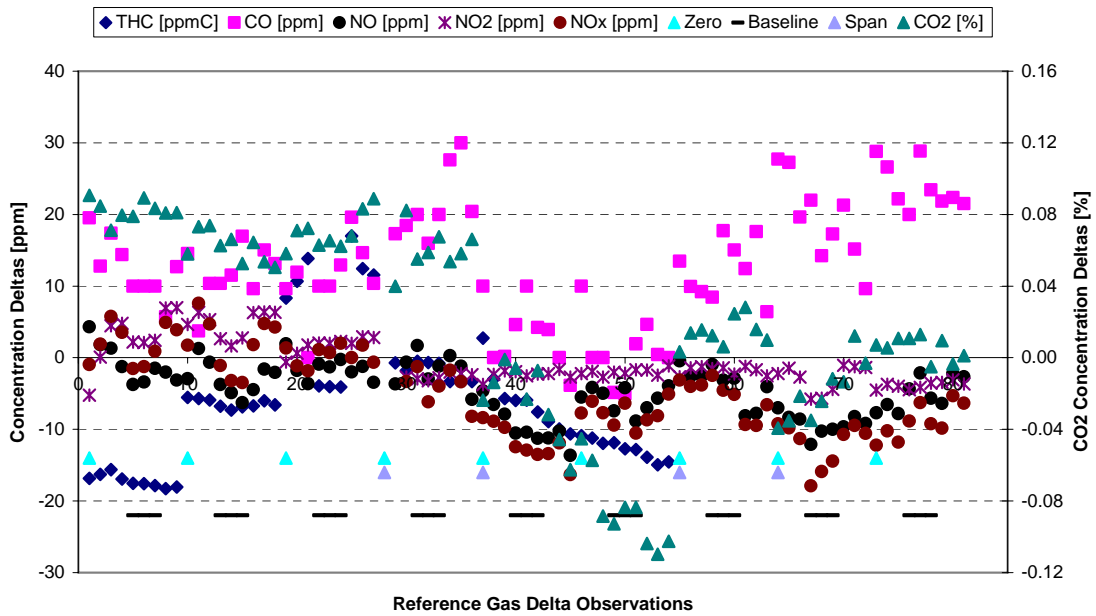
5-INCH EFM ENVIRONMENTAL RADIATION CONDUCTED TRANSIENT ZERO DELTA MEASUREMENTS



PEMS 3 ENVIRONMENTAL VIBRATION ZERO DELTA MEASUREMENTS



PEMS 3 ENVIRONMENTAL VIBRATION AUDIT DELTA MEASUREMENTS



PEMS 3 ENVIRONMENTAL VIBRATION SPAN DELTA MEASUREMENTS

APPENDIX L
MEASUREMENT ALLOWANCE TEST PLAN
FINAL VERSION – OCTOBER, 2005

Test Plan to Determine PEMS Measurement
Allowances for the Gaseous Emissions
Regulated under the Manufacturer-Run
Heavy-Duty Diesel Engine In-Use Testing
Program

Developed by:

United States Environmental Protection Agency,
California Air Resources Board, and
Engine Manufacturers Association

October 25, 2005

Executive Summary

This test plan sets forth the agreed upon processes and methodologies to be utilized to develop additive, brake-specific, data-driven measurement allowances for gaseous emissions measured by PEMS (NO_x, NMHC and CO) as required under the HDIUT regulatory program. A separate test plan will be developed and agreed upon for the determination of the PM measurement allowance.

As detailed in this test plan, there is a clear consensus on what components of measurement error are intended to be covered by the measurement allowances. Namely, the allowances are to be calculated in a manner that subtracts lab error from PEMS error. Specifically, utilizing Part 1065 compliant emissions measurement systems and procedures for both the lab and PEMS, the lab error associated with measuring heavy-duty engine emissions at stabilized steady-state test points within the NTE zone, sampled over 30-second durations will be subtracted from the PEMS error associated with measuring heavy-duty engine emissions utilizing PEMS over 30-second transient NTE sampling events under a broad range of environmental conditions. This subtraction will yield “PEMS minus laboratory” measurement allowances. The error model will not subtract any laboratory accuracy or precision that is determined from laboratory measurements of transient ~30-second NTE events. The experimental methods and procedures specified in this test plan for determining, modeling, and comparing each of the various components of measurement error are designed to generate statistically robust data-driven measurement allowances for each of the gaseous emissions, namely NO_x, NMHC, and CO.

Successful completion of this test plan is part of the resolution of a 2001 suit filed against EPA by EMA and a number of individual engine manufacturers. The suit challenged, among other things, certain supplemental emission requirements referred to as “not-to-exceed” (NTE) standards. On June 3, 2003, the parties finalized a settlement of their disputes pertaining to the NTE standards. The parties agreed upon a detailed outline for a future regulation that would require a manufacturer-run heavy-duty in-use NTE testing (“HDIUT”) program for diesel-fueled engines and vehicles. One section of the outline stated:

“The NTE Threshold will be the NTE standard, including the margins built into the existing regulations, plus additional margin to account for in-use measurement accuracy. This additional margin shall be determined by the measurement processes and methodologies to be developed and approved by EPA/CARB/EMA. This margin will be structured to encourage instrument manufacturers to develop more and more accurate instruments in the future.”

Given the foregoing, the work to be completed under this test plan is a vital component to the fulfillment of the settlement agreement, and it is vital to the successful implementation of a fully-enforceable HDIUT program. Because of this significance, it is critically important that the work detailed in this test plan be carried out in as thorough, careful and timely a manner as possible.

Table of Contents

1	Introduction.....	6
2	Monte Carlo Error Model and Measurement Allowance	8
2.1	Objective.....	8
2.2	Background.....	8
2.3	Methods and Materials.....	13
2.4	Data Analysis.....	13
3	Engine Dynamometer Laboratory Tests	19
3.1	Preliminary Audits.....	19
3.1.1	Objective.....	19
3.1.2	Background.....	19
3.1.3	Methods and Materials.....	19
3.1.4	Data Analysis.....	20
3.2	Bias and Precision Errors under steady state engine operation	20
3.2.1	Objective.....	20
3.2.2	Background.....	20
3.2.3	Methods and Materials.....	20
3.2.4	Data Analysis.....	24
3.3	Precision Errors under transient engine operation (dynamic response).....	26
3.3.1	Objective.....	26
3.3.2	Background.....	26
3.3.3	Methods and Materials.....	26
3.3.4	Data Analysis.....	29
3.4	Exhaust Flow Meter Installation.....	32
3.4.1	Objective.....	32
3.4.2	Background.....	32
3.4.3	Methods and Materials.....	32
3.4.4	Data Analysis.....	34
3.5	ECM Torque and BSFC.....	37
3.5.1	Objective.....	37
3.5.2	Background.....	37
3.5.3	Methods and Materials.....	39
3.5.4	Data Analysis.....	42
4	Environmental Chamber Tests.....	45
4.1	Data Analysis for all Environmental Tests	46
4.2	Baseline.....	47
4.2.1	Objective.....	47
4.2.2	Background.....	47
4.2.3	Methods and Materials.....	47
4.2.4	Data Analysis.....	48
4.3	Electromagnetic Radiation.....	48
4.3.1	Objective.....	48
	Ba.....	49
4.3.2	ckground	49
4.3.3	Methods and Materials.....	49

4.3.4	Data Analysis	50
4.4	Atmospheric Pressure	52
4.4.1	Objective	52
4.4.2	Background	52
4.4.3	Methods and Materials.....	53
4.4.4	Data Analysis	54
4.5	Ambient Temperature	55
4.5.1	Objective	55
4.5.2	Background	55
4.5.3	Methods and Materials.....	56
4.5.4	Data Analysis	57
4.6	Orientation, Shock, and Vibration	58
4.6.1	Objective	58
4.6.2	Background	58
4.6.3	Methods and Materials.....	59
4.6.4	Data Analysis	59
4.7	Ambient Hydrocarbons.....	60
4.7.1	Objective	60
4.7.2	Background	60
4.7.3	Methods and Materials.....	61
4.7.4	Data Analysis	63
5	Model Validation and Measurement Allowance Determination	64
5.1	Model validation	64
5.1.1	Objective	64
5.1.2	Background	64
5.1.3	Methods and Materials.....	65
5.1.4	Data Analysis	66
5.2	Measurement Allowance Determination	70
5.2.1	Objective	70
5.2.2	Background	70
5.2.3	Methods and Materials.....	70
5.2.4	Data Analysis	70
6	Time and Cost	71
7	Appendices.....	73
7.1	Description of Spreadsheet provided by Matt Spears.....	73
7.2	Abbreviations used in Brake Specific Equations (Table 3.3.4-a).....	75

Table of Figures

Fig 9
 2.4-a. PDF. 9
 Table 2.2-a: Example of Calculation/Selection of Measurement Allowance 12
 Figures 2.4 a, b, and c: Construction of an Error Surface..... 15
 Table 3.2.3-a: Steady State Operating Conditions for 40 point matrix 23
 Table 3.2.4-a: Steady State Error Surfaces (Refer to section 2.4) 25
 Table 3.3.3-a: Dynamic Response NTE Events..... 27
 Table 3.3.3-b: Dynamic Response Inter-NTE Events 28
 Figure 3.3.3-a: Example of Transient Test Cycle 28
 Table 3.3.4-a: Methods for Calculation of Brake Specific Emissions....**Error! Bookmark not defined.**
 Table 3.3.4-b: Dynamic response (Transient) Error Surfaces 31
 Table 3.4.4.1-a: Exhaust Flow Configuration Error Surfaces (Refer to section 2.4) 35
 Table 3.5.3.1-a: DOE Engine Operating Conditions (%speed, and %torque respectively) 40
 Table 3.5.3.1-b: DOE Parameter Set Points 40
 Table 3.5.3.3-a: Sensitivity Engine Operating Conditions (%speed, and %torque respectively)..... 41
 Table 3.5.3.3-b: Sensitivity Parameter Set Points..... 41
 Tables 3.5.4.1 through 3.5.4.6: Torque Error Surfaces..... 43
 Table 4-a: Gas Cylinder Contents for 5 of 6 Environmental Tests..... 45
 Table 4-b: Gas Cylinder Contents for Ambient Hydrocarbons 46
 Table 4.3.4-a: EMI / RFI Pooled Error Surface 51
 Atmospheric Pressure Test Sequence 53
 Time Series Chart of Atmospheric Pressure Test 53
 Ambient Temperature Test Sequence 56
 Time Series Chart of Ambient Temperature Test..... 56
 Table 4.6.4-a: Shock and Vibration Pooled Error Surface 60
 Table 4.7.3-a: Ambient Hydrocarbon Error Test Sequence 62
 Table 5.1.3-a: CE-CERT Model Validation Test Sequence 66
 Chart of Model Validation NTE Events 67
 Chart of PEMS vs Tow-along lab Results 68
 Budget 71
 Timeline 72

1 Introduction

This test plan will establish PEMS measurement allowances for the gaseous emissions regulated by the manufacturer-run on-highway heavy-duty diesel engine in-use test program. The measurement allowances will be established using various laboratory facilities and PEMS. The measurement allowances will be established in units of brake-specific emissions (g/hp-hr), and they will be added to the final NTE standard for a given emission, after all the other additive and multiplicative allowances have been applied. This test plan will establish three measurement allowances; one for NOx, one for NMHC, and one for CO.

The PEMS used in this test plan must be standard in-production makes and models that are for sale as commercially available PEMS. In addition, PEMS and any support equipment must pass a “red-face” test with respect to being consistent with acceptable practices for in-use testing. For example, use of large gas bottles that can not be utilized by the EPA/ARB/EMA HDIU enforceable program is unacceptable. Furthermore, the equipment must meet all safety and transportation regulations for use on-board heavy-duty vehicles.

Even though the PEMS can not be “prototypes” nor their software “beta” versions, the steering committee has already agreed that after delivery of PEMS to the contractor, there may be a few circumstances in which PEMS modifications might be allowed, but these modifications must meet certain deadlines, plus they are subject to approval by the steering committee. Also, any implementation of such approved modifications will not be allowed to delay the test plan, unless the steering committee specifically approves such a delay. Table 1 summarizes these allowable modifications and their respective deadlines:

Table 1: Allowed Modifications	Before start of...
Steering committee approved hardware and software modifications that affect emissions results; including but not limited to fittings, components, calibrations, compensation algorithms, sampling rates, recording rates, etc.	Section 3.2
Steering committee approved hardware modifications for DOT approval or any other safety requirement approval	Section 4.3
Delivery of any environmental / weather enclosure to contractor	Section 4.3
Post-processing software to determine NTE results	Section 5.1
DOT approval and documentation	Section 5.1
Steering committee approved hardware or software that improves the contractor’s efficiency to conduct testing and data reduction	Always Allowed

This test plan describes a computer model, a series of experiments that are used to calibrate the model, and another series of experiments that are used to validate the calibrated model.

The test plan first describes the computer model. The computer model statistically combines many sources of PEMS and lab error, which are nearly impossible to capture simultaneously in a single test. The model will use statistics to apply the errors in a way that simulates actual running of a PEMS in-use. The model will also consider only the portion of error that is attributable to PEMS, and it will subtract the error that is already tolerated in an emissions lab today. The model will also calculate and validate results according to 40 CFR Part 1065.

The test plan then describes the series of experiments. These tests will characterize the many sources of PEMS and lab error so that the specific nature of the errors can be programmed into the computer model. The nature of the error has to do with the way PEMS and the lab react to certain conditions. For example, under varying environmental conditions such as temperature or vibration, a PEMS might exhibit signal drift, or it may record noise that is not a part of the true emissions.

Next the experimental results will be entered into the computer model, and the measurement allowances are calculated by the model. The model uses a "reference" PEMS data set, which will have many "reference NTE events." The model statistically applies all the errors to the reference data set, calculates results, and saves the results. Then the model will be run with all errors set to zero to calculate the ideal results of the reference data set. Each difference between a reference NTE event's result with errors and its respective ideal result will be a brake-specific difference that is recorded for later use. Then the process repeats using the same reference data set, to which new, statistically selected errors are applied, and thus another unique set of differences is calculated. As the model continues to iterate and generate more and more results, patterns are expected to appear in the output data. These patterns should be the distributions of differences, based upon the error that was statistically and repeatedly applied to the reference data set. Many difference distributions will be determined: for each reference NTE event, for each three regulated gaseous emissions, and for each of three brake-specific calculation methods. It has been agreed that the 95th percentile values of these distributions will be taken as reasonable "worst case" results for each reference NTE event. Details on how all these distributions will be reduced to determine the three gaseous measurement allowances are given in the "Error Model" section of this test plan.

Finally, the test plan describes how the computer model will be validated against real-world over-the-road in-use PEMS operation as well as additional lab testing. For the over-the-road testing, PEMS emissions measurements will be conducted, while at the same time a reference laboratory will be towed along to measure the same emissions. For the lab testing, an attempt will be made to simulate real-world engine operation to "replay" an over-the-road test in the lab. Data from these final experiments will be used to validate the model, which must be done in order to gain sufficient confidence that the model did not establish unreasonable measurement allowances.

The following sections of this test plan are written as instructions to the contractor or contractors who will complete the test plan.

2 Monte Carlo Error Model and Measurement Allowance

2.1 Objective

Use Monte Carlo (e.g. random sampling) techniques in an error model to simulate the combined effects of all the agreed-upon sources of PEMS error incremental to lab error. Create error “surfaces” for the Monte Carlo simulation to sample, based upon results from the experiments described in Sections 3 and 4. Exercise the model over a wide range of NTE events, based on a single, reference data set of at least 100 unique NTE events. Determine the pollutant-specific brake-specific additive measurement allowances for NO_x, NMHC, and CO.

2.2 Background

The error model uses Monte Carlo techniques to sample error values from “error surfaces” that are generated from the results of each of the experiments described in Section 3: lab tests, and Section 4: environmental tests. The lab test error surfaces cover the domain of error versus the magnitude of the signal to which the error is to be applied (i.e. 5th to 95th percentile error vs. concentration, flow, torque, etc.). This is illustrated later in this section. The environmental test error surfaces for shock & vibration and electromagnetic & radio frequency interference (EMI/RFI) cover the same domain as the lab tests, but only for concentration. The environmental test for ambient hydrocarbons is similar but the error surface does not change as a function of concentration. The environmental test error surfaces for pressure and temperature are characteristically different because they cover the domain of environmental test cycle time versus the magnitude of the signal to which the error is to be applied (i.e. error at a selected time vs. concentration). Details on how each surface is generated are given in each of the respective sections. These surfaces will already be adjusted to represent PEMS error incremental to lab error; therefore, these surfaces are sampled directly by the model.

The error model will use two different probability density functions (PDFs) to sample the error surfaces, depending upon which experiment the surface represents. To sample error surfaces that are generated from all the laboratory test results (Section 3), and the environmental test results for shock & vibration; EMI/RFI; and ambient hydrocarbons, the model will use a truncated normal PDF because these tests are designed to evenly cover the full, but finite, range of engine operation and ambient conditions.

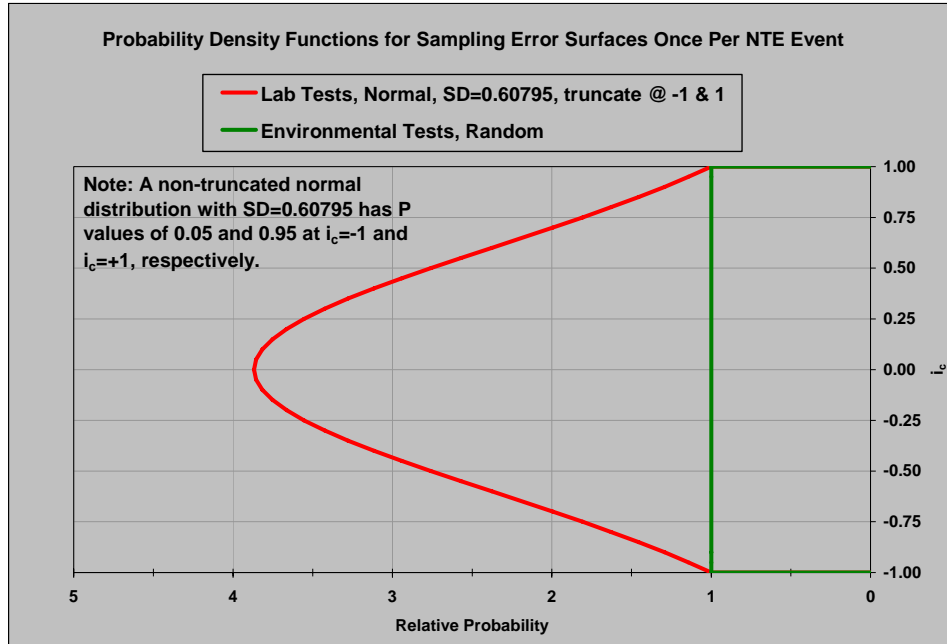


**Fig
2.4-a. PDF.**

To sample error surfaces that are generated from the pressure and temperature environmental test results (Section 4), the model will use a random PDF because these tests are already designed to cover the typical range and frequency of the respective conditions. Note that the lab’s normal PDF samples i_c , from -1 to 1, including -1 and 1, and the pressure and temperature environmental tests use a random PDF to sample test time, from which the nearest (in time) calculated errors are used. The errors from the other tests will be aligned with the normal PDF such that each of the 50th percentile values at each of the tested signal magnitudes is centered at the median of the PDF and the 5th and 95th percentile error values at each of the tested signal magnitudes will be aligned with the extreme negative ($i_c = -1$) and positive ($i_c = +1$) edges of the PDF, respectively.

Each error surface will be sampled along its i_c axis (y-axis) once per reference NTE event, and it will be sampled along its parameter value axis (x-axis, e.g., concentration, flow, torque, etc...) once per second, within a given reference NTE event. An error will be determined for a given second and parameter along the error axis (z-axis) at the intersection of an i_c value and a parameter value.

To ensure that the magnitudes of the error surfaces are appropriate, each data point used to generate the surfaces will be a mean or a weighted mean of 30 seconds of sampling.

Interpolation will be performed by first linearly interpolating error values at each tested magnitude along the selected line perpendicular to the i_c axis. Then from that line of errors, individual error values will be linearly interpolated at each second-by-second signal magnitude of the given NTE event in the reference data set. If good engineering

judgment dictates that unevenly spaced data, sparse data, or other data irregularities warrant more sophisticated interpolation techniques, the steering committee will consider alternatives and provide guidance to the contractor.

The reference data set to which all errors will be applied will be a large data set of engine operation over a wide range of NTE events. This reference data set will be initially generated from collections of real-world PEMS data sets. The reference data set should contain at least 100 unique NTE events. Parameters in the reference data set may be scaled in order to exercise the model through a more appropriate range of parameters (i.e. concentrations, flows, ambient conditions, etc.). If the parameters are scaled, care should be taken to maintain the dynamic characteristics of the reference data set.

After the errors are applied, NTE brake-specific emissions results are calculated for NO_x, CO and NMHC, using each of the three agreed-upon NTE calculation methods. Next, the NTE events are calculated by each of the three calculation methods, but with no error sampled or applied to the reference data set. These results are considered the “ideal” results of the reference NTE events. These ideal results are subtracted from each respective NTE event, and the difference is recorded. Then a new set of errors are sampled and applied to the reference data set, and the NTE results are calculated again. The ideal results are again subtracted, and the difference is recorded. This is repeated thousands or possibly even millions of times so that the model converges upon distributions of brake-specific differences for each of the original NTE events in the reference data set. Then the 95th percentile difference value is determined for each NTE event’s distributions of brake-specific differences for each emission (NO_x, NMHC, and CO) for each calculation method.

The three different brake-specific emission calculation methods referred to in this test plan are i) Torque-Speed Method, ii) BSFC method, and iii) Fuel Specific method, and these are illustrated in the same order in Figure 2.4-b, below. The symbol notation for these equations is described in 40 CFR Part 1065 Subpart K.

Figure 2.4-b: The three brake-specific emission calculation methods.

$$e_{NO_x} \text{ (g/ hp-hr)} = \frac{M_{NO_2} \sum_{i=1}^N x_i g_i \Delta t}{\sum_{i=1}^N f_{ni} \mathcal{G}_i \Delta t}$$

$$e_{NO_x} \text{ (g/ hp-hr)} = \frac{M_{NO_2} \sum_{i=1}^N x_i g_i \Delta t}{\frac{M_C}{W_{fuel}} \sum_{i=1}^N \frac{x_{Cproddryi}}{1 + x_{H2Oi}} e_{fueli} \Delta t}$$

$$e_{NO_x} \text{ (g/ hp-hr)} = \frac{M_{NO_2} W_{fuel} \sum_{i=1}^N x_i g_i \frac{n_{fueli} (1 + x_{H2Oi})}{x_{Cproddryi}} \Delta t}{M_C \sum_{i=1}^N f_{ni} \mathcal{G}_i \Delta t}$$

$$\Delta t = \frac{1}{f_{record}}$$

At this point there are nine distributions of 95th percentile differences, where all the NTE events are pooled by the three emissions (NOx, CO, NMHC) times three different calculation methods. Each of the 95th percentile distributions represents a range of possible measurement allowances.

From each of these nine distributions of possible measurement allowances, one measurement allowance per distribution must be determined. First the correlation between measurement allowance values versus the ideal result values is tested. For each data set, if a least squares linear regression of measurement allowances versus ideal results has an $r^2 > 0.9$ and an $SEE < 5\%$ of the median ideal result, then that linear regression equation will be used to determine the measurement allowance for that data set at the following NTE thresholds:

NOx = 2.0 g/hp-hr

NMHC = 0.21 g/hp-hr

CO = 19.4 g/hp-hr

In cases where extrapolation is required to determine the measurement allowance at the NTE threshold, the measurement allowance will be determined using the linear regression, but evaluated at the ideal result that is closest to the NTE threshold, not extrapolated to the NTE threshold itself.

If the linear regression does not pass the aforementioned r^2 and SEE statistics, then the median value of the distribution is used as the single measurement allowance for that distribution. Once all data distributions are evaluated, there will be nine measurement allowances for three emissions times the three different calculation methods.

Next, the calculation method is selected. First the nine measurement allowances are normalized by their respective NTE thresholds and expressed as a percent of that threshold.

Table 2.2-a below illustrates the selection of the calculation method for all of the measurement allowances. The example is based on a hypothetical set of nine measurement allowances for the three emissions and the three calculation methods. The calculation method is selected by first picking the maximum allowances of all the emissions for each of the given calculation methods. For each column the maximum value is selected (highlighted in yellow). Then the minimum of these maximums is used to select the best method (highlighted in blue). In this hypothetical case, the BSFC method would be selected.

Table 2.2-a: Example of Calculation/Selection of Measurement Allowance			
	Measurement Errors at respective NTE threshold (%)		
Calc. Method ==>	Torque-Speed	BSFC	ECM fuel specific
BSNOx	18 %	18 %	20 %
BSNMHC	19 %	17 %	14 %
BSCO	3 %	2 %	1 %
max error ==>	19 %	18 %	20 %
min of max ==>		18%	
selected method==>	"BSFC" method		

Therefore, 18%, 17%, and 2% would be selected as the best measurement allowances for NOx, NMHC, and CO, respectively. And thus, the additive brake-specific measurement allowances would be:

$$\begin{aligned}
 \text{NOx} &= 18 \% * 2.0 \text{ g/hp-hr} = 0.36 \text{ g/hp-hr} \\
 \text{NMHC} &= 17 \% * 0.21 \text{ g/hp-hr} = 0.0357 \text{ g/hp-hr} \\
 \text{CO} &= 2 \% * 19.4 \text{ g/hp-hr} = 0.388 \text{ g/hp-hr}
 \end{aligned}$$

Each of these values would be very last value added to the actual brake-specific NTE threshold for a given engine, based on actual family emissions limit, mileage, model year, etc.

Note that if any measurement allowance is determined to have a value less than zero, then that measurement allowance will be set equal to zero.

2.3 Methods and Materials

Exercise the model using three different calculation methods: a) torque and speed method, b) BSFC method, and c) ECM - fuel specific method. Determine which calculation method is the most accurate, and use it to estimate the measurement allowance. Each calculation method is described in Table 3.3.4-a

Prepare an Excel spreadsheet model for use with Crystal Ball Monte Carlo software for error analysis of brake specific emissions, BSE, as outlined in section 2.4. Changes to the model's specifications may be requested as agreed upon by the steering committee. Prepare the spreadsheet in a modular structure following the specified model outline, and make provisions for the identified calculation modules. Additionally, clearly identify and easily locate input cells to the model to facilitate any revisions that may become necessary for user's who want to exercise the model with other Monte Carlo add-ins such as @Risk or the newest versions of Crystal Ball. Test the spreadsheet with controlled test cases of simplified input distributions with the Crystal Ball add-on to confirm correct model implementation in accordance with this test plan. Run at least one typical analysis as an additional confirmation.

Deliver the electronic spreadsheet and a brief report describing the model; presenting the test cases and describing pertinent information including the Crystal Ball version, Excel version, operating system and computer. Use standard spreadsheet calculations so that no serious difficulties will be anticipated regarding application in other spreadsheet versions. Use Crystal Ball 2000, and confirm test cases using Excel 97 and Excel 2003.

Control revisions of the spreadsheet model using descriptive file names. Extensive revisions or testing with other software versions beyond that initially proposed may be re-proposed by the steering committee if and when a need for such additional work is identified.

2.4 Data Analysis

For each of the measurement errors in section 3, create an error surface and sample it according to the aforementioned PDFs. Each error surface represents an additive error—or a subtractive error if the sign is negative—relative to the reference value to which it is applied. Figures 2.4-(a),(b), and (c) serve as a hypothetical example of how these error surfaces should be created for every error. The example applies to the error module for steady state bias and precision NO_x concentration errors (section 3.2). The plots shown correspond to hypothetical NO_x emissions concentration data acquired with 3 PEMS and three engines, with all nine sets of PEMS data pooled together. These figures will be referenced by each “Data Analysis” section, for the various errors discussed in this test plan.

Errors from Sections 3 and 4 are combined by adding all of the sampled error once per NTE event. For example, in order to assess the errors in NO_x concentration, several modules will be created such that:

$$\text{NO}_x \text{ PPM} = \text{NO}_x \text{ PPM}_{\text{reference}} + \Delta(\text{PPM})_1 + \Delta(\text{PPM})_2 + \Delta(\text{PPM})_3 + \dots$$

Where,

$\Delta(\text{PPM})_1$ = NOx concentration errors due to steady state bias and precision errors,
 $\Delta(\text{PPM})_2$ = NOx concentration errors due to ambient temperature,
 $\Delta(\text{PPM})_3$ = NOx concentration errors due to ambient pressure,
etc....

Fig 2.4-a: raw data PEMS vs Lab:

Acquire raw data with the PEMS at various average concentration levels (NOx ppm) as per section 3.2. Plot the “PEMS” signals versus the corresponding “lab” signals that were measured using lab equipment. This plot pools all bias and precision errors for all 3 PEMS and for all data from all engines for all steady-state modes. Shown are the 5th 50th and 95th percentiles at each measured concentration level (note that the distribution of data at each level is not necessarily Gaussian). If the 50th percentile is different than the line of perfect agreement (diagonal), the data suggests that there is a bias error between PEMS and Lab. In essence this graph shows the statistical distribution measured by the PEMS at each concentration level sampled. The example shows only 6 discrete concentration levels (ranging from 100-350ppm). However the actual number of discrete levels will be determined by the total number of operating conditions actually run for all the tests of all the engines. Section 3.2 for example will select 10 operating conditions from an initial number of 40 operating conditions. Thus the actual plot for section 3.2 will likely have 30 discrete concentration levels (10 operating conditions x 3 engines).

Figures 2.4 a, b, and c: Construction of an Error Surface

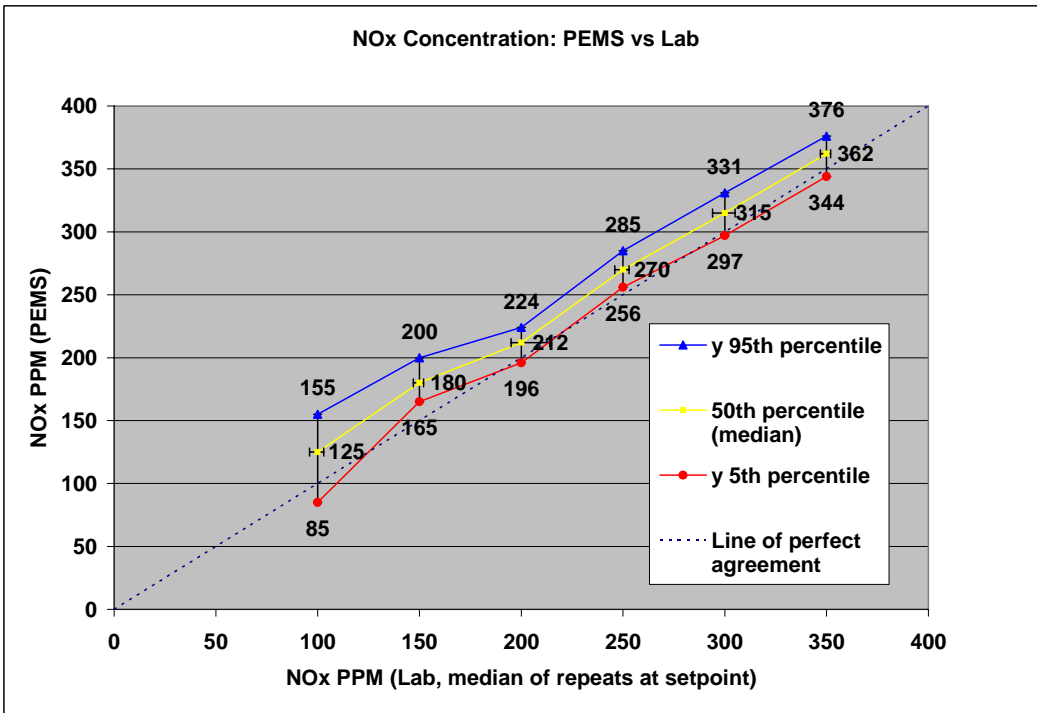


Fig 2.4-a

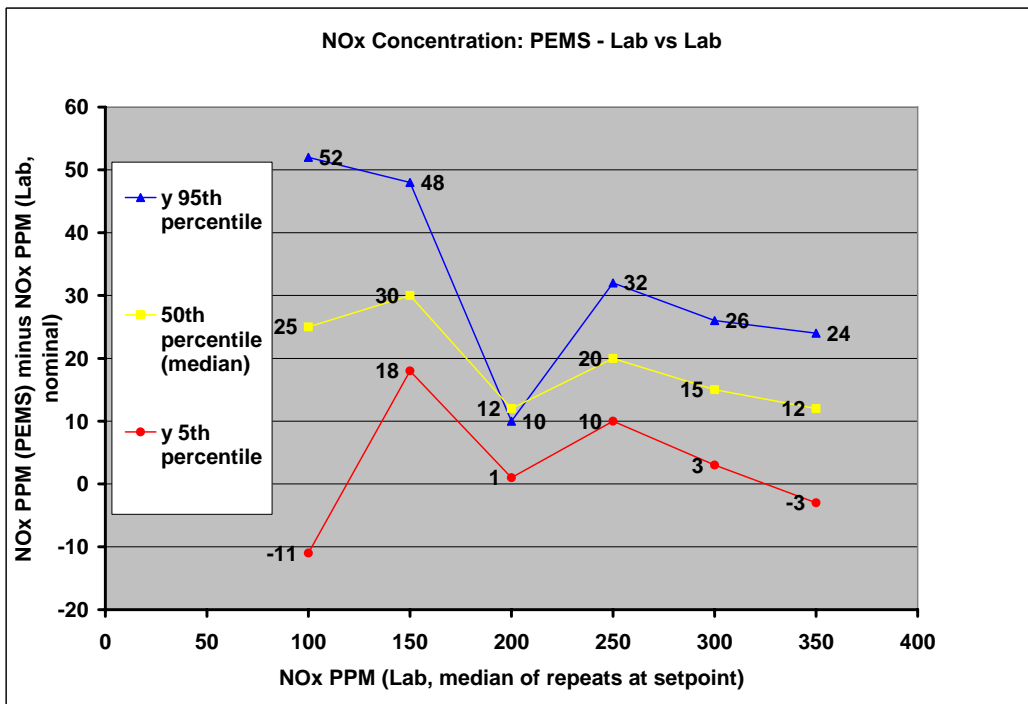


Fig 2.4-b

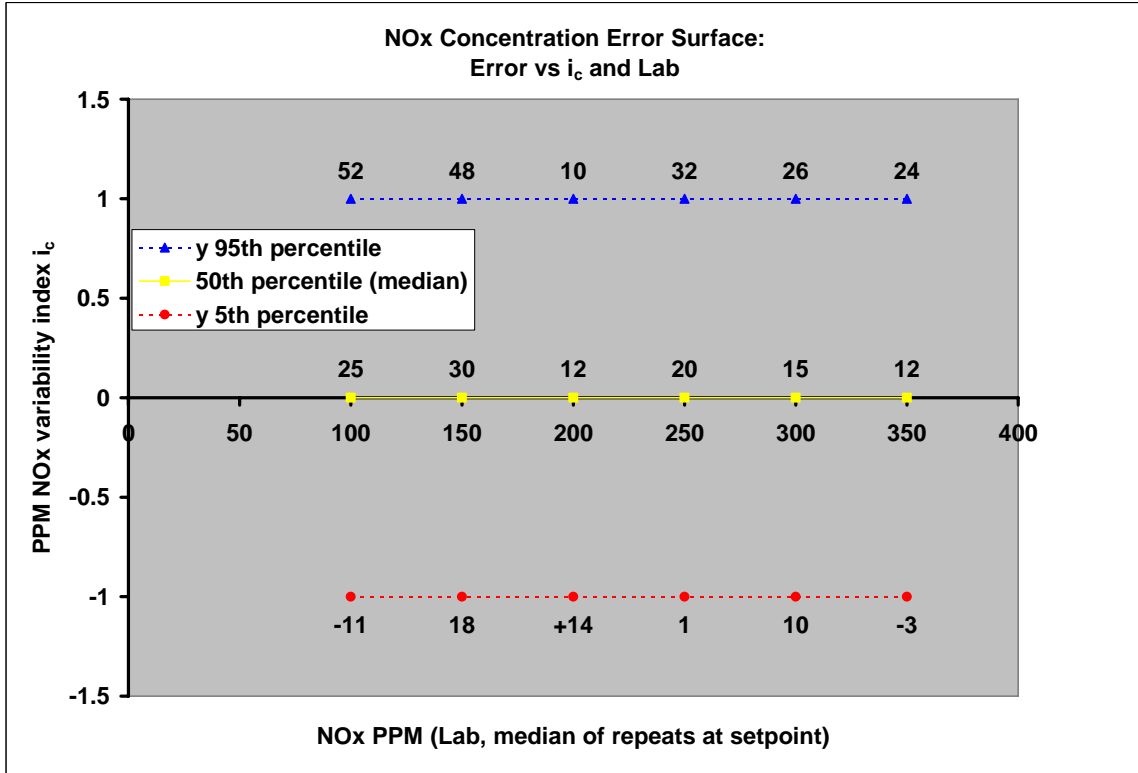


Fig 2.4-c

Fig 2.4-b: (PEMS minus lab) vs lab level

This plot basically shows the “additive error band” measured during testing. The plot is created by subtracting the “lab” 95th, 50th, and 5th percentile values from the “PEMS” 95th, 50th, and 5th percentile values, respectively; displayed in Fig 4.2-a. Notice that if lab error exceeds PEMS error at a given percentile, crossover of values can occur. This is acceptable because the crossover effectively reduces PEMS error whenever lab error exceeds PEMS error.

Fig 2.4-c: Error Surface

This step normalizes the previous plot using what is called a “variability index (i_c)”, which represents the “dice to be rolled” by the Monte Carlo technique, in order to select a given error level. This variability index is allowed to vary from -1 to $+1$. The likelihood of “ i_c ” being any value between -1 through $+1$ is specified by a “probability density function (PDF)” assigned to i_c . In the case of the example given, i_c is assumed to vary according to a normal distribution during Monte Carlo calculations. This is because it is believed that the distribution of errors due to steady state bias and precision will be centered about the 50th percentile of the full range of conditions measured according to section 3.2. The pressure and temperature environmental error modules use flat (random) probability density functions for their respective variability index. Each set of data for each lab setpoint median (i.e., lab reference value) in Figure 2.4-b’s is normalized by aligning the 5th percentile error with $i_c=-1$, the 50th percentile error with $i_c=0$, and the 95th percentile error with $i_c=+1$. Notice that the 5th, 50th, and 95th percentile values remain equivalent between 2.4-b and 2.4-c.

Error surfaces such as the one presented in Fig 4.2-c are the input modules that the Monte Carlo simulation program will use during calculations of brake-specific emissions. For example, for a given NTE calculation the dice will be rolled once per valid NTE event. Let us assume that the dice were rolled (by the computer program) the first time and $i_c = 0.5$. Let us also assume that during this valid NTE event, the reference NOx concentration measured at a given second in time is 100ppm. In this case:

$$\Delta(\text{PPM})_1 = (25+55)/2 = 40\text{ppm}$$

(from Fig 4.2-c, for $i_c = 0.5$, Reference NOx = 100)

For that step in the calculation, the Monte Carlo approach will add this “delta” to the reference concentration value of 100ppm (100ppm+40ppm = 140ppm) to represent errors in steady state bias and precision for $i_c = 0.5$, and NOx_reference = 100ppm. If during the same NTE event in the reference data set, a reference concentration of 225 ppm is read, then,

$$\Delta(\text{PPM})_1 = ((30+42)/2+(20+35)/2)/2 = 31.75\text{ppm} \quad (\text{from Fig 4.2-c})$$

Note that first, the error along the i_c line perpendicular to the i_c axis (in this case the line along 0.5) is linearly interpolated at each discrete concentration level, then, those interpolated values are themselves linearly interpolated to determine the error corresponding to each reference concentration in the NTE event. Note that the dice are rolled once per reference NTE event, but the error along that i_c line is applied to every second-by-second value within the given NTE event.

Now let us assume that the error in NO_x concentration is composed of only 3 deltas: $\Delta(\text{PPM})_1$, $\Delta(\text{PPM})_2$, and $\Delta(\text{PPM})_3$. And let us assume that for one second of a given reference NTE event, the reference value of NO_x = 300ppm ; and:

$$\Delta(\text{PPM})_1 = 36\text{ppm}, \quad \Delta(\text{PPM})_2 = -20\text{ppm}, \quad \Delta(\text{PPM})_3 = -2\text{ppm}.$$

Then, when the model calculates brake-specific emissions by each of the three calculation methods, it will use the following NO_x value, which has all of its error applied:

$$\text{NO}_x\text{_PPM} = 300 + 36 - 20 - 2 = 314 \text{ ppm}$$

The application of error at the selected i_c continues during the entire NTE event without having to “roll the dice” again. In other words, i_c will not change. However, as the reference NO_x concentration values change during the reference NTE event, $\Delta(\text{PPM})_1$, $\Delta(\text{PPM})_2$, and $\Delta(\text{PPM})_3$ will take on different values, depending on the reference value of NO_x_ppm at each second in the reference NTE event.

This same approach would be used for other the other deltas such as ambient temp, ambient pressure, shock and vibration, BSFC interpolation, torque, exhaust flow rate, etc.)

3 Engine Dynamometer Laboratory Tests

Utilize engine dynamometer laboratory testing to establish the difference between PEMS emissions analyzers and flow-meters against lab grade instruments. Also establish how exhaust flow meter installation affects performance, and establish how well ECM parameters can be used to estimate torque and BSFC.

First, however, audit all the PEMS and lab equipment to ensure that they are operating properly, according to 40 CFR Part 1065 Subpart D. Next, conduct steady-state engine dynamometer tests to establish PEMS steady-state bias and precision relative to the lab. Then, conduct transient engine dynamometer testing to determine PEMS transient precision by repeating transient NTE events. Afterward, investigate the effects of exhaust flow meter installation. Finally, compare ECM derived torque and BSFC to laboratory measured torque and BSFC.

3.1 Preliminary Audits

3.1.1 Objective

Conduct 40 CFR Part 1065 Subpart D audits of all engine dynamometer laboratory systems and all PEMS.

3.1.2 Background

Because the overall purpose of this entire test plan is to establish measurement allowances that account for the incremental difference in the performance of PEMS versus engine dynamometer laboratory systems, the first task is to audit all of the measurement systems to ensure that the specific systems used for testing meet EPA's minimum performance requirements. The audits also help to minimize bias errors between PEMS and lab systems measurements.

On-site meeting to establish 1065 compliance requirements

In order to clarify what are all the requirements expected from the lab-grade instrumentation and PEMS equipment, with respect to 1065 compliance, a meeting will be held between the test plan steering committee and the contractor at the contractor site to provide the contractor with guidance regarding which specific sections of Part 1065 Subpart D are required and which are optional.

3.1.3 Methods and Materials

Use the methods and materials described in 40 CFR Part 1065 Subpart D to conduct audits of all lab and PEMS measurement systems. Even if lab systems and PEMS pass initial Subpart D audits, allow lab operators and PEMS manufacturers to make on-site adjustments to improve the performance of their systems prior to engine testing. Allow adjustments to be based on recalibrations with reference signals that are allowed in 40 CFR Part 1065. Do not allow recalibrations based on a comparison between lab audit results and PEMS audit results. The steering committee may direct the contractor to calibrate or adjust the laboratory sampling system based on audit results. The steering

committee may also suggest that a PEMS manufacturer calibrate or adjust one or more PEMS based on lab audits.

3.1.4 Data Analysis

Use the data analyses described in CFR Part 1065 Subparts D, J and G. For all subsequent testing, use only those measurement systems that pass the minimum performance criteria in Subpart D, unless a deficiency is deemed acceptable in writing by all parties including PEMS manufacturers.

3.2 Bias and Precision Errors under steady state engine operation

3.2.1 Objective

Evaluate the bias and precision of repeatedly measuring 10 different steady-states NTE over a 30-minute cycle. Repeat this test for three different engines. Determine the Δ_{SS} surface plot for the error model based upon all data pooled.

- a) Obtain data for torque mapping and test matrix selection (40 data points)
- b) Quantify bias and precision errors of gaseous emissions concentration measurements (ppm raw and fuel-specific dilute), under standard laboratory conditions.
- c) Quantify bias and precision errors in exhaust flow measurement measurements using PEMS' portable flow-meters, under standard laboratory conditions.
- d) Quantify bias and precision errors in gaseous emissions flow rate measurements (e.g. g/hr NO_x).

3.2.2 Background

Testing will be conducted to capture bias and precision errors in PEMS' emissions analyzers and flow meters, versus lab grade instruments. The tests will be steady-state only. In essence, testing under this section will use a methodology consistent with that currently used and tolerated by engine manufacturers during certification and compliance with respect to the supplemental emissions test (SET).

Note: Section 3.3 (next section) will evaluate precision errors (not bias) due to the dynamic response of the PEMS instrumentation, with respect to those of lab grade analyzers. The precision error captured during steady state testing (section 3.2) will have to be subtracted from the overall precision error captured in section 3.3 in order not to double-count the steady state precision errors of PEMS instrumentation. This process is detailed in Section 3.3.

3.2.3 Methods and Materials

Use the following systems:

- a) Three (3) heavy duty diesel engines (1 HHDE--DDC, 1 MHDE-Cat, 1 LHDE-International)
- b) Three (3) PEMS analyzers (3 Sensors Semtech-DS models with NMHC capability)
- c) Up to nine (9) PEMS exhaust flow-meters (from Sensors, Inc. for each of three engines)

d) Three (3) oversized passive diesel particulate filters (DPFs) for each engine. Select DPF's to be attached to the exhaust of each engine. Establish a procedure to ensure that the DPF's are cleaned at the beginning of each test, and remain clean in order to make their impact on emissions variability negligible.

Use the following overall guidelines:

- e) Measure raw as well as CVS-dilute emissions
- f) Measure engine inlet airflow through use of LFE or equivalent
- g) Measure instantaneous fuel consumption and torque
- h) Analyze fuel for at least atomic hydrogen-to-carbon ratio, specific gravity, and sulfur mass fraction
- i) Ensure regeneration of the DPF system as often as needed in order to ensure negligible impact on emissions variability
- j) Capture ECM broadcast channels and other common diagnostic channels, as recommended by engine manufacturer(s), to ensure proper engine operation
- k) Do not measure PM.
- l) Stabilization time = 120 seconds. Data acquisition = 30 seconds, after stabilization. Dwell time between points = 30 seconds (total time per point = 180 sec. = 3 min)
- m) Zero and span PEMS at beginning of day following manufacturer's guidelines. Do not re-span PEMS analyzers again during the day, unless PEMS manufacturer provides a way to do this automatically, so it is realistic with real-life in-use testing practices. Re-zeroing should be allowed if and only if done automatically by the PEMS for the same reasons. Use zero gases for automatic PEMS re-zeros, and use purified FID burner air for all FIDs, including PEMS FIDs.
- n) Zero and spanning of lab analyzers can be repeated between each 30-minute test.
- o) Perform carbon balance checks on CVS emissions data to ensure data quality according to Part 1065.
- p) Always power off PEMS equipment at end of each day, according to PEMS manufacturer instructions. Re-start start-up process every day according to PEMS manufacturer instructions and Part 1065, Subpart J.

40 point selection testing:

- q) Map each engine lug curve according to the variable speed engine sweep map test procedures in Part 1065 Subpart F and follow the applicable calculations in Part 1065 Subpart G to transform the normalized steady-state modes into steady-state reference commands for each engine. Use the spreadsheet provided by the steering committee to transform modes. E-mail the transformed 40-pt matrix to the steering committee for approval before starting the 40-pt emissions testing. The steering committee may adjust one or more points to maximize the utility of the 40 points.
- r) Measure 40 points spanning the NTE zone. These points are listed in Table 3.2.3-a (no repeats).
- s) Verify that none of these test points have triggered emissions deficiencies (this will have to be accomplished with assistance from the respective engine manufacturer)
- t) Stop testing, analyze 40 points of emissions and examine data for overwhelming biases. For example: i) One of three PEMS is very different than the other two from a given PEMS manufacturer; ii) Lab raw vs lab dilute is very different from one

another (i.e. questionable reference); iii) One flow meter seems very different than all others; iv), etc.

- u) Spend minimum amount of time to determine source of bias, correct if possible via adjustments to the experimental setup, Part 1065 calibration specifications, PEMS manufacturer-specified calibrations, lab system manufacturer specifications, contractor QA/QC procedures. Under no circumstances will PEMS be calibrated to lab instruments or vice versa, and under no circumstances will lab equipment be calibrated to any other lab equipment that is also used to validate results, such as carbon balance or propane-check validations (i.e., no circular calibration-validation procedures) . However, torque/BSFC tables will be created (i.e. calibrated) based on mapped data.
- v) During the 40 point selection testing, all PEMS analyzers and flow meters can be connected at the same time in series (daisy chain fashion) if PEMS manufacturers agree. This would allow evaluation of interactions between PEMS. Testing in the next portion of testing will not allow daisy chaining of PEMS, unless agreed upon in advance by the steering committee, the PEMS manufacturer, and the contractor.

10 point cycle repeat-testing, evaluate bias and precision errors:

- w) The steering committee will select 10 operating conditions for repeat testing, based upon the results from the 40 points. The points will be selected to appropriately span the range of expected emissions concentrations and exhaust flow rates obtained during 40 point test set. The points should also represent the highest degree of bias errors with respect to the lab measurements. The ten points do not have to be only a subset of the 40 tested points; the ten points can include previously untested points.
- x) Create a test cycle consisting of the ten selected points, using the criteria described above (l). As this cycle is tested a second time however, the order in which each operating condition is entered into the cycle needs to be changed randomly. Keep randomizing the order of the operating conditions during all subsequent cycle tests.
- y) Repeat each cycle a total of 20 times, where each repeat is in a different mode order.
- z) Each test will use one PEMS at a time, to measure emissions concentration and exhaust flow rate (unless otherwise agreed to by PEMS manufacturer)
- aa) Expected test duration: 10 points x 3 minutes x 20 repeats = 600 minutes (10 hrs). This assumes that the DPF will not need to be purged during testing.
- bb) Each engine will have to be run on 3 different days to obtain data from all 3 PEMS unless the PEMS can be tested simultaneously.

Table 3.2.3-a: Steady State Operating Conditions for 40 point matrix					
NTE Event	¹Speed % Range	²Torque % Range	NTE Event	¹Speed % Range	²Torque % Range
NTE ₁	Governor Line	25% * Peak	NTE ₂₁	NTE _{min} + 0.5* (MTS-NTE _{min})	NTE ₆
NTE ₂	Governor Line	NTE _{min}	NTE ₂₂	NTE _{min} + 0.5* (MTS-NTE _{min})	NTE ₄
NTE ₃	Governor Line	Ave(NTE ₁ ,NTE ₄)	NTE ₂₃	NTE _{min} + 0.5* (MTS-NTE _{min})	NTE ₃
NTE ₄	Governor Line	Ave(NTE ₁ ,NTE ₅)	NTE ₂₄	NTE _{min} + 0.5* (MTS-NTE _{min})	NTE _{min}
NTE ₅	MTS	Max	NTE ₂₅	NTE _{min} + 0.5* (MTS-NTE _{min})	NTE ₁
NTE ₆	MTS	Ave(NTE ₄ ,NTE ₅)	NTE ₂₆	NTE _{min} + 0.25* (MTS-NTE _{min})	NTE ₁
NTE ₇	MTS	NTE ₄	NTE ₂₇	NTE _{min} + 0.25* (MTS-NTE _{min})	NTE _{min}
NTE ₈	MTS	NTE ₃	NTE ₂₈	NTE _{min} + 0.25* (MTS-NTE _{min})	NTE ₃
NTE ₉	MTS	NTE _{min}	NTE ₂₉	NTE _{min} + 0.25* (MTS-NTE _{min})	NTE ₄
NTE ₁₀	MTS	NTE ₁	NTE ₃₀	NTE _{min} + 0.25* (MTS-NTE _{min})	NTE ₆
NTE ₁₁	NTE _{min} + 0.75* (MTS-NTE _{min})	NTE ₁	NTE ₃₁	NTE _{min} + 0.25* (MTS-NTE _{min})	NTE ₅
NTE ₁₂	NTE _{min} + 0.75* (MTS-NTE _{min})	NTE _{min}	NTE ₃₂	NTE _{min} + 0.25* (MTS-NTE _{min})	Ave(NTE ₅ ,Max)
NTE ₁₃	NTE _{min} + 0.75* (MTS-NTE _{min})	NTE ₃	NTE ₃₃	NTE _{min} + 0.25* (MTS-NTE _{min})	Max
NTE ₁₄	NTE _{min} + 0.75* (MTS-NTE _{min})	NTE ₄	NTE ₃₄	NTE _{min}	Max
NTE ₁₅	NTE _{min} + 0.75* (MTS-NTE _{min})	NTE ₆	NTE ₃₅	NTE _{min}	NTE ₅
NTE ₁₆	NTE _{min} + 0.75* (MTS-NTE _{min})	NTE ₅	NTE ₃₆	NTE _{min}	NTE ₆
NTE ₁₇	NTE _{min} + 0.75* (MTS-NTE _{min})	Ave(NTE ₅ ,Max)	NTE ₃₇	NTE _{min}	NTE ₄
NTE ₁₈	NTE _{min} + 0.75* (MTS-NTE _{min})	Max	NTE ₃₈	NTE _{min}	NTE ₃
NTE ₁₉	NTE _{min} + 0.5* (MTS-NTE _{min})	Max	NTE ₃₉	NTE _{min}	NTE _{min}
NTE ₂₀	NTE _{min} + 0.5* (MTS-NTE _{min})	NTE ₅	NTE ₄₀	NTE _{min}	NTE ₁

Peak = peak torque of engine along lug curve
NTE_{min} for speeds = nlo+0.15*(nhi - nlo)
Ave = average of values in parentheses
MTS = Maximum Test Speed, as defined per part 1065, subpart F
Max = maximum torque at speed
NTE_{min} for torques = max of 30% peak torque AND torque at speed and 30% peak power

3.2.4 Data Analysis

Use the acquired data to create the “error surfaces” to be used by the Monte Carlo simulation. Refer to section 2.4 for description and example of an error surface. Using Figure 2.4-(c) as reference, create the error surfaces for steady state bias and precision errors using the parameters indicated in Table 3.2.4-a.

3.3 Precision Errors under transient engine operation (dynamic response)

3.3.1 Objective

Evaluate the precision of measuring 30 different 32-second NTE events in different orders over a 20-minute cycle. Determine the Δ_{Trans} surface plot for the error model. Carry out this evaluation both for engine emissions and exhaust flow rate.

3.3.2 Background

PEMS are expected to operate in a repeatable manner over NTE events as short as 30 seconds. Two sources of PEMS precision error are hypothesized: 1) dynamic response to rapidly changing signals, and 2) susceptibility to “history” effects. Dynamic response error includes error due to measurement signal time alignment, and the dissimilarity of the dynamic response and aliasing of signals that are combined on a second-by-second basis; including those signals used to determine entry into and exit from the NTE zone. History effects include the effects of previously measured quantities on currently measured quantities. For example, this may be caused by ineffective sample exchange in the gaseous emissions sampling volumes, or it may be caused by one or more sensors’ characteristic rise time or fall time. To account for any dynamic response precision error, the increase in precision error incremental to the steady-state emissions measurement precision will be incorporated into the overall error model.

Selection of short NTE cycles (each 32 seconds) maximizes the sensitivity of this test to effects of dynamic response. Thirty-two seconds was chosen as the minimum instead of thirty seconds, which is the shortest NTE event time, to ensure that 1 Hz ECM updating of torque and speed values would be unlikely to interfere with capturing NTE events. For each repeat of the test cycle, the order of the 30 different NTE events will be randomly rearranged. In addition the 29 different intervals separating each NTE event from the next will have a range of durations and these will be randomly arranged in each test cycle as well. Random rearrangement of the NTE events and the inter-NTE events will maximize the sensitivity of this test to dynamic response and history effects.

3.3.3 Methods and Materials

- a) Use a transient engine dynamometer emissions laboratory.
- b) Use a laboratory that can accommodate at least three PEMS, their power supplies, the PEMS flow meters, cables and lines.
- c) Use same 3 engines from steady state testing, section 3.2
- d) Use same overall guidelines described in section 3.2, but applied to transient engine testing.
- e) Ensure that PEMS systems are not spanned more than once per day, and re-zeroed unless PEMS software allows this to be done automatically. Use zero air for zeroing analyzers and for FID burner air.

Challenge PEMS to 30 different 32-second NTE events over a 20 minute test cycle (see Table 3.3.3-a). Repeat the test cycle 20 times for a total of 600 measured NTE events.

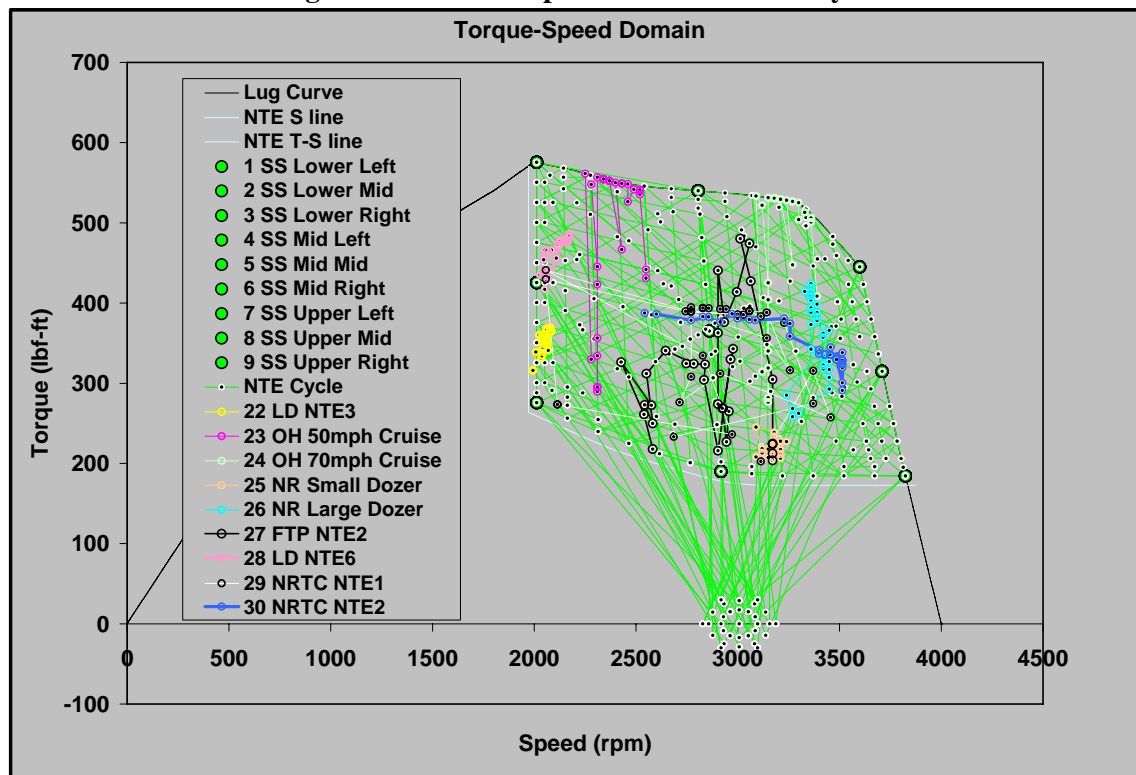
Repeat the test cycle such that it occurs 4 to 5 times per day and over 4 to 5 different days. Create unique cycles for each repeat by first randomly sampling the order of NTE events from the NTE event table. Separate each NTE event with a randomly sampled inter-NTE event from the inter-NTE event table (Table 3.3.3-b). Regardless of the descriptions in the summary table (Table 3.3.3-b), use the provided spreadsheet (author: Matt Spears, EPA) with the engine maps generated in 3.2.3 to create 20 unique second-by-second de-normalized test cycles, and use one unique cycle for each repeat of this test. Note that for any torque command that is less than zero, command closed throttle (i.e. zero or minimum fuel command), and motor the engine at the commanded speed for that data point.

Table 3.3.3-a: Dynamic Response NTE Events			
NTE Event	¹Speed % Range	²Torque % Range	Description
NTE ₁	17%	³ 32%	Steady speed and torque; lower left of NTE
NTE ₂	59%	³ 32%	Steady speed and torque; lower center of NTE
NTE ₃	Governor line	³ 32%	Steady speed and torque; lower right of NTE
NTE ₄	17%	66%	Steady speed and torque; middle left of NTE
NTE ₅	59%	66%	Steady speed and torque; middle center of NTE
NTE ₆	Governor line	66%	Steady speed and torque; middle right of NTE
NTE ₇	17%	100%	Steady speed and torque; upper left of NTE
NTE ₈	59%	100%	Steady speed and torque; upper center of NTE
NTE ₉	100%	100%	Steady speed and torque; upper right of NTE
NTE ₁₀	Lower third	³ 32% - 100%	Highly transient torque; moderate transient speed
NTE ₁₁	Upper third	³ 32% - 100%	Highly transient torque; moderate transient speed
NTE ₁₂	Middle third	³ 32% - 100%	Highly transient torque; moderate transient speed
NTE ₁₃	17% - governed	Lower third	Highly transient speed; moderate transient torque
NTE ₁₄	17% - governed	Upper third	Highly transient speed; moderate transient torque
NTE ₁₅	17% - governed	Middle third	Highly transient speed; moderate transient torque
NTE ₁₆	Lower right diagonal		Transient; speed increases as torque increases
NTE ₁₇	Upper left diagonal		Transient; speed increases as torque increases
NTE ₁₈	Full diagonal; lower left to upper right		Transient; speed increases as torque increases
NTE ₁₉	Lower left diagonal		Transient; speed decreases as torque increases
NTE ₂₀	Upper right diagonal		Transient; speed decreases as torque increases
NTE ₂₁	Full diagonal; lower right to upper left		Transient; speed decreases as torque increases
NTE ₂₂	Third light—heavy-duty NTE event from International, Inc. data set		Sample from LHDE
NTE ₂₃	Cruise; ~ 50 mph		Sample from HDDE
NTE ₂₄	Cruise; ~ 75 mph		Sample from HDDE
NTE ₂₅	Small bulldozer		Sample from NRDE
NTE ₂₆	Large bulldozer		Sample from NRDE
NTE ₂₇	Second of three NTE events in FTP		Seconds used from FTP: 714-725, 729-743, 751-755
NTE ₂₈	Third light—heavy-duty NTE event from International, Inc. data set		Sample from LHDE
NTE ₂₉	First of two NTE events in NRTC		Seconds used from NRTC: 423-430, 444, 448-450, 462-481, increased 464 speed from 40% to 42%
NTE ₃₀	First of two NTE events in NRTC		Seconds used from NRTC: 627-629, 657-664, 685-696, 714-722
¹ Speed (rpm) = Curb Idle + (Speed % * (MTS - Curb Idle)) ² Torque (lbf-ft) = Torque % * Maximum Torque At Speed (i.e. lug curve torque at speed) ³ Torque (lbf-ft) = Maximum of (32 % * peak torque) and the torque at speed that produces (32 % * peak power)			

Table 3.3.3-b: Dynamic Response Inter-NTE Events			
INT Event ¹	Duration (s)	Frequency	Description
INT ₁	10	1	Initiation of cycle; INT ₁ is always first
INT ₂₋₆	2	5	Shortest and most frequent inter-NTE events
INT ₇₋₁₀	3	4	Short and frequent inter-NTE events
INT ₁₁₋₁₄	4	4	Short and frequent inter-NTE events
INT ₁₅₋₁₈	5	4	Short and frequent inter-NTE events
INT ₁₉₋₂₁	6	3	Short and frequent inter-NTE events
INT ₂₂	7	1	Medium inter-NTE event
INT ₂₃	8	1	Medium inter-NTE event
INT ₂₄	9	1	Medium inter-NTE event
INT ₂₅	11	1	Medium inter-NTE event
INT ₂₆	13	1	Long inter-NTE event
INT ₂₇	17	1	Long inter-NTE event
INT ₂₈	22	1	Long inter-NTE event
INT ₂₉	27	1	Long inter-NTE event
INT ₃₀	35	1	Longest inter-NTE event
INT ₃₁	5	1	Termination of cycle; INT ₃₁ * is always last

Interval speeds and torques are not identical, but they are clustered around zero torque and the speed at which 15% of peak power and 15% of peak torque are output.

Figure 3.3.3-a: Example of Transient Test Cycle



Prior to executing the first repeat, setup each PEMS and stabilize engine operation at the first inter-NTE operating point. Setup the PEMS according to 40 CFR Part 1065 and PEMS manufacturer instructions, including any warm-up time, zero-spans of the

analyzers and the setup of all accessories including flow meters, ECM interpreters, etc. Then, when the test cycle starts, switch the PEMS' to sample emissions from the engine. When the test cycle ends, switch the PEMS back to ambient sampling. Complete all post-test lab and PEMS validations according to 40 CFR Part 1065 and according to PEMS manufacturer instructions.

3.3.4 Data Analysis

- a) Discard from further data analysis any NTE events invalidated by any criteria in 40 CFR Part 1065 subpart J.
- b) For each NTE_i event (i=1 to 30), which was repeated 20 times (j = 1 to 20), calculate the transient median absolute deviation, MAD_{TRi}, for each of the parameters in Table 3.3.4-b (ppmNO_x, ppmCO, ppmNMHC, ppm0.98*THC, exhaust flow, speed, torque, fuel, and bsfc), where for each NTE_i event, MAD_{TRi} = median(| NTE_{ij} – median (NTE_{ij}) |).
- c) Next calculate the difference of MAD by subtracting a corresponding steady-state MAD, MAD_{SSi}. MAD_{TRi-SSi} = MAD_{TRi} – MAD_{SSi}. To determine a corresponding MAD_{SSi}, calculate the PEMS MAD_{SS} at each steady-state median lab value, and then use the median PEMS NTE_i value along the median lab value's axis to find MAD_{SSi} for the corresponding MAD_{TRi}. Do not extrapolate any MAD_{SSi} beyond the minimum or maximum median lab values. Note that some MAD_{SSi} values might be zero because the lab data for that median failed the F-test in the previous section.
- d) For any MAD_{TRi-SSi} less than zero, set that MAD_{TRi-SSi} equal to zero.
- e) Create a transient error surfaces using all of the MAD_{TRi-SSi}. Be sure to include any MAD_{TRi-SSi} data points that are equal to zero because they will affect the 5th and 95th percentile values.
- f) Using Figure 2.4-(c) as reference, create the error surfaces for the parameters indicated in Table 3.3.4-b.
- g) To evaluate lab performance under transient NTE conditions according to the MOA, perform the following:
 - a. For every repeated steady-state NTE event (from all engines and for NO_x, CO, and NMHC), subtract the corresponding brake-specific 50th percentile value from every brake-specific value. Pool all resulting deltas by emission, calculation method, and raw or dilute lab sampling. Determine the 99th percentile value for each emission by calculation method and raw or dilute sampling.
 - b. For every repeated transient NTE event (from all engines and for NO_x, CO, and NMHC), subtract the corresponding brake-specific 50th percentile value from every brake-specific value. Pool all resulting deltas by emission, calculation method, and raw or dilute lab sampling. Determine the 95th percentile value for each emission by calculation method and raw or dilute sampling.
 - c. For each emission, subtract the 99th percentile steady-value from the 95th percentile transient value. If the result is positive for a particular emission, for all calculation methods and for both raw and dilute sampling, the following provisions of the MOA will apply: EMA will work with EPA

and CARB to optimize laboratory NTE measurement specifications and procedures. This work will primarily be in the form of participating in and supporting joint laboratory NTE test procedure development efforts and meetings. Also, EPA would intend to issue a guidance document and/or propose changes to Part 1065 to reflect any optimized specifications and procedures for laboratory NTE testing as a result of those efforts and meetings no later than the end of calendar year 2008.

Table 3.3.4-b: Dynamic response (Transient) Error Surfaces

For use in Measurement Allowance Determination		For use in Measurement Allowance Determination	
Error Surface for TR Exhaust molar flowrate			
Fig 2.4-a		Fig 2.4-a	
x-axis	mol/s (PEMS NTE median) / mol/s_max -[%]	x-axis	NOx ppm (PEMS NTE flow-wtd median)
y-axis	NOx mol/s (PEMS) / mol/s_max -[%]	y-axis	NOx ppm (PEMS)
Fig 2.4-b		Fig 2.4-b	
x-axis	mol/s (PEMS NTE median) / mol/s_max -[%]	x-axis	NOx ppm (PEMS NTE flow-wtd median)
y-axis 5th percentile	(5th mol/s (TR pems) - 5th mol/s (SS lab @ PEMS NTE median)) / mol/s_max -[%]	y-axis 5th percentile	5th NOx ppm (TR pems) - 5th NOx ppm (SS lab @ PEMS NTE median)
	if result >=0 and result <=50th then = 0		if result >=0 and result <=50th then = 0
y-axis 50th percentile	0	y-axis 50th percentile	0
y-axis 95th percentile	(95th mol/s (TR pems) - 95th mol/s (SS lab @ PEMS NTE median)) / mol/s_max -[%]	y-axis 95th percentile	95th NOx ppm (TR pems) - 95th NOx ppm (SS lab @ PEMS NTE median)
	if result <=0 and result <=50th then = 0		if result <=0 and result <=50th then = 0
Fig 2.4-c		Fig 2.4-c	
x-axis	mol/s (PEMS NTE median) / mol/s_max -[%]	x-axis	NOx ppm (PEMS NTE flow-wtd median)
y-axis	I_{t, TR_flow}	y-axis	I_{t, TR_NOx}
z-axis = ΔTR_flow	mol/s (5th 50th, & 95th) / mol/s_max -[%]	z-axis = ΔTR_NOx,ppm	ppm (5th 50th, & 95th)
I _t sample frequency	once per NTE event	I _t sample frequency	once per NTE event
I _t sample distribution	Gaussian (normal distribution)	I _t sample distribution	Gaussian (normal distribution)
	Note: mol/s_max = PEMS flowmeter max rating, mol/s		Reference: PEMS f.w median
Error Surface for TR NOx Concentration			
Fig 2.4-a		Fig 2.4-a	
x-axis	Nm (PEMS NTE spd-wtd median lookup Torque) / Torque_max -[%]	x-axis	CO ppm (PEMS NTE flow-wtd median)
y-axis	Torque Nm (PEMS recorded lookup) / Torque_max -[%]	y-axis	NOx ppm (PEMS)
Fig 2.4-b		Fig 2.4-b	
x-axis	Nm (PEMS NTE spd-wtd median lookup Torque) / Torque_max -[%]	x-axis	CO ppm (PEMS NTE flow-wtd median)
y-axis 5th percentile	(5th Nm (TR pems) - 5th Nm (SS lab @ PEMS NTE median)) / Torque_max -[%]	y-axis 5th percentile	5th CO ppm (TR pems) - 5th CO ppm (SS lab @ PEMS NTE median)
	if result >=0 and result <=50th then = 0		if result >=0 and result <=50th then = 0
y-axis 50th percentile	0	y-axis 50th percentile	0
y-axis 95th percentile	(95th Nm (TR pems) - 95th Nm (SS lab @ PEMS NTE median)) / Torque_max -[%]	y-axis 95th percentile	95th CO ppm (TR pems) - 95th CO ppm (SS lab @ PEMS NTE median)
	if result <=0 and result <=50th then = 0		if result <=0 and result <=50th then = 0
Fig 2.4-c		Fig 2.4-c	
x-axis	Nm (PEMS NTE spd-wtd median lookup Torque) / Torque_max -[%]	x-axis	CO ppm (PEMS NTE f.w median)
y-axis	I_{t, TR_torque}	y-axis	I_{t, TR_CO}
z-axis = ΔTR_torque	Torque Nm (5th 50th, & 95th) / Torque_max -[%]	z-axis = ΔTR_CO,ppm	ppm (5th 50th, & 95th)
I _t sample frequency	once per NTE event	I _t sample frequency	once per NTE event
I _t sample distribution	Gaussian (normal distribution)	I _t sample distribution	Gaussian (normal distribution)
	Notes: Torque_max = peak lookup torque; speed-wtd median torque = time-wtd median power / time-wtd median speed		Reference: PEMS f.w median
Error Surface for TR CO Concentration			
Fig 2.4-a		Fig 2.4-a	
x-axis	rpm (PEMS NTE torque-wtd median ECM speed) / Speed_max -[%]	x-axis	THC-CH4 ppm (PEMS NTE flow-wtd median)
y-axis	Speed rpm (PEMS recorded ECM speed) / Speed_max -[%]	y-axis	THC-CH4 ppm (PEMS)
Fig 2.4-b		Fig 2.4-b	
x-axis	rpm (PEMS NTE torque-wtd median ECM speed) / Speed_max -[%]	x-axis	THC-CH4 ppm (PEMS NTE flow-wtd median)
y-axis 5th percentile	(5th rpm (TR pems) - 5th rpm (SS lab @ PEMS NTE median)) / Speed_max -[%]	y-axis 5th percentile	5th THC-CH4 ppm (TR pems) - 5th THC-CH4 ppm (SS lab @ PEMS NTE median)
	if result >=0 and result <=50th then = 0		if result >=0 and result <=50th then = 0
y-axis 50th percentile	0	y-axis 50th percentile	0
y-axis 95th percentile	(95th rpm (TR pems) - 95th rpm (SS lab @ PEMS NTE median)) / Speed_max -[%]	y-axis 95th percentile	95th THC-CH4 ppm (TR pems) - 95th THC-CH4 ppm (SS lab @ PEMS NTE median)
	if result <=0 and result <=50th then = 0		if result <=0 and result <=50th then = 0
Fig 2.4-c		Fig 2.4-c	
x-axis	rpm (PEMS NTE torque-wtd median ECM speed) / Speed_max -[%]	x-axis	THC-CH4 ppm (PEMS NTE flow-wtd median)
y-axis	I_{t, TR_speed}	y-axis	$I_{t, TR_THC-CH4}$
z-axis = ΔTR_speed	Speed rpm (5th 50th, & 95th) / Speed_max -[%]	z-axis = ΔTR_THC-CH4,ppm	ppm (5th 50th, & 95th)
I _t sample frequency	once per NTE event	I _t sample frequency	once per NTE event
I _t sample distribution	Gaussian (normal distribution)	I _t sample distribution	Gaussian (normal distribution)
	Notes: Speed_max = max ECM speed; torque-wtd median speed = time-wtd median power / time-wtd median torque		Reference: PEMS f.w median
Error Surface for TR THC-CH4 Concentration			
Fig 2.4-a		Fig 2.4-a	
x-axis	g/hp-hr PEMS NTE fuel-wtd median lookup BSFC	x-axis	0.98*THC ppm (PEMS NTE f.w median)
y-axis	BSFC g/hp-hr PEMS recorded lookup	y-axis	0.98*THC ppm (PEMS)
Fig 2.4-b		Fig 2.4-b	
x-axis	g/hp-hr PEMS NTE fuel-wtd median lookup BSFC	x-axis	0.98*THC ppm (PEMS NTE flow-wtd median)
y-axis 5th percentile	5th g/hp-hr (TR pems) - 5th g/hp-hr (SS lab @ PEMS NTE median)	y-axis 5th percentile	5th 0.98*THC ppm (TR pems) - 5th 0.98*THC ppm (SS lab @ PEMS NTE median)
	if result >=0 and result <=50th then = 0		if result >=0 and result <=50th then = 0
y-axis 50th percentile	0	y-axis 50th percentile	0
y-axis 95th percentile	95th g/hp-hr (TR pems) - 95th g/hp-hr (SS lab @ PEMS NTE median)	y-axis 95th percentile	95th 0.98*THC ppm (TR pems) - 95th 0.98*THC ppm (SS lab @ PEMS NTE median)
	if result <=0 and result <=50th then = 0		if result <=0 and result <=50th then = 0
Fig 2.4-c		Fig 2.4-c	
x-axis	g/hp-hr PEMS NTE fuel-wtd median lookup BSFC	x-axis	0.98*THC ppm (PEMS NTE flow-wtd median)
y-axis	I_{t, TR_BSFC}	y-axis	$I_{t, TR_0.98*THC}$
z-axis = ΔTR_BSFC	BSFC g/hp-hr (5th 50th, & 95th)	z-axis = ΔTR_0.98*THC,ppm	ppm (5th 50th, & 95th)
I _t sample frequency	once per NTE event	I _t sample frequency	once per NTE event
I _t sample distribution	Gaussian (normal distribution)	I _t sample distribution	Gaussian (normal distribution)
	Note: fuel-wtd median BSFC = time-wtd median (fuel rate/BSFC) / time-wtd median fuel rate		Reference: PEMS f.w median
Error Surface for TR 0.98*THC Concentration			
Fig 2.4-a		Fig 2.4-a	
x-axis	g/s (PEMS NTE time-wtd median ECM fuel rate) / fuel rate_max -[%]	x-axis	g/s (PEMS NTE time-wtd median ECM fuel rate) / fuel rate_max -[%]
y-axis	fuel rate g/s (PEMS recorded ECM fuel rate) / fuel rate_max -[%]	y-axis	fuel rate g/s (PEMS recorded ECM fuel rate) / fuel rate_max -[%]
Fig 2.4-b		Fig 2.4-b	
x-axis	g/s (PEMS NTE time-wtd median ECM fuel rate) / fuel rate_max -[%]	x-axis	g/s (PEMS NTE time-wtd median ECM fuel rate) / fuel rate_max -[%]
y-axis 5th percentile	(5th g/s (TR pems) - 5th g/s (SS lab @ PEMS NTE median)) / fuel rate_max -[%]	y-axis 5th percentile	(5th g/s (TR pems) - 5th g/s (SS lab @ PEMS NTE median)) / fuel rate_max -[%]
	if result >=0 and result <=50th then = 0		if result >=0 and result <=50th then = 0
y-axis 50th percentile	0	y-axis 50th percentile	0
y-axis 95th percentile	(95th g/s (TR pems) - 95th g/s (SS lab @ PEMS NTE median)) / fuel rate_max -[%]	y-axis 95th percentile	(95th g/s (TR pems) - 95th g/s (SS lab @ PEMS NTE median)) / fuel rate_max -[%]
	if result <=0 and result <=50th then = 0		if result <=0 and result <=50th then = 0
Fig 2.4-c		Fig 2.4-c	
x-axis	g/s (PEMS NTE time-wtd median ECM fuel rate) / fuel rate_max -[%]	x-axis	g/s (PEMS NTE time-wtd median ECM fuel rate) / fuel rate_max -[%]
y-axis	I_{t, TR_fuel}	y-axis	I_{t, TR_fuel}
z-axis = ΔTR_fuel	fuel rate g/s (5th 50th, & 95th) / fuel rate_max -[%]	z-axis = ΔTR_fuel	fuel rate g/s (5th 50th, & 95th) / fuel rate_max -[%]
I _t sample frequency	once per NTE event	I _t sample frequency	once per NTE event
I _t sample distribution	Gaussian (normal distribution)	I _t sample distribution	Gaussian (normal distribution)
	Notes: Fuel_max = ECM max fuel rate		
Error Surface for TR ECM Speed			
Fig 2.4-a		Fig 2.4-a	
x-axis	rpm (PEMS NTE torque-wtd median ECM speed) / Speed_max -[%]	x-axis	rpm (PEMS NTE torque-wtd median ECM speed) / Speed_max -[%]
y-axis	Speed rpm (PEMS recorded ECM speed) / Speed_max -[%]	y-axis	Speed rpm (PEMS recorded ECM speed) / Speed_max -[%]
Fig 2.4-b		Fig 2.4-b	
x-axis	rpm (PEMS NTE torque-wtd median ECM speed) / Speed_max -[%]	x-axis	rpm (PEMS NTE torque-wtd median ECM speed) / Speed_max -[%]
y-axis 5th percentile	(5th rpm (TR pems) - 5th rpm (SS lab @ PEMS NTE median)) / Speed_max -[%]	y-axis 5th percentile	(5th rpm (TR pems) - 5th rpm (SS lab @ PEMS NTE median)) / Speed_max -[%]
	if result >=0 and result <=50th then = 0		if result >=0 and result <=50th then = 0
y-axis 50th percentile	0	y-axis 50th percentile	0
y-axis 95th percentile	(95th rpm (TR pems) - 95th rpm (SS lab @ PEMS NTE median)) / Speed_max -[%]	y-axis 95th percentile	(95th rpm (TR pems) - 95th rpm (SS lab @ PEMS NTE median)) / Speed_max -[%]
	if result <=0 and result <=50th then = 0		if result <=0 and result <=50th then = 0
Fig 2.4-c		Fig 2.4-c	
x-axis	rpm (PEMS NTE torque-wtd median ECM speed) / Speed_max -[%]	x-axis	rpm (PEMS NTE torque-wtd median ECM speed) / Speed_max -[%]
y-axis	I_{t, TR_speed}	y-axis	I_{t, TR_speed}
z-axis = ΔTR_speed	Speed rpm (5th 50th, & 95th) / Speed_max -[%]	z-axis = ΔTR_speed	Speed rpm (5th 50th, & 95th) / Speed_max -[%]
I _t sample frequency	once per NTE event	I _t sample frequency	once per NTE event
I _t sample distribution	Gaussian (normal distribution)	I _t sample distribution	Gaussian (normal distribution)
	Notes: Speed_max = max ECM speed; torque-wtd median speed = time-wtd median power / time-wtd median torque		
Error Surface for TR ECM Fuel Rate			
Fig 2.4-a		Fig 2.4-a	
x-axis	g/s (PEMS NTE time-wtd median ECM fuel rate) / fuel rate_max -[%]	x-axis	g/s (PEMS NTE time-wtd median ECM fuel rate) / fuel rate_max -[%]
y-axis	fuel rate g/s (PEMS recorded ECM fuel rate) / fuel rate_max -[%]	y-axis	fuel rate g/s (PEMS recorded ECM fuel rate) / fuel rate_max -[%]
Fig 2.4-b		Fig 2.4-b	
x-axis	g/s (PEMS NTE time-wtd median ECM fuel rate) / fuel rate_max -[%]	x-axis	g/s (PEMS NTE time-wtd median ECM fuel rate) / fuel rate_max -[%]
y-axis 5th percentile	(5th g/s (TR pems) - 5th g/s (SS lab @ PEMS NTE median)) / fuel rate_max -[%]	y-axis 5th percentile	(5th g/s (TR pems) - 5th g/s (SS lab @ PEMS NTE median)) / fuel rate_max -[%]
	if result >=0 and result <=50th then = 0		if result >=0 and result <=50th then = 0
y-axis 50th percentile	0	y-axis 50th percentile	0
y-axis 95th percentile	(95th g/s (TR pems) - 95th g/s (SS lab @ PEMS NTE median)) / fuel rate_max -[%]	y-axis 95th percentile	(95th g/s (TR pems) - 95th g/s (SS lab @ PEMS NTE median)) / fuel rate_max -[%]
	if result <=0 and result <=50th then = 0		if result <=0 and result <=50th then = 0
Fig 2.4-c		Fig 2.4-c	
x-axis	g/s (PEMS NTE time-wtd median ECM fuel rate) / fuel rate_max -[%]	x-axis	g/s (PEMS NTE time-wtd median ECM fuel rate) / fuel rate_max -[%]
y-axis	I_{t, TR_fuel}	y-axis	I_{t, TR_fuel}
z-axis = ΔTR_fuel	fuel rate g/s (5th 50th, & 95th) / fuel rate_max -[%]	z-axis = ΔTR_fuel	fuel rate g/s (5th 50th, & 95th) / fuel rate_max -[%]
I _t sample frequency	once per NTE event	I _t sample frequency	once per NTE event
I _t sample distribution	Gaussian (normal distribution)	I _t sample distribution	Gaussian (normal distribution)
	Notes: Fuel_max = ECM max fuel rate		

3.4 Exhaust Flow Meter Installation

3.4.1 Objective

Evaluate potential bias errors of PEMS exhaust flow sensor due to exhaust system installation related factors; measuring 10 different steady-state NTE over a 30-minute cycle, and under different installation configurations. Determine the $\Delta_{\text{cfg_pulse}}$ and $\Delta_{\text{cfg_swirl}}$ surface plots for the error model.

This part of the test program extends the exhaust flow sensor evaluation conducted in Section 3.2, which assessed the bias and precision characteristics of the exhaust flow sensor.

3.4.2 Background

The PEMS exhaust flow sensors rely upon stable uniform exhaust velocity profiles near the flow sensor in order to provide the best opportunity for accurate flow measurements. When applying PEMS exhaust flow metering systems to actual in-use vehicles, a wide variety of exhaust system designs will likely be encountered, which could expose the flow sensor to exhaust plumes that are not fully established or altered from the case in which the flow sensor was calibrated. In such situations, a decrease in the accuracy or precision of the exhaust flow metering would result.

In order to evaluate the sensitivity of the exhaust flow sensors to installation effects, the PEMS exhaust flow sensor will be installed in test set-ups where the sensor will be exposed to factors intended to alter the exhaust velocity profiles approaching the sensor to see if the reported flow rate changes from baseline data. The installation factors to be assessed are i) pulsating exhaust flow, ii) non-uniform velocity profile (swirl), and iii) wind effect on the exhaust tailpipe exit.

3.4.3 Methods and Materials

The following items apply to each of the test set-up phases of this program. The only difference between each test phase is the configuration of the exhaust system near the PEMS exhaust flow sensor.

- a) Perform the flow sensor evaluation on only one (1) of the test program engines. Engine selection will be based upon project schedule efficiency, but the HHDE engine is desired due to its higher exhaust flow range.
- b) Use two PEMS for this testing (one Sensors Semtech-D, and one Horiba OBS-2000). Test each PEMS individually to eliminate the chance of one flow sensor influencing the other.
- c) Do not connect the exhaust (after the PEMS flow meter) to a CVS tunnel. It is desired to discharge the exhaust flow to the cell ambient. As in section 3.2.3, it is imperative to measure engine inlet air flow and fuel flow rate in order to calculate exhaust flow rate using lab-grade instrumentation.

- d) Follow the same testing guidelines of Section 3.2.3 for determining engine stability time, logging duration, test mode dwell time, and engine test conditions (inlet temperatures, restrictions, etc)
- e) Use the same 10 NTE zone test points selected in Section 3.2.3. These test points are the final reduced set test point matrix derived from the initial 40 point test point map. NOTE: the 10 NTE test points are nominal engine speed/load targets. It is important to fine adjust the engine speed and/or load to achieve the same Laboratory exhaust flow rates observed for the 10 NTE zone test points selected in Section 3.2.3.
- f) Repeat the test matrix 5 times for each test set-up. For each repeat of the test matrix, alter (randomize) the sequence of the engine operation test points. If after 3 repeats of the test point matrix the data suggests no significant difference between the PEMS flow rate data observed in this section and the PEMS flow rate data reported in Section 3.2.3, halt further testing of the specific test set-up.
- g) At minimum record the following data:
 - 1. Laboratory exhaust mass and volume flow rate (kg/hr)
 - 2. PEMS indicated exhaust mass and volume flow rate (kg/hr)
 - 3. Engine speed (rpm) and engine torque (N-m)
 - 4. Engine intake air mass flow rate (kg/hr)
 - 5. Engine fuel consumption mass rate (kg/hr)
- h) Do not record raw PEMS gaseous emissions unless the PEMS requires these measurements in order to report the exhaust flow rate.
- i) Expected test matrix time duration:
 - 3 min/point x 10 points x 5 repeats = 150 min (or 2.5 hrs) per test configuration
 - 3 Test configurations = 3 x 2.5 hrs = 7.5 hrs per PEMS
 - 2 PEMS evaluations = 2 x 7.5 hrs = 15 hrs = total engine running time.

Allocate additional time for fabrication of needed test set-up components, installation of the PEMS exhaust flow sensors, and pre-test instrumentation check-out.

3.4.3.1 Pulsation Test

Utilizing the exhaust configuration used in Section 3.2.3 (sensor bias and precision evaluation), remove the aftertreatment device and replace it with an unobstructed full flow exhaust pipe of the same diameter as the entrance and exit of the aftertreatment device. The intent of this set-up is to expose the exhaust flow sensor to higher pulsations than found in typical exhaust systems by eliminating the pulse attenuating characteristics of the aftertreatment device.

Conduct the testing following the provisions of Section 3.4.3 items (g-n).

3.4.3.2 Non-Uniform Velocity Test (swirl)

Utilizing the same exhaust configuration used in Section 3.2.3, (including the aftertreatment device), install two 90° elbows connected in series, in non-parallel planes, immediately upstream of the exhaust flow metering device supplied by the PEMS manufacturer. Connect the two elbows together in a manner such that their axial planes are 90° to each another. The intent of this set-up is to induce swirl into the exhaust flow stream to produce non-uniform flow velocity profiles across the exhaust pipe prior to the PEMS flow metering system.

Conduct the testing following the provisions of Section 3.4.3 items (g-n).

3.4.3.3 Tailpipe Wind Test

- a) For this test set-up utilize an exhaust system set-up in which the exhaust can freely exit the PEMS flow metering device and form a typical exhaust plume. Utilize the same exhaust configuration utilized in Section 3.2.3., including the aftertreatment device.
- b) Operate the engine at the exhaust flow rates established in Section 3.4.3 item d (10 NTE test points). For each of these test points, use a common leaf blower, or perhaps a carpet dryer blower (or other high velocity/high volume air source) to blow air across the tailpipe exit in an attempt to see if the PEMS indicated exhaust flow rate shows any noticeable change.
- c) Set the test-points by directing the high velocity air at the tailpipe exit from a wide variety of angles, perpendicular and non-perpendicular to the exhaust axial flow.
- d) Adapt to the blower exit and connect a flexible hose, of at least 5 in. dia. Attach to the flexible hose a short section of solid thin-wall tubing (material of steel, aluminum, or plastic), that will provide the ability to be portable and direct the air flow at the exhaust plume from various directions. The outlet of the blower, at the point the air is directed at the exhaust plume, should be at least 5 in. diameter.
- e) Ensure that the air velocity directed on the exhaust plume is in the range of 60-65 mph (88 ft/sec – 95 ft/sec). A second PEMS exhaust flow sensor may be useful in determining the blower air velocity.
- f) At each test point, obtain two 30 sec. average data logs of the PEMS indicated flow rate. Obtain one average log without the blower air impinging on the exhaust plume, and obtain a second log with the blower air impinging on the exhaust plume.

Notes:

- g) The intent of this effort is to detect any significant change in the exhaust flow rate reported by the PEMS due to the air being blown across the tailpipe. If initial efforts do not show significant changes, this phase of the test program is to be terminated.
- h) However, should the PEMS exhaust flow sensor show sensitivity to air currents moving across the tailpipe exit, this information is to be noted and communicated to the project director in a timely manner. In such a case, request discussions with the steering team to determine if more extensive and quantitative testing is warranted.

3.4.4 Data Analysis

3.4.4.1 Pulsation and Swirl Effects -- Data Analysis

- a) For each test matrix data point, calculate the difference between the PEMS reported exhaust flow rate and the flow rate reported by the baseline PEMS data reported for Section 3.2.3. This will be an indication of potential biases due to exhaust flow-meter configuration
- b) Also calculate the difference between the PEMS reported exhaust flow rate and the Laboratory reported exhaust flow rate. If the magnitude of these differences are

similar to those measured under section 3.2, then the effect of these configuration factors is negligible.

- c) Use the data in (a) above to create the “error surfaces” to be used by the Monte Carlo simulation. Refer to section 2.4 for the description and an example of an error surface. Using Figure 2.4-(c) as reference, create the error surfaces for exhaust flow configuration bias errors using the parameters indicated in the table below (Table 3.4.4.1-a). Note that examples are given only for exhaust mass flow, but the same could be used for volumetric flow rate if needed:

Table 3.4.4.1-a: Exhaust Flow Configuration Error Surfaces (Refer to section 2.4)

<u>Error Surface for Pulsation effects on Exhaust Mass Flowrate</u>	
Fig 2.4-a	
x-axis	$\text{exh_flow (pems,ss)} / \text{exh_flow_max} \text{ -[\%]}$
y-axis	$\text{exh_flow (pems,pulse)} / \text{exh_flow_max} \text{ -[\%]}$
Fig 2.4-b	
x-axis	$\text{exh_flow (pems,ss)} / \text{exh_flow_max} \text{ -[\%]}$
y-axis	$[\text{exh_flow (pems,pulse)} - \text{exh_flow(pems,ss)}] / \text{exh_flow_max} \text{ -[\%]}$
Fig 2.4-c	
x-axis	$\text{exh_flow (pems,ss)} / \text{exh_flow_max} \text{ -[\%]}$
y-axis	$i_{c_cfg_pulse}$
z-axis = Δ_{cfg_pulse}	$[\text{exh_flow (pems,pulse)} - \text{exh_flow(pems,ss)}] / \text{exh_flow_max} \text{ -[\%]}$
i_c sample frequency	once per NTE event
i_c sample distribution	random (same chance to roll any number between -1 to +1)
<u>Note:</u> exh_flow_max = PEMS flowmeter maximum exhaust flowrate (@ max density)	
<u>Error Surface for Swirl effects on Exhaust Mass Flowrate</u>	
Fig 2.4-a	
x-axis	$\text{exh_flow (pems,ss)} / \text{exh_flow_max} \text{ -[\%]}$
y-axis	$\text{exh_flow (pems,swirl)} / \text{exh_flow_max} \text{ -[\%]}$
Fig 2.4-b	
x-axis	$\text{exh_flow (pems,ss)} / \text{exh_flow_max} \text{ -[\%]}$
y-axis	$[\text{exh_flow (pems,swirl)} - \text{exh_flow(pems,ss)}] / \text{exh_flow_max} \text{ -[\%]}$
Fig 2.4-c	
x-axis	$\text{exh_flow (pems,ss)} / \text{exh_flow_max} \text{ -[\%]}$
y-axis	$i_{c_cfg_swirl}$
z-axis = Δ_{cfg_swirl}	$[\text{exh_flow (pems,swirl)} - \text{exh_flow(pems,ss)}] / \text{exh_flow_max} \text{ -[\%]}$
i_c sample frequency	once per NTE event
i_c sample distribution	random (same chance to roll any number between -1 to +1)
<u>Note:</u> exh_flow_max = PEMS flowmeter maximum exhaust flowrate (@ max density)	

3.4.4.2 Tailpipe Wind Velocity Effects – Data Analysis

Create a table showing the following information:

Test Point Number	Blower Orientation Description	PEMS Flow No Wind kg/hr	PEMS Flow with Wind kg/hr	Difference w/wind – no wind Δ_{efwind}
1	90° to axial flow horizontal to exhaust pipe			
2	45° to axial flow horizontal to exhaust pipe			
3,4,5,...8,9				
10				

If the differences are of a magnitude equal to or greater than 1%, call a meeting with the in-use testing steering team, to decide how to proceed in the creation of an error surface for tailpipe wind velocity effects.

3.5 ECM Torque and BSFC

3.5.1 Objective

Evaluate the performance of engine torque and BSFC through ECM-based parameters (speed, fuel commanded).

Evaluate bias and precision errors from ECM-broadcast Torque and BSFC. Determine the $\Delta_{\text{cfg_pulse}}$ and $\Delta_{\text{cfg_swirl}}$ surface plots for the error model.

This part of the test program relies on data acquired from section 3.2 for Torque and BSFC mapping.

3.5.2 Background

Data for this section will come from two sources: contractor engine dynamometer testing and the engine manufacturers themselves. Additional errors not evaluated at the contractor's will be evaluated at engine manufacturer labs (involving testing that would be considered confidential for each engine manufacturer). Examples of such errors include, among others, non-deficiency AECD strategies that are not captured in the contractor's evaluation, and others, as listed in Task 3.5.2.5. Note that the accuracy of the torque/BSFC maps is only relevant to in-use emissions testing when under the NTE zone, and in operating conditions not declared as deficiencies. Also, it is not the intent of this task to "minimize" torque/BSFC mapping errors by developing more sophisticated mapping techniques as that would impose new demands in normal engine development processes, for every engine rating.

During this section, five different tasks will be used to evaluate the impact of various parameters on the accuracy of ECM-broadcast torque and BSFC (maps). The first four will be performed at a contractor's facility. The first task will evaluate parameters that are likely to interact with each other, and thus a Design of Experiments (DOE) approach will be used. The second task will evaluate temperature-related parameters that cannot be independently controlled, using an engine warm-up test. The third task will evaluate parameters that are not likely to have strong interactions, using a sensitivity analysis. The fourth task will evaluate the effect of interpolating torque and BSFC from discrete data sets of (speed, fuel, torque) and (speed, fuel, BSFC). The fifth task is open-ended in that manufacturers have the option to submit additional data for consideration for an additional Δ in the error model. The parameters to be used in the investigation of their corresponding effects on torque/BSFC map accuracy are listed below:

Task 1: (1) Intake air restriction; (2) Exhaust gas restriction; (3) Barometric pressure (altitude); (4) Charge air cooler out temperature

Task 2: (1) Oil viscosity (weight); (2) Fuel temperature; (3) Oil temperature; (4) Coolant temperature

Task 3: (1) Intake air humidity; (2) Fuel properties (cetane number, viscosity, API density, etc.)

Task 4: (1) Estimation of engine torque/BSFC through ECM-based parameters

Task 5: (1) Non-deficiency AECD strategies that are not captured by the contractor's evaluation; (2) Effect of multi-torque engine software on torque/BSFC maps; (3) Effect of production variability on torque/BSFC; (4) Effect of engine deterioration on torque/BSFC; (5) Any parameters not covered under 3rd party lab testing that are deemed important by any engine manufacturer.

Note 1: All measurements uncertainties associated with Task 5 are the burden of the engine manufacturers only. If engine manufacturers fail to provide this data 1 month before the beginning of the validation testing tasks (section 5), a zero contribution to the torque/BSFC error will be assessed under this task.

3.5.2.1 Interacting parameters - DOE

The DOE will evaluate the effect of the following parameters on torque/BSFC map errors:

(1) intake air restriction; (2) exhaust gas restriction; (3) barometric pressure (altitude); (4) Charge air cooler out temperature. Only operating conditions not declared as deficiencies will be evaluated.

3.5.2.2 Interacting parameters – Warm-up

The warm-up test will evaluate the effect of the following parameters on torque/BSFC map errors:

(1) oil viscosity (weight); (2) fuel temperature; (3) oil temperature; (4) coolant temperature

3.5.2.3 Independent parameters

The sensitivity test will evaluate the effect of the following parameters on torque/BSFC map errors:

(1) intake air humidity; (2) fuel properties (cetane number, viscosity, API density, etc.)

3.5.2.4 Interpolation

The HDIU testing program will not require ECMs to be programmed to transmit torque and BSFC values, which are needed for the work calculation as well as the calculation of brake-specific emissions. It was determined that this requirement would place an unnecessary burden on the engine manufacturers, who are only required to test a relatively small number of engines each year for this program (25% of an engine manufacturer's families, with a maximum of 20 vehicles tested per family). Instead, torque and BSFC will be mapped as a function of speed and fuel commanded with the engine installed in a dyno prior to any in-use testing of the same engine family and rating. Data for the mapping exercise is actually acquired as part of section 3.2. Since the mapping process is time consuming and is required for each engine family and rating tested in the HDIU testing program, it would be advantageous to reduce the number of points required for a torque/BSFC map to a minimum, striking a balance between mapping effort and limiting errors due to linearly interpolating torque and BSFC on a coarser grid. Map interpolation errors will be quantified in this task.

3.5.2.5 Other parameters

As stated above, each engine manufacturer will be responsible for this task, and thus the structure of testing and reporting will be communicated as CBI (confidential business information) to the EPA.

A list of anticipated parameters (not all inclusive) envisioned being a part of this task is shown below:

- Non-deficiency AECD strategies that are not captured by tasks 1-4 above
- Effect of multi-torque engine software on torque/BSFC maps
- Effect of production variability on torque/BSFC
- Effect of engine deterioration on torque/BSFC
- Any parameters not covered under 3rd party lab testing

The methods and materials for evaluating these “other parameters” are left up to the individual manufacturers to determine.

EPA and CARB will accept manufacturer-supplied information for an additional allowance according to the terms agreed upon in the Memorandum of Agreement.

3.5.3 Methods and Materials

Use the following systems:

- a) Two (2) heavy duty diesel engines (1 HHDE, 1 LHDE) for Subtask 3.5.2.1.
- b) Three (3) heavy duty diesel engines (1 HHDE, 1 MHDE, 1 LHDE) for Subtask 3.5.2.2.
- c) One (1) heavy duty diesel engine (1 MHDE) for Subtask 3.5.2.3.
- d) Three (3) heavy duty diesel engines (1 HHDE, 1 MHDE, 1 LHDE) for Subtask 3.5.2.4.
- e) Each engine will be mapped as per section 3.2. It is likely that these data points will be down sampled to 20 points to create the map for each engine.

3.5.3.1 Interacting Parameters Test - DOE

- a) Evaluate torque/BSFC map errors due to intake air restriction, exhaust gas restriction, barometric pressure, and charge air cooler out temperature using a Design of Experiments (DOE) test matrix (half factorial), with resolution IV, 4 factors, and 1 center point (9 pts).
- b) Evaluate each parameter two conditions (min and max) plus a center point, to investigate nominal conditions.
- c) Evaluate accuracy of the Torque and BSFC map under five (5) steady-state engine operating conditions, as shown in Table 3.5.3.1-a (which are a subset of the 40-point map evaluated in Task 3.2)
- d) For each operating condition, use closed loop control on engine speed and load cell torque.
- e) At each condition, measure torque, fuel flow rate, and BSFC. Also, record ECM speed and fuel commanded (in order to infer broadcast torque and BSFC).

- f) This will result in a total number of points of $9 \times 5 = 45$ / engine. No repeats of this test are needed, unless necessary to establish that the precision error is less than the variability for the above task.
- g) Use the parameter settings given in Table 3.5.3.1-b for the DOE matrix
- h) Note that this test must be performed in an altitude cell so that barometric effects may be studied. For example, hook up a CVS tunnel to simulate the barometric pressures at engine inlet and exhaust.

Table 3.5.3.1-a: DOE Engine Operating Conditions (%speed, and %torque respectively)				
17%, 32%	100%, 100%	59%, 49%	100%, 32%	100%, 100%

Table 3.5.3.1-b: DOE Parameter Set Points		
Parameter	Minimum	Maximum
Intake air restriction	Minimum capable*	Max. allowed by manufacturer*
Exhaust gas restriction	Minimum capable*	Max. allowed by manufacturer*
Barometric pressure	82.7 kPa	105 kPa
Charge air cooler out temperature	Minimum per manufacturer specifications and ambient conditions**	Maximum per manufacturer specifications and ambient conditions**

* Consider removing aftertreatment to extend range of restrictions

** Assume that a 1 deg. change in ambient temperature corresponds to a 1 deg. change in charge air cooler out temperature

3.5.3.2 Interacting Parameters Test - Warm-up

- a) Evaluate torque/BSFC map errors due to oil viscosity (weight), fuel temperature, oil temperature and coolant temperature.
- b) Since these parameters cannot easily be independently controlled, they will be evaluated during an engine warm-up cycle.
- c) Install the Caterpillar (non-EGR) engine in cell capable of controlling ambient temperature, preferably at 0 deg C [this may be not feasible]. Warm up the engine until the coolant temperature reaches above 212 deg. F.
- d) Install the International and DDC engines will be installed in a standard test cell at ambient temperature, and perform the same type of warm up test.
- e) You will receive the speed/torque schedule to be used during the warm-up cycle from the CSTF in-use testing steering team.
- f) Sample engine torque at 5 Hz and fuel flow at 1 Hz (per Part 1065 recommendations)
- g) Record fuel temperature, oil temperature, and coolant temperature, along with the ECM channels of speed and fuel commanded.
- h) Resample and/or bin data as deemed appropriate.

- i) Record data throughout the engine warm-up, but use only data obtained when the engine’s operating conditions meet the criteria for a valid NTE event, for the measurement allowance.
- j) Warm up all three engines in the same manner, which is to be established by the contractor and agreed on by the engine manufacturers. This test does not need to be repeated, unless it becomes necessary to establish that the precision error is less than the variability for the above task.

3.5.3.3 Independent Parameters Test

- a) Evaluate torque/BSFC map errors due to intake air humidity and fuel properties (cetane number, viscosity, API density, etc.) using a sensitivity analysis with 5 total points.
- b) Evaluate each parameter at two or three conditions (min, mid and max, or 1 and 2).
- c) Set engine to three (3) steady state operating conditions which are a subset of those tested in Task 3.5.3.1. and given in Table 3.5.3.3-a.
- d) For each operating condition, use closed loop control on engine speed and load cell torque.
- e) At each condition, measure torque, fuel flow rate, and BSFC. Also, record ECM speed and fuel commanded (in order to infer broadcast torque and BSFC).
- f) This will result in a total number of points of $5 \times 3 = 15$ data pts/ engine.
- g) Use parameter settings specified in Table 3.5.3.3-b.
- h) Perform only minimal repeat testing to establish that the precision error is less than the variability observed in the above subtasks, as explained in Note 3.
- i) Note: One or two additional sensitivity parameters may be added to Table 3.5.3.3-b. In that case you will be asked to test those conditions also. The steering committee will finalize any additional sensitivity parameters prior to signature of the Memorandum of Agreement. If no additional parameters are added prior to Memorandum of Agreement signature, additional parameters may be added by written mutual agreement of all parties.

Table 3.5.3.3-a: Sensitivity Engine Operating Conditions (%speed, and %torque respectively)		
17%, 32%	59%, 49%	100%, 100%

Table 3.5.3.3-b: Sensitivity Parameter Set Points			
Parameter	Minimum (#1)	Mid. (#2)	Maximum (#3)
Intake air humidity	Minimum possible (@30 deg. C); 0 grains/lb dry air	50% RH (@30 deg. C); 95 grains/lb dry air	95% RH (@30 deg. C)*; 180 grains/lb dry air
Fuel properties	Fuel used in program	Fuel selection #2	California ULSD

*Run charge air cooler water inlet temperature of 30 deg. C

3.5.3.4 Interpolation Test

- a) Evaluate torque/BSFC errors due to interpolating map values.
- b) To quantify interpolation errors, down-sample the 40 steady-state points taken in Task 3.2 to 20 points (used to create the torque/BSFC maps)
- c) Quantify interpolation errors by subtracting the subset of the 40 points that were NOT used to create the 20-point map.

Note 3: the methodology used in the preceding tasks does not separate bias and precision errors. Both types of errors will be coupled together. In order to better assess precision errors, repeat testing would be necessary. However, it is expected that the variability in ECM mapped torque and mapped BSFC will be greater than the precision interval on a repeated test for the above Subtasks . It is also expected that the precision error (as percent of point) in Subtask 3.5.2.3 will be less than the variability interval (as percent of point) of Subtask 3.5.2.1.

If this does not hold, a modification to the test plan may be needed, which may include repeated testing.

3.5.4 Data Analysis

Use the acquired data to create the “error surfaces” to be used by the Monte Carlo simulation. Refer to section 2.4 for description and example of an error surface.

Assume the errors to be independent and additive unless determined otherwise. The following sub-sections will describe the error surfaces for ECM-based torque. Construct BSFC models in a similar fashion, based on BSFC data.

Determine mean of the ten steady-state torque variances, where each of the ten variances is calculated from the 20 repeats of each of the points in the 10-point steady-state matrix in 3.2.3. Subtract this mean torque variance from each of the respective ECM deltas.

3.5.4.1 Interacting Parameters Analysis DOE

Refer to section 2.4 for description and example of an error surface. Using Figure 2.4-(c) as reference, create the error surface $\Delta_{\text{Torque_DOE}}$ using the parameters indicated in Table 3.5.4.1-a.

Tables 3.5.4.1 through 3.5.4.6: Torque Error Surfaces

<p>Table 3.5.4.1-a: Error Surface for Torque (interacting parameters - DOE)</p> <p>Fig 2.4-a</p> <table border="1"> <tr> <td>x-axis</td> <td>% Peak Torque (load cell)</td> </tr> <tr> <td>y-axis</td> <td>% Peak Torque (ECM map)</td> </tr> </table> <p>Fig 2.4-b</p> <table border="1"> <tr> <td>x-axis</td> <td>% Peak Torque (load cell)</td> </tr> <tr> <td>y-axis</td> <td>% Peak Torque (ECM map) - % Peak Torque (load cell)</td> </tr> </table> <p>Fig 2.4-c</p> <table border="1"> <tr> <td>x-axis</td> <td>% Peak Torque (load cell)</td> </tr> <tr> <td>y-axis</td> <td>i_c Torque DOE</td> </tr> <tr> <td>z-axis = $\Delta\%Torque_{DOE}$</td> <td>% Peak Torque (ECM map) - % Peak Torque (load cell)</td> </tr> <tr> <td>i_c sample frequency</td> <td>once per NTE event</td> </tr> <tr> <td>i_c sample distribution</td> <td>random (same chance for i_c: -1 to +1)</td> </tr> <tr> <td>Data:</td> <td>All parameters sampled in DOE matrix</td> </tr> </table>	x-axis	% Peak Torque (load cell)	y-axis	% Peak Torque (ECM map)	x-axis	% Peak Torque (load cell)	y-axis	% Peak Torque (ECM map) - % Peak Torque (load cell)	x-axis	% Peak Torque (load cell)	y-axis	i_c Torque DOE	z-axis = $\Delta\%Torque_{DOE}$	% Peak Torque (ECM map) - % Peak Torque (load cell)	i_c sample frequency	once per NTE event	i_c sample distribution	random (same chance for i_c : -1 to +1)	Data:	All parameters sampled in DOE matrix	<p>Table 3.5.4.2-a: Error Surface for Torque (interacting parameters - warm up)</p> <p>Fig 2.4-a</p> <table border="1"> <tr> <td>x-axis</td> <td>% Peak Torque (load cell)</td> </tr> <tr> <td>y-axis</td> <td>% Peak Torque (ECM map)</td> </tr> </table> <p>Fig 2.4-b</p> <table border="1"> <tr> <td>x-axis</td> <td>% Peak Torque (load cell)</td> </tr> <tr> <td>y-axis</td> <td>% Peak Torque (ECM map) - % Peak Torque (load cell)</td> </tr> </table> <p>Fig 2.4-c</p> <table border="1"> <tr> <td>x-axis</td> <td>% Peak Torque (load cell)</td> </tr> <tr> <td>y-axis</td> <td>i_c Torque warm-up</td> </tr> <tr> <td>z-axis = $\Delta\%Torque_{warmup}$</td> <td>% Peak Torque (ECM map) - % Peak Torque (load cell)</td> </tr> <tr> <td>i_c sample frequency</td> <td>once per NTE event</td> </tr> <tr> <td>i_c sample distribution</td> <td>random (same chance for i_c: -1 to +1)</td> </tr> <tr> <td>Data:</td> <td>warm-up cycle. Discretize data at different torque levels</td> </tr> </table>	x-axis	% Peak Torque (load cell)	y-axis	% Peak Torque (ECM map)	x-axis	% Peak Torque (load cell)	y-axis	% Peak Torque (ECM map) - % Peak Torque (load cell)	x-axis	% Peak Torque (load cell)	y-axis	i_c Torque warm-up	z-axis = $\Delta\%Torque_{warmup}$	% Peak Torque (ECM map) - % Peak Torque (load cell)	i_c sample frequency	once per NTE event	i_c sample distribution	random (same chance for i_c : -1 to +1)	Data:	warm-up cycle. Discretize data at different torque levels
x-axis	% Peak Torque (load cell)																																								
y-axis	% Peak Torque (ECM map)																																								
x-axis	% Peak Torque (load cell)																																								
y-axis	% Peak Torque (ECM map) - % Peak Torque (load cell)																																								
x-axis	% Peak Torque (load cell)																																								
y-axis	i_c Torque DOE																																								
z-axis = $\Delta\%Torque_{DOE}$	% Peak Torque (ECM map) - % Peak Torque (load cell)																																								
i_c sample frequency	once per NTE event																																								
i_c sample distribution	random (same chance for i_c : -1 to +1)																																								
Data:	All parameters sampled in DOE matrix																																								
x-axis	% Peak Torque (load cell)																																								
y-axis	% Peak Torque (ECM map)																																								
x-axis	% Peak Torque (load cell)																																								
y-axis	% Peak Torque (ECM map) - % Peak Torque (load cell)																																								
x-axis	% Peak Torque (load cell)																																								
y-axis	i_c Torque warm-up																																								
z-axis = $\Delta\%Torque_{warmup}$	% Peak Torque (ECM map) - % Peak Torque (load cell)																																								
i_c sample frequency	once per NTE event																																								
i_c sample distribution	random (same chance for i_c : -1 to +1)																																								
Data:	warm-up cycle. Discretize data at different torque levels																																								
<p>Table 3.5.4.3-a: Error Surface for Torque (independent parameters -</p> <p>Fig 2.4-a</p> <table border="1"> <tr> <td>x-axis</td> <td>% Peak Torque (load cell)</td> </tr> <tr> <td>y-axis</td> <td>% Peak Torque (ECM map)</td> </tr> </table> <p>Fig 2.4-b</p> <table border="1"> <tr> <td>x-axis</td> <td>% Peak Torque (load cell)</td> </tr> <tr> <td>y-axis</td> <td>% Peak Torque (ECM map) - % Peak Torque (load cell)</td> </tr> </table> <p>Fig 2.4-c</p> <table border="1"> <tr> <td>x-axis</td> <td>% Peak Torque (load cell)</td> </tr> <tr> <td>y-axis</td> <td>i_c Torque_hum [Discrete Range: 1, or 2, or 3]</td> </tr> <tr> <td>z-axis = $\Delta\%Torque_{hum}$</td> <td>% Peak Torque (ECM map) - % Peak Torque (load cell)</td> </tr> <tr> <td>i_c sample frequency</td> <td>once per NTE event</td> </tr> <tr> <td>i_c sample distribution</td> <td>random (same chance for i_c: 1, or 2, or 3)</td> </tr> <tr> <td>Data:</td> <td>3 different humidity levels will need to be pooled at each of the 3 torque levels</td> </tr> </table>	x-axis	% Peak Torque (load cell)	y-axis	% Peak Torque (ECM map)	x-axis	% Peak Torque (load cell)	y-axis	% Peak Torque (ECM map) - % Peak Torque (load cell)	x-axis	% Peak Torque (load cell)	y-axis	i_c Torque_hum [Discrete Range: 1, or 2, or 3]	z-axis = $\Delta\%Torque_{hum}$	% Peak Torque (ECM map) - % Peak Torque (load cell)	i_c sample frequency	once per NTE event	i_c sample distribution	random (same chance for i_c : 1, or 2, or 3)	Data:	3 different humidity levels will need to be pooled at each of the 3 torque levels	<p>Table 3.5.4.3-b: Error Surface for Torque (independent parameters - fuel type)</p> <p>Fig 2.4-a</p> <table border="1"> <tr> <td>x-axis</td> <td>% Peak Torque (load cell)</td> </tr> <tr> <td>y-axis</td> <td>% Peak Torque (ECM map)</td> </tr> </table> <p>Fig 2.4-b</p> <table border="1"> <tr> <td>x-axis</td> <td>% Peak Torque (load cell)</td> </tr> <tr> <td>y-axis</td> <td>% Peak Torque (ECM map) - % Peak Torque (load cell)</td> </tr> </table> <p>Fig 2.4-c</p> <table border="1"> <tr> <td>x-axis</td> <td>% Peak Torque (load cell)</td> </tr> <tr> <td>y-axis</td> <td>i_c Torque_fuel [Discrete Range: 1, or 2, or 3]</td> </tr> <tr> <td>z-axis = $\Delta\%Torque_{fuel}$</td> <td>% Peak Torque (ECM map) - % Peak Torque (load cell)</td> </tr> <tr> <td>i_c sample frequency</td> <td>once per NTE event</td> </tr> <tr> <td>i_c sample distribution</td> <td>random (same chance for i_c: 1, or 2, or 3)</td> </tr> <tr> <td>Data:</td> <td>3 different fuel types will need to be pooled at each of the 3 torque levels</td> </tr> </table>	x-axis	% Peak Torque (load cell)	y-axis	% Peak Torque (ECM map)	x-axis	% Peak Torque (load cell)	y-axis	% Peak Torque (ECM map) - % Peak Torque (load cell)	x-axis	% Peak Torque (load cell)	y-axis	i_c Torque_fuel [Discrete Range: 1, or 2, or 3]	z-axis = $\Delta\%Torque_{fuel}$	% Peak Torque (ECM map) - % Peak Torque (load cell)	i_c sample frequency	once per NTE event	i_c sample distribution	random (same chance for i_c : 1, or 2, or 3)	Data:	3 different fuel types will need to be pooled at each of the 3 torque levels
x-axis	% Peak Torque (load cell)																																								
y-axis	% Peak Torque (ECM map)																																								
x-axis	% Peak Torque (load cell)																																								
y-axis	% Peak Torque (ECM map) - % Peak Torque (load cell)																																								
x-axis	% Peak Torque (load cell)																																								
y-axis	i_c Torque_hum [Discrete Range: 1, or 2, or 3]																																								
z-axis = $\Delta\%Torque_{hum}$	% Peak Torque (ECM map) - % Peak Torque (load cell)																																								
i_c sample frequency	once per NTE event																																								
i_c sample distribution	random (same chance for i_c : 1, or 2, or 3)																																								
Data:	3 different humidity levels will need to be pooled at each of the 3 torque levels																																								
x-axis	% Peak Torque (load cell)																																								
y-axis	% Peak Torque (ECM map)																																								
x-axis	% Peak Torque (load cell)																																								
y-axis	% Peak Torque (ECM map) - % Peak Torque (load cell)																																								
x-axis	% Peak Torque (load cell)																																								
y-axis	i_c Torque_fuel [Discrete Range: 1, or 2, or 3]																																								
z-axis = $\Delta\%Torque_{fuel}$	% Peak Torque (ECM map) - % Peak Torque (load cell)																																								
i_c sample frequency	once per NTE event																																								
i_c sample distribution	random (same chance for i_c : 1, or 2, or 3)																																								
Data:	3 different fuel types will need to be pooled at each of the 3 torque levels																																								
<p>Table 3.5.4.4-a: Error Surface for Torque (interpolation effects)</p> <p>Fig 2.4-a</p> <table border="1"> <tr> <td>x-axis</td> <td>single point</td> </tr> <tr> <td>y-axis</td> <td>% Peak Torque (ECM map) - % Peak Torque (load cell)</td> </tr> </table> <p>Fig 2.4-b</p> <table border="1"> <tr> <td>x-axis</td> <td>single point</td> </tr> <tr> <td>y-axis</td> <td>% Peak Torque (ECM map) - % Peak Torque (load cell)</td> </tr> </table> <p>Fig 2.4-c</p> <table border="1"> <tr> <td>x-axis</td> <td>single point</td> </tr> <tr> <td>y-axis</td> <td>i_c Torque_intp</td> </tr> <tr> <td>z-axis = $\Delta\%Torque_{intp}$</td> <td>% Peak Torque (ECM map) - % Peak Torque (load cell)</td> </tr> <tr> <td>i_c sample frequency</td> <td>once per NTE event</td> </tr> <tr> <td>i_c sample distribution</td> <td>random (same chance for i_c: -1 to +1)</td> </tr> <tr> <td>Data:</td> <td>results from all 20 points will be pooled under a single point in the x-axis (unless data shows clear trend with</td> </tr> </table>	x-axis	single point	y-axis	% Peak Torque (ECM map) - % Peak Torque (load cell)	x-axis	single point	y-axis	% Peak Torque (ECM map) - % Peak Torque (load cell)	x-axis	single point	y-axis	i_c Torque_intp	z-axis = $\Delta\%Torque_{intp}$	% Peak Torque (ECM map) - % Peak Torque (load cell)	i_c sample frequency	once per NTE event	i_c sample distribution	random (same chance for i_c : -1 to +1)	Data:	results from all 20 points will be pooled under a single point in the x-axis (unless data shows clear trend with	<p>Table 3.5.4.5-a: Error Surface for Torque (engine manufacturer data)</p> <p>Fig 2.4-a</p> <table border="1"> <tr> <td>x-axis</td> <td>% Peak Torque (load cell)</td> </tr> <tr> <td>y-axis</td> <td>% Peak Torque (ECM map)</td> </tr> </table> <p>Fig 2.4-b</p> <table border="1"> <tr> <td>x-axis</td> <td>% Peak Torque (load cell)</td> </tr> <tr> <td>y-axis</td> <td>% Peak Torque (ECM map) - % Peak Torque (load cell)</td> </tr> </table> <p>Fig 2.4-c</p> <table border="1"> <tr> <td>x-axis</td> <td>% Peak Torque (load cell)</td> </tr> <tr> <td>y-axis</td> <td>i_c Torque_eng-man</td> </tr> <tr> <td>z-axis = $\Delta\%Torque_{eng-man}$</td> <td>% Peak Torque (ECM map) - % Peak Torque (load cell)</td> </tr> <tr> <td>i_c sample frequency</td> <td>to be specified by engine manufacturer</td> </tr> <tr> <td>i_c sample distribution</td> <td>to be specified by engine manufacturer</td> </tr> <tr> <td>Data:</td> <td>to be specified by engine manufacturer</td> </tr> </table>	x-axis	% Peak Torque (load cell)	y-axis	% Peak Torque (ECM map)	x-axis	% Peak Torque (load cell)	y-axis	% Peak Torque (ECM map) - % Peak Torque (load cell)	x-axis	% Peak Torque (load cell)	y-axis	i_c Torque_eng-man	z-axis = $\Delta\%Torque_{eng-man}$	% Peak Torque (ECM map) - % Peak Torque (load cell)	i_c sample frequency	to be specified by engine manufacturer	i_c sample distribution	to be specified by engine manufacturer	Data:	to be specified by engine manufacturer
x-axis	single point																																								
y-axis	% Peak Torque (ECM map) - % Peak Torque (load cell)																																								
x-axis	single point																																								
y-axis	% Peak Torque (ECM map) - % Peak Torque (load cell)																																								
x-axis	single point																																								
y-axis	i_c Torque_intp																																								
z-axis = $\Delta\%Torque_{intp}$	% Peak Torque (ECM map) - % Peak Torque (load cell)																																								
i_c sample frequency	once per NTE event																																								
i_c sample distribution	random (same chance for i_c : -1 to +1)																																								
Data:	results from all 20 points will be pooled under a single point in the x-axis (unless data shows clear trend with																																								
x-axis	% Peak Torque (load cell)																																								
y-axis	% Peak Torque (ECM map)																																								
x-axis	% Peak Torque (load cell)																																								
y-axis	% Peak Torque (ECM map) - % Peak Torque (load cell)																																								
x-axis	% Peak Torque (load cell)																																								
y-axis	i_c Torque_eng-man																																								
z-axis = $\Delta\%Torque_{eng-man}$	% Peak Torque (ECM map) - % Peak Torque (load cell)																																								
i_c sample frequency	to be specified by engine manufacturer																																								
i_c sample distribution	to be specified by engine manufacturer																																								
Data:	to be specified by engine manufacturer																																								

3.5.4.2 Interacting Parameters Analysis – Warm-up

Refer to section 2.4 for description and example of an error surface. Using Figure 2.4-(c) as reference, create the error surface Δ_{Torque_warmup} using the parameters indicated in Table 3.5.4.2-a.

3.5.4.3 Independent Parameters Analysis

Refer to section 2.4 for description and example of an error surface. Using Figure 2.4-(c) as reference:

a) create the error surface Δ_{Torque_hum} using the parameters indicated in Table 3.5.4.3-a

b) create the error surface $\Delta_{\text{Torque_fuel}}$ using the parameters indicated in Table 3.5.4.3-b

3.5.4.4 Interpolation Analysis

Refer to section 2.4 for description and example of an error surface. Using Figure 2.4-(c) as reference, create the error surface $\Delta_{\text{Torque_intp}}$ using the parameters indicated in Table 3.5.4.4-a.

3.5.4.5 Analysis for Torque/BSFC errors provided by engine manufacturers

Refer to section 2.4 for description and example of an error surface. Using Figure 2.4-(c) as reference, engine manufacturers can create the various error surfaces $\Delta_{\text{Torque_eng-man}}$ using the parameters indicated in Table 3.5.4.5-a.

It must be emphasized that these error surfaces will not be determined by the contractor. Engine manufacturers can supply as many error surfaces as deemed appropriate, so long as they back up their claims with data and/or engineering judgment. This data, and error surfaces must be supplied by the engine manufacturers to the contractor on or before one month prior to the beginning of the validation test work (section 5)

4 Environmental Chamber Tests

The environmental chamber tests challenge PEMS to a variety of environmental disturbances, namely electromagnetic interference, atmospheric pressure, ambient temperature, vibration, and ambient hydrocarbons. During each of the tests, plus a baseline test, PEMS will sample a series of reference gases, and errors quantifying the reference values will be calculated. Each test is designed to mimic real-world environmental disturbances with the magnitude and frequency of the disturbance adjusted to real-world conditions. Because of this, error from these tests can be sampled randomly, from any minute of the test. By randomly sampling from the minutes of these tests the magnitude and frequency of the real-world error will be built into the error model, which is described in Section 2.

All of the testing will be done with reference gases during application of the ambient conditions. All tests will use the same gases, except for the ambient hydrocarbons test. The following tables list the gases:

Table 4-a: Gas Cylinder Contents for 5 of 6 Environmental Tests	
Gas	Number of AL size cylinders ¹
1. purified air	5, +1 spare
2. quad-blend span: CO ₂ , CO, NO, C ₃ H ₈ , balance N ₂	5, +1 spare
3. CH ₄ span, balance N ₂	5, +1 spare
4. NO ₂ span, balance N ₂	5, +1 spare
5. quad-blend audit: CO ₂ , CO, NO, C ₃ H ₈ , balance N ₂	5, +1 spare
6. CH ₄ audit, balance N ₂	5, +1 spare
7. NO ₂ audit, balance N ₂	5, +1 spare
¹ AL size compressed gas cylinders are high pressure (2000 psi full) and hold 29.5 liters of water. Considering the compressibility (Z) of certain gases, a safe approximate supply from one full AL cylinder is 4,000 liters at atmospheric conditions. Assuming 6 PEMS consuming 40 lpm total for a given test, times 8 hr 20 min equals 20000 liters per day or 5 cylinders per day. Because a minimum of 7 cylinders are used each day (one for each of 7 mixtures), only 1 of each cylinder is needed per day—as long as full cylinders are used each day.	

N₂ is not in the gas cylinder matrix as a zero quantity since N₂ would be just like the CH₄ or NO₂ cylinders for the other gases, and the quad-blends are just like N₂ for CH₄ and NO₂. Gas cylinder concentrations will be selected so that the audit values are near the flow-weighted average concentration of emissions in the raw exhaust at the NTE standards, span values will be about twice the audit values, NO₂ will be at half the concentration of NO, and CH₄ will be at half the concentration of C₃H₈. The gas cylinders purity and accuracy do not have to meet 1065 Subpart H specifications because PEMS outputs will only be used for relative differences.

Table 4-b: Gas Cylinder Contents for Ambient Hydrocarbons	
Gas	Number of AL size cylinders ¹
1. purified air	2, +1 spare
2. C6H14 span, balance N2	2, +1 spare
3. CH4 span, balance N2	2, +1 spare
¹ AL size compressed gas cylinders are high pressure (2000 psi full) and hold 29.5 liters of water. Considering the compressibility (Z) of certain gases, a safe approximate supply from one full AL cylinder is 4,000 liters at atmospheric conditions. Assuming 6 PEMS consuming 40 lpm total for a given test, times 8 hr 20 min equals 20000 liters per day or 5 cylinders per day. Because a minimum of 3 cylinders are used each day (one for each of 3 mixtures), 2 of each cylinder are needed to complete the test day.	

Cylinder concentrations of the ambient hydrocarbons will be selected to allow adjustment to the concentrations specified in the ambient hydrocarbons test cycle.

4.1 Data Analysis for all Environmental Tests

Refer to the spreadsheet prepared for performing this data analysis. The spreadsheet describes the schedule to be used with the various gas bottles, during the 8hr (480min) tests. Reduce data by first calculating means for each 30-second period of stabilized measurements. Subtract from each mean the respective reference concentration. The results are errors or “deltas”. Group the errors by the categories of zero errors, mid-span errors, and span errors. Correct each of these three error distributions by removing their respective baseline biases and variances, which were determined in section 4.1. To remove the baseline bias from each distribution, subtract the respective median baseline error from each of the errors in each respective distribution. This shifts each error distribution to null out any respective baseline zero, mid-span, or span bias. Next calculate the variance of each of the distributions. Subtract the respective baseline variance from each calculated variance. Use the resulting difference in variance as the target variance for adjusting the error distributions. If the target variance is zero or negative, set all error values of the distribution to the corrected bias value and do not proceed to the next step. If the target variance is positive, iteratively solve to find a single numerical value that can be used to divide each error in a given distribution such that the resulting distribution has a variance equal to the target variance. Now each of the errors is corrected for baseline bias and variance.

Sample the errors by randomly selecting a number between 1 and 480, which represent the minutes of the actual test. For the selected minute, record the most recent past set of baseline corrected errors for each emission. Wrap backwards to the end of the data set (i.e. 480) if a complete set of recent errors are not available. Do this by going backward from minute 1.

For each nominal NTE event, randomly sample one minute’s error. Then, second-by-second use the nominal second-by-second concentrations to linearly interpolate between the respective zero, mid-span, and span error values for each emission as a function of concentration to find the error associated with that second’s nominal concentration.

Apply this error as a “delta” to the nominal concentration for that second. Calculate the brake-specific NTE event once all errors are applied.

Next calculate whether or not a periodic drift check would have invalidated the NTE event. Simulate drift check results by subtracting from each of the zero, mid-span, and span error values a single delta that would result in the zero error value being zero. Then subtract from the span error a value that would result in the span error being zero. Divide that value by the span reference value, multiply it by the mid-span reference value and subtract the result from the mid-span error. The results are three values for zero, mid-span, and span error, where zero and span errors are zero. The mid-span may have a positive or negative value, which would indicate a non-linearity that was not checked by the pre-test 0-span maneuver. Use the three values to recalculate the NTE event, but use all of the other original flow and torque errors. If the NTE result with all of the errors applied is more than $\pm 4\%$ different than the NTE event with the errors decreased, discard the results. Then calculate the NTE result with all errors, including torque and flow errors set to zero. This is the true value. Then for each of the validated results, subtract the true NTE value and record this difference in one of the eighteen measurement allowance distributions: three emissions (NO_x, CO, NMHC) times three calculation methods (torque-speed, fuel-specific * BSFC, ECM fuel flow) times two PEMS manufacturers. Then proceed to the next NTE event in the nominal data set. Repeat the entire nominal data set over and over until all 18 measurement allowance distributions converge. Follow the data reduction steps set out in Section 2 to select the final measurement allowances.

4.2 Baseline

4.2.1 Objective

Evaluate the baseline repeatability and bias of PEMS with ambient conditions held constant. Determine the medians and variances for each baseline error for each emission. Use the medians and variances to correct all other environmental test results according to Section 4.1, Data Analysis for All Environmental Tests.

4.2.2 Background

All of the other environmental tests inherently incorporate the baseline bias and variance of the PEMS. Because the Monte Carlo simulation model adds all the errors determined from the various environmental tests, it would add the baseline bias and variance of PEMS to the model too many times. In order to compensate for this in the model, the baseline bias and variance of PEMS is determined and subtracted from each of the environmental tests' results.

Note that the baseline bias and variance of PEMS is measured and modeled (i.e. added) once as part of the steady-state engine dynamometer laboratory experiment.

4.2.3 Methods and Materials

For this experiment use a well ventilated EMI/RFI shielded room capable of maintaining reasonably constant temperature and pressure. Use a room that can house all six PEMS,

their power supplies, the PEMS flow meters, cables and lines, plus seven different zero, audit, and span gas cylinders, and a gas switching system.

Prior to executing the baseline test, setup each PEMS and stabilize the PEMS in the room. Perform PEMS setup according to 40 CFR Part 1065 Subpart J and PEMS manufacturer instructions, including any warm-up time, zero-span-audits of the analyzers and the setup of all accessories including flow meters, ECM interpreters, etc. Then supply the PEMS' overflow sample ports with the sequence of gases from the seven gas cylinders described at the beginning of Section 4.

Flow each cylinder long enough so that at least 30 seconds of stable readings are recorded for the slowest responding gas concentration output of all the PEMS. Position PEMS and configure gas transport tubing to minimize transport delays. Target to sample about 1 minute per cylinder (30 seconds to stabilize + 30 seconds to record stable readings), or 7 minutes to cycle through all 7 cylinders. Repeat this 7-minute cycle over the 8-hr test cycle. Note that this results in about 68 repeats per cylinder.

Perform this test once for each of the six PEMS with as many PEMS tested at once. Test at least one PEMS from each PEMS manufacturer simultaneously so at most repeat this test three times to test each of the three pairs of PEMS once.

Zero and span PEMS at beginning of day following manufacturer's guidelines. Do not re-span PEMS analyzers again during the day, unless PEMS manufacturer provides a way to do this automatically, so it is realistic with real-life in-use testing practices. Re-zeroing should be allowed if and only if done automatically by the PEMS for the same reasons.

4.2.4 Data Analysis

Reduce data by first calculating means for each 30-second period of stabilized measurements. Subtract from each mean the respective reference concentration. The results are errors or "deltas". Group the errors by the categories of zero errors, mid-span errors, and span errors for each emission. Calculate each error distribution's median and variance and use these values in the data reduction of the remaining environmental tests.

4.3 Electromagnetic Radiation

4.3.1 Objective

Evaluate the effect of Electromagnetic Interference (EMI) and Radio frequency Interference (RFI) on the performance of the PEMS and determine error factors for the PEMS due to these effects. Determine Δ_{EMI} .

4.3.2 Background

The performance of the PEMS could be affected by being in a vehicle which is traveling on the roadway and is subject to interferences from surrounding EMI/RFI signals – from the vehicle itself and from items external to the vehicle.

There were many EMI/RFI tests considered for this program. They include the following list

1. Radiated Immunity – This test method is used to verify the ability of the PEMS and associated cabling to withstand electric fields
2. Radiated Emissions – This test method is used to verify that the electric field emissions from the PEMS and its associated cabling do not exceed specified requirements
3. Conducted Immunity – This test method is used to verify the ability of the PEMS to withstand signals coupled onto input power leads
4. Conducted Emissions – This test method is used to verify that electromagnetic emissions from the PEMS do not exceed the specified requirements for power input leads, including returns
5. Electrostatic Discharge – This test method is used to verify the ability of the PEMS to withstand electrostatic discharge from the human body
6. Conducted Transient Immunity – This test method is used to verify the ability of the PEMS to withstand electrical transients
7. Electrical fast transients – This test method is used to verify the ability of the PEMS and associated cabling to withstand short transients
8. Surge Immunity – This test method is used to verify the ability of the PEMS and associated cabling to withstand surges caused by switching and lightning transients
9. Alternator Noise – This test method is used to verify the ability of the PEMS to withstand transients where voltage differences are developed across different current return paths through the chassis
10. Magnetic field immunity – This test method is used to verify the ability of the PEMS and associated cabling to withstand magnetic fields resulting from nearby wiring carrying high current.

After consulting with an expert at The contractor facility, four tests were selected based on SAE standards. Those tests are listed below along with a time estimate for each test.

Standard	Description	Calibration Time	Test time
J1113-4	Bulk Current Injection	0.5 day	1 day
J1113-11	Conducted Transients		0.5 day
J1113-13	Electrostatic Discharge		0.5 day
J1113-21	Radiated Immunity	1 day	1 day

4.3.3 Methods and Materials

Use an EMI test facility capable of running the SAE tests listed above. This would include: Signal generators, Power amplifiers, Transmit antennas, Electric Field Sensors,

Measurement Receiver, Data recording device, LISNs (Line Impedance Stabilization Networks) and shielded enclosure.

Because of the length of these tests, test only one PEMS from each of the two manufacturers. Normally these tests are run separately on each unit under test. Under this scenario, it will take 4.5 days for each PEMS for a total of 9 days. This does not include PEMS set up time. Test multiple PEMS simultaneously on the -4 and -21 tests if the EMI facility can accommodate multiple PEMS. If both PEMS can be tested together on the -4 and -21 tests, then the estimated test time for both PEMS drops to 5.5 days. Since the PEMS output is not expected to deteriorate with prolonged exposure to EMI tests, the test times for any of the four tests may be reduced to the time it takes to collect at least 30 samples of each of the seven gas cylinders. This is only appropriate for EMI tests that have either steady inputs or repetitive input cycles 30 seconds or shorter. If it takes 7 minutes to sample all 7 cylinders, then the test time for each test needs to be at least 210 minutes (3.5 hrs). For EMI tests that sweep the input, run the full test time. There is no requirement to synchronize the sweeping of EMI inputs with the sampling of gases. Suspend the PEMS data logging whenever the EMI inputs are suspended to adjust parameter or conditions such as antennas.

Where the standard includes various severity levels, choose the one most appropriate for the purpose of this program, which is to subject the unit under test to typical levels for normal operation (normally the lowest severity level).

For each EMI test, setup the PEMS according to 40CFR1065, Subpart J and the PEMS manufacturer instructions, including any warm-up time, and zero-spans of the analyzers. Begin the data logging functions, then begin the EMI inputs, then supply the PEMS' overflow sample ports with the sequence of gases from seven gas cylinders described in the beginning of section 4. Flow each cylinder long enough so that at least 30 seconds of stabilized readings are recorded for the slowest responding analyzer. Target to sample about 1 minute from each cylinder (30 seconds to stabilize and 30 seconds to record stable readings), or 7 minutes to cycle through all 7 cylinders. Repeat this 7-minute cycle over the duration of each test.

4.3.4 Data Analysis

Subtract baseline variances according to Section 4.1. Also, when subtracting the baseline biases and variances at zero, mid and span levels, use the baseline data from the same PEMS under test. Treat each set of EMI test results as part of a single environmental test. In other words, after calculating baseline adjusted deltas for zero, audit and span, pool all zero, audit, and span deltas, respectively. Then use the same error surface generation technique that was used in Section 3 for the engine dynamometer tests, where the error is ranked from 5th to 95th percentile and centered with the truncated normal PDF at the 50th percentile error.

Table 4.3.4-a: EMI / RFI Pooled Error Surface

<u>Error Surface for EMI/RFI effect on NOx concentration</u> <u>(Repeat for CO and NMHC)</u>	
Fig 2.4-a	
x-axis	NOx ppm (pems, nom)
y-axis	NOx ppm (pems,EMI)
Fig 2.4-b	
x-axis	NOx ppm (pems, nom)
y-axis	NOx ppm (pems,EMI) - NOx ppm (pems,baseline)
Fig 2.4-c	
x-axis	NOx ppm (pems, nom)
y-axis	$i_c_{EMI_pooled_NOx}$ [Range: $t_{initial}$ through t_{final}]
z-axis = $\Delta_{EMI_pooled_NOx}$	NOx ppm (pems,EMI) - NOx ppm (pems,baseline)
i_c sample frequency	once per NTE event
i_c sample distribution	Gaussian (normal distribution)

4.4 Atmospheric Pressure

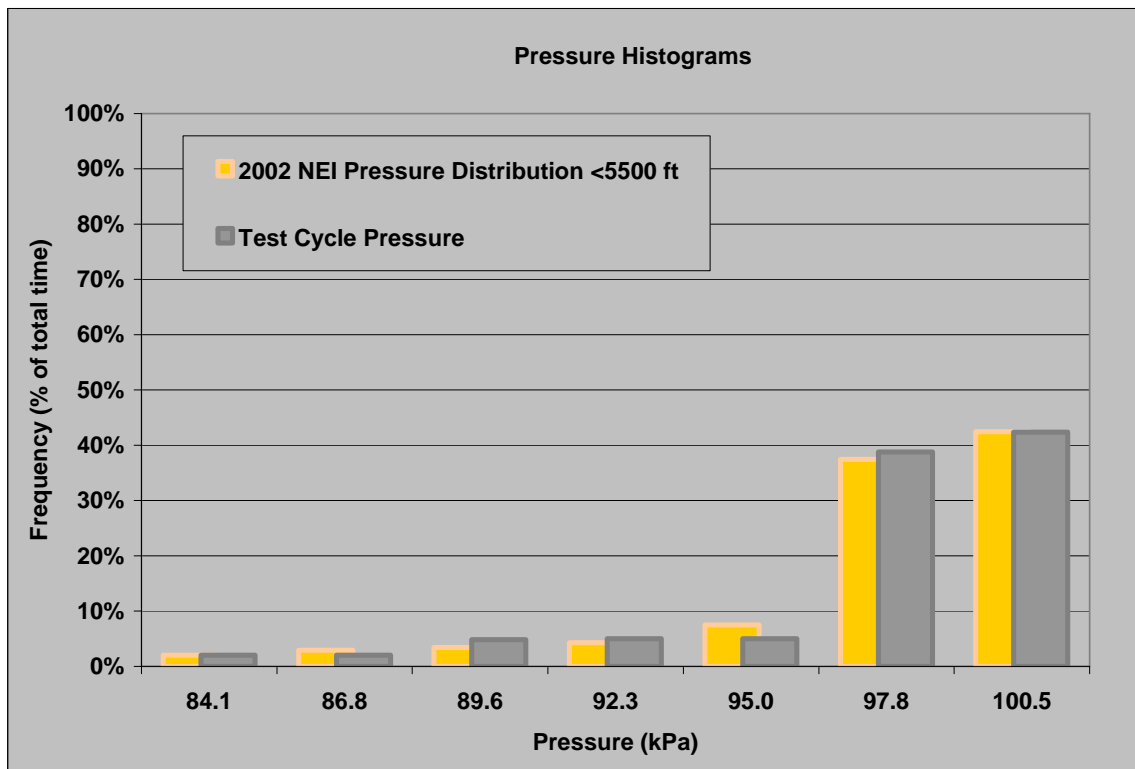
4.4.1 Objective

Evaluate the effects of ambient pressure on PEMS gas concentration outputs.

- Determine Δ_{P_NOx} , Δ_{P_NMHC} , and Δ_{P_CO} , as a function of test time and concentration for use in the error model.
- Also determine $\Delta_{P_exhflow}$ as a function of test time only. This error only needs to be quantified if the flow meter zero flow reading during these tests change due to various atmospheric pressures.

4.4.2 Background

PEMS are expected to operate over ranges of ambient pressures. It is hypothesized that some of the errors of the PEMS concentration outputs may be a function of ambient pressure. Therefore, this experiment will change the ambient pressure surrounding PEMS to evaluate its effects on PEMS measured concentrations and flow meter transducer outputs. As with all of the environmental tests, the test cycle for this test is based on the best-known distribution of real world conditions. For this test, the test cycle pressure distribution was matched to the county-by-county annual average atmospheric pressure distribution in EPA's 2002 National Emissions Inventory (NEI) model. The following table depicts the NEI data distribution (based on 3149 data points) and the test cycle pressure distribution.



4.4.3 Methods and Materials

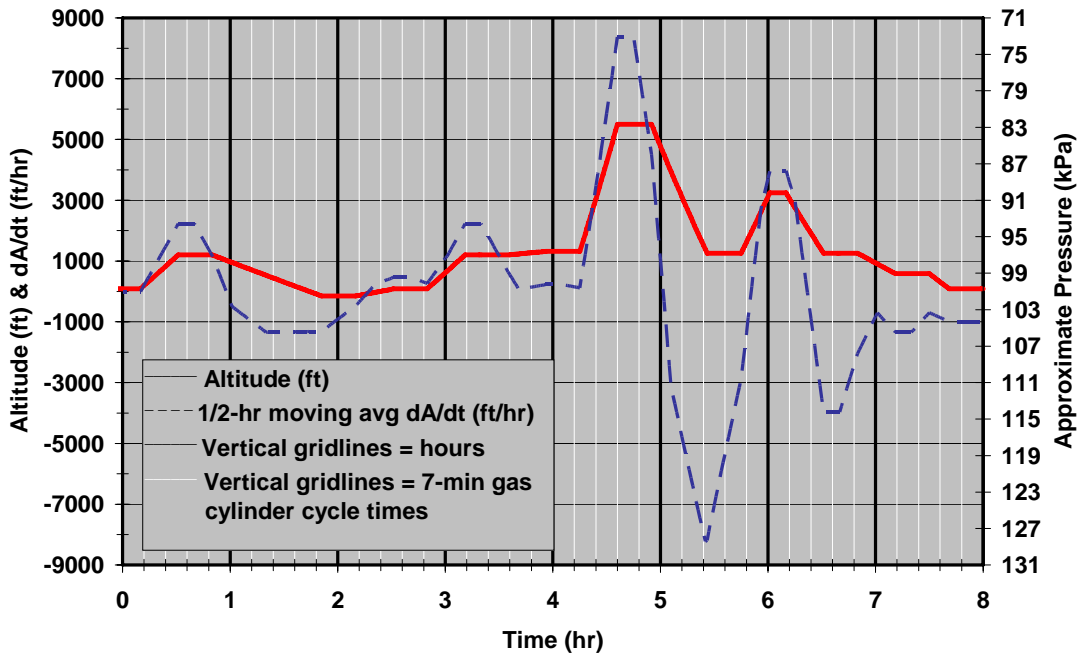
Use a barometric chamber that can be well ventilated and capable of controlling a wide range of pressure changes (82.74 to 101.87 kPa). Use a chamber that can house at least two PEMS at a time, one of each PEMS manufacturer, their power supplies, the PEMS flow meters, cables and lines, plus seven different zero, audit, and span gas cylinders, and a gas switching system.

Follow a pattern of first soaking the PEMS at a constant pressure, then ramp the pressure to a new pressure, soak the PEMS at that new pressure, and then ramp to another pressure. Use the following sequence of pressures and times to simulate a typical distribution of real-world pressures and changes in pressure, which are believed to be dominated by changes in altitude during driving in the United States.

Atmospheric Pressure Test Sequence					
Phase	Pressure		Time	Rate	Comments
	kPa	Alt. ft.	min	ft/min	
1 Soak	101	89	10	0	Flat near sea-level
2 Ramp	101-97	89-1203	20	56	Moderate hill climb from sea level
3 Soak	97	1203	20	0	Flat at moderate elevation
4 Ramp	97-101.87	1203- -148	60	-23	Moderate descent to below sea level
5 Soak	101.87	-148	20	0	Flat at extreme low elevation
6 Ramp	101.87-101	-148-89	20	12	Moderate hill climb to near sea level
7 Soak	101	89	20	0	Flat near sea level
8 Ramp	101-97	89-1203	20	56	Moderate hill climb from sea level
9 Soak	97	1203	25	0	Flat at moderate elevation
10 Ramp	97-96.6	1203-1316	20	6	Slow climb from moderate elevation
11 Soak	96.6	1316	20	0	Flat at moderate elevation
12 Ramp	96.6-82.74	1316-5501	20	209	Rapid climb to NTE limit
13 Soak	82.74	5501	20	0	Flat at NTE limit
14 Ramp	82.74-96.8	5501-1259	30	-141	Rapid descent from NTE limit
15 Soak	96.8	1259	20	0	Flat at moderate elevation
16 Ramp	96.8-90	1259-3244	15	132	Rapid hill climb to mid elevation
17 Soak	90	3244	10	0	Flat at mid elevation
18 Ramp	90-96.8	3244-1259	20	-99	Rapid descent within middle of NTE
19 Soak	96.8	1259	20	0	Flat at moderate elevation
20 Ramp	96.8-99.2	1259-586	20	-34	Moderate descent to lower elevation
21 Soak	99.2	586	20	0	Flat at lower elevation
22 Ramp	99.2-101	586-89	10	-50	Moderate decent to near sea-level
23 Soak	101	89	20	0	Flat near sea-level

Time Series Chart of Atmospheric Pressure Test

Pressure-Time Environmental Test Cycle



Prior to executing this pressure sequence, setup each PEMS and stabilize the PEMS in the chamber's first pressure. Perform PEMS setup according to 40 CFR Part 1065 Subpart J and PEMS manufacturer instructions, including any warm-up time, zero-span-audits of the analyzers and the setup of all accessories including flow meters, ECM interpreters, etc. Then supply the PEMS' overflow sample ports with the sequence of gases from the seven gas cylinders described at the beginning of Section 4.

Flow each cylinder long enough so that at least 30 seconds of stable readings are recorded for the slowest responding gas concentration output of all the PEMS. Position PEMS and configure gas transport tubing to minimize transport delays. Target to sample about 1 minute per cylinder (30 seconds to stabilize + 30 seconds to record stable readings), or 7 minutes to cycle through all 7 cylinders. Repeat this 7-minute cycle over the 8-hr test cycle. Note that this results in about 68 repeats per cylinder or about 480 minutes of data points per day per concentration output recorded.

Perform this test once for each of the six PEMS with as many PEMS tested at once. Test at least one PEMS from each PEMS manufacturer simultaneously so at most repeat this test three times to test each of the three pairs of PEMS once.

4.4.4 Data Analysis

Perform data analysis according to Section 4.1.

4.5 Ambient Temperature

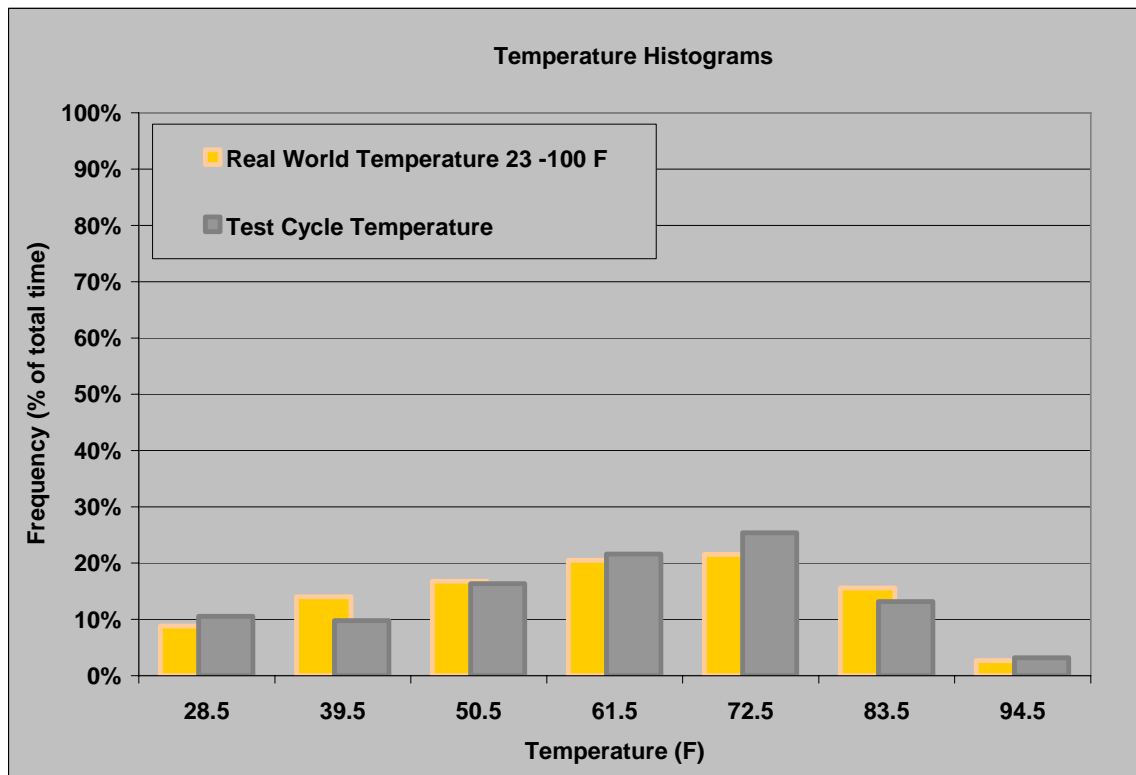
4.5.1 Objective

Evaluate the effects of ambient temperature on PEMS gas concentration outputs.

- Determine Δ_{T_NOx} , Δ_{T_NMHC} , and Δ_{T_CO} , as a function of test time and concentration for use in the error model.
- Also determine $\Delta_{T_exhflow}$ as a function of test time only. This error only needs to be quantified if the flow meter zero flow reading during these tests change due to various ambient temperatures.

4.5.2 Background

PEMS are expected to operate over a wide range of changing ambient temperatures. It is hypothesized that some of the errors of the PEMS outputs may be a function of changes in ambient temperature. Therefore, this experiment will change the ambient temperature surrounding PEMS to evaluate its effects on PEMS measured concentrations and flow meter transducer outputs. As with all of the environmental tests, the test cycle for this test is based on the best-known distribution of real world conditions. For this test, the test cycle temperature distribution was matched to the hour-by-hour county-by-county average atmospheric temperature distribution, weighted by vehicle miles traveled according to EPA's 2002 National Emissions Inventory (NEI) model. The following table depicts the NEI data distribution (based on over 900,000 temperatures and over 270 trillion vehicle miles) and the test cycle temperature distribution.



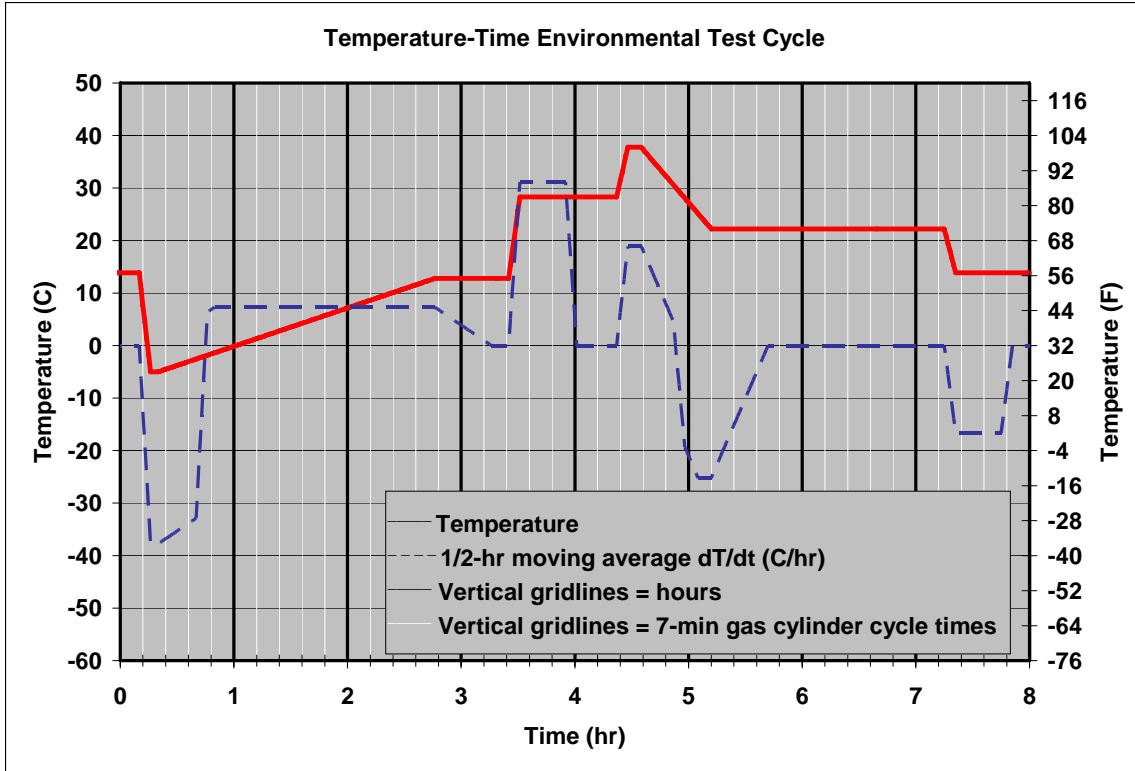
4.5.3 Methods and Materials

Use a well ventilated room capable of controlling a wide range of temperature changes (-23 to 100 °F). Use a room that can house at least six PEMS, their power supplies, the PEMS flow meters, cables and lines, plus seven different zero, audit, and span gas cylinders, and a gas switching system.

Follow a pattern of first soaking the PEMS at a constant room temperature, then ramping the room temperature to a new temperature, soaking the PEMS at that new temperature, and then ramping to another temperature. Use the following sequence of temperatures and times to simulate the range of real-world temperatures and changes in temperature:

Ambient Temperature Test Sequence					
Phase	Temperature		Time min	Rate °C/min	Comments
	°C	°F			
1 Soak	13.89	57	10	0.00	Cool in-garage pre-test PEMS operations
2 Ramp	13.89-5.00	57-23	5	-3.78	Leaving cool garage into cold ambient
3 Soak	-5.00	23	5	0.00	Operating at cold temperature outside of vehicle
4 Ramp	-5.00-12.78	23-55	145	0.12	Diurnal warming during cool day
5 Soak	12.78	55	40	0.00	Steady cool temperature during testing
6 Ramp	12.78-28.33	55-83	5	3.11	Return to hot garage on a cool day
7 Soak	28.33	83	52	0.00	Hot in-garage pre- post- test PEMS operations
8 Ramp	28.33-37.78	83-100	5	1.89	Leaving ho garage into hot ambient
9 Soak	37.78	100	8	0.00	Operating at hot temperature outside of vehicle
10 Ramp	37.78-22.22	100-72	100	-0.16	Diurnal cooling during hot day
11 Soak	22.22	72	60	0.00	Steady moderate temperature during testing
12 Ramp	22.22-13.89	72-57	5	-1.67	Return to cool garage on a moderate day
13 Soak	13.89	57	40	0.00	Cool in-garage post-test PEMS operations

Time Series Chart of Ambient Temperature Test



Prior to executing this temperature sequence, setup each PEMS and stabilize the PEMS in the chamber's first temperature. Perform PEMS setup according to 40 CFR Part 1065 Subpart J and PEMS manufacturer instructions, including any warm-up time, zero-span-audits of the analyzers and the setup of all accessories including flow meters, ECM interpreters, etc. Then supply the PEMS' overflow sample ports with the sequence of gases from the seven gas cylinders described at the beginning of Section 4.

Flow each cylinder long enough so that at least 30 seconds of stable readings are recorded for the slowest responding gas concentration output of all the PEMS. Position PEMS and configure gas transport tubing to minimize transport delays. Target to sample about 1 minute per cylinder (30 seconds to stabilize + 30 seconds to record stable readings), or 7 minutes to cycle through all 7 cylinders. Repeat this 7-minute cycle over the 8-hr test cycle. Note that this results in about 68 repeats per cylinder or about 480 minutes of data points per day per concentration output recorded.

Perform this test once for each of the six PEMS with as many PEMS tested at once. Test at least one PEMS from each PEMS manufacturer simultaneously so at most repeat this test three times to test each of the three pairs of PEMS once.

4.5.4 Data Analysis

Perform data analysis according to Section 4.1.

4.6 Orientation, Shock, and Vibration

4.6.1 Objective

Evaluate the effect of vehicle vibration on the performance of the PEMS and determine error factors for the PEMS due to these effects.

- a) Determine $\Delta_{\text{Vib_pooled_NOx}}$, $\Delta_{\text{Vib_pooled_NMHC}}$, and $\Delta_{\text{Vib_pooled_CO}}$.
- b) Also determine $\Delta_{\text{Vib_pooled_exhflow}}$ as a function of test time only. This error only needs to be quantified if the flow meter zero flow reading during these tests change due to vibration level.

4.6.2 Background

The performance of the PEMS could be affected by being in a vehicle which is traveling on the roadway and is subject to roadway irregularities resulting in the transmission of shock and vibration to the PEMS. The location/orientation of the PEMS in the vehicle could also be a factor.

Several vibration tests were considered, including random vibration, sine sweep, and resonate dwell tests. Experts in this field recommended the random vibration test as the most appropriate vibration test for this program. This kind of testing is run with electrodynamic shakers with controllers that can input a broad range of frequencies of varying amplitudes. These controllers are generally programmed with the desired Power Spectral Density (g^2/Hz versus Hz).

Three different approaches were considered for identifying appropriate Power Spectral Density - 1) use a proprietary PSD's or proprietary vehicle accelerometer data from either an EMA member or a vehicle manufacturer; 2) collect vehicle accelerometer data and reduce it down to a PSD; and 3) use a standard. Although some limited vehicle accelerometer data was available, experts at The contractor and Cummins Inc. agreed that the Mil Standard 810, method 514.5, appendix C, p 514.5c-8, US Highway Truck Vibration Exposure was a representative vibration profile based on a larger data set and has been widely used. It is also more cost effective and less ambiguous to use an existing vibration profile from a standard than to develop a custom profile from limited vehicle accelerometer data. The PSD from the Mil Standard includes vibration PSD in three axes – vertical, longitudinal and transverse. These three PSD's are run one at a time, i.e. vibration is applied to the unit under test one axis at a time.

Shock is short term, high level pulses that are generally unusual events. With the adsorbing action of vehicle suspensions, shock testing was deemed to not be applicable for the purposes of this test plan. The PSD of the Mil Standard was judged to adequately cover the normal range of vibrations.

Orientation of the PEMS vertical axis with respect to gravity was also deemed to be adequately covered in the vibration test. Since PEMS are typically mounted top up (one PEMS manufacture even requires this), the angle of the PEMS vertical axis with respect to gravity will be limited to road grades. This angle would create small static side loads,

but these were judged to be too small to include in the test plan. The transverse and longitudinal axis vibration profiles will be applied and are expected to provide adequate testing of dynamic side loads that were of more concern. Since the PEMS can be rotated to any position around its vertical axis when it is mounted in the vehicle, differences in the transverse and longitudinal axis PSD are not appropriate. Rather than test both horizontal axis of the PEMS with both PSD's, use a single PSD for both horizontal axes that contains the PSD of both the longitudinal and transverse PSD's in the Mil Standard.

Two locations on the vehicle was also considered – in-cab and on the frame rails for an outside installation. In-cab installations are not possible on many vehicles and operators often object to the in-cab installations. So a special PSD for the in-cab location was not pursued. The PSD of the Mil Standard was judged to be adequately representative of the frame rail location..

4.6.3 Methods and Materials

Use a shaker test facility capable of running the Mil Standard 810, version F, method 514.5, appendix C, p 514.5C-8, US Highway Truck Vibration Exposure. A total of four test days are allocated for this test. This does not include set up time. Test multiple PEMS simultaneously if the shaker table can accommodate multiple PEMS. If not, test a minimum of two PEMS – one from each manufacture. Run the vertical axis test for a minimum of 6, and preferably 8 hours. Run each of the transverse and longitudinal axes of the PEMS for a minimum of 3, and preferable 4 hours.

Take appropriate measures to shield the PEMS from EMI from the shaker table. Fabricate the fixture to mount the PEMS to the shaker table. Use any isolation/mounting device recommended by the PEMS manufacturer for the frame rail.

Setup the PEMS according to 40CFR1065, Subpart J and the PEMS manufacturer instructions, including any warm-up time, and zero-spans of the analyzers. Begin the data logging functions, then begin the vibration inputs, then supply the PEMS' overflow sample ports with the sequence of gases from seven gas cylinders described in the beginning of section 4. Flow each cylinder long enough so that at least 30 seconds of stabilized readings are recorded for the slowest responding analyzer. Target to sample about 1 minute from each cylinder (30 seconds to stabilize and 30 seconds to record stable readings), or 7 minutes to cycle through all 7 cylinders. Repeat this 7-minute cycle over the duration of each test. Suspend the PEMS data logging whenever the vibration inputs are suspended to adjust the test rig such as switching axes.

4.6.4 Data Analysis

Subtract baseline variances according to Section 4.1. Also, when subtracting the baseline biases and variances at zero, mid and span levels, use the baseline data from the same PEMS under test. Treat each set of EMI test results as part of a single environmental test. In other words, after calculating baseline adjusted deltas for zero, audit and span, pool all zero, audit, and span deltas, respectively. Then use the same error surface generation technique that was used in Section 3 for the engine dynamometer tests, where the error is

ranked from 5th to 95th percentile and centered with the truncated normal PDF at the 50th percentile error.

Table 4.6.4-a: Shock and Vibration Pooled Error Surface

<u>Error Surface for Vibration effect on NOx concentration</u> <u>(Repeat for CO and NMHC)</u>	
Fig 2.4-a	
x-axis	NOx ppm (pems, nom)
y-axis	NOx ppm (pems,vibration)
Fig 2.4-b	
x-axis	NOx ppm (pems, nom)
y-axis	NOx ppm (pems,vibration) - NOx ppm (pems,baseline)
Fig 2.4-c	
x-axis	NOx ppm (pems, nom)
y-axis	$i_{c_vibration_pooled_NOx}$ [Range: $t_{initial}$ through t_{final}]
z-axis = $\Delta_{Vib_pooled_NOx}$	NOx ppm (pems,Vibration) - NOx ppm (pems,baseline)
i_c sample frequency	once per NTE event
i_c sample distribution	Gaussian (normal distribution)

4.7 Ambient Hydrocarbons

4.7.1 Objective

Evaluate the effects of ambient hydrocarbons on PEMS FID zero error, and establish error as a function of time. Determine Δ_{HC} for use in the error model.

4.7.2 Background

PEMS are expected to operate over ranges of ambient hydrocarbons. It is hypothesized that zero error of the PEMS FID outputs may be a function of ambient hydrocarbons. Therefore, this experiment will change the ambient hydrocarbons surrounding PEMS to evaluate its effects on PEMS FID zero error.

There are two reasons why a FID might be affected by ambient hydrocarbons:

1. The FID uses ambient air as FID burner air. This introduces hydrocarbons into the detector chamber from a source other than raw engine exhaust. Because a FID uses

burner air continuously, ambient air hydrocarbons from the burner air will also be present in the reaction chamber.

2. The FID may use ambient air as zero air during over-the-road periodic zeroing. This introduces into the detector a second source of ambient hydrocarbons during a FID zeroing procedure, in addition to the burner air ambient hydrocarbons.

Furthermore, these effects become more complicated when one considers that EPA regulations set HDDE standards on a non-methane hydrocarbons (NMHC) basis. Because there is no real-time instrument that directly measures NMHC, NMHC is determined by subtracting a real-time methane measurement from a real-time total hydrocarbons (THC) measurement.

This means two things:

1. Ambient hydrocarbons will have different effects on the net results, depending upon what fraction of the total ambient hydrocarbons is methane.
2. A PEMS will have to quantify exhaust NMHC, which by regulation can be done in real-time by using two FIDs; one with a non-methane hydrocarbon catalytic cutter that measures only methane (CH₄), and one without a cutter so that it measures total hydrocarbons (THC). EPA specifies that NMHC shall be reported as the lower of $NMHC = THC - CH_4$ or $NMHC = 0.98 * THC$. This provision will be incorporated into the model.

4.7.3 Methods and Materials

Use a well ventilated temperature-controlled room at nearly constant pressure. Use a room that is able to house two PEMS (one from each manufacturer), their power supplies, the PEMS flow meters, cables and lines, plus different zero, audit, and span gas cylinders, and two gas dividers.

Follow burner air hydrocarbons changes in a pattern of stabilizing the PEMS FIDs' burner air to one of nine hydrocarbon combinations output to an ambient pressure overflow. After stabilizing each burner air hydrocarbon concentration, set zero for the THC and CH₄ FIDs using a zero gas cylinder. Operate the PEMS to quantify zero air from a gas cylinder at each of ten (9, plus repeat of 1st) different burner air hydrocarbon combinations. Record at least 30 seconds of values at each combination. Then switch to the next of the nine ambient hydrocarbons combinations. Reset zero with the new burner air hydrocarbons concentration overflowing to the burner air port.

Repeat the entire zero quantification sequence after zeroing with the latest ambient hydrocarbons concentration. Continue this series of sequences until all combinations have been quantified and recorded (see table 4.7.3-a below)

Table 4.7.3-a: Ambient Hydrocarbon Error Test Sequence

Ambienet Hydrocarbons Test Sequence					Ambienet Hydrocarbons Test Sequence				
Phase	Burner air hydrocarbons during		Burner air hydrocarbons during		Phase	Burner air hydrocarbons during		Burner air hydrocarbons during	
	Hexane, ppm	Methane, ppm	Hexane, ppm	Methane, ppm		Hexane, ppm	Methane, ppm	Hexane, ppm	Methane, ppm
1			0	0	51			8	8
2			2	2	52			0	0
3			8	8	53			2	2
4			0	2	54			8	0
5	0	0	2	8	55	8	0	0	2
6			8	0	56			2	8
7			0	8	57			8	2
8			2	0	58			0	8
9			8	2	59			2	0
10			0	0	60			8	8
11			2	2	61			0	0
12			8	8	62			2	2
13			0	0	63			8	8
14			2	8	64			0	2
15	2	2	8	0	65	0	8	2	8
16			0	2	66			8	0
17			2	0	67			0	8
18			8	2	68			2	0
19			0	8	69			8	2
20			2	2	70			0	0
21			8	8	71			2	2
22			2	2	72			8	8
23			0	0	73			0	0
24			8	2	74			2	8
25	8	8	2	0	75	2	2	8	0
26			0	8	76			0	2
27			8	0	77			2	0
28			2	8	78			8	2
29			0	2	79			0	8
30			8	8	80			2	2
31			0	0	81			8	8
32			2	2	82			0	0
33			8	8	83			2	2
34			0	2	84			8	0
35	0	2	2	8	85	8	0	0	2
36			8	0	86			2	8
37			0	8	87			8	2
38			2	0	88			0	8
39			8	2	89			2	0
40			0	0	90			8	8
41			2	2					
42			8	8					
43			0	0					
44			2	8					
45	2	8	8	0					
46			0	2					
47			2	0					
48			8	2					
49			0	8					
50			2	2					

Prior to executing this ambient hydrocarbons sequence, setup each PEMS and stabilize the PEMS at the zero methane, zero hexane FID burner air condition. Perform PEMS setup according to 40 CFR Part 1065 Subpart J and PEMS manufacturer instructions, including any warm-up time, zero-span-audits of the analyzers and the setup of all accessories including flow meters, ECM interpreters, etc. Then supply the PEMS' overflow sample ports with the sequence of gases from the seven gas cylinders described at the beginning of Section 4.

Flow each cylinder long enough so that at least 30 seconds of stable readings are recorded for the slowest responding gas concentration output of all the PEMS. Position PEMS and configure gas transport tubing to minimize transport delays. Target to sample about 1 minute per cylinder (30 seconds to stabilize + 30 seconds to record stable readings). Expect that this test cycle will take about 5 hours to complete, which should be completed in one day:

9 separate zero setting procedures at 4 minutes each ($9 \times 4 = \sim 1/2$ hr)

90 phases where hydrocarbons are switched and zero air must be stabilized and quantified; 3 minutes each ($90 \times 3 = 4.5$ hr).

Ambient hydrocarbons concentrations will be controlled by a gas divider to the values specified in table 4.7.3-a. Unless new information about the range of ambient hydrocarbons dictates a change in the test matrix's values. Such information could come from the UCR Ce-Cert results of Ce-Cert trailer continuous CVS background measurements.

This test should be replicated only once.

4.7.4 Data Analysis

Perform data analysis according to Section 4.1, noting that only the zero error will be determined. This means that there will be no "surface" to sample. There will be just a line to sample. Use this error for all second-by-second concentrations

5 Model Validation and Measurement Allowance Determination

5.1 Model validation

5.1.1 Objective

Validate the Monte Carlo model by

- a) Testing the PEMS in parallel with the CE-CERT trailer, and
- b) Replaying tests in a laboratory.

5.1.2 Background

5.1.2.1 Validation with CE-CERT Trailer

Previous tests are designed to evaluate the effect of various potential noise parameters on PEMS units. These effects have are then incorporated into a Monte Carlo model (section 2). The testing in this section is designed to verify the model by comparing the in-use differences between the PEMS system and the CE-CERT trailer in relation to model predicted differences. Test routes will be designed to meet the limits reasonable expected to be found in use testing, and to appropriately cover NTE operation.

Several weeks worth of testing are necessary to validate the Monte Carlo Model. The 1065 audit of the CE-CERT trailer may take several weeks in itself. The NTE cycle test will consist of a 20-minute cycle repeated 20 times on one engine, a total of approximately 2 test days. For the on-road portion of the testing, it is likely that Route 1 will take a complete test day and that Routes 2 and Route 3 can be completed in one test day. This requires 2 test days per PEMS, per mounting location, plus 2 days of on-road CE-CERT validation testing, for a total of 10 test days of on-road CE-CERT trailer operation. If more then one PEMS is available, several systems could be tested in parallel. While two flow meters in the exhaust could affect results, it is likely that this measurement already experiences reduced ambient effects because the CE-CERT trailer captures the exhaust and that any further deviation from the true operating conditions is immaterial.

5.1.2.2 Validation in dyno test cell

Additional testing will be conducted in a laboratory, where selected tests will be “replayed,” while the PEMS is maintained at laboratory conditions.

The engine will be operated as close as possible to previously recorded tests from the on-road portion of the validation testing. Controlled conditions will include engine speed/load, ambient conditions, and any other condition that can be repeated with a reasonable level confidence. For each PEMS, two test days will be replayed, for a total of 4 test days.

5.1.3 Methods and Materials

5.1.3.1 CE_CERT Trailer validation

- a) Use two PEMS units, one Sensors and one Horiba, in parallel with the CE-CERT emissions trailer.
- b) Ensure that the trailer is able to measure regulated emissions and CO₂, ambient hydrocarbons (methane and NMHC), humidity, temperature, and pressure and have adequate data acquisition capabilities to capture the additional measurements discussed herein.
- c) Acquire ECM data to allow “re-play” of engine conditions during section 5.1.3.2 (Dyno cell validation). Work with engine manufacturer to ensure enough data is capture, using proprietary tools if needed for subsequent re-play of conditions.
- d) Test the trailer at Contractor facility to insure that a reasonable level of confidence can be placed on the reported NTE results. As part of these tests include a 1065 audit.
- e) In addition, validate the trailer by testing over the conditions present during the over-the-road test by measuring zero, span, and audit gases while traveling over the designated routes. Ensure that the CE-CERT trailer emissions measurements are insensitive to these over-the-road changing conditions
- f) Install and calibrate the PEMS as specified by the manufacturer in a Class 8 truck.
- g) Install temperature sensors inside the protective enclosure housing PEMS analyzers, near exhaust flow meter, and in the ambient air stream.
- h) Use a Rohde & Schwarz Spectrum Analyzer FSH3 or similar unit to measure electromagnetic spectrum and power.
- i) Use Two 3-axis vibration/shock transducers to measure vibration/shock for the PEMS analyzer unit and the flow meter. Note: The accelerometers and the spectrum analyzer should have previously been used during section 4.6 of this test plan.
- j) Mount the PEMS in two locations: inside the cab and behind the cab, in order to maximize environmental differences.
- k) Drive the vehicle over 3 routes, each design to test particular limits that are expected to simulate conditions imposed the environmental tests of sections 4.3-4.7

Use the following Routes:

- l) Route 1--Route starts in the morning in room temperature garage. Vehicle is driven into cold ambient conditions of less than 32 deg F. Vehicle is operated throughout day in a warm location where temperatures exceed 100 deg F. Vehicle returns to cooler ambient temperatures.
- m) Route 2--Vehicle travels from sea level to a high altitude exceeding 6000 ft and returns to sea level.
- n) Route 3--Vehicle is operated in locations were following conditions are known to exist: high ambient HC, high EMI/RFI, and rough road surface.

CE-CERT Validation		Test Day
Contractor CE-CERT Validation	1065 Audit	xx
	NTE Cycle	xx
On-Road CE-CERT Validation	Route 1	xx+1
	Route 2, Route 3	xx+2
On-Road CE-CERT Tests		Test Day
Sensors/ Behind Cab	Route 1	xx+3
	Route 2, Route 3	xx+4
Sensors/ In Cab	Route 1	xx+5
	Route 2, Route 3	xx+6
Horiba/ Behind Cab	Route 1	xx+7
	Route 2, Route 3	xx+8
Horiba/ In Cab	Route 1	xx+9
	Route 2, Route 3	xx+10
Laboratory Replay		Test Day
Sensors	Simulate Route 1	xx+11
	Simulate Routes 2 & 3	xx+12
Horiba	Simulate Route 1	xx+13
	Simulate Routes 2 & 3	xx+14

5.1.3.2 Dyno test cell validation

- a) Remove engine from chassis and install in dyno test cell
- b) Select portions of the CE-CERT tests that are deemed appropriate for “re-play” in a dyno test cell. These portions of test should be limited to about 30-60 minutes in duration
- c) Operated engine as close as possible to previously recorded conditions
- d) Control engine boundary conditions (charge cooler outlet temperature, intake/exhaust restrictions, ambient pressure, etc.) tests from the on-road portion of the validation testing.
- e) Control engine operating conditions (torque, speed, AECDC’s if active, etc.) to mimic operating conditions that can be repeated with a reasonable level of confidence.
- f) For each PEMS, perform testing during two days, for a total of 4 test days.
- g) Record emissions data with PEMS and lab-grade analyzers, and compare the two.

5.1.4 Data Analysis

5.1.4.1 CE-CERT Validation

The difference between the PEMS results and the CE-CERT trailer results will be compared to the error predicted by the Monte Carlo model. Data on ambient conditions must be analyzed to insure that the model was fully exercised. Special consideration will be paid to conditions where the PEMS was found to be sensitive to its environment. If it

was found that the PEMS did not see conditions that are likely to occur in the field that are known to increase erroneous reporting, then more testing is required.

To validate the Monte Carlo Model data must be run through the model and the model's results must predict the actual test results. To run data forwards through model, raw concentration must be known. This requires the CE-CERT trailer to either measure raw exhaust concentration or determine dilution ratio accurately enough to calculate the raw concentration. If concentration can be established with a reasonable level of confidence, then the model can be validated as follows by comparing data in brake specific units (using the work recorded by the PEMS for both the CE-CERT and PEMS data) or in fuel specific units. Raw exhaust concentration, ambient conditions, and exhaust flow are fed to the model. Since ambient effects are incorporated as a distribution of error, the model must be run many times for each NTE event. The model then produces a likely distribution of error expected from the PEMS. If 95% (or maybe 90%-99%) of the PEMS recorded NTE events fit within the model predicted NTE distribution then the model can be considered validated. Data from 20 pseudo NTE events are plotted below in the graph titled "Brake Specific NTE Events." The "model" predicted a likely error distribution from the CE-CERT measured data and ambient conditions. The PEMS data is compared to the error distribution, and if enough NTE events are within the range the model is deemed validated.

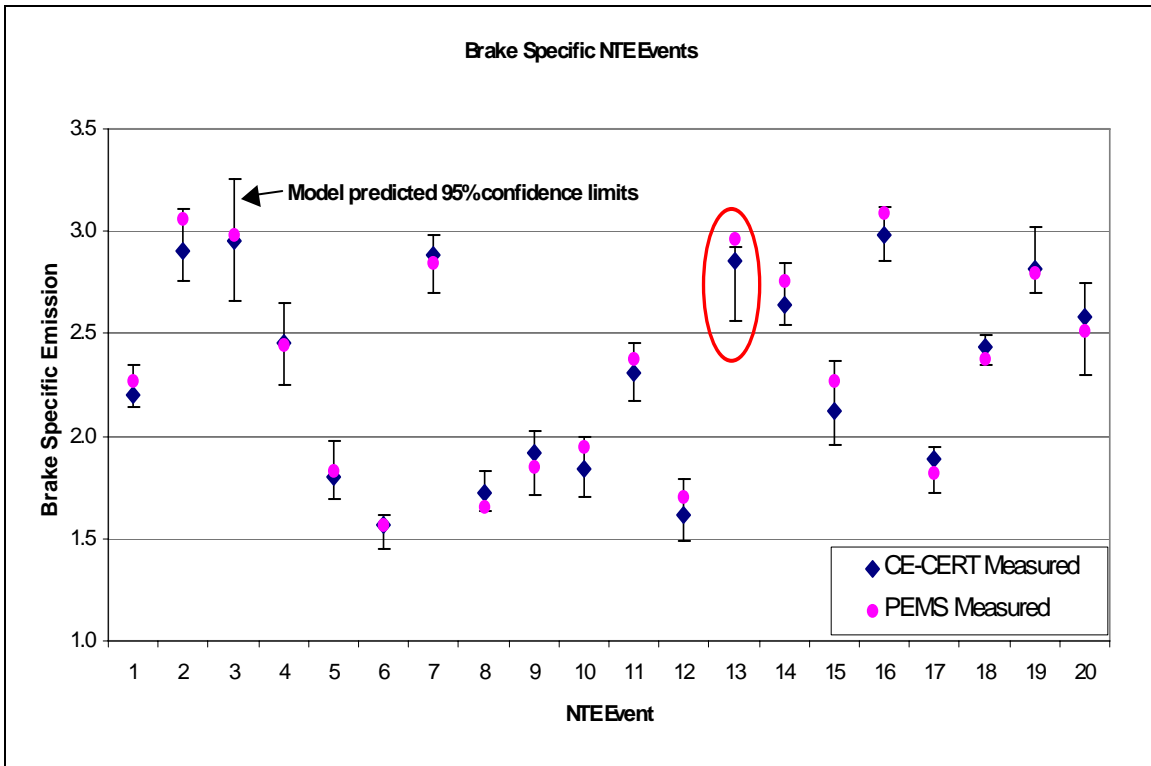


Chart of Model Validation NTE Events

If it is determined that the CE-CERT trailer is unable to accurately determine raw exhaust concentration then the model cannot be run forward. Instead the PEMS recorded data can be run through the model as if it were absolutely correct. Then the model will predict a distribution of error that is likely to occur. This error distribution should overlap with CE-CERT recorded data as long as the error is random. If there is a bias, then the PEMS will record the bias and the model will predict a further bias in the same direction, misrepresenting the comparison—not preferred.

One could also compare the NTE events recorded by the PEMS and the CE-CERT trailer. Below is a graph that shows PEMS NTE events minus the Accuracy Margin versus the CE-CERT trailer results. If 95% (or maybe 90%-99%) of the PEMS values are less than the CE-CERT NTE events, then the margin seems to be correct. Unfortunately this does not incorporate the model directly, but it gives evidence that the model's end result, the Accuracy Margin, is suitable. This test fails to test the intricacies of the model and may be too broad for comfort.

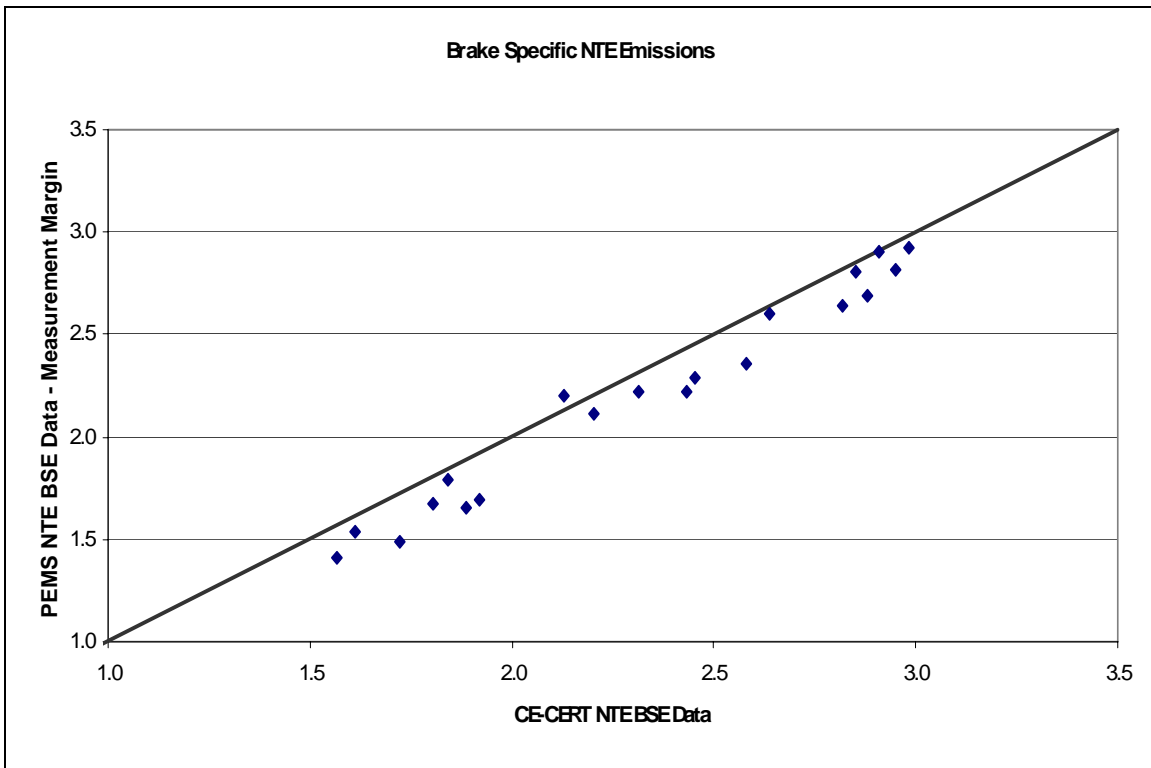


Chart of PEMS vs Tow-along lab Results

5.1.4.2 Dyno Test Cell Validation

Compare brake specific emissions from each valid NTE event between the PEMS and lab-grade analyzers. Confirm that differences fall within the expected ranges as predicted by the Monte Carlo simulation. If they do not, conduct further investigation to try to understand and resolve the discrepancies.

5.2 Measurement Allowance Determination

5.2.1 Objective

Use the Monte Carlo simulation program developed with data from sections 2, 3 and 5, and validated with section 5.1 to determine the measurement allowances for all regulated emissions, at 2007 emissions standards

5.2.2 Background

After the Monte Carlo model has been validated and confidence in its ability to predict errors from PEMS instrumentation, the last step in this program will be to actually calculate a single set of measurement allowances for BSNO_x, BSNMHC, and BSCO.

5.2.3 Methods and Materials

Using the criteria explained in section 2.2 calculate the various levels of measurement accuracy corresponding to the two PEMS manufacturers and the three different brake specific emissions calculations, for all three regulated emissions. Use all the various error surfaces developed during this test program, including those provided by engine manufacturers to the EPA and ARB.

5.2.4 Data Analysis

Use the methodology explained in section 2.2, and Table 2.2-a to arrive at the final measurement allowance.

6 Time and Cost

Budget

Contractor to provide independent estimate.

Timeline

Contractor to provide independent estimate.

Timeline			
	Weeks	Date	Year
Model creation			
Lab Audit			
PEMS audits			
Engine setup			
PEMS setup			
Steady-state testing			
Steady-state data reduction			
Transient testing			
Transient data reduction			
Exhaust flow meter test setup			
Exhaust flow meter testing			
Exhaust flow meter data reduction			
ECM torque bsfc setup			
ECM torque bsfc testing			
ECM torque bsfc data reduction			
Baseline environmental test setup			
Baseline environmental testing			
Baseline environmental data reduction			
Pressure environmental test setup			
Pressure environmental testing			
Pressure environmental data reduction			
Temperature environmental test setup			
Temperature environmental testing			
Temperature environmental data reduction			
EMI/RFI environmental test setup			
EMI/RFI environmental testing			
EMI/RFI environmental data reduction			
Vibration environmental test setup			
Vibration environmental testing			
Vibration environmental data reduction			
Ambient HCs environmental test setup			
Ambient HCs environmental testing			
Ambient HCs environmental data reduction			
Model Validation			
Final Report preparation and publication			
Submission of Final Report to EPA/EMA/ARB			

7 Appendices

These appendices provide additional detailed information and descriptions of spreadsheets and other sources of information.

7.1 Description of Spreadsheet provided by Matt Spears

To use the spreadsheet, here's a description of the various worksheets:

1. Input lug curve: paste any speed-torque lug curve up to 5000 data points long into this worksheet. Make sure the lug curves last data point is where the governor line intersects exactly 0 torque. Tweak your lug curve so that this is the case.
2. Interpolated lug curve: don't do anything here.
3. Cycles: here is where the data for the On-highway, Non-road, condensed on-highway+non-road, and dynamic response NTE cycles are. The SET RMC is also here. The upper part of the spreadsheet has NTE and SET calculations. I think the column headings for the cycles are self-explanatory. I haven't created the random cycle generator for the "NTE cycle", which is for the dynamic response test. The cycle just currently sequences the events and inter-NTE events in the order that I'm building them. Note that only 12 of the 30 events are complete in this spreadsheet.
4. 32 s Events: here is where I'm building the dynamic response NTE events. The first 9 are steady-state. The next three (10-12) are "vertical" NTEs in the lower, mid, and upper third of the zone. For NTEs 13-15 I plan to do the same horizontally, and then 16-18 will be diagonal from low speed & torque to high speed and torque. 19-21 will be diagonal from high speed & low torque to low speed and high torque. 22-24 will be 32 second samples from HDDE PEMS testing, 25-27 will be from LHDDE, and 28-30 will be 3 from non-road operation. Note I made these 32 seconds long to account for 1-second ECM under-sampling on the entry and exit of each event. That way even if the ECM is 1-second off the wrong way on the entry and exit, PEMS will still ID an NTE event. If the ECM is worse, then we'll see that.
5. INT events: here are the inter-NTE events on a second-by-second basis. Note that I took Bill Trestrail's suggestion to scramble up the origin a little. This scrambling is easily tweaked and/or eliminated, but it's easier to build the NTE cycles when the cycle traces (in the charts) don't overlap.
6. NTE event finder: I cut and paste the last column of this spreadsheet "as values" into the first column of each cycle in "Cycles" to ID the NTE events. I have to tweak the second column each time I name the NTE events in different cycles.
7. Histogram data: supplies data to the speed, torque, and power histograms. Nothing to do here.

8. dHistogram data: work in progress, I plan to repeat the histograms as first derivatives: dspeed, dtorque, dpower to visualize how the different cycles compare.
9. Speed, torque, and power histograms: self explanatory. Note that because the “NTE Cycle” is only 1/3 complete, the histograms are skewed because they are counting unfinished NTE events. They’re counted at the lowest bins in torque and power.
10. T-S domain & P-S domain: good visualization of all the cycles.
11. dT-dS domain: visualization of “transientness” of cycles. Note that currently the “NTE Cycle” is the most severe. I hope the engine/dyno can do this. If not the NTEs can be tweaked.
12. All the cycles vs time: self explanatory. You can see that the “NTE Cycle” is not complete.]

7.2 Abbreviations used in Brake Specific Equations (Table 3.3.4-a)

Method 1:

e_{NO_x} = brake-specific emission, NO_x (g/hp-hr)
 M_{NO_2} = Molecular weight, NO_2 (~46 g/mol)
 N = total number (of time intervals) in series
 x = amount of substance fraction (mol NO_x /mol exhaust; note that 1 μmol (emission constituent)/mol (exhaust) = 1ppm (part per million))

\dot{n} = amount of substance rate (mol/sec, in this case, mol (exhaust)/sec)
 Δt = time interval (sec)
 f_n = rotational frequency (shaft), rev/min
 T = torque (N-m)

NOTE: The units of the numerator work out to g_{emission} as is. However, using the units given for the denominator (RPM * N-m * s), you would still need to divide by 1.978 to get to hp-hr (using RPM * N-m = kW * 9550, 1 hour = 3600 sec, and kW = hp*0.7457)

Method 2:

e_{NO_x} = brake-specific emission, NO_x (g/hp-hr)
 M_{NO_2} = Molecular weight, NO_2 (~46 g/mol)
 N = total number (of time intervals) in series
 x = amount of substance fraction (mol NO_x /mol exhaust; note that 1 μmol (emission constituent)/mol (exhaust) = 1ppm (part per million))

\dot{n} = amount of substance rate (mol/sec, in this case, mol (exhaust)/sec) that is linearly proportional to \dot{n} (Note: this is a proportional sample, which means that you may use a flow meter that has a span error, as long as its calibration is linear)
 Δt = time interval (sec)
 M_C = Atomic weight of carbon (~12 g/mol)
 w_{fuel} = g (carbon)/g (fuel); Note fuel is roughly 86% carbon by mass
 x_{Cproddry} = amount of carbon products on a C1 basis per dry mol of measured flow (exhaust), mol/mol, solved iteratively per 1065.655
 $x_{\text{H}_2\text{O}}$ = amount of water in measured flow, mol/mol (see 1065.645 for calculations)
 e_{fuel} = brake-specific fuel consumption (g (fuel)/hp-hr)

Method 3:

e_{NO_x} = brake-specific emission, NO_x (g/hp-hr)
 M_{NO_2} = Molecular weight, NO_2 (~46 g/mol)
 w_{fuel} = g (carbon)/g (fuel); Note fuel is roughly 86% carbon by mass
 M_C = Atomic weight of carbon (~12 g/mol)
 N = total number (of time intervals) in series

x = amount of substance fraction (mol NO_x /mol exhaust; note that 1 μmol (emission constituent)/mol (exhaust) = 1ppm (part per million))

\dot{m}_{fuel} = mass rate of fuel (g/sec)
 $x_{\text{H}_2\text{O}}$ = amount of water in measured flow, mol/mol (see 1065.645 for calculations)
 x_{Cproddry} = amount of carbon products on a C1 basis per dry mol of measured flow (exhaust), mol/mol
 Δt = time interval (sec)
 f_n = rotational frequency (shaft), rev/min
 T = torque (N-m)
 Δt = time interval (sec)

NOTE: The units of the numerator work out to g_{emission} as is. However, using the units given for the denominator (RPM * N-m * s), you would still need to divide by 1.978 to get to hp-hr (using RPM * N-m = kW * 9550, 1 hour = 3600 sec, and kW = hp*0.7457)

APPENDIX M

CE-CERT ON-ROAD VALIDATION TESTING REPORT

Final Report

**Measurement Allowance Project –
On-Road Validation**

August 2007

Prepared for:

The Measurement Allowance Steering Committee

Principal Investigator J. Wayne Miller

Authors: Kent Johnson, Tom Durbin, David Cocker

College of Engineering-Center for Environmental Research and Technology

University of California

Riverside, CA 92521

(951) 781-5791

(951) 781-5790 fax

Disclaimer

The statements and conclusions in this report are those of the contractor and not necessarily those of California Air Resources Board, the United States Environmental Protection Agency (EPA), or the Measurement Allowance Steering Committee (MASC). The mention of commercial products, their source, or their use in connection with material reported herein is not to be construed as actual or implied endorsement of such products.

Acknowledgments

The authors thank the following organizations and individuals for their valuable contributions to this project.

The authors acknowledge the support of the Measurement Allowance Steering Committee (MASC) that includes EPA, CARB, and the Engine Manufacturers Association (EMA) for assistance in developing and carrying out this program.

The authors acknowledge Mr. Chris Sharp of the Southwest Research Institute and his associates for their assistance in carrying out the program and in performing the cross laboratory testing.

The authors acknowledge Sensors Inc. for providing a PEMS as an in-kind contribution to the program and assistance and training during the set up of the on-road testing.

The authors acknowledge Caterpillar for providing a truck for use in the on-road testing portion of this work as an in-kind contribution. The authors acknowledge the International Engine Company for providing a diesel particulate filter for the in-use measurements.

We acknowledge funding from the California Air Resources Board (CARB).

We acknowledge Mr. Donald Pacocha, University of California, Riverside for his contribution in setting up and executing this field project, the data collection and quality control.

Table of Contents

Disclaimer	ii
Acknowledgments.....	ii
Table of Contents	iii
Table of Tables	iv
Table of Figures	v
Abstract.....	vi
Executive Summary	vii
1.0 Background	1
2.0 1065 Audit CE-CERT Mobile Emissions Laboratory (MEL)	2
2.1 1065 Audit Overview.....	2
2.2 1065 Audit Results.....	2
2.3 CARB Audit Bottle Comparisons.....	8
3.0 Cross Correlation Testing with SwRI and CE-CERT.....	9
3.1 Experimental Procedures	9
3.2 Calibration Bottle Results.....	9
3.2 Correlation Testing Results.....	11
4.0 On-Road Testing of the PEMS vs. the CE-CERT MEL – Experimental Procedures	14
4.1 Test Vehicle	14
4.2 PEMS Operation	15
4.3 MEL Operation	20
5.0 On-Road Testing of the PEMS vs. the CE-CERT MEL – Experimental Results.....	29
5.1 Audit Run Results.....	29
5.2 Calculation Methods	30
5.3 Summary of NTE Events	34
5.4 NO _x Emission Results.....	36
5.5 CO ₂ Emission Results	43
5.6 NMHC Results.....	45
5.7 CO Emission Results	48
5.8 Exhaust Concentration Levels	51
5.9 Zero and Span Calibration Comparisons	53
6.0 Summary and Conclusions.....	56
Appendix A – Background Information on UCR’s Mobile Emission Lab.....	1
Appendix B – Description of PEMS Instrument.....	1
Appendix C – Test File Names and Descriptions.....	1
Appendix D – Brake Specific Emissions Calculations.....	1
Appendix E – NO_x Emissions by NTE Event and Calculation Method.....	1
References.....	1

Table of Tables

Table 2-1 Summary of 1065 Audit Results	2
Table 2-2 H ₂ O Interference Check for CO ₂	3
Table 2-3 H ₂ O and CO ₂ Interference Check for CO.....	3
Table 2-4 FID Methane Response	4
Table 2-5 Non-Methane Cutter Penetration Fractions.....	4
Table 2-6 CO ₂ and H ₂ O Quench Verification for NO _x CLD.....	5
Table 2-7 CARB Audit Bottle Checks.....	8
Table 3-1 CE-CERT MEL Audit Bottle Results	10
Table 3-2 Correlation Results Between SwRI and CE-CERT MEL – NTE Engine cycle.....	12
Table 3-3 Correlation Results Between SwRI and CE-CERT MEL – Ramped Modal cycle.....	13
Table 5-1. MEL audit and calibration ranges for on road tests audits.....	29
Table 5-2. Ambient Background Levels Over Different Test Routes	30
Table 5-3. Summary of NTE Events for Each Test Day	34
Table 5-4. Summary of Deviations in % vs. Standard for NO _x Emissions	40
Table 5-5. Summary of Deviations in % vs. Point for NO _x Emissions	41
Table 5-6. Summary of Deviations for NO _x Emissions with Dispersion	42
Table 5-7. Summary of Deviations for NMHC Emissions.....	48
Table 5-8. Summary of Deviations for CO Emissions	51
Table 5-9. MEL calibration ranges.	52
Table 5-10. PEMS Calibration Ranges.....	52

Table of Figures

Figure 4-1. Installation of Diesel Particulate Filter	14
Figure 4-2 Picture of In Cab PEMS Installation.....	15
Figure 4-3 Picture of Out-of-Cab PEMS Installation.....	16
Figure 4-4. Picture of Exhaust Connection for PEMS.....	17
Figure 4-5. Installation of Relative Humidity Sensor.....	18
Figure 4-6. Driver’s Aid	21
Figure 4-7. Environmental Conditions for Testing along Route 1.	22
Figure 4-8. Route 3: Riverside to San Diego round trip – distance 197 miles.	23
Figure 4-9. Route 2,3: Riverside to Mammoth Mountain via US 395.	25
Figure 4-10. EMF Interference During Routes 2/3.....	26
Figure 4-11. Railroad Crossing During Route 2/3.....	26
Figure 4-12. Environmental Conditions for Test Runs over Route 2.....	27
Figure 4-13 Local temperature and RH data near Mammoth Mt.	28
Figure 5-1. Comparison of Real-Time CO ₂ Emissions (a) Before Dispersion is Compensated for and (b) After Dispersion is Compensated for.	33
Figure 5-2. Real-time ECM % actTorque for both MEL and PEMS.	35
Figure 5-3. Real-time ECM % actTorque for both MEL and PEMS.	35
Figure 5-4. NO _x Mass Emissions (g/bkW-hr) for PEMS Relative to MEL.....	36
Figure 5-5. NO _x Mass Emissions (g) for PEMS Relative to MEL.....	37
Figure 5-6. Deviations in % Relative to the Standard for NO _x on an NTE Event Basis.....	38
Figure 5-7. Absolute Differences for NO _x (g/bkW-hr) Compared to NO _x Emission Level (g/bkW-hr)	38
Figure 5-8. Deviations in % of Point for NO _x on an NTE Event Basis.....	39
Figure 5-9. Deviations in % Relative to the Standard for NO _x on an NTE Event Basis for Dispersion Data.....	42
Figure 5-10. CO ₂ Mass Emissions (g/bkW-hr) for PEMS Relative to MEL.....	43
Figure 5-11. CO ₂ Mass Emissions (grams) for PEMS Relative to MEL.....	44
Figure 5-12. CO ₂ Mass Emissions (g/bkW-hr) for PEMS Relative to MEL.....	44
Figure 5-13. Absolute Deviations and Deviations Relative to NTE Standard for NMHC on an NTE Event Basis.....	46
Figure 5-14. NMHC Mass Emissions (g/bkW-hr) for PEMS Relative to MEL.....	47
Figure 5-15. Absolute and Relative to NTE Standard Deviations for CO on an NTE Event Basis	49
Figure 5-16. CO Mass Emissions (g/bkW-hr) for PEMS Relative to MEL.....	50
Figure 5-17. MEL Concentration Data as Measured by Instruments for All Primary Species	52
Figure 5-18. PEMS concentration data as measured by instrument for all primary species.....	53
Figure 5-19. MEL Calibrations for (a) zero and (b) span.	54
Figure 5-20. PEMS Calibrations for (a) zero and (b) span.....	55

Abstract

Regulations were promulgated requiring the measurement of emissions from diesel engines while operating within the Not-To-Exceed (NTE) control area of the engine map. These measurements require the use of portable emissions measurement systems (PEMS) rather than traditional laboratory methods. To provide input into the determination of a measurement “allowance” that would account for differences between a laboratory measurement and PEMS, a comprehensive Measurement Allowance testing project was set-up and governed by the Measurement Allowance Steering Committee (MASC). In the first phase of the project emissions measured with PEMS and federal reference were compared for an engine on a dynamometer while the environmental conditions were changed for the PEMS unit. These data were fitted to a Monte Carlo model. In a second phase, the goal was to compare the measurements from PEMS with federal reference methods during actual in-use driving using the University of California, Riverside (UCR) Bourns College of Engineering – Center for Environmental Research and Technology’s (CE-CERT) Mobile Emissions Laboratory (MEL). Prior to the on-road testing portion, MEL underwent an audit following 40CFR Part 1065 and a side-by-side comparison with emissions measured at the SwRI laboratory. Results were viewed to be comparable. This report focuses on the on-road comparison of the PEMS measuring in the raw exhaust with gaseous instruments measuring flow and concentrations from a full dilution tunnel according to the Code of Federal Regulations (CFR). For comparison, simultaneous emissions measurements using MEL and PEMS were carried out over three routes designed to capture different driving and environmental conditions, such as temperature and elevation. The results of this program were used to validate the Monte Carlo model by comparing over-the-road results against the Monte Carlo model predictions and evaluating if the model correctly predicted the PEMS error relative to the CFR-compliant MEL.

Executive Summary

In recent years, the US Environmental Protection Agency (EPA) and the California Air Resources Board (CARB) have promulgated regulations to further control diesel emissions. Recent regulations have targeted in-use emissions and the protocols required to make those measurements. The requirement to measure in-use emissions means that portable emissions monitoring systems (PEMS) will be needed in place of the traditional fixed laboratories and more information was needed about the variation of measurement during in-use operation. In response to this need, a Measurement Allowance Steering Committee (MASC) and comprehensive Measurement Allowance testing program were established to determine the “allowance” for compliance purposes when PEMS are used for in-use testing. Members of the MASC include EPA, ARB, and the Engine Manufacturers Association (EMA).

Part of the Measurement Allowance program required the in-use emissions by the federal reference instruments in UCR’s Mobile Emissions Laboratory (MEL) and compared with those of a PEMS unit. Before carrying out the in-use emissions measurements, MEL underwent a 40CFR Part 1065 audit and side-by-side comparison of emissions measurements with an engine operated on a dynamometer at SwRI. After establishing the emissions measured by UCR and SwRI were equivalent, the in-use measurement portion of the program began and that work is described in this report.

1065 Audit

The first step in the project required that UCR’s MEL undergo a 40CFR Part 1065 self-audit using the protocol developed by SwRI and agreed to by the US EPA. The 1065 self audit of MEL included water (H₂O) and carbon dioxide (CO₂) interference/quench checks, nitrogen dioxide (NO₂) to nitrogen oxide (NO) converter efficiency checks, non-methane hydrocarbons (NMHC) cutter penetrations fractions. In addition the linearity of all analyzers, mass flow controllers, and temperature and pressure sensors was verified. All checks were found to pass and the system to comply with 40CFR Part 1065.

Cross Correlation with Southwest Research Institute Engine Laboratory

In the next step, a cross correlation of measured emissions concentrations and flow rates was conducted between an engine dynamometer test cell at SwRI and UCR’s MEL. For this task, the MEL was towed to SwRI in San Antonio and set-up such that UCR’s MEL could make measurements from the same engine dynamometer test cell being used by SwRI. This represented a unique opportunity to evaluate the comparison between two 1065 compliant laboratories under the same conditions including the test engine and dynamometer, test location, and test cycles. This setup was selected to demonstrate that in-lab and on-road measurement platforms would give equivalent results.

The correlation was performed for two cycles: one cycle based on a series of NTE events and another based on the Ramped Modal Cycle (RMC). Testing was performed on a 2005, 14 liter Detroit Diesel Corporation (DDC) Series 60 engine. For the NTE emissions cycle, the MEL was 2.1% higher than the SwRI measurement for oxides of nitrogen (NO_x) and 2.7% higher than

SwRI for CO₂. For the RMC, the MEL was 3.8% higher than the SwRI measurement for NO_x and 2.3% higher than SwRI for CO₂. THC and CO emissions were at relatively low levels and showed larger deviations (-65 to -92% for THC and -16 and -24% for CO). The members of the MASC concluded the results were acceptable to allow continuation of the on-road portion of the measurement allowance program.

On-Road Comparisons between the MEL and the PEMS

On-road comparisons of the MEL and the PEMS measurements were made over three different driving routes. The routes included round trips to a San Diego and Bishop, CA. The tests were conducted using a truck that was equipped with a 475 hp Caterpillar C-15 ACERT engine and a diesel particulate filter to provide emission levels comparable to those anticipated for 2007 for PM, THC, and CO. A total of 6 test runs and 3 audits runs were conducted during the on-road testing phase, including:

1. Three Audit runs without the PEMS
2. Three runs with PEMS positioned inside the cab
3. Three runs with PEMS positioned outside the cab.

During the audit runs, the measured values were compared to the audit bottle concentrations over the course of the test route. For NO_x and CO₂, the measurements were both within 2% of the audit bottle concentration over the course of the three different test runs. THC and CO audits were within ~ 1 ppmv or 5% of the audit bottle concentrations, even though these bottles were at the low levels expected for a DPF equipped vehicle. Ambient background levels for NO_x and CO₂ were relatively low compared to the diluted exhaust levels. THC and CO background concentrations were comparable to those found in the diluted exhaust of the DPF equipped vehicle.

Over the course of the six test runs, a total of 426 NTE events were identified. Of these 426 events, 26 events were identified by only the MEL or PEMS, but not by both. For an additional 57 events, the start of the NTE events between the MEL and PEMS differed by more than 3 seconds or the duration of the NTE event differed by more than 1 second. NTE events where the data did not pass the drift limit validity check were also excluded. This included all the data from the first test day since the post-test zero span data were not available. The on-road test results presented below are based on this subset of data.

It is important to note the routes for the on-road validation were structured to emphasize data collection within the NTE zone of engine operation. That is, while the overall driving routes included some stop-and-go vehicle/engine operation, data were generally recorded only during higher speed, quasi-steady-state engine operation. Very little data collection occurred during vehicle/engine operation under stop-and-go driving conditions, which generate few NTE events.

The brake specific emission comparisons for NO_x, THC, and CO were calculated using three different methods:

1. based on engine speed and torque

2. based on brake specific fuel consumption
3. based on mass fuel flow or a fuel specific method.

The brake specific NO_x emissions for matching NTE events are provided in Figure ES-1 and values for the PEMS measurements were consistently higher than those for the MEL, with a correlation of R²~0.84/0.85 between the measurement methods. The deviations relative to the NTE NO_x standard of 2.0 grams per brake horsepower-hour or 2.68 grams per brake kW-hour are presented in Figure ES-2. The absolute deviations as a function of the total NO_x emissions as measured by the MEL are provided in Figure ES-3. The deviations were greatest for Method 1 with an average deviation of +8%±4% relative to the standard, where the error represents one standard deviation. The deviations for Methods 2 and 3 were +4%±5% and +3%±5%, respectively, at one standard deviation. The differences in deviations for the three calculation methods could be related to the incorporation of CO₂ exhaust measurements into calculation methods 2 and 3, which are also biased high for the PEMS, or to the impacts of differences in analyzer dispersion on the calculations. Some differences appeared between the different test runs/days, although overall these trends were weak for different environmental conditions (in cab vs. out of cab) or between the different routes (i.e., San Diego, Riverside to Bishop, and Bishop to Riverside).

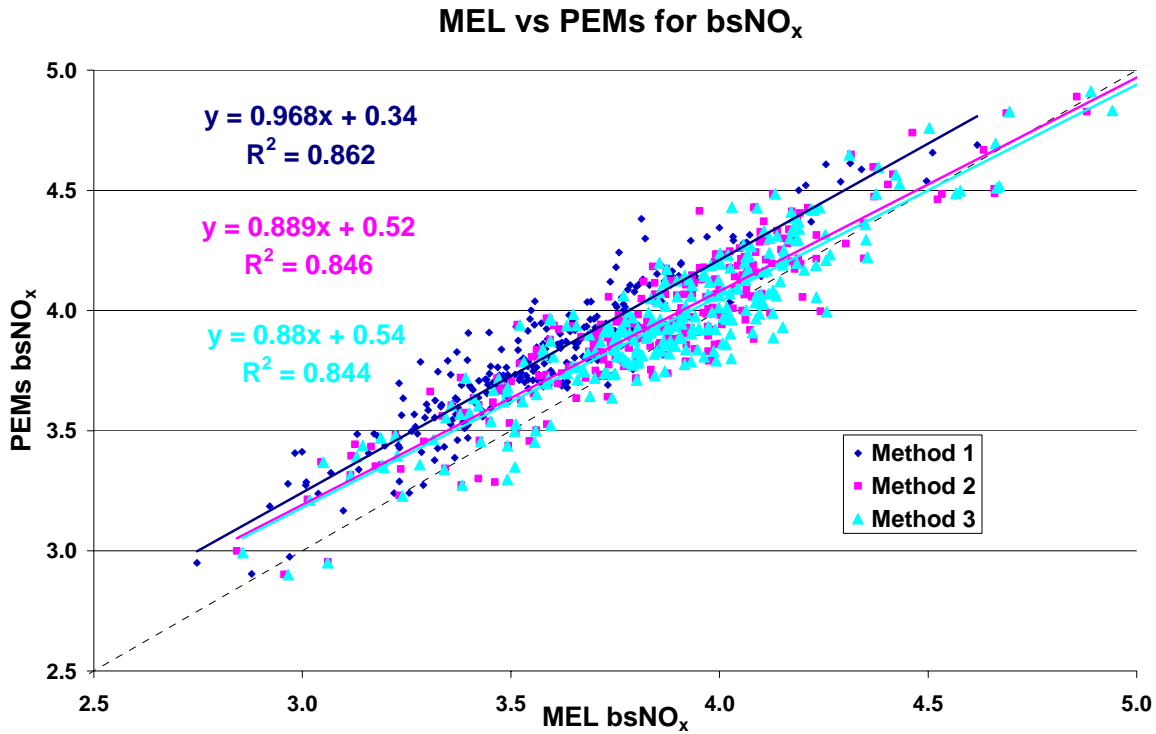


Figure ES-1. NO_x Mass Emissions (g/bkW-hr) for PEMS Relative to MEL

Method 1,2,& 3 Brake Specific kNO_x PEMS vs MEL Deltas

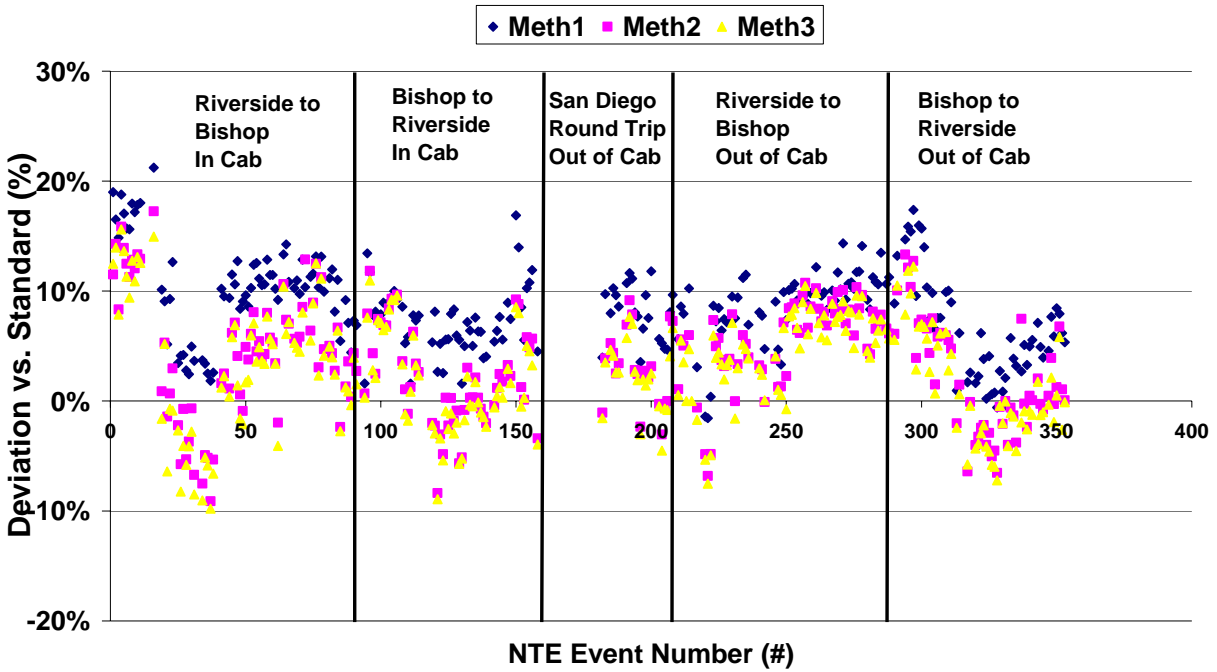


Figure ES-2. Relative Deviations vs. NTE Standard for NO_x on an NTE Event Basis

Differences in bsNO_x vs. MEL NO_x Level

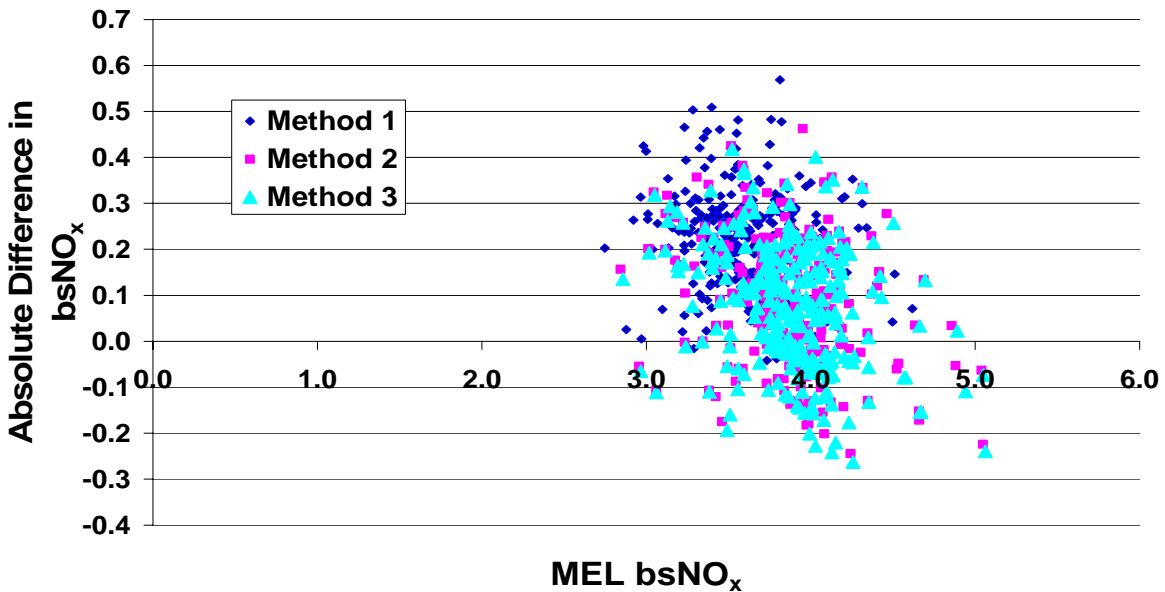


Figure ES-3. Absolute Differences for NO_x (g/bkW-hr) Compared to NO_x Emission Level (g/bkW-hr)

The correlation for brake specific CO₂ emissions for matching NTE events is provided in Figure ES-4. The method 1 brake specific CO₂ emissions for the PEMS were consistently biased high relative to the MEL, with an average deviation of +4%±2%. There was a good correlation

between the MEL and PEMS method 1 CO₂ measurements ($R^2 = 0.97$). Note for the methods 2 and 3, the resulting brake specific CO₂ emissions primarily represent the values derived from the mass fuel flow from the ECM for both the MEL and PEMS since the measured CO₂ concentrations cancel out of the equation.

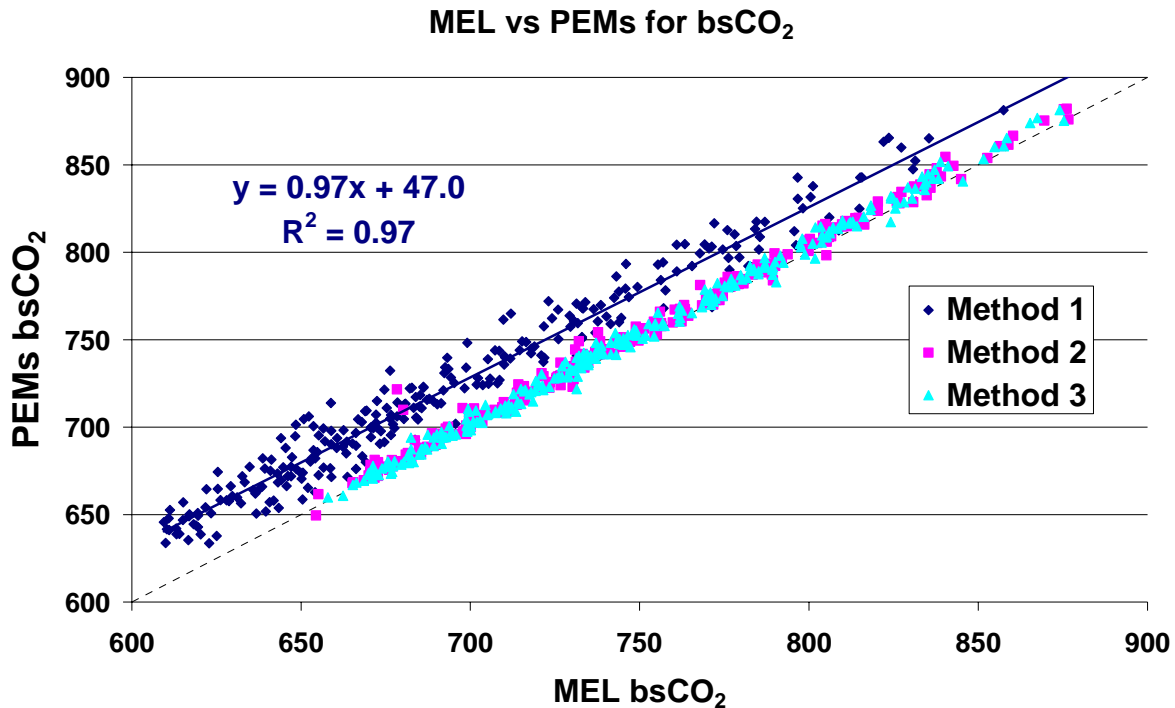


Figure ES-4. CO₂ Mass Emissions (g/bkW-hr) for PEMS Relative to MEL

As a consequence of the installed diesel particulate filter, the NMHC and CO emissions levels were consistently low. For the MEL, the diluted exhaust concentrations were comparable to those of the ambient background. The average emission rates for NMHC were 0.003 g/bkW-hr or below, which is approximately 1% of the anticipated NTE standard of 0.28 g/bkW-hr. There is not consistent bias for NMHC emissions between the different analyzers, with the PEMS higher for some tests and lower for others, albeit at very low levels. Average differences for the different test runs were $\pm 0.5\%$ or less of the NTE standard. There was a weak correlation ($R^2 \sim 0.36/0.37$) between the MEL and PEMS measurements due to the low level measurements.

CO emissions levels were also consistently low during the on-road measurements. For the MEL, the diluted exhaust concentrations were comparable to those of the ambient background. The PEMS measurements were consistently higher than those of the MEL. The CO emissions levels were on the order of 0.1% of the anticipated NTE standard of 26.01 g/bkW-hr for CO for the MEL measurements. The absolute differences represented approximately 1% of the NTE standard, although the PEMS measurements were approximately an order of magnitude higher than those for the MEL. The correlation analysis showed that there was essentially no correlation between the measurement methods ($R^2 = 0.0011$ or less) at these low levels.

1.0 Background

Diesel engines are one the most important emissions sources to control for continued improvement in air quality due to their contribution to the emissions inventory for oxides of nitrogen (NO_x) and particulate matter (PM). In recent years, the US Environmental Protection Agency (EPA) and the California Air Resources Board (CARB) have promulgated regulations to further control diesel emissions. The most recent regulation has targeted in-use emissions in a defined portion of the engine map known as the Not-To-Exceed (NTE) control area and the protocols required to make those measurements.

The new requirement to measure in-use emissions means that portable emissions measurement systems (PEMS) will be needed rather than the fixed laboratory measurements. However, as comparative data for Federal Reference Methods and PEMS were scarce, the regulatory agencies and engine manufacturers created the Measurement Allowance Steering Committee (MASC) to develop a comprehensive testing program for determining the measurement allowance. From the MASC evolved the design of a comprehensive program that was published on the EPA web site on June 3, 2005 (<http://www.epa.gov/otaq/hd-hwy.htm>). The program includes engine testing, environmental testing and Monte Carlo modeling. A key objective of the Measurement Allowance Program is to determine the “allowance” for compliance purposes when PEMS are used for in-use testing.

One of the main components of the Measurement Allowance test program is the comparison of PEMS and a mobile laboratory platform under in-use conditions. The University of California at Riverside (UCR) Bourns College of Engineering – Center for Environmental Research and Technology’s (CE-CERT) Mobile Emissions Laboratory (MEL) was incorporated into the Measurement Allowance test plan for this task. The in-use comparisons include simultaneous measurements by the MEL and the PEMS under different in-use driving conditions designed to generate NTE events and provide a range of environmental conditions, such as temperature and altitude. The results of this in-use comparison will be used to, in part, validate the sensitivity analysis and resultant model based on Monte Carlo simulations of a number of key parameters that are expected to contribute to the measurement allowance. Prior to conducting the on-road tests, a cross laboratory correlation was performed between the MEL and an engine test cell at the Southwest Research Institute (SwRI) in San Antonio, Texas. A 1065 audit of the MEL was also conducted.

2.0 1065 Audit CE-CERT Mobile Emissions Laboratory (MEL)

2.1 1065 Audit Overview

As part of the validation of the CE-CERT MEL for the on-road testing, a 1065 self-audit for gaseous emissions was performed on the CE-CERT MEL. A description of the MEL is provided in Appendix A. Prior to conducting the audit, the 1065 regulations were reviewed and the MEL trailer subsystems were modified as needed.

The 1065 self audit of the trailer included water (H₂O) and carbon dioxide (CO₂) interference/quench checks, nitrogen dioxide (NO₂) to nitrogen oxide (NO) converter efficiency checks, nonmethane hydrocarbons (NMHC) cutter penetration fractions. The linearity of all analyzers, mass flow controllers, and temperature and pressure sensors was also verified. The template used for the audit was the same as that used at SwRI and was designed by EPA in conjunction with the Measurement Allowance program.

2.2 1065 Audit Results

A summary of the interference and quenching effects and flame ionization detector (FID) response checks is provided below. All checks were found to pass and the system to be in 1065 compliance.

Verification Description	Measurement		Verification Value	Pass/Fail
1065.350 H ₂ O interference for CO ₂ NDIR [%]	0.001%	±	0.02%	Pass
1065.355 H ₂ O and CO ₂ interference for CO NDIR [ppm]	0.1	±	5.6	Pass
1065.360 FID optimization (methane response)	1.10		N/A	N/A
1065.370 CO ₂ and H ₂ O quench verification for NO _x CLD [%]	-1.71%	±	2.00%	Pass
1065.378 NO ₂ -to-NO converter conversion [%]	96.4%	±	95%	Pass
1065.365 Nonmethane cutter penetration fractions [%]	1.0%	<	2.0%	Pass

Table 2-1 Summary of 1065 Audit Results

1065.350 H₂O Interference Check for CO₂.

H₂O can interfere with a nondispersive infrared (NDIR) analyzer's response for CO₂. A CO₂ NDIR must have an H₂O interference that is less than 2% of the lowest flow-weighted average CO₂ concentration expected during testing, although an interference of less than 1% is recommended. This test is conducted by bubbling zero gas through a water to create a water saturated test gas that creates a response in the NDIR.

1065.350 H₂O interference for CO₂ NDIR [%]			Notes
Dry Zero Air	0.000%		CO ₂ conc
Wet Zero Air	0.001%		CO ₂ conc
Interference	0.001%		
Dew Point	24.97	degC	DP of wet zero air
Exp. Mean CO ₂ Conc.	0.81%		Transient cycle
Criteria	0.016%		±2% of the flow-weighted mean CO ₂ conc. at the standard

Table 2-2 H₂O Interference Check for CO₂

1065.355 H₂O and CO₂ Interference Check for CO NDIR Analyzers.

H₂O and CO₂ can positively interfere with an NDIR analyzer by causing a response similar to carbon monoxide (CO). A CO NDIR analyzer must have combined H₂O and CO₂ interference that is less than 2% of the flow-weighted average concentration of CO expected at the standard, though it is recommended that the interference be less than 1%. This test is conducted by bubbling CO₂ span gas through a water to create a water saturated test gas that creates a response in the NDIR.

1065.355 H₂O and CO₂ interference for CO NDIR [ppm]			
Wet CO ₂ Span Gas	0.58945634	ppm	CO conc meas with wet CO ₂ span gas
CO ₂ Span Conc	3.580%		CO ₂ span gas conc
Dew Point	28.47	degC	DP of wet CO ₂ span gas
Exp. CO ₂ Mean Conc.	0.81%		Transient cycle
Ratio CO Conc.	0.133	ppm	
CO Mean Conc.	25.4	ppm	1.399
Exp. CO at Standard	281	ppm	15.5
Criteria	5.6	ppm	±2% of the flow-weighted mean CO conc at the standard

Table 2-3 H₂O and CO₂ Interference Check for CO

1065.360 FID Optimization (Methane Response).

FIDs respond differently to methane than other hydrocarbons, and this factor must be incorporated into emissions calculations. For this exercise, the response of FID to a methane calibration gas was determined to provide a methane response factor.

1065.360 FID optimization (methane response)

	Methane Actual	Measured	CH4 RF	point vs ave
10	104.09	115.16	1.11	0.2%
9	94.40	104.43	1.11	0.2%
8	81.79	90.35	1.10	0.0%
7	71.95	79.43	1.10	0.0%
6	61.18	67.49	1.10	-0.1%
5	51.29	56.57	1.10	-0.1%
4	40.46	44.52	1.10	-0.4%
3	29.73	33.08	1.11	0.8%
2	19.84	21.91	1.10	0.0%
1	14.34	15.76	1.10	-0.5%
	Average		1.10	

Table 2-4 FID Methane Response

1065.365 Nonmethane Cutter Penetration Fractions Determination.

A nonmethane cutter removes nonmethane hydrocarbons from the exhaust stream before the FID analyzer measures hydrocarbon concentrations. It is recommended that the nonmethane cutter be optimized by adjusting the catalyst temperature such that the penetration factor for CH₄ is >0.9 while the penetration factor for C₂H₆ is <0.1.

1065.365 Nonmethane cutter penetration fractions [%]

Ethane Conc.	362	ppmC1
Cutter response	3.568	ppmC1
Ethane penetration fraction	0.99%	

Table 2-5 Non-Methane Cutter Penetration Fractions

1065.370 CLD CO₂ and H₂O Quench Check.

H₂O and CO₂ can negatively interfere with a chemiluminescence detector (CLD)'s NO_x response by collisional quenching, which inhibits the chemiluminescent reaction that a CLD utilizes to detect NO_x. The calculations in 1065.672 are used to determine the impact of H₂O and CO₂ in quenching the chemiluminescent signal in a NO span. The procedure and the calculations scale the quench results to the water vapor and CO₂ concentrations expected during testing. A CLD analyzer must have a combined H₂O and CO₂ quench of less than ±2%, though it is recommended that quench be below ±1%. This check is performed by introducing CO₂ into an NO calibration gas and by bubbling an NO calibration gas through water.

1065.370 CO₂ and H₂O quench verification for NO_x CLD [%]

NO _x wet	245.77	ppm	NO conc with wet NO _x span gas
NO _x dry	259.93	ppm	NO conc with dry NO _x span gas
dewTemp	28.47	C	
satPres		at	
dewTemp	3893.04	Pa	
Local Baro Press	98737.64	Pa	
H ₂ Omeas	3.94%		H ₂ O conc of wet NO _x span gas
H ₂ Oexp	3.50%		Max water conc expected during test
NO, CO ₂	129.25	ppm	NO conc with 50% CO ₂ span gas and 50% NO _x span gas
NO, N ₂	129.84	ppm	NO conc with 50% N ₂ and 50% NO _x span gas
CO ₂ meas	3.58%		CO ₂ conc with 50% CO ₂ span gas and 50% NO _x span gas
CO ₂ exp	2.50%		Max CO ₂ conc expected during test
H ₂ O Quench	-1.39%		
CO ₂ Quench	-0.32%		
Quench	-1.71%		

Table 2-6 CO₂ and H₂O Quench Verification for NO_x CLD*1065.378 NO₂ to NO Converter Efficiency Check.*

An NO₂ to NO converter allows an analyzer that measures only NO to determine to NO_x by converting NO₂ in exhaust to NO. The converter was found to convert NO₂ to NO with an efficiency of 96.4%.

Linearity Checks

Linearity checks were performed on all analyzers, temperature sensors, pressure sensors, and mass flow controllers (MFCs).

Sensor Name	Slope			Intercept			SEE			r ²			Overall Pass/Fail	Units
	Value	Criteria	Pass/Fail	Value	Criteria	Pass/Fail	Value	Criteria	Pass/Fail	Value	Criteria	Pass/Fail		
CO	0.999	0.99 / 1.01	Pass	-0.002	1.162	Pass	0.212	1.162	Pass	1.0000	0.998	Pass	Pass	ppm
CO2	1.001	0.99 / 1.01	Pass	-0.004	0.057	Pass	0.006	0.057	Pass	1.0000	0.998	Pass	Pass	%
NOx	1.000	0.99 / 1.01	Pass	-0.234	4.645	Pass	0.365	4.645	Pass	1.0000	0.998	Pass	Pass	ppm
THC	1.000	0.99 / 1.01	Pass	-0.086	2.452	Pass	0.148	2.452	Pass	1.0000	0.998	Pass	Pass	ppm
CH4	1.000	0.99 / 1.01	Pass	-0.094	2.265	Pass	0.178	2.265	Pass	1.0000	0.998	Pass	Pass	ppm
TC_room	tbd													C
TC_Hxout	tbd													C
TC_Hxin	tbd													C
TC_cont	tbd													C
TC_oven	tbd													C
TC_split	tbd													C
TC_filter	tbd													C
T_CVSd	0.999	0.99 / 1.01	Pass	0.067	0.992	Pass	0.035	0.992	Pass	1.0000	0.998	Pass	Pass	C
T_CVSt	0.993	0.99 / 1.01	Pass	-0.125	2.990	Pass	0.208	2.990	Pass	1.0000	0.998	Pass	Pass	C
T_CFO	tbd													C
TC_exh	tbd													C
TC_CVSt	tbd													C
P_CVSt	1.000	0.99 / 1.01	Pass	-0.076	7.622	Pass	0.083	7.622	Pass	1.0000	0.998	Pass	Pass	mmHg
P_CVSd	1.000	0.99 / 1.01	Pass	-0.030	7.622	Pass	0.079	7.622	Pass	1.0000	0.998	Pass	Pass	mmHg
P_amb	1.000	0.99 / 1.01	Pass	-0.003	0.300	Pass	0.004	0.300	Pass	1.0000	0.998	Pass	Pass	inHg
P_CFO	0.996	0.99 / 1.01	Pass	0.057	0.651	Pass	0.019	0.651	Pass	1.0000	0.998	Pass	Pass	psig
dP_CVSt	1.004	0.99 / 1.01	Pass	-0.015	0.500	Pass	0.011	0.500	Pass	1.0000	0.998	Pass	Pass	inH2O
dP_CVSd	1.003	0.99 / 1.01	Pass	-0.031	0.500	Pass	0.030	0.500	Pass	1.0000	0.998	Pass	Pass	inH2O
dP_Filter	1.001	0.99 / 1.01	Pass	-0.315	2.000	Pass	0.121	2.000	Pass	1.0000	0.998	Pass	Pass	inH2O +/-
dP_CVS_stack	1.001	0.99 / 1.01	Pass	0.020	0.200	Pass	0.021	0.200	Pass	1.0000	0.998	Pass	Pass	inH2O
dP_CVS_exh	1.001	0.99 / 1.01	Pass	0.476	1.000	Pass	0.338	1.000	Pass	1.0000	0.998	Pass	Pass	inH2O
T_RH_amb	1.000	0.99 / 1.01	n/a	0.749	0.722	n/a	1.070	0.722	n/a	0.9990	0.998	n/a	n/a	RH
T_RH_cond	1.000	0.99 / 1.01	n/a	0.902	0.714	n/a	1.104	0.714	n/a	0.9990	0.998	n/a	n/a	RH
T_dew	1.001	0.99 / 1.01	Pass	0.586	3.012	Pass	0.595	3.012	Pass	0.9993	0.998	Pass	Pass	K
Speed	tbd													mph
MFC41	1.005	0.99 / 1.01	Pass	-0.352	1.027	Pass	0.315	1.027	Pass	0.9999	0.998	Pass	Pass	sccm

MFC42	1.000	0.99 / 1.01	Pass	0.000	0.010	Pass	0.001	0.010	Pass	1.0000	0.998	Pass	Pass	slpm
MFC43	0.999	0.99 / 1.01	Pass	0.003	0.098	Pass	0.005	0.098	Pass	1.0000	0.998	Pass	Pass	slpm
MFC44	1.001	0.99 / 1.01	Pass	-0.001	0.017	Pass	0.002	0.017	Pass	1.0000	0.998	Pass	Pass	slpm
MFC45	1.001	0.99 / 1.01	Pass	0.009	0.286	Pass	0.051	0.286	Pass	1.0000	0.998	Pass	Pass	slpm
MFC46	0.998	0.99 / 1.01	Pass	0.000	0.048	Pass	0.011	0.048	Pass	1.0000	0.998	Pass	Pass	slpm
														slpm
														20C 1
MFC47	0.998	0.99 / 1.01	Pass	0.077	0.285	Pass	0.085	0.285	Pass	1.0000	0.998	Pass	Pass	atm
MFC61	1.001	0.99 / 1.01	Pass	-0.130	1.081	Pass	0.185	1.081	Pass	1.0000	0.998	Pass	Pass	slpm
MFC62	1.000	0.99 / 1.01	Pass	-0.083	1.059	Pass	0.195	1.059	Pass	1.0000	0.998	Pass	Pass	slpm
MFC63	1.000	0.99 / 1.01	Pass	0.003	0.273	Pass	0.045	0.273	Pass	1.0000	0.998	Pass	Pass	slpm
MFC64	1.002	0.99 / 1.01	Pass	-0.012	0.269	Pass	0.065	0.269	Pass	1.0000	0.998	Pass	Pass	slpm
MFC65	1.000	0.99 / 1.01	Pass	-0.006	0.282	Pass	0.029	0.282	Pass	1.0000	0.998	Pass	Pass	slpm
MFC66	1.001	0.99 / 1.01	Pass	0.005	0.068	Pass	0.019	0.068	Pass	1.0000	0.998	Pass	Pass	slpm
MFC67	1.000	0.99 / 1.01	Pass	-0.002	0.016	Pass	0.003	0.016	Pass	1.0000	0.998	Pass	Pass	slpm
MFC68	1.004	0.99 / 1.01	Pass	-0.091	0.527	Pass	0.115	0.527	Pass	1.0000	0.998	Pass	Pass	slpm
MFC69	1.001	0.99 / 1.01	Pass	-0.049	0.521	Pass	0.095	0.521	Pass	1.0000	0.998	Pass	Pass	slpm

Standard conditions at 20C, 1 atm

2.3 CARB Audit Bottle Comparisons

CARB staff from El Monte did some cross checks of the CE-CERT analyzers with calibration bottles that they provided. These audit bottles showed some differences slightly greater than 2% for CO and NO_x. The reason for the high audit response was that a new purge process was being implemented that at the time did not provide sufficient stabilization time. The implementation of the purge process was completed by the time testing was conducted at SwRI and included longer purge times. The audit bottle cross calibrations made at SwRI did not indicate any further issues. The longer purge times improved the stabilization for CO and NO_x by approximately 1 ppm.

UCR CE-CERT MOBILE LABORATORY - JUNE 2006 TEST RESULTS:

TYPE OF ANALYZERS CALIFORNIA ANALYTICAL INSTRUMENT

(NIST) REFERENCE GAS	CYLINDER I.D.	REF. Conc. ppm	LAB. Conc. ppm	CONC. Difference %	LAB. Span Value	ANALYZER Range ppm/%
C3H8	FF28567	8.646	8.57	-0.88	94.70	100
		8.646	8.67	0.28	94.70	100
CO	CAL011764	25.05	24.40	-2.59	94.60	100
	XF000386B	48.76	47.60	-2.38	94.60	100
CO ₂	CAL013669	0.4795	0.478	-0.31	3.72	4%
	CAL013725	0.9710	0.966	-0.51	3.72	4%
NO _x	CAL015570	48.52	47.40	-2.31	202.00	250

Table 2-7 CARB Audit Bottle Checks

3.0 Cross Correlation Testing with SwRI and CE-CERT

A complete cross-laboratory correlation was conducted between the CE-CERT MEL and an engine dynamometer laboratory at the Southwest Research Institute (SwRI) in San Antonio, TX. The CE-CERT MEL was towed to the SwRI facility in San Antonio, TX from Riverside, CA for this testing, such that the testing was conducted side-by-side. This exercise was carried out prior to the on-road testing of the PEMS to ensure comparability of the on-road measurements with those collected in the main engine dynamometer testing portion of the Measurement Allowance program.

3.1 Experimental Procedures

The cross correlation exercise was performed at SwRI at the engine dynamometer facility being used for the engine testing portion of the Measurement Allowance program. A 2005, 14 liter Detroit Diesel Series 60 engine was used as the test engine. This was one of the three test engines being used by SwRI on the main engine testing portion of the Measurement Allowance program. The CE-CERT MEL was positioned external to the engine laboratory and the transfer tube was routed from the engine cell to the MEL.

Emissions testing was conducted using two cycles, an NTE engine cycle, which is an engine cycle that was designed for the main portion of the engine testing, and the Ramped Modal cycle (RMC). For each day of testing, three iterations of the NTE cycle and two iterations of the Ramped Modal cycle were performed using each of the emissions analyzer benches, i.e., the SwRI emissions benches for the test cell and the CE-CERT MEL. The order of testing for the SwRI emissions equipment and the MEL was reversed on alternating test days. For the first day testing was performed using the SwRI emissions benches followed by the MEL. For the second day of testing, this order was reversed so that testing was conducted on the MEL followed by the SwRI emissions benches. For the final day, the SwRI emissions benches were used first followed by the MEL benches.

After the arrival of the CE-CERT MEL, but prior to the emissions test, a full calibration of system analyzers and a propane recovery test were conducted with the MEL. This included cross calibration of the SwRI and MEL with calibration bottle from the other laboratory. After arrival at the SwRI facility, there was a failure with a computer board related to the MEL dilution tunnel. This board was replaced prior to testing and propane recovery checks showed the dilution tunnel was operating with no issues.

3.2 Calibration Bottle Results

Cross correlations between the CE-CERT and SwRI audit bottle were conducted prior to beginning testing. The CE-CERT MEL audit bottle results are provided in Table 3-1. The audit bottles included a THC bottle and a combination CH₄, CO, NO_x, and CO₂ bottle from CE-CERT, and two NO_x and one CO₂ concentration bottle from SwRI. Comparison of the measurements with the audit bottle standard concentrations indicated that all measurements were within 2% of the audit bottle concentrations, with all but a few CO₂ measurements within 1%.

File Name		Measured					Bottle Primary Standard					Percent Deviation from Standard					
n/a	Bottle Supplier	THC ppm	CH ₄ ppm	CO Ppm	NO _x ppm	pCO ₂ %	THC ppm	CH ₄ ppm	CO ppm	NO _x ppm	CO ₂ %	THC	CH ₄	CO	NO _x	pCO ₂	
200506010933	CECERT	184.57					185.15					-0.3%					
200505091012	CECERT		9.266	91.22	100.2	1.536		9.27	90.6	100	1.554		0.0%	0.7%	0.2%	-1.2%	*
200506010933	SwRi				27.16					27.08					0.3%		*
200506010940	SwRi					1.784					1.815					-1.7%	*
200506211255	SwRi				88.03					87.45					0.7%		*
200506211255	CECERT		9.292	91.03	100.4	1.532		9.27	90.6	100	1.554		0.2%	0.5%	0.4%	-1.4%	*
200506291452	CECERT		9.266	91.22	100.2	1.555		9.27	90.6	100	1.554		0.0%	0.7%	0.2%	0.1%	**
200506291459	SwRi				27.2					27.08					0.3%		**
200506291452	SwRi					1.802					1.815					-0.7%	**
200506291459	SwRi				88.0					87.45					0.7%		**
200508120923	CECERT		9.292	91.03	100.4	1.554		9.27	90.6	100	1.554		0.2%	0.5%	0.4%	0.0%	**

* = uncorrected CO₂ curve; ** = linearized CO₂ typical calibration

Table 3-1 CE-CERT MEL Audit Bottle Results

3.2 Correlation Testing Results

Overall, the MEL showed good correlation with the emissions measurements made in the SwRI test cell. A summary of the results is provided in Table 3-2 for the NTE cycle and Table 3-3 for the RMC. For the NTE emissions cycle, the MEL was 2.1% higher than the SwRI measurement for NO_x and 2.7% higher than SwRI for CO₂. For the RMC, the MEL was approximately 3.8% higher than the SwRI measurement for NO_x and 2.3% higher than SwRI for CO₂. THC and CO emissions were at relatively low levels and showed larger deviations (-65 to -92% for THC and -16 and -24% for CO). These results were reviewed with the MASC and it was agreed they were acceptable for the measurement allowance program.

Test Day	Test Date	Test Number	Transient Emissions, g/hp-hr					
			THC	CH ₄	NMHC	CO	NO _x	CO ₂
1	6/29/2006	SwRI-NTE-1	0.003	-0.005	0.008	0.057	1.99	540.4
1	6/29/2006	SwRI-NTE-2	0.003	0.001	0.002	0.057	1.97	540.9
1	6/29/2006	SwRI-NTE-3	0.004	0.003	0.001	0.057	1.99	542.0
		Mean	0.003	0.000	0.004	0.057	1.98	541.1
1	6/29/2006	CE-CERT-NTE-1	0.001	0.001	-0.001	0.044	2.03	557.6
1	6/29/2006	CE-CERT-NTE-2	0.001	0.002	-0.001	0.044	2.03	558.0
1	6/29/2006	CE-CERT-NTE-3	0.001	0.002	-0.001	0.042	2.04	557.8
		Mean	0.001	0.002	-0.001	0.043	2.03	557.8
Day 1 Difference (%point)			-288%	119.7%	546.0%	-31.7%	2.4%	3.0%
2	6/30/2006	SwRI-NTE-1	0.004	0.001	0.003	0.058	2.04	541.5
2	6/30/2006	SwRI-NTE-2	0.003	0.002	0.001	0.054	2.01	543.0
2	6/30/2006	SwRI-NTE-3	0.003	0.002	0.001	0.057	2.02	542.4
		Mean	0.003	0.002	0.002	0.056	2.02	542.3
2	6/30/2006	CE-CERT-NTE-1	0.002	0.001	0.000	0.041	2.04	554.2
2	6/30/2006	CE-CERT-NTE-2	0.001	0.002	-0.001	0.040	2.05	551.7
2	6/30/2006	CE-CERT-NTE-3	0.001	0.002	-0.001	0.041	2.04	551.1
		Mean	0.001	0.002	0.000	0.041	2.04	552.3
Day 2 Difference (%point)			-148.3%	8.2%	556.3%	-38.2%	1.0%	1.8%
3	7/5/2006	SwRI-NTE-1	0.005	-0.007	0.012	0.055	2.01	539.5
3	7/5/2006	SwRI-NTE-2	0.003	0.002	0.001	0.052	1.99	540.4
3	7/5/2006	SwRI-NTE-3	0.003	0.002	0.001	0.053	2.00	541.2
		Mean	0.004	-0.001	0.005	0.053	2.00	540.4
3	7/5/2006	CE-CERT-NTE-1	0.001	0.002	-0.001	0.042	2.06	558.5
3	7/5/2006	CE-CERT-NTE-2	0.001	0.002	-0.001	0.043	2.05	558.0
3	7/5/2006	CE-CERT-NTE-3	0.002	0.002	0.000	0.042	2.07	554.8
		Mean	0.001	0.002	-0.001	0.042	2.06	557.1
Day 3 Difference (%point)			-159.4%	152.1%	960.2%	-26.2%	2.9%	3.0%
Standard for 2005 DDC Series 60 Engine			0.14	0.14	0.14	15.5	2.2	
NTE SwRI	Mean		0.004	0.000	0.004	0.056	2.001	541.3
	Stdev		0.001	0.004	0.004	0.002	0.020	1.1
	CE-CERT Mean		0.001	0.002	-0.001	0.042	2.044	555.7
	Stdev		0.000	0.000	0.000	0.001	0.014	2.9
	%point		-65.1%	2336.2%	-117.4%	-24.2%	2.1%	2.7%
	%standard		-1.6%	1.3%	-2.9%	-0.1%	1.9%	n/a

Table 3-2 Correlation Results Between SwRI and CE-CERT MEL – NTE Engine cycle

Test Day	Test Date	Test Number	Transient Emissions, g/hp-hr					
			THC	CH ₄	NMHC	CO	NO _x	CO ₂
1	6/29/2006	SwRI-RMC-1	0.004	0.000	0.004	0.054	1.79	499.8
1	6/29/2006	SwRI-RMC-2	0.003	0.002	0.001	0.057	1.80	499.8
		Mean	0.004	0.001	0.003	0.055	1.80	499.8
1	6/29/2006	CE-CERT-RMC-1	0.000	0.001	-0.002	0.048	1.88	511.7
1	6/29/2006	CE-CERT-RMC-2	0.000	0.001	-0.001	0.052	1.88	510.5
		Mean	0.000	0.001	-0.002	0.050	1.88	511.1
Day 1 Difference (%point)			-109%	23%	-160%	-9.5%	4.6%	2.3%
2	6/30/2006	SwRI-RMC-1	0.002	0.000	0.002	0.054	1.83	500.6
2	6/30/2006	SwRI-RMC-2	0.002	0.000	0.002	0.053	1.84	501.1
		Mean	0.002	0.000	0.002	0.053	1.84	500.8
2	6/30/2006	CE-CERT-RMC-1	0.001	0.002	-0.001	0.043	1.90	508.1
2	6/30/2006	CE-CERT-RMC-2	0.000	0.002	-0.001	0.041	1.91	509.0
		Mean	0.001	0.002	-0.001	0.042	1.90	508.5
Day 2 Difference (%point)			-72%	1586%	-161%	-21%	3.6%	1.5%
3	7/5/2006	SwRI-RMC-1	0.002	0.002	0.000	0.052	1.84	498.9
3	7/5/2006	SwRI-RMC-2	0.002	0.002	0.001	0.052	1.85	499.0
		Mean	0.002	0.002	0.000	0.052	1.85	499.0
3	7/5/2006	CE-CERT-RMC-1	0.000	0.002	-0.002	0.041	1.92	514.2
3	7/5/2006	CE-CERT-RMC-2	0.000	0.001	0.000	0.045	1.89	514.6
		Mean	0.000	0.001	-0.001	0.043	1.91	514.4
Day 3 Difference (%point)			-84%	-35%	-314%	-17%	3.2%	3.1%
Standard for 2005 DDC Series 60 Engine			0.14	0.14	0.14	15.5	2.2	
Overall Results RMC Cycle								
RMC	SwRI	Mean	0.003	0.001	0.002	0.053	1.827	499.9
		Stdev	0.001	0.001	0.001	0.002	0.024	0.9
	CE-CERT	Mean	0.000	0.002	-0.001	0.045	1.897	511.3
		Stdev	0.000	0.001	0.001	0.004	0.015	2.7
		% of Point	-92.6%	42.9%	-171.9%	-16%	3.8%	2.3%
		% of Standard	-1.8%	0.3%	-2.1%	-0.1%	3.1%	n/a

Table 3-3 Correlation Results Between SwRI and CE-CERT MEL – Ramped Modal cycle

4.0 On-Road Testing of the PEMS vs. the CE-CERT MEL – Experimental Procedures

Comparisons were made between the CE-CERT MEL and the PEMS under in-use conditions designed to generate NTE events and provide a variety of conditions such as temperature, elevation, etc. The experimental procedures and test routes are described in this section.

4.1 Test Vehicle

The test truck for the on road testing was provided by Caterpillar. The truck was equipped with a 475 hp Caterpillar C-15 ACERT engine with 200 hours or about 5,000 miles on it since being rebuilt. The engine was certified to the 2.5 g/bhp-hr NO_x + NMHC and 0.1 g/bhp-hr PM standard. The engine was equipped with dual exhausts and originally had a pair of oxidation catalysts. In order to achieve emissions levels representative of 2007 standards, the oxidation catalysts were removed and were replaced with a diesel particulate filter (DPF). The DPF was provided by International Truck and Engine Corp. and had an effective volume of 1391.6 in³, which was deemed to provide sufficient capacity for the test engine. The DPF was configured to meet the Caterpillar specifications for recommended back pressure with DPF installed of 35 – 50 inches. Preliminary on-road tests showed that the measured back pressure with the DPF installed was approximately 45 inches at high speed/high loads, with the back pressure measured 12 inches from turbo and 3 feet before the DPF. The DPF installation is shown in Figure 4-1.



Figure 4-1. Installation of Diesel Particulate Filter

4.2 PEMS Operation

A SEMTECH DS PEMS unit was used for the on-road testing. This is the same model being used for the main portion of the engine and environmental testing at SwRI, and this specific unit was used for a segment of the environmental testing at SwRI prior to being shipped to CE-CERT. A description of the PEMS is provided in Appendix B.

The PEMS was utilized in two different locations for the on-road testing, one inside the cab and one outside the cab. Pictures of the in and out of cab installation are shown below in Figures 4-2 and 4-3, respectively. The in cab runs were performed with the PEMS placed on the aluminum flooring of the air ride cab. The out of cab runs were performed with the PEMS mounted in a frame that was specially constructed behind the driver side fuel tank. The Sensors Inc. environmental case was used for the out of cab testing as pictured in Figure 4-3, whereas the case was not used for the in cab installation.

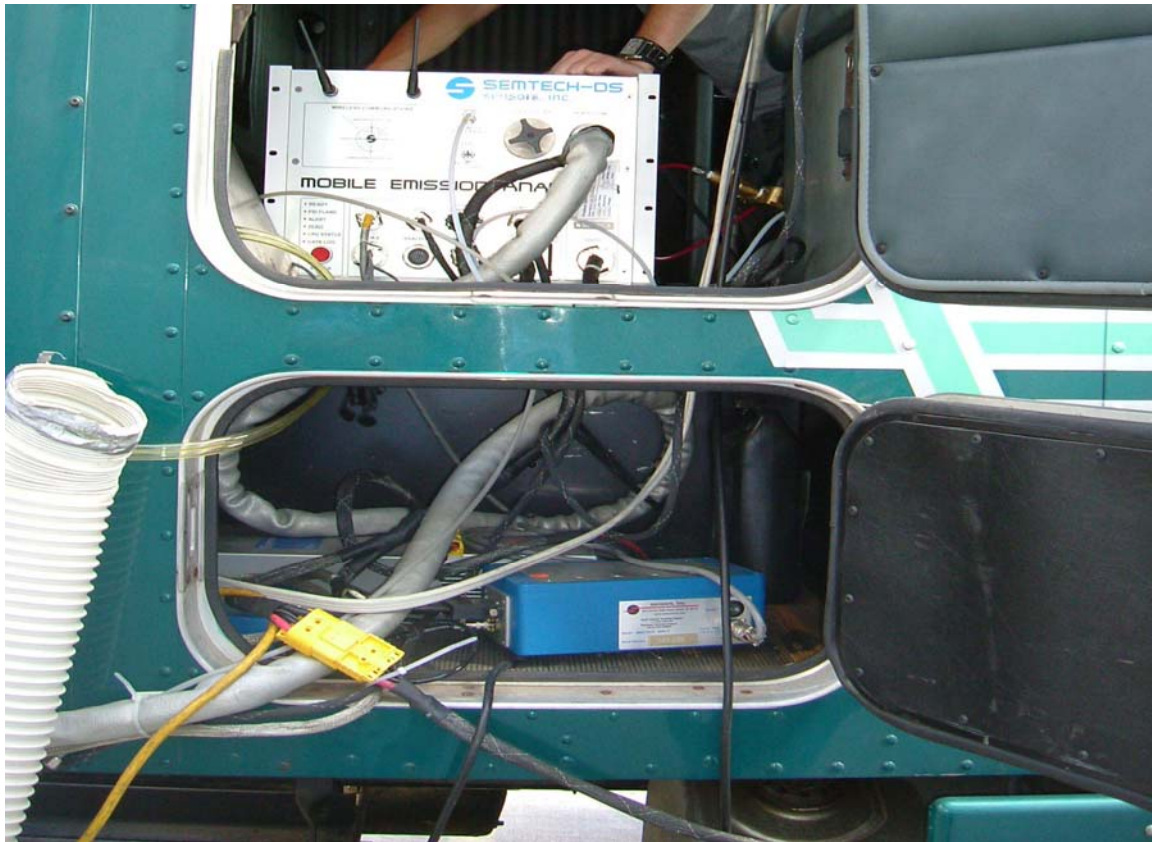


Figure 4-2 Picture of In Cab PEMS Installation

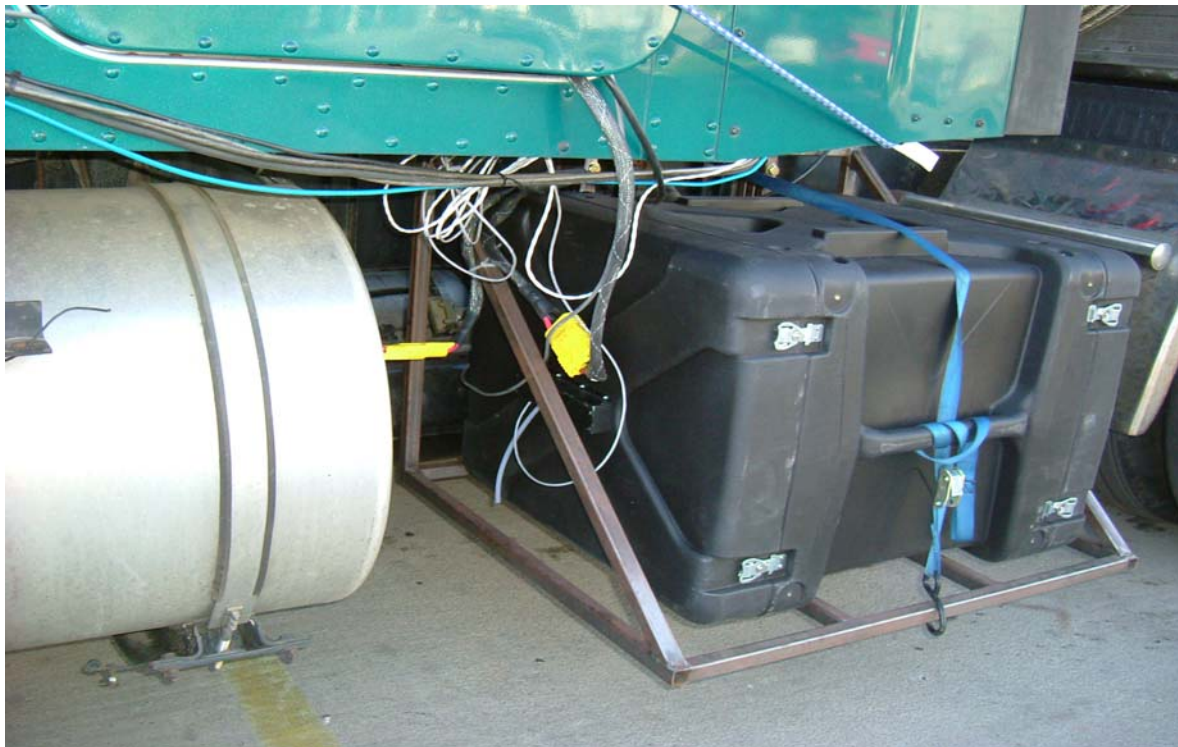


Figure 4-3 Picture of Out-of-Cab PEMS Installation

The set up included the installation of the flow meter, sample lines, and required sensors for the PEMS. The flow monitoring and sample probe was installed in roughly the middle of a straight pipe section leading from the end of the exhaust towards the dilution tunnel. The sample probe and exhaust flow meter (EFM) were installed approximately 10 exhaust pipe diameters (50 inches) after the final exhaust hookup to ensure full mixing prior to the sample point. This point was not originally specified in the manual but was agree to following subsequent conversations with the steering committee. An additional straight section of 6 exhaust pipe diameters was also added after the sample probe prior to the dilution tunnel. A picture of the exhaust connection is provided in Figure 4-4. The relative humidity (RH) sensor was mounted vertically on the outside the cab on the driver's side, as shown in Figure 4-5. The use of a UV or weather shield on the RH sensor was discussed with the steering committee prior to the on-road tests, since the PEMS manual provides some flexibility on when the shield is or is not need. Based on this discussion, it was decided not to employ the weather shield during the on-road testing. During testing the RH ambient temperature seemed higher than other ambient temperature measurements. The post calculated humidity correction factors also showed differences between the MEL and PEMS. As such, for the final calculations the temperature and humidity corrections for the MEL were used for both the MEL and the PEMS. A standard 104 liter FID fuel bottle, typical of that used with this particular PEMS was used. The PEMS was loaded with the Lug Curve used in previous tests with this same C15 engine. The ECM module was set up for J1939 and a GPS for the PEMS was installed.

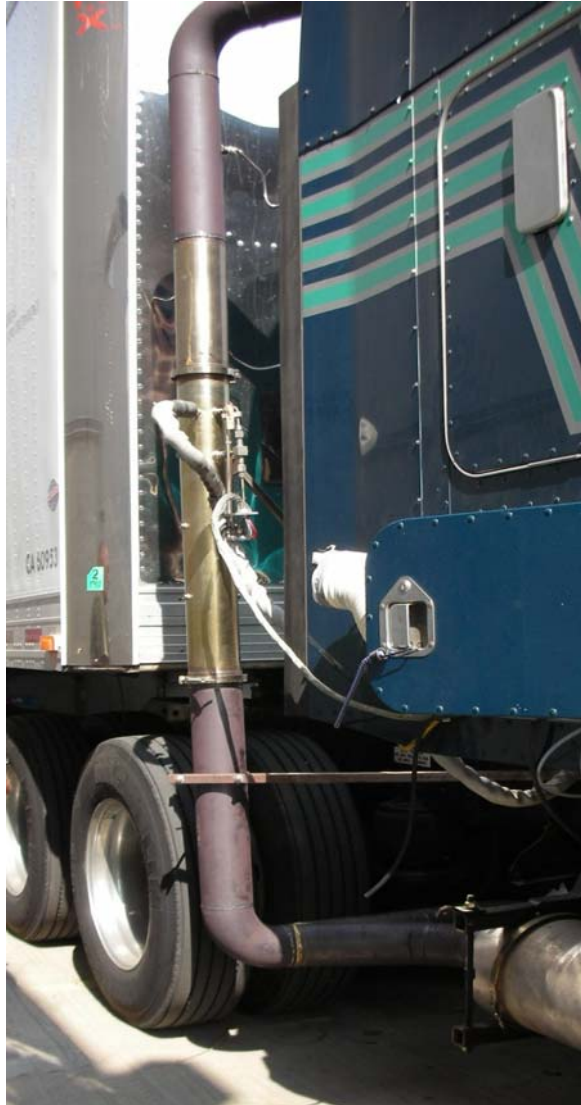


Figure 4-4. Picture of Exhaust Connection for PEMS



Figure 4-5. Installation of Relative Humidity Sensor

Prior to beginning the on-road testing, a representative of Sensors Inc. visited CE-CERT and provided one day of training. Although several CE-CERT staff were already familiar with the general Semtech operation, the additional day of training provided assurances that the instrument was operated properly and that CE-CERT staff were current on the latest software and hardware with the Semtech DS system. The newest version of software that was available at the time of testing (version 10.05SP2) was used during the testing.

The PEMS was operated in a manner consistent with the manufacturers manual and the procedures being used by SwRI, except for some changes to facilitate on-road testing in conjunction with the MEL. The PEMS is typically operated in auto-zero and auto-exhaust flow meter (EFM) purge mode. The PEMS automatic procedures were turned off to facilitate the MEL triggering automatically. CE-CERT staff manually zeroed and purged the EFM at the end of each 50 minute sample period. The zero calibration and EFM purge were performed while progressing through the routes at the flow of traffic or in local conditions such as waiting in truck scales or at traffic lights. In the event of a 10 minute delay to start the next test cycle, a zero and EFM purge were performed prior to starting the next test segment to capture the data within an approximate one hour zero calibration and EFM purge.

In order to maintain data integrity and clarity of file names, CE-CERT chose to operate the PEMs using the session manager available in the supplied software. Each session was set up using the route name and each test was identified by the MEL test name. The MEL test name is number representing year, month, day, hour, and minute (i.e., 200611051232 is year 2006,

month 11, day 05, hour 12, and minute 32). The session manager was successful on all tests except the first day in-cab Route 1. The session manager was not utilized during that test because the test was performed prior to identifying this particular feature of the software. The session manager has the advantage of maintaining pre- and post-zero drift information and pre- and post-audit calibrations. A list of the raw XML (Extensible Markup Language) file names is listed in Appendix C. The table of file names describes all the details of that test segment and any issues or details regarding that data set.

One other operational difference was FID bottle changes. The committee decided to change the FID fuel bottle when the pressure was below 300 psi. The bottle pressure was checked before starting each test segment. If the bottle pressure was less than 300 psi the bottle was changed. If the pressure was greater than or equal to 300 psi, the next one hour segment would be started. If a bottle change occurred in the middle of a route, CE-CERT performed a zero, span, and audit before and after the bottle change. CE-CERT experienced three mid-bottle changes on the first three in-cab routes. During a bottle change on Route 1 in-cab, the PEMS software froze and CE-CERT was unable to perform a post zero, span, and audit calibration. CE-CERT adapted by selecting bottles above 1700 psi to prevent bottle changes during a test. For all the out-of-cab tests, there were no in-test bottle changes during the entire route.

CE-CERT started the PEMS from cold start conditions each day. A cold start is defined where the PEMS is turned on after being left off over night. CE-CERT staff turned on the PEMS and waited for the ready status indication from the software before beginning calibration. Warm-up is completed when all heater temperatures meet PEMS tolerances and the red status lights turn green. The in-cab PEMS power supply was connected directly to the truck's alternator and not the batteries. On Route 3, the in-cab test PEMS unit took approximately 2 hours to warm up because the ambient temperature was cold and the supply voltage to the power inverter was low, around 13 volts. All in-cab tests were performed with the power supplied by the vehicle.

For the out-of-cab installation, CE-CERT initially moved the power supply from the alternator to the battery pack. The power supply voltage dropped from 13 volts to 12.6 volts at idle. At this voltage, the heaters could not reach tolerances even after two hours. The steering committee and PEMS manufacture recommended connecting the power supply to the MEL generator for out-of-cab correlation tests. All the out-of-cab routes were operated with power supplied by the MEL generator and there were no further issues in warming up the PEMS with this configuration.

Once the PEMS system warmed up, CE-CERT performed a zero, span, and audit check on all systems. If the audit check failed, the zero and span were repeated until the audit passed. The PEMS failed the audit check a few times. It only took one calibration repeat to pass the audit during the correlation exercise. All zero calibrations were performed on ambient air throughout all the routes for both in-cab and out-of-cab installations. At the end of each day a final zero, span and audit were performed. During the post calibration on the Route 3 out-of-cab test, CE-CERT performed the standard zero calibration then did an audit check before the span calibration. It was found that many of the gas concentrations were out of tolerance. The final calibration was performed with the audit check and the post calibration audit met all the tolerances.

4.3 MEL Operation

The MEL was operated using procedures similar to those used at SwRI correlation. A standard zero span calibration was performed every hour and before each test throughout the correlation. An audit was performed once each day to verify proper calibration operation. All daily audit checks were within 2% of point throughout the on-road testing program. The MEL did not fill or analyze bags for ambient level concentrations. The steering committee decided to use default ambient concentrations for background corrections. The default concentrations came from averages from the audits for each route. Details can be found in the ambient audit data section. Average ambient concentrations from Route 1 were used on Route 1 and averages from Routes 2 and 3 were used on Routes 2 and 3.

Since the MEL system triggered the PEMS, the order of testing went as follows. First the MEL and PEMS were calibrated and verified. Then the PEMS session manager was started using the route name. Next, the MEL was initiated and a file name was generated. Then the PEMS test segment was started using the MEL file name. Then the MEL was started with a control button available to the driver in the cab. When the button was pressed, a data flag was set and the MEL triggered the PEMS start-sampling flag. The MEL had a specific countdown where both the PEMS and MEL stop flags were set at the end of the 50 minutes. At the end of the test, the PEMS was manually calibrated and the MEL performed a zero and span calibration. The PEMS unit was typically ready two minutes earlier than the MEL. At the end of each sequence, the process was repeated until the end of the route. PM was not measured by the MEL for these on-road tests segments.

A complete audit run was performed over each of the test routes prior to the on-road tests with the PEMS. The audit runs included sampling of audit gases and ambient background. The audit runs included repeat runs alternating sampling of ambient and audit gases. The sequence consisted of 60 seconds of stabilization with ambient air followed by 510 seconds of sampling and measurement of ambient air followed by 30 seconds of stabilization with audit gases followed by 30 seconds of sampling and measurement of audit gases. For each test segment, this sequence was repeated five times for approximately 1 hour. The test segments were then repeated over the course of each route. A zero and span was performed between each test segment.



Figure 4-6. Driver's Aid

Route 1 – Riverside to San Diego Round Trip

The first route for the on-road testing consisted of driving from Riverside to San Diego and then returning to Riverside. This route utilizes Interstate-15 (I-15) and I-5, which are two of California's major freeways. Driving on this route is more rural with possible congestion around the San Diego region and around the Riverside area on the return trip. This route also included some power line crossings and potholes which contributed to road vibrations. This route has many elevation changes, which ensured sufficient generation of NTE events, due to uphill grades that caused the engine to operate in the NTE zone for long periods of time. The total trip distance is approximately 200 miles. The actual trip driving began at approximately 9 AM and went to approximately 1 PM.

The environmental conditions for route 1 are provided in Figure 4-7 for the two test runs. The temperature ranged from approximately 65°F in morning to 87°F in mid day. The elevation extends from approximately 1500 feet (ft.) to down to sea level, with some elevation changes along the route. A map of the route is provided in Figure 4-8.

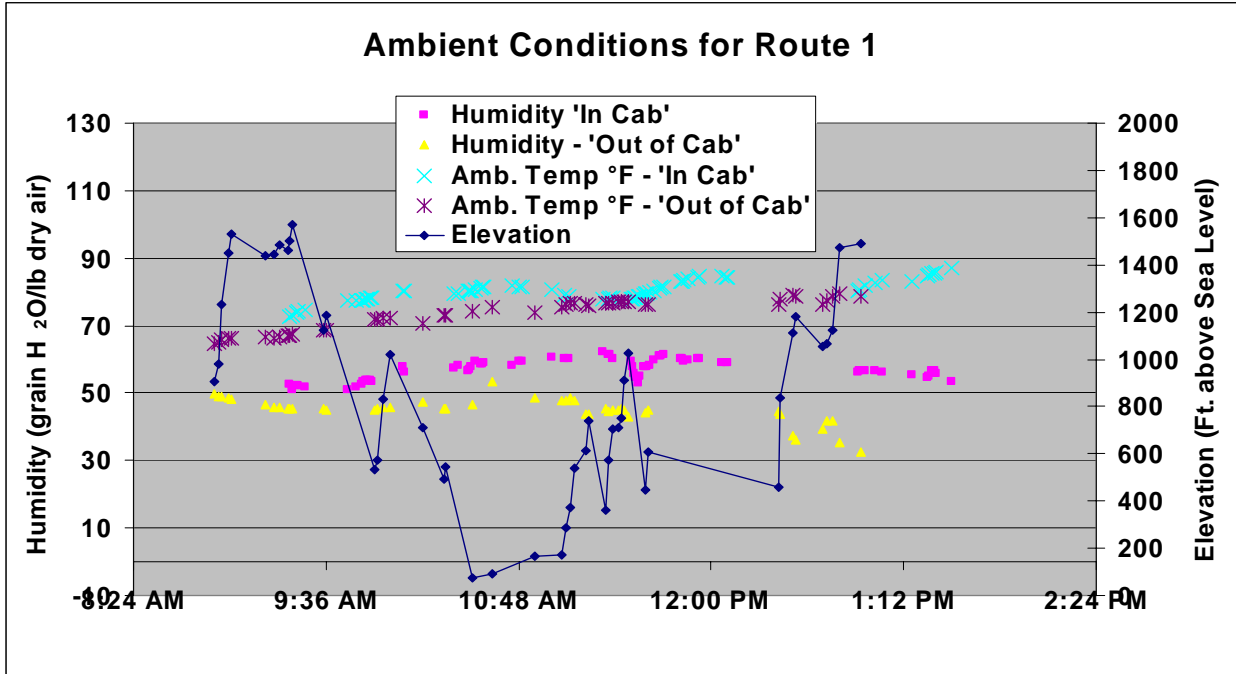


Figure 4-7. Environmental Conditions for Testing along Route 1.

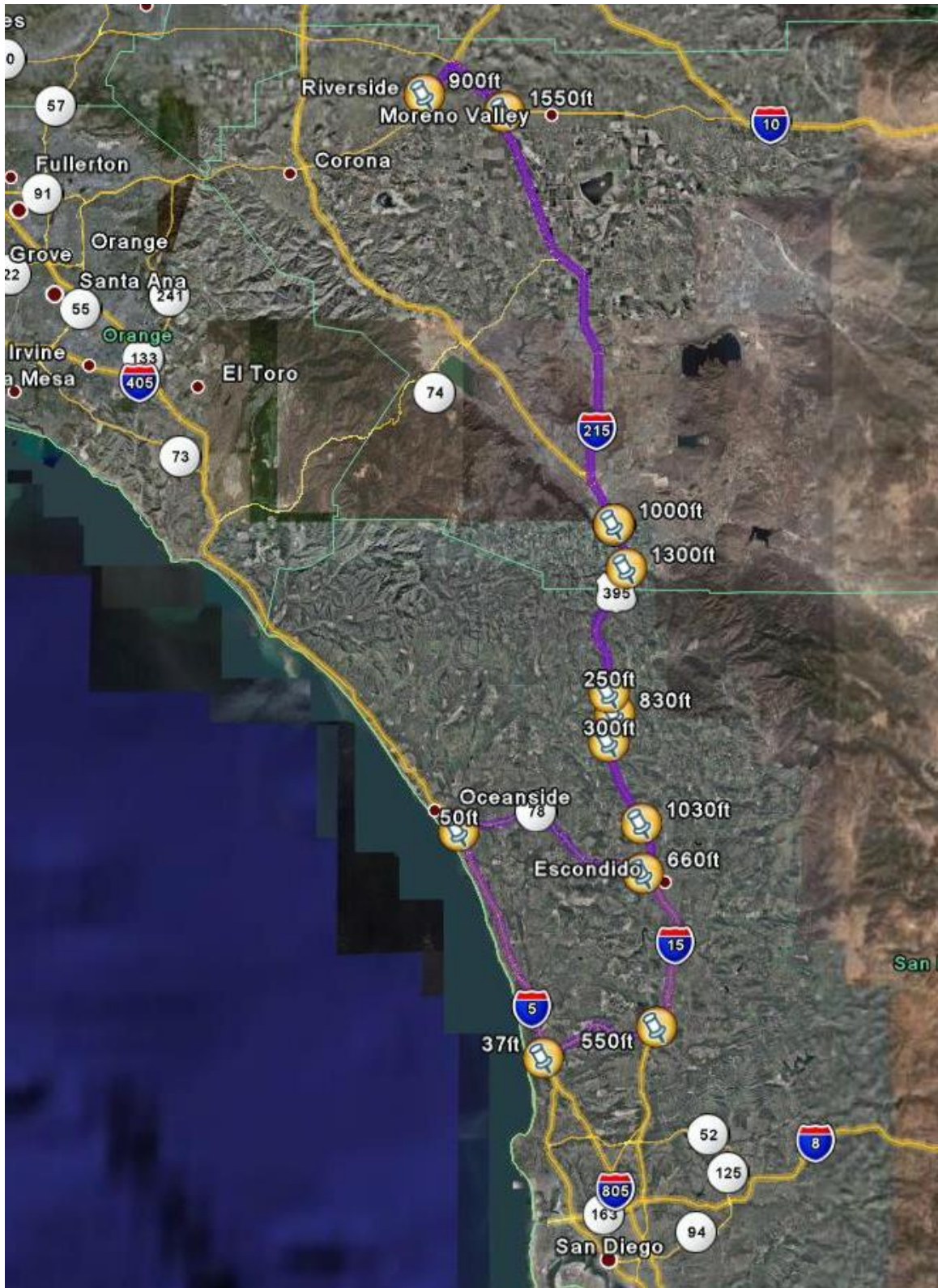


Figure 4-8. Route 3: Riverside to San Diego round trip – distance 197 miles.

Route 2 – Riverside, CA to Bishop/Mammoth Mountain, CA

The second route consisted of driving from Riverside to Bishop/Mammoth Mountain, CA. This route is mostly rural driving along US-395 with some driving on the I-15 at the start of the route. A map of the route is provided in Figure 4-9. Parts of this route carry a significant amount of truck traffic in California. The route has many elevation changes, which created a sufficient number of NTE events, and reaches an elevation above 5000 feet. One section of the road also has high power transmission lines to provide some measure of EMF interference, as shown in Figure 4-10. One railroad crossing provided some measure of road vibration over the route, as shown in Figure 4-11. The total trip distance is approximately 300 miles. Testing was conducted between approximately 9:30 AM and 5 PM on the test day.

The environmental conditions for route 2 are provided in Figure 4-12 for the two test runs. The temperature ranged from 67°F in morning to 88°F in midday and then started to cool back down to the high 70s/low 80s. The elevation extended from approximately 1000 ft. to above 5000 ft. and was generally up hill for a majority of the route. The route included a climb out of Bishop to Mammoth Mountain to ensure the 5000 ft elevation was reached.



Figure 4-9. Route 2,3: Riverside to Mammoth Mountain via US 395.



Figure 4-10. EMF Interference During Routes 2/3



Figure 4-11. Railroad Crossing During Route 2/3

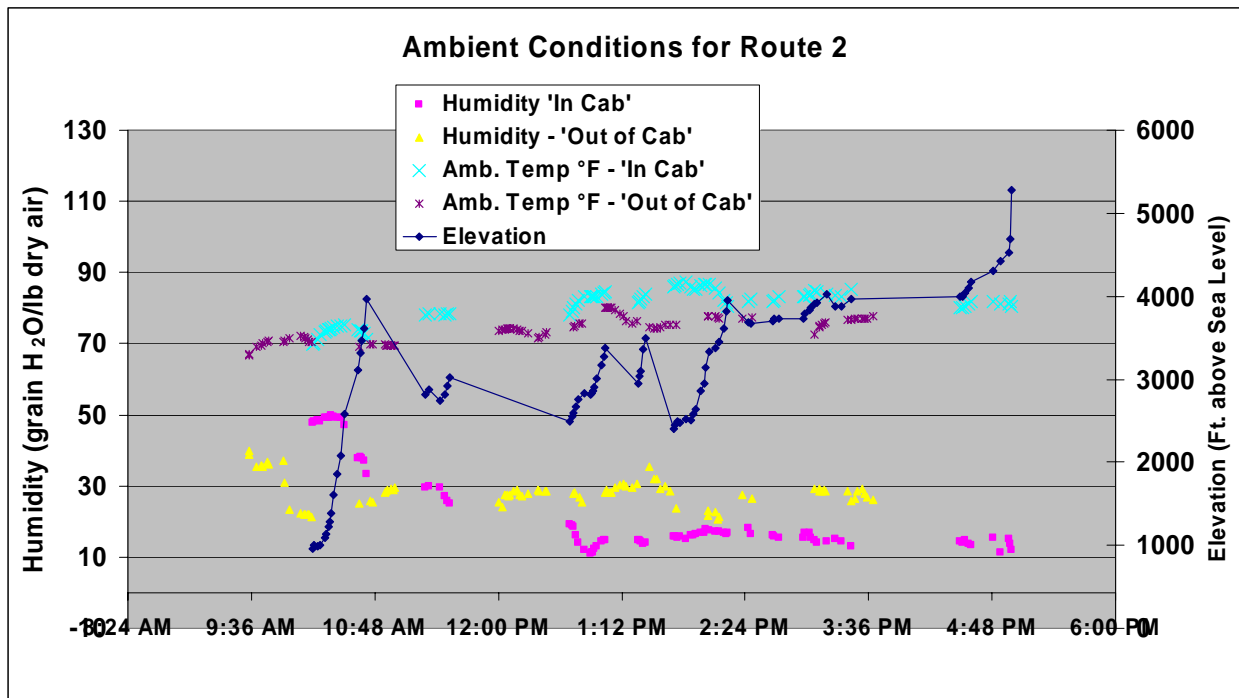


Figure 4-12. Environmental Conditions for Test Runs over Route 2

Route 3 – Return trip from Bishop/Mammoth Mountain, CA to Riverside, CA

The third route is the return trip from Bishop/Mammoth Mountain, CA to Riverside, CA (see Figure 4-9). This route is mostly downhill driving along the I-395 starting from an elevation of approximately 5000 ft., repeating the course for route 2. In the early morning, an extra climb out of Bishop at 4500 ft. towards Mammoth Mountain to above 5000 ft. was performed to provide information under low ambient temperature conditions and corresponding elevation information. The environmental conditions for route 3 are provided in Figure 4-13 for the two test runs. The temperature ranged from just below 50°F in morning to the high 70s/low 80s near the mid day end of the run. The elevation extends from approximately 5000 ft. to approximately 1000 ft. and is generally downhill for a majority of the route. Testing was conducted between approximately 6-7 AM and 1-2 PM on the test day.

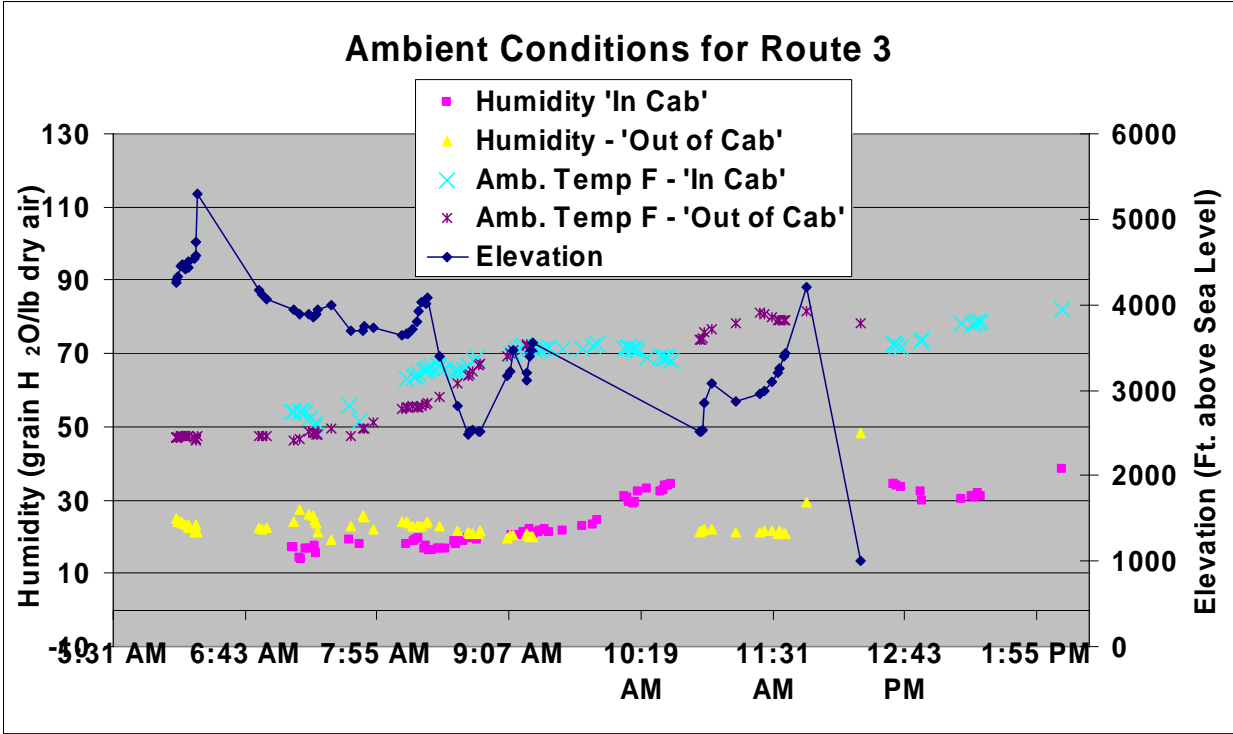


Figure 4-13 Local temperature and RH data near Mammoth Mt.

5.0 On-Road Testing of the PEMS vs. the CE-CERT MEL – Experimental Results

A total of 6 test runs and 3 audits runs were conducted for the on-road testing. The runs included a trip to San Diego, CA and back, a trip from Riverside to Bishop, CA, and a trip returning to Riverside from Bishop, CA. The trips were conducted with the PEMS positioned inside the cab, with the PEMS positioned outside the cab, and as an audit run without the PEMS.

5.1 Audit Run Results

CE-CERT performed audit tests over the selected routes using three different quad blend audit bottles for CH₄, CO, NO and CO₂ and one single blend for THC. See Table 5-1 for audit blends and calibration set points. The reason multiple audit blends were used was a result of the analyzer consumption rate and the 20 hour duration to run all three routes. One bottle was consumed on each route for the quad species sample stream. For NO_x and CO₂, the audit checks were within 2% of the bottle value over all three routes. Some of the quad blends were low concentrations and the effects of elevation changes were significant enough to prevent meeting the 2% specification in the CFR for CO, CH₄ and THC. THC was within 3% and CO and CH₄ were within 5% for all test routes. If the audit bottles with the lower concentrations are excluded, then the remaining CO and CH₄ audits were within the 2% CFR specification.

Test Date	Audit/cal	Route	THC	CH ₄	CO	NO	CO ₂
9/22/2006	audit1	1a	47.7	n/a	25.1	148	1.43
9/26/2006	audit2	1b	47.7	n/a	25.1	148	1.43
9/27/2006	audit3	2	47.7	9.27	90.6	100	1.554
9/28/2006	audit4	3	47.7	23.73	229	271.8	3.63
9/22/2006	cal1	1a	89.4	27.83	70.5	278.9	2.604
9/26/2006	cal2	1b	47.9	14.93	37.8	150.1	1.667
9/27/2006	cal3	2	47.9	14.93	37.8	150.1	1.667
9/28/2006	cal4	3	47.9	14.93	37.8	150.1	1.667

Table 5-1. MEL audit and calibration ranges for on road tests audits.

The gaseous instruments are affected by changes in barometric pressure. CE-CERT found that NO_x was not affected by barometer changes but CO₂, CO, THC and CH₄ were affected by the change in barometric pressure. The CO₂ and CO instruments used had a reference cell that was open to the atmosphere and corrected for most of the deviations but needed some additional corrections. THC and CH₄ zero and span were affected by changes in pressure. The pressure effect on FID zero and span made it hard to correct the FID data at the low concentration levels measured during the correlation. The FID zero changed 2-3 ppm and the span changed 6 ppm with a difference in 6000 feet of elevation. Based on the low levels measured during the correlation and the ability to make barometer corrections, the THC and CH₄ data may have had larger deviations than is expected in the CFR.

The ambient background levels for each emissions component were measured along the test route. These results are summarized in Table 5-2. The background levels are relatively low for NO_x and CO₂. THC and CO levels were comparable to the exhaust sample levels for the DPF equipped vehicle.

Date	Test Run		THC ppm C1	CH ₄ ppm C1	CO ppm	NO _x ppm	CO ₂ %
9/22/06	San Diego, CA (round trip)	Ave.	2.26	2.27	0.83	0.24	0.04
		Stdev.	0.09	0.16	0.34	0.11	0.00
9/27/06	Riverside, CA to Bishop, CA	Ave.	2.19	1.91	0.46	0.12	0.04
		Stdev.	0.09	0.13	0.17	0.08	0.00
9/28/06	Bishop, CA to Riverside, CA	Ave.	2.12	1.97	0.99	0.07	0.03
		Stdev.	0.08	0.12	0.31	0.05	0.00

Table 5-2. Ambient Background Levels Over Different Test Routes

5.2 Calculation Methods

The NTE data are calculated using three different methodologies to obtain brake specific emission factors for NO_x, NMHC, CO, and CO₂. The calculations for each of the three methods are presented in Appendix D and are briefly summarized below. The calculations use slightly different methodologies to determine the emissions factors. The first method utilizes the straight speed and torque to determine the brake specific emission factors. The second method uses the brake specific fuel consumption to determine the brake specific emission factors. The third method uses the mass fuel flow or a fuel specific method to determine the brake specific emission factors. It should be noted that while these calculations provide a generalized perspective of the different calculations, there are important differences in how these calculations are applied and the order in which different values are summed that are more readily apparent in the full calculations in Appendix D.

$$Method\ 1 = \frac{\sum g}{\sum Work}$$

$$Method\ 2 = \frac{\sum g}{\sum \left[\frac{CO_2\ fuel}{ECM\ fuel} \times Work \right]}$$

$$Method\ 3 = \frac{\sum \left[g \times \frac{ECM\ fuel}{CO_2\ fuel} \right]}{\sum Work}$$

The data from the test runs was compiled by CE-CERT for both the MEL and the PEMS. All calculations for the MEL data were performed by the CE-CERT. The data files for the PEMS were subsequently time aligned and corrected for drift by the PEMS manufacturer. The time alignment was performed using the standard post processing feature in the PEMS software. The drift correction was performed using a beta software version that is not yet commercially available.

In comparing the humidity correction factors for the MEL and PEM, differences ranging from 0-2.5% were found over the course of the testing. After reviewing the ambient data and corresponding humidity correction factors, it was speculated that absence of the weather shield may have impacted the ambient measurements made by the PEMS. This, in turn, could adversely affect the biases between the PEMS and MEL. It was decided by the steering committee that for the final data set, the humidity correction factors for the MEL system would be used for both the MEL and PEMS to eliminate this source of error. As such, the resulting comparisons do not account for any errors that might be associated with the humidity correction factors determinations between the different systems.

For the PEMS, the drift correct values were compared against the uncorrected values by the PEMS manufacturer to determine the validity of the test for each NTE event. In accordance with §1065.672 [Federal Register / Vol. 70, No. 133 / Wednesday, July 13, 2005], The drift limit between the corrected and uncorrected values can not excel 4% of the NO_x NTE threshold or 4% of point if the BS NTE values is greater than the NTE threshold (here 2 g/hp-hr). The 4% threshold also applies for CO emissions, while the threshold for THC is slightly higher at 10%. The current beta version of the PEMS software makes all comparisons based on % of point, which is consistent with the 1065 requirements for NO_x, since all measured NO_x emissions values were above the NO_x NTE threshold. Based on these comparison checks, 16 events were found to fail for the PEMS based on the drift limit. Additionally, all the test values for the day one round trip to San Diego (in-cab) were excluded since the drift correction comparison could not properly be performed. For CO and NMHC, the measured values were all considerably below the NTE thresholds, hence not tests were invalidated based on the drift limit for these species. For the MEL system zero and span checks were performed hourly, hence the results over the course of the day were considered drift correct. A separate attempt was not made to generate an “undrift corrected” data set for the MEL for comparison. Separate comparisons were made of the system drift over the data, however, as discussed below, and the drift was found to be much less than the 1065 drift limits that would invalidate any test runs.

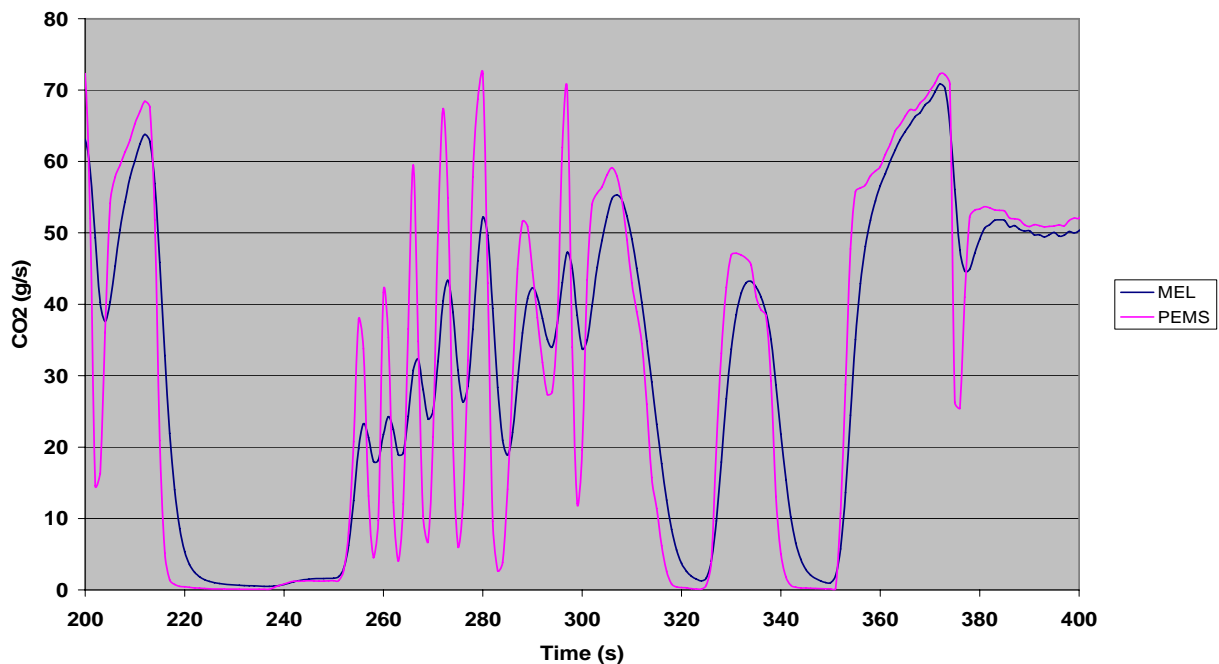
One additional set of calculations was also performed using a dispersion model to account for the differences in the time constants for the analyzer responses. Specifically, the configuration for the MEL sampling system and associated dilution tunnel has a longer time constant for CO₂ than that for the PEMS, and as such shows some peak broadening that can impact the analyzer comparisons. This effect is shown in Figure 5-1(a), which shows a second by trace of CO₂ emissions for the MEL vs. the PEMS for one test file. While the MEL peaks are broader than those of the PEMS, they are still well within the limits specified in 1065, with a rise time from the 10% to 90% level of 2.7 seconds for CO₂ compared to the maximum allowable time of 5 seconds. The time constant for NO_x is less than that for CO₂, hence the results are less impacted by the dispersion. While the impact of dispersion on the analyzer comparisons is relatively minor

for the method 1 calculations, this impact can be greater for methods 2 and 3 since these calculation methods require the calculations of ratios of either the ECM mass fuel rate or BSFC to the CO₂ mass emission rate on a second by second basis.

For the data calculations with dispersion, EPA utilized a dispersion model based on analyzer broadening to disperse the PEMS data such that dispersion differences between the PEMS and MEL were minimized or nearly eliminated. This model was based on a previous investigation of analyzer dispersion by Ganesan and Clark (2001). A comparison of the data after dispersion is provided in Figure 5-1(b) CE-CERT also examined a subset of NTE events using a separate but similar dispersion model and found the impacts on the percentage differences to be similar to those from the EPA (Truex et al., 2000).

One additional item on the calculations is worth noting. Methods 2 and 3, as shown in Appendix D, utilize the brake specific fuel consumption (BSFC) and fuel mass flow, respectively, in the calculations for determinations related to fuel usage. For the present testing, BSFC values were not available over the entire range needed for the calculations. As such, BSFC was determined using a combination of the mass fuel flow and work for method 2 instead of BSFC. This would lead to a closer agreement between the method 2 and 3 calculations than would likely be found if the actual BSFC values were available.

CO2 Time Aligned without Dispersion 200610041004



CO2 Post Drift Correction Time Aligned and Dispersed 200610041004

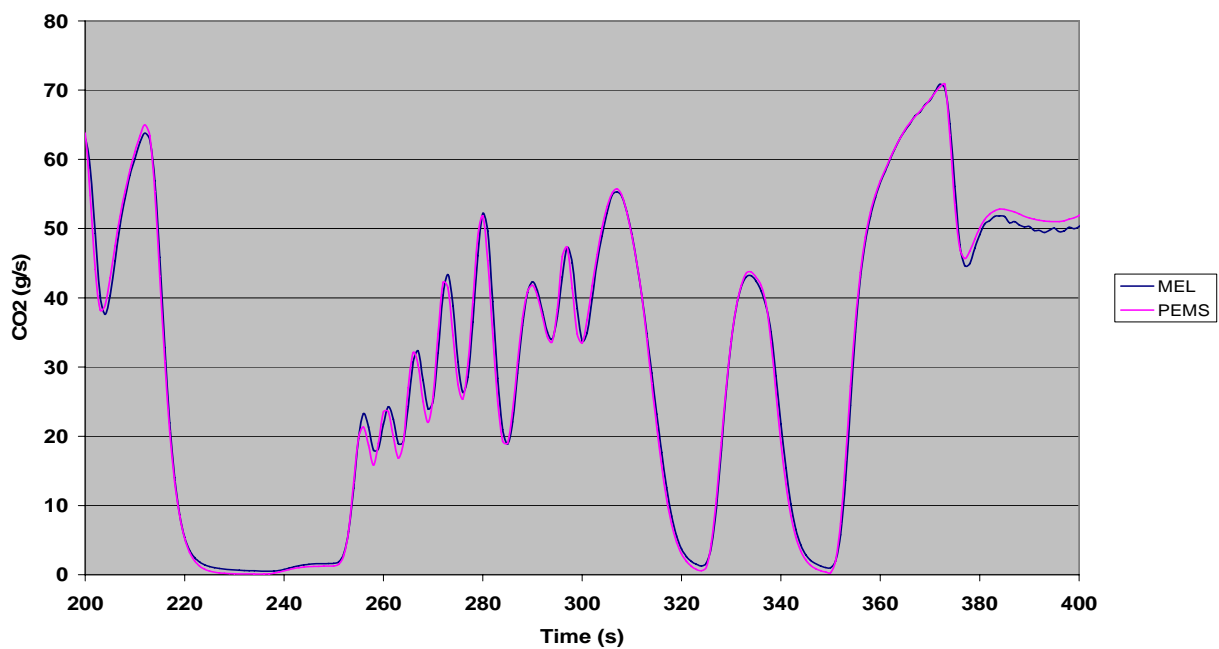


Figure 5-1. Comparison of Real-Time CO₂ Emissions (a) Before Dispersion is Compensated for and (b) After Dispersion is Compensated for.

5.3 Summary of NTE Events

A total of 6 comparisons runs were conducted with the PEMS in either the in cab or out of cab position. The number of NTE events identified in total and for the individual MEL and PEMS units are summarized in Table 5-3. Total number of identified NTE events varied for different test days between 48 and 87. Over the course of the daily test runs, the number of mismatched events (i.e., events identified by either the MEL or PEMS but not both) varied from 3 to 7.

Date	Test Run	PEMS Position	Total NTE	CE-CERT NTE	PEMS NTE	Mismatched Events
10/3/06	San Diego, CA (round trip)	in cab	70	69	65	6
10/4/06	Riverside, CA to Bishop, CA	in cab	87	85	82	7
10/5/06	Bishop, CA to Riverside, CA	in cab	71	68	70	4
10/10/06	San Diego, CA (round trip)	out of cab	48	47	46	3
10/11/06	Riverside, CA to Bishop, CA	out of cab	83	83	80	3
10/12/06	Bishop, CA to Riverside, CA	out of cab	67	66	64	4

Table 5-3. Summary of NTE Events for Each Test Day

Over all six days of sampling, a total of 426 NTE events were identified by either the MEL, the PEMS or both. Of these events, there were a number of NTE events that had differences in start time or event duration as well as events that were not identified by both the MEL and PEMS.

Figures 5-2 and 5-3 show typical examples of mismatched NTE events. In Figure 5-2 both the MEL and PEMS starting at the same time, but the PEMS ended after 60 seconds and the MEL continued. For this event the MEL had one NTE and the PEMS had two NTE's. On a different test, as shown in Figure 5-3, the MEL ended and PEMS continued. One reason for early dropout could be attributed to averaging differences. The ECM broadcast J1939 torque and rpm data rate is typically 10 Hz, but could fluctuate from 5 to 10 Hz on the vehicle network. If the PEMS samples the first five records and the MEL samples the last five records of a 10 record per second data set, then different averages will be calculated by each system. The difference in these calculated averages could cause one system to dropout while the other remains in the event. The calculated averaged differences will be largest on rapid torque transitions. Notice in Figures 5-2 and 5-3 that the dropout by one of the two systems occurred during a rapid torque condition.

Real Time ECM % actTorque for both MEL and PEMs

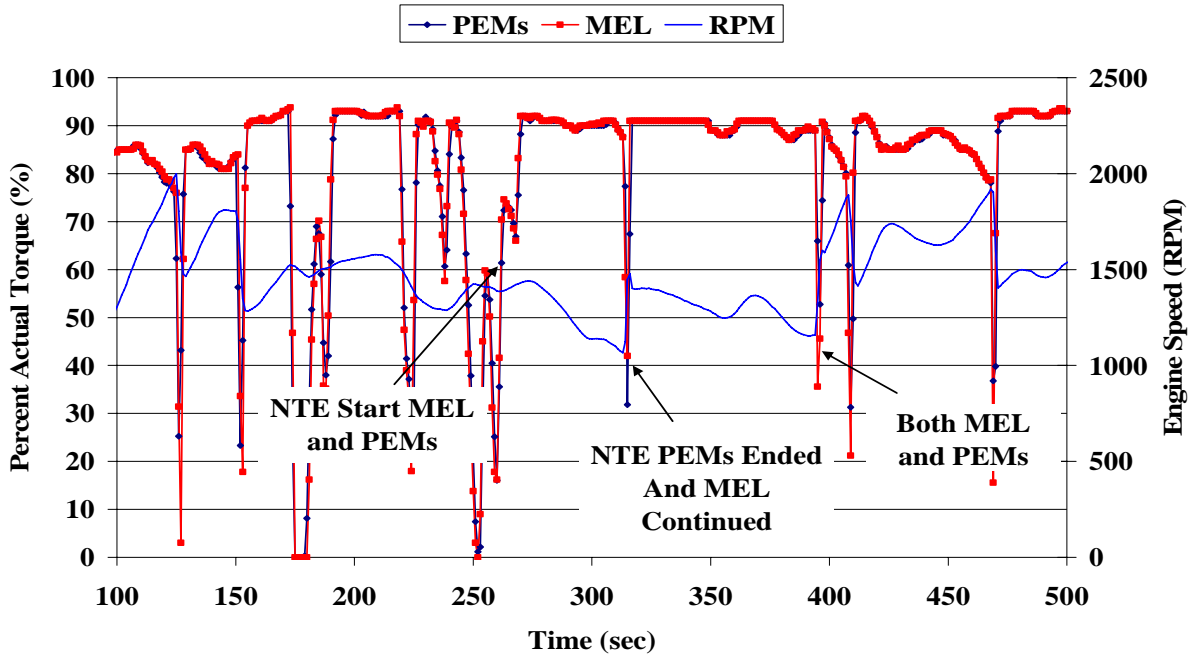


Figure 5-2. Real-time ECM % actTorque for both MEL and PEMS.

Real Time ECM % actTorque for both MEL and PEMs

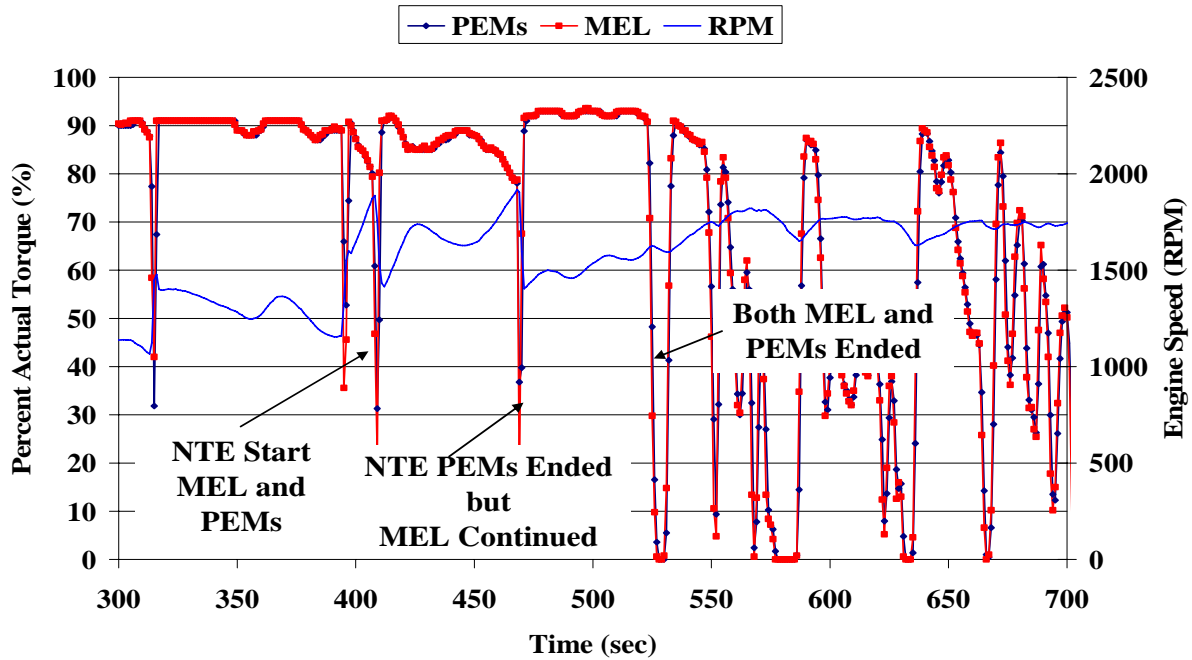


Figure 5-3. Real-time ECM % actTorque for both MEL and PEMS.

In order to compare identical events, NTE events that have common start and duration times must be matched. For the remaining analyses in this section, the analyses were limited to those NTE events where the start time for the NTE event matched to within 3 seconds or less and the event duration matched to within 1 second or less between the MEL and the PEMS. This represented a total of 343 events. This essentially eliminates the errors associated with NTE events of different start times or durations and allows a straight comparison in the emissions differences between the MEL and PEMS. NTE events where the data did not pass the drift limit validity check, as discussed in the previous section, were also excluded. This included all the data from the first test day since the post-test zero span data were not available. All of the remaining Figures in this section are based on only this subset of NTE events.

5.4 NO_x Emission Results

Correlation plots for NO_x emissions between the MEL and PEMS are provided for the common NTE events for brake specific emissions in Figure 5-4 and for total grams in Figure 5-5. The brake specific emissions are shown for each of the calculation methods. An event by event comparison of NTE events for brake specific NO_x emissions for the MEL and PEMS is provided in Appendix E. This appendix also indicates the points that were eliminated due to failed drift correction. The results show the PEMS measurements are generally biased high relative to the MEL, with the largest bias seen for the method 1 calculations.

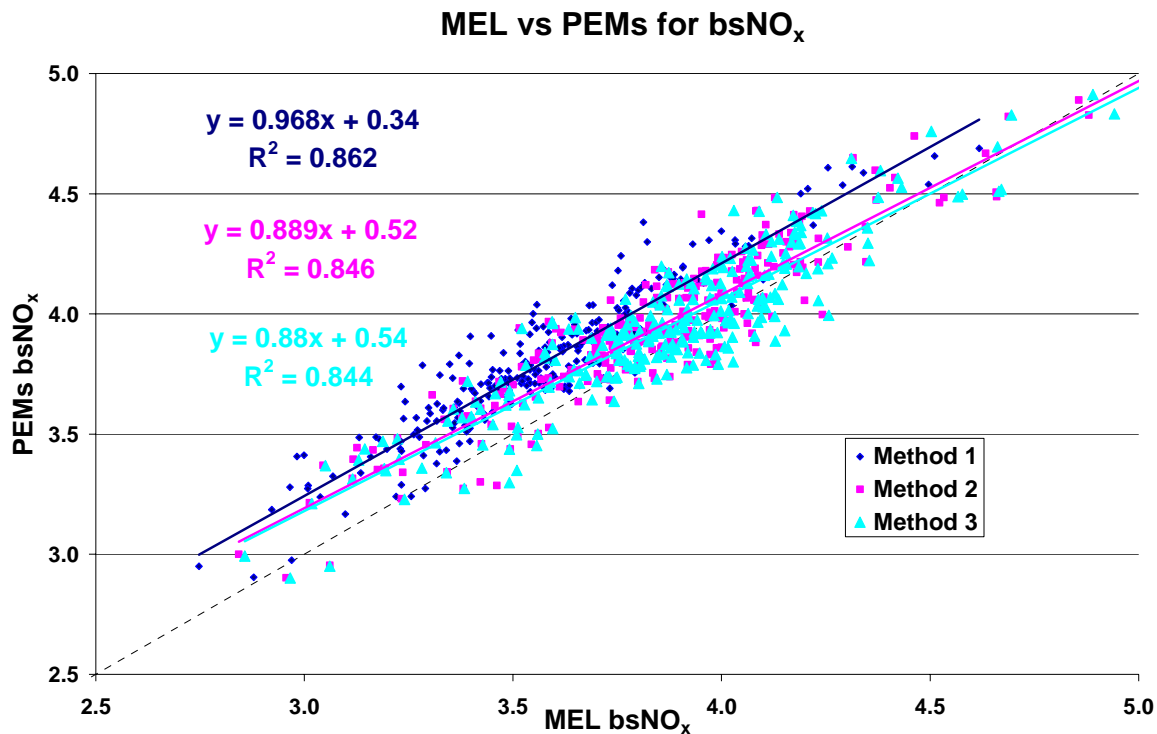


Figure 5-4. NO_x Mass Emissions (g/bkW-hr) for PEMS Relative to MEL

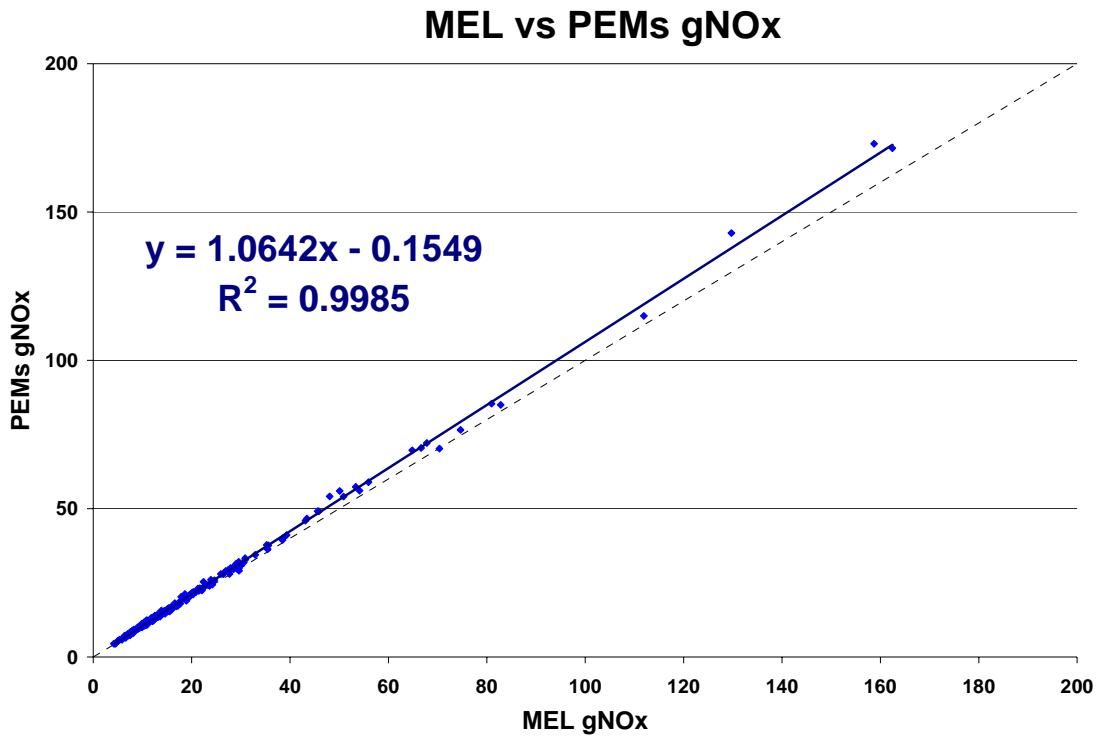


Figure 5-5. NO_x Mass Emissions (g) for PEMS Relative to MEL

The deviations in the brake specific emissions relative to the NTE NO_x standard (2.0 grams per brake horsepower-hour or 2.68 grams per brake kW-hour) are provided in Figure 5-6 on an event by event basis. The absolute deviations as a function of the total NO_x emissions as measured by the MEL are provided in Figure 5-7. The results are summarized in Table 5-4 on a relative basis to the NTE standard and for the absolute differences. The deviations are shown for the 3 different calculation methodologies. The deviations were greatest for the method one calculation, with an average deviation of $+8\% \pm 4\%$ of the NTE standard over all points, where the error represents one standard deviation. The deviations for methods 2 and 3 were $+4\% \pm 5\%$ and $+3\% \pm 5\%$, respectively, over all points. The differences in the deviations for the different calculation methods could be related to the incorporation of CO₂ exhaust measurements into calculations 2 and 3. As the CO₂ is also biased high, as shown in the next subsection, this should have the effect of normalizing the emissions differences. Methods 2 and 3 are also somewhat impacted by analyzer dispersion, as will be discussed further below. The deviations relative to the proposed NTE NO_x standard (2.68 grams per brake kW-hour) are slightly higher than those on a relative basis, since the emissions measurements were generally above the NTE standard. On a relative basis, the deviations were $+6\% \pm 3\%$, $+3\% \pm 4\%$, and $+2\% \pm 4\%$, respectively, for calculation method 1, 2 and 3. The results for the relative percent deviations of point are provided in Figure 5-8 and in Table 5-5.

Method 1,2,& 3 Brake Specific kNO_x PEMs vs MEL Deltas

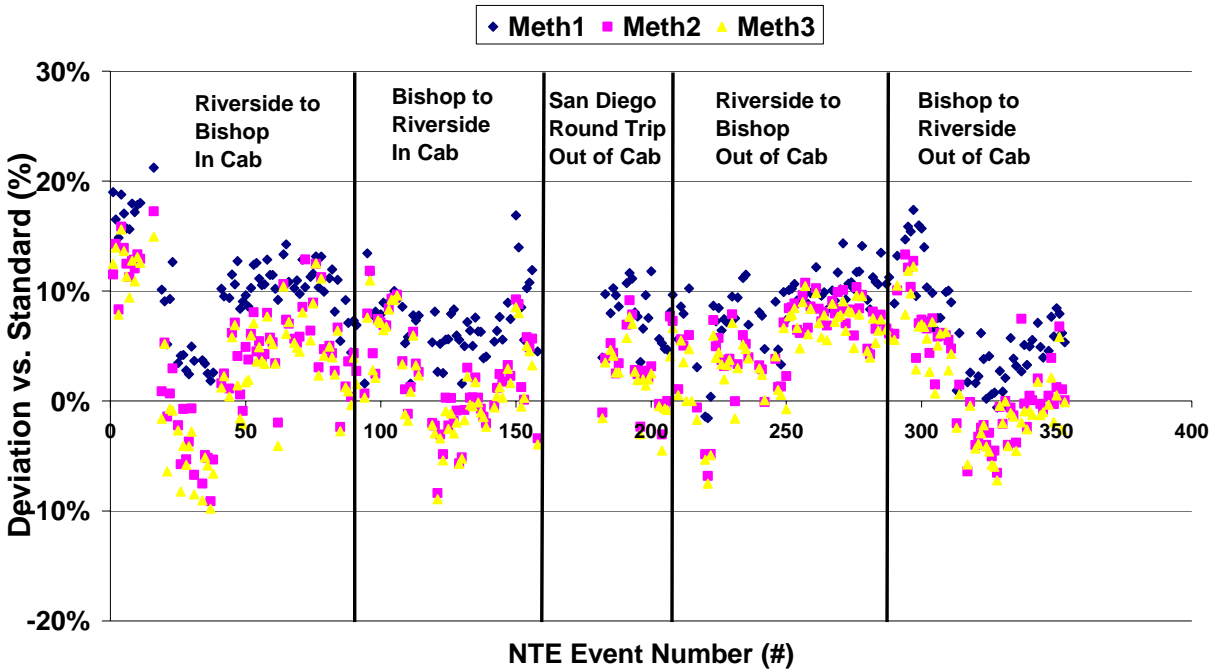


Figure 5-6. Deviations in % Relative to the Standard for NO_x on an NTE Event Basis

Differences in $bsNO_x$ vs. MEL NO_x Level

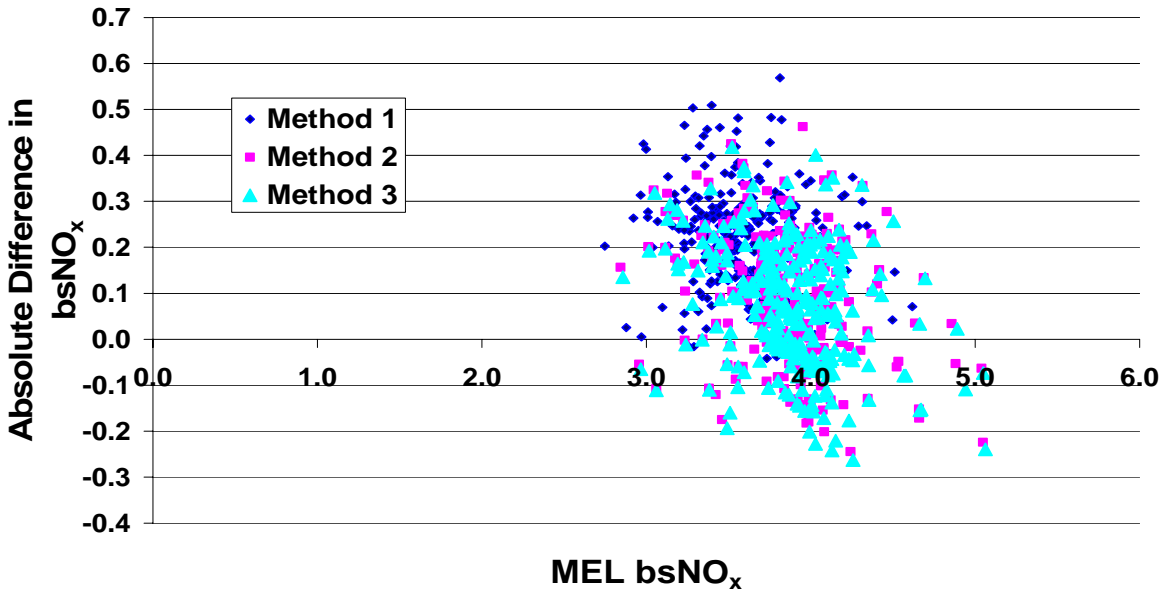


Figure 5-7. Absolute Differences for NO_x (g/bkW-hr) Compared to NO_x Emission Level (g/bkW-hr)

Method 1,2,& 3 Brake Specific kNO_x PEMs vs MEL Deltas

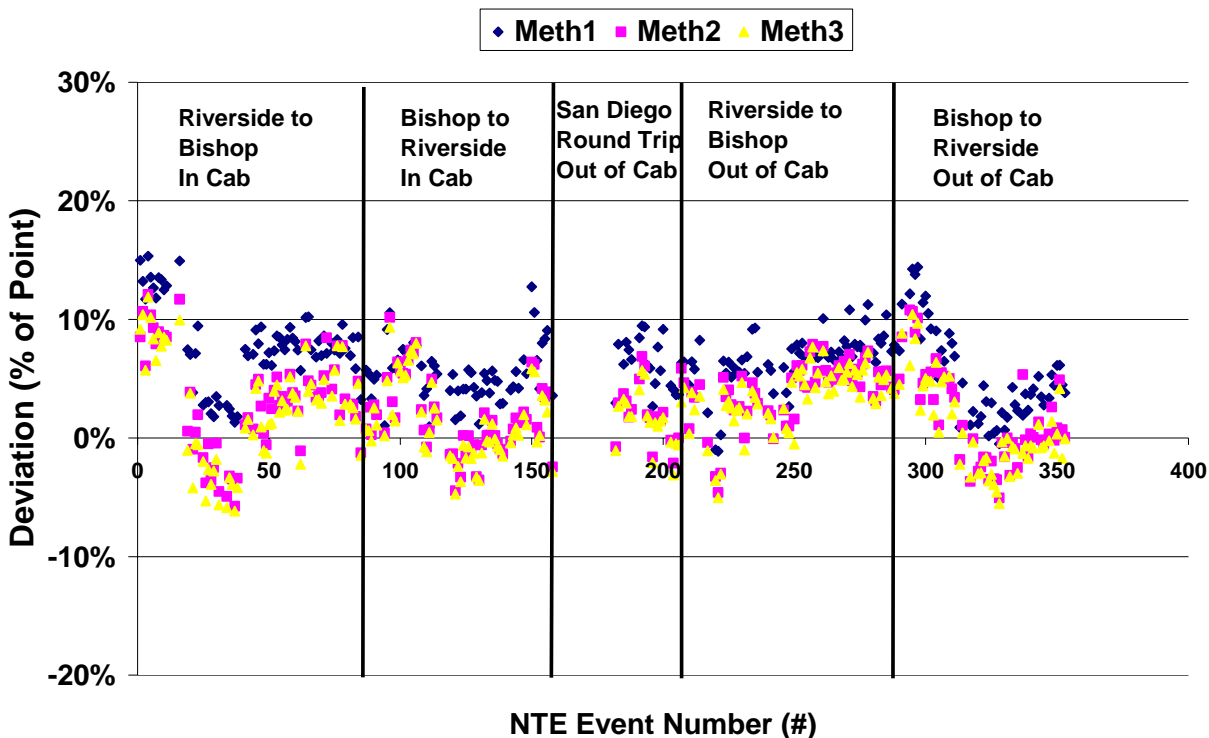


Figure 5-8. Deviations in % of Point for NO_x on an NTE Event Basis

There were some differences for the deviations between the different test runs or segments/days, which could be due to a variety of factors such as environmental conditions, altitude, and analyzer drift. These data were not analyzed in detailed, although there is some indications that zero drift for the PEMS may have contributed to variability within the testing. In general, comparisons between test days or routes indicate most of the conditions were comparable within the experimental variability. A two-tailed, paired t-test between the MEL and PEMS NO_x results for individual NTE events, as provided in Table 5-4, showed that the differences in emissions between the MEL and PEMS were highly statistically significant for nearly all test conditions. The only comparisons that were not statistically significant for at least the 95% confidence level were the method 3 calculations for the out of cab Bishop, CA to Riverside, CA run.

Test day/points	Trip	PEMS Position	Average Difference vs.		Absolute Difference (g/kW-hr)	t-test	
			Method	Standard			St Dev
All points			1	8%	4%	0.22	4.97E-99
			2	4%	5%	0.10	3.56E-26
			3	3%	5%	0.07	5.67E-17
10/4/2006	Riverside, CA to Bishop, CA	in cab	1	11%	5%	0.28	7.90E-30
			2	5%	6%	0.12	3.237E-08
			3	4%	6%	0.09	2.59E-05
10/5/2006	Bishop, CA to Riverside, CA	in cab	1	7%	3%	0.19	2.23E-26
			2	2%	4%	0.06	2.80E-04
			3	2%	4%	0.04	9.25E-03
10/10/2006	San Diego, CA (round trip)	out of cab	1	8%	3%	0.21	3.51E-11
			2	3%	3%	0.07	0.00194
			3	2%	3%	0.05	0.0118
10/11/2006	Riverside, CA to Bishop, CA	out of cab	1	9%	3%	0.24	8.21E-33
			2	6%	4%	0.15	1.56E-18
			3	5%	4%	0.13	7.28E-16
10/12/2006	Bishop, CA to Riverside, CA	out of cab	1	6%	5%	0.17	4.89E-14
			2	2%	5%	0.05	0.00701
			3	1%	5%	0.03	0.135

Table 5-4. Summary of Deviations in % vs. Standard for NO_x Emissions

Test day/points	Trip	PEMS Position	Method	Average % Difference vs. Point	St Dev
All points			1	6%	3%
			2	3%	4%
			3	2%	4%
10/4/2006	Riverside, CA to Bishop, CA	in cab	1	8%	3%
			2	3%	4%
			3	2%	4%
10/5/2006	Bishop, CA to Riverside, CA	in cab	1	5%	2%
			2	2%	3%
			3	1%	3%
10/10/2006	San Diego, CA (round trip)	out of cab	1	6%	2%
			2	2%	2%
			3	1%	2%
10/11/2006	Riverside, CA to Bishop, CA	out of cab	1	7%	2%
			2	4%	3%
			3	3%	3%
10/12/2006	Bishop, CA to Riverside, CA	out of cab	1	5%	4%
			2	2%	4%
			3	1%	4%

Table 5-5. Summary of Deviations in % vs. Point for NO_x Emissions

The deviations for the data generated from the dispersion model are shown in Figure 5-9 in the brake specific emissions relative to the NTE NO_x standard. The results are summarized in Table 5-6 on a relative basis to the NTE standard and for the absolute differences. The results from the dispersion model were fairly similar to those found for the baseline data set. The deviations for the method one calculation were slightly less than those for the baseline data set, with an average deviation of +7%±5% of the NTE standard over all points. The deviations for methods 2 and 3 over all points were +4%±5% and +4%±6%, respectively, with a slight tendency for higher differences than for the baseline data set.

Method 1,2,& 3 Brake Specific kNO_x PEMs vs MEL Deltas

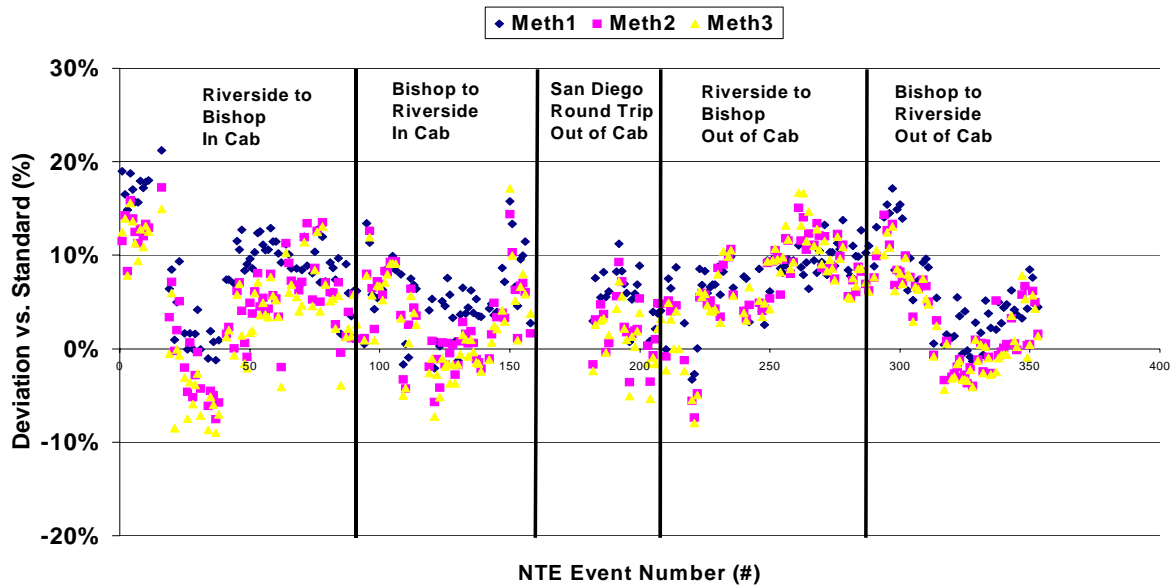


Figure 5-9. Deviations in % Relative to the Standard for NO_x on an NTE Event Basis for Dispersion Data

Test day/points	Trip	PEMS Position	Average Difference vs. Standard		Absolute Difference (g/kW-hr)	t-test	
			Method	St Dev			
All points			1	7%	5%	0.19	7.16E-74
			2	4%	5%	0.12	2.80E-34
			3	4%	6%	0.10	8.72E-24
10/4/2006	Riverside, CA to Bishop, CA	in cab	1	9%	5%	0.25	3.52E-22
			2	5%	6%	0.14	7.90E-10
			3	4%	7%	0.10	1.70E-05
10/5/2006	Bishop, CA to Riverside, CA	in cab	1	6%	4%	0.15	1.32E-16
			2	3%	4%	0.08	2.26E-06
			3	2%	5%	0.06	4.16E-04
10/10/2006	San Diego, CA (round trip)	out of cab	1	6%	3%	0.15	7.37E-08
			2	2%	3%	0.05	0.0128
			3	1%	3%	0.03	0.181
10/11/2006	Riverside, CA to Bishop, CA	out of cab	1	8%	3%	0.21	1.24E-27
			2	7%	4%	0.19	2.32E-19
			3	7%	5%	0.19	1.07E-17
10/12/2006	Bishop, CA to Riverside, CA	out of cab	1	6%	5%	0.17	2.58E-12
			2	3%	5%	0.05	2.73E-05
			3	3%	5%	0.03	2.25E-04

Table 5-6. Summary of Deviations for NO_x Emissions with Dispersion

One other factor that could influence the deviations between the systems is the NO_x converter efficiency. For the MEL, the NO_x converter efficiency for NO₂ to NO was found to be 96.4%. Based on the relative NO₂ values measured in the exhaust by the PEMS, this could result in a 'loss' of 1.8 to 0.8% of NO_x during the MEL measurements, potentially biasing the system low.

5.5 CO₂ Emission Results

The brake specific and total gram CO₂ emissions for the common NTE events are provided in Figure 5-10 and Figure 5-11, respectively. The method 1 results show the PEMS measurements are consistently biased high relative to the CE-CERT MEL, with an R² = 0.97. The percentage deviations for method 1 CO₂ for the PEMS relative to the MEL value are shown in Figure 5-12. The percentage differences averaged +4%±2%. This is consistent with the correlation plot for grams of CO₂ which shows a slight high bias with an R² = 1.0. Note that for the method 2 and 3 calculations, the resulting brake specific CO₂ emissions are primarily representative of the values derived from the mass fuel flow from the ECM for both the MEL and PEMS since the measured CO₂ emissions or concentrations largely cancel out of the equation.

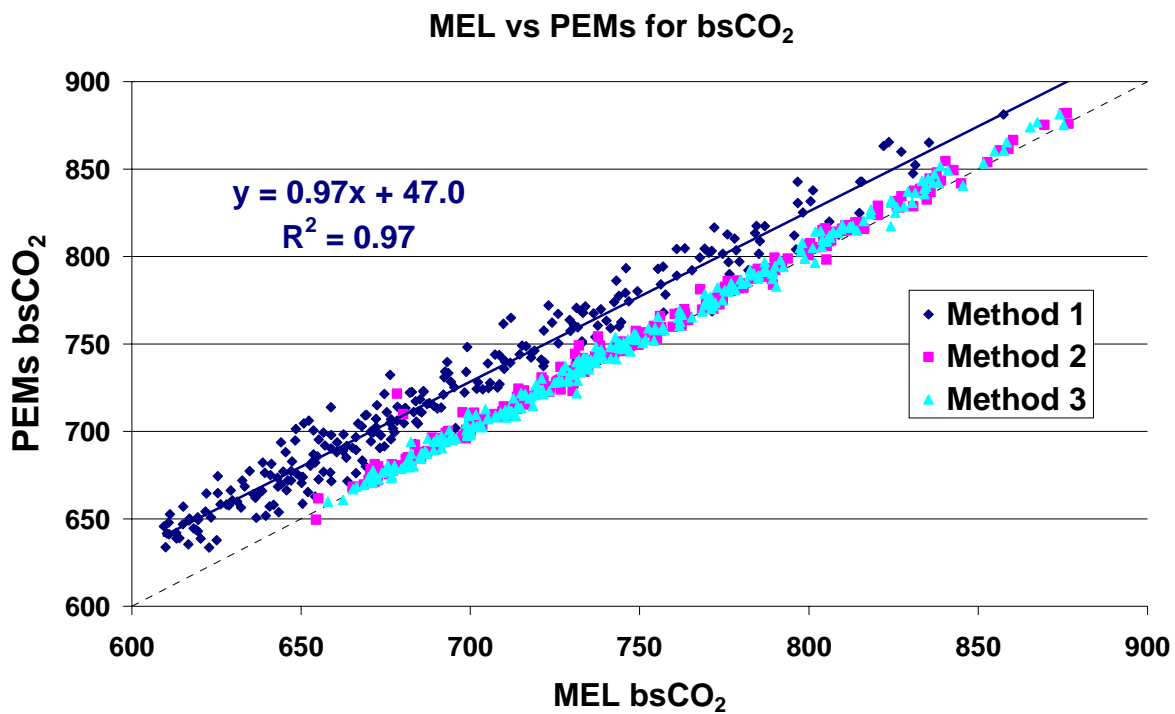


Figure 5-10. CO₂ Mass Emissions (g/bkW-hr) for PEMS Relative to MEL

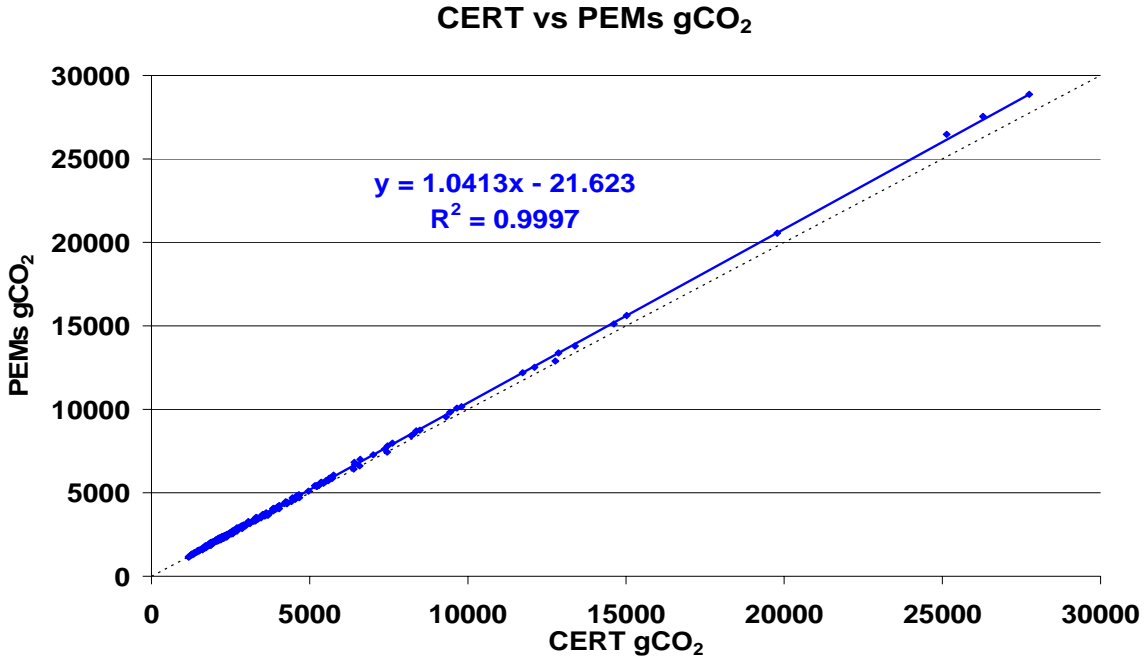


Figure 5-11. CO₂ Mass Emissions (grams) for PEMS Relative to MEL

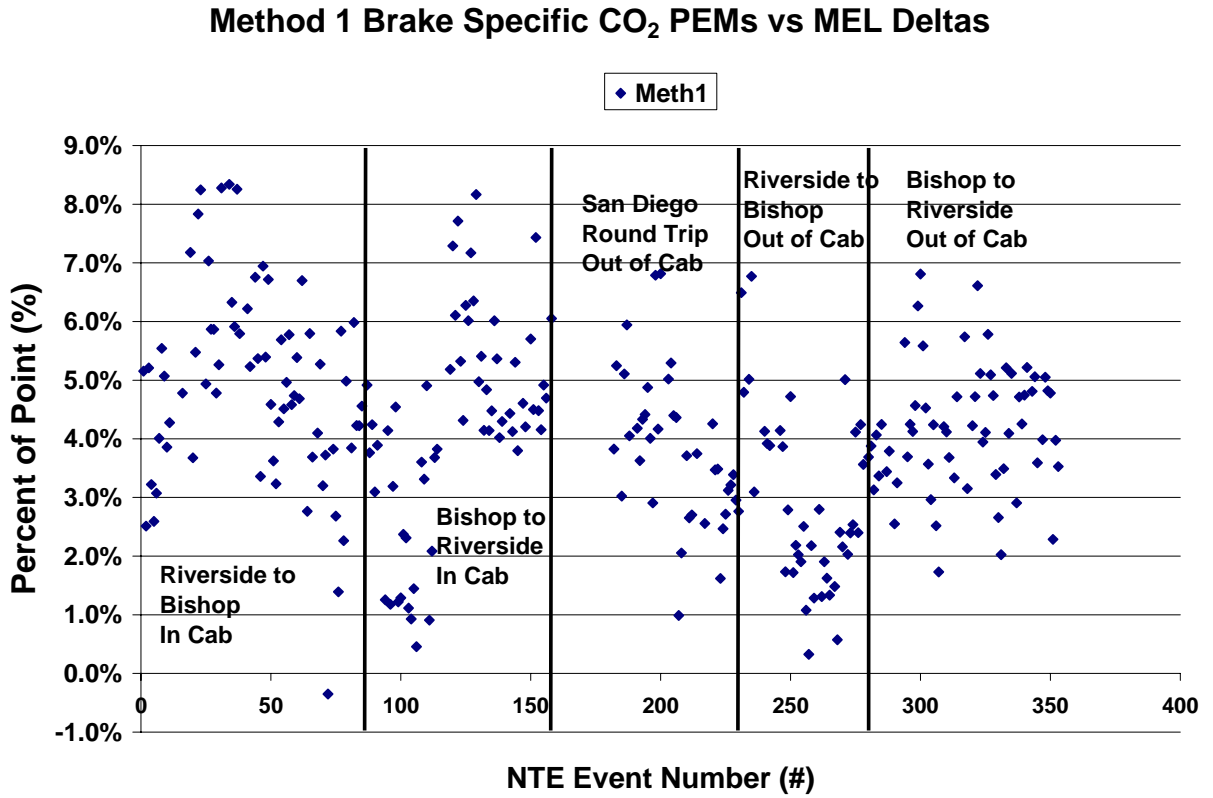
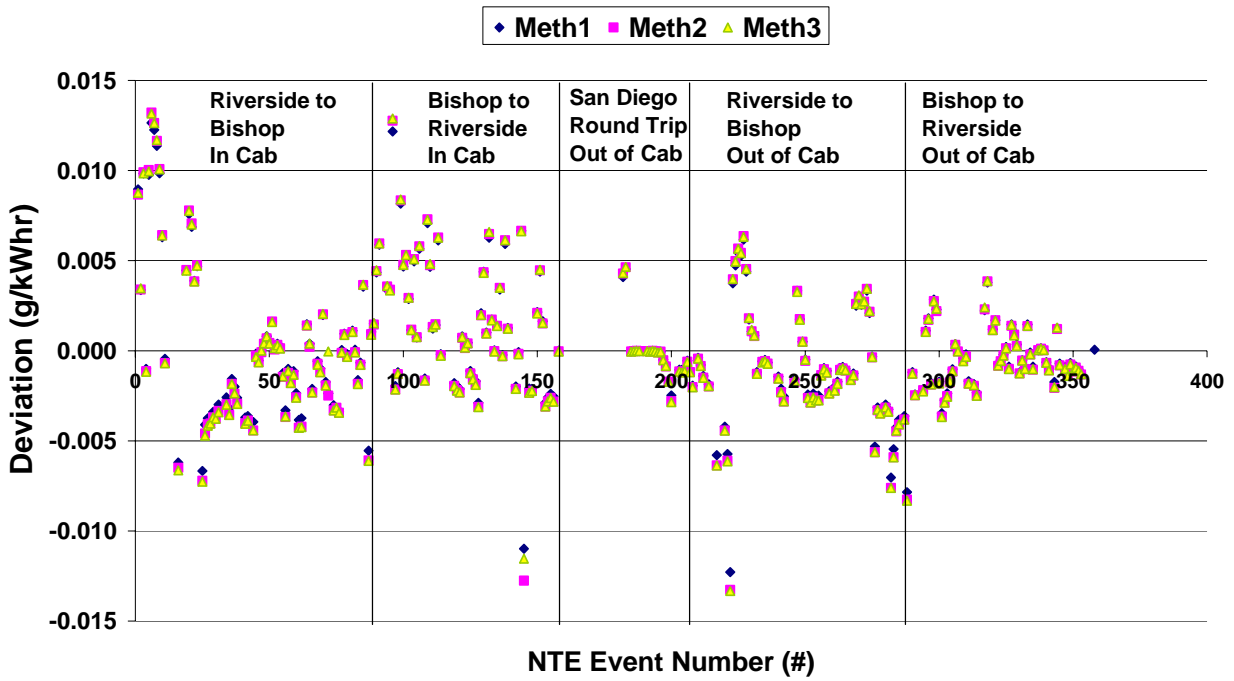


Figure 5-12. CO₂ Mass Emissions (g/bkW-hr) for PEMS Relative to MEL

5.6 NMHC Results

NMHC emissions levels were consistently low for the on-road measurements. The average emission rates for NMHC was 0.003 g/bkW-hr or below, which is around 1% of the anticipated NTE standard of 0.28 g/bkW-hr. For the MEL, the diluted exhaust NMHC concentration levels were comparable to those of the ambient background. The concentration levels are discussed further in section 5.8. The deviations of the NMHC measurements between the PEMS and the MEL are plotted in Figure 5-13 in terms of absolute differences and on a relative basis compared to the NTE standard. There is not consistent bias for NMHC emissions between the different analyzers, with the PEMS higher for some tests and lower for others, albeit at very low levels. Average differences for the different test runs were $\pm 0.5\%$ or less of the NTE standard. The correlation analysis in Figure 5-14 shows relatively weak correlation of $R^2 \sim 0.36/0.37$ due to the low level measurements. A summary of the absolute differences and the differences relative to the NTE standard for different test runs is provided in Table 5-7. The t-test comparisons showed that the differences between the analyzers were statistically significant for some test runs but not for others. Over all NTE events, the differences were not found to be statistically significant.

Method 1,2,& 3 Brake Specific NMHC PEMs vs MEL Deltas



Method 1,2,& 3 Brake Specific NMHC PEMs vs MEL Deltas

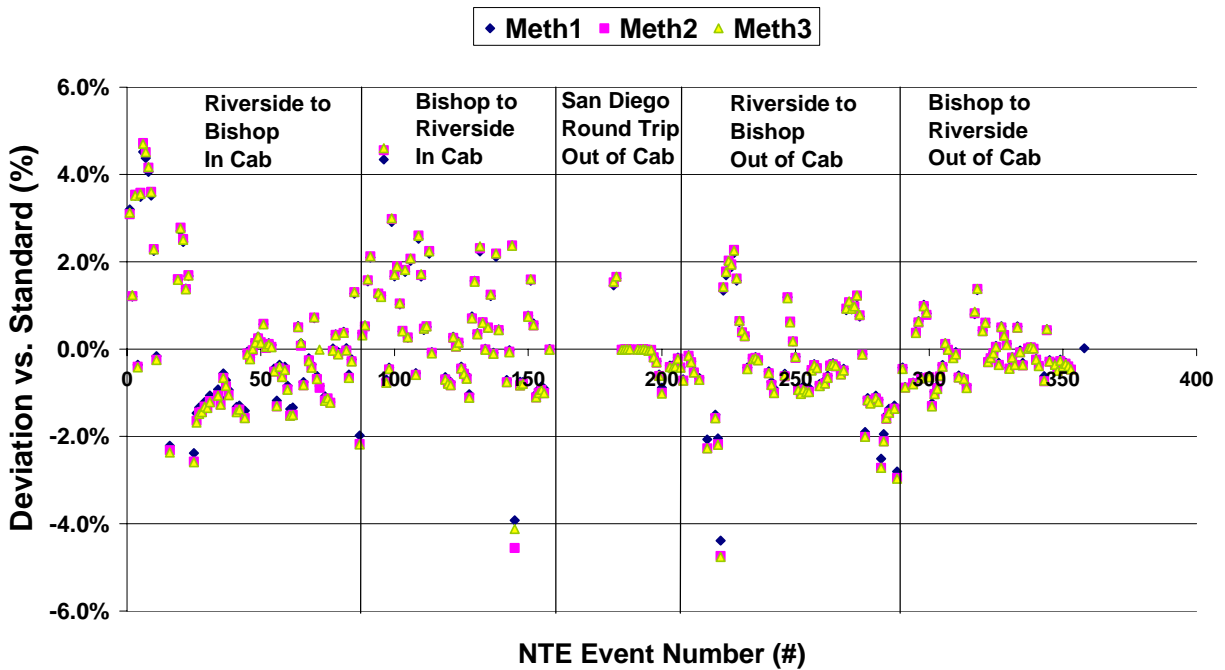


Figure 5-13. Absolute Deviations and Deviations Relative to NTE Standard for NMHC on an NTE Event Basis

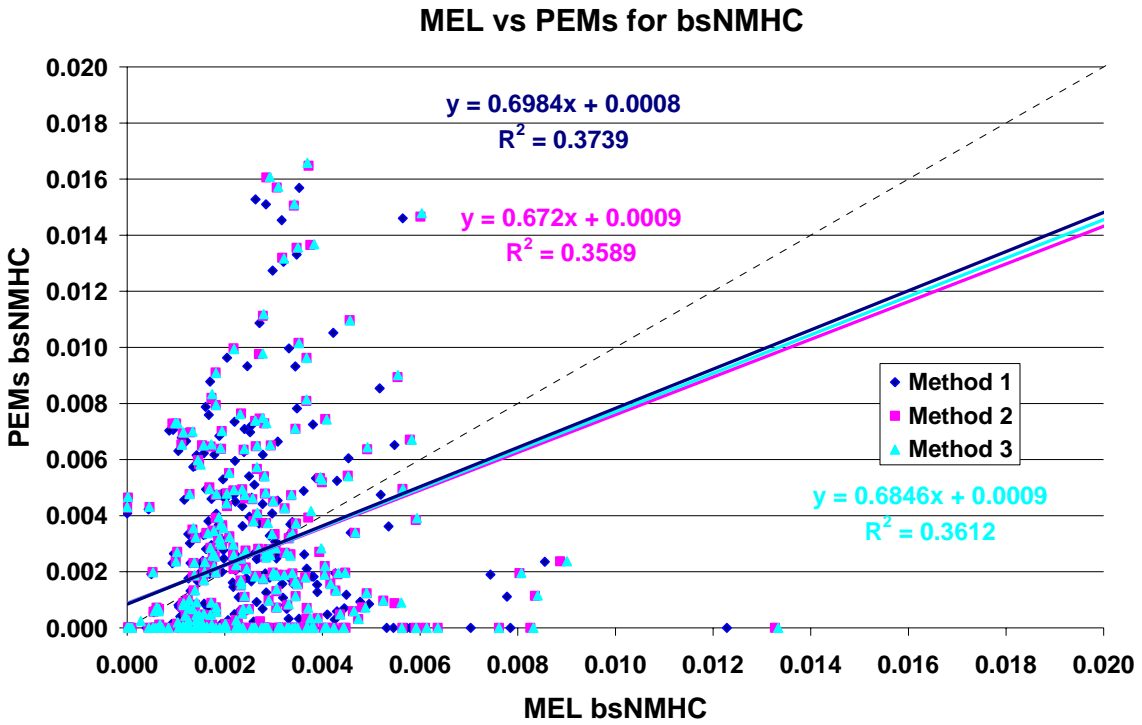


Figure 5-14. NMHC Mass Emissions (g/bkW-hr) for PEMS Relative to MEL

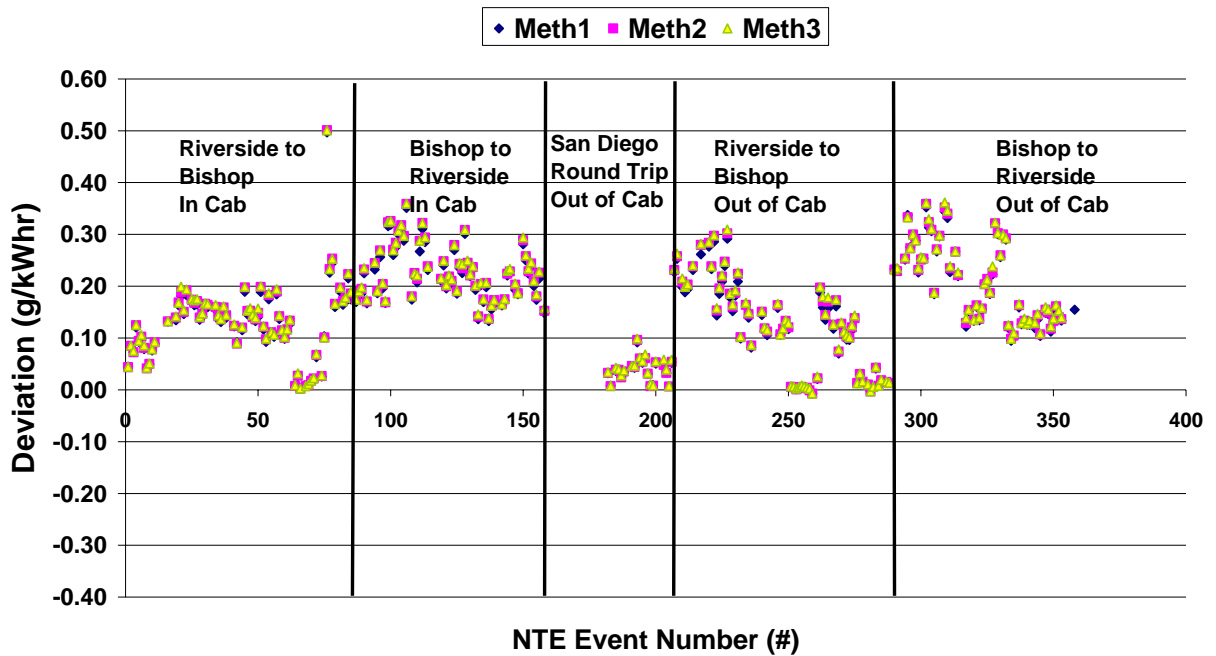
Test day/points	Trip	PEMS Position	Method	Average Difference (g/kW-hr)	St Dev (g/kW-hr)	% Diff vs. Standard	t-test
All points			1	0.000	0.004	0.0%	0.797
			2	0.000	0.004	0.0%	0.861
			3	0.000	0.004	0.0%	0.905
10/4/2006	Riverside, CA to Bishop, CA	in cab	1	0.000	0.005	0.1%	0.556
			2	0.000	0.005	0.1%	0.752
			3	0.000	0.005	0.1%	0.716
10/5/2006	Bishop, CA to Riverside, CA	in cab	1	0.001	0.004	0.5%	0.00449
			2	0.001	0.004	0.5%	0.00963
			3	0.001	0.004	0.5%	0.00762
10/10/2006	San Diego, CA (round trip)	out of cab	1	0.000	0.002	0.0%	0.917
			2	0.000	0.002	0.0%	0.857
			3	0.000	0.002	0.0%	0.850
10/11/2006	Riverside, CA to Bishop, CA	out of cab	1	-0.001	0.003	-0.4%	0.0121
			2	-0.001	0.004	-0.4%	0.00896
			3	-0.001	0.004	-0.4%	0.00891
10/12/2006	Bishop, CA to Riverside, CA	out of cab	1	0.000	0.001	-0.1%	0.0613
			2	0.000	0.002	-0.2%	0.0269
			3	0.000	0.002	-0.2%	0.0308

Table 5-7. Summary of Deviations for NMHC Emissions

5.7 CO Emission Results

For CO emissions, the MEL emissions measurements were very low and the PEMS measurements were consistently higher than those of the MEL. The CO emissions levels were on the order of 0.1% of the anticipated NTE standard of 26.01 g/bkW-hr for CO for the MEL measurements, although the PEMS measurements were higher than this. For the MEL, the diluted exhaust CO concentration levels were comparable to those of the ambient background. The concentration levels are discussed further in section 5.8. The deviations of the CO measurements between the PEMS and the MEL are plotted in Figure 5-15 in terms of absolute differences and on a relative basis compared to the NTE standard. These Figures show that CO emission levels for the PEMS were consistently higher than those for the MEL. The absolute differences represented 1% or less of the NTE standard, although the PEMS measurements were approximately an order of magnitude higher than those for the MEL. The correlation analysis in Figure 5-16 shows again that the PEMS had considerably higher readings than the MEL and that there was essentially no correlation between the measurement methods ($R^2 = 0.0011$ or less) at these low levels. A summary of the absolute differences and the differences relative to the NTE standard for different test runs is provided in Table 5-8. The t-test comparisons showed that all differences were highly statistically significant.

Method 1,2,& 3 Brake Specific CO PEMs vs MEL Deltas



Method 1,2,& 3 Brake Specific CO PEMs vs MEL Deltas

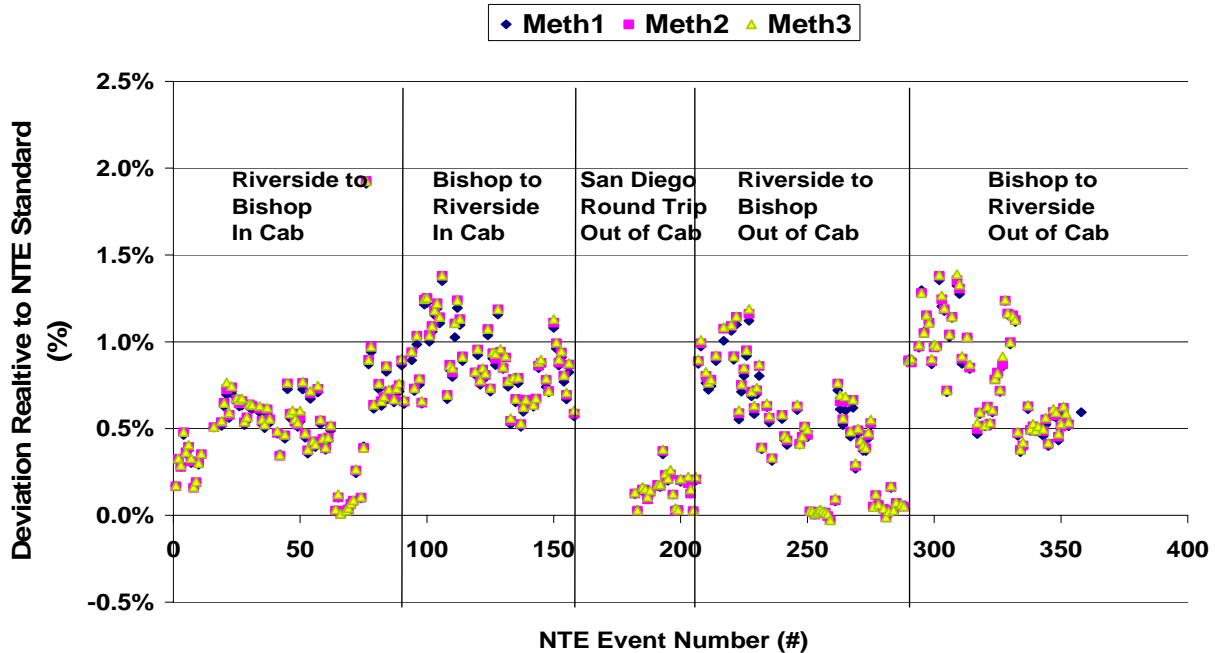


Figure 5-15. Absolute and Relative to NTE Standard Deviations for CO on an NTE Event Basis

MEL vs PEMs for bsCO

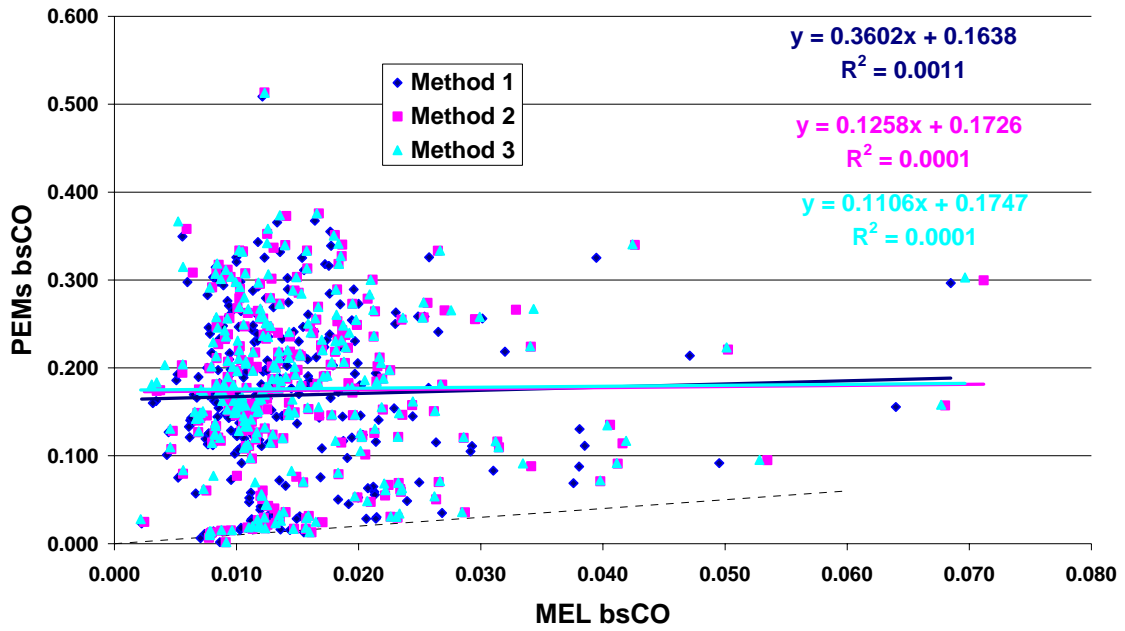


Figure 5-16. CO Mass Emissions (g/bkW-hr) for PEMS Relative to MEL

Test day/points	Trip	PEMS Position	Method	Average Difference (g/kW-hr)	St Dev (g/kW-hr)	% Diff vs. Standard	t-test
All points			1	0.155	0.090	0.6%	1.62E-81
			2	0.159	0.092	0.6%	3.59E-82
			3	0.161	0.092	0.6%	2.98E-83
10/4/2006	Riverside, CA to Bishop, CA	in cab	1	0.126	0.072	0.5%	5.45E-23
			2	0.131	0.074	0.5%	3.97E-23
			3	0.132	0.074	0.5%	2.23E-23
10/5/2006	Bishop, CA to Riverside, CA	in cab	1	0.223	0.050	0.9%	4.99E-40
			2	0.229	0.052	0.9%	5.32E-40
			3	0.231	0.051	0.9%	2.17E-40
10/10/2006	San Diego, CA (round trip)	out of cab	1	0.038	0.021	0.1%	1.41E-07
			2	0.039	0.022	0.1%	2.48E-07
			3	0.042	0.023	0.1%	1.41E-07
10/11/2006	Riverside, CA to Bishop, CA	out of cab	1	0.115	0.087	0.4%	1.03E-15
			2	0.120	0.091	0.5%	1.00E-15
			3	0.122	0.092	0.5%	6.59E-16
10/12/2006	Bishop, CA to Riverside, CA	out of cab	1	0.207	0.078	0.8%	6.12E-26
			2	0.210	0.077	0.8%	2.45E-26
			3	0.2136	0.077	0.8%	1.13E-26

Table 5-8. Summary of Deviations for CO Emissions

5.8 Exhaust Concentration Levels

Concentrations measured by PEMS and MEL are within reasonable ranges for the instruments for NO_x and CO₂. CO, THC and CH₄ are below 10% of the instruments span points. The span, audit, and average NTE measured values are shown in Tables 5-9 and 5-10, respectively, for the MEL and PEMS. The measured concentration levels for specific NTE events for the MEL and PEMS are shown in Figures 5-17 and 5-18, respectively. Note that the MEL levels represent diluted exhaust while the PEMS levels represent raw exhaust. Also, values for all tests except those on the first day of testing were used for these tables and figures, as these data are provided to show typical levels rather than detailed comparisons between the MEL and PEMS. The PEMS instrument was zeroed on ambient air while the MEL was zeroed on bottled air or nitrogen depending on the species. Ambient levels of THC were on the same order as the measured NTE exhaust levels for the MEL.

	CO ppm	CO ₂ %	NO _x ppm	THC ppmC1	CH ₄ ppmC1
ZERO	bottle	bottle	bottle	bottle	bottle
CAL	71.47	3.68	280.2	89.39	27.60
AUDIT	19.07	3.63/0.307	271.8	27.37	23.73
AVE NTE	1.37	2.68	137.01	1.92	2.03
STD NTE	0.64	0.39	28.68	0.49	0.18

Table 5-9. MEL calibration ranges.

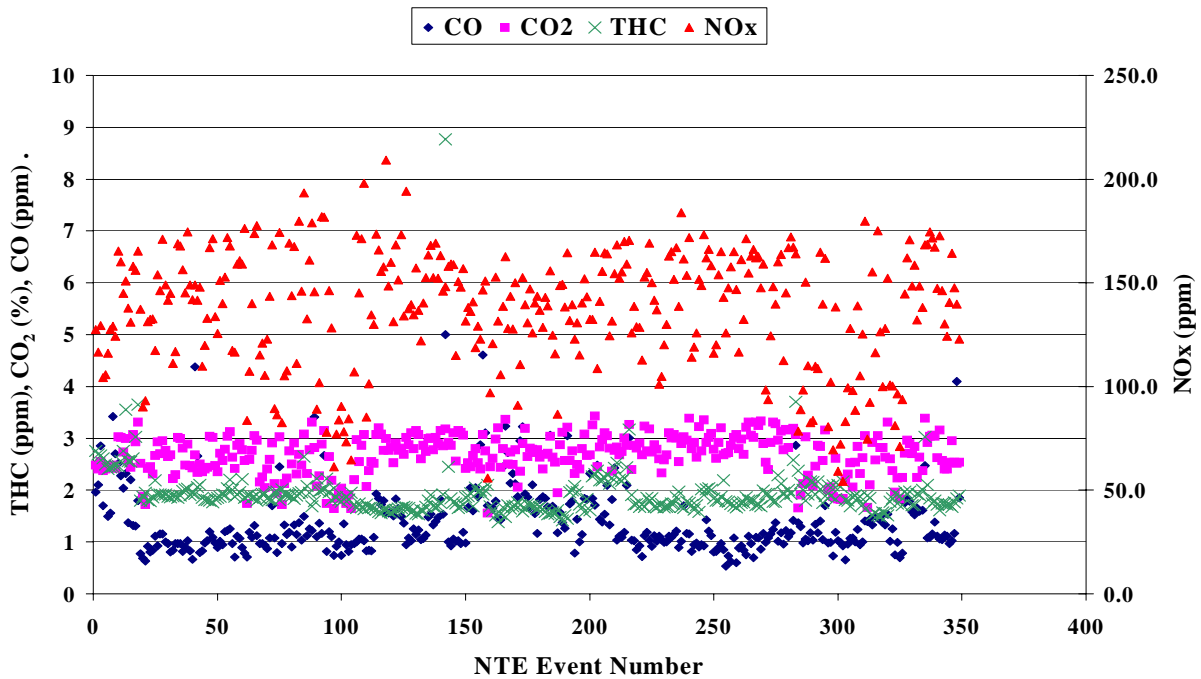


Figure 5-17. MEL Concentration Data as Measured by Instruments for All Primary Species

	CO ppm	CO ₂ %	NO ppm	NO ₂ ppm	THC ppm
ZERO	amb	amb	amb	amb	amb
CAL	1204	12.00	1503	253	198.0
AUDIT	200	6.03	298	60	50.5
AVE NTE	29.4	8.36	304	147	0.8
STD NTE	14.3	0.95	84	23	1.6

Table 5-10. PEMS Calibration Ranges.

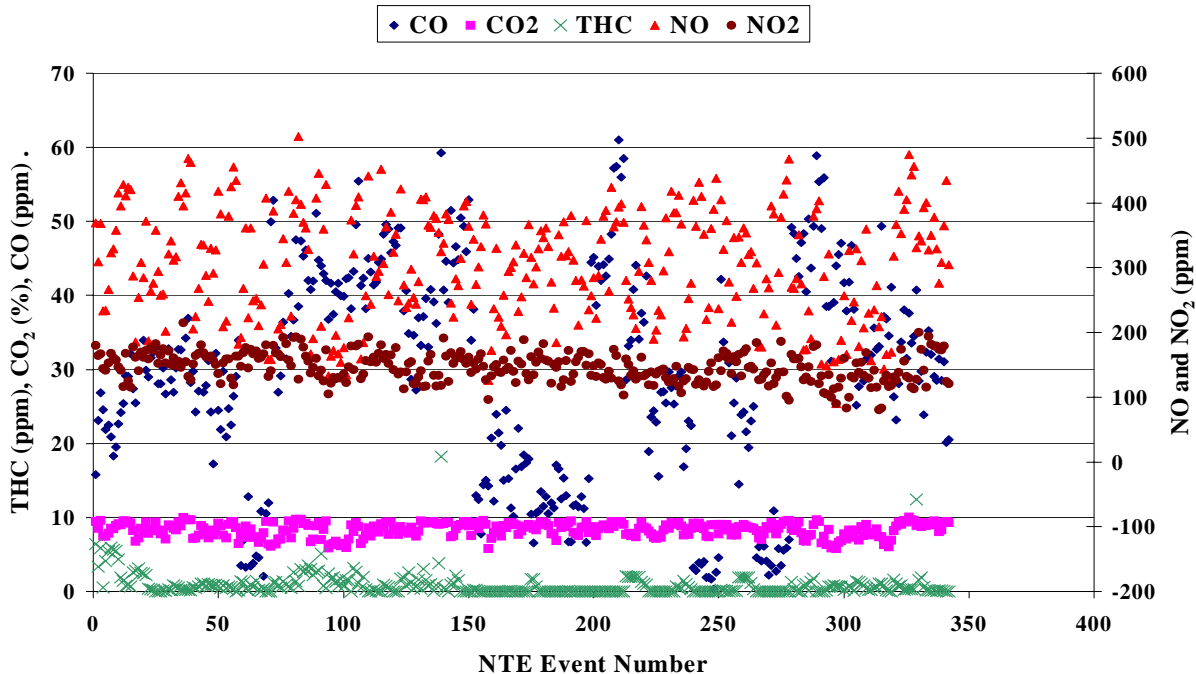


Figure 5-18. PEMS concentration data as measured by instrument for all primary species

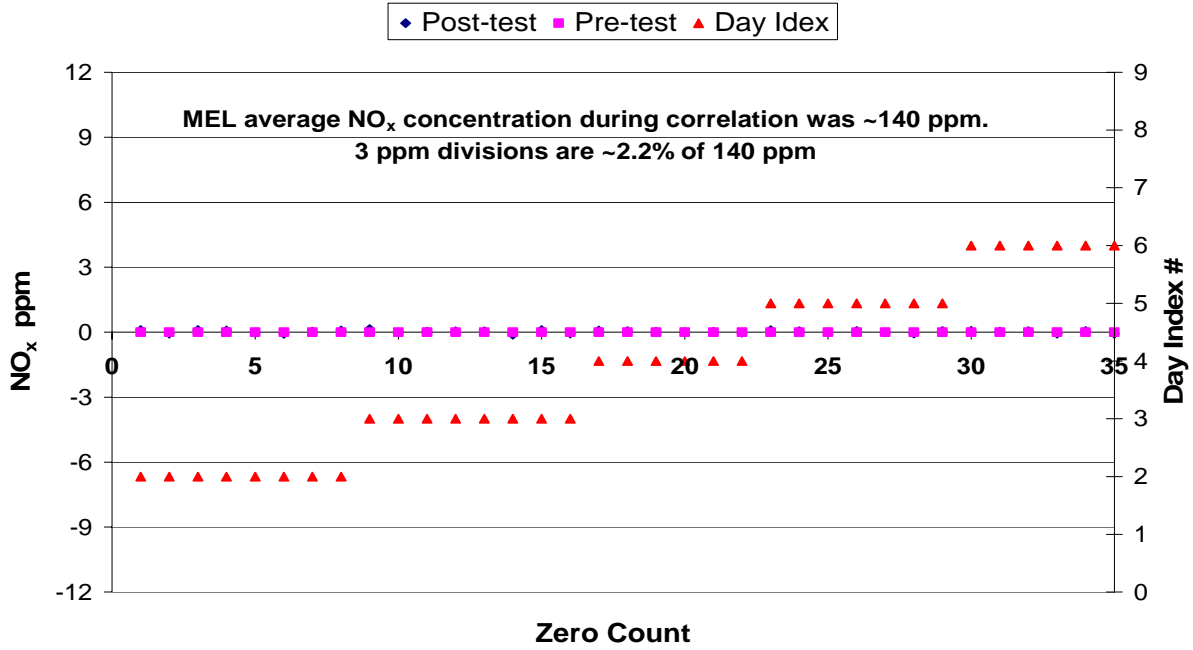
5.9 Zero and Span Calibration Comparisons

Some additional analyses of the zero and span data through the course of the test runs was also performed as part of the evaluations for the drift limit correction and validation and to better understand the differences between the MEL and PEMS. Comparisons of pre and post zero and span data for NO_x for the MEL and PEMS are provided in Figures 5-19 and 5-20, respectively. The day index markers provide a reference as to which testing day the corresponding calibrations were conducted.

The MEL zero and spans were relatively stable over the testing period and showed little drift. It should be noted that the MEL analyzers were rezeroed and span hourly, so large drift over the testing day would not be expected. The MEL zeros showed an average drift over of the 1 hour period of less than 0.02% of the typical concentration value of 140 ppm. The span calibrations showed an average drift of 0.22%. Span drifts of over 2% were seen for only two tests with a maximum drift of 2.47%.

The PEMS showed an average pre-/post-span deviation of -0.21% with a range from -3.11% to +2.85% relative to the bottle concentration. The deviations did show greater differences relative to the average concentration levels in the exhaust with an average deviation relative to the 300 ppm concentration level of -1.04%, with a range from -15.5% to +14.7%. The zeros also showed some drift during course of testing with an average deviation of 1.0% of the average exhaust concentration (300 ppm), but a range from -12.2% to +14.7% of 300 ppm. This could indicate that addition stabilization/purge time is needed for the zero measurements.

MEL Total NO_x Zero Calibrations



MEL Total NO_x Span Calibrations

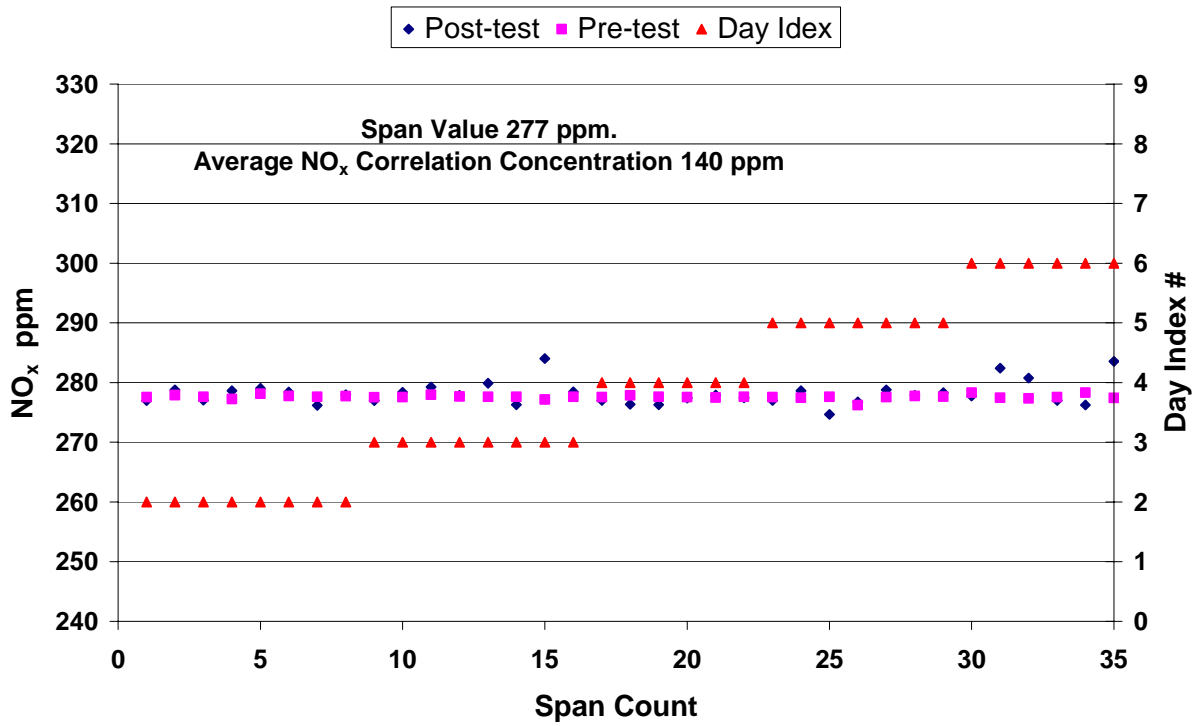
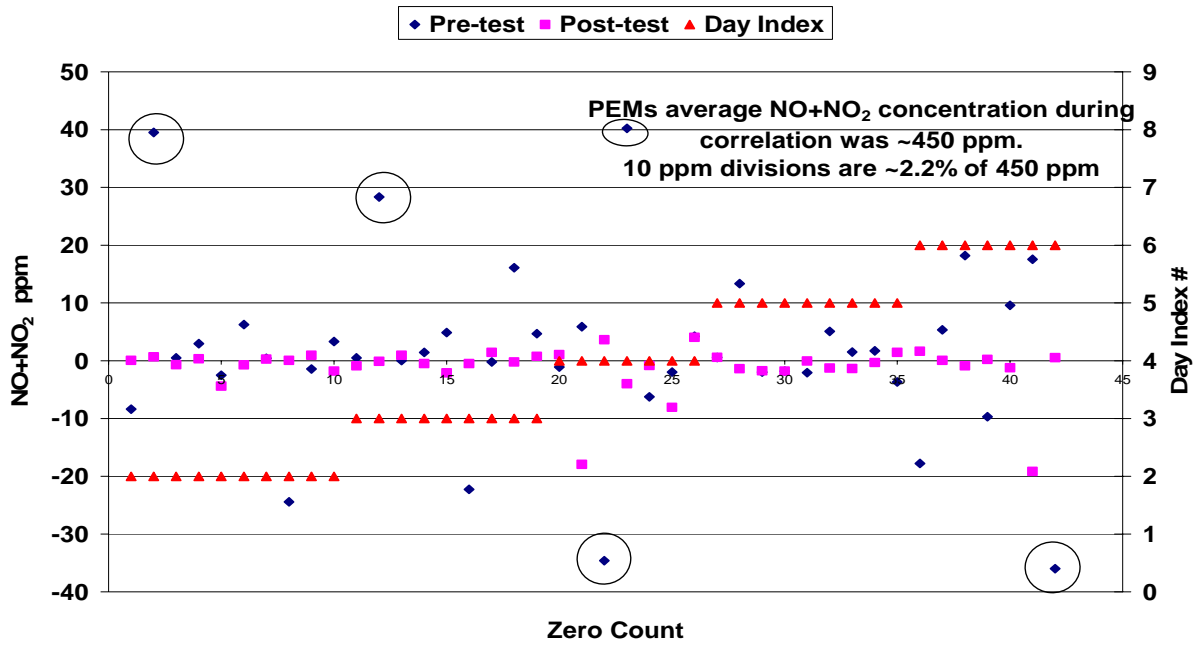


Figure 5-19. MEL Calibrations for (a) zero and (b) span.

PEMs Total NO+NO₂ Zero Calibrations



PEMs NO Span Calibrations

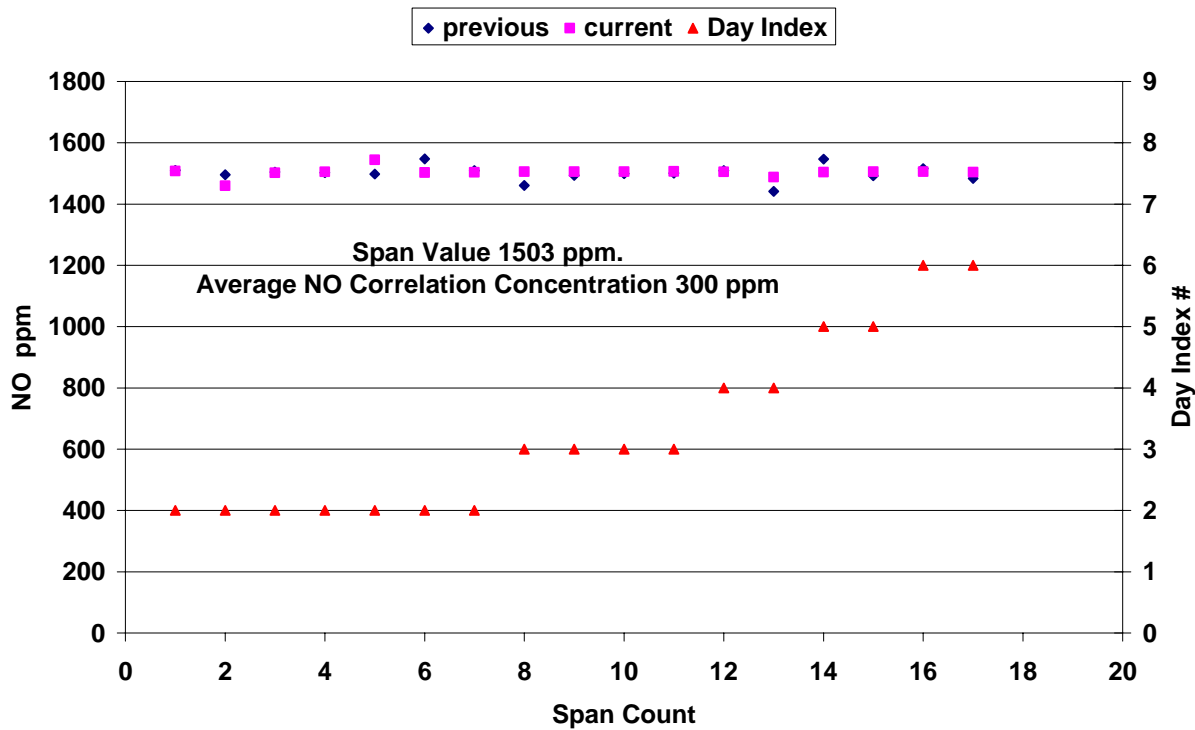


Figure 5-20. PEMS Calibrations for (a) zero and (b) span.

6.0 Summary and Conclusions

For diesel engines, soon to be implemented regulations will require the measurement of in-use emissions within the Not-To-Exceed (NTE) control area of the engine map. This will require the use of portable emissions monitoring systems (PEMS) as opposed to more traditional laboratory methods. The US EPA, CARB, and the EMA have worked together to develop a comprehensive program to determine the “allowance” for compliance purposes when PEMS are used for in-use testing. This program incorporates engine testing and environmental testing to evaluate PEMS together with a Monte Carlo simulation to evaluate and predict the anticipated error for the PEMS in the field.

An important element of this program is on-road comparisons between PEMS and the CE-CERT Mobile Emissions Laboratory (MEL), which is a full dilution tunnel system on a mobile platform. On-road comparisons were made between the MEL and the PEMS over three different courses. The courses included a trip to San Diego, CA and back, a trip from Riverside to Bishop, CA, and a trip returning to Riverside from Bishop, CA. A total of 6 test runs and 3 audits runs were conducted for the on-road testing. The runs included a trip with the PEMS positioned inside the cab, a trip with the PEMS positioned outside the cab, and a trip as an audit run without the PEMS. In conjunction with this program, a complete a cross-laboratory emissions correlation with the MEL was conducted with an engine dynamometer laboratory at the Southwest Research Institute (SwRI) in San Antonio, Texas, as well as a full 1065 audit of the MEL.

This report describes the on-road comparisons between the CE-CERT MEL and the PEMS and associated 1065 audit of the MEL and cross correlation with SwRI. The results of this study are summarized below as follows:

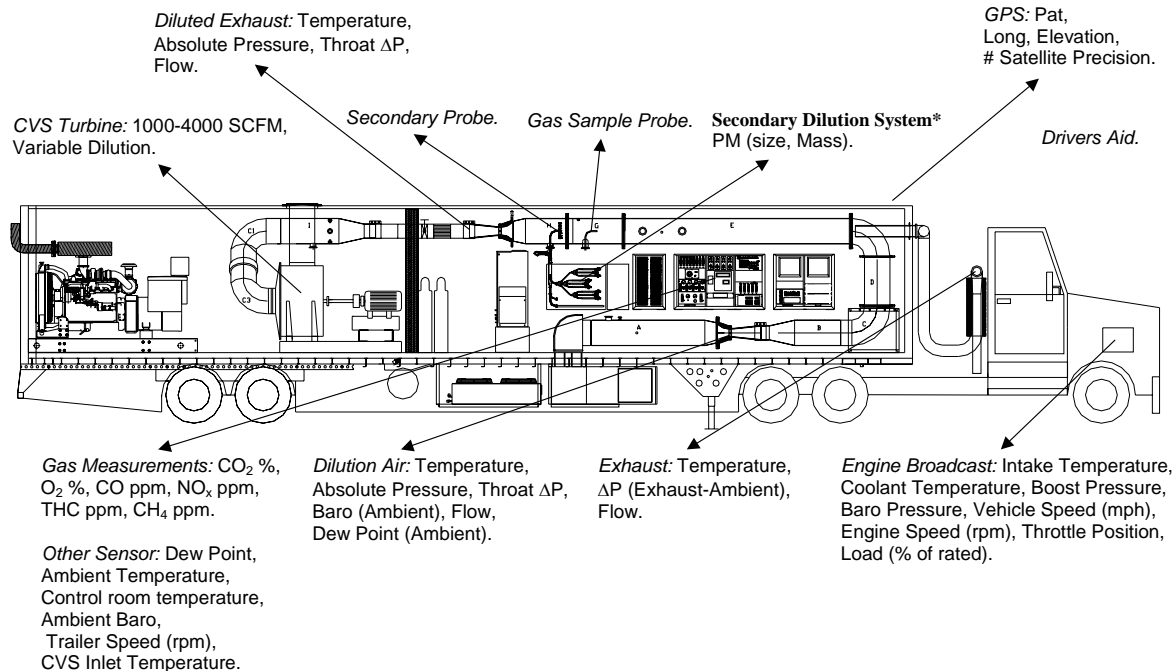
- As part of the validation of the CE-CERT MEL for the on-road testing, a 1065 self-audit was performed on the CE-CERT MEL. The 1065 self audit of the trailer included H₂O and CO₂ interference/quench checks, NO₂ to NO converter efficiency checks, NMHC cutter penetrations fractions. Also the linearity of all analyzers, mass flow controllers, and temperature and pressure sensors was verified. All checks were found to pass and the system to be in 1065 compliance.
- The cross correlation between an engine dynamometer test cell at SwRI and UCR’s MEL represented a unique opportunity to evaluate the comparison between two 1065 compliant laboratories under the same conditions including the test engine and dynamometer, test location, and test cycles. For the NTE emissions cycle, the MEL was approximately 2% higher than the SwRI measurement for NO_x and 2.7% higher than SwRI for CO₂. For the Ramped Modal Cycle, the MEL was approximately 4% higher than the SwRI measurement for NO_x and 2.3% higher than SwRI for CO₂. These results were deemed to be acceptable to allow continuation of the on-road and engine dynamometer portions of the measurement allowance program.

- For the on-road audit runs, the measurements were compared with the audit bottle concentrations over the course of the test route. For NO_x and CO₂, the audit bottle measurements were both within 2% of the audit bottle concentration over the course of the three different test runs. THC and CO audits were within ~ 1 ppm or 5% of the audit bottle concentrations, although these bottles were at the low levels expected for a DPF equipped vehicle. Ambient background levels for NO_x, CO, and CO₂ were relatively low compared to the expected exhaust levels. THC background levels represented x% of the exhaust levels.
- Over the course of the 6 test runs, a total of 426 NTE events were identified by either the MEL, the PEMS or both systems. Of these 426 events, 26 events were identified by only the MEL or PEMS, but not by both systems. For an additional 57 events, the start of the NTE events between the MEL and PEMS differed by more than 2 seconds or the duration of the NTE event differed by more than 1 second. The remaining 343 NTE events represent matching NTE events that were identified by both the MEL and the PEMS, and these events form the basis of the emissions comparisons between the MEL and PEMS.
- Brake specific emissions for NO_x, THC, and CO were calculated using three different methodologies. This included one method based on speed and torque, one method based on brake specific fuel consumption, and one method based on mass fuel flow or a fuel specific method.
- The brake specific NO_x emissions for the PEMS measurements are consistently higher than those for the MEL, with a correlation of $R^2 \sim 0.84/0.85$ between the measurements methods. The deviations were greatest for the method one calculation with an average deviation of $+8\% \pm 4\%$ relative to the NTE NO_x standard (2.0 grams per brake horsepower-hour or 2.68 grams per brake kW-hour), where the error represents one standard deviation. The deviations for methods 2 and 3 were less at $+4\% \pm 5\%$ and $+3\% \pm 5\%$, respectively. The differences in the deviations for the different calculation methods could be related to the incorporation of CO₂ exhaust measurements into calculations 2 and 3, which are also biased high for the PEMS, or to the impacts of differences in analyzer dispersion on the calculations.
- The brake specific CO₂ emissions for the PEMS were consistently biased high relative to the MEL, with a average deviation of $+4\% \pm 2\%$. There was a good correlation between the MEL and PEMS CO₂ measurements ($R^2 = 0.97$).
- NMHC emissions levels were consistently low for the on-road measurements. The average emission rates for NMHC were 0.003 g/bkW-hr or below, which is approximately 1% of the anticipated NTE standard of 0.28 g/bkW-hr. For the MEL, the diluted exhaust concentrations were comparable to those of the ambient background. There is not consistent bias for NMHC emissions between the different analyzers, with the PEMS higher for some tests and lower for others, albeit at very low levels. Average differences for the different test runs were $\pm 0.5\%$ or less of the NTE standard. There was a weak correlation ($R^2 \sim 0.36/0.37$) between the MEL and PEMS measurements due to the low level measurements.

- CO emissions levels were also consistently low for the on-road measurements. For the MEL, the diluted exhaust concentrations were comparable to those of the ambient background. The PEMS measurements were consistently higher than those of the MEL. The CO emissions levels were on the order of 0.1% of the anticipated NTE standard of 26.01 g/bkW-hr for CO for the MEL measurements. The absolute differences represented approximately 1% of the NTE standard, although the PEMS measurements were approximately an order of magnitude higher than those for the MEL. The correlation analysis showed that there was essentially no correlation between the measurement methods ($R^2 = 0.0011$ or less) at these low levels.

Appendix A – Background Information on UCR’s Mobile Emission Lab

Extensive detail is provided in Reference 2; so this section is provided for those that may not have access to that reference. Basically the mobile emissions lab (MEL) consists of a number of operating systems that are typically found in a stationary lab. However the MEL lab is on wheels instead of concrete. A schematic of MEL and its major subsystems is shown in the figure below. Some description follows.



Major Systems within the Mobile Emission Lab

The primary dilution system is configured as a full-flow constant volume sampling (CVS) system with a smooth approach orifice (SAO) venturi and dynamic flow controller. The SAO venturi has the advantage of no moving parts and repeatable accuracy at high throughput with low-pressure drop. As opposed to traditional dilution tunnels with a positive displacement pump or a critical flow orifice, the SAO system with dynamic flow control eliminates the need for a heat exchanger. Tunnel flow rate is adjustable from 1000 to 4000 scfm with accuracy of 0.5% of full scale. It is capable of total exhaust capture for engines up to 600 hp. Colorado Engineering Experiment Station Inc. initially calibrated the flow rate through both SAOs for the primary tunnel.

The mobile laboratory contains a suite of gas-phase analyzers on shock-mounted benches. The gas-phase analytical instruments measure NO_x, methane (CH₄), total hydrocarbons (THC), CO, and CO₂ at a frequency of 10 Hz and were selected based on optimum response time and on road stability. The 200-L Tedlar bags are used to collect tunnel and dilution air samples over a complete test cycle. A total of eight bags are suspended in the MEL allowing four test cycles to

be performed between analyses. Filling of the bags is automated with Lab View 7.0 software (National Instruments, Austin, TX). A summary of the analytical instrumentation used, their ranges, and principles of operation is provided in the table below. Each modal analyzer is time-corrected for tunnel, sample line, and analyzer delay time.

Gas Component	Range	Monitoring Method
NO _x	10/30/100/300/1000 (ppm)	Chemiluminescence
CO	50/200/1000/3000 (ppm)	NDIR
CO ₂	0.5/2/8/16 (%)	NDIR
THC	10/30/100/300/1000 & 5000 (ppmC)	Heated FID
CH ₄	10/30/100/300/1000 & 5000 (ppmC)	HFID

Summary of gas-phase instrumentation in MEL

Quality Assurance and Quality Control Requirements

Internal calibration and verification procedures are performed regularly in accordance with the CFR. A partial summary of routine calibrations performed by the MEL staff as part of the data quality assurance/quality control program is listed in the table below. The MEL uses precision gas blending to obtain required calibration gas concentrations. Calibration gas cylinders, certified to 1 %, are obtained from Scott-Marrin Inc. (Riverside, CA). By using precision blending, the number of calibration gas cylinders in the lab was reduced to 5 and cylinders need to be replaced less frequently. The gas divider contains a series of mass flow controllers that are calibrated regularly with a Bios Flow Calibrator (Butler, New Jersey) and produces the required calibration gas concentrations within the required ± 1.5 percent accuracy.

In addition to weekly propane recovery checks which yield >98% recovery, CO₂ recovery checks are also performed. A calibrated mass of CO₂ is injected into the primary dilution tunnel and is measured downstream by the CO₂ analyzer. These tests also yield >98% recovery. The results of each recovery check are all stored in an internal QA/QC graph that allows for the immediate identification of problems and/or sampling bias.

An example shown below is for propane mass injected into the exhaust transfer line while sampling from raw and dilute ports (three repeats) to evaluate exhaust flow measurement on steady state basis (duration = 60 sec, Date completed January 2005).

Tests	Raw C3H8 g	Dil C3H8 g	CVS DF	Raw C3H8 est	Diff
1	2522	608	4.11	2499	-0.9%
2	2485	598	4.10	2454	-1.2%
3	2462	601	4.13	2484	0.9%
ave	2490	602	4.12	2479	-0.4%
stdev	30	5	0.01	23	
COV	1.2%	0.8%	0.3%	0.9%	

Recent example of propane quality control check

EQUIPMENT	FREQUENCY	VERIFICATION PERFORMED	CALIBRATION PERFORMED
CVS	Daily	Differential Pressure	Electronic Cal
	Daily	Absolute Pressure	Electronic Cal
	Weekly	Propane Injection	
	Monthly	CO ₂ Injection	
	Per Set-up Second by second	CVS Leak Check Back pressure tolerance ±5 inH ₂ O	
Cal system MFCs	Annual	Primary Standard	MFCs: Drycal Bios Meter
	Monthly	Audit bottle check	
Analyzers	Pre/Post Test		Zero Span
	Daily Monthly	Zero span drifts Linearity Check	
Secondary System Integrity and MFCs	Semi-Annual	Propane Injection: 6 point primary vs secondary check	
	Semi-Annual		MFCs: Drycal Bios Meter & TSI Mass Meter
Data Validation	Variable	Integrated Modal Mass vs Bag Mass	
PM Sample Media	Per test	Visual review	
	Weekly	Trip Tunnel Banks	
	Monthly	Static and Dynamic Blanks	
Temperature	Daily	Psychrometer	Performed if verification fails
Barometric Pressure	Daily	Aneroid barometer ATIS	Performed if verification fails
Dewpoint Sensors	Daily	Psychrometer Chilled mirror	Performed if verification fails

Sample of Verification and Calibration Quality Control Activities

Appendix B – Description of PEMS Instrument

SEMTECH-DS is a complete, fully integrated portable emissions measurement system (PEMS) for testing all classes of vehicles and equipment under real-world operating conditions. SEMTECH-DS measures emissions at the tailpipe, engine-out, or at any stage of after-treatment from vehicles powered by diesel, biodiesel, gasoline, CNG, propane, and even hydrogen fuel. A data logger records the vehicle emissions, environmental conditions, and the output of a vehicle’s on-board electronic control system to compact flash removable storage while the vehicle is in operation. The optional exhaust mass flowmeter and GPS are also fully integrated with the SEMTECH-DS data logger and post-processing software. Engine and vehicle-related parameters are combined with gaseous emissions on a real-time basis to determine in-use emissions levels in g/sec, g/g-fuel, g/Bhp-hr, and g/mile. Not to Exceed (NTE) vehicle operation and emissions results are also determined on a real-time basis. Test results can also be viewed subsequently with the user-configurable post-processor application.

Access to the central processor is provided through LabView™ PC host software. The user interface is designed to provide immediate feedback to the user. There are over 150 different fault codes that the SEMTECH will automatically report to the user if a problem occurs. In addition, there are 24 warning codes that will also automatically be reported when potential problems exist. They indicate to the user when to change filters, when to change the FID fuel bottle, when to zero the instrument. In addition, many of the routine tasks that are required to operate the system are fully automated, requiring minimal effort for the user.

The SEMTECH-DS system comprises of eight individual analyzers, all integrated into a single package and controlled from a central processor/data logger. The following table describes the subcomponents and system features.

SEMTECH-D Subsystem	Specifications
Sample Line & Filter	Heated (191 °C)
THC	Heated FID (191 °C), Wet sample measurement, autoranging, max 4 Hz data rate
NO ₂	NDUV resonant absorption spectroscopy
NO	NDUV resonant absorption spectroscopy
CO and CO ₂	CO and CO ₂ through NDIR spectroscopy
O ₂	Electrochemical Cell
Methane	Unheated FID with cutter, external to SEMTECH
Exhaust flow rate and temperature	Sensors Exhaust Flow Meter (averaging Pitot tube)
Vehicle speed and position	Garmin 16-HVS GPS, WAAS supported
Ambient temperature, relative humidity, barometric pressure	Vaisla remote temperature and humidity monitor; on-board barometric pressure sensor, max 4 Hz data rate
Vehicle Interface (VI) Protocols	Heavy-Duty: SAE-J1708, SAE-J1939 Light-Duty: SAE-J1850 VPW, SAE-J1850 PWM, ISO-9141-2, ISO-14230-4, ISO-11898, ISO-15765
Engine torque	VI (if available from equipment’s CAN/ECM)
Engine RPM	VI (if available from equipment’s CAN/ECM), or through use of an optical tachometer probe on mechanically-controlled equipment
Air-fuel ratio	Determined per ISO 16183 carbon balance method
Size	14”H x 17”W x 22”D
Weight	approximately 75 lbs
Communications	Wired and wireless Ethernet, 8.0211g
Host Software	Sensor Tech suite using Labview™

SEMTECH-D Subsystem	Specifications
Analog output	8-channels, 0 – 5V
Analog input	3-channels, $\pm 5V$, $\pm 10V$, $\pm 10V$ with programmable transform functions
Digital input	2-channel
Digital output	1-channel
Data Storage	Up to 1 Gb Compact Flash cards. Adequate to hold one full week of data.
Data rate	Configurable 1 – 4 Hz for most channels

Appendix C – Test File Names and Descriptions

Test File Name	Description
200610030817.XML	<i>In-cab Route 1 Riverside to San Diego:</i> Session manager not setup properly. Figured out for Route 2 and on. All in-cab Route 1 have individual tests sessions. In-cab Route 2 and later tests have one session for the day.
200610030910.XML	<i>In-cab Route 1 Riverside to San Diego:</i> Session manager not setup properly.
200610031016.XML	<i>In-cab Route 1 Riverside to San Diego:</i> Session manager not setup properly.
200610031117.XML	<i>In-cab Route 1 Riverside to San Diego:</i> Software hang-up prevented pre FID bottle change zero, span and audit test. Post bottle swap zero span audit test was successful.
200610031247.XML	<i>In-cab Route 1 Riverside to San Diego:</i> Software hang-up prevented pre FID bottle change zero, span and audit test. Post bottle swap zero span audit test was successful.
ROUTE2A.XML	<i>In-cab Route 2 Riverside to Mammoth. Part A.</i> FID bottle change one hour before end of test. Successful pre and post FID bottle change zero, span, and audit test.
ROUTE2B.XML	<i>In-cab Route 2 Riverside to Mammoth. Part B.</i> FID bottle change one hour before end of test. Successful pre and post FID bottle change zero, span, and audit test.
ROUTE3A.XML	<i>In-cab Route 3 Mammoth to Riverside. Part A.</i> FID bottle change one hour before end of test. Successful pre and post FID bottle change zero, span, and audit test. 2 hour to warm up because power from engine.
ROUTE3B.XML	<i>In-cab Route 3 Mammoth to Riverside. Part B.</i> FID bottle change one hour before end of test. Successful pre and post FID bottle change zero, span, and audit test.
ROUTE1OUT.XML	<i>Out-of-cab Route 1 Riverside to San Diego:</i> Took more than two hours to warm up because power supplied by batteries (12.6 volts). Moved to generator power with committee approval. No FID bottle change.
ROUTE2OUT.XML	<i>Out of cab Route 2 Riverside to Mammoth.</i> Power supplied by generator power. No FID bottle change.
ROUTE3OUT.XML	<i>Out of cab Route 3 Mammoth to Riverside.</i> Power supplied by generator power. No FID bottle change.

Appendix D – Brake Specific Emissions Calculations

Notes:

1. The PEMS sample data file contains the information necessary to perform the three brake-specific emission calculations as stated in the work assignment. After a discussion with Matt Spears (EPA) we have modified the emission equations as shown below.
2. The ECM fuel rate is broadcast in L/hr, so we will need to convert that measurement into g/s with density data for the fuel. The fuel density is 851.0 g/L.
3. The PEMS sample data did not include NMHC or ECM fuel rate. These values were estimated and added to the file. It is still unclear what the units of some of the channels will be as we do not have a recent PEMS sample file.
4. CO₂ error surfaces were added for all steady state, transient and environmental tests.
5. In calculation methods #2 and #3, assume HC=NMHC (i.e., 0.98*THC = NMHC).

METHOD #1 EQUATIONS

Data from reference NTE event:

1. Exhaust flow rate (scfm)
2. Emission Concentration: NO(ppm), NO₂(ppm), CO(%), NMHC(ppm)
NOTE: Compute NMHC = 0.98 * THC from reference NTE.
3. Fuel rate (L/h)
4. Speed (rpm)
5. Torque values (N·m)

Convert *exhaust flow rate* from SCFM to mol/s:

$$\dot{n}_i \left(\frac{\text{mol}}{\text{s}} \right) = \frac{\dot{n}_i (\text{SCFM}) * \frac{1}{35.31467} \left(\frac{\text{m}^3}{\text{ft}^3} \right) * \frac{1}{60} \left(\frac{\text{min}}{\text{s}} \right) * 101325 (\text{Pa})}{293.15 (\text{K}) * 8.314472 \left(\frac{\text{J}}{\text{mol} * \text{K}} \right)}$$

Brake Specific NOx Calculation for Method #1

$$\Delta t = 1 \text{ (sec)}$$

$$M_{NO_2} = 46.0055 \left(\frac{g}{mol} \right)$$

$$e_{NO_x} (g/kW \cdot hr) = \frac{M_{NO_2} * \sum_{i=1}^N \left[(xNO_{2i} (ppm) + xNO_i (ppm)) * 10^{-6} * \dot{n}_i \left(\frac{mol}{s} \right) * \Delta t \right]}{\sum_{i=1}^N \left[\frac{Speed_i (rpm) * T_i (N \cdot m) * 2 * 3.14159 * \Delta t}{60 * 1000 * 3600} \right]}$$

In the MC simulation, the following deltas (error surface number) will be added to the above parameters:

xNO ₂ + xNO	<=	SS (1) + TR (2) + EMI (3) + Pressure (4) + Temp (5) + Shock/Vib (6)
Exhaust Flow	<=	SS (20) + TR (21) + Pulse (22) + Swirl (23) + Wind (24) + EMI (25) + Shock/Vib (26) + Temp (27) + Pressure (28)
Torque	<=	DOE (30) + Warm-up (31) + Humidity (32) + Fuel (33) + Manuf (35)
Speed	<=	Dynamic Speed (43)

Brake Specific CO Calculation for Method #1

$$\Delta t = 1 \text{ (sec)}$$

$$M_{CO} = 28.0101 \left(\frac{g}{mol} \right)$$

$$e_{CO} (g/kW \cdot hr) = \frac{M_{CO} * \sum_{i=1}^N \left[(xCO_i (\%)) * 10^{-2} * \dot{n}_i \left(\frac{mol}{s} \right) * \Delta t \right]}{\sum_{i=1}^N \left[\frac{Speed_i (rpm) * T_i (N \cdot m) * 2 * 3.14159 * \Delta t}{60 * 1000 * 3600} \right]}$$

In the MC simulation, the following deltas (error surface number) will be added to the above parameters:

xCO	<=	SS (7) + TR (8) + EMI (9) + Pressure (10) + Temp (11) + Shock/Vib (12)
Exhaust Flow	<=	SS (20) + TR (21) + Pulse (22) + Swirl (23) + Wind (24) + EMI (25) + Shock/Vib (26) + Temp (27) + Pressure (28)
Torque	<=	DOE (30) + Warm-up (31) + Humidity (32) + Fuel (33) + Manuf (35)
Speed	<=	Dynamic Speed (43)

Brake Specific NMHC Calculation for Method #1

$$\Delta t = 1 \text{ (sec)}$$

$$M_{NMHC} = 13.875389 \left(\frac{g}{mol} \right)$$

$$e_{NMHC} (g / kW \cdot hr) = \frac{M_{NMHC} * \sum_{i=1}^N \left[(x_{NMHC_i} (ppm)) * 10^{-6} * \dot{n}_i \left(\frac{mol}{s} \right) * \Delta t \right]}{\sum_{i=1}^N \left[\frac{Speed_i (rpm) * T_i (N \cdot m) * 2 * 3.14159 * \Delta t}{60 * 1000 * 3600} \right]}$$

In the MC simulation, the following deltas (error surface number) will be added to the above parameters:

xNMHC	<=	SS (13) + TR (14) + EMI (15) + Pressure (16) + Temp (17) + Shock/Vib (18) + Ambient (19)
Exhaust Flow	<=	SS (20) + TR (21) + Pulse (22) + Swirl (23) + Wind (24) + EMI (25) + Shock/Vib (26) + Temp (27) + Pressure (28)
Torque	<=	DOE (30) + Warm-up (31) + Humidity (32) + Fuel (33) + Manuf (35)
Speed	<=	Dynamic Speed (43)

Method #2 Equations

Data from reference NTE event:

1. Exhaust flow rate (scfm)
2. Emission Concentration: NO(ppm), NO₂(ppm), CO(%), CO₂(%), NMHC(ppm)
NOTE: NMHC = 0.98 * THC from the reference NTE
3. Fuel rate (L/h)
4. Speed (rpm)
5. BSFC values (g/kW·hr)

Convert *exhaust flow rate* from SCFM to mol/s:

$$\dot{n}_i \left(\frac{mol}{s} \right) = \frac{\dot{n}_i (SCFM) * \frac{1}{35.31467} \left(\frac{m^3}{ft^3} \right) * \frac{1}{60} \left(\frac{min}{s} \right) * 101325 (Pa)}{293.15 (K) * 8.314472 \left(\frac{J}{mol * K} \right)}$$

Brake Specific NOx Concentration for Method #2

$$w_{fuel} = 0.869 \quad \text{Mass fraction of carbon in the fuel.}$$

$$\Delta t = 1 \text{ (sec)}$$

$$M_C = 12.0107 \left(\frac{g}{mol} \right)$$

$$M_{NO_2} = 46.0055 \left(\frac{g}{mol} \right)$$

$$e_{NO_x} (g / kW \cdot hr) = \frac{M_{NO_2} * \sum_{i=1}^N \left[(xNO_{2_i} (ppm) + xNO_i (ppm)) * 10^{-6} * \dot{n}_i \left(\frac{mol}{s} \right) * \Delta t \right]}{\frac{M_C}{w_{fuel}} * \sum_{i=1}^N \left[\frac{\dot{n}_i \left(\frac{mol}{s} \right) * \left[xNMHC_i (ppm) * 10^{-6} + (xCO_i (\%) + xCO_{2_i} (\%)) * 10^{-2} \right] * \Delta t}{BSFC_i \left(\frac{g}{kW \cdot hr} \right)} \right]}$$

In the MC simulation, the following deltas (error surface number) will be added to the above parameters:

xNO ₂ + xNO	<=	SS (1) + TR (2) + EMI (3) + Pressure (4) + Temp (5) + Shock/Vib (6)
xCO	<=	SS (7) + TR (8) + EMI (9) + Pressure (10) + Temp (11) + Shock/Vib (12)
xNMHC	<=	SS (13) + TR (14) + EMI (15) + Pressure (16) + Temp (17) + Shock/Vib (18) + Ambient (19)
Exhaust Flow	<=	SS (20) + TR (21) + Pulse (22) + Swirl (23) + Wind (24) + EMI (25) + Shock/Vib (26) + Temp (27) + Pressure (28)
BSFC	<=	DOE (37) + Warm-up (38) + Humidity (39) + Fuel (40) + Manuf (42)
xCO ₂	<=	SS (45) + TR (46) + EMI (47) + Pressure (48) + Temp (49) + Shock/Vib (50)

Brake Specific CO Concentration for Method #2

$w_{fuel} = 0.869$ Mass fraction of carbon in the fuel.

$\Delta t = 1$ (sec)

$$M_C = 12.0107 \left(\frac{g}{mol} \right)$$

$$M_{CO} = 28.0101 \left(\frac{g}{mol} \right)$$

$$e_{co}(g / kW \cdot hr) = \frac{M_{co} * \sum_{i=1}^N \left[(xCO_i (\%)) * 10^{-2} * \dot{n}_i \left(\frac{mol}{s} \right) * \Delta t \right]}{\frac{M_C}{w_{fuel}} * \sum_{i=1}^N \left[\frac{\dot{n}_i \left(\frac{mol}{s} \right) * [xNMHC_i (ppm) * 10^{-6} + (xCO_i (\%) + xCO_2 (\%)) * 10^{-2}] * \Delta t}{BSFC_i \left(\frac{g}{kW \cdot hr} \right)} \right]}$$

In the MC simulation, the following deltas (error surface number) will be added to the above parameters:

xCO	<=	SS (7) + TR (8) + EMI (9) + Pressure (10) + Temp (11) + Shock/Vib (12)
xNMHC	<=	SS (13) + TR (14) + EMI (15) + Pressure (16) + Temp (17) + Shock/Vib (18) + Ambient (19)
Exhaust Flow	<=	SS (20) + TR (21) + Pulse (22) + Swirl (23) + Wind (24) + EMI (25) + Shock/Vib (26) + Temp (27) + Pressure (28)
BSFC	<=	DOE (37) + Warm-up (38) + Humidity (39) + Fuel (40) + Manuf (42)

$$xCO_2 \leq SS (45) + TR (46) + EMI (47) + Pressure (48) + Temp (49) + Shock/Vib (50)$$

Brake Specific NMHC Concentration for Method #2

$$w_{fuel} = 0.869 \quad \text{Mass fraction of carbon in the fuel.}$$

$$\Delta t = 1 \text{ (sec)}$$

$$M_C = 12.0107 \left(\frac{g}{mol} \right)$$

$$M_{NMHC} = 13.875389 \left(\frac{g}{mol} \right)$$

$$e_{NMHC} (g / kW \cdot hr) = \frac{M_{NMHC} * \sum_{i=1}^N \left[(x_{NMHC_i} (ppm)) * 10^{-6} * \dot{n}_i \left(\frac{mol}{s} \right) * \Delta t \right]}{\frac{M_C}{w_{fuel}} * \sum_{i=1}^N \left[\frac{\dot{n}_i \left(\frac{mol}{s} \right) * \left[x_{NMHC_i} (ppm) * 10^{-6} + (x_{CO_i} (\%) + x_{CO_2_i} (\%)) * 10^{-2} \right] * \Delta t}{BSFC_i \left(\frac{g}{kW \cdot hr} \right)} \right]}$$

In the MC simulation, the following deltas (error surface number) will be added to the above parameters:

$$\begin{aligned}
 xCO &\leq SS (7) + TR (8) + EMI (9) + Pressure (10) + Temp (11) + Shock/Vib (12) \\
 xNMHC &\leq SS (13) + TR (14) + EMI (15) + Pressure (16) + Temp (17) + Shock/Vib (18) + Ambient (19) \\
 Exhaust Flow &\leq SS (20) + TR (21) + Pulse (22) + Swirl (23) + Wind (24) + EMI (25) + Shock/Vib (26) + Temp (27) + Pressure (28) \\
 BSFC &\leq DOE (37) + Warm-up (38) + Humidity (39) + Fuel (40) + Manuf (42) \\
 xCO_2 &\leq SS (45) + TR (46) + EMI (47) + Pressure (48) + Temp (49) + Shock/Vib (50)
 \end{aligned}$$

Method #3 Equations

Data from reference NTE event:

1. Exhaust flow rate (scfm)
2. Emission Concentration: NO(ppm), NO₂(ppm), CO(%), CO₂(%), NMHC(ppm)
NOTE: NMHC = 0.98 * THC from the reference NTE
3. Fuel rate (L/h)
4. Speed (rpm)
5. Torque values (N·m)

Brake Specific NOx Concentration for Method #3

$$w_{fuel} = 0.869 \quad \text{Mass fraction of carbon in the fuel.}$$

$$M_C = 12.0107 \left(\frac{g}{mol} \right)$$

$$M_{NO_2} = 46.0055 \left(\frac{g}{mol} \right)$$

$$\Delta t = 1 \text{ (sec)}$$

Example mass fuel mass rate calculation :

$$\dot{m}_{fuel_i} \left(\frac{g}{s} \right) = Fuelrate_i \left(\frac{L}{hr} \right) * 851.0 \left(\frac{g}{L} \right) * \frac{1}{3600} \left(\frac{hr}{s} \right)$$

$$e_{NO_x} \left(g / kW \cdot hr \right) = \frac{\frac{M_{NO_2} * w_{fuel}}{M_C} * \sum_{i=1}^N \left[\frac{(xNO_{2_i} (ppm) + xNO_i (ppm)) * 10^{-6} * \dot{m}_{fuel_i} \left(\frac{g}{s} \right)}{xNMHC_i (ppm) * 10^{-6} + (xCO_i (\%) + xCO_{2_i} (\%)) * 10^{-2}} * \Delta t \right]}{\sum_{i=1}^N \left[\frac{Speed_i (rpm) * T_i (N \cdot m) * 2 * 3.14159 * \Delta t}{60 * 1000 * 3600} \right]}}$$

In the MC simulation, the following deltas (error surface number) will be added to the above parameters:

xNO ₂ + xNO	<=	SS (1) + TR (2) + EMI (3) + Pressure (4) + Temp (5) + Shock/Vib (6)
xCO	<=	SS (7) + TR (8) + EMI (9) + Pressure (10) + Temp (11) + Shock/Vib (12)
xNMHC	<=	SS (13) + TR (14) + EMI (15) + Pressure (16) + Temp (17) + Shock/Vib (18) + Ambient (19)

Torque	<=	DOE (30) + Warm-up (31) + Humidity (32) + Fuel (33) + Manuf (35)
Speed	<=	Dynamic Speed (43)
Fuel Rate	<=	Dynamic Fuel Rate (44)
xCO2	<=	SS (45) + TR (46) + EMI (47) + Pressure (48) + Temp (49) + Shock/Vib (50)

Brake Specific CO Concentration for Method #3

$w_{fuel} = 0.869$ Mass fraction of carbon in the fuel.

$$M_C = 12.0107 \left(\frac{g}{mol} \right)$$

$$M_{CO} = 28.0101 \left(\frac{g}{mol} \right)$$

$$\Delta t = 1 \text{ (sec)}$$

Example mass fuel mass rate calculation :

$$\dot{m}_{fuel_i} \left(\frac{g}{s} \right) = Fuelrate_i \left(\frac{L}{hr} \right) * 851.0 \left(\frac{g}{L} \right) * \frac{1}{3600} \left(\frac{hr}{s} \right)$$

$$e_{co}(g/kW \cdot hr) = \frac{\frac{M_{CO} * w_{fuel}}{M_C} * \sum_{i=1}^N \left[\frac{(xCO_i(\%)) * 10^{-2} * \dot{m}_{fuel_i} \left(\frac{g}{s} \right)}{xNMHC_i(ppm) * 10^{-6} + (xCO_i(\%) + xCO_{2_i}(\%)) * 10^{-2}} * \Delta t \right]}{\sum_{i=1}^N \left[\frac{Speed_i(rpm) * T_i(N \cdot m) * 2 * 3.14159 * \Delta t}{60 * 1000 * 3600} \right]}$$

In the MC simulation, the following deltas (error surface number) will be added to the above parameters:

xCO	<=	SS (7) + TR (8) + EMI (9) + Pressure (10) + Temp (11) + Shock/Vib (12)
xNMHC	<=	SS (13) + TR (14) + EMI (15) + Pressure (16) + Temp (17) + Shock/Vib (18) + Ambient (19)
Torque	<=	DOE (30) + Warm-up (31) + Humidity (32) + Fuel (33) + Manuf (35)
Speed	<=	Dynamic Speed (43)
Fuel Rate	<=	Dynamic Fuel Rate (44)
xCO2	<=	SS (45) + TR (46) + EMI (47) + Pressure (48) + Temp (49) + Shock/Vib (50)

Brake Specific NMHC Concentration for Method #3

$w_{fuel} = 0.869$ Mass fraction of carbon in the fuel.

$$M_C = 12.0107 \left(\frac{g}{mol} \right)$$

$$M_{NMHC} = 13.875389 \left(\frac{g}{mol} \right)$$

$$\Delta t = 1 \text{ (sec)}$$

Example mass fuel mass rate calculation :

$$\dot{m}_{fuel_i} \left(\frac{g}{s} \right) = Fuelrate_i \left(\frac{L}{hr} \right) * 851.0 \left(\frac{g}{L} \right) * \frac{1}{3600} \left(\frac{hr}{s} \right)$$

$$e_{NMHC} (g / kW \cdot hr) = \frac{\frac{M_{NMHC} * w_{fuel}}{M_C} * \sum_{i=1}^N \left[\frac{(x_{NMHC_i} (ppm)) * 10^{-6} * \dot{m}_{fuel_i} \left(\frac{g}{s} \right)}{x_{NMHC_i} (ppm) * 10^{-6} + (x_{CO_i} (\%) + x_{CO_2_i} (\%)) * 10^{-2}} * \Delta t \right]}{\sum_{i=1}^N \left[\frac{Speed_i (rpm) * T_i (N \cdot m) * 2 * 3.14159 * \Delta t}{60 * 1000 * 3600} \right]}$$

In the MC simulation, the following deltas (error surface number) will be added to the above parameters:

xCO	<=	SS (7) + TR (8) + EMI (9) + Pressure (10) + Temp (11) + Shock/Vib (12)
xNMHC	<=	SS (13) + TR (14) + EMI (15) + Pressure (16) + Temp (17) + Shock/Vib (18) + Ambient (19)
Torque	<=	DOE (30) + Warm-up (31) + Humidity (32) + Fuel (33) + Manuf (35)
Speed	<=	Dynamic Speed (43)
Fuel Rate	<=	Dynamic Fuel Rate (44)
xCO2	<=	SS (45) + TR (46) + EMI (47) + Pressure (48) + Temp (49) + Shock/Vib (50)

Appendix E – NO_x Emissions by NTE Event and Calculation Method

Shaded areas are where drift correction failed

Unique ID for NTE event	MEL	PEMS	MEL	PEMS	MEL	PEMS	MEL start	PEMS start	MEL dur	PEMS dur	MEL bhp	PEMS bhp
	Meth 1 NOx g/kWhr	Meth 1 NOx g/kWhr	Meth 2 NOx g/kWhr	Meth 2 NOx g/kWhr	Meth 3 NOx g/kWhr	Meth 3 NOx g/kWhr						
10041004_1	3.40	3.91	3.62	3.92	3.65	3.98	379	376	38	39	3.176	3.166
10041004_2	3.35	3.79	3.59	3.97	3.59	3.97	419	416	38	38	2.946	2.929
10041004_3	3.40	3.79	3.67	3.89	3.69	3.90	530	528	34	33	2.884	2.833
10041004_4	3.28	3.79	3.52	3.94	3.52	3.94	648	646	77	76	5.445	5.363
10041004_5	3.37	3.83	3.59	3.96	3.60	3.96	798	796	34	33	2.376	2.326
10041004_6	3.32	3.75	3.60	3.94	3.63	3.94	867	864	32	32	2.487	2.478
10041004_7	3.55	3.96	3.82	4.12	3.87	4.12	918	915	44	44	3.527	3.516
10041004_8	3.56	4.04	3.84	4.18	3.86	4.20	964	961	38	39	3.078	3.073
10041004_9	3.45	3.91	3.73	4.06	3.77	4.06	1006	1003	50	51	4.018	4.014
10041004_10	3.82	4.30	4.13	4.48	4.13	4.48	1094	1092	136	135	13.11	13.02
10041004_11	3.76	4.24	4.08	4.43	4.09	4.43	1243	1240	135	136	12.79	12.77
10041004_12	3.58	4.11	3.87	4.18	3.89	4.18	1379	1377	106	378	9.515	34.12
10041004_13	3.66	#N/A	3.85	#N/A	1.49	#N/A	1486	#N/A	271	#N/A	24.64	#N/A
10041004_14	3.57	4.07	3.85	4.21	3.86	4.21	1957	1955	82	142	6.8	11.42
10041004_15	3.59	#N/A	3.80	#N/A	3.81	#N/A	2040	#N/A	59	#N/A	4.619	#N/A
10041004_16	3.81	4.38	3.95	4.41	4.03	4.43	2100	2098	55	55	4.893	4.856
10041004_17	3.71	4.50	3.97	4.64	3.98	4.64	2157	2154	82	277	7.385	24.32
10041004_18	4.00	#N/A	4.30	#N/A	4.31	#N/A	2240	#N/A	194	#N/A	17.01	#N/A
10041105_1	3.64	3.91	4.06	4.09	4.13	4.08	615	613	37	37	2.952	2.939
10041105_2	3.46	3.70	3.69	3.83	3.68	3.82	772	769	35	36	1.927	1.948
10041105_3	3.60	3.74	3.95	3.91	4.08	3.91	1151	1149	36	35	1.969	1.935
10041105_4	3.48	3.73	3.83	3.85	3.88	3.86	1300	1298	45	45	3.567	3.542
10041105_5	3.59	3.92	4.05	4.13	4.15	4.12	1415	1413	42	42	3.249	3.202
10041105_6	3.47	3.88	3.87	3.95	3.92	3.96	1470	1467	35	65	2.791	5.451
10041237_1	3.34	3.43	3.59	3.53	3.60	3.52	208	205	73	73	5.302	5.248
10041237_2	3.69	3.80	4.07	3.92	4.15	3.93	294	291	47	47	4.057	4.023
10041237_3	3.70	3.81	4.00	3.98	4.10	3.99	353	351	40	39	3.263	3.212
10041237_4	3.62	3.70	3.97	3.83	3.99	3.83	412	409	63	63	6.103	6.07
10041237_5	3.62	3.69	3.94	3.84	3.95	3.84	498	495	91	91	7.646	7.597
10041237_6	3.81	3.94	4.08	4.06	4.14	4.06	700	698	34	34	2.567	2.551
10041237_7	3.59	3.69	3.99	3.81	4.03	3.80	926	924	34	34	2.772	2.765
10041237_8	3.67	3.69	4.05	3.85	4.11	3.85	963	961	40	103	2.451	6.546
10041237_9	3.61	#N/A	3.95	#N/A	3.96	#N/A	1004	#N/A	63	#N/A	4.125	#N/A
10041237_10	3.63	3.73	4.08	3.88	4.13	3.89	1070	1068	35	34	3.31	3.246
10041237_11	3.72	3.81	4.12	3.99	4.13	3.99	1129	1126	104	105	9.539	9.547
10041237_12	3.63	3.70	4.00	3.86	4.02	3.86	1302	1299	93	93	8.152	8.083
10041237_13	3.76	3.81	4.24	4.00	4.26	3.99	1400	1398	36	36	2.835	2.814
10041237_14	3.83	3.90	4.20	4.06	4.23	4.06	1437	1435	68	67	6.314	6.254
10041237_15	#N/A	4.24	#N/A	4.44	#N/A	4.43	#N/A	1517	#N/A	35	#N/A	3.096
10041237_16	3.72	#N/A	4.02	#N/A	4.07	#N/A	2603	#N/A	30	#N/A	2.455	#N/A
10041237_17	3.65	3.93	3.93	3.97	3.94	3.97	2639	2636	52	52	4.121	4.103
10041237_18	3.68	3.93	3.91	3.97	3.91	3.97	2692	2690	102	101	8.414	8.35
10041237_19	3.73	4.05	4.05	4.11	4.09	4.11	2795	2792	32	60	2.471	4.753
10041237_20	3.56	3.81	3.96	3.99	3.98	3.99	2869	2867	63	62	5.326	5.253

10041338_1	3.38	3.69	3.70	3.87	3.71	3.87	210	207	35	36	2.329	2.354
10041338_2	3.58	3.86	3.85	4.04	3.85	4.04	270	267	80	80	5.495	5.467
10041338_3	3.64	3.98	4.08	4.19	4.15	4.19	355	352	36	36	2.697	2.656
10041338_4	3.62	3.84	3.97	3.99	4.02	3.98	422	419	33	33	3.118	3.088
10041338_5	3.90	4.14	4.30	4.28	4.35	4.29	671	668	37	37	3.323	3.294
10041338_6	3.58	3.84	3.93	4.06	4.02	4.07	826	823	48	48	3.674	3.647
10041338_7	3.77	4.00	4.11	4.21	4.16	4.21	919	916	37	38	2.532	2.568
10041338_8	3.75	4.03	4.06	4.22	4.06	4.22	1003	1000	148	148	12.23	12.2
10041338_9	3.86	4.19	4.21	4.43	4.24	4.43	1181	1178	101	102	7.526	7.494
10041338_10	3.97	4.31	4.40	4.52	4.43	4.53	1285	1282	34	34	2.686	2.668
10041338_11	3.80	4.10	4.16	4.30	4.17	4.30	1321	1319	151	151	14.04	13.99
10041338_12	3.80	4.08	4.15	4.25	4.15	4.25	1480	1477	63	63	5.709	5.684
10041338_13	3.42	3.71	3.71	3.83	3.75	3.84	1680	1677	36	36	2.527	2.511
10041338_14	3.69	4.04	3.99	4.20	4.00	4.20	1814	1812	113	112	7.293	7.19
10041338_15	3.65	3.96	4.02	4.18	4.03	4.18	1957	1954	91	92	8.107	8.11
10041338_16	3.78	4.09	4.04	4.19	4.06	4.20	2050	2047	65	66	5.631	5.635
10041338_17	3.69	3.96	4.06	4.15	4.06	4.16	2117	2114	134	135	11.77	11.78
10041338_18	4.34	4.59	4.88	4.83	4.94	4.83	2825	2822	35	35	2.908	2.866
10041338_19	3.55	3.90	3.77	4.11	3.78	4.10	2904	2902	36	34	1.725	1.635
10041438_1	3.52	3.87	3.59	3.88	3.59	3.87	13	11	34	34	2.108	2.091
10041438_2	3.74	4.12	4.10	4.30	4.18	4.34	54	51	38	39	2.9	2.899
10041438_3	3.91	4.20	4.23	4.41	4.23	4.42	217	214	57	58	5.157	5.176
10041438_4	#N/A	3.98	#N/A	4.19	#N/A	4.17	#N/A	288	#N/A	30	#N/A	1.875
10041438_5	4.03	4.31	4.42	4.57	4.42	4.56	1074	1071	34	35	3.04	3.052
10041438_6	3.59	3.88	3.99	4.13	4.00	4.13	1132	1130	34	34	2.224	2.207
10041438_7	3.75	4.01	4.09	4.24	4.12	4.24	1290	1288	43	43	2.821	2.793
10041438_8	4.00	4.34	4.37	4.60	4.38	4.60	1340	1338	36	35	1.924	1.871
10041438_9	3.89	4.16	4.09	4.43	n/a	4.43	1496	1493	58	59	3.719	3.737
10041438_10	4.12	4.44	4.59	4.73	4.63	4.74	1557	1555	41	35	2.889	2.555
10041438_11	3.81	4.11	4.17	4.34	4.19	4.34	1924	1922	44	43	3.945	3.894
10041438_12	4.19	4.50	4.17	4.41	4.17	4.41	2210	2207	50	50	2.159	2.131
10041438_13	4.26	4.61	4.31	4.65	4.31	4.65	2415	2413	60	59	2.459	2.397
10041438_14	3.88	4.15	4.23	4.31	4.25	4.32	2786	2784	45	45	4.08	4.063
10041628_1	3.68	4.04	3.87	4.17	3.87	4.17	9	7	38	37	1.717	1.675
10041628_2	3.52	3.79	3.83	3.95	3.84	3.95	94	91	34	34	2.048	2.022
10041628_3	3.86	4.20	4.08	4.28	4.08	4.28	162	139	42	63	2.366	3.656
10041628_4	4.31	4.61	4.69	4.82	4.70	4.83	279	277	47	46	3.72	3.667
10041628_5	3.79	4.11	4.18	4.29	4.18	4.29	370	367	32	32	2.451	2.424
10041628_6	3.73	3.95	4.05	4.13	4.06	4.13	1136	1134	165	164	15.01	14.94
10041628_7	3.47	3.76	3.74	3.92	3.74	3.91	1403	1400	37	38	2.372	2.38
10041628_8	4.51	4.66	5.04	4.98	5.05	4.98	1708	1706	34	33	2.736	2.701
10041628_9	3.69	3.80	3.89	3.88	3.93	3.89	1757	1747	33	40	2.625	3.102
10041628_10	4.29	4.54	4.63	4.67	4.66	4.70	1791	1788	420	420	37.86	37.81
10050703_1	3.52	3.71	3.72	3.82	3.80	3.82	132	130	35	34	2.685	2.648
10050703_2	3.58	3.69	3.88	3.89	3.91	3.90	169	166	34	35	3.11	3.125
10050703_3	3.94	4.14	4.16	4.28	4.19	4.29	358	356	36	36	3.293	3.295
10050703_4	3.49	3.68	3.72	3.80	3.77	3.81	396	393	43	43	3.622	3.603
10050703_5	3.07		3.24		3.25		557		148		8.686	
10050703_6	3.12		3.33		3.34		708		63		4.169	
10050703_7	4.10	4.14	4.35	4.36	4.35	4.36	852	849	43	43	3.873	3.846

10050703_8	3.93	4.29	4.19	4.41	4.22	4.42	896	893	434	435	40.38	40.34
10050703_9	2.97	3.28	3.13	3.44	3.14	3.44	2006	2004	34	34	1.816	1.795
10050703_10	3.55	3.76	3.81	3.93	3.84	3.92	2329	2327	31	30	2.592	2.554
10050807_1	3.69	3.91	3.89	3.96	3.91	3.96	212	210	33	33	2.341	2.333
10050807_2	3.04	3.24	3.12	3.32	3.12	3.31	445	443	35	34	1.442	1.393
10050807_3	3.28	3.49	3.38	3.57	3.38	3.57	521	518	60	60	2.887	2.867
10050807_4	3.20	3.44	3.39	3.58	3.40	3.57	586	583	57	57	3.059	3.027
10050807_5	3.26	3.50	3.42	3.61	3.42	3.60	800	797	45	45	2.54	2.516
10050807_6	3.32	3.55	3.41	3.64	3.41	3.63	866	864	69	68	3.309	3.25
10050807_7	3.27	3.52	3.36	3.61	3.36	3.60	940	938	103	102	4.679	4.603
10050807_8	3.33	3.60	3.47	3.72	3.47	3.72	1046	1043	169	169	8.688	8.613
10050807_9	3.16	3.41	3.22	3.48	3.22	3.48	1256	1254	48	47	1.996	1.945
10050807_10	3.49	3.73	3.67	3.86	3.67	3.85	1308	1306	163	161	10.17	10.03
10050807_11	3.78	4.01	4.07	4.16	4.07	4.16	1472	1469	75	75	6.993	6.978
10050807_12	3.93	4.07	4.19	4.22	4.27	4.23	1791	1788	35	35	2.643	2.609
10050807_13	3.77	3.92	4.10	4.07	4.12	4.07	1830	1827	36	36	3.345	3.336
10050807_14	4.50	4.54	4.86	4.89	4.89	4.91	1958	1955	30	30	2.697	2.674
10050807_15	3.23	3.44	3.40	3.57	3.40	3.56	2071	2068	101	101	5.455	5.422
10050807_16	3.23	3.43	3.45	3.54	3.45	3.54	2248	2246	81	80	5.193	5.126
10050807_17	3.86	4.06	4.13	4.20	4.15	4.21	2408	2405	63	63	4.508	4.478
10050807_18	3.79	5.07	4.06	5.49	4.09	5.48	2549	2514	47	30	3.305	2.734
10050807_19	#N/A	3.96	#N/A	4.12	#N/A	4.12	#N/A	2546	#N/A	47	#N/A	3.305
10050907_1	3.73	3.91	4.03	3.97	4.04	3.98	1	1	34	93	3.258	8.534
10050907_2	3.73	#N/A	4.02	#N/A	4.06	#N/A	36	#N/A	61	#N/A	5.57	#N/A
10050907_3	3.59	3.73	3.87	3.82	3.88	3.82	189	186	73	73	6.5	6.493
10050907_4	4.07	4.28	4.52	4.46	4.57	4.49	313	310	54	55	4.311	4.309
10050907_5	4.62	4.69	5.05	4.82	5.06	4.82	421	419	40	39	3.732	3.678
10050907_6	3.49	3.63	3.80	3.72	3.80	3.71	613	611	36	36	3.158	3.13
10050907_7	3.64	3.70	3.92	3.79	3.93	3.79	756	753	89	89	8.053	8.044
10050907_8	3.63	3.78	3.92	3.93	3.95	3.93	869	866	62	62	4.615	4.592
10050907_9	3.65	3.80	3.98	3.92	3.99	3.92	938	935	111	112	10.55	10.54
10050907_10	3.70	3.91	4.06	4.07	4.10	4.07	1064	1061	79	79	6.663	6.625
10050907_11	4.06	4.28	4.53	4.49	4.58	4.50	1235	1232	47	48	4.134	4.148
10050907_12	3.74	3.90	4.03	4.01	4.09	4.03	1700	1697	31	32	2.293	2.311
10050907_13	4.22	4.37	4.66	4.51	4.67	4.52	2335	2332	34	35	3.255	3.253
10050907_14	3.66	3.70	3.88	3.74	3.92	3.78	2657	2654	38	38	2.979	2.961
10050907_15	3.49	3.63	3.66	3.64	3.69	3.64	2809	2806	55	56	4.602	4.602
10051009_1	3.54	3.73	3.80	3.88	3.83	3.89	16	13	73	74	5.909	5.889
10051009_2	3.54	3.71	3.86	3.87	3.88	3.87	96	93	47	47	4.431	4.403
10051009_3	3.54	3.68	3.72	3.73	3.75	3.73	145	142	74	75	6.053	6.066
10051009_4	3.59	3.80	3.87	3.92	3.88	3.92	254	251	41	41	2.95	2.919
10051009_5	3.49	3.66	3.81	3.82	3.82	3.81	297	295	47	47	4	3.953
10051009_6	3.53	3.70	3.85	3.83	3.86	3.83	347	344	102	103	9.327	9.317
10051009_7	3.66	3.76	3.97	3.93	3.97	3.93	452	449	322	323	30.62	30.59
10051009_8	3.71	3.81	4.05	4.00	4.06	4.00	776	774	209	208	20.15	20.09
10051009_9	3.62	3.65	3.90	3.82	3.92	3.82	1213	1210	83	49	7.432	4.36
10051009_10	3.89	3.85	4.06	3.92	4.12	3.92	1297	1260	40	74	3.7	6.757
10051009_11	3.57	3.72	3.80	3.79	3.81	3.79	1339	1336	88	88	7.987	7.949
10051009_12	3.96	4.13	4.17	4.20	4.19	4.20	1428	1426	62	62	5.449	5.443
10051009_13	3.66	3.86	3.88	3.94	3.91	3.94	1545	1543	47	47	3.984	3.973

10051233_1	3.56	3.71	3.70	3.75	3.73	3.74	54	52	34	33	3.028	2.958
10051233_2	3.65	3.92	3.96	4.13	3.97	4.13	89	87	96	101	8.9	9.222
10051233_3	3.63	3.87	4.00	4.09	4.01	4.09	194	191	127	128	11.88	11.88
10051233_4	3.69	3.89	3.87	3.93	3.89	3.93	322	320	116	115	10.65	10.57
10051233_5	#N/A	4.17	#N/A	4.41	#N/A	4.43	#N/A	923	#N/A	34	#N/A	2.384
10051233_6	3.55	4.00	3.87	4.12	3.92	4.15	964	962	33	32	2.278	2.215
10051233_7	3.54	3.92	3.81	4.05	3.84	4.05	1018	1015	52	52	4.68	4.635
10051233_8	3.49	3.72	3.76	3.80	3.79	3.78	2299	2297	30	30	2.692	2.67
10051233_9	3.59	3.74	3.85	3.86	3.87	3.87	2629	2626	44	44	4.067	4.018
10051233_10	3.44	3.71	3.73	3.89	3.75	3.89	2724	2722	78	77	6.297	6.233
10051233_11	3.45	3.74	3.77	3.90	3.78	3.91	2838	2835	82	83	6.941	6.965
10051233_12	3.52	3.84	3.92	4.07	3.97	4.06	2951	2948	36	36	2.938	2.936
10051335_1	#N/A	3.75	#N/A	3.94	#N/A	3.93	#N/A	1870	#N/A	32	#N/A	2.398
10051335_2	3.39	3.51	3.73	3.64	3.74	3.64	1988	1985	37	37	3.353	3.348
10100845_1	3.38	3.66	3.49	3.65	3.50	3.64	91	92	36	33	2.827	2.752
10100845_2	3.45		3.77		3.77		183		41		3.417	
10100845_3	3.51	3.55	3.72	3.66	3.73	3.66	262	261	148	53	11.53	3.97
10100845_4	#N/A	3.83	#N/A	3.86	#N/A	3.86	#N/A	315	#N/A	93	#N/A	7.487
10100845_5	3.51	3.83	3.75	3.95	3.76	3.96	411	409	59	116	5.486	10.61
10100845_6	3.60	#N/A	3.97	#N/A	3.98	#N/A	471	#N/A	55	#N/A	5.133	#N/A
10100845_7	2.83		3.06		3.07		1241		33		1.44	
10100845_8	3.26		3.46		3.49		1415		37		2.432	
10100845_9	3.30		3.60		3.62		1541		45		3.632	
10100845_10	3.61		3.91		3.95		1735		36		3.362	
10100845_11	3.25		3.51		3.53		1790		44		3.93	
10100845_12	3.15		3.48		3.50		1847		55		4.076	
10100845_13	3.48		3.76		3.76		2543		75		6.611	
10100845_14	3.86		4.07		4.07		2619		36		3.353	
10100952_1	3.31		3.66		3.67		60		59		5.063	
10100952_2	3.55	3.42	3.84	3.55	3.87	3.55	121	120	76	59	6.816	5.216
10100952_3	3.51		3.80		3.81		230		164		13.26	
10100952_4	3.68		4.10		4.12		396		38		3.442	
10100952_5	3.27	3.72	3.53	3.88	3.53	3.87	1141	1145	35	34	2.167	2.131
10100952_6	3.19	3.45	3.44	3.57	3.44	3.56	1608	1612	35	40	2.695	2.942
10100952_7	3.58	3.96	3.87	4.13	3.92	4.13	1644	1654	34	34	3.222	3.214
10100952_8	3.46	3.87	3.58	3.89	3.58	3.89	2235	2244	41	42	3.69	3.689
10100952_9	3.30	3.70	3.60	3.81	3.62	3.81	2700	2709	36	37	3.21	3.212
10101053_1	3.58	3.68	3.89	3.86	3.89	3.85	21	18	91	91	8.382	8.373
10101053_2	3.29	3.55	3.52	3.63	3.53	3.62	634	631	41	42	3.497	3.506
10101053_3	3.56	3.78	3.87	4.00	3.88	3.99	726	707	51	68	4.497	5.838
10101053_4	3.44	3.66	3.78	3.92	3.80	3.93	828	826	39	39	3.641	3.637
10101053_5	3.40	3.68	3.74	3.86	3.75	3.86	918	916	85	85	7.622	7.607
10101053_6	3.47	3.73	3.82	3.88	3.83	3.90	1177	1174	39	39	3.201	3.179
10101053_7	3.48	3.71	3.83	3.92	3.85	3.92	1249	1246	65	65	5.903	5.896
10101053_8	3.43	3.79	3.74	3.91	3.74	3.91	1621	1618	50	117	4.501	10.7
10101053_9	3.64	#N/A	3.80	#N/A	3.83	#N/A	1672	#N/A	65	#N/A	6.179	#N/A
10101053_10	3.40	3.69	3.74	3.92	3.77	3.92	1769	1766	48	49	3.901	3.919
10101053_11	3.30	3.61	3.57	3.81	3.60	3.81	1896	1894	55	54	4.279	4.194
10101053_12	3.18	3.48	3.48	3.69	3.49	3.68	1979	1977	55	54	3.316	3.252
10101053_13	3.52	3.74	3.83	3.91	3.84	3.91	2036	2033	108	108	10.1	10.06

10101053_14	3.50	3.71	3.86	3.93	3.87	3.92	2145	2143	43	43	4.045	4.023
10101053_15	3.56	3.65	3.92	3.86	3.92	3.84	2521	2518	57	57	4.915	4.922
10101053_16	3.86	4.04	4.09	4.16	4.11	4.17	2579	2576	84	84	7.935	7.911
10101221_1	3.37	3.63	3.78	3.85	3.80	3.84	10	8	34	34	2.957	2.936
10101221_2	3.56	3.76	3.75	3.81	3.75	3.81	47	44	263	263	22.74	22.7
10101221_3	3.45	3.77	3.90	3.99	3.92	3.99	350	348	35	35	2.71	2.7
10101221_4	3.52	3.76	3.83	4.00	3.84	4.00	409	394	68	80	5.467	5.981
10101221_5	3.33	3.56	3.67	3.79	3.68	3.78	998	996	30	35	2.267	2.452
10101221_6	3.43	3.58	3.73	3.73	3.75	3.74	1102	1099	40	40	3.595	3.53
10101221_7	3.45	3.59	3.84	3.75	3.87	3.75	1222	1219	34	35	3.288	3.313
10101221_8	3.50	3.62	3.79	3.77	3.79	3.77	1385	1382	175	176	15.48	15.48
10101221_9	3.43	3.56	3.77	3.77	3.80	3.78	1873	1870	52	53	4.299	4.3
10110924_1	3.42	3.64	3.50	3.71	3.59	3.70	417	415	34	33	2.884	2.854
10110924_2	4.03	4.29	4.19	4.38	4.19	4.37	454	452	38	37	3.391	3.336
10110924_3	3.26	3.41	3.43	3.56	3.45	3.55	680	707	73	44	5.281	3.275
10110924_4	3.38	3.54	3.71	3.73	3.72	3.74	886	883	36	36	3.245	3.212
10110924_5	3.58	3.81	3.87	4.02	3.87	4.02	926	923	151	152	14.21	14.19
10110924_6	3.66	3.88	3.93	4.07	3.97	4.07	1078	1076	61	61	5.941	5.936
10110924_7	3.76	4.03	4.12	4.28	4.13	4.29	1141	1138	59	75	5.574	6.968
10110924_8	3.33	3.61	3.57	3.73	3.59	3.72	1616	1613	44	45	3.559	3.561
10110924_9	3.65	3.83	3.89	3.96	3.92	3.96	1661	1659	172	519	13.23	43.4
10110924_10	3.69	#N/A	3.89	#N/A	3.90	#N/A	1834	#N/A	326	#N/A	28.55	#N/A
10110924_11	3.86	3.94	4.23	4.22	4.26	4.21	2239	2236	45	45	4.087	4.056
10110924_12	3.54	3.70	3.86	3.87	3.87	3.87	2366	2363	50	136	4.464	11.79
10110924_13	3.75	#N/A	4.00	#N/A	4.01	#N/A	2417	#N/A	85	#N/A	7.311	#N/A
10110924_14	3.79	3.75	3.99	3.86	4.01	3.86	2503	2500	44	45	4.094	4.088
10110924_15	3.73	3.69	3.97	3.79	3.99	3.79	2549	2547	90	89	7.943	7.89
10110924_16	4.02	4.03	4.35	4.22	4.35	4.22	2640	2638	200	199	17.49	17.42
10111027_1	3.58	3.81	3.87	4.07	3.90	4.06	661	658	35	35	2.581	2.535
10111027_2	3.55	3.75	3.83	3.96	3.86	3.96	1029	1026	77	77	6.3	6.237
10111027_3	3.54	3.77	3.79	3.94	3.84	3.96	1122	1119	42	43	3.208	3.214
10111027_4	3.36	3.53	3.55	3.65	3.56	3.65	1560	1557	52	53	4.207	4.208
10111027_5	3.37	3.57	3.61	3.70	3.66	3.71	1617	1614	38	38	2.692	2.675
10111027_6	3.49	3.68	3.74	3.84	3.75	3.84	1656	1654	86	86	7.969	7.924
10111027_7	3.58	3.78	3.91	4.01	3.92	4.02	1789	1787	59	58	5.398	5.346
10111027_8	3.87	4.12	4.05	4.26	4.08	4.27	1849	1846	31	32	2.865	2.882
10111027_9	3.70	3.90	4.19	4.19	4.23	4.19	1889	1887	34	34	2.911	2.88
10111150_1	3.68	3.93	3.97	4.06	3.98	4.06	6	4	36	35	2.91	2.845
10111150_2	3.67	3.98	3.92	4.19	3.94	4.20	125	115	51	59	3.982	4.496
10111150_3	3.27	3.57	3.46	3.62	3.48	3.62	215	212	35	35	2.28	2.259
10111150_4	3.32	3.63	3.69	3.83	3.70	3.83	287	285	30	30	1.999	1.972
10111150_5	3.36	3.55	3.63	3.74	3.64	3.74	340	338	56	55	4.212	4.148
10111150_6	3.40	3.56	3.70	3.77	3.70	3.77	401	399	136	57	10.94	4.02
10111150_7	3.61	3.70	3.94	3.88	3.95	3.88	539	457	90	77	8.582	6.734
10111150_8	3.63	3.83	3.97	4.03	3.98	4.04	630	536	76	167	7.29	15.82
10111150_9	3.49	3.71	3.79	3.88	3.80	3.88	722	720	90	90	8.235	8.186
10111150_10	3.65	3.86	3.99	4.07	4.00	4.06	815	812	190	191	18.24	18.24
10111150_11	3.40	3.52	3.77	3.77	3.78	3.78	1048	1045	37	37	3.172	3.151
10111150_12	4.11	3.98	4.62	4.11	4.64	4.12	1387	1384	44	213	4.157	19.52
10111150_13	3.70	#N/A	3.87	#N/A	3.90	#N/A	1432	#N/A	167	#N/A	15.38	#N/A

10111150_14	3.55	3.83	3.79	3.94	3.81	3.95	1620	1598	39	58	3.546	4.914
10111150_15	4.07	4.31	4.37	4.47	4.38	4.48	1661	1658	62	62	5.515	5.472
10111150_16	3.29	3.41	3.42	3.46	3.43	3.46	2627	2624	37	38	2.716	2.724
10111150_17	3.37	3.46	3.50	3.53	3.51	3.53	2674	2672	67	66	5.006	4.941
10111150_18	3.52	3.79	3.78	3.97	3.79	3.97	2835	2832	71	71	5.344	5.294
10111150_19	3.52	3.72	3.78	3.84	3.85	3.83	2908	2906	35	35	3.169	3.161
10111300_1	3.44	3.71	3.72	3.94	3.73	3.94	42	40	65	65	5.926	5.915
10111300_2	3.83	4.11	4.01	4.23	4.02	4.23	109	106	42	43	4.002	4.001
10111300_3	3.56	3.85	3.89	4.12	3.90	4.12	153	151	78	77	7.475	7.387
10111300_4	3.62	3.87	3.96	4.13	3.96	4.14	233	230	56	56	5.414	5.377
10111300_5	3.54	3.79	3.90	4.06	3.93	4.06	293	291	46	46	4.324	4.338
10111300_6	3.36	3.61	3.55	3.81	3.58	3.82	414	411	112	113	8.16	8.119
10111300_7	3.41	3.67	3.65	3.94	3.66	3.94	570	568	139	138	10.35	10.3
10111300_8	3.47	3.70	3.80	3.98	3.83	3.99	712	710	74	73	6.946	6.877
10111300_9	3.88	4.15	4.10	4.33	4.11	4.33	789	786	195	195	17.45	17.4
10111300_10	3.69	4.09	4.08	4.42	4.13	4.42	986	984	59	41	4.824	3.746
10111300_11	3.24	3.56	3.56	3.84	3.58	3.84	1157	1154	34	35	2.786	2.802
10111300_12	3.70	3.96	3.95	4.18	4.00	4.19	1607	1604	59	59	5.022	5.004
10111300_13	3.77	4.03	4.14	4.33	4.18	4.33	1754	1751	36	36	3.189	3.178
10111300_14	3.65	3.92	3.96	4.18	3.98	4.19	1867	1864	58	58	5.555	5.536
10111300_15	3.37	3.60	3.72	3.91	3.76	3.91	1972	1970	35	34	3.207	3.16
10111300_16	3.37	3.62	3.52	3.80	3.52	3.80	2147	2145	42	40	3.058	2.977
10111300_17	3.71	3.98	3.99	4.23	4.00	4.24	2308	2306	59	59	5.395	5.364
10111300_18	3.61	3.86	3.93	4.15	3.96	4.16	2553	2551	34	33	2.59	2.551
10111401_1	3.82	4.13	4.11	4.37	4.18	4.39	9	7	35	34	3.249	3.202
10111401_2	3.53	3.80	3.76	3.98	3.78	3.99	46	43	34	34	3.093	3.083
10111401_3	3.56	3.94	3.84	4.11	3.87	4.11	294	292	39	39	3.7	3.667
10111401_4	3.61	3.86	3.92	4.11	3.93	4.10	362	359	36	36	3.41	3.392
10111401_5	3.62	3.90	3.84	4.07	3.86	4.08	399	396	42	42	3.882	3.864
10111401_6	3.77	4.06	4.02	4.25	4.06	4.27	1226	1223	82	83	7.422	7.413
10111401_7	3.49	3.76	3.70	3.86	3.75	3.88	1578	1575	33	34	2.916	2.924
10111501_1	4.21	4.52	4.46	4.74	4.50	4.76	68	65	36	37	2.859	2.876
10111501_2	3.17	3.49	3.34	3.56	3.34	3.55	221	218	34	35	2.215	2.227
10111501_3	3.36	3.73	3.52	3.78	3.53	3.79	259	256	40	40	2.345	2.316
10111501_4	3.51	3.85	3.65	3.91	3.69	3.92	305	303	45	49	3.348	3.51
10111501_5	3.44	3.69	3.64	3.77	3.65	3.77	398	396	48	47	4.331	4.255
10111501_6	3.51	3.73	3.65	3.77	3.66	3.76	463	460	53	53	4.419	4.386
10111501_7	3.61	3.92	3.91	4.13	3.93	4.13	1210	1207	136	136	12.63	12.55
10111501_8	3.64	3.93	3.94	4.11	3.98	4.12	1348	1345	34	34	3.186	3.142
10111501_9	3.30	3.59	3.47	3.67	3.49	3.66	1487	1485	44	44	3.122	3.124
10111501_10	3.48	3.84	3.71	3.92	3.73	3.93	1583	1580	40	40	3.494	3.459
10111501_11	3.96	4.17	4.34	4.38	4.37	4.40	1741	1738	44	68	3.877	5.939
10111501_12	3.91	4.19	4.11	4.29	4.14	4.31	1810	1807	86	87	7.904	7.941
10111501_13	3.85	4.15	4.05	4.22	4.07	4.22	1906	1904	187	186	16.84	16.78
10111501_14	3.74	4.04	3.94	4.11	3.95	4.12	2117	2092	105	127	9.507	10.92
10120600_1	3.23	3.47	3.29	3.46	3.31	3.46	10	7	37	37	1.857	1.84
10120600_2	3.13	3.49	3.16	3.43	3.19	3.47	49	46	41	42	2.406	2.41
10120600_3	3.04	3.38	3.12	3.38	3.14	3.38	100	91	60	67	4.016	4.368
10120600_4	3.44	3.70	3.47	3.62	3.49	3.63	175	159	36	49	3.256	4.147
10120600_5	3.24	3.64	3.31	3.66	3.46	3.67	234	232	36	35	2.523	2.456

10120600_6	2.98	3.41	3.04	3.37	3.05	3.37	343	341	58	58	3.304	3.276
10120600_7	3.00	3.41	3.12	3.40	3.13	3.39	403	400	37	37	2.122	2.099
10120600_8	3.23	3.70	3.38	3.72	3.39	3.72	442	440	99	98	6.939	6.859
10120600_9	3.07	3.32	3.24	3.34	3.28	3.36	600	598	31	30	2.25	2.203
10120600_10	3.75	4.18	4.10	4.29	4.12	4.30	644	641	35	36	3.153	3.165
10120600_11	3.51	3.93	3.70	3.90	3.72	3.91	681	678	36	37	2.948	2.969
10120600_12	3.57	3.95	3.76	3.95	3.77	3.95	718	716	392	392	36.31	36.22
10120600_13	3.01	3.29	3.18	3.35	3.20	3.35	2716	2714	31	31	1.712	1.702
10120600_14	3.42	3.61	3.62	3.74	3.67	3.74	2857	2855	34	33	2.099	2.047
10120600_15	2.92	3.19	3.01	3.21	3.02	3.21	2960	2957	35	35	1.713	1.693
10120705_1	3.48	3.66	3.68	3.72	3.70	3.72	256	254	35	35	2.885	2.886
10120705_2	2.75	2.95	2.84	3.00	2.86	2.99	451	449	34	34	1.528	1.512
10120705_3	3.14	3.34	3.19	3.36	3.19	3.36	751	749	69	68	3.31	3.255
10120705_4	2.79	3.27	2.83	3.35	2.85	3.40	908	947	31	40	1.248	2.289
10120705_5	3.01	3.27	3.19	3.35	3.23	3.40	949	947	41	40	2.346	2.289
10120705_6	3.37	3.64	3.58	3.73	3.67	3.75	992	990	44	43	2.697	2.63
10120705_7	3.49	3.73	3.74	3.87	3.76	3.87	1057	1055	101	100	7.625	7.565
10120705_8	3.45	#N/A	3.64	#N/A	3.68	#N/A	1478	#N/A	32	#N/A	1.865	#N/A
10120705_9	2.88	2.90	2.96	2.90	2.97	2.90	2116	2114	60	59	3.818	3.763
10120705_10	3.57	3.73	3.73	3.77	3.78	3.79	2520	2518	37	36	3.009	2.94
10120705_11	3.20	3.36	3.43	3.51	3.43	3.51	2585	2582	64	62	4.387	4.277
10120705_12	3.34	3.48	3.54	3.54	3.56	3.54	2877	2875	44	51	3.408	3.795
10120805_1	4.16	4.20	4.66	4.49	4.66	4.51	183	180	41	42	3.686	3.697
10120805_2	3.10	3.17	3.23	3.23	3.24	3.23	321	319	38	37	1.9	1.84
10120805_3	3.20	#N/A	3.38	#N/A	3.40	#N/A	381	#N/A	30	#N/A	1.797	#N/A
10120805_4	3.63	3.68	3.84	3.73	3.85	3.73	528	526	59	58	5.212	5.161
10120805_5	3.32	3.38	3.54	3.46	3.56	3.45	661	658	66	66	4.79	4.756
10120805_6	3.75	3.91	4.10	4.03	4.11	4.03	729	726	53	54	5.126	5.125
10120805_7	3.32	3.43	3.56	3.50	3.56	3.50	823	820	58	58	4.554	4.521
10120805_8	2.97	2.97	3.06	2.95	3.06	2.95	940	938	32	31	2.23	2.181
10120805_9	3.70	3.81	3.97	3.90	4.03	3.90	990	988	40	39	2.871	2.821
10120805_10	3.72	3.73	3.92	3.79	3.96	3.81	1419	1416	43	44	3.656	3.657
10120805_11	3.22	3.24	3.42	3.30	3.51	3.35	1997	1994	37	38	2.406	2.406
10120805_12	3.29	3.27	3.46	3.29	3.49	3.30	2344	2342	36	35	2.278	2.227
10120805_13	3.40	3.47	3.51	3.50	3.51	3.50	2388	2386	59	59	2.926	2.9
10120805_14	3.37	3.39	3.49	3.44	3.49	3.44	2499	2496	73	73	4.345	4.318
10120805_15	3.23	3.29	3.34	3.34	3.34	3.34	2679	2677	31	30	1.412	1.369
10120805_16	3.26	3.24	3.38	3.27	3.38	3.27	2735	2733	42	42	2.511	2.496
10120905_1	3.60	3.75	3.92	3.90	3.93	3.90	19	17	65	65	5.395	5.342
10120905_2	3.69	3.80	4.01	3.97	4.01	3.97	87	85	115	115	10.43	10.4
10120905_3	3.71	3.79	4.06	3.96	4.09	3.97	210	208	67	66	6.373	6.327
10120905_4	#N/A	3.61	#N/A	3.76	#N/A	3.76	#N/A	526	#N/A	34	#N/A	2.277
10120905_5	3.79	3.86	3.75	3.95	4.02	3.96	632	629	34	34	2.76	2.758
10120905_6	3.67	3.81	3.89	3.88	3.91	3.88	668	665	62	63	5.532	5.534
10120905_7	3.76	3.85	4.01	3.94	4.03	3.96	760	758	44	43	3.183	3.144
10120905_8	3.64	3.77	3.80	3.82	3.84	3.82	805	802	53	54	4.455	4.475
10120905_9	3.59	3.74	3.91	3.91	3.95	3.92	860	858	67	66	5.318	5.224
10121047_1	3.81	3.88	3.91	3.95	3.94	3.94	167	150	40	55	3.675	4.879
10121047_2	3.66	3.85	4.04	4.09	4.04	4.09	210	207	43	44	4.119	4.115
10121047_3	3.79	3.92	4.18	4.17	4.20	4.17	255	252	36	37	3.452	3.452

10121047_4	3.82	3.92	4.08	4.06	4.09	4.06	296	293	232	232	21.7	21.66
10121047_5	3.75	3.98	4.13	4.06	4.16	4.12	530	526	36	38	3.334	3.363
10121047_6	3.64	3.76	3.91	3.93	3.93	3.93	1353	1351	43	42	3.611	3.565
10121047_7	3.85	4.06	4.04	4.14	4.10	4.16	2099	2097	36	36	3.343	3.334
10121047_8	3.55	3.71	3.92	3.91	3.97	3.92	2248	2246	36	35	3.083	3.025
10121047_9	3.70	3.93	3.97	4.01	4.00	4.01	2495	2492	38	39	2.771	2.789
10121047_10	3.47	3.68	3.71	3.89	3.76	3.92	2702	2700	31	31	2.301	2.303
10121047_11	3.70	3.87	3.98	4.01	4.10	4.03	2761	2758	42	43	3.301	3.309
10121047_12	3.76	3.91	3.99	3.99	4.02	4.01	2913	2910	36	36	3.25	3.241
10121047_13	3.60	#N/A	3.98	#N/A	4.00	#N/A	2951	#N/A	48	#N/A	4.068	#N/A
10121148_1	3.50	3.84	3.95	4.08	3.96	4.09	14	11	40	53	3.35	4.221
10121148_2	3.29		3.52		3.51		1814		47		3.918	

References

Ganesan, B. and Clark, N.N. (2001) Relationships Between Instantaneous and Measured Emissions in Heavy-Duty Applications. SAE Technical Paper No. 2001-01-3536.

Truex, T.J., Collins, J.F., Jetter, J.J., Knight, B., Hayashi, T., Kishi, N., and Suzuki, N. (2000) Measurement of Ambient Roadway and Vehicle Exhaust Emissions – An Assessment of Instrument Capability and Initial On-Road Test Results with an Advanced Low Emission Vehicle. SAE Technical Paper No. 2000-01-1142.